MINUTES
OF THE SEVENTEENTH
EXPLOSIVES SAFETY SEMINAR

VOLUME I

AD A036015



DDC
RECEIVED
FEB 25 1977
C

REGENCY INN
DENVER, COLORADO
14-16 SEPTEMBER 1976

COPY AVAILABLE TO DDC DOES NOT
PERMIT FULLY LEGIBLE PRODUCTION

SPONSORED BY

DEPARTMENT OF DEFENSE EXPLOSIVES SAFETY BOARD

WASHINGTON, D.C. 20314

DISTRIBUTION STATEMENT A
Approved for public release;
Distribution Unlimited

(6)

MINUTES OF THE

~~SEVENTEENTH~~ EXPLOSIVES SAFETY SEMINAR (17th)

~~Volume I~~

Held at

Regency Inn,

Denver, Colorado,

on

14-~~15~~16 September 1976.

Volume I.

DDC
RECEIVED
FEB 25 1977
C

Sponsored by

(11) 1976

Department of Defense Explosives Safety Board

Washington, D. C. 20314

(12) 980 p.

Approved for public release; distribution unlimited

034 850
bpk

PREFACE

This Seminar is held as a medium by which there may be a free exchange of information regarding explosives safety. With this idea in mind, these minutes are being provided for ~~your~~ public information. The presentations made at this Seminar do not imply indorsement of the ideas, accuracy of facts presented, or any product, by either the Department of Defense Explosives Safety Board or the Department of Defense.

P. G. KELLEY, JR.
Colonel, USA
Chairman

PRECEDING PAGE BLANK-NOT FILMED

These proceedings are published for information as an accommodation to the participants at the Seminar. The Department of Defense Explosives Safety Board cannot accept responsibility for the correctness of those papers which have been directly reproduced from copy furnished by the authors.

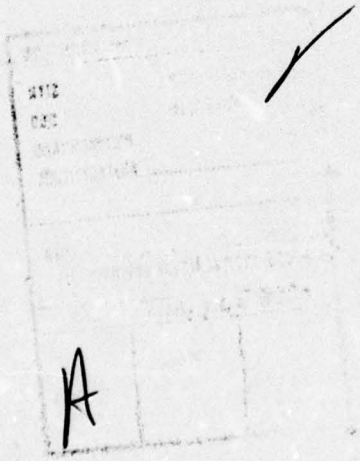


TABLE OF CONTENTS

VOLUME I

EXPLOSIVES SAFETY MANAGEMENT - 50 YEARS AFTER LAKE DENMARK
Mr. Perry J. Fliakas, Deputy Asst Secretary of Defense (Installations and Housing), Washington, D. C. 1

ESKIMO TEST SERIES
Dr. T. A. Zaker, DDESB, Washington, D. C. 7

ELECTROLYTIC LEAD AZIDE DISPOSAL SYSTEM
Mr. J. E. Jamison, Mason & Hanger-Silas Mason Co., Inc., Iowa Army Ammunition Plant, Middletown, IA 21

JOINT CONVENTIONAL AMMUNITION PROGRAM - DEMIL & DISPOSAL TASK GROUP
Mr. J. L. Byrd, Jr., USA Materiel Development & Readiness Command Ammunition Center, Savanna, IL 39

THE ADDITION OF POLLUTION ABATEMENT EQUIPMENT TO EXISTING NAVSEA DEMILITARIZATION PROCESSES
Mr. P. J. Barker, Naval Weapons Support Center, Crane, IN 45

USING CAVITATING WATER JETS FOR DEMILITARIZATION
Messrs. A. F. Conn & S. L. Rudy, Hydronautics Inc., Laurel, MD 51

EXPLOSIVE/FLAMMABILITY CHARACTERISTICS OF VINYL CHLORIDE MONOMER (VCM)-AIR-WATER VAPOR MIXTURES
Messrs. J. C. Hokanson & A. B. Wenzel, Southwest Research Institute, San Antonio, TX 85

HEAT GENERATION MEASUREMENTS FOR THE STABILITY CONTROL OF NITRATE ESTER PROPELLANTS
J.L.C.van Geel, J. Verhoeff, Th.M.Groothuizen, Technological Laboratory TNO, Rijswijk, The Netherlands 121

PHYSICAL PROCESSES CAUSING LOX/LH_2 AUTOIGNITION
Mr. W. H. Boggs, J.F. Kennedy Space Center, NASA, FL 135

THERMAL BEHAVIOR OF A PLASTICS FOAMING AGENT p,p'-Oxy-bis (benzene sulphonhydrazide) Fison's Industrial Chemicals, OBSH
Messrs. J.M. Pakulak, Jr. & C.M. Anderson, NWC China Lake, CA 143

THE PLANNING REQUIRED FOR, AND THE PROBLEMS ASSOCIATED WITH THE CONVERSION IN THE UNITED KINGDOM TO THE UN SYSTEM OF CLASSIFICATION OF EXPLOSIVES
Air Vice-Marshal P M S Hedgeland, RAF, VP (Air) Ordnance Board & Chairman, Explosives Storage & Transport Committee, United Kingdom 165

PRACTICAL PROBLEMS OF IMPLEMENTING THE UNITED NATIONS SYSTEM OF CLASSIFICATION OF EXPLOSIVES
R R Watson, Esq., Explosives Storage & Transport Committee, Ministry of Defence, United Kingdom 171

EXPLOSIVES ON MOTOR VEHICLES AN UPDATE OF DOT REGULATIONS
Mr. D. W. Morrison, Federal Highway Admin, DOT, Wash, DC 185

ADAPTATION OF COMMERCIAL INTERMODAL FREIGHT CONTAINERS FOR CARRIAGE OF AMMUNITION
Mr. D. I. Willis, DARCOM Ammunition Center, Savanna, IL 191

TRAILER-MOUNTED CHAMBER FOR CONTAINMENT OF 40 POUNDS OF TNT
B.D. Trott, J.E. Backofen, Jr., & J.J. White, III, Battelle-Columbus Laboratories, Columbus, OH 229

TESTS ON A NEW TYPE OF BUILDING FOR STORAGE OF PROPELLANTS
J. J. Roure, Ingenieur General de l'Armement, Inspection Technique de l'Armement, pour les Poudres et Explosifs, France 265

ANALYSIS OF CONCRETE ARCH MAGAZINE TO LONG DURATION OVERPRESSURE
Mr. J. M. Ferritto, Civil Engineering Lab, Port Hueneme, CA 275

DYNAMIC ANALYSIS OF MAGAZINE HEADWALL IN ESKIMO IV TEST
Mr. D. P. Reddy, Agbabian Associates, El Segundo, CA 287

DEFLAGRATION TO DETONATION OF SMOKELESS BALL POWDERS AND THE MEANS USED TO REDUCE A DETONATION OCCURRENCE
Mr. E. A. Andrew, Olin Corp., East Alton, IL 319

PRESSURE RELIEF VENTING CONCEPTS FOR ELIMINATING AN EXPLOSIVE HAZARD IN AUTOMATED SINGLE-BASE OPERATIONS
Messrs. C.H. Johnson & F.T. Kristoff, Hercules Inc., Radford Army Ammunition Plant, Radford, VA 339

EFFECT OF CONFINEMENT ON PYROTECHNIC REACTION RATES AND OUTPUT ENERGY
Mr. G.L. McKown, USA Edgewood Arsenal Resident Laboratory, National Space Technology Labs, Bay St. Louis, MS 357

TRENDS IN ELECTROSTATIC PRECAUTIONS IN FILLING FACTORIES
Mr. D. P. Donegan, Royal Ordnance Factory, Chorley, England 363

THE ROLES OF DEFLAGRATION AND EXPLOSIVENESS IN HAZARD ASSESSMENT
Messrs. P J Hubbard & P R Lee, Royal Armament Research and Development Establishment, Royal Arsenal, Woolwich, UK 385

GUIDELINES FOR EVALUATING CONDUCTIVE FLOOR COATINGS
Mr. G. C. Pritchard, NWC China Lake, CA 409

SAFETY HIGHLIGHTS OF THE FIFTH QUADRIPARTITE AMMUNITION CONFERENCE
Mr. L. W. Saffian, Picatinny Arsenal, Dover, NJ 423

ELIMINATION OF BASE SEPARATION IN CAST LOADED PROJECTILES
E. A. Place & J. E. Jamison, Mason & Hanger-Silas Mason Co., Inc., Iowa Army Ammunition Plant, Middletown, IA 427

NOISE ABATEMENT PROGRAM FOR EXPLOSIVE OPERATIONS AT NSWC/DL
Dr. L. L. Pater, NSWC Dahlgren, VA 467

THE NOISE STANDARD REVISITED
Mr. W. V. Hollander, Olin Corporation, New Haven, CT 479

ENVIRONMENTAL QUALITY STANDARDS FOR MUNITIONS-UNIQUE POLLUTANTS
CPT J.P. Glennon & LTC L.H. Reuter, USA Medical Bioengineering Research & Development Lab, Fort Detrick, MD 489

GUIDELINES FOR ENVIRONMENTAL IMPACT STATEMENTS ON NOISE (Airblast)
Mr. J. W. Reed, Sandia Laboratories, Albuquerque, NM 503

DESIGN OF STEEL, MASONRY AND PRECAST CONCRETE STRUCTURES TO RESIST THE EFFECTS OF H.E. EXPLOSIONS
J.J. Healey, Samuel Weissman, & Norval Dobbs, Ammann & Whitney and Paul Price, Picatinny Arsenal 511

SHEAR STRESS IN ONE-WAY SLABS SUBJECTED TO BLAST LOAD
Mr. W. A. Keenan, Civil Engineering Laboratory, Port Hueneme, CA 553

AN ECONOMIC STUDY OF BLAST RESISTANT BUILDINGS
Mr. C. C. Huang, USA CofEngineers, Huntsville, AL 569

METHODS FOR UPGRADING BLAST RESISTANCE OF EXISTING STRUCTURES
Kenneth Kaplan, Scientific Service, Inc., Redwood City, CA and Dr. B. L. Gabrielsen, San Jose State University, CA 593

A REPORT ON U.S. COAST GUARD EXPLOSION-SUPPRESSION TESTS
Mr. T. E. Larsen, Detector Electronics Corp, Minneapolis, MN 615

A WATER DELUGE FIRE SUPPRESSION SYSTEM FOR CONVEYOR LINES TRANSPORTING HIGH EXPLOSIVES
W.H. McLain & Alex Wenzel, Southwest Research Institute and W.O. Seals & Richard Rindner, Picatinny Arsenal 623

DYNAMIC PROCESSES IMPORTANT TO THE SUPPRESSION OF PROPELLANTS AND EXPLOSIVES BY WATER DELUGE ACTION
W. H. McLain, Southwest Research Institute, San Antonio, TX 643

THE CONTROL AND MONITORING OF EXPLOSIVES SAFETY IN THE BRITISH ARMY
Brigadier J H Lawrence-Archer, Chief Inspector Land Service Ammunition, United Kingdom 651

PSYCHOLOGICAL BEHAVIOR OF EXPLOSIVE WORKERS
Mr. A. D. Workum, McDonnell Douglas Astronautics Co, FL 675

REPORT OF ABSENCE OF HEALTH HAZARDS ASSOCIATED WITH RDX MANUFACTURE AND USE IN SHELL-LOADING PLANTS
Drs. J.A. Hathaway & C.R. Buck, USA Environmental Hygiene Agency, Aberdeen Proving Ground, MD 683

TRINITROTOLUENE: A REVIEW OF REPORTED DOSE-RELATED EFFECTS PROVIDING DOCUMENTATION FOR A WORKPLACE STANDARD
Dr. J.A. Hathaway, USA Environmental Hygiene Agency, Aberden PG 693

A DESIGN-AID & COST ESTIMATE MODEL FOR SUPPRESSIVE SHIELDING STRUCTURES
G.D.C. Chiang & R.S.K. Pei, USDARCOM Intern Training Center, Red River Army Depot, Texarkana, TX 707

ANALYSIS OF THE LOADING AND RESPONSE OF A SUPPRESSIVE SHIELD WHEN SUBJECTED TO AN INTERNAL EXPLOSION
Mr. F.H. Gregory, Ballistic Research Laboratory, Aberdeen PG, MD 743

VIRTUAL VELOCITY-STATIONARY MODE TECHNIQUES FOR THE DESIGN OF SUPPRESSIVE SHIELD STRUCTURES
Messrs. A.S. Kushner & M.E. Giltrud, NSWC Silver Spring, MD 761

STRUCTURAL ANALYSIS EMPHASIZING ENERGY METHODS: SOME COMPARISONS WITH SUPPRESSIVE SHIELD EXPERIMENTS
P.S. Westine, P.A. Cox, E.D. Esparza, Southwest Research Institute 777

AIRBLAST AND STRUCTURAL RESPONSE TESTING OF A 1/4 SCALE CATEGORY I SUPPRESSIVE SHIELD
R.N. Schumacher & C.N. Kingery, Ballistic Research Laboratory 811

SYSTEM SAFETY THE KEY TO EFFECTIVE ACCIDENT PREVENTION ON R&D PROJECTS
Mr. R. B. Gordon, Aeronutronic Ford Corp., Newport Beach, CA 903

HARPOON SYSTEM SAFETY PROGRAM
Mr. W. J. Smith, McDonnell Douglas Corp., St. Louis, MO 913

IMPROVED SAFETY FOR SMALL ARMS AMMUNITION ASSEMBLY, INSPECTION AND PACKAGING
Mr. C. S. Skinner, Booz, Allen & Hamilton, Inc., Cleveland, OH 917

THE THERMAL PROTECTION OF IN-SERVICE AIR LAUNCHED NAVAL WEAPONS
Mr. P. B. McQuaide, Pacific Missile Test Center, Point Mugu, CA 931

Volume II contains pages 973 thru 1916

EXPLOSIVES SAFETY MANAGEMENT - 50 YEARS AFTER LAKE DENMARK

Mr. Perry J. Fliakas
Deputy Assistant Secretary of Defense
(Installations and Housing)

Ladies and Gentlemen:

In the overall excitement and fascination of celebrating the 200th birthday of the United States of America, we have passed with little notice another significant anniversary which, while not as meaningful of course, is nonetheless of some importance to the Department of Defense and to persons like yourselves who are in the explosives safety business.

July 10, 1976 was the fiftieth anniversary of the disaster at the Naval Ammunition Depot, Lake Denmark, New Jersey, which set in motion a chain of events which brought about the establishment by the Congress of the Ammunition Storage Board - what we now know as the Department of Defense Explosives Safety Board your host today.

This is not the type of golden anniversary we like to celebrate. There was nothing pleasurable about it, and there are many people who do not wish to be reminded of it.

It is desirable and necessary, however, to occasionally take note of history and to refresh our memories with the lessons to be learned from it.

After the cessation of hostilities in Europe in 1918, large quantities of ammunition backed up at coastal ammunition depots, at ports of embarkation, and in manufacturing plants because of the immediate halt in shipments. This excess explosive material continued to build up for some time and caused severe overcrowding of available storage facilities. One of the magazines involved in the Lake Denmark disaster contained approximately three times the amount of high explosives that is permitted today. Thus, when an explosion did occur, this overstocking and the lack of separation between explosives caused a chain reaction of explosions from one storage magazine to another greatly increasing the amount of property damage and the number of injuries and deaths.

As you have heard so often in the past, that episode brought about the establishment of firm standards for the storage and handling of ammunition and the creation of the forerunner of the Department of Defense Explosives Safety Board.

The United States has recently been again in a position of winding down from a period of active hostilities much as it was after World War I. The same problems again were evident, with ammunition in pipelines headed for

overcrowded terminals. There was also the necessity to review stocks versus requirements, adjust production schedules to rebuild strategic inventories, to modernize our plants and to look at ways of disposing of surplus items with all the environmental considerations such actions now demand.

In any human activity, a time of change is a time of danger. This is particularly true in the explosives business where danger and hazard are our day-to-day companions.

But we have not had another Lake Denmark and the Department of Defense Explosives Safety Board and the Safety Offices of the Armed Services at all levels are to a large extent responsible though seldom do they receive sufficient credit.

It is difficult to work in an organization and to remain dedicated day after day to your profession when the highest praise that can be given your efforts is to say that "Nothing Happened."

It is also very difficult to compete for funds and other resources when nothing has happened. The one sure way to bring top management attention to explosives safety is to have a disaster - yet this is what we are all here to prevent.

Certainly top management - Congress - became interested after Lake Denmark. A lengthy and sometimes acrimonious investigation was held which rivalled some investigations of today - and there were no televised hearings then to stimulate rhetoric and debate - the Congress was thoroughly concerned as it should have been.

As an outgrowth of that investigation Congress directed the adoption of certain quantity-distance tables to keep supplies of ammunition properly separated and to assure that a reasonable and practicable degree of safety was provided. Congress then defined "safe." The definition is interesting and bears repeating.

"As regards the 'safety' of individuals and structures outside the boundaries of ammunition depots, the word 'safety' is a relative term. No one is ever absolutely safe from injury. The average chance of the average individual of escaping injury has, by custom, been termed 'safe'."

In approving the results of this investigation and establishing the Ammunition Storage Board, the committee chairman expressed the view that it should become the agency to guard against a repetition of the "conditions now confronting us", that is, the undesirable concentration of large quantities of explosive stores in facilities not adequate for them with a consequent high risk to personnel and to valuable military supplies and equipment.

While the Congress defined safety 50 years ago and charged us with assuring it, the problem is not that simply solved. When they defined "safe" as the average risk of an average person did they mean we should not take any action that would increase that risk? Probably not. Our general counsel tells us that it is an accepted practice for the Government to take "reasonable" risks in the conduct of its lawful business. What then is reasonable?

The problem arises frequently. It is common to design such mundane facilities as drainage systems to accommodate the worst rain storm that may be expected in 10 years, or 25 years or 50 years depending on the estimated damage that a flood would cause.

In the design of buildings in earthquake prone areas there is continuing debate as to how safe a building should be. At least one proposal has been made that would determine acceptable safety by adding up all the chances of an individual being accidently killed or severely injured in an average lifetime. It would then specify that the building would be acceptable if it did not more than double all the other risks. Clearly this philosophy would accept a very high risk.

Now, as I understand it, in the explosives safety business, safety standards are not predicated on the probability of an accident occuring. Perhaps these probabilities do influence the deliberation, but the usual procedure is to take every action possible to minimize the probability of an accident and then to establish safety standards which assume that an accident will nevertheless occur and which provide "reasonable" safety in that event.

Perhaps the probability of occurrence should be included in the computations of safety standards and we should adopt that most misused of military concepts -- the calculated risk. Misused because it frequently refers to a guess, not to a calculation - and the means of calculating the risk are often not known. This has been suggested before but it is a subject that needs consideration in the years ahead. It may be a means of achieving reasonable safety standards that are also, and I think this is very important, attainable.

The second involves building a magazine or other container for the explosives that is so strong that the effects of an explosion are substantially suppressed, or, building protection around facilities that are nearby in order that they and the people within them may be protected. This takes construction effort.

Both real estate and construction are programmed through my office and both are very expensive in today's market. Further, the resources of the Department of Defense are essentially limited. Although the Congress has approved a substantial Defense budget this year, and is generally sympathetic to our requirements - there is never enough to do everything we would like.

In addition, the Military Construction budget is considered separately from other Defense budgets by the Congress and we therefore have our own ceiling imposed on the total money we can spend in any year. A dollar allocated to safety cannot be used to build a runway, a tank repair shop, a drydock, or a school.

Unattainable standards tend to be ignored and rather than contributing to safety probably detract from it because they foster an attitude that if the standard cannot be achieved, nothing need be done.

Why am I talking about attainable and unattainable positions, reasonable and unreasonable standards? It is because I and my associates in the Office of the Secretary of Defense, are always faced with decisions as to how scarce Department of Defense funds will be spent. On safety matters for example or on other vital and competing areas such as support of operational weapons and vehicles or, and I know a little about this, visible and necessary improvements in our facilities and bases.

We have today primarily two ways of keeping the public safe from supplies of ammunition and explosives.

The first involves separation between magazines to prevent propagation of explosions from one to another and large clear or safety zones around them which keep the public far enough away from the site of the explosives to be relatively safe should an explosion occur. This takes real estate.

This allocation of limited resources to competing requirements is one of the most frequent and difficult management actions I must take and this is of course true for the Department of Defense and the Government in general.

Because of the nature of this constant competition, my office sometimes must act as an arbiter between the requirements of safety and the demands of operational procedures and readiness. When this occurs I look to the Department of Defense Explosives Safety Board to be a strong and effective advocate of safety. If I err in any direction I intend to err on the side of safety and when such debate arises the Explosives Safety Board's view usually prevails.

Lest anyone be led to believe that safety does not get a large amount of our dollars let me assure you that every Military Construction Program contains money for the specified purpose of safety.

This frequently occurs because of our direction that all construction projects or acquisition or disposal of real estate involving explosives or projects near explosives facilities be cleared with the Explosives Safety Board before they are programmed. Thus, any resiting or other requirements imposed by the Board will be in the project by the time we see it.

Many projects are undertaken for the specific and single purpose of safety. An example is in Apra Harbor on Guam. For some time the Navy, the Air Force and ourselves have been concerned with the crowded conditions of Apra Harbor, the proximity of the ammunition pier to commercial facilities, and the necessity to truck ammunition through congested business and residential areas to Andersen Air Force Base.

Several hundred thousand dollars have been spent on feasibility studies and environmental studies of ways to alleviate these problems. A solution was found involving a new pier, a new harbor entrance and a barge pier at Andersen Air Force Base. The Government of Guam approved and the Navy recently requested and received my approval to spend over five million dollars on subsurface exploration and design. The whole project when carried out will probably cost between 40 and 50 million dollars.

Another recently undertaken project is the construction of new homeports for ammunition ships on both coasts away from busy commercial ports. We originally estimated that some $20 million dollars would be involved in this program (which was started this year) but with rising costs of construction the total will probably far exceed that.

The Navy should be congratulated for their commitment of funds to these projects as well as to their entire explosives safety program.

And since I, as a member of the Office of the Secretary of Defense, cannot show favortism, and also because they fully deserve it, I would like to compliment the Army and the Air Force as well on their dedication and support of explosives safety programs.

Adequate safety depends as much or more upon proper management of our existing resources as it does on obtaining new funds. We are frequently advised or requested to give up land used for safety zones since empty land appears underutilized - this is true for aircraft flight safety clearance areas as well as explosives - or to tear down currently unutilized ammunition igloos to make room for other new construction.

We have resisted these pressures in several cases but it is true that empty land or igloos are underutilized. The ideal solution is to find a use that is compatible with the safety requirements yet preserves the ability to make full use of the facilities for ammunition if necessary. Grazing and other agriculture seem compatible with some safety zones - but also compatible are certain unattended power stations or communication facilities - sanitary land fills or even sewage sludge drying beds.

The risk of a small number of people intermittently exposed may be acceptable where danger to larger numbers is not.

Again I have suggested that one degree of danger may be acceptable and another may not. To be able to make such a determination, one must have knowledge. One must be able to truly calculate a risk.

This is why it is so urgently necessary that the Explosives Safety Board continue its program of research into the nature and extent of hazards and means to alleviate them. The Board's budget in this area has been small and when it must support a test program and be spent to buy explosives, build test facilities, provide instruments and so forth, there is very little left with which to buy brain power. And until about 10 years ago we had no coordinated research program in this field at all. Perhaps this explains in large measure why there are many unanswered questions remaining 50 years after Lake Denmark.

In an ideal world we could plan ahead with such enlightened wisdom that we could avoid the necessity of choosing between competing objectives. We do our best and we attempt to look 5 years ahead with some certainty and even 20 years ahead when we can. Again, to do such planning in any reasonable way, we must have knowledge.

It is in both these areas, knowledge and planning, that seminars of this type can be effective.

Seldom, except for a rare flash of inspiration, will "new" knowledge result. But knowledge will be exchanged and what may have been old to one person is new to another.

Since we need knowledge, and as I have previously stated our budget to obtain it is limited -- we must make maximum use of our available resources. And you here today, are a resource.

The Department of Defense looks to the Explosives Safety Board and to the rest of you to share with each other -- whether in formal session or informal -- that information which will let us make the hard decisions and yet assure that adequate safety is always programmed into our plans and projects. We owe it to ourselves. We owe it to the American people.

I wish you luck and success in your conference.

Thank you.

ESKIMO TEST SERIES

Dr. T. A. Zaker
Department of Defense Explosives Safety Board
Washington, D, C.

Beginning in late 1971, a series of explosion tests of full-scale earth-covered ammunition storage magazines has been sponsored by the Department of Defense Explosives Safety Board and conducted at the Naval Weapons Center, China Lake, California. These tests have had the general objective of rationalizing the quantity-distance standards for magazines. The results justified significant reductions of the distances formerly applied to situations involving exposure of the headwall of one magazine to the earth-covered side or rear of another (1)*. The performance of several different headwall and door combinations under explosive blast loading was evaluated (2,3). During the course of the program a noncircular corrugated steel arch magazine was designed under the supervision of the Army Corps of Engineers.

The oval arch magazine was subjected in ESKIMO III to lateral blast loading from a full-size donor igloo filled with bombs at the minimum side-to-side distance permitted between earth-covered magazines (4,5,6). The standard for that orientation had been established by a series of tests of circular steel arch magazines at the Naval Weapons Center in 1962-63. The reinforced concrete headwall of this magazine is fitted with a single-leaf steel door suspended from an overhead track. Prior to ESKIMO IV, this combination had not been tested at the minimum front-to-rear separation distance of 0.8 $m/kg^{1/3}$ now permitted by standards.

ESKIMO IV Test Design

In ESKIMO IV, conducted in September 1975, the oval arch magazine was subjected to face-on blast from a bare hemispherical explosive charge designed to produce the loading expected on a headwall facing the rear of a full-size earth-covered magazine at 0.8 $m/kg^{1/3}$. The test structure is located northeast of the explosion source in the test area layout, Figure 1. Exposed also at the same distance, west of the source, was a circular steel arch magazine with a lighter headwall, fitted with the same single-leaf sliding door, and one east of the source having the two-leaf hinged door normally provided in that design.

---

*Numbers in parentheses designate references.

Free-field pressure-time histories had been recorded by transducers mounted on the flat ground surface to the rear of the donor igloo in ESKIMO III. The donor contained 159,000 kg of tritonal in M117 bombs. At 0.8 $m/kg^{1/3}$, the peak overpressure was found to be about 3.8 bars and the side-on overpressure impulse about 40 bar-ms.

The explosion source for ESKIMO IV designed to produce this free-field pressure and impulse was a 16,800-kg hemisphere built up of 3.6-kg TNT blocks, located at the center of the 45-m radius circular array of the three target structures (Figure 2). At this distance, a 3.8-bar shock striking the headwall at normal incidence will be reflected to about 16 bars. The impulse loading on the front wall depends on the shape and dimensions of the wall.

Piezoelectric transducers were installed at several locations on the headwall and door of the oval arch igloo to obtain a fairly complete picture of the blast loading as a function of position on the wall. Their locations are shown in Figure 3. A few such gages were also mounted on the headwalls of the other exposed igloos.

Linear motion transducers (LVDT's) were mounted on an inertial platform consisting of a massive structural steel framework suspended from the arch behind the headwall and door of the oval arch igloo. Accelerometers were fastened to the wall at essentially the same locations as the LVDT's, making possible a direct comparison of the velocities derived from the two instruments at each such point. The locations of these instruments are shown in Figures 4 and 5. A few linear motion gages were also positioned at selected points behind the headwalls of the other acceptors.

The ESKIMO IV detonation on 10 September 1975 was recorded photographically from directly overhead by means of a helicopter-borne high-speed camera, as well as from ground stations. (A 13-min, 16mm color sound motion picture produced by the Naval Weapons Center was shown, summarizing the principal qualitative findings of the ESKIMO IV test.)

ESKIMO IV Results

Maximum permanent deflection at the bottom edge of the door of the oval arch igloo was about 30 cm, and permanent displacements of the headwall slab ranged up to about 5 cm (Figure 6). The test demonstrated this headwall and door design to be well balanced and completely effective in preventing communication of an explosion to ammunition stored in the magazine.

Pressure-time histories recorded by gages mounted on the oval arch magazine headwall exhibit maximum values ranging from 14 to 19 bars and load durations of about 15 ms. Records from a vertical array of gages are reproduced in Figure 7. The impulse load per unit area was about 80 bar-ms.

The complicated structure of the first millisecond or so of the waveforms from the bottom and middle thirds of the headwall may be due to the projection of the pilasters and lintel beam about 46 cm forward of the otherwise flat slab around the 3.05-m square opening.

Comparison With Predicted Response

Independent calculations of the response to the measured loading were made using a nonlinear, dynamic finite-element computer program. The computation mesh and the predicted displacement contours at 158 ms are shown in Figure 8. The behavior of reinforced concrete was described by a bilinear moment-curvature relationship, and the supporting soil was simulated by nonlinear springs and dampers. The duration of the computed transient response is about 100 ms. Predicted deformations after, say, 150 ms are considered to be the permanent ones. The computed time history of the response at a particular node is shown in Figure 9.

Computed motions compared favorably with the response measured by instruments which were located at nodes of the computing mesh so as to facilitate this comparison. Records from a few of the linear motion gages are reproduced in Figure 10. The purpose of independent calculations of the response to the measured loads was to gain confidence in modeling the behavior of magazine structures. Since scale-model experiments with instrumented, nonresponding acceptors can be used to determine structure loadings, this has provided a tool for evaluation of magazine designs with reduced reliance on expensive full-scale testing.

Future Plans

The oval arch igloo design includes structural features known as thrust beams of reinforced concrete cast along the exterior of the corrugated steel arch at the regions of maximum curvature in the cross section. These are intended to ensure the development of adequate horizontal thrust to resist downward load on the shallow arch segment above the beams. They contribute significantly to the cost of construction, and the need for them is questionable in view of the mode of permanent deformation observed in ESKIMO III, which was a flattening of the arch on the side toward the donor, and a slight upward movement at the crown.

In ESKIMO V, planned for mid-1977, the thrust beams will be stripped from the oval arch magazine, the earth fill restored, and the structure retested against lateral explosive blast loading using a bare aboveground charge, probably a hemisphere, designed to produce the levels of peak pressure and impulse measured in ESKIMO III on the surface of the earth fill over the top of the arch. These were about 6 bars and about 45 bar-ms. In the same test, a reinforced concrete igloo of noncircular cross section will be exposed to the same levels of pressure and impulse. It will be constructed on or near the site of the light-gage circular steel arch acceptor

in ESKIMO III. This will demonstrate the applicability of the side-to-side intermagazine distance standard to concrete igloos. This standard was established in tests conducted exclusively on steel-arch igloos. The concrete test igloo is of relatively recent design and has an internal cross section quite comparable in usable storage space to the oval steel arch, and may be competitive with it in some localities from an economic standpoint. The explosion source for ESKIMO V is currently being designed with the aid of model simulation experiments, and is expected to be in the range of 20 to 30 metric tons of TNT.

References

1. F. H. Weals, "ESKIMO I Magazine Separation Test," NWC TP 5430, April 1973.

2. T. A. Zaker, "ESKIMO II: Summary of Results and Damage Observations," Minutes, 15th DDESB Seminar, 139-148, September 1973.

3. F. H. Weals, "ESKIMO II Magazine Separation Test," NWC TP 5557, September 1974.

4. T. A. Zaker, "Summary Report, *ESKIMO III Test*," *Minutes*, *16th* DDESB Seminar, 3-7, September 1974.

5. T. A. Zaker, "ESKIMO III: Magazine Structure Damage Observations," Minutes, 16th DDESB Seminar, 179-183, September 1974.

6. F. H. Weals, "ESKIMO III Magazine Separation Test," NWC TP 5771, February 1976.

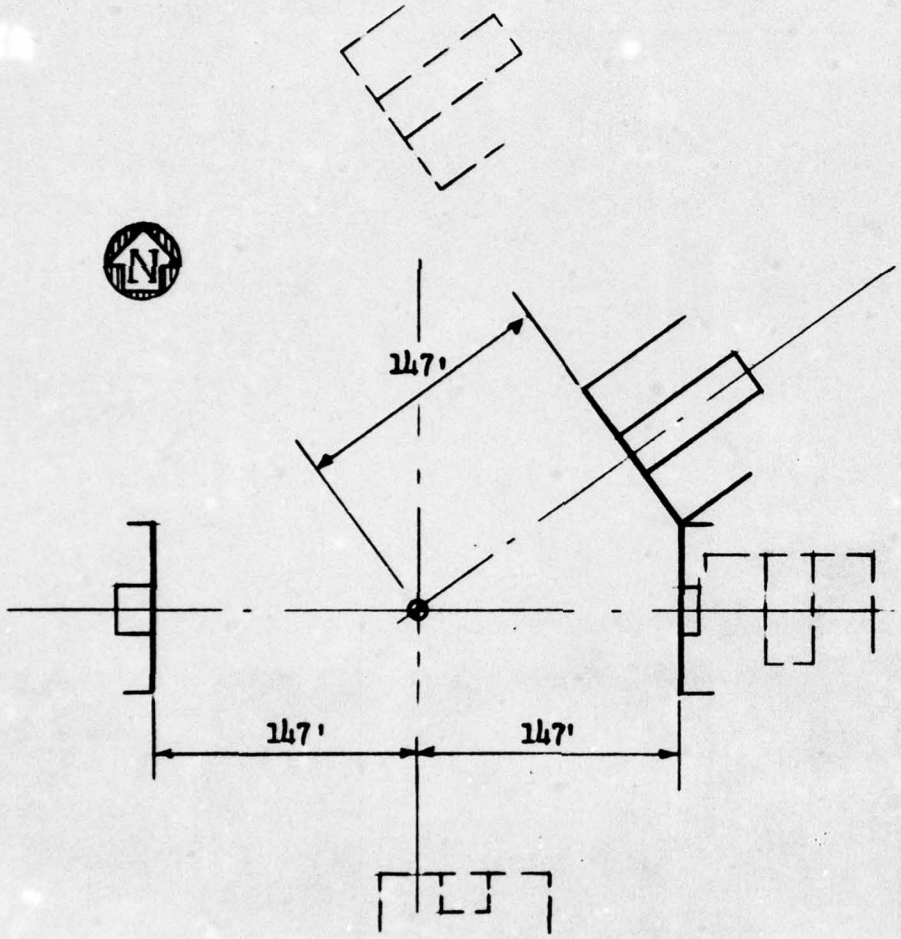


Figure 1 ESKIMO IV Test Area Layout

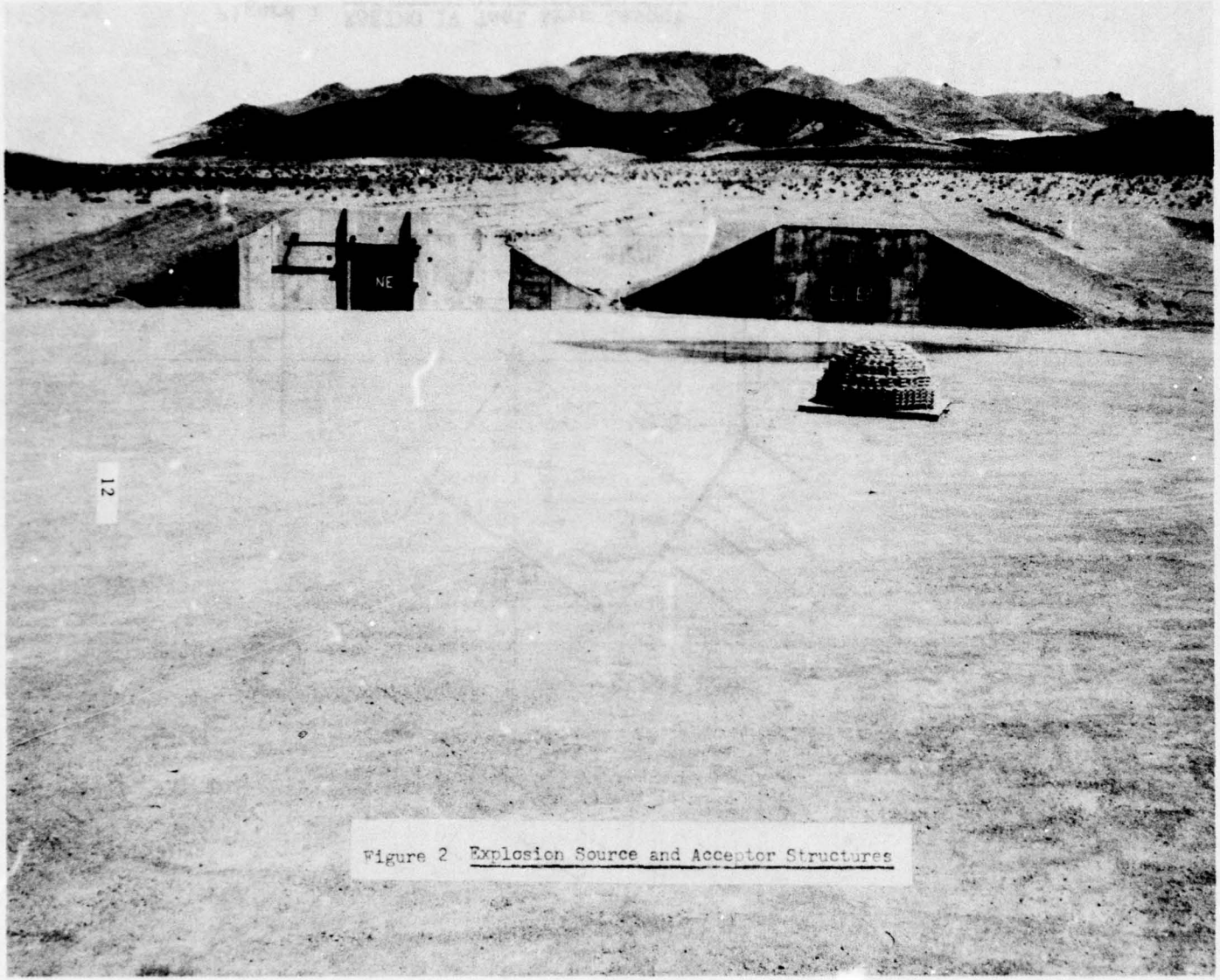


Figure 2 Explosion Source and Acceptor Structures

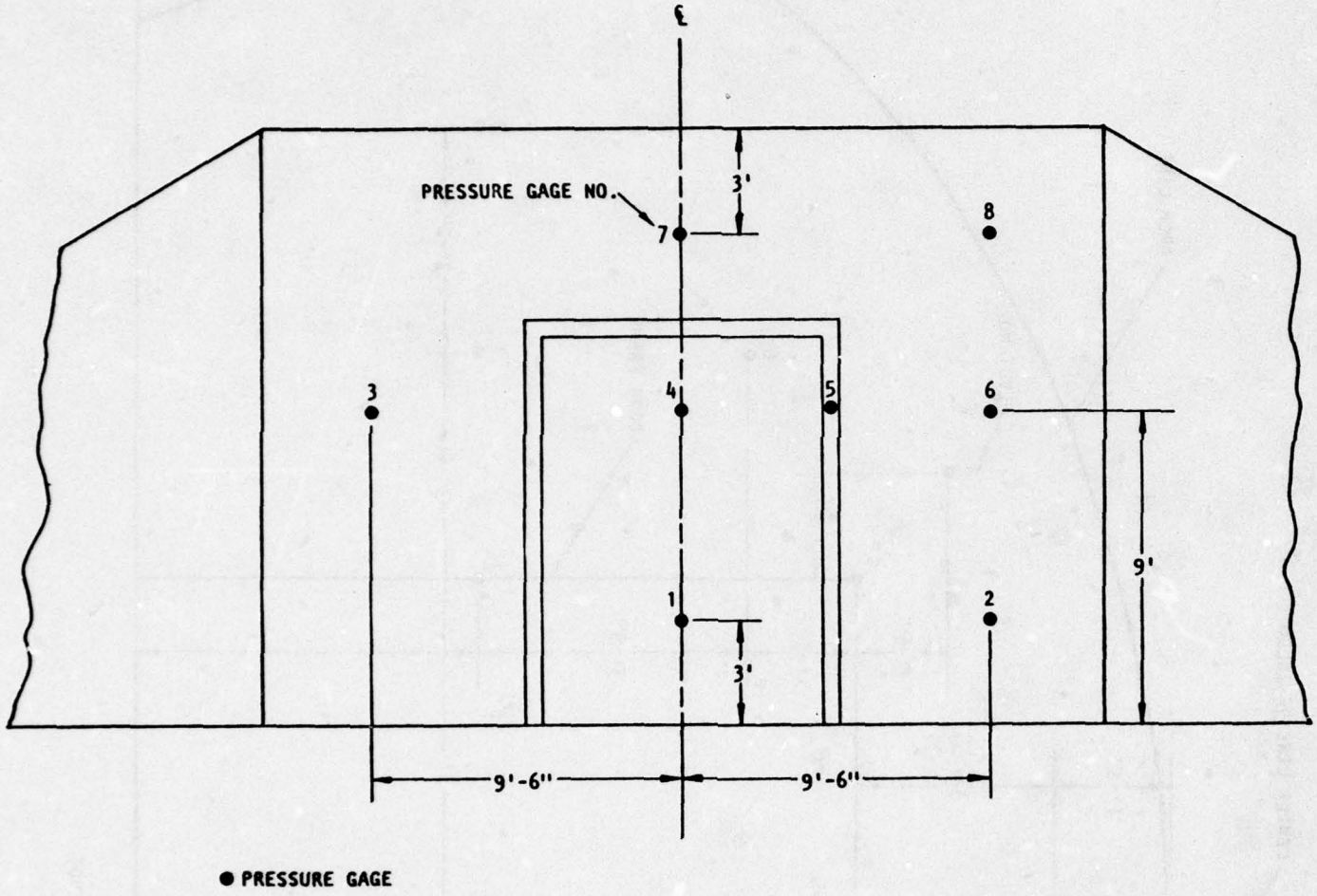


Figure 3 Pressure Gage Positions on Oval Arch Igloo

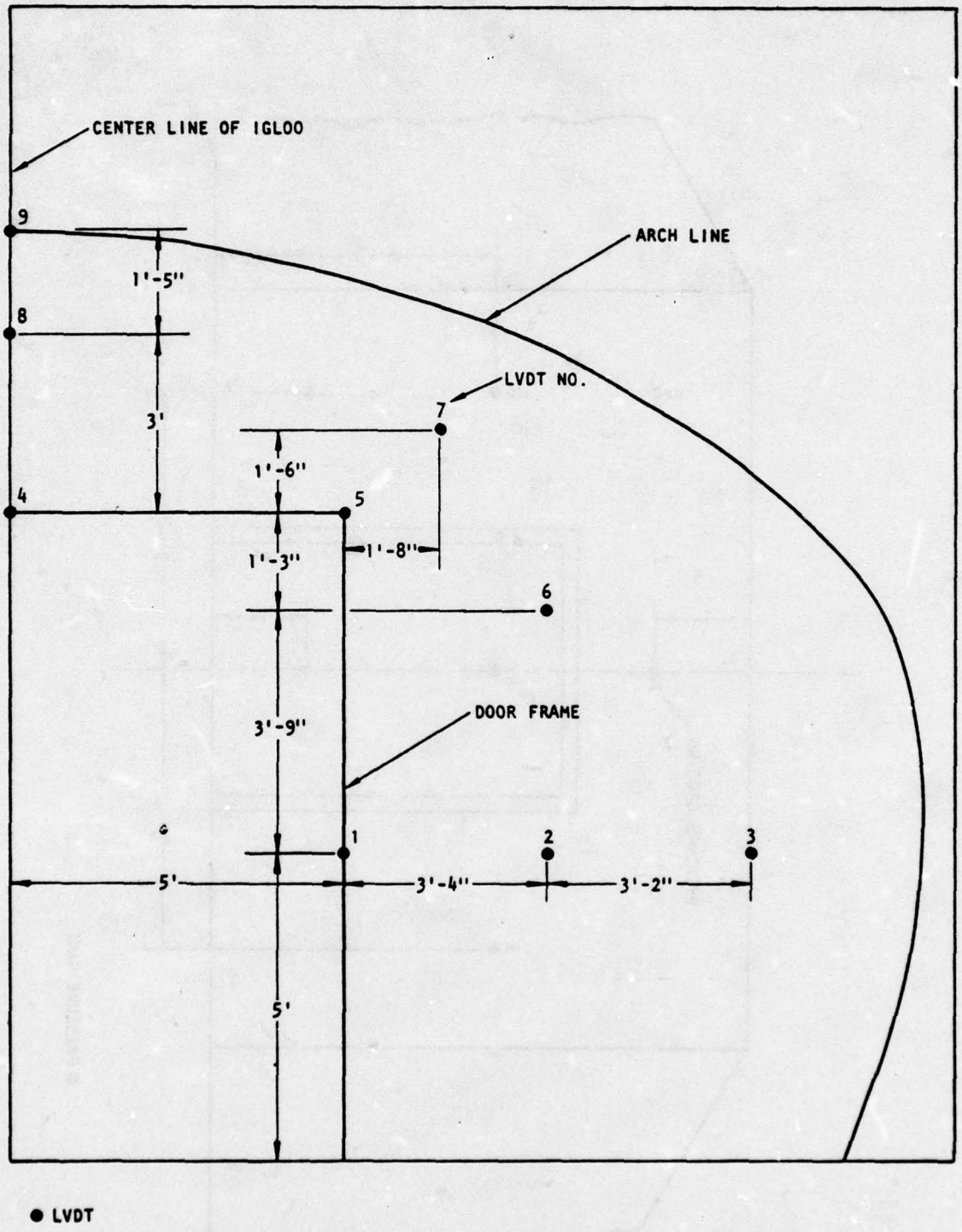


Figure 4 Positions of Linear Motion Gages on Oval Arch Igloo

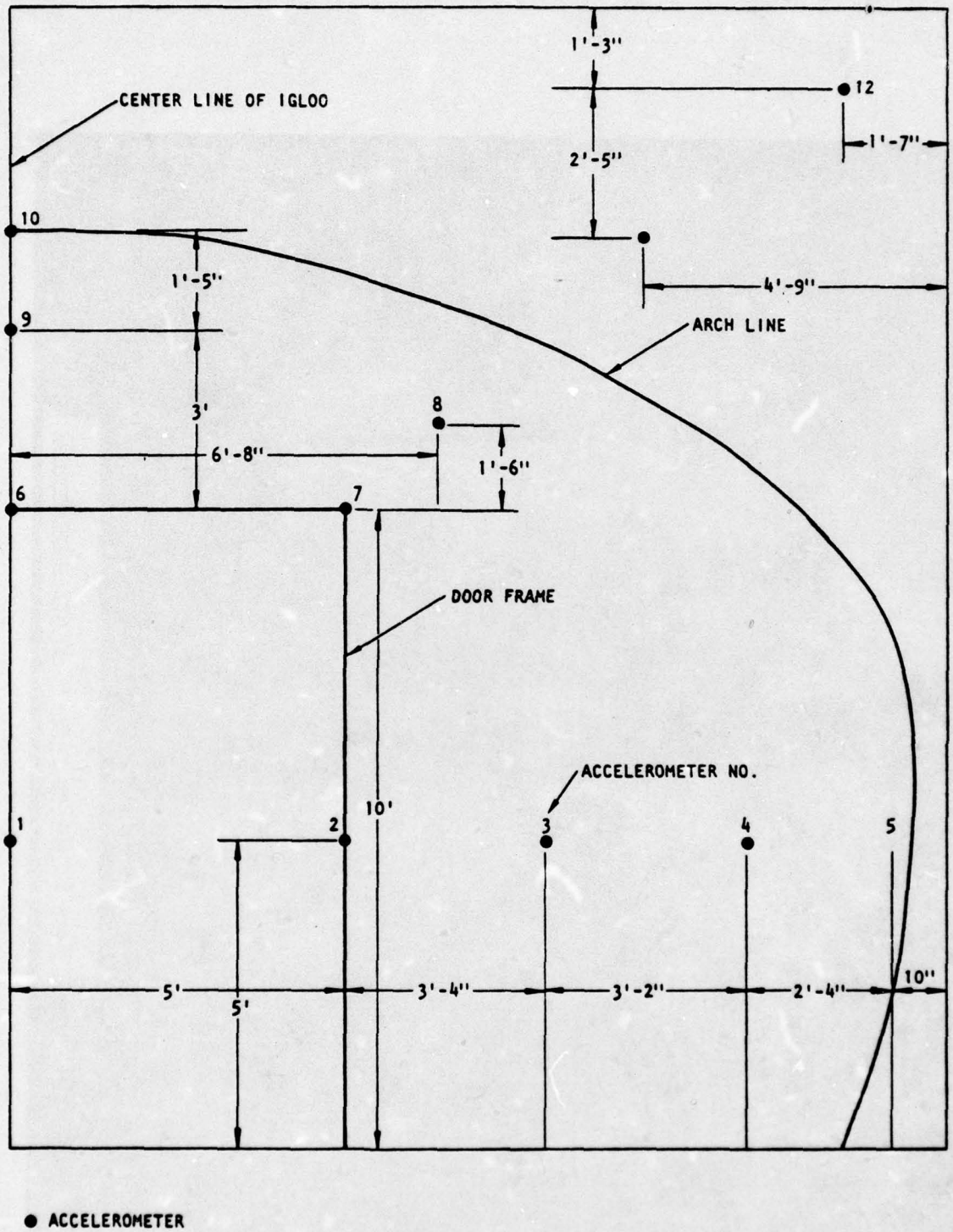


Figure 5 Accelerometer Locations on Oval Arch Igloo

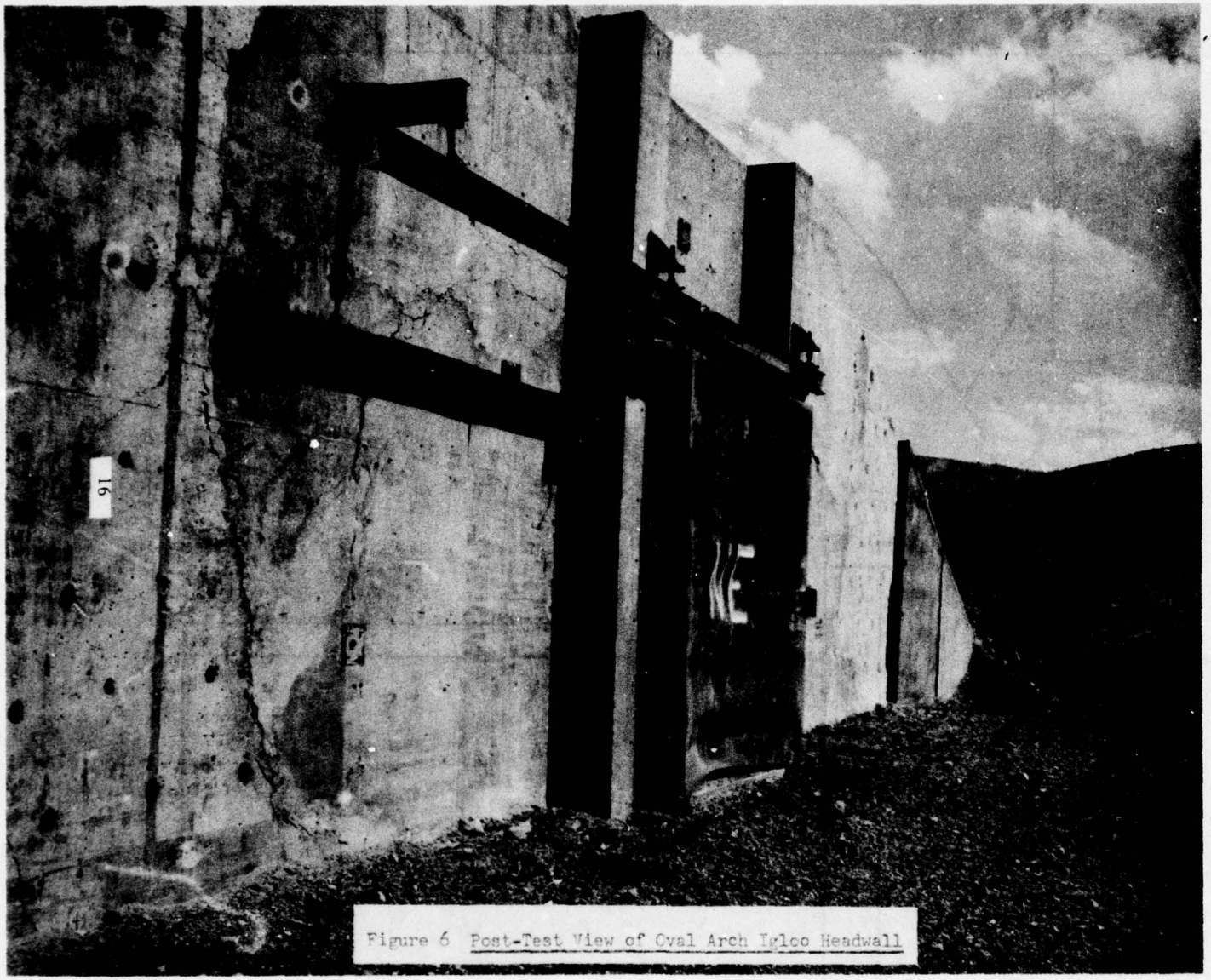


Figure 6 Post-Test View of Oval Arch Igloo Headwall

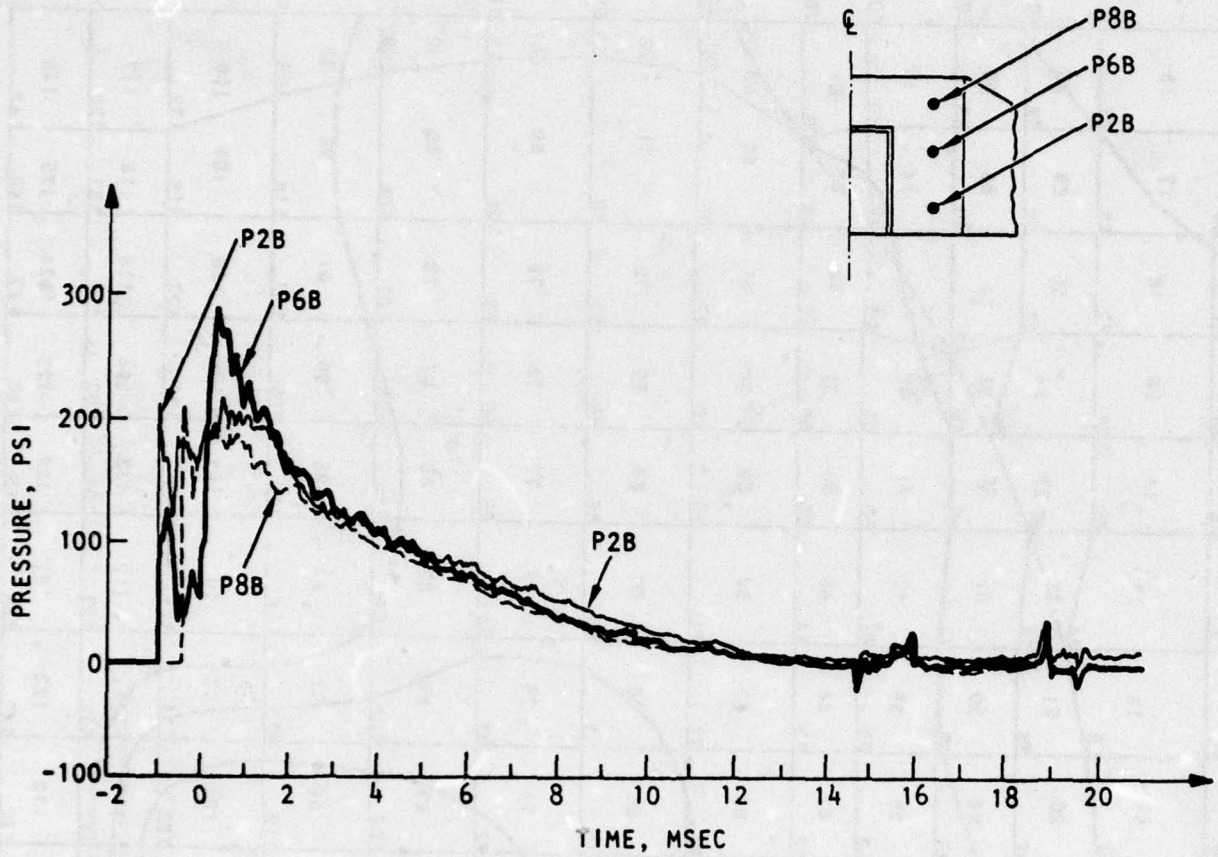


Figure 7 Pressure-Time Histories on Oval Arch Igloo Headwall

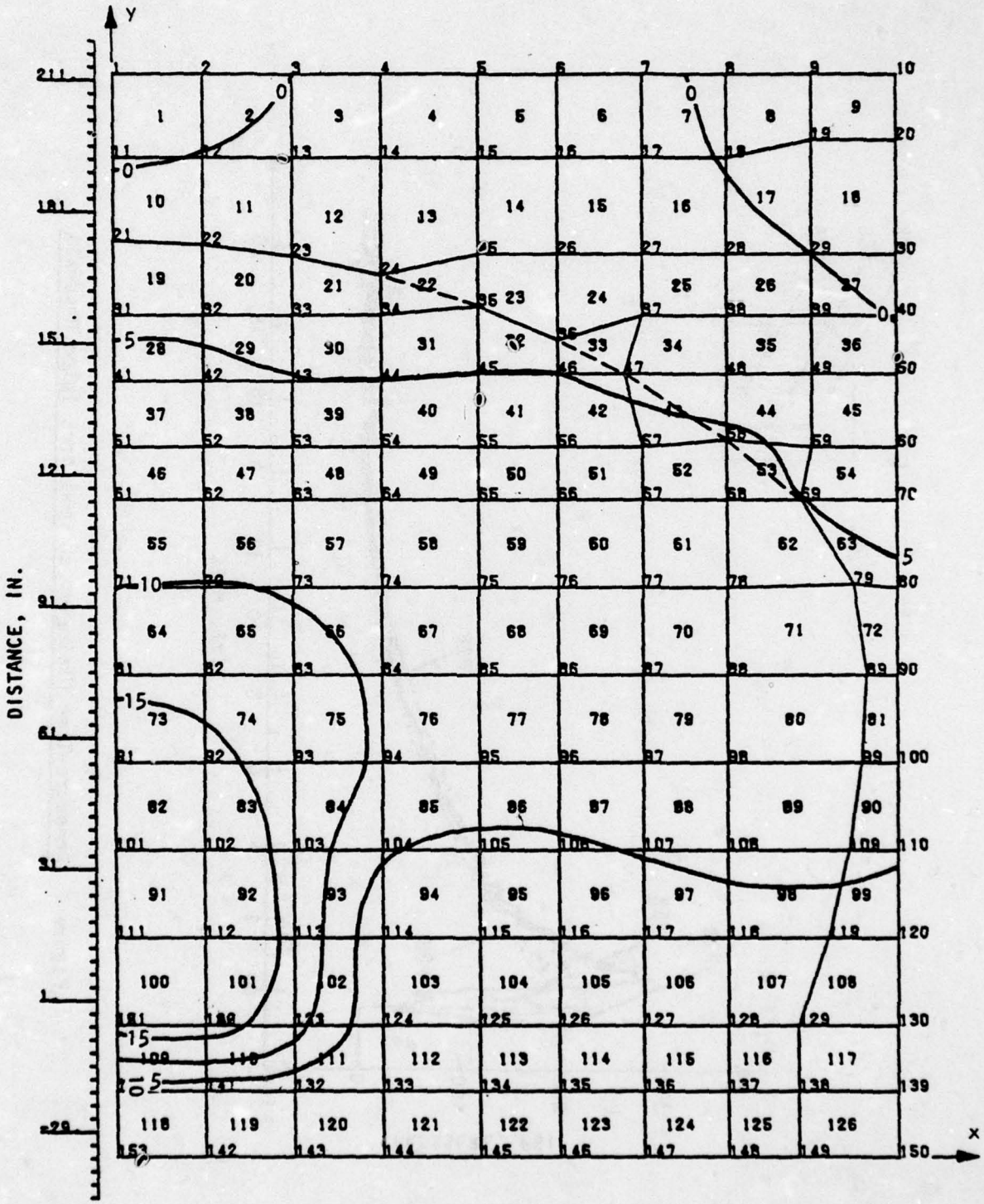
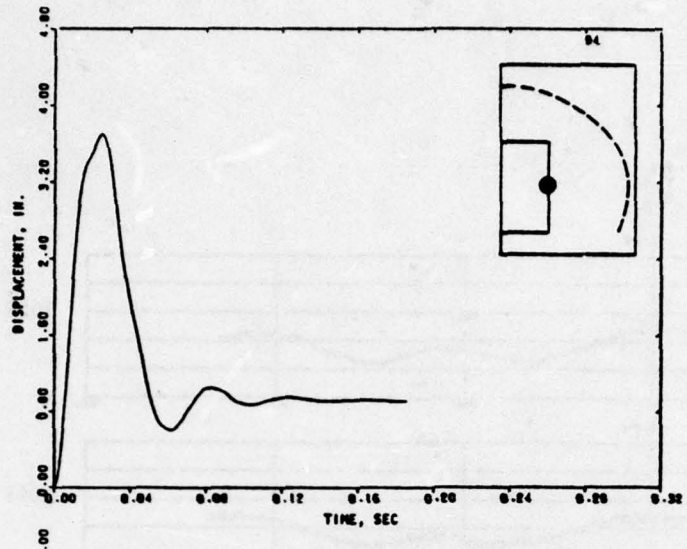
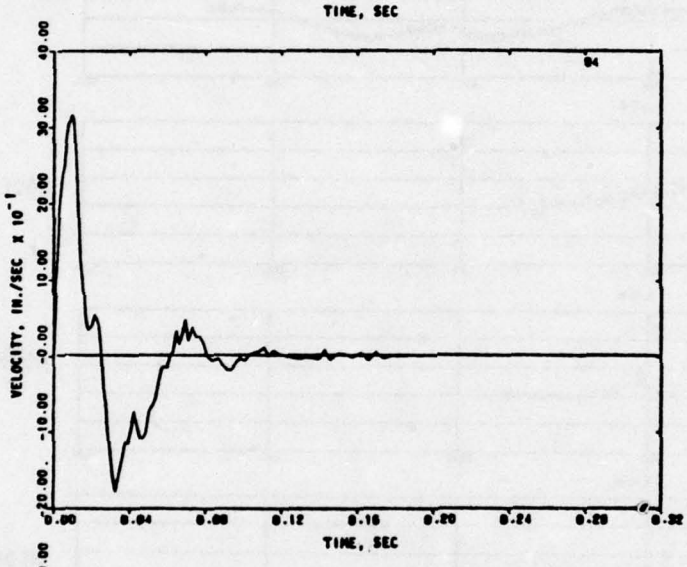


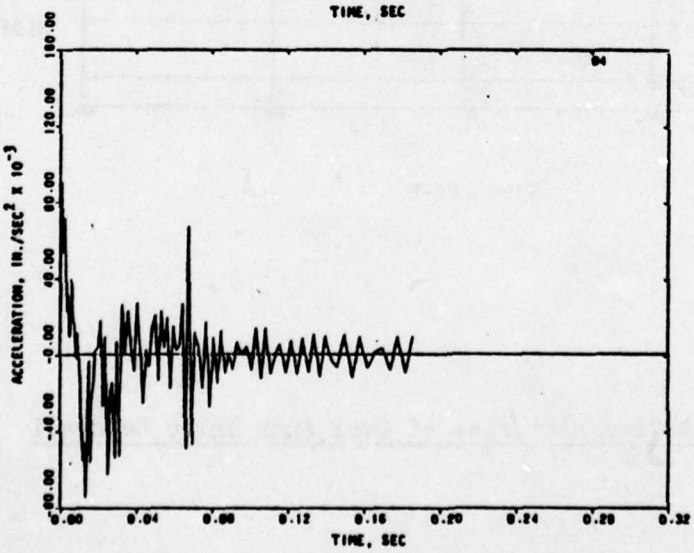
Figure 8 Displacement Contours at 158 ms (Units: 0.01 ft)



(a) Displacement



(b) Velocity



(c) Acceleration

Figure 9 Computed Motion of Oval Arch Igloo Headwall at Node 94

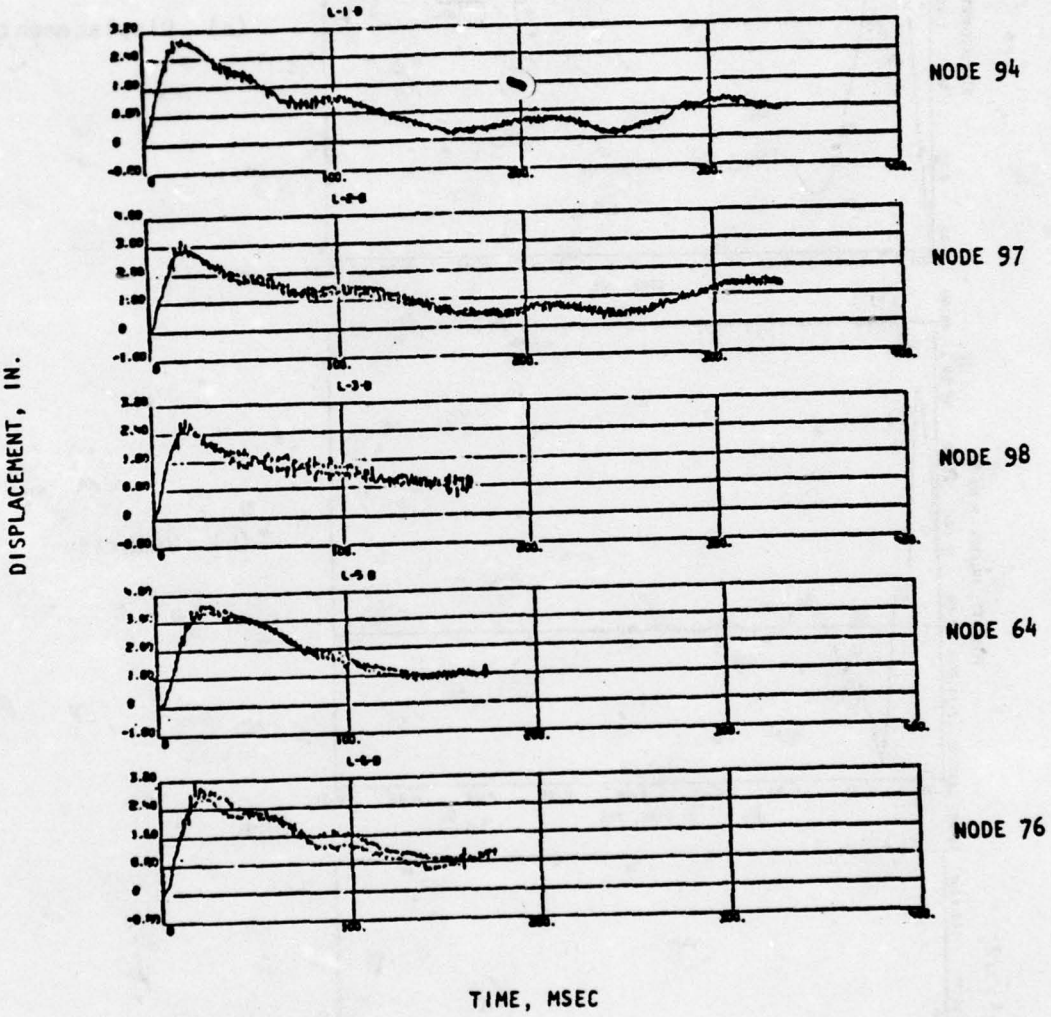


Figure 10 Displacement-Time Histories of Oval Arch Igloo Headwall

ELECTROLYTIC LEAD AZIDE DISPOSAL SYSTEM

J. E. Jamison
Mason & Hanger-Silas Mason Co., Inc.
Iowa Army Ammunition Plant
Middletown, Iowa

Mason & Hanger-Silas Mason Co., Inc., operating contractor at the Iowa AAP has developed a pollution-free lead azide disposal system.

The Electrolytic Lead Azide Disposal System was invented in 1969 by J. R. Polson, Manager, Technical Service. Laboratory work carried out under his direction led to the initial proposal which was submitted to Picatinny Arsenal in May of 1970. Later a Pilot Scale Study was funded under a MM&T Project No. 5734114 and following this, a full scale 25 lb/hr system was developed and installed at Iowa AAP.

This presentation will review the development of the Electrolytic Lead Azide disposal system. (Due to the short time allotted for this presentation, many of the development details will be omitted.) It begins with the problem of lead azide disposal.

The Army has approximately 347,000 lbs. of Special Purpose Lead Azide to destroy. A pound of lead azide is approximately 71% lead. Present disposal methods are costly, not pollution free and hazardous. Today, disposal of lead azide by detonation is frowned upon by the EPA and is costly and hazardous.

The goal of this project was the achievement of a pollution-free 25 lb/hr electrolytic disposal system for lead azide and the efficient recovery of lead as pure metal. This method when compared to all other disposal methods is an economical system for the disposal of lead azide.

In this system lead azide is chemically disassociated in an electrolyte and the lead is plated at the cathode and nitrogen is evolved at the anode.

Electrolysis has advantages because chemical cost is reasonable (a single solution may be reused many times), and a salable product is obtained.

The cost of material and power consumption per pound of lead azide destroyed is about $0.06. This is significant in view of the comparative costs for other chemical methods which are as high as $68.10 per pound of lead azide destroyed for the Ceric Ammonium Nitrate Method.

Here are some slides which I hope will be beneficial to those present who have never seen lead azide handled or packaged.

Slide 1 - standard packing barrel of lead azide, lid being removed.

Slide 2 - removal of liquid solution (50% alcohol water) from barrel by siphoning.

Slide 3 - removal of sawdust packing from barrel.

Slide 4 - untieing the outer cloth bag which contains smaller cloth bags of lead azide. Also shows larger plastic bag with solution inside.

Slide 5 - cloth bag containing 15 lbs of lead azide being removed from barrel and is being placed in a 5-gallon stainless steel container in water. (Some cloth bags contain 25 lbs of lead azide.) Total explosive weight in barrel is 150 lbs.

Slide 6 - bag of lead azide has been transferred from 15-gallon container into a stainless steel tub and is being kneaded to break it up for removal from the bag.

Slide 7 - bag has been opened and lead azide is being flushed from the sides of the bag.

Sodium hydroxide was the most promising. Various concentrations were tested to obtain optimum plating conditions. The 10% solution had the lead density but the 20% solution was the most efficient.

During development optimum operating temperature was determined. The quality and yield of the lead deposit, the type of electrodes, cathode-anode area ratio, operating current and potential, electrochemical efficiency, heat of solution experiments, addition of lead azide to the electrolyte, and other variables were also investigated.

As the product obtained in the beginning was of poor quality the next goal was to improve the quality of lead.

With the addition of sodium-potassium tartrate and commercial rosin to the electrolyte a product of desired quality was produced.

The next goal was to install a large system to plate the lead at the rate of 25 lbs of lead azide per hour.

Slide 8 - a stainless steel tank which had a volume of 1600 gallons, 2.5 inches from the top, was designed and purchased.

Slide 9 - a 3000 ampere 0-9 volt power supply, all the necessary cable, electrical connection insulators, and panel bars were purchased and installed.

Slide 10 - stainless steel sheets were purchased and electrodes were fabricated from them. Stainless steel steam heating panels were installed.

After installation of the equipment was completed, the electrolyte was prepared directly in the tank. The electrolyte composition was as follows: 20 per cent by weight sodium hydroxide, 5 per cent sodium-potassium tartrate, and 0.2 per cent commercial rosin. Approximately one thousand gallons of water was added to the tank. The sodium hydroxide was added in two increments on successive days as the reaction is very exothermic. Two days after the last addition of sodium hydroxide the 5 per cent sodium potassium tartrate was added. The next working day the tank was heated up to 180°F and the rosin was added. This added temperature is necessary to get the rosin in solution. When all the ingredients were in the tank it was filled to within three inches of the top with water.

One primary consideration had to be solved before a 25 lb/hr system was to be workable. This was the method of lead azide addition. The process of addition of small quantities at a time from a rubber cup was not feasible as it was too slow and it was not possible to see if all of it was dissolved. Therefore, it was desirable to devise a way of adding larger quantities and to insure dis-association of the lead azide. An external addition vessel was a logical addition device.

Slide 11 - after some pondering, it was decided to modify 10 gallon stainless steel can with lid by putting an overflow outlet 6.5 inches above the bottom. This is enough depth to keep 30 lbs. of azide under water. An air-powered pump was acquired and a flushing head fabricated for use with the can. Tygon tubing was attached from the can outlet into the plating tank. The pump then transferred hot electrolyte from the top of the tank and flushed it through the can and back to the tank.

Slide 12 - a small quantity of lead azide was put in the flushing can to test the system and the pump was turned on. The lead azide was readily dissolved, and it was decided that this would be the general method to add the lead azide. To determine the amount of lead azide that could be disassociated, laboratory experiments were performed. The tank of 1600 gallons of electrolyte and 553 pounds of disassociated lead azide was heated to 180°F. Power was turned on and plating was started.

It should be noted that at 0.100 amperes per square inch (Amp^2), some sponge lead was noted and at .085 Amp^2 the yield was approximately the same with good lead quality. This indicates that 0.100 Amp^2 is too much current. The first run made at $0.100_2 Amp^2$ showed considerable sponge lead so a second run was made at 0.085 Amp^2. On this particular test, seven panels did not hold lead. An investigation was made to try to determine why this happened and to devise a way to correct it. It was found that etching the panels before they are put in the tank with a HCl solution would eliminate the problem.

Therefore, for the remainder of this experiment the panels were always re-etched. The average for the five runs with good plate adhesion was 28.6 lbs of lead azide per hour.

The planned plating capability goal has been reached and exceeded. A safe method of lead azide addition on a large scale was developed.

Slide 13 - a stainless steel electrode which has been removed from the tank after plating shows how the lead can be stripped off of electrode.

A practical, efficient, safe, economical and pollution-free disposal system has been developed.

Thank you very much for your attention and I will be glad to answer any questions you may have.



Slide 1

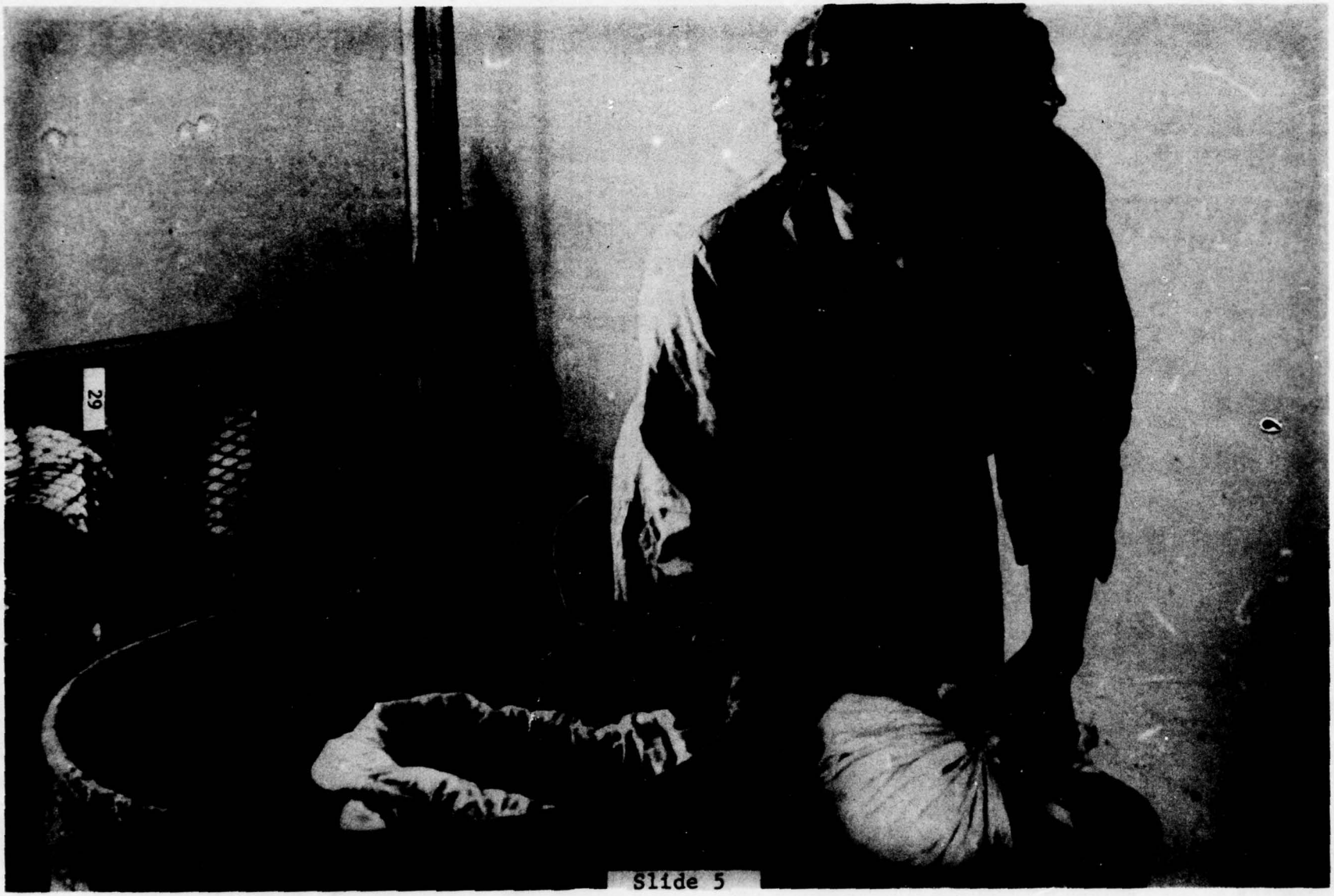


Slide 2

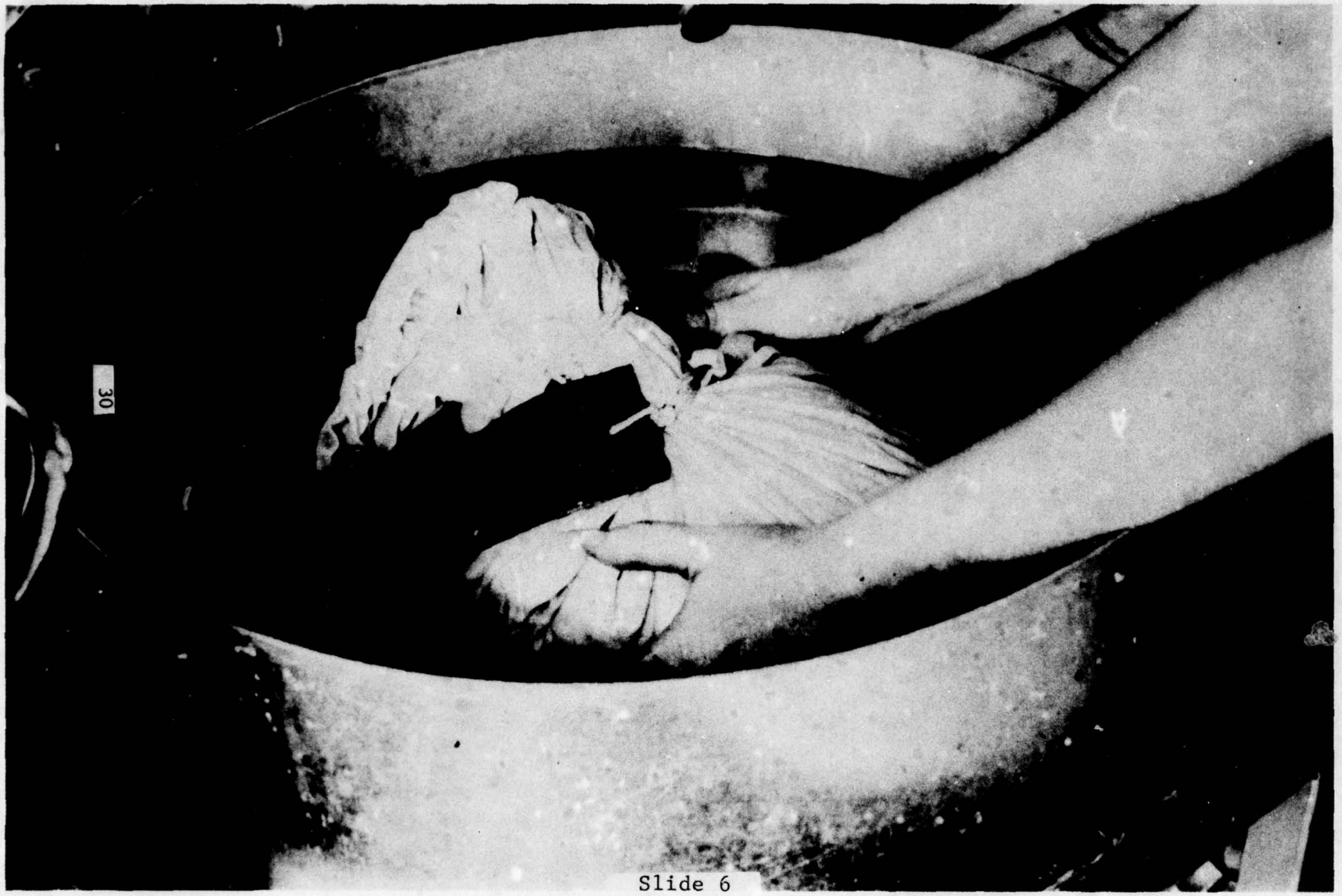

Slide 3
27



Slide 4



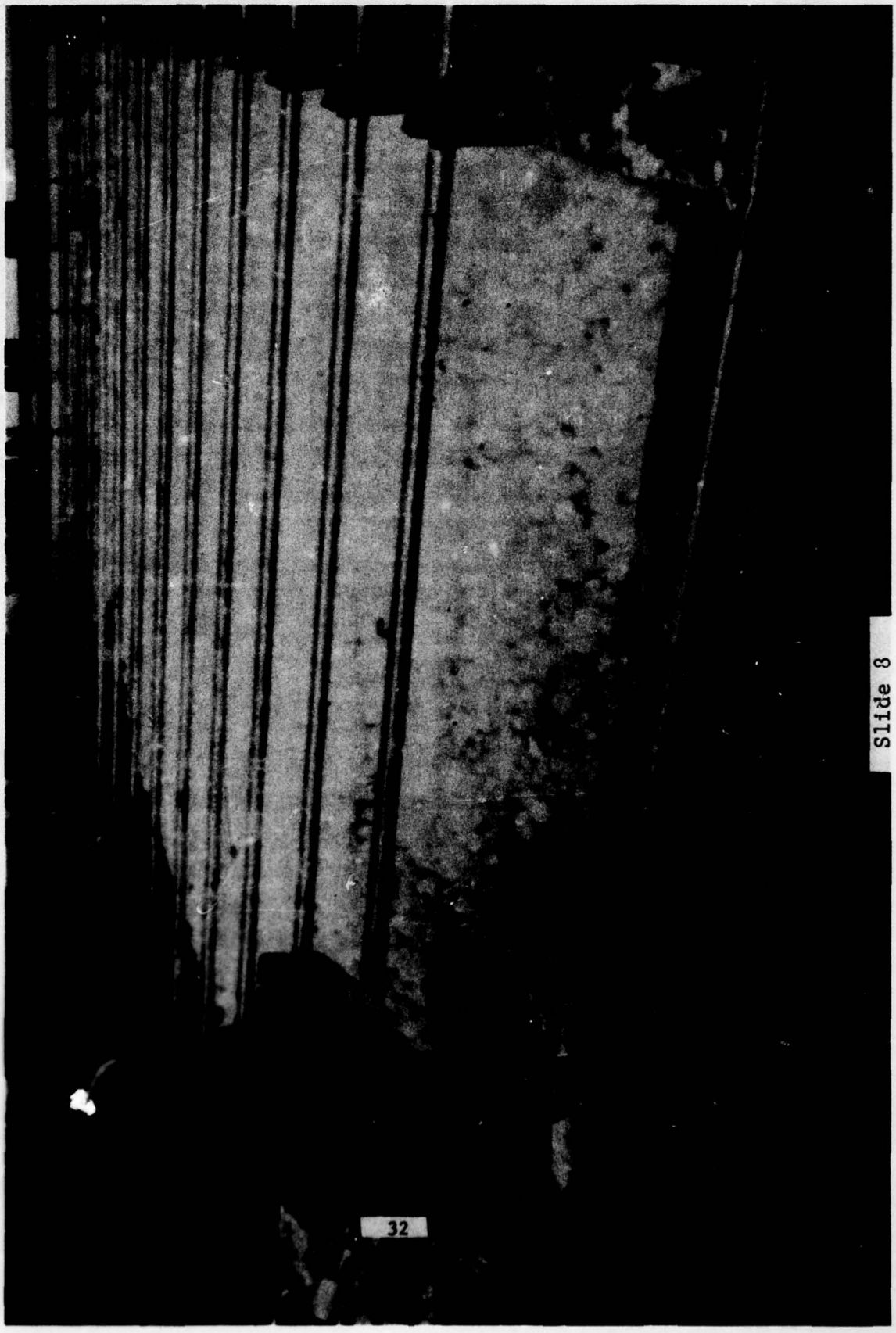
Slide 5



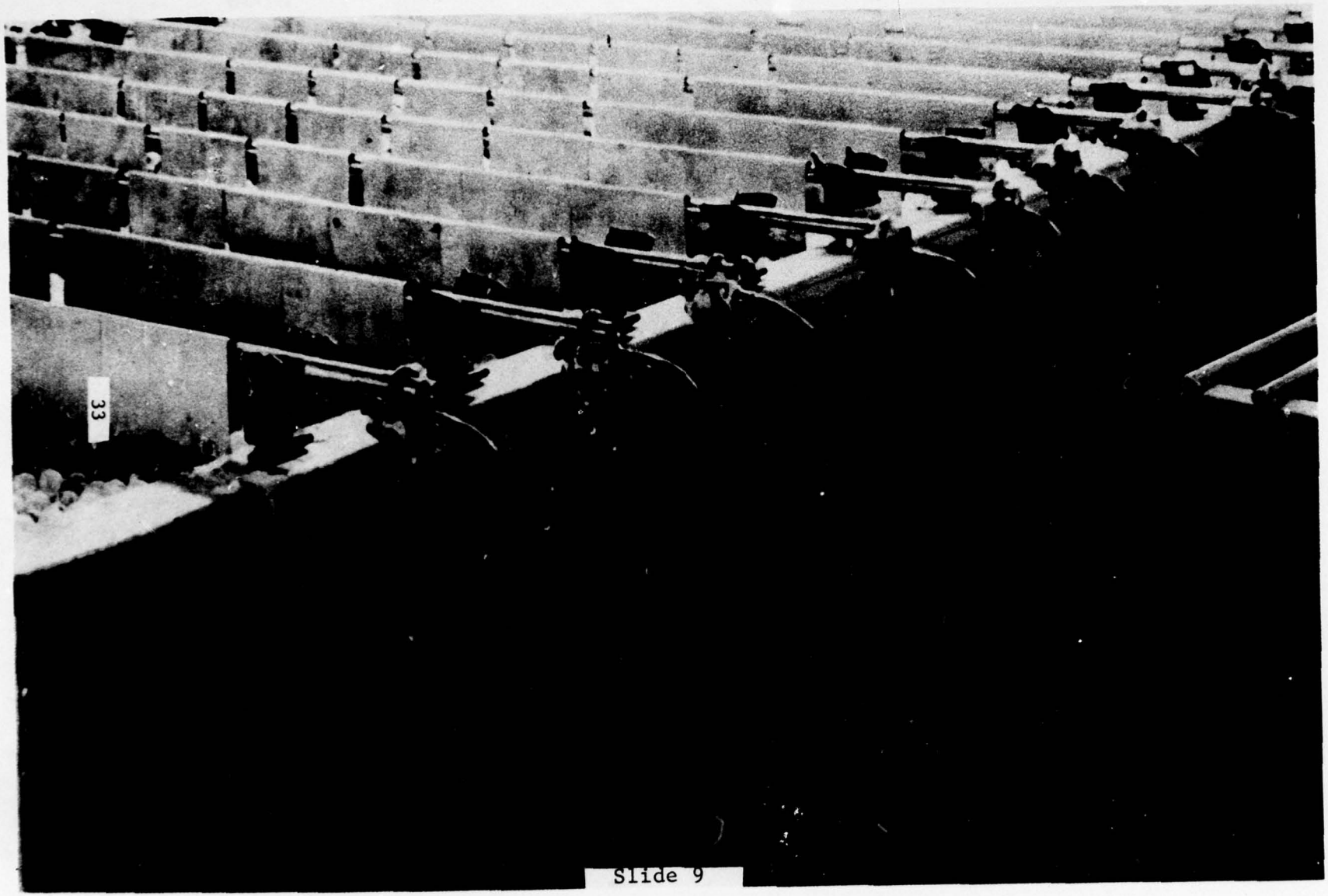
Slide 6



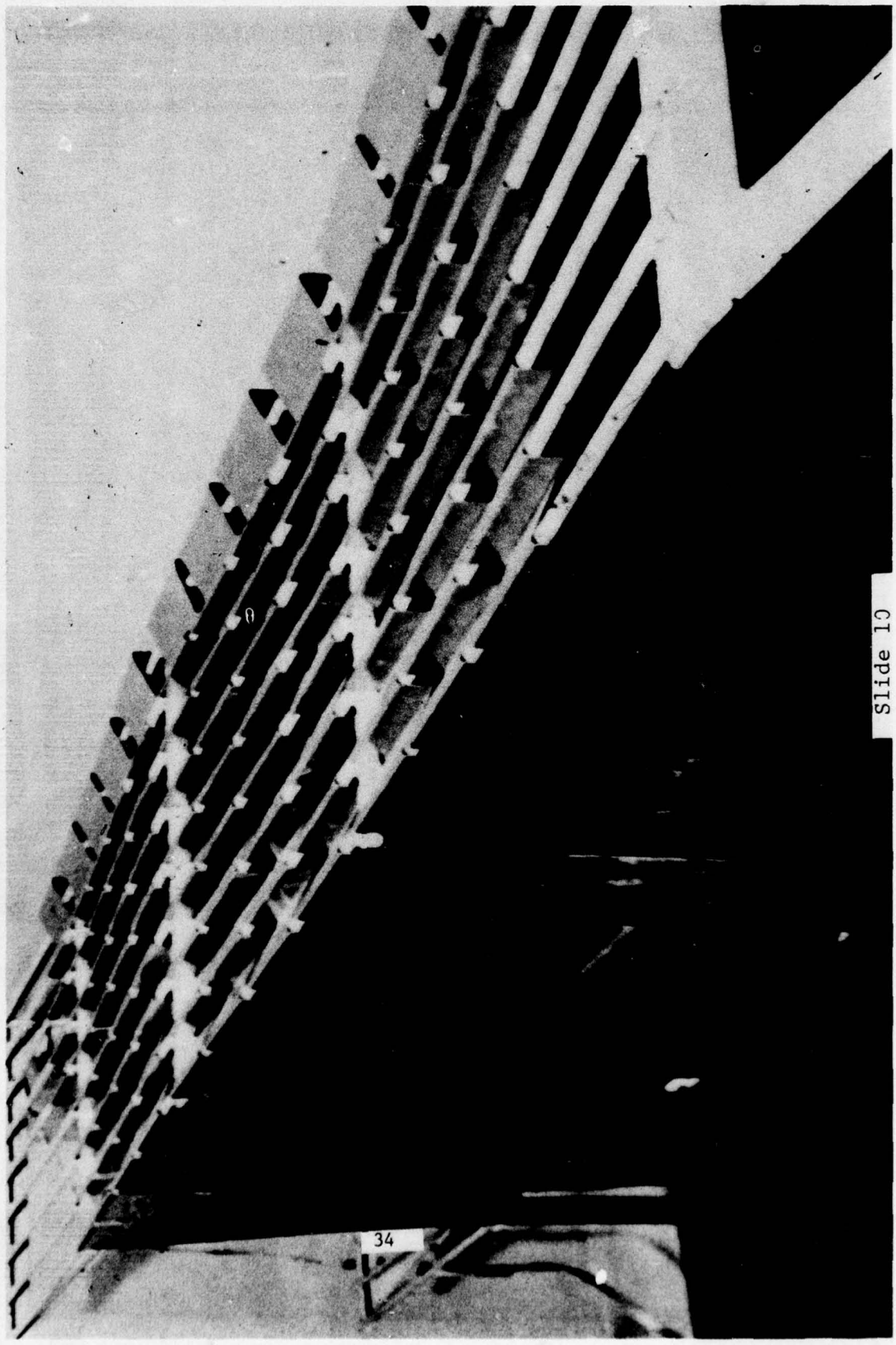
Slide 7

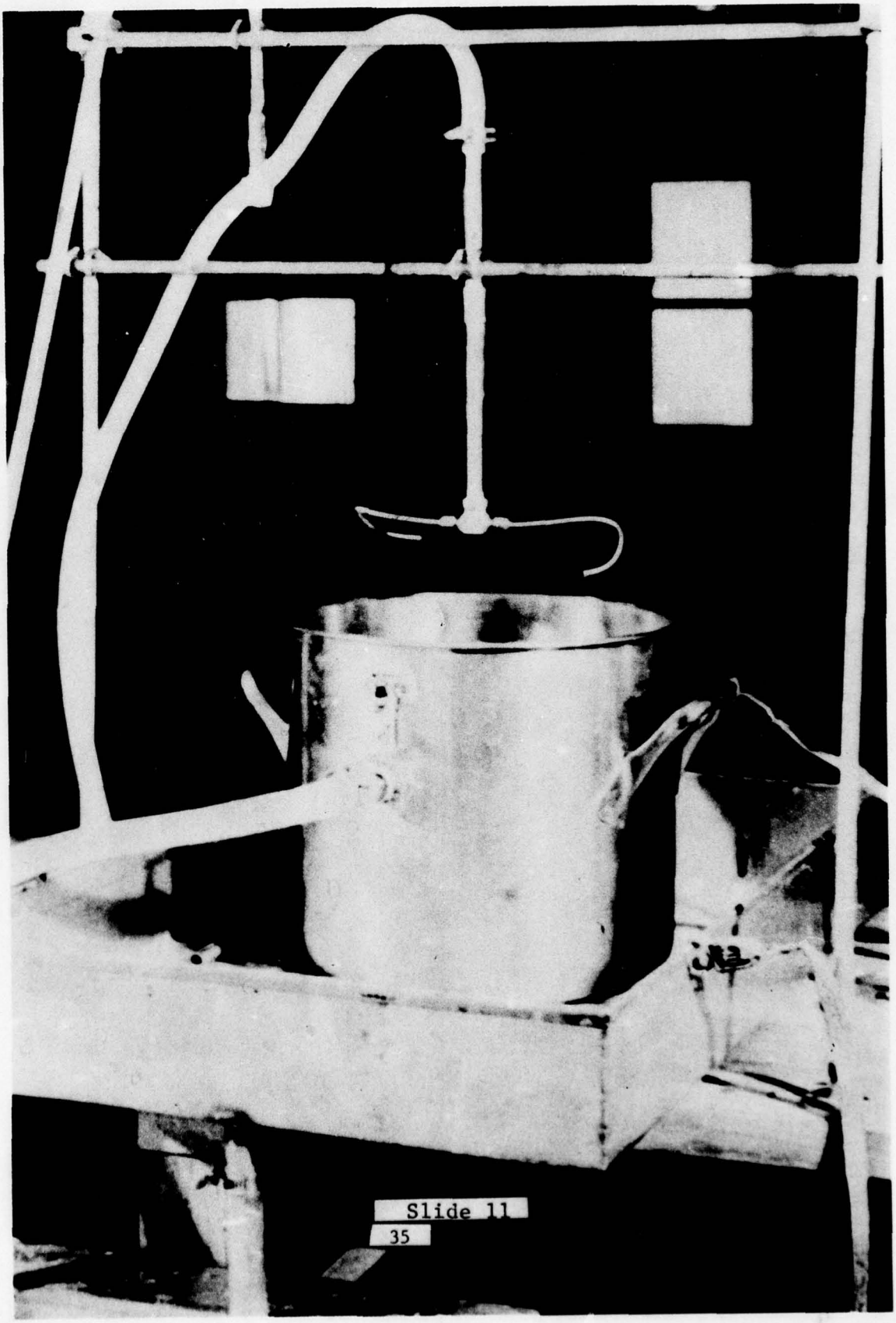


Slide 8



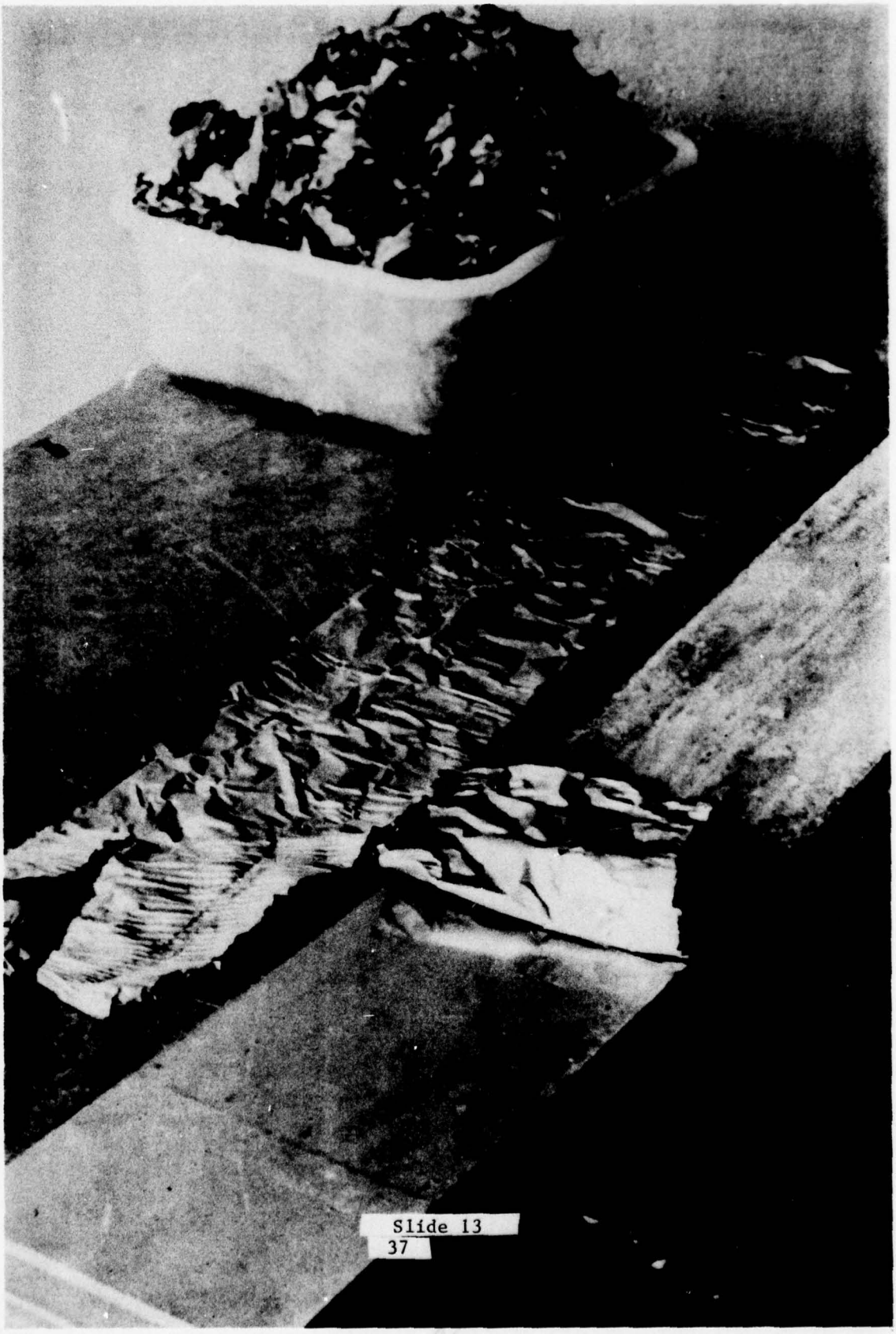
Slide 9


Slide 10
34



Slide 11


Slide 12



Slide 13
37

Joint Conventional Ammunition Program

DEMIL AND DISPOSAL TASK GROUP

John L. Byrd, Jr., Chairman
US Army Materiel Development & Readiness Command Ammunition Center
SAVANNA, IL

The purpose of this briefing is to review the activities of the JCAP Demil and Disposal Task Group and discuss on going actions being accomplished.

As seen on the organization chart, the Demil and Disposal Task Group is one of several groups reporting to the JCAP Operating Group. The JCAP OG consists of representatives from all the Services who are normally full colonel level. The next group in the organizational ladder consists of flag officers at the two star general level and is called the JCAP Coordinating Group. This Coordinating Group reports to the Logistics Commanders who are at the four star general level. While I have briefly touched on the upper organization of JCAP, let's look at the organization of the Demil and Disposal Task Group.

The Task Group consists of a Chairman and principal members from the Services. These personnel also serve on Subtask Groups and are responsible for certain functions. Within the Demil and Disposal Task Group, two Subtask Groups have been formed and are referred to as the Technology Subtask Group and Current Subtask Group. Each Subtask Group has representatives from all the Services.

PRECEDING PAGE BLANK-NOT FILMED

The next chart provides an overview of the Demil and Disposal Program. There are four major categories of items that must be investigated in the demilitarization area. R & D items being developed provide an indication of the technology that will be required in the future to dispose of these items. A Joint Service Agreement has been reached that will require material developers in all Services to develop a disposal plan during the R & D stage. Field Service Stocks, as shown on the chart, represent those items in the active inventory. These items require review to determine if technology and capability exist for disposal at a future date. Once an item has been declared excess, it starts through the disposal process as shown on the right hand side of the chart. First actions in the disposal process consist of screening the stocks for potential reuse of end items and components. There are several avenues for disposal, such as sales, donations, and transfers to other agencies. Those items not consumed during this process are authorized for demilitarization. Four primary methods are utilized for demilitarization and are open burning, open demolition, washout or steam out, and thermal deactivation in the furnaces. The products of demilitarization are sold through the Property Disposal Officers as agents of the Defense Supply Agency. As shown on the chart, the Current Subtask Group's functions deal with today's problems, such as inventory, capabilities, constraints, and disposal plans. Those items requiring demil for which no capability exists are referred to the Technology Subtask Group. The Technology Subtask Group has an active interest in the active inventory of munitions and research and development programs that will provide technology for demilitarization.

For the moment let's look at what the Current Subtask Group has accomplished. This chart is a simplified diagram of the current inventory plan and identifies data that is required to manage the demilitarization process. The first task to accomplish was to identify what has to be demilled within DOD. This task has been accomplished and a DOD inventory listing is now being published on a quarterly basis. The inventory listing identifies the Federal Stock Number, quantity, location, and value of the material to be disposed. The listing is divided into groups of munitions by weight which is related to carload lots, truckload lots, dromedary lots, and small quantities. This inventory data has been extremely useful for ammunition managers in that components can be identified and retrieved, which precludes procurement in many cases.

The second task accomplished was to develop a catalog of the existing DOD capability. This has been accomplished and the capability catalog identifies each installation's capability for disposal by mode. As an example, the catalog indicates that an installation can demil an item by burning and shows the man-hours per unit and cost per unit to accomplish the process. This capability catalog will be updated annually and as demil processes occur, capabilities for each activity will be updated.

The third task relates to the constraints at a given installation. A listing of all of the applicable State, local, and Federal regulations by location has been collected and is in the process of being printed.

These constraints identify environmental restrictions that may affect the capability of an installation to accomplish the demilitarization program.

Transportation costs required to move an item from a location that has no capability to a location that has capability has been included in the plan. With modeling techniques available, JCAP has the capability of determining the cost to demil a total inventory in the shortest time possible and also determine the cost of demilitarization at the most optimum location with no time constraints. It must be recognized that the demilitarization workload at an installation has traditionally been utilized as a workload leveling program. As such there has been no major effort in transferring stocks of ammunition to be demilled from one location to another.

The next chart shows the general process of how the Technology and Current Subtask Groups interface. Those items found in the current inventory that have no capability are referred to the Technology Subtask Group to determine if research and development is required or if the capability can be provided through applied engineering and modernization efforts. To accomplish this task the Technology Subtask Group has developed an analysis of all research and development projects identified within the Department of Defense. The listing of R & D projects that impact on demilitarization have been cataloged and published by JCAP. This publication is one year old and is currently being updated. The updated listing will have an analysis of the R & D efforts, summary charts, and a narrative executive summary for managers to utilize. Publication of this data will be accomplished in November 1976.

Another action taken by the Demil and Disposal Task Group was to develop a Demil and Disposal Roster of personnel that are actively engaged in demil programs within the Department of Defense. A prototype edition has been published. The roster will be updated as required.

An example of interchange of technical data that has resulted from JCAP activities is shown on the next viewgraph. Letterkenny Army Depot developed a demolition method utilizing an auger to drill holes in the earth for detonation . These slides show the method of operation. This system has been reviewed by the DOD Explosives Safety Board and comments provided by Army safety agencies, including an SOP, have been provided to Service representatives. Additional information can be provided by Letterkenny Army Depot personnel.

Another major effort to be discussed is the development of Joint Operating Policies and Procedures, commonly referred to as JOPP's. The Task Group is in the process of developing the procedures that will be utilized in the implementation of the Single Manager for Conventional Ammunition. This represents a major effort in that demilitarization is a worldwide program and many interfaces are required.

The last major effort is the development of a common reporting system that will support the single manager concept.

THE ADDITION OF POLLUTION ABATEMENT EQUIPMENT TO EXISTING NAVSEA DEMILITARIZATION PROCESSES

P. J. Barker
Naval Sea Systems Command (NAPEC)
Naval Weapons Support Center
Crane, Indiana

I. Rotary Demil Furnace at Naval Weapons Support Center, Crane, Indiana

This rotary demil furnace facility was installed in the early 1960's. It has been used to dispose of small arms including 20mm, 30 and 50 caliber, and certain igniters, fuzes, and similar components. In recent years, it has become necessary to control the pollution to the atmosphere from such operations as the furnace operation. In the incidence of the Crane facility (which was the first Navy furnace facility to be fitted with pollution abatement equipment), it was decided to attempt to control the particulate emission and the gaseous emission as much as possible. Hence, the pollution abatement equipment includes the "bag house" type of equipment for particilate control and wet scrubber type of equipment for gaseous emission control.

The facility consists of three rotary furnaces (two large and one small). Each furnace is equipped with a bag house and scrubber. It was expected that the bag house/scrubber combination pollution equipment would control particulate sizes from 1/2 micron to 5 micron and absorb CO2 and NOx's gases. The federal, local and state of Indiana calls for a minimum control of .1 grain/SCF of particilate and no present control on gaseous discharge. The residue from the bag house and scrubber is planned to be deposited in a sanitary land fill.

The impact upon production capability is expected to be very little, if any. It is estimated that the cost of operating the pollution abatement equipment will be $3.50 per hour. The capital cost of the pollution abatement equipment was $237,000.

Checkout of the pollution equipment is expected to be completed by 30 September 1976. The pollution equipment is scheduled to be in production operation during the early first quarter of fiscal year 1977.

PRECEDING PAGE BLANK-NOT FILMED

II. Rotary Demil Furnace at NAVWPNSTA Earle, New Jersey.

Currently, a rotary furnace being installed at Earle is basically the same as the Crane furnaces; however, the pollution equipment is modified from the pollution equipment that has been installed at Crane. Pollution abatement equipment is being installed as part of the facility installation.

Pertinent to the pollution abatement equipment, there is a difference as compared to the Crane installation. In the case of the Earle installation, only a bag house is being installed. The reasons for installing only the bag house are basically two: First, at the time the planning took place for the installation, the pollution standards relative to Earle required only that particilate material from such a process be controlled (no requirement or forseeable regulation concerning gaseous discharge); secondly it was considered feasible to control the temperature of the gases entering the bag house.

The operating costs are expected to be $3 per hour. The expected date for starting operations is November 1976.

III. AEDA Demil Box Incinerator for Small Explosive Loaded Items.

1. The box incinerator came into being as a result of a need at the Naval coastal activities for a means to dispose of a small quantity of items such as small arms ammunition (including .22 caliber, 30 caliber and 50 caliber), ignitions, primers, activating devices and small pyrotechnic items.

2. The incinerator consists of a steel box with 1" thick steel walls divided into two compartments (detonation and afterburner). Each compartment has a burner with a combined output of 3 million btu's. In addition, a feed tube and associated safety devices, barricade, pollution abatement equipment with a marble bed scrubber and associated water treatment equipment to facilitate the recirculating of the water in a closed loop are included to make up the complete incinerator.

3. At present, some of the pollution abatement equipment has not been finalized. As a result, specific feed rates for certain items have yet to be determined. A number of tests have been conducted on a prototype incinerator installed at NAD McAlester. The McAlester incinerator has a marble bed scrubber installed but does not have the water treatment equipment installed.

4. Plans call for the incinerators to be located at the coastal locations which include California. The pollution limitation regulations require that no more than .1 grain/SCF, corrected to 12% CO2, particilate be discharged to the atmosphere from an incinerator of this type. The regulations call for a limit of combustion gases including SO2 and NOx of 1000 ppm and 150 ppm respectively. Since the water is circulated through a closed loop and none is discharged to the environment, the only question still remaining is what is done with the sludge from the water treatment equipment. (Sludge is removed from the clarifier, dried and placed in plastic bags to be deposited in a sanitary land fill.) Tests to date have indicated exhaust gases contain less than 1000 ppm SO2 and 150 ppm NOx's.

5. The tests that have been conducted to date indicate the particilate rate is in excess of the allowable limit. The first tests (3) were conducted in June 1976. The tests utilized 80 rounds of 50 caliber incinerary type. The 80 rounds were deposited into the feed tube of the incinerator as one batch feed at intervals of 2 1/2 minutes. The results were as follows:

	Inlet	Outlet*	Efficiency
First Run -	1.91 grain/SCF	.42 grain/SCF	77.0%
Second Run -	1.94 grain/SCF	.56 grain/SCF	72.0%
Third Run -	1.78 grain/SCF	.33 grain/SCF	81.6%

* Preliminary tests indicate, by reducing the feed rate, the pollution code can be satisfied.

6. In analyzing the results of the tests, it was determined that a number of alterations to both the incinerator and the scrubber could improve the performance of the incinerator/scrubber significantly. The alterations include the re-design of the grate assembly to permit a periodic remote emptying or "dumping" of the material on the grates. Certain alterations to the scrubber to increase the efficiency (variable orifice in the discharge side of the scrubber and increase the pressure drop through the venturi section).

7. Tests are being conducted this week as to the effectiveness of the incinerator/scrubber to satisfy the pollution code requirements.

8. The initial cost of the unit (including equipment and installation) totals approximately $250,000. Operating costs have not been determined; however, it is expected that operating costs will be approximately $10 per hour, exluding operator costs. Process rates have not been finalized to date but are expected to be available within six to eight months.

IV. High Pressure Water Washout for Composition A-3 Loaded Projectiles.

1. Until recently, the process for removing Composition A-3 explosive from projectiles was first to contour drill and finally burn or flash out the "rine" left by the drill. However, more recently, to eliminate atmospheric pollution, a process for avoiding the burning or flashing of the "rine" was sought; hence, the high pressure water washout process. Although the air pollution problem is eliminated, a water pollution problem exists. Consequently, a water treatment system is necessary for a "closed loop" recirculation of the water used in the washout process.

2. The equipment consists of two high pressure pumps, a projectile holder with special nozzle and feed, a water and explosive collection trough to empty into a head box that flows over a hydrosieve, an explosive collector, a clarifier, and a clearwell (1,100 gallon).

3. The pumps are capable of 10,000 psi at 22 gpm/pump and are driven by 150 horse power electric motors. The projectile holder positions the projectile in an inclined position 45° from the horizontal. The nozzle is fed from the nose end of the projectile to the full length of the projectile cavity in 30 seconds. During the washout of the explosive, the projectile is rotated at the rate of 200 rpm. The nozzle design is such that, at present, it is necessary to make one additional pass into the projectile with a separate nozzle designed to clean the interior surface of the projectile. The eroded explosive material is in the form ranging from irregular chunks, weighing 4 to 5 ounces, to fine particles. The hydrosieve separates the material that is 100 micron size and larger. The separated material goes to the explosive package station. The material that is not separated by the hydrosieve continues on into the clarifier where the suspended solids settle out (a holding time of 57 minutes to pass through the clarifier). From the clarifier the water returns through duplex filter and clearwell to the high pressure pumps. Tests of water samples taken from similar water treatment systems indicated that the saturated water leaving the water treatment system contains suspended solids not larger than 5 microns. Under controlled conditions, 9,000 gallons of water (with controlled explosive suspended and dissolved solids) have been circulated through high pressure pumps. After these tests, the pumps were disassembled and examined. The accumulation of explosive film on the internal pump surfaces was visible and therefore were considered safe for continuous use.

4. The cost of the initial equipment and its installation that is located at Crane amounted to $150,000 and is expected to process 400 5" projectile/shift. Tooling can be attached to handle different size projectiles ranging from 3" to 8".

USING CAVITATING WATER JETS

FOR DEMILITARIZATION

by

Andrew F. Conn and S. Lee Rudy
HYDRONAUTICS, Incorporated
Laurel, MD

ABSTRACT

A test and evaluation program is described, which examined the use of the CAVIJET™ cavitating water jet method for cutting and removing propellants and liners from Navy missile motor casings. Laboratory and field trials were conducted. A three-nozzle CAVIJET cutting head, operating at 2600 psi, removed the propellant and liner from the TARTAR motor casing at a rate one-third faster than the present non-cavitating water jet system which operates at 5000 psi. Thus, cavitating water jets required one-third of the energy that was needed to clean a casing by the conventional water jet method.

PRECEDING PAGE BLANK-NOT FILMED

INTRODUCTION

High pressure water jets have been used for many years for various demilitarization applications such as the removal of propellant and liner materials from missile casings. The advantages over mechanical techniques are well established, in particular the minimization of spark creation. However, the use of these high pressures, typically in the range of 5,000 to 10,000 psi, creates many disadvantages. These include: clogging of the extremely small jet orifices which are usually found in such systems, thereby often blowing out pump packings; the wear of the nozzles due to the high velocities of the water through these orifices, necessitating frequent expensive shutdowns and replacement of the nozzles; and the expense and inherent increased danger related to the use of high pressure water. All fittings, connections and related hardware must be rated for high pressure use, and regular maintenance and replacement of critical components are an important safety aspect for the operation of such a system.

Within the Mechanical Design Branch at the Naval Ordnance Station at Indian Head, Maryland, a high pressure water jet system, known as the "HOGOUT", was developed as a prototype for clearing the propellant and liner materials from case-bonded missile motors such as the SIDEWINDER and TARTAR. This prototype system was placed into production usage and has been operated for several years in this manner. Frequent shutdowns have been experienced with this system, typically caused by clogging of the small (30 to 60 mil diameter) nozzle orifices which then cause the pump packings to blow out; in turn contaminating the flow and frequently replugging the orifices and again blowing the packings. Also, as the system was designed to operate

effectively only at or near 5,000 psi, any wear of these small nozzle orifices causes a decrease in the system pressure, with the associated loss in effectiveness in cutting power of the jets. Thus, unless frequent monitoring of the system pressure is enforced, the rate of cleaning has been found to fall off drastically; hence, increasing the cost per missile.

After becoming aware of this use of steady (i.e., non-cavitating) water jets for the removal of missile propellant and liner materials, HYDRONAUTICS, Incorporated suggested that the patented CAVIJET™, cavitating water jet method, might provide important improvements in any existing water jet systems being used for this purpose. This paper describes the results of a two-phase program which was successfully completed, demonstrating that the CAVIJET technology provides improved performance in all categories over the present operation of the steady jet, HOGOUT system. The first phase, conducted in the HYDRONAUTICS laboratories, had the objective of determining what rates of cutting of inert, simulated propellant and liner materials for the SIDEWINDER and TARTAR missiles might be achieved with the CAVIJET, and what system parameters, i.e., pressures and flow rates, would be required. The next objective, after successful completion of this first phase in our laboratory, was to evaluate a CAVIJET prototype cutting head. This head consisted of a holder, compatible with the existing HOGOUT system, supporting three CAVIJET nozzles, and was used in actual field trials at Indian Head in a final feasibility determination.

THE CAVIJET™ TECHNOLOGY

The cavitating water jet represents one of the few successful attempts to harness the destructive power of cavitation

which for decades has plagued the designers of hydrodynamic equipment. In its most basic conceptualization, the CAVIJET technology involves the growth of vapor filled cavities within a relatively low velocity jet, which later collapse in the high pressure stagnation region where the jet impacts the material. Since the collapse energy is concentrated over many very small areas of collapse, extremely high localized stresses are produced. This local pressure amplification provides the cavitating water jet with a great advantage over steady noncavitating jets operating at equivalent pump pressures and flow rates.

Further details of the cavitation phenomena in general, and of the specific HYDRONAUTICS CAVIJET test method and facility (see Figures 1, 2, and 3), can be found in Appendix A, and in References 1 - 12. The work summarized in this paper has been abstracted from the various reports (References 13 - 15) for the program.

DISCUSSION OF LABORATORY TESTS

Tests were conducted within the HYDRONAUTICS CAVIJET test facility on inert specimens of simulated missile propellant material and liners using two sizes of jet orifices, namely, 1/8-in. and 1/4-in. diameters. Nozzle configurations suitable for tests which were conducted both in air and submerged were used. It is felt that the situation within the actual missile casing is such that submerged operation of the jet flow can be provided, thus taking full advantage of the CAVIJET method which is considerably more effective when used in the submerged mode. Some typical cut specimens are shown in Figures 4 and 5. Due to the relative ease of cutting of the SIDEWINDER propellant and liners, and the smaller size of these missiles, subsequent efforts were concentrated on the TARTAR.

Depth of Cuts

The relative performance of the 1/8-in. CAVIJET vs the 1/4-in. CAVIJET are summarized in Figure 6. The curves which are faired through the data points are merely intended to show the relative trends, and are not to be taken as an exact indication of these nozzle performances, due to the limited amount of data obtained. However, at any given set of test specifications, sufficient replication has been obtained so that those values are quite well established. It is seen, for instance, at a translation rate of about 20 ipm (inches per minute), the 1/4-in. CAVIJET provides a depth of cut which is more than twice that achieved by the 1/8-in. CAVIJET at the same translation rate. Similarly, at about 50 ipm the 1/4-in. CAVIJET achieves a cutting depth of about 3-3/4-in. while the 1/8-in. CAVIJET provides only about 1-3/8-in. depth.

The curves presented in Figure 6 do indicate a trend which was observed as lower rates are utilized: a rather small increase in the relative depths achieved for large decreases in the translation rate, thus approaching a plateau for very slow rates. Similarly, at the higher translation rates, namely, well above 100 ipm, there is a gradual decrease in the cut depth for large increases in rate. Indeed, even at the extremely high rate of 250 ipm, a one-half inch depth of cut was obtained.

Also indicated in Figure 6 are some of the effects of decreasing the operating pressure. Several points are shown for the 1/4-in. CAVIJET operated at 1800 psi in comparison to 2000 psi for the other 1/4-in. CAVIJET tests. It is seen that considerably smaller cut depths were obtained for this lower pressure. Similarly, for the 1/8-in. CAVIJET operated at 1000 psi at about 20 ipm, depths about half of those obtained at 2000 psi were achieved for this 1/8-in. diameter nozzle.

In Figure 7, a comparison is presented of the relative performance of the 1/8-in. CAVIJET, operated while in air and while submerged. It is seen that the same basic trends are obtained for this nozzle when operated in these two modes, with a fairly consistent larger depth of cut achieved in the submerged mode. For instance, at about 20 ipm, the submerged mode provides a depth of about 2-1/4-in. vs the 1-3/4-in. achieved with this same 1/8-in. jet operated in air, that is, a performance over 25% better for the submerged mode. The same relative difference of about 1/2-in. less depth of cutting seems to be achieved over the entire range of translation rates which were used in these tests. The data shown in Figure 7 contains tests conducted both at 1800 and 2000 psi, a pressure difference which for the 1/8-in. jet is of much less influence than is observed for the 1/4-in. jet (as discussed above in relation to the data presented in Figure 7 for this larger nozzle).

Width of Cuts

The surface of the cuts made within the TARTAR propellant material are typically quite jagged (see the photograph in Figure 5), hence making it more difficult to exactly determine a width for these cuts, i.e., of the material which was actually reduced to extremely fine particles. Also, the cuts were frequently made at the end of the block of material; hence, causing the cut off piece to fall away and making it impossible to determine the width of cut. However, as shown in Table 1, certain trends have been observed in these cut widths. For the in-air operation of the CAVIJET, the slower translation rates produced somewhat wider cuts relative to those produced at the higher rates - that is, above 90 ipm. A similar trend was also observed for the tests with the 1/8-in. CAVIJET which were run

in the submerged mode. It is seen in Table 1 that the tests at high rates produced slots which were somewhat narrower than those at the lower rates. However, the overall slot widths of those tests run in the submerged mode were consistently larger relative to those measured for the tests run in air with the 1/8-in. CAVIJET.

A similar dependency on translation rate was also observed for the width of cuts obtained with the 1/4-in. CAVIJET - that is, a tendency for the slot width to decrease with increasing rate. The slots cut with the 1/4-in. nozzle were considerably wider however, ranging for the submerged tests from about 1/4-in. at the high translation rates to about 1/2-in. at the lower rates.

DISCUSSION OF FIELD TESTS

HOGOUT Facility

The components of the HOGOUT facility at the Naval Ordnance Station, Indian Head, Maryland, are shown schematically in Figure 8. The speed of rotation and the feed rate for the water jet cutter may be independently varied. The system is remotely operated from a control station several hundred yards away, with closed circuit T.V. monitoring. The steady (i.e., non-cavitating) jet cutting head has six nozzles, with orifice diameters of 0.030 in. to 0.060 in., and operates at 5000 psi. The system is usually run at a fixed speed of 6 rpm and a fixed feed of 7.2 ipm, which, although not optimum for all cleaning passes, greatly simplifies the operation. Seven "passes", i.e., runs up and down the length of the casing, are required to clean the propellant and liner from a TARTAR motor, which is about one foot in diameter and over six feet long.

CAVIJET Cutting Head

A nozzle holder, designed for use in the existing HOGOUT system, was fabricated during this phase of the program. Photographs of the complete cutting head, with the three CAVIJET nozzles installed, are shown in Figure 9. It was concluded that the optimum use of the available 57 gpm flow capacity from the HOGOUT pump would be a cutter with three CAVIJET nozzles, each having an orifice diameter of 0.14 in. This was based on the decrease in cutting width and depth as nozzle diameter is decreased, as shown, for instance, in Figure 6, comparing the 1/8-in. and 1/4-in. CAVIJETS for cutting inert TARTAR propellant.

A drawing which specifies the nozzle orientations for the CAVIJET cutter is given in Figure 10. The circumferential orientation of the nozzles is as follows: Nozzles 1 and 3 are 180° apart, i.e., at opposite positions on the same diameter. The angle between Nozzles 2 and 3 is 108°. The first nozzle, that seen to the left side in the smaller leading section in Figure 9(a), is oriented at an angle of 45° forward. The second nozzle, shown pointing upward in Figure 9(b), is oriented perpendicular to the axis of the holder. The third nozzle is oriented at an angle of 16° backwards from the perpendicular to the nozzle axis.

The second two nozzles can be extended out about 2.0 in. from the nozzle holder by the use of extension fittings. Thus, for later passes, in order to place these nozzles nearer to the receding cylindrical surface of the propellant, these threaded extensions were placed between the holder and Nozzles 2 and 3.

Field Test Results

The CAVIJET cutting head was installed in the HOGOUT system, and used to clean the propellant and liner from TARTAR missile

motor casings. Due to the larger nozzle orifices, the CAVIJET cutter operates at 2600 psi. The first trials were run at the same 6 rpm speed and 7.2 ipm feed used with the steady jet cutter. The CAVIJETS required seven passes, the same as for the steady jets, to remove the propellant and liner from a TARTAR casing, but at about one-half the pressure. Due to the orientations of the nozzles, some material could not be effectively reached at the closed end of the casing.

After analysis of these initial trials and comparisons with the laboratory test results, it was concluded that the volume removal rates could be increased for this cutter if the speed was reduced to 4 rpm, and the feed reduced to the range of 2.3 to 4.6 ipm. These conclusions were borne out in subsequent trials, wherein essentially all of the propellant and liner was removed from the TARTAR in only two passes.

Although the orientations of the nozzles in the prototype CAVIJET cutter were by no means optimum, the results of using it in these field trials have demonstrated that the CAVIJET method can provide savings in time and energy over the current methods. As summarized in Table 2, an optimized, three-nozzle CAVIJET cutter, in comparison to the present operation of the HOGOUT system, should completely clean a TARTAR casing at about half the pump pressure, in one-third less time, therefore using one-third of the energy per casing. And, modifications to the HOGOUT pump, which could then provide double the present flow at 2720 psi, would allow the use of a six-jet CAVIJET cutter, thus potentially halving the present CAVIJET cleaning time.

CONCLUDING REMARKS

The results of laboratory and field trials with the CAVIJET method have demonstrated that a systematic test and evaluation

program of this new technique can provide important improvements to demilitarization efforts such as the removal of propellants from Naval missile motor casings.

As shown in Table 2, the CAVIJET cavitating water jet technology can provide a safer, more efficient demilitarization operation, with overall savings in labor and energy per missile. There are ongoing efforts to develop operational equipment for this application.

ACKNOWLEDGEMENTS

The work described in this paper was supported by the U. S. Naval Ordnance Station, Indian Head, Maryland, under Contract N00174-74-C-0465. The authors wish to thank the Technical Program Manager, Mr. Bob Skinner, for his valuable advice and guidance throughout this project. The analyses and suggestions provided by our colleagues, Dr. T. R. Sundaram, Dr. Laskar Wechsler, and Mr. Norman I. Shapira, are also gratefully acknowledged.

TABLE 1

Width of Cuts for 1/8-Inch CAVIJET™
Operated at 1800 psi and 2000 psi,
1/4-Inch Stand Off, TARTAR Propellant

Mode	Translation Velocity, ipm	Width of Cut, in.
In Air	20 to 60	1/8 to 1/4
	90 to 144	1/16 to 3/32
Submerged	20 to 60	3/16 to 1/4
	90 to 240	3/32 to 5/32

Table 2

Comparison of the HOGOUT (Steady Jet) and CAVIJET™ (Cavitating Water Jet) Methods

For: Cleaning TARTAR Missile Motor Casings

Parameter	HOGOUT	CAVIJET*	Comparing CAVIJET to HOGOUT	Remarks
Pressure, psi	5000	2600	Pressure almost half	Lower jet velocities; longer nozzle life; safer; longer life of all components.
Flow, gpm.	54	54	Same flow	Full available pump capacity was used for both methods.
Hydraulic Power delivered, hp	157	82	About one-half the power	Less cost per motor cleaned
Nozzles	Six @ 0.030" to 0.060" diameters	Three @ 0.14" dia.	Orifice areas: 5 to 22 times larger	Larger nozzles: less likely to clog and cause blowouts of seals and packings
Number of passes with cutter	7	2	Five less passes	Simpler operation with less passes.
Rate of feed of cutter, in./min.	7.2	1st pass: 2.3 2nd pass: 4.6	Slower feeds	Optimum feeds for each pass, to minimize overall cleaning time
Cutter rotation speed, rpm	6	4	Two-thirds of the rotation speed	More effective cutting with CAVIJET at slower speeds
Total time to clean, hrs.	3.0	1.92	Over 1/3-less time	Less labor cost per motor
Total hydraulic energy per motor, kw-hr.	351	117	One-third of the energy	Less energy cost per motor

*Based on results from tests on actual TARTAR motors, at Indian Head Naval Ordnance Station, November 17 and 26, 1975.

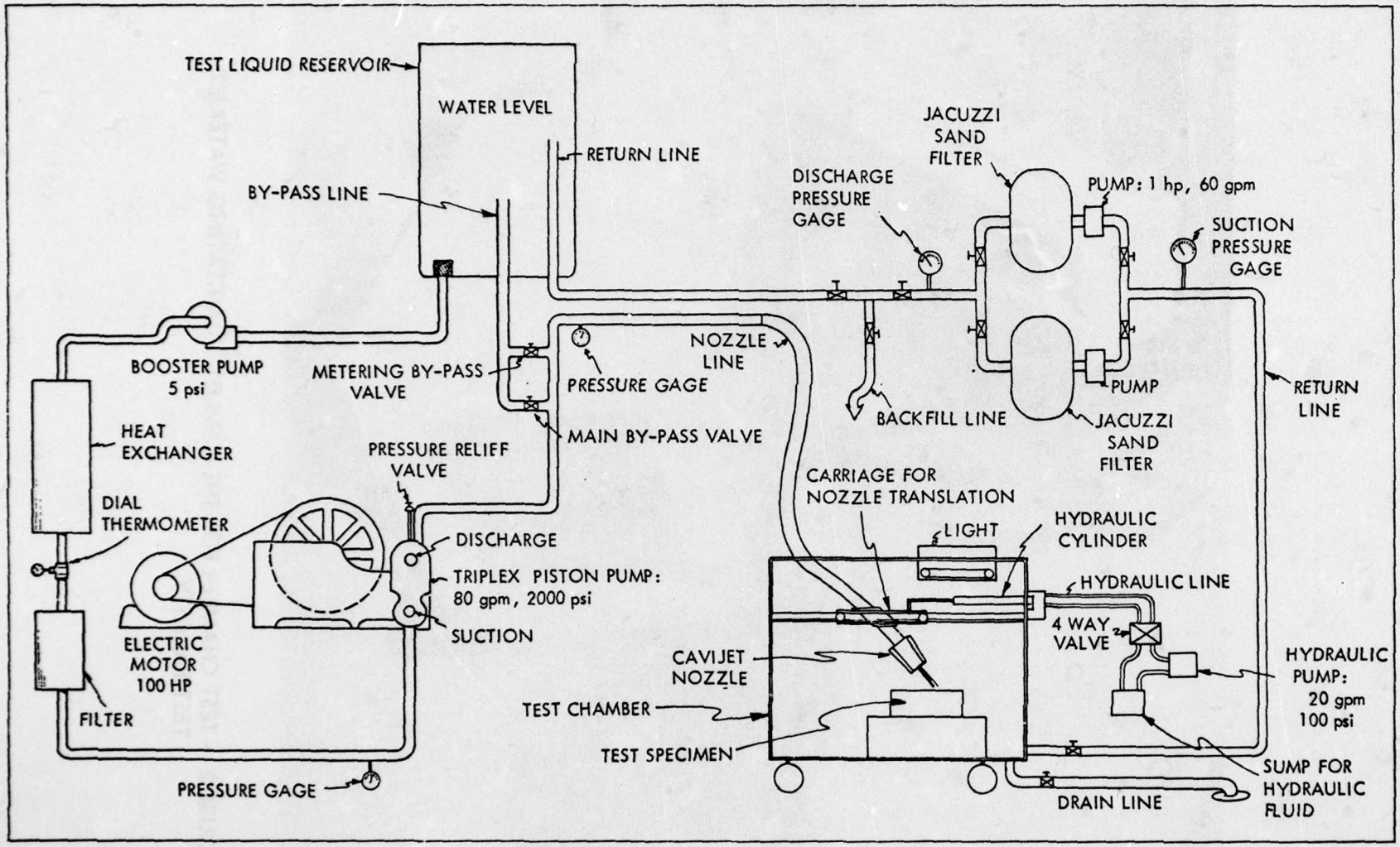


FIGURE 1 - SCHEMATIC OF CAVIJET™ CAVITATING WATER JET TEST FACILITY

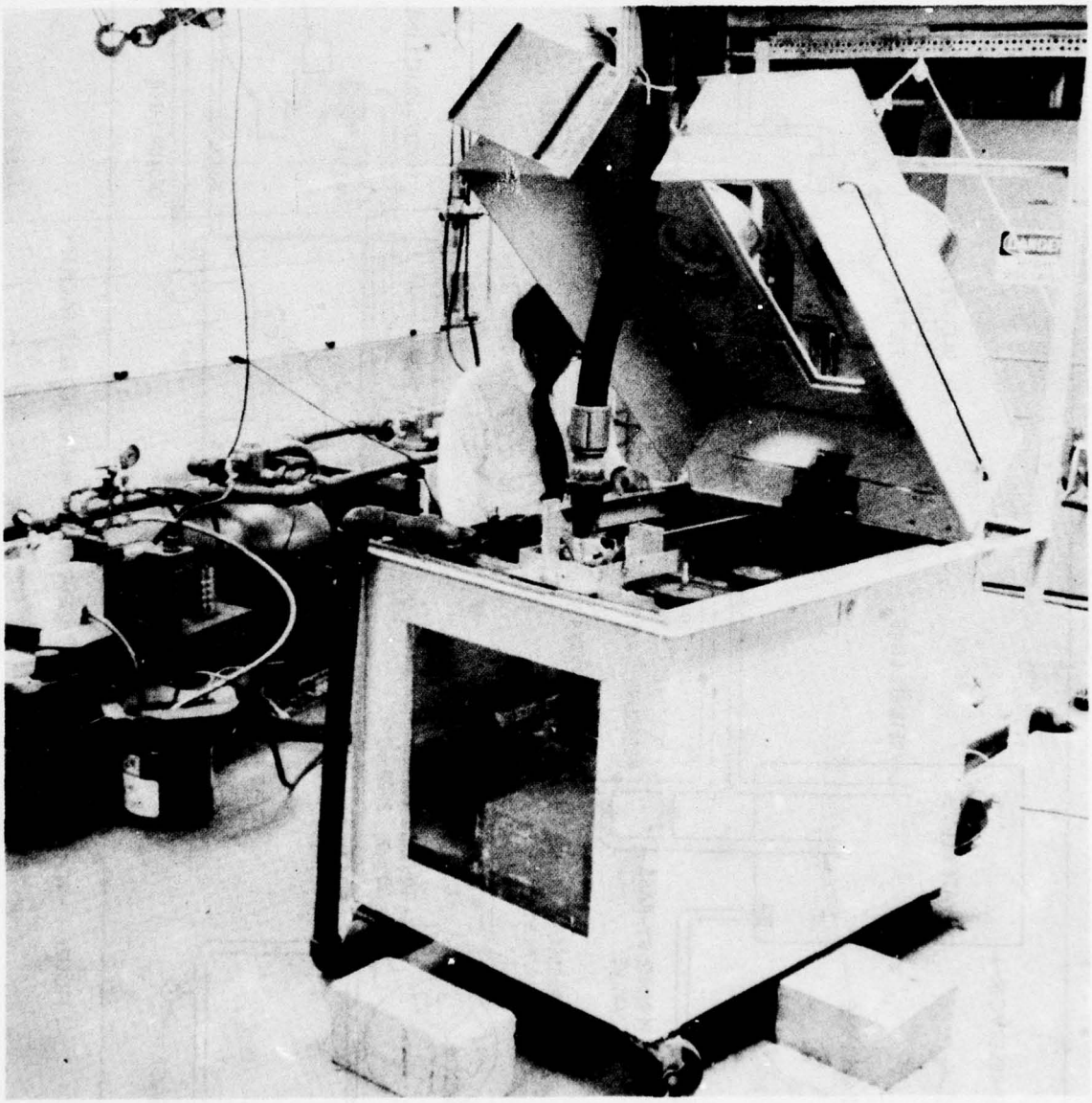


FIGURE 2 - TEST CHAMBER FOR THE CAVIJET™ CAVITATING WATERJET TEST FACILITY

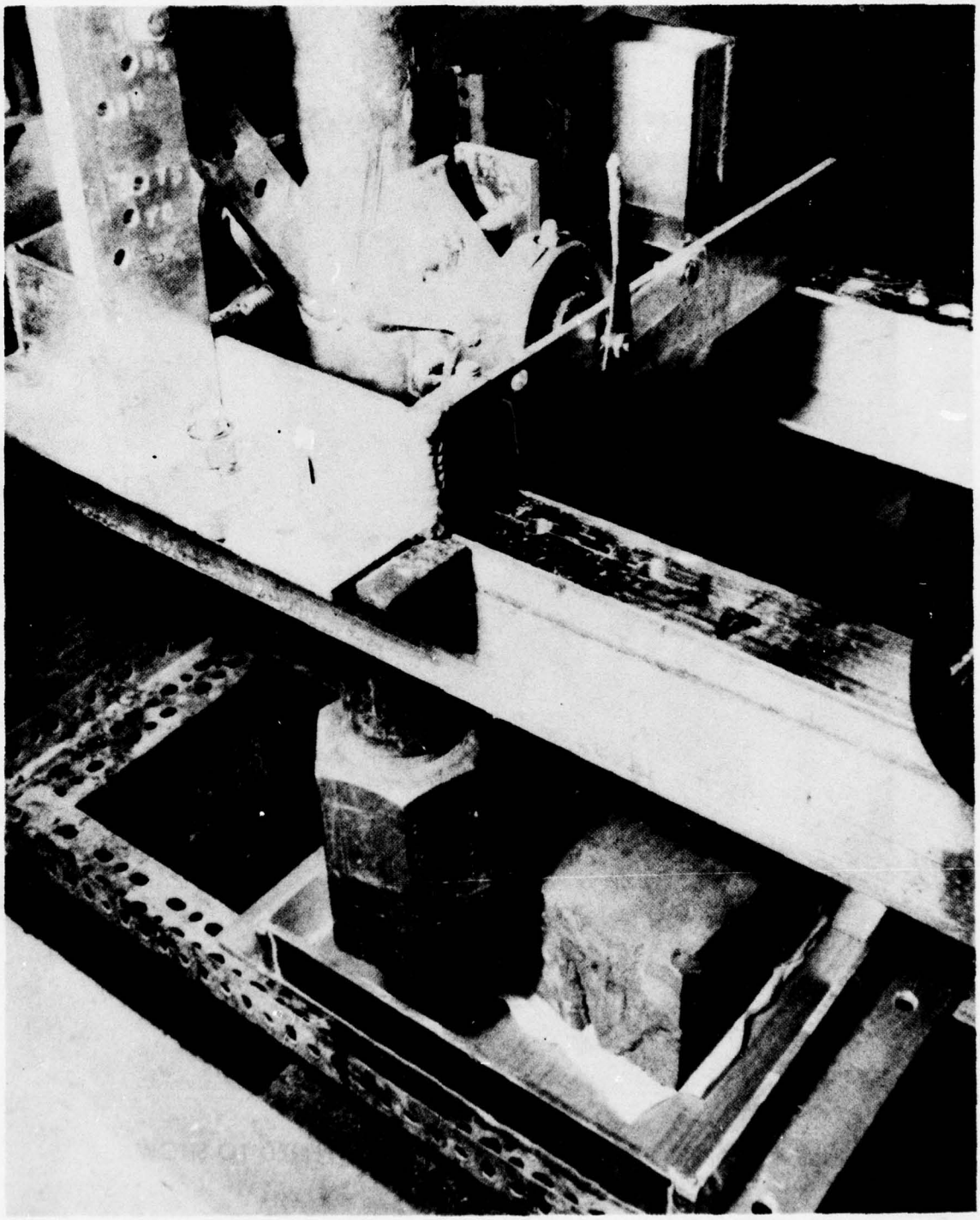


FIGURE 3 – CLOSE-UP OF TEST CHAMBER FOR THE CAVIJET™ CAVITATING WATERJET TEST FACILITY

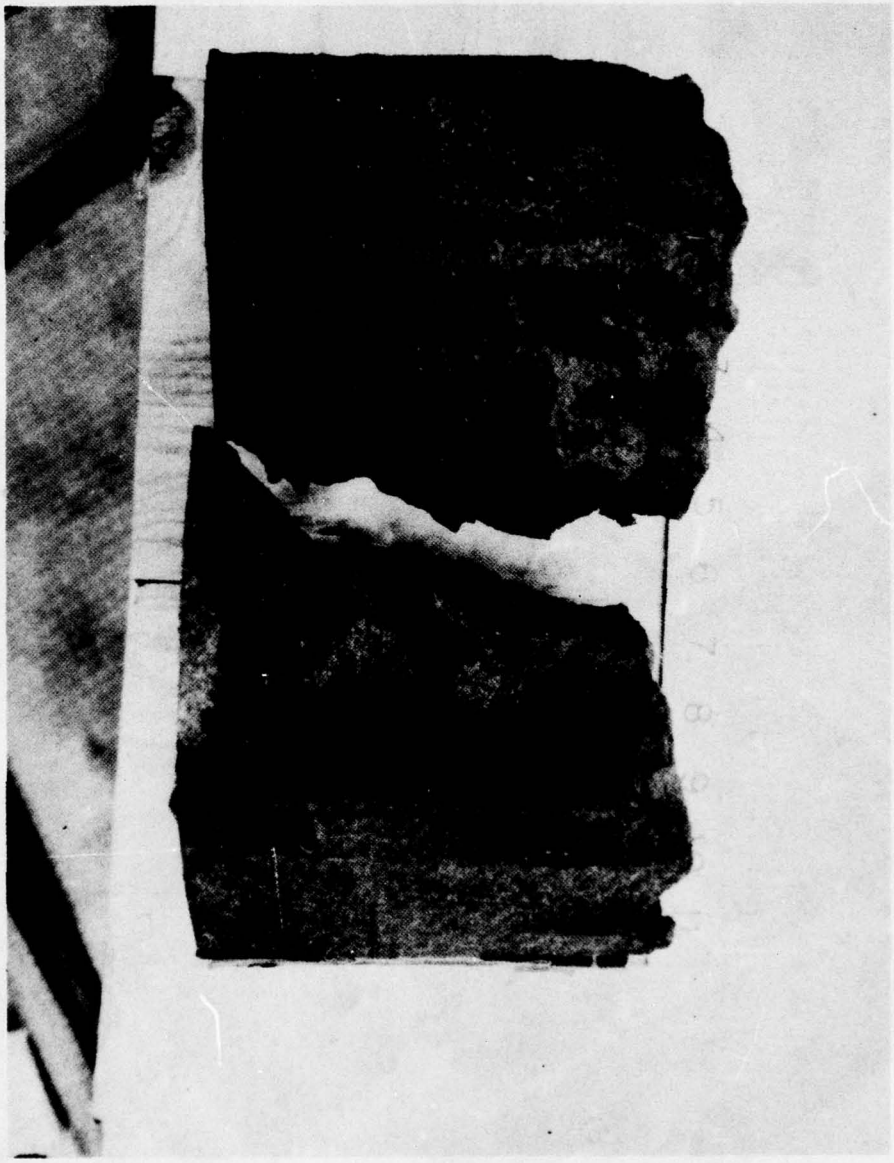


FIGURE 4 - TARTER PROPELLANT: TOP VIEW, OPENED TO SHOW CUT SURFACES

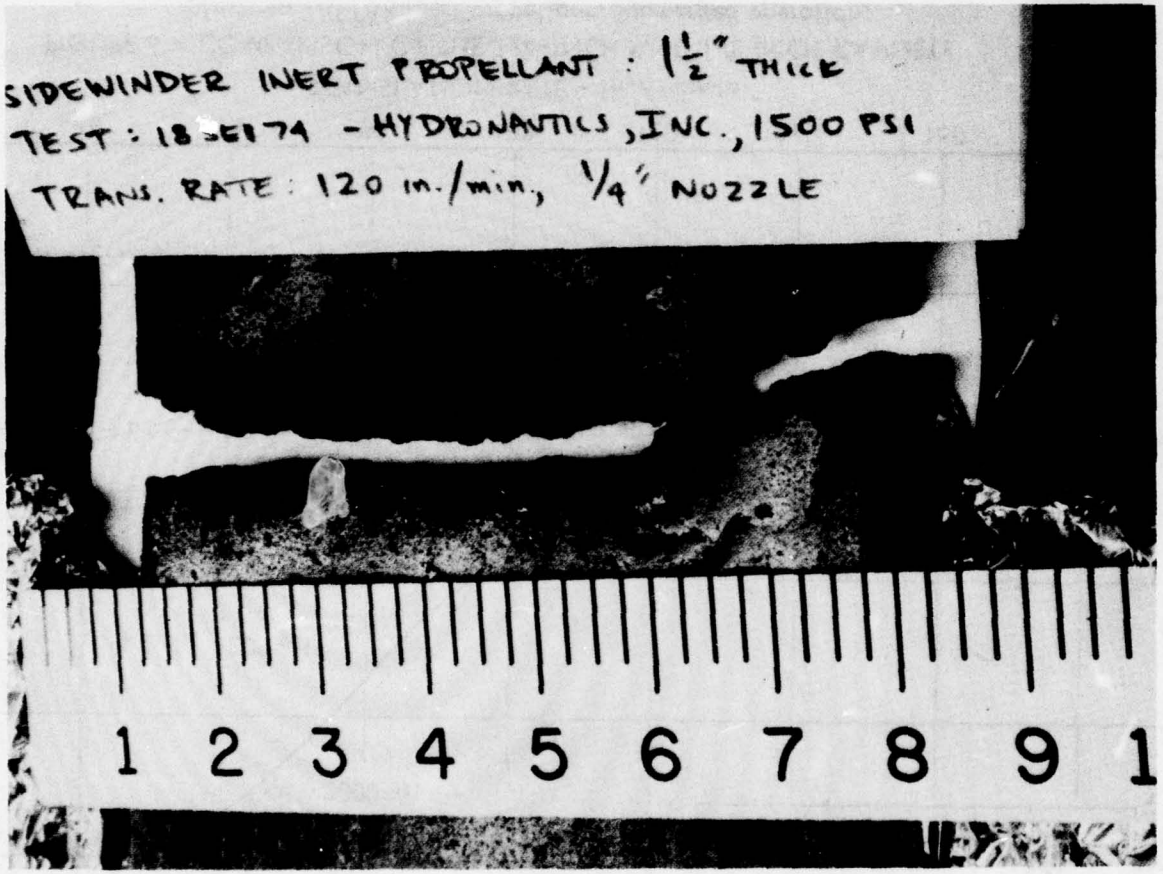


FIGURE 5 - SIDEWINDER PROPELLANT

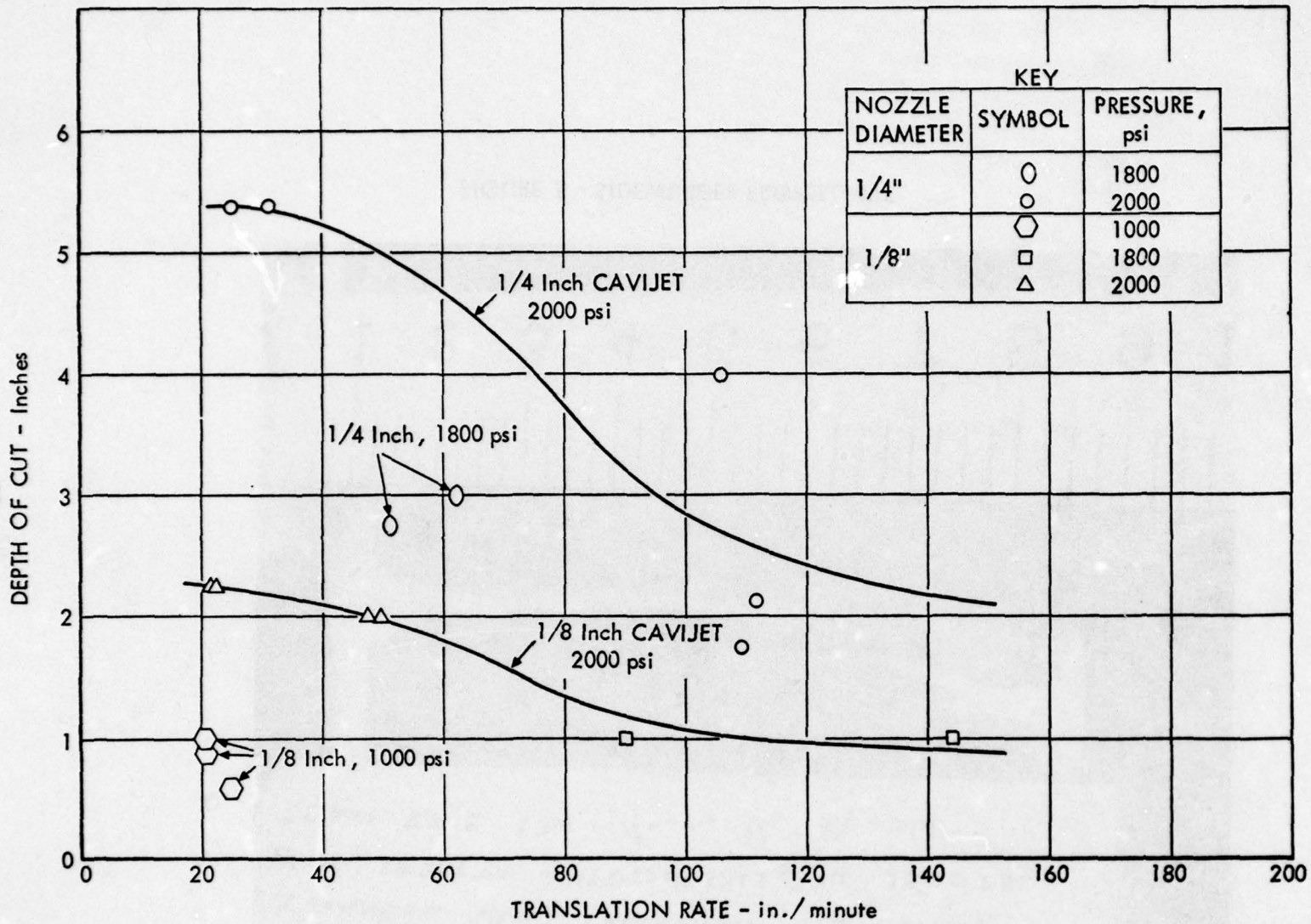


FIGURE 6 - COMPARISON OF THE 1/4-INCH AND 1/8 INCH CAVIJET:
Tests on TARTAR inert propellant, submerged operation;
1/4-in. stand off distance.

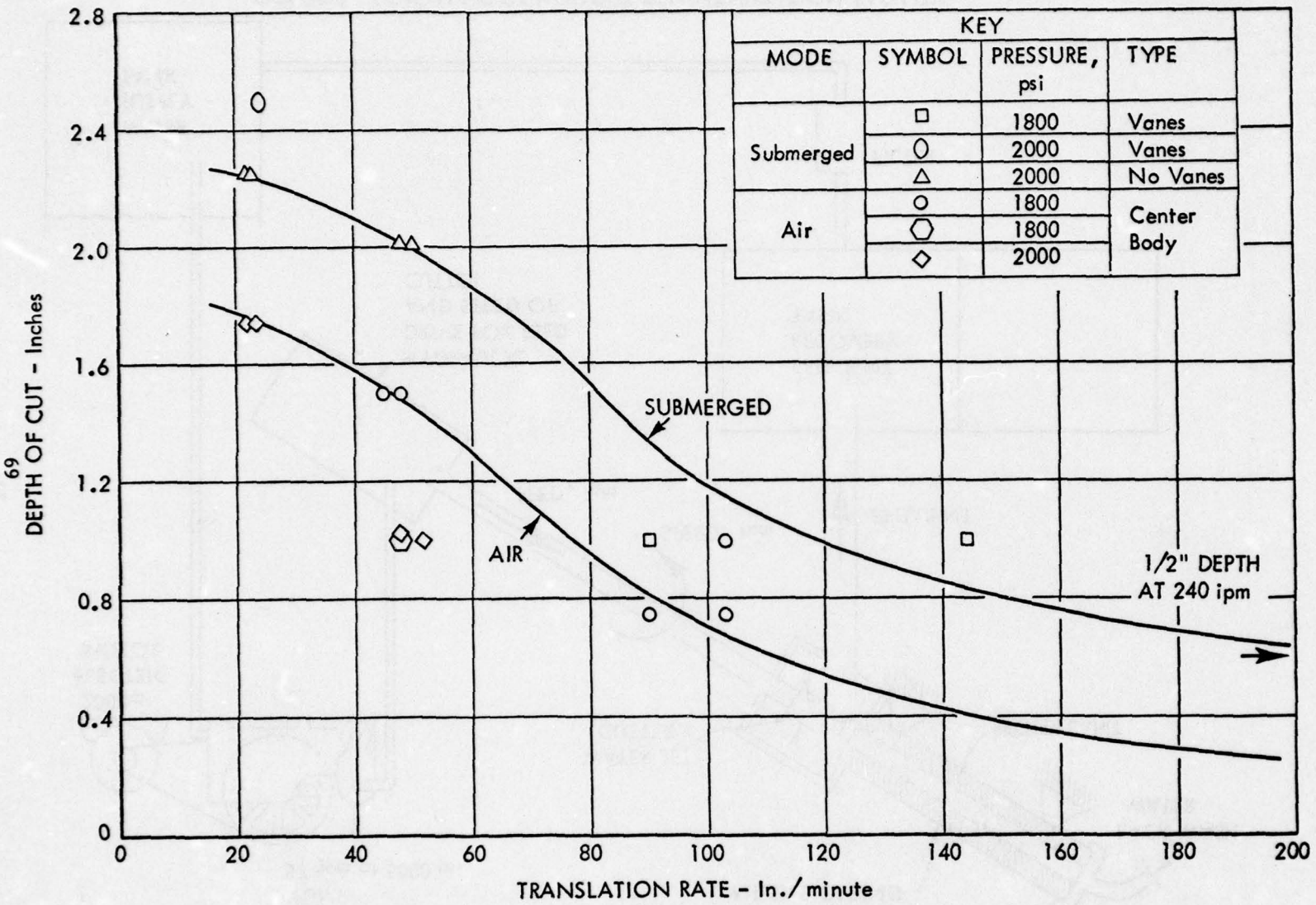


FIGURE 7 - EFFECT OF SUBMERGED AND IN AIR OPERATION OF 1/8-INCH CAVIJET:
Tests on TARTAR inert propellant; 1/4-Inch stand off distance

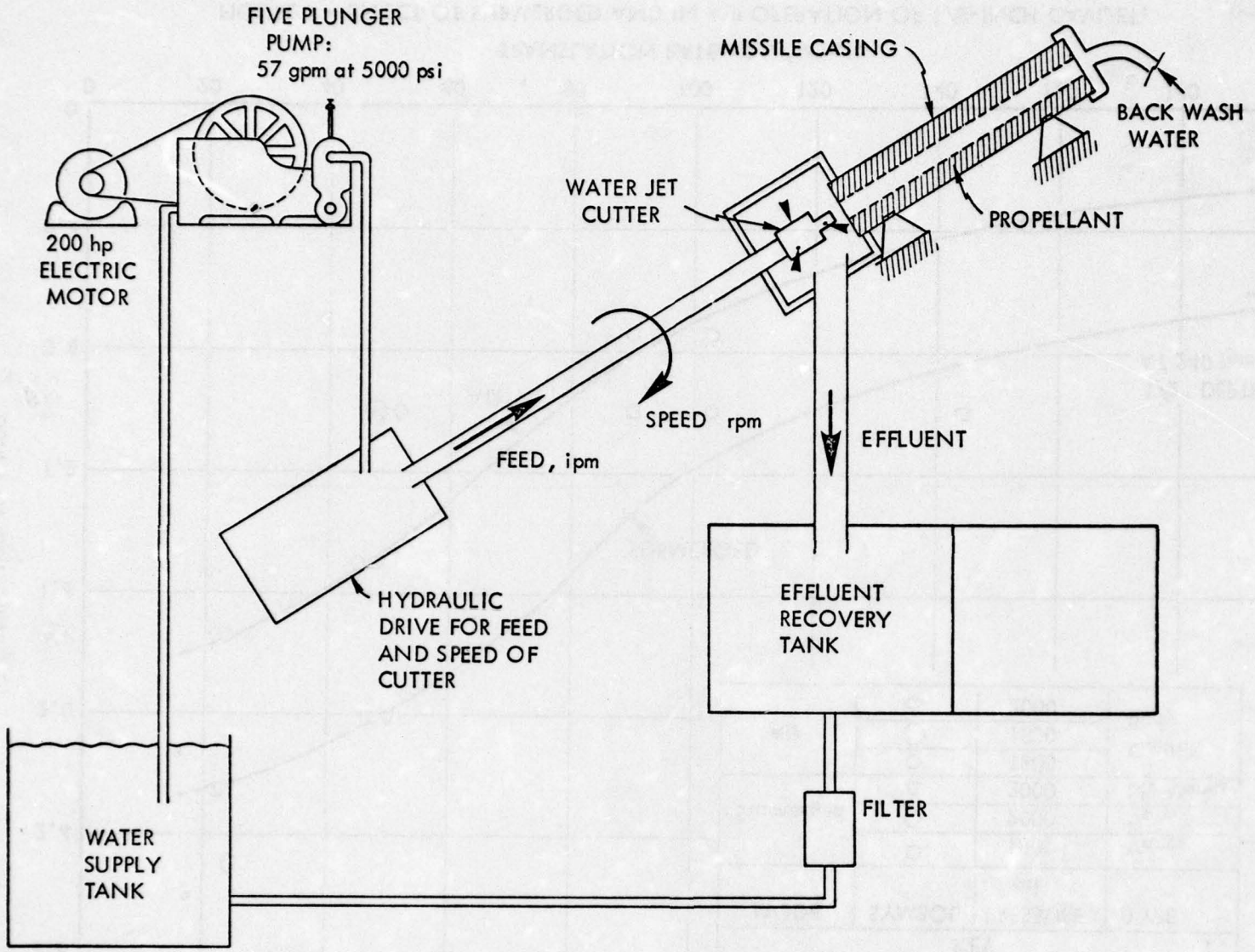
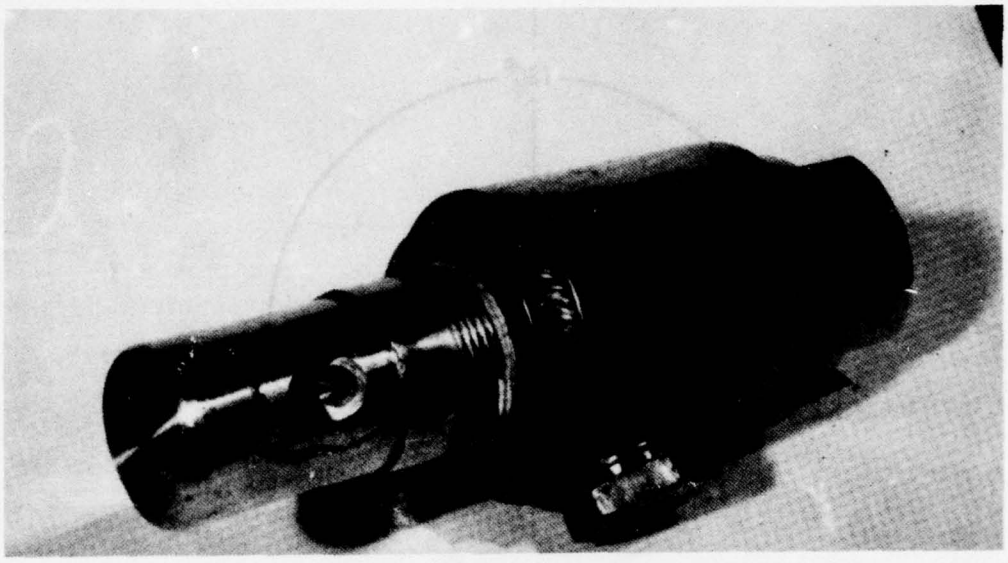
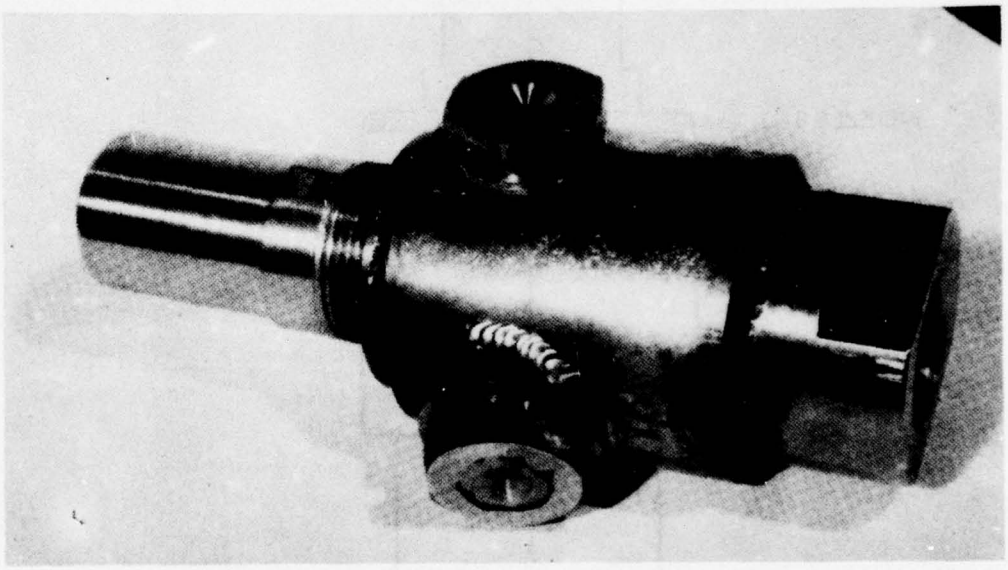


FIGURE 8 - SCHEMATIC OF HOGOUT DEMILITARIZATION FACILITY

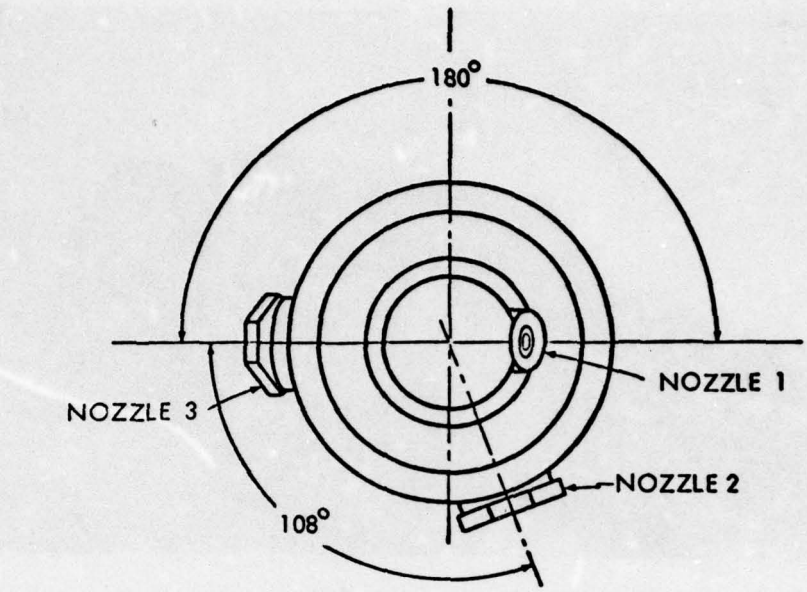


a. Showing leading section, with forward directed nozzle

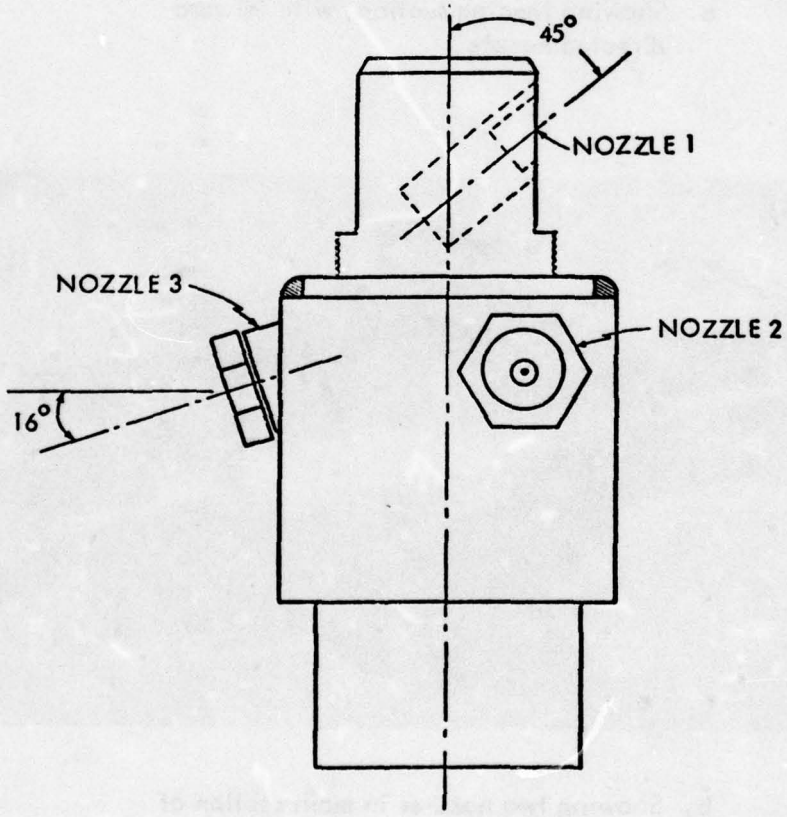


b. Showing two nozzles in main section of nozzle holder

FIGURE 9 - CAVIJET™ CUTTING HEAD FOR PROPELLANT REMOVAL



a. CIRCUMFERENTIAL POSITIONS



b. LATERAL POSITIONS

FIGURE 10 - ORIENTATION OF NOZZLES IN CAVIJET™ CUTTING HEAD

APPENDIX A

THE HYDRONAUTICS CAVIJET™ CAVITATING WATER JET METHOD AND TEST FACILITY

A.1 THE CAVIJET METHOD

The following background information is appended for those readers unfamiliar with cavitation erosion or the CAVIJET cavitating water jet method.

Figure A-1 provides an indication of the ability of a cavitating water jet to amplify the available free stream pressure, and therefore deliver a considerably higher impact pressure to a surface than does a steady jet at the same velocity. The curve for impact pressure, p_i , for the steady jet was calculated from the equation for the stagnation pressure:

$$P_i = p_o = \tfrac{1}{2}\rho v^2 \qquad [A\text{-}1]$$

where

ρ = mass density of water
v = velocity of the jet.

The envelope of curves in Figure A-1 for the cavitating water jet is based on Rayleigh's (1) single cavity spherical collapse theory, with gases in the cavity assumed to follow an isothermal compression. Thiruvengadam (2,3) has studied the thermodynamics of this process, and presents a relationship for the collapse pressure as a function of gas content in the cavities. This was then used to calculate the curves for p_i, the impact pressure reaching the surface, shown in Figure A-1 for the cavitating water jet:

$$p_i = \frac{p_o}{6.35} \exp\left(\frac{2}{3\alpha}\right) \qquad [A\text{-}2]$$

where $\alpha = Q_o/p_o$ is the gas content of the cavities, expressed as the ratio of the partial pressure of the gas, Q_o , to the local pressure, p_o , surrounding the cavity at the beginning of the collapse. Near the surface p_o is the local value of the stagnation pressure. The damping effect of gases in the cavities

is clearly shown in Figure A-1, where at any given velocity, a decrease in α allows a substantial increase in the impact pressure.

In order to compare the CAVIJET with a steady jet, due to differences in discharge coefficients, nozzle sizes providing the same flow rate should be considered. Only then, for a given pressure, the delivered horsepower would be the same for each system. For example, at 83.8 m/sec (275 ft/sec) the impact pressure for the steady jet is about 3.4 MPa (500 psi). Whereas, if we assume that the cavitating water jet operates with an $\alpha \simeq 1/8$, which experience indicates is typical for several practical cases, then this would produce a local (in space and time) impact pressure of about 114.5 MPa (16,600 psi) at the same nozzle pressure of 3.4 MPa (500 psi). In order for the steady jet to deliver the same impact pressure, it would have to operate with a pump discharge pressure of 114.5 MPa (16,600 psi).

It should be emphasized that, although the foregoing discussion of pressure provides an indication of the erosion potential of the cavitating water jet, the effect of other parameters such as cavitation number, collapse frequency, degree of cavitation, Weber number, mean nuclei size, gas content of nuclei, and impact pressure should also be included. Thiruvengadam[3] proposed a theory which describes the role of these parameters on thé erosion intensity which is actually imparted to the material surface. Interactions of the jet with the particular surface being eroded also contribute to the effectiveness of this device, which must be determined empirically for each specific application.

A measure of the relative ability of cavitating devices to erode materials is given by the cavitation erosion intensity, I_e.

This parameter is defined (2,3) by

$$I_e = \frac{\Delta y}{\Delta t} \cdot S_e$$

where

I_e = Cavitation erosion intensity (power/area), the power being absorbed by a unit area of the eroded portion of the material.

Δt = time interval of exposure to the cavitation.

Δy = depth of the eroded region of the material, during Δt.

S_e = Erosion strength of the material (energy/volume, or force/area), defined (2,3) as the energy absorbing capacity of the material under the action of erosion. The value of S_e are empirical, and fixed for a given material. Using a standard material, the intensity, I_e , of various erosive devices may be determined.

An indication of the effect of the cavitation erosion intensity parameter, I_e , may be seen in Figure A-2. Here the results of drilling tests on concrete are plotted for various CAVIJET configurations. (See Refs. 6-8 for a discussion of these configurations.) It is seen that in this concrete an increase in the drilling rate of several orders of magnitude may be achieved by varying the nozzle configuration or the mode of operation.

In many situations, an increase in the cavitation erosion intensity has been observed to be proportional to the sixth power of the velocity (3,4,5). This should be compared with a steady jet where, as shown by Equation [A-1], the pressure is proportional to the second power of velocity only. Earlier work on the CAVIJET (6,7,8) also showed a sixth power dependence

for the cavitating water jet, when operated in air. Recent developments, under water, have indicated a much higher velocity dependence of the cavitation erosion intensity (9,10). This increased intensity may also be achieved, when eroding surfaces not actually submerged, by creating an "artificial submergence" of the CAVIJET either by encasing the jet within a rigid sleeve or by causing a flow of low velocity water to surround the high velocity cavitating jet.

However, although the intensity of the CAVIJET has been seen to increase very rapidly with increasing jet velocity, the power required to drive the cavitating water jet shows the same dependence on velocity as does the steady jet, namely, velocity to the third power. The relationships for the cavitation erosion intensity and power are plotted, for a 6.4 mm (1/4-in.) CAVIJET operated in air, in Figure A-3. These data, from drilling tests on aluminum, clearly indicate how a cavitating water jet becomes increasingly more efficient as higher velocities are achieved. As erosion intensity is a property of the device, the same curves are obtained for any material which is being eroded.

This increase in volume effectiveness (and decrease in specific energy; see the definitions in Reference 9), as indicated by results of tests with concrete, is shown in Figure A-4. Here a comparison is made between the relative improvements in specific energy, with increases in pressure, for the CAVIJET and for a steady water jet (11). It is seen that, because of the large increases in the intensity of the CAVIJET, this method shows a much stronger dependence on pressure than does the steady water jet. Thus, a cavitating water jet system provides the capability for efficient cutting of materials with moderate power and water flow requirements.

A.2 TEST FACILITY

The facility which was constructed to study the principles of a cavitating water jet, and which has provided the basis for the development of a wide variety of systems, includes the following equipment and features (see Figures 1 and 2).

1. Pump. An electrically driven piston pump delivers a constant flow of 303 ℓ/min (80 gpm) at 13.8 MPa (2000 psig). With the present nozzle design, this pump provides a 6.4 mm (1/4") diameter jet at a velocity of over 152 m/sec (500 ft/sec). The pressure range of 13.8 MPa (2000 psig) covers physical parameters of considerable interest, while still remaining within an economic framework.

2. Test Chambers. Two mobile chambers are available for conducting test and evaluations of the CAVIJET for various applications. One is 0.91 m wide, 1.22 m long and 0.91 m deep (three feet wide, four feet long, and three feet deep), has a 946 ℓ (250 gallons) capacity. A new, larger tank is 1.5 m wide, 1.8 m long, and 1.2 m deep (5 ft by 6 ft by 4 ft deep), and has a working capacity of 2,840 ℓ (750 gallons). These tanks are used for either stationary, translating, or manual operation of the cavitating water jet, which has been extended by 5.1 cm (2 in.) flexible high-pressure hose for any of these modes of usage. These chambers are fitted with removable wooden covers which serve to retain the splash to facilitate in-air testing. The smaller chamber also contains two lights to permit viewing or photography during the testing. Hydraulic systems for controlling nozzle translation are also a part of each chamber (see below).

3. Nozzle Translator. Hydraulic cylinders, affixed to the carriages which support the CAVIJET nozzle, provide controlled translations of the jet relative to the specimens in each test

chamber. A gear pump, sump, and four-way control valve complete these systems, which provide translation velocities from less than 2.5 cm/sec (1 in./sec) to well over 90 cm/sec (36 in/sec) in either direction.

4. Test Liquid Reservoir. A water tank is provided which serves as a reservoir for the pump and a return basin for the nozzle effluent. The tank's size and equipment auxiliaries are designed to permit careful control of the water quality. The upper part of the tank is equipped with quick access viewing ports in the top and around the circumference, which were formerly used to permit easy specimen exchange and photography when this tank served as the test chamber. Screens are available, if required, to catch eroded particles removed from specimens.

5. Valves. A remotely controlled bypass valve located between the main line to the nozzle and a bypass line permits limited surging of the jet. Also located between these two lines is a metering valve which provides fine control of the flow in the main line and therefore the jet velocity. Other valves are provided to allow rapid backfilling of the test chamber, draining, and for backwashing the sand filters.

6. Heat Exchanger. A shell and tube heat exchanger located in the suction line of the pump controls the water temperature.

7. Filters. Also located in the pump suction line is a filter which will trap any small eroded particles missed by the main filters. This filter provides extra protection for the pump. The main filtration is provided by two parallel Jacuzzi sand filters. Each of these filters is equipped with a 227 ℓ/min (60 gpm) pump which will allow rapid draining of the test chamber for specimen viewing or removal. These filters effectively capture even large particles from the various

test specimens which are cut, fractured or cleaned by the CAVIJET, and backwashing capability allows periodic removal of these particles without opening the filter tank.

8. Nozzle. Orifices in the nozzle of 6.4, 3.2, or 1.6 mm (1/4, 1/8, or 1/16-inch) diameter, or any interim size may be used. The nozzle system is so designed that by the exchange of several inserts, the types and length of cavity produced can easily be altered.

9. Gages. A gage is located in the suction end of the main pump to be sure that a net positive head is maintained there. A gage located in the nozzle line is used to monitor the pressure on the discharge side of the pump. Gages are also placed in the suction and discharge lines for each Jacuzzi filter.

10. Booster Pump. Located in the suction line of the main pump is a small booster pump so that the space above the water in the tank can be evacuated without losing the required positive head on the main pump.

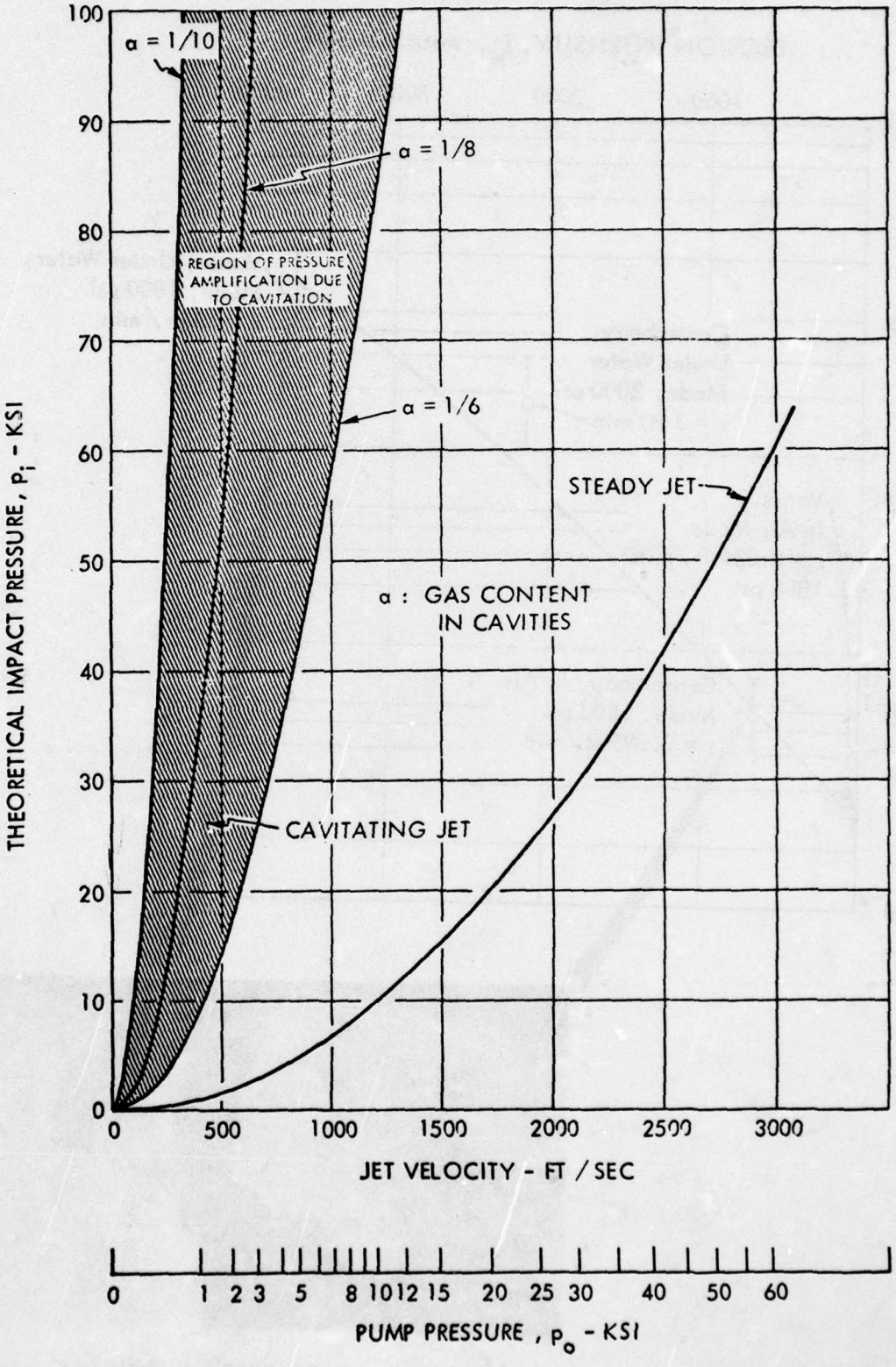


Figure A-1. Theoretical Comparison of Cavitating and Steady Water Jets

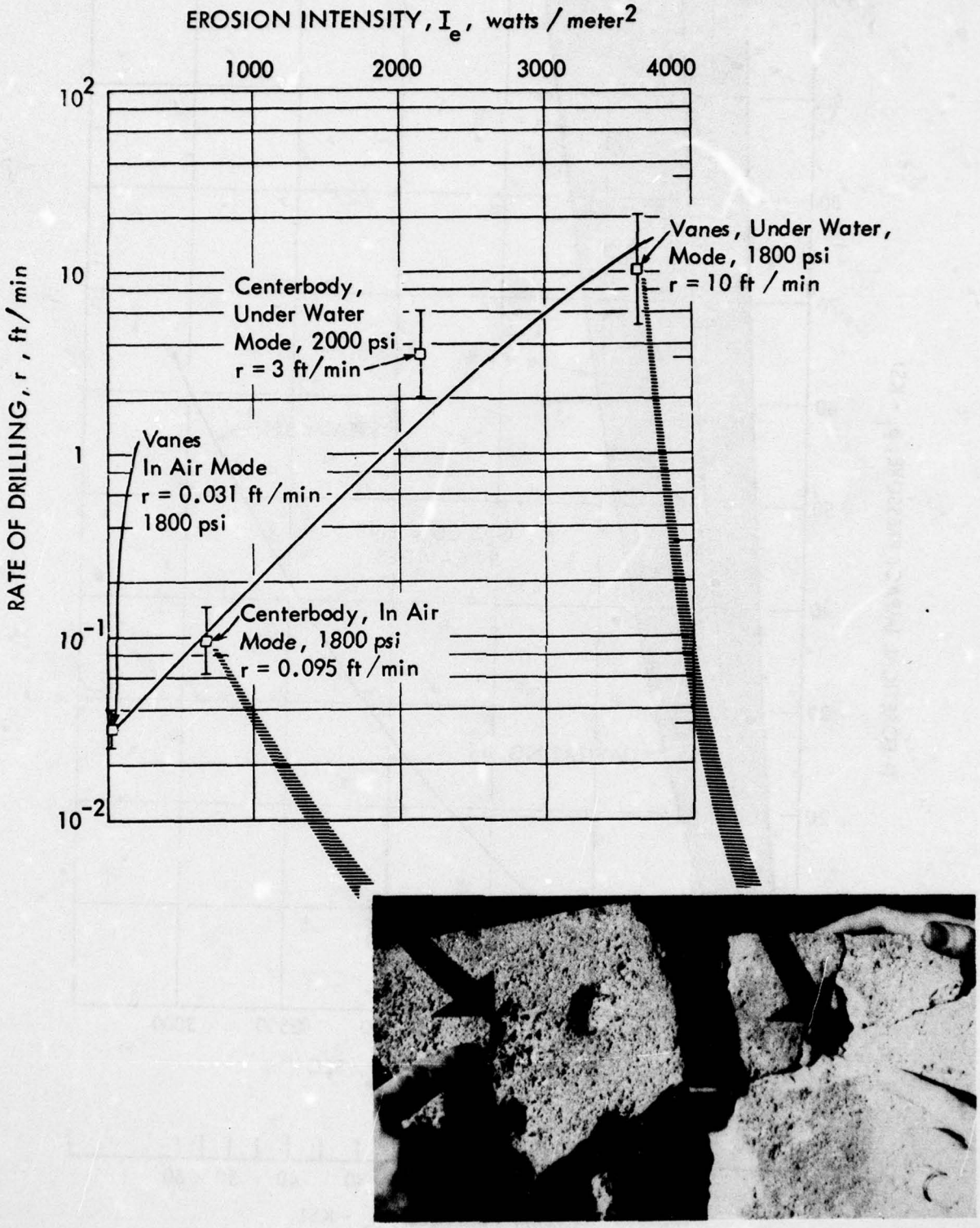


Figure A-2. Performance of the $\frac{1}{4}$-in. Diameter CAVIJET™ In Drilling Concrete (Compressive Strength: 5,000 – 10,000 psi)

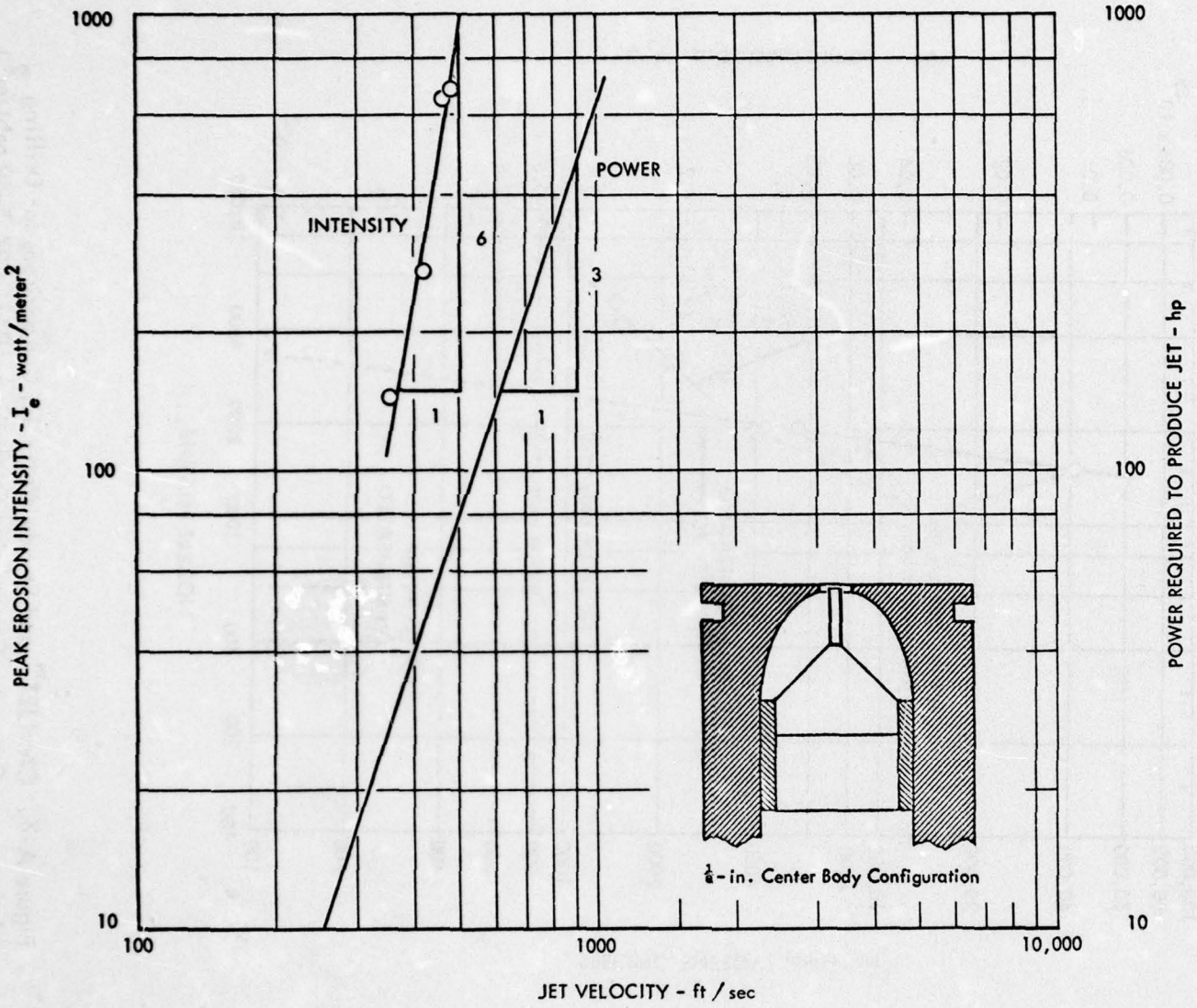


Figure A-3. Peak Erosion Intensity and Power Vs. Jet Velocity for the ¼-in. Diameter CAVIJET™, in Air Mode, Drilling 1100 Aluminum Alloy

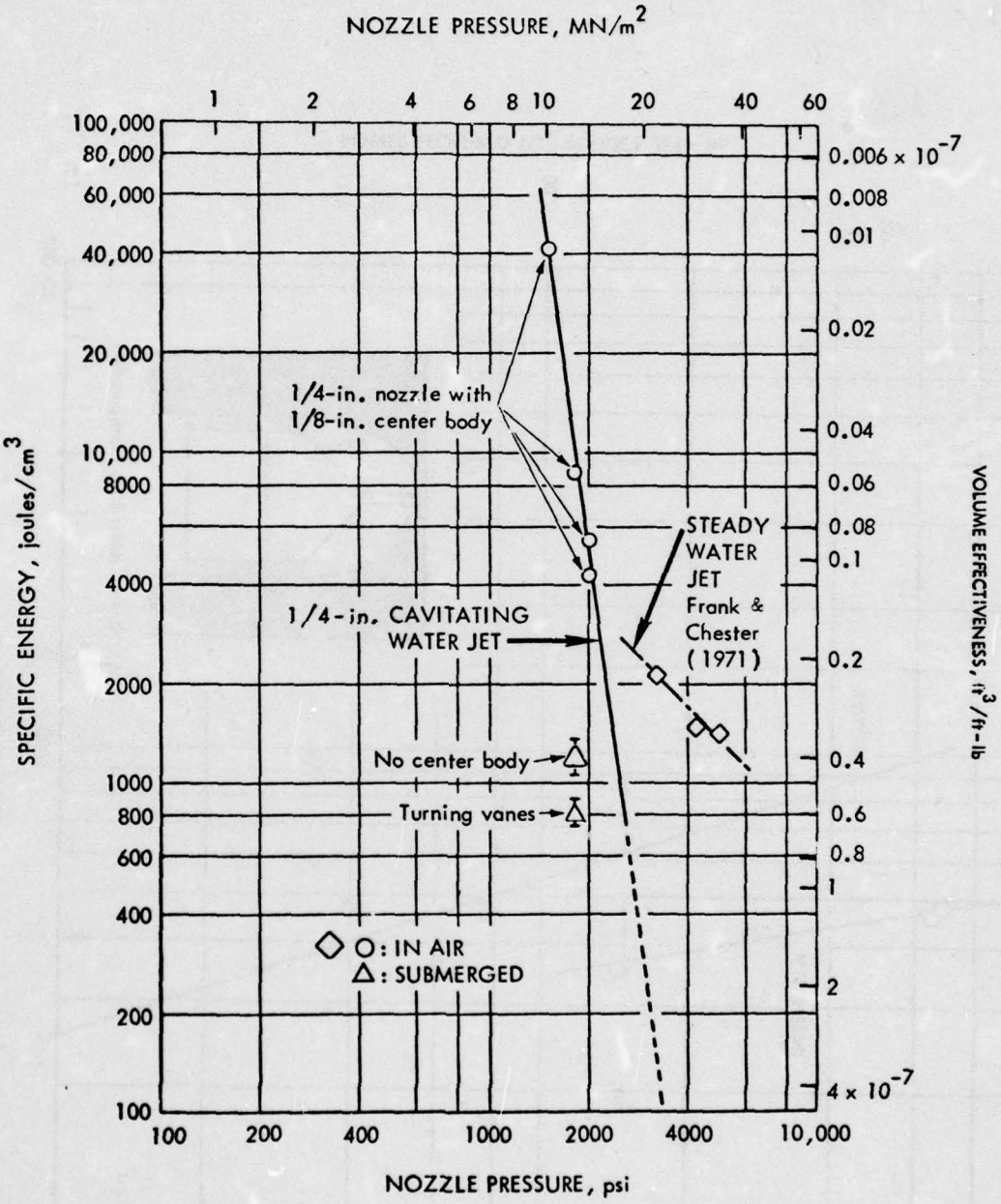


Figure A-4. CAVIJET™ and Steady Water Jet Comparisons for Drilling Concrete; Compressive Strength: 5-10 ksi (34.5-69 MN/m²)

EXPLOSIVE/FLAMMABILITY CHARACTERISTICS OF VINYL CHLORIDE MONOMER (VCM)-AIR-WATER VAPOR MIXTURES

J. C. Hokanson
A. B. Wenzel

Southwest Research Institute
San Antonio, Texas

ABSTRACT

The measurement of pressures and velocities associated with the reaction front of various VCM-Air and VCM-water vapor mixtures as a function of ignition sources and temperature was conducted for Continental Oil Company. The mixtures tested varied from 2% to 30% vinyl chloride in air. Ignition sources used in these tests were a double squib using a pyrophoric material (ignition source A),a propellant boosted squib (ignition source B), and a detonator (ignition source C). The temperature was maintained constant at 82° ± 5°F, except for one test which was conducted at 142°F. For the VCM-Air-Water Vapor Tests, initiators B & C were used in tests with water vapor saturated stoichiometric mixtures of VCM and air. The temperature was varied from 80°F to 160°F in these tests. A total of 53 tests were conducted in this program.

From the results obtained, the following observations are made:

- No detonations were experienced in these experiments.
- Within the range of temperatures tested, there appear to be no significant effects in the reaction intensity as a function of temperature.
- The flammability characteristics are significantly affected by the ignition source. Sparks or hot sources will yield low reactions with low rise-times capable of generating up to 4 times atmospheric pressures. Blast sources such as detonators increase the reaction rates and shorten the rise-time significantly, generating up to 6 times atmospheric pressures.
- Water vapor mixtures significantly reduce the reaction times. For the case of hot ignition sources the reaction intensity is greatly reduced with water vapor mixtures. For the case of blast ignition sources, the results are not as conclusive. We experienced both a very low reaction and a high reaction. This implies that, given a strong ignition source, water-vapor may not have a significant effect on the reaction intensity.

VCM should be treated as a flammable gas even in the presence of water vapor.

I. INTRODUCTION

This paper describes an experimental program conducted at Southwest Research Institute (SwRI) for Continental Oil Company (CONOCO). The primary objective of this program was to measure the "Explosive/Flammability Characteristics of Vinyl Chloride Monomer (VCM)-Air-Water Vapor Mixtures". This condition represents the most hazardous operating condition encountered in the proposed CONOCO technique for the polymerization of VCM to produce polyvinyl chloride (PVC). To accomplish the above objective, the following tasks were conducted:

- Measure the pressures and velocities associated with the reaction front of various VCM-air mixtures as a function of ignition sources.
- Determine the effects of introducing water vapor to the stoichiometric mixture as a function of ignition sources and temperature.

For the first task, various VCM-air mixtures at ambient temperatures were initiated to demonstrate that the laboratory test apparatus agreed with the explosive limits found in the literature. Three different initiators were used in these tests. The ignition sources used in these tests were a double squib using a pyrophoric material (ignition source A), a propellant boosted squib (ignition source B), and a detonator (ignition source C). The second task consisted of initiating water vapor saturated stoichiometric VCM-air mixtures at temperatures in the range, of 130 to 160°F. The two most energetic initiators (ignition sources B and C) were used in these tests. In both cases pressure and or strain recordings in the laboratory test apparatus were used to determine if the gas mixtures detonated, and where detonation occurred, the relative severity of the detonation. Section III describes the details of the experimental apparatus, the instrumentation system and the initiators, which were used to accomplish the objectives of the program.

The test results are described in Section IV using graphs, tables and illustrations. For each test, the reactions, if any, are described qualitatively, identified as to low-order combustion, combustion, deflagration or detonation, and described quantatively using the pressure measurements. Conclusions and recommendations are given in Section V.

II. TECHNICAL DISCUSSION

A. Literature Review

Because vinyl chloride is so widely used in the plastics industry, many investigators have studied the physical properties, explosive and flammable limits of vinyl chloride monomer (VCM). Prior to this program, personnel at Continental Oil Company conducted an extensive search of the technical literature for material dealing with the explosibility of VCM in air. The results of this search, given in Table 1, are briefly outlined in this section of the report. The methods generally used to measure the explosive and flammable limits are based on the observation that dilution with an excess amount of fuel (rich mixture) or oxidizer (lean mixture) causes the burning velocity and flame temperature of the mixture to decrease until at some limit concentration, the reaction ceases to propagate. Experimentally this point is not well defined, but depends to a large extent on the experimental apparatus, temperature, pressure, direction of flame propagation and the mode of initiation.

Of the references cited in Table 1, only three[2, 3, 5] describe how the tests were conducted. Generally the experimental apparatus consisted of a long slender tube mounted vertically. The bottom of the tube is open. The explosive limit concentration is determined by observation of flame propagation in the tube from the open end towards the closed top. Initiation is usually achieved by means of an electric spark or with a heating coil. Although the references cited in Table 1 refer to the explosive limits of VCM, close examination reveals that the authors are referring to the flammability limits of VCM -- the lowest and highest VCM concentrations for which a flame will propagate the length of the tube. Only references 5 and 7 report the maximum pressures attained in a chamber after ignition. Reference 5 reports that a maximum pressure of 120.5 psig was attained in a 0.18 ft^3 cylindrical chamber. Although a typical pressure-time trace is given, a time scale is not provided. Reference 7 reports a maximum pressure of 165 psig but, like reference 5, does not explain how this figure was obtained.

The burning velocity of VCM in air is only reported by L. A. Eggleston[8], et al. In this report a test program to explore the use of a water spray system for removal of VCM vapors, inhibition of flame speeds and restriction of vapor flow is described. Full scale experiments showed that water spray at normal application rates could not quench ignition nor reduce burning velocity. It changed conditions and resulted in nonluminous combustion and increased flame speeds. During the course of this investigation, two control tests were conducted which are of interest to this program. In each test the detonation chamber consisted of a wooden frame covered with a layer of 8 mil clear vinyl plastic. The volume of the enclosure was 2300 cubic feet. The vinyl

TABLE 1. PHYSICAL PROPERTIES OF VCM

Heat of Combustion	508, 141 Btu/lb · mole
Latent Heat of Evaporation	128.25 Btu/lb
Latent Heat of Fusion	32.65 Btu/lb
Self Ignition Temperature	881.6°F
Heat of Formation	1.620×10^7 Btu(lb_m · mole)

Flammability Limits in Air[1]

Reference	Chamber Volume (ft^3)	VCM Limit Concentration[2] Lean (%)	Rich (%)
1	--	4.0	20.0
2	1.1 (cylinder)	4.0	21.7
3	- (cylinder)	4.0	22.0
4	--	4.0	22.0
5	0.18 (cylinder)	3.65	26.6[3]
5	5.65	4.35	25.2
6	--	3.6	33.0

Maximum Explosive Pressure

Reference	Chamber Volume (ft^3)	VCM Concentration (%)	P_{max} (psig)
5	0.18 (cylinder)	10.0	120.5
7	--	7.0	165.0[4]

Burning Velocity 40.8-50.2 fps (reference 8)

---

[1] According to Reference 1, the most readily ignitable mixture is 7% VCM.
[2] Percent by volume.
[3] This value was increased to 33% with the addition of nitrocelluose fibers in the initiator.
[4] This may be a calculated maximum pressure.

chloride concentration for each test was about 7% by volume in air; initiation was achieved by igniting 10 to 15 inches of black powder saturated cord with an electric squib. The flame velocity was measured in these tests with a high speed camera. From frame to frame measurements of the flame front and the time between subsequent frames, the burning velocity was obtained. The burning velocity reported by L. A. Eggleston et al.[8] was 40.8 to 50.2 fps. In both tests the flame front was described as a yellowish-smoky flame. Internal chamber pressures were not sufficiently high enough to rupture the plastic enclosure.

B. The Combustion Process

Once a flammable gaseous mixture has been successfully ignited, the resulting flame will propagate away from the ignition source. If the rate of propagation is subsonic*, the reaction is called deflagration. If the rate of propagation is supersonic*, the reaction is considered to be a detonation. In deflagration, the rate of propagation is so slow that the chamber pressure, although increasing, is at any instant practically equalized throughout the vessel. Thus, the pressure differential across the combustion front is relatively small. Slow burning or low-order combustion is a similar process, but the propagation velocity is even slower than for deflagration. For this reason, the pressure rise is lower than for deflagration. In detonation the initial pressure will equalize at a rate appreciably less than the propagation velocity, resulting in a significant pressure drop across the flame front. For most combustible air mixtures at ambient temperatures, the peak pressure caused by deflagration will not usually exceed about 8 times the initial pressure. However, if ignition results in detonation the peak pressure may exceed 40 times the initial pressure. Detonation is usually obtained by one of two processes. First, detonation in a closed chamber may occur after deflagration has caused a large pressure buildup. The point at which deflagration becomes detonation depends on the fuel concentration, temperature, pressure, ignition source and the geometry of the test chamber. Second, with a sufficiently intense ignition source detonation may occur immediately after ignition, even when the mixture is not confined. The ignition energy required to initiate a detonation is several orders of magnitude greater than that required to propagate a deflagration.

C. Calculation of the Maximum Pressure Rise for Deflagration

The propagation of a flame from ignition at a point source through the contents of a closed vessel is a problem that has been widely studied. By far, the simplest closed vessel explosion is that following ignition at the center of the vessel. Lewis and von Elbe[10] have presented an extensive analysis of this system and have reached the following conclusions:

---

*Relative to the sonic velocity of the unburned mixture.

- Throughout the propagation process, the flame may be assumed to be burning in a constant pressure environment.
- The early pressure rise is a cubic function of time.
- Burning velocity is not constant during the entire propagation process. This is a result of adiabatic compression which significantly raises the temperature and pressure of the outer shell of gas before it is reached by the combustion process.
- The combustion process produces a gas sample which is significantly hotter at the center of the vessel.

The above results imply that with sufficient information concerning the burning velocity and the thermodynamic properties of the gas, the combustion process, as it occurs in a spherical vessel may be described analytically for central ignition. This is not true for an arbitrarily shaped vessel because the expansion process associated with flame propagation leads to complex flame behaviors which are not easily generalized. The maximum pressure achieved during deflagration of VCM-air mixtures in a spherical vessel will be calculated in this section of the report. Although the detonation chamber used on this program was cylindrical, the calculated maximum pressure will serve to give an indication of order of magnitude to be expected.

The balanced combustion reation for the burning of VCM in air is given by the following chemical equation:

$$CH_2 = CHCl + 2.5O_2 + 9.4N_2 \longrightarrow 2CO_2 + HCl + H_2O + 9.4N_2 \quad (1)$$

In order to calculate the flame temperature for a stoichiometric mixture of VCM in air, the method outlined by Woinsky[7] will be used. The flame temperature is calculated for a constant volume system, starting at 77°F and 1 atmosphere. The net heat of combustion of vinyl chloride monomer is H_N = 508, 141 Btu/mole. The enthalpy of the combustion products at 4060° R is

$$H_{4060} = \underbrace{36,700}_{\text{water}} + \underbrace{2(46,000)}_{CO_2} + \underbrace{9.4(28,150)}_{N_2} + \underbrace{27,500}_{HCl} = 420,810 \text{ Btu}$$

The specific heat of the combustion products at 4060° R is:

$$C_p = 12.5 + 2(15.0) + 9.4(8.5) + 8.6 = 131.0 \text{ Btu/°R}$$

Then using the definition of the enthalpy of reaction, eq. 2, the formula

$$\Delta H = C_p \Delta t \tag{2}$$

for the flame temperature may be obtained:

$$t_f = \frac{H_N - H_{4060}}{C_p} + 4060\ °R = \frac{508,141\ (\text{Btu/mole})(1\ \text{mole}) - 420,810\ \text{Btu}}{131\ \text{Btu}/°R} + 4060\ °R$$

$$t_f = 4726.65\ °R = 4266\ °F$$

Using this calculated flame temperature and the ideal gas law, the pressure associated with the flame can be calculated.

$$P_{max} = P_1 \frac{\overline{M}_1}{\overline{M}_2} \frac{T_F}{T_1} \tag{3}$$

where P_1 = initial pressure in the chamber = 14.7 psi

T_1 = initial temperature in the chamber = 77 °F = 537 °R

M_1 = average molecular weight of the initial mixture

= 31.44

and M_2 = average molecular weight of the burned mixture

= 30.28

so

$$P_{max} = (14.7\ \text{psi})(\frac{31.44}{30.28})(\frac{4726.65\ °R}{537\ °R}) = 134.3\ \text{psi}$$

Although this is not the pressure which was measured in this program, it is indicative of the magnitude of the pressure produced by initiation of VCM in a cylindrical chamber. The pressure measured in our experiments was less than the value obtained above because heat is transferred from the flame to the tube walls by radiation, convection and conduction.

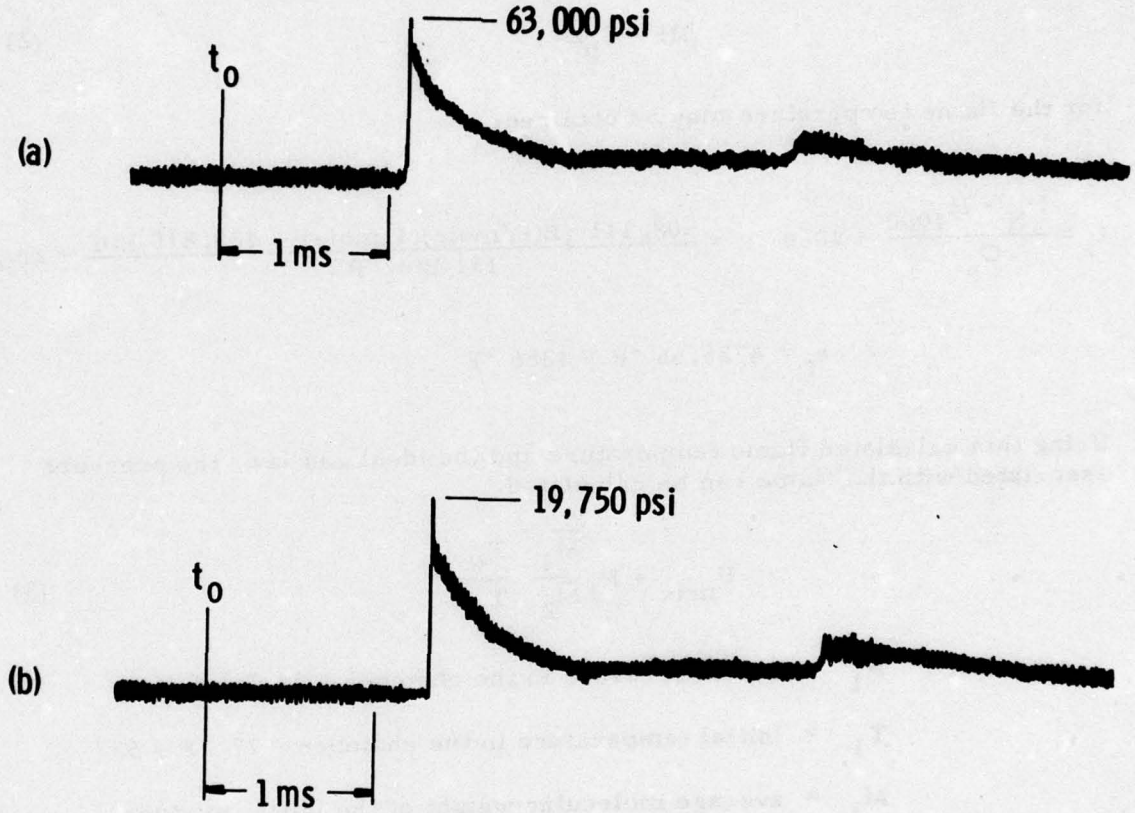


Figure 1. Typical Pressure-Time Measurements for Gaseous Detonation for Methane-Oxygen Mixtures

Zabetakis[6] provides a rule of thumb for calculating the minimum elapsed time required for the pressure to reach a maximum value. For paraffin hydrocarbons and fuel blends such as gasoline, the minimum rise time (in milliseconds) is approximately $75\sqrt[3]{V}$; where V is the chamber volume in cubic feet. Thus, for the test chamber used in this program, using the above relation, the minimum rise time should be about 190 msec for deflagration reactions. Although this rule of thumb does not apply directly to the combustion of VCM, it does provide an indication of the order of magnitude of the rise times which should be encountered in the field experiments.

D. Measurement of Gaseous Detonation Pressures

On a previous SwRI program conducted for CONOCO[11], explosive parameters of gaseous mixtures of methane and oxygen were measured. In particular the reflected pressure and the detonation wave arrival time were measured. Many of the techniques developed on the previous program for CONOCO were implemented in this study of the explosibility of VCM. For instance, the initiating mechanism, the strain gage velocity measurement system and the pressure measurement systems were nearly identical between programs. Detonation of the methane-air mixtures was very definitely achieved on the previous program as evidenced by the traces shown in Figure 1. Note that the ratio of the peak pressure recorded to the initial chamber pressure was approximately 80 for both tests shown in the figure. Second, the rise time of the traces is on the order of 0.3 μsec. Finally, the propagation velocity of the detonation wave was between 7500 and 9300 which is much higher than the sonic velocity (≈1100 fps) of the unburned mixture. The description of the detonation of methane-air mixtures is given in this report to show in a qualitative way characteristics of detonation of gaseous mixtures.

III. EXPERIMENTAL SETUP

The tests described in this report were conducted at the explosive facilities of the Engineering Sciences Division. The test apparatus was housed in a metal building located on a remote portion of the Institute. The instrumentation was located in a trailer approximately 20 feet from the metal building. The test apparatus was designed so that the detonation chamber could be charged from outside the metal building, and subsequently initiated from the instrumentation trailer, thereby reducing personnel exposure to VCM. Details of the experimental system consisting of the detonation chamber and charging system, initiator and instrumentation are described in the following subsections.

A. Detonation Chamber and Charging System

Considerable effort was invested on this program in sizing the detonation chamber. Zabetakis[6] has shown that many complications arise when flame propagation and flammability limits are studied in small cylindrical chambers. Heat transfer from the flame to the chamber walls by means of conduction, convection and radiation may cause a flame to be quenched by the surrounding walls. Therefore, flammable limit determinations should be made in a chamber of sufficient size to minimize quenching effects. Zabetakis reports that a 2 in.inside diameter vertical tube is suitable for use with paraffin hydrocardons (methane, ethane, etc.) at atmospheric pressure and room temperature. However, such a tube is not satisfactory for many halogenated hydrocarbons under the same initial conditions. In order to ensure that the tube diameter was greater than the critical diameter, 12 in.was chosen for the chamber diameter. Strehlow[9] reports successful initiation of carbon monoxide-oxygen-saturated water vapor mixtures in closed cylindrical tubes of length-to-diameter (l/d) ratios ranging from about 2.0 to 4.0. Jones, et al.[2] measured the flammability limits of VCM in a tube with an l/d of 9.5, while Urbancova and Gregor[5] report similar tests in a l/d = 27.0 tube. Since successful initiation of gaseous mixtures has been achieved over such a wide range of tube sizes, it was felt that the tube could be arbitrarily sized. Thus, a length of 62.0 inches was chosen for the following reasons. First, a 62.0 inch length gives an l/d of about 5.0, which is in the range of tube sizes used by other researchers for flammability limit determinations. Second, the tube could be instrumented at 4 locations, 15 inches apart or 5 locations, 12 inches apart, yielding what was believed to be sufficient resolution for propagation velocity measurements. Third, the 62.0 inch tube was as long as possible, while still remaining manageable in the field experiments. Lewis and von Elbe[10] have shown that the flammability limits are widest and the propagation velocity greatest when the flame is initiated from the bottom of a vertical tube. Conversely, the flammability limits are narrowest and the propagation velocity is lowest when the flame is initiated from the top of a vertical tube. For horizontal mounting the flammability limits and propagation velocity are intermediate between those for upward and downward flame propagation. For these reasons, and because a tube of this size is more manageable when mounted horizontally, this arrangement was chosen.

Thus, the detonation chamber used on this program consisted of a 62.0 in long, 12 in O.D. steel pipe, with 3/8 inch walls. Slip-on flanges were welded to either end of the pipe to close both ends of the tube. The wall thickness was chosen to withstand pressures generated by the TNT equivalent of the maximum VCM concentration tested, while permitting the detection of longitudinal strains due to internal chamber pressures below 100 psi. A photograph of the detonation chamber is shown in Figure 2. Note that the chamber was instrumented at four equally spaced intervals with strain gages, and at six locations with pressure transducers (transducer No. 1 is not shown in the

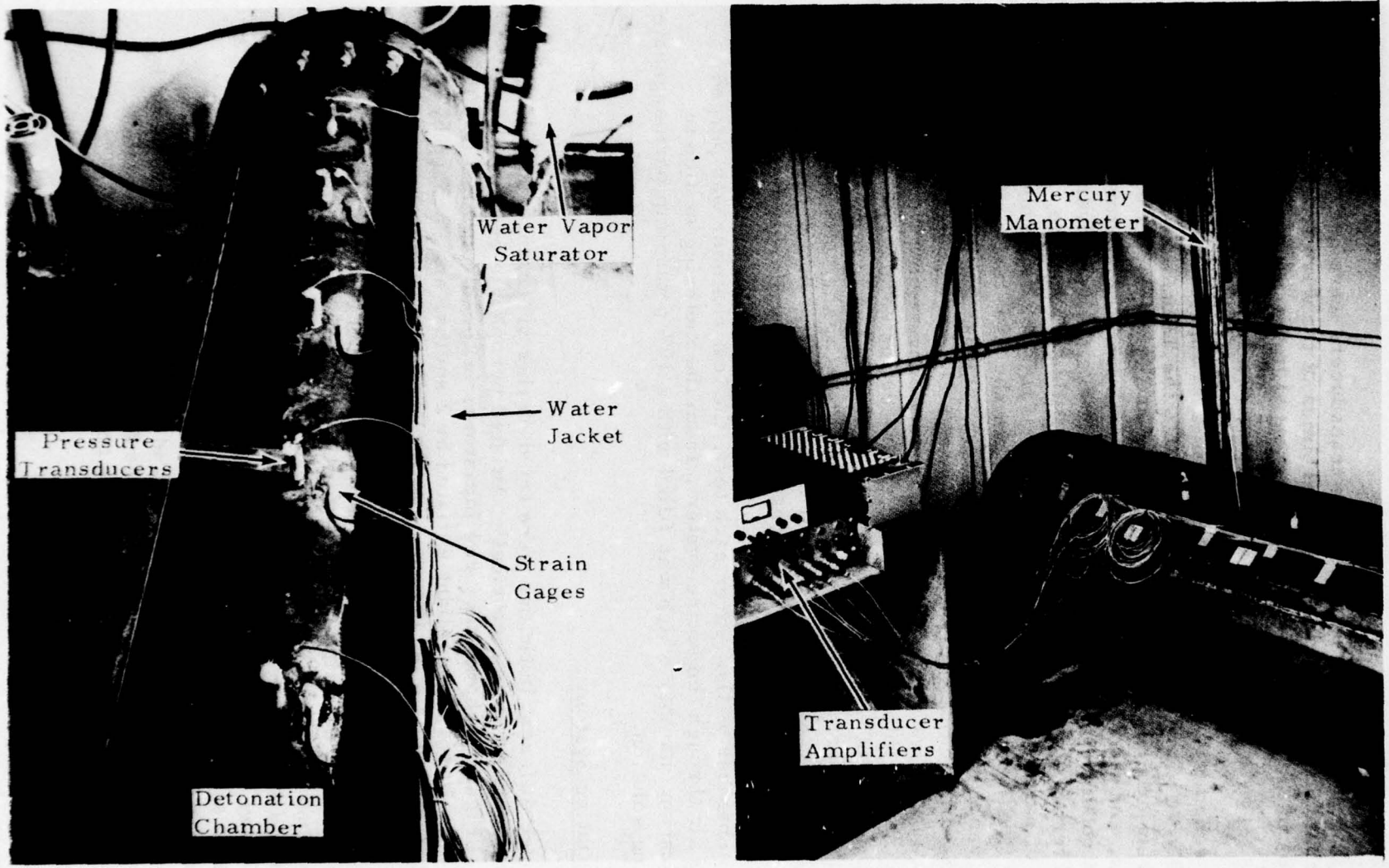


Figure 2. Two Views of the Experimental Test Apparatus

figure). The strain gages and pressure transducers were used to measure internal chamber pressures, and arrival times of the wave front. Further description of the transducers will be presented in the section of instrumentation.

A schematic diagram of the experimental apparatus is given in Figure 3. Initially VCM and air were introduced into the detonation chamber via the metering orifice. This orifice functions on the principles of critical mass flow, and the relative orifice sizes determined the mixture of VCM and air introduced into the test chamber. However, after several unsuccessful initial tests, a more direct and accurate filling procedure, based on the principle of partial pressures, was devised. From the metering orifice, the gases flow into the detonation chamber for the first test series, or into the water vapor saturator for the second test series. The saturator was kept at the same temperature as the detonation chamber (100-170 °F) by circulating the water in the jacket through a conventional water heater and into a coiled, thin wall aluminum tube inside the saturator. The jacket surrounding most of the detonation chamber served two important purposes; in the initial test series, the jacket was used to keep the detonation chamber at a uniform temperature (82 ± 5 °F) from test to test. In the saturated air tests, the jacket was to keep the detonation chamber walls warmer than the incoming gas. This prevented the water vapor from condensing on the detonation chamber walls. After each test, the test chamber was purged by flowing air through the entire system, from the metering orifice to a neutralization chamber which was filled with a 10% potassium permanganate neutralizing solution.

B. Initiating System

Three different initiators were tried on this program. In each case the device consisted of an electrically initiated pyrophoric or explosive material. Figure 4 shows the three initiators: a) double squibs, b) 60 grains of WC 870 solid propellant initiated by 2 squibs, and encased by a paper cylinder, and c) E-81 blasting cap. The two squib initiators were soldered onto a spark plug as shown in Figure 4 and inserted into the test chamber at the point shown on Figure 3. The squib leads were 8 inches long, so the initiating material was inserted into the chamber about 4 inches beyond the inside face of the slip-on flange. The E-81 detonator was used for all tests beyond test 34. In this case, the detonator was suspended 1/2 way into the tube from the hole normally occupied by the transducer located at position G on Figure 3. This was done to minimize the possibility that fragments from the detonator would impact any of the remaining transducers. Both the squibs and the detonator were initiated by current supplied from a 45 volt battery; the firing switch, as indicated before, was located in the instrumentation trailor.

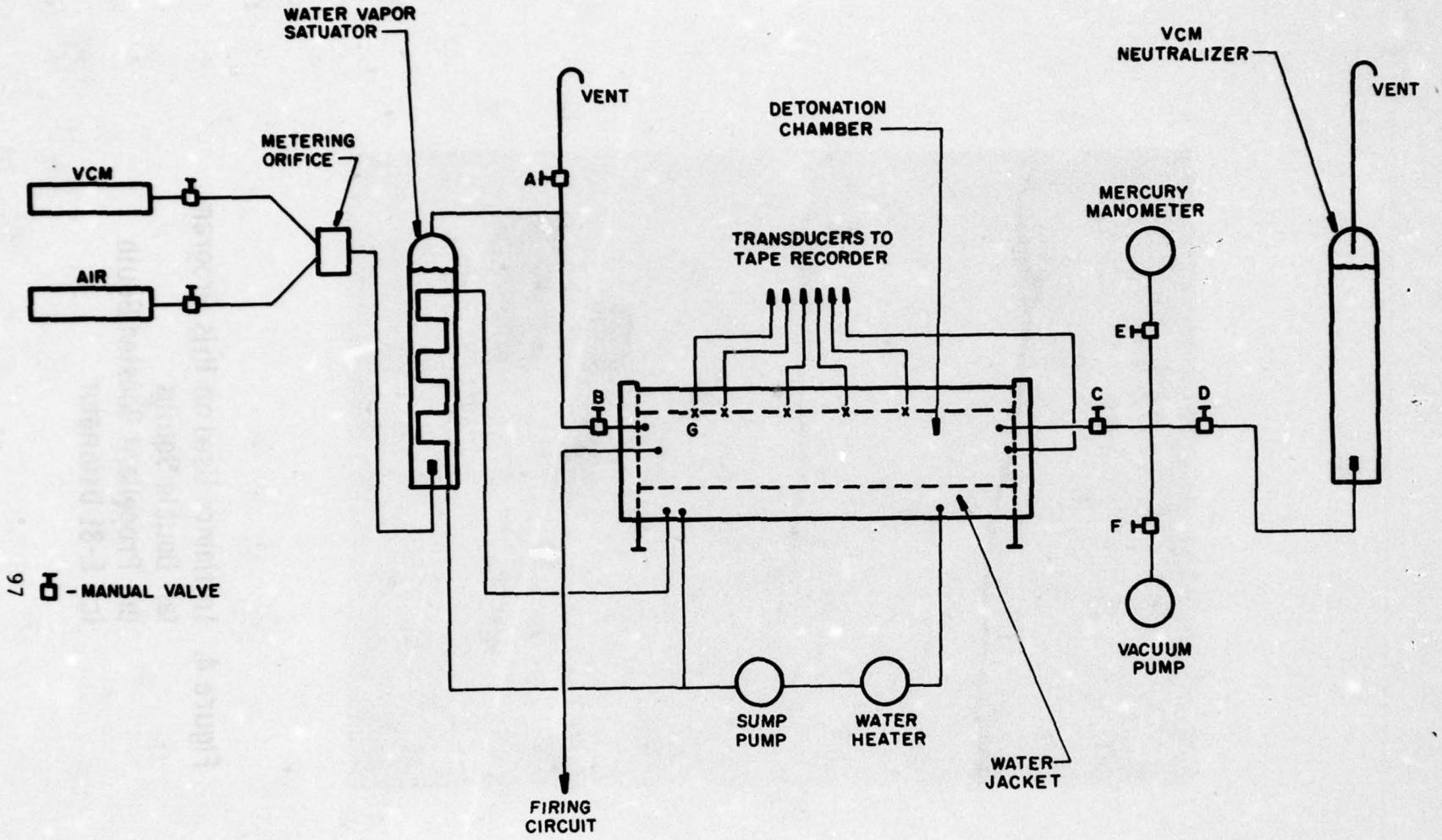


Figure 3. Schematic Diagram of the Test Apparatus

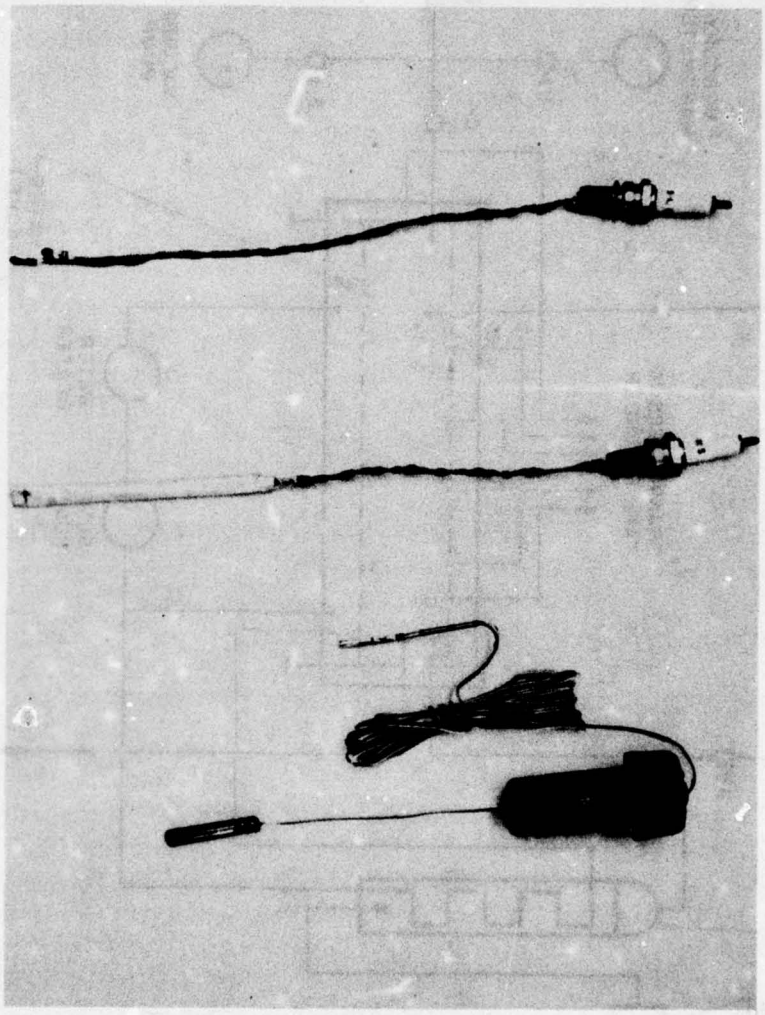


Figure 4. Initiators Used on this Program
(a) Double Squibs
(b) Propellant Boosted Squib
(c) E-81 Detonator

D. Instrumentation System

The purpose of the instrumentation system was to determine if a reaction occurred and when it occurred to assess the relative severity of the reaction. For this purpose, initially four semiconductor strain gages were mounted on the outside of the detonation chamber, and a piezoelectric pressure transducer was mounted in the center of the slip-on flange opposite the initiator. In order to increase the sensitivity of the leading wave arrival time measurement, the four strain gages were replaced by five pressure transducers for all tests after test 14. A schematic diagram of the instrumentation system is given in Figure 5. Notice that the strain gage or the pressure transducer output is recorded after the appropriate amplification and signal conditioning on an Ampex FR-1900 wide band tape recorder. Data for each test was recorded at 120 ips, and replayed at the same speed into the recording oscillograph. The oscillograph recorded at either 1 7/8 or 64 ips using galvanometers with a frequency response of DC to 500 Hz. In addition to the strain gage or the pressure transducer output, the detonation time and a time reference or time base were also recorded.

The pressure transducers used on this program were Susquehanna model ST-2, piezioelectric gages. These transducers have a sensitive surface or diaphragm which displaces under an applied pressure. This pressure is transmitted by the diaphragm to an interior piezioelectric element which responds with an output proportional to the applied pressure. The ST-2 transducers are designed for reflected pressures in the range of 0-500 psi and to minimize acceleration and transient temperature sensitivity. In order to install the ST-2 in the detonation chamber, the gage was molded into a standard 1 in. pipe nipple using soft-selastic. This procedure was used to ensure that shock waves propagated through the chamber walls would not be transmitted to the transducer. The sensitive portion of the gage was positioned flush with the lower portion of the nipple, and when installed in the test chamber was placed as nearly flush with the chamber walls as possible. Figure 6 shows two ST-2 transducers; the upper one has been molded as described above into a one inch pipe nipple.

Each pressure transducer was dynamically calibrated during this program using a drop weight calibrator. This device employs a weight which is dropped onto a piston mounted in an oil filled cavity. The ST-2 transducer and a Kulite reference transducer are also mounted in the cavity. By comparing the output of the Kulite reference gage and the ST-2 for a wide variety of drop heights and weights, the sensitivity (volts/psi) of each transducer was determined.

Typical pressure-time traces obtained with the instrumentation system on this program are found on Figure 7. Notice that the pressure trace (7a) is different from the usual pressure traces associated with

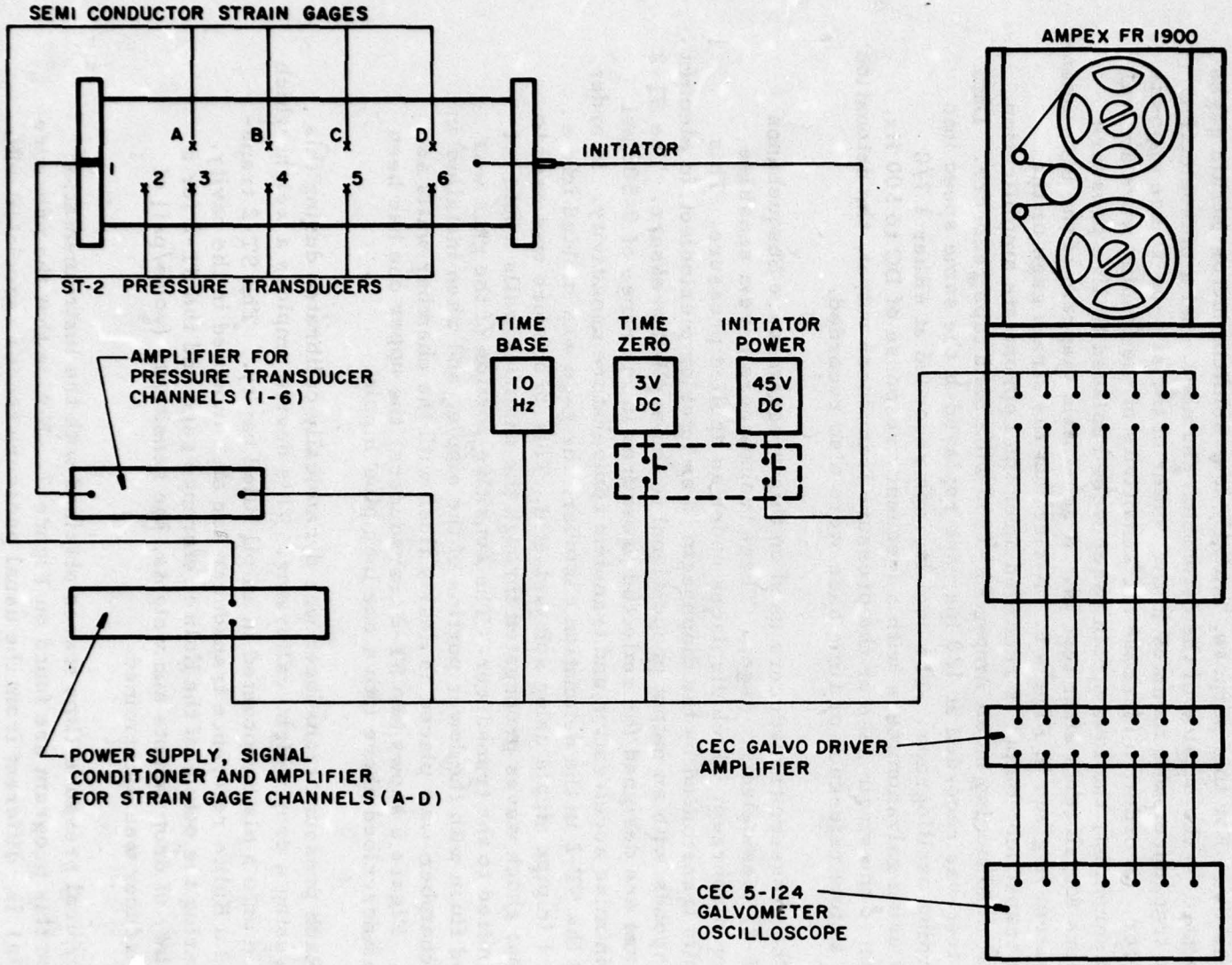


Figure 5. Schematic Diagram of Data Acquisition System

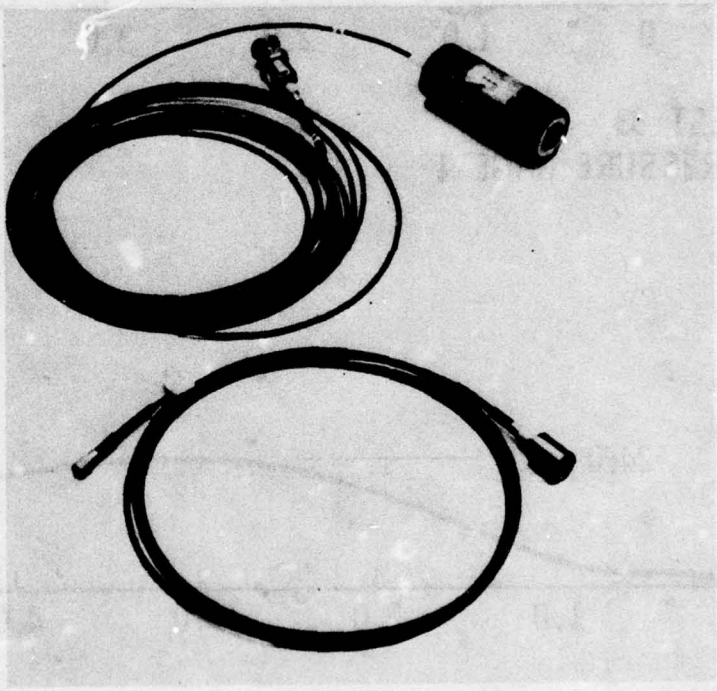
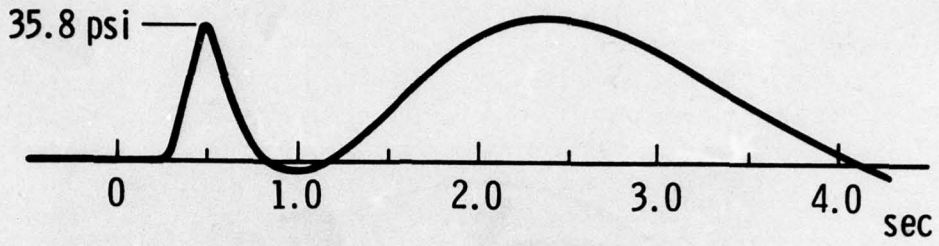
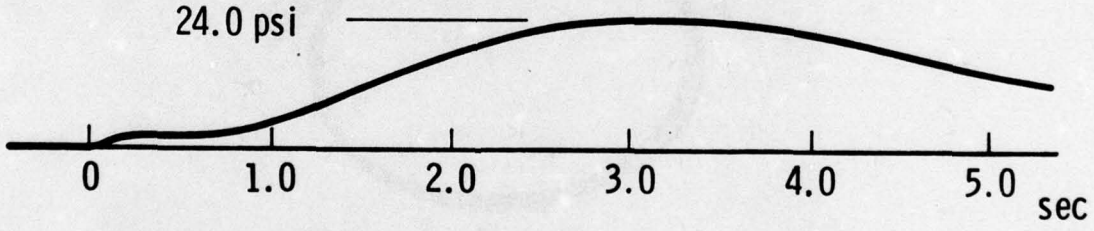


FIGURE 6. ST-2 PRESSURE TRANSDUCERS



a) TEST 33
PRESSURE GAGE 1



b) TEMPERATURE TEST

Figure 7. Typical ST-2 Response to (a) Pressure-Thermal Loading, and (b) Thermal Loading

detonation. Two major differences are evident. First, the rise time of the trace is approximately 0.20 seconds, which is much longer than the rise times associated with detonation (~10 μsec). Second, although the first peak is associated with the internal chamber pressure, the second peak is associated with the internal chamber temperature. As mentioned previously, the ST-2 gage is designed to minimize transient thermal response. For short-term (on the order of a few tenths of a second or less) temperature fluctuations, the output of the ST-2 varies only 1% per 10° C of temperature change. However, for the long-term (on the order of 0.5 to 2.0 seconds) temperature variations that are apparently occurring in the chamber, ST-2 temperature response is significant. In order to verify the assumption that the second peak was associated with the combustion temperature and not with the chamber pressure, the following simple test was devised. An ST-2, still linked to the entire instrumentation chain, was slowly immersed in a water bath (50° F above ambient temperature) for 0.5 seconds and slowly removed. The resulting trace is shown in Figure 7b. Since the transducer was subjected only to the hydrostatic pressure of the water, the deflection shown in Figure 7b must be entirely due to the thermal response of the gage. Notice that the general shape and duration of the second peak of Figure 7a resemble to a remarkable degree the shape and duration of 7b. In addition the pressure equivalent of the peak thermal response as indicated on Figure 7b is about 24 psi. Based on this test, only the first peak of the pressure-time trace was measured and discussed in later sections of this report.

IV. TEST PROGRAM AND RESULTS

A. Test Program

During the course of this investigation approximately 53 tests were conducted. Of these, the first ten tests were non-instrumented tests, and were conducted to establish a workable filling procedure. The VCM concentration in the chamber after filling was determined by gas chromatograph analysis for five of the first nine tests. These tests demonstrated that the orifice method of filling the chamber resulted in extremely rich VCM concentrations. At this point it became obvious that to obtain the correct VCM concentration using the orifice method would require a trial and error process involving the construction of several orifice plugs and many gas chromatograph tests. Therefore it was decided to use an alternative procedure of filling the chamber based on the method of partial pressures.

The remaining 43 tests were instrumented either with strain gages or pressure transducers. Twenty-seven of these tests involved varying the VCM-air concentration at ambient temperature (80°F). Twelve tests in which the VCM-air-water vapor system at different temperatures in the range of 110-165°F were conducted. Finally, four tests were conducted to determine the contribution to the internal pressure due to the various initiators (in air). Table 4 summarizes the test program.

TABLE 4. SUMMARY OF TEST PROGRAM

VCM-AIR TESTS

Test No.	% VCM	Initiator
1	2.5	
2, 5-7	7.7	A(double squib)
3, 4	15.0	
8, 9, 16-21, 32, 33	7.7	
10, 11, 15	15.0	B(propellant boosted squib)
	30.0	
39	2.0	
34, 36, 37	7.7	C(detonator)
14, 40	30.0	

VCM-AIR-WATER VAPOR TESTS

Test No.	Temperature (°F)	Initiator
23, 27, 28	110	
29, 28, 30, 31	130	B(propellant boosted squib)
22, 24-26	160	
41	135	
42, 43	160	C(detonator)

DETONATOR TESTS

Test No.	Initiator
12, 13	B
35, 38	C

B. Test Results

1. VCM-air tests

As mentioned earlier, the purpose of this series of tests was to demonstrate that the explosive limits obtained with the test apparatus used on this program agreed with the results reported by other researchers. In this section, the results of the VCM-air tests will be described in detail. Because several different types of initiators were used in the program, the results for each type of initiator will be described separately. The results of these tests are summarized in Table 5. Basically these tests substantiate the explosibility-flammability limits obtained by other researchers, given in Table 1. Tests were conducted at 2.5, 7.7, 15.0, 30.0% VCM in air. The results indicate that for VCM concentrations of 7.7 and 15.0% definite reactions were obtained. The severity of the reaction depended on the initiator used. At VCM concentrations of 2.5 and 30% either no or very low order reactions were recorded. These results agree very well with the flammability limit concentrations given in Table 1; 3.6 to 4.0% for the lean limit, and 20.0-33% for the rich limit.

a. Double Squib Initiator

Seven tests were conducted in this series, with three different VCM concentrations. In each of these tests the waiting period between completion of the fill procedure and initiation was less than 15 minutes. Instrumentation for these tests consisted of pressure transducer number 1, and the 4 strain gages. Tests numbered 1(2.5%) and 3(15%) resulted in no discernible reaction. The squibs had detonated, but no residue characteristic of combustion was observed on the squib leads. No pressure increase or strain deflection was recorded. Tests numbered 4(15%), 5(7.7%) and 7(7.7%) resulted in a very low order combustion. In this case, the squib leads were slightly charred or coated with a black residue. The internal chamber pressure, as recorded by gage number 1, was between 2.5 and 9.2 psi. The time for the pressure to reach a maximum was between 0.2 and 0.35 seconds. Rise times for the strain gage channels were between 0.3 to 1.0 seconds. Because the rise times of the pressure and strain-time traces were of the same magnitude as the arrival times, no combustion velocity could be measured for these tests. It should be emphasized here that the relatively slow rise times recorded on these tests are characteristic of the VCM-air reaction being studied and not due to inadequacies in the instrumentation system. Rise times on the order of tenths of milliseconds have been easily resolved on previous programs with instrumentation systems essentially identical to the one used on this program. Finally, test number 2(7.7%) resulted in a low order combustion. The pressure recorded by transducer number 1 was 15.3 psi, and the rise times for both the pressure and strain gages were the same as for the previous tests.

TABLE 5. SUMMARY OF INSTRUMENTED TEST RESULTS FOR VCM-AIR TESTS

Test No.	% VCM	Detonator	Chamber Temp(°F)	Holding Time (min)	Peak Pressure (psi) 1	2	3	4	5	6	Average
1	2.5	A	80	--	No Reaction						--
2	7.7		85	--	15.3						15.3
5			82	15	2.5						2.5
6			80	10	Very Low Reaction						--
7	7.7		80	15	6.3						6.3
3	15.0		88	--	No Reaction						--
4	15.0	A	80	7	9.2						9.2
8	7.7	B	83	122	61.1						61.1
9			81.5	110	29.2						29.2
15			80	30	19.6	20.0	16.9	17.8	23.9	11.5	18.3
16			80	30	No Reaction						--
17			80	60	47.0	59.2	57.4	52.4	71.7	53.2	56.8
18			80	60	9.3	8.9	8.7	8.6	11.8	8.3	9.3
19			80	75	No Reaction						--
20			102	45	45.1	51.7	45.6	44.9	60.8	48.3	49.4
21			142	140	48.8	--	42.3	49.7	71.3	46.1	51.4
32			82	100	33.0	56.7	68.0	74.3	65.9	70.1	61.3
33	7.7		80	60	35.8	--	73.4*	59.2	52.9	58.6	56.0
10	15.0		83	--	53.5						53.5
11	15.0		80	120	53.7						53.7
14	30.0		81	--	Very Low Reaction						--
30	30.0	B	130	30	No Reaction						--
39	2.0	C	75	60	Very Low Reaction						--
34	7.7		80	--	65.5	--	--	76.4	86.0		76.0
36	7.7		80	60	78.1	76.4	--	65.5	90.8		77.7
37	7.7		82	--	--	88.9	76.5	60.0	89.2		78.7
40	30.0	C	80	105	Very Low Reaction						--

*Stratham strain gage pressure transducer.

The data presented in this section is summarized in Figure 8. Here the average peak pressure recorded by the ST-2 transducer is plotted as a function of the VCM concentration. Different symbols are used on the figure to differentiate between the low and very low reactions. The line shown on Figure 8 is given to emphasize the trend of the results. As expected the greatest reaction occurred when the VCM concentration was stochiometric (7.7%). Lower or no reaction was recorded at 2 and 15% VCM concentrations. The pressure-time trace shown as an insert on Figure 8 is typical of the traces obtained on the tests resulting in low order combustion. In every case where some reactions occurred, the pressure or strain rise times were relatively long, about 0.1 to 0.35 seconds, which prevented measurement of the combustion velocities. Based on this information, it was concluded that the VCM mixture burned, but did not detonate.

b. Propellant Boosted Squib Initiator

As a result of the tests described in the previous section, it was decided to use an initiator consisting of two squibs surrounded by 60 grains of solid propellant to obtain a more energetic source. Fifteen tests were conducted in this series, again at three different VCM concentrations. In each of these tests, the waiting period between completion of the filling procedure and initiation was much longer than on the previous series. Since the pressure recorded on these tests was generally higher than for the double squib tests, it was concluded that the effect of the increased holding time was to allow the gas, which cools while expanding into the evacuated chamber, sufficient time to equilibrate with the chamber walls. The higher gas temperatures, coupled with the more energetic initiator, resulted in the higher reactions. Instrumentation for the majority of these tests consisted of the six channels of ST-2 pressure transducers. The results of the propellant boosted tests are summarized in Figure 9 where the average peak pressures recorded by the six transducers are plotted as a function of the VCM concentration. It is appropriate to plot the average peak pressure because, as shown in Table 5, the pressures do not vary significantly from recording station to recording station. As seen in the figure, consistantly higher pressures were recorded in the propellant boosted tests than in the double squib tests. However, the time for the pressure to reach a maximum was still on the order of 0.2 to 0.4 seconds. Therefore, no accurate combustion velocities could be obtained for these tests.

On test number 33, ST-2 number 3 was replaced by a Statham pressure transducer. This pressure transducer has a strain gage bridge mounted on the diaphram as its sensing element. This particular transducer is particularly suited for tests such as these because the frequency response is DC to about 20 Khz, and the thermal effect on sensitivity is less than 0.01% of the reading per °F.

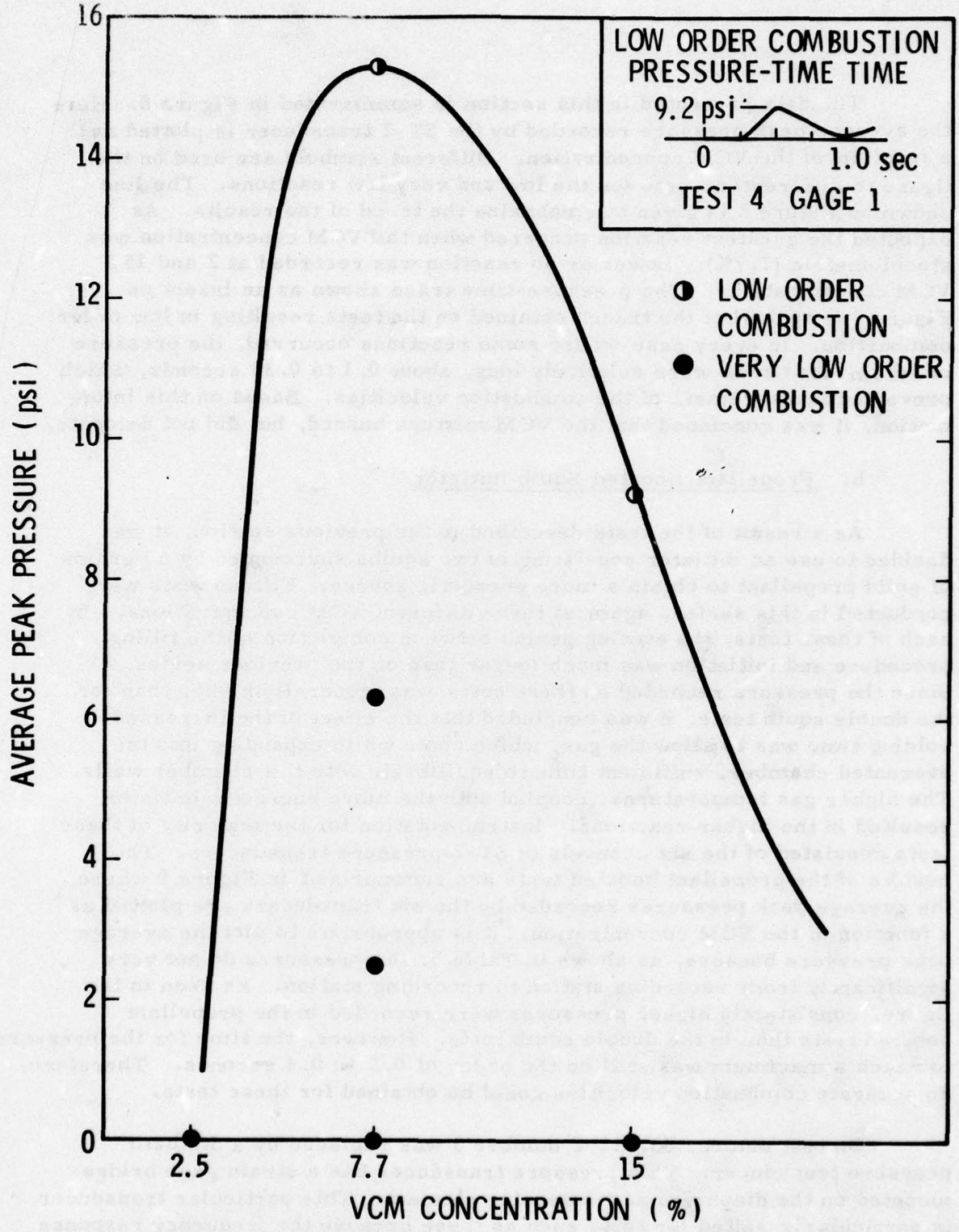


Figure 8. Variation in Pressure with VCM Concentration for Double Squib Tests

The trace obtained with this transducer is shown in the upper right corner of Figure 9. Notice that both the magnitude of the peak pressure and the general shape of the trace agree quite well with the only pressure-time trace reported in the literature. Urbancova and Gregor[5] did not present a time scale on their figure, so that a comparison of rise time and total event duration cannot be made. Unfortunately, the Statham gage failed on test 34, and because a replacement was not available, an ST-2 was again installed at station 3.

Based on the data presented in this section several observations can be made. First, as expected, the highest pressures were measured when the VCM concentration was stochiometric. Generally, lower pressures were recorded at 15% VCM concentrations, while no reactions were observed when the VCM concentration was 30%. In every case the rise time of the pressure trace was on the order of 0.2-0.4 seconds, which prevented an accurate measure of the combustion velocity.

Although higher pressures were recorded with the propellant boosted squibs, it was determined that the VCM mixture burned, but did not detonate on these tests.

c. Detonator Tests

Because detonation had not been achieved to date in the VCM-air tests, it was decided to use an initiator which was still more energetic than the squibs. An E-81 detonator was chosen as the iniation source for the tests summarized in this section. Detonators had not been used previously in the program because on initiation they scatter fragments radially from the sides and axially from the bottom of the casing at high velocities. Obviously, the potential for transducer damage on these tests was considerably higher than on the previous tests. Therefore, the detonator was suspended into the chamber from station 6, to minimize the probability of transducer damage. Five tests were conducted on this series, at three different VCM concentrations. The results of these tests are summarized on Figure 10 where the average peak pressures recorded in each test are plotted as a function of the VCM concentration. As seen in the figure, little or no reaction was observed when the VCM concentration was 2 or 30%. However, at stociometric concentrations peak pressures consistently averaged about 75.0 psi. Although the peak pressure is not significantly higher than that recorded for the propellant boosted tests, it is believed that the VCM mixtures deflagrated on these tests. Three observations justify this belief. First, notice the pressure time trace shown on the insert of Figure 10. The rise time of the trace and of all the stochiometric detonator tests is about 0.09 sec., which is about 2 times faster than for the propellant boosted squib tests. Second, the pressure is not significantly higher than for the squib tests. The third justification is given as Figure 11. Here the arrival time of the flame front at the pressure transducer locations (relative to transducer 6) is plotted with the transducer position. The slope of the line represents the average flame front velocity. Although most of the points on Figure 11

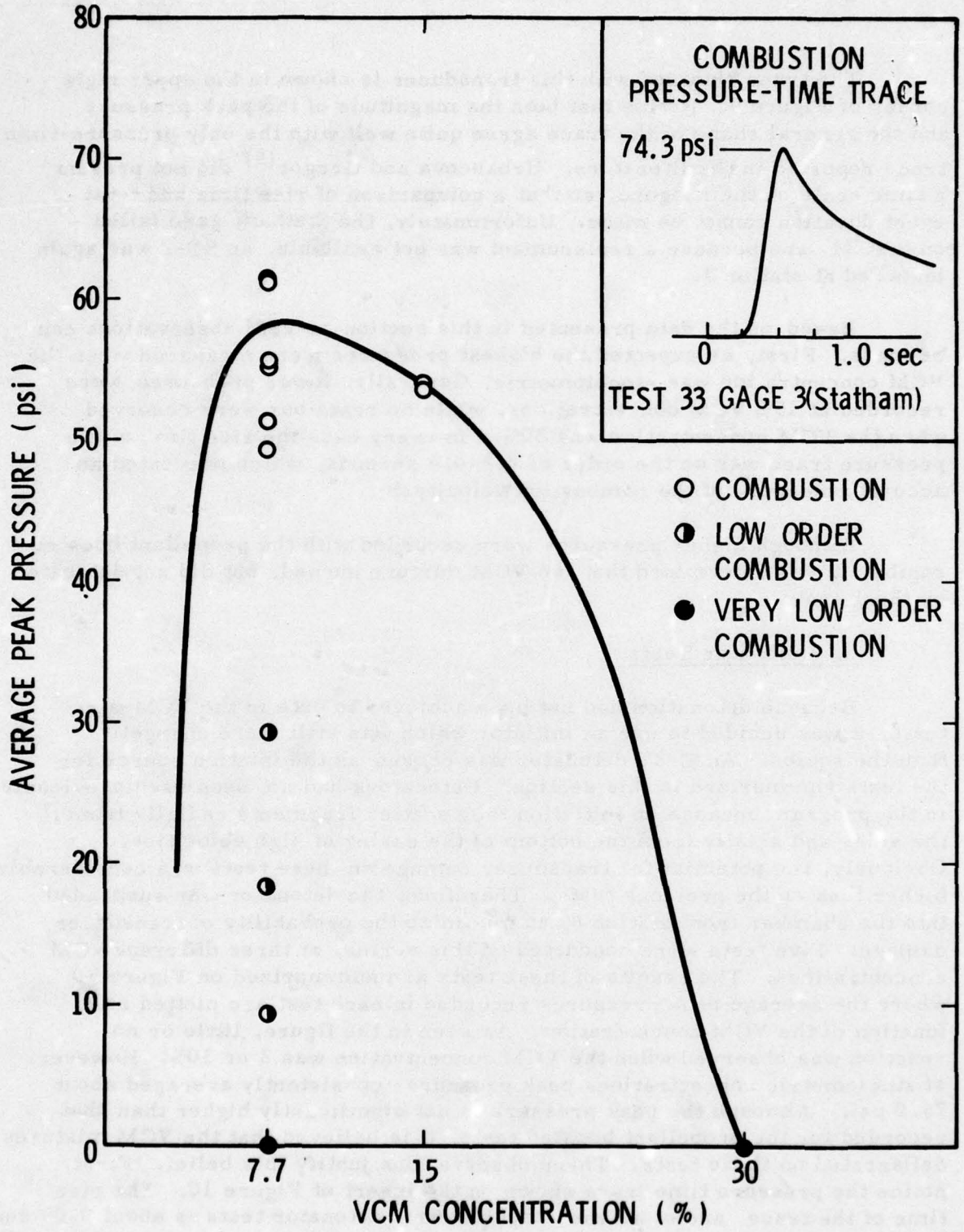


Figure 9. Variation in Pressure with VCM Concentration for Propellant Boosted Tests

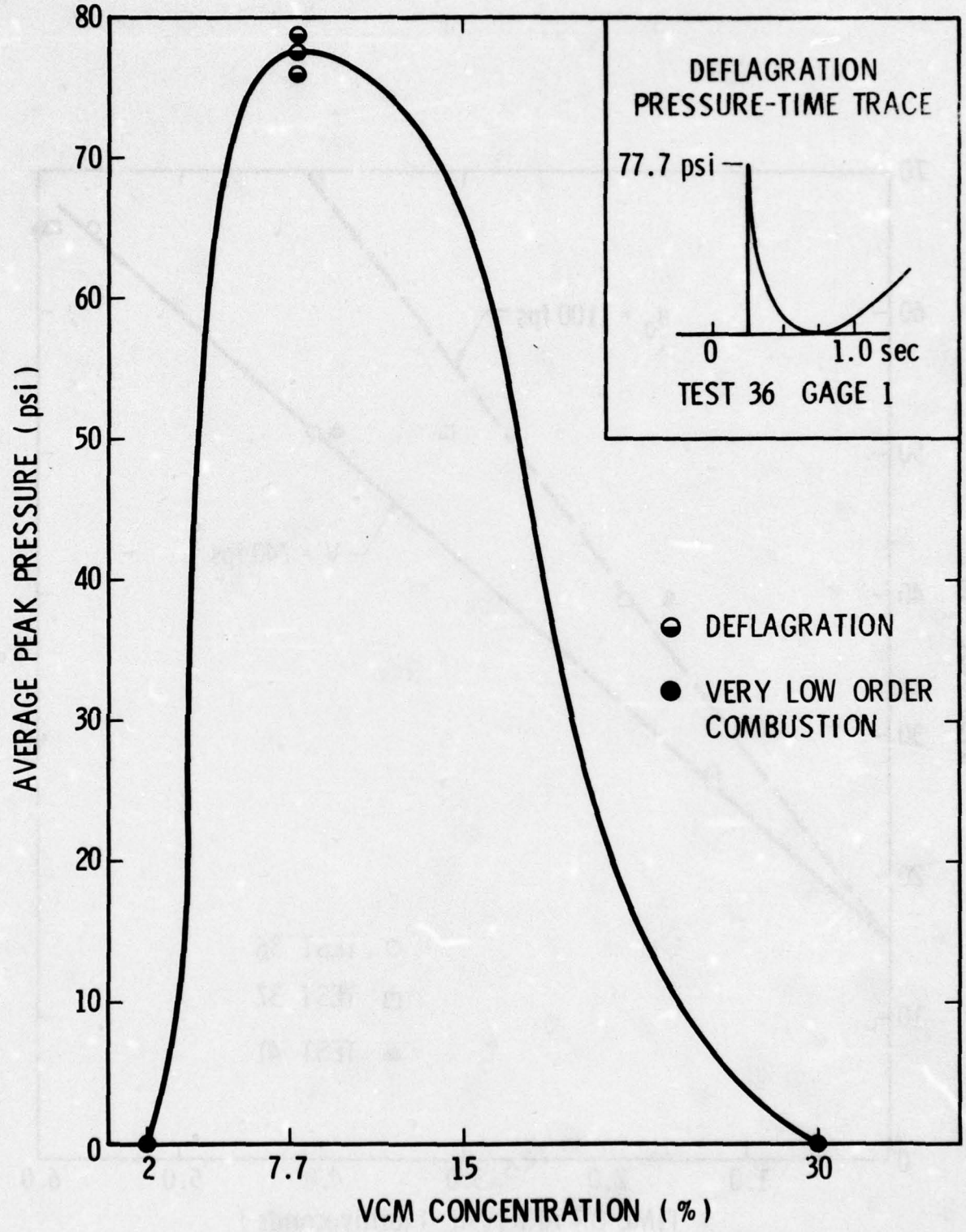


Figure 10. Variation in Pressure with VCM Concentration for E-81 Detonator Tests

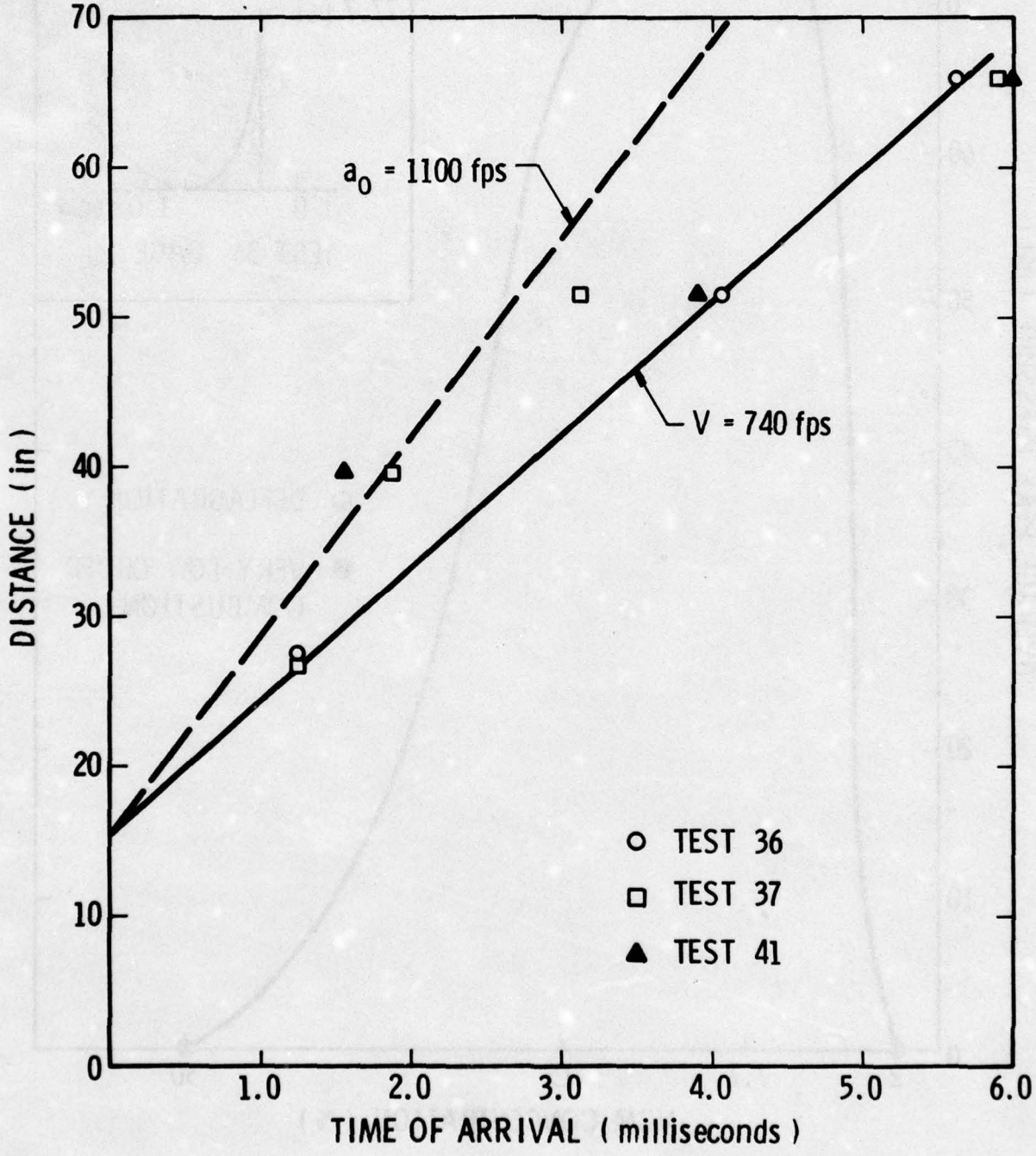


Figure 11. Arrival Time Measurements for VCM-Air Mixture Tests

fall very near the 740 fps line, three do not. The rise time of the traces is so slow, it is difficult to determine when the trace begins to deviate from the base line. Errors in the location of the break from the baseline of only 0.05 inches translate to about 0.75 milliseconds. To further complicate the problem, the baselines prior to initiation were particularly noisy for the three points in question, making the arrival time measurement more difficult. Thus, the choice of a constant propagation velocity of 740 fps is reasonable. Since the average velocity obtained in this manner, about 740 fps, is less than the sonic velocity of the unburned mixture (about 1080 fps) the conclusion that the mixture deflagrated on these tests is justified.

2. VCM-air-water vapor tests

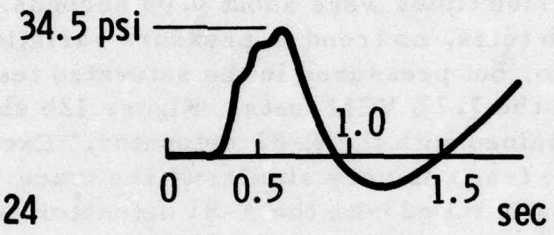
In this section the results of the VCM-air-water vapor tests will be described. Because of the experience gained in the previous tests, two initiators were used in the saturated tests--the propellant boosted squib and the E-81 detonator. All tests were conducted at stochiometric mixtures of VCM and air, while the temperature was varied from 110 to 160°F. The results of these tests are summarized in Table 6.

a. Propellant boosted squib tests

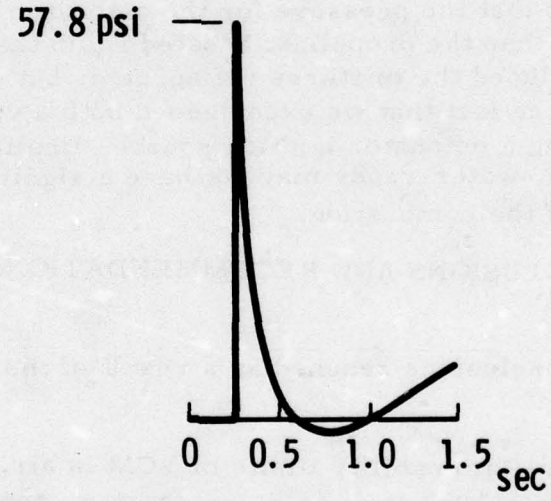
Ten tests were conducted in this series, with essentially three different temperatures. In each of these tests the waiting time after introduction of the VCM and air was at least an hour. No reaction was observed on four tests. At 160° F, one test resulted in a low order combustion (average peak pressure was 10.3 psi), while two tests resulted in moderate reactions (peak pressures averaged 37.7 psi). At 130 and 146° F only one test at each temperature was successfully initiated, yielding average peak pressures of 28.4 and 34.5 psi, respectively. The time for the pressure to reach a maximum was between about 0.3 and 0.7 seconds for those tests in which reactions were observed. No significant trend in the variation of pressure with temperature can be deduced from these tests. However, the effect of the introduction of water vapor is to first of all make it harder to achieve a successful initiation of the mixture. Secondly, the presence of the water vapor apparently reduces the peak pressure. Pressures recorded on the VCM-saturated air tests average approximately 30% less than the corresponding pressures for the 7.7% VCM-air tests (for the propellant boosted squib tests). Typical pressure-time trace is given in Figure 12. Notice that the time for the pressure to reach a maximum is longer than for the corresponding VCM-air test (see the insert on Figure 9). Based on the data presented in this section it was concluded that the VCM-air-water vapor burned but did not detonate on these tests.

TABLE 6. SUMMARY OF INSTRUMENTED TEST RESULTS FOR VCM-AIR-WATER VAPOR TESTS

Test No.	Detonator	Chamber Temp(°F)	Holding Time (min)	Peak Pressure (psi) 1	2	3	4	5	6	Average
23	B	110	60	7.4	--	10.1	10.6	9.9	13.5	10.3
27	↑	110	60	33.9	45.3	46.7	33.2	31.2	46.3	39.4
28	↑	110	75	39.5	48.1	49.2	37.0	39.6	--	36.0
29	↑	132	60	No Reaction						
30	↑	130	30	Very Low Reaction						
31	↑	130	--	25.6	--	31.7	24.3	25.3	35.1	28.4
22	↑	154	120	No Reaction						
24	↑	146	60	31.2	--	33.9	35.6	33.0	38.8	34.5
25	↓	162	60	No Reaction						
26	B	157	60	No Reaction						
41	C	135	60	58.5	72.2	50.4	51.1	57.0	--	57.8
42	C	160	60	62.7	68.6	53.5	48.1	57.9	--	58.2
43	C	160	60	6.0	5.6	5.5	5.8	5.4	--	5.7



a) TEST 24
GAGE 1



b) TEST 41
GAGE 1

Figure 12. Typical Pressure-Time Traces for the VCM-Air-Water Vapor Tests Using (a) Propellant Boosted Squib Initiator and (b) E-81 Detonator

b. Detonation tests

Three tests were conducted with VCM-air-water vapor mixtures initiated by the E-81 detonator at two temperatures. One test at 160° F resulted in a low order combustion in which the average peak pressure was 5.7 psi. At 130° F and on another test at 160° F, high order reactions were obtained. Peak pressures for these tests averaged 57.8 and 58.2 psi, respectively, while rise times were about 0.09 seconds. As for the propellant boosted squib tests, no trend in pressure variation with temperature can be seen, but pressures in the saturated tests averaged about 20% less than for the 7.7% VCM tests. Figure 12b shows a typical pressure time trace obtained with the E-81 detonator. Except for the lower peak pressure the trace is very similar to the trace obtained with 7.7% VCM-air-mixtures initiated with the E-81 detonator (see the insert on Figure 10). Flame front arrival times could only be measured on Test 41, and these points are presented on Figure 11. Generally, these points fall very near the arrival times measured with VCM-air mixtures initiated by the E-81 detonator. Based on the low propagation velocity (about 740 fps), the fact that the pressure for the detonator tests was not significantly higher than the propellant boosted squib tests, and the long rise times, it was concluded the mixtures deflagrated, but did not detonate on these tests. Also, the fact that we experienced both a very low reaction and a high reaction using a detonator ignition source, implies that given a strong ignition source, water-vapor may not have a significant effect on the reaction intensity of the combustion.

V. CONCLUSIONS AND RECOMMENDATIONS

The principal conclusions reached as a result of the tests conducted on this program are:

- The explosive-flammability limits of VCM in air, obtained with the experimental apparatus, are 2.5% to 30%. These values agree with the flammability limits measured by other researchers.

- No detonations were observed in the experiments. This is substantiated by several observations. First, reaction velocities were under the speed of sound in the VCM-air mixture (~1100 fps) Second, peak pressures were relatively low--average pressures were no greater than 62 psi for the VCM-air tests or 59 psi for the VCM-air-water vapor tests. Finally, the rise time of the pressure traces was substantially longer than would be expected if the mixture had detonated.

- Within the range of temperatures tested, there appear to be no significant effects in the reaction intensity as a function of temperature.

- The flammability characteristics are significantly affected by the ignition source. The maximum pressure achieved with the double squib initiator was 6.3 psi for 7.7% VCM concentrations. For the same mixture, 61.3 psi was achieved using the propellant boosted squib initiator. Finally, 78.7 psi was obtained under similar conditions with an E-81 detonator. In addition to the effect on pressure, initiators affect the time for the pressure to reach a maximum value. Although this effect is not as dramatic as for pressure it is certainly true that more energetic detonators shorten the rise time.

- The presence of water vapor in the VCM mixture reduces the reaction rise time and peak pressure. Generally, the peak pressure was reduced by 20% from the peak pressure in similar VCM-air tests. For the most energetic ignition source a low and high order ignition was recorded. This implies that, given a strong enough ignition source, water vapor may not have a significant effect on the reaction intensity.

- VCM should be treated as a flammable gas even in the presence of water vapor.

In order to design a safe reactor for the production of PVC slurry, the following recommendations are made:

- The tests conducted to date show that no detonations are achieved using ignition sources which are more intense than would be encountered in actual operations. However, the reaction caused by ignition from potential electrostatic discharge sources should be quantified by additional tests.

- During the production of PVC slurry the pressure in the reactor is as high as 200 psi at 200° F. Previous work with methane-oxygen mixtures[11] indicates that the reaction intensity increases significantly as the initial pressure increases. Therefore, additional tests should be conducted at initial pressures and temperatures corresponding to those encountered in actual service to ensure that the most hazardous operating conditions have been identified.

- Eliminate any potential electrical, frictional, or electrostatic ignition sources in or around the reactor.

- Because shock waves were never developed in this program, the design of the reactor can be based on static applied pressures. This, however, may not apply if shock waves are developed at higher initial pressures.

- Since difficulties arose in the measurement of propagation velocities on this program, another measurement technique should be tried on any further experiments. Photographic procedures offer the most attractive alternative. In this case the reaction in a clear detonation chamber would be recorded with a high speed camera. In addition to recording the travel of the flame front, such phenomena such as spinning detonation, transition from flame to deflagration or detonation, and quenching should be observable in the film.

ACKNOWLEDGMENTS

The authors are grateful to Dr. Dave Porchey and Dr. Kang Yang, of Continental Oil Company, for furnishing the VCM used on the tests and an extensive literature review on VCM explosibility. In addition, Mr. Porchey and Dr. Yang provided many helpful comments and suggestions during the course of this investigation.

The work conducted at Southwest Research Institute was performed for Continental Oil Company, Ponca City, Oklahoma, under SwRI Project No. 02-4326. Also, the authors wish to acknowledge the following SwRI personnel for their contribution to this program: Messrs. E. D. Esparza, W. D. Rumbaugh, E. R. Garcia Jr., M. Rumbaugh, J. W. Rhoades and J. Miller. The cooperation of these individuals and others who are always inadvertently overlooked is greatly appreciated.

REFERENCES

1. D. W. F. Hardie, "Chlorocarbons and Chlorohydrocarbons", Kirk-Othmer Encyclopedia of Chemical Technology, 2nd edition, Vol. 5, p. 171-172, 1964.

2. G. W. Jones, W. E. Miller, and H. Seaman, "Explosive Properties of Propylene Dichloride-Air Mixtures", Industrial and Engineering Chemistry, Vol. 25, p. 771-773, July 1933.

3. Associated Factory Mutual Fire Insurance Companies, "Properties of Flammable Liquids, Gases and Solids", Industrial and Engineering Chemistry, Vol. 32, June 1940, p. 880-884.

4. C. A. Brighton, "Vinyl Chloride Polymers", Encyclopedia of Polymer Science and Technology, Vol. 14, p. 318, 1971.

5. L. Urbancova and F. Gregor, "The Explosibility of Vinyl Chloride", Plastie and Kautschuk, Vol. 10, No. 9, p. 532-534, 1963.

6. M. G. Zabetakis, "Flammability Characteristics of Combustible Gases and Vapors", Bureau of Mines Bulletin No. 627, p. 116, 1965.

7. S. G. Woinsky, "Predicting Flammable-Material Classifications", Chemical Engineering, p. 81-86, November 27, 1972.

8. L. A. Eggleston, W. R. Herrera and M. D. Pish, "The Use of Divided Water to Reduce the Hazard Potential of Vapor Clouds", Final Report for Project No. 3-3274, for an Ad Hoc Committee representing a Chemical Industry Group, Southwest Research Institute, San Antonio, Texas, March 10, 1975.

9. R. A. Strehlow, Fundamentals of Combustion, International Textbook Company, Scranton, Pennsylvania, p. 275, 1968.

10. B. Lewis and G. von Elbe, Combustion, Flames and Explosions of Gases, Second Edition, Academic Press Inc., New York, p. 312, 1961.

11. A. B. Wenzel, "Feasibility Studies of Gaseous Explosive Mixtures as a Secondary Gas-Oil Recovery Technique", Final report for project no. 02-3567, for Continental Oil Company, Southwest Research Institute, San Antonio, Texas, October 1973.

HEAT GENERATION MEASUREMENTS FOR THE STABILITY CONTROL OF NITRATE ESTER PROPELLANTS

J.L.C.van Geel, J.Verhoeff, Th.M.Groothuizen
Technological Laboratory TNO
Rijswijk, The Netherlands

Abstract

In the Netherlands the judgement of the stability of nitrate ester propellants is based on the results of the heat generation test. With this stability test the heat generation of the propellant is measured at 358K (85°C) during one week.

It will be explained that the test gives information about the self-ignition hazard and the ballistic stability.

For a number of propellants the results of the heat generation test will be shown.

Further the influence of several factors on the course of the heat generation will be discussed. In this connection special attention is paid to the so-called initial heat effect and to the heat generation during autocatalysis following depletion of the stabilizer.

Attention will also be given to the relation between the heat generation test and other stability tests.

Finally, proposals are given for further investigations.

PRECEDING PAGE BLANK-NOT FILMED

1. Introduction

The judgement of chemical stability plays an important part in the quality control of nitrate ester propellants, because two significant phenomena are connected with it, viz.

- self-ignition and
- ballistic stability

These two aspects are closely related to the exothermal decomposition to which the propellants are subjected at normal storage temperatures [1].

If the heat generation of this exothermal decomposition exceeds the heat loss to the surroundings, the temperature of the propellant will rise, which may eventually lead to self-ignition.

The ballistic stability is also connected with the exothermal decomposition process because owing to the heat release during storage the caloric value of the propellant will decrease.

The chemical stability of these propellants may be controlled by means of several tests which generally involve artificial aging at elevated temperature. The tests are based on the detection of distinct degradation products or such phenomena as for instance the decrease in stabilizer content, the loss in weight, the evolution of nitrous gases or other gaseous degradation products. The results are compared with those of reference propellants which are known to be sufficiently stable for safe storage.

Problems arise, however, when the stability of new propellant compositions has to be examined for which no reference propellant is available.

From the foregoing it follows, that the stability tests mentioned give only indirect information on the hazard of self-ignition. Therefore we have developed a new stability test: the heat generation test. With this test the heat generation is measured as a function of time at a constant temperature, and it is possible to determine the self-ignition hazard and ballistic stability of the propellants for a storage period of at least 10 years.

2. Short description of the heat generation test

The heat generation test is a standardized test under isothermal conditions at 85°C during one week, and is performed in the heat generation meter (Figure 1).

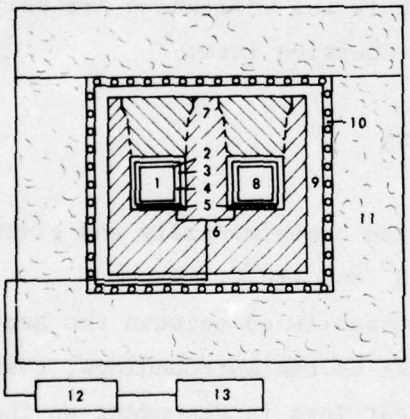


Figure 1. Arrangement of heat generation meter. (Arch.no.710825).

The heat generation meter consists of a thermostated aluminium block in which a sample vessel is placed on a so-called heat-flow meter (peltier element). If the sample generates heat a small temperature difference between sample and block will establish which is directly proportional to

the heat generation. The voltage generated by the peltier element is monitored via an amplifier after subtracting the voltage of a second peltier element, on which a vessel with inert substance is placed. This compensation is done to eliminate environmental disturbances. A 5 gram sample of propellant is introduced into the perfectly gastight sample vessel of about 60 ml. The vessel is quickly heated till the required temperature of 85°C and after that placed into the meter. A period of about 6 hours is then needed before getting a reproducible heat generation. This period after inserting the sample is necessary to restore the thermal equilibrium in the apparatus.

3. Theoretical background

The basis of this test is the well-known Arrhenius' equation. We modified this equation into:

$$q = F(Q) \exp(-E/RT) \qquad (1)$$

This equation has been tested experimentally and given very reliable results between 60° and 110°C. [1]

If an equilibrium is established between the heat generation and the heat loss to the surroundings, there will be no self-ignition. The heat loss is dependent on the storage temperature, the heat conductivity and the dimensions of the propellant mass, i.e. diameter of the container.

Frank Kamenetzkii [2] has determined a so-called critical diameter (of an infinitely long cylindrical container), which is defined as the smallest diameter at which self-ignition takes place:

$$D = \sqrt{\frac{4\delta_c \lambda RT_A^2}{\rho_b E q_{TA}}} \qquad (2)$$

To predict the stability of a propellant during a storage period of at least ten years, it was necessary to assume a temperature-time course over that period [3]. In accordance with the NATO-requirement, that ammunition has to withstand temperatures up to 71°C during short periods, we calculated from the forementioned modified Arrhenius' equation (1) a corresponding aging period of seven days at a temperature of 85°C.

Since for practical reasons the heat generation is measured at a higher temperature, viz. 85°C, than the expected storage temperature, we had to transform, the equation for the critical diameter (2) into the following formula:

$$D_{safe} = 12.1 \sqrt{\frac{\delta_c \cdot \lambda}{\rho_b \cdot (q_{85^oC})_{max}}} \qquad (3)$$

In this formula we have included the maximum heat generation at the measured temperature during the first seven days. This is done for safety reasons, because this maximum rate presents the worst situation. Therefore the critical diameter is changed into the safe diameter.

The chemical stability of the propellant under investigation is determined by comparing the safe diameter and the actual diameter.

With respect to the ballistic stability it can be said that this stability decreases as a result of the decrease in the caloric value. This decrease in caloric value is directly proportional to the total amount of heat released during the storage period. For quality control the ballistic stability is also determined for a storage period of ten years. In this case, however, a distinction is made between storage in a moderate climate and in the tropics, assuming a constant temperature of 20°C and 30°C respectively. In the heat generation test at 85°C an aging period of 1.5 and 6 days corresponds with an aging period of 10 years at 20°C and 30°C respectively. The corresponding decrease in caloric value is determined by integration of the heat generation versus time curve.

4. Experimental results

During the experimental program a decision had to be taken on the physical state of the propellant. Several stability tests use ground propellant, others do not. We investigated the influence of this physical state and found that the initial heat generation of ground propellant was much higher than that of unground propellant: compare curves 1 and 2 in Figure 2. This initial effect, however, was not observed in triple base propellants.

We also studied the effect of moisture and air and found that the moisture content has hardly any influence. The influence of air, on the other hand, is considerable as is shown by curves 2 and 3 in Figure 2.

Since the most important information of these curves is the maximum heat generation, and this parameter appeared to be dependent on the physical state of the propellant and on the presence of air, we decided to imitate the situation, which simulates best the storage situation in practice, viz. unground propellant grains in air.

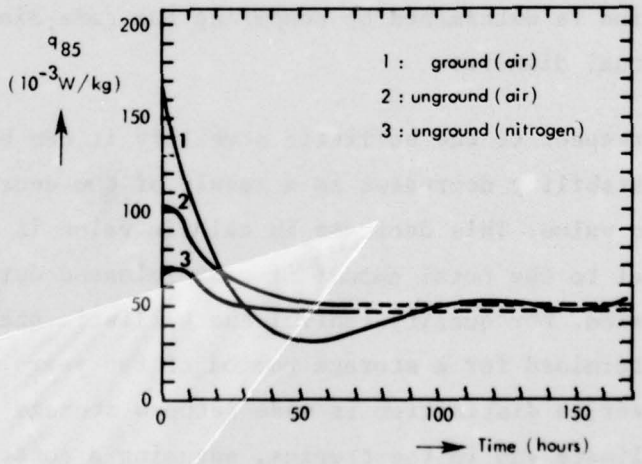


Figure 2. Heat generation versus time of a propellant under several physical conditions. (Arch.no.760833).

The heat generation as a function of time of ten different propellants is given in Figure 3.

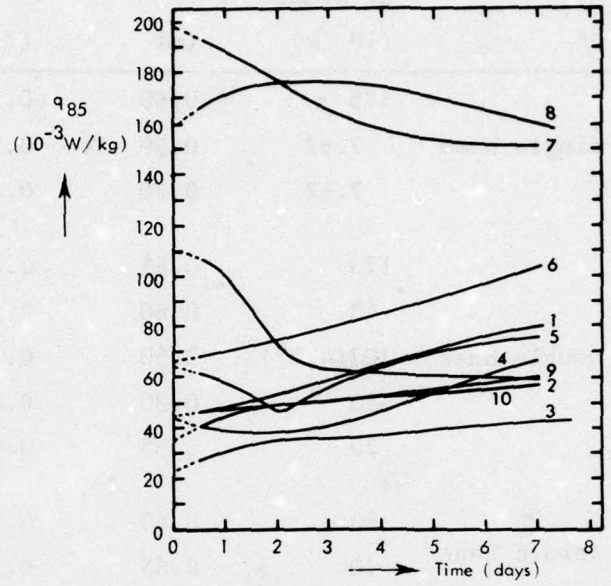


Figure 3. Heat generation versus time of ten different propellant samples. (Arch.no.711193-2).

In this Figure curves 1, 2 and 3 are single base propellants, curves 4, 5, 6, 7 and 8 double base, and curves 9 and 10 triple base propellants.

From these measurements we determine the maximum heat generation and calculated the safe diameter. By integration we determined the decrease in caloric value at 20°C and 30°C. The results are given in Table 1.

Table 1. Safe diameter and ballistic stability of the tested propellants.

Propellant		Calibre of weapon (10^{-3}m)	D_{safe} (m)	$(\Delta Q_{ex})_{20}$ (%)	$(\Delta Q_{ex})_{30}$ (%)
1		175	0.60	0.24	1.0
2	single base	7.62	0.50	0.34	1.0
3		7.62	0.70	0.10	0.5
4		175	0.65	0.15	0.7
5		40	0.60	0.12	0.6
6	double base	107(4,2")	0.50	0.17	0.8
7		150	0.30	0.48	1.7
8		20	0.35	0.61	2.5
9		90	0.60	0.16	0.7
10	triple base	90	0.65	0.14	0.7

Comparing the values of the safe diameter with the dimensions in practice it may be concluded that the safe diameter of all investigated propellants is sufficiently large compared with the calibre of the weapon used.

As can be noticed the calculated decrease in caloric value differs markedly from propellant to propellant.

5. Autocatalysis

After a prolonged measurement in the heat generation meter the rate of heat generation increases sharply by autocatalysis. This effect is caused by the depletion of stabilizer. In Figure 4 the heat generation is given of two single base propellants with nearly the same composition. The only difference between the two propellants was the type of stabilizer, but the stabilizer content was the same.

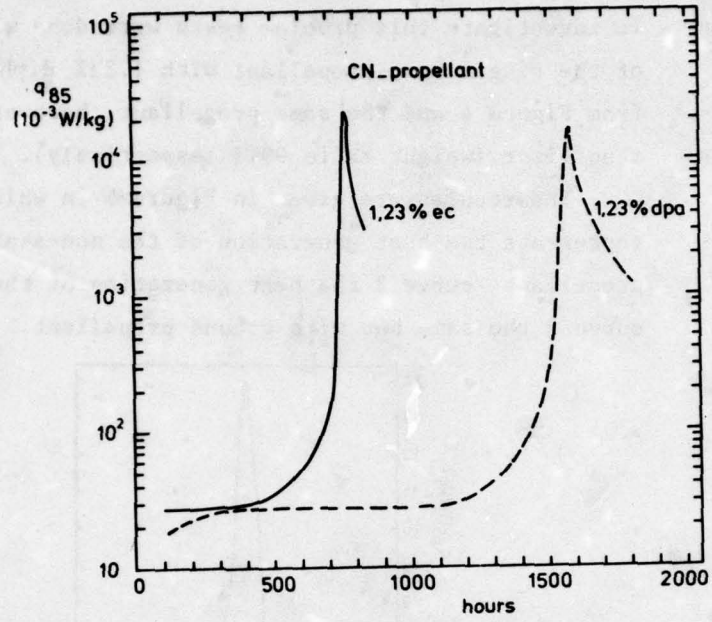


Figure 4. Heat generation at 85°C of two samples of single base propellant with different stabilizers. (Arch.no.760445).

From Figure 4 it follows that diphenylamine has a better stabilizing effect than the same amount of ethyl centralite for this type of propellant. So it is also possible to investigate the influence of the type and the quantity of stabilizer on a propellant with this meter.

As has been discussed before the heat generation of most propellants is less than 100 mW/kg during the first week at 85°C. This means that the safe diameter is at least 0.5 m for most propellants. However, when the period of autocatalysis is reached the safe diameter will decrease sharply. Because of this effect the question arose whether an inhomogeneous stabilizer distribution may give rise to self-ignition.

To investigate this problem tests were done with a mixture of the single base propellant with 1.23% diphenylamine from Figure 4 and the same propellant, however without stabilizer (weight ratio 99:1 respectively).

The results are given in Figure 5 in which curve 1 represents the heat generation of the non-stabilized propellant, curve 2 the heat generation of the mixture, and curve 3 the same but with ground propellant.

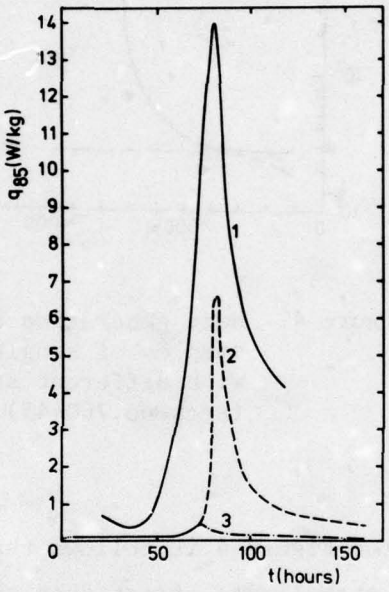


Figure 5. Heat generation at 85°C of a non-stabilized single base propellant.
1. the propellant alone
2. the propellant mixed with 99% CN propellant stabilized with 1.23% dpa
3. the ground propellant mixed with 99% ground CN propellant stabilized with 1.23% dpa.

From Figure 5 it follows that there is a stabilizing effect from the surrounding stabilized grains on the unstabilized propellant and that this effect becomes stronger with decreasing grain size. At the moment we are studying the influence of the degree of inhomogeneity of the stabilizer distribution in the propellant on both the self-ignition hazard and the ballistic stability.

6. Conclusions

Summarizing we may conclude, that it is possible to predict the self-ignition hazard and ballistic stability for a storage period of 10 years by measuring the heat generation at 85°C in the heat generation meter during 7 days.

The safe diameter of most types of propellants is about 0.5 m, which is sufficiently large compared with the calibre of the weapon used.

The influence of the type of stabilizer and the inhomogeneous distribution of stabilizer can also be studied by this test. The investigation will be continued.

Literature

1. Van Geel, J.L.C., Thesis on self-ignition hazard of nitrate ester propellants, Technological Laboratory TNO, Rijswijk, The Netherlands, thesis dated 12-1-1969.
2. Frank Kamenetzkii, D.A., Acta physicochim, URSS, X, 3, 365-370 (1939).
3. Van Geel, J.L.C., The heat generation test for the determination of the self-ignition hazard and the ballistic stability of nitrate ester propellants, Technological Laboratory TNO, Rijswijk, The Netherlands. Report TL 1971-1, 7360-I.

List of symbols

D	- critical diameter	(m)
D_{safe}	- safe diameter for acceptance and surveillance control of nitrate ester propellants	(m)
E	- activation energy of the rate determining reaction of the decomposition process of a propellant	(J/mole)
$F(Q)$	- heat generation factor, a function of Q	(W/kg)
q	- heat generation per unit weight of propellant	(W/kg)
Q	- total quantity of heat generated per unit of weight of propellant	(J/kg)
ΔQ_{ex}	- percentual decrease of caloric value	
q_{85}	- heat generation per unit weight of propellant at 85°C (358 K)	(W/kg)
R	- gas constant	(J/mole K)
T	- absolute temperature	(K)
T_a	- ambient absolute temperature	(K)
δ_c	- dimensionless critical diameter	
λ	- overall heat conductivity coëfficiënt of the propellant (bulk)	(W/m K)
ρ_b	- bulk density of the propellant	(kg/m^3)

PHYSICAL PROCESSES CAUSING LOX/LH_2 AUTOIGNITION

Wallace H. Boggs
Advanced Engineering Section
John F. Kennedy Space Center, NASA

ABSTRACT

Autoignition of liquid hydrogen/liquid oxygen mixtures has been demonstrated in DOD/NASA explosive yield tests and determined to be a self limiting phenomenon. This phenomenon has been reported previously, and the predictive relationships for explosive yield have been generally accepted. Yields on the order of several thousands of pounds are expected in failure of a space launch vehicle in modes that rupture propellant tankage containing quantities to the million pound order.

This paper will describe analytical efforts to determine the physical process or processes responsible for the initiation of the explosive reaction in the dynamic fluid mix region. It covers research performed by the University of Florida under Contract NAS10-1255, completed in 1973, and by Battelle Pacific Northwest Laboratories under NAS10-8591, completed in 1975.

Fundamental physical/chemical process models were constructed for dynamic liquid-liquid and liquid-gas interfaces and were examined, along with certain external influences, for potential of creating the localized energy concentration and continuous physical environment that would produce initiation. Several processes were found to produce expected energy conditions from one to three orders of magnitude greater than initiation requirements.

BACKGROUND

Over the 1960's, during tests conducted for the purpose of establishing explosive yield (TNT equivalence) of rocket propellants, existence of a self limiting process became apparent. Knowledge of the yield (TNT equivalence) and other characteristic properties of explosions of liquid rocket propellants is needed in siting and operations safety planning during space launch systems design.

Liquid fuel rocket stages had grown to appreciable sizes over the years leading to the Apollo program. The NASA Saturn V booster used upper stages having propellant capacities of 930,000 pounds (422,000 Kg) and 230,000 pounds (105,000 Kg) respectively of liquid oxygen (LOX) and liquid hydrogen (LH_2) in 5:1 weight ratio.

The first stage had a capacity of 4,400,000 pounds LOX and fuel similar to jet aircraft fuel, RP-1. Even a brief historical review of the tests carried out to establish a predictive relationship for explosive yield would be lengthy and superfluous here. Simply important is that yields anywhere near the theoretical thermodynamic yield of approximately 200 percent would require large areas of land for launch complexes. Equipment would need to be "hardened" and excessive piping/ducting/cabling distances from control and support facilities would be levied on systems designs for the safety of personnel. For these reasons it was incumbent that NASA establish the predicted yield as accurately as possible for all reasonable failure modes.

Studies and tests by NASA and DOD led to the establishment of a linear 60 percent yield prediction for missile and booster stages/vehicles based on total propellant weight as "workable" restriction.

Continuing test analysis led to realization that the larger geometric scale under most feasible failure modes would not allow mixing of large amounts of cryogenic propellants. Dr. Erich A. Farber of the University of Florida conducted a lengthy study of liquid propellant explosive phenomena, including much modeling development, that helped establish a better prediction of propellant mixing under such conditions as common bulkhead rupture in space vehicle tankage. His work under Contract NAS10-1255 was under technical cognizance of J. H. Deese of Kennedy Space Center and later under the author. The study also produced models of spill dynamics and fireball growth dynamics under certain projected failure modes.

The most significant result, however, was establishment of existence of an "autoignition" process that occurs in LOX/LH_2 mixtures. The process is mix energy dependent but for most projected failure modes of interest, does limit the reacting region to several thousand pounds and disperses the remaining propellant, a beneficial effect not generally expected. The cause was only categorically attributed to electrostatic charge buildup within the mix region and gas bubble breakdown as the trigger mechanism. Farber's study of the mixing dynamics for LOX/LH_2 and LOX/RP-1 were of particular importance to follow-up analytical work now described.

SCOPE

This paper reports the work that was done for Kennedy Space Center by Battelle Pacific Northwest Laboratories under Contract NAS10-8591. It further places the findings of that study effort in the overall context of other previous efforts particularly NAS10-1255 and of present interest. The final report of the Battelle effort was issued in May 1975. Dr. David H. Lester was Principal Investigator and

PRECEDING PAGE BLANK-NOT FILMED

the author was the government's Technical Representative. Battelle was given the task of examining the processes taking place in regions from the microscale up to the scale at which the explosive reaction autoignited. Laboratory or field tests were not desired, but physical-chemical analytical modeling was desired, to enable assertions concerning the likelihood of various possible causes. The work was directed primarily to LOX/LH_2 with LOX/RP-1 secondary interest and other useful safety observations extractable from the analysis being the remaining interests.

Figure 1 shows the Saturn V launch vehicle with locations of propellant dispersal openings cut if destruct systems were to be needed and initiated. Figure 2 shows the yield as a function of total propellant weight out past the approximately 6,000,000 pounds (2,700,00 Kg) Saturn V total, according to Farber's analysis. The PYRO data is extracted from the final report, Reference 1, and the Arthur D. Little test data from Reference 2. The final reports of the two NASA contracts previously mentioned are listed as Bibliography and are quoted freely.

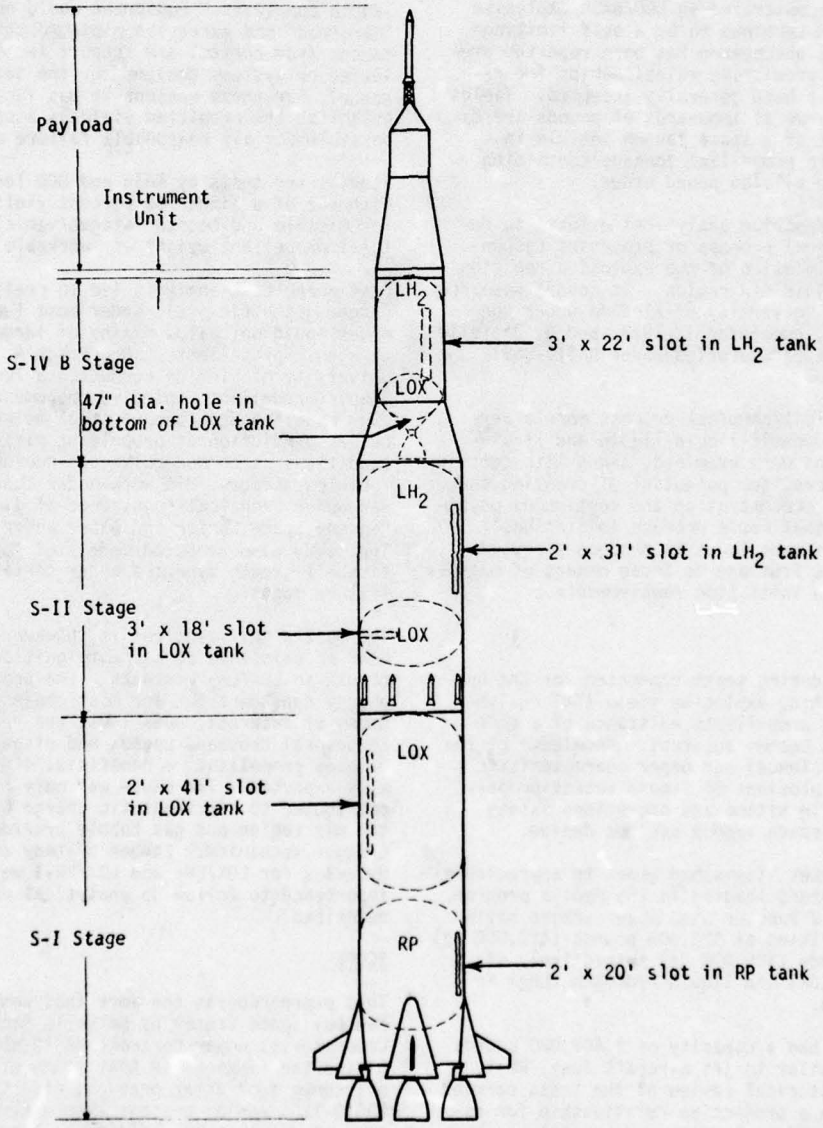


FIGURE 1 Schematic Diagram of Saturn V, with Effects of Destruct Initiation Indicated

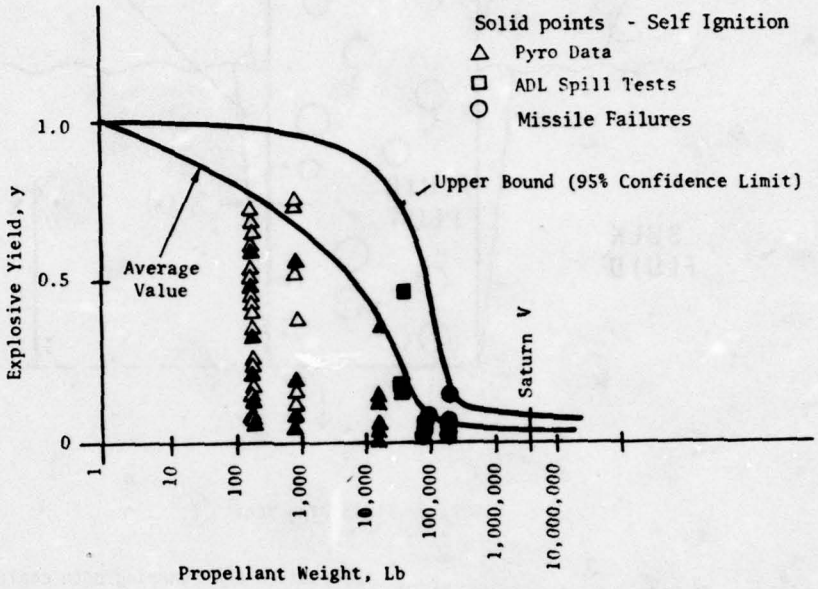


FIGURE 2 Estimated Explosive Yield as a Function of Propellant Weight

POSSIBLE PROCESSES CONSIDERED

In order to clarify the electrostatic breakdown postulate sufficiently to assess its validity, two tasks were initiated. The first sought to define the physical environment of the mixing region. The second examined the mechanics of electrostatic change generation and accumulation within the region. A third task considered alternate explanation and a final task to compare the relative probabilities was planned. The first two tasks received priority because of Farber's postulate that the cause was likely breakdown of H_2 gas bubbles approximately .25 inches (.6 cm) in diameter by charge accumulated from relative motion of dielectric fluids in the mixing turbulence. He made measurements of average potential gradients in turbulent regions with electrode probes. He further developed a model of the general overall behavior of the mixing region under the relatively low mixing energy resulting from gravity fall following a common bulkhead(s) rupture failure mode. Farber showed the mixing to be strongly dependent on the ratio "total mixing energy to boiling energy contribution". His predictive equation for yield is

$$M = \frac{K_1}{E} + K_2 E^2 \qquad \text{where}$$

E is this dimensionless energy ratio, K_1 and K_2 are empirical constants and M is the so called critical mass at which autoignition is a certainty.

His model of the mixing region was that of a "fluid plug" of less dense liquid falling into a more dense liquid, to a depth greater than equilibrium, then oscillating in damped sinusoidal fashion due to bubbles of LH_2 causing buoyancy change. Most important was his demonstration that the plug persisted "intact" for several seconds. Figure 3 illustrates the fluid plug model.

With reasonable persistence in the confines of the mixing region, focus could be shifted to the formation and behavior of vapor bubble populations and the formation of solid particles of the second reactant. A model of the total mixing process could then be envisioned that would include the vapor and solid formation dynamics and total energy relations of turbulent mixing.

Bubble population dynamics can be described by a general model including five basic processes: (1) bubble production by nucleate boiling, (2) bubble flow into and out of a region, (3) bubble growth into and out of a size range, (4) bubble breakup, and (5) coalescense of two or more bubbles. A general expression which includes all these factors is:

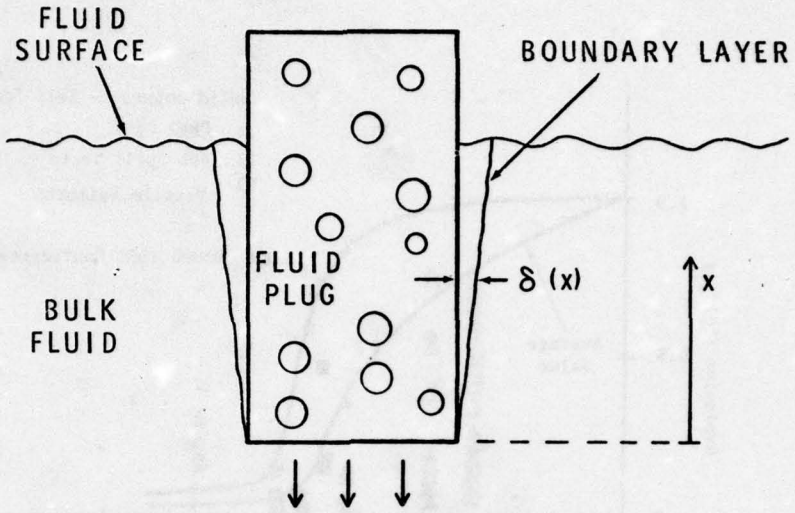


FIGURE 3 Fluid Plug Model

$$\frac{\partial n}{\partial t} + G(R)\frac{\partial n}{\partial R} + B(R)n = -\nabla \cdot \underline{j} + s(r,t)f(R) + \int_R^\infty n(R')B(R' \to R)dr' + \int_0^R \int_0^R n(R')n(R'')C(R', R'' \to R)dR'dR'' - n(R)\int_0^\infty n(R')C(R,R')dR'$$

where $\underline{j}$ = the flow of bubbles (bubble current)
s = nucleation probability
f(R) = nucleation size distribution
B = breakup probability
C = coalescence probability
G = growth probability

This expression will require solution by involved numerical analysis and does not provide a convenient approach without simplifying restriction. Frequency functions for nucleation, coalescence and breakup would otherwise be needed along with the relationship between bubble velocity, size and position and the relationship between bubble growth rate, size, and position. Discontinuities would need to be resolved. Two simplifications possible are: (1) neglect coalescense and breakup, a reasonable approach when number of bubbles is low and (2) consider bubble velocity to depend only on size. Writing $\underline{j}$ as n $\underline{V}(R)$ into the former equation and ignoring both coalescence and breakup the result is

$$\frac{\partial n}{\partial t} + G(R)\frac{\partial n}{\partial t} + \underline{V}(R) \cdot \nabla n = S(r,t)f(R)$$

Expressions for G(R), $\underline{V}$ (R) S (r, t) and f(R) are needed to make the equation a first order partial differential equation for n (V, R, t).

Two regions must be considered when two liquids come into contact with one boiling: one where bubble evolution and growth occur in a boundary layer under a supersaturated condition and one where the surrounding liquid is saturated but not superheated. The growth in a boundary region was shown to be $R = \bar{K}t^{\frac{1}{2}}$ where $\bar{K}$ is a constant and is given by

$$\bar{K} = \left[\left(\frac{12}{\pi}\right)^{1/2} \frac{K}{P_v Q a^{1/2}}\right] \xi_o$$

where K = conductivity, Pv = vapor density, Q = latent heat, a = thermal diffusivity, ξ_o = superheat and t = time. If it is assumed that buoyancy is the chief impetus in the boundary region the problem simplifies to one of vertical motion, and on expression for n (z, R, t) can be obtained. Picking an arbitrary value for superheat of 5^oC in liquid hydrogen and a reasonable nucleation rate of $S = 1 \times 10^6$ nuclei/sec-m^3, boundary regions of approximately 8 cm would be required to produce a .25 in. (.6 cm) bubble as observed by Farber, and concentration of 1×10^5 $\frac{.25 \text{ in bubbles}}{\text{sec-m}^3}$ near the

interface. An expression for the plug requires numerical solution but would be bounded by the solution for the interface region.

Solid oxygen is likely to be formed. The largest (limiting) crystal of oxygen will be formed when all heat to form a bubble of H_2 is taken from the freezing colume, not from total surroundings. This can be shown to be at a ratio $M_H/Mo = 0.156$, $V_H/Vo = 183$ and molar ratio of 2.5. The crystal formed in such a manner to pair with a 0.25 in. hydrogen bubble would be 0.02 inches in diameter, if spherical. Oxygen crystals would then account for very little of the volume of mixed hydrogen, but could be important if not essential to detonation. An A. D. Little study report, Reference 3, found that when a nitrogen/oxygen mixture of at least 75% oxygen was mixed with liquid hydrogen, sufficient solid oxygen was formed to support detonation by a spark. The system could be modeled as follows. The hydrogen mass is a plug of fluid entering the oxygen pool. As the plug enters, hydrogen bubbles and solid oxygen crystals are formed and dispersed through the hydrogen (because of the small size of the oxygen crystals). Arcs across bubbles from bubble to bubble must be in the presence of oxygen close to the bubbles, in order to vaporize some of the oxygen mixture. After examining the implications of turbulence, more analysis of the electrostatic charge buildup mechanisms that might clarify the arcing process was attempted.

Farber's critical mass hypothesis was derived in large part from studies of mixing behavior under turbulence created by allowing free fall of the less dense propellant. He used inert referee fluids to obtain visual demonstration and derived a mixing function dependent on the ratio total mixing energy to boiling energy. On examining the Kolmogoroff theory of turbulent mixing, the ratio of amount of a fluid mixed in another to the total amount of the first fluid is

$$\frac{m}{M} = 1 - e^{\frac{t}{\gamma}}$$

where $$\gamma = \frac{\rho}{6u}\left[\frac{u^{3/4}}{\rho^{1/2}}\right]\left(\frac{\rho}{V}\right)^{1/4}$$

and $\frac{P}{V}$ = power/unit volume

Integration of this relationship over a period of time where inflow is at a constant rate and a constant energy (for Farber's case $E = MgX$, X representing the ullage space height in a tank) give a mixing function with first term $K E^2$ where K is a constant. This term derived from first principles appears to support the semi-empirical form for the high energy term in the critical mass equation, $m = \frac{K_1}{E} + K_2 E^2$.

This term is dominant for the cases of interest.

A number of electrical ignition mechanisms can be postulated in the rapid mixing of liquid oxygen with liquid hydrogen or liquid hydrocarbon fuels. These include

1. electrical discharge across fuel/oxygen vapor mixtures
2. liquid dielectric breakdown discharge across both fuel and oxygen, releasing a combustible vapor mix and
3. electric discharge through combustible vapor from or among droplets ejected from the surface in boiling.

The streaming potential was shown to generate estimated electric fields of 1×10^8 volt/cm. A resistivity estimate of 10^{17} ohm cm was used for hydrogen. This number was reported in Reference 4, but is admittedly changed by impurities as is the zeta potential. It is not clear what level of impurities might be introduced in an actual test or tankage failure but they are likely low and poorly distributed. Figure 4 illustrates charge accumulation and transport in a general fashion. Gradients approximately equal to 1×10^8 volts/cm can also be generated by this mechanism. Since the dielectric breakdown field is 1×10^5 volts/cm for H_2 gas at 20^0K, this suggests that discharge across rising hydrogen bubbles is likely.

Electrostatic effects at surfaces were examined as follows: (1) discharge between an oxygen droplet and the bulk liquid as droplet is ejected or falls back (2) discharge between flying droplets of dissimilar charge level, or droplets oppositely charged by induction effects, and (3) miniature "lightning"flashes between charged oxygen droplets and oppositely charged hydrogen gas surrounding. More assumptions that cannot be rigorously demonstrated are required in this analysis but indications are that a cloud of suspended droplets only a few inches in depth would give electric breakdown field at the surface. Figure 5 illustrates the surface behavior.

Two other sources were considered. Even though the cosmic rays were thought to be much too low in total energy they were considered. Ortho-para H_2 state conversion was known to be catalysed rapidly by oxygen and its concurrent heat release was examined as a cause. Cosmic rays were found to be eight orders of magnitude too low. Ortho-para conversion is not a plausible cause since stored H_2 is 99+% para state already. One percent would give just the minimum 13.6 joules/mole, in total absence of heat loss. Heat loss from evaporation will preclude heat buildup.

SUMMARY

It seems quite clear that electrostatic charges arising in dielectric liquids and vapor bubbles therein, can, due to mixing and boiling turbulence, reach a gradient level sufficient to cause breakdown of hydrogen gas bubbles, possibly breakdown of the liquids. The former appears more likely. Surface and vapor droplet charging phenomena are less easily quantitatively described, but are judged a less likely initiation cause for LOX/LH_2. Solid oxygen crystals of small dimension are likely generated and dispersed in the liquid hydrogen,

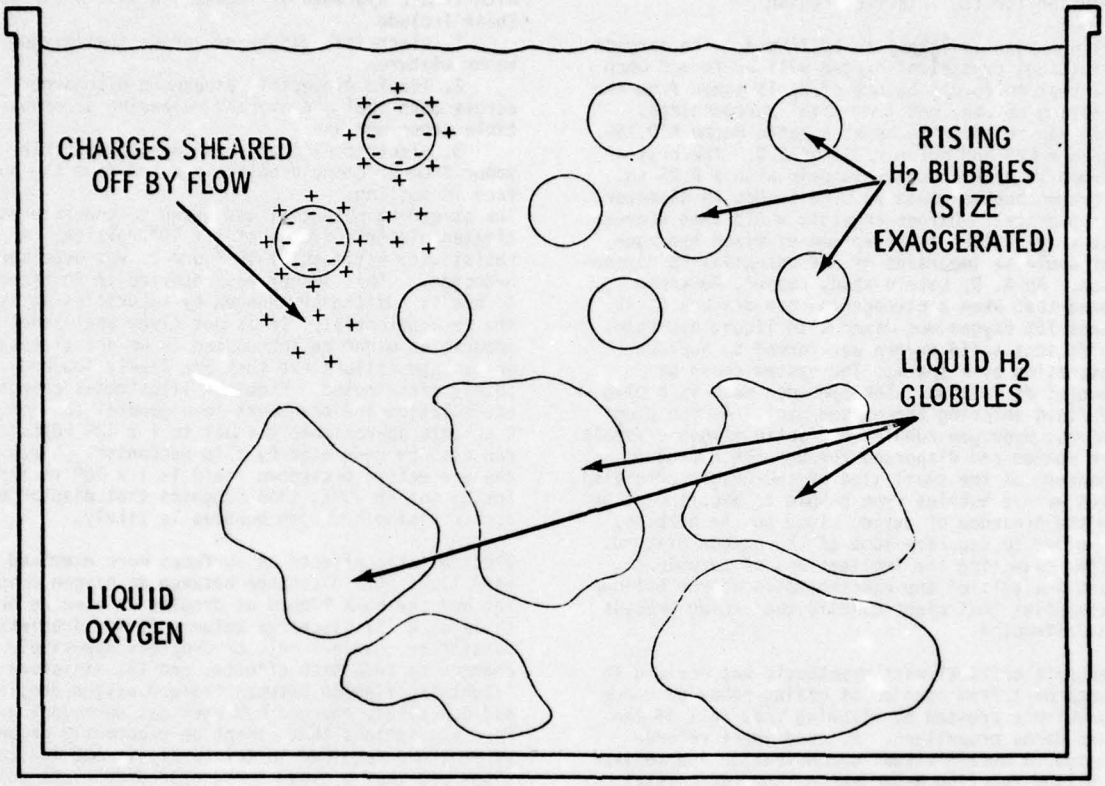


FIGURE 4 Rising Bubble Charge Transport

perhaps held to bubbles of H_2 by surface effects. These can supply the oxygen vapor when discharge occurs across a bubble at breakdown field gradient.

For LOX/RP-1 the potential gradients are not so high and breakdown potential is greater. Waxlike hydrocarbon solids slow the turbulence. The surface vapor phenomena seem more a likely cause of initiation.

The form of the high energy term from Dr. Farber's critical mass equation was verified. No further quantitative relations could be determined by analytical development.

The assertions that LOX/LH_2 autoignition takes place in the body of the liquid is supported by visual observations of one test at Kennedy Space Center, in which initiation appeared to take place deep within the mixing dewar.

No autoignition has been observed for LOX/RP-1 but the Farber critical mass hypothesis predicts it at about 3000 pounds (1350 Kg). No reasons were found to dispute the prediction from model analysis. Surface region potential gradients could conceivably reach breakdown levels.

Current plans are to use 20% TNT equivalence for LOX/LH_2 on the Space Shuttle. No further analysis to lower the yield prediction are planned unless a detonation hazard to other potential new propellants within the Space Transportation System warrants closer scrutiny.

No further work is planned for LOX/RP-1 (or other hydrocarbon) unless new space booster or energy system reactant storage dictates.

REFERENCES

1. Project PYRO Final Reports, "Liquid Propellant Explosive Hazards", Vols. 1, 2, and 3, December 1968. AFRPL-TR-68-92; URS 652-35. Prepared under contract AF 04 (611) 10739 for Air Force Rocket Propulsion Laboratory, Air Force Systems Command USAF, Edwards, CA.

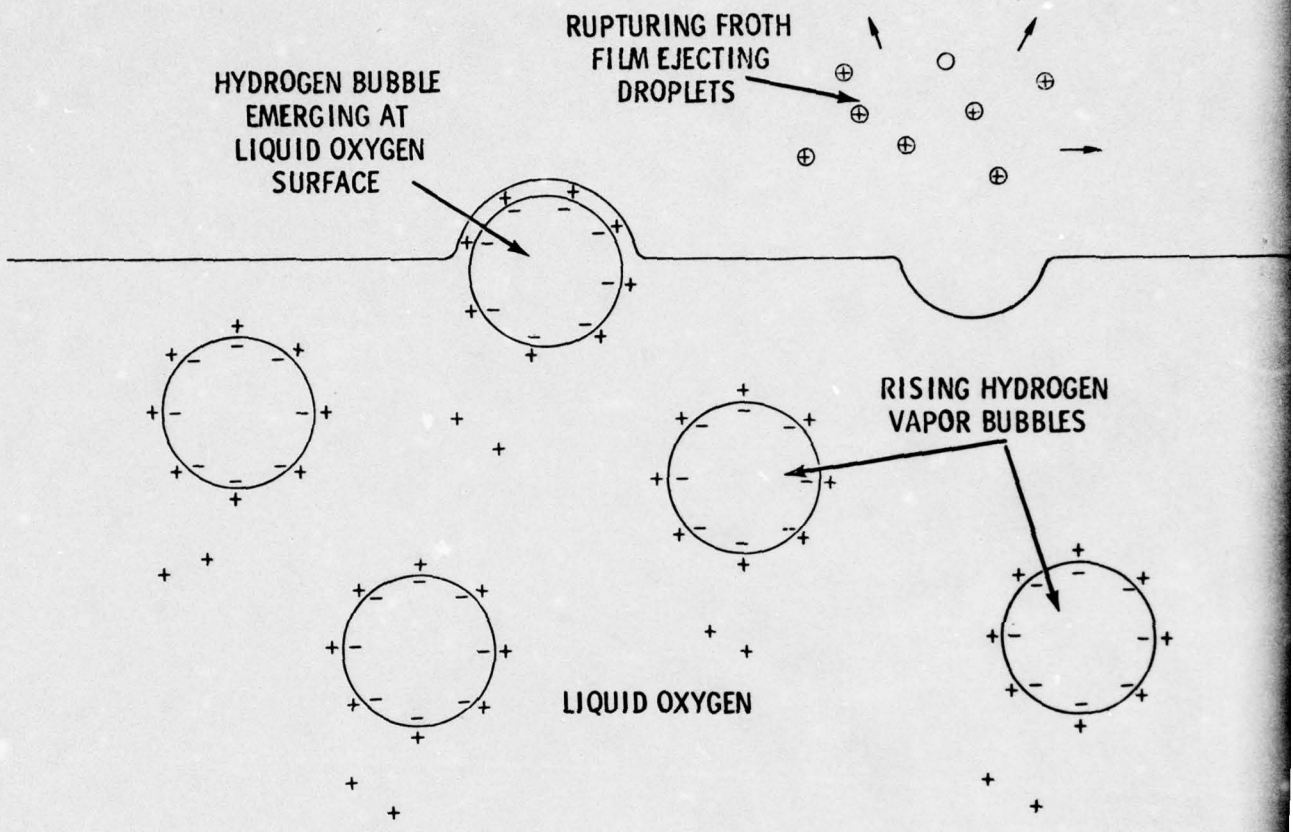


FIGURE 5 Surface Froth Droplet Charging Effects

2. Arthur D. Little, Inc., "Electrostatic Hazards Associated with the Transfer and Storage of Liquid Hydrogen", Final Report, Contract No. AF 18(600)-1687, May 1961.
3. A. D. Little, Inc., Interim Report on an Investigation of Hazards Associated with Liquid Hydrogen Storage and Use, Contract No. AF 18(600)-1687 C-61092, January 15, 1959.

BIBLIOGRAPHY

1. D. H. Lester, A. G. Gibbs, D. L. Lesser, "Study of Liquid Propellant Autoignition", Battelle Pacific Northwest Laboratories, Contract No. NAS10-8591, May 1975.
2. E. A. Farber, J. H. Smith, and E. H. Watts, "Final Report, Prediction of Explosive Yield and Other Characteristics of Liquid Rocket Propellant Explosions", Contract No. NAS10-1255, June 30, 1973.

THERMAL BEHAVIOR OF A PLASTICS FOAMING AGENT

p,p'-Oxy-bis (benzene sulphonhydrazide)
Fison's Industrial Chemicals, OBSH

by

Jack M. Pakulak, Jr. and Carl M. Anderson
Propulsion Development Department

ABSTRACT. A brief study is reported of the application of experimental and computational procedures developed for explosives and propellants to other exothermally unstable materials. A plastics "blowing agent", OBSH, a product of Fison's Industrial Cehmicals, was used as an example for the test application.

The study indicates that explosives theories and techniques can be applied, at least to OBSH, for prediction of safety limits for storage and shipping of materials other than explosives/propellants.

NAVAL WEAPONS CENTER
China Lake, California 93555

PRECEDING PAGE BLANK-NOT FILMED

INTRODUCTION

This report is concerned with the application of experimental procedures to define thermal hazards and of techniques for prediction of conditions for safe handling developed for explosive and propellant compositions to other materials being shipped, stored, and used in quantity. The Navy Department's problem is well stated in the following:

> "Several serious fires aboard aircraft carriers have focused attention on the need for intensified research and development in fire-fighting technology and the effects of fires on ordnance items carried aboard attack aircraft. Although the explosives can create a very hazardous situation when they are subjected to elevated temperatures, the hazard may be partially mitigated if existing ordnance items could be modified so that additional fire-fighting time would be made available. This would allow the fire fighters to cool the heated ordnance items so that runaway decomposition reactions would not set in, allowing sufficient time for the disposal team to jettison the items over the side". (reference 1).

As an example of a thermal hazard with a material of commerce:

> "The explosion that devastated a square-block industrial area in downtown Los Angeles last week was caused by prolonged exposure of organic peroxides to high temperatures, fire officials have tentatively determined .....
>
> Suspected source of the blast was a truck trailer loaded with several thousand pounds of methyl ethyl ketone peroxide and tertbutyl hydroperoxide-70, officials say. Reportedly, the trailer had been parked in a lot outside a warehouse for a day and a half. During that time, officials speculate, the sun heated the chemicals in the trailer to the point where they exploded. Organic peroxides are identified as 'oxidizing materals,' not explosives, in California, and therefore are not controlled under the Los Angeles municipal code. Responsibility for transportation and storage of such chemicals rests with the state's Transportation Dept." (reference 2). Fortunately, the event occured when the plant, and its neighbors, were unoccupied."

Rather than use one of the peroxide catalyst substances for this study, one of the "blowing agents", gas generators for plastic foams, etc., was chosen as an apparently innocuous material that is potentially dangerous when stored/shipped in large containers. In this preliminary report, the thermal stability of OBSH, [4,4'oxy-bis (benzene sulfonyl hydrazide)] was determined. OBSH has been reported to melt with decomposition at 157-160°C according to the mechanism (reference 3)

$$NH_2\text{-}NH\text{-}SO_2\text{-}\emptyset\text{-}O\text{-}\emptyset\text{-}SO_2\text{-}NH\text{-}NH_2 \xrightarrow{\Delta} (\text{-}S\text{-}\emptyset\text{-}O\text{-}\emptyset\text{-}S\text{-})_{\frac{n}{2}} + (\text{-}S\text{-}\emptyset\text{-}O\text{-}\emptyset\text{-}SO_2\text{-})_{\frac{n}{2}}$$

$$2nN_2 + 3nH_2O$$

with the implication that the material is safe below this temperature. The exact decomposition mechanism is stated as being uncertain but is assumed to react, according to Ref. 3, by analogy to the thermal decomposition of benzene sulphonyl hydrazide.

$$\emptyset\text{-}SO_2\ NHNH_2 \xrightarrow{\Delta} \emptyset\text{-}SS\text{-}\emptyset + \emptyset\text{-}SSO_2\text{-}\emptyset + N_2 + 2H_2O$$

Both of these compounds are chemical reducing agents and the decomposition rate could be affected in the presence oxidizing agents.

Although the current study was limited to thermal effects, studies of this kind should include the effects of fires, impacts such as produced by dropping or bullet and missile impact, sliding friction, etc.

EXPERIMENTAL TECHNIQUES

ANALYTICAL

The Mettler Model No. 2 Thermoanalyzer[1] is used to obtain true simultaneous measurements on the effect of heat on a single sample under precisely defined conditions. Differential thermal analysis (DTA), thermogravimetric analysis (TGA), and derivative thermogravimetry (DTG) data are obtained on one sample in one single run. The DTA is a record of the temperature changes and the TGA is the weight gained or lost, while the sample is being heated at a constant rate. The DTG indicates the rate at which the weight is being lost at that temperature. The heating rate is usually 3°C per minute, chart speed 12 inches per hour, temperature span 10-millivolt full scale, and runs made under atmosphere of air. (On the original chart, the distance between two numbered horizontal lines (e.g., 50 and 60) is one inch. This vertical distance is equal to ~1°C on the DTA curve and 1 mg on the TGA (10x) curve.) Indium metal is used on the reference side to give a temperature calibration by producing a small exothermic blip at the melting point, 156°C.

The other analytical techniques employed are: differential scanning calorimetry (DSC), infrared spectrophotometry (IR), and mass spectrophotometry.

---

[1] Mettler Instrument Corp., Princeton, New Jersey.

Two different techniques are used for isothermal analysis. Both techniques are not always employed on the candidate material.

The decomposition rates of explosives and other hazardous mixtures, 5 to 8 milligram sample, are measured at temperatures ranging to 260°C. The differential pressure measurement can be used for the determination of kinetic parameters and for compatibility studies (reference 4).

The second technique uses 1 to 2 grams of material contained within a 45-milliliter stainless steel bomb. This small-scale pressure bomb (SPB) and heating block are shown schematically in Figure 1. The heating block was machined from a 5 1/2-inch-diameter piece of solid cylindrical aluminum stock. The material sample container was a commercially available 45-milliliter T303 stainless steel general purpose bomb[2] with Parr type A7AC7 head. The overall length of the bomb was 4.6 inches. Additional items are required for the basic bomb configuration: gage block, Parr type 4316 with needle valve, and pressure sensor. Two cartridge-type heaters rated at 230 watts at 120 volts were used. The heating block was insulated with a 1/2-inch layer of asbestos ribbon around the sides of the block and a 1 1/2-inch-thick asbestos pad on the bottom. Additional insulation was provided by placing the completed assembly within a cylindrical enclosure of asbestos with a cover placed on top of the enclosure, allowing the sensor and valve to be readily accessible above the enclosure. Pressure and temperature data are recorded continuously. Decomposition products are analyzed by transferring a gas sample from the bomb into the mass spectometer and/or the infrared spectrophotometer or by any other convenient technique after the block has returned to ambient temperature.

FAST COOK-OFF

Fast cook-off tests are used to study the dynamic thermal response of explosives or hazardous materials when contained within a closed vessel and subjected to a rapid increase in temperature. The technique uses a small-scale cook-off bomb (SCB), Figure 2, consisting of a 2.5-inch ID by 5 inches long stainless steel cylinder with 0.12 inch walls instrumented with a plate-type thermocopule spot welded to the wall and a pressure sensor take off in the cover. The bomb is electrically heated at a rate of 0.2° to 3°C per second. Each bomb was filled with approximately two pounds of explosive or hazardous material, and heated until destruction. The time-temperature and pressure data are recorded on strip-chart recorder. The bomb reaction and fragmentation are noted and recorded for each test. The type of reaction obtained is reported in accordance with reference 5.

---

[2]Part No. 4712, Manufactured by the Parr Instrument Co., Moline, Illinois.

SLOW COOK-OFF

Cook-off tests are made with samples of various sizes and configurations, weighing up to ten pounds, in ovens that will withstand repeated deflagrations of hazardous materials. The standard cook-off oven has been 7.65-inch ID and four feet long made from 8-inch steel pipe, designed to test samples up to 6-inch OD. Lightweight fiberglass plugs are used in each end of the oven, made so that they are a tight fit to prevent convection heat losses and yet give quick release for the hot gases during a deflagration. In a standard test, the oven is brought to the desired temperature with a dummy set-up. The test specimen, implemented with thermocouples, is then placed in the oven and the test is monitored remotely until deflagration occurs.

The general practice has been to select such temperatures that deflagration occurs in one to five days. Plots of data obtained from these tests show a linear relationship between the log of the time to deflagration and the reciprocal of the absolute temperature. In exploratory tests, five to ten samples are generally required to establish the trends. Size of sample may be 100 grams during the development phase and 3.0 kilograms at later stages in the testing of a specific material. This covers the range of diamensions (1 to 5 inches) normally used in development work. With larger ovens propellant samples up to 30 inch diameter have been tested. Since deflagration occurs to terminate each test and occasional detonations may be expected, the ovens are monitored by remote control and are propertly barricaded.

MISCELLANEOUS TECHNIQUES

Although not used in this study, there are other Navy tests that may be directly adaptable to other hazardous materials. They are listed without detail.

1. Vibration, surface and airborne transportation.

2. Forty-foot free fall drop onto a steel plate.

3. Ten foot drop on to steel plate with spikes.

4. Fragment-impact tests. This includes bullet impact.

ANALYSIS OF EXPERIMENTAL DATA

Two methods are used for the analysis of experimental data and to estimate the time to cook-off. The first method involves a simple constant-heating rate and is only an approximation and cannot be applied in every case. It can only be used where the ignition of the material occcured at some specific heating rate at the inside surface of the bomb. A plot of such data is shown in Figure 3. This plot

does not consider a mass effect, which should be small at a high heating rate. The temperature data is for the material surface in contact with a metal. The reaction temperature at a given heating rate would be lower for an explosive in contact with an insulating material. The insulating material would also affect the heating rate.

The second method is derived from the general heat-flow equation:

$$-\lambda\nabla^2 T + \rho c\left(\frac{\partial T}{\partial t}\right) = QAe^{-E/RT} \qquad (1)$$

where the first term, $-\lambda\nabla^2 T$ describes the temperature profile within the material and is dependent on the transfer of heat to the mass. The second term involves the heating rate and the third term involves the heat generated in the sample by chemical reaction. For an adiabatic situation, which is described as a no-heat-transfer condition from the center of the charge to some other point in the charge, Eq. (1) then reduces to

$$k = \frac{c}{Q}\left(\frac{dT}{dt}\right) \qquad (2)$$

when $-\lambda\nabla^2 T$ equals zero. Under steady-state conditions, where $\rho c\,(\partial T/\partial T)$ equals zero, a heat balance can be calculated at some "critical" temperature, T_m, by an iteration on Eq. (3) using data derived from the variety of thermal measurements.

$$T_m = \frac{E}{2.303R \log\left(\frac{\rho a^2 QAE}{\lambda RT_m^2 \delta}\right)} \qquad (3)$$

When the surface temperature (T_1) exceeds T_m under steady-state conditions, and a zero-order reaction rate model is considered, the time to deflagration, t_e, is given by

$$\frac{t_e \lambda}{\rho c a^2} = F\left(\frac{E}{T_m} - \frac{E}{T_1}\right), \qquad (4)$$

where the dimensionless time, t_e/τ (first term reduced), is a function of $(E/T_m - E/T_1)$. The reduced time, τ, is defined as

$$\tau = \frac{a^2}{\alpha} = \frac{\rho c a^2}{\lambda}, \qquad (5)$$

where α is the thermal diffusivity ($\alpha = \lambda/\rho c$) and a is a radius or half-thickness of the sample.

From a plot of Eq. 4 (Figure 3), a value of X in

$$\frac{1}{T_m} = \frac{1}{T_1} + \frac{X}{E} \qquad (6)$$

can be found for some ratio of

$$\frac{t_e}{\tau} , \qquad (7)$$

thereby calculating the time to cook-off, t_e, from Eq. 6. A more complete treatment on reaction kinetics is given in Ref. 6

RESULTS

Samples of the "blowing agent" OBSH (reference 3) were treated as outlined in the Experimental Techniques Section of this report.

DTA/TGA

A portion of the Mettler Thermoanalyzer-2 Strip-chart record is reproduced as Figure 4. At a heating rate of 3°C per minute with a 31.7 milligram sample, OBSH begins to lose weight noticeably at about 125°C. From 125°C to 155°C, 1.5 milligrams of the material leave the balance. At 155°, an exothermic reaction occurs involving a weight loss of 9.2 milligrams; this is the gas release reaction used for expanding plastics. This reaction is sudden and strongly exothermic producing a temperature increase on the sample side of 15 to 25°C. (The instrument uses a multi-point chart recorder with a 24 second cycle time and a 10° span on the DTA record and an automatic scale stepper so that the very abrupt temperature change cannot be surely defined.)

DSC

A reproduction of the DSC record of runs at varying heating rates is presented here as Figure 5. Using the Kissinger method of the change in peak temperature with heating rate, $\emptyset$, a plot of $\log \emptyset/T^2$ vs. 1/T should produce a line (Figure 6) with a slope of E/R.

$$\frac{E}{R} \quad \frac{\emptyset}{T^2} = A\exp(-E/RT)$$

From Figure 6, the slope defines an activation energy, E, of 32.7 kcal per mole and an Arrhenius frequency factor, A, of 2.67×10^{14} sec^{-1}.

SCB

A sample, 248 grams, of OBSH (nitropore) powder was packed into the SCB and heated until the system opened. Gas released by OBSH produced sufficient pressure to bulge the 1/8-inch stainless steel wall of the vessel and burst the pressure hose lead to the pressure sensor. This event occurred at 50 seconds with a wall temperature of 193°C. The entire sample then burned. Figure 7 is a reproduction of the time-vs-temperature and pressure recorded for this experiment.

It is of interest that the heating rate-temperature function for this SCB run with a large powdered sample and a high heating rate should fall near the line defined by the DSC and DTA data using samples of <2 mg and 31 mg at much lower heating rates. This suggests that the DSC/DTA data could be used to estimate the reaction temperature and time for large samples under rapid heating such as in a fire.

SCO

For this brief preliminary investigation, two runs were made with OBSH powder in 2" x 6" vertical ovens at temperatures of 125°C and 110°C. Figures 8 and 9 give the time-temperature records of these runs. The time to reaction, t_e, under isothermal conditions is derived by calculating the time for an equivalent amount of reaction to take place as that which occurs while the sample is warming to the oven temperature. An estimate is made of the thermal diffusivity, α (Eq. (5)) from the temperature lag during the warm-up period, which then allows an estimate of the thermal conductivity of the powder.

Two items are derivable from this data that should be of concern for shipping/storage of this material. First, this material is reacting at an appreciable rate even at 110°C, 45°C below the published decomposition temperature, as evidenced by the self heating that occurred before the sample destroyed itself. Second, a plot of the logarithm of the time-to-reaction vs. the reciprocal of the absolute temperature (Figure 10) allows for an extrapolation for prediction of time-to-reaction at other temperatures for this size of container. Experience with other materials indicates that with larger sizes, times-to-reaction are shorter but roughly parallel to this 2-inch line. To make a reasonable prediction of time-to-reaction for other sizes and temperatures will require further data.

ISOTHERMAL DECOMPOSITION

Rather than use the Parr bomb instrumentation, the data in the supplier's literature on rate of gas generation was used. Half-life times, i.e., time to produce one-half the maximum pressure were estimated from the published curves. A plot of log $t_{\frac{1}{2}}$ vs. 1/T produced

a line whose slope yields an activation energy of 43 kcal/mole and the intercept, a frequency factor of 4.2×10^{19} sec^{-1}.

DISCUSSION

Calculation of a critical temperature, T_m, of 105°C was made on the OBSH from Eq. (3) and the following physical and chemical data at a diameter of two inches (steady-state conditions).

δ = 2

ρ = 1.43 g/cm^3

a = 2.54 cm radius (2-inch diameter)

c = 0.21 cal/gram-°C

Q = (est) 150 cal/gram

α = 0.00136 cm^2/sec

R = 1.987 cal/mole-°K (gas constant)

λ = 0.0005 cal/cm-sec-°C

E = 43 kcal/mole
log A = 19.62/sec
} (reference 3)

E = 32.7 kcal/mole
log A = 14.43/sec
} DSC

E = 41.6 kcal/mole (half-life)

The second method was used to determine the critical temperature of a 2-inch diameter sample and this prediction was checked by a comparison to the experimental T_m via Eqs. (6) and (7) (references 7 and 8 for value of X). Using experimental values of T_1 and t_e (isothermal conditions)

T_1 = 110.6°C

t_e = 355 minutes

T_1 = 125°C

t_e = 26 minutes

and a plot of log time vs. $1/T_1$ for a value of t_e at $t_e = \tau$

where

$$\tau = \frac{a^2}{\alpha} = \frac{(2.54)^2}{(0.00136)(60)} = 79 \text{ minutes}$$

and $1/T_1 = 0.00246$ at $t_e = 79$ minutes

and $T_1 = 118°C$

This compares favorably with the predicted value of 111°C from about 10-40 mg samples and available data from literature. Had the decomposition of this material been purely a zero order reaction, no cook-off could have occurred below the T_m value ($t_e = \infty$ for $T_1 < T_m$). For a first order reaction model, cook-off can occur for $T_1 < T_m$ but the mass effect drops off rapidly for this condition and a plot of T_1 (where $T_1 < T_m$) vs. log t_e should be independent of mass.

CONCLUSIONS

Blowing agent, OBSH, behaves much as do explosives and propellants in tests developed for these materials. The equations applicable to explosives/propellants fit the decomposition of OBSH quite well.

This study has shown that kinetic data from DTA and isothermal analysis studies can be used to predict the thermal stability of a selected hazardous material. These techniques have been used to predict the thermal stability of explosives, pyrotechnics, and other materials that exhibit exothermic reactions, provided the kinetic parameters can be determined by thermal analysis. The results of a prediction can be given in precise terminology, e.g., terms that relate geometry (mass), time, and temperature. This will eliminate the possibility of performing tests under a set of conditions which could yield the type of data desired. It is possible, however, to relate and correlate results from data obtained by different persons with different types of instrumentation.

The experience developd at the Naval Weapons Center with explosives and propellants is of value and can be used outside of DoD for safety in production and use and transportation of hazardous materials.

REFERENCES

1. Naval Weapons Center. "Termperature Data on MK 82 Bombs used in CASS Mini-Deck Tests", by Jack M. Pakulak, Jr. and Edward Kuletz. NWC, China Lake, CA. October 1970 (NWC TP 4967)

2. Chemical Week, 8/28/74, Page 16

3. Fison's Industrical Chemical Literature on Blowing Agent, Sobin Chemical Inc., Sobin Park, Boston, Mass. 02210

4. Naval Weapons Center. "Thermal Decomposition of Explosives. Part 9. The Decomposition of Destex, Tritonal and D-2 Wax", by Taylor B. Joyner, NWC, China Lake, CA. 1974. (NWC TP 4709, Part 9)

5. Naval Ordnance Systems Command, Navy Department. "Standard Technology for Ordnance Explosives Reactions Obtained by Cook-off". (NAVORDNOTE 8020, ORD-93221, 23 April 1969)

6. Naval Weapons Center. "Thermal Analysis Studies on Candidate Solid JPL Propellants for Heat Sterilizable Motors", by Jack M. Pakulak, Jr. and Edward Kuletz. NWC, China Lake, CA. July 1970. (NWC TP 4258)

7. Zinn and Rogers. "Thermal Initiation of Explosives", J. Phys. Chem., Vol. 66 (1962), p2646

8. Naval Weapons Center. "Cook-off Predictions of Explosives by Thermal Analysis Techniques", by Carl M. Anderson, NWC, China Lake, CA. July 1972. (NWC TP 5245)

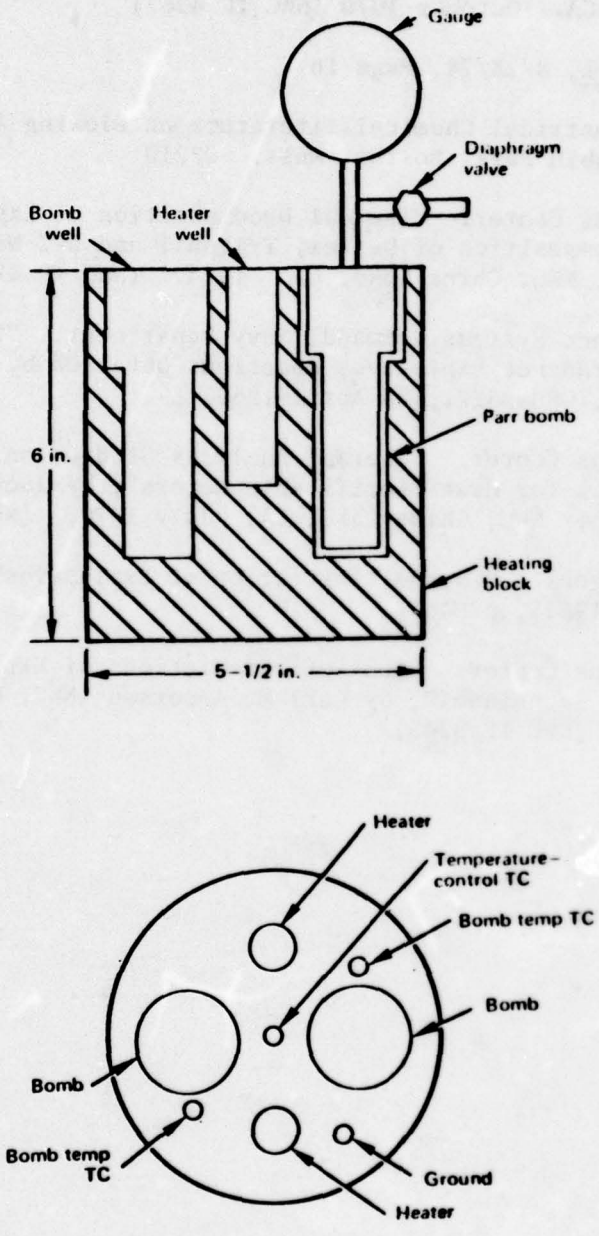


FIG. 1. Schematic Diagram of Small-Scale Pressure Bomb (SPB) Setup.

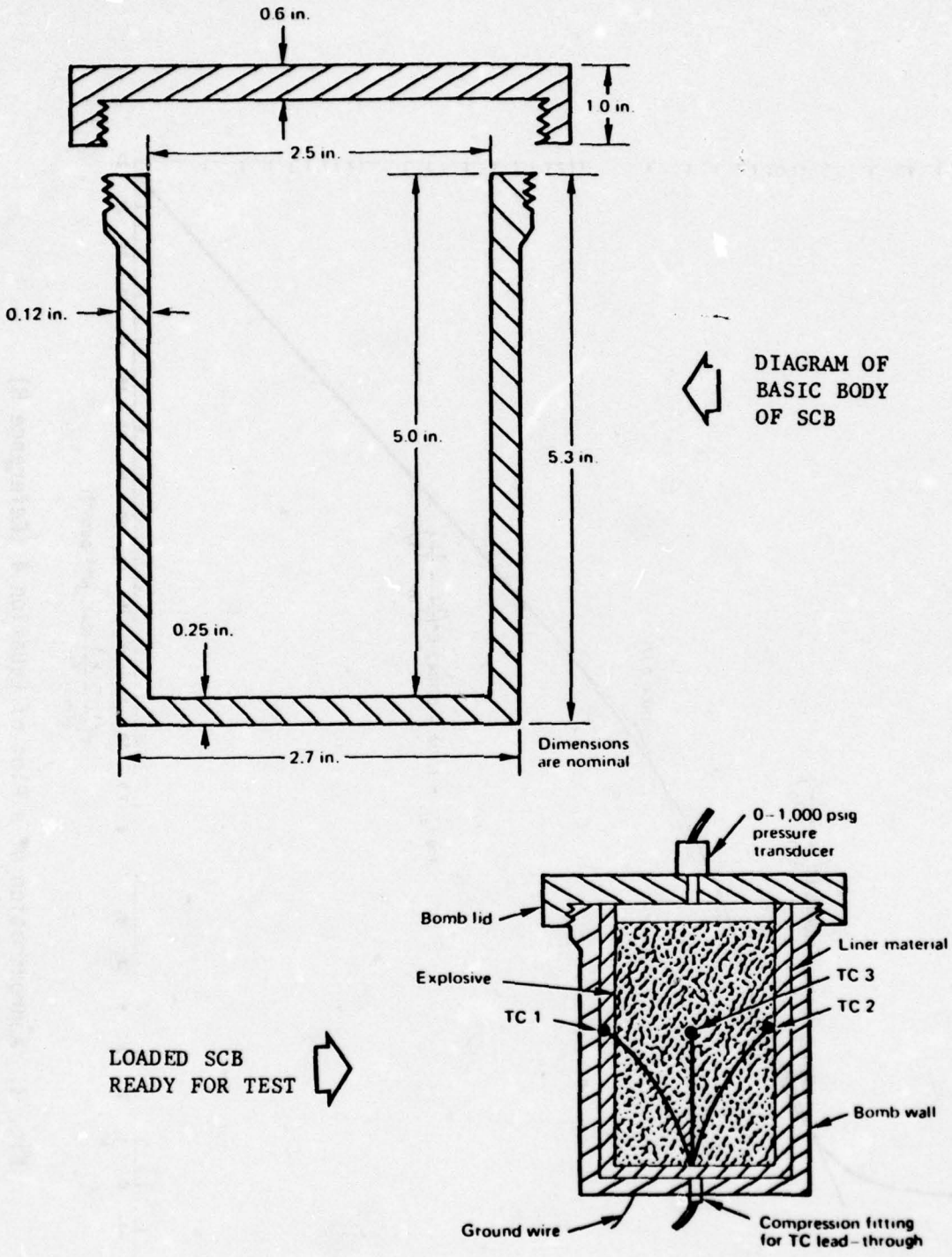


FIG. 2. Small-Scale Cookoff Bomb (SCB).

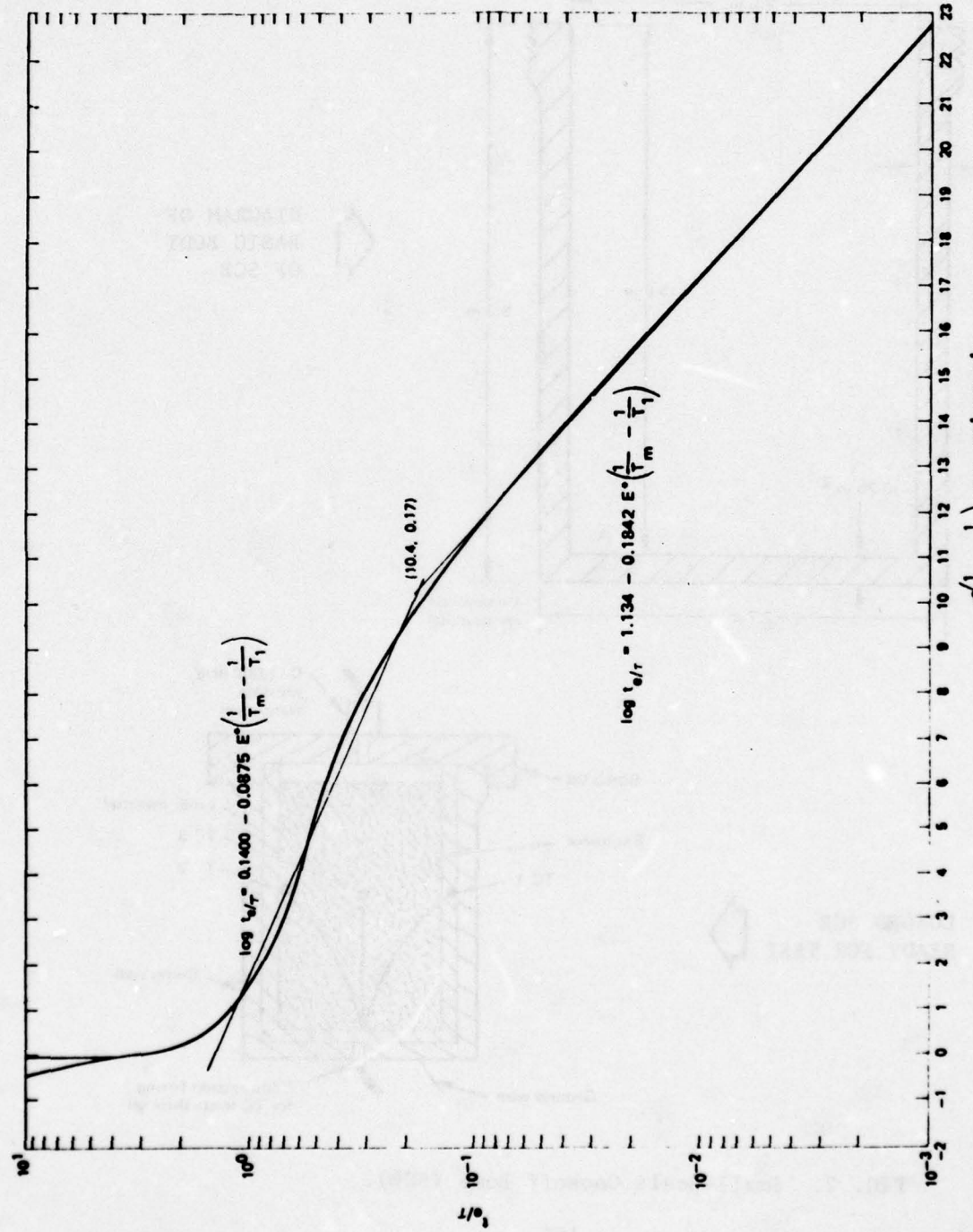


Fig. 3. Approximation of a Plot of Equation 4 (Reference 8)

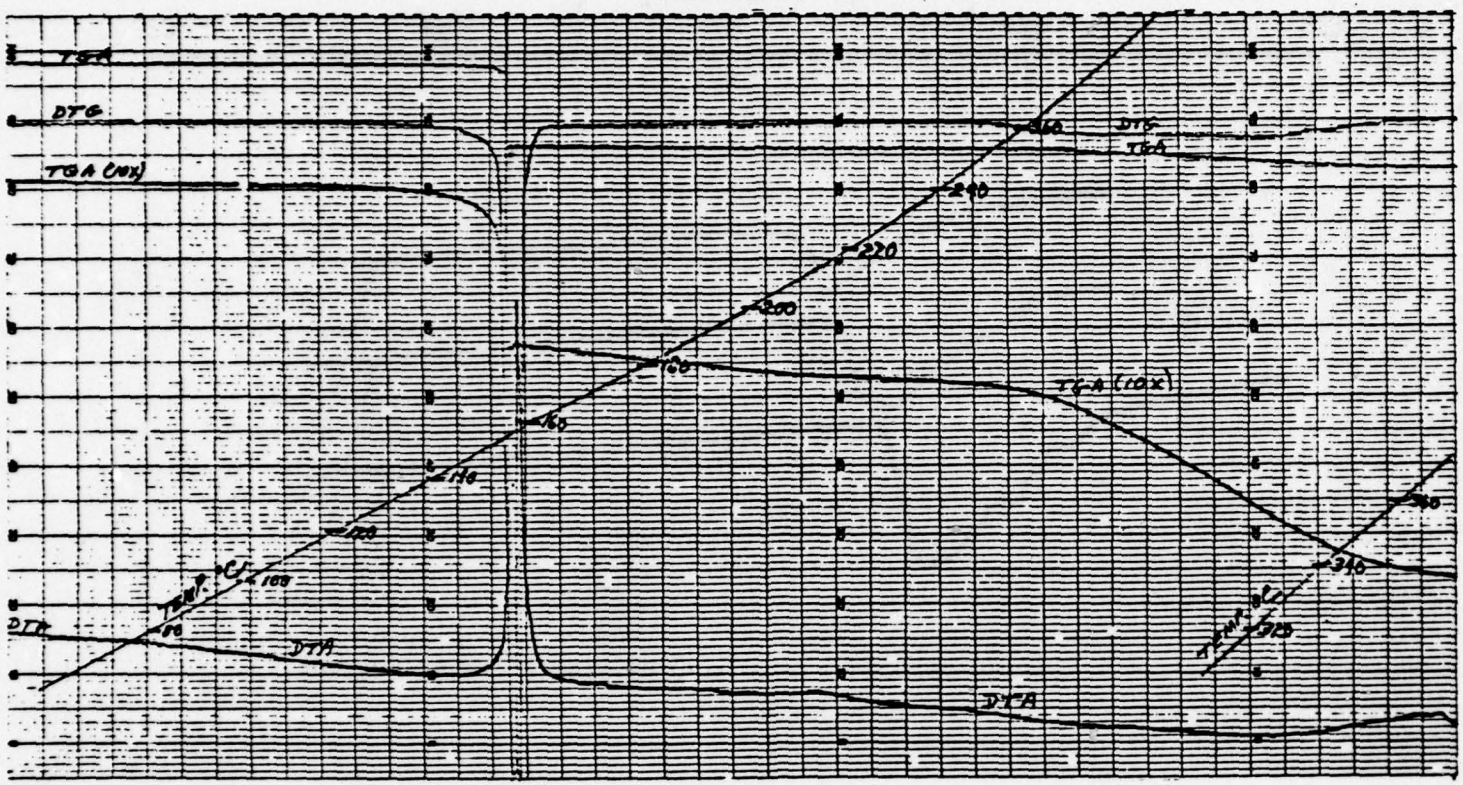


Fig. 4. Thermal Patterns of NP Nitropore OBSH at Heating Rate of 3°C/min. (Sample wt.: 31.7 mg; Run No. 2-39-2.)

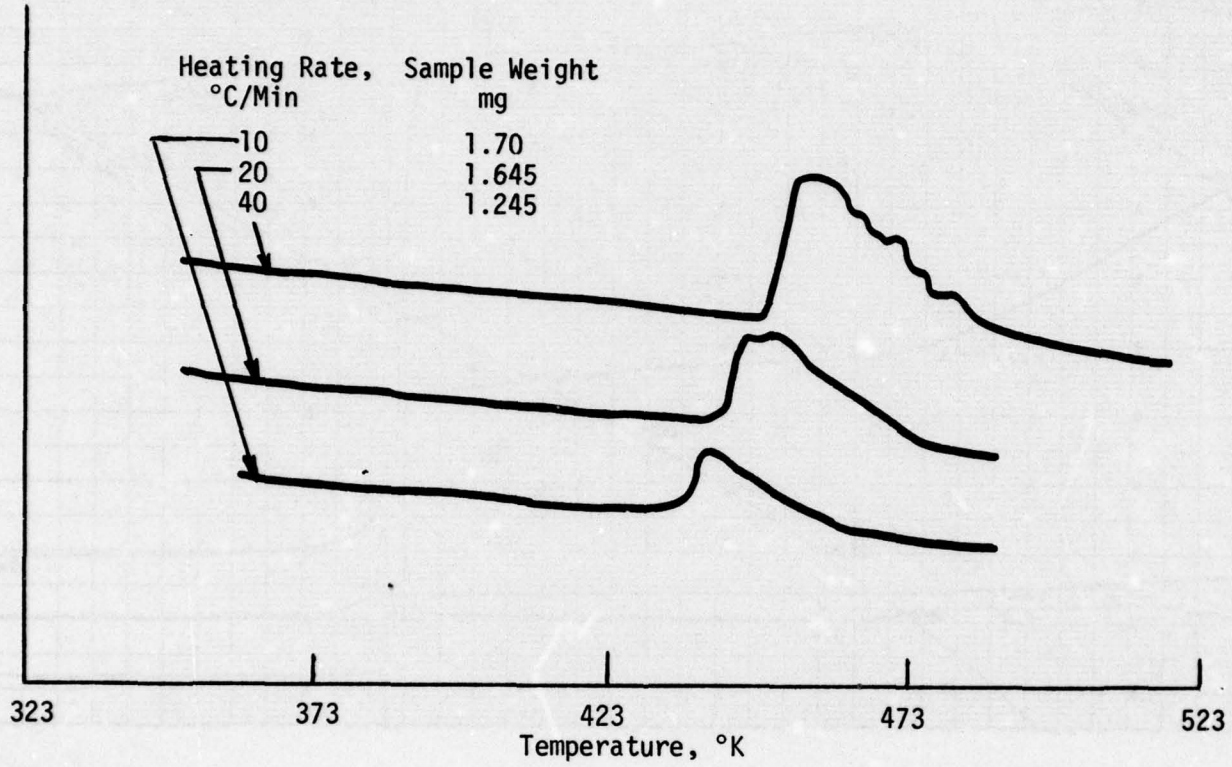


Fig. 5. DSC Results for Nitropore OBSH

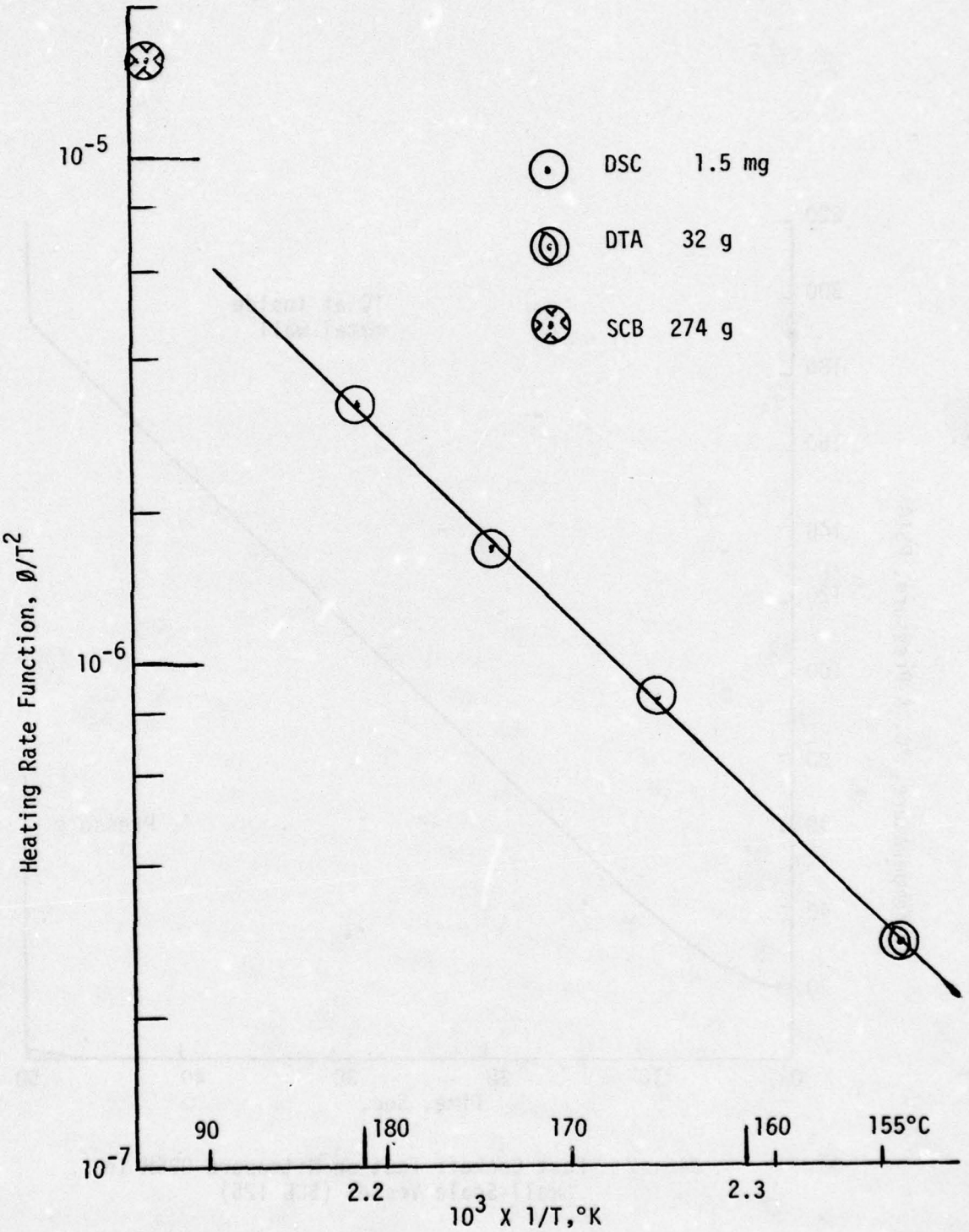


Fig. 6. Plot of Heating Rate Function for Nitropore OBSH

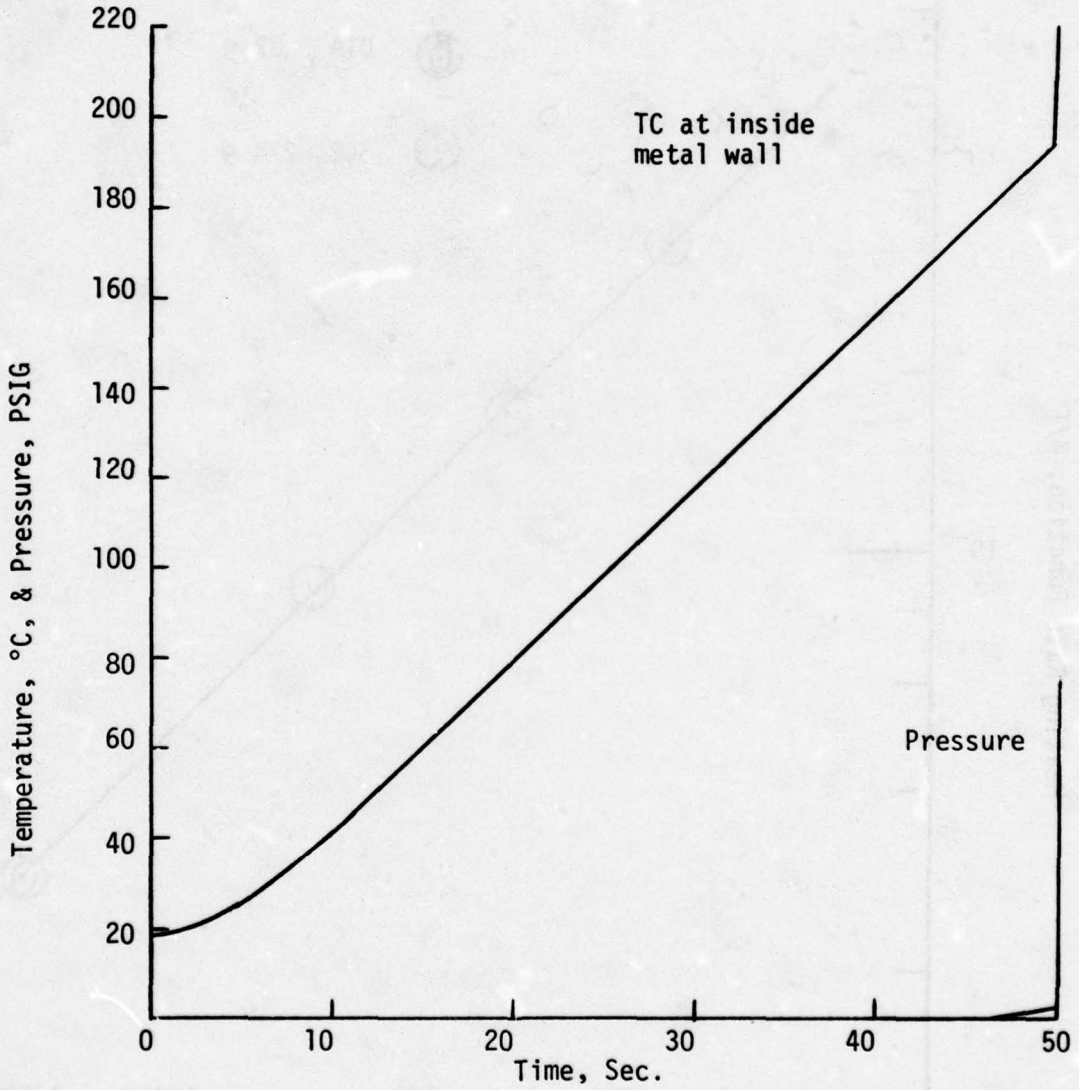


Fig. 7. Fast Cookoff Test on Nitropore OBSH in Small-Scale Vessel (SCB 125)

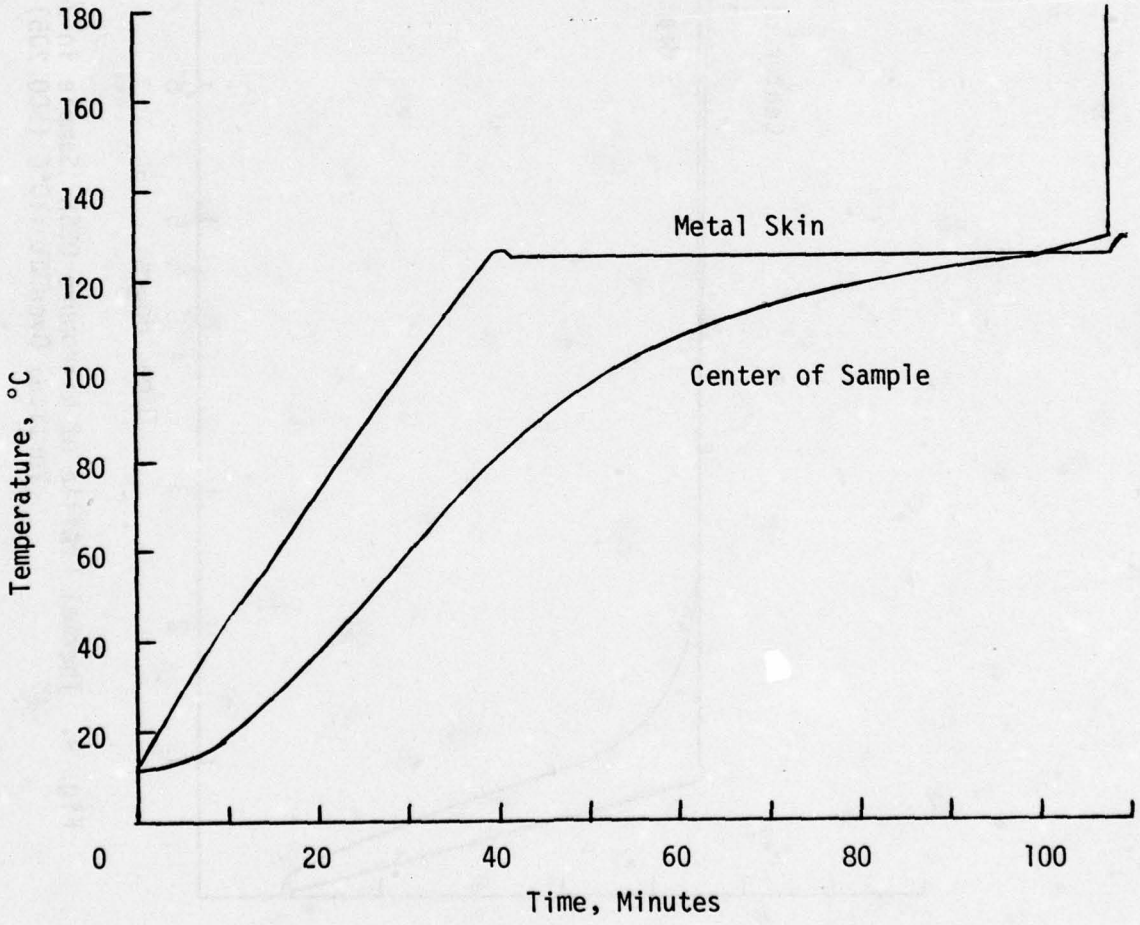


Fig. 8. Thermal Profile of Nitropore OBSH Sample in 2-inch-diameter Vertical Oven at 125°C (SCO 204)

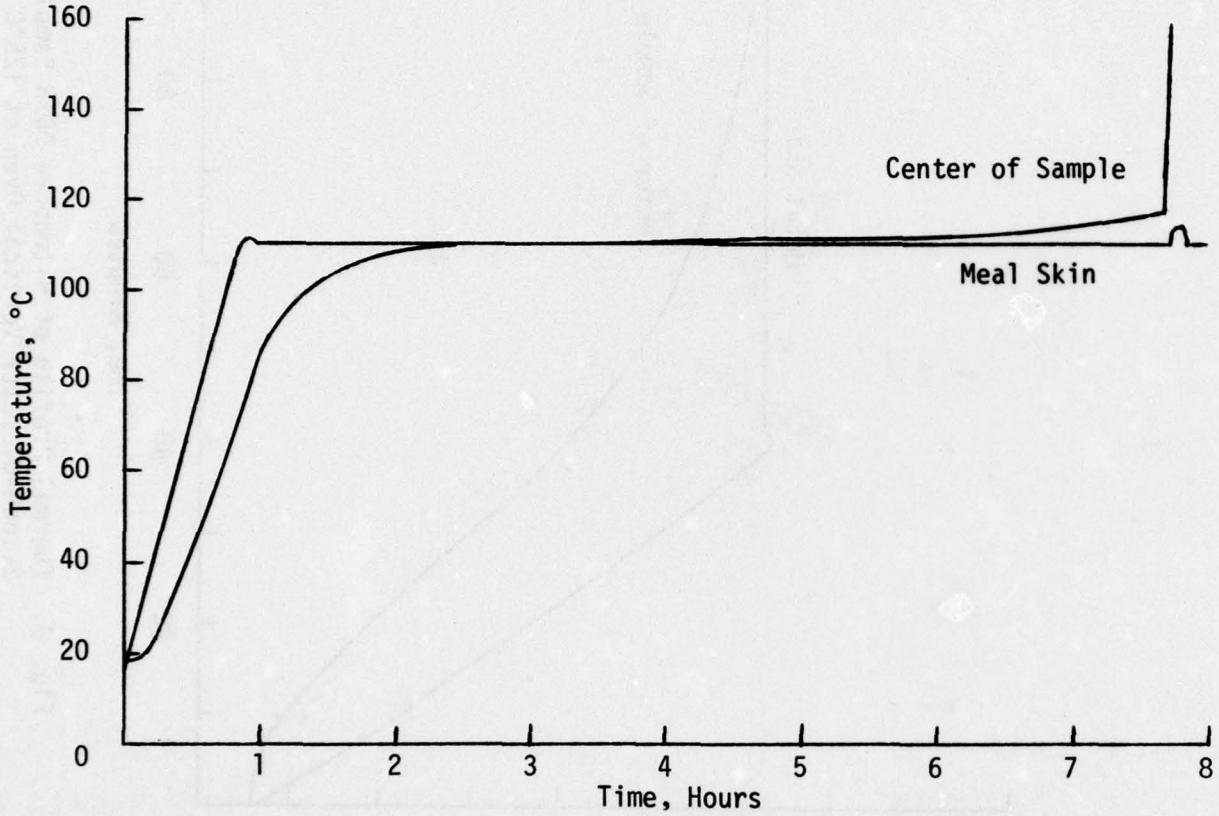


Fig. 9. Thermal Profile of Nitropore OBSH Sample in 2-inch-diameter Vertical Oven at 110°C (SCO 205)

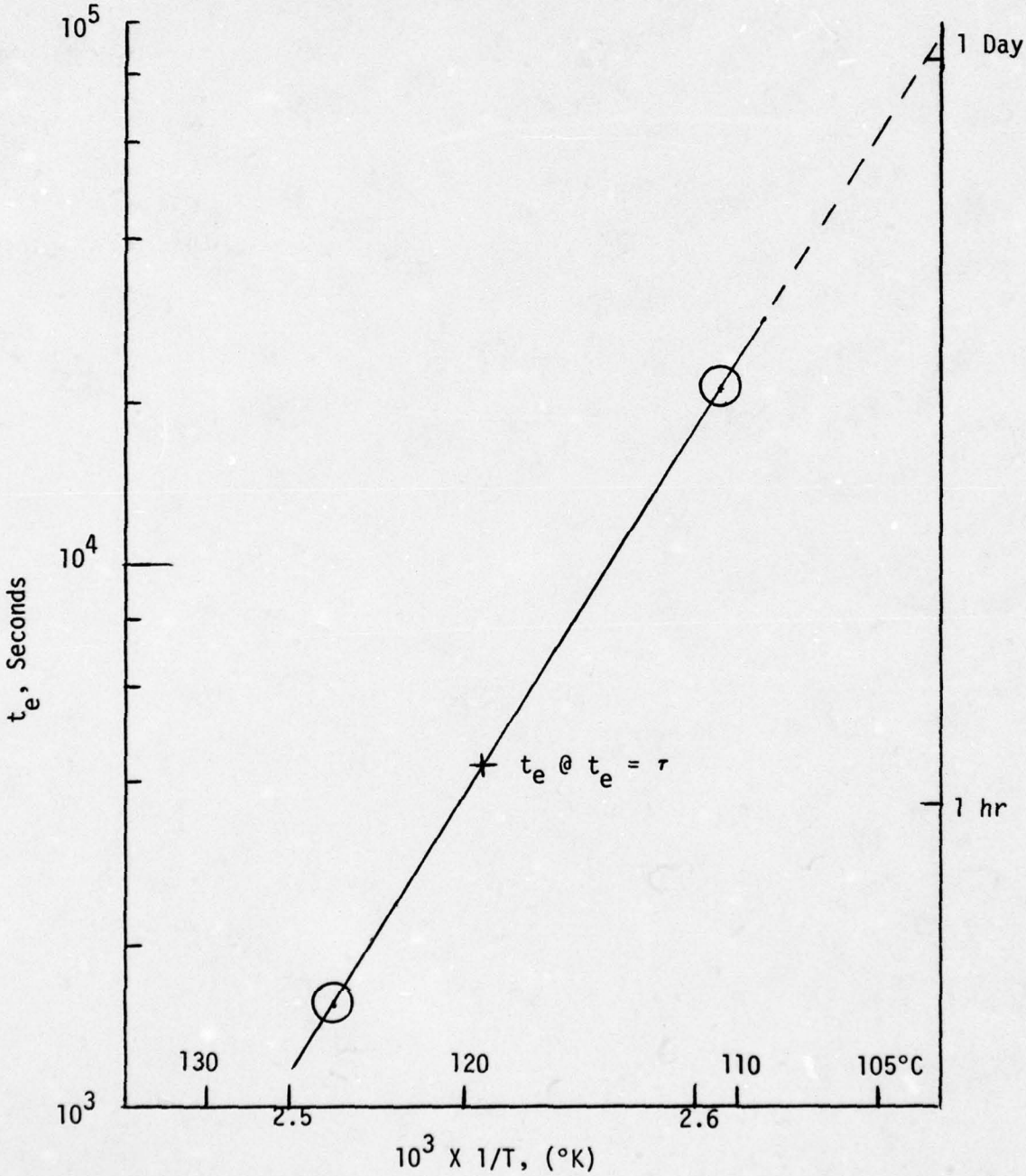


Fig. 10. Plot of Time-to-Reaction for Nitropore OBSH (SCO Runs)

THE PLANNING REQUIRED FOR, AND THE PROBLEMS ASSOCIATED WITH THE CONVERSION IN THE UNITED KINGDOM TO THE UN SYSTEM OF CLASSIFICATION OF EXPLOSIVES

Air Vice-Marshal P M S Hedgeland, RAF
Vice-President (Air) Ordnance Board and
Chairman, Explosives Storage and Transport Committee
United Kingdom Ministry of Defence

At the 16th Department of Defense Explosives Safety Seminar, my former colleague, Major General Pellereau, as some of you may recall, presented a paper on the history, role and organisation of the Ordnance Board. In his talk he touched upon the work of the Explosives Storage and Transport Committee and Mr R R Watson expanded on this in a later paper. I shall not, therefore, spend long in introducing myself as a Vice-President of the Board and Chairman of the Committee but it might be helpful if I showed you an up-to-date version of the Organisation Chart for Explosives Safety in the United Kingdom which Mr Watson presented two years ago. Brigadier Lawrence-Archer will be referring to the subject in full session tomorrow morning, so I shall keep my remarks brief.

The 1875 Explosives Act (of which I shall say more later) remains the legal basis in the United Kingdom for the movement and storage of explosives: but there have always been exceptions from its provisions for the military who operate under Statutory Instruments approved by Parliament and enacted by the Secretary of State for Defence. The safety of commercial explosives is now in the hands of the Health and Safety Executive, created by the Health and Safety at Work Act of 1974. The Ordnance Board itself is concerned with the operational safety and suitability for service of military explosives and the Explosives Storage and Transport Committee, as its name implies, with their storage and movement.

The ESTC (for short) is chaired by a Vice-President of the Ordnance Board, has a small permanent Secretariat and is composed of representatives from the departments shown on the slide, plus technical advisers on particular aspects (of which Mr Watson is one). You will note that the Health and Safety Executive provides a member, in fact Mr George Whitbread, because the armed services have to keep constantly in mind their responsibilities to the general public.

Thus the ESTC is an inter-departmental committee and its primary function is to provide the Secretary of State for Defence with the means of discharging his legal responsibilities under the Statutory Instruments. The committee classifies all explosives and prescribes conditions for safe storage and movement which are translated by the individual Service departments into regulations. Its functions are thus very similar to those of the Department of Defense Explosives Safety Board.

PRECEDING PAGE BLANK-NOT FILMED

As you can see, the committee is served, not only by its technical advisers but also by a number of specialist sub-committees whose proceedings are discussed and endorsed by the main committee.

The short paper which I am presenting today was, in fact, prepared by the Secretary, ESTC, Air Commodore H E Barker, who, but for problems of our travel budget, would have introduced it himself. It recapitulates the history of, and reasons for the adoption by the UK, and then by NATO, of a classification system for both storage and transportation, based on the United Nations classification system of dangerous goods which, as you have heard at previous seminars, was designed to produce a system that would enable world-wide transportation of these commodities to be conducted in a safe and orderly fashion. The paper goes on to discuss the planning required for, and the problems encountered in changing over to this system in the UK.

Planning for the transfer from the current system, which has been in use for some 50 years, has, in fact, been proceeding for some time past. It was originally intended that we should go over to the new system on 1 July 1976, i.e. this year. However, the need to reach agreement on some vitally important issues has meant that the conversion date in the United Kingdom will now be 1 July 1977, that is one year later than originally intended. As a consequence, the decision by your United States Department of Defense Explosives Safety Board that the United States Defense Services will be using the system for storage purposes from 1 January 1977 means that you have, to a degree, stolen a march on us. It shows however that the United Kingdom Ministry of Defence are in good company, for most of the NATO nations have already decided that they too will go over to the new system as soon as practicable.

The present United Kingdom system of classification of military explosives was originally developed by the ESTC and consequently is known as the "ESTC System". It has been widely used by other nations with whom the United Kingdom had ties, for instance Canada, Australia, New Zealand, India, Malaysia and Pakistan; it was also used by certain of the Scandinavian countries. However during the 1960s it became known in the United Kingdom Ministry of Defence that the United Nations at Geneva had instituted a "Committee of Experts" to prepare a classification system for dangerous goods which was to provide guidance on the means of regulating the packaging and transport of these commodities to developing countries, who did not possess the necessary technical facilities nor the required experience. In particular it would prescribe for the packaging and transportation of explosives, both commercial and military. At an early stage the United Kingdom Ministry of Defence arranged for representation on the United Kingdom delegation to the key committee concerned, which was, and is, the "Group of Experts on Explosives". This consisted of representatives from the United States of America, France and the United Kingdom, with Germany originally co-opted as observers. More recently, Canadian explosives experts have also participated in the work of

the group. During the course of their meetings the group of experts pooled the knowledge of the various systems in use in their countries and eventually developed a system of classification which was suitable for universal use for the transportation of all explosives, military and commercial. It became clear that although it had been originally intended as an aid for developing countries, so much effort had been put into the new system by the explosives experts of the countries participating in the group, that in the interests of facilitating world wide transportation of explosives, it would be to everybody's advantage if a single classification system could be adopted in place of the various national systems currently in use. The UN classification system was designed to cater for all modes of transportation - land, sea and air - so that its inter-modal character can help to iron out the difficulties which may exist between the various modes at present.

The first break through occurred in 1970 when the Inter-Governmental Maritime Consultative Organisation (IMCO) decided to adopt the United Nations dangerous goods classifications in respect of all dangerous goods. In the same year NATO agreed in principle to the use of the system for the classification of military explosives. The IMCO decision was a crucial one because their International Maritime Dangerous Goods Code, issued in 1972 and recently revised, is increasingly used by the maritime countries of the world for the regulation of the shipment of all dangerous goods, including explosives. The IMCO prescriptions for stowage conditions on ships, and for hazard labels based on United Nations practice, and the use of the United Nations serial number for dangerous goods, are increasingly required by shipping lines, port authorities, etc. in place of the various national hazard codes, where these exist. The United Kingdom authorities intend to use the International Maritime Dangerous Goods Code from 1977 onwards.

I mentioned earlier that in 1970 NATO had agreed in principle to use the UN classification system for all military explosives. Based on United Nationals and NATO work, the United Kingdom in 1971 produced a universal classification system for storage and transport of explosives, both military and commercial. Each element of the system represents a unique combination of explosives characteristics relevant to safe storage or transport and provides a common framework for safety regulations concerning storage and all modes of transport. There are differences within this framework, as at present. For example, certain Groups are permitted to be loaded together into a rail wagon for transport, although they are normally segregated for storage purposes. The system states which Groups may be mixed. Furthermore, it provides the elements to construct safety criteria for each mode of conveyance or storage.

The principles on which this classification system was based were agreed by NATO in 1974 and have been used by the NATO Group of Experts on Safety Conditions for Storage and Transportation of Military Explosives, AC/258, as the basis for the revised NATO Manual of Safety Principles for Storage of Military Ammunition and Explosives, which will be published early

in 1977. The associated NATO transportation manuals for the carriage of military explosives by rail, by road, by military aircraft and through harbours are now in preparation.

One of the problems in converting the military classification system for explosives to the United Nations code is that of ensuring compatibility, or compliance with, the national code of regulations. However, the explosives experts at the United Nations, and by an amazing coincidence, the explosives experts at IMCO, are the same group of people. This all sounds very cosy, but it does ensure that the systems keep in step. In the main, the delegations are derived from the departments concerned with the regulation of explosives movements in the various countries, with representatives from industry and from the Defence Departments. The fact that the makers of regulations for the conveyance of dangerous goods such as explosives in the nations concerned have been associated with the production of the international code, seems to indicate that at some time what they have agreed is suitable for universal use, will also be deemed suitable for use at home! Their efforts to make the system workable should eventually show dividends. It is, of course, often the case that change-over is not an easy process because of the need to prepare the necessary legislation and to repeal the old provisions.

And now returning to this point of legislation, as I indicated earlier, in the United Kingdom the movement and storage of military explosives is based on legislation just over 100 years old, the Explosives Act of 1875. This was instituted after an accident in October 1874 when a barge containing 5 tons of gunpowder, black powder, part of a train of 4 other barges loaded with grain, sugar, barrels of petroleum, and general cargoes, being towed by a steam tug in a canal in London, exploded under a road bridge, which disintegrated, with casualties and considerable damage to the neighbourhood. As a result of public outcry, Parliament passed the Explosives Act in June 1875. The Act contained special legislative conditions for the manufacture, storage and conveyance of military explosives which provided a form of exemption from the provisions of the Act. It empowered the Secretary of State for Defence to make regulations for the safe conduct of military explosives affairs in the United Kingdom. We are therefore separate from, but we think, stricter in many respects than the commercial explosives world. Our packaging of explosives items for instance is to a much higher standard because it has to withstand the rigours of a military environment. The ESTC, as I said earlier, is the instrument of the Secretary of State for performing many of the functions delegated to him by the Explosives Act. The necessary Statutory Instruments for the various modes of transportation by road, by rail and in harbours - are couched in legal terminology. We have had to re-write all these documents to delete all references to the existing classifications and to cater for the United Nations terminology. Lawyers being what they are, and Government lawyers in particular, this is a long-winded process.

Apart from the legal processes, arrangements have had to be made for the design and printing of various new labels, for example for packages, for the production of new hazard warning signs in the vicinity of storage buildings and so on: but the biggest problem of course, and this has been a considerable task, is the revision of the various ESTC guidance publications. These have had to be produced in their final agreed formats one year in advance of the conversion, or "C" Day, to enable the Services to revise their explosives regulations and to commence training courses for the new system. It has been said that there will not be much bother in the United Kingdom in changing to the new system as the older, experienced element in the Services, imbued and steeped in the traditional methods, are determined to retire before the changeover date so they will not be on hand to criticise and make invidious comparisons. It will be left to the younger element to cope with the new system. Be that as it may, we have the greatest confidence that the new system will be as satisfactory as the present one, with all the added advantages of it being truly international.

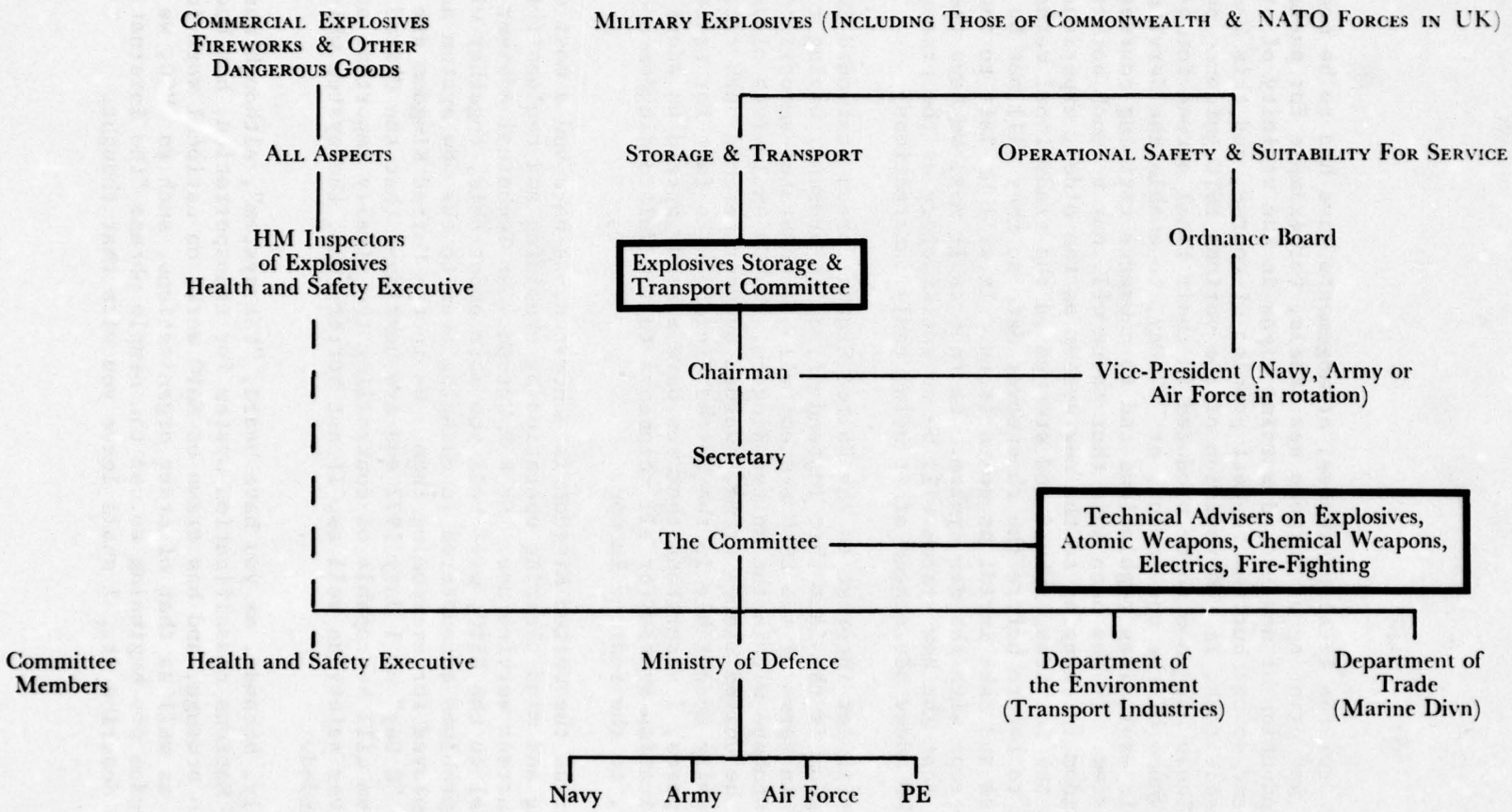
Of particular interest to the United States forces stationed in the United Kingdom is the fact that instead of, as at present, having to reclassify in terms of the ESTC system, all United States ammunition in use or in storage within the United Kingdom, the UN explosives classifications for the United States items, awarded by your Defense authorities, will be legally acceptable in the United Kingdom. In fact for transportation purposes, I understand that you have already agreed to adopt the UN classification system for all shipments to the United Kingdom and, presumably, to the rest of Europe.

So far as the United Kingdom is concerned, we have had a most useful stocktaking and mind clearing operation by examining and reclassifying all items in current service use. Mr R R Watson, our Technical Adviser (Explosives) to the ESTC, will tell you more about this, together with the technical problems encountered in changing over to the new system and the methods employed for overcoming them. We in the United Kingdom are looking forward to "C Day" on 1 July 1977 and are confident that the United Nations based system will be capable of controlling the vitally important aspects of explosives safety as well as, if not better than, the system which it has superseded.

Finally, because, as you have heard, "the system", although based on the United Nations classification system for transportation, has been extended to storage, and has drawn on NATO work, on national work in various countries, as well as that of other organisations, such as IMCO, we in the United Kingdom are beginning to use the simple phrase "the International System" to describe it. I shall leave you with that thought.

ORGANISATION CHART

EXPLOSIVES SAFETY IN THE UK



PRACTICAL PROBLEMS OF IMPLEMENTING THE UNITED NATIONS SYSTEM OF CLASSIFICATION OF EXPLOSIVES

R R WATSON
Explosives Storage & Transport Committee
Ministry of Defence
United Kingdom

SUMMARY

1. The paper discusses some of the technical and practical problems encountered by the explosives safety authorities in the United Kingdom, the United States and other NATO countries during their preparations for changing over to the UN system in 1977/78. It describes proposed solutions and assesses the relative importance of the outstanding matters. After indicating the much greater problems which would result from not changing to the international system, the paper concludes that the proposed conversion dates are remarkably opportune.

INTRODUCTION

2. In a small way the conversion of military explosives to a new system of classification resembles the conversion of pounds, shillings and pence in Britain to decimal currency. Many of the problems are similar. Careful planning is necessary to ensure a smooth change-over, statutory regulations have to be amended, labels and other tags have to be printed, and particular care must be given to training of people. There is an added complication in the conversion of explosives inasmuch as the UN authorised names and serial numbers do not quite cover all the requirements for the more exotic types.

3. An important lesson from decimalisation of the currency was that the older folk found it very difficult to change their ways. Even today in some remote areas one sees shop windows with price tags in £sd. This resistance to change is already evident in some quarters of the Services; the ESTC has been requested to produce a "backwards conversion chart" so that after July 1, 1977 personnel may work out what the old classification would have been!

4. The human problems and the need for adequate training programmes are thus quite obvious and this paper will not dwell upon them. It is the technical problems which may not be evident which will be discussed today.

CATALOGUING

5. The first step was to list all the items to be converted. If modern methods of codification and cataloguing had been universal this would have presented no problem at all. Unfortunately ESTC records, which started when the Committee was set up in 1925, rely entirely on names and sorting

by alphabetical order of key words or initial words. It took a working group three years to produce an agreed list of items to be converted. The Services had variants in terminology for the same item. Some items listed proved to be obsolete. Others in current use appear never to have been classified at all which, strictly, is illegal; thus the preparation for conversion has been a useful exercise if only to put our records in good order.

6. Ideally the final lists should show the NATO Stock Numbers and corresponding ADAC, DODAC etc codes. There has not been time to insert these so the interim lists, published on August 19, 1976 still rely on alphabetical order except that guided missiles have been grouped separately by name.

7. The traditional card index system of the ESTC is to be supplemented, perhaps even supplanted, by a computer file to facilitate the up-dating of records and to ensure that never again do we have the task of sorting out incomplete records. A bonus will be the ability to call for lists according to hazard division or compatibility group or UN Serial Number.

CONVERSION AB INITIO

8. The original concept was to convert only the generalised "Transport Designations" of the former ESTC system. Under this sytem, every item with broadly similar characteristics such as % explosive content, function and susceptibility to mass explosion or not, was listed under a single shipping name. Initially, conversion would have been simple but the old framework for classifications is now so strained, by assimilation of exotic items never foreseen in 1925, that conversion on the basis of generic names is quite misleading. To quote just one example, our Rapier missile warhead bears the shipping title "Shell, HE, boxed"! -- that is not a sound starting point for conversion to the UN classifications!

9. Reluctantly therefore the ESTC decided that every one of the two thousand or so items in current service should be reviewed ab initio to select the appropriate UN division, compatibility group and authorised name on the basis of its actual characteristics. For this reason the work was undertaken by the writer in conjunction with technical experts from the Service concerned, who had access to publications and people with detailed knowledge of components and ingredients. The advantage of this approach, which involved much more work than a general conversion would have done, is that we are confident that the UN classifications chosen are realistic in every case.

10. Informal discussion with Explosives Safety Board staff indicates that a similar problem may exist where the US Services have converted directly from DoT Class A, B or C to UN Division 1.1, 1.2, 1.3 or 1.4. In many cases one can say, for example, that Class A becomes Division 1.1, but not in all. Class A includes items which are not susceptible to mass explosion and are therefore not Division 1.1. Of course the DoD Hazard Class would indicate

this unequivocally (Class 7 is mass detonating) but it is less easy to decide whether to assign items of DoT Class C to UN classification codes 1.3G, 1.4G or 1.4S. Many pyrotechnic articles have only a moderate fire hazard and a small projection hazard, but how moderate and how small must they be to qualify as "Safety Explosives, 1.4S"?

FUZED ITEMS

11. It is a traditional feature of safe practice that one doesn't carry blasting explosives with blasting caps assembled. This concept of denying means of initiation during transportation was extended by the European railroad regulations (RID) to items such as fuzed shell; shell above a certain gross weight are prohibited in the fuzed state. One cannot deny the wisdom of this restriction in the case of fuzed 20mm HE rounds which, bulk packed, are a mass explosion hazard. It seems an outdated concept however when applied to the 155mm FH 70 shell which has a high standard of safety in the S & A mechanism. The presence of this fuze, even when assembled to the shell, does not significantly increase the risk during transport so why prohibit it?

12. NATO Group of Experts AC/258 foresaw this problem some years ago and managed to persuade the UN Group of Experts to make a realistic provision in its system of classification. Some very careful wording was inserted in the definitions of Compatibility Group F (with its means of initiation) and of "means of initiation" in the UN Glossary. In effect, shuttered fuzes are not penalised and rocket igniters don't count as means of "initiation". Note however the need to use the words "ignition" and "initiation" carefully in order to maintain this distinction. In common parlance, unfortunately, the words are often interchangeable.

13. Some teething pains are likely in the application of this rather subtle distinction. Already it has been noticed that the German MOD appears not to be taking full account of it: a remarkably high proportion of its items are still in Compatibility Group F. Once there has been a general exchange of conversion lists, it should be possible in a forum like the NATO Group AC/258 to eliminate any differences in interpretation and application of the classification criteria.

IDEAL AND ACTUAL ITEMS

14. The NATO participants in the UN Group of Experts tried hard to anticipate practical problems but one was not foreseen. This relates to the difference between what the designer of ammunition sees on his drawing board and what the Service user sees in his incident report. The designer may assure the classification authority that a fuze has two independent safety devices, according to his drawings, but the user may point out from bitter experience that, due perhaps to mis-assembly at the factory, the fuze can be actuated by accident and may not properly seal. In this situation, does the classification authority assign the item to Compatibility Group F or not? Is he

classifying the item as it should be or as it is in fact? Or, even more difficult to say, is he to assess the statistical likelihood of there being a certain percentage of mis-assembled fuzes in service and classify accordingly.

15. In the UK it has been decided that prudence requires a third course of action. In the few cases where serious malfunction or mis-assembly has been reported, a "Pink Card" classification has been assigned. This requires that all transportation shall be under the direct physical control of the MOD. In practice this means by Service vehicles as opposed to common carriers. Only after the safety problem has been cleared up will the ESTC issue an orthodox classification within the UN system.

16. Even this procedural device did not entirely obviate the problem. Recently it was found to be necessary to recall stocks of a certain item from Units scattered world wide, in order to radiograph them to assess the incidence of mis-assembly of components. The ESTC prescribed that, in view of the evident doubts on safety, they could only be transported by Service vehicle. A practical solution was worked out by CILSA's staff who pointed out that by packaging the items to qualify for code 1.4S (Safety Explosive), one could with a clear conscience ask the RAF to transport them. If the consequences of accidental actuation are not significant, the likelihood of such an event in transport is immaterial.

CONFUSING TERMINOLOGY

17. In the course of assessing UK ammunition and selection of appropriate UN authorised names, the writer came across some remarkable differences among the use of terms by the three Services. Examples appear in some of the Figures. If one imagines these differences to be compounded by the differences in American and English usage, the scope for misunderstanding among NATO countries becomes evident. The French speaking members of NATO have often made good natured complaints about the number of interpretations of the words "primer", "primed", "priming" and "primary" in connection with explosives. At least the adoption of standard UN Serial Numbers will eliminate the need to rely on words and doubtful translations.

LACK OF SUITABLE UN ENTRIES

18. When the UK began conversion two years ago it soon became apparent that the existing 340 or so UN Serial Numbers were insufficient to cater for all the more exotic items used in guided missiles and the aerospace industry. Many of the smaller components are not complete end-products so it is difficult to assign meaningful names to complement their catalogue numbers. This problem was solved at the meeting of the UN Group of Experts from August 9 to 13th, 1976 when joint US/UK proposals were adopted for rather flexible entries "Articles, explosive, not otherwise specified" in Division 1.4 and various compatibility groups. The restriction to Division 1.4 is

intended to prevent abuse of so general an entry. Another important innovation is "Articles, explosive, not otherwise specified" in Compatibility Group L and Divisions 1.1, 1.2 and 1.3. This will enable the competent national authority to classify even the most awkward items pending submission to the UN of a case for a new specific entry; the penalty will be acceptance of rather stringent conditions for transportation provisionally.

NAMES AND SERIAL NUMBERS

19. The original aim - and this is still the long term goal - was to reduce the plethora of national designations and classifications to the absolute minimum of information really necessary for normal transportation and immediate response in an emergency. For this purpose, the 31 classification codes (1.1A to 1.4S) should suffice. These codes avoid problems of language and are admirably terse for use by computers and by telephone or radio in an emergency.

20. To abandon the traditional several hundred shipping titles, used for regulatory purposes, was just too radical a step so the UN provided about 340 internationally agreed "authorised names" to cover all military and commercial explosives. Serial numbers were also assigned, in line with the procedure for other classes of dangerous goods.

21. The British Army had resisted the use of anything beyond the basic 31 classification codes but latterly has reluctantly accepted the proposition that the conversion lists should show the UN Serial Number since IMCO and other authorities are recommending this be shown on shipping papers. It is understood that a similar difference of opinion exists in the US where the USAF has worked out the UN Serial Numbers for every item in its inventory but the other Services feel that this can be added later if necessary.

22. The list of authorised names, with alternatives in some instances, which the UN published in 1973 left much to be desired. It had evolved through the interaction of national representatives each putting forward names akin to their own shipping names. There has been considerable consolidation recently and the list to be published late in 1976 or early in 1977 is much more acceptable. Consequently the ESTC believes that the Services should, in their own interests, publish lists showing UN Serial Numbers as well as the basic classification codes. There is no need to publish the authorised names in stock lists since each Serial Number, to be shown in Statutory Instruments, corresponds uniquely to one name.

OUTSTANDING MATTERS

23. Up to last month a cause for some serious concern was the lack of any means for securing UN approval for additional entries (names and Serial Numbers) in the event that some novel explosive device should not fit into the existing system. There had been from one to two years delay because the

UN Group of Experts was not authorised to meet more frequently, for financial reasons which are related to UN politics. It is gratifying to report that two blanket entries mentioned earlier will avoid acute problems. There remains a long term need for some review body or standing committee which could regularly update the list and take account of developing explosives technology. However this is not a serious problem now.

24. Variations in the interpretation of the definitions of the compatibility groups are likely to create anomalies until a general exchange of lists and ideas can harmonise national practices. Countries like the US and UK can play a leading role here and assist countries which do not have bodies like the Explosives Safety Board and the Explosives Storage and Transport Committee. The anomalies are likely to be irksome rather than hazardous.

THE FUTURE

25. Now that some countries have implemented the IMCO IMDG Code, it is becoming more and more frequent a requirement for the consignor to provide the UN classification on shipping papers. The adoption of the UN system for storage by many NATO countries, as a means for specifying quantity-distances criteria, will soon make it imperative that visiting forces can quote UN classification details for their stocks. At previous seminars the writer has urged the US DoD to consider the benefits of adopting the UN system. Now it remains only to remind the DoT of the disadvantages of not using for transportation the system which DoD has adopted for storage from January 1977, which the UK has adopted for storage and transport from July 1977, and which Germany has adopted for harbours (already) and storage (1977). Other NATO countries have given declarations of intent to change in the next few years.

UK SERVICE DESIGNATION	CODE	UK SHIPPING TITLE
Cartirdge, cockpit, canopy jettison No.2	6X	Tubes, percussion
Remover with cartridge, aircraft canopy	$6^{SC}X$	Cartridges, SA separate
Cartridge,seat ejection(Folland)drogue No.1	$6^{SC}X$	Cartridges, shot gun
Cartridge,separation,drogue, SKT - 197	6X	Igniters, electric
Grenade, hand, No. 75 anti-tank	7Z	Mines, contact
Grenade, rifle, HE/AT, Energa Type G	8Z	Grenades, HE/HC
Grenade, rifle, Energa Type H1	8X	Rockets, training
Grenade, rifle, Energa Type H2	6X	Fuzes
Grenade, rifle, Energa Type H3	$6^{SC}X$	Cartridges, SA separate
Release fuze, DM 39	8X	Mines, anti-personnel
Mine, anti-personnel, buried	8Z	Mines, anti-personnel
Mine, AP, Airburst, X12 E1	8X	Mines, land
Mine, Anti-tank, Mk 7	7Z	Mines, contact
Mine, limpet	7Z	Charges, demolition
Mine, jumping	6X	Shell, HE (boxed)

Figure 1 Some Confusing Shipping Names (para 8)

COMPATIBILITY GROUP 'F'

ARTICLE CONTAINING A SECONDARY DETONATING EXPLOSIVE SUBSTANCE,

WITH MEANS OF INITIATION,

WITH OR WITHOUT A PROPELLING CHARGE

Figure 2 A Crucial Definition (para 12)

UK SERVICE DESIGNATION	CODE	UK SHIPPING TITLE
Cartirdge, cockpit, canopy jettison No.2	6X	Tubes, percussion
Remover with cartridge, aircraft canopy	$6^{SC}X$	Cartridges, SA separate
Cartridge,seat ejection(Folland)drogue No.1	$6^{SC}X$	Cartridges, shot gun
Cartridge,separation,drogue, SKT - 197	6X	Igniters, electric
Grenade, hand, No. 75 anti-tank	7Z	Mines, contact
Grenade, rifle, HE/AT, Energa Type G	8Z	Grenades, HE/HC
Grenade, rifle, Energa Type H1	8X	Rockets, training
Grenade, rifle, Energa Type H2	6X	Fuzes
Grenade, rifle, Energa Type H3	$6^{SC}X$	Cartridges, SA separate
Release fuze, DM 39	8X	Mines, anti-personnel
Mine, anti-personnel, buried	8Z	Mines, anti-personnel
Mine, AP, Airburst, X12 E1	8X	Mines, land
Mine, Anti-tank, Mk 7	7Z	Mines, contact
Mine, limpet	7Z	Charges, demolition
Mine, jumping	6X	Shell, HE (boxed)

Figure 1 Some Confusing Shipping Names (para 8)

WITH ITS MEANS OF INITIATION

" ... THE CONTRIVANCE HAS ITS NORMAL INITIATING DEVICE ASSEMBLED TO IT AND THIS DEVICE IS CONSIDERED TO PRESENT A SIGNIFICANT RISK DURING TRANSPORT."

WITHOUT ITS MEANS OF INITIATION

" THE MEANS OF INITIATION CAN EVEN BE ASSEMBLED TO THE CONTRIVANCE PROVIDED THERE ARE PROTECTIVE FEATURES SUCH THAT THE DEVICE IS VERY UNLIKELY TO CAUSE DETONATION OF THE CONTRIVANCE IN CONDITIONS WHICH ARE ASSOCIATED WITH TRANSPORT."

(NB AN IGNITING FUZE IS NOT A MEANS OF INITIATION)

Figure 3 Shuttered Fuzes etc are not Penalized (para 12)

SOME VERY RECENT ADDITIONS TO THE UN LIST

AMMUNITION, PRACTICE	1.4 G
AMMUNITION, PROOF	1.4 G
DETONATORS FOR AMMUNITION	1.2 B, 1.4B & 1.4 S
PROJECTILES, with burster or expelling charge	1.2 D & 1.4 D
PRIMERS, CAP TYPE	1.1 B, 1.4 B & 1.4 S
PRIMERS, TUBULAR	1.3 G, 1.4 G & 1.4 S
COMPONENTS, EXPLOSIVE TRAIN, not otherwise specified	1.2 B, 1.4 B & 1.4 S
ARTICLES, EXPLOSIVE, not otherwise specified	1.4 (B, C, D, G & S)
ARTICLES, EXPLOSIVE, not otherwise specified	1.1 L, 1.2 L & 1.3 L

Figure 4 (para 18)

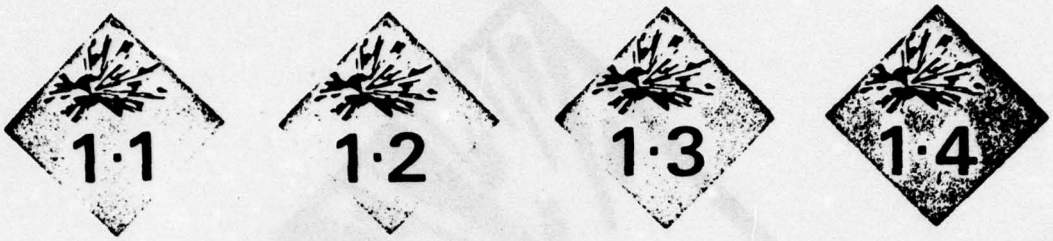


Figure 5 Final Version of Package Label (August 1976)

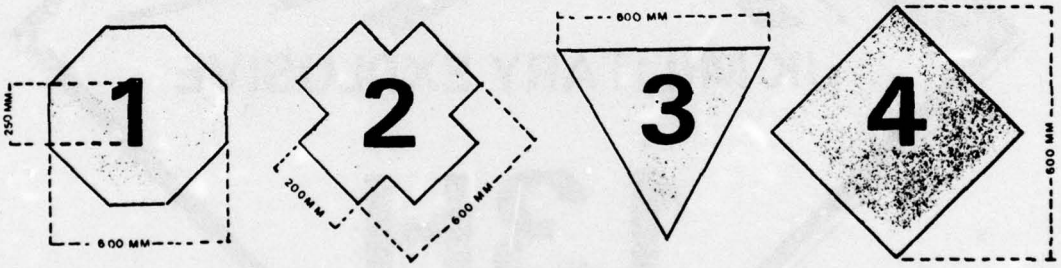
FIRE SYMBOLS

1. FIRE DIVISION SYMBOLS

a For use on road and rail transport



b For use on buildings and stacks

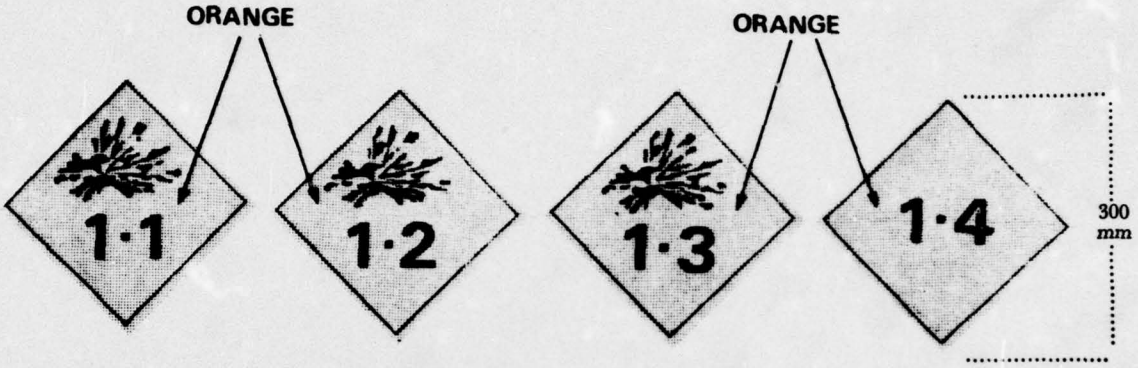


2. SUPPLEMENTARY FIRE SYMBOLS

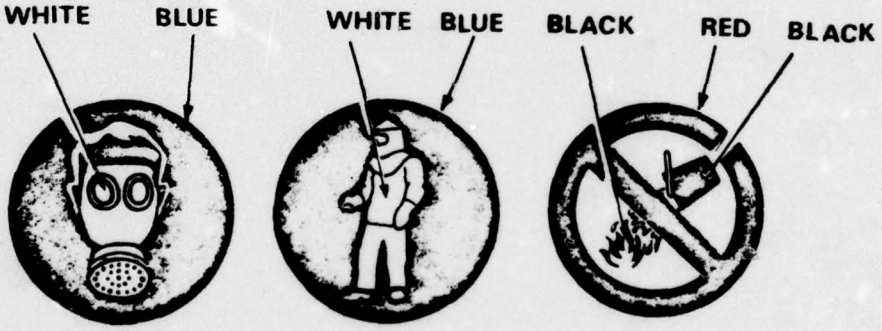
Advisory	Advisory	Advisory	Prohibitive
			
Radiological Hazard	Breathing Apparatus	Protective Clothing	No Water to be used

Figure 6 Original UK proposals (1975) before Modification

1. FIRE DIVISION SYMBOLS FOR USE ON ROAD AND RAIL TRANSPORT:



2. SUPPLEMENTARY FIRE SYMBOLS:



BREATHING APPARATUS PROTECTIVE CLOTHING NO WATER TO BE USED

Symbols are on a white background 300 mm square.

Figure 7 Final UK Proposals to NATO (August 1976)

EXPLOSIVES ON MOTOR VEHICLES

AN UPDATE OF DOT REGULATIONS

D. W. MORRISON
Federal Highway Administration
Department of Transportation
Washington, D. C.

In considering the remarks that I would make this morning at this Explosives Safety Board Seminar, I thought that it was best to give an overview of the Department of Transportation (DOT) and the statutory authorities under which the Bureau of Motor Carrier Safety (BMCS) of the Federal Highway Administration operates. Also of interest would be the mission of the BMCS.

The mission of the Bureau is:

1. To reduce deaths and injuries from commercial vehicle involvement.
2. To increase the public safety in the movement of hazardous materials by highway.
3. Provide technical assistance to motor carriers in reducing cargo theft and losses.
4. Enforcing the Environmental Protection Agency's Motor Carrier Noise Standards.

PRECEDING PAGE BLANK-NOT FILMED

The authority under which the Bureau operates includes the Department of Transportation Act, the Interstate Commerce Act, and the Explosives and Combustibles Act. In addition, there are delegations of authority and agreements with many of the several States and various subdivisions thereof.

The Bureau consists of a Headquarters organization, with the Office of the Director, a Regulations Division and a Compliance Division. Field Staff is located in each Regional Federal Highway Administrator's office and technical guides are provided to these offices by Headquarters' staff.

The magnitude of the task which the Bureau has facing it is quite large, and in order to give you some idea, the following statistics are provided for your information. We have approximately 160,000 motor carrier entities with 4 million commercial vehicle drivers and 3 million commercial vehicles operating under our safety jurisdiction.

The Regulations enforced by the BMCS are the Federal Motor Carrier Safety Regulations, the DOT's Hazardous Materials Regulations especially as they relate to motor vehicles and the Interstate Motor Carrier Noise Emission Compliance Standards.

Those of you associated with Department of Defense, well know the only thing permanent in Government is change. At DOT, it is no different. We are constantly making changes, especially in our Hazardous Materials and Federal Motor Carrier Safety Regulations.

We do not make changes just for the sake of doing so. We realize that many provisions in our regulations are now outmoded. Technology has brought us new containers, new techniques for packaging, and new means of conveying material. We have become more aware of the need to better communicate the dangers associated with materials classified as hazardous. We are also aware of the ever changing patterns of distribution associated with highway transportation. These are a few of the reasons why the Department's Hazardous Materials Regulations are continually being changed. With these thoughts in mind, let us review some of the recent changes and, if time permits, some of the changes that are planned for the near future.

During April of this year the Department published several rule changes that related to explosives. Docket No. HM-116, published April 9, amended § 173.86 which pertained to procedures for defining, approving and classifying new explosives. It should be noted that this section

requires the filing of certain information with DOT before new explosives may be shipped. These requirements do not apply to shipments consigned to a laboratory for examination. The filing requirement is not new. It has been in existence since about 1970. If you have not already done so, I would suggest that those of you who are responsible for shipping new explosives check your records to make sure you have complied with the filing requirements. You should check back to, at least, 1970.

On April 15 the Department published its most far reaching, and probably most controversial amendments. I am speaking, of course, of Docket Nos. 103 and 112. Included in these amendments are new placarding requirements, including format, and new shipping paper requirements. The new requirements affect both the shipper and carrier. These new rules generally became effective July 1, 1976. However, the mandatory date for use of the new placards and the new shipping paper format is July 1, 1977. Preprinted shipping papers containing the previously authorized shipper's certificate may be used until July 1, 1979. Time does not permit a detailed analysis of these new regulations but it behooves each of you to become thoroughly familiar with them.

Presently, the Department is considering the creation of a new class of explosive material. The new classification, if adopted, would be called

"Blasting Agents." This new class of material would most likely include some of the materials now classified as oxidizers.

In the new future Docket HM-110 will be reopened insofar as it concerns maintenance and repair to motor vehicles containing hazardous materials. § 177.854(g) and (h) will ultimately be amended to deal more realistically with repairs made to vehicles while ladened with hazardous materials. We sincerely hope that you will respond to the Notice and share your thoughts with us.

An Advance Notice of Proposed Rulemaking was published last February. It dealt with Part 395 of the Motor Carrier Safety Regulations. That is the Hours of Service Regulations. The closing date for comments was July 31. A Notice of Proposed Rulemaking will be published as soon as our staff review of the comments received is completed. Any changes in the Hours of Service Regulations could dramatically affect your distribution systems. I would strongly suggest that once the Notice is published, you carefully study the entire proposal and reply to it according to your needs.

Finally, I wish to remind you that once the Transportation Safety Act of 1974 (Public Law 93-633) is fully implemented, the Department's Hazardous Materials Regulations will apply to any hazardous material that

is in commerce. That means that they will apply to each and every shipper, carrier, and consignee. Each of you will have a vested interest in every new rule that is promulgated. I urge you to participate in our rulemaking process every time the occasion arises.

ADAPTATION OF COMMERCIAL INTERMODAL FREIGHT
CONTAINERS FOR CARRIAGE OF AMMUNITION

Donald I. Willis
DARCOM Ammunition Center
Savanna IL

VG 1

ADAPTATION OF COMMERCIAL INTERMODAL FREIGHT CONTAINERS FOR THE CARRIAGE OF AMMUNITION

VG 2

The US Army Materiel Development and Readiness Command (DARCOM) Ammunition Center is located in the northwestern corner of Illinois, on the banks of the Mississippi River about 150 miles west of Chicago, and approximately 70 miles north of the Rock Island Arsenal. Although we are located with the Savanna Army Depot Activity, we are a tenant organization, functioning as a separate Class II Activity.

One of the major missions assigned to the Center and one which has been performed for over 35 years is the development of storage and outloading procedures for Army ammunition. This presentation relates to that mission.

Basically, this presentation will address the use of commercial intermodal containers for shipping DOD ammunition, and will specifically address:

VG 3

The development of wooden dunnage cargo restraint systems, and:

The evaluation of the wooden dunnage systems through accomplishment of standard dynamic tests and a trial shipment program.

Also, the effort toward developing a DOD container inspection criteria handbook will be discussed briefly.

Why is there a need to move ammunition in commercial containers?

It is for two reasons.

We have lost our breakbulk ship capability, and DOD does not own a sufficient number of Milvan containers to support a major contingency. Additionally, the current DOD policy restricts the purchase of additional containers.

VG 4

If all US flag ships were called back to port today, about 70% of those ships would be containerships. By 1985 the 70% figure is expected to climb to 85%. Therefore, it can be readily determined that ammunition will have to be containerized to support a large deployed force - at least during the early months of a conflict. A significant amount of time would be required to outfit available but "mothballed" breakbulk type ships, should it be desirable to revert to breakbulk shipping. Even after the additional breakbulk ships are put into service, some ammunition might still have to be containerized to achieve the desired logistic objectives. A combined breakbulk/containerized posture certainly will depend on shipping priorities, but cannot be ignored when recognizing that ammunition is expected to be more than one-third of the total tonnage moved in support of a large deployed force.

VG 5

Where will the commercial containers come from?

There are 220,000 plus US-owned 20-foot containers available. These containers are represented on the right side of this viewgraph, with those in the lower left-hand corner marked to indicate the quantity required to support a possible contingency. The three small, grouped squares on the left side represent the DOD-owned Milvans. It is apparent from this display that the use of commercial containers is a necessity.

VG 6

(blank) How did the Ammunition Center get involved with developing the wooden dunnage cargo restraint systems?

Our Center has been involved with the ammunition containerization program since 1969.

The loading and bracing procedures used for the 226-container test shipment which was successfully delivered to Vietnam in January 1970 were designed and tested at the Center.

The configuration of the mechanical type cargo restraint system installed in the 4,500 ammunition Milvans was recommended by the Center, and subsequently validated through the accomplishment of test programs designed to satisfy regulatory requirements.

Many test programs have also been conducted to evaluate and prove the validity of loading and bracing procedures applicable to Milvan loads of ammunition.

Additionally, several contractor-designed cargo restraint systems installed in commercial containers have been tested.

Therefore, it was logical that the DOD project manager for containerization task the Center to investigate the feasibility of using wooden dunnage to secure loads of ammunition in commercial containers for shipment by all surface modes of transport. This assignment was received at the beginning of 1975, with preliminary analysis and design completed for evaluation testing during the spring months.

VG 7

Acceptable intermodal containers are constructed in accordance with American National Standards Institute (ANSI) or International Organization of Standardization (ISO) specifications. Also, depending on the material used in fabrication, these containers can be grouped into three broad categories; steel, aluminum or fiberglass reinforced plywood. All three types were used in our program, and all three were found to be acceptable.

The depiction on this viewgraph is supposed to represent a floor, an end wall and a side wall of a container. Although there are numerous pertinent ANSI/ISO design values which apply to containers, only three are indicated on this picture. The design values 0.4 (indicating the strength of an end wall) and 0.6 (indicating the strength of a side wall) are of paramount importance. The 0.4 end wall strength is an important factor because the resultant load on an end wall is 2.5 when a loaded container is subjected to a rail impact test in accordance with the requirements specified within Title 49 Code of Federal Regulations. Also, the 0.6 side wall strength is an important factor because the resultant load on a side wall is 1.0 when a loaded container is subjected to a tilt test as required by the US Coast Guard.

Although not indicated on this viewgraph, containers are built with a strong vertical frame member at each corner. These members are called corner posts. They are fastened into a relatively strong floor structure and connected at the top through substantial eave rail frame members. Analysis and tests proved that the corner posts were adequate to support the largest longitudinal forces expected during transport. Wooden dunnage was arranged to transfer load-induced lengthwise forces to the corner posts. Similarly, analysis and tests proved that the upper side rails and the bottom side rails of the floor structure were adequate to support the largest lateral forces expected during transport. Again, wooden dunnage was arranged to transfer load-induced crosswise forces to the upper and lower side rails.

VG 8

This is a side view of a typical dunnaging system. The diagram shows the use of heavy forward and rearward load-supporting bulkheads, and side-strength augmenting dunnage assemblies.

VG 9

Here is a photograph of a steel container. Corner posts can be seen at the four corners, and the upper and lower side rails are also shown.

VG 10

This is a fiberglass reinforced plywood container. Again the strong frame members can be identified in this photograph.

VG 11

Wooden dunnage assemblies were constructed in sections to the maximum extent possible. This permitted the prefabrication and stock piling of dunnage assemblies so that a minimum amount of time was required during actual container stuffing operations. A partial load of inert palletized 155MM separate loading projectiles are seen here with some of the required dunnage sections in place.

VG 12

This is a view of a partial load of inert unitized 105MM howitzer ammunition. It can be seen that the units are loaded two-high. This could not be done in an 8-foot high container such as a Milvan. The depicted container is an eight and one-half-foot high unit, as are about 45% of the commercial containers. Containers higher than 8 feet can enhance containerization of many standard unit loads such as the 105MM unit.

VG 13

This viewgraph and the next one depict full loads of separate loading projectiles and howitzer ammunition ready for test.

VG 14

Some containers have rear corner posts which project one inch into the doorway on each side. This projection is used to capture the blocking. However, some containers do not have projecting corner posts, as the container shown here. For these types of containers it was necessary to use some Z-shaped metal blocks to capture the rear blocking. The front portion of a block fits into a groove ahead of a post and the rear portion of the block provides a ledge to support the rear blocking.

VG 15

This is an aerial view of the area where we conduct our dynamic type tests. Three different types of tests were conducted in this area. The oval track supports part of a standard truck test procedure. Rail impact testing is conducted on the railroad line shown at the right, and containers are tilt-tested in the middle area.

VG 16

Two test specimens are shown here on a railcar in a trailer-on-flatcar (TOFC) configuration, ready to be rail impact tested. Rail impact testing is accomplished by rolling a specimen car into a line of stationary railcars at speeds of 4, 6 and 8 miles per hour (MPH) and at 8 MPH with the opposite end of the specimen car striking into the line of stationary cars.

VG 17

Here is a container on chassis ready to traverse a hazard course which is step one of the standard 5-step road test procedure. Road test environments include hazard courses, over the road travel and forward and rearward panic stops. The hazard course provides the most severe environment. Hazards impart high vertical shocks and side to side rolling reactions to a test specimen. The US Coast Guard, as well as the Bureau of Explosives of the Association of American Railroads, relies on the road test to evaluate the effectiveness of loading, blocking and bracing methods.

VG 18

A tilt test is unique to the US Coast Guard. They require the test to evaluate the strength of conainer side walls and the effectiveness of sway brace type blocking used within a load. To accomplish a tilt test, a container is picked up and rotated 80 degrees to one side as seen here.

VG 19

(blank) Following the successful completion of all of the tests which were witnessed by representatives from various agencies, including the Bureau of Explosives and the US Coast Guard, some apprehension was expressed by the representatives from the two identified agencies. This apprehension was based primarily on one factor - the workmanship of the crews applying the wooden dunnage. It was a valid point, therefore, as an on-going action to further evaluate the system, a trial shipment program was implemented.

The trial shipment involved a round trip movement of four instrumented container loads from CONUS installations to Germany, where the containers were stripped and restuffed using European lumber, and then returned to the original shippers in CONUS.

All containers were loaded and dunnaged by inexperienced crews in CONUS and in Germany.

Two container loads of palletized inert 500-pound MK82 bombs were shipped in a container-on-flatcar (COFC) configuration from the Naval Weapons Station Earle to the Military Ocean Terminal Sunnypoint.

Two container loads of palletized inert 105MM and 155MM ammunition were shipped in a trailer-on-flatcar (TOFC) configuration from the Savanna Army Depot to the Military Ocean Terminal Sunnypoint.

VG 20

After the loads arrived at Sunnypoint they were inspected and the instrumentation was serviced in preparation for the ocean voyage.

VG 21-22

Nothing was found out of order except in one of the Navy loads.

VG 23

The inexperienced-crew theory came into play. For some unknown reason, the loading crew had shimmed the rear blocking outward almost completely free from the dunnage restraining corner post at one side of the container.

This deficiency can be seen at the left side of this photograph. Although the rear blocking still restrained the load, it had slipped slightly rearward. No corrective changes were made to the blocking, and the container doors were reclosed in preparation for the next leg of the voyage.

VG 24-25-26-27-28-29-30

These next few viewgraphs show container handling at Sunnypoint, from a container holding area, to ship side, to stowed positions aboard the American Ranger.

As shown, the containers were weather deck stowed in positions believed to provide the roughest ride.

The ship sailed for Nordenham, Germany, during the latter part of February this year, arriving during early March without incident.

VG 31

The ocean voyage was intentionally scheduled to hopefully encounter a North Atlantic storm. Although an all-out storm was not met, the voyage was not entirely smooth sailing all the way. Even though a prolonged period of substantial roll was experienced, the instrumentation on the test loads only showed minor traces of imparted forces.

VG 32

(blank) At Nordenham the containers were offloaded and moved to Miesau Army Depot in southern Germany on European container railcars.

A visit was made to Miesau to inspect the arrival condition of the loads and to service the instrumentation, and to ensure that the loads were properly prepared for their return to the states.

Returning, the containers left Miesau during the latter part of April moving under the same routing used to ship them to Germany, except in reverse order.

Their home stations were reached during the last part of May or early June in excellent condition - you could not determine that the loads had been shipped even one mile, although they had moved several thousand.

What did all this prove?

Basically, containerizing ammunition with wooden dunnage in commercial containers can provide a viable and responsive logistic system to fill an existing gap.

Dunnage costwill vary between loads. For the trial shipment loads, the cost ran between $150 to $250 per container - not too bad when compared to a $1,500 figure for a mechanical type cargo restraint system.

Improvement to the rear blocking retention method is required. An improved, fool-proof method has been designed, and is to be tested at our Center as an on-going action.

After this evaluation test, our proposal will be - now let us ship some live ammunition in commercial containers to gain system expertise.

VG 33

Quality of commercial containers used for shipping ammunition is a major controlling factor - it can make or break the system.

Recognizing this factor during the early development stages, our command took action to establish a workable quality control system. Under a joint Army/Navy program a DOD inspection criteria handbook has been drafted. Our Center submitted this handbook for review action earlier this year.

On 23 and 24 September a joint meeting is scheduled in the DC area. Several representatives from private industry will attend the meeting on the first day, and on the second day DOD attendees are expected to establish guide line parameters to facilitate the development of a final draft.

This handbook is to be used by both container owners and DOD inspectors.

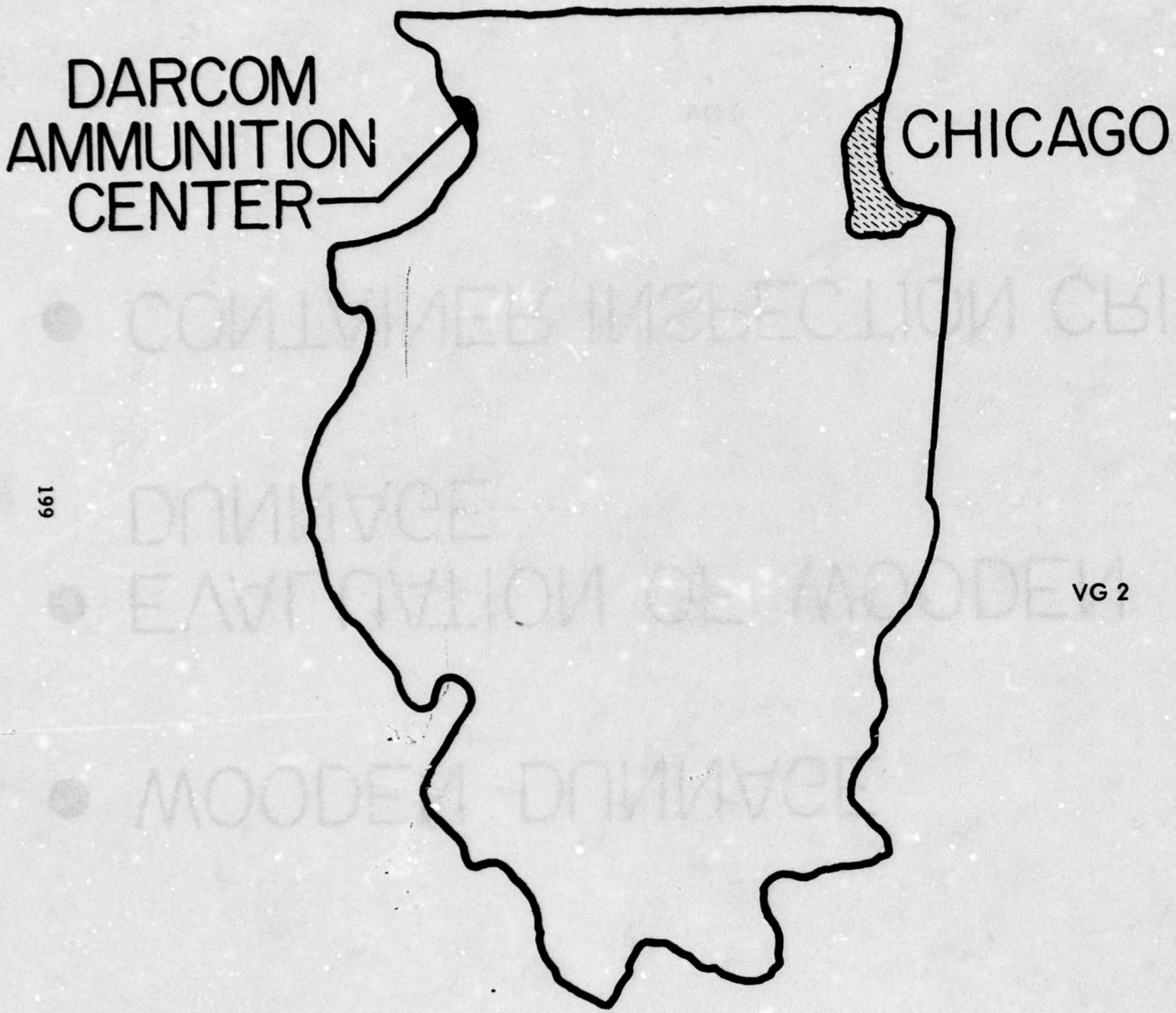
The handbook will be the vehicle which will ensure the use of safe containers for shipments of ammunition, without being unduly restrictive, which would negate the effectiveness of our commercial resources.

VG 34
(blank)

DODESB 17TH EXPLOSIVES SAFETY SEMINAR
14-16 SEPTEMBER 1976

ADAPTATION OF COMMERICAL INTERMODAL FREIGHT CONTAINERS FOR CARRIAGE OF AMMUNITION

VG 1

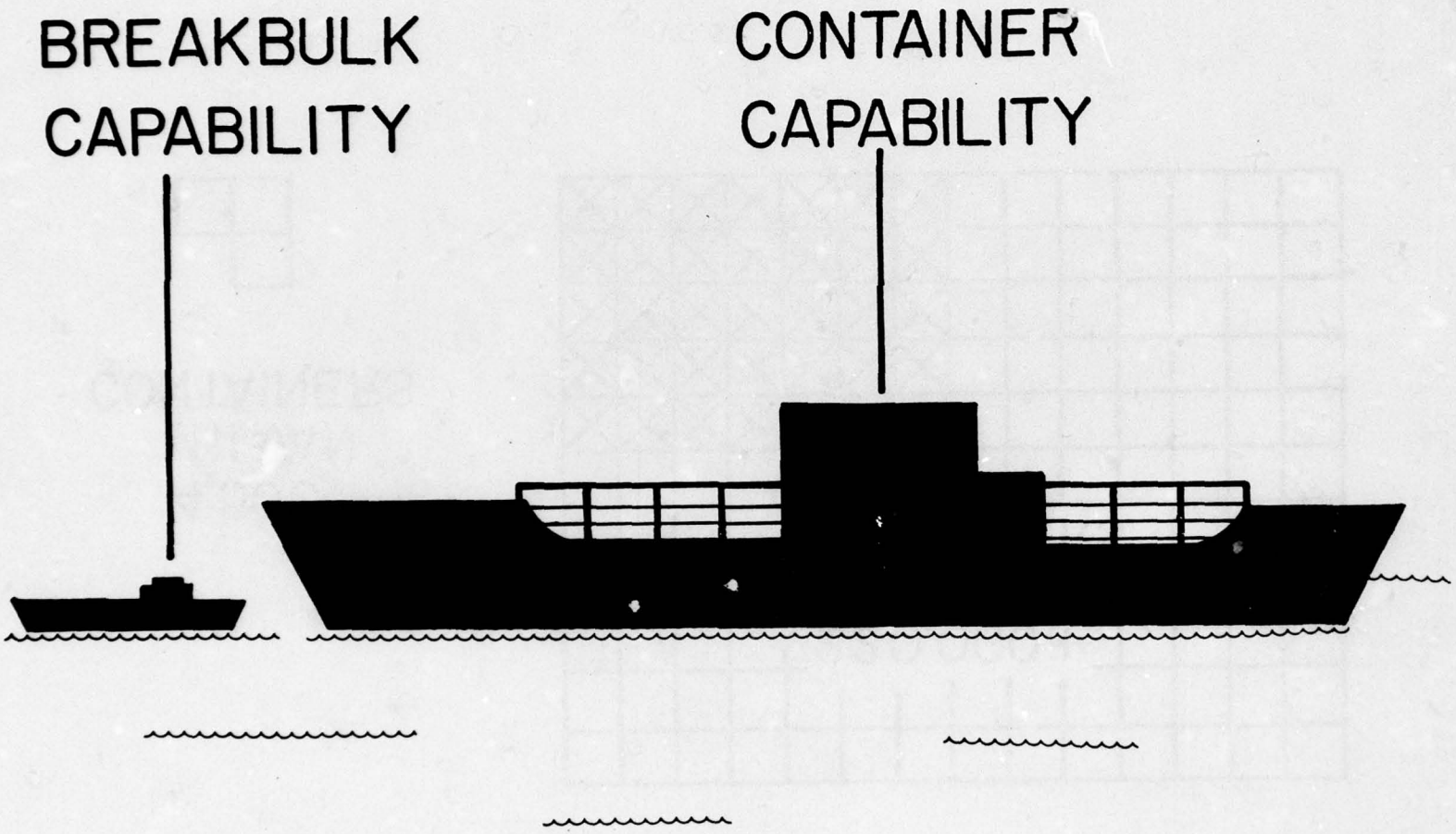


199

VG 2

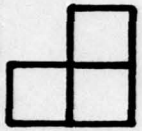
- WOODEN DUNNAGE
- EVALUATION OF WOODEN DUNNAGE
- CONTAINER INSPECTION CRITERIA

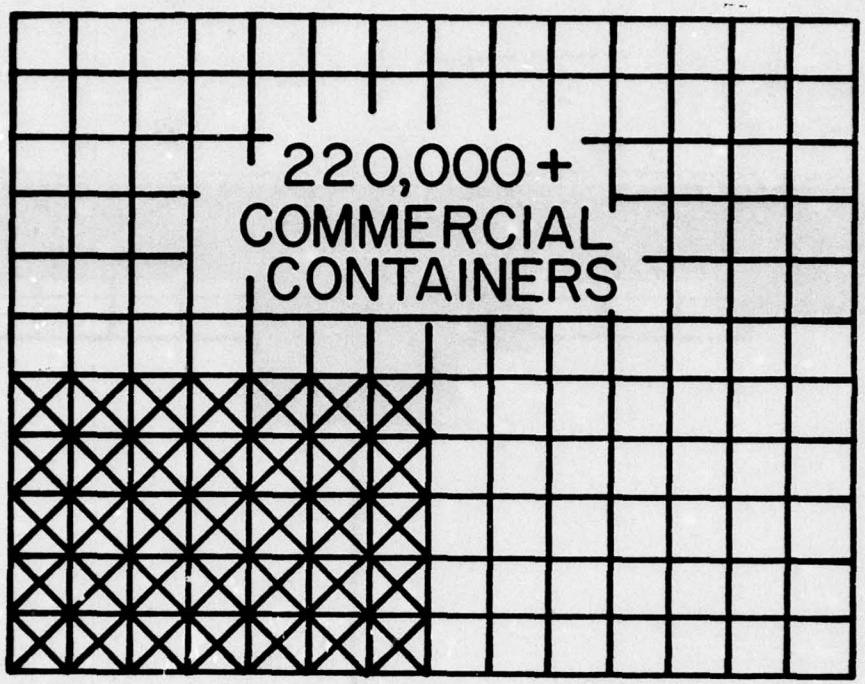
200



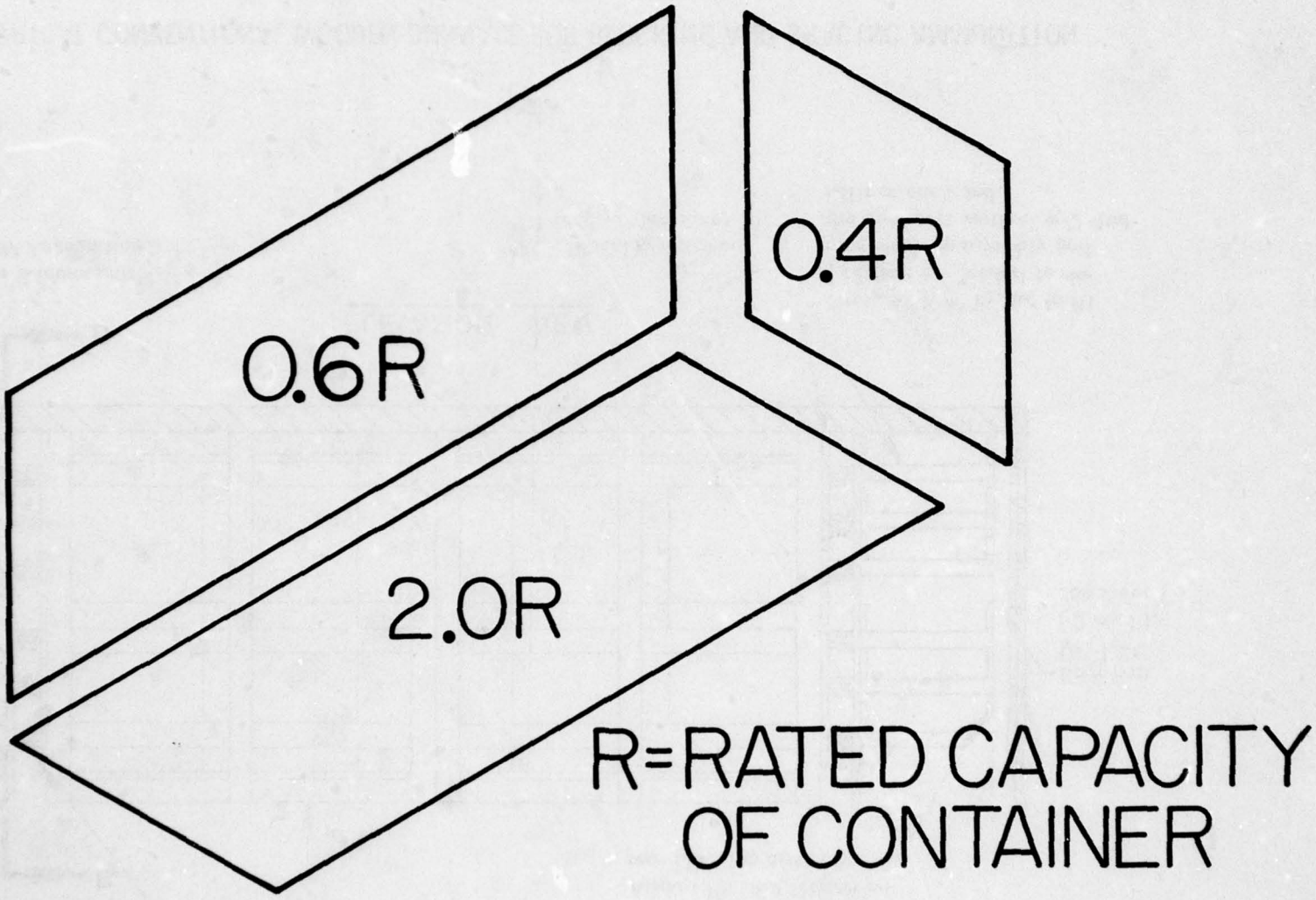
VG 4

4,500
MILVAN
CONTAINERS

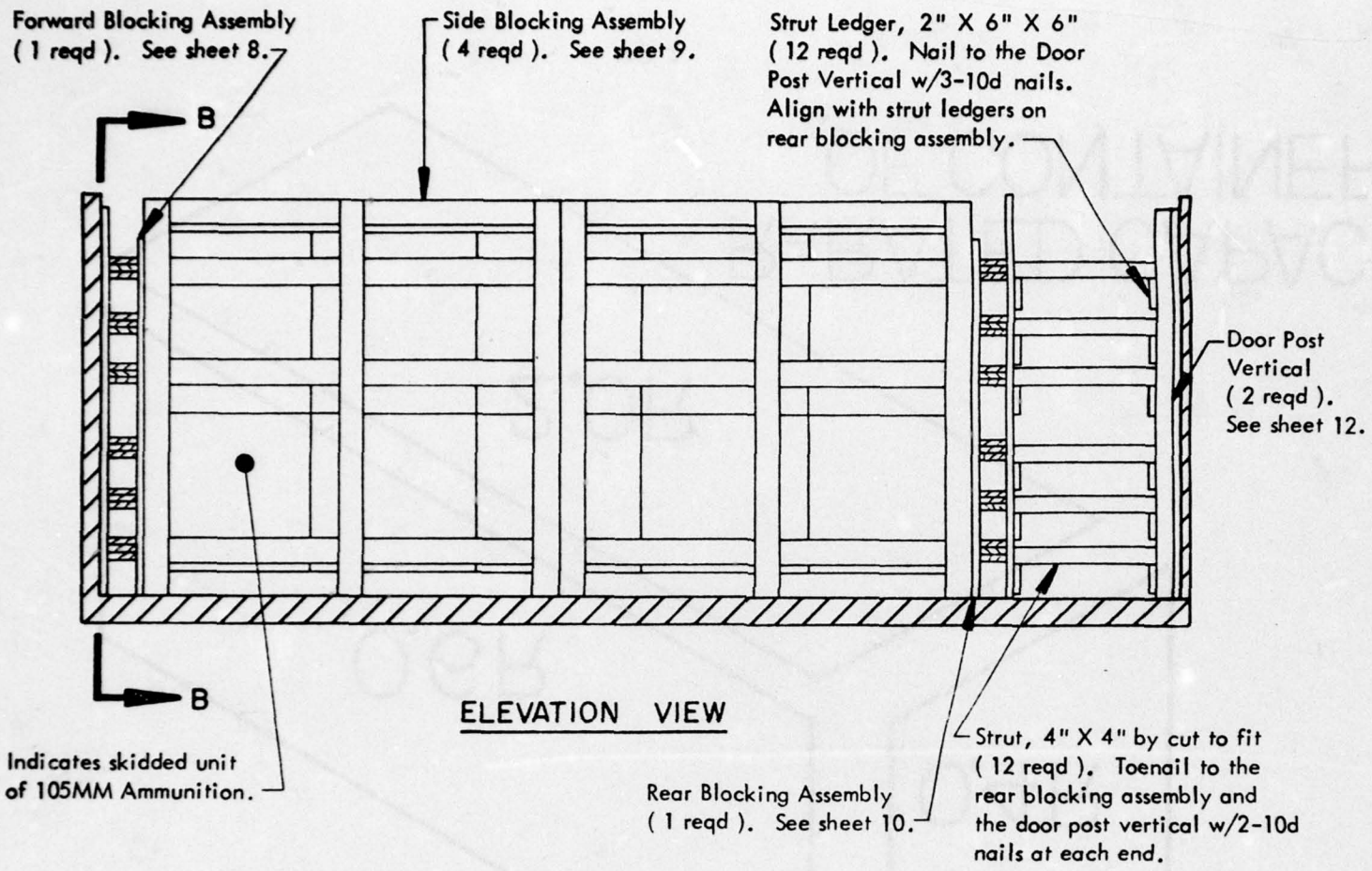




VG 5



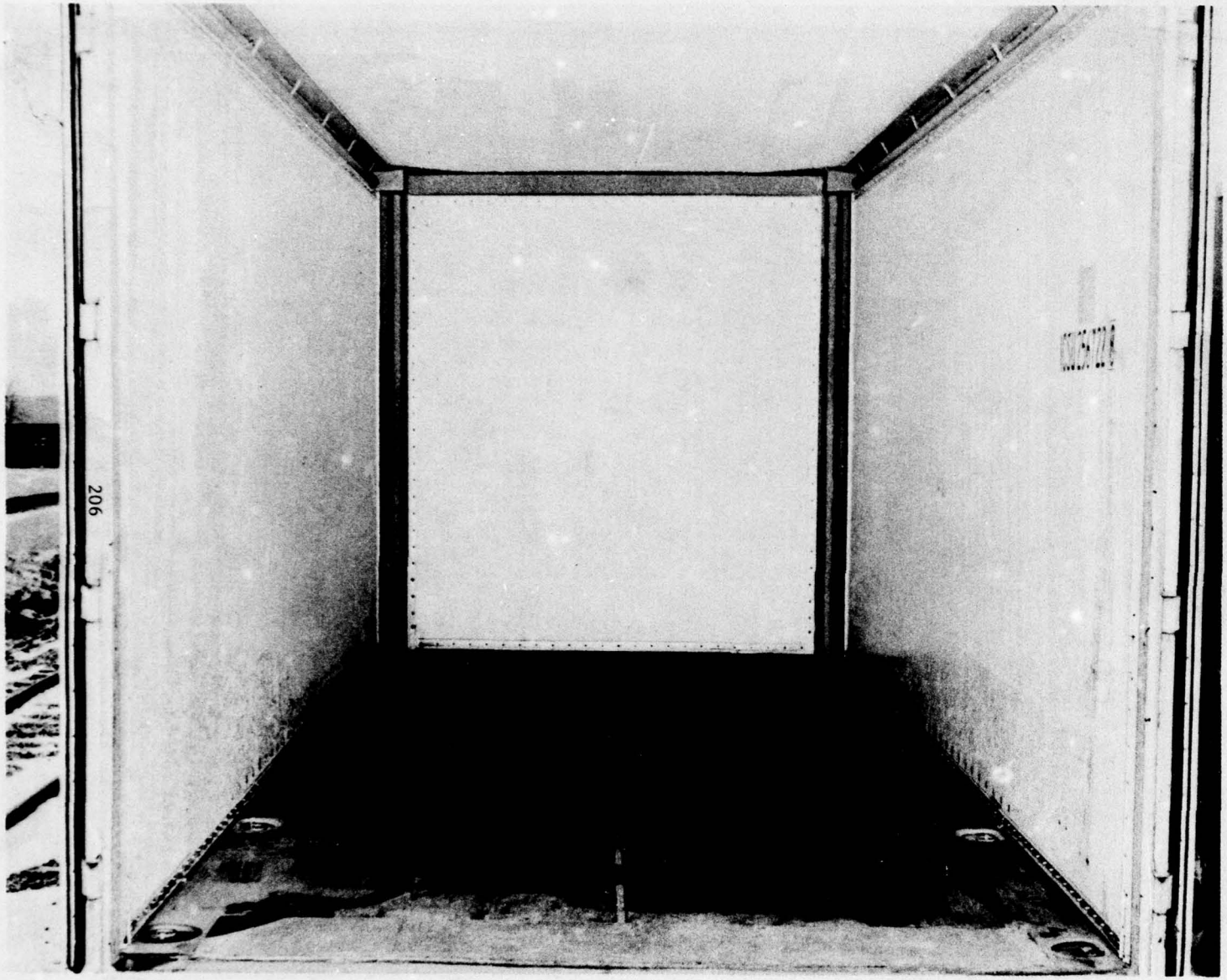
VG 7



VG 8

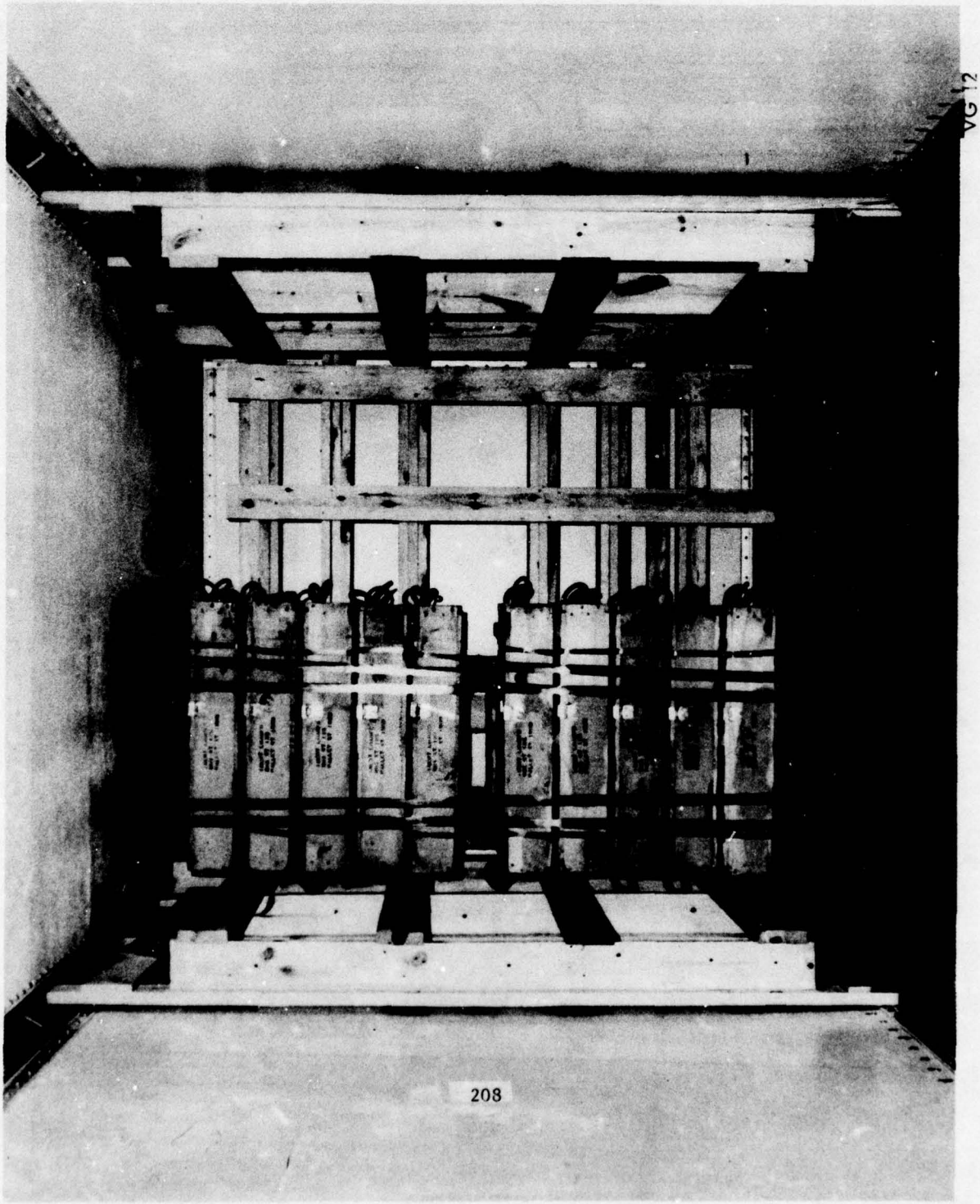
TYPICAL CONVENTIONAL WOODEN DUNNAGE FOR BLOCKING AND BRACING AMMUNITION IN 20-FOOT ISO COMMERCIAL CONTAINERS FOR ALL SURFACE MODES OF TRANSPORT

VG 6

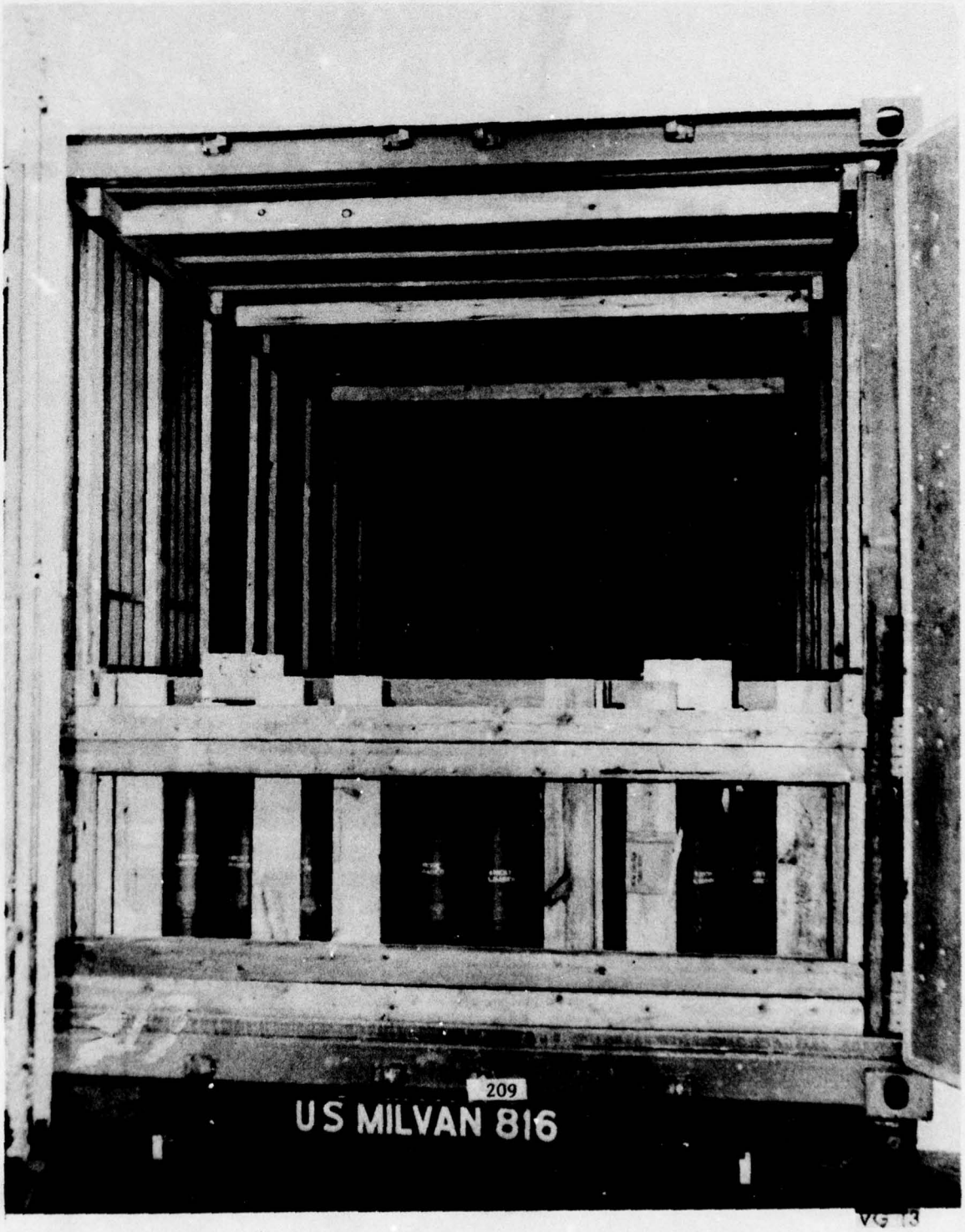


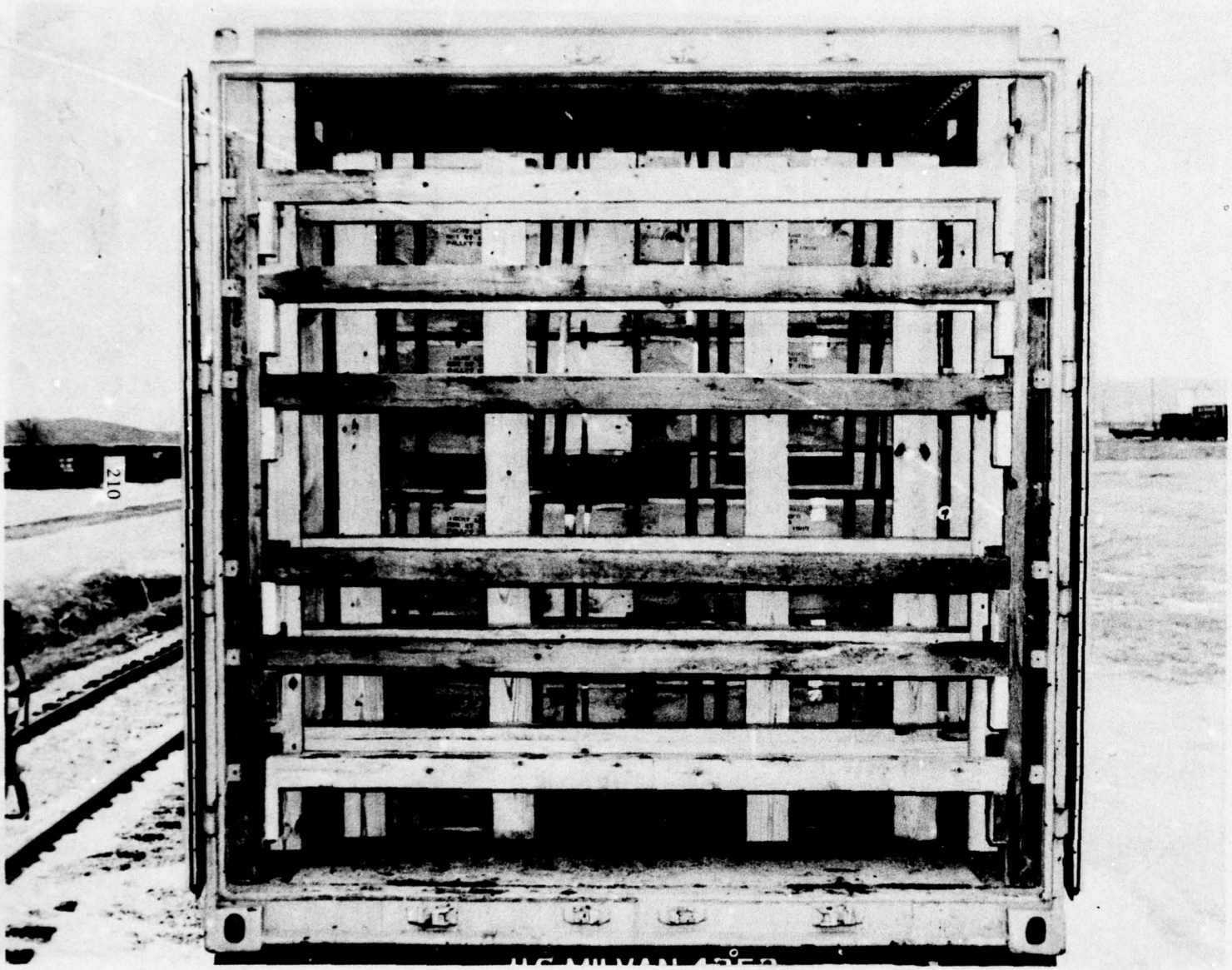
VG 10

VG 11

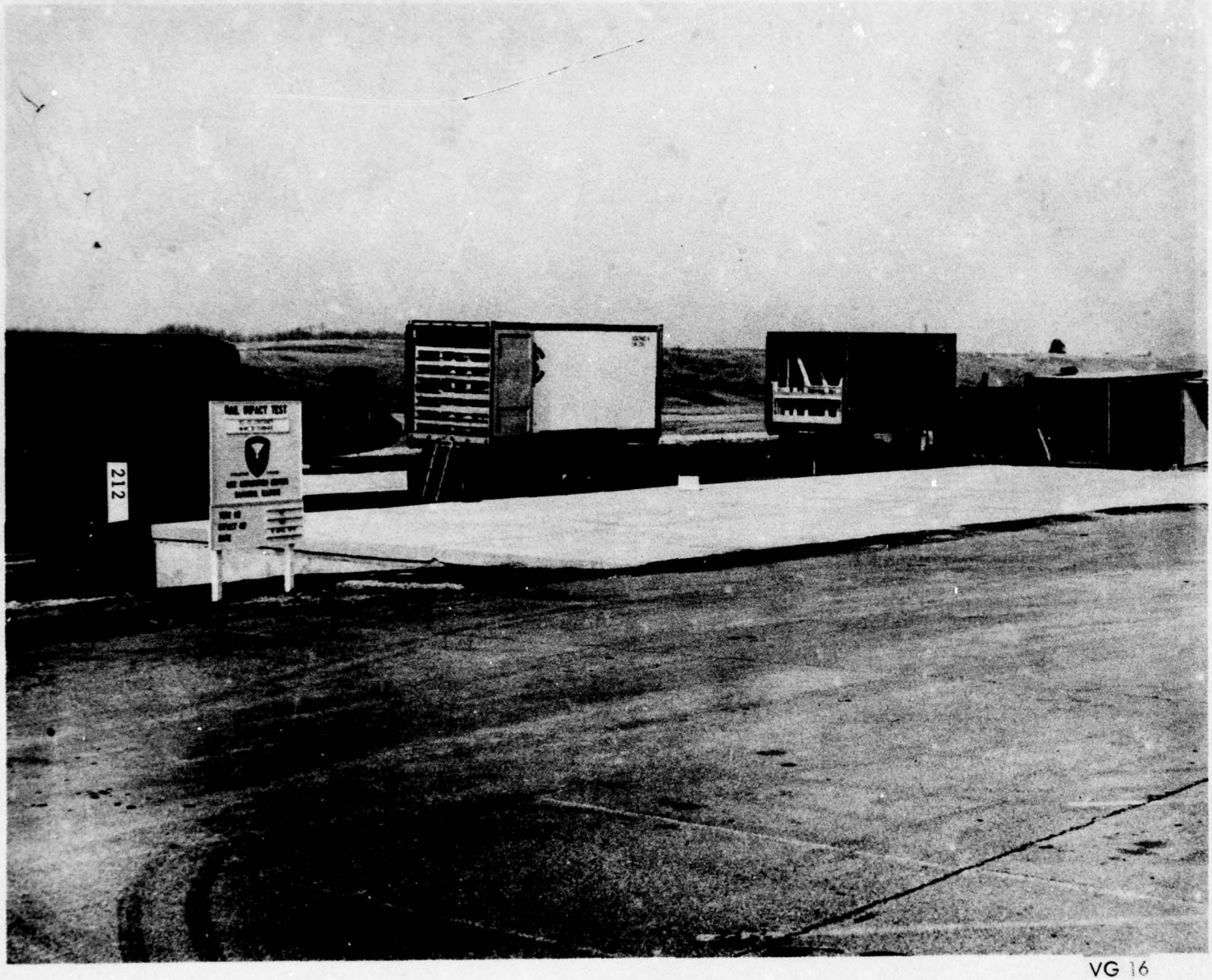


VG 12


209
US MILVAN 816

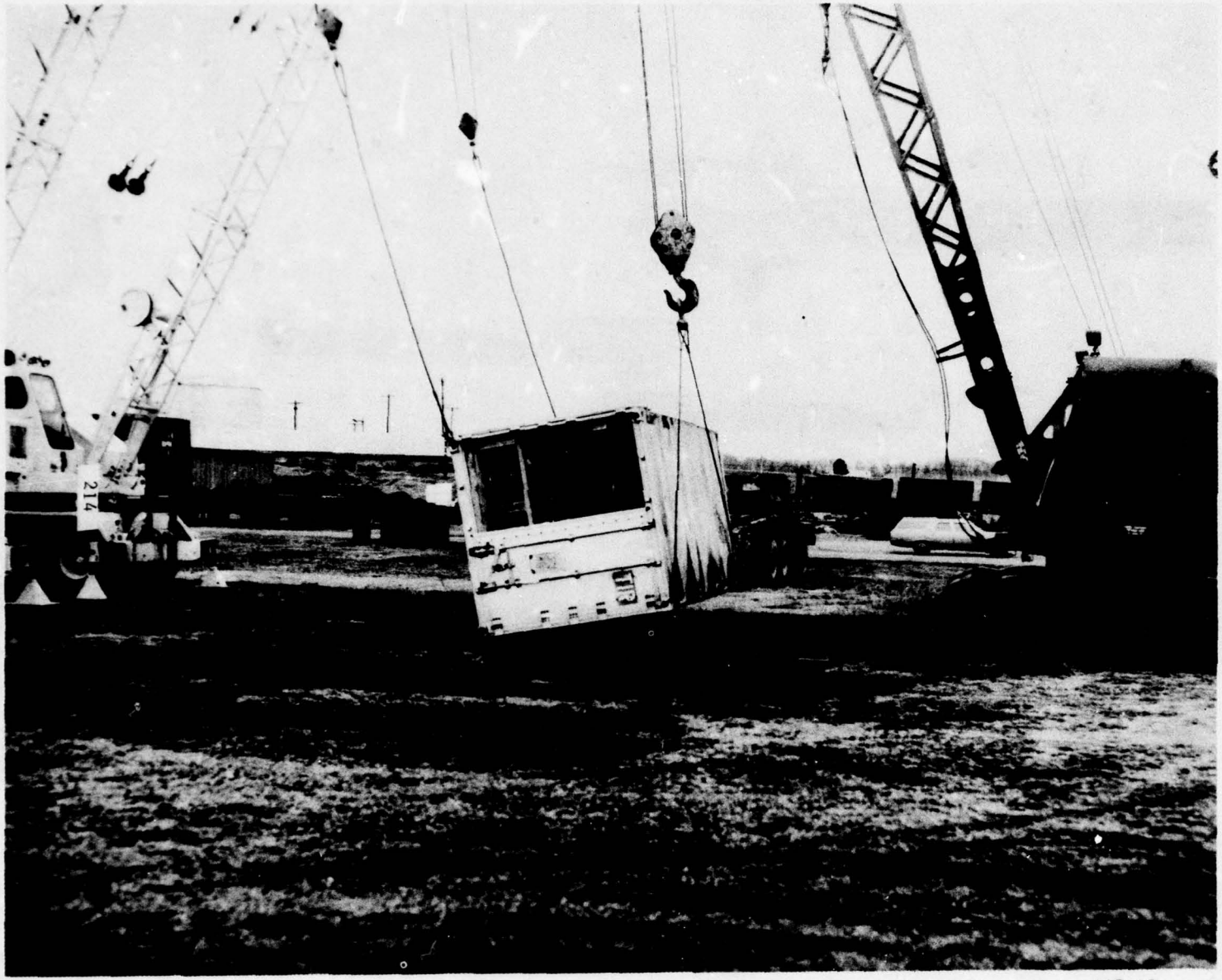

210

211

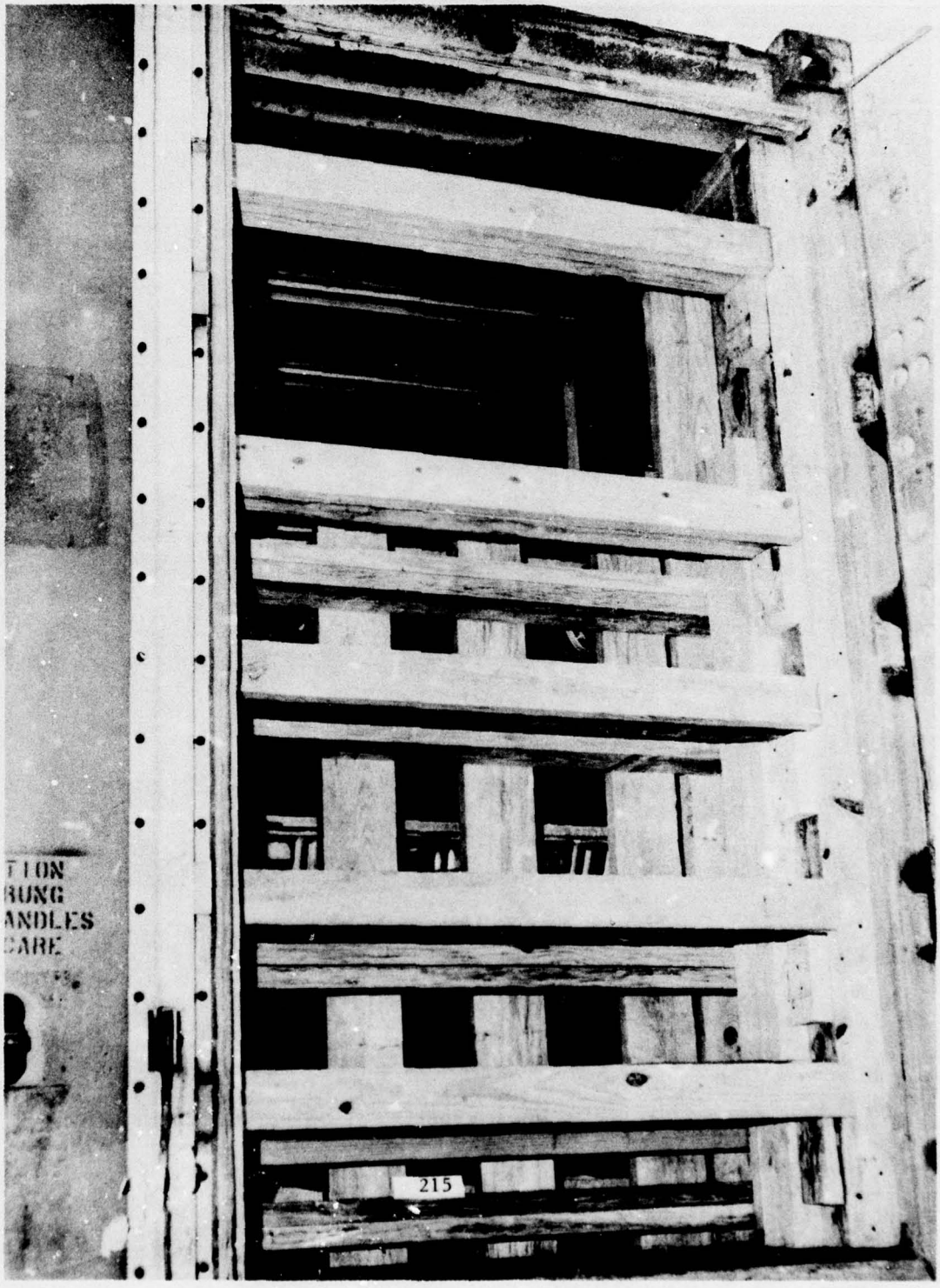


VG 16

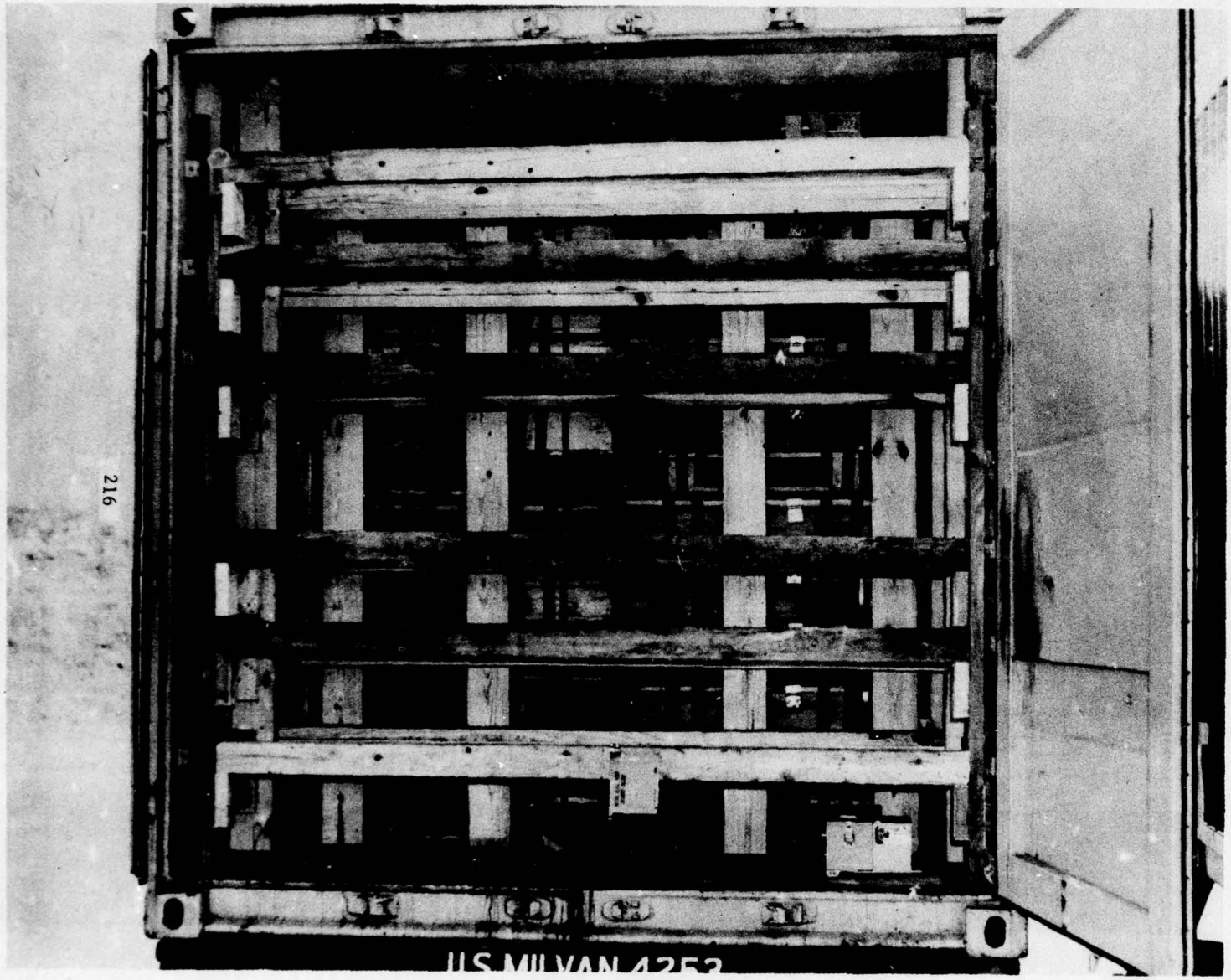

213



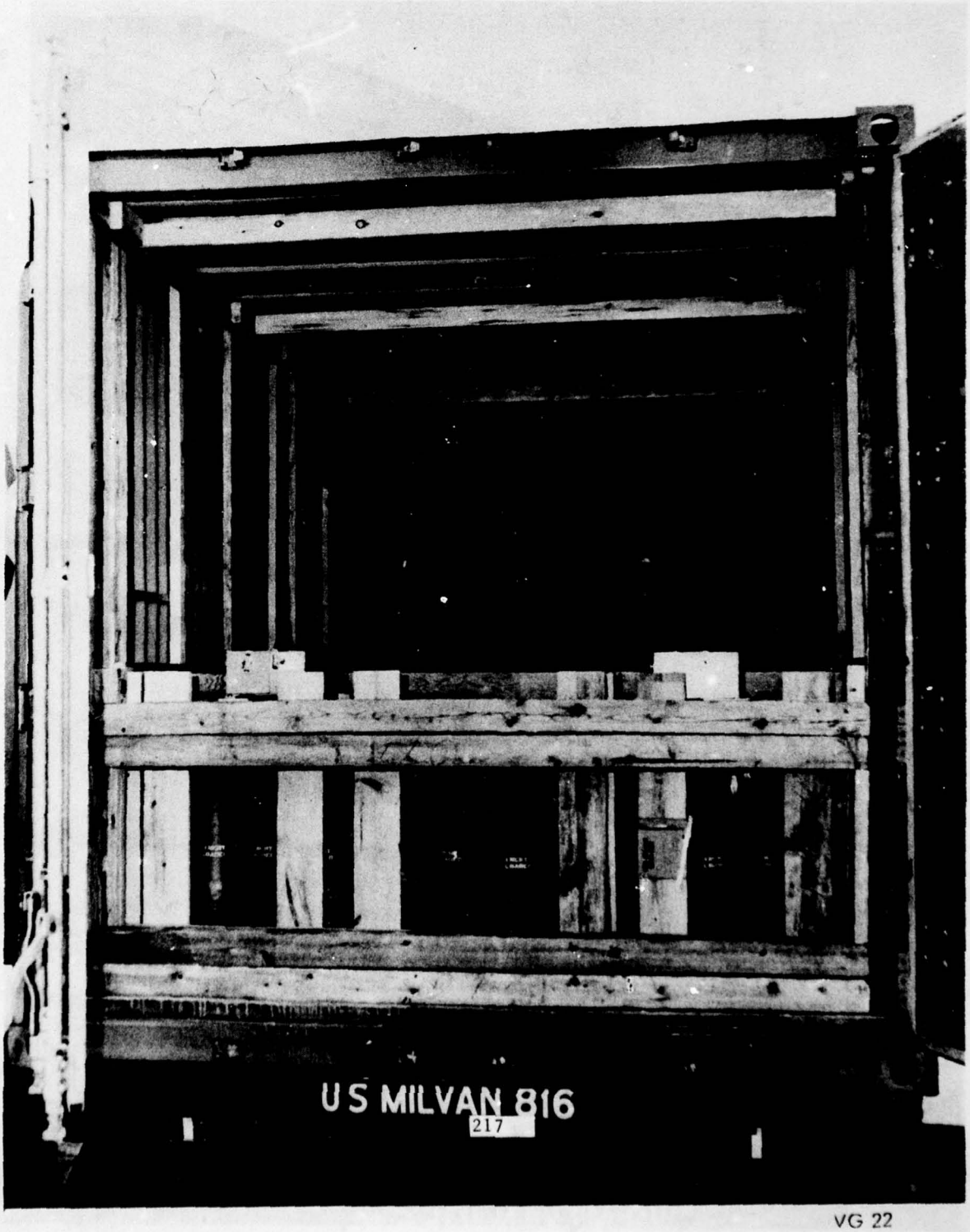
VG 18



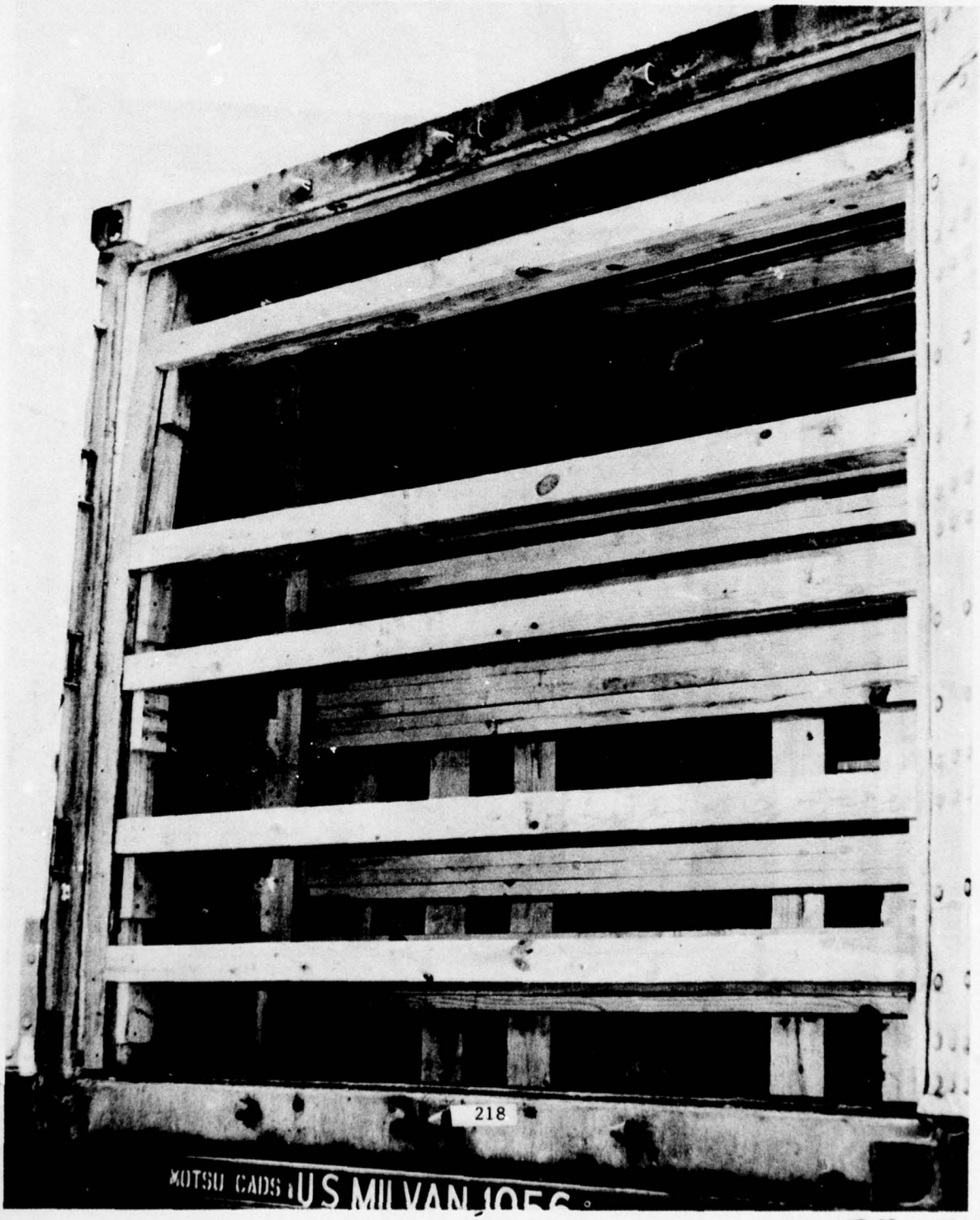
VG 2



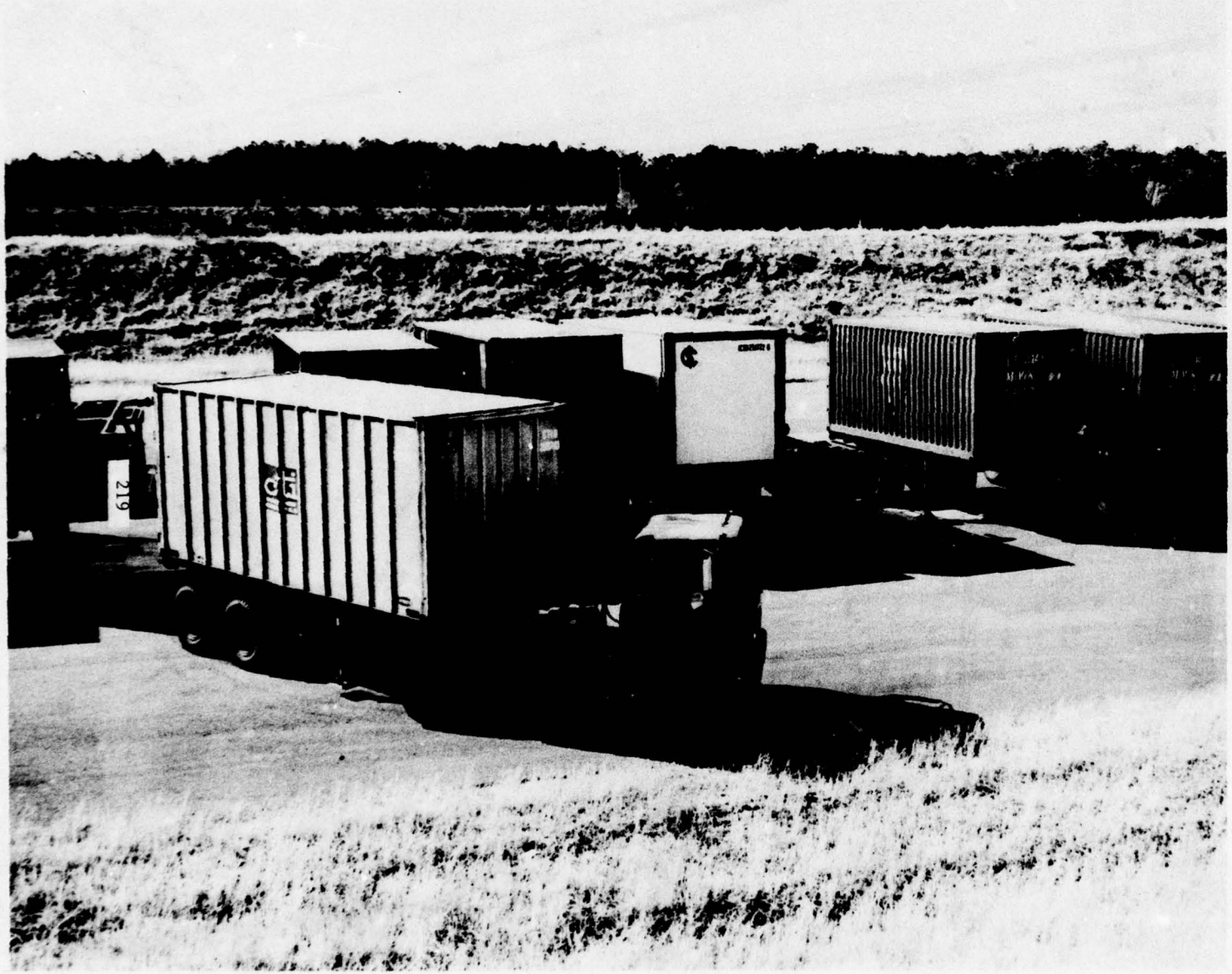
VG 2



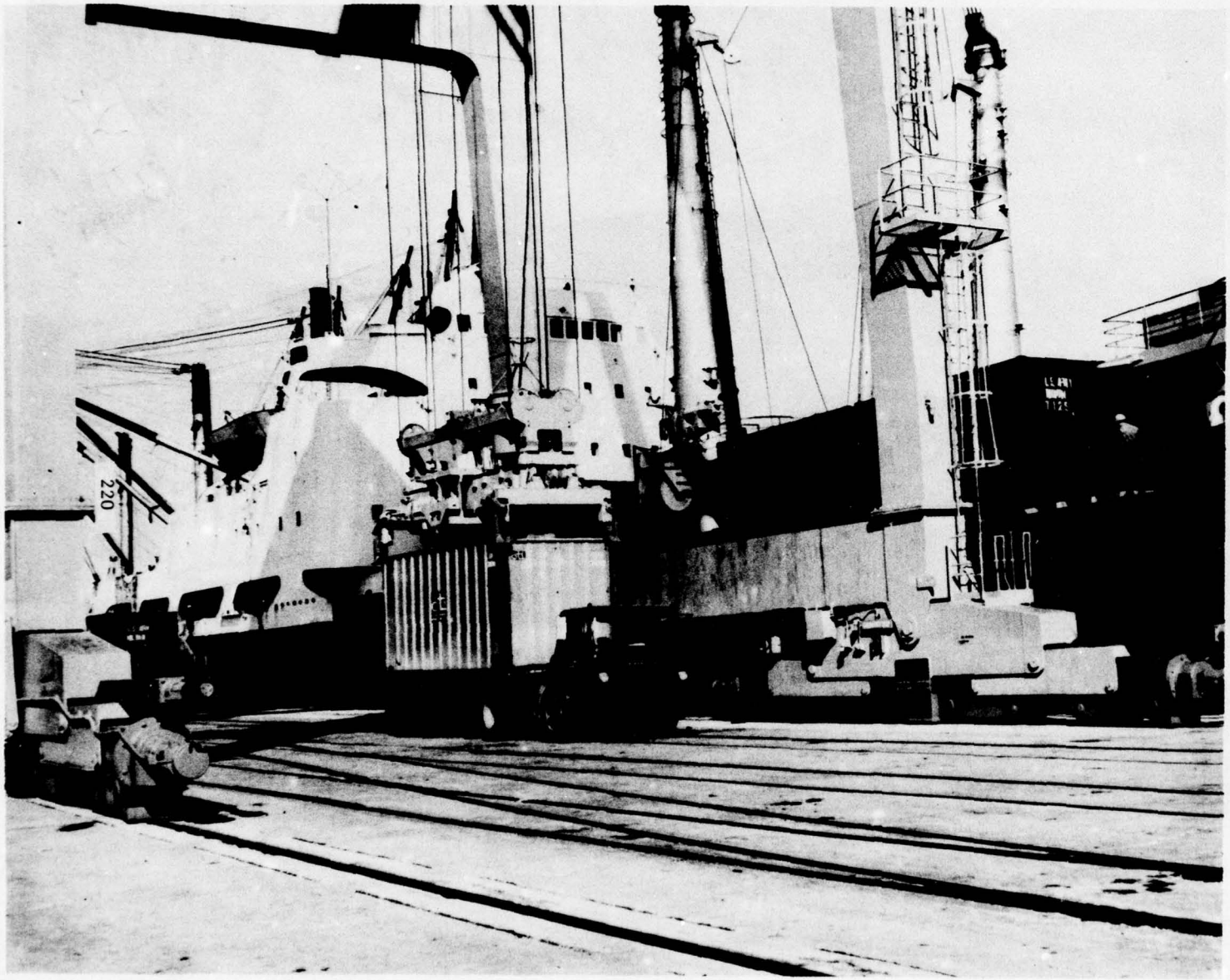
VG 22



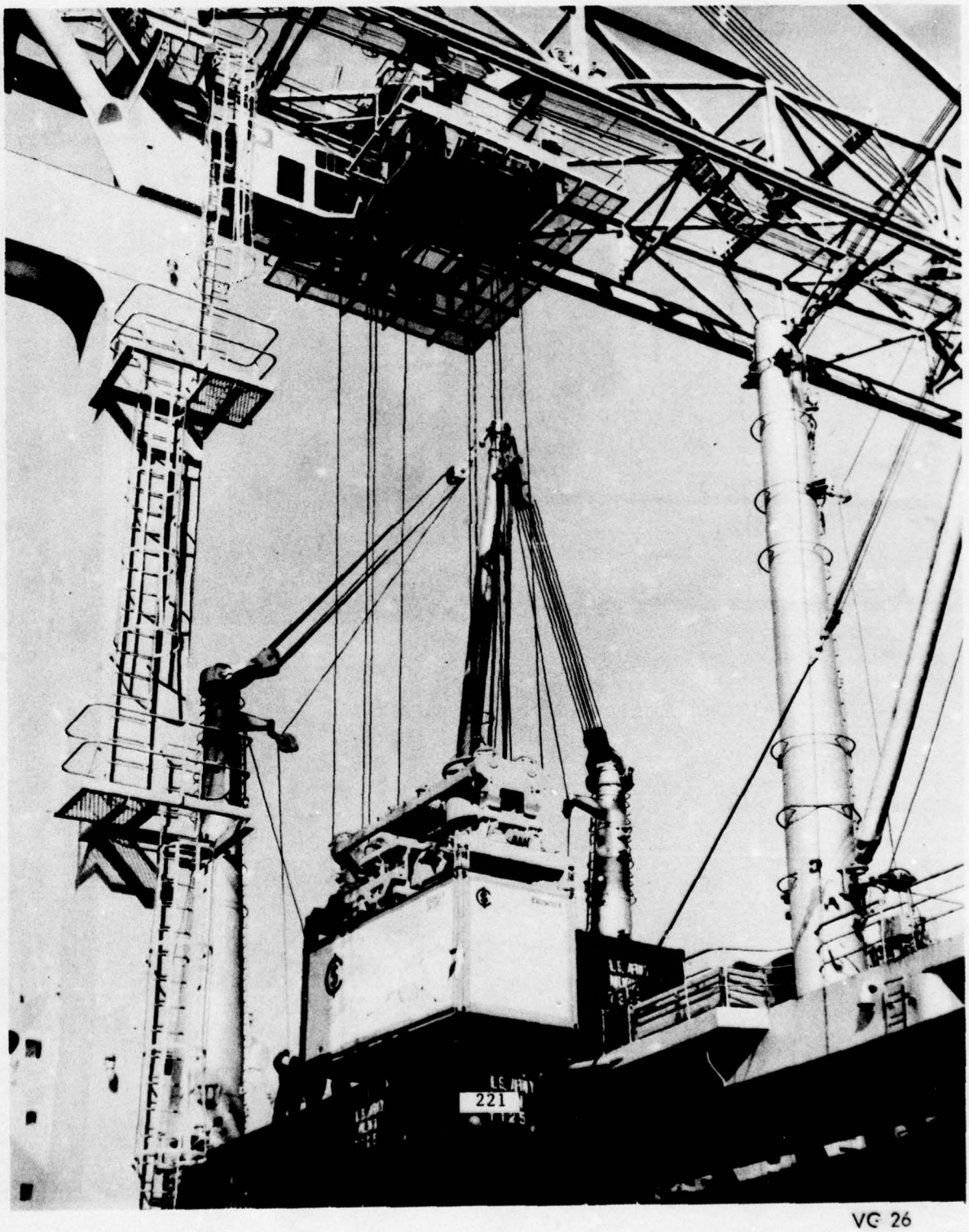
VG 23



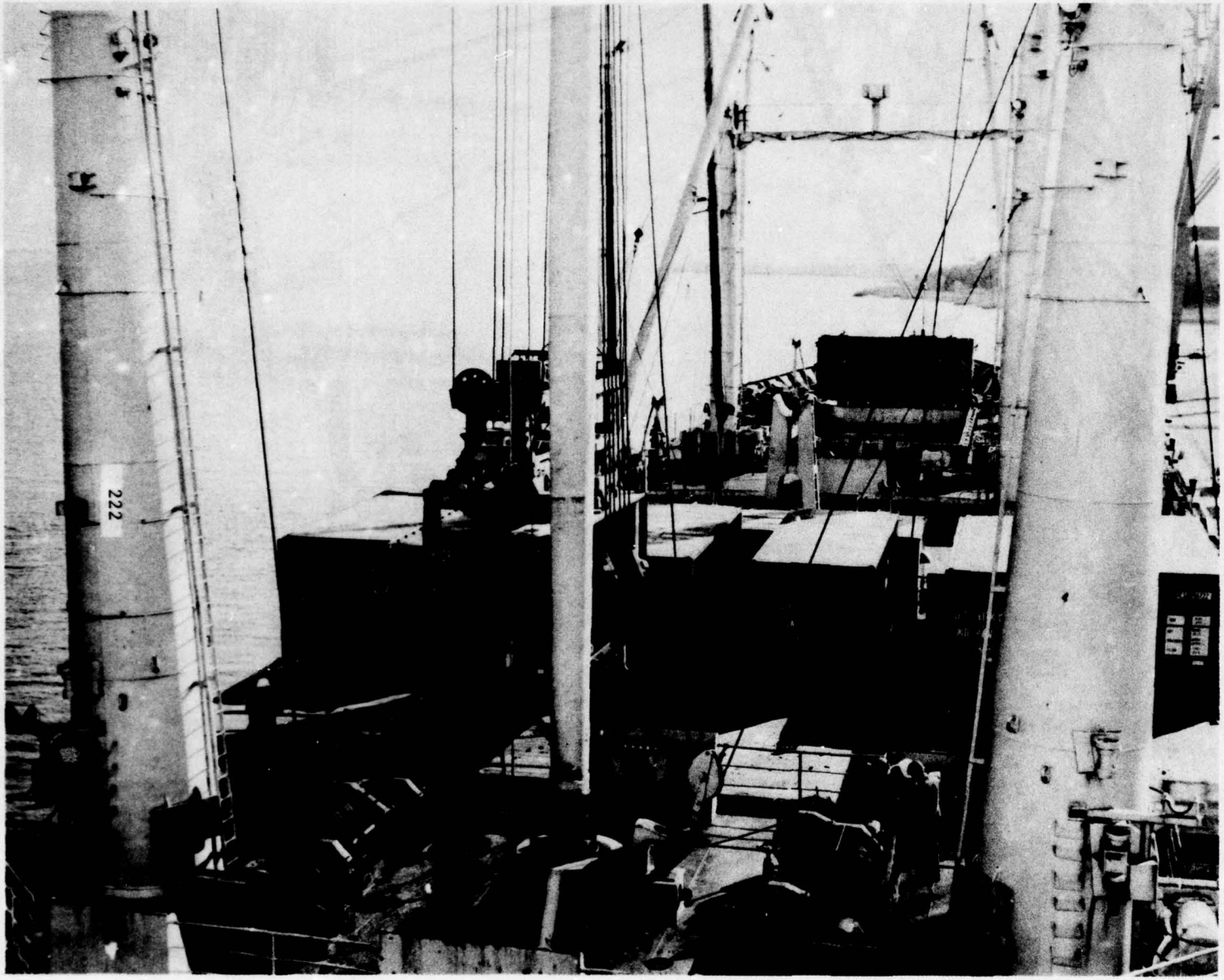
VG 21



VG 25



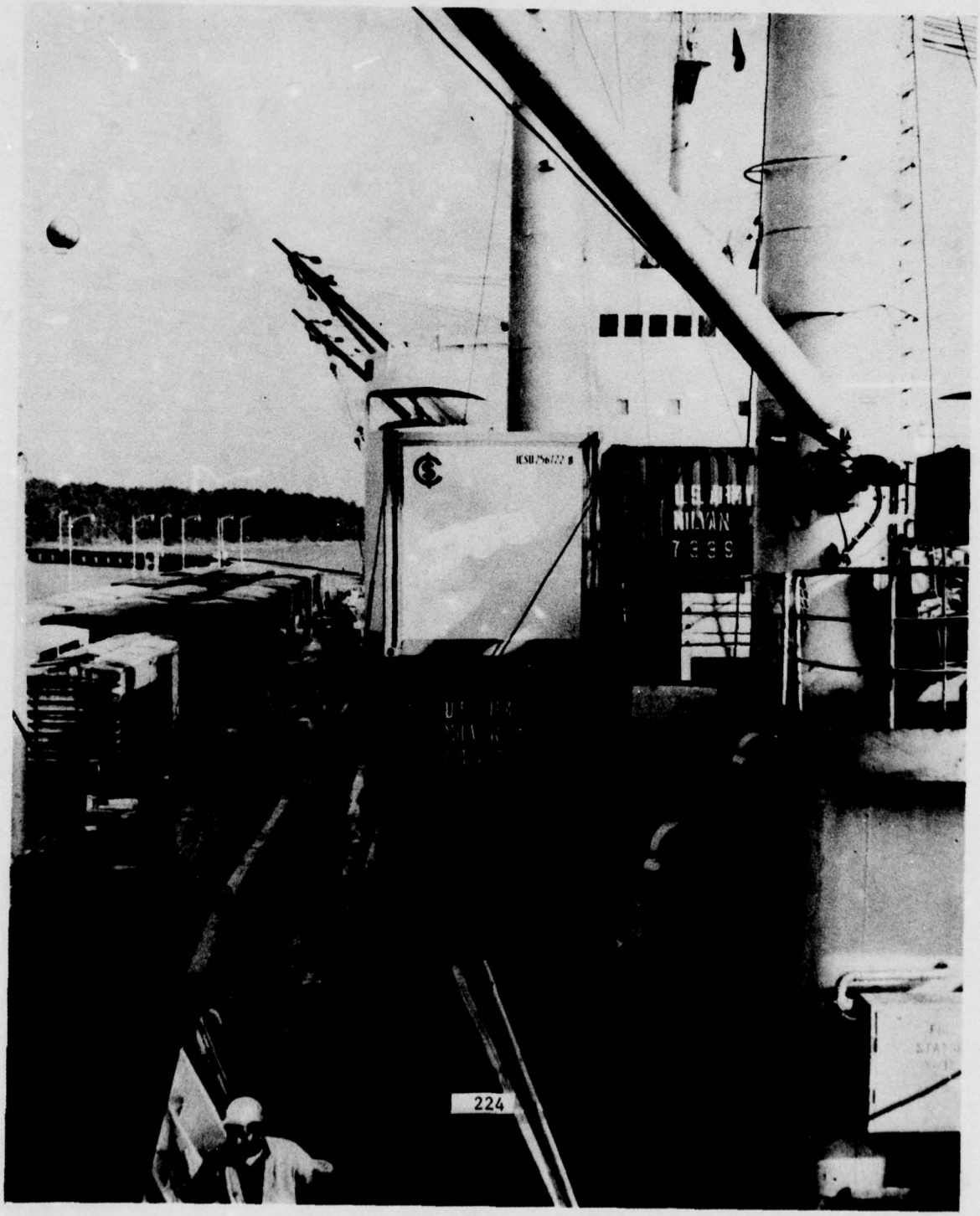
VG 26



VG 27

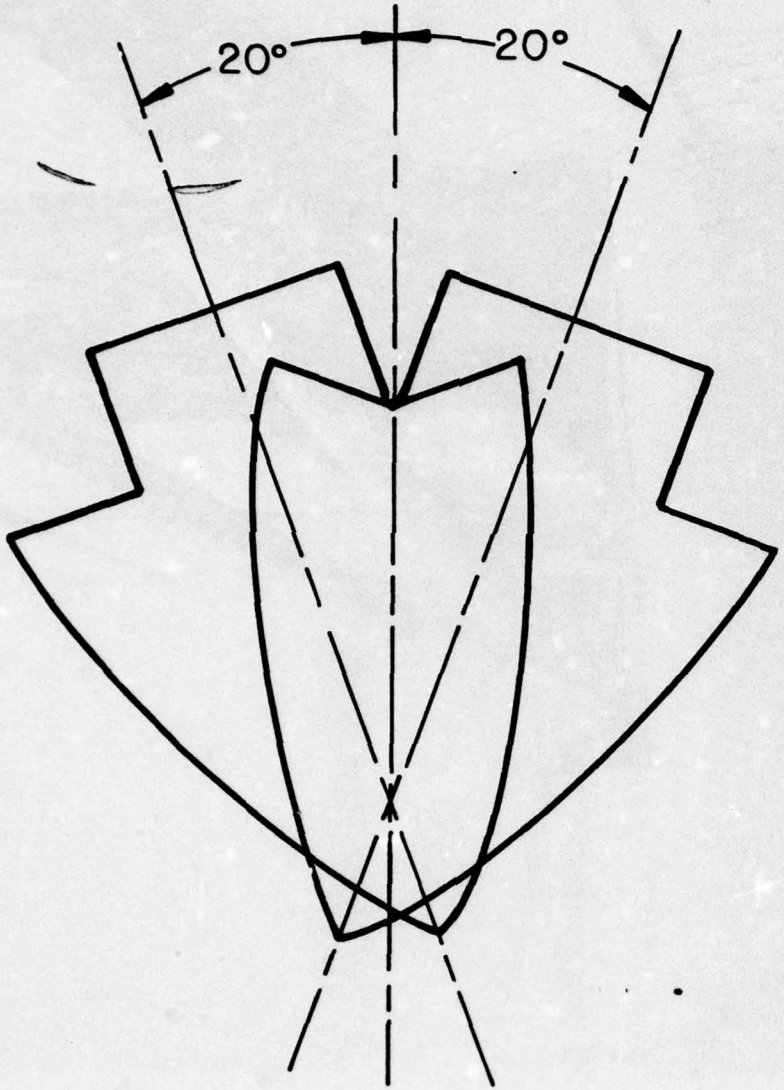


VG 28



VG 22

VG 30



VG 31

MILITARY STANDARDIZATION

HANDBOOK

FOR INSPECTION

OF COMMERCIAL INTERMODAL CONTAINERS

FOR AMMUNITION SHIPMENTS

VG 33

TRAILER-MOUNTED CHAMBER FOR CONTAINMENT OF 40 POUNDS OF TNT *

by

B. D. Trott, J. E. Backofen, Jr., and J. J. White, III
Battelle-Columbus Laboratories
Columbus, Ohio

and

L. J. Wolfson
U. S. Naval Explosive Ordnance Disposal Facility
Indian Head, Maryland

ABSTRACT

A 5-ft diameter, spherical blast-containment chamber fabricated from ASTM A-537-72A, Class 1 steel was designed for the repeated containment of 40-lb charges of TNT. The vessel included a reinforced access port 18 in. in diameter closed by a pair of inward-swinging cafe doors which overlapped the port reinforcing ring all around the edges. Four vessels were built to this design. As fabricated, the vessel wall thickness varied from 1.26 to 1.52 in. with an average of 1.40 in. as determined from one of the vessels.

The vessels were supported on cradles designed for a flat surface interface. Two of the cradle-mounted vessels were experimentally evaluated for their blast-containment capability. Two vessels were mounted on special modified commercial four-wheel trailers equipped with large toolboxes and shipped to NEODF for further evaluation as prototypes.

A total of 14 charges were detonated in the first vessel, including seven 35-lb spherical charges of Composition C-4 and one 47.5-lb charge of 60 percent strength commercial dynamite. At the conclusion of this test series the vessel was still in good condition and had swelled an average of 1 percent over the vessel surface. Three 35-lb spherical charges of C-4 were fired in the second vessel, producing an accumulated plastic strain of 0.6 percent average over the vessel surface. This is in reasonable agreement with the observed strain on the first vessel after three 35-lb shots. Measured peak free air-blast overpressures successively decreased from 3.4 to 1.6 psi at 5-1/2 ft from the vessel port for the three shots. Likewise, the peak blast overpressures decreased from 0.95 to 0.53 psi at a distance of 13-1/2 ft from the port. This decrease is attributed to better seating of the doors being achieved by the blast loading.

* Sponsored by the U.S. Naval Explosive Ordnance Facility, Indian Head, Maryland, under Contract No. N00174-74-C-0218.

PRECEDING PAGE BLANK-NOT FILMED

INTRODUCTION

Completely closed explosion-containment structures have found an increasing number of applications in both the defense and civilian and sectors of society. Typical applications include confinement and transport of improvised explosive devices[1-3] (typically pipe bombs), unsafe conventional ordnance, and nuclear weapons[4,5], nuclear-reactor safety[6-8], ammunition manufacture, ammunition disposal (demilitarization), explosive forming, explosive welding, and research utilizing explosives[9-12]. Advantages include safety, noise reduction, environmental control, elimination of off-site facilities, integration with nonexplosive activities, and cost-effectiveness. Partially open chambers[13,14] avoid the complication of port closure schemes, however they are less satisfactory in several respects, including safety, noise propagation[15], and detonation-product confinement. Partially open designs[16,17] may offer advantages in certain situations, particularly large-scale operations, however they are not competitive with total containment in terms of cost and weight in applications where safe transport of explosive devices is required[18,19].

This paper describes the development of a trailer-mounted chamber capable of complete containment of the blast from 40 lbs of TNT or the equivalent for several repetitions. This work was initiated to provide Armed Services explosive-ordnance disposal teams with a vessel design which had been tested and two trailer-mounted prototype vessels for further evaluation.

A spherical vessel design was developed which was predicted to attain a small fraction of 1 percent plastic strain during a containment of each 40-lb blast of TNT. By designing the vessel to operate in the plastic-strain regime, rather than providing sufficient vessel strength and weight to provide blast containment without plastic strain, a weight reduction estimated to be near 40 percent was achieved. A blast chamber designed for a limited number of uses and having minimum weight appears to

be quite cost-effective for this application where few actual contained detonations are expected.

This paper describes the vessel design, the fabrication procedures used, the experimental technique applied in evaluating the chamber performance, and the achieved performance of the two vessels evaluated during the development program. This work[20] was conducted under the sponsorship of the Naval Explosive Ordnance Disposal Facility, Indian Head, Maryland.

CHAMBER DESIGN AND FABRICATION

This section contains the design criteria for the selection of the chamber size, the design criteria for the port reinforcing ring and door, the reasons for the selection of the materials used, and the description of the fabrication method employed. Figure 1 shows the appearance of the trailer-mounted chamber.



FIGURE 1. FIVE-FOOT-DIAMETER PROTOTYPE CHAMBER MOUNTED ON TRAILER

Chamber Size

The selection of the chamber size in this development was based on the predictions of a one-dimensional, elastic-plastic analysis of a spherical chamber[9]. This analysis was extended both to include the effects of confined static gas pressure[21] following shock loading and to provide values for the maximum residual plastic strain to be expected. The analysis was programmed for evaluation by computer to allow quick parametric analyses. The program[22] included the shock-wave loading data for Pentolite as tabulated by Goodman[23]. The chamber size was selected to be 5 ft in diameter with a 1.25-in.-wall-thickness. This chamber was predicted to strain plastically 0.46 percent per 40-lb TNT shot based on the conservative value of 50,000 psi for the material yield strength. This value corresponds to the minimum static yield strength permissible for the selected chamber material. In practice the hemispherical heads ordered for the chambers were specified at 1-1/8-in. minimum wall thickness with the expectation of obtaining the desired average wall thickness. The actual minimum and average wall thicknesses for the one chamber ultrasonically surveyed were 1.29- and 1.40-in., respectively.

Later estimates of the proper dynamic yield strength to be used for the chamber material based on the testing of smaller vessels[3] suggested that 80,000 psi would more closely predict the chamber performance. Also, using more realistic TNT/Pentolite/Composition C-4 equivalent weights, and the actual chamber wall thickness, the predicted plastic strain per shot was reduced to between 0.1 and 0.2 percent, in agreement with the experimental results.

Reinforcing Ring and Door Design

The cross-sectional area for the reinforcing ring was determined by matching the radial deflection of the ring with the radial component of

deflection of the sphere at the ring location using elastic formulas[2]. The trapezoidal shape of the reinforcing ring was determined by engineering layout and calculation to minimize the net toroidal twisting moment from the sphere and door loadlines about the centroid of the ring cross-section.

The door closure design chosen for this chamber consisted of a pair of cafe doors mounted on vertical hinge pins allowing an inward swing from the port opening and arranged to overlap the reinforcing ring around its entire circumference. To prevent possible fragment ejection along the split between the two doors, the junction between the doors was made along an offset line as shown in Figure 2 and further covered by a heavy strap bolted to the door which is closed last.

The thickness of the door was chosen on the basis that the maximum stress on the outer surface of the doors due to bending under an applied internal hydrostatic load should not exceed the stress in the chamber wall. To evaluate this thickness, the structure whose stress analysis is desired is a semicircular plate, loaded with a uniform load per unit surface area, simply supported around the circumferential edge, and not supported along the linear edge. It was necessary to utilize an approximate basis for this solution because the exact structure desired could not be located in standard stress-analysis sources. Solutions were found for a simply supported square plate under hydrostatic load, and for a rectangular plate simply supported around three edges[24]. By choosing the dimensions of the rectangle to make them a half-square, and taking the ratio of the derived thicknesses for the half-square and full-square plates, it was found that approximately 12 percent additional thickness was required for the half-square over the full-square plate. Next, the thickness of the full-circular door required for the design vessel port was determined on the basis of equal stresses in the outer fiber of the central portion of the door and the chamber wall proper[24]. The door thickness so obtained was increased by 12 percent obtaining a value of 3.67-in., which was reduced to 3.50 in. for ordering, as previous experience[2] had shown the circular plate door criterion to be conservative. The details of the above analysis may be found in Reference 20.

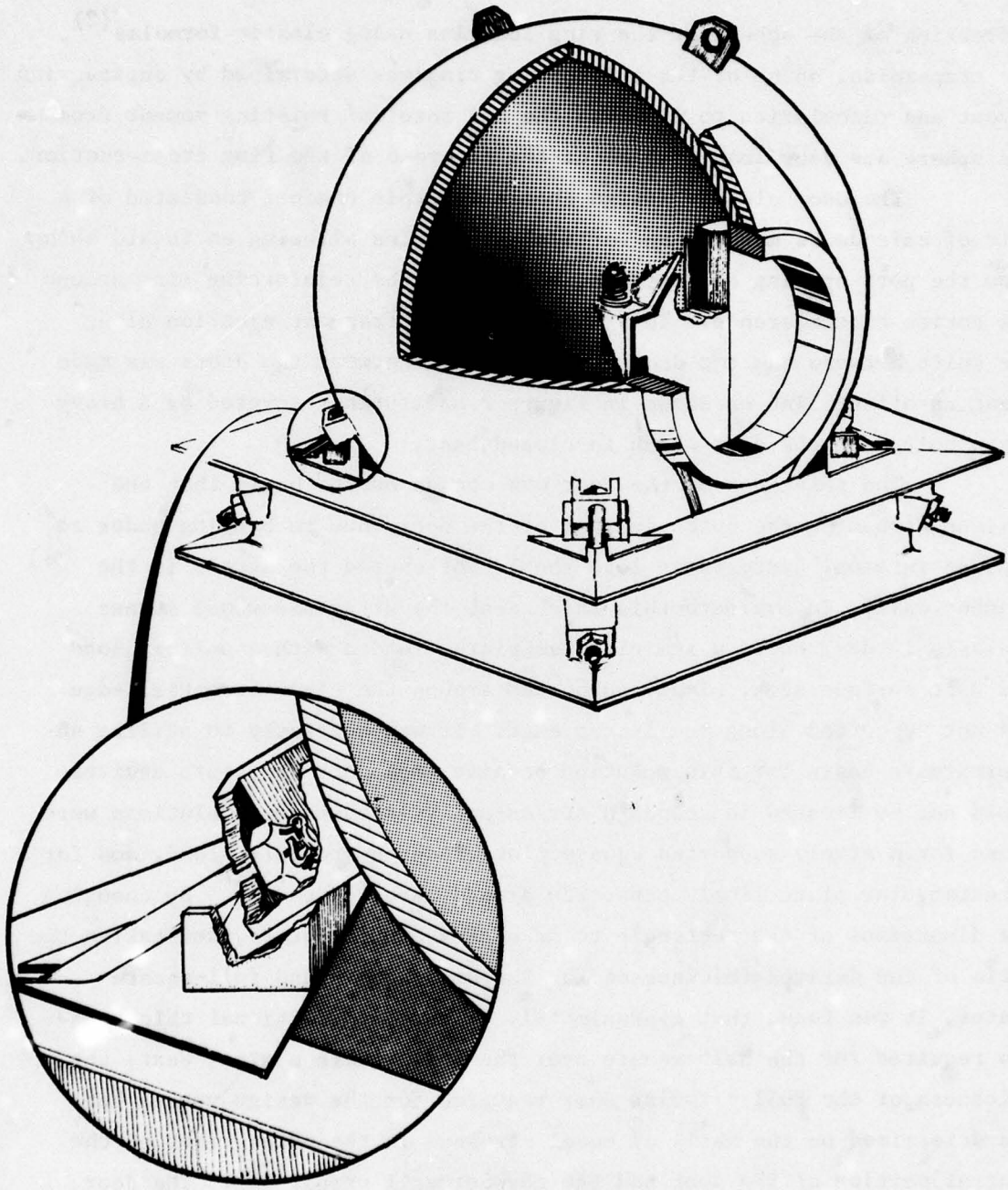


FIGURE 2. SCHEMATIC VIEWS OF CHAMBER AND MOUNTING

Separation of the circular closure piece into two semicircular doors introduced a bending moment in the ring and chamber. This bending moment could lead to a stress concentration in the chamber wall adjacent to the ring and opposite the split in the chamber closure. To reduce this stress concentration doubler plates, sized to make maximum use of the spherical cap removed from the sphere for the entry port, were used to reinforce the sphere at these locations, as shown in Figure 2.

Door-Hinge Mechanism Design

The door hinges were designed to allow the ring and door to deflect and move a limited distance during explosive loading without mechanical failure, while maintaining a close tolerance fitup of the doors during operation and road travel. The design chosen to satisfy these requirements consisted of a spring-loaded hinge that utilized a floating conical bearing to provide the necessary alignment of the door and yet allow lightly restrained movement during explosive loading. The design allowed 3/16 in. of spring-restrained motion in any direction about the hinge axis. For the cone angle chosen a spring load of 1,000 lb was determined to be required to keep the doors in proper alignment for 6-G road travel loads. Belleville springs to provide this preload on the mechanism were sized so that they would not bottom out before the design 3/16-in. motion occurred.

Vessel-Support Cradle Design

The vessel-support system was designed to allow the free radial expansion of the chamber under blast loading without transferring large impulsive loads to the support structure. To achieve this, the bearing support surfaces between the "feet" welded to the chamber, and the supports attached to the cradle were arranged to lie along a radius of the chamber as shown in Figure 2. The surfaces were designed to allow at least 1 in.

of sliding in the radial direction without mechanical interference to permit operation with expansion of the blast-containment chamber. The tie-downs selected for the chamber were bolts extending outward from the chamber feet to the cradle under the chamber. These bolts were also arranged to lie along a radius of the chamber so that the expansion of the chamber could occur without interference from the bolts. The bolts were sized to support a basic road loading of 6 G's in the vertical direction and 4 G's in any horizontal direction.

Material Selection

The material selected for the chamber shells was a steel designated as ASTM-537-72A, Class 1, or ASME boiler steel SA-537A. This selection was made on the basis of past experience[2] in blast-containment application. Its original selection was based on its toughness at low temperatures, weldability, cost, and availability. This steel is a higher quality carbon steel with a nominal chemical composition of 0.15 to 0.2 percent carbon, 1.2 percent manganese, 0.2 percent silicon, less than 0.02 percent sulfur, and less than 0.01 percent phosphorus. It has a minimum yield strength of 50,000 psi and a minimum ultimate strength of 80,000 psi with a minimum of 18 percent elongation in 8 in. In addition it will have a guaranteed minimum Charpy notched-bar impact strength value of 12 ft-lb at -75 F. Nominal values for impact strength at -75 F are about 30 ft-lb and at -50 F about 55 ft-lb. The shells of all four chambers were constructed of this material.

At the time of fabrication of these chambers, U.S. economic conditions were such that steel availability was less than normal. The only suitable material which could be located for fabrication of the rings and doors for the chambers was a lot of ASTM-A-350, Grade LF3 available from a single supplier. At delivery time for this material, however, only two of the four required reinforcing rings could be supplied. Eventually material specified as ASTM-537-72A, Class 2 (except for gage) was obtained

to fabricate the remaining two reinforcing rings. The mechanical properties of both of these steel grades equal or exceed those of the chamber shell material.

The remaining small parts for the vessels were constructed of mild steel or cold-rolled mild steel. The cradles were constructed of standard structural grade 10-in.-wide flange steel I-beams.

Fabrication and Welding

After machining, the doors and hinge parts were assembled to the inner side of a reinforcement ring; and the hinge parts were welded in place to the reinforcement ring. The ring and door assembly was then welded into the port machined into a hemisphere. After the main girth weld joining the two hemispherical shells into a spherical chamber was completed, the doubler plates, lifting lugs, and support feet were welded to the outside of the vessel.

A weld preheat temperature of at least 250 F was used for all welds. The main structural welds for the reinforcing ring and main girth joint were performed using qualified welding procedures established for these vessels. Briefly these structural welds consisted of a number of small passes to minimize the heat-affected zone with careful grinding and cleaning procedures used between passes as necessary. Complete details of the welding processes used may be found in Reference 20. All main structural welds were 100 percent inspected radiographically.

Trailer Mounting

Two of the cradle-supported chambers were mounted on specially modified, industrial trailers manufactured by the Fayette Division of the Dayton-Walther Corporation. The special modifications of the Fayette Model No. 12010-215 trailers with a rated capacity of 12,000 lb. consisted of shortening the trailer bed forward of the support wheels and removing the sloping aft end of the standard trailer to allow direct access from

the ground to the vessel port which was mounted facing the rear of the trailer. In addition reinforced tie-down brackets were welded to the trailer frame underneath the deck to allow secure anchoring of the chamber cradle on the trailer bed. A large toolbox was mounted across the front of the trailer as shown in the photograph of Figure 1.

EXPERIMENTAL TECHNIQUES

Two of the four chambers fabricated during this development were evaluated by firing of a series of explosive detonations inside the chambers. This section describes the experimental techniques used in conducting these evaluations.

Charge Preparation

All of the test detonations in this series used charges of Composition C-4 except one of 60 percent strength special gelatin dynamite (commercial). The Composition C-4 charges were tightly hand-packed into special molds to an average density of 1.55 g/cm^3. The first five shots in the first chamber evaluated ranged from 10 to 30 lb in weight and were in the form of cubes with the corners truncated to the center line of each edge as an approximation to a spherical shape. After deformation measurements revealed a definite charge-shape effect associated with charges of this shape, all remaining charges were packed into spherical shapes. All Composition C-4 charges were fitted with a Detasheet* "C" booster charge of $\sim$ 0.14 lb. The 47.5-lb gelatin dynamite charge was too weak to support itself in a spherical shape and required support provided by a ribbed structure formed of 1-inch Styrofoam sheet. The charges were supported at the center of the test chamber by means of a small table formed of a 1/4-in. plywood top supported by 1 x 2-in. wooden legs. As

*Registered Trademark, E. I. DuPont, de Nemours & Co., Inc.

noted later, the center portion of the plywood tabletop was removed for the final shots in the second vessel.

Strain-Gage Installation and Measurement

A total of six strain gages were installed on the first chamber evaluated at various locations around the vessel shell and one gage was mounted on the port reinforcing ring. Standard constantan strain gages were bonded to the vessel with EPY 500 epoxy manufactured by the Baldwin-Lima-Hamilton Corporation. This cement was used because of its superior bond strength, which prevented the gages from popping off the vessel surface during the explosive testing. The strain gages were attached to the shielded lead wires by means of short lengths of 34-gage enameled wire to minimize the mass attached to the gages. This bonding and lead-wire technique proved to be quite successful in maintaining the strain-gage integrity during the severe loading conditions encountered.

The dynamic response of the vessel strain gages was recorded photographically from an oscilloscope trace. The trigger for the oscilloscope was provided by a foil switch mounted on the blasting cap used to detonate the charge.

Static readings of the strain gages were made between shots with a Vishay Instruments Model SB-1 switch and balance unit and a Budd Model P-350 strain indicator.

To determine the heating effect of the explosive charge, an ISA Type K Chromel-Alumel thermocouple was spot welded to the surface of the chamber well away from disturbing influences of the supports or port. The temperature rise from the thermocouple was recorded using a strip-chart recorder to obtain the time history of the chamber temperature following a test detonation.

Measurement of Plastic Deformation

In order to measure the plastic deformation of the chamber shell, a series of fiducial marks were placed on the surface arranged in three

orthogonal great circles around the chamber. The distance between adjacent marks ranged from 22 to 25 in. The marks consisted of small punch impressions plus sharp scribed lines placed on the chamber surface. The distance between adjacent marks was monitored using a specially constructed tool with a punch point at one end and a steel scale calibrated in hundredths of an inch at the other end of the tool. Distances were measured between one punch mark and the adjacent mark scribed line with the aid of a hand lens. These measurements proved to be reproducible to within 0.005-in. or approximately 0.02 percent for the nominal 24-in. gage lengths employed. The actual fiducial-mark arrangements are presented with the experimental results for ease in comparing the data with the corresponding location on the chamber surface.

Wall-Thickness Measurements

Figure 3 summarizes the ultrasonic thickness measurements on the first chamber evaluated. These measurements used an ultrasonic pulse reflection technique, which was calibrated for thickness using a test specimen removed from the port of the chamber being measured. Precision of 0.01 in. was obtained. The measurements were taken in a pattern identical with the layout of the fiducial marks. The variations of the thickness with location confirm previous experience with hot-pressed hemispheres[2]. Note that the shell is thinnest near (but not at) the pole and is thickest near the main equatorial weld. The measured thicknesses ranged from 1.29 to 1.52 in. By weighting the data based on assumed cylindrical symmetry, the average thickness of this chamber was calculated to be 1.40 in.

CHAMBER PERFORMANCE

Tables 1 and 2 present summaries of the explosive testing conducted on the two 5-ft-diameter explosive-containment chambers. They show the accumulated strain readings calculated from measurements between adjacent fiducial marks located on the chamber surfaces as shown schematically in Figures 4 and 5 for the two chambers. The two chambers

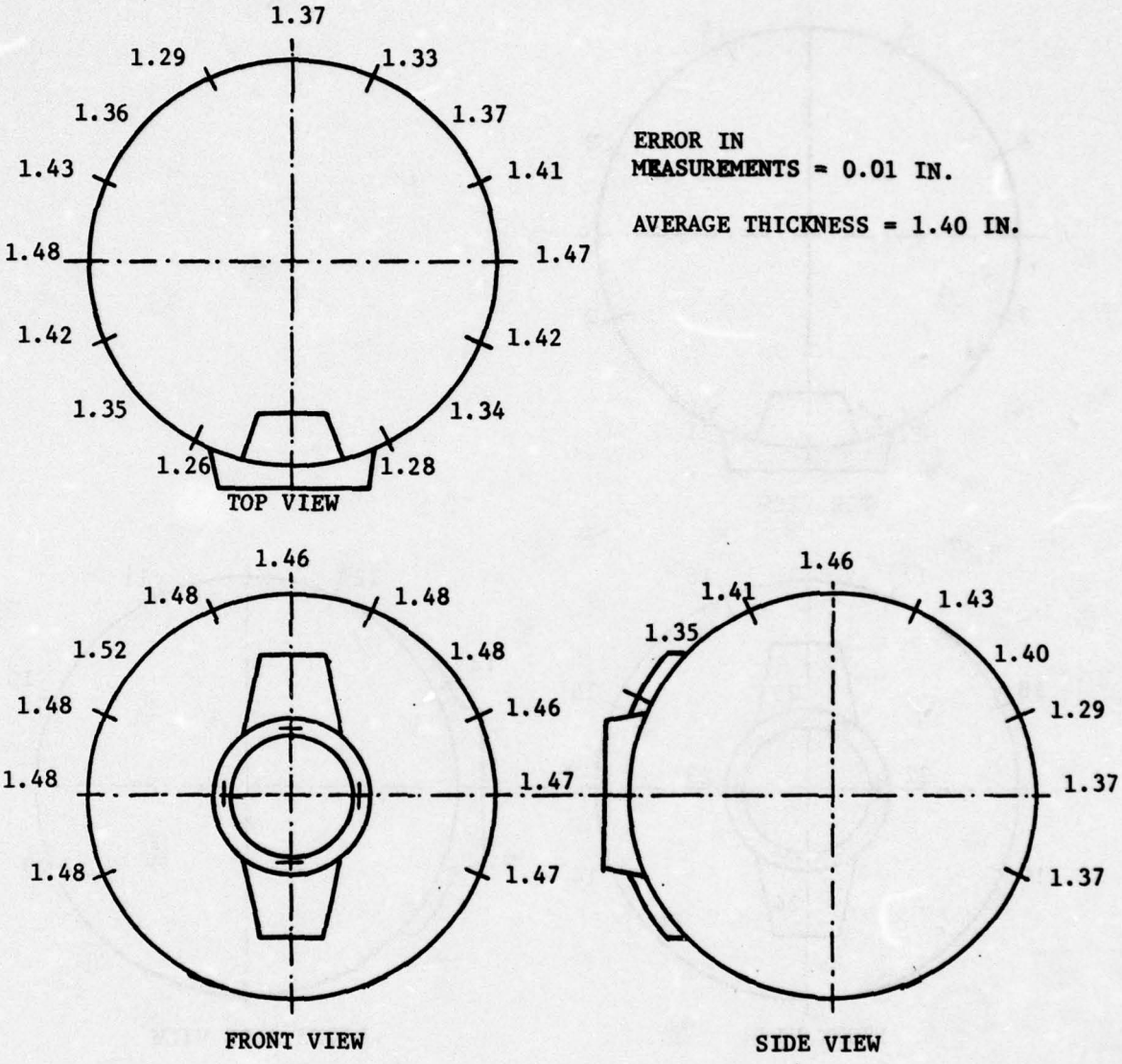


FIGURE 3. ULTRASONIC WALL THICKNESS MEASUREMENTS IN INCHES ON THE FIRST FIVE-FOOT DIAMETER CHAMBER

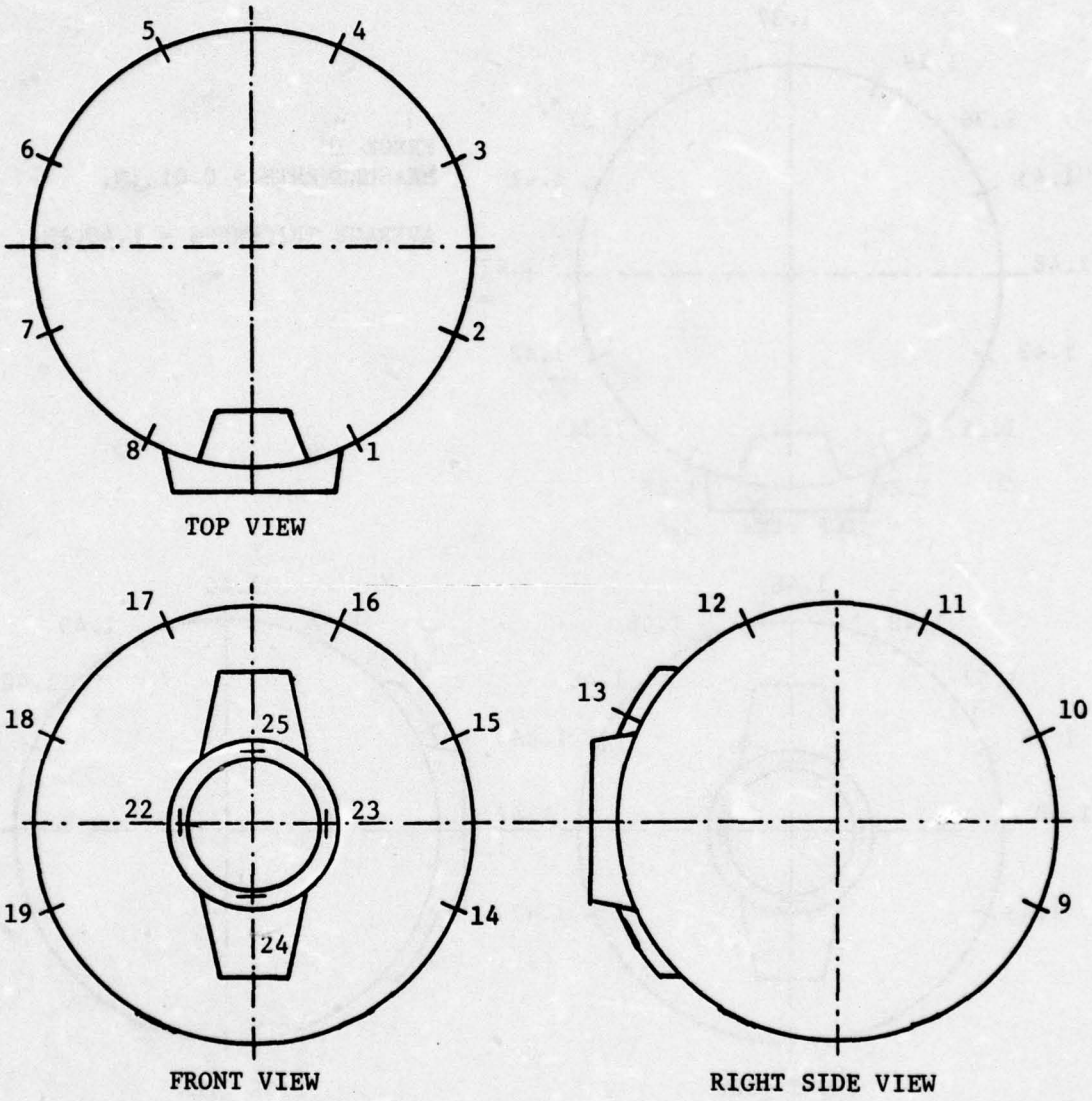


FIGURE 4. LOCATION OF FIDUCIAL MARKS ON THE FIRST FIVE-FOOT DIAMETER CHAMBER

TABLE 1. ACCUMULATED PLASTIC STRAIN ON THE FIRST FIVE-FOOT DIAMETER CHAMBER, IN PERCENT

Shot No.	1	2	3	4	5	6	7	8	9	10	11	12	13	14
Explosive Wt., lb[a]	10	10	20	25	30	20	35	35	35	35	35	35	35	47.5
Marks[b]														
1-2	0.01	0.04	0.01	0.01	0.32	--	0.50	0.68	0.84	1.05	1.24	1.38	1.40	1.45
2-3	--	--	--	0.30	0.32	--	0.35	0.41	0.47	0.54	0.65	0.69	0.75	0.74
3-4	--	--	--	-0.04	0.10[d]	--	0.28[d]	0.45[d]	0.58[d]	0.74	0.90	1.02	1.06	1.15
4-5	--	--	--	0.48	-0.38[d]	--	0.40[d]	0.24[d]	0.33[d]	0.43	0.57	0.68	0.76	0.84
5-6	--	--	--	0.02	0.46	--	0.65	0.78	0.88	0.96	1.09	1.21	1.28	1.29
6-7	--	--	--	0.28	0.26	--	0.33	0.38	0.47	0.54	0.67	0.72	0.76	0.73
7-8	--	--	--	0.03	0.30	--	0.44	0.59	0.80	0.92	1.12	1.16	1.21	1.19
9-10	--	--	--	0.53	0.05[d]	--	0.40[d]	0.27[d]	0.40	0.56	0.58	0.63	0.70	0.79
10-11	--	--	--	0.03	0.05	--	0.14	0.26	0.60	0.77	0.96	1.09	1.21	1.23
11-12	--	--	--	0.31	0.45	--	0.69	0.83	0.88	0.96	1.01	1.03	1.09	1.15
12-13	--	--	--	0.02	0.10	--	0.36	0.53	0.73	0.86	0.98	1.13'	1.16	1.19
14-15	--	--	--	0.21	0.16	--	0.30	0.33	0.42	0.52	0.52	0.58	0.60	0.61
15-16	--	--	--	0.02	-0.03	--	0.08	0.15	0.34	0.43	0.53	0.72	0.80	0.82
16-17	--	--	--	0.25	0.50	--	0.68	0.76	0.92	0.98	1.03	1.06	1.06	1.17
17-18	--	--	--	0.00	0.00	--	0.03	0.06	0.17	0.33	0.43	0.54	0.60	0.63
18-19	--	--	--	0.20	0.28	--	0.37	0.42	0.49	0.56	0.65	0.66	0.64	0.63
Avg. (Marks 1-19)[c]				0.17	0.23		0.37	0.47	0.60	0.70	0.81	0.89	0.94	0.98
22-23	0.03	0.03	0.03	0.17	0.10	--	0.09	0.10	0.13	0.04	0.09	0.13	0.43	0.12
24-25	0.03	0.04	0.06	0.10	0.00	--	-0.15	-0.19	-0.21	-0.24	-0.25	0.32	0.24	-0.31

(a) Explosive was C-4 except Shot No. 14 was 60 percent strength dynamite. Charges 1 through 5 were corner-truncated cubes. Charges 6 through 14 were spheres. All were centrally initiated.
(b) Refer to Figure 4 for locations.
(c) Doubtful readings marked (d) excluded from average.
(d) Doubtful meaning due to dent at the pole.

NOTE: (1) The estimated error in the cumulative strain from fiducial readings is 0.03 percent.

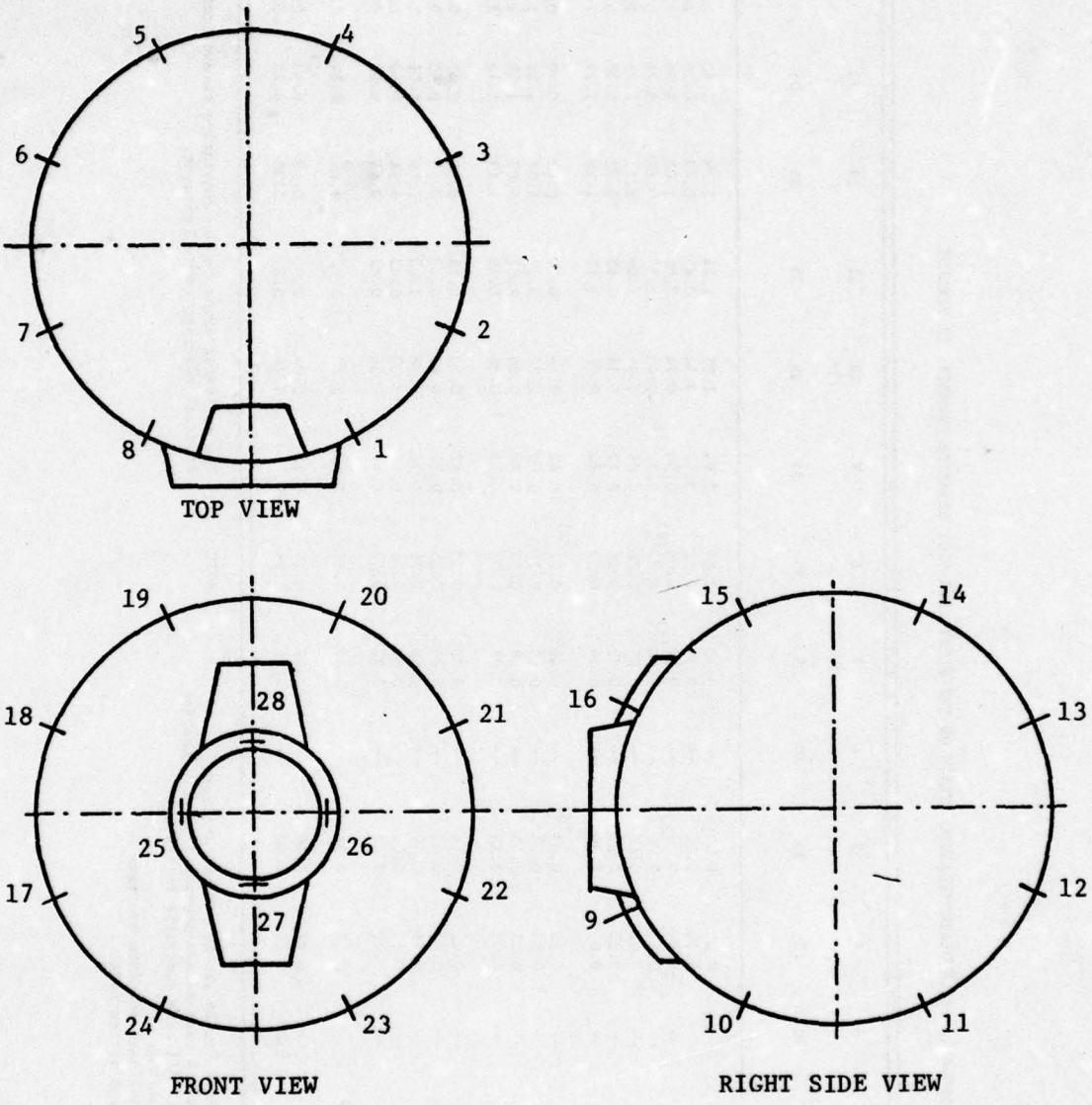


FIGURE 5. LOCATION OF FIDUCIAL MARKS ON THE SECOND FIVE-FOOT DIAMETER CHAMBER

TABLE 2. ACCUMULATED PLASTIC STRAIN ON THE SECOND FIVE-FOOT DIAMETER CHAMBER, IN PERCENT

Marks[a]	After Shot 1 %	After Shot 2 Individual %	After Shot 2 Cumulative %	After Shot 3 Individual %	After Shot 3 Cumulative %
1-2	.26	.37	.64	.27	.91
2-3	-.004	.02	.02	.01	.03
3-4	.17	.21	.37	.28	.66
4-5	-.04	.05	.01	.11	.12
5-6	.16	.20	.37	.15	.52
6-7	-.004	.03	.02	.03	.05
7-8	.24	.26	.50	.22	.72
9-10[b]	.31	.43	.74	.45	1.20
10-11[b]	.75	.20	.94	.32	1.26
11-12[b]	.21	.33	.54	.39	.93
12-13	-.05	.10	.05	.14	.19
13-14	.07	.15	.22	.27	.49
14-15	.42	.26	.68	.43	1.11
15-16	.17	.26	.44	.23	.67
17-18	.004	-.02	-.02	.12	.11
18-19	.06	.05	.11	.0	.13
19-20	.37	.09	.46	.68	1.14
20-21	.03	-.01	.02	.16	.18
21-22	.02	.02	.04	.02	.05
22-23[b]	.11	.26	.36	.28	.65
23-24[b]	1.02	.18	1.19	.20	1.40
24-17[b]	.11	.21	.32	.09	.41
Ave. #1[c]	.199	.166	.365	.223	.588
Ave. #2[d]	.117	.129	.246	.197	.443
25-26	.02	-.03	-.01	-.02	-.03
27-28	-.10	-.09	-.19	.005	-.19

NOTE:

(a) Refer to Figure 5 for location of marks.
(b) These gage marks were used on No. 2 chamber only.
(c) Average of all gage marks on chamber skin.
(d) Average of same 16 gage marks as used on chamber No. 1.

tested were mounted on cradles identical to those used for the trailer-mounted versions but due to the design of the cradle support it was deemed unnecessary to conduct the testing with the chambers actually mounted on trailers. Chamber No. 1 was tested with the cradle essentially on the floor of the test containment building. The cradle for Chamber No. 2 was supported along two edges by several railroad ties to allow access to the bottom surface of the chamber for observation and measurement. For clarity, the results of the tests on the two chambers will be discussed serially in the following paragraphs.

Explosive Testing of the First Chamber

As shown in Table 1, Shots Nos. 1 and 2 employed 10 lb charges, and the vessel response was elastic. Shot No. 3 used 20 lb of explosive and the result was on the threshold of plastic response. Shots Nos. 4 and 5 used 25 and 30 lb of C-4, respectively, and a small plastic response was obtained. The doors of the chamber were not closed for Shot No. 5. The chamber recoiled about 18 in., due to the blast exiting the open port, whereupon it collided with the flat vertical concrete wall of the test containment building[12], producing a flat area ~11-1/2 in. across on the spherical surface opposite the port. The door hinge bolts were sheared off but both door halves were retained inside the vessel. Minor damage, mostly in the form of bending, also occurred in the cradle region under the support feet, but the chamber was retained on the cradle.

The dent in the area of gage lengths 4-5 and 9-10 (see Figure 4) made these particular gage lengths of little value for several subsequent shots; nevertheless a significant charge-shape effect was evident. In Shot No. 4, the major flat surfaces of the truncated cubical charge were oriented as shown in Figure 6. The nonuniform strain distribution noted led to the hypothesis that the shape of the charge was affecting the results. To test this hypothesis, the orientation of the charge for Shot No. 5 was rotated 45 deg as shown by the dashed lines in Figure 6 with the result that the locations of maximum and minimum strains also shifted by 45 deg as

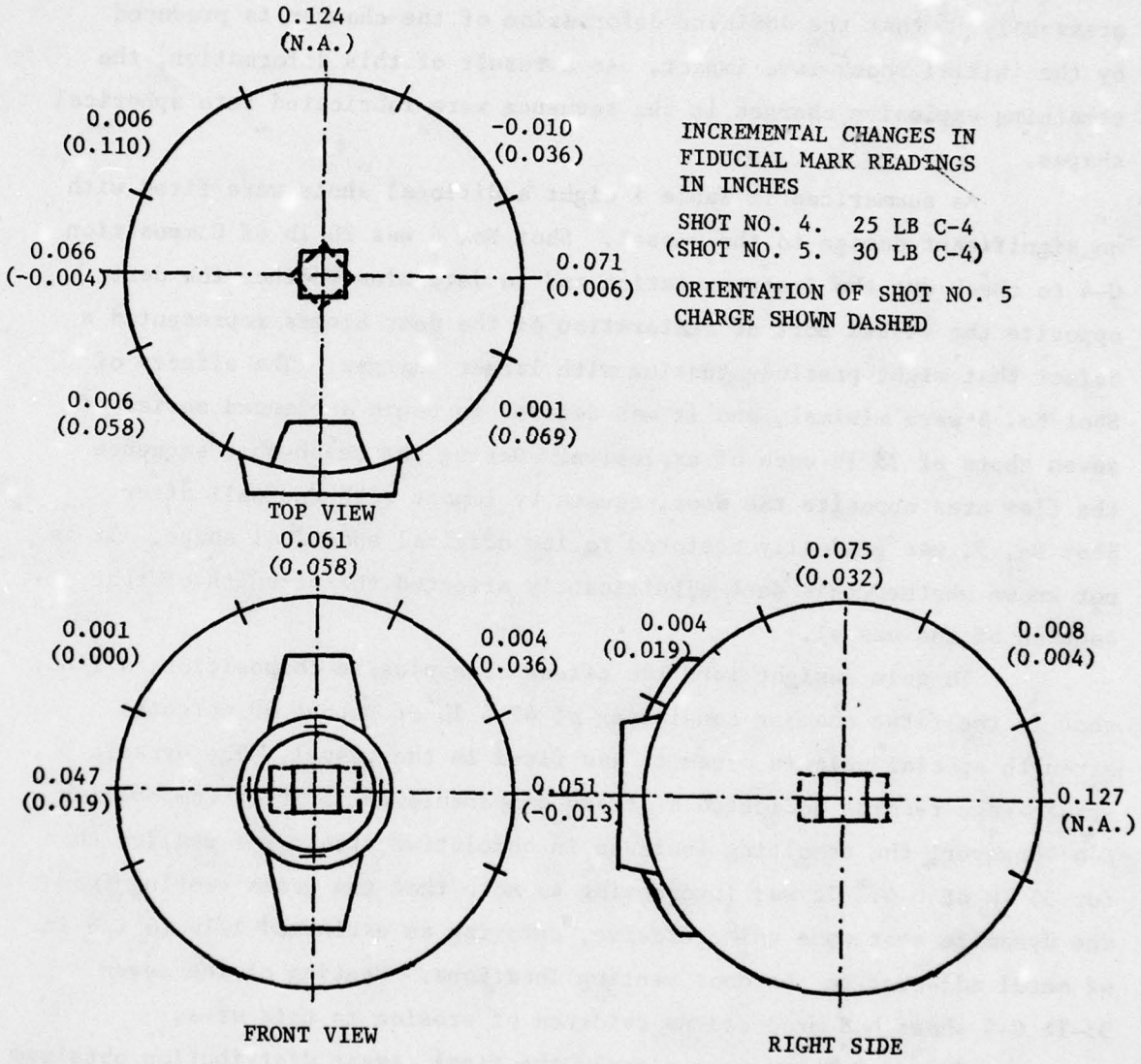


FIGURE 6. EFFECT OF CHARGE SHAPE AND ORIENTATION ON INCREMENTAL STRAIN DISTRIBUTION IN THE FIRST FIVE-FOOT DIAMETER CHAMBER

shown in the figure, thus demonstrating the charge-shape effect. These results may also be taken as further confirmation of effects noted previously[2] that the dominant deformation of the chamber is produced by the initial shock-wave impact. As a result of this information, the remaining explosive charges in the sequence were fabricated into spherical shapes.

As summarized in Table 1 eight additional shots were fired with no significant damage to the vessel. Shot No. 6 was 20 lb of Composition C-4 to check out the instrumentation and to determine whether the dent opposite the vessel port or restoration of the door hinges represented a defect that might preclude testing with larger charges. The effects of Shot No. 6 were minimal, and it was decided to begin a planned series of seven shots of 35 lb each of explosive. During the seven-shot sequence the flat area opposite the door, caused by impact with the wall after Shot No. 5, was gradually restored to its original spherical shape. It is not known whether this dent significantly affected the strength of that section of the vessel.

To gain insight into the effect of explosive composition, a final shot in the first chamber consisting of 47.5 lb of Dupont 60 percent strength special gelatin dynamite was fired in the vessel. The dynamic strain-gage records indicated a strain comparable to 35 lb of Composition C-4; however, the resulting increase in cumulative strain was smaller than for 35 lb of C-4. It was interesting to note that the gases venting from the dynamite shot were quite erosive, removing an estimated 1/16 to 1/8-in. of metal adjacent to the door venting locations. Venting of the seven 35-lb C-4 shots had produced no evidence of erosion in this area.

Figure 7 shows more clearly the final strain distribution obtained on Chamber No. 1. With the exception of the somewhat exaggerated strain which occurred at the top of the chamber, the strain distribution generally follows the variation in wall thickness as shown in Figure 3. These strains are all well within the capability of this chamber material[2]. The average accumulated strain observed by the static measurements of the strain gages

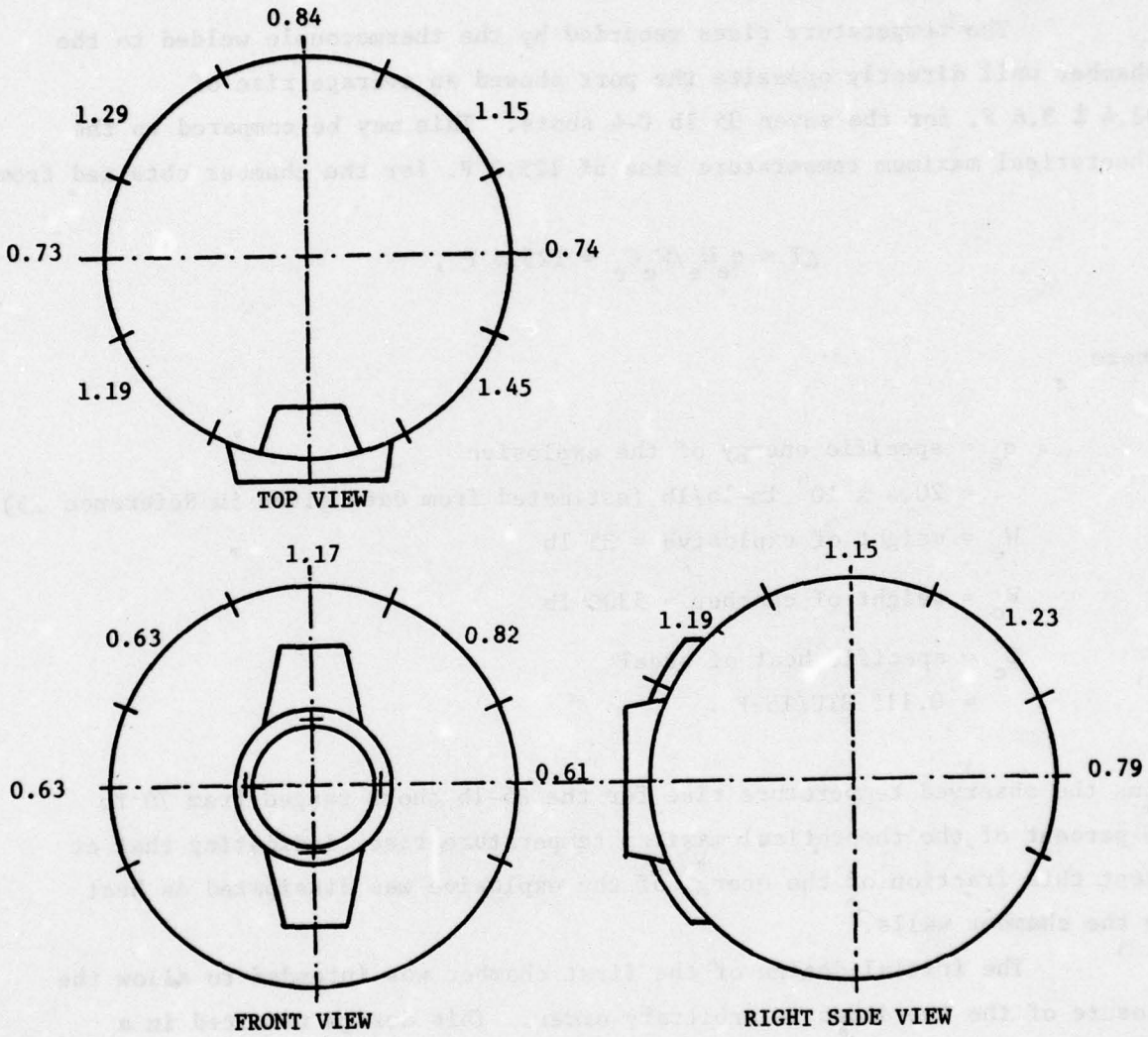


FIGURE 7. ACCUMULATED STRAIN DISTRIBUTION IN PERCENT ON THE FIRST FIVE-FOOT DIAMETER CHAMBER AFTER SHOT NO. 14

installed on the chamber was in general agreement with direct measurements on the chamber surface, although some uncertainties exist owing to damage to the strain-gage leads after Shot No. 5.

The temperature rises recorded by the thermocouple welded to the chamber wall directly opposite the port showed an average rise of 92.4 ± 3.6 F. for the seven 35 lb C-4 shots. This may be compared to the theoretical maximum temperature rise of 125.5 F. for the chamber obtained from

$$\Delta T = q_e W_e / W_c C_c = 125.5 \text{ F} ,$$

where

q_e = specific energy of the explosive
= 20.4×10^6 in-lb/lb (estimated from data given in Reference 25)

W_e = weight of explosive = 35 lb

W_c = weight of chamber = 5300 lb

C_c = specific heat of steel
= 0.115 BTU/lb-F .

Thus the observed temperature rise for the 35-lb shots ranged from 70 to 85 percent of the theoretical maximum temperature rise, indicating that at least this fraction of the energy of the explosive was dissipated as heat in the chamber walls.

The initial design of the first chamber was intended to allow the closure of the two doors in arbitrary order. This design resulted in a wedge-shaped notch along the outer face of the doors, which allowed venting of the contained gases to the outside at the top and bottom of the doors. After firing each of the first five charges, the venting gases burned with a bright noisy flame several feet in length extending from the port of the vessel as viewed by movie and closed-circuit TV camera coverage.

During the repair after Shot No. 5 additional metal was added near the top and bottom of one of the doors by welding to completely fill the original wedge-shaped notch and thus to reduce the venting rate. Also, an overlapping strap was fastened to the back of the other door to cover the small gap between the doors. After these modifications venting was still severe enough to produce a noisy hot flame at the port, but much smaller than the original flame noted. For the 35-lb shots, the venting time increased from 2 minutes 15 seconds for Shot No. 7 up to 3 minutes 20 seconds for Shot No. 10, then decreased with each successive shot to 2 minutes 15 seconds again at Shot No. 13. The 47.5-lb dynamite Shot No. 14 vented in 25 seconds with little or no flame at the port.

At the conclusion of testing there was no evidence of cracking or failure of any of the main structural welds, or of the vessel surface or reinforcing ring of any kind. In the first vessel design a vertical reinforcing plate extended all the way between the two hinge pivot straps. This vertical reinforcing plate was bowed inward gradually during the progress of the tests to contact the outer edges of the doors and caused minor difficulty in opening and closing the doors. The bowing of these plates also pulled the inner ends of the hinge pivot straps slightly closer together, initiating small cracks at the welds at the outside corners of three of the four hinge pivot straps where they were welded to the reinforcing ring. However, none of these cracks propagated far enough to produce any significant failure.

After shipment of the first 5-ft chamber to the Naval Explosive Ordnance Disposal Facility an exaggerated swelling on the bottom surface of the vessel was noted which was not visible with the vessel on its cradle. As a result of this finding, the second chamber and cradle were mounted higher during testing to provide access to its bottom surface for overall measurements.

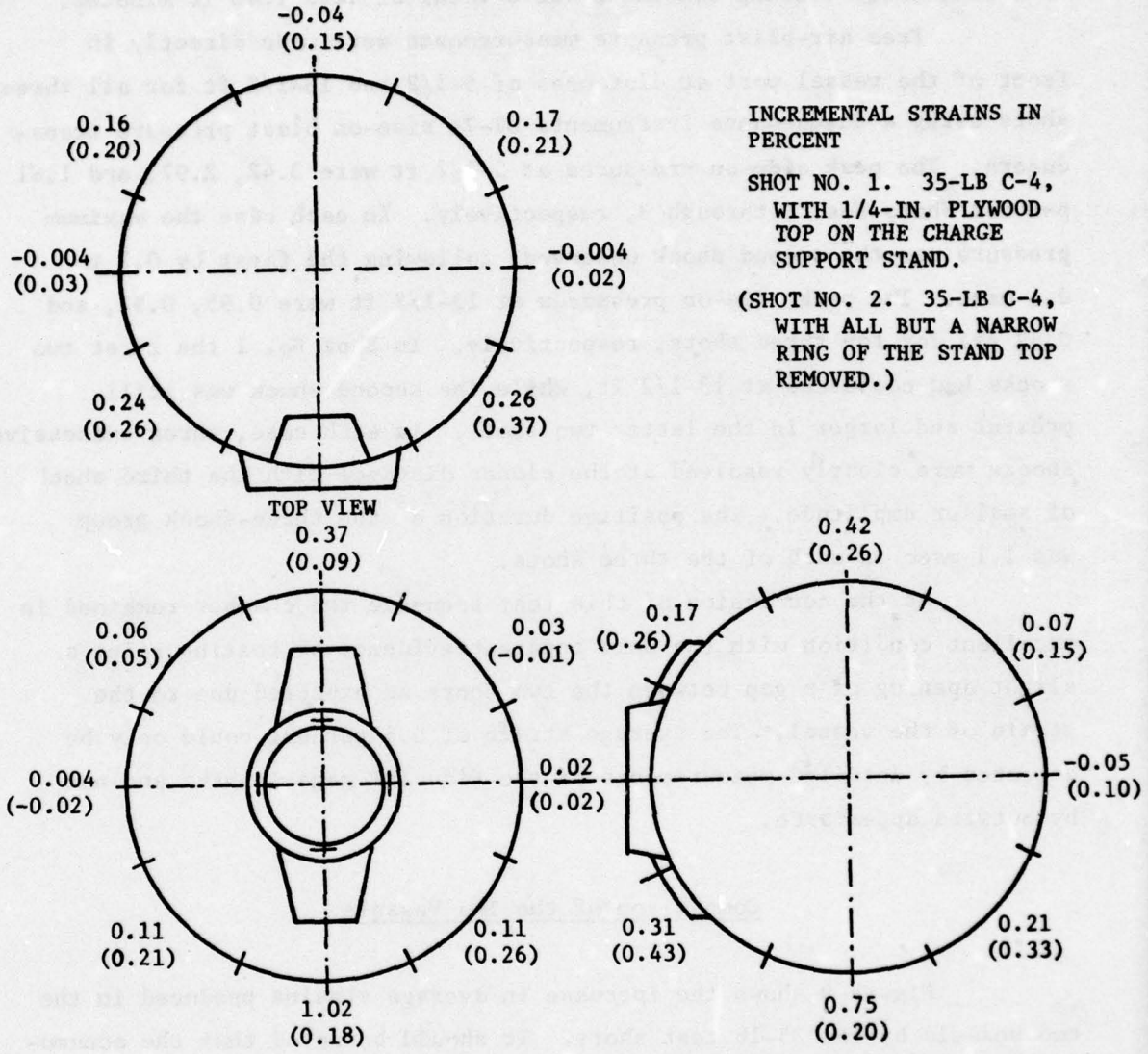
Explosive Testing of the Second Chamber

This chamber had a reinforcing ring of A537-72A Class 2 material, whereas the first chamber tested had a reinforcing ring of A-350A Class LF3 material. In this chamber as well as the trailer-mounted chambers delivered, the door design was altered to that shown in Figure 2. In addition, special spring-loaded blocks overlapping the joint between the doors at their top and bottom were installed to effect a better seal. The hinge support plate, which was bent during the first test, was modified as shown in Figure 2 to reduce the blast loading on it and to provide the maximum possible clearance between it and the door.

Table 2 shows the strains calculated from the changes in fiducial gage lengths for the three 35-lb charges fired in this chamber. Figure 5 shows the modified set of fiducial marks used on this chamber.

The charge for Shot No. 1 was supported on the same design stand used in the testing of the first chamber, i.e., a 10-in. square, 1/4-in. plywood top supported on 24-in.-long, 1 x 2-in.-thick legs. For this shot relatively larger strain was produced on the bottom of the vessel than at other locations. As a check on whether the plywood top on the charge-support stand was responsible for this observation, all but a narrow strip around the edge was cut away from the top of the similar stand prepared for Shot No. 2. To maintain the charge in the vessel center without direct support under the bottom, 1 x 2-in. strips of Styrofoam were taped to the remaining edges of the stand top. The strain distributions resulting from these two shots are shown in Figure 8. It will be noted that the exaggerated strains at the bottom and top of the vessel were eliminated by this modification in the charge support. A similar open topped support stand was used for Shot No. 3 with similar results.

The modifications to the doors to effect a better seal were fairly effective. The escaping detonation-product gas did not ignite, and venting of the gases continued for about 13 minutes after the first shot. After Shot No. 2, the escaping gases ignited and burned at the port for about 10 minutes with flames about 3 ft in length, much less than noted



INCREMENTAL STRAINS IN PERCENT

SHOT NO. 1. 35-LB C-4, WITH 1/4-IN. PLYWOOD TOP ON THE CHARGE SUPPORT STAND.

(SHOT NO. 2. 35-LB C-4, WITH ALL BUT A NARROW RING OF THE STAND TOP REMOVED.)

FIGURE 8. EFFECT OF 1/4-INCH PLYWOOD CHARGE SUPPORT ON INCREMENTAL STRAIN DISTRIBUTION OF THE SECOND FIVE-FOOT DIAMETER CHAMBER

previously. After the third shot, the gases burned for 6 seconds and then went out, while venting continued for a total of less than 10 minutes.

Free air-blast pressure measurements were made directly in front of the vessel port at distances of 5-1/2 and 13-1/2 ft for all three shots using a Susquehanna Instruments ST-7A side-on blast pressure transducers. The peak side-on pressures at 5-1/2 ft were 3.42, 2.97, and 1.61 psi for Shots Nos. 1 through 3, respectively. In each case the maximum pressure was the second shock observed, following the first by 0.2 to 0.4 msec. The peak side-on pressures at 13-1/2 ft were 0.95, 0.92, and 0.52 psi for the three shots, respectively. In Shot No. 1 the first two shocks had coalesced at 13-1/2 ft, while the second shock was still present and larger in the latter two shots. In each case, three successive shocks were clearly resolved at the closer distance with the third shock of smaller amplitude. The positive duration of the three-shock group was 1.1 msec in each of the three shots.

At the conclusion of this test sequence the chamber remained in excellent condition with the only apparent evidence of testing being a slight opening of a gap between the two doors as expected due to the strain of the vessel. The average strain of 0.6 percent could only be detected by detailed measurements of the fiducial gage lengths and not by outward appearance.

Comparison of the Two Vessels

Figure 9 shows the increase in average strains produced in the two vessels by the 35-lb test shots. It should be noted that the accumulated strain of 0.32 percent for Chamber No. 2 on the ordinate was produced by the previous testing with smaller explosive charges. Also it should be recalled that no strain measurements were made across the bottom of Chamber No. 1 and that later examination showed that some exaggerated strain in this area had taken place. Thus it is felt that the agreement in the strains observed on the two vessels is quite reasonable, considering the

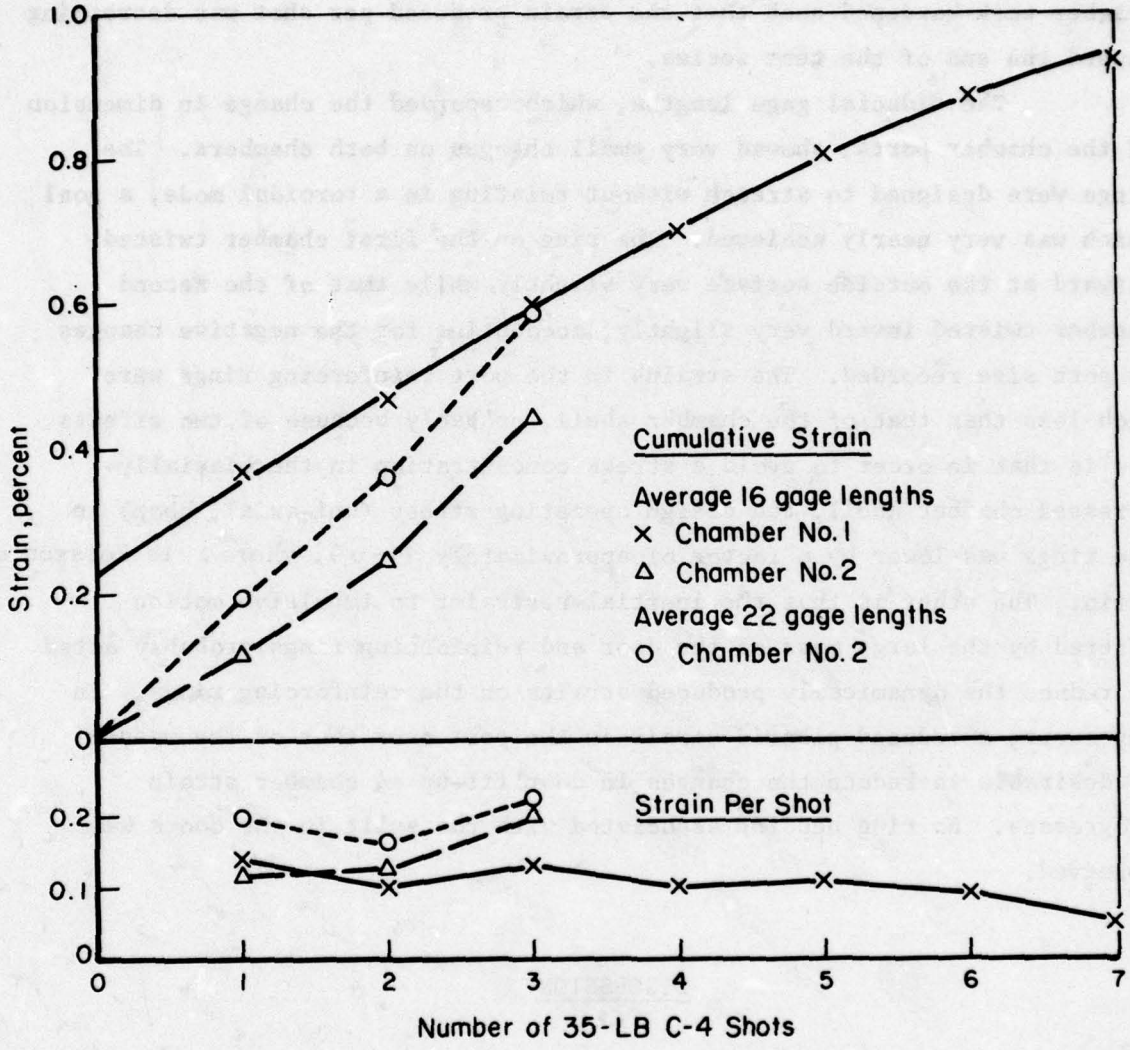


FIGURE 9. COMPARISON OF AVERAGE STRAIN ON CHAMBERS 1 AND 2 PRODUCED BY 35-LB COMPOSITION C-4 SHOTS

differences in the test histories and the charge support mechanisms used. From the extended testing sequence in Chamber No. 1, it appears that the chamber work-hardened such that the strain produced per shot was decreasing toward the end of the test series.

The fiducial gage lengths, which recorded the change in dimension of the chamber ports, showed very small changes on both chambers. The rings were designed to stretch without twisting in a toroidal mode, a goal which was very nearly achieved. The ring on the first chamber twisted outward at the outside surface very slightly, while that of the second chamber twisted inward very slightly, accounting for the negative changes in port size recorded. The strains in the port reinforcing rings were much less than that of the chamber shell, probably because of two effects. One is that in order to avoid a stress concentration in the biaxially-stressed chamber shell, the design operating stress (uni-axial, hoop) in the rings was lower by a factor of approximately $(1-\nu)$, where ν is Poisson's ratio. The other is that the inertial restraint to impulsive motion offered by the large mass of the door and reinforcing rings probably acted to reduce the dynamically produced strains on the reinforcing rings. In any event, a reduced plastic strain in the port over that of the vessel is desirable to reduce the changes in door fit-up as chamber strain progresses. No ring bending associated with the split in the doors was observed.

DISCUSSION

Complete containment of the blast from an explosion has been achieved in many installations for a number of years.[9,10,26] However, the usual approach is to design the chamber to keep the maximum stresses in the elastic response region of the structure. When the containment of many repeated blast loadings are part of the design criteria, such as for explosive welding, research and development, or testing applications, an elastic design, with consideration of possible fatigue failure effects,[2,19] becomes a necessity.

For several other applications, where a blast containment structure may be necessary or desirable for the provision of safety but where no intentional detonations are to be conducted and the frequency of accidental detonations is quite low, such as the present explosive ordnance disposal application or some hazardous manufacturing or demilitarization operations, the design of a blast containment chamber to take advantage of the appreciable savings possible through use of plastic deformation of the structure becomes quite attractive.

At the outset of this effort, however, there were no known applications in which plastic deformation of a complete containment structure was included as part of its design. Due to the requirement that containment was to be achieved while maintaining a high level of safety, a conservative design was selected for this program which depended on the successful achievement of only very modest plastic strains.

Through use of the well-known[7,22] impulse approximation, and an elastic perfectly plastic constituitive model, it is easy to show the weight savings potentially achievable using chambers designed for plastic deformation. Table 3 shows the chamber wall thicknesses, weights, and weight savings for several levels of plastic strains which might be chosen as design points. It will be noted that the original design of the vessels actually built was based on 50,000 psi yield strength material and a predicted 0.46 percent strain per shot, which yields a predicted weight savings of $\sim$ 68 percent, over a chamber designed for incipient yield. Under the conditions evaluated, which lead to $\sim$ 0.15 percent strain per shot, using the estimated dynamic yield strength[2] of the shell material of 80,000 psi and the delivered average shell thickness of 1.40 in., yields a calculated weight savings of $\sim$ 39 percent over a chamber designed for incipient yield at this higher yield strength.

Since the inception of this program, several 2-ft.-diameter vessels[2,3] of a similar design have demonstrated the capability to absorb over 1 percent plastic strain per shot, and in one case, 3.8 percent plastic strain in a single shot. Thus, the large weight savings shown in Table 3 for 1 percent design plastic strain appear to be achievable. Of course,

TABLE 3. POTENTIAL WEIGHT SAVINGS FOR A FIVE-FOOT DIAMETER BLAST CONTAINMENT CHAMBER DESIGNED FOR PLASTIC STRAIN

Design Plastic Strain, percent	Required Wall Thickness, inches	Spherical Shell Weight, pounds[a]	Weight Savings Over Elastic Design, percent
	For An Assumed 50,000 psi Yield Strength		
0[b]	3.66	13,200	--
0.1	2.25	7,750	41
0.2	1.77	6,000	55
0.4	1.33	4,450	66
0.46	1.25	4,150	68
0.6	1.11	3,700	72
1.0	0.87	2,900	78
	For An Assumed 80,000 psi Yield Strength		
0[b]	2.23	7,700	--
0.1	1.57	5,300	31
0.15	1.40	4,700	39
0.2	1.28	4,250	44
0.4	0.99	3,250	57
0.6	0.83	2,750	64
1.0	0.66	2,200	72

NOTES:

(a) Weights given are spherical shells only. Total chamber weights are greater but will approximately scale with the shell weight.

(b) Designed for maximum elastic stress equal to the yield stress.

good materials and fabrication quality control practices must be maintained, as well as proper materials selection for the expected temperature of operation to succeed with the application of such designs.

CONCLUSIONS

(1) The concept of complete blast containment utilizing a design for plastic strain was proven in the chamber design developed in this program for 35-lb charges of Composition C-4.

(2) The average plastic strain increments per 35-lb shot were small, 0.045 to 0.223 percent. In smaller chambers, single shot plastic strain increments up to 3.8 percent have been successfully contained[3]. Thus it seems highly probable that considerably larger charges could be contained for a limited number of shots in chambers of the size built during this program. A spherical charge in the range of 70 to 80 lb of Composition C-4 is predicted to produce only approximately one percent plastic strain, which should still be a safe situation.

(3) Where limited numbers of detonations are to be contained, 40 percent or more savings in containment chamber weight can be realized by designing for plastic deformation of the containment chamber.

(4) For a containment chamber designed for plastic deformation, the occurrence of small, 1 to 1-1/2 percent strains has been proven not to impair a chamber's containment capability for a blast which will produce small ($\sim$ 0.2 percent) additional plastic strain increments.

(5) Both charge-shape effects and the presence of lightweight material surrounding the charge have both been shown to be significant. Further work is needed however to fully characterize these effects.

* * *

ACKNOWLEDGMENTS

Several persons on the Battelle staff made valuable contributions to the success of this program. These include Dr. Joe H. Brown, Jr., for his encouragement, Mr. H. W. Mishler for establishment and supervision of the welding procedures used in the fabrication of the containment chambers, Mr. A. S. Chace for technical support, Mr. W. H. Stefanov and others of the welding laboratory for conduct of the welding, Messrs. J. W. Neutzling, H. C. Burchfield and others of the machine shop for fabrication and fit-up of the chamber, cradle, tool boxes and trailer modifications, and Messrs. W. F. Schola and S. C. Green for assistance in the conduct of the explosive experiments.

REFERENCES

(1) Rogers, B. T., and Taylor, R. W., *Total Confinement of Clandestine Device Explosions*, FBI Law Enforcement Bulletin (August 1973), p 2.

(2) Trott, B. D., Backofen, J. E., and White, J. J., *Design of Explosion Blast Containment Vessels for Explosive Ordnance Disposal Units*, Final Report to Picatinny Arsenal, Dover, N. J., Contract No. DAAA21-72-C-0129, Battelle, Columbus Laboratories, Columbus, O. (June 1975).

(3) Trott, B. D., Backofen, J. E., and White J. J., *Blast and Fragment Capability of Portable Chambers*, Final Report to Naval Explosive Ordnance Disposal Facility, Indian Head, Md., Contract No. N00174-74-C-0219, Battelle, Columbus Laboratories, Columbus, O. (September 1975), AD A024 493.

(4) Barr, G. E., and Dahlgren, D. A., *Confinement of a Detonation*, Report SC-RR-72-0748, Sandia Laboratories, Albuquerque, N. M. (May 1973).

(5) Baker, W. E., Silverman, S., Briggs, E. M., and Pickett, A. G., *Engineering Feasibility of Contained Detonation (U)*, Report AFWL-TR-65-96, Final Report to Air Force Weapons Laboratory, Kirtland AFB, N. M., Southwest Research Institute, San Antonio, Tex. (October 1965), Secret.

(6) Wise, W. R., and Proctor, J. F., *Explosion Containment Laws for Nuclear Reactor Vessels*, Report NOLTR-63-140, Naval Ordnance Laboratory, Silver Spring, Md. (1965).

(7) Duffey, T., and Mitchell, D., *Containment of Explosions in Cylindrical Shell*, Int. J. Mech. Sci, 15, 237 (1973).

(8) Benham, R. A., and Duffey, T. A., *Experimental-Theoretical Correlation on the Containment of Explosions in Closed Cylindrical Vessels*, Int. J. Mech. Sci, 16, 549 (1974).

(9) Baker, W. E., *The Elastic-Plastic Response of Thin Spherical Shells to Internal Blast Loading*, J. Appl. Mech., 27, 139 (1960).

(10) Ivanov, A. G., Novikov, S. A., and Sinitsyn, V. A., *The Behavior of Steel Shells When Charges of Explosive Detonate Inside Them*, J. Appl. Mech. and Tech. Phys., 9, 706 (1968).

(11) Ivanov, A. G., Novikov, S. A., and Sinitsyn, V. A., *Scale Effect of the Explosive Destruction of Closed Steel Vessels*, Combustion, Explosion, and Shock Waves, 8, 101 (1972).

REFERENCES (Continued)

(12) Fling, R. S., and Linse, V., *Design and Operation of a Blast Containment Structure*, in *Behavior and Utilization of Explosives in Engineering Design*, edited by L. Davison and J. E. Kennedy; New Mexico Section of ASME (1972), p 167.

(13) Goddard, S., and Dunleavy, J. G., *The Experimental Design and Evaluation of a Bomb Disposal Unit*, Final Report to the International Association of Chiefs of Police, Gaithersburg, Md., Battelle, Columbus Laboratories, Columbus, O. (September 1971).

(14) Collett, R. W., and Griffin, C. J., *Testing of Open Spherical Shells for Possible Explosive Disposal*, Report 2051, Picatinny Arsenal, Dover, N. J. (October 1972).

(15) Collett, R. W., *External Blast and Blast Reduction from Explosives Suspended in Steel Pipes*, Report 4466, Picatinny Arsenal, Dover, N. J. (January 1973).

(16) King, P. V., *An Overview of the Suppressive Shielding Program*, in *Minutes of the Sixteenth Explosives Safety Seminar*, Hollywood, Fla., 24-26 September, 1974, Vol I, p 91.

(17) Cox, P. A., and Esparza, F. D., *Design of a Suppressive Structure for a Melt Loading Operation*, in *Minutes of the Sixteenth Explosives Safety Seminar*, Hollywood, Fla., 24-26 September, 1974, Vol II, p 793.

(18) Huffington, N. J., and Robertson, S. R., *Structural Analysis of Containment Structures*, in *Minutes of the Sixteenth Explosives Safety Seminar*, Hollywood, Fla., 24-26 September, 1974, Vol II, p 817.

(19) Huffington, N. J., and Robertson, S. R., *Containment Structures Versus Suppressive Structures*, Report 2597, Ballistic Research Laboratories, Aberdeen Proving Ground, Md. (February 1976).

(20) Trott, B. D., Backofen, J. E., and White, J. J., *The Design, Evaluation, and Delivery of a Prototype, Trailer-Mounted Chamber Capable of Complete Containment of the Blast From Forty Pounds of TNT*, Final Report to Naval Explosive Ordnance Disposal Facility, Indian Head, Md., Contract No. N00174-74-C-0218, Battelle, Columbus Laboratories, Columbus, O. (September 1975), AD A026 290.

(21) Proctor, J. F., *Internal Blast Damage Mechanisms Computer Program*, Report NOLTR 72-231, Naval Ordnance Laboratory, Silver Spring, Md (August 1972).

(22) Trott, B. D., and White, J. J., *Elastic-Plastic Response of a Spherical Vessel to Shock Loading*, Bull. Am. Phys. Soc., 2C, 812 (1975).

(23) Goodman, H. J., *Compiled Free-Air Blast Data on Bare Spherical Pentolite*, Report 1092, Ballistic Research Laboratories, Aberdeen Proving Ground, Md. (February 1960), AD 235 278.

(24) Roark, R. J., *Formulas for Stress and Strain*, 4th Edition, McGraw-Hill, N. Y. (1965), p 225, Case 36.

(25) Baker, W. E., *Explosions in Air*, University of Texas Press, Austin, Tex. (1973), p 152.

(26) MacKenzie, A., Dalrymple, E. W., and Schwartz, F., *Design of Pressure Vessels for Containing Explosives*, Report 1643, Picatinny Arsenal, Dover, N. J. (July 1965), AD 467 730.

TESTS ON A NEW TYPE OF BUILDING FOR STORAGE OF PROPELLANTS

Jean J. ROURE
Ingénieur Général de l'Armement
Inspection Technique de l'Armement
pour les Poudres et Explosifs
France

The building to be tested had a rectangular section with the two side walls and the rear wall strong, the front wall replaced by an iron grid, and a roof of concrete tiles. It is intended that in case of propellant fire inside, the pressure will be discharged first through the iron grid of the front operture and if pressure will increase, by the roof, the concrete tiles being blown out. Conversely in case of fire outside the concrete tiles will protect propellant inside against fragments and brands coming from outside.

Tests performed gave evidence that this type of building is adequate up to about 50 tons of gun propellant in plywood drums or 33 tons of gun propellant in bags.

PRECEDING PAGE BLANK-NOT FILMED

TESTS OF A NEW TYPE OF BUILDING FOR STORAGE OF PROPELLANT

Jean J. ROURE, Ingénieur Général de l'Armement
Inspection technique de l'Armement pour les Poudres
et Explosifs (France) and

Pierre H. FONTAINE, Assistant Safety Manager,
Société Nationale des Poudres et Explosifs, Paris, (France).

The magazines for propellants CAPTIEUX type are designed for a more efficient use of land in case of propellant storage by

(1) reducing the rear and side extension of exposed surface outside the magazine

(2) increasing the protection of the propellant against fragments and brands coming from outside.

Each magazine may consist in single cell or a row of several cells. A description of a single cell magazine is given in Annex I.

Purpose of the tests:

(1) to test the building with artillery gun propellants in bulk (bags) and small arms propellant in plywood drums and/or in bulk (bags),

(2) to verify that the fire propagation to the side or the rear of the building is unlikely,

(3) to settle the safety distance to apply between two rows of such magazines.

Scope:

Tests were made with quantities of propellants from 6 up to 60 tons.

- temperature measured by thermocouples near to the side or rear walls, never exceeded 100°C even when wind was blowing frontward.

- temperature measured by thermocouples, at 60 m in front of the building never exceeded 160°C (at 40 m mean temperature was about 250°C)

- at 40 m frontward of the building maximum speed of combustion gases never exceed 10m/s

- whatever was the quantity and the web of the propellant, combustion lasted about 30s for tests on propellant in bulk (bags) and about 3 to 4 mn for tests on propellant in drums

- concrete was more damaged by tests on bags than by tests on drums

- projections of brands from polyethylene bags, depends heavily on speed and direction of wind

- for a quantity of 40 t gun propellant in bulks almost all the concrete tiles were blown out; for a quantity of 20 t small arms propellant in bulk not all tiles were blown out.

Conclusions:

The tests result in the proposal of adoption of the below value for the main parameters of the magazines:

- in case of storage of propellant in bulk (bags)

  Internal volume of the building ..... 10 m^3/ton of propellant

  Front wall aperture ..... 1 m^2/ton of propellant

  Pressure discharge surface from the roof ..... 3 m^2/ton of propellant

  So for the type of cell described in annex I, the quantity would be 50 t

- in case of storage of propellant in plywood drums

  Internal volume of the building ..... 6,5 m^3/ton of propellant

  Front wall aperture ..... 0,65 m^2/ton of propellant

  Pressure discharge surface from the roof ..... 2 m^2/ton of propellant

In case of storage of propellant porous or with very high vivacity the quantity to be stored would be reduced by 20%. So for the type of cell described in annex I, the quantity would be 33 t.

The cells would be constructed side to side provided that the side wall would be of reinforced concrete (30cm thick) and would outpass the front wall and the roof of more than 1 m.

But the number of cell adjacent in a single building must be limited to about 3 or 4, due to difficulties they offer to handling. Between building of a same row a distance of 25 m appears as safe.

Between front and rear of the parallel rows of building 40 m appears as a safe distance for the above given quantities.

Between two rows of such building which would be near to row a distance of 25 m may be sufficient.

For exterior quantity-distances, the below values would be adopted for the above given quantities:

- in the front wall direction:

  . workshop distance 80 m

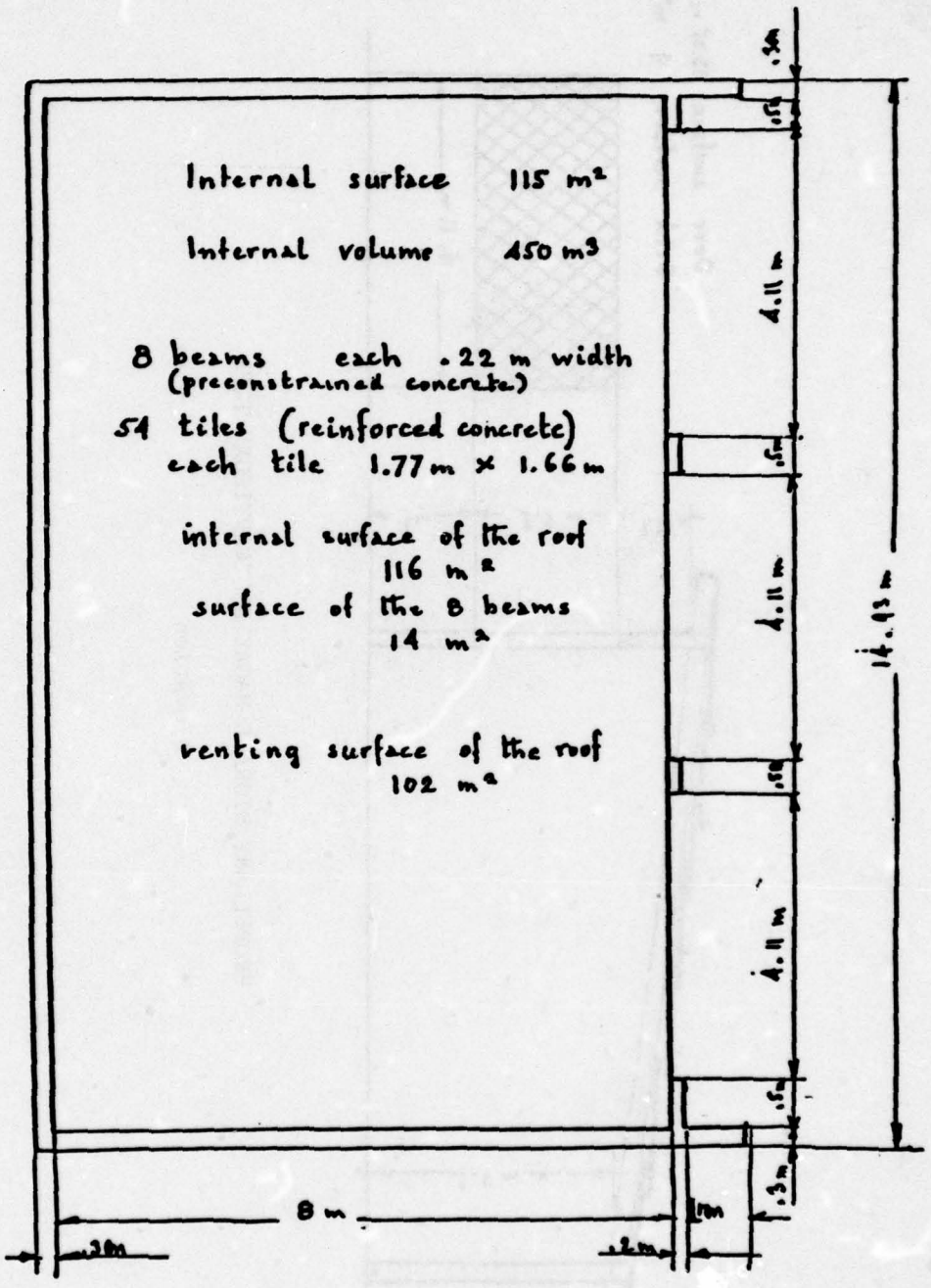
  . inhabited buildings, and highway distances 100 m

- in the side or near walls directions:

  . workshop distance 40 m

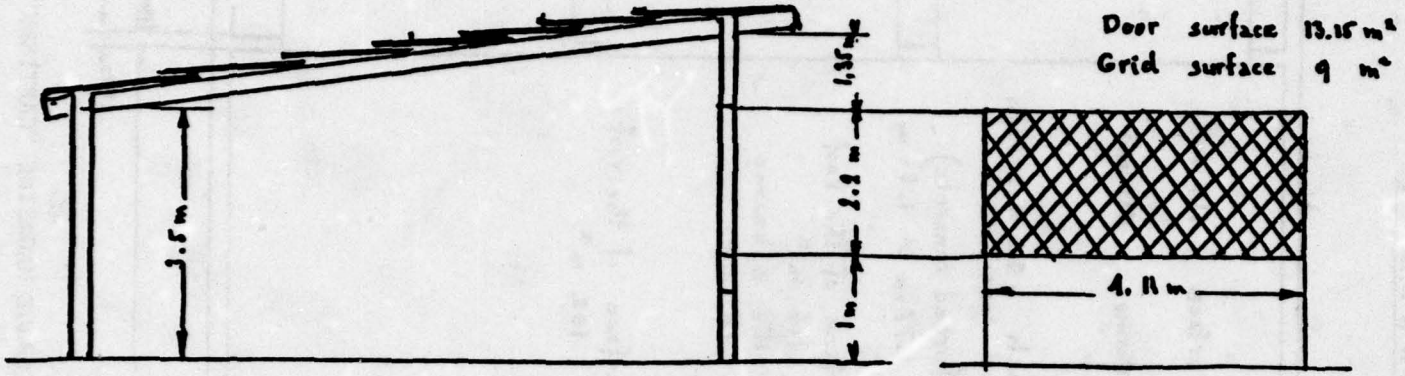
  . inhabited building distances 60 m

ANNEXE I



PROPELLANT STORAGE MAGAZINE "CAPTIEUX" TYPE

Plan View



PROPELLANT STORAGE MAGAZINE "CAPTIEUX" TYPE

Elevation

A N N E X E II

Translation of commentaries on the motion picture presented with the paper. SNPE/SE/pf 76-54 du 2.8.76

DESCRIPTION OF CAPTIEUX CAMP

Captieux Camp is an annex of the Landes Test Center with a surface of 10,000 Hectares. It lies at 100 km from Bordeaux. The size of the Camp allows the tests to be conducted on an actual operating scale without any danger for environment.

Firing station is approximately located in the middle of the Camp, in prolongation of an old igloos row.

Three storage buildings of the "Captieux" type have been built, just in front of the igloo row.

Each building is 15 m long and 8 m wide. The front wall is 4,60 m high and the back 3,50 m.

Openings are provided in the front wall of the building for the doors of which size is 4 m by 3 m each. Each door is partly made of solid metal and of a 9 sq m surface fitted with wire screen. Reinforced concrete walls are 30 cm thick. The roof is covered with 54 concrete slabs of 1,80 m by 1,60 m each of them approximately weighing 400 kg. The slabs, overlap each other. The roof surface is 100 sq m covering an inside volume of 450 cubic m.

Our control station is located in an igloo, 900 m from the firing station.

200 m from the firing station, cameras remote controlled from the control station are in a small building.

STORAGE AND TESTING FACILITIES OF THE "CAPTIEUX" TYPE

Various tests on combustion of powder in polyethylene bags and in barrels made of fine board have been carried out in buildings of the "Captieux" type.

The powder has been fired in various points by means of igniters fitted with small packs of igniting powder.

TEST WITH 6 TONS IN BAGS

The test with six tons in bags that you will see have been carried out with 3 tons of gunpowder in bags of 50 kg and 3 tons of Single Base powder in bags of 60 kg.

Combustion has been 30 s long, 20 meters ahead temperature of 700 °C has been reached, and 40 m ahead a 100° C have been reached. Flame front shown up by sawdust train burning has covered a distance of 50 m ahead.

The roof slabs have been lifted up by fire power. About ten of them have been removed.

TEST WITH 20 TONS IN BAGS

The following test has been carried out with 20 tons of gunpowder in bags of 68 kg.

This time, all the slabs have been blown over.

20 m and 40 m from the fire same temperatures as in the six tons test have been noted, that is to say 700°C and a 100°C respectively.

Combustion has not been longer than about 30 seconds and flame front has reached 30 m only (against 50 m in the previous test). This effect is probably due to the escape of the flames by the roof.

The fire has spread to bushes around the building, but the powder contained in concrete cells located 20 m ahead of the building and facing the opposite direction has not been reached by the flames.

In a test with 40 tons in bags, which has not been longer than 30 s, following temperatures have been obtained: 800° 20 m ahead and 150° 40 m ahead, that is to say slightly higher than in the test with 20 tons. Flame front has reached 100 m in this test with 40 tons, but there was no heat transfer through building walls.

The pine tree you can see on the right side of the screen, about 50 m behind the building, has not been damaged.

TEST WITH 20 TONS IN BARRELS

When powder is stored in barrels, combustion is much longer.

In 20 tons test in barrels, gunpowder in barrels of 68 kg has been used.

To make firing easier, 25 bags of powder, that is to say 1.7 tons, have been taken out from the barrels.

To follow flames development, the following sequences have been filmed through a very dark screen.

In this 20 tons test, first, igniting powder in bags has burnt for 1 minute, then the fire has spread to the powder in barrels, and combustion has been 4 mn long.

Right now you are seeing firing bags combustion.

The flames are decreasing, and because of the screen the fire seems to be dead (in fact, some flames are still burning). Then the fire is spreading to the barrels. Real combustion is beginning.

Temperatures of 450°C have been reached 20 m ahead the building and of 70°C 40 m ahead. They are slightly lower than those of the tests in bags.

Flame front has not been over 30 m ahead.

Many barrel covers have been blown up to 30 m.

The bright vertical line which can be seen on the building wall is caused by the reflection of electric aluminum armoured cables.

Under pressure, the roof slabs have been lifted up and the flames have been released.

In spite of long combustion time, the walls have only been slightly crumbled inside the building, but this time a slight heat transfer through the walls has been noted.

TEST WITH 60 TONS IN BARRELS

A test with 60 tons has been carried out with gunpowder in barrels of 50 kg, 80 powder bags, that is to say 4 t have been taken out from barrels for igniting.

This time, some slabs have been removed and burning powder has been thrown up through the roof.

As in the previous test, combustion has been 4 mn long and very violent.

The flames, moving ahead, have made a strong noise, like a jet motor.

In a while, a slab will come down, getting off a part of the roof, and releasing the flames. The slab has been found by the side of the building.

Barrel covers have been blown over up to 50 m. In spite of barrel position along the walls (about 50 cm), the building has remained undamaged after the test.

In a similar test carried out with 40 tons of gunpowder in barrels, a guinea pig has been put near the building, close by a side wall. The fire has remained guinea pig untouched, and now it has a wide offspring.

The difference between bags combustion and barrels combustion is to be noted. In the case of bags, combustion time is not long (about 30 s) and there is no heat transfer through the walls. In the case of barrels, combustion time is much longer (about 4 mn) and heat has run through the walls. However, in the latter case, temperatures higher than a 100°C have not been noted.

During these various tests, building walls have resisted the fire and elastic strains only have been produced by heat. Sometimes cracks have been noted after combustion, but they have disappeared when cooling.

In the middle of the building, reflections due to electric aluminum armoured cables can be seen again.

In every test, gaz speed has never been quicker than 10m/s at 40 m, and beyond, a material having the same reactions to the fire as human skin, has never been damaged.

In this 60 tons test in barrels, some slab have been removed.

The Safety Environment Department of the SNPE has concluded from these tests some safety rules concerning maximum admitted quantities and regarding the distances to be complied with for isolating buildings of the "Captieux" Type.

ANALYSIS OF CONCRETE ARCH MAGAZINE TO LONG DURATION OVERPRESSURE

J. M. Ferritto
Civil Engineering Laboratory
Naval Construction Battalion Center
Port Hueneme, California

INTRODUCTION

The Department of Defense has for many years stored explosive components of various weapon systems in earth-mounded arch magazines or igloos. Several varieties of reinforced concrete arch igloos have been used; one of the most prevalent used has been the circular barrel arch such as the Department of the Army, Office of the Chief Engineer's standard igloo, OCE Drawing Number 33-15-06.

The arch spans about 27 feet (8.22 m) and has a height at the crown of about 13 feet (3.96 m). The thickness of the reinforced concrete varies from 16 inches (0.4 m) at the base to 6 inches (0.15 m) at the crown. Reinforcing steel in the direction of the arch consists of No. 5 bars at 12-inch (0.30 m) centers on eacy face with a uniform concrete cover of 1-5/8 inches (0.041 m).

The arch igloos are covered with 2 feet (0.6 m) of soil, forming an earth berm sloping outward with a horizontal-to-vertical ratio of 2:1.

The objective of this project was to examine and upgrade the blast resistance of this arch to long-duration loading effects produced by a detonation of a nuclear weapon. The relatively steep slope of the earth berm results in an increase in loading from the reflection of the side-on overpressure blast wave and from the dynamic drag forces caused by the blast wind pressure. Further, the loading is principally on the side of the structure, producing a significantly asymmetrical loading condition on the arch. An approximate analysis indicated that the structure in its existing configuration would fail at a very low overpressure (less than 10 psi (69 kPa) side-on overpressure, equal to 25 psi (172 kPa) total dynamic pressure). To upgrade the hardness of the structure, it would be necessary to decrease the reflected pressure wave, the dynamic drag pressure, and/or the asymmetrical characteristics of the load applications. To achieve these results, it was proposed to flatten the slope to as near horizontal as possible (less than 4:1) and to increase the height of soil cover over the arch. The hardness level of the modified structure was evaluated using the finite element technique. This paper presents the results of the finite element analysis and the recommended modifications to the existing structure to upgrade its hardness to a side-on overpressure level of 100 psi (690 kPa).

ANALYSIS OF ARCH STRUCTURE

Finite Element Technique

The finite element method idealizes a continuum as an assemblage of a finite number of discrete structural elements interconnected at a number of joints or nodal points. This discussion considers planar sections idealized by being segmented into quadrilaterals. The program used in this study was NONSAP [1,2], a structural analysis program for static and dynamic analysis of nonlinear structural systems. The University of California at Berkeley (under sponsorship of the Bureau of Mines) and Engineering/Analysis Corporation (under contract from CEL) developed the program.

Two element types were used in this study – the truss and the two-dimensional continuum. The truss element has two nodes and is capable of transmitting axial force only. The lumped mass matrix technique was used which lumps half of the element's mass at each of the two nodes. The two-dimensional continuum element is an arbitrary quadrilateral shape used in this case to represent the plane strain idealization. The element may have any number of nodes between four and eight. Nodes above four are considered as midside nodes. Displacement interpolation functions are written to include midside nodes and are omitted when not used. The mass of the element is lumped equally at all of its node points. The program can perform a dynamic analysis by either numerical time integration or an eigenvalue method of mode superposition.

Material Models

Linear material properties were defined using a Young's modulus for truss elements and by a Young's modulus and Poisson's ratio for two-dimensional continuum elements. Nonlinear properties for the truss elements were defined by a series of stress and strain points. Nonlinear two-dimensional continuum elements were defined by a series of points at which the loading bulk modulus, unloading bulk modulus, and shear modulus were defined as functions of the volumetric strain. Tensile stresses were limited to set values in nonlinear concrete and soil elements.

The nonlinear two-dimensional continuum material model used incorporates crack propagation capability. Initially, the element material is treated as isotropic. When a principal tensile stress exceeds the allowed limit, the material becomes orthotropic; and the modulus in the "cracked" direction is divided by 100 to simulate the presence of a crack.

Arch Without Soil Cover

As a preliminary step in developing an understanding of the behavior of the structure, it was decided to study the arch by itself without any soil cover. A model was developed having 72 two-dimensional continuum

elements to represent the concrete and 72 truss elements tc represent the reinforcing steel (Figure 1). The base of the arch was restrained (or fixed) against translation and rotation.

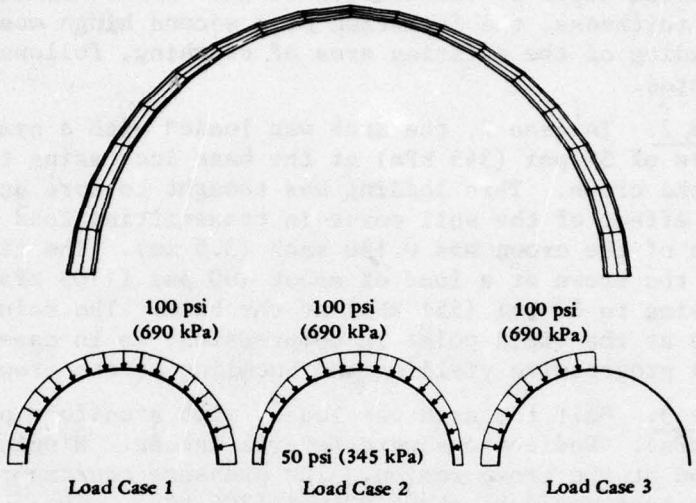


Figure 1. Finite element mesh of arch without soil cover.

The material properties of the arch were considered to be linear. The Young's modulus of steel reinforcing was assumed to be 29,000,000 psi (2.0×10^8 kPa), and the area of the truss elements representing the steel was determined by dividing the actual bar area by the bar spacing. In this manner, the steel reinforcement was represented as a continuum through the length of the arch, allowing, the use of a planar model. The dynamic concrete material in the two-dimensional continuum elements was modeled by an average Young's modulus of 3,000,000 psi (2.06×10^7 kPa) and a Poisson's ratio of 0.17.

Load Case 1. A uniform static pressure of 100 psi was applied around the arch. The thrust at the crown was computed by integrating the element stress contributions over the cross section. This value was found to be approximately equal to the thrust computed by simple pipe formula.

The deflection of the crown of the arch was 0.0506 inch (1.42 mm). This demonstrates the inherent stiffness of the arch section in symmetrical ring compression. The region with highest stress was the crown section. The arch structures were constructed a number of years ago with a design concrete strength of 2,500 psi (17,240 kPa). Applying a dynamic increase factor of 1.25 plus an age factor, ultimate concrete strengths of 4,000 psi (27,580 kPa) would not be considered excessive. By assuming a 4,000-psi (27,580-kPa) dynamic concrete strength, one would expect that the formation of the first hinge point at the crown would occur at a uniform pressure of 140 psi (965 kPa). This is based

on the stress in element 27 (2,840 psi, 19,581 kPa) and assumes crushing of the concrete cover. The steel stress would be above dynamic yield in compression (assumed to be 48,000 psi, 330,960 kPa). The ductility of this section is severely limited by the buckling of the reinforcement and by the minimum depth of the section at the crown. Because the arch has a varying thickness, the formation of a second hinge would not occur; rather a spreading of the existing area of crushing, followed by collapse, would be expected.

Load Case 2. In case 2, the arch was loaded with a symmetrical static pressure of 50 psi (345 kPa) at the base increasing to 100 psi (690 kPa) at the crown. This loading was thought to more accurately represent the effect of the soil cover in transmitting load to the arch. The deflection of the crown was 0.138 inch (3.5 mm). The first hinge would form at the crown at a load of about 160 psi (1103 kPa) at the crown, decreasing to 80 psi (551 kPa) at the base. The reinforcing steel would be at the yield point in compression; as in case 1 failure would occur as progressive yielding and buckling at the crown.

Load Case 3. Half the arch was loaded with a uniform pressure of 100 psi (690 kPa). Deflections were several inches. Hinging would occur at the base and at the crown region. The pressure causing the first hinge to form at the base would be about 30 psi (206 kPa). The data from the elastic analysis of the arch half loaded was very difficult to interpret. To obtain a better understanding of the failure mechanism under gross asymmetric loading, a static nonlinear analysis was performed. A bilinear concrete model with compression yielding at 4,000 psi (27,580 kPa) and tensile cracking at 400 psi (2,758 kPa) was used. The steel reinforcement was also a bilinear model both in tension and compression. Figure 2 gives the deflection of the structure. Figure 3 summarizes the arch behavior for various increments of load. The maximum static resistance of the arch is about 25 psi (172 kPa). This loading condition closely represents the arch in its existing condition with minimum soil cover.

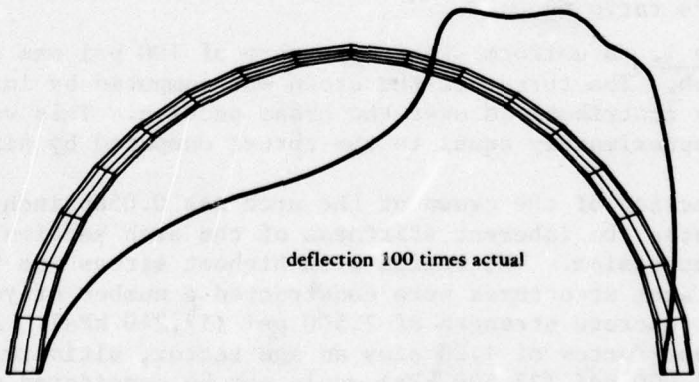


Figure 2. Deflection of arch under load case 3.

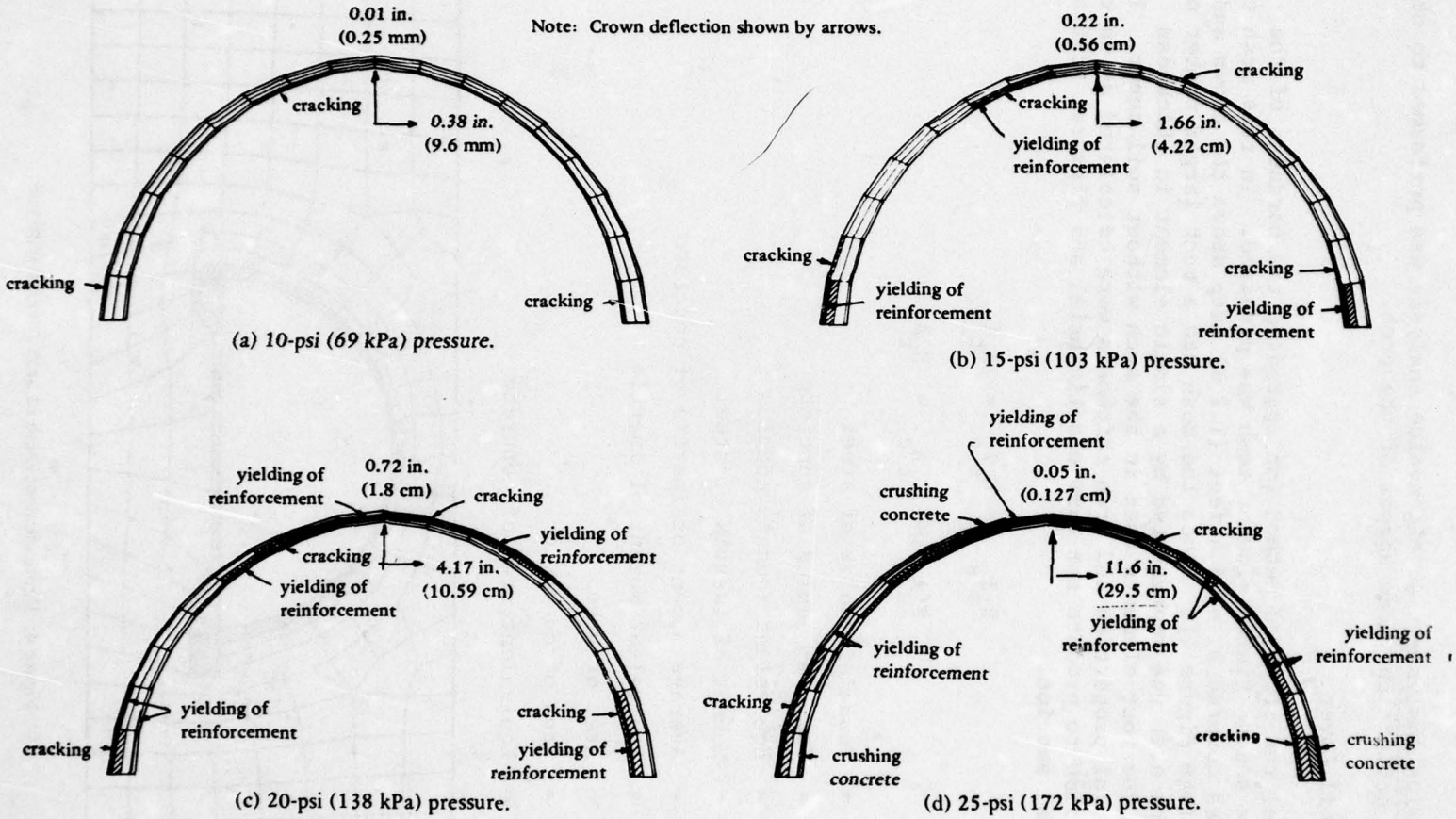


Figure 3. Behavior of arch under asymmetric load for various load increments.

Eigenvalue Analysis. An eigenvalue analysis was performed to obtain the natural periods and mode shapes of the arch.

Arch With Soil Cover

To model the proposed method for upgrading the hardness of the structure, a second finite element mesh was prepared. In this mesh the structure was covered by soil 4 feet (1.2 m) deep above the crown and horizontal (see Figure 4). Since the mesh had a much larger number of elements, the arch was represented by a single element in thickness rather than the four elements used in the arch without soil cover. The linear material properties and arch thickness were calculated as in the equations below to produce the same elastic axial and flexural stiffness as the actual section.

$$E_s I_s + E_c I_c = E_t I_t$$

$$E_s A_s + E_c A_c = E_t A_t$$

where E_s = Young's modulus of steel

E_c = Young's modulus of concrete

E_t = Equivalent Young's modulus

I_s = Moment of inertia of steel

I_c = Average moment of inertia of concrete

I_t = Equivalent moment of inertia

A_s = Area of steel

A_c = Area of concrete

A_t = Equivalent area of concrete

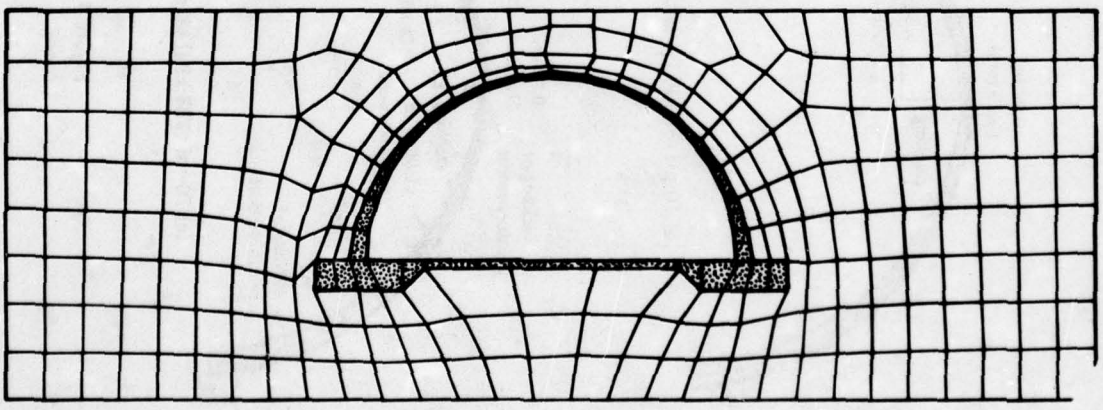


Figure 4. Finite element mesh of arch covered with soil.

As shown in Figure 4, a total of 266 elements and 307 node points were used in the mesh.

The portion of the mesh representing the ground surface was loaded with a 100-psi (690 kPa) static load. The thrust and moment along the arch are shown in Figure 5. Figure 6 gives the thrust-moment capacities of various sections of the arch.

The critical section is the crown section governed by thrust. By comparison of the calculated thrust-moment loading (196 kips (0.87 N) at 100 psi (690 kPa)) with the allowable thrust-moment capacity (270 kips (1.2 N)) at which yielding occurs, the pressure on the ground surface at which yield occurs is 138 psi. Since the pressure loading is nearly hydrostatic in this case, the load capacity of the arch should agree with that computed above when the arch was modeled by four elements in thickness without soil. The agreement is excellent – 138 psi (951 kPa) to 140 psi (965 kPa) – indicating the modeling of the arch by one-element-thick sections was accurate enough.

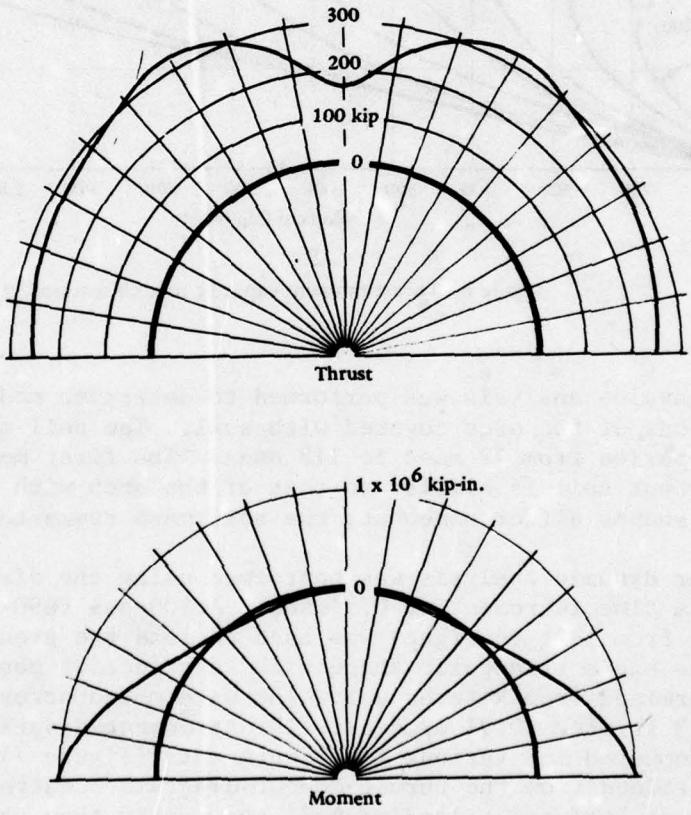


Figure 5. Thrust and moment of arch covered with soil, 100-psi static load.

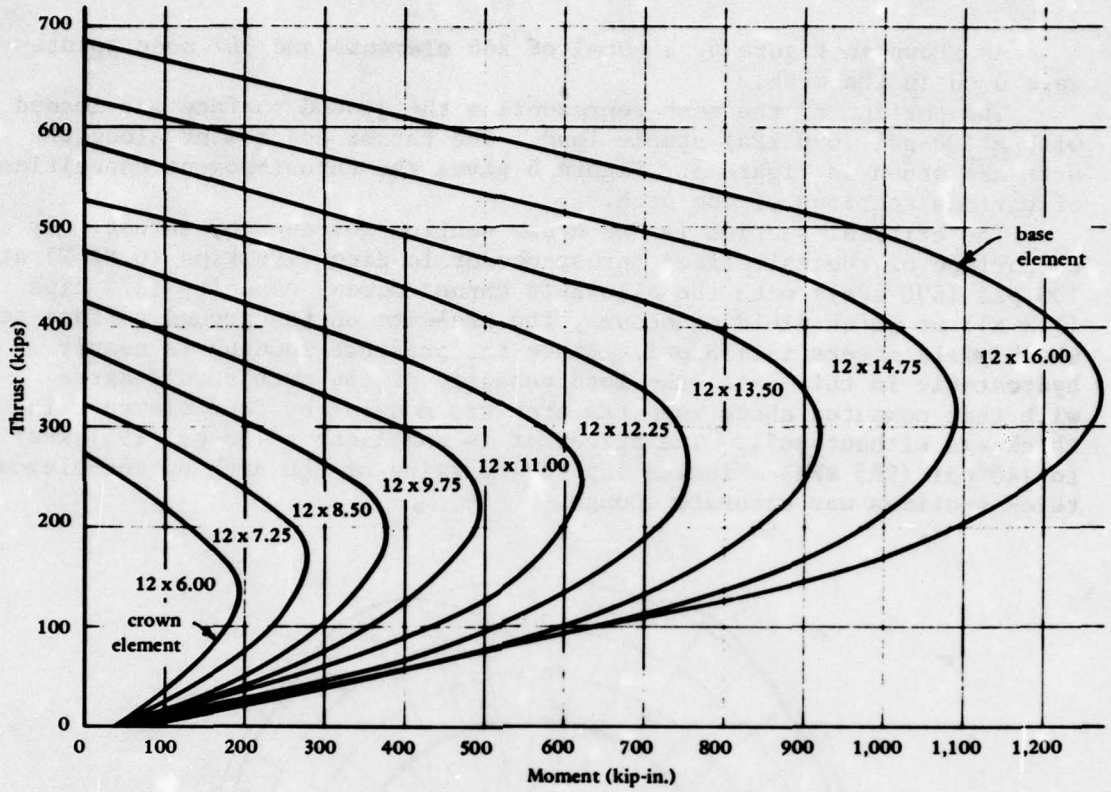


Figure 6. Thrust-moment capacity of arch sections.

An eigenvalue analysis was performed to determine mode shapes and natural periods of the arch covered with soil. The soil mass increases the natural period from 72 msec to 118 msec. The first mode shape of the arch without soil is similar to that of the arch with soil. However, higher mode shapes differ somewhat; the soil mass seems to restrain the arch.

A linear dynamic analysis was performed using the direct-integration method with a time increment of 0.5 msec. A 100-psi (690-kPa) traveling wave (moving from left to right) was used to load the ground surface; the pressure wave had a triangular shape with an effective positive wave duration as determined from Reference 3. The wave moved across the ground at the rate of 3 ft/msec (0.91 m/msec). Thrust-moment diagrams and pressure loads were computed for various time increments (Figure 7). The peak loading determined from the thrust-moment diagrams occurred at 34 msec. The moving wave produced a loading more asymmetric than the static loads. By using the thrust-moment loadings it was determined that the load at which the structures became inelastic (formed a first hinge) was 80 psi (551 kPa). Points of high stress (hinge formation) are shown in Figure 8.

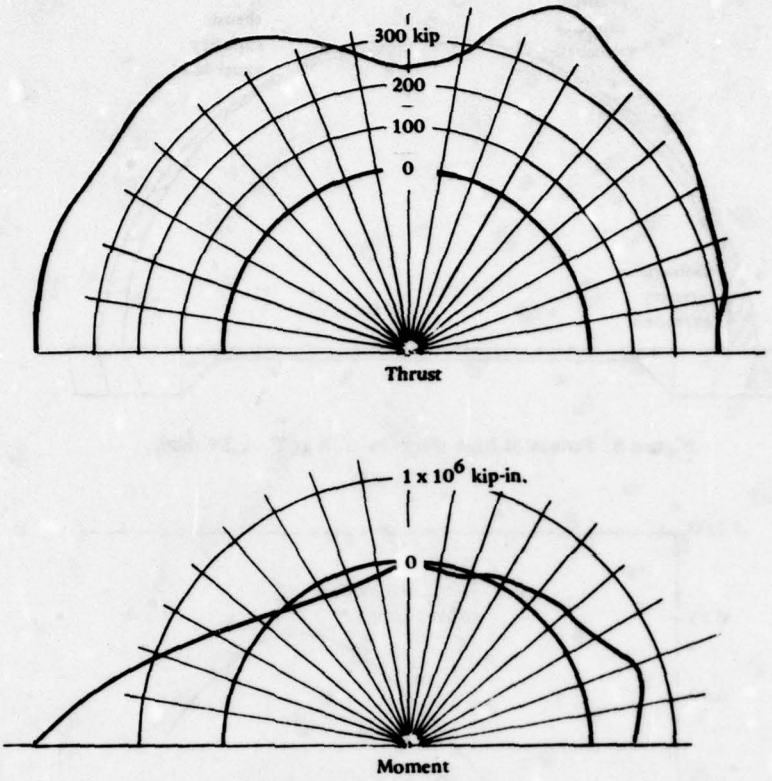


Figure 7. Thrust and moment of arch for time T = 34 msec, 100-psi (690-kPa) dynamic wave on surface.

If the structure were considered as a single-degree-of-freedom system with a natural period of 118 msec, the required structural resistance for a structure to remain elastic would be 1.8 times the load or 144 psi (993 kPa) (1.8 x 80 psi (551 kPa)). Since the stresses approach the ultimate capacity of the concrete (thrust rather than moment), the probability of failure over large areas of the arch is high. Therefore, it is necessary that the ductility factor allowed must be low - 1.3 to 1.5 [3]. Using the response of a single-degree-of-freedom system with a structural resistance of 144 psi (993 kPa) and a ductility factor of 1.4, the maximum total load capacity of the arch is 105 psi (724 kPa). Eliminating the dead load, the arch would be able to carry about 100 psi (690 kPa) side-on overpressure on the ground surface. This represents the maximum pressure that can be carried without structural modification of the arch. The deflection history of the crown of the arch is given in Figure 9.

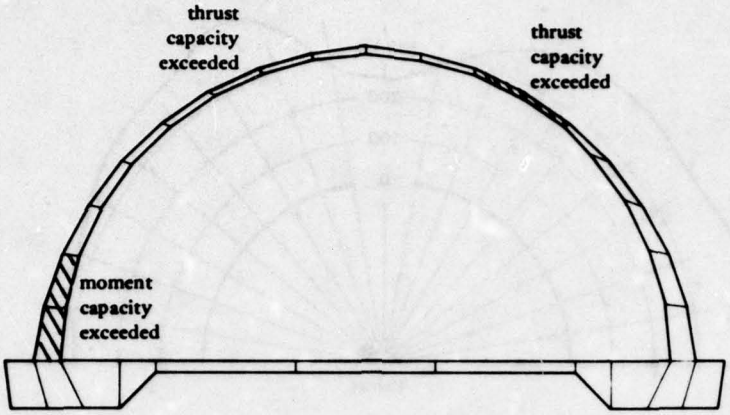


Figure 8. Points of high stress in arch at T = 34 msec.

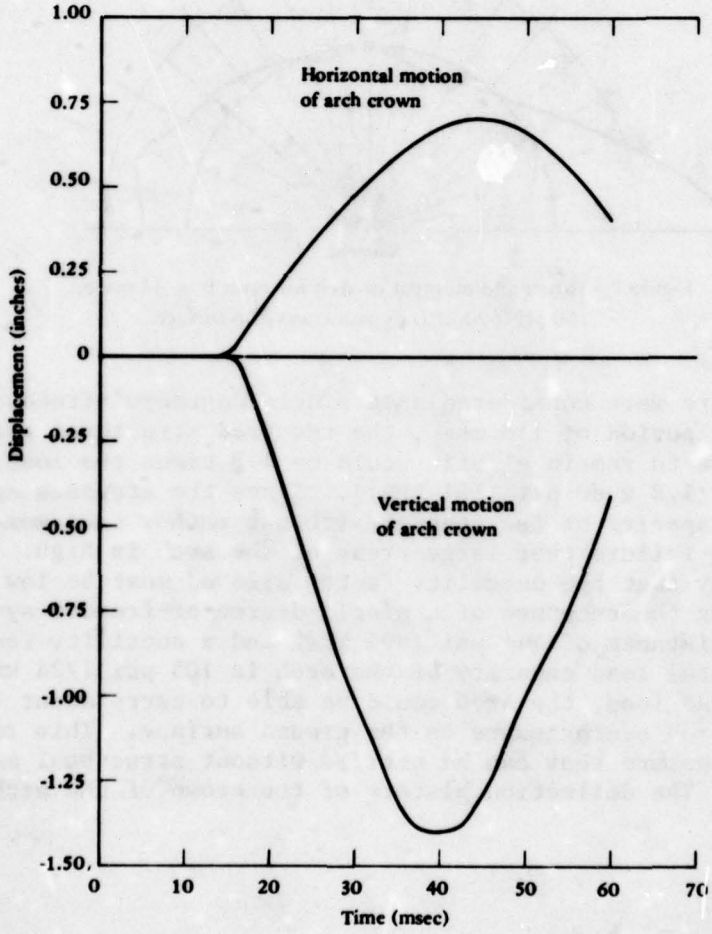


Figure 9. Deflection of crown of arch.

SUMMARY

The standard earth-covered arch was analyzed in its existing configuration and found capable of resisting a total dynamic long duration pressure of only 25 psi (172 kPa) (10 psi (69 kPa) overpressure). The loading produces an asymmetric condition mainly caused by the reflected pressure wave and the drag pressure. The soil cover above the arch was widened to flatten the slope to as near horizontal as possible. The structure was found to be capable of resisting a side-on overpressure of 100 psi.

REFERENCES

1. Engineering Analysis Corporation. E/AC Report 74-2: User's manual for N NONSAP, by K. J. Bathe and F. E. Peterson. Berkeley, CA (CEL Contract No. N62399-73-C0019) (under preparation).

2. Engineering Analysis Corporation. E/AC Report 73-3: July 1974. Theoretical basis for NONSAP, by K. J. Bathe and F. E. Peterson. Berkeley, CA (CEL Contract N62399-72-C0010) (under preparation).

3. Air Force Special Weapons Center. AFSWC TDR 62-138: Air Force Design Manual: Principles and practices for design of hardened structures. Kirtland Air Force Base, NM.

DYNAMIC ANALYSIS OF MAGAZINE HEADWALL IN ESKIMO IV TEST

D. P. Reddy
Agbabian Associates
El Segundo, California

The Department of Defense Explosives Safety Board (DDESB) has been conducting a general program to determine safe intermagazine separation distances for various orientations of magazines for storing chemical explosives. The main objective of the program is to determine the minimum intermagazine separation distances so that an explosion in one magazine (donor) will not cause an explosion in an adjacent magazine (acceptor).

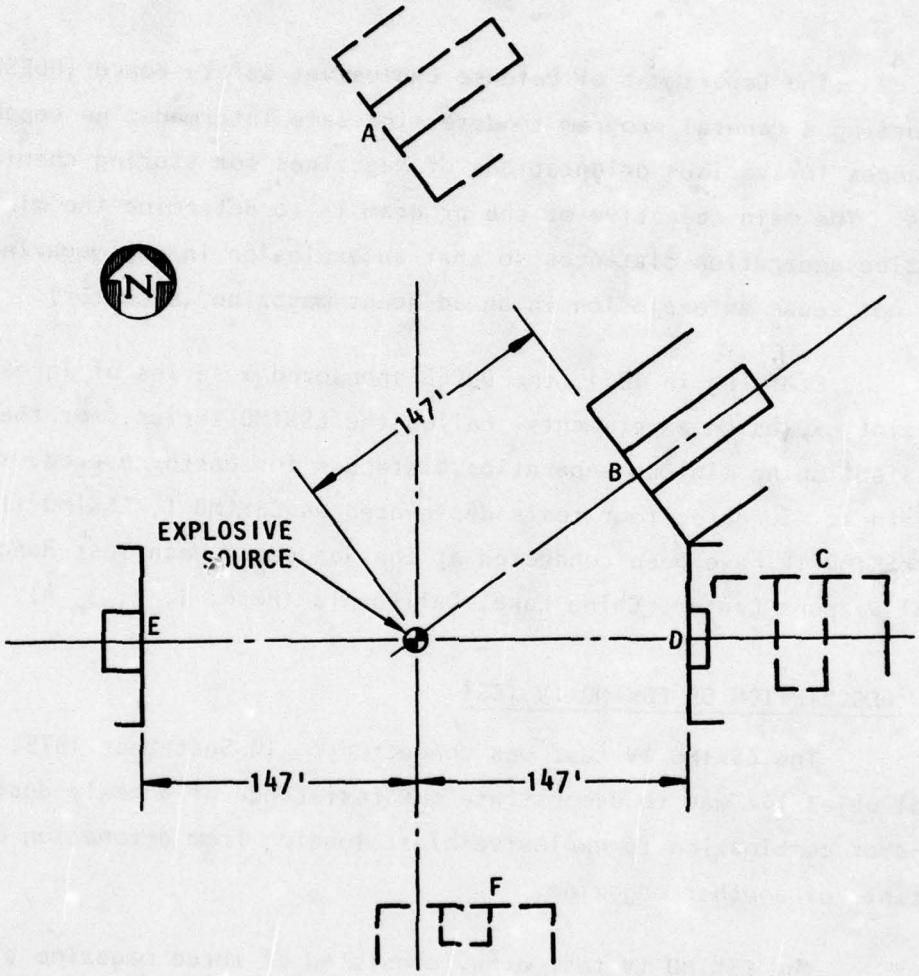
Starting in 1971, the DDESB sponsored a series of large-scale magazine explosion experiments, called the ESKIMO series, for the purpose of establishing minimum separation distances for earth-covered, steel-arch magazines. To date, four tests designated as ESKIMO I, ESKIMO II, ESKIMO III, and ESKIMO IV have been conducted at the Randsburg Wash Test Range of the Naval Weapons Center, China Lake, California (Refs. 1, 2, 3, 4).

1.1 DESCRIPTION OF ESKIMO IV TEST

The ESKIMO IV test was conducted on 10 September 1975. Its principal objective was to demonstrate the resistance of a newly designed headwall-and-door combination to explosive blast loading from detonation of the contents of another magazine.

The ESKIMO IV test array consisted of three magazine structures, each facing the explosion source 147 ft away, as shown in Figure 1. The primary target structure was Igloo B to the northeast, consisting of a single-leaf sliding door, horizontally spanned, mounted on a modified headwall of the standard Stradley magazine. This paper deals with the analysis of only this headwall.

PRECEDING PAGE BLANK-NOT FILMED



NOTE: IGLOOS A, C, AND F WERE OLD STRUCTURES FROM THE PREVIOUS ESKIMO TESTS THAT WERE NOT CONSIDERED IN ESKIMO IV.

FIGURE 1. LAYOUT OF TEST STRUCTURES FOR ESKIMO IV MAGAZINE SEPARATION TEST

Igloos D (east) and E (west) were left over from the previous ESKIMO tests. Igloo D was rebuilt with the two-leaf, hinged, steel-plate door and the headwall of the standard circular steel-arch magazine. Exposed to the same level of loading as the primary target, it served as a control structure to demonstrate directly the relative strength of the primary target (Igloo B). Igloo E was rebuilt with the headwall of the standard circular steel-arch magazine, but fitted with a single-leaf sliding door. The present study does not include analyses of the headwalls of these two igloos.

The test utilized a nearly ideal explosion source to generate blast loadings. It afforded the opportunity for more extensive source diagnostics and dynamic response measurements on the target structures than in previous tests of the ESKIMO series. This in turn would enable an extensive correlation between measured and calculated responses.

The explosion source consisted of 8-lb rectangular blocks of TNT stacked in the form of a hemisphere, containing a total of 37,000 lb of TNT. The explosives were left exposed, rather than surrounded by an earth cover or barriers.

Pressure gages were installed in the headwalls and in the ground nearby to measure blast pressures on the headwalls. Accelerometers and linear displacement transducers (LVDTs) were used to measure structure-response time histories of the headwalls. Self-recording pressure gages were installed to measure pressure loading at the far-field stations. Locations of the pressure gages, accelerometers, and LVDTs for the northeast igloo are shown respectively in Figures 2, 3, and 4. The northeast headwall was instrumented more heavily than the other headwalls so that the calculated response could be compared with measurements at several locations.

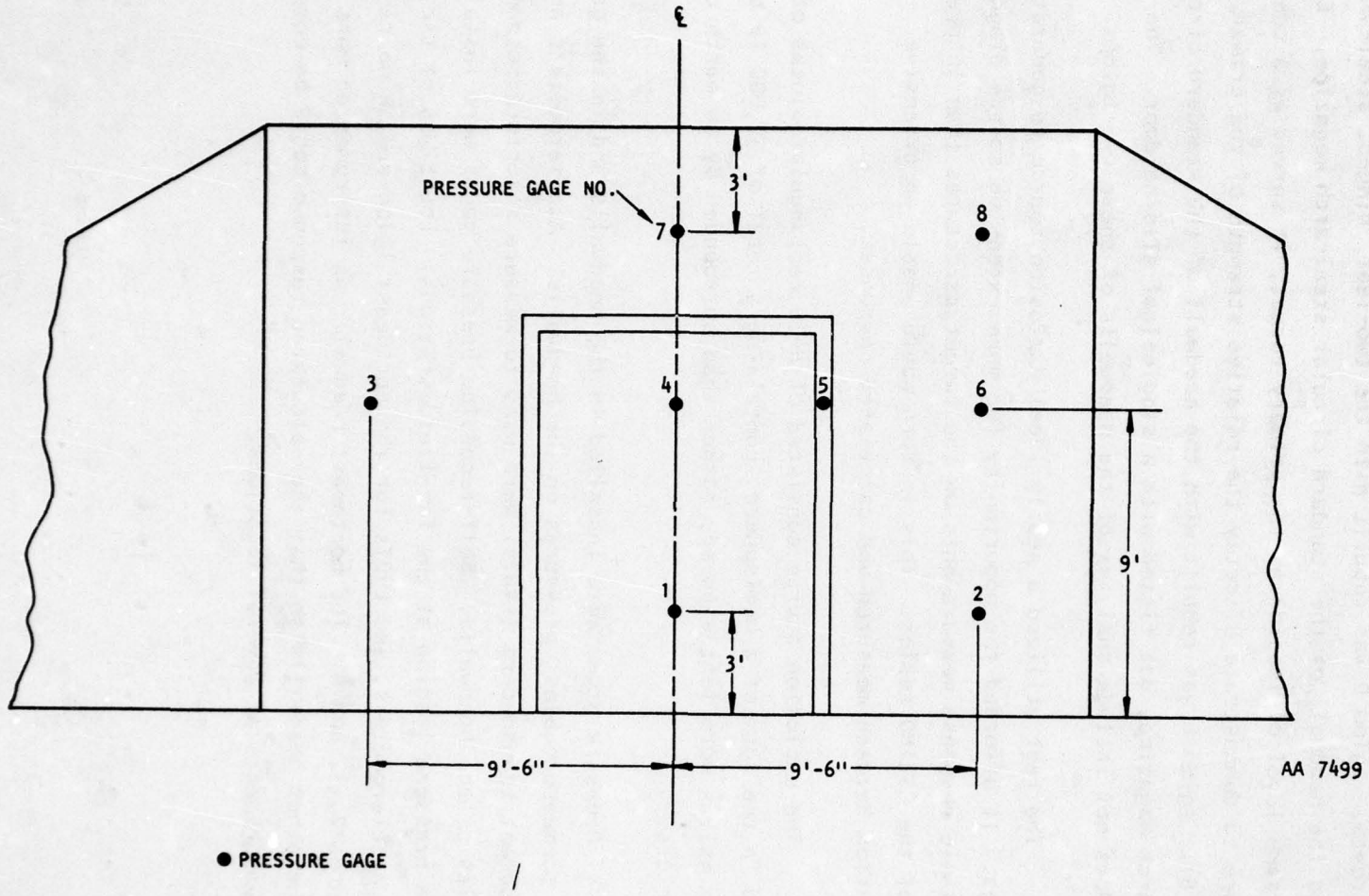


FIGURE 2. PLACEMENT OF PRESSURE GAGES ON NORTHEAST (B) IGLOO, ESKIMO IV

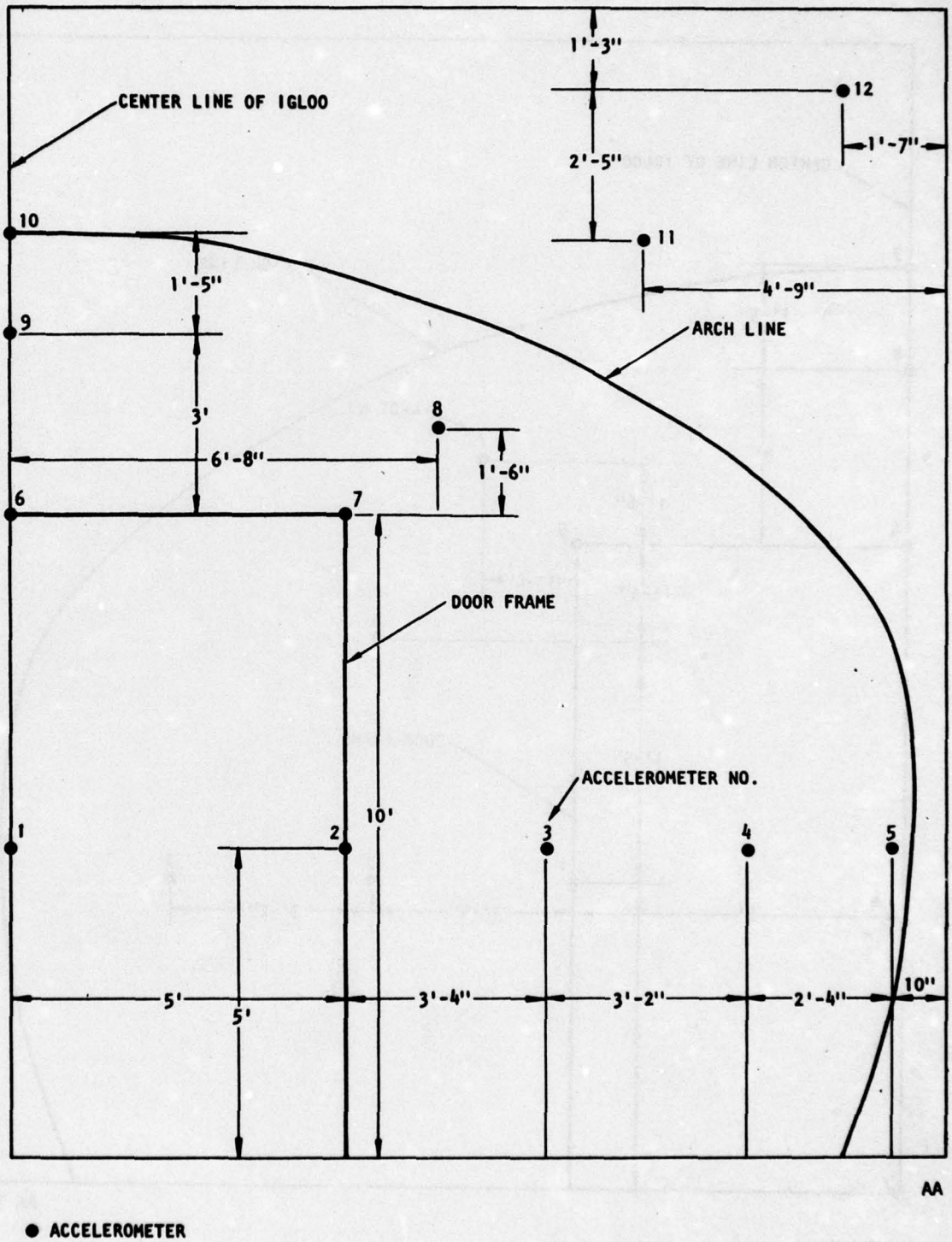


FIGURE 3. PLACEMENT OF ACCELEROMETERS ON HEADWALL OF NORTHEAST IGLOO, ESKIMO IV

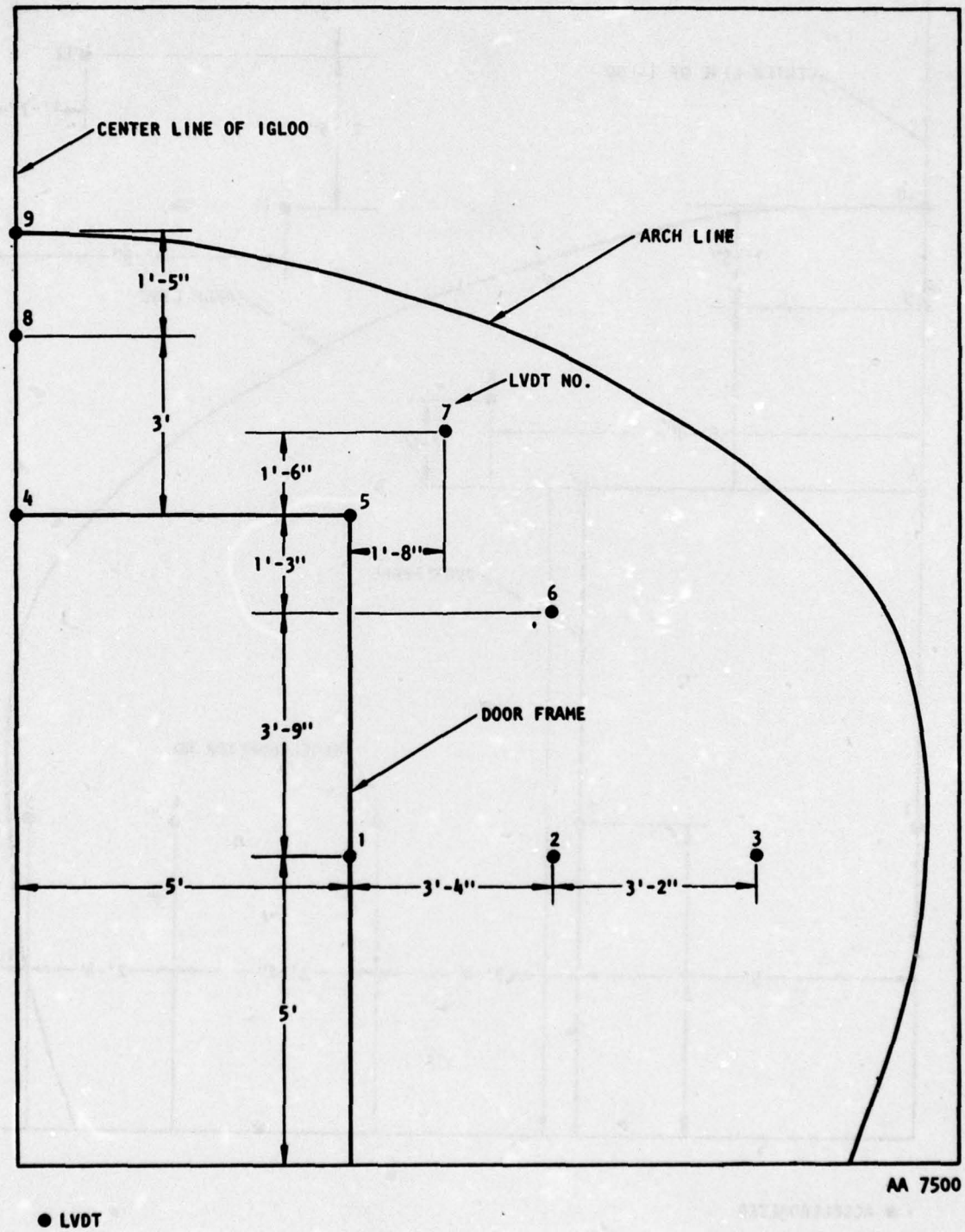


FIGURE 4. PLACEMENT OF LVDT TRANSDUCERS ON HEADWALL OF NORTHEAST IGLOO IN ESKIMO IV

FINITE ELEMENT ANALYSIS OF HEADWALL

The finite element method is an established structural analysis technique that is well documented (e.g., Ref. 5). Basic to the method is the preparation of a mathematical model of the structure to be analyzed. The mathematical model is constructed by an assembly of individual elements such as beams, plates, and membranes. The dynamic properties (such as the mass and stiffness) of the individual elements can be obtained easily. The mass and stiffness properties of the individual finite elements are appropriately added together to obtain the total mass and stiffness characteristics of the complex structure to be analyzed. The individual finite elements interconnect at the joints or nodes.

MATHEMATICAL MODEL OF HEADWALL

Figure 5 shows the finite element model of the headwall of the northeast igloo in the ESKIMO IV test. An oval-shaped steel arch supports the soil for this igloo. The door opening in the headwall is strengthened with concrete beams. The vertical beam extends to the top of the headwall. The model of this headwall represents the above beams by separate elements so that the actual beam properties can be assigned only to the elements representing the beams. An effort was made, as far as possible, to place the arch line on the edges of the finite elements. However, in order to minimize the use of triangular elements, the arch line was permitted to run across Elements 22, 33, 43, and 53, as shown in Figure 5. The finite element mesh for this headwall is designed so that the locations of the accelerometers and the LVDT transducers (Figs. 3 and 4) generally correspond to nodes in the mesh. This facilitates a direct comparison of the test and calculated results. The finite element mesh of the headwall shown in Figure 5 consists of a total of 126 elements and 150 nodes.

The single-leaf sliding steel door of this headwall consists of a 3/8-in. plate and a 1/4-in. plate, strengthened by four 6WF25 wide-flange sections and two 6 [13 channels, all running horizontally. Two 6 [13 channels also run vertically along the two ends. The door is represented by

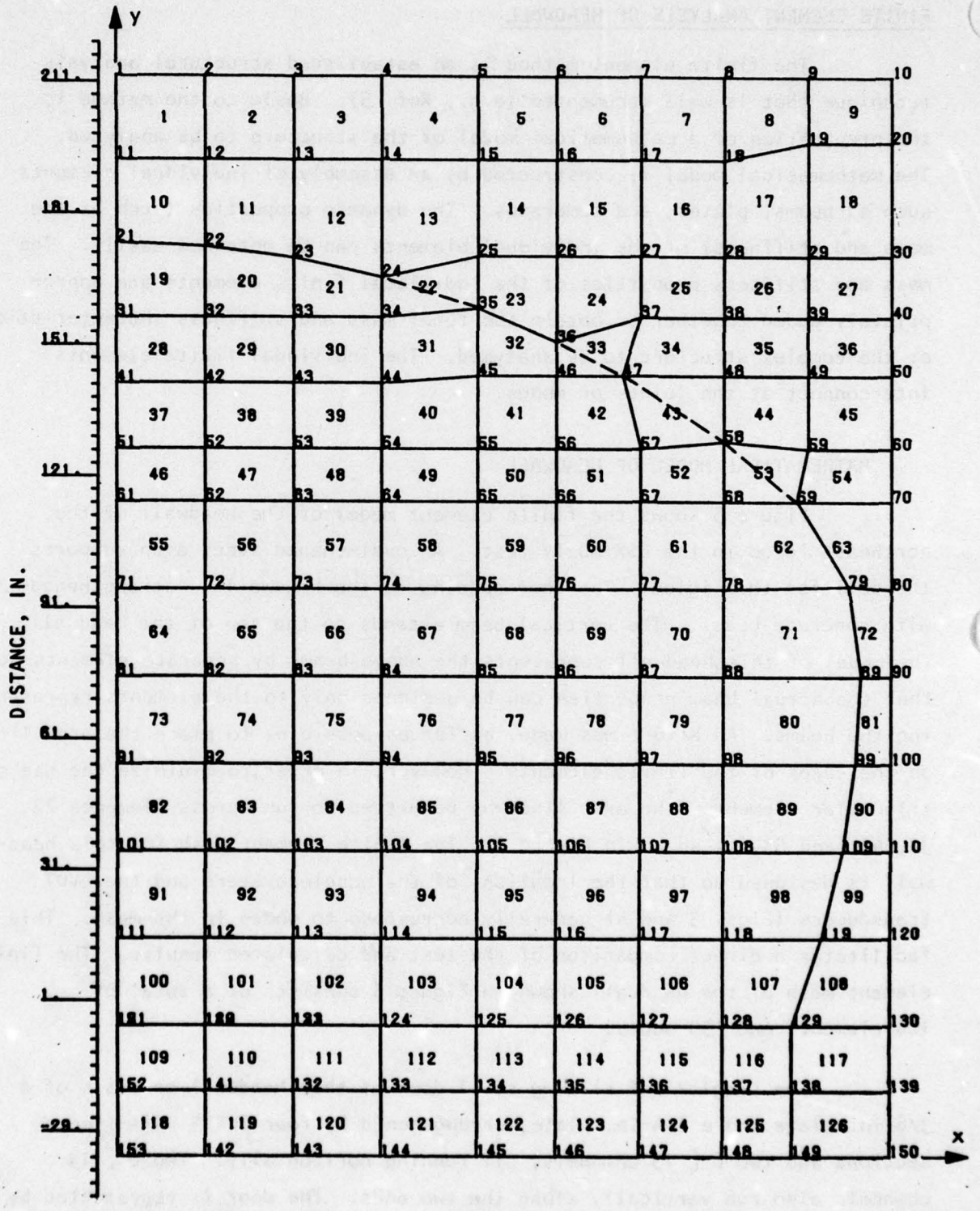


FIGURE 5. FINITE ELEMENT MODEL OF NORTHEAST HEADWALL, ESKIMO IV

uniform, orthotropic plates whose equivalent properties are computed following the procedures described in Reference 6.

The ESKIMO tests showed, in general, a gap of the order of several inches between the headwall and the earth fill (Ref. 7). This indicated that the soil was subjected to large deformations and its behavior was highly nonlinear. Therefore, the interaction of the soil with the headwall was modeled by representing the soil by a series of linear dampers and nonlinear springs. Reference 7 provides additional information on the nonlinear springs.

The pressure history to be used in simulation of the ESKIMO IV event is developed on the basis of the measured data in the test and the analytical and empirical data for chemical explosions in air. Figure 6 shows the proposed pressure history for use in the calculations. Also shown in the figure are the measured pressure histories at three locations on the headwall. The proposed pressure pulse shown in Figure 6 has a peak value of 290 psi and a rise time of 1 msec.

ANALYSIS TECHNIQUES

The dynamic analysis using the finite element model of the headwall is performed using the INSLAB computer program (Ref. 8). INSLAB is a dynamic, nonlinear finite element program in which the force equilibrium equations at any time are expressed as:

$$[M]\{\ddot{X}_t\} + [C]\{\dot{X}_t\} + [K]\{X_t\} = \{P_t\} \qquad (1)$$

in which $\{\ddot{X}_t\}$, $\{\dot{X}_t\}$, $\{X_t\}$ are the nodal acceleration, velocity, and displacement vectors at time t; $[M]$, $[C]$, $[K]$ are the mass, damping, and stiffness matrices; and $\{P_t\}$ is the nodal point force vector at time t. For linearly elastic problems the mass, damping, and stiffness matrices in Equation 1 remain constant so that they are evaluated only once.

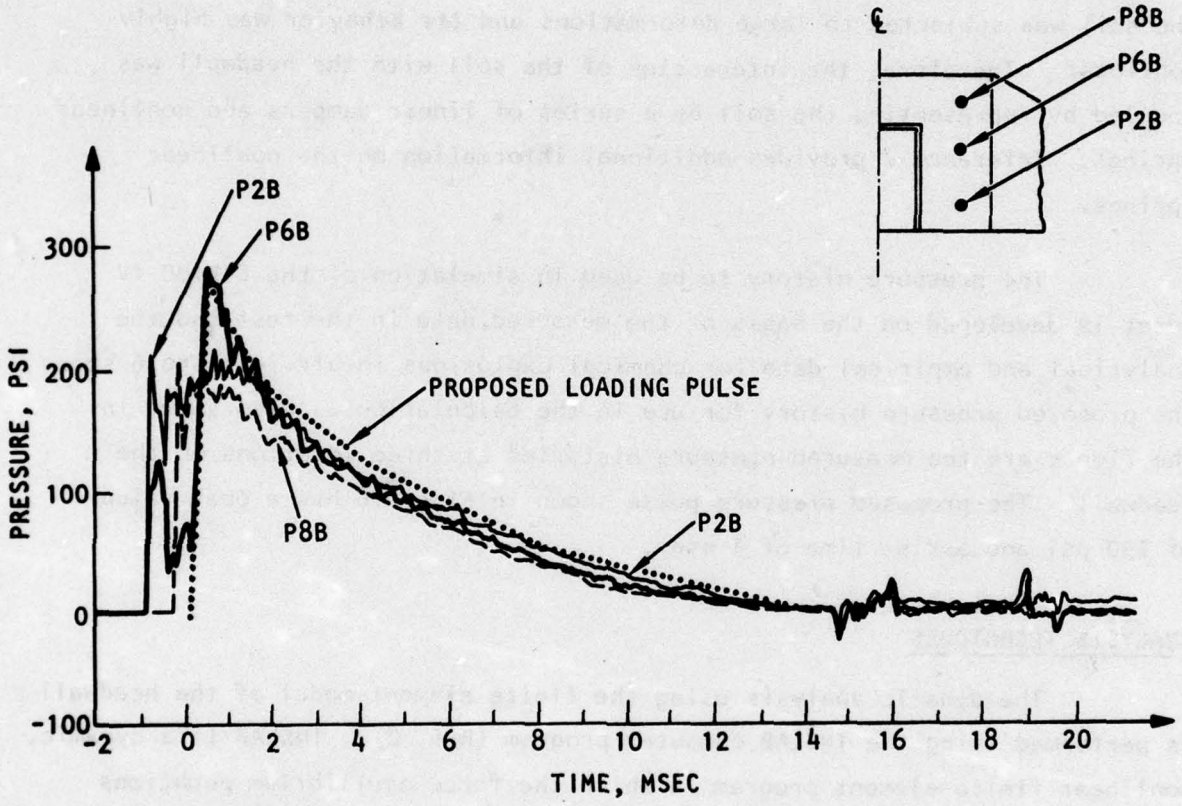


FIGURE 6. COMPARISON OF PRESSURE HISTORIES FOR A VERTICAL ARRAY OF GAGES WITH THE PROPOSED LOADING PULSE FOR RESPONSE ANALYSIS OF IGLOO B, ESKIMO IV

The ESKIMO test data showed that all headwalls and doors in the test experienced large permanent deflections. This suggests that the analysis must consider the yielding of the headwall and door. To accomplish this, a bilinear moment-curvative relationship (Fig. 7) is assumed for the headwall and door.

The INSLAB code solves the nonlinear equations of motion (Eq. 1) by a step-by-step numerical integration procedure that assumes a constant acceleration between successive time increments (Fig. 8). Further details on the numerical integration procedure may be found in Reference 8.

DYNAMIC RESPONSE OF HEADWALL

The response calculation of the northeast headwall, ESKIMO IV, was to have been performed before the test was conducted on 10 September 1975, so that the analytical results could be used to predict the behavior of the headwall and door system in the test. Because of tight schedules, the above calculation could not be completed before the test; but the calculation was performed before any results from the test were available. This assured that the calculation was performed independently of the test and was not subject to any bias that could have resulted from reviewing the test results before performing the calculation.

As of the writing of this paper, the data from the ESKIMO IV test are available only in preliminary form. Therefore, the test results reflect raw data that may be subject to future corrections. This fact should be kept in mind when comparing the analytical results with the test data.

Figures 9 through 15 show displacement, velocity, and acceleration time histories computed at several locations on the northeast headwall of the ESKIMO IV event. The motion time histories shown in Figures 9 through 15 reflect calculations with a duration of 186 msec. The displacement time histories at most locations show a single peak at about 25 msec and become steady state after about 100 msec.

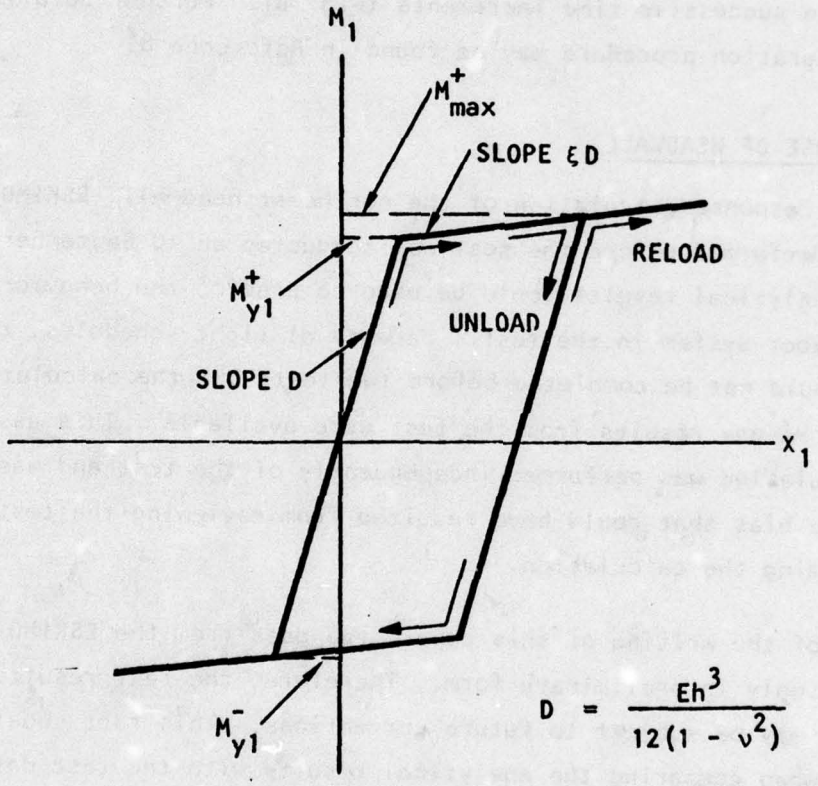
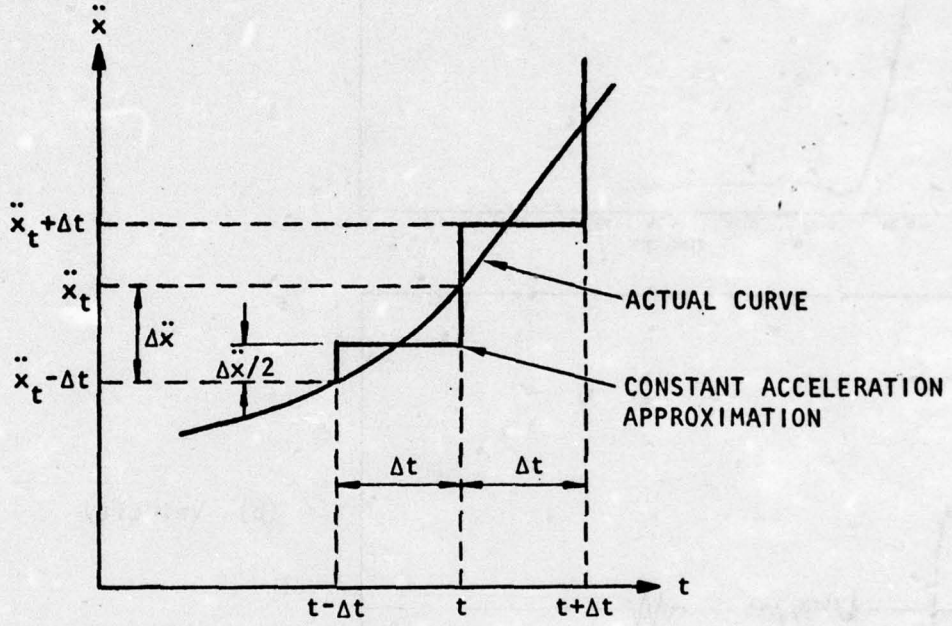


FIGURE 7. BILINEAR MOMENT-CURVATIVE RELATIONS IN INSLAB



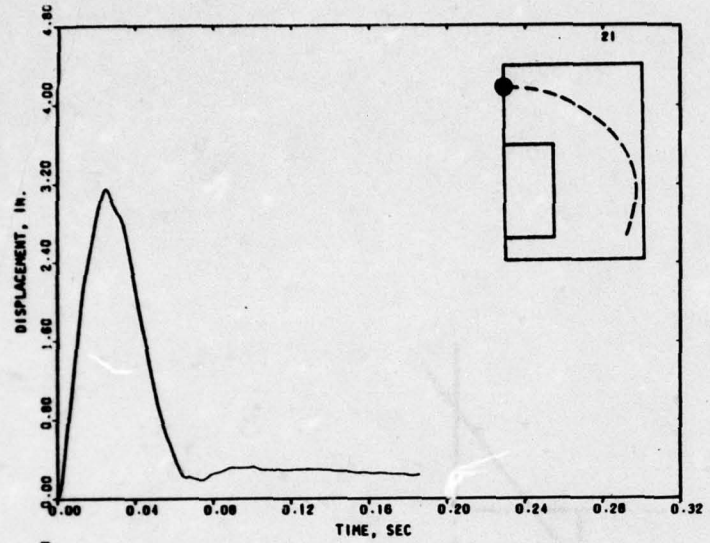
NOTE: FOR CONSTANT ACCELERATION METHOD:

$$\ddot{x}(t) = \ddot{x}_{t-\Delta t} + \Delta\ddot{x}$$

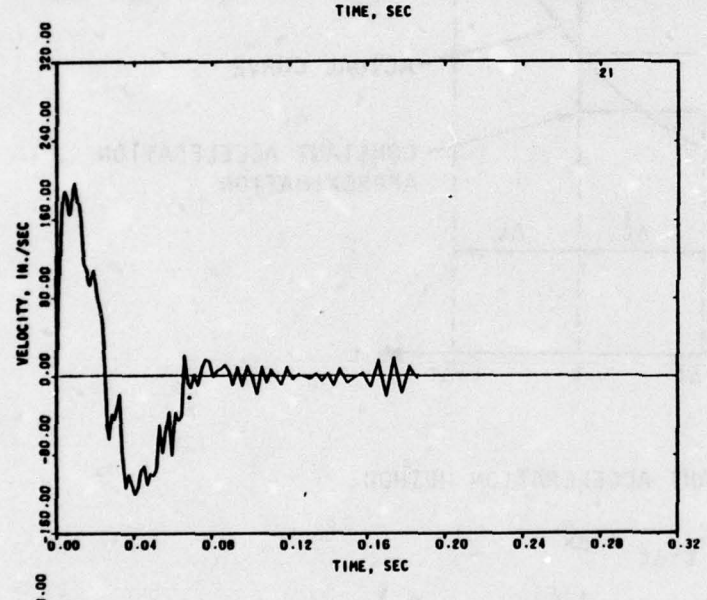
$$\dot{x}(t) = \dot{x}_{t-\Delta t} + \frac{1}{2}\left(\ddot{x}_{t-\Delta t} + \ddot{x}_t\right)\Delta t$$

$$x(t) = x_{t-\Delta t} + \dot{x}_{t-\Delta t}\,\Delta t + \frac{\Delta t^2}{4}\left(\ddot{x}_t + \ddot{x}_{t-\Delta t}\right)$$

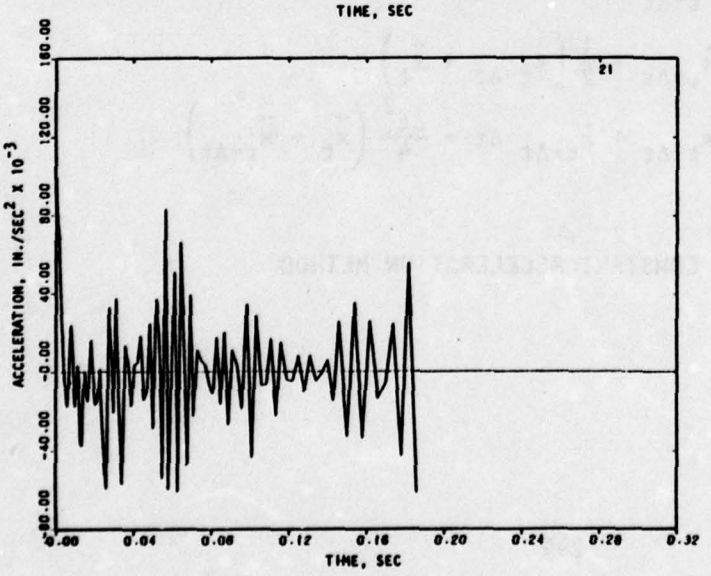
FIGURE 8. CONSTANT ACCELERATION METHOD



(a) Displacement

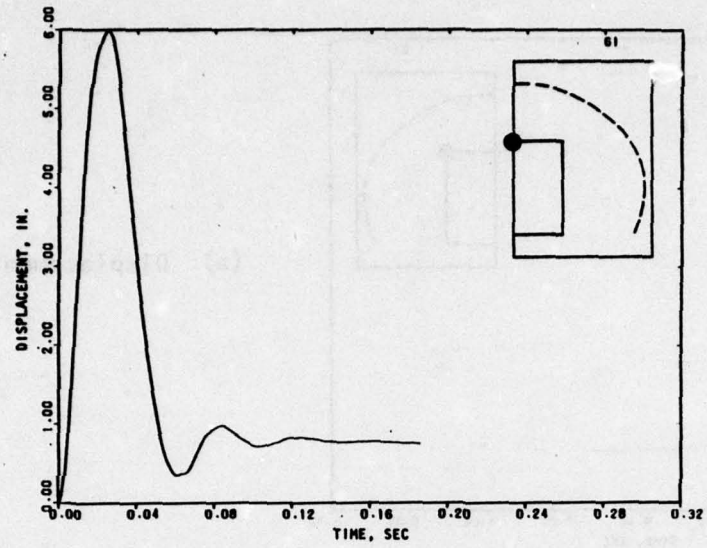


(b) Velocity

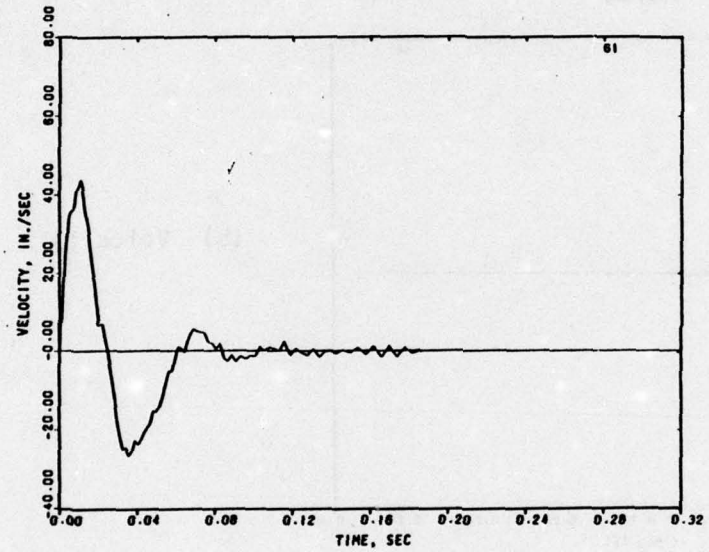


(c) Acceleration

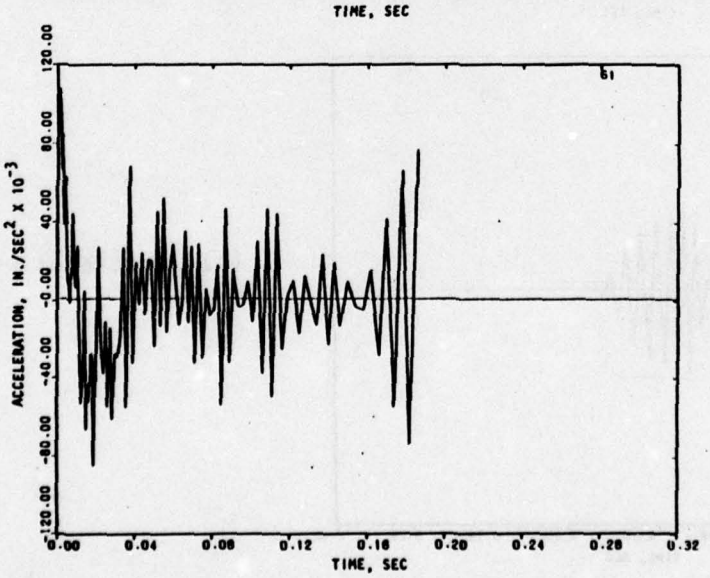
FIGURE 9. COMPUTED MOTION OF NORTHEAST IGLOO (ESKIMO IV) AT NODE 21



(a) Displacement

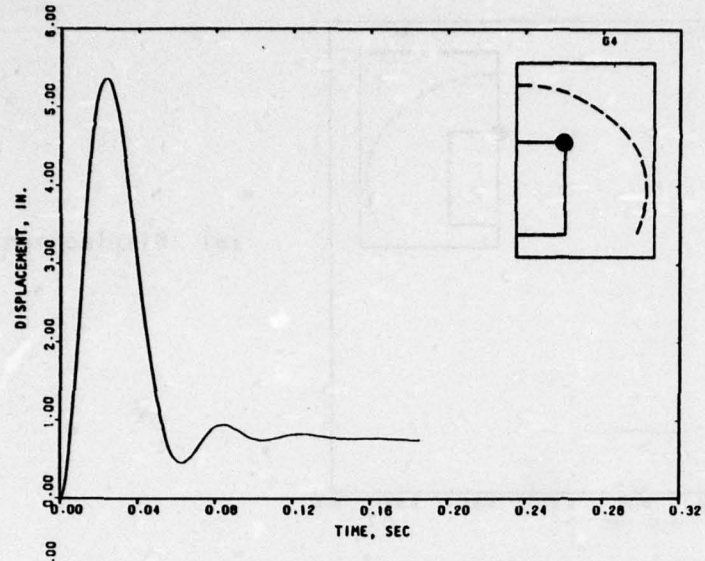


(b) Velocity

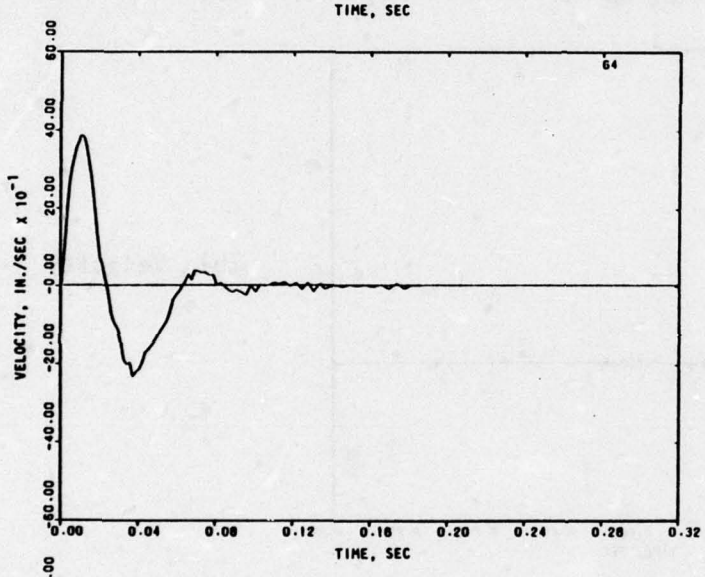


(c) Acceleration

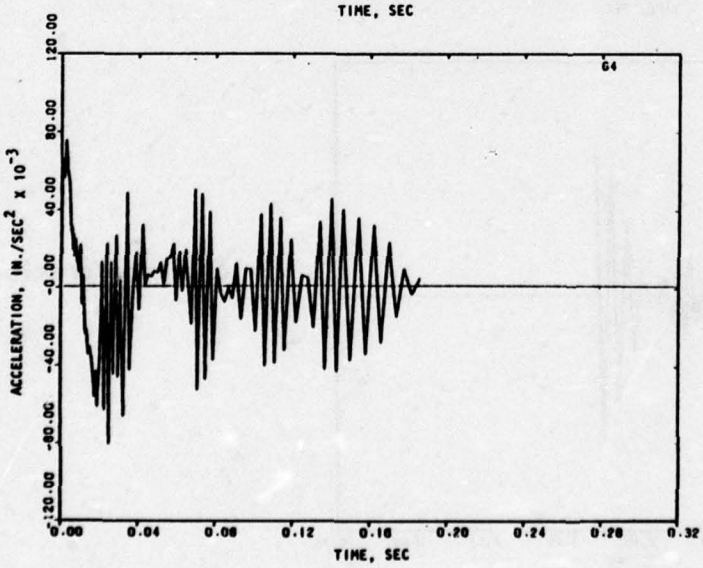
FIGURE 10. COMPUTED MOTION OF NORTHEAST IGLOO (ESKIMO IV) AT NODE 61



(a) Displacement

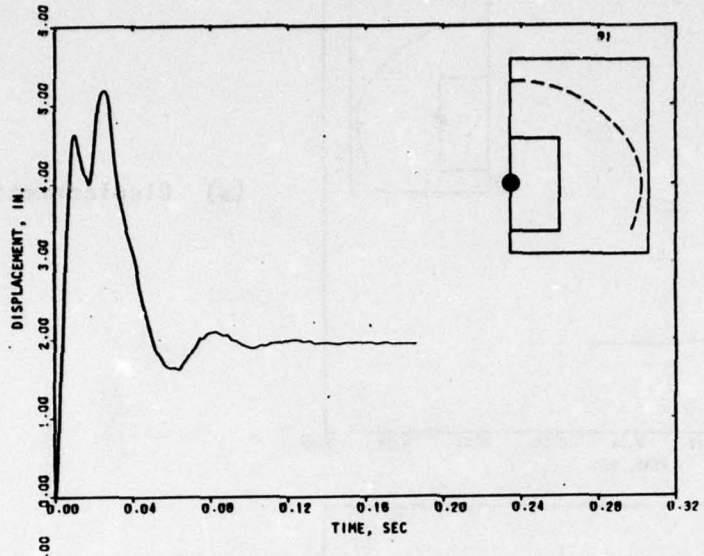


(b) Velocity

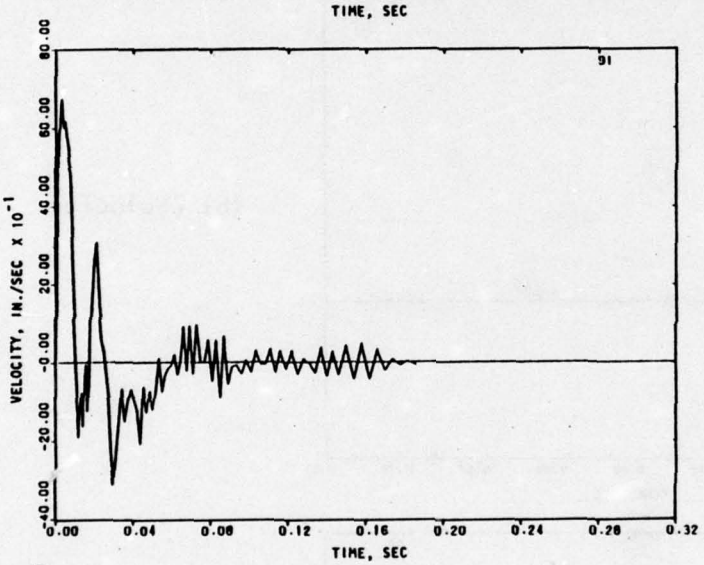


(c) Acceleration

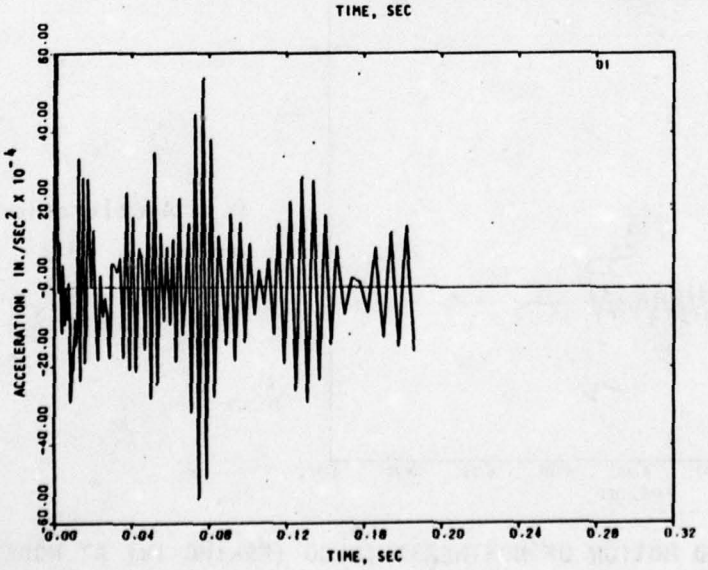
FIGURE 11. COMPUTED MOTION OF NORTHEAST IGLOO (ESKIMO IV) AT NODE 64



(a) Displacement

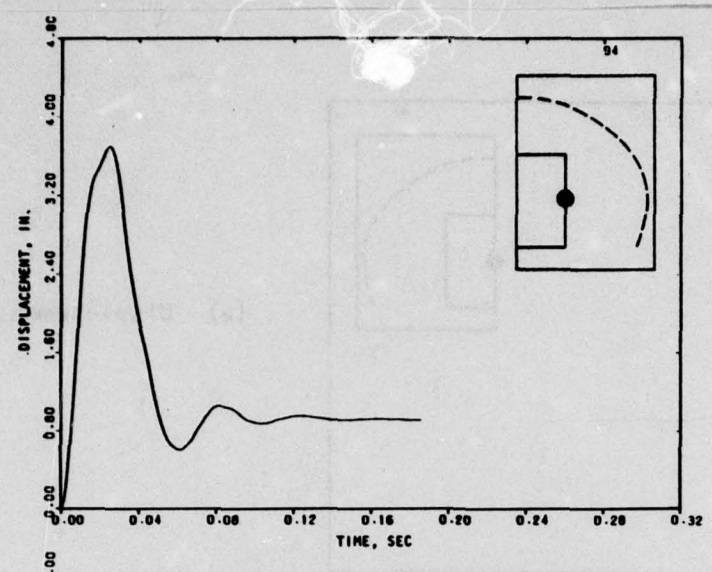


(b) Velocity

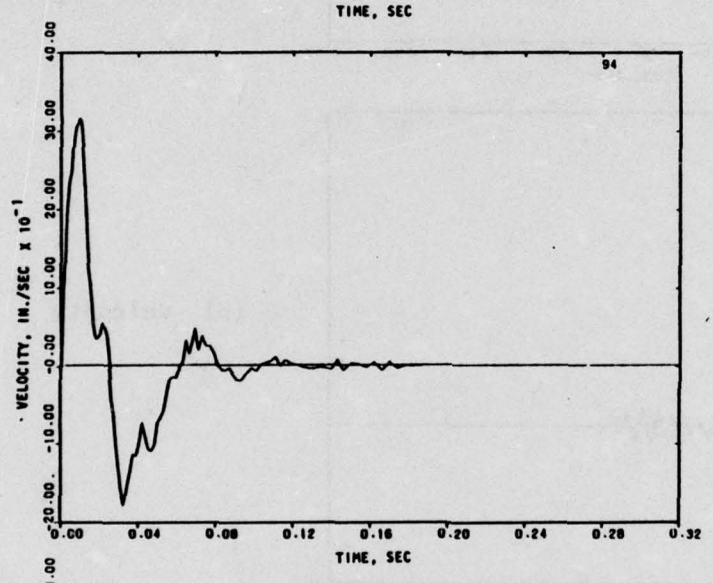


(c) Acceleration

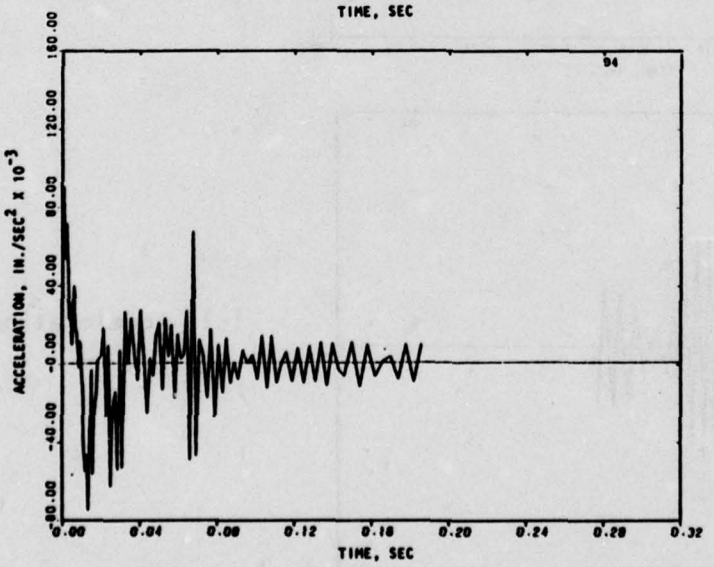
FIGURE 12. COMPUTED MOTION OF NORTHEAST IGLOO (ESKIMO IV) AT NODE 91



(a) Displacement

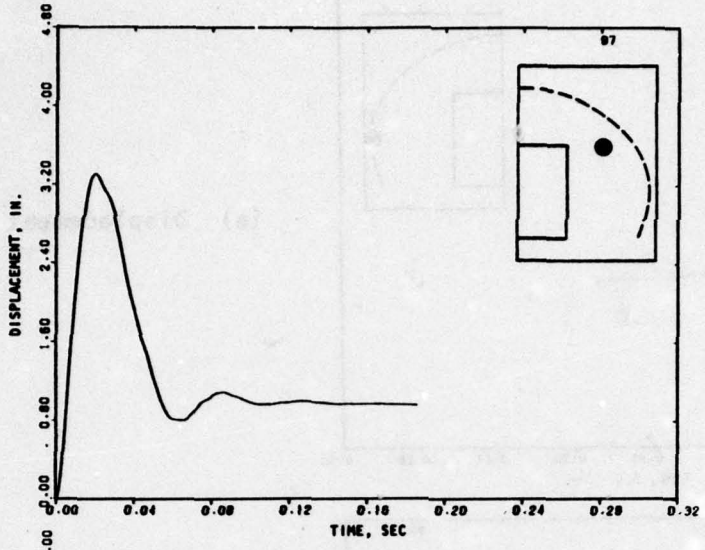


(b) Velocity

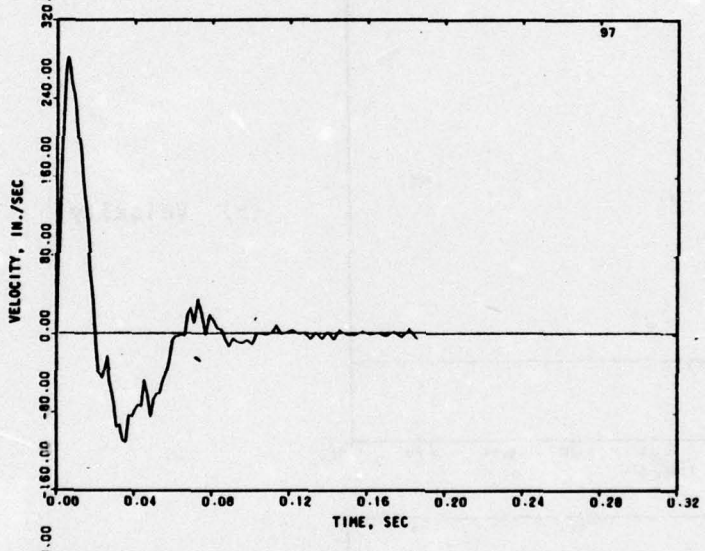


(c) Acceleration

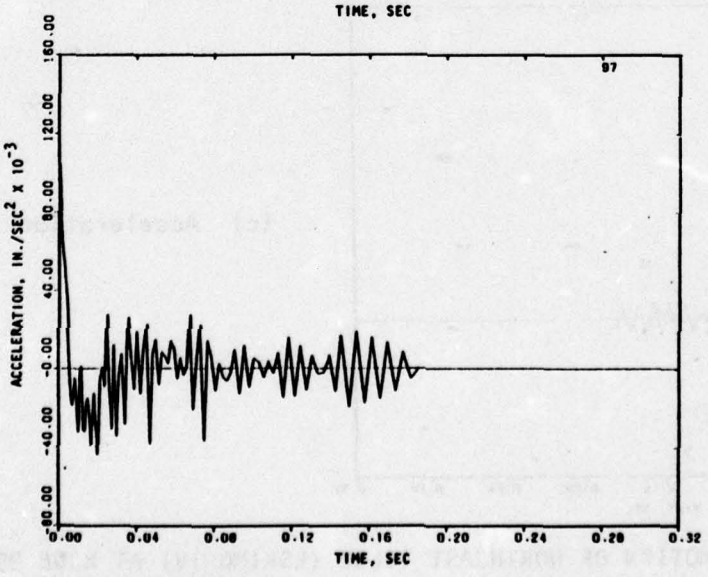
FIGURE 13. COMPUTED MOTION OF NORTHEAST IGLOO (ESKIMO IV) AT NODE 94



(a) Displacement

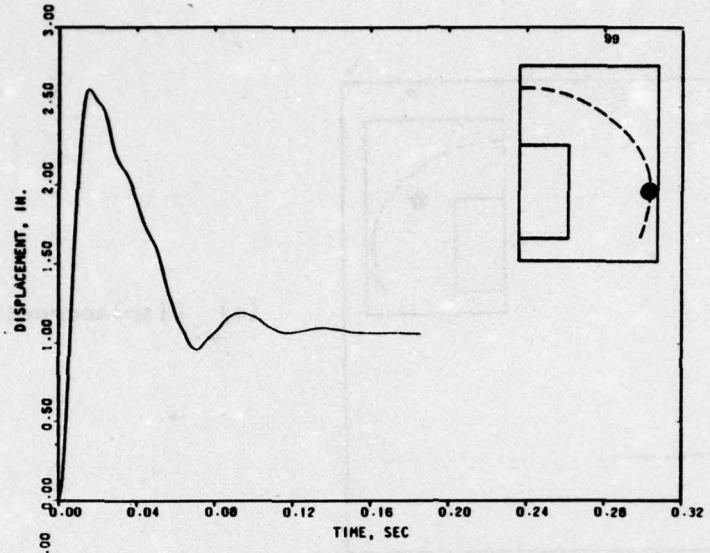


(b) Velocity

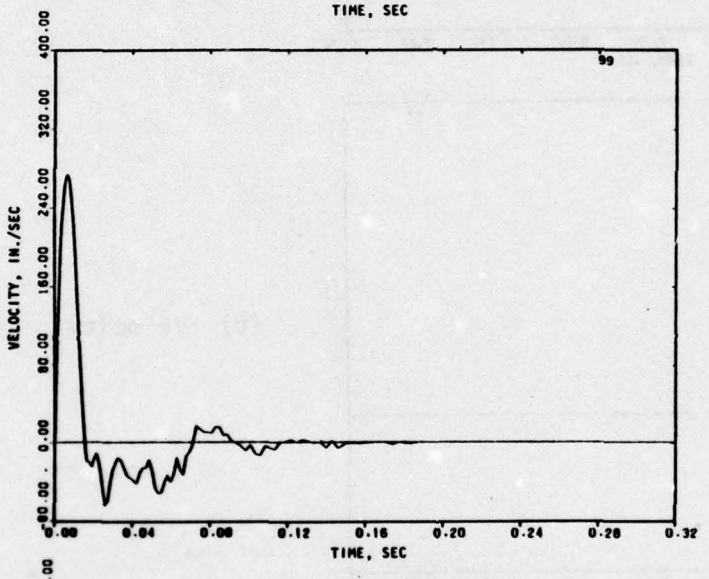


(c) Acceleration

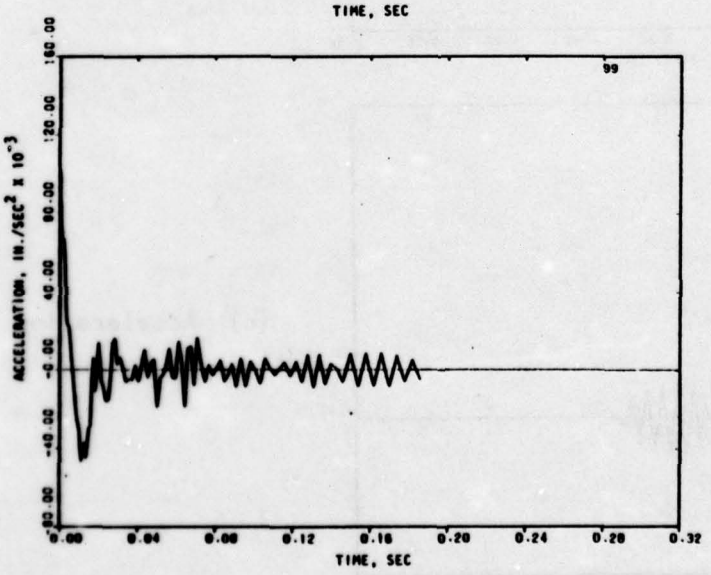
FIGURE 14. COMPUTED MOTION OF NORTHEAST IGLOO (ESKIMO IV) AT NODE 97



(a) Displacement



(b) Velocity



(c) Acceleration

FIGURE 15. COMPUTED MOTION OF NORTHEAST IGLOO (ESKIMO IV) AT NODE 99

COMPARISON OF COMPUTED RESULTS WITH TEST DATA

As in the case of the other ESKIMO tests, posttest measurements were made on the headwalls of the ESKIMO IV test (Ref. 4), in order to obtain permanent displacements of the headwalls. Figure 16 shows the permanent displacement contour lines of the northeast headwall based on the average of two measured values due to the symmetry of the headwall at the vertical centerline. The computed displacement contours at time $t = 158$ msec are shown in Figure 17. As noted before, the computed displacements became steady state after about 100 msec and therefore the displacements of the headwall at 158 msec represent the permanent displacements. A comparison of the computed and measured contours shows that the computed displacements generally are smaller than those measured. However, the differences are not great and are not significant because the magnitudes of the permanent displacements are small. The contours do not indicate any strong influence of the arch on the headwall response.

Figures 3 and 4 show the locations of the accelerometers and the linear motion transducers mounted on the headwall and door. The measured acceleration and displacement time histories for the headwall are shown respectively in Figures 18 and 19. These records are reproduced from the preliminary report (Ref. 4) on the test. As such, these records have not been corrected for drifts and other random errors. This fact should be kept in mind in the following discussion involving the measured time histories.

The measured displacement time histories at several locations on the headwall and door are shown in Figure 19. The displacements shown are in inch units and are plotted as functions of time expressed in msec unit. next to each time history the node in the finite element mesh of the headwall (Fig. 5), to which the time history corresponds, is shown. Of the eight measured displacement time histories, direct comparison with the calculated histories is possible at only four locations. These are at Nodes 21, 64, 94, and 97; and the corresponding time histories are shown respectively in Figures 9, 11, 13, and 14. A comparison of the calculated and measured

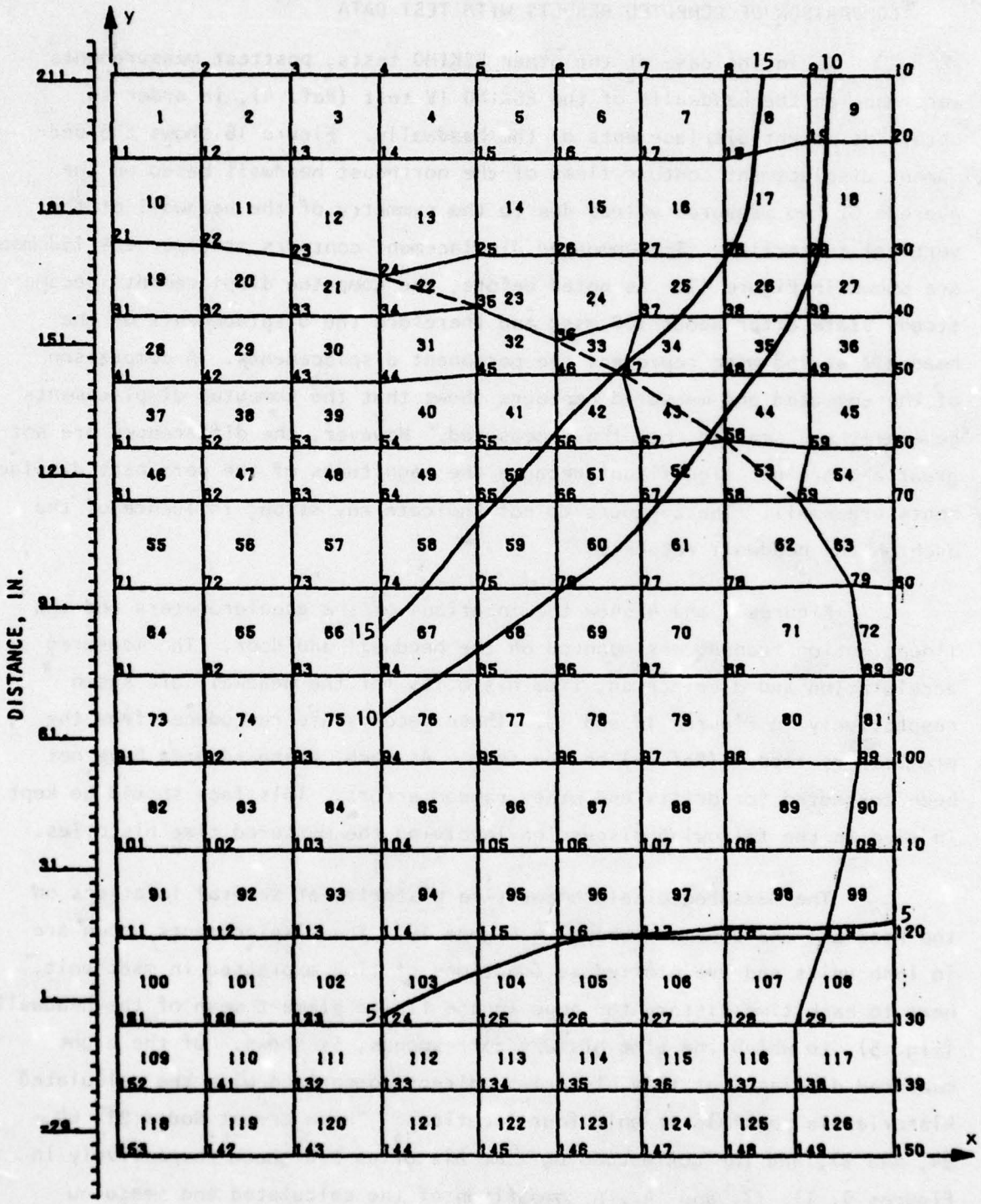


FIGURE 16. MEASURED PERMANENT DISPLACEMENT CONTOURS OF NORTHEAST HEADWALL OF ESKIMO IV (IN HUNDREDTHS OF FEET)

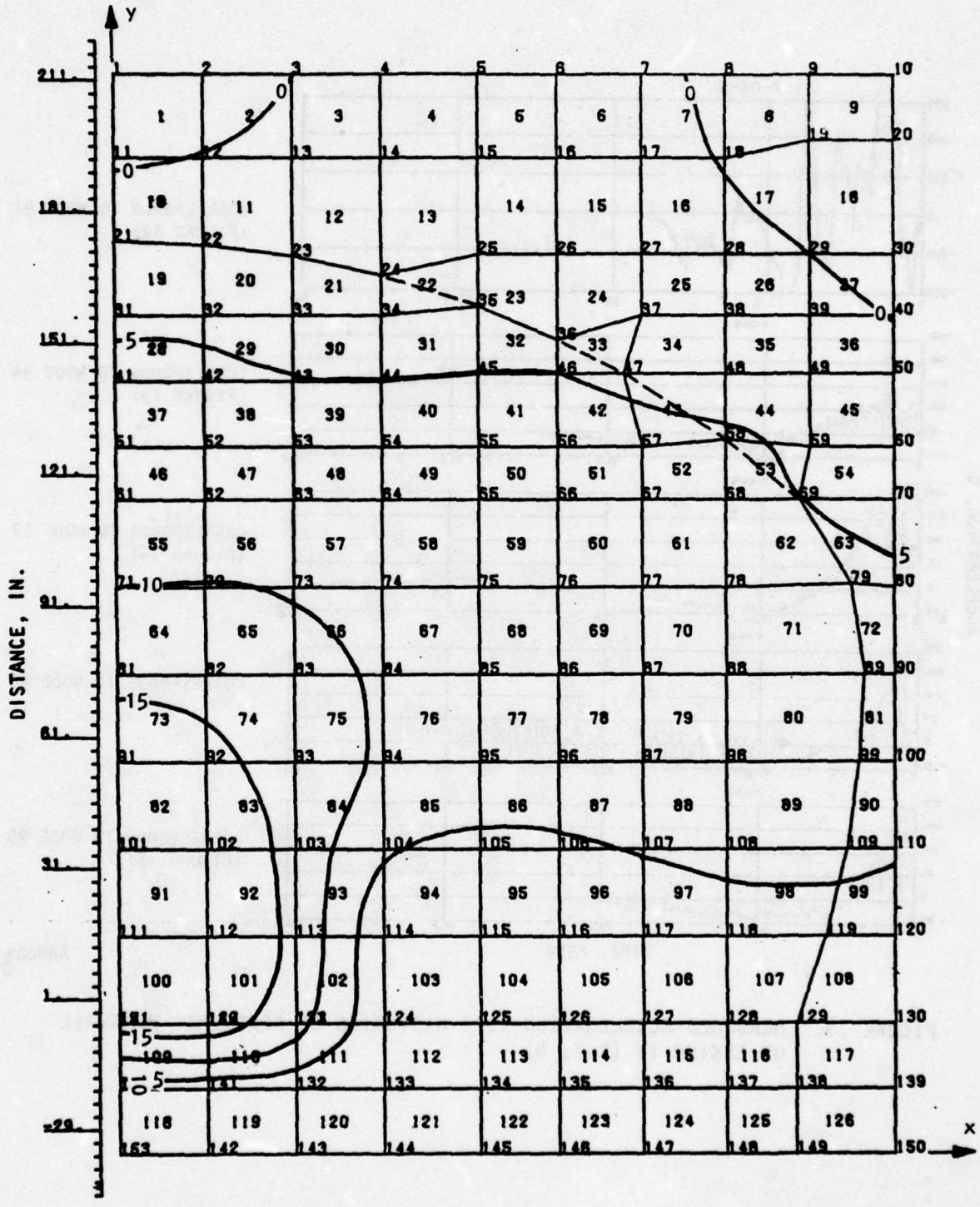


FIGURE 17. COMPUTED DISPLACEMENT CONTOURS OF NORTHEAST HEADWALL OF ESKIMO IV AT 158 MSEC (IN HUNDREDTHS OF FEET)

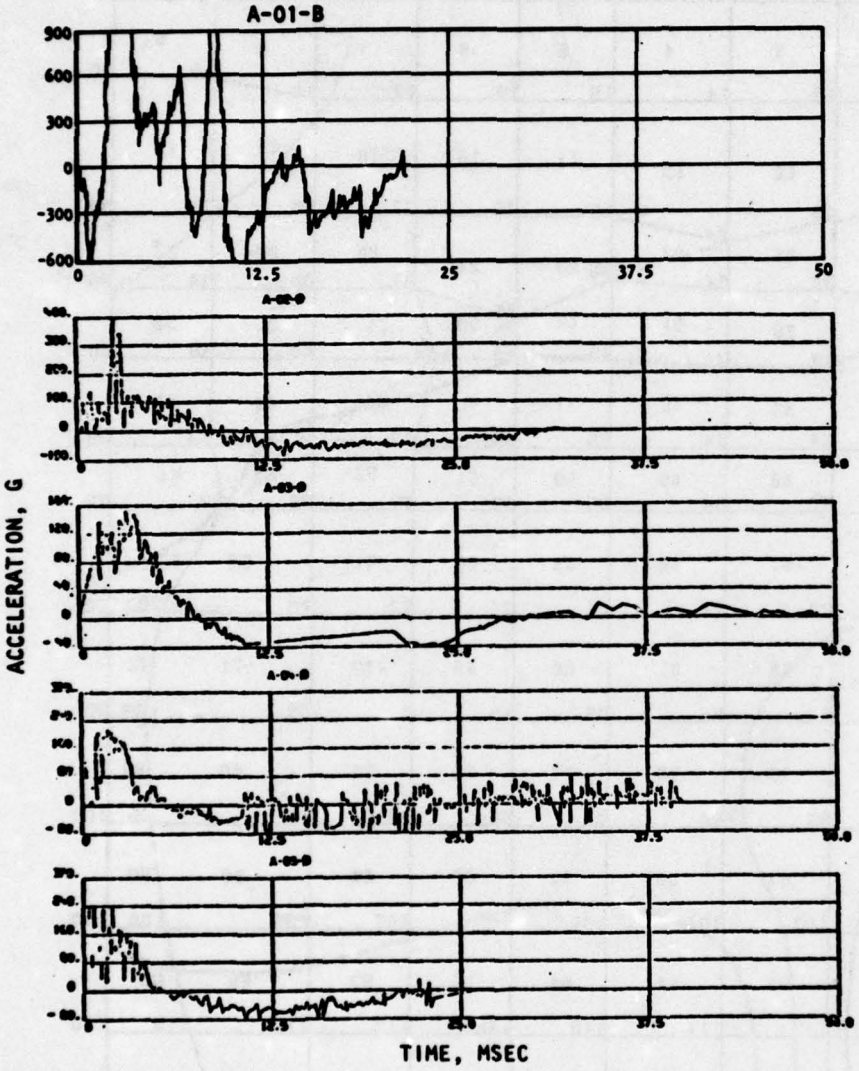


FIGURE 18. MEASURED ACCELERATION TIME HISTORIES OF NORTHEAST HEADWALL OF ESKIMO IV (Ref. 4)

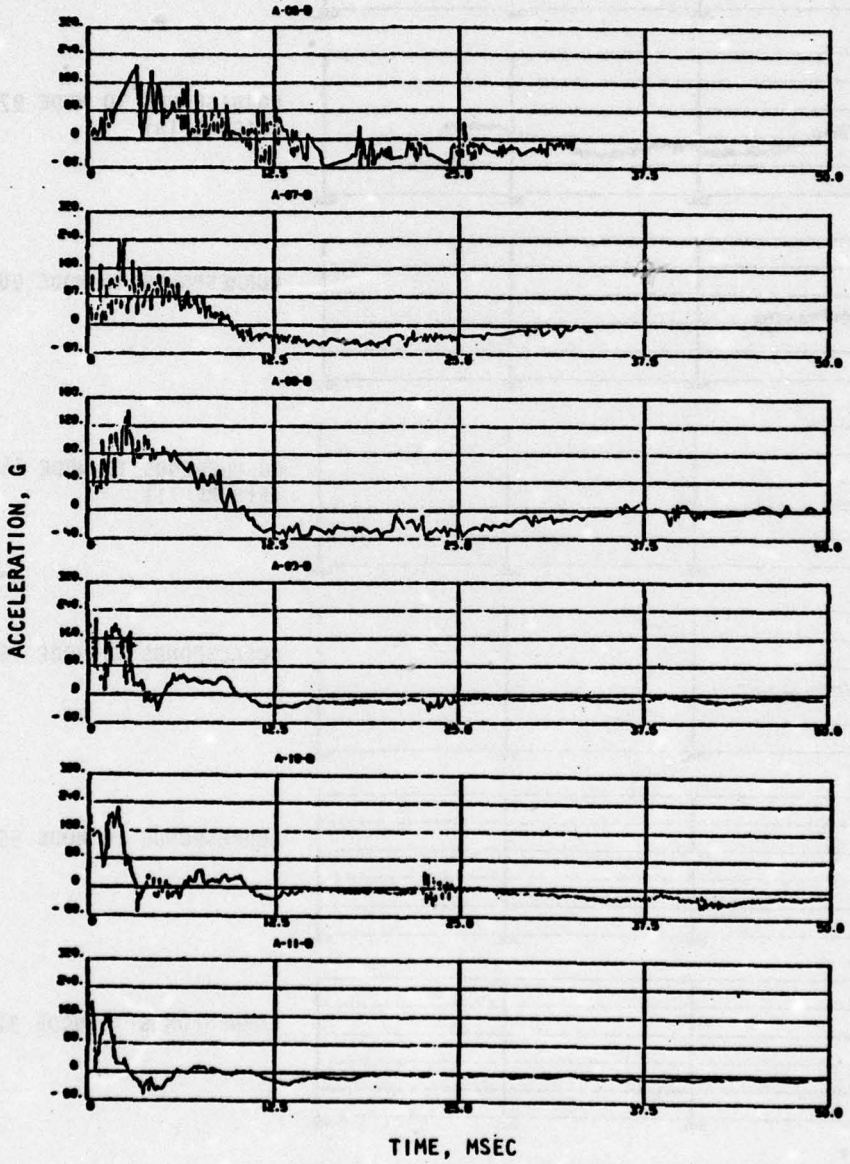


FIGURE 18. (CONCLUDED)

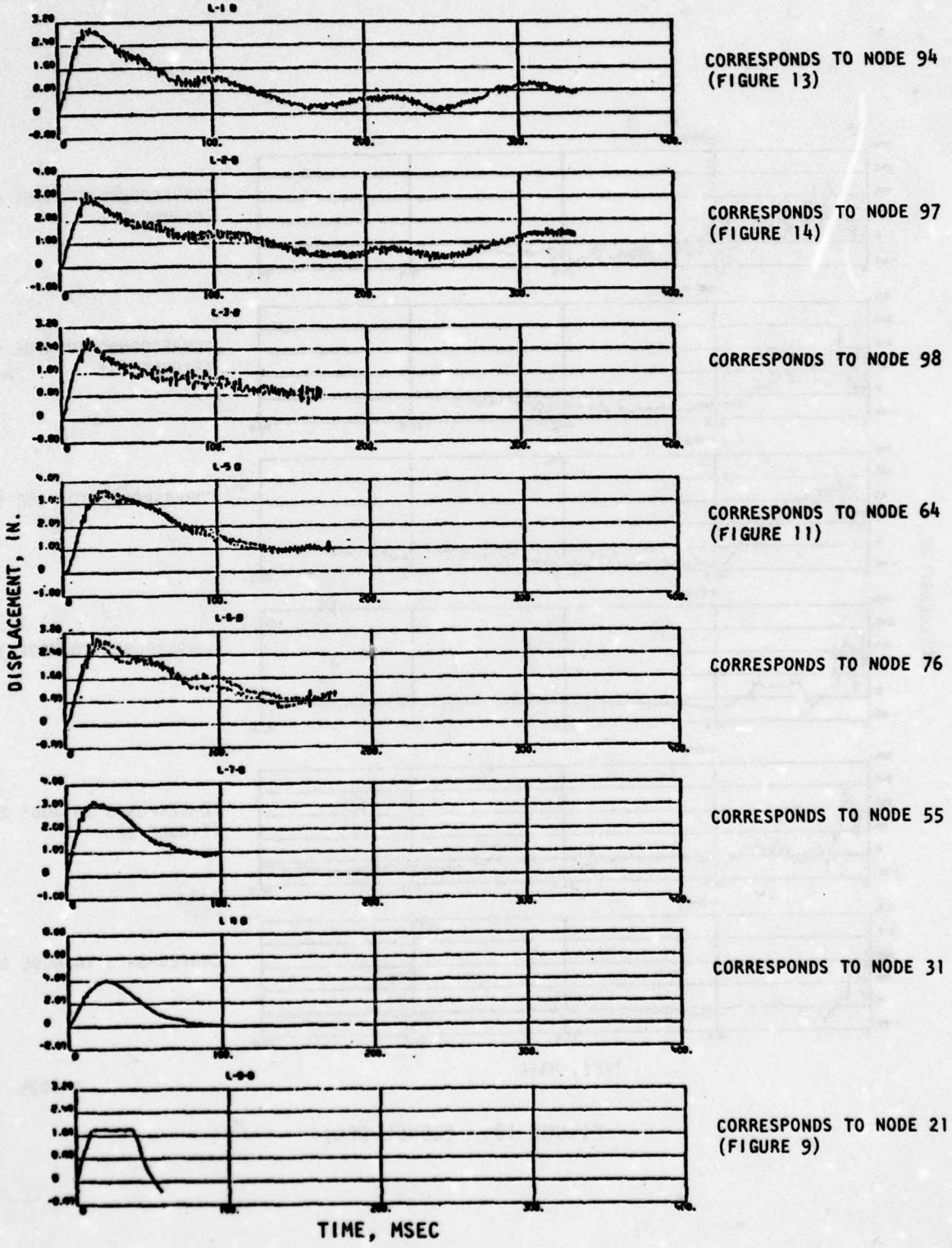


FIGURE 19. MEASURED DISPLACEMENT TIME HISTORIES OF NORTHEAST HEADWALL (Ref. 4)

displacement at the four locations shows that the shapes of the pulses are in good agreement. Table 1 shows a comparison of the maximum displacements and permanent displacements. The agreement between the computed and measured permanent displacements is very good, although the computed maximum displacements are somewhat higher than those measured. Nevertheless, the differences between the computed and measured values are small in comparison with those found for the headwalls in the ESKIMO I and II tests (Ref. 7).

The measured acceleration time histories at several locations on the headwall and door are shown in Figure 18. The accelerations are given in the units of g (gravity constant) and the time is expressed in millesecond units. For each record the corresponding node in the finite element mesh (Fig. 5) is identified. Out of a total of 11 records, the computed pulses are available only at seven locations. These are at Nodes 21, 61, 64, 91, 94, 97, and 99 and the corresponding acceleration pulses are given respectively in Figures 9 through 15. The measured pulses are shown up to a maximum of 50 msec, while the duration of the computed time histories is 186 msec. The general shapes of the computed pulses are different from those computed. The measured records show small motions after about 25 msec. In contrast, the computed acceleration records show strong motions even after 150 msec. This is attributable to the fact that in the actual test, cracking and crushing of concrete dissipates large amounts of energy. Although the INSLAB code accounts for the energy dissipation through the yielding of concrete, it is not intended to consider the crushing of concrete. Therefore, the energy dissipation model in the calculation may underestimate the actual energy loss. A comparison of the computed and measured maximum accelerations at various locations on the headwall and door is shown in Table 2. The agreement between the measured and computed values is good.

In ESKIMO IV, unlike in the previous ESKIMO tests, the headwalls were heavily instrumented to measure pressure, acceleration, and displacement time histories on the headwall and door systems. The northeast headwall was instrumented with seven pressure gages, twelve accelerometers, and nine

TABLE 1. COMPARISON OF MAXIMUM AND PERMANENT DISPLACEMENTS OF NORTHEAST IGLOO, ESKIMO IV

Location		Maximum Displacements, in.		Permanent Displacements, in.	
Node	Gage I.D.	Measured	Computed	Measured	Computed
94	L-1-B	3.0	3.7	0.8	0.9
97	L-2-B	3.2	3.3	1.0	1.0
64	L-5-B	3.6	5.3	1.0	0.8
21	L-9-B	1.9	3.1	*	0.3

*The transducer seemed to have failed after recording about 50 msec of motion.

TABLE 2. COMPARISON OF MAXIMUM ACCELERATION OF NORTHEAST IGLOO, ESKIMO IV

Location		Maximum Accelerations, g	
Node	Gage I.D.	Computed	Measured
21	A-10-B	258	225
61	A-6-B	280	208
64	A-7-B	196	238
91	A-1-B	1550	1250*
94	A-2-B	236	395
97	A-3-B	272	151
99	A-5-B	264	241

*Estimated value, since the gage exceeded the rating limit

linear motion transducers. This provided for the first time an opportunity to compare the computed and measured time histories of accelerations and displacements at several locations on the headwall. The information contained in the measured records can be used to adjust the parameters of soil models in any future calculations to improve the analytical prediction capabilities.

CONCLUSIONS

The present study consisted of a dynamic analysis of the northeast magazine headwall subjected to blast loadings in the ESKIMO IV test. The analysis was performed using the INSLAB code, a nonlinear finite element computer program. The computed results were compared with available test data. The following is a summary of conclusions of the study.

a. The INSLAB computer program is capable of analytically predicting the behavior of the magazine headwalls used in the ESKIMO tests.

b. The nonlinear material model to represent the soil behind the headwalls appears to be satisfactory.

c. The general behavior of the headwalls predicted by the calculation agreed well with the actual behavior of the headwall in the test.

d. The corrugated steel arch does not appear to provide any significant resistance to the motion of the headwall.

e. The magnitudes and general shapes of the computed displacement time histories are in good agreement with those measured by the linear motion transducers.

f. The computed acceleration time histories look somewhat different from those measured by the accelerometers; however, the computed maximum accelerations are in good agreement with those measured.

ACKNOWLEDGMENTS

The work reported herein was performed under Contract No. DAAB09-75-C-0025 with the Department of Defense Explosive Safety Board. Dr. T.A. Zaker was technical monitor of the contract for the Department of Defense Explosives Safety Board. Major contributions to the study were made by D. Van Dillen, H.S. Ts'ao, B. Barclay, and J.W. Workman of the Agbabian Associates staff.

REFERENCES

1. Weals, F.H. *ESKIMO I Magazine Separation Test,* NWC TP 5430. China Lake, CA: Naval Weapons Center, April 1973.

2. ----. *ESKIMO II Magazine Separation Test,* NWC TP 5557. China Lake, CA: Naval Weapons Center, September 1974.

3. ----. *ESKIMO III Magazine Separation Test,* NWC TP 5771. China Lake, CA: Naval Weapons Center, February 1976.

4. Weals, F.H., and Wilson, C.H. *Preliminary Report, ESKIMO IV.* China Lake, CA: Naval Weapons Center, 1976.

5. Zienkiewicz, O.C., and Chung, Y.K. *The Finite Element Method in Structural and Continuum Mechanics.* New York: McGraw-Hill, 1967.

6. Ts'ao, H.S.; Reddy, D.P.; and Dowdy, R.D. *Magazine Headwall Response to Explosive Blast,* R-7336-3284. El Segundo, CA: Agbabian Associates, January 1974.

7. *Dynamic Analyses of Magazine Headwalls in the ESKIMO Tests,* R-7556-1-4182. El Segundo, CA: Agbabian Associat-s, May 1976.

8. *User's Guide for INSLAB Code,* U-7556-1-4001. El Segundo, CA: Agbabian Associates, September 1975.

TITLE: DEFLAGRATION TO DETONATION OF SMOKELESS BALL POWDERS AND THE MEANS USED TO REDUCE A DETONATION OCCURRENCE

Mr. E. A. Andrew
Olin Corporation
East Alton, IL

ABSTRACT

- Chemical explosions are described and a typical explosion reaction is followed from an initial fire to a detonation.

- Several hazard classifications for smokeless powders are briefly covered and a definition of confinement (the chief cause of detonation) is presented.

- The contributing factors that accelerate the rate reaction of smokeless BALL POWDERS are combined into an overall factor, and an empirical relationship with relative quickness is described.

- Several means of reducing detonations of smokeless BALL POWDER are discussed and a typical application is shown.

DEFLAGRATION TO DETONATION OF SMOKELESS BALL POWDERS

AND THE MEANS USED TO REDUCE A DETONATION OCCURRENCE

1. Chemical explosions are characterized by

   - very high rate of reaction and
   - very high temperatures and pressures.

- Explosive undergoes the chemical reaction within a peculiar type of shock wave or detonation wave.
- Detonation wave propagates thru the explosive, supported and reinforced by the chemical reaction at velocities of from 1 to 6 miles per second.
- In general, the wave travels thru the column of explosive at a constant speed.

Figure 1

This reaction starts as a slow combustion but builds up

- thru the stages of explosive deflagration and
- finally undergoes a sudden transition to the detonation reaction.
- This is preceded sometimes by pulsating reactions and shock interactions (generally in a gaseous state).

- Low and high explosives differ in several respects. These differences may be seen in

Table 1

- Commonly accepted classification of explosives is shown in

Table 2

- Our particular interest in this presentation is with the hazards associated with the use, storage and physical processing of BALL POWDER, although the information would probably be similar for extruded small arms propellant powder.

- There are several publications that are available for determining the degree of hazard of Smokeless Powder. These are:

1. "Contractors Safety Manual for Ammunition, Explosives and Related Dangerous Materials"

   Dept. of Defense DOD 4145.26M (Oct. '68)

   Defines 2 classes of dangerous materials:

   Fire Hazard (Class 2)

   - Pressure rupture of container, but
   - no propagating shock waves, and
   - no damaging blast pressure beyond magazine distances,
   - but fire may be spread by tossed containers.

   Mass Detonation Hazard (Class 7)

   - Entire quantity explodes instantaneously.
   - Causes severe structural damage to adjacent objects.
   - Initiates simultaneous explosions of separated explosives sufficiently close to initially exploding pile.

2. Army Materials Command Regulation "Safety Manual" No. 385-100 (April '70).

   Class 7 (detonation hazard) powders:

   - Contains > 20% NG
   - Gravimetric Density is 0.750 or less
   - Web is 0.0075" or less
   - Or web is 0.0090 or less & GD is < .900

3. "Ordnance Safety Manual" ORDM 7-224
   Dept. of Army (1951 and revised May 15, 1958)

   - Forerunner of above safety manual and categorizes explosives into 12 classes. Contains considerable detailed information on explosive materials.

Table 3

4. The relative quickness of a smokeless powder is a measure of the rate at which the powder will burn.

   - It is a comparative value and measured against another powder called a "reference" or "base".

   - To develop the RQ data, 5 grams of powder is fired in a 200 cc heavy walled pressure vessel and a photograph trace of the firing is made.

   - A tabulation of the relative quickness (RQ) of BALL POWDERS is shown in

FIGURE 2

5. Empirical burn rate factor:

   I would like to propose at this time a quick and simple method for approximating the relative quickness value of BALL POWDERS or the relative rate which these powders will burn. This method is an attempt to calculate a relative quickness when the physical and chemical properties of the BALL POWDERS are known.

   We know the effect of certain factors on the burn rate of Smokeless Powder:

Increased	Decreased
Higher N %	High Grain Density
Low Grav. Density	Added Deterrent
High N.G.	
Small Webs	
Small Ball Diameter	

   - Now, if we plot the R.Q. against the calculated factor -

$$\text{Burn Rate Factor} = \frac{\%\ \text{Nitroglycerin}^*}{\text{Web} \times \text{Grav. Density}}$$

$$\text{(For Example)} = \frac{15}{.010" \times 0.600}$$

$$R = 2500$$

we see a definite correlation emerge. This correlation is really not surprising since the 3 main factors affecting burning rate are in the equation. This is different from previous methods which considered only % NG, GD, web, web and GD and web and NG.

*Applicable for nitroglycerin values of 10% or greater.

- The RQ:Burn Rate factor correlation is graphed in:

FIGURE 3, FIGURE 4

- Several discernable conclusions can be drawn from the graph:

1. There is good correlation between the RQ determined from bomb firings and the burn rate factor calculated from the BALL POWDER properties. (Variation is $\pm$ 8% of the nominal value.)

2. Class 2:Class 7 powders are separated fairly clearly from each other at -

   RQ = 187 or
   Burn Factor = 2000

3. All deterred BALL POWDERS occur below a factor of 2000.

4. Density lowered deterred WC452 - WC472 series are an errant, separate consideration.

- Winchester-Western's major source of first hand information on the deflagration: detonation reaction of Smokeless Powder is based on studies made at our St. Marks Plant between Dec. '70 and Dec. '71.

- A fire and explosion at this plant in Sept. '70 resulted in detonations that would not have been predicted by criteria in use at that time.

- The objective of the undertaken Safety Testing Program was to:

1. Obtain test data to establish permissible configurations of in-process containers for the transfer and storage of Class 2 and 7 propellants.

2. Learn more about the initiation phase prior to the detonation.

3. Further define the criteria for classifying powders as Class 2 or Class 7.

- Briefly, the program was to:

1. Reassess the hazards associated with bulk powder handling and storage and --

2. Determine the means necessary to reduce the hazards of:

   A. Powder in tubes or pipes.

   B. Fibre paks in various stacking configurations and degrees of confinement.

   C. Kingsmill powder hoppers.

   D. Bulk tote bin storage.

- Up to the time of the tests most dry powder operations were governed in part by the widely accepted 30" critical height theory which in simple form said, "Smokeless powder will burn and will not detonate if the powder height or depth is maintained less that 30 inches."

- The open tube tests were conducted to determine the effect of:

    1. Different degrees of wall stiffness (fibreboard, aluminum, black iron).

    2. Different powder heights - 50" to 5".

    3. Differences between Class 2 and Class 7 powders.

- These test data are summarized in:

TABLE 4

- Results from these tests simply stated are:

    1. Class 2 Smokeless BALL POWDER -

        Upon ignition, the powder doesn't even completely burn regardless of the degree of wall confinement. The pressure of burning causes unburned powders to spew out of the top of the tube.

    2. Class 7 Smokeless BALL POWDER -

        There is enough wall confinement in 4" and 1" diameter iron pipe to cause a detonation of the entire powder mass.

- The fibrepak tests are summarized in:

TABLE 5

and adopted stacking for in-process storage is shown in:

FIGURE 5

- Testing was also made on the hazards associated with the storage of powder in a Kingsmill powder hopper:

FIGURE 6

The results were:

Powder	Ignition Point	Results
150 lbs. - Class 7	B - Surface of Powder	Fire only
150 lbs. - Class 7	A - Bottom of Supply Tube	Fire only
150 lbs. - Class 7	C - Apex of Cone	Detonation with complete destruction of hopper.

- The St. Marks study caused revision of our earlier thinking on powder hazards and we developed a hypothesis on the mechanism of the deflagration to detonation reaction in smokeless powders with the following factors considered important in the deflagration: detonation reaction:

    1. The rate of reaction is determined by:

        1) The thermoconductivity of the solid:vapor interface of the burning propellant,

        2) The pressure, and

        3) The temperature.

    2. The rate increases with both pressure and temperature increase.

    3. Rate increase factors are:

        1) High NG content.

        2) Small webs.

        3) Low GD

        4) Or combinations thereof.

    4. Rate decreasing factors are:

        1) Increase of previously mentioned factors.

        2) Increase in deterrent level.

- Drawing on the above factors and their effect on the rate of reaction and the knowledge gained in the actual testing program, the hypothesis was drawn that confinement of either the heat or pressure source upon ignition leads the reaction thru the deflagration to detonation transition zone.

- Now this confinement in a relatively low pressure system is of two types:

    1. Pressure Confinement.

        1) Powder weight or height above the ignition source.

        2) Physical wall strength of the container.

    2. Heat Confinement.

        1) Thermoconductivity of powder and powder container material.

- To reduce the probability of a deflagration:detonation event, you must resort to reducing the two aforementioned confinement factors of pressure and heat.

- This can best be done by the engineering design of the following mechanical means into the powder system:

Means	Results
1. Vent Tube	Reduces pressure & heat at ignition source.
2. Blow out panels where vent tubes are not possible	"
3. Reduction of powder height	"
4. Use very thin or weak walls for containers	"
5. Interrupted powder height or flow	Reduces & limits fuel source.

- Successful corroboration of the pressure:heat reduction hypothesis was made by 10 full scale Kingsmill hopper test firings. A 3" cardboard vent tube was installed approximately 2" from the sides of the cone (at apex) and ignition was made at the cone apex.

FIGURE 6

No detonation occurred in 5 out of 5 trials. The same results were obtained with the use of blow out panels installed on the cone.

U.S. Patents 3,730,049 and 3,713,359 were granted for the protection of smokeless powder hoppers employing the blow out panel and vent tube principle.

SUMMARY

1. Smokeless BALL POWDERS can be catagorized into Class 2, a fire hazard or Class 7, a mass detonation hazard based on whether the powder is above or below a relative quickness of approximately 187.

2. If the relative quickness of the BALL POWDER is unknown, a good approximation as to its fire or mass detonation property can be made by the formula:

$$R = \frac{\% \text{ NG}}{\text{Web} \times \text{G.D.}}$$

If $R < 2000$, BALL POWDER is Class 2.

If $R > 2000$, BALL POWDER is Class 7.

3. Reduction of (1) the heat ignition source and/or (2) the pressure source can reduce the probability of a deflagration:detonation reaction.

4. A physical means of accomplishing item 3 (above) in storage containers has been developed.

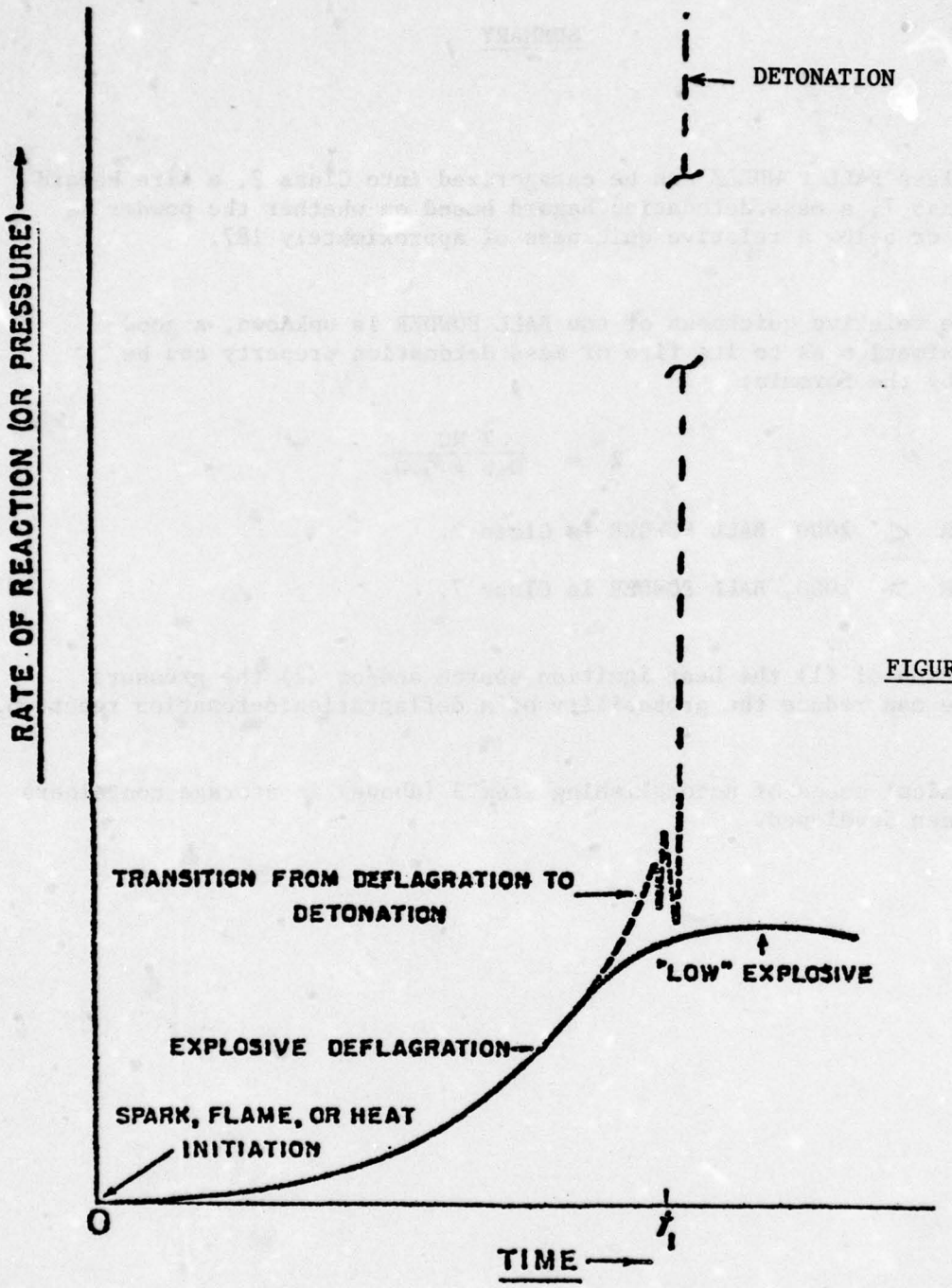


FIGURE 1

EXPLOSIVE DEFLAGRATION VERSUS DETONATION
AND
TRANSITION FROM DEFLAGRATION TO DETONATION

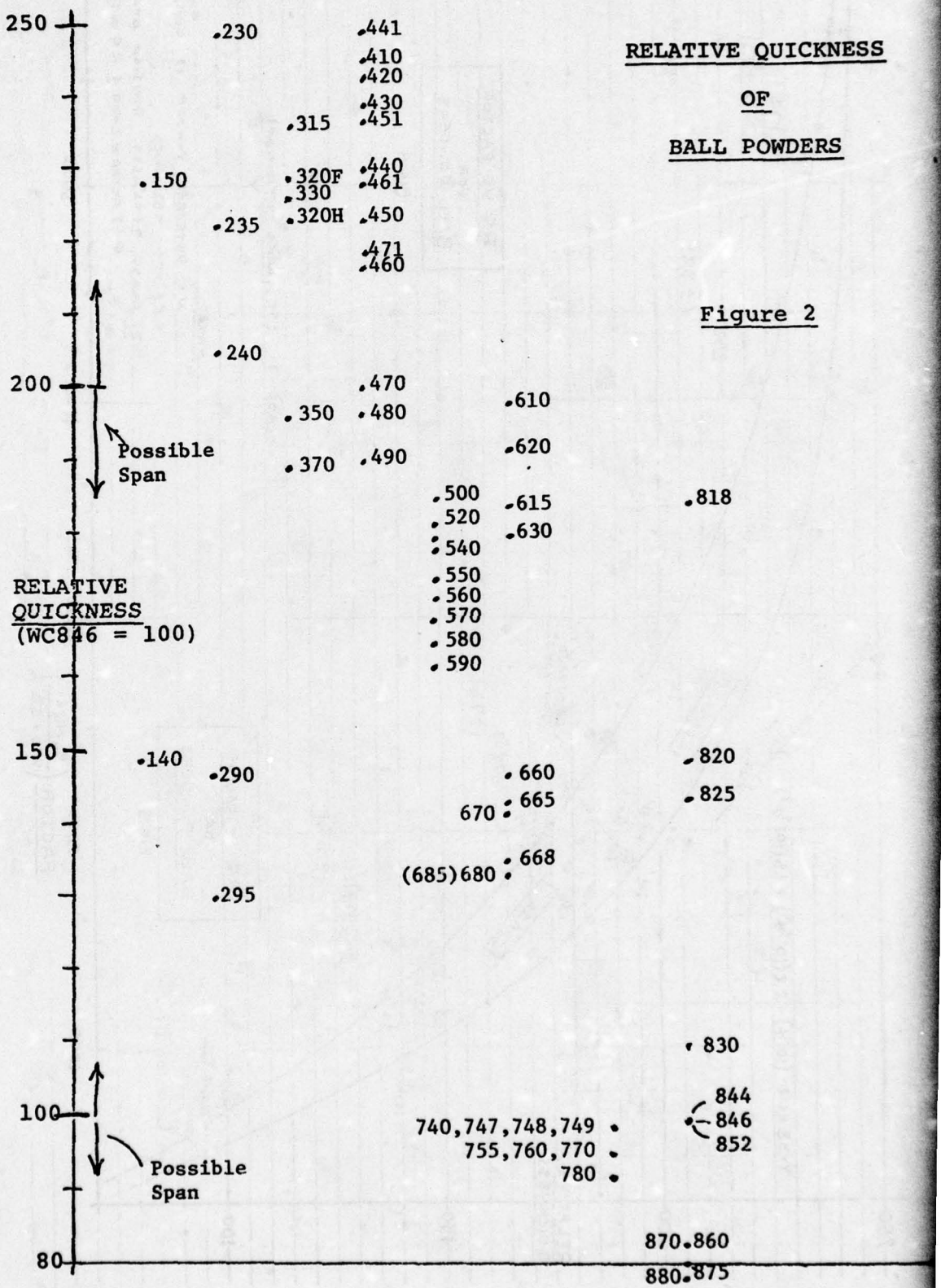
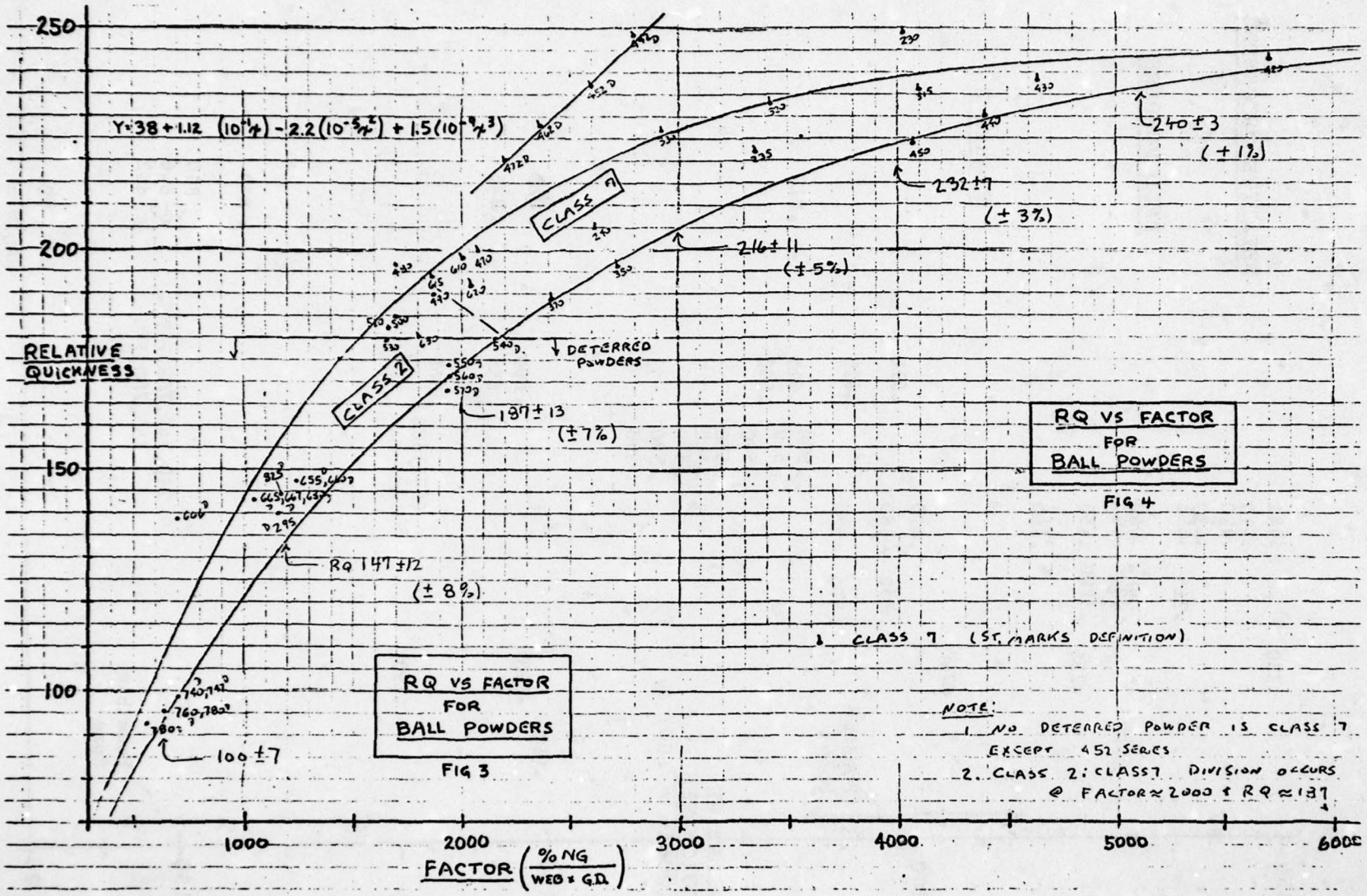

RELATIVE QUICKNESS
OF
BALL POWDERS
250
200
150
100
80
RELATIVE
QUICKNESS
(WC846 = 100)
Possible
Span
Possible
Span
.230
.441
.410
.420
.430
.315
.451
.150
.320F
.440
.461
.330
.235
.320H
.450
.471
.460
.240
.470
.610
.350
.480
.620
.370
.490
.500
.615
.818
.520
.630
.540
.550
.560
.570
.580
.590
.140
.290
.660
.820
.665
.825
670
.668
(685)680
.295
.830
.844
.846
740,747,748,749
.852
755,760,770
780
870.860
880.875

Figure 2



RQ VS FACTOR FOR BALL POWDERS

FIG 3

RQ VS FACTOR FOR BALL POWDERS

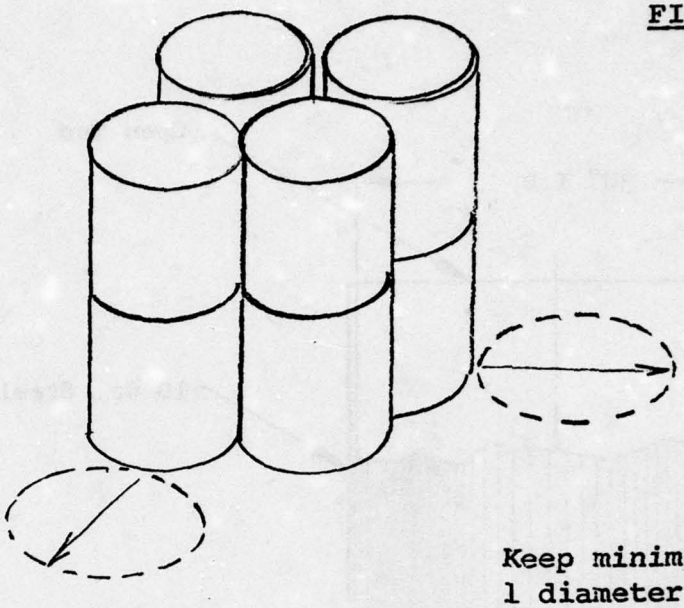
FIG 4

NOTE:
1. NO DETERRED POWDER IS CLASS 7 EXCEPT 452 SERIES
2. CLASS 2 : CLASS 7 DIVISION OCCURS @ FACTOR ≈ 2000 & RQ ≈ 137

MAXIMUM STACKING FOR CLASS 7 IN PROCESS STORAGE

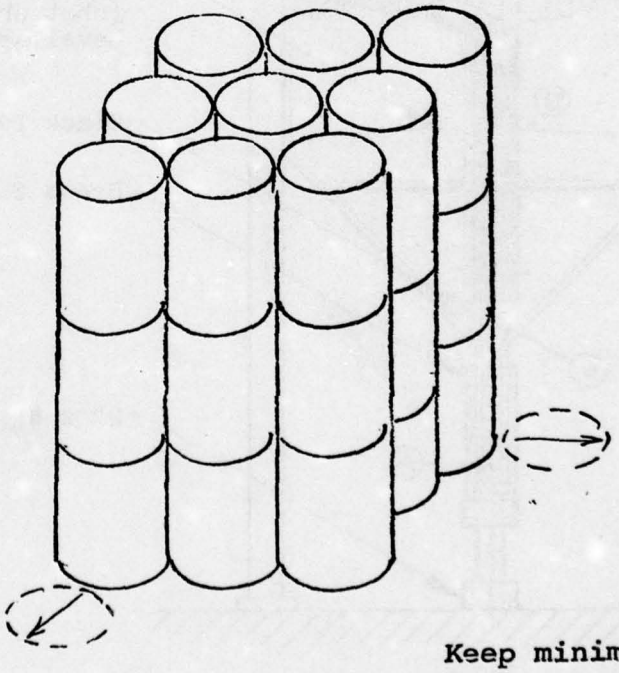
FIGURE 5

LARGE FIBREPAKS



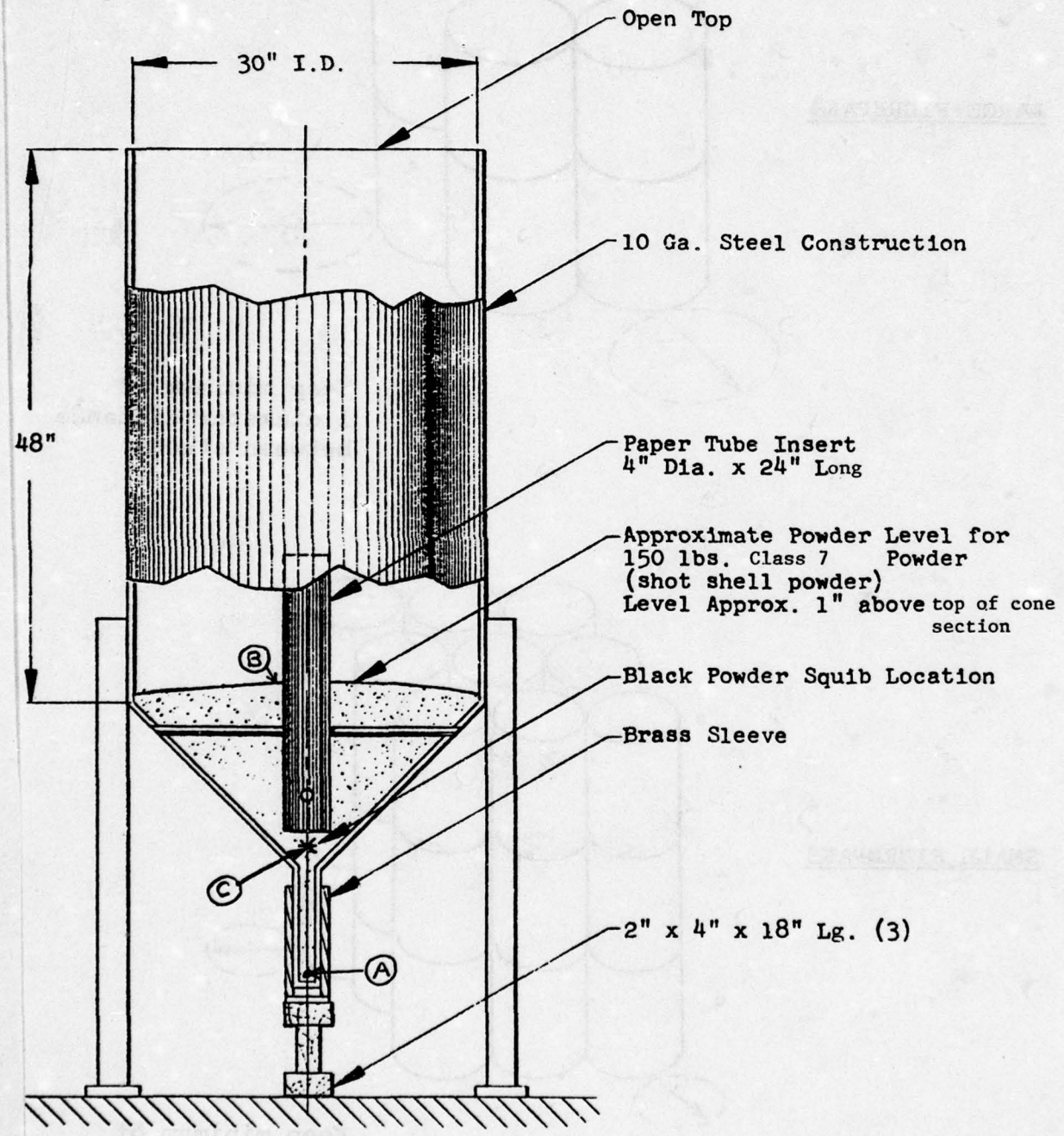
Keep minimum of
1 diameter distance
between stacks

SMALL FIBREPAKS



Keep minimum of
1 diameter distance
between stacks

FIGURE 6



KINGSMILL HOPPER

TABLE 1

CHARACTERISTICS OF LOW AND HIGH EXPLOSIVES

	Low	High
Rate of reaction	1 to 4	1000
Time of complete conversion of explosive to gaseous products	Milliseconds	Microseconds
% of conversion of solid explosive to gaseous products	100	100
Velocity of consumption of explosive grains	A few inches to feet per sec	1 to 6 miles/sec
Velocity of flame front	1/3 to 1 mi/sec	1 to 6 miles/sec
Pressure of explosion	Up to about 60,000 psi	100,000 to 4,000,000 psi

TABLE 2

COMMONLY ACCEPTED CLASSIFICATIONS OF EXPLOSIVES

LOW	HIGH	
	SECONDARY	PRIMARY
Smokeless Powder	Trinitrotoluene	
Black Powder	Tetryl	Lead Azide
Nitroglycerine	RDX	Lead Styphnate
	PETN	Tetracene
	Ammonium Picrate	Mercury Fulminate
	Ammonium Nitrate	Diazodinitrophenol
Method of ignition:		
Spark, flame, impact or heat	Requires booster	Spark, flame, impact or heat

TABLE 3

ORDINANCE SAFETY MANUAL ORD M7-224

Class 2	- Material in approved storage containers, bulk storage or cartridge cases. - Single base with web less than .019".
Class 2A	- Double base with not more than 20% NG and a web 0.0075" or less. - Single base powders.
Class 9	- Class 2A powders in all metal containers not designed for quick pressure release. - Double base with web less than 0.0075" regardless of NG content. - Double base powders containing more than 20% NG. - Single base with 98% or more NC. - RDX - TNT

TABLE 4

ST. MARKS TEST OF BALL POWDERS IGNITED IN OPEN TUBES

Type of Tube	Powder Height	Class 2 Powder	Class 7 Powder
8" Diameter	50"		30' Flame
Fibre Board	30" (1)		Report & 25'Fireball
8" Diameter	60" (1)	Tube split with 2/3 of powder unburned	
Aluminum	60" (2)		Tube cut into two Very rapid burn
	50"		Report - 20'Fireball 20" of tube folded
4" Fibre Board	60"		Quietly burned
4" Black Iron	20"		20" pipe gone Crater formed
1" Black Iron	41"	24" Peeled - Unburned powder	
	23"	Unburned powder	23" pipe gone
	10"		10" pipe gone
	5"		5" pipe gone
1 quart cardboard container with No. 6 blasting cap	Full		Hole cut through 1/4" steel plate

(1) aluminum disc + 4" sand

(2) squib located @ 30"

Detonation occurred

TABLE 5

FIBRE PAK TESTING

Class	Pak Size	Stack	Ignition	1/4" Witness Plate Damage	Results
2A	Large	2 High	Squib	None	No report, 8' flame for 16 seconds.
2A	Large	2 High	Bonfire	None	Burned quietly for 8 seconds.
2A	Large	1 Buried	Squib	-	15' Flame.
7	Large	2 High	Squib	2½" Bow	Very heavy report with 30' flame. Debris thrown 150'.
7	Small	2 High	Squib	2" Bow	Very heavy report with 40' flame. Debris thrown 100'.
7	Small	1 Buried	Squib	-	Heavy concussion. 13' dia. crater x 6' deep. Time less than .030 seconds.

DETONATION

PRESSURE RELIEF VENTING CONCEPTS FOR ELIMINATING AN EXPLOSIVE HAZARD IN AUTOMATED SINGLE-BASE OPERATIONS

C. H. Johnson and F. T. Kristoff

Hercules Incorporated
Radford Army Ammunition Plant
Radford, Virginia

ABSTRACT

The adequacy of a propellant storage hopper was established for venting burning reaction gases to preclude an explosive reaction in the air-dry operation of the Automated Single-Base Line (ASBL). Full-scale tests with 450 pounds of M1SP f/105mm propellant did not transit from burning to an explosion when bottom flame initiated in a specially designed hopper incorporating pressure relief venting. Implementation of this hopper design reduced an assessed Class 7 explosive hazard to a Class 2 burning hazard in Automated Single-Base Line finishing operations.

Application of the propellant surface area to hopper vent area ratio established in this study provides basic safety design information for preventing flame initiated explosive reactions in single-base propellant processing vessels.

PRECEDING PAGE BLANK-NOT FILMED

INTRODUCTION

As part of the overall Army modernization program, a new continuous automatic facility is being constructed at Radford Army Ammunition Plant (RAAP) for manufacturing single-base cannon propellants. When completed, this new production plant will be capable of manufacturing 2.5 million pounds per month of single-base propellant. In this plant, new equipment and manufacturing technology have been advanced to produce propellants more economically and with a much lower level of personnel exposure than in the conventional batch process.

The process flow begins with the metering of preconditioned propellant ingredients into a compounder where ingredient blending and some mix consolidation begins (see Figure 1). From the compounder, an uninterrupted flow is maintained through mixing, extruding, cutting, solvent recovery, water dry, air dry, and finally the pack-out operations. The propellant is maintained solvent-wet or surface water-wet in all processing steps until it is discharged from the air-dry module into discharge hoppers. At this point, the finished propellant exists in a dry state and is governed by the safety regulations established for dry propellants.

A safety problem evolved when the original M6 mission of the ASBL was expanded to include M1 single perf (SP) propellant manufacturing capability. This change resulted in the thin web SP propellant bed depth exceeding the maximum limit of 18 inches (AMCR 385-229) in the air-dry modular discharge hoppers. Exceeding this limit introduced a Class 7 explosive hazard in this processing phase. However, the manufacturing and support facilities within the ASBL have been sited for propellant quantities posing a Class 2 burning hazard only. Therefore, without design changes, imposition of a Class 7 in-process hazard rating would seriously curtail propellant manufacture in the present ASBL complex. Changes in the mode of operation to eliminate the potential explosive hazard by maintaining the propellant bed depth below 18 inches or provide Class 7 protective barricading would require extensive costly modifications to existing structures or equipment, new construction, and extended delay in project completion. Therefore, a hopper design incorporating pressure relief venting capability was introduced together with a confirmatory prototype hopper test program.

The purpose of this report is to present the findings and conclusions regarding (1) the design and venting adequacy of the proposed

propellant surge hopper for precluding explosive reactions when expected quantities of 450 pounds is flame initiated, and (2) the in-process hazard classification for 450 pounds of M1SP f/105mm propellant in these hoppers for ASBL air-dry finishing operations.

This test program was conducted at Hercules Incorporated test facilities at Frackville, Pennsylvania and was funded by Picatinny Arsenal.

DISCUSSION

HOPPER DESIGN/TEST

Engineering design information is not available to design pressure relief panels for venting burning propellant gases to preclude destructive pressures, or propellant transition from burning to explosive reactions in finely packed beds. In the absence of such information as (1) venting requirement, and (2) pressure relief panel location, size, mass, and materials of construction, the approach employed in designing the hopper was to introduce maximum venting without jeopardizing the structural integrity of the equipment iteself. The prototype hopper shown in Figure 2 was designed with an effective vent area of 9.69 ft^2. As seen from data in Figure 3, the hopper top opening has an apparent 9 square foot area; however, the effective area for pressure relief purposes is 2.25 ft^2 which is the cross-sectional area limited by an inner, upper baffle. An additional 0.35 square foot of venting is provided by the 8-inch diameter bottom discharge port. To maximize venting of the hopper design, additional venting in the form of 16 side vent panels was incorporated to increase the effective vent area to 9.69 ft^2 (Figure 4).

Although the need did not arise, an alternate hopper design provided for four additional pressure relief panels in the hopper bottom conical section. This design feature provided for 3.86 ft^2 of additional venting if needed (see Figure 4).

The internal baffles were incorporated to prevent propellant from flowing out the side vent panels and to aid in directing burning gases and propellant from the hopper interior after ignition.

The side vent lids were fabricated of neoprene rubber with a steel plate bonded on the outside to enhance the stability and sealing capability. The hinges of the lids were an integral part of the neoprene to eliminate the possibility of a malfunction of a mechanical joint (see Figure 5). Since the AMCR 385-229 requirement restricted propellant height to 18 inches, the first module consisting

of eight vent panels was located 17 inches above the hopper discharge outlet. The second module of eight vents was positioned approximately 17 inches above the first module to be consistent with AMCR 385-229 criteria (Figure 6).

The discharge hopper was evaluated with up to 450 pounds of M1SP f/105mm propellant in flame-initiated tests. Initial tests were performed at reduced propellant quantities of 250 and 350 pounds in 1/2-inch thick mild steel hopper to check out instrumentation and assess hopper component exposure to flame reactions.

Provisions were incorporated in the hopper design to obtain data on internal pressure magnitudes and pressure rate of rise at various locations so correlation with propellant surface area and venting could be made. Additionally, to define vent panel dynamic response to the pressure/time profile of the burning propellant in the test hopper, suitable accelerometers were mounted on the exterior of the vent panels. All test trials were monitored by high-speed and real-time photographic coverage.

Results of full-scale hopper tests are presented in Table I. As seen, the data reveal that 450 pounds of M1SP f/105mm propellant reacts by <u>burning only</u>, when flame initiated in the specially designed hopper incorporating pressure relief venting. The hopper vent panel design functioned, as intended, to prevent internal destructive pressure buildup and/or propellant transition from burning to an explosive reaction. In these tests, pressure relief venting was provided by the sixteen side vents plus the effective vent area provided by the hopper top and bottom openings. High-speed photographic coverage together with visual examination showed that no noticeable damage such as warping or flame erosion occurred to the stainless steel prototype hopper or neoprene vent panel in the ten full-scale tests performed. Figure 7 shows the prototype hopper after ten trials.

A propellant surface-to-hopper vent area ratio of approximately 660:1 established in the full-scale hopper test is more than adequate for preventing violent explosive reaction for 450 pounds of M1SP f/105mm propellant.

High-speed film coverage at 500 and 1,000 frames/second was studies and functioning times for pressure relief locations established on the basis of panel movement and/or appearance of smoke or flame. The reaction times for the lower boot, side vent panels, and top lid are listed in Table II. Examination of functioning times shows pressure venting occurs immediately and

is first observed at the bottom boot, then at the lower side vents, upper side vents, and the top lid vent areas. Functioning times in terms of smoke and flame are not constant but are reasonably close as seen by time ranges for each location.

In the prototype hopper tests with 450 pounds of M1SP, the time from ignition to the first observation of propellant or gases ranged from 24 to 60 milliseconds at the hopper discharge opening (see Table II). A portion of this time is consumed in ignition of the igniter. Flame was observed earliest at the hopper discharge opening approximately 140 milliseconds after ignition and at the hopper lid approximately 330 milliseconds after ignition. The total burning time ranged from 9.2 to 12.9 seconds; however, these times include the slow burning of propellant in the simulated discharge conveyor at the hopper bottom.

The overlapping of data only signifies differences in propellant burning characteristics within the bed and passage of smoke/flame through the interstices to the observed venting location.

Of particular interest is that hopper venting is accompanied by the initial spewing of unburned propellant granules out of the lower and upper pressure relief panels. Upon ignition, the propellant bed is apparently fluidized and pressurized with a force sufficient to propel large amounts of unburned propellant granules as far as 20 to 25 feet from the hopper. A typical chronological time sequence of this and other events, taken from high-speed film, is depicted pictorially in Figures 8a - 8f. As can be seen, unignited propellant granules are expelled from the lower vent panels almost simultaneously with the rupture of the hopper discharge boot. This action is followed by internal pressure forcing propellant out of the hopper top inlet port in the center of the lid. Next the lid is forced off followed by flame exiting out the hopper top opening. This action occurs simultaneously with gases venting out the uppermost side vent panels.

It is obvious from study of high-speed film coverage that unignited propellant spewing from the hopper is contributing to the overall dimension of the resulting fireball sized at 40 to 50 feet in diameter (see Figure 8f). The flame emanating from the hopper eventually extends upward to approximately 150 feet in height and terminates into a mushroom-shaped fireball approximately 100 feet in diameter. However, it appears at this time that the fireball created must be contained in order to minimize facility damage. Some proposed remedies to this problem are the use of flame

arresting screens located around the hopper, fire walls, or a system to direct unignited or burning propellant granules funneled out of the pressure relief vent ports into a water bath or moat. The feasibility and suitability of these methods need to be explored.

Although not studied in detail, it appears that application of Primac-operated deluge systems would not aid in preventing growth or containment of the ensuing fireball.

CONCLUSIONS

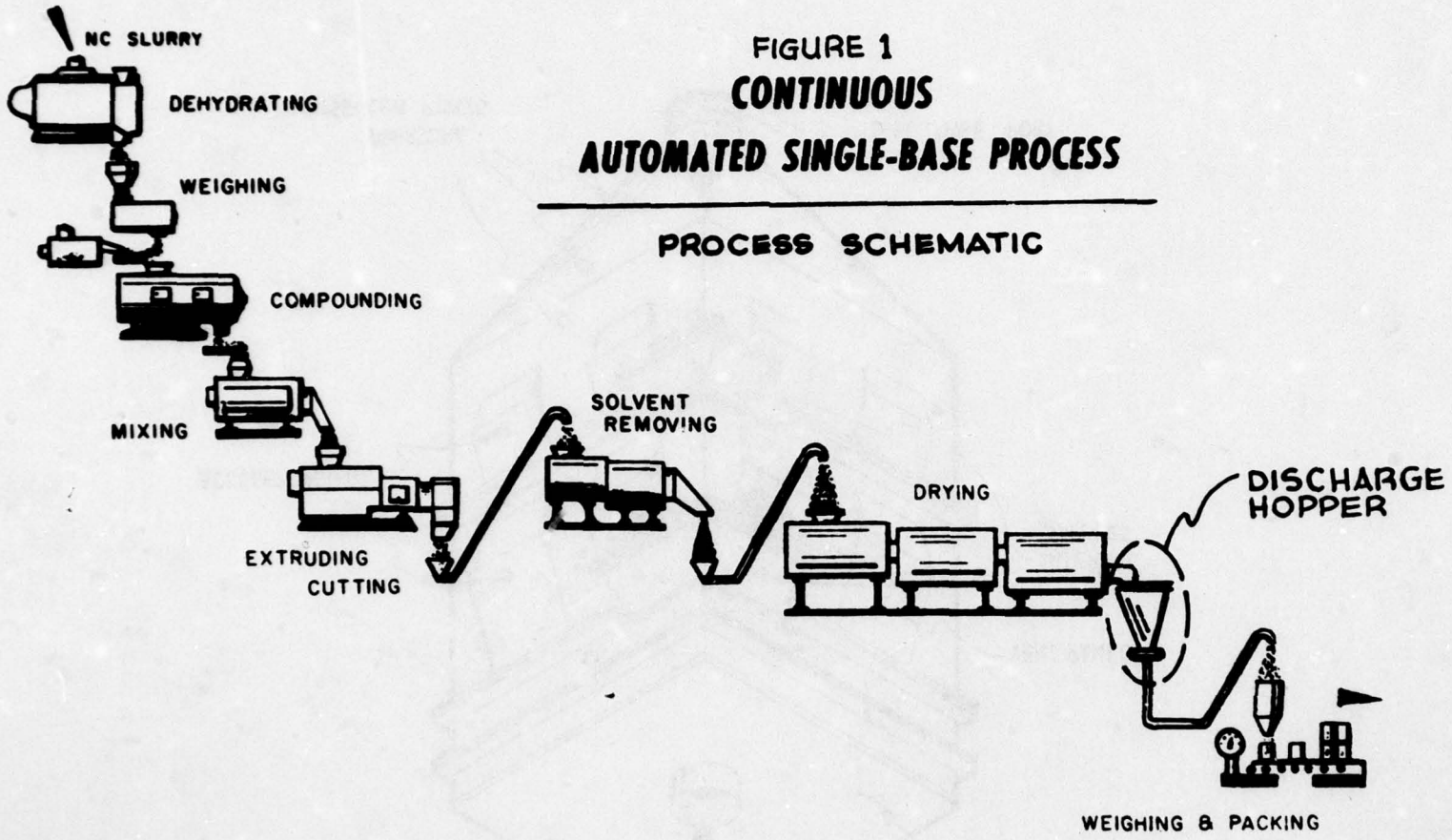
Ten full-scale hopper tests have confirmed a Class 2 propellant burning hazard for 450 pounds of M1SP f/105mm propellant in a specially designed hopper incorporating pressure relief venting. The hopper-pressure-relief venting design functioned as intended and will preclude 450 pounds of M1SP propellant from transiting from slow burning to an explosive reaction if initiated. On the basis of the successful results achieved in these full-scale tests, the pressure relief venting design has been incorporated on the air-dry modular discharge hopper in ASBL finishing operations to eliminate a Class 7 propellant explosive hazard posed by the M1SP f/105mm formulation. A propellant surface to hopper vent area ratio of approximately 660 was established for venting reaction gases to prevent transition from burning to an explosion in this hopper for 450 pounds of M1SP propellant. Application of this ratio provides basic safety design information which can prevent flame initiated explosive reactions in single-base propellant processing and storage vessels.

FIGURE 1

CONTINUOUS

AUTOMATED SINGLE-BASE PROCESS

PROCESS SCHEMATIC



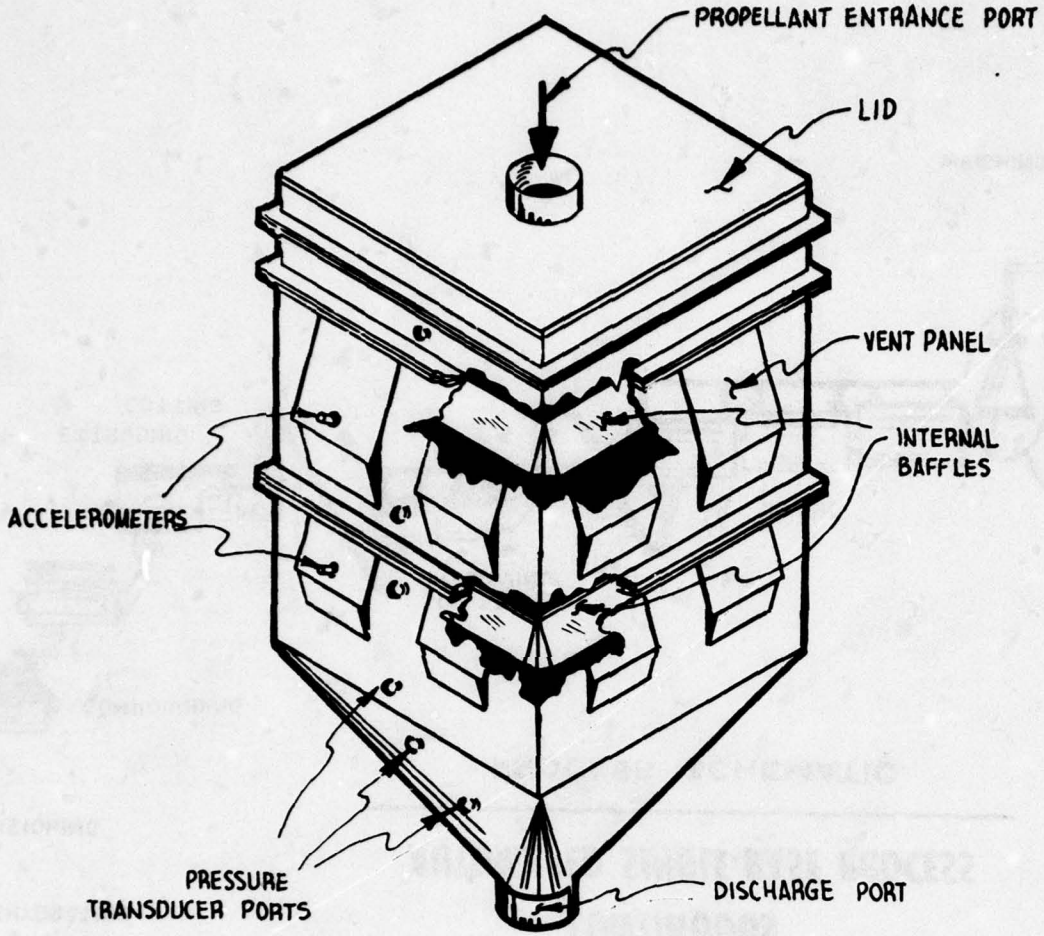
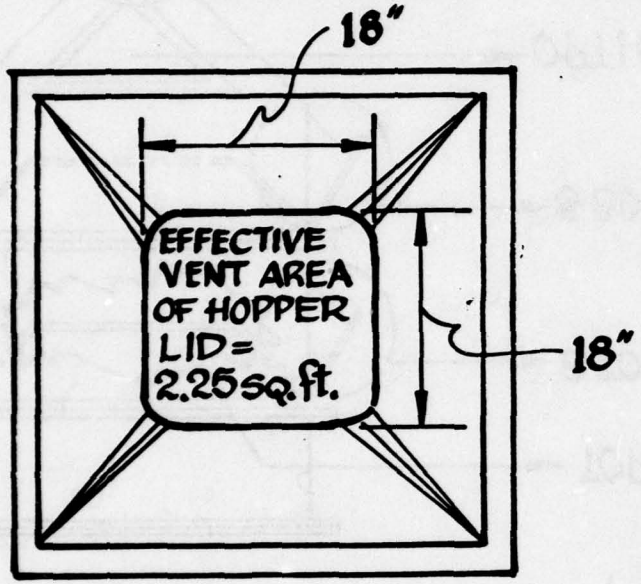


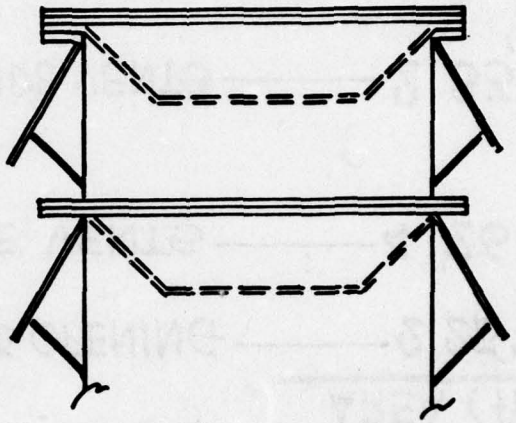
FIGURE 2

ISOMETRIC VIEW OF HOPPER

FIGURE 3
PRESSURE RELIEF AREA LIMITATIONS IMPOSED by UPPER BAFFLE



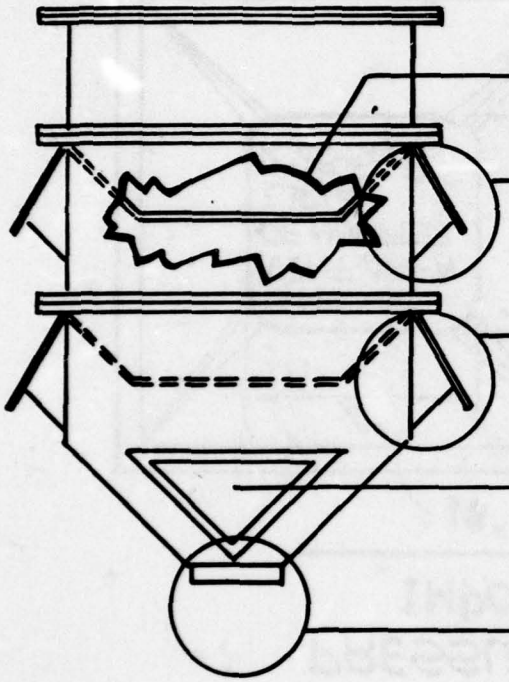
TOP VIEW



PARTIAL SIDE VIEW

FIGURE 4

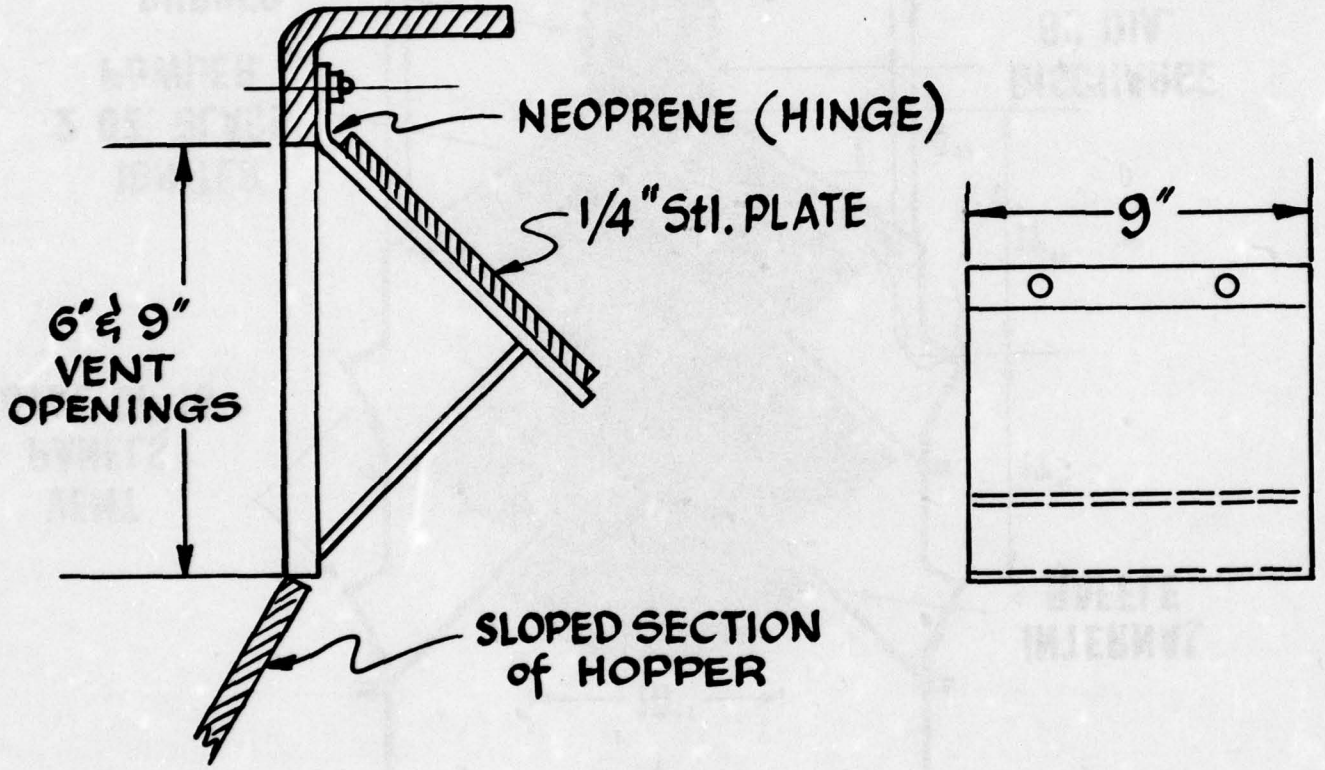
HOPPER EFFECTIVE VENT AREA



	EFFECTIVE VENT AREA (ft^2)
TOP BAFFLE OPENING	2.25
8 TOP SIDE VENTS	4.26
8 BOTTOM SIDE VENTS	2.83
OPTIONAL (3.86 SQ.ft.)	--
DISCHARGE OPENING	0.35
TOTAL EFFECTIVE VENT AREA	9.69 ft^2

FIGURE 5

SIDE VENT PANEL LID



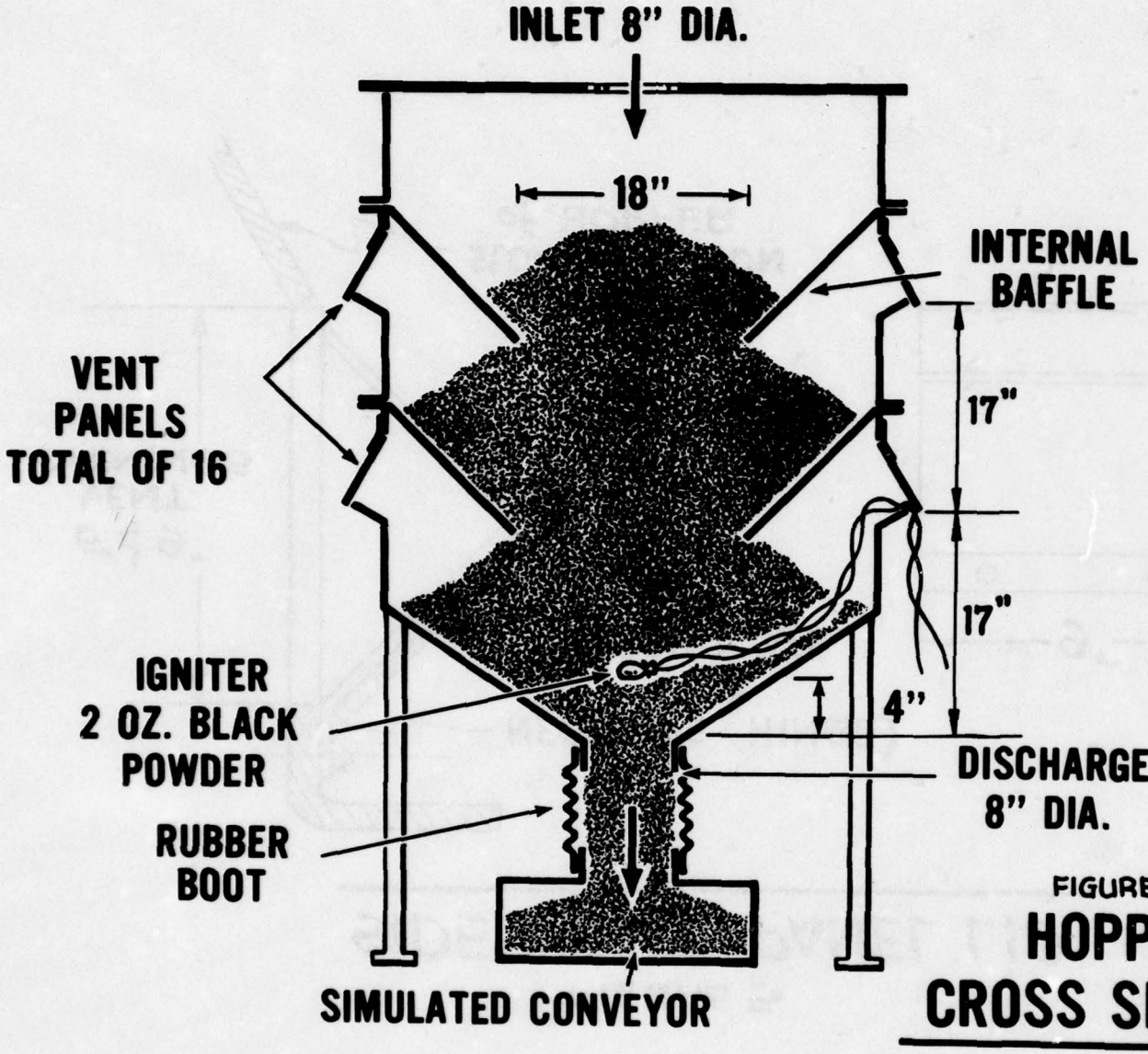


FIGURE 6

HOPPER CROSS SECTION

TABLE I

LARGE-SCALE VENTED HOPPER TESTS

HOPPER	No. TRAILS	PROP. Wt. lbs.	PROP. Bed Depth in.	REACTION
MILD STEEL	1	250	19	ORDERLY BURNING with HUGE FIREBALL
	1	350	23	
	1	450	29	
STAINLESS STEEL	10	450	29	ORDERLY BURNING with HUGE FIREBALL

*MISP f/105

TABLE II
VENTED HOPPER FILM ANALYSIS

TIME FROM IGNITION, sec.

Trial No.	Prop. Wt. lbs.	PROPELLANT GASES HOPPER Disćhg.	VENTS Lower	VENTS Upper	FLAME HOPPER Lid	Total Burning Time,
4	450	0.024	0.084	*	0.576	10
5			0.108	0.220	0.342	9.2
8		0.036	0.082	*	0.410	12.9
10		0.060	0.108	*	0.330	12.9
13		0.032	0.084	*	0.510	11.2

* UPPER VENTS OBSCURED by SMOKE and FLAME

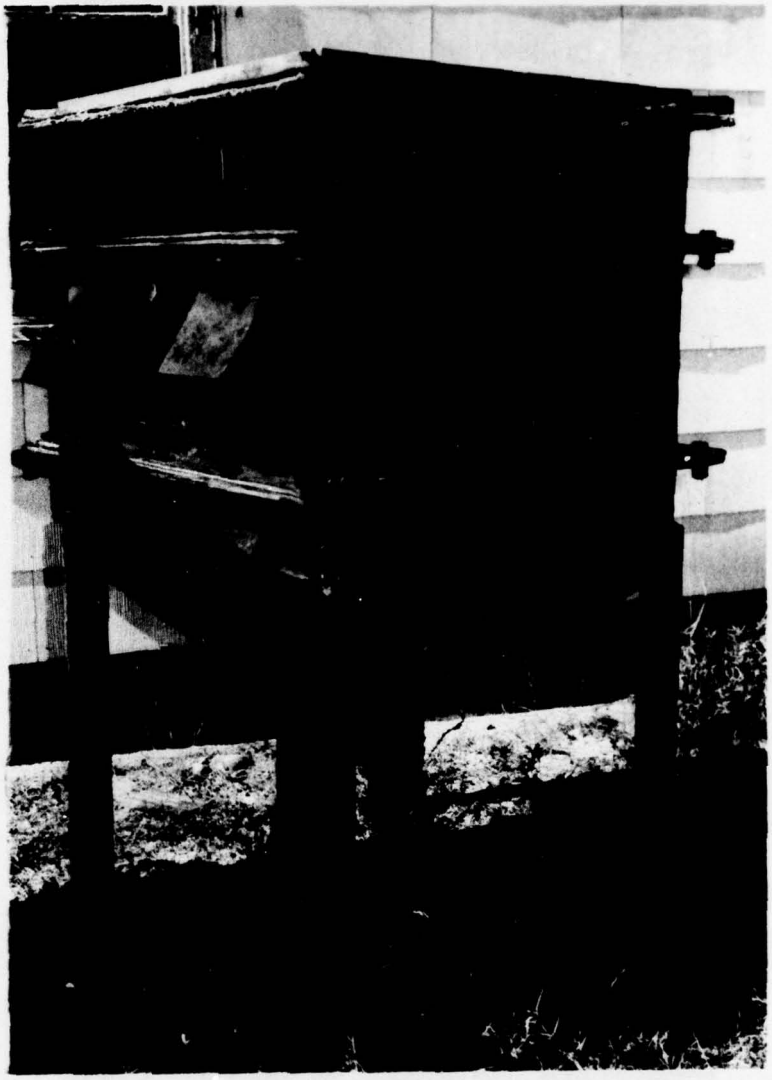
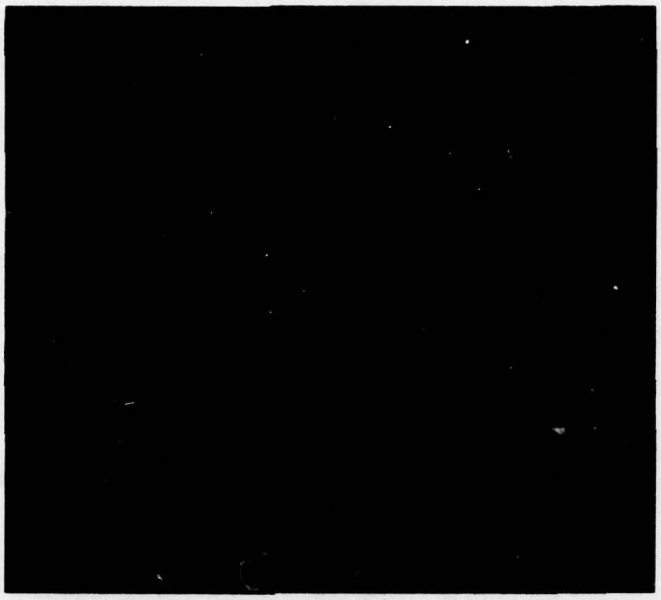


Figure 7

Prototype Hopper After Ten Tests

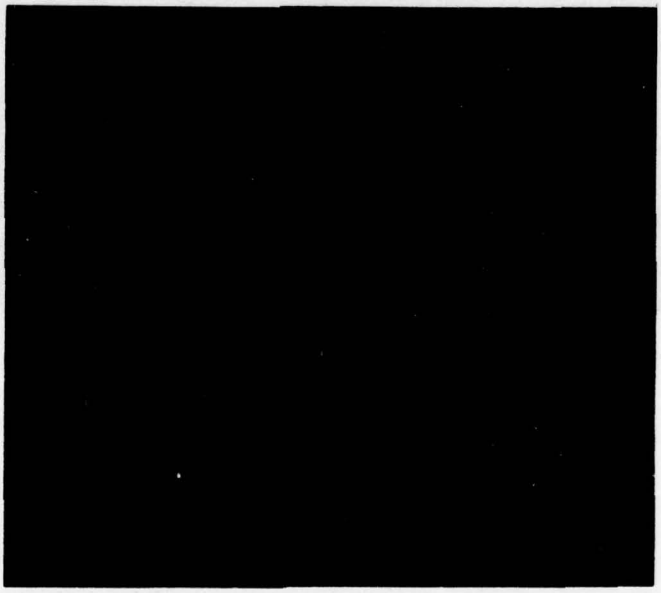
Figure 8

Sequence of Events During Testing



8a

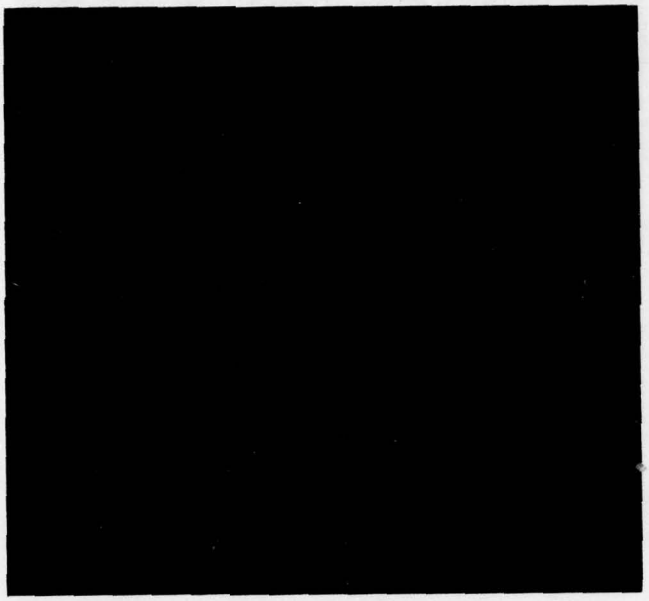
Loaded Hopper Ready for Test



8b

64 Milliseconds After Ignition

Figure 8 (continued)



8c

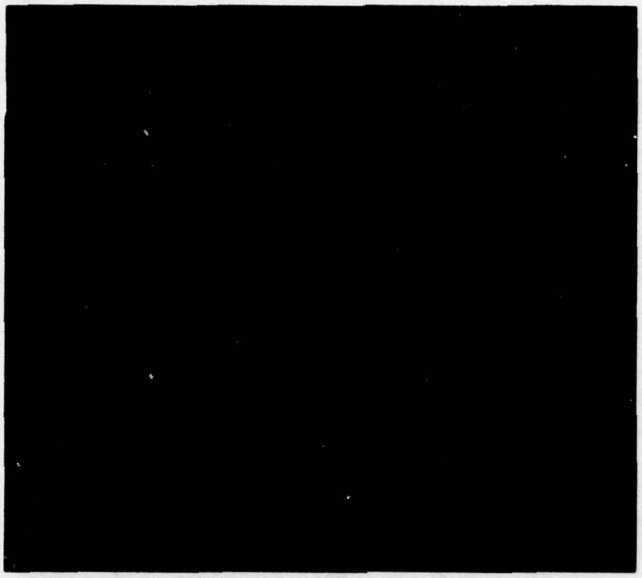
125 Milliseconds After Ignition



8d

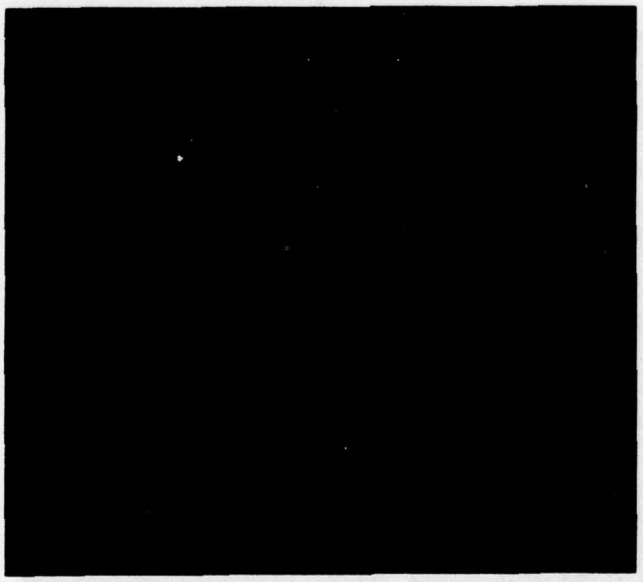
225 Milliseconds After Ignition

Figure 8 (continued)



8e

5 Seconds After Ignition



8f

View Showing Height of Fireball

EFFECT OF CONFINEMENT ON PYROTECHNIC REACTION RATES AND OUTPUT ENERGY

Gary L. McKown
US Army Edgewood Arsenal Resident Laboratory
National Space Technology Laboratories
Bay St. Louis, Mississippi 39520

ABSTRACT

This paper discusses experimental evidence that confinement afforded by enclosures or containers may have a dramatic effect on reaction rate and output energy of deflagrating pyrotechnic materials. Tests in apparatus that represent a closed structure, self-confinement, and a vented enclosure are described. Results obtained in the form of reaction rates from measurement of temperature, pressure, heat flux, reaction duration and fireball size are given.

1. INTRODUCTION

Several experimental and engineering programs have been conducted by this Laboratory in development of basic data for evaluation of the hazards involved in production and distribution of pyrotechnic materials and end item munitions. The primary emphasis of the past work has been on determination of the hazardous characteristics of a given process or on development of enclosures to contain the effects of a reaction. Thus the majority of testing has been performed to evaluate the effect of a reaction on the surroundings, particularly where the latter is represented by a vessel, structural enclosure or other containment barrier. During the course of these studies, evidence has been obtained to indicate that the rate of a reaction and resultant output energy can depend on details of the surroundings such as the extent of confinement afforded by an enclosure. This paper describes some preliminary experiments that have been performed to evaluate the effect of structural confinement on pyrotechnic reactions.

2. EXPERIMENTAL PROCEDURES

2.1 TOTAL CONFINEMENT EXPERIMENTS

An important performance criterion of pyrotechnic materials is the thermal energy released during reaction. Prior efforts have employed Parr Bomb calorimeters to determine the quantity[1], but the high pressure, oxygen-rich atmosphere and small sample size employed render the standard laboratory apparatus unsuitable for evaluation of operational situations[2]. Accordingly, the apparatus shown in figure 1 has been developed for large scale calorimetry of bulk

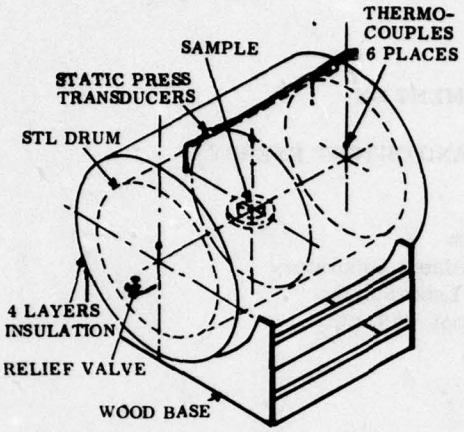


Figure 1. Bomb Calorimeter Apparatus

compositions and end items. The reaction vessel is a cylindrical steel tank with an internal volume of 30.5 liters and a wall thickness of .076 cm, providing a heat capacity of 310 calories/°K at 25°C and 1 atm pressure.

The tank is insulated from the surroundings by four layers of 2.5 cm thick aluminum-backed fiberglass insulation, and instrumented with six thermocouples and two static pressure gauges. The system has been shown to be sufficiently adiabatic, over a typical 2-4 minute reaction and equilibration time, to be usable for calorimetric measurements.

The bomb calorimeter represents a scale model of a sealed, total enclosure, and was used for experiments to demonstrate that effect. The fifty gram samples of sulfur-based pyrotechnic mixtures that were burned in the calorimeter represent a charge to volume ratio of 1.4×10^{-3} gm/cm^3. Thermal and pressure data were recorded during the course of reaction to yield overall reaction rate (energy output per unit time) and total output energy as a function of initial air pressure within the tank.

2.2 SELF-CONFINEMENT TESTS

In connection with recent tests to determine whether critical masses are exceeded in pyrotechnic processing equipment[3, 4], studies have been performed to determine whether reaction kinetics can be deduced from internal measurements of temperature or pressure in a reacting mass of material. The aim of experimentation is to determine whether the reaction front velocity increases within a material as the reaction proceeds, and whether extrapolation of these rate measurements will indicate whether a critical mass is expected. Critical mass tests have been performed with the experimental configuration shown in figure 2.

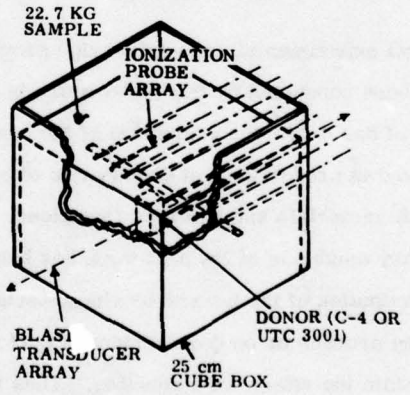


Figure 2. Configuration for Critical Mass Test

A thin plywood or fiberboard box containing 22.7 kg of pyrotechnic material is ignited either thermally or explosively by a small charge placed in the center. Carbon resistor pressure probes [3] and capacitive discharge ionization probes have been used in the internal arrays to determine velocity of the reaction front, and external

blast pressure gauges measure gross residual blast overpressure due to material detonation.

The critical mass test setup is of interest since confinement is a critical parameter in the experiment. For the cases studied, the container affords negligible resistance, and confinement in these experiments is postulated to be due entirely to the mass of material. From the standpoint of the reaction, the charge to volume ratio of these tests is equal to the material density. However, if effects on the surroundings are of primary interest, the charge to volume factor could be considered equal to zero since the mass of material reacts in free field.

2.3 PARTIAL CONFINEMENT TESTS

Reactions under conditions of partial confinement have been observed in two situations:

(a) Ignition tests of smoke materials in a large-scale blending operation

(b) Suppressive shielding tests

As part of a program to evaluate the hazards involved in the use of the Jet Airmix process for blending pyrotechnic materials, large scale burn tests were performed in partially closed containers, as shown in figure 3. Violet smoke mix (227 kg) was burned in this apparatus, the charge/volume ratio of which was 1050 kg/M^3. The fixture is vented by two 10.2 cm diameter holes and the area vent ratio is 8.0 x 10^{-3} cm^2/cm^2. A burn test was also performed in the full scale Jet Airmix simulator, figure 4, using 454 kg of violet smoke material. In this case the charge/volume ratio was 258 kg/M^3 and the vent ratio was 9.6 x 10^{-4} cm^2/cm^2. The burn rates from these

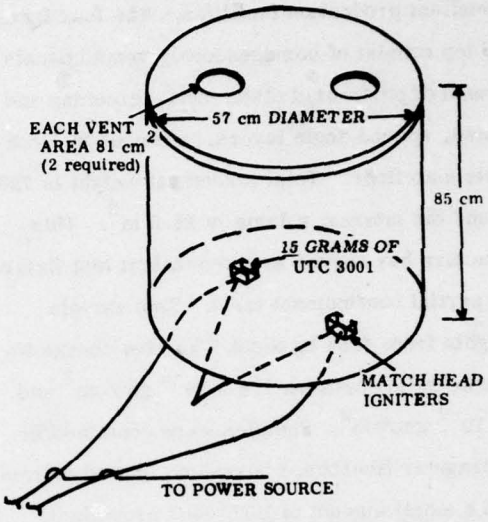


Figure 3. Thermal Initiation Test, Violet Smoke Mix

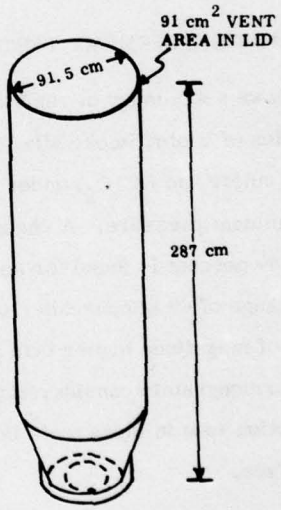


Figure 4. Full Scale Jet Airmix Simulator

experiments were compared to that for violet smoke in an open-air trough, the "vent ratio" afforded by the open top being 0.42 cm^2/cm^2.

The Group V suppressive shield [5] is a 3m x 3m x 3m enclosed steel structure, designed to protect equipment and personnel in pyrotechnic and

propellant production facilities. The four faces and top consist of homogeneously vented panels formed of perforated plate, wire screening and nested, spaced angle layers, anchored to a concrete slab floor. Total structural weight is 7250 kg and the internal volume is 28.3 m^3. This structure has served as a convenient test fixture for partial confinement tests. Test sample weights from 4.54 kg to 22.7 kg give charge to volume ratios between 1.6×10^{-4} gm/cm^3 and 8×10^{-4} gm/cm^3. Samples were contained in rectangular fiberboard boxes and ignited thermally with a small amount of UTC 3001 propellant. Similar tests were conducted in free field.

3. RESULTS

3.1 TOTAL CONFINEMENT TESTS

Figure 5 shows a summary of results using 50 gram samples of Violet Smoke Mix IV (active ingredients sulfur and $KClO_3$) under varying conditions of ambient pressure. A change in heat of reaction of 40 percent is found for an ambient pressure change of 69 kilopascals (10 psi), which is an order of magnitude higher than predictions based on thermodynamic considerations. The overall reaction rate in these tests is on the order of 0.003 kg/sec.

3.2 SELF-CONFINEMENT TESTS

Test results for 22.7 kg quantities of a 45 percent magnesium/55 percent sodium nitrate illuminant composition are given in table 1. In the case of thermal ignition using a small quantity of UTC 3001 propellant a moderate burning rate was observed, and there was no indication that the reaction rate increased as the reaction front

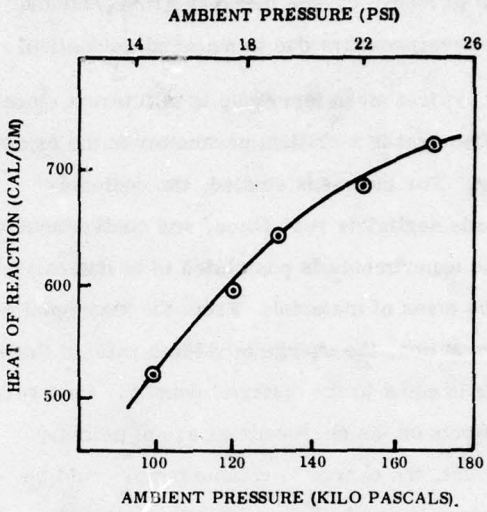


Figure 5. Bomb Calorimeter Results

Table 1. Self-Confinement Tests on 22.7 kg Quantities of $Mg/NaNO_3$ Mixture

INITIATION SOURCE	THERMAL (UTC 3001)	EXPLOSIVE (C-4)
HE EQUIVALENCY (PERCENT)	<3	48 ± 4
MAXIMUM FIREBALL DIAM. (M)	12.2	13.7
TIME TO MAXIMUM FIREBALL (SEC)	0.55	0.23
TOTAL REACTION TIME (SEC)	2.4	0.9
RADIANT HEAT FLUX AT 2.5 METERS (cal/cm^2 sec.)	14.1	---
INTERNAL REACTION VEL. (M/SEC)	50 ± 20	600
GROSS REACTION RATE (Kg/SEC)	9.5	25

diameter expanded. The gross reaction rate of 9.5 kg/second agrees well with other experiments to be discussed in a subsequent paragraph.

Conversely, the mixture when ignited with a small explosive charge showed evidence of a supersonic reaction front velocity with resultant high explosive equivalency of about 50 percent by weight. The gross reaction rate was approximately three times that of a normal deflagration.

3.3 PARTIAL CONFINEMENT TESTS

Gross reaction rate data for both the free field and suppressive shield tests using thermally initiated $Mg/NaNO_3$ illuminant are shown in figure 6. The increasing reaction rate with charge size in the free field case probably shows the effect of self-confinement by the reacting mass, and a dramatic four-fold increase in the reaction rate is observed when the reacting medium is partially confined within the suppressive shield. In fact, the rate of reaction for thermally initiated 22.7 kg charges in this experiment is nearly double that observed for the high order detonation given in table 1. A potentially catastrophic (i.e., high order detonation) reaction could thus be postulated for thermally initiated material under confinement conditions approached by these vented enclosure tests.

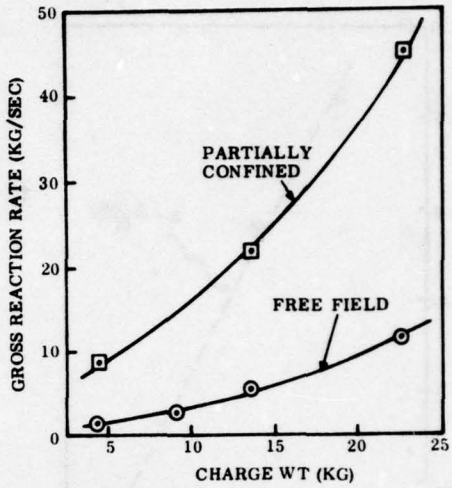


Figure 6. Reaction Rates of $Mg/NaNO_3$ Under Conditions of Partial Confinement

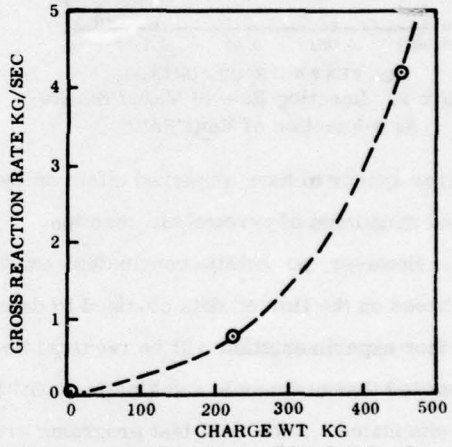


Figure 7. Reaction Rate of Violet Smoke as a Function of Charge Weight

Figure 7 shows the burning rate for violet smoke mix as a function of charge weight. The same type variation, i.e., an increasing function as the charge increases, is obtained as in the case of the $Mg/NaNO_3$ mixtures, although the overall reaction rate is much lower. Again, the possibly asymptotic increase in reaction rate would indicate caution with regard to the use of very large quantities of this material in a manufacturing or storage situation. Any direct conclusions here are hampered by the fact that the vent characteristics in these experiments varied considerably. Figure 8 shows the reaction rate data plotted as a function of container venting ratio, which function fits a simple hyperbolic equation. It is noted that these tests simulate the worst possible operational situation, i.e., larger charges were burned in containers with smaller venting. Further tests will be required to isolate the two effects.

4. POSTSCRIPT

Confinement by process containers or facility

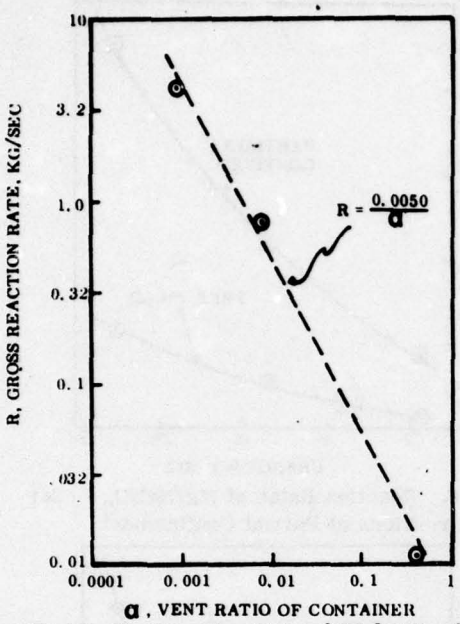


Figure 8. Reaction Rate of Violet Smoke *as a Function of Vent Ratio*

structures appear to have a marked effect on the form and magnitude of pyrotechnic reaction energy. However, no definite conclusions can be drawn based on the limited data obtained to date, and further experimentation will be required before detailed thermodynamic and kinetic quantities can be elucidated. Additional test programs are currently being conducted in unvented, homogeneously vented and nonhomogeneously vented structural entities, from which the compatibility of pyrotechnic materials with surrounding enclosures may be determined.

REFERENCES

1. Edgewood Arsenal Contractor Report, EM-CR-75017, Compilation and Preliminary Analysis of Sensitivity Data for Pyrotechnics, R. E. Schmidt, A. Dabul, and F. L. McIntyre, August 1975.

2. Edgewood Arsenal Technical Report, in preparation, Bomb Calorimetry for Evaluation of Pyrotechnic Materials, G. L. McKown and K. Nimitz.

3. Edgewood Arsenal Contractor Report, EM-CR-75001, Identification and Evaluation of Hazards Associated with Blending of HC White Smoke Mix by Jet Airmix Process, F. L. McIntyre, January 1974.

4. Edgewood Arsenal Contractor Report, EM-CR-75001, Identification and Evaluation of Hazards Associated with Blending of Violet Smoke Mix by Jet Airmix Process, F. L. McIntyre, March 1974.

5. Edgewood Arsenal Technical Report, EM-TR-76001, Category 5 Suppressive Shield Test Report, D. M. Koger and G. L. McKown, October 1975.

TRENDS IN ELECTROSTATIC PRECAUTIONS IN FILLING FACTORIES

D P Donegan,
Royal Ordnance Factory,
Chorley, Lancashire
England

Précis

A brief history is given of the various techniques employed to reduce potentials achieved due to electrostatic charge generation in explosives environments, leading up to current practice where, for work on electrically sensitive primary explosives, atmospheric humidification and the use of antistatic materials are mandatory in UK.

The electrostatic behaviour of explosives powders is reviewed, and the concepts of "electrostatically safe explosives" and "electrostatically safe quantity of explosives" are introduced. These concepts are used to define locations where the introduction of atmospheric humidification would reduce hazard. An analysis of data on charge generation during the transfer of primary explosives powder under various atmospheric conditions is employed to derive minimum safe levels of humidity at various temperatures.

The effect of the capacitances of explosives containers, etc, is considered, and a case is presented for the use of a mixed conducting/insulating environment, rather than a totally conducting environment, using insulating containers and tools of relative low effective capacitance.

Note

The views presented in this paper are those of the author, and do not represent the official position in UK. They are proposed to stimulate interest in techniques for reduction of electrostatic charge in explosives environments with the aim of establishing precautionary practice on sound scientific bases.

LIST OF CONTENTS

1. INTRODUCTION

2. HISTORY

3. CURRENT PRACTICE

   3.1 Earthing of plant, etc
   3.2 Earthing of production tools
   3.3 Earthing of operatives
   3.4 Other earthing precautions
   3.5 Atmospheric humidification

4. HAZARD REAPPRAISAL

   4.1 Background
   4.2 Operatives
   4.3 Acceptable circuit breaks
   4.4 Humidification

5. THE ALTERNATIVE ENVIRONMENT

   5.1 Non-conducting items
   5.2 Humidity

6. ACKNOWLEDGEMENTS

APPENDICES

1. References indicating the scope of work on and control precautions for the undesirable properties of electrostatic charges since 1930.

2. Electrostatic charges associated with operatives.

3. Analysis of data on electrostatic charges generated during the pouring of primary explosives powders under various conditions of atmospheric humidity and temperature.

4. Practical considerations in atmospheric humidification practice.

1. INTRODUCTION

In the last 10 years, standardised precautions against electrostatic hazards brought in in the early 1960's have been tested under practical production conditions, and application problems and residual hazards have crystallised.

This paper has been assembled on the basis of a new look at electrostatic hazards, necessitated by a need to reconsider the areas in which atmospheric humidification should be applied and to relate permissible humidity levels to atmospheric temperature. The hazard review has thrown new light on the fully conducting environment used for work on electrically sensitive explosives materials and explosives stores, and suggests that established practice may be responsible for new hazards. An alternative environment containing non-conducting items is proposed for consideration.

Although there has been improvement in lightning protection practice, current standards closely follow trends in US and elsewhere, and have therefore not been included.

2. HISTORY

Electrostatic hazards associated with explosives were recognised in the 18th century, when lightning protection was first considered. Hazards due to electrostatic charge generation on plant, personnel and explosives powders were appreciated during the 1914-1918 war, but the only precautions in general use up to the 1930's were the use of lightning protection, the earthing of metal plant and furniture and artificial humidification of the atmosphere.

Appendix 1 is a list of related references since 1930. The studies seem to have been sponsored mainly by textiles institutes and national safety authorities.

Antistatic footwear and flooring became available in Europe in about 1938, but the use of these was introduced in hospitals, research laboratories and non-explosives establishments before they were generally adopted for explosives work: application in areas handling sensitive explosives powders and stores did not become mandatory in UK until the early 1960's.

3. CURRENT PRACTICE

3.1 Earthing of Plant, etc

240-V electrical supplies in explosives buildings are carried in conduit which is assembled to high standards to give complete enclosure of wiring or metal sheathing and good continuity earthing.

All metal plant, furniture and similar items are connected to the building earthing tape: the principle is extended to quite small items such as weighing scales.

Where conducting floors are installed, a matrix of tape, bonded to the building earthing system, is first laid in the installation area.

Workbenches are often covered with conducting working surfaces (generally conducting rubber) laid on a metal matrix bonded to the earthing network.

3.2 Earthing of production tools

Although some production tools such as detonator tweezers are still made from wood, there has been a definite trend in the last 10 years towards the use of conducting plastics and conducting rubber. This trend has permitted the use of metal scoops and scrapers etc, metal-to-metal nip and friction hazard being avoided by the use of coatings or coverings of non-metallic conductors. Items manufactured from non-metallic conducting materials now include "jelly mould" mixer bowls, initiator pots, detonator trays and detonator wallets. Earthing is achieved by metal bonding for fixed items such as mixers or by the use of conducting working surfaces for portable items.

3.3 Earthing of operatives

The hazards presented by operatives are considered in Appendix 2, showing that an electrically isolated worker represents a capacitance to earth of 500 picofarads capable of releasing an electrostatic spark discharge of about 0.02 joules.

For explosives materials and items where the minimum ignition energy exceeds this value, earthing of operatives is not considered necessary.

The earthing standards applied for workers on more sensitive materials and filled stores were introduced when portable electric tools were virtually unknown and the total enclosure of electrics for dust-tightness or flameproofing made electric shock risk unlikely. It was therefore possible to employ an environment in which, tested under standard conditions, flooring had a resistance less than 50,000 ohms and footwear a resistance of less than 150,000 ohms. The test criterion applied to operatives in such an environment is a maximum resistance of 10° ohms measured from the hand to earth when the worker is standing on a representative section of the conducting flooring.

Portable electric tools, introduced since the 1960's, are operated by low-voltage supplies to eliminate electric shock risk.

3.4 Other earthing precautions

Most processes in which powder is transferred are carried out under earthed conditions. As an example, donor and receptor powder cans are earthed before transfer of material from the one to the other.

There has also been a trend to the use of conducting rubber or conducting plastic hoses where powders are dried by passage of dry air through a container, or in vacuum cleaning facilities.

3.5 Atmospheric Humidification

Atmospheric humidification is used to reduce electrostatic potentials generated during the transfer of electrically sensitive primary explosives powders. Until very recently the standard employed was an environment in the range 65% to 75% RH, but recent work has resulted in the introduction of minimum permissible humidity values dependent on air temperature in accordance with the following table:-

Temperature ^{o}C	15	20	25	30	35	40
Minimum permissible humidity level %RH	70	65	61	57	54	52

An upper limit of 75% is applied for practical applicability and comfort.

Humidification is generally restricted to explosives materials having a minimum ignition energy less than 0.02 joules; experience over 10 years has shown a negligible ignition frequency due to electrostatic discharge where humidification is not applied.

4. HAZARD REAPPRAISAL

4.1 Background

Since the mid 1960's, trials at ERDE Waltham Abbey were sponsored by Royal Ordnance Factory Chorley with the aim of relating safe values of atmospheric humidity to air temperature and to the type of process being undertaken. The results of some of the trials are reported in reference 33.

The ERDE data is analysed in Appendix 3. The chief findings are

(a) Lead styphnate generates more electrostatic charge per gram poured than other primary explosives tested. Since under certain discharge conditions lead styphnate is the most electrically sensitive powder in general use, it can be used as a basis for the establishment of safe working conditions.

(b) The electrostatic potential generated during transfer of m grams of lead styphnate is not likely to exceed the value given by the equation

$$v = m(95.4 - 0.778h - 0.663T) \text{ volts},$$

where h is the percentage relative humidity and T is the atmospheric temperature in degrees C.

(c) Up to about 1.7 grams of lead styphnate can be poured without significant risk of ignition due to electrostatic discharge. The figure includes substantial safety factors and could be appreciably increased for less sensitive explosives powders.

This finding introduces the concept of a "safe pouring quantity" of explosives powder.

(d) It is safe to transfer ¼lb (113 grams) of explosives powder under any atmospheric conditions of air temperature and relative humidity likely to be encountered in practice provided that the minimum ignition energy of the material exceeds about 1400 microjoules.

(e) Electrostatic potentials generated during the pouring of lead styphnate could be as high as 7.5KV under cold and dry atmospheric conditions.

It should be noted that the pouring of only a few grams of lead styphnate can be sufficient to generate hazardous potentials even at 75% RH, so that the imposition of artificial humidification gives no guarantee that ignitions will be eliminated or even significantly reduced in frequency. In addition, the application of the fully conducting environment outlined in section 3 above provides excellent earth paths for the discharge.

The fact that there have been no ignitions during the transfer of explosives powders of minimum ignition energy exceeds 0.02 joules in areas where artificial humidification is not applied suggests that humidification is not necessary for such materials.

4.2 Operatives

Appendix 2 shows that the operative in a fully-conducting environment could be a capacitance of about 1000 picofarads charged to perhaps 5 microjoules.

The table below lists some primary explosives which could be ignited by a spark discharge of this order.

Name of Material	Reference Number	Minimum ignition energy, Microjoules	Remarks
Normal lead styphnate	RD 1367	Less than 0.3	Conducting rubber/metal electrodes. Associated capacitance not known.
Service lead azide		2	Metal/metal electrodes. Capacitance 400 picofarads
Silver azide	RD 1336	2.5	Metal/metal electrodes. Capacitance 500 picofarads
Lead azide	RD 1343	2.5	Metal/metal electrodes. Capacitance 500 picofarads
Monobasic lead 4:6 dinitroresorcinate	RD 1353	4	Conducting rubber/metal electrodes. Capacitance 150 picofarads.
Monobasic lead styphnate	RD 1346	4.5	Metal/metal electrodes. Capacitance 8 picofarads

Although conducting bracelets connected to an earth point by a flexible connector have been introduced to minimise this hazard in certain processes, there are objections with loose powder because of nip and friction hazards, and in fine work they result in unacceptable restrictions of movement.

4.3 Acceptable circuit breaks

One technique to avoid igniferous electrostatic discharges is to include a high resistance in the earth path. The high resistance object could itself be a potential source of electrostatic charge, so that some limitation in size and shape is necessary to ensure that the energy available is not hazardous.

Experience at ROF Chorley suggests that most of the small containers and tools used for initiator work would be too small to generate a hazardous electrostatic charge if manufactured from non-conducting material, and consideration is being given to the use of a material which has only a low surface charge density. The items would all be hand tools such as scoops, scoop tappers, detonator trays, detonator wallets, tweezers.

Because of the quantity of powder involved, there is no proposal at present to use non-conducting initiator pots, although trials could show that the possibility of an igniferous spark might be reduced if these were introduced.

The use of these small non-conducting tools and containers would introduce acceptable circuit breaks into the fully conducting environment. A charged operative, for example, could not discharge through non-conducting tweezers to a detonator sitting in a non-conducting wallet standing on an earthed conducting working surface.

4.4 Humidification

Atmospheric humidification is considered from a practical point of view in Appendix 4. This uses the formula of 4.1 (b) above,

$$v = m(95.4 - 0.778h - 0.663T) \text{ volts}$$

and known safe values of 65% RH, 16°C to derive a formula for minimum permissible relative humidity:-

$$h = 77.8 - 0.80T$$

It is possible that the base 65% RH at 16° may be unnecessarily restrictive, when a more relaxed formula for h could be applied.

SUMMARY

5. THE ALTERNATIVE ENVIRONMENT

5.1 Non-conducting items

The introduction of safe non-conducting tools and containers will result in "acceptable circuit breaks" in an otherwise fully-conducting environment, reducing earth leakage paths and therefore reducing the chance of ignition caused by discharge of electrostatic energy from powder during transfer or from an operative.

5.2 Humidity

Humidification will not be necessary in the following areas:-

a. Locations where only wet explosives are handled.

b. Storage locations where the explosives powders remain in closed containers, unless humidification is necessary for maintenance of moisture content.

c. Locations where the operations involve transfer of less than the "safe pouring quantity" of explosives powder (eg scoop filling) (Appendix 3 section 6).

d. Locations where the minimum ignition energy of the explosives powder exceeds about 0.02 joules.

Where humidification is applied, practical minimum permissible humidity levels for lead styphnate are given by the formula

$$h = 77.8 - 0.80T \quad \%RH$$

where T is the atmospheric temperature in degrees C (Appendix 4). This equation gives the table

Temperature ^{o}C	10	15	20	25	30
Minimum permissible humidity level % RH	69.8	65.8	61.8	57.8	53.8

More detailed work on the potentials generated during the pouring of primary explosives powders might permit significant reduction in these humidity values.

Lower humidity levels may be safe with explosives materials and less sensitive than lead styphnate.

6. ACKNOWLEDGEMENTS

The author is very grateful to the staff of ERDE, Waltham Abbey, England for permission to use reference 33 and for the data on minimum ignition energies reproduced in the table in section 4.2.

APPENDIX 1

LIST OF REFERENCES INDICATING THE SCOPE OF WORK ON AND CONTROL PRECAUTIONS FOR THE UNDESIRABLE PROPERTIES OF ELECTROSTATIC CHARGES SINCE 1930

1. "Electrification and the electrical conductivity of wool", S G Barker, British Research Association for the Woollen and Worsted Industry, No 133, June 1930.

   Suggests a "series" in which textile materials could be placed in order, in accordance with the case with which they are electrified. Recommends artificial humidification as a means of reducing charge accumulation.

2. "The ignition of firedamp-air mixture by sparks produced by the self-electrification of coal dust". S C Blacktin and H Robinson, Safety in Mines Research Board, Buxton, paper No 71 March 1931.

   Indicates that static charges can be dissipated through quite high resistance leakage paths (about 2 megohms) and suggests that multiple-point "static dischargers" are therefore often sufficient to minimise ignition risks.

3. "Electrification of dust particles by air blast", U Nakaya and T Terada, Phil Mag No 124, 115 123, January 1935.

   The microscopic method of measuring the charge of individual dust particles is described. The report suggests that although particles in an air stream would have a net charge as a cloud with respect to earth, some of the individual particles will be of opposite charge.

4. "Report of Committee on static electricity". National Fire Protection Association, 41st Annual Meeting, Chicago, May 10-14 1937.

   Surveyed many instances in industry of hazard due to the accumulation of electrostatic charge. Recommended artificial humidification (50% to 75% RH), the use of comb point dischargers for conveyor belts, the use of "static neutralisers" (pointed electrodes charged to a high alternating potential) and earthing wires for the use of personnel.

5. "Origin of static electricity on the surfaces of solid dielectrics". J Strachan, "Nature" No 3523, Vol 139, May 1937.

   A letter to "Nature" reporting the detection of charges on the surfaces of two sheets of the same insulating material after having been forced in contact under pressure.

6. "Frictional electricity in buildings, specially considering ignition sparks in hazardous workshops and storage places" (in German). W. Starck and H Gross - July 1937.

Various cases are mentioned in which electrostatic charges of persons and metallic objects caused spark discharges. Potential of 6000 to 7000 volts were measured on patients in hospitals, and potentials of up to 14,000 volts were detected under dry conditions on persons walking on woollen carpeting in a centrally heated Berlin dwelling. The increased incidence of electrostatic phenomena in the lower humidity conditions prevailing in winter were observed. Recommendations for the reduction of undesired electrostatic charges including earthing of plant and equipment, the earthing of metal parts of wooden utensils, the installation of electrical switchgear, control gear, lighting and motors outside hazardous rooms, the use of conducting floors and artificial humidification.

7. "Static Electricity in industry". E S Hodges, "Electrical Times", page 683, 18 November 1937.

   Discusses the reduction of electrostatic charges on paper, mainly in the printing trade. Methods suggested include discharge points mounted near the paper surface, ionisation of neighbouring air by the flames of gas jets and the use of pointed electrodes connected to a high-voltage alternating source.

8. "The risk of explosion due to electrification in operating theatres of hospitals". E H Rayner, National Physical Laboratory; The Institute of Electrical Engineers, the "Electrical Review", March 1938.

   A very thorough treatise introducing conducting flooring, both of metal and of conducting rubber, which had only become available at about that time. The capacitance of a man in parallel with a trolley carrying anaesthetic equipment was quoted as 500 picofarads: this value is now used as the average capacitance of an operative in Filling Factories. Reduction of hazards at atmospheric humidities of about 65% RH was mentioned.

   In discussion on this paper the use of conducting tyres for trolley buses was mentioned by a Mr H W Swann of the Home Office.

9. "Electrically conducting rubber; a new material with extensive safety uses". The Electrical Review, 3 June 1938.

   Reviews the properties of conducting rubber, which had recently become available.

10. "Static electricity in nature and industry", US Department of Commerce, Bureau of Mines, Bulletin 368, 1939.

    Gives a comprehensive review of the history and of the investigations carried out on electrification, and a detailed account of industrial hazards and safeguards. The precautions include notes on lightning conductors, earthing and humidification.

11. "Static Risks in Ordnance Factories" WDE Thomas and A R Ubbelohde, Ministry of Supply ARD Report 390/43 November 1943.

Mainly deals with sensitive initiatory powders. Suggests the use of radioactive isotapes and artificial humidification as means of control.

12. "The static hazard in industry". G Morris, "Engineering", July 1947 page 49.

13. "Static electricity and explosives". R E Stainton and J B Tindale, Process Research Department Report No 41, Royal Ordnance Factory, Chorley August 1954.

Summarises areas in Explosives Filling Factories in which accumulation of static charges causes hazard. Suggests the use of conducting additives to non-conducting explosives powders, earthing, and the measurement and maintenance of atmospheric humidity as precautionary measures.

14. "The electrostatic spark sensitivity of initiators, Part I", Moore, Sumner and Wyatt, ERDE Report No 4/R/56, 1956.

15. Ditto, Part II, ERDE Report No 5/R/56, 1956.

16. Ditto, Part III, P W J Moore, ERDE Report No 22/R/56, 1956.

17. Electrostatic hazards with initiators: notes of a meeting held at Waltham Abbey on 18 February 1958. Ministry of Supply ERDE note XR/300/61.

Page 3 recommends 60% RH as an acceptable humidity level.

18. "Electrostatic risks and precautions in processes and operations in Filling Factories". H G Ward, Ministry of Supply DOF/F Report No 64 May 1958.

19. "Method of overcoming dangers from electrostatic charges in Filling Factories". A R Ubbelohde, W D E Thomas Ministry of Supply Monograph 15/351.

Recommends 65-75% RH as a means of minimising static hazards with sensitive explosives.

20. "Specification for electrically conducting rubber flooring". BS 3187 of 1959.

21. Appendix II to Ordnance Board Proceeding Q8,858 (Special) Part I, September 1959.

22. "Standard specification for static earthing systems and the protection of structures against lightning at Royal Ordnance Factories (Filling and Explosive Groups)" Ministry of Supply DOF/E Standard Specification No EL/1, October 1959.

23. "The electrostatic spark sensitiveness of initiators, Part V, further study of ignition risk with metallic and antistatic rubber electrodes" R M H Wyatt, Ministry of Supply ERDE Report 24/R/59, October 1959.

24. The Factories Act, 1961 Part IV, Section 68, limitations of humidity.

25. "Specification for the electrical resistance of conductive and antistatic products made from flexible polymeric material". BS 2050 of 1961.

26. "Specification for antistatic rubber flooring" BS 3398 of 1961.

27. "The protection of structures against lightning for Filling and Explosives Groups" Ministry of Defence (Army Department) CROF Code of Practice No 5, May 1964.

28. "Specification for antistatic rubber footwear" BS 2506 of 1964.

29. "Specification for electrically conducting footwear" BS 3825 of 1964.

30. "Recommendations to minimise electrostatic hazards to stores containing electrically initiated explosive devices during handling, testing and assembly". (Restricted). Annexe A to Ordnance Board Proceeding 40,225, March 1965.

    Lays down requirements for conducting flooring, conducting footwear and earthing, particularly of mobile equipment.

31. "Changing to the metric system". Conversion factors, symbols and definitions," Ministry of Technology, National Physical Laboratory, 1966 reprint: HMSO 17p net.

32. Restriction of carrying primary explosives powders when the atmospheric temperature is below 320°F or when the humidity is less than 50% RH: example ROF Chorley DSO 1E 62 Part II, paragraph C, for compositions RD 1651, RD 1337 and RD1339/graphite.

33. ERDE Offprint 24, February 1972: The effect of temperature and relative humidity on the accumulation of electrostatic charges and primary explosives, by A C Cleves, J F Sumner and R M H Wyatt.

APPENDIX 2

ELECTROSTATIC CHARGES ASSOCIATED WITH OPERATIVES

1. INSULATING ENVIRONMENT

The human body is usually regarded as having an effective capacitance to earth of 500 picofarads in an insulating environment.

Earth leakage resistance is mainly via perspiration and humid footwear, and tends to be very high. Values over 10 megohms are common. Under these conditions the electrostatic potentials which can be generated may be as high as 9 KV in UK.

The stored electrostatic energy is given by

$$E = \tfrac{1}{2} CV^2 \text{ joules},$$

where C is the capacitance in farads and V is the charge potential in volts. Substituting values,

$$E = \tfrac{1}{2} 500 \times 10^{-12} \times (9 \times 10^3)^2$$

$$= \underline{0.02 \text{ joules}}$$

2. CONDUCTING ENVIRONMENT

The use of conducting footwear and flooring can give an effective increase in the body capacitance to earth, and it is possible that values in the order of 1000 picofarads could be achieved.

The residual resistance of the operative to earth in a conducting environment means that electrostatic potentials on the body are not completely eliminated. Work by ERDE and other researchers supports the view that the maximum electrostatic potential which can be generated is not likely to exceed 100 volts: indeed, the "maximum probable" value is in the order of 50 volts.

Using C = 1000 picofarads and V = 100 volts, the stored energy is

$$E = \tfrac{1}{2}(1000 \times 10^{-12}) \times (100)^2 \text{ joules}$$

$$= \underline{5 \text{ microjoules}}$$

APPENDIX 3

ANALYSIS OF DATA ON ELECTROSTATIC CHARGES GENERATED DURING THE POURING OF PRIMARY EXPLOSIVES UNDER VARIOUS CONDITIONS OF ATMOSPHERIC HUMIDITY AND TEMPERATURE

LIST OF CONTENTS

1. BACKGROUND THEORY.

2. ESTIMATION OF POTENTIAL GENERATED BASED ON ERDE 0.4 GRAM POUR.

3. ESTIMATION OF POTENTIAL GENERATED BASED ON ERDE 28 GRAM POUR.

4. CONCLUSIONS:

   RELATION OF POTENTIAL GENERATED TO MASS POURED, HUMIDITY AND TEMPERATURE

5. SAFE ELECTROSTATIC POTENTIALS FOR LEAD STYPHNATE.

6. SAFE POURING QUANTITIES FOR LEAD STYPHNATE.

7. NOTE ON "SAFE" EXPLOSIVES POWDERS.

1. BACKGROUND THEORY

The Langmuir adsorption isotherm theory suggests that

$$v = A - Bh - CT \text{ volts},$$

where v is the electrostatic potential which can be generated during transfer of a powder, h is % RH, T is atmospheric and powder temperature, and A, B and C are constants.

The analyses below assume that the electrostatic potential generated is also proportional to the quantity of powder transferred. In practice, this seems to be true with fairly small quantities of powder where the time required for pouring is short; for larger quantities, charge generated at the beginning of the pour is being lost from the poured powder at a significant rate by the end of the pour, so that the actual potential generated is less than that calculated on the basis of proportional dependence. A comparison of derived data included in the work below suggests that the proportional dependence assumption gives results over 50% too high for potentials generated when ¼ lb of lead styphnate is poured. Action levels based on the forecast potentials therefore contain an inherent safety factor.

It is also evident that the electrostatic potential generated is some function of the capacitance to earth of the equivalent electrical circuit of the pouring apparatus. Insufficient is known about the relationship between potential and capacitance to be able to take capacitance properly into account in the considerations below: the assumptions made, however, always err towards a forecast potential higher than that which would be expected in practice, thereby improving the inherent safety factor.

2. ESTIMATION OF POTENTIAL GENERATED BASED ON ERDE 0.4 GRAM POUR

The ERDE note of reference 33 gives, in Fig 5 on page 231, a graph showing the variation of potential on pouring 0.4 grams of lead styphnate into an apparatus whose capacitance to earth is 420 picofarads, under various conditions of humidity and temperature.

Mathematical analysis of this graph on the basis of the Langmuir relationship gives

$$v = 38.15 - 0.311h - 0.249T, \qquad (A)$$

a relation which fits the graphs closely for temperatures up to over 30°C.

This equation can be used to forecast the electrostatic potential generated on 0.4 grams of lead styphnate poured into a 420-pf apparatus at any values of h and T.

An estimate of the electrostatic potential generated when other quantities are poured can be made on the basis of proportional dependency:-

$$0.4 \text{ grams generate } v \text{ volts}$$
$$\text{hence m grams generate } \frac{vm}{0.4} = 2.5\ vm \text{ volts}$$

The relation for m grams of lead styphnate corresponding to equation A is therefore:-

$$v = 2.5\ (38.15 - 0.311h - 0.249T)\ m$$
$$= m\ (95.38 - 0.7775h - 0.6225T) \text{ volts} \qquad (B)$$

applicable for a related capacitance of 420 picofarads.

3. ESTIMATION OF POTENTIAL GENERATED BASED ON ERDE 28-GRAM POUR

The bulk pouring trials reported in reference 33 were carried out using barium styphnate for safety reasons. Page 2 of the reference gives Table 2 as follows:

28 grams of barium styphnate poured:
associated capacitance 50 picofarads

Temperature °C	% RH	Potential generated v
13	65	250
15	60	200
21	44	200
27	36	300
28	36	300
24	75	250

Unfortunately, these results are insufficiently distributed to give reliable graphs of v against h at various temperatures. Application of the data in the Langmuir relation has, however, been attempted, and it has been found that a very approximate relation can be developed as follows:

$$v = 793 - 6.41h - 9.7T \text{ volts} \qquad (C)$$

This equation gives values of potential equal to or higher than those in the table above, ie it errs in the direction of safety.

Applying proportional relation to convert from 28 grams to m grams,

$$v = \frac{m}{28} (793 - 6.41h - 9.7T)$$

$$- m (28.3 - 0.229h - 0.346T) \text{ volts} \qquad (D)$$

applicable for a related value of 50 picofarads.

4. CONCLUSIONS:

RELATION OF POTENTIAL GENERATED TO MASS POURED, HUMIDITY AND TEMPERATURE

The only correlation between the barium styphnate and lead styphnate data in reference 33 is the following sentence on page 230:-

"Similar results were found for lead azide and barium styphnate except that the voltages obtained at 65% relative humidity and 20°C were roughly one tenth and one third that for lead styphnate respectively".

Substituting m = 0.4 grams, h = 65% and T = 20° in equation D,

v for barium styphnate

= 0.4 (28.3 - 0.229 x 65 - 0.346 x 20)

= 0.4 x 6.495

= 2.6 volts (A graphical estimate from a plot of the table in section 3 above gives 2.5 volts).

Equation A for 0.4 grams of lead styphnate gives, with h = 65% and T = 20°,

$$v = 38.15 - 0.311 \times 65 - 0.249 \times 20$$

$$= 13 \text{ volts}$$

It will be noted that the latter figure is much more than three times the figure calculated from the bulk barium styphnate pour. Use of equation B thus contains a considerable safety factor, and in using this equation the effect of related capacitance can be ignored up to 420 picofarads.

5. SAFE ELECTROSTATIC POTENTIALS FOR LEAD STYPHNATE

Lead styphnate can be regarded as having a minimum ignition energy of 0.3 microjoules (for discharge sparks between conducting rubber and metal electrodes).

The energy stored on a capacitance of C farads charged to a potential difference of V volts is

$$E = \tfrac{1}{2} CV^2 \text{ joules}$$

Using C = 50 picofarads and E = 0.3 microjoules,

$$0.3 \times 10^{-6} = \tfrac{1}{2} (50 \times 10^{-12}) V^2$$

$$\text{whence } V^2 = \frac{2 \times 0.3 \times 10^6}{50} = 12{,}000$$

and V is approximately 110 volts

A capacitance of 50 picofarads charged to less than 110 volts is thus unlikely to cause an ignition of lead styphnate by spark discharge. The "safe electrostatic potential" value would be proportionately lower for larger capacitances.

6. SAFE POURING QUANTITIES FOR LEAD STYPHNATE

Assuming a protective system could be employed in which the maximum stray capacitance likely to be encountered was 50 picofarads, the maximum electrostatic potential which would be tolerated would be 110 volts from Section 5.

Using equation B

$$110 = m(95.38 - 0.7775h - 0.6225T)$$

whence the safe pouring quantity m grams can be derived:

$$m = \frac{110}{95.38 - 0.7775h - 0.6225T}$$

The worst likely atmospheric conditions in practice would be h - 30% RH and T = 10°C; substituting these values,

$$m = \frac{110}{95.38 - 0.7775 \times 30 - 0.6225 \times 10}$$

$$= \frac{110}{65.83} = \underline{1.67 \text{ grams}}$$

7. NOTE ON "SAFE" EXPLOSIVES POWDERS

A "safe" explosives powder could be defined as one which is not likely to generate its minimum ignition energy when ¼ lb is poured.

Equation B gives

$$v = m\,(95.38 - 0.7775h - 0.6225T)$$

Substituting m - 113.5 grams (¼ lb) and the worst likely atmospheric conditions h = 30% RH and T = 10°C, the maximum voltage likely to be generated in practice is given by

$$\begin{aligned} v &= 113.5\,(95.38 - 0.7775 \times 30 - 0.6225 \times 10) \\ &= 113.5\,(65.83) \\ &= 7472 \text{ volts,} \end{aligned}$$

a value which errs considerably in the direction of safety.

Assuming a related capacitance of 50 picofarads,

$$\begin{aligned} E &= \tfrac{1}{2}\,CV^2 \\ &= \tfrac{1}{2}\,(50 \times 10^{-12})\,(7472)^2 \text{ joules} \\ &= 1400 \text{ microjoules} \end{aligned}$$

An explosives powder whose minimum ignition energy is 1400 microjoules or more is therefore unlikely to ignite due to electrostatic energy generated when ¼ lb is poured under any conditions of humidity and temperature likely to be encountered in practice, provided that the related capacitance is 50 picofarads or less.

APPENDIX 4

PRACTICAL CONSIDERATIONS IN ATMOSPHERIC HUMIDIFICATION PRACTICE

1. "SAFE" POINT OF HUMIDITY AND TEMPERATURE

Conditions currently applied permit carriage of certain primary explosives only at temperatures above 0°C and humidities above 50% RH (reference 32).

Until recently, workshop practice for operations on primary explosives was to set the humidity in the range 65% to 75% RH regardless of temperature: work could, and occasionally does, carry on down to about 10°C (50°F).

In the light of these practices and the low incidence of electrostatic ignitions over many years, it would seem reasonable to regard a minimum humidity of 65% RH at a shop temperature of 16°C (60.8°F) as "acceptable" conditions.

2. CALCULATIONS

a. Using Equation B (Section 2 of Appendix 1), ie

$$v = m(95.38 - 0.7775h - 0.6225T) \text{ volts} \qquad (B)$$

and substituting h = 65, T = 16 from (b) above,

$$v = m(95.38 - 0.7775 \times 65 - 0.6225 \times 16) \text{ volts} \qquad (C)$$

b. Equation C may be re-substituted in equation B to result in a relation between h and T:

$$m(95.38 - 0.7775 \times 65 - 0.6225 \times 16) = m(95.38 - 0.7775h - 0.6225T)$$

whence $(0.7775 \times 65) + (0.6225 \times 16) = 0.7775h + 0.6225T$,
giving $h = 77.8 - 0.08T$

This equation gives the minimum permissible values of h for safety at various temperatures corresponding to the "acceptable" value 65% RH at 16°C.

c. The equation may therefore be employed to calculate the "minimum permissible" values of h to retain ignition frequency at its present level. A table derived from the equation is reproduced below.

Temperature °C	10	15	20	25	30
Min permissible humidity level, % RH	69.8	65.8	61.8	57.8	53.8

It should be noted that, if some lower value of atmospheric humidity could be shown to give safe working conditions at 16°C, the revised safe working point would result in relaxations of the minimum permissible humidity levels given in the table.

THE ROLES OF DEFLAGRATION AND EXPLOSIVENESS IN HAZARD ASSESSMENT

P J Hubbard and P R Lee
Royal Armament Research and Development Establishment
Royal Arsenal
Woolwich, UK

1. INTRODUCTION

Although the term "explosiveness" has been in use for a number of years, it can be interpreted in more than one way because of the lack of quantitative factors in its definition. It is associated with the behaviour of explosives after initiation by mechanical or thermal stimuli which are not energetic enough to initiate detonation directly. Such stimuli arise in a large proportion of accidents in which high explosives or weapons function prematurely in a non-design mode. The hazard involved is a function of the explosiveness of the system which can be very great (as Figure 1 shows) despite the fact that the explosive is deflagrating rather than detonating.

The Explosives Branch, RARDE is concerned with the causes of munition malfunctions and accidents involving high explosives in general and it was as a result of investigations into premature initiation of shell in guns that the aspects of explosiveness reviewed in this paper have been examined.

2. EXPERIMENTS RELATED TO PREMATURES

Prior to about 1965, nearly all premature initiations of shell in gun barrels were believed to have been due to fuze malfunction. Subjective assessment of the fragments recovered after a premature (Figure 2), tended to confirm the view that the fuze was the culprit. It was argued that such devastation could only have been caused by the detonation of the filling and at the time it was considered that this could only have been caused by the fuze. Filling defects were not regarded as important, since simple calculations showed that the shocks resulting from firing were insufficient to initiate detonation of the main filling or booster charge independently of the fuze. However, when shells were deliberately detonated in gun barrels, both statically and dynamically, some via the fuze and booster and some by means of a demolition detonator placed at various positions in the shell filling, the damage and nature of the fragments were different both macroscopically and microscopically from those recovered after premature events. The main differences were that detonation produced a zone of scabbing around the barrel (Figure 3) and the shell fragments exhibit shear failure, (Figure 5) whereas the result of a shattering in-bore event is petalling of the gun barrel (see Figures 2 and 4) and the shell fragments show evidence of brittle fracture on the edges (see Figure 5). Fuze involvement was finally eliminated when overseas experience of prematures in unfuzed shell was reported.

PRECEDING PAGE BLANK-NOT FILMED

Alternative mechanisms were therefore examined experimentally on the basis that a deflagration could have occurred after initiation either as a result of adiabatic heating of air compressed within a cavity at the explosive-shell liner interface or by intrusion of hard, gritty particles into the explosive. Deflagrations were initiated in shell confined in gun barrels by means of hot wires embedded at the base of the filling. Shell ignited in this manner deflagrated violently, producing fragment and damage patterns identical with those obtained in premature events (Figure 6).

A study was also begun to examine the sensitiveness of shell fillings to stimuli similar to those they would experience on firing. The equipment used is known as the vertical activator and its test assembly is shown diagrammatically in Figure 7. Small pellets (12.7 x 12.7mm) of explosive are subjected to the effects of adiabatically compressed air cavities or the rapid ingress of grit, or both, followed by confinement resulting from the impact of the movable punch driven by a falling 10 kg weight. The events produced are deflagrations, for, despite the heavy confinement, there is insufficient explosive present for the deflagration-detonation transition to be achieved, at least for the relatively insensitive explosive compositions employed as high explosive shell fillings.

High speed cine films of the events produced show great variations in characteristics from explosive to explosive. In particular, RDX/TNT (60/40) produces a cloud of glowing reaction products whereas TNT appears to burn more slowly with much more smoke, as shown in Figure 8. These differences give an indication of the relative explosiveness of each explosive under these particular conditions of confinement.

In general explosiveness is directly related to the speed of deflagration of the explosive involved, but it is not necessarily a property of the explosive alone. Many explosives used in munitions systems cannot be ignited readily in the massive form when unconfined, and even when they do ignite they may burn quietly. The confinement not only aids ignition and propagation but also, if it is in the form of a metallic casing, provides a simple means of comparing the damaging effect of the event through the mode of failure of the casing and the size, shape and number of fragments produced.

The activator is unsuitable for measuring deflagration velocities, but the results obtained led to the design of equipment for such a purpose.

3. BURNING TUBE EXPERIMENTS

3.1 Experimental

High speed photographic studies have been made of the deflagration of various high explosives in mild steel tubes 500 mm long by 38 mm external diameter with 9 mm thick walls, as shown in Figure 9. The explosive was ignited by a hot wire in early experiments; later, however, a small propellant/fuzehead

system was used. This avoided synchronisation problems. The charges were designed to be sufficiently small to be fired conveniently but to have confinement representative of that of explosive in shell.

Originally, attempts were made to follow the burning front along the tube by means of ionisation probes, but they proved to be unsuccessful because the ionisation level was too low to short the probes reliably. Further, the processes are relatively slow, so that the pressure wave preceding the burning front often caused sufficient deformation in its vicinity for the probe to be rendered useless. Instead 2 mm diameter holes were drilled in the curved wall of the tube in a line parallel to the longitudinal axis. Another set of holes was drilled along a line diametrically opposite the first with their individual positions off-set from the others. Each of these holes was tapped and fitted with a bolt with a 2 mm diameter hole drilled axially through it. The ends of these bolts were so arranged as to lie along the central axis of the tube.

As the burning process travelled down the tube, its progress was marked by the emergence of puffs of reaction products which were clearly visible on a high speed film with the burning tube silhouetted by photoflood bulbs mounted behind a diffusing screen. The velocity of the process was obtained by reference to the timing marks on the film and the known distance apart of the holes. The arrangement allowed the determination of burning velocities along the axis of the tube and at its outer surface; it was thought that any differences between the two would be indicative of flaws in the filling of the tubes or a peripheral gap between the explosive and the cylinder wall.

The fragments produced after each event were collected and examined.

3.2 Results

The burning of RDX/TNT (60/40) and TNT were studied first. The events showed similar characteristics to those observed in the activator tests and representative examples are shown in Figures 10 and 11. The average burning velocity of RDX/TNT (60/40) was found to be about 1400 m/s compared with 700 m/s for TNT. The RDX/TNT (60/40) burned at the same rate at both the centre and the surface of the charge, whereas the TNT initially burned more rapidly along the centre of the charge than at the surface.

3.3 Discussion

The anomalous burning of the TNT may be due to the production of imperfect charges with a region of low density along the axis, where increased porosity would be expected to accelerate burning. This effect would be expected to become less significant as the burning front progressed down the tube and the whole of the burning tube became pressurised.

The explosiveness of RDX/TNT (60/40) is clearly greater than that of TNT under the experimental conditions described in Section 3.1. The velocity of the

deflagration in RDX/TNT (60/40) was greater than that in TNT and this was manifested by the smaller fragments produced from RDX/TNT (60/40) filled tubes. The burning rate is one factor which governs the violence of the event, and this in turn accounts for the different types of events that have been recorded for munitions filled with these explosives. This is neatly illustrated in Figure 12 where the incidence of premature initiation of obsolete 25 pdr. L6 and L7 shell filled TNT and RDX/TNT (60/40), respectively is tabulated. The position at which the premature initiation of a shell is observed is dependent upon the time whether initiation of deflagration and expansion of the shell body is so rapid that the shell is stopped in its motion down the bore or whether reaction occurs more slowly so that the shell bursts out of the bore. If the shell becomes jammed, the rate of burning of the explosive determines the extent of damage to the barrel. The data for the 25 pdr. shell are entirely consistent with the more rapid deflagration of RDX/TNT (60/40) compared with TNT under the same confinement.

4. CONFINEMENT EFFECTS

The velocity of deflagration increases with increasing confinement, due to the achievement of higher pressures, and deflagration can take place so rapidly that the deflagration/detonation transition occurs. Conversely, as confinement is progressively reduced a detonation may undergo transition to a deflagration which may fade entirely if insufficient confinement is maintained or the charge diameter is less than some limiting value.

4.1 Experimental

Two simple experiments have been chosen to illustrate the effects of confinement on explosiveness. An Activator test cartridge was modified as shown in Figure 13 in which a Perspex window was keyed into the steel. Samples of RDX/TNT (60/40) were ignited and photographed with a high speed cine camera.

Another series of trials was conducted using large burning tubes, examples of which are shown in Figure 14. RDX/TNT (60/40) and RDX/PU (88/12) were compared. The tubes were 750 mm long, 150 mm outside diameter with 10mm thick walls in which a line of holes was set at 50 mm intervals. They contained about 10 kg of explosive.

4.2 Results

The modified activator cartridge provided sufficient confinement to permit initiation of the RDX/TNT (60/40) as is shown in Figure 15 by the appearance of pin-points of light. These arose from the sites of hot-spots from which, under normal circumstances, the burning process would have grown, but later frames show that in this arrangement they faded due to the failure of the Perspex window which was ejected, along with molten explosive.

The results of the firings of the large burning tubes were complementary. When RDX/TNT (60/40) was fired, a high velocity deflagration was initiated

which resulted in numerous small fragments of the casing and the charge was completely consumed. On the other hand, the RDX/PU (88/12) appeared to ignite normally, but the tube was split open rather than fragmented and only about 2 kg of the explosive charge was consumed since the deflagration was extinguished with rupture of the tube.

4.3 Discussion

The two experiments described in Section 4.2 show that explosiveness is as much a function of the whole explosive system as it is of individual explosives. The RDX/TNT (60/40) was extinguished soon after initiation in the modified activator, whereas the RDX/PU (88/12) was extinguished at a time at which it could reasonably be assumed that the material was properly ignited. These two phenomena have a common factor, namely the relatively slow velocity of deflagration with which either process would have been travelling at the time damage began to occur to the system. If the deflagration velocity is sufficiently slow, it is more susceptible to the decelerative action of the release of confinement than if it is more rapid. This may be due partly to the chemistry of the decomposition process being inherently unstable but it is more probably physical rather than chemical in origin. The high-speed deflagration of RDX/TNT (60/40) does not fade despite the extensive fragmenting of the tube because the inertia of the fragments maintains the confinement while the burning front is in the vicinity of the portion of the tube being fragmented at a given time. On the other hand, in the case of RDX/PU (88/12), or in the activator test with the plastic insert, the burning process is taking place at a speed which is of the same order or less than that with which the confinement may be removed from the vicinity of the reaction.

This concept of the explosiveness of a system, is illustrated by studies on the occurrence of bulged barrel prematures which have been noted occasionally in guns of medium calibre firing RDX/TNT filled shell at proof or in service. Although the damage produced by these events is considerably less severe than those shown in Figures 2 and 4 it is generally sufficient to render the gun useless. Investigations into events of this type suggest that initiation occurs in the nose region of the RDX/TNT (60/40) filled shells, most probably at the base of the exploder, as a result of compression ignition possibly aggravated by dusting of the explosive. Soon after initiation occurred, the pressure would have been sufficient either to strip the fuze threads or expand the ogive sufficiently to release the fuze and eject it from the shell. The shell would probably only stop momentarily before it was swept on out of the bore by the effect of the propellant gases. The hypothesis was tested with shell of similar calibre the filling of which was ignited at a position just beneath the exploder pellet. The result is shown in Figure 16 in which the steel casing was recovered virtually welded to the bore of the gun. In this experiment the shell was static so there was no propellant gas to eject the damaged shell.

The conclusion to be drawn is that explosives have different levels of explosiveness depending upon the confinement, which can be different depending upon the point of ignition of the explosive within a munition.

5. DEFLAGRATION AS A HAZARD ASSESSMENT TOOL

The burning tube experiments described earlier were designed to give information upon which the design of a standard tube would be based. Such a tube is shown alongside the other types in Figure 14. It does not carry the drilled bolts, since they would not allow pressed explosives to be studied. In any case they were not essential.

5.1 Experimental

The dimensions of the standard burning tube are 300 mm overall length, 45 mm external diameter with 4.5 mm thick walls. The technique of initiation was exactly as described earlier and the process were followed with a high speed camera.

5.2 Results

A number of different pressed and cast explosives were studied and the results are summarised in Table 1.

5.3 Discussion

The evidence obtained from these experiments, in addition to experience gained with earlier burning tube work and activator studies, permits the construction of a rough table of explosiveness of a number of common warhead, bomb and shell filling explosives. This is shown in Table 2 in decreasing order of hazard.

This order was derived by a process involving some comparison of quantitative data and some subjective assessment.

6. CONCLUSIONS

The hazards arising from the accidental initiation of a high explosives by stimuli less energetic than those necessary to cause detonation directly is dependent upon the rate of deflagration of the explosive under a given confinement and the confinement the explosive experiences in the hazard situation. The experiments described here have been aimed at quantifying explosiveness both for different explosives under a given confinement and for a given explosive confined in different ways.

At present, the most useful comparisons between explosives have been achieved by examination of the velocity of deflagration, examining the fragment patterns and the ease of extinguishment of the process on removal of the confinement.

Already the work has enabled consistent explanations to be proposed for a number of accidents.

TABLE 1

Hazard Assessment of Some Explosives

Explosive	Time to Explosion, 10^{-3}s	Fragments Type Number	Amount of Explosive left, %	Remarks
RDX/TNT (55/45)	0.7	Small 17 - 20	0	Typical of all other RDX/TNT firings. Ignition within 100 us
RDX/TNT (55/45) Fibre reinforced	1.25	Small 15 - 20	0	Apparently indistinguishable from RDX/TNT (55/45) except velocity halved
TNT	1.5-2	About 10	0	Larger fragments than with RDX/TNT
TORPEX 4D	10, induction period included, 4 otherwise	Medium sized up to 10	Up to 10%	Variable induction period before burning began
RDX/PU (88/12)	3 - 5	2 or 3	About 75-90%	Tube opened up
TORPEX 4D Fibre reinforced	-	Tube unfragmented	About 90%	Ignition faded without rupturing tube, three out of 4 trials. 4th trial similar to Torpex 4D.
RDX/WAX/Al (68/12/20)	5.5	End caps only	25%	Tube unfragmented. End caps sheared off
RDX/WAX/Al (68/12/20) Reinforced	5 to 10	End caps only up to 5	Up to 80%	Tube unfragmented. End caps sheared off
PE4	-	-	100%	Ignition could not be effected

TABLE 2

Order of Explosiveness for some Common Explosives

RDX/TNT 60/40)
RDX/TNT 55/45)

RDX/TNT 55/45 Fibre reinforced

TNT

TORPEX 4D

RDX/WAX/Al 68/12/20

Decreasing Explosiveness

RDX/WAX/Al 68/12/20 Fibre reinforced

RDX/PU 88/12

TORPEX 4D Fibre reinforced

PLASTIC EXPLOSIVE PE4



FIGURE 1 EFFECT OF THE RAPID DEFLAGRATION OF A 5.5 in HE BL SHELL DURING A REWORKING OPERATION



FIGURE 2 TYPICAL EFFECT OF A GUN PREMATURE AT PROOF

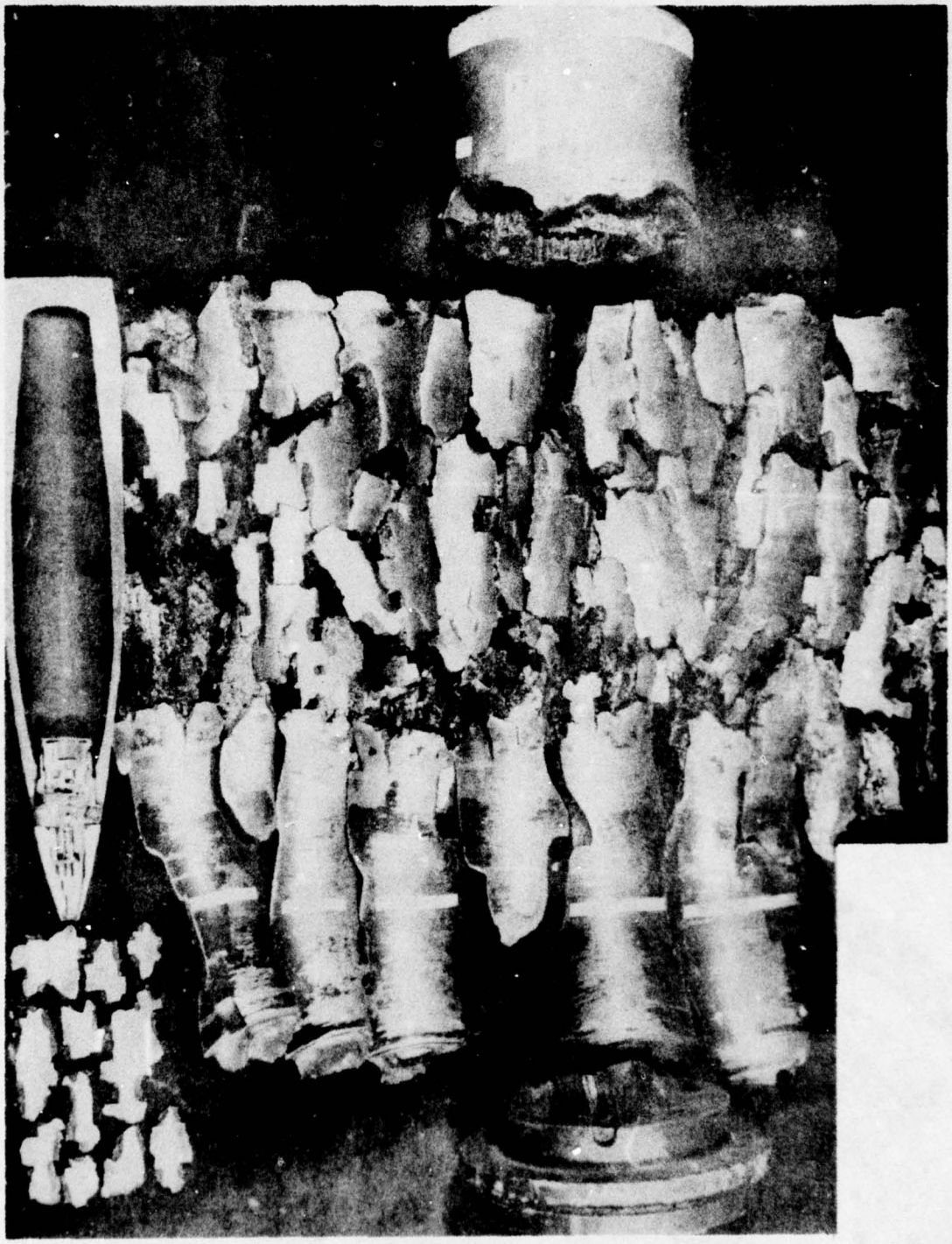


FIGURE 3 BARREL FRAGMENTS FROM A SHELL PURPOSELY DETONATED BY THE FUZE

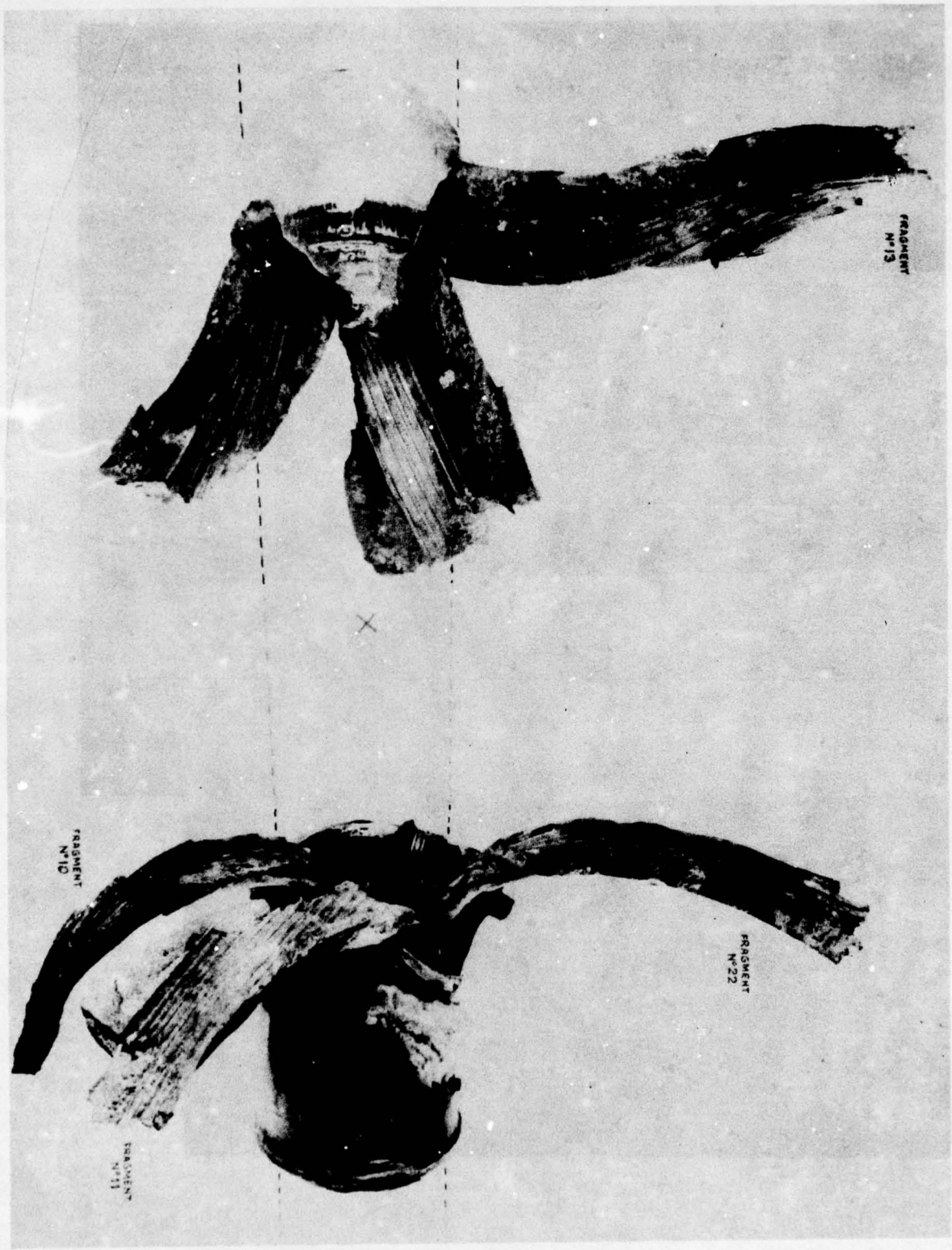


FIGURE 4 BARREL FRAGMENTS FROM A PREMATURE AT PROOF



FIGURE 5 SHELL FRAGMENTS A, B, C AND DYN FROM DETONATIONS
SHELL FRAGMENT D FROM HOT WIRE IGNITED ROUND
SHELL FRAGMENT 13 FROM A PREMATURE EXPLOSION DURING PROOF FIRING

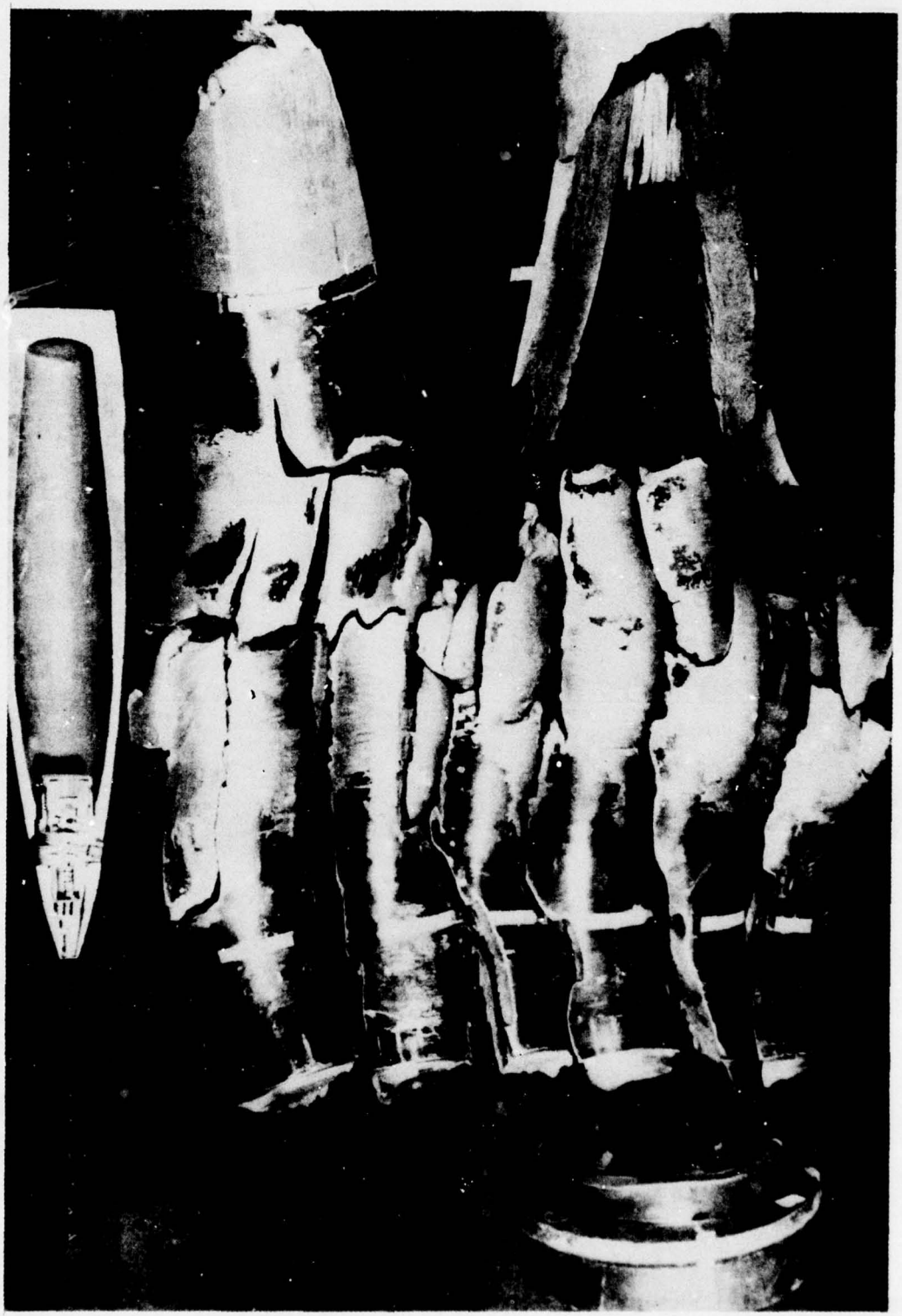


FIGURE 6 BARREL FRAGMENTS PRODUCED BY A HOT WIRE IGNITED ROUND

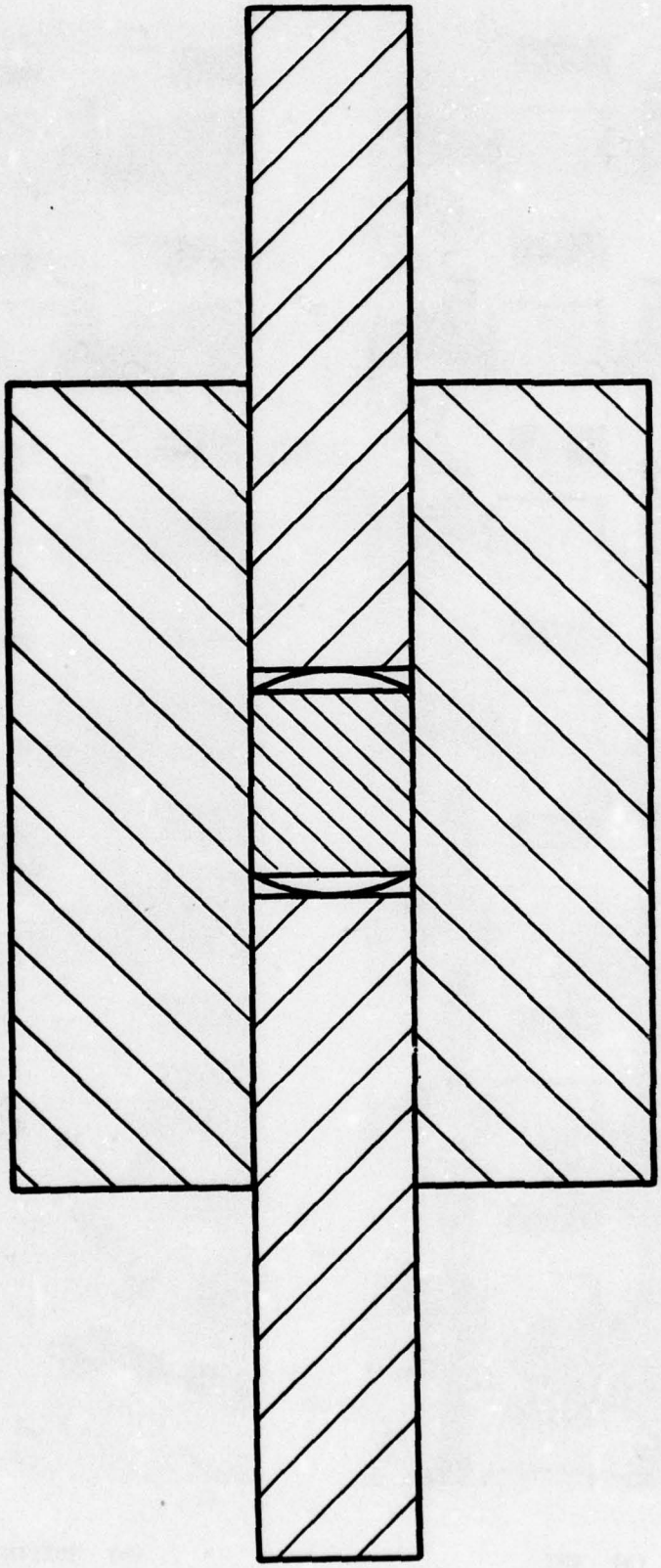
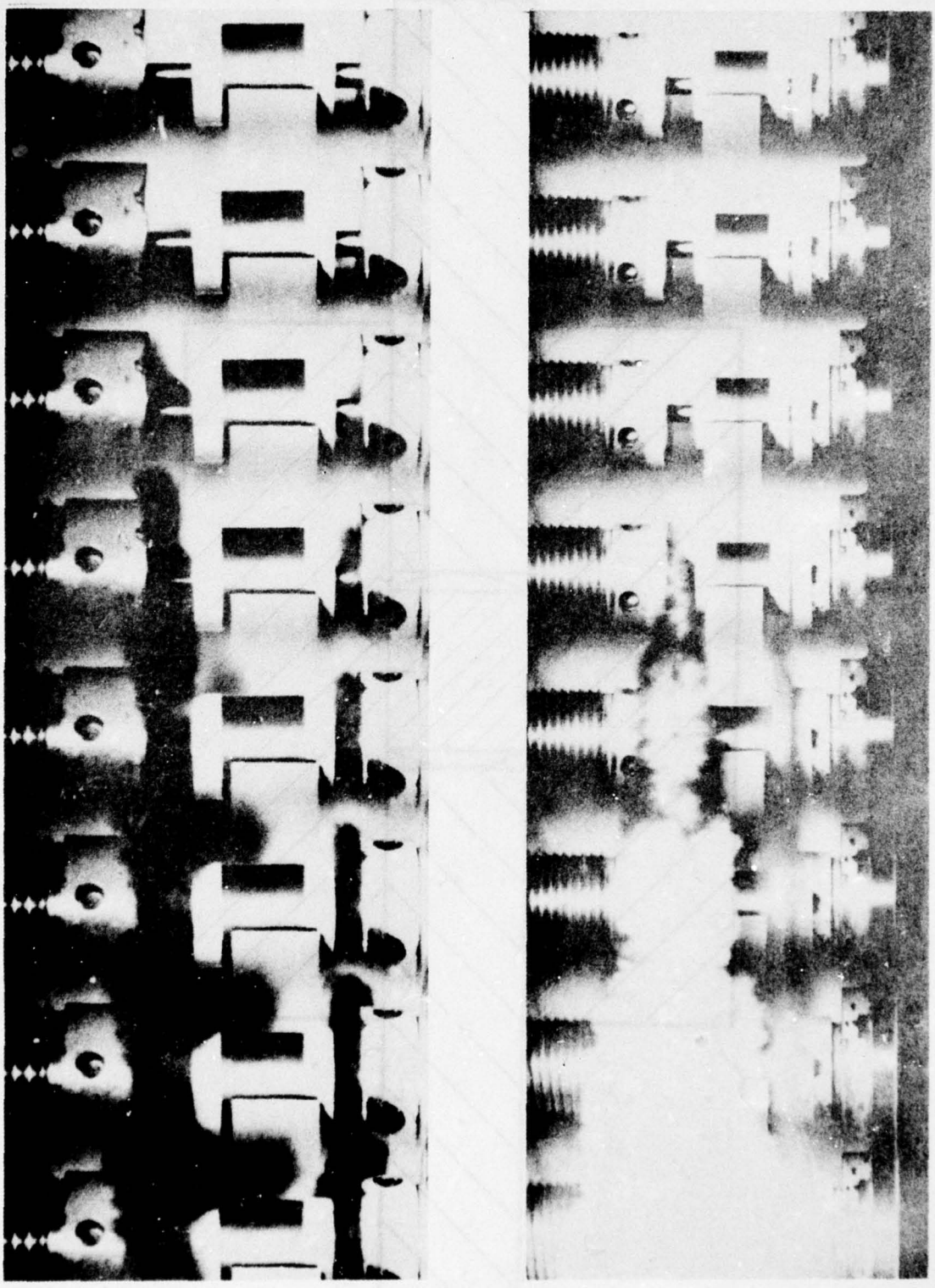


FIGURE 7 TEST SECTION OF THE ACTIVATOR



(a) TNT

(b) RDX/TNT (60/40)

FIGURE 8 REACTIONS OBSERVED IN THE ACTIVATOR

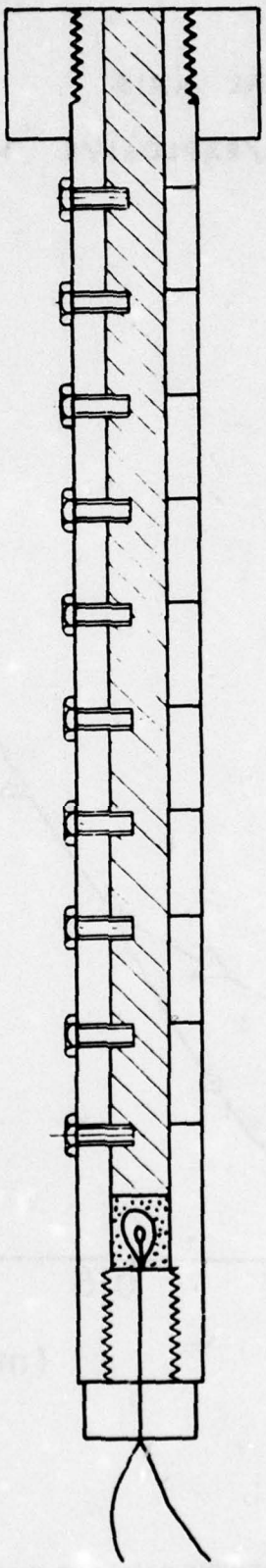


FIGURE 9 EXPERIMENTAL ARRANGEMENT TO DETERMINE BURNING VELOCITIES

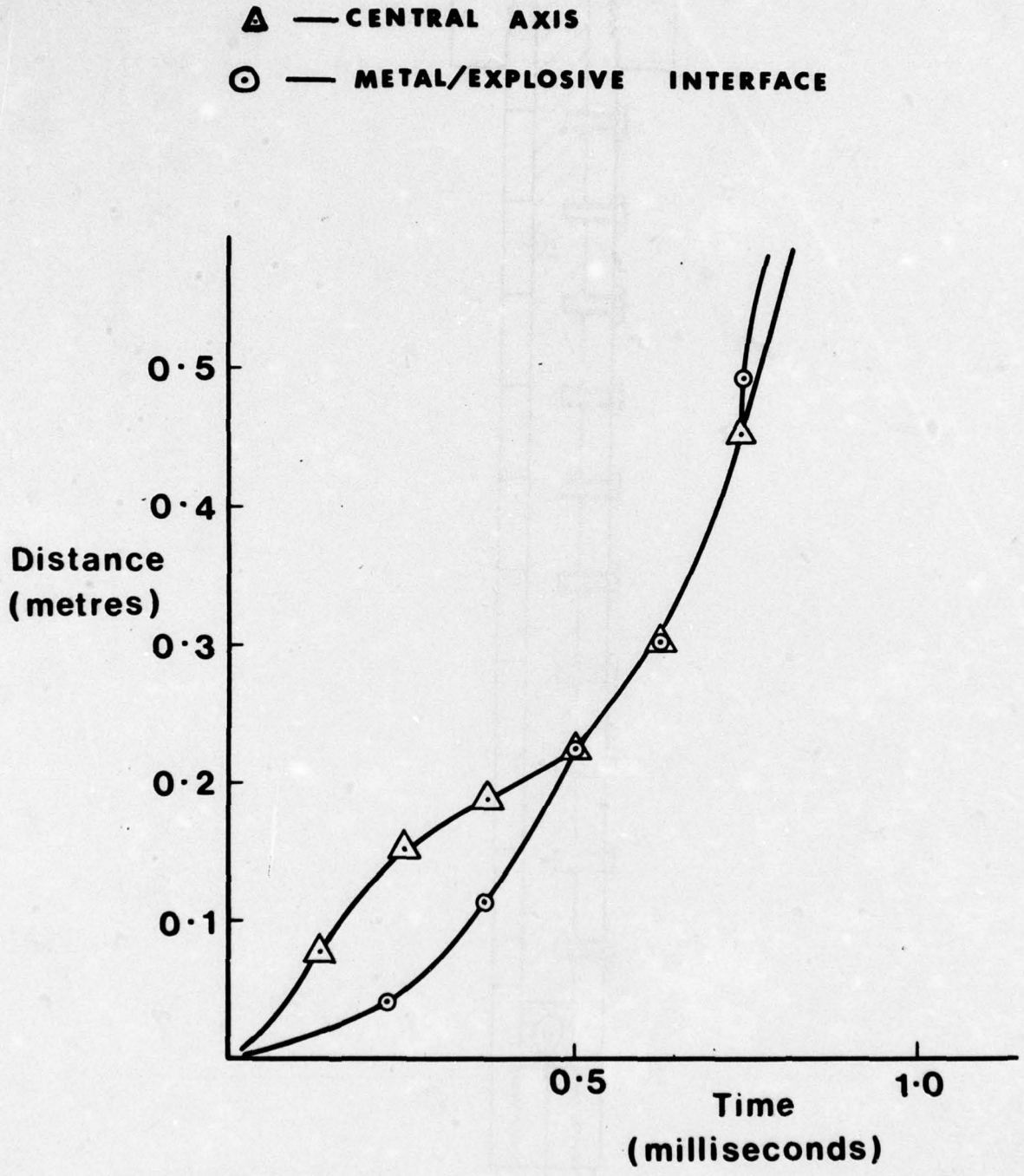


FIGURE 10 BURNING RATE FOR CONFINED TNT

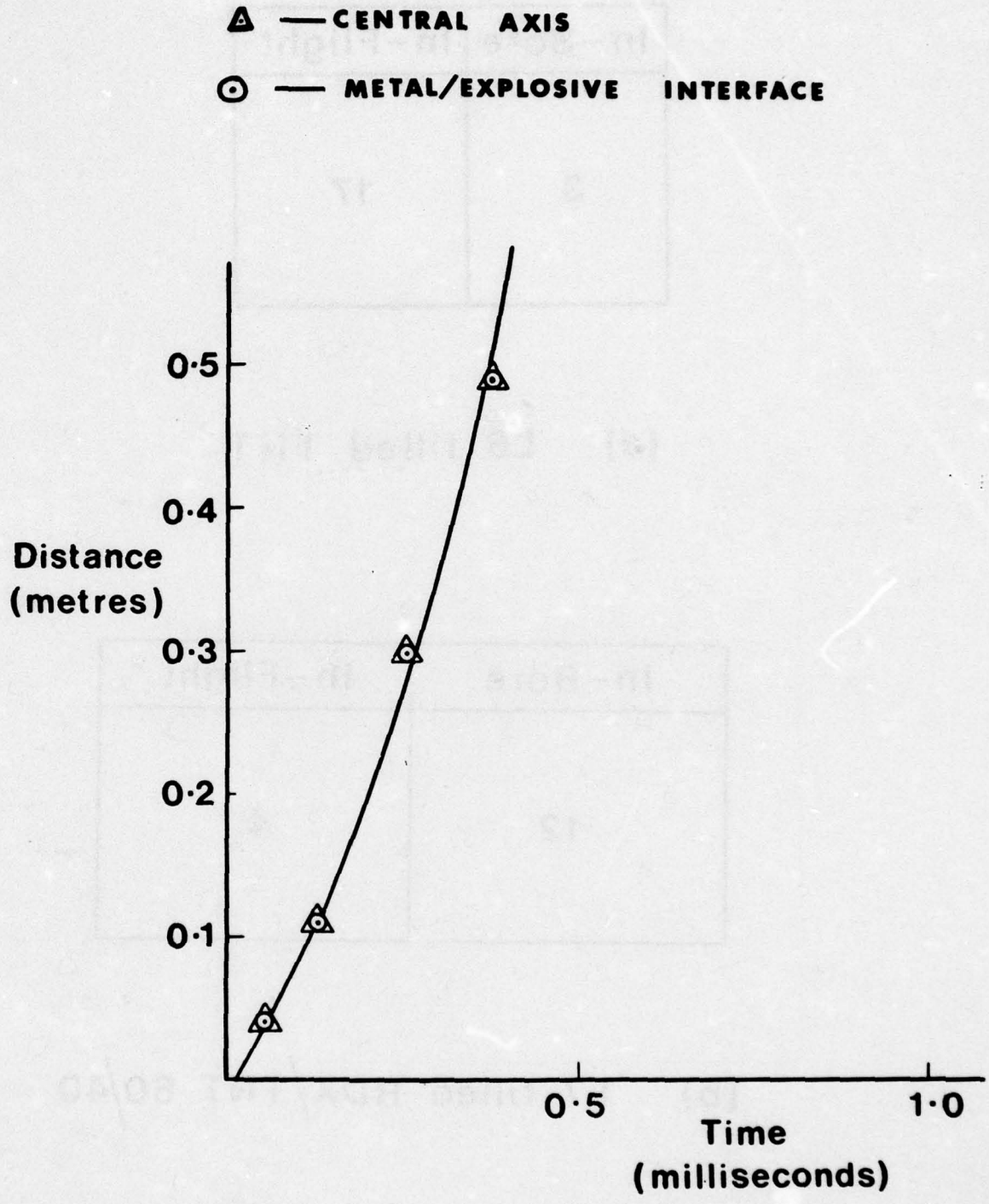


FIGURE 11 BURNING RATE FOR CONFINED RDX/TNT 60/40

In-Bore	In-Flight
3	17

(a) L6 filled TNT

In-Bore	In-Flight
12	4

(b) L7 filled RDX/TNT 60/40

FIGURE 12 POST-WAR PREMATURELY EXPLODING 25 pdr AMMUNITION L6 AND L7 SHELL

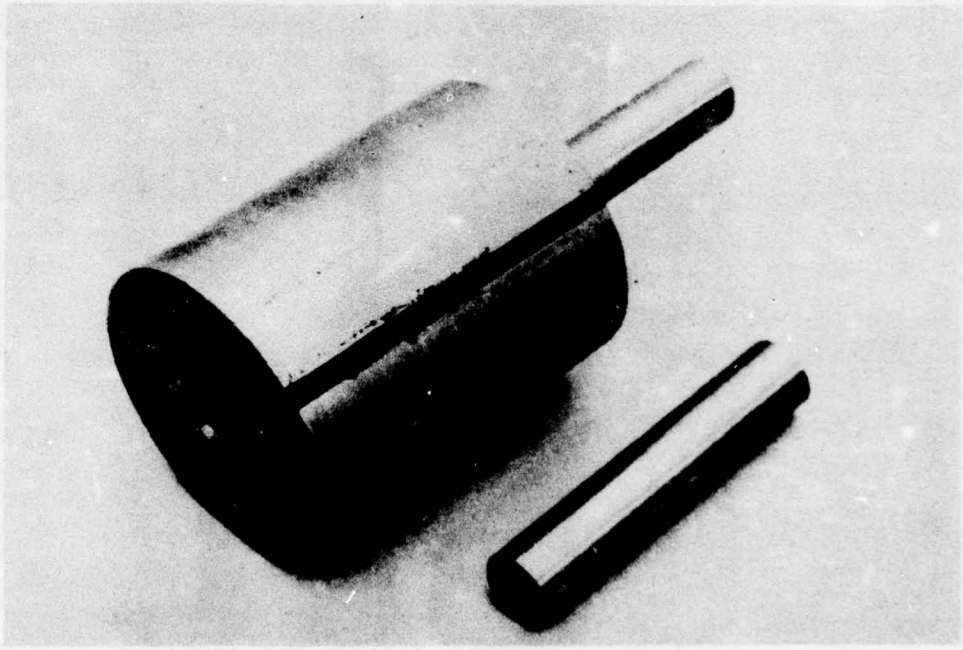
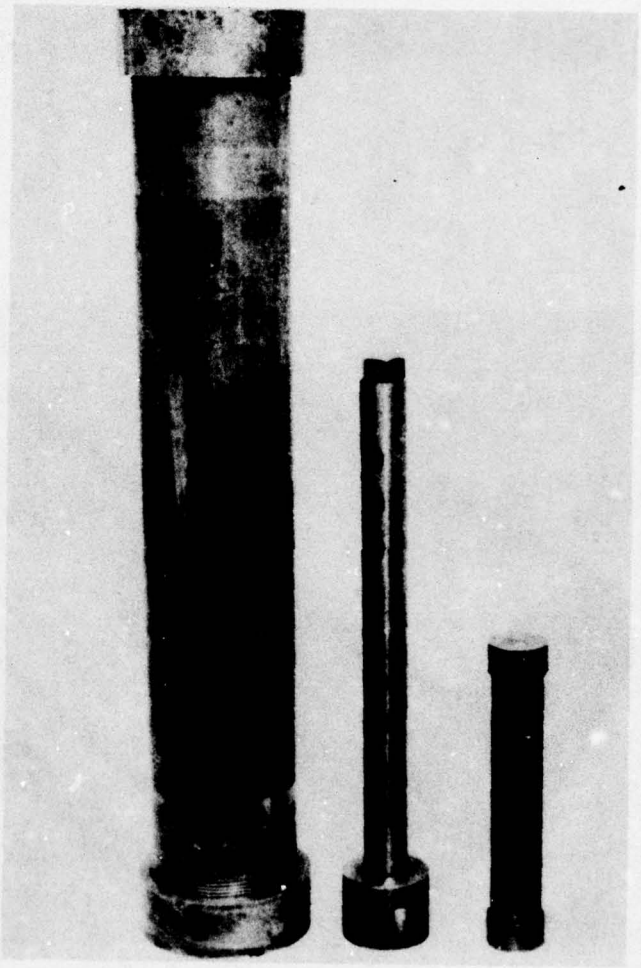


FIGURE 13 ACTIVATOR TEST SECTION MODIFIED BY THE INSERTION OF A PERSPEX WINDOW



(a) (b) (c)

FIGURE 14 COMPARATIVE SIZES OF BURNING TUBES USED IN EXPERIMENTS

(a) 750 × 150 mm containing 12 kg of HE
(b) 500 × 38 mm containing 0.34 kg of HE
(c) 300 × 45 mm containing 0.34 kg of HE

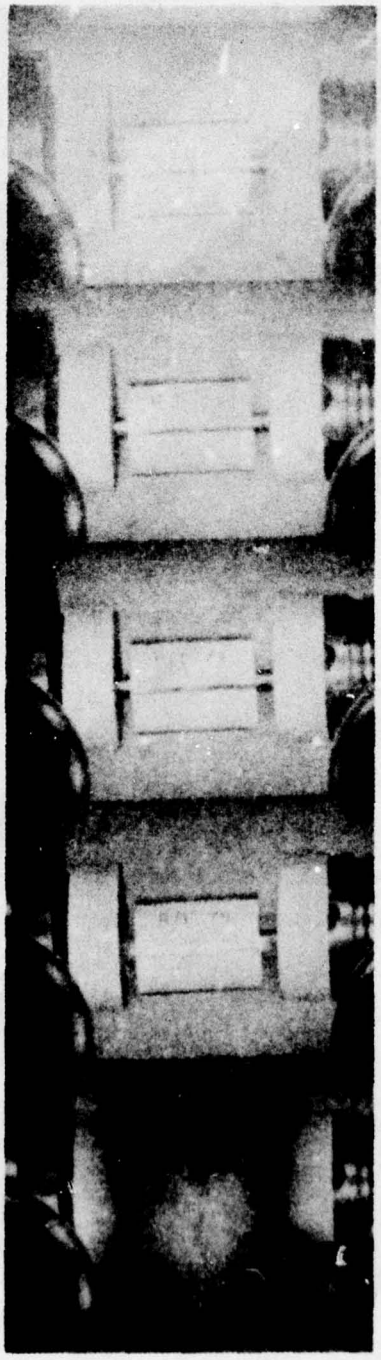


FIGURE 15 RDX/TNT (60/40) EVENT PRODUCED IN AN ASSEMBLY WITH A PERSPEX WINDOW

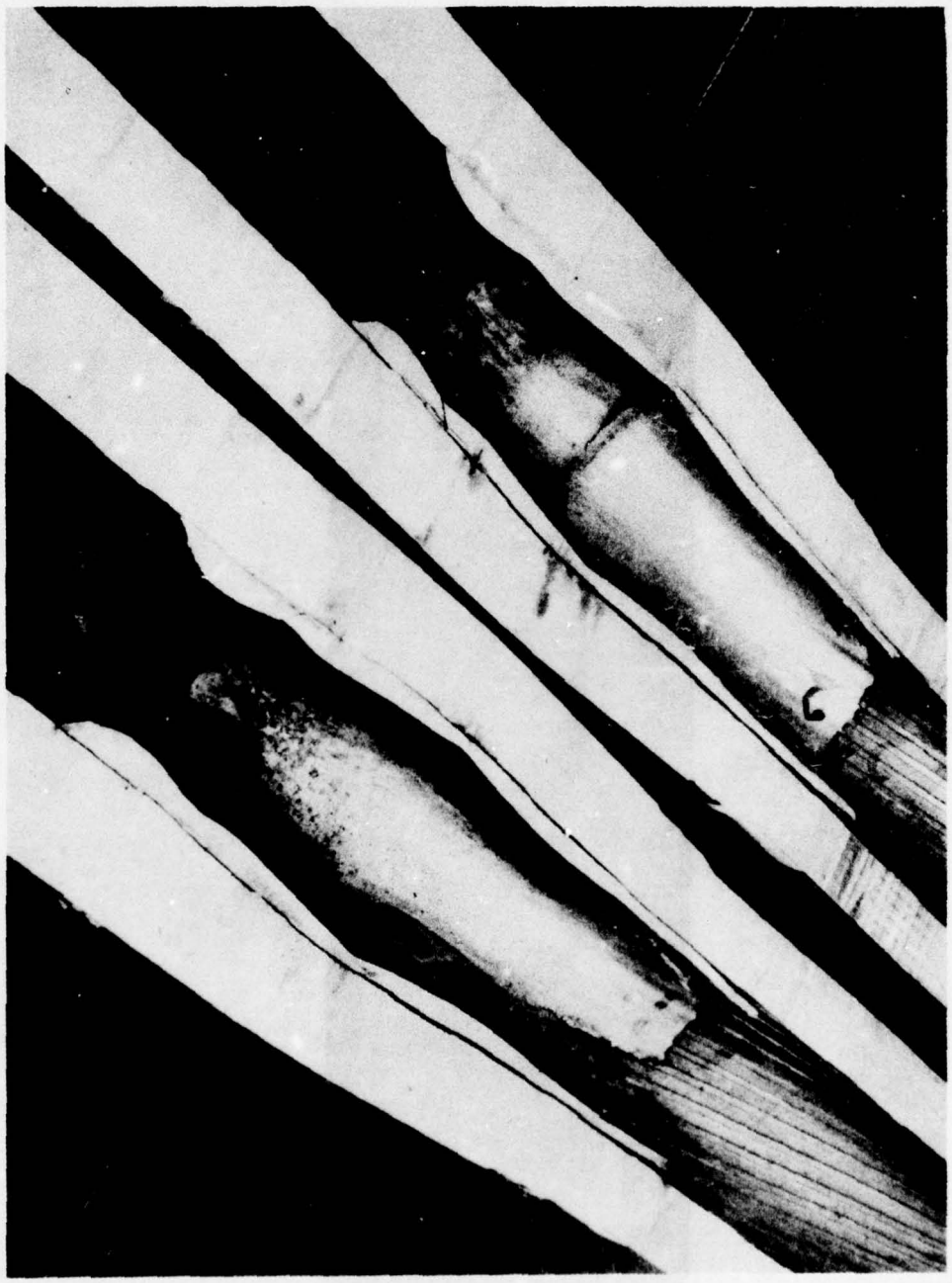


FIGURE 16 SECTIONED GUN BARREL SHOWING BULGE PRODUCED BY AN IGNITION BENEATH THE EXPLODER

GUIDELINES FOR EVALUATING CONDUCTIVE FLOOR COATINGS

Glenn C. Pritchard
Naval Weapons Center
China Lake, California

ABSTRACT

Literature over the past several decades has called attention to the electrostatic ignition hazard in ordnance and explosive research facilities. One such method of coping with this particular problem has been the utilization of conductive flooring. In many instances, however, insufficient time or money may preclude the installation of such flooring needed to meet current governmental specifications.

As a result, research at the Naval Weapons Center, China Lake, was initiated to study the efficacy of conductive coatings (paints, cleaners, and toppings) on deficient floors in explosive areas. This paper concerns itself with a segment of this research. Specifically, it deals with the criteria used to evaluate the coatings during initial selection or subsequent use, and variables needing control during the evaluation phase.

INTRODUCTION

Current regulations require the use of electrically conductive flooring at ordnance and explosive research facilities to prevent accidental initiation of high-energy materials. To comply with the regulations ordinary floors may need to be made electrically conductive and those floors that are already electrically conductive must be satisfactorily maintained. However, malfunctions of conductive flooring occasionally occur. Age, attrition, soaps not specifically designed to retain conductivity, and wax carried on mobile equipment or the shoes of personnel are usually responsible for electrical resistance readings in excess of the maximum acceptable NAVSEA requirement of 1,000,000 ohms. When resistance is too high, static electricity can accumulate, and exposed explosives, propellants and pyrotechnics, flammable mixtures of solvents and air, and electroexplosive devices can be initiated by energy released from this static accumulation. Conversely, condensation under and on top of floors or excessive conductive elements in the floor are usually responsible for electrical resistance readings below the minimum acceptable NAVSEA requirement of 5,000 ohms for 110-volt service and 10,000 ohms for 220-volt service. When resistance is too low, the potential for electrical shock increases.[1] (NFPA requirements prohibit a resistance of less than 25,000 ohms regardless of voltage.)[2]

In each of the above situations there may not be sufficient time or money available to install new conductive flooring; therefore conductive coatings such as paints, cleaners, and toppings must be substituted to bring the resistance readings to a safe level.[3,4]

EVALUATION CRITERIA

Eleven criteria were used at the Naval Weapons Center, China Lake[5], to evaluate a number of conductive floor coatings, either during their initial selection or subsequent use. Since limited funding and time precluded extensive analysis on the many coatings currently available on the market, only the more desirable as determined by the list below were chosen for the entire evaluation period of two years. Following is a list of these criteria, not necessarily in order of importance.

1. The coating must be acceptable from a cost (material and labor) standpoint.
2. It must be compatible with modern day explosives, propellants, pyrotechnics, and other high-energy materials.
3. It must be easily mixed and applied.
4. It must meet the necessary and acceptable resistance requirements, as as specified by NAVSEA.[1]
5. It must bond or adhere properly.
6. It must be able to withstand pedestrian and materials loading traffic over an acceptable time period.
7. It must exhibit nontoxic properties.
8. It must accept the inadvertent spillage of cleaning or thinning solvents without significant physical deterioration.
9. It must withstand washing with water or detergent.
10. It must have the desired color.
11. It must exhibit nonsparking characteristics.

Once the more desirable coatings were selected for evaluation, the following steps were taken. A number of rooms in explosive operating buildings were selected. Each room was typical of those found in explosive facilities. Resistance measurements were made with a 500-volt DC ohmmeter at six carefully selected places on the floor of each room evaluated. These places remained unchanged during a two-year evaluation period.

The procedures outlined in Appendix A were followed during the entire evaluation period.

DISCUSSION OF VARIABLES

Many variables were found that affect the adequacy or efficiency afforded by conductive coatings. In order to obtain future, more reliable information that can be applied over a wide variety of conditions, one must attempt to sucessfully control these variables. Variables that merit consideration are listed below and are covered under the general headings of installation, maintenance, factors influencing resistance measurements, traffic, and hazardous material compatibility. These variables are not considered to be all-inclusive.

INSTALLATION

Floor Preparation

Before coating an ordinary floor to create conductivity or to improve a malfunctioning conductive floor, the floor must be prepared in some fashion. In some cases the floor is steam-cleaned and subsequently dried. In other cases the floor is acid-etched (e.g.,50% hydrochloric acid, 50% water). Acid etching appears to create very good bonding due to its cleansing action on the surface to be coated. As a minimum, the floor may be only swept clean, or wet-mopped and then dried.

Floor Preparer

The knowledge and skill of personnel preparing the floor will certainly determine the degree of success one will have with a conductive coating (e.g., coating endurance, resistance fluctuation, adherence). If cost is no obstacle, it is desirable to request assistance from a manufacturing representative of the product, if not to lay the actual coating, at least to supervise its installation. If it is financially prohibitive to do this, then a facilities public works department or even personnel employed in the cognizant code may be called upon to do the job.

Coating Thickness

With most coatings, resistance can be varied by simply varying the coating thickness. This is not easily achieved since large fluctuations in resistance may occur as a result of only a 2-to 5-mil thickness differential.

Floor Type

Success or failure of a particular coating is dependent upon the type of floor onto which the coating is to be applied. Some coatings work exceptionally well on concrete, metal, or wood. Others may be designed to be used with vinyl or linoleum flooring. A thorough evaluation should be made prior to purchase.

MAINTENANCE

Floor Maintenance

The type of cleaning agent used on a floor after it has received a conductive coating must be controlled. Steam cleaning, solvent cleaning, wet mopping, and dry sweeping are only a few methods employed. Harsh agents will deteriorate a coated floor rapidly, but will provide substantial cleaning in most cases. On the other hand, weak agents will cause only minimal deterioration, but adequate cleaning may be sacrificed. Careful evaluation of the advantages and disadvantages of various cleaning agents is needed.

FACTORS INFLUENCING RESISTANCE MEASUREMENTS

Floor Preparation

Prior to conducting floor resistance measurements, the floor will be prepared in some manner, or not prepared at all. *Dirt, grime, grease, and wax* are just a few of the materials that may provide sufficient insulative effects to prevent reliable and accurate resistance readings if not removed from the floor. However, cleaning the floor prior to conducting resistance measurements, may not simulate the floor resistance during normal working periods in which ordnance operations are being performed.

NAVSEA[1] requires that the room be cleaned before testing.

Frequency and Method of Cleaning

Cleaning a coated floor on a daily basis as opposed to a weekly or monthly basis, will probably cause a faster deterioration of the floor coating and thus create more drastic, less acceptable changes in resistance readings. The method of cleaning (wet mopping, steam cleaning, or dry sweeping) will also influence resistance measurements. If wet mopping or steam cleaning is the technique employed, the floor must be allowed to dry properly before resistance measurements are taken.

Humidity

Relative humidity must be controlled in order to obtain reliable resistance measurements over a period of time. A high humidity may cause enough moisture on the floor to affect the ohmmeter reading, causing the meter to show a lower resistance than there is normally. Similarly, a low humidity may cause an incorrect resistance indication. Theses readings may not reflect the nominal humidity conditions in the area. Therefore, maximum resistance should be determined under the driest condition and minimum resistance should be determined under the wettest condition.

Resistance Test Instruments

Resistance measurements in the electrode-to-electrode mode have proven to be higher, in some cases dramatically, than those in the electrode-to-ground mode. The former involves test current flowing from one electrode through the conductive surface to the other electrode, while the latter involves current flowing through the conductive surface to ground. Since the current has less distance to travel when going to ground than when going from one electrode to another (i.e., 3 feet), the resistance would be expected to be lower. It is postulated that this may be one of the major reasons for the difference in readings.

Two other reasons for differences in readings were noted. When two resistance-to-ground measurements were made at the same location, but with the leads interchanged between measurements, there was a noticeable difference between readings. Electrodes without a surface of tinfoil backed by a layer of rubber (i.e., nonresilient electrodes) provide readings significantly different in some cases from those provided by electrodes with the foil and rubber additions. Resilient electrodes give more valid and reliable measurements. They more nearly fit the contour of the floor being measured and thus allow not only more but also better surface area contact.

NAVSEA[1] requires resilient electrodes during measurements.

Several different types of ohmmeters are available for use in taking resistance measurements. Although all must operate on a nominal open-circuit output voltage of 500 volts DC, some meters are battery powered and have a tendency to drift. Others require hand cranking at a specified number of

revolutions per minute (e.g., 160 rpm) to provide the correct readings. When compared, differences in readings between the above mentioned meters were found to be as large as 3,000 ohms and as little as 1,000 ohms.

Location of Readings

Resistance measurements taken at various places throughout the room should be located to approximate the normal traffic pattern. Readings taken in room corners having very little or nothing to do with ordnance operations, even though adequate from a requirement standpoint, are not appropriate. In addition, these readings when averaged with others taken around the room in question may effectively change an otherwise unacceptable floor to an acceptable floor, or vice versa.

TRAFFIC

Pedestrian Traffic

The amount of pedestrian traffic across a floor painted with a conductive coating needs to be determined, controlled and evaluated as light, moderate, or heavy. Naturally, light traffic should lead to a better resistance and endurance evaluation over any given period of time than moderate or heavy traffic.

Materials Loading

The weight applied to a conductive coating and the manner in which it is applied affects endurance, deterioration, and thus resistance. As may be expected, light to moderate items with rubber wheels are less likely to damage a coating than heavy items with metallic wheels.

HAZARDOUS MATERIALS COMPATIBILITY

A single, yet satisfactory, method of determining and evaluating the compatibility or chemical reactivity of a particular conductive coating with propellant, high explosives, pyrotechnics or other high-energy materials must be determined and agreed upon. Currently, one method of evaluation is the 80°C oven-heat analysis, in which a coating sample is placed in physical contact with an explosives sample, usually in equal parts, left overnight in an 80°C oven, then analyzed for color changes and outgassing. Another method that is frequently used is a thermogram analysis, where exothermic

changes, decomposition peak changes, and phase changes are analyzed for peculiarities. Neither method, however, indicates the extent or seriousness of the problem caused by the incompatibility. In addition, the degree to which these tests actually simulate environmental conditions is not fully known.

SUMMARY

Research has shown that conductive floor coatings can effectively meet governmental conductive flooring specifications and thus can be substituted for actual conductive flooring, especially where limited time and money are factors. Criteria have also been presented whereby conductive coatings can be evaluated during initial selection or subsequent use.

Research programs are needed, however, to obtain data in which variables intervening during the evaluation phase of conductive coatings are controlled.

REFERENCES

[1]Naval Sea Systems Command. Ammunition and Explosives Ashore Safety Regulations for Handling, Storing, Production, Renovation and Shipping. Volume 1. (NAVSEA OP-5, Vol. 1, Fourth Revision, 15 October 1974.)

[2]National Fire Protection Association. Standard for the Use of Inhalation Anesthetic, Boston, Mass. 1970. (Standard No. 56A.)

[3]Naval Civil Engineering Laboratory. Conductive Flooring for Ordnance Activities and Hospitals, by Peter J. Hearst, Port Hueneme, Calif., NCEL, June 1972. (Technical Note N-1235, publication UNCLASSIFIED.)

[4]Naval Civil Engineering Laboratory. Electrical Resistance Measurement of Conductive Flooring, by Peter J. Hearst, Port Hueneme, Calif., NCEL, June 1973. (Technical Note N-1289, publication UNCLASSIFIED.)

[5]Naval Weapons Center. Safety Evaluation Tests of Conductive Floor Coatings for Ordnance Facilities, by Glenn C. Pritchard, China Lake, Calif., NWC, September 1975. (Technical Publication TP 5786, publication UNCLASSIFIED.)

Appendix A

EXCERPTS FROM AMMUNITION AND EXPLOSIVES ASHORE SAFETY REGULATIONS FOR HANDLING, STORING, PRODUCTION, RENOVATION AND SHIPPING. VOLUME 1, FOURTH REVISION (NAVSEA OP-5.)

The following excerpts are from Chapter 4, "Electrical Requirements."

4-7.2.4 CONDUCTIVE FLOORS

a. Specifications. Conductive floors may be made of lead, conductive rubber or plastic, conductive masonry material, or conductive composition material. Floors must comply with the following requirements:

(1) The surface of the floor must be free from cracks and reasonably smooth. If washing of floors is necessary, the material as installed must be capable of withstanding repeated washing with hot water. If conductive floors are to be waxed, a conductive wax which provides the same conductive characteristics shall be used.

(2) The material must not produce sparks when stroked briskly and firmly with a hardened steel file.

(3) The material must not slough off, wrinkle, or buckle under normal conditions of use.

(4) The resistance of the conductive floor shall be less than 1,000,000 ohms as measured between two electrodes placed three feet apart at any points on the floor. The resistance of the conductive floor to ground shall also be less than 1,000,000 ohms.

(5) The resistance of the floor shall be more than 5,000 ohms in areas with 110-volt service and 10,000 ohms in areas with 220-volt service, as measured between a permanent ground connection and an electrode placed at any point on the floor, and also as measured between two electrodes placed three feet apart at any points on the floor. This minimum is specified as an additional protection against electrical shock.

(6) Where conductive floors and conductive shoes are required, table tops on which exposed explosives or electroexplosive devices are handled or where explosive dust is encountered shall be covered with properly grounded, conductive, sparkproof material.

b. Use of Conductive Floors. Conductive floors are mandatory in areas where personnel work with or are exposed to contact with the materials listed in paragraphs 4-6.4.1 through 4-6.4.3 or other materials known to be static sensitive. Conductive shoes or other devices providing similar protection shall be worn in areas where conductive floors are mandatory. Sparkproof shoes should be worn in conjunction with steel reinforced concrete floors. Where the need for conductive floors is localized, they need not be installed throughout the building.

4-8.2.2 CONDUCTIVE FLOOR TESTING

a. General Requirements. Conductive floors shall be tested at time of installation and at least semiannually thereafter. In areas exposed to large variations in relative humidity, additional measurements should be made during times of lowest relative humidity and highest relative humidity to ensure adequate floor conductivity. The tests shall determine if the floors meet the requirements of paragraph 4-7.2.4a. The results of these tests shall be posted in a log and maintained on file.

b. Method of Test.

(1) The floor shall be clean and dry and the room shall be free of flammable gas mixtures or explosive dusts.

(2) Each electrode shall weigh five pounds and shall have a dry, flat, circular contact area 2-1/2 inches in diameter, which shall comprise a surface of aluminum or tinfoil 0.0005 to 0.001 inch thick, backed by a layer of rubber 1/4 inch thick and measuring betwen 40 and 60 durometer hardness as determined with a Shore Type A durometer (ASTM D-2240-68).

(3) Resistance shall be measured with a suitably calibrated ohmmeter which shall operate on a nominal open-circuit output voltage of 500 volts DC and a short-circuit current of 5 millamperes with an effective internal resistance of 100,000 ohms ±10%.

(4) For both electrode-to-electrode and electrode-to ground, measurements shall be made at five or more locations in each room and the results averaged. For compliance with paragraph 4-7.2.4a(4), the average shall be below the limits specified and no value shall be greater than five megohms. For compliance with paragraph 4-7.2.4a(5), no location shall have a resistance less than that specified. Where resistance to ground is measured, two measurements shall be made at each location, with the test leads interchanged at the instrument between measurements; the average of the two measurements is to be taken as the resistance to ground at that location. All readings may be taken with the electrode or electrodes more than three feet from any ground connection or grounded object resting on the floor. If the resistance changes appreciably with time during a measurement, the value observed after the voltage has been applied for about five seconds shall be considered to be the measured value.

c. Use of Test Instruments. Instruments for testing the conductivity of floors shall be used inside the room only if the room is free of explosives and no exposed electroexplosive devices are present; otherwise, the test instrument shall be placed outside the room. In any case, the floor in the immediate area of the electrode contact shall be thoroughly cleaned of all explosive material and the air purged of explosive dust or vapors.

Safety Highlights of the Fifth Quadripartite Ammunition Conference

Leon W. Saffian
Picatinny Arsenal
Dover, New Jersey

ABSTRACT:

The Fifth Quadripartite Ammunition Conference, held in Australia in October, 1975, covered various selected aspects of technology relating to the manufacture of munitions. One area of particular emphasis was explosives safety. This presentation is a very brief summary of nine papers presented at this conference dealing with safety of explosive systems.

INTRODUCTION:

The Quadripartite Ammunition Conferences have resulted in a useful exchange of information relating to various aspects of munitions manufacture. The papers presented have covered a broad range of subjects of direct interest to those involved in process engineering for the production of munitions. Typical themes have included manufacture and loading of energetic materials, automated assembly of munitions, design of protective structures and other safety engineering matters, and pollution abatement.

The first conference, proposed by Australia, was held there in 1968. It was devoted primarily to manufacturing technology for loading of munitions, and was considered to be highly successful by all four countries (Australia, United Kingdom, Canada and United States). This conference led to the subsequent meetings in 1969, 1971, 1973 and 1975 sponsored by the U.S., U.K., Canada and Australia, respectively.

It is tentatively planned to have the Sixth Quadripartite Ammunition Conference in the U.S., sometime in 1977.

DISCUSSION:

The Fifth Quadripartite Ammunition Conference included six sessions dealing with different aspects of munitions and their manufacture. These were:

1. Environmental Aspects
2. Explosives Safety

PRECEDING PAGE BLANK-NOT FILMED

3. Explosive Materials and Their Properties

4. New Devices Related to Ammunition, Explosives or Pyrotechnics

5. Testing, Evaluation and Quality Assurance

6. New or Improved Processes or Equipment

The session presentations were complemented by a series of visits to Australian munitions plants and research and development centers for first-hand observation and discussion of current activities.

The Conference was very well organized and resulted in a valuable exchange of information among the representatives of the four nations in attendance.

Following are synopses of nine papers, on various subjects relating to safety of explosive systems, which were presented at the Fifth Quadripartite Ammunition Conference:

1. (U.S.) "Systems Safety as Applied to Explosives Loading and Processing Facilities" -- E. Daugherty, NAVSEA Safety Office, Washington, D.C.

Emphasis is placed on designing safety into a munition. Safety must be considered at the inception of the program and implemented throughout the life cycle. Personnel aware of all safety requirements for fuzing, safety and arming devices, explosive formulations, explosive loading techniques, etc. must provide the necessary inputs to produce a safe, reliable product. The only requisites for performing a useful hazard analysis are sound reasoning and logic coupled with an understanding of the effect of a hazard on system operation. There is no substitute for experience in the safety engineer.

2. (U.S.) "Advanced Safety Concepts in a Modernized 105mm Load, Assembly and Packout Line" -- I. Forsten, Picatinny Arsenal, Dover, NJ

Attention is focused on the modernization of the 105mm load, assemble and pack line at the Lone Star Army Ammunition Plant. Recently developed safety concepts related to wall design for close-in blast effects, optimum quantity-distance building layouts, separation distances of explosive items, explosive waste collection, safe building-access designs and earth mounded structures, are discussed.

3. (U.S.) "Hazards Analysis Studies of a Modernized U.S. Navy Bomb Plant" -- W. McBride, Naval Weapons Station, Yorktown, VA

A Safety Review Panel was established to review the design concepts and criteria for process equipment and building modifications at Crane, Indiana. The preliminary safety review and, more specifically, tests of proposed methods to feed bulk explosive to the explosive melt buildings are discussed.

4. (Canada) "Testing Electrostatic Sensitiveness of Primary Explosives" -- R. M. Ferguson, Canadian Arsenals Ltd.

Electrostatic sensitivity test parameters cannot be chosen arbitrarily. However, sensitiveness data should be used with caution in assessing hazardous situations or in investigating causes of explosions. Different situations require different test methods, e.g. testing of loose powders is done with fixed gap, time varying gap or vibrating contact testers, while testing of consolidated powders is done with electro-explosive devices or directly in contact with needle/plane or parallel plane testers.

5. (U.K.) "The Possible Advantages of Using Non-Conducting Containers for Electrically Sensitive Compositions" -- R. Davies, R.O.F., Chorley, Lancashire, England

This paper suggests that, in certain circumstances, a non-conducting condition might provide greater security against electrostatic spark ignition than the rigid application of an all-conducting system.

6. (U.S.) "Pyrotechnic Hazard Classification Investigations" -- W. Junkin, Edgewood Arsenal, Edgewood, MD

An improved approach and tests to classify pyrotechnic hazards are discussed. The following instrumented test procedures are proposed: differential thermal analysis, Parr bomb calorimetry, electrostatic spark sensitivity, propagation rate, mass effects test, and friction sensitivity.

7. (U.K.) "Explosive Fillings for Thin-Cased Warheads" -- N. Griffiths, R.A.R.D.E., Fort Halstead

The paper outlines work in the U.K. to produce a large blast warhead in which the thermo-mechanical properties of the explosive filling are well defined so that the warhead meets stringent safety requirements, and performance is satisfactory. The work was one in support of the Martel "AR" Warhead program.

8. (U.S.) "Suppressive Shielding Applications to Manufacture, Transportation and Storage Operations" -- W. P. Junkin, Edgewood Arsenal, Edgewood, MD

Problems directly associated with the installation and use of particular category shields in munitions plants are discussed. Areas considered include tie-down for the shield, access doors and conveyor doors, effect of installation in existing building, heating and ventilation systems, and the effect of venting of blast overpressure by the shield.

9. (U.S) "Acceptor Structure Design for the Blast Environment" -- I. Forsten
Picatinny Arsenal, Dover, NJ

Inadequacies of structures designed for conventional loadings to provide acceptable protection to personnel and/or equipment when subjected to blast pressures are discussed. Problems relating to the design of safe structures to resist blast loadings, utilizing available construction materials are covered.

CLOSING COMMENTS:

Clearly, the very brief statements in this presentation give only a general idea of the useful information contained in the complete papers as presented at the Fifth Quadripartite Ammunition Conference. Copies of the full text of any paper can be furnished to those who are interested.

ELIMINATION OF BASE SEPARATION IN CAST LOADED PROJECTILES

Prepared by: Edward A. Place, Senior Engineer
Presented by: John E. Jamison, Safety Engineer
MASON & HANGER-SILAS MASON CO., INC.
IOWA ARMY AMMUNITION PLANT
Middletown, Iowa

SLIDE #1

Since late in 1974, a study has been conducted by Mason & Hanger-Silas Mason Co. Inc., in conjunction with Picatinny Arsenal, to develop a reliable process for eliminating base separation in cast loaded projectiles without compromising cast tightness or quality.

SLIDE #2

Base Separation is a gap between the explosive cast and the steel shell casing which is caused by contraction of the explosive as it cools after pouring. Base Separation is believed to be a contributor to premature detonations, and is therefore the subject of much concern.

SLIDE #3

The method currently prescribed for treating base separation requires that all projectiles be processed at alternating temperatures of 150 and 75 degrees Farenheit for 12 hour periods. This process is called post cyclic heat. It's purpose is to eliminate base separation and produce a tighter cast. The effectiveness of the treatment is determined by placing eight projectiles which are known to contain base separation in each oven to represent all projectiles in that oven. At the completion of the cycle, these samples are sectioned and the amount of base separation is measured. This is necessary because even though base separation is discernable at x-ray, it cannot be measured accurately by nondestructive techniques. If any sample contains base separation in excess of .015 thousandths of an inch, the entire oven load of projectiles is recycled and resampled.

SLIDE #4

After treatment, sample projectiles are sectioned on this remotely controlled saw while being observed on closed circuit television.

SLIDE #5

At Iowa Army Ammunition Plant, post cyclic heating is accomplished in these four ovens which are modified 26 X 80 foot igloo type storage magazines, using forced air as the treatment medium.

SLIDE #6

Each oven holds 5440 155MM, M107 Projectiles, or five rail car loads. It takes 12 hours to load or unload one oven. One typical post heat cycle takes between 70 and 80 hours, or more than three days.

SLIDE #7

This slide shows the typical oven loading pattern. Post cyclic heat is not only slow, it also requires large amounts of energy. Furthermore, it is often ineffective, which means that entire ovenloads are sometimes rejected and recycled several times. Because of these inadequacies, a project was undertaken at Iowa to develop a process that would reliably eliminate base separation as well as produce a tight cast, and which could be performed on line as a part of the production process, thereby eliminating the use of post cyclic heat.

SLIDE #8

At the inception of the project it was assumed that the desired results could be obtained by heating the projectile until the explosive adjacent to the inner wall of the shell casing was remelted as shown on this slide, while at the same time expanding the shell casing, thereby allowing the cast to reseat itself. When the projectile cooled, the remelted layer would solidify and the shell casing would contract to lock the resized cast tightly in its new position.

SLIDE #9

Hot water was selected as the treatment medium because it is easier to control than steam or hot air in a continuous process, and because of its superior heat transfer qualities. A conveyor was selected to assure uniform immersion times and because it simulates an actual production process.

SLIDE #10

This prototype treatment facility was designed and fabricated especially for this project. The speed of the conveyor is variable to achieve immersion times of 1 to 3 minutes. The tank will accomodate any caliber projectile up to and including 8 inch.

SLIDE #11

In this system, the water temperature is controllable within $\pm$ 2° up to 200°F. by means of this steam heat exchanger with built in controller.

SLIDE #12

The ability of this system to maintain a uniform water temperature is enhanced by insulating the tank on all sides and by the use of these balls which minimize heat loss at the exposed water surface.

SLIDE #13

After the equipment was installed and tested, we began to treat shells in an effort to achieve our previously established goal of remelting the cast adjacent to the inner wall of the shell casing. These tests revealed that remelt did in fact cure base separation, as anticipated. However, when the remelted layer solidified and the shell casing contracted, the cast was gripped so tightly that severe cracking occurred. A crack is defined as a separation in the cast of sufficient magnitude to be visible by x-ray.

SLIDE #14

As it became obvious that remelt was not the solution, we began to search for other methods of treatment which would not crack the cast. Projectiles were treated by dipping only the first 6 to 8 inches of the base end in heated water, without success. The dipped shells contained both cracks and stress lines. A stress line is a minor imperfection in the cast which is not visible on x-ray. Furthermore, these shells were not cured of base separation. The shell on the right has a gap of .010 thousandths.

SLIDE #15

Other shells were treated at water temperatures ranging as low as 120°F. In every case, stress lines were present in the cast. Even though these stress lines meet existing acceptance criteria, we continued in our efforts to eliminate them.

SLIDE #16

We then began to treat shells that were still warm from the pouring process, before the cast had completely cooled. At this point we achieved our first success. The casts of these shells were of excellent quality. However, many of them still contained base separation. The shell on the right has a gap of .011 thousandths.

SLIDE #17

Since the start of the project, it had been our practice to install a dial indicator in the nose of one shell in each treatment group to monitor the position of the cast during treatment. At about this point in time, we observed that the cast of one shell suddenly dropped approximately .020 thousandths of an inch while the shell was immersed in the tank. When sectioned, the projectile had neither base separation nor stress lines.

SLIDE #18

We theorize that the steel shell casing expands as it absorbs heat from the water, which releases its grip on the cast and allows the cast to reseat itself. However, the cast must drop at precisely the right moment, because as the heat continues to transfer into the explosive, the cast begins to expand at five times the rate of the steel, causing it to be held more firmly than before. In a completely solidified round, this expansion causes the stress lines.

SLIDE #19

In order to assure that sufficient force is present when the cast is released, this device was designed and built to force the cast down during treatment utilizing the weight of the projectile in conjunction with a system of levers.

SLIDE #20

The dial indicator is used to monitor cast movement. This lever plug has been quite successful and is now used on all shells treated. It applies 180 lbs. force to the cast when the shell is immersed and 230 lbs. when the shell is in the air.

SLIDE #21

A series of experiments was conducted to determine the optimum parameters for treating hot shells, using the lever plug. The results show that we can reliably cure base separation without damaging the cast by treating the projectiles in 180° water for 1 1/2 minutes, as long as the surface temperature of the projectile remains at or above 110° prior to treatment. Although this method allowed us to cure base separation, there remained another problem inherent in treating hot shells. If the surface temperature falls below 110° the projectiles could not be treated without causing stress lines. This means that any shells which were by-passed for any reason, such as mechanical problems, end of shift carryover, etc. could not be treated without stress lining the cast.

SLIDE #22

Once again we tried treating cold projectiles, in the hope that with the aid of the lever plug, we could shorten the immersion time required to release the cast sufficiently to avoid stress lines. After running a series of tests, we concluded that we could readily cure base separation by treating the projectiles in 180° water for 1 1/2 minutes, using the lever plug. When x-rayed, the casts of these projectiles showed no defects. Upon sectioning, however, the casts still contained some stress lines.

SLIDE #23

Further experiments revealed that we could indeed treat cold shells and eliminate base separation without stress lining the cast if we immersed the projectile in room temperature water immediately after removal from the hot water tank. This quench cycle removes the heat from the steel shell casing before it can migrate into the explosive to the extent that stress lines are formed. Another series of experiments designed to establish treatment parameters revealed that cold shells can be successfully treated in 180° water for 1 1/2 minutes, using the lever plug, followed immediately by a two minute quench in room temperature water. However, this process is not desirable from a production standpoint for several reasons:

FIRST Two tanks and two temperature control systems are required.

SECOND The quenched projectile does not have sufficient heat to cause the water to evaporate quickly from its surface when it emerges from the tank, which could cause a rusting problem.

THIRD The conveyor speed required to move the projectile quickly from one tank to the next could make loading a problem.

SLIDE #24

As this slide shows, there is little doubt that base separation can be eliminated by use of the hot water treatment. There is also little doubt that the cast quality of hot water treated shells is equal to or better than those which have undergone post cyclic heat. The shell on the left is from our current post cyclic heating process. We feel that the best process is one in which either hot or cold projectiles are treated in 180° water for 1 1/2 minutes prior to fuze well drilling using the lever plug, then allowed to cool normally, without quenching. This method is reliable, well suited for mass production, and inexpensive to install. Even though this treatment produces stress lines in cold projectiles, these stress lines are of a cosmetic nature only, and meet all current acceptance criteria.

SLIDE #25

After developing a satisfactory process which would cure base separation, we devised a test to compare the cast tightness of shells treated by the hot water method to shells treated by post cyclic heat. Since no standard test for determining cast tightness has been developed which yields quantitative results, this tester was designed and built by Mason & Hanger. In use, the specially sawed projectile is clamped in the fixture which grips the shell ahead of the rotating band. The plunjet is attached magnetically to the shell casing and set to zero while in contact with the cast.

SLIDE # 26

The cast is then forced forward by a standard Porta Power with a calibrated pressure gage while motion of the cast relative to the shell casing is monitored using a Precisionaire column. This test is performed immediately after the shell is sawed to assure uniform results.

SLIDE #27

Four groups of sixteen projectiles were treated by each of the following methods prior to testing for cast tightness.

Hot shells in 180° water for 1 1/2 minutes,

Cold shells in 180° water for 1 1/2 minutes followed by a 2 minute quench,

Cold shells in 180° water for 1 1/2 minutes, and

Post Cyclic Heat.

A control group of sixteen shells which received no treatment was also included in the test.

Comparisons of the cast tightness of the five categories are shown on this chart, which shows the average amount of force required to move the cast forward . 001 thousandth of an inch. As you can see, both the hot and cold treatments produce tighter casts than post cyclic heat, while the cold treatment with quench and post cyclic heat are both tighter than the untreated shells.

SLIDE #28

Now, let's take a look at cost. A modernization proposal has been submitted to construct a new automated post cyclic heat facility, shown on the left center of the screen which would give us the capability to meet existing post cyclic heat requirements on line, in-process at a cost of 7. 5 million dollars.

SLIDE #29

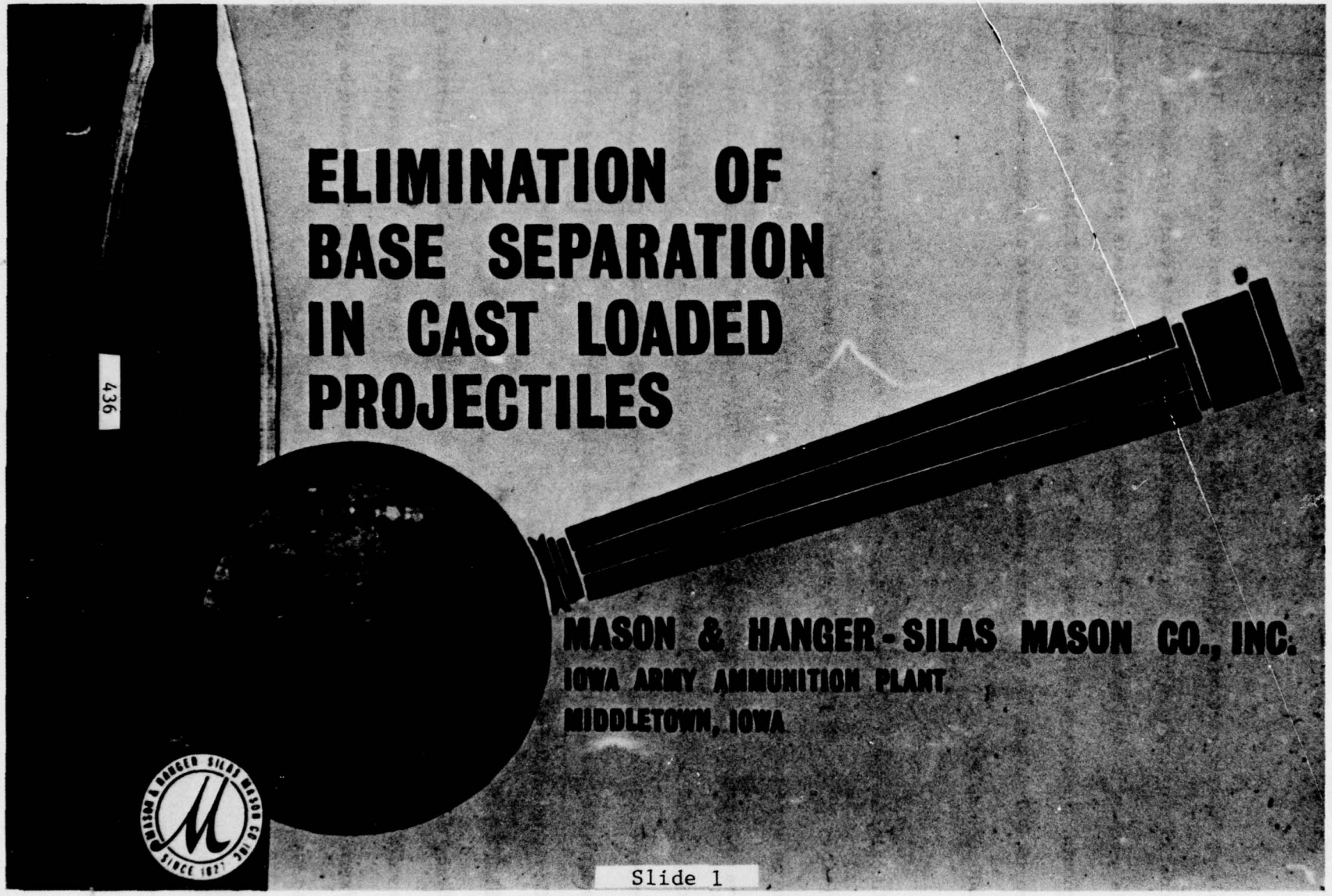
By comparison, the hot water treatment facility can be installed in existing buildings without construction. If we estimate the installation cost extremely high at one million dollars, this still results in a saving of 6. 5 million dollars.

Using current methods, it costs 54 cents per round for post cyclic heat. The cost of the proposed hot water treatment is estimated at 4 cents per round, which is a saving of 50 cents per round. Based on a production rate of 100,000 rounds per month, the annual cost of post cyclic heat would be 648,000 dollars, as compared to 48,000 dollars for hot water treatment. This amounts to an annual saving of 600,000 dollars.

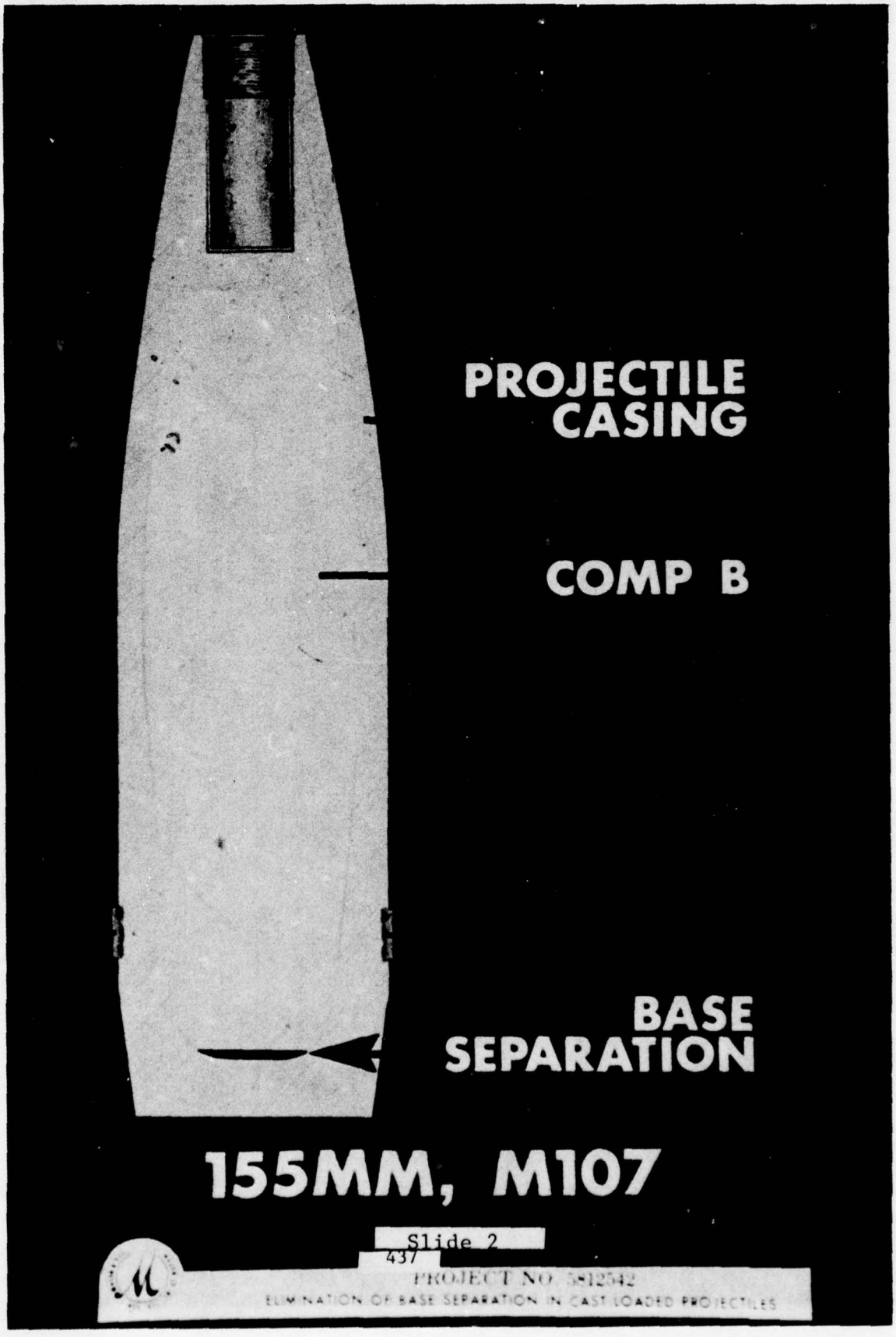
In calendar year 1975 approximately 950,000 rounds were subjected to post cyclic heat at Iowa. Of these, 27% were recycled because the samples representing the oven were not cured of base separation. If this 27% recycle rate is projected forward based on a production rate of 1,200,000 rounds per year, an additional saving of 174,960 dollars would be realized. Total first year savings are estimated at oven 7 million dollars for the 155MM at Iowa. We believe that this process is adaptable to all cast loaded projectiles at all plants with similar savings to the Government for each item.

SLIDE #30

Since the final report for this project is not complete, there will be no literature available at this time. Upon completion, copies of the report will be available from Picatinny Arsenal. Thank you very much for your attention. I would be glad to try to answer an questions that you may have.


436
ELIMINATION OF
BASE SEPARATION
IN CAST LOADED
PROJECTILES
MASON & HANGER - SILAS MASON CO., INC.
IOWA ARMY AMMUNITION PLANT
MIDDLETOWN, IOWA
MASON & HANGER SILAS MASON CO INC
SINCE 1827

Slide 1

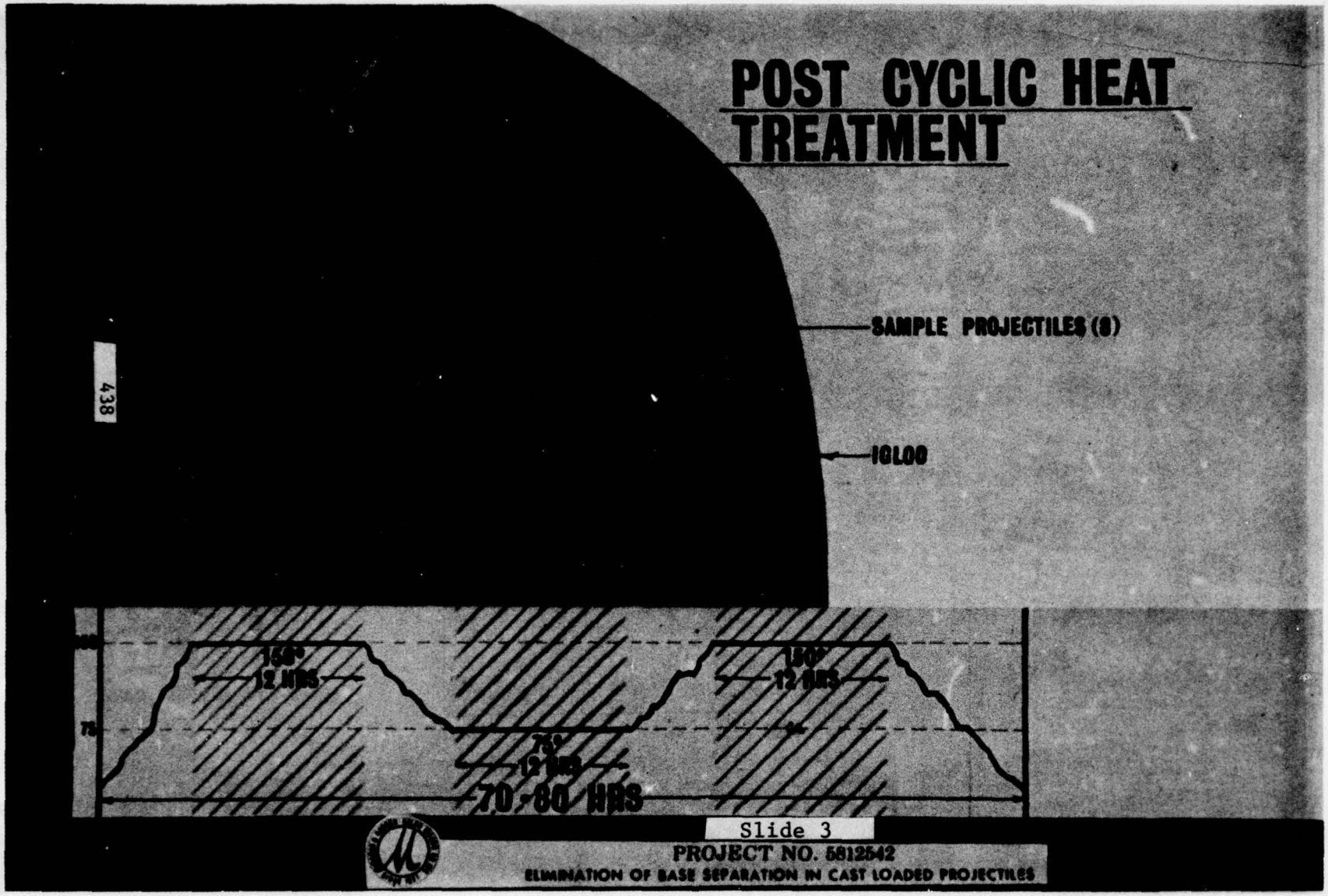


Slide 2

PROJECT NO. 3A12542

ELIMINATION OF BASE SEPARATION IN CAST LOADED PROJECTILES

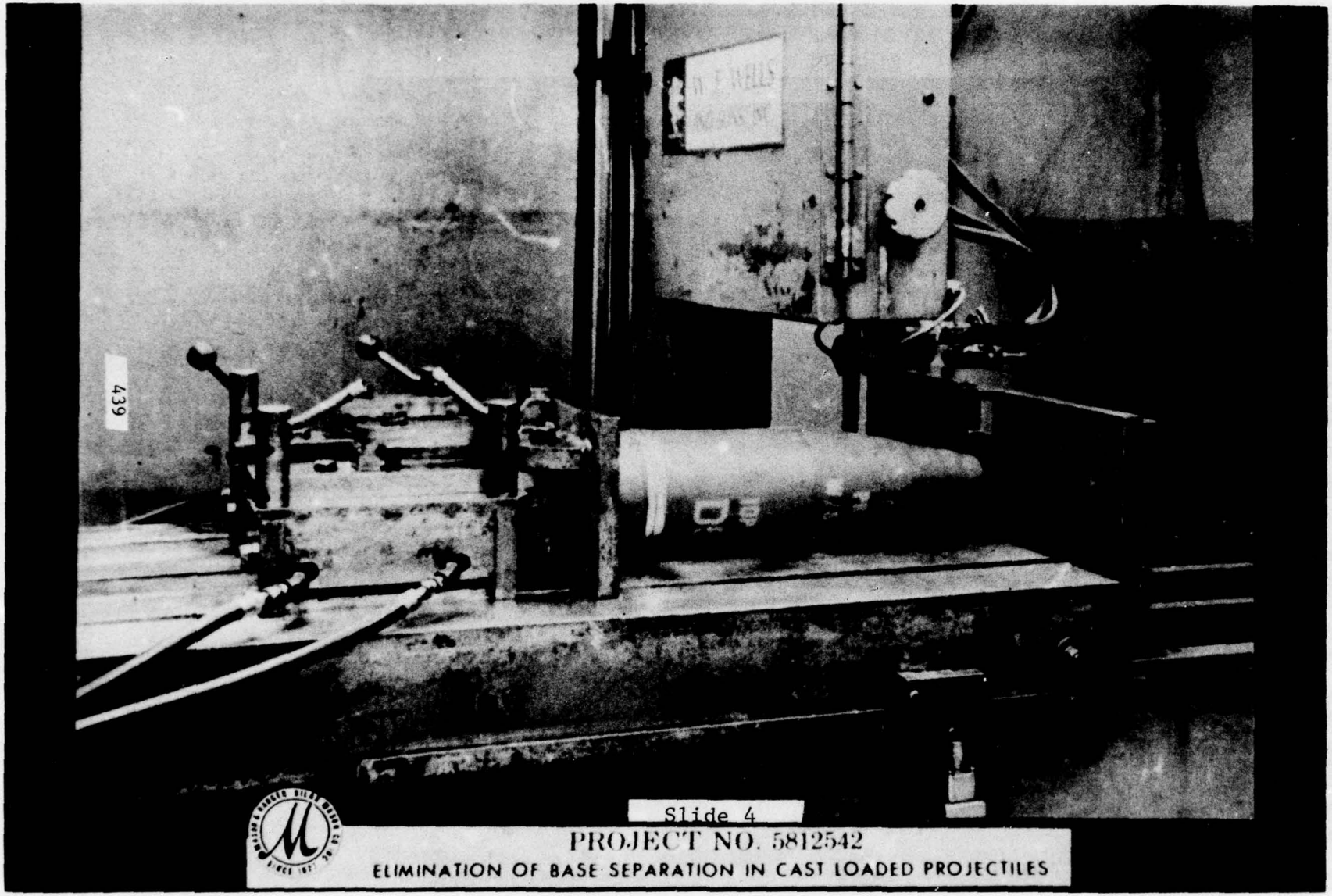
POST CYCLIC HEAT TREATMENT



Slide 3

PROJECT NO. 5812542

ELIMINATION OF BASE SEPARATION IN CAST LOADED PROJECTILES


439
Slide 4
PROJECT NO. 5812542
ELIMINATION OF BASE SEPARATION IN CAST LOADED PROJECTILES

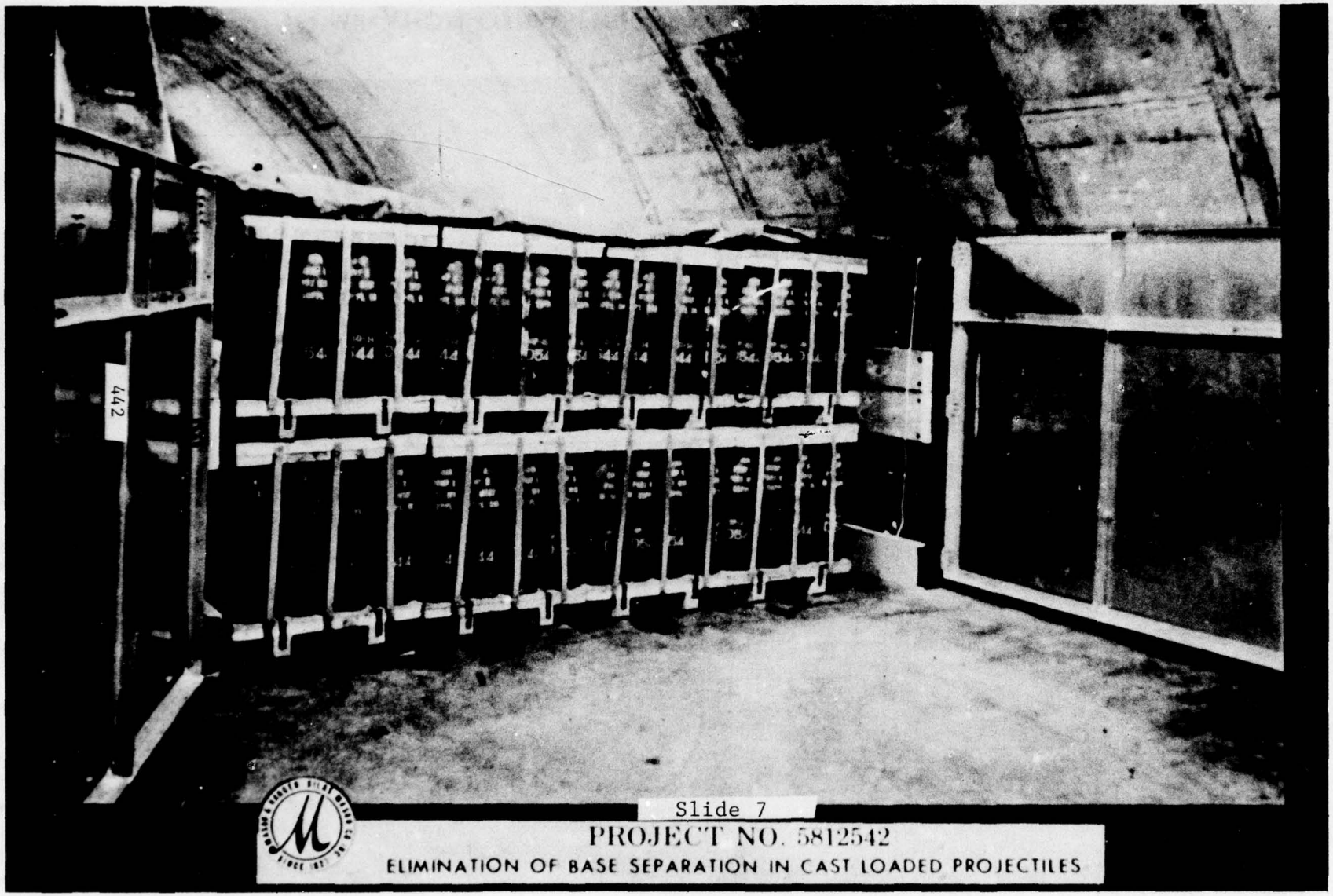

470
Slide 5
PROJECT NO. 5812542
ELIMINATION OF BASE SEPARATION IN CAST LOADED PROJECTILES

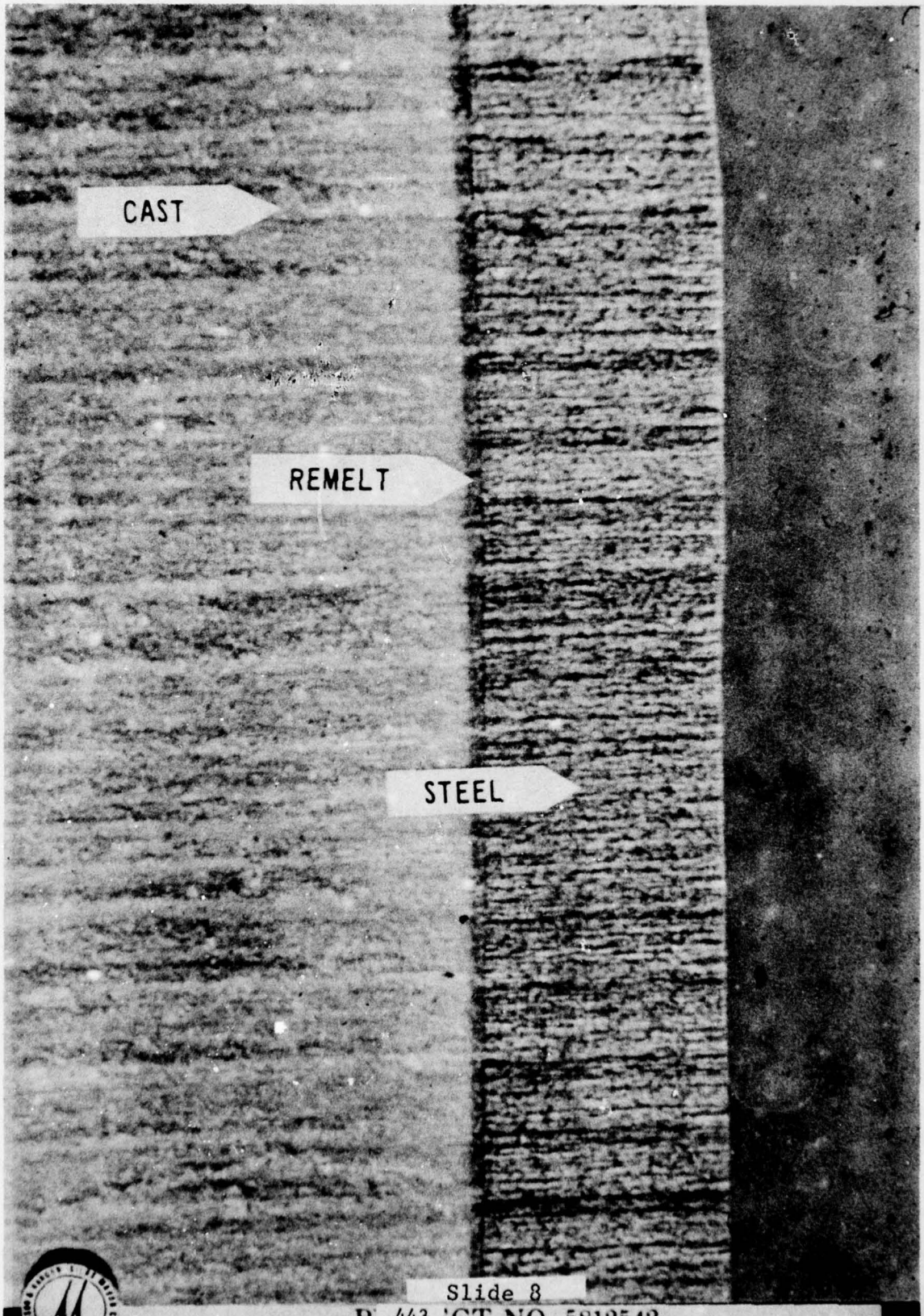


Slide 6

PROJECT NO. 5812542

ELIMINATION OF BASE SEPARATION IN CAST LOADED PROJECTILES


442
Slide 7
PROJECT NO. 5812542
ELIMINATION OF BASE SEPARATION IN CAST LOADED PROJECTILES

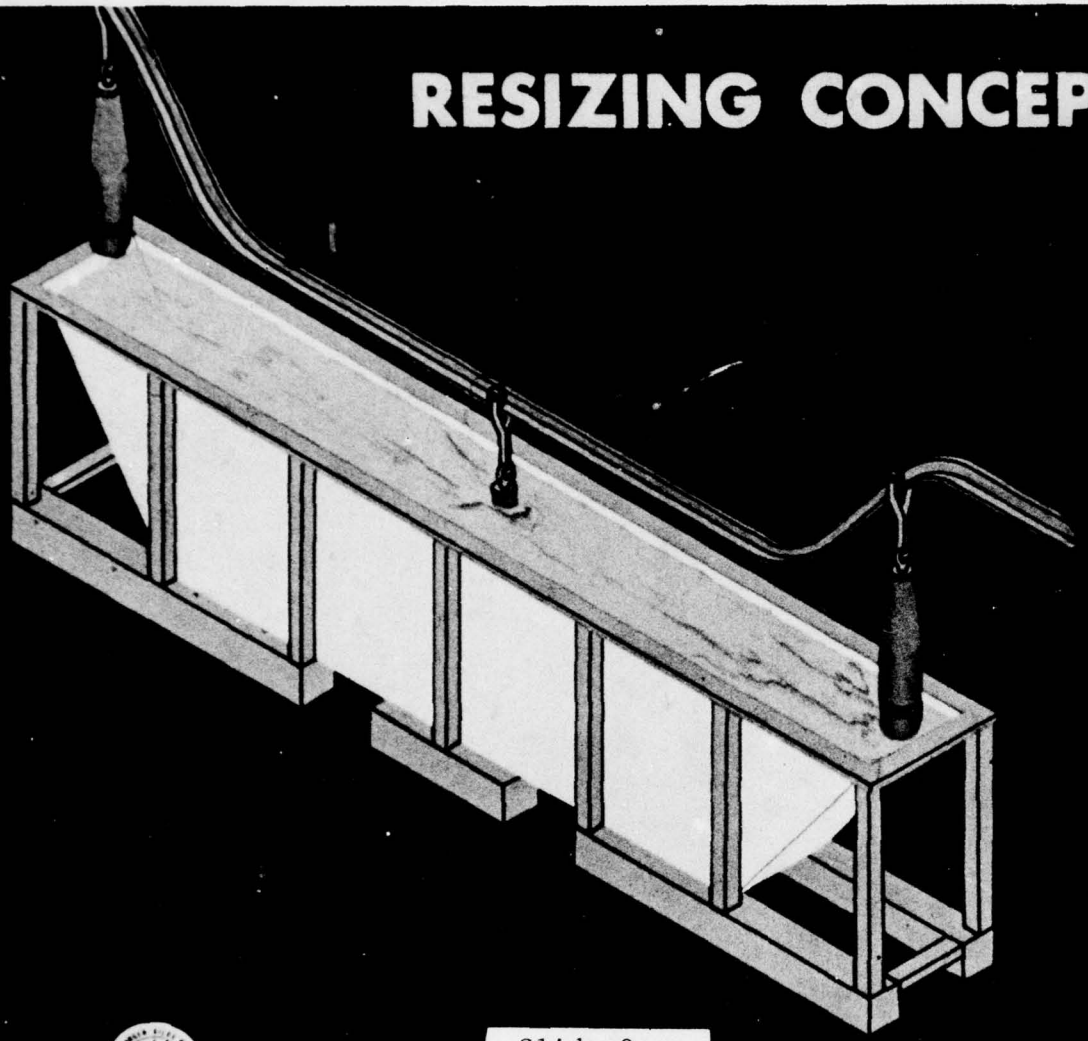


Slide 8

PROJECT NO. 5812542

ELIMINATION OF BASE SEPARATION IN CAST LOADED PROJECTILES

RESIZING CONCEPT

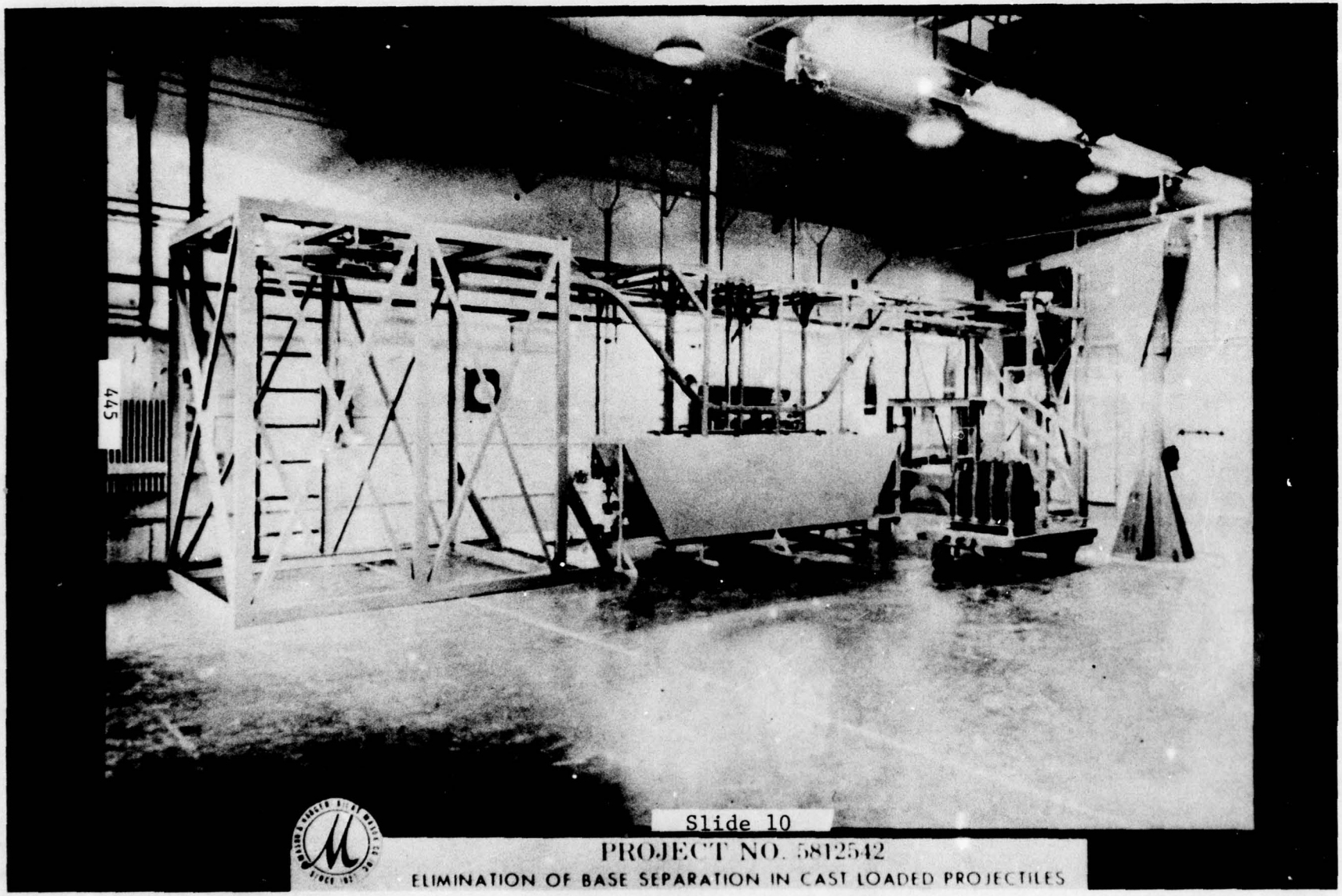


444

Slide 9

PROJECT NO. 581242

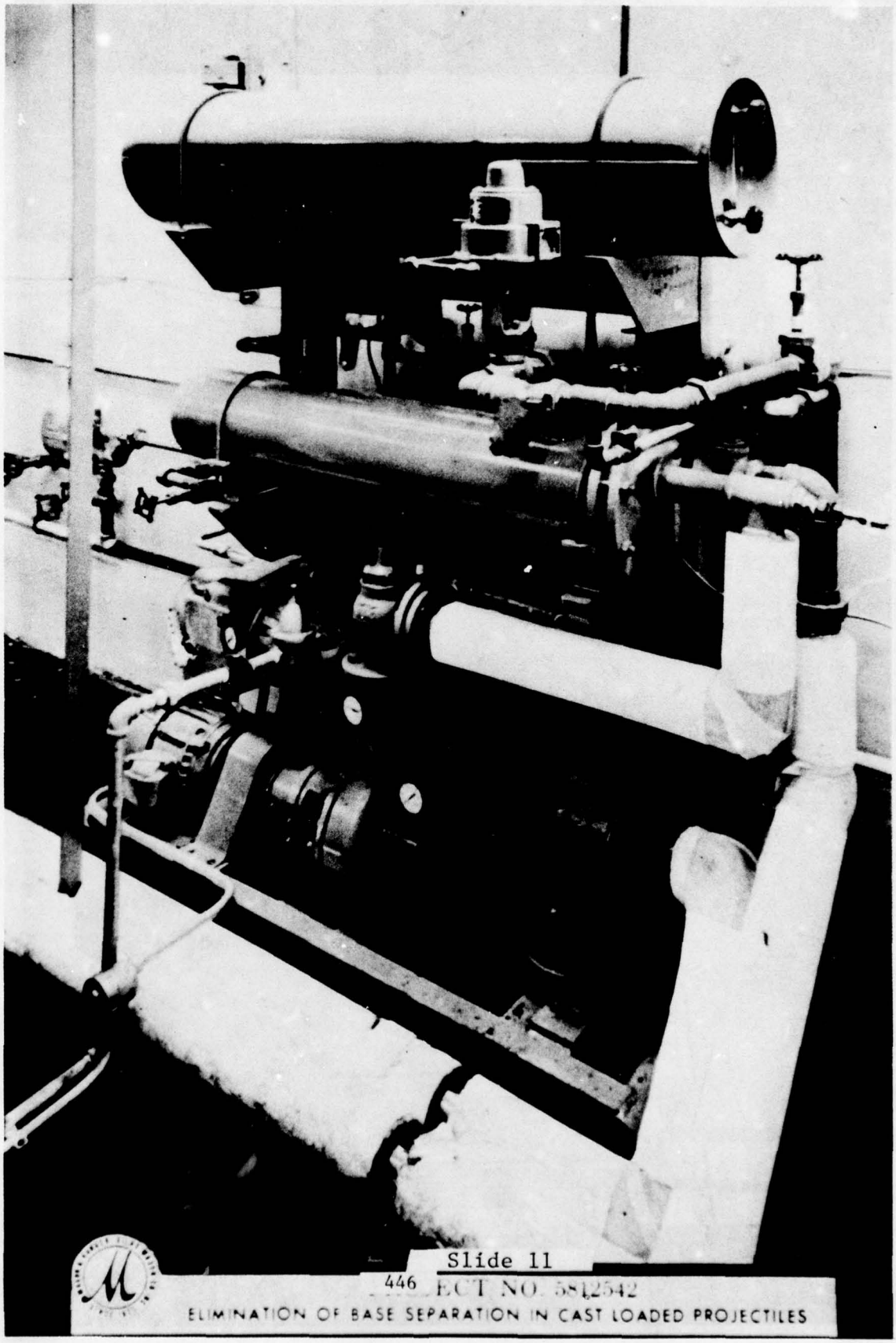
ELIMINATION OF BASE SEPARATION IN CAST LOADED PROJECTILES



Slide 10

PROJECT NO. 5812542

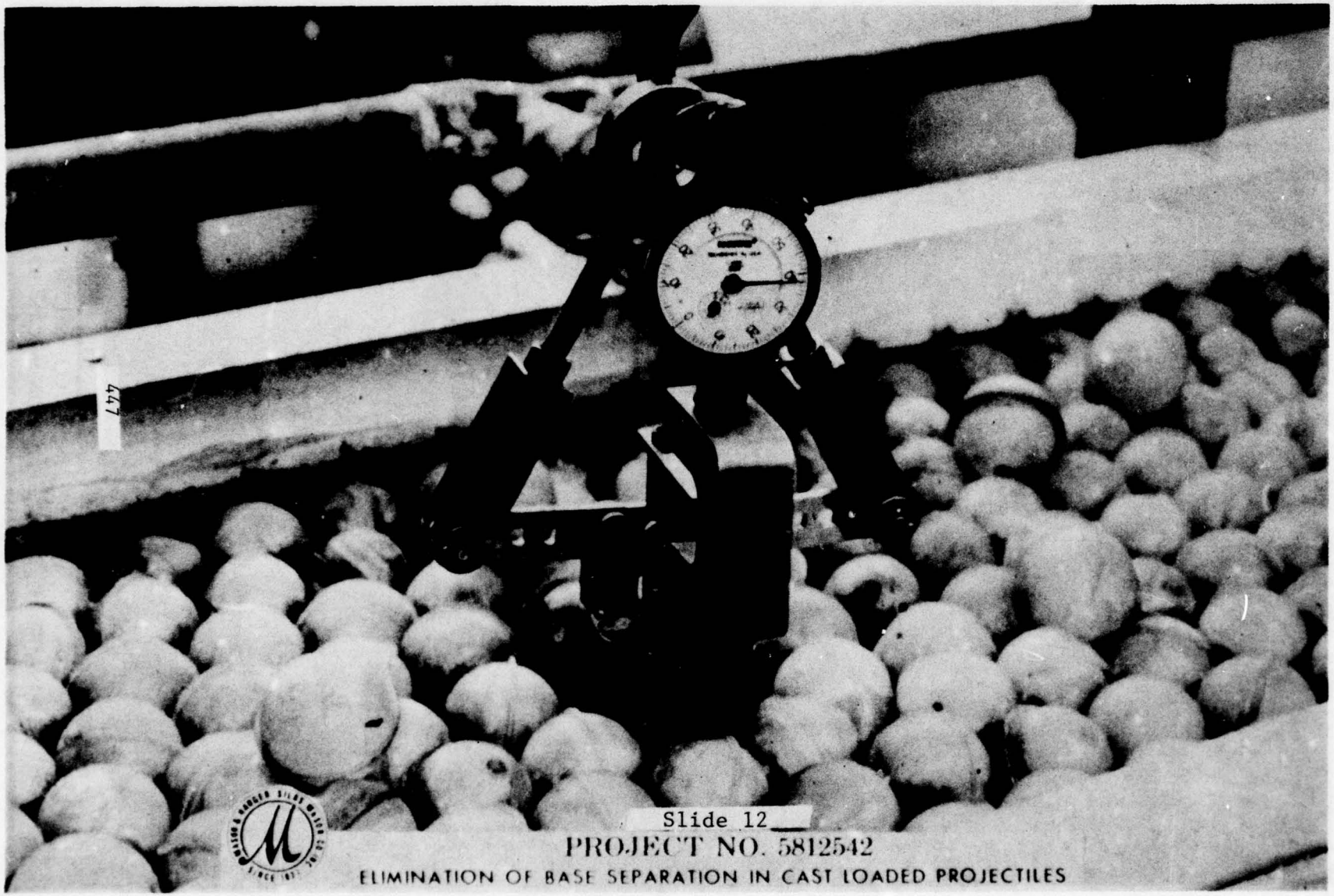
ELIMINATION OF BASE SEPARATION IN CAST LOADED PROJECTILES



Slide 11

446 PROJECT NO. 5812542

ELIMINATION OF BASE SEPARATION IN CAST LOADED PROJECTILES

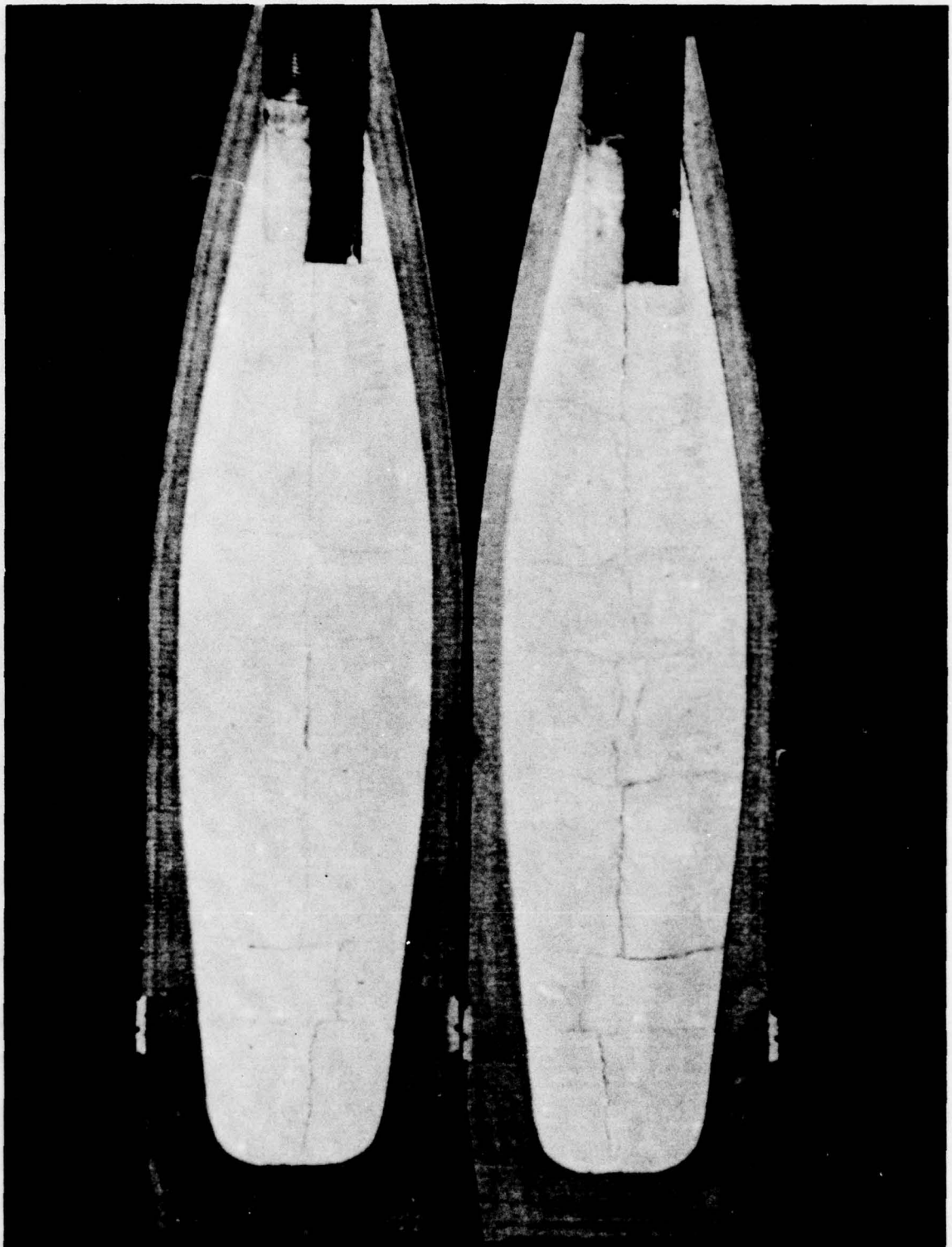


447

Slide 12

PROJECT NO. 5812542

ELIMINATION OF BASE SEPARATION IN CAST LOADED PROJECTILES

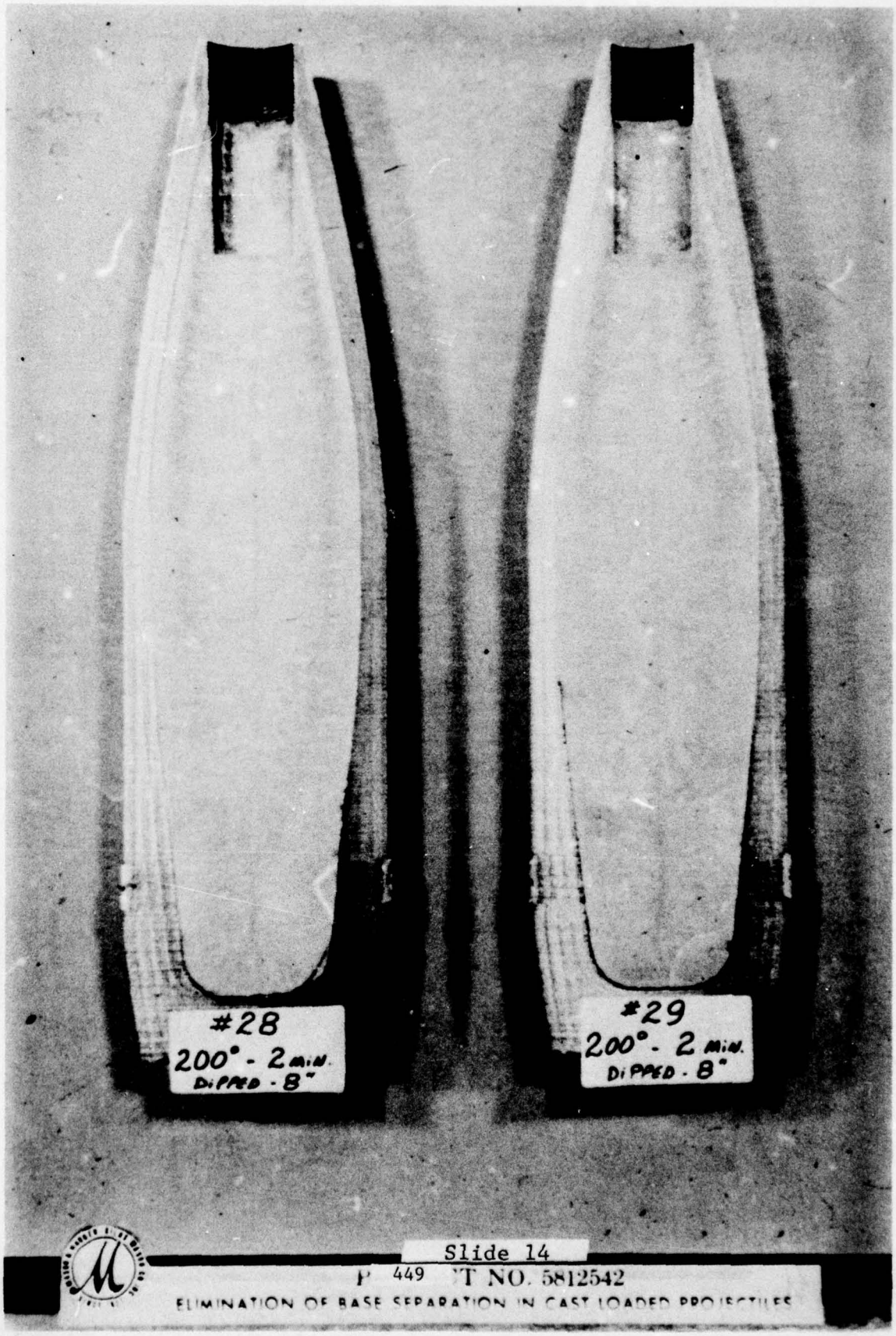


Slide 13

448

PROJECT NO. 5812542

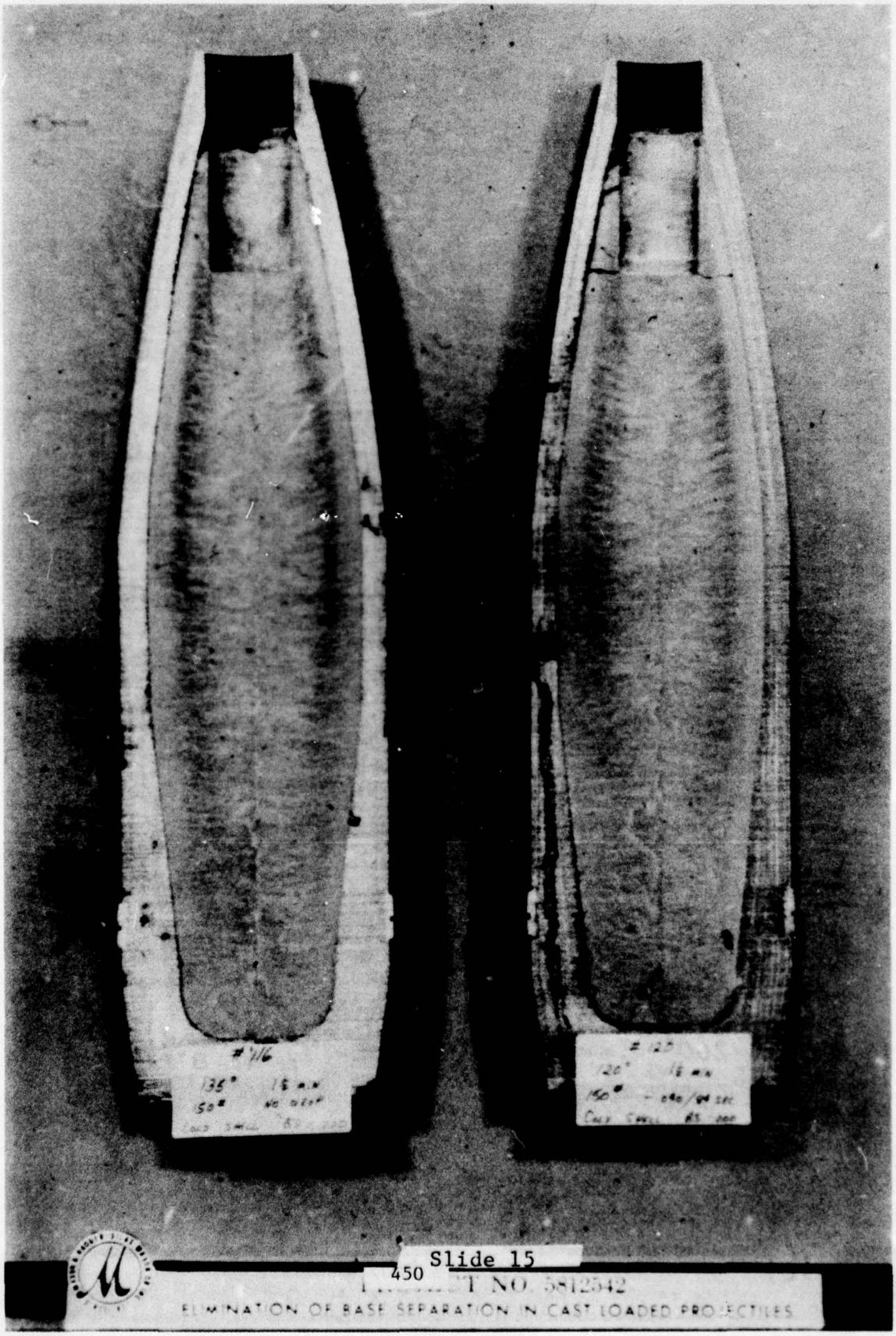
ELIMINATION OF BASE SEPARATION IN CAST LOADED PROJECTILES



Slide 14

P 449 VT NO. 5812542

ELIMINATION OF BASE SEPARATION IN CAST LOADED PROJECTILES

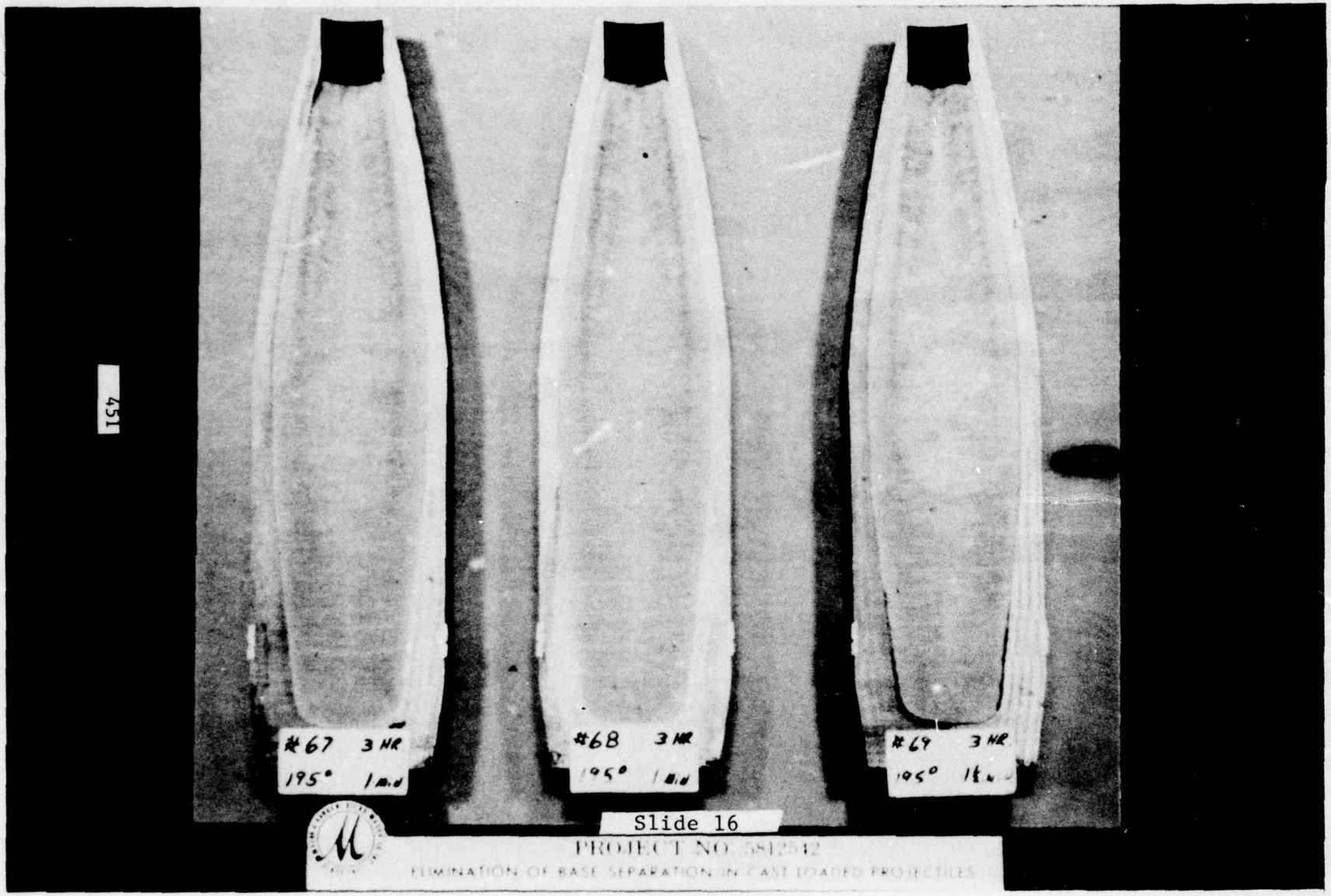


Slide 15

450

PATENT NO. 5812542

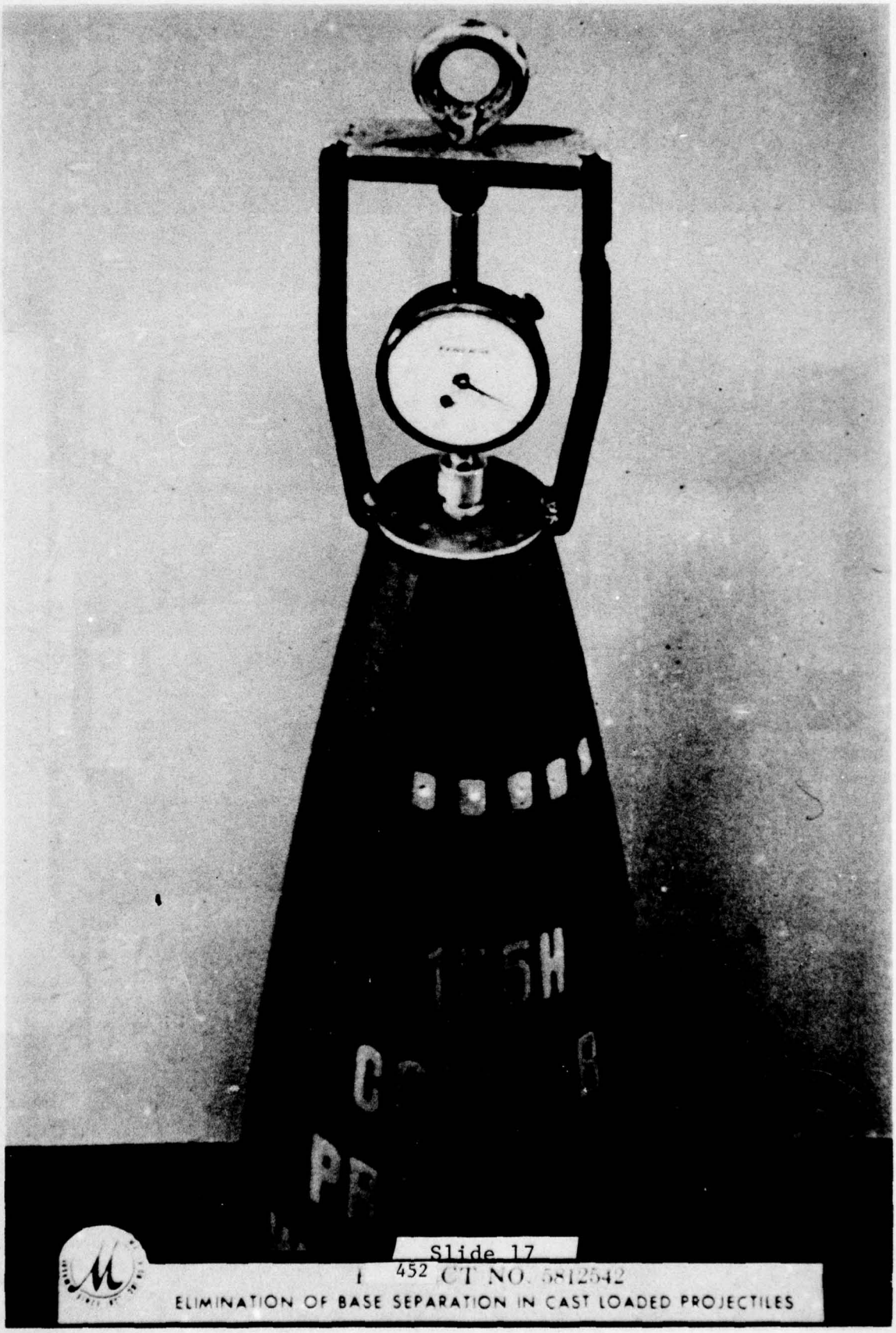
ELIMINATION OF BASE SEPARATION IN CAST LOADED PROJECTILES



Slide 16

PROJECT NO. 581242

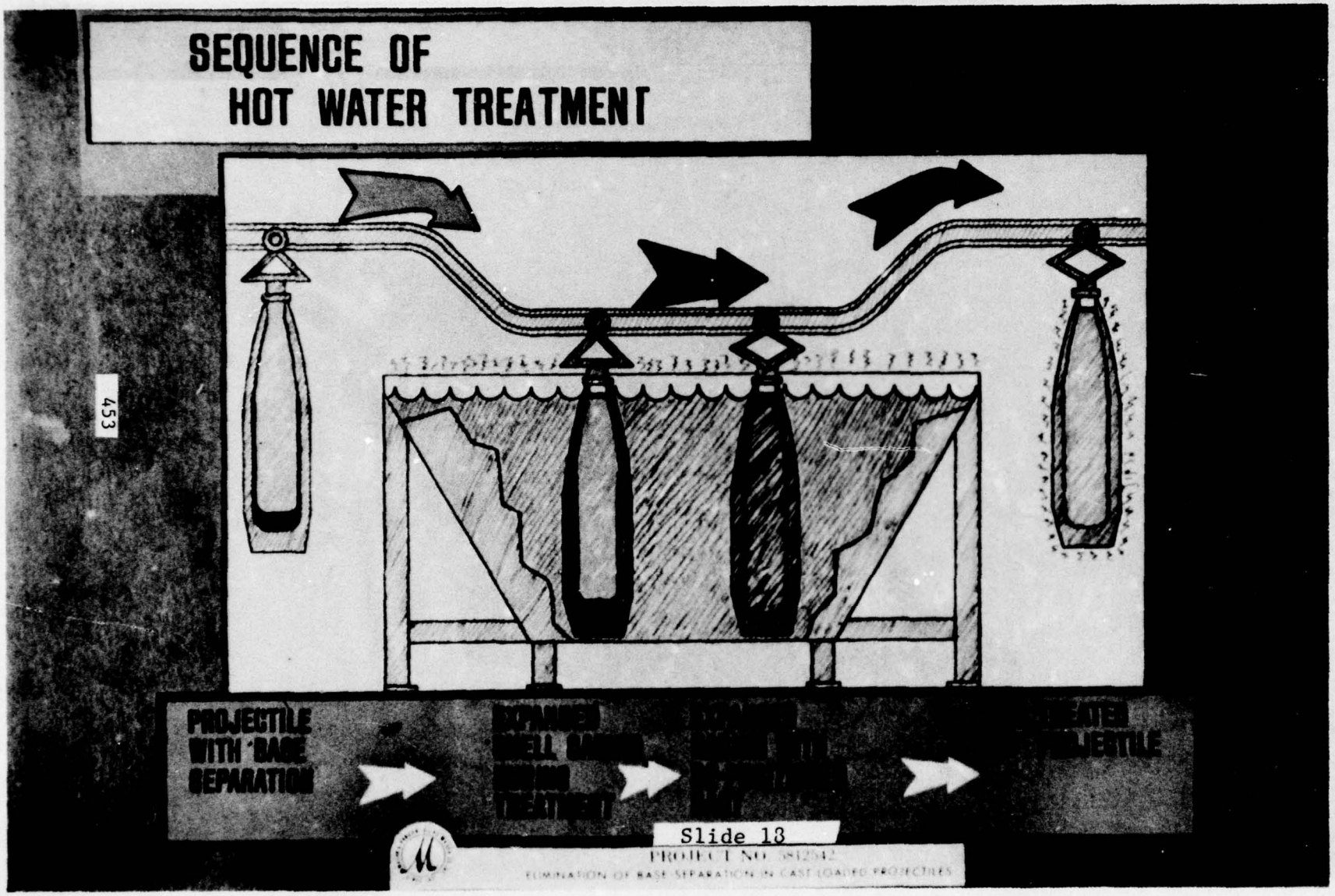
ELIMINATION OF BASE SEPARATION IN CAST LOADED PROJECTILES

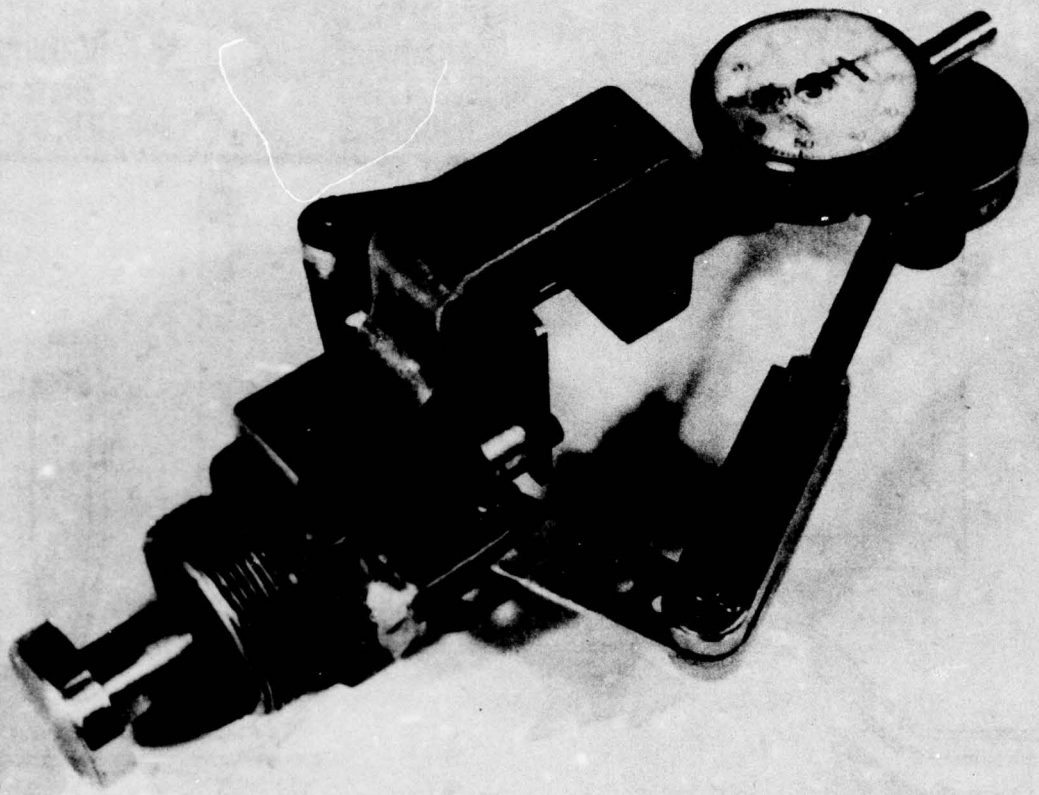


Slide 17

452 CT NO. 5812542

ELIMINATION OF BASE SEPARATION IN CAST LOADED PROJECTILES


SEQUENCE OF
HOT WATER TREATMENT
453
PROJECTILE
WITH BASE
SEPARATION
Slide 13
PROJECT NO. 681254
ELIMINATION OF BASE SEPARATION IN CAST LOADED PROJECTILES

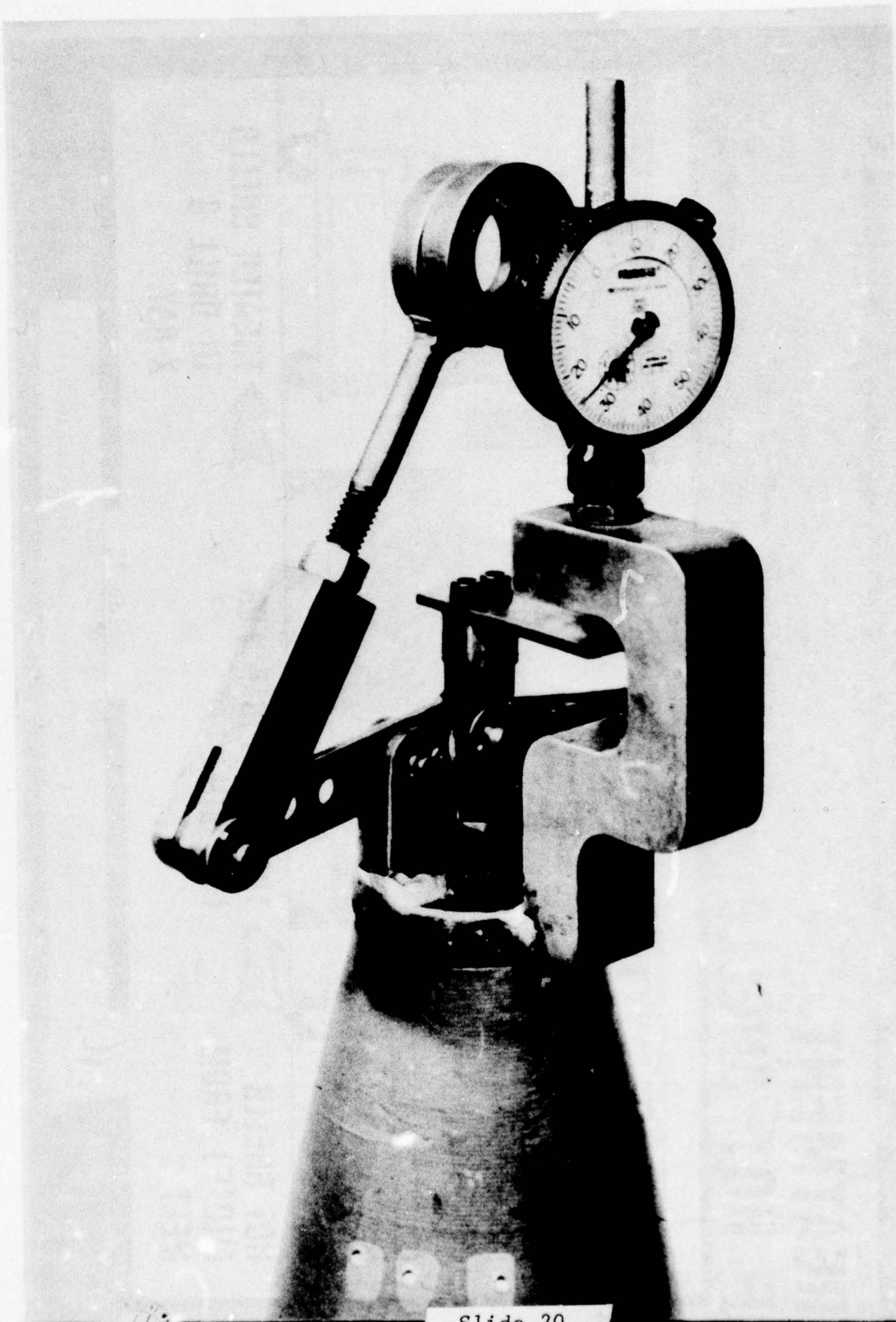


454

Slide 19

PROJECT NO. 5812542

ELIMINATION OF BASE SEPARATION IN CAST LOADED PROJECTILES

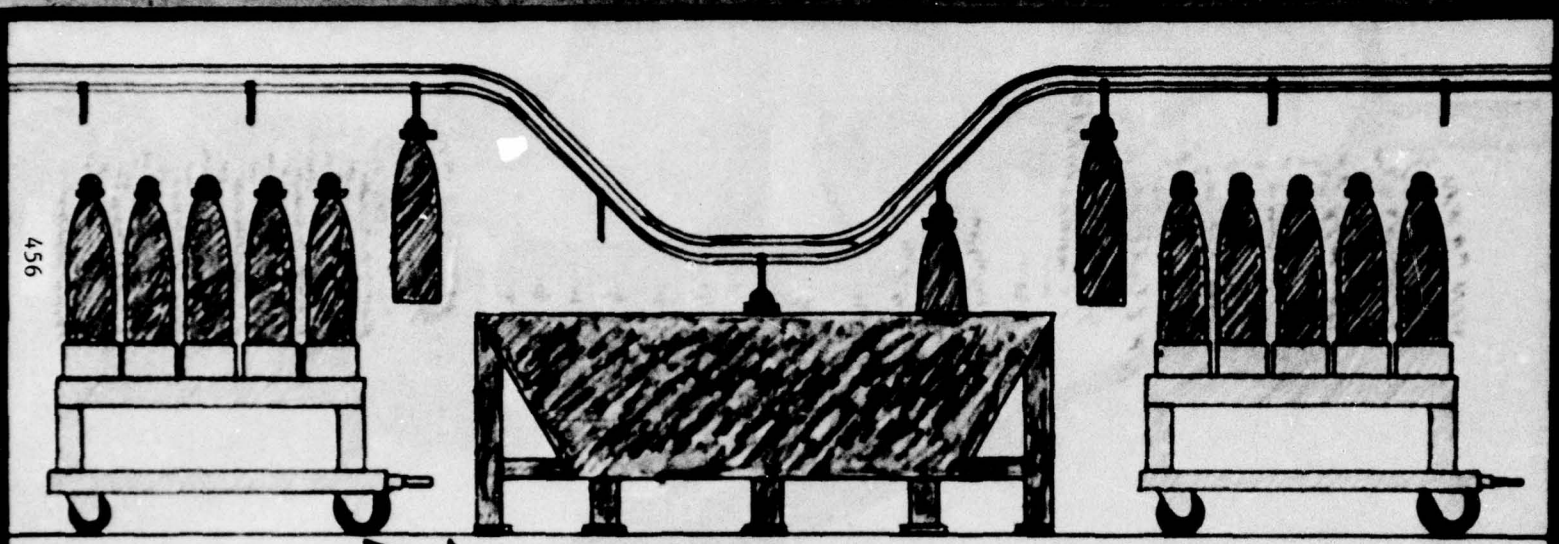


Slide 20

PROJECT NO. 9120-02

ELIMINATION OF BASE SEPARATION IN CAST LOADED PROJECTILES

TREATMENT OF HOT SHELLS

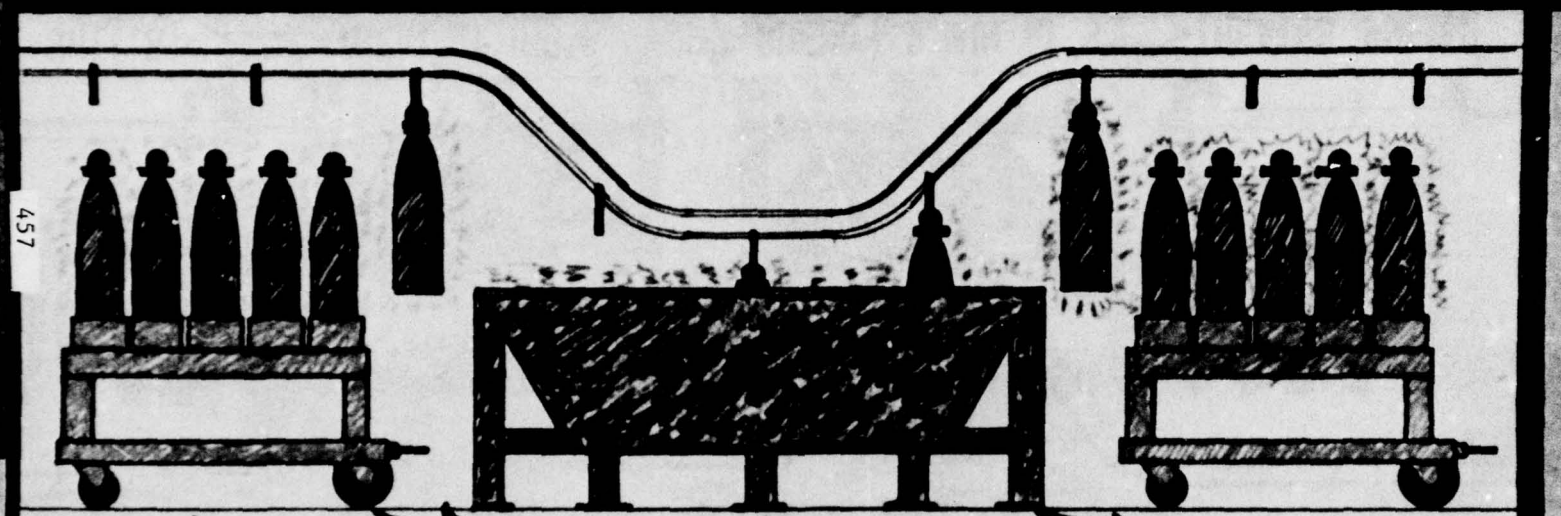


Slide 21

PROJECT NO. 581242

ELIMINATION OF BASE SEPARATION IN CAST LOADED PROJECTILES

TREATMENT OF COLD SHELLS

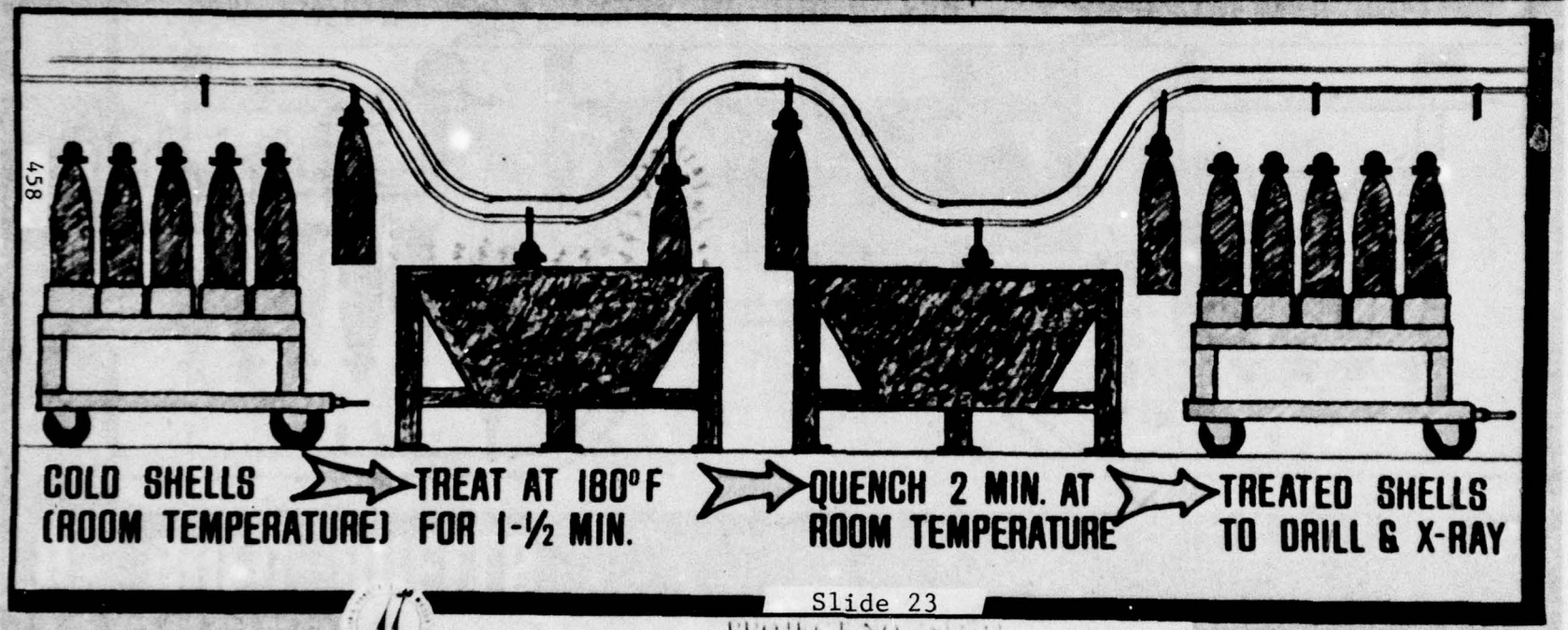


Slide 22

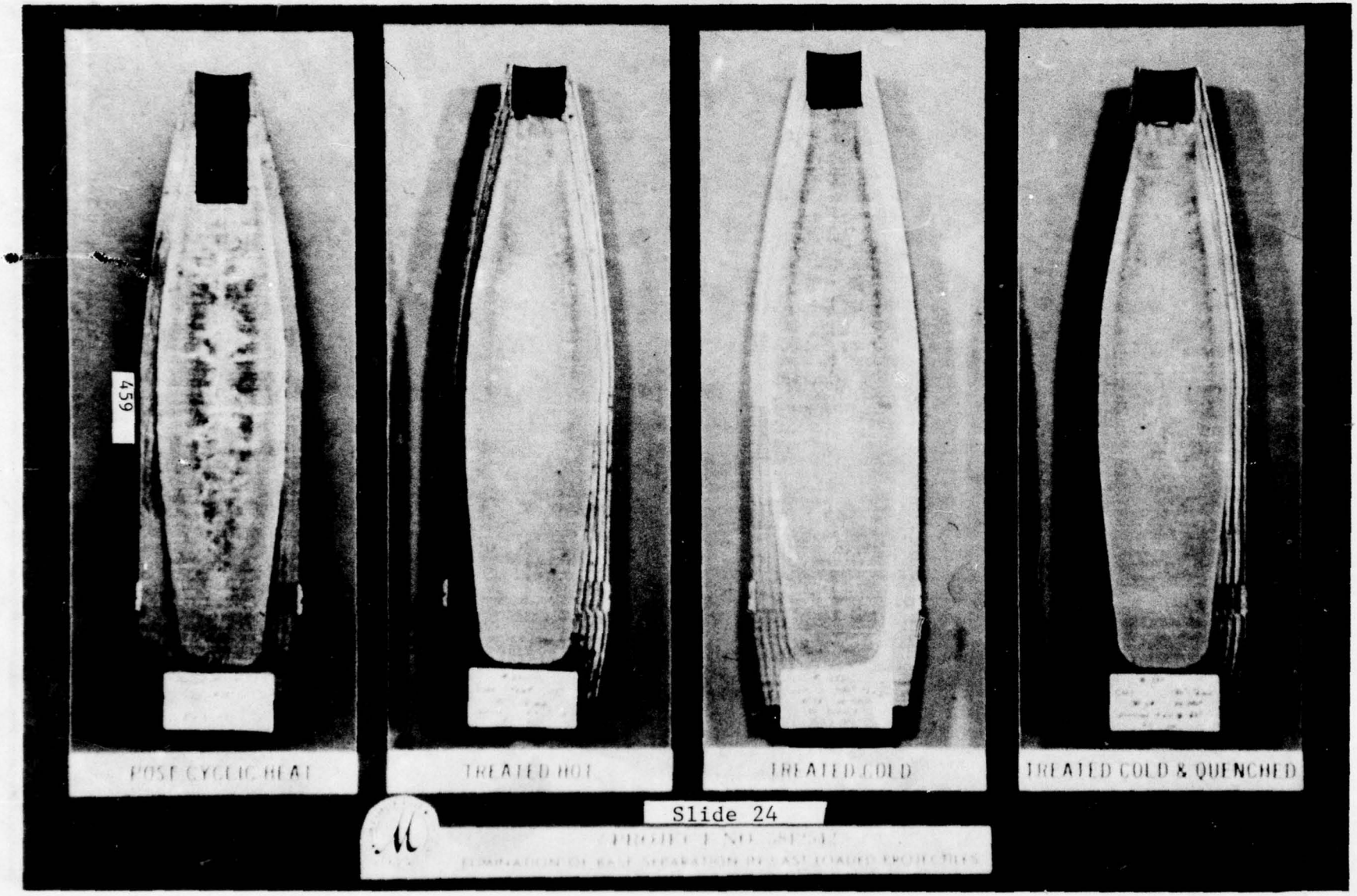
PROJECT NO. 581242

ELIMINATION OF BASE SEPARATION IN CAST LOADED PROJECTILES

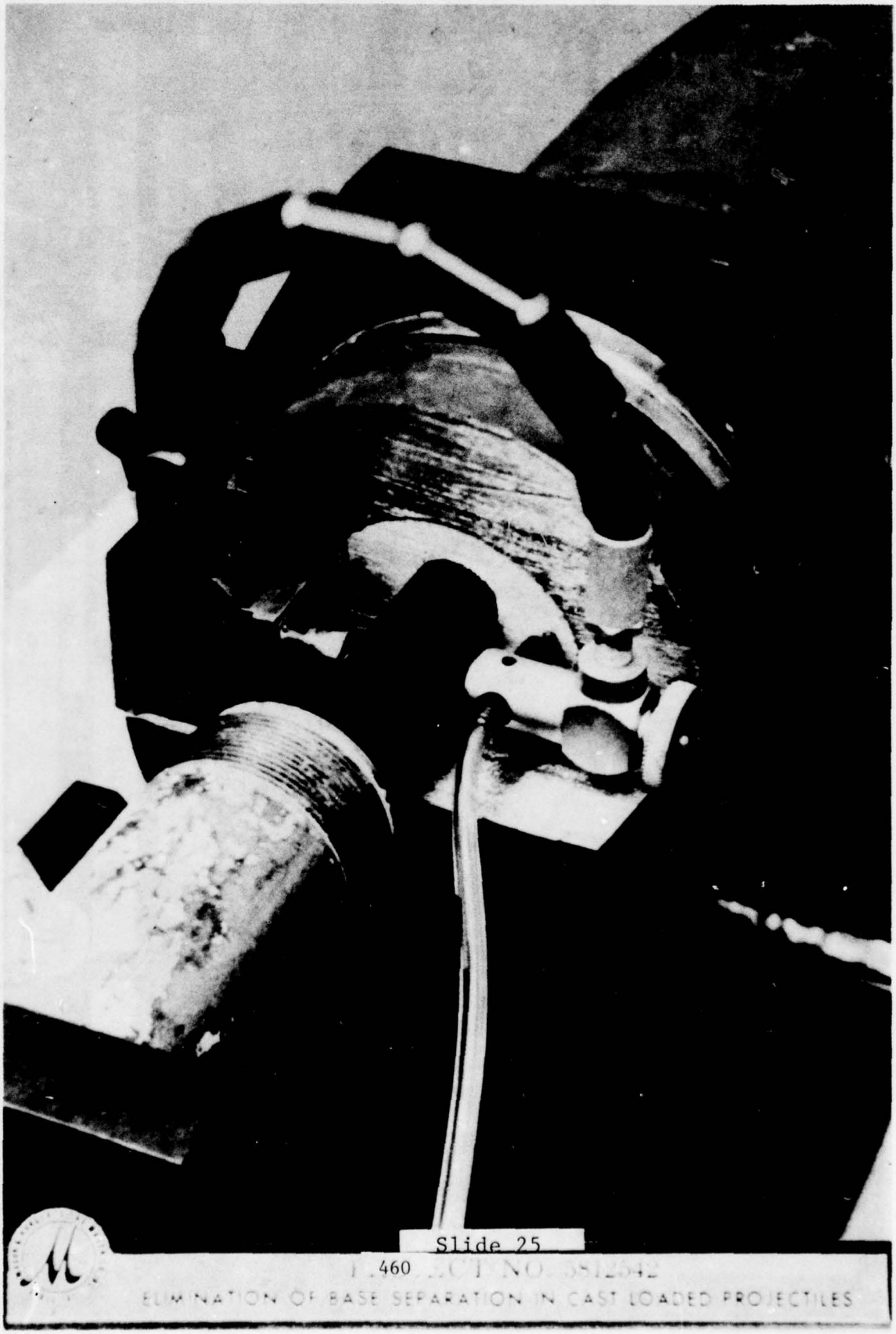
QUENCH TREATMENT OF COLD SHELLS



Slide 23


459
POST CYCLIC HEAT
TREATED HOT
TREATED COLD
TREATED COLD & QUENCHED

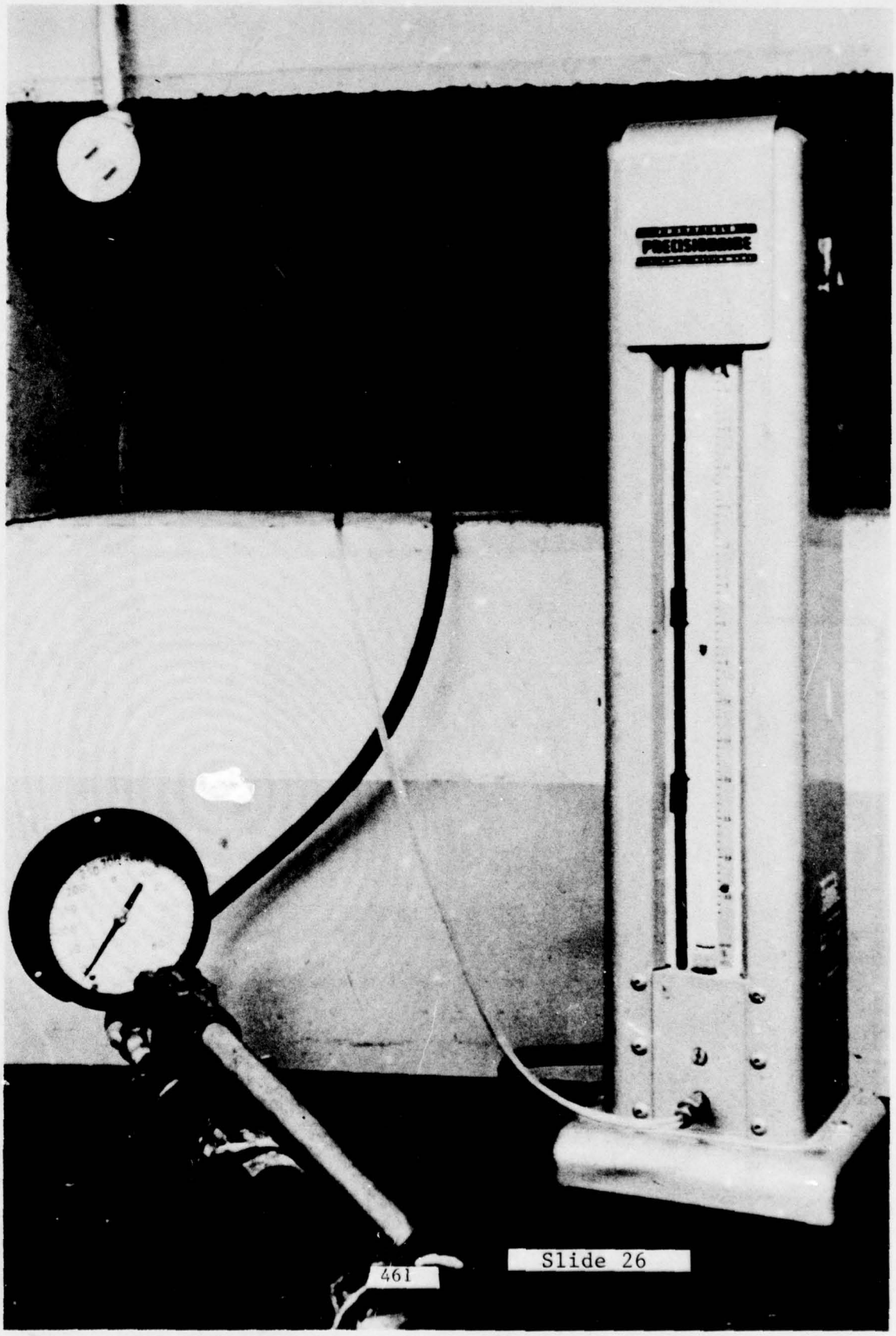
Slide 24



Slide 25

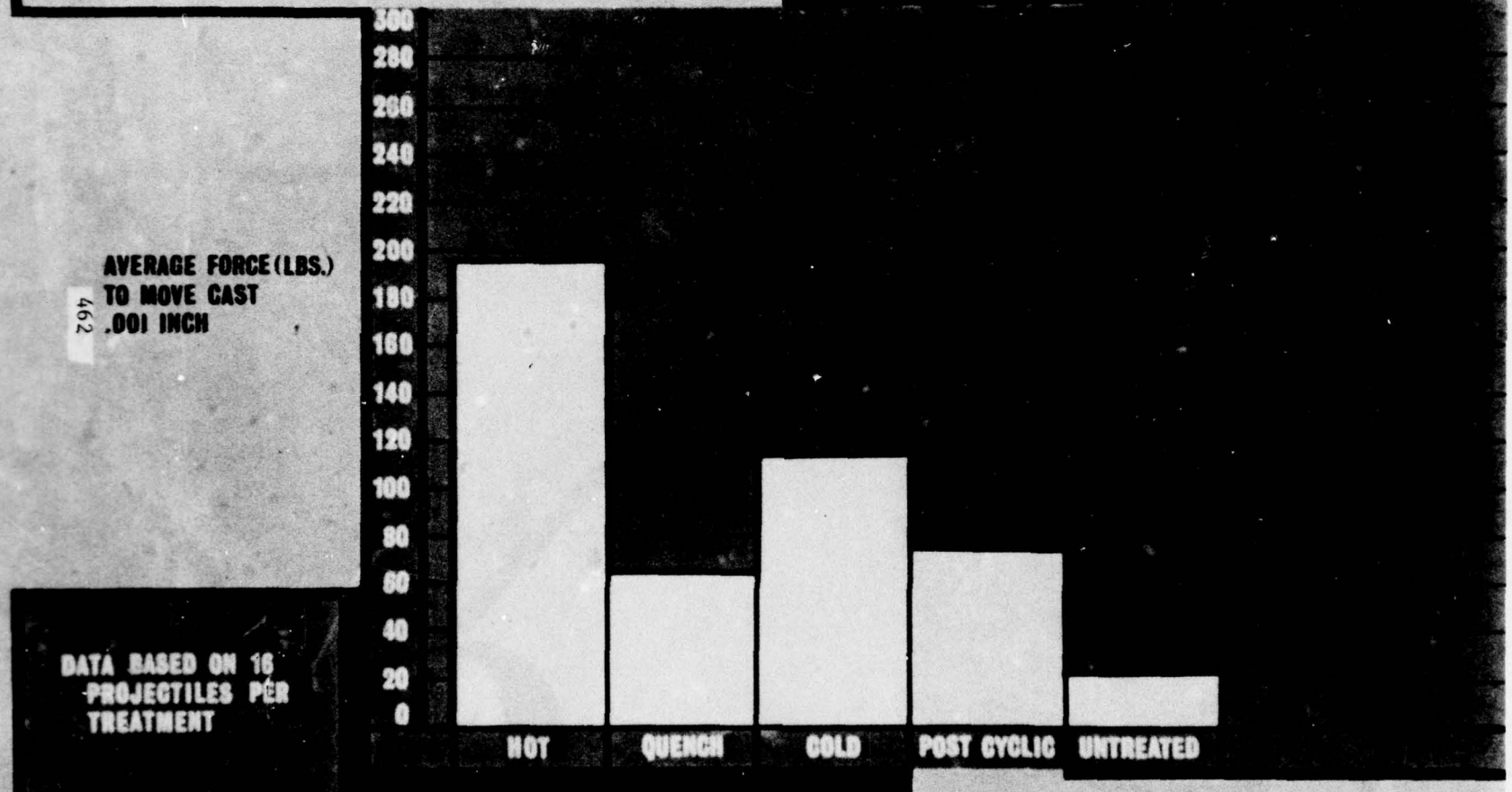
1.460 PROJECT NO. 581242

ELIMINATION OF BASE SEPARATION IN CAST LOADED PROJECTILES



Slide 26

M107 CAST TIGHTNESS



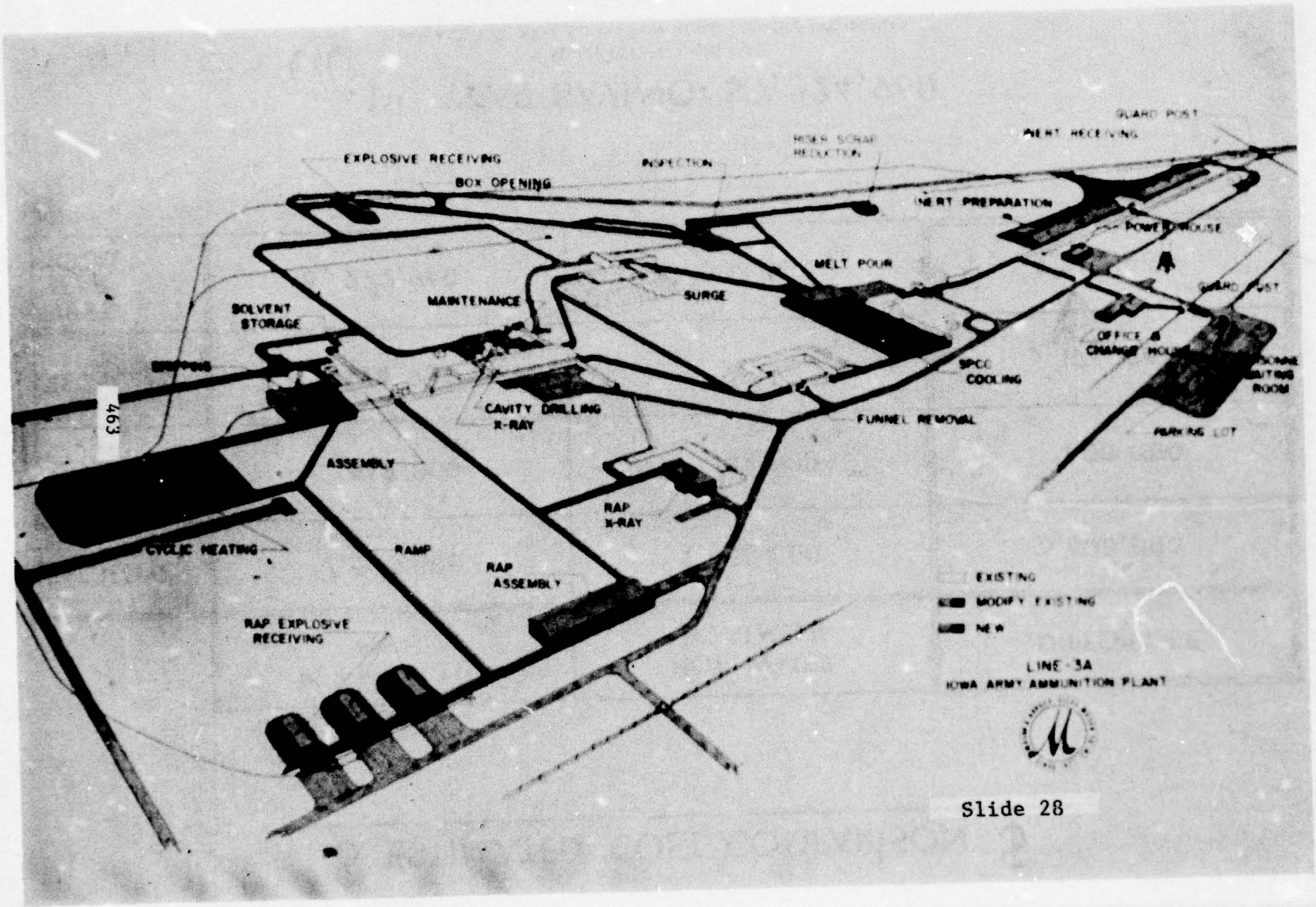
462

DATA BASED ON 16 PROJECTILES PER TREATMENT

Slide 27

PROJECT NO. 581242

ELIMINATION OF BASE SEPARATION IN CAST LOADED PROJECTILES


EXPLOSIVE RECEIVING
BOX OPENING
INERT PREPARATION
MELT POUR
SURGE
MAINTENANCE
SOLVENT STORAGE
CAVITY DRILLING X-RAY
FUNNEL REMOVAL
SPCC COOLING
ASSEMBLY
RAP X-RAY
CYCLIC HEATING
RAMP
RAP ASSEMBLY
RAP EXPLOSIVE RECEIVING
463
EXISTING
MODIFY EXISTING
NEW
LINE 5A
IOWA ARMY AMMUNITION PLANT

Slide 28

$ ESTIMATED COST COMPARISON $

	POST CYCLIC HEAT	HOT WATER TREATMENT	DIFFERENCE
FACILITIES	7,500,000	1,000,000	6,500,000
ANNUAL TREATMENT COST	648,000	48,000	600,000
RECYCLES	174,960	0	174,960
FIRST YEAR TOTAL	8, 272,960	1, 048,000	7,224,960

464

Slide 29

1st YEAR SAVING: $ 7,224,960

PROJECT NO. 5812542

ELIMINATION OF BASE SEPARATION IN CAST LOADED PROJECTILES

IOWA ARMY AMMUNTION PLANT



465

Slide 30

ENGINEERS AND CONTRACTORS

NOISE ABATEMENT PROGRAM FOR EXPLOSIVE OPERATIONS AT NSWC/DL

by

L. L. Pater, Ph.D.
Naval Surface Weapons Center
Dahlgren, VA

ABSTRACT

This paper is a summary and description of noise abatement research, procedures and results at the Naval Surface Weapons Center/Dahlgren Laboratory, Dahlgren, Virginia. The type of noise of concern is impulse noise resulting from explosive operations and gunfire. Topics discussed include atmospheric sound focusing, noise abatement procedures and facilities, and noise limit criteria.

Cleared for open publication 13 Sept 1976 -
Directorate for Freedom of Information and
Security Review (DASD-PA), Department of Defense
Review of this material does not imply Department of
Defense endorsement of factual accuracy or opinion.

PRECEDING PAGE BLANK-NOT FI

NOISE ABATEMENT PROGRAM FOR EXPLOSIVE OPERATIONS AT NSWC/DL

INTRODUCTION

The production of excessive noise, or "noise pollution", is an important operational consideration for most activities that involve explosive operations. Requirements for control and reduction of noise pollution have recently increased as a result of increased population awareness of and concern for environmental quality. This paper is a summary of noise abatement research, procedures and accomplishments at the Naval Surface Weapons Center, Dahlgren Laboratory (NSWC/DL) (formerly Naval Weapons Laboratory), Dahlgren, Virginia.

BACKGROUND

Explosive operations at NSWC/DL range from unique research and development experiments to routine "proof and acceptance" testing. These explosive operations include: firing of guns ranging in size from small arms to 16-inch (406mm) Naval guns; static detonation of explosives ranging in size from a few grams to over 1000 lbs. (454 Kg) (TNT equivalent) for some bomb/warhead cook-off and sympathetic detonation experiments; and firing of rocket motors. NSWC/DL is located along the Potomac River in a rural area of moderate but increasing population density.

Active efforts to reduce noise from explosive operations at NSWC/DL began in 1970. As a first step, sound pressure level measurements were made at many locations, including locations at distances up to 20 miles (32 kilometers) from NSWC/DL. The measured sound pressure levels were sometimes significantly higher or lower than expected, as compared to predictions of sound pressure level for appropriate range and explosive weight. It was quickly determined that the explanation for such discrepancies between predicted and measured sound pressure levels is a refraction phenomenon known as "atmospheric sound focusing".

ATMOSPHERIC SOUND FOCUSING

The predicted sound pressure levels mentioned above were "free air" predictions. The free air prediction (reference 1) is the expected surface air blast pressure from an explosion in an atmosphere that is uniform and stationary, so that sound rays travel along straight lines (no refraction occurs). In the real atmosphere, variations in sound propagation velocity cause sound rays to travel along curved lines (refract). Thus, atmospheric sound focusing is a refraction phenomenon resulting from variations of sound propagation velocity in the atmosphere.* The sound propagation velocity is primarily a function of temperature and

*Similar refraction phenomena are of importance for SONAR, involving the propagation of sound through water, and RADAR, involving the propagation of electromagnetic radiation through the atmosphere.

wind speed and direction. Certain atmospheric structures can result in focusing of considerable amounts of sound energy onto a relatively small region of the earth's surface. The sound levels in such focal regions can be considerably greater than would otherwise be expected. On the other hand, atmospheric structures which reduce surface sound levels also occur. Atmospheric conditions that result in focusing are dynamic, varying seasonally, daily, and even hourly. Accurate prediction of atmospheric sound focusing, and curtailment of explosive operations during periods when resulting noise levels would be high in sensitive areas, can result in significantly reduced numbers of noise complaints. Conversely, atmospheric conditions which result in significantly reduced noise levels (sound energy refracted away from the earth's surface, into the upper atmosphere) present opportunities to detonate large amounts of explosives with significantly reduced risk of noise disturbance.

SOUND INTENSITY PREDICTION SYSTEM

Having recognized the importance and possible consequences of atmospheric sound focusing, the objective became to develop a capability to predict atmospheric sound focusing effects. In particular, it was desired to be able to accurately predict the location and sound level of focal regions. This objective was realized by development of the Sound Intensity Prediction System (SIPS), a computer code which is described in detail, along with a mathematical model for atmospheric sound focusing, in reference 2. Required input data for the SIPS computer code are current meteorological data, specifically temperature, wind speed and wind direction as functions of altitude. These data are used to generate profiles of sound speed as a function of altitude. Wind causes the sound speed profile to be in general different for each azimuthal direction of interest. Horizontal variations in sound speed are not accounted for; such variations were found to be generally small compared with vertical variations, and their inclusion would very greatly increase the complexity of the calculation procedures.

The sound speed profiles calculated from the meteorological data are used in what is basically a ray-tracing calculation procedure, with the effect of atmospheric refraction on spherical energy spreading accounted for, to calculate predicted overpressure levels as a function of range and azimuthal direction for the geographical region surrounding the detonation site. A requirement for short calculation time (short turn-around time) dictated that a somewhat simplified mathematical model be used. A consequence of the simplified model is that the predicted over-pressure levels at focal points are somewhat higher than the overpressure levels that actually occur. During validation of the SIPS computer code, in which predictions and field measurements were compared (reference 3), a semi-empirical method of interpreting the predicted overpressure levels was developed and incorporated into the computer code. The resulting output of the SIPS computer code gives accurate predictions of overpressure

levels in the surrounding area due to explosive operations, in a format that is easily understandable without extensive technical knowledge or background.

NOISE ABATEMENT PROGRAM

There are basically two methods of reducing noise levels due to explosive operations. One method is to reduce the amount of sound energy generated at the source; that is, to reduce the amount of explosive detonated. This technique should be pursued when feasible, but often involves serious operational restrictions. The second, more subtle but often more fruitful, method is to avoid the deleterious effects and take advantage of the beneficial effects of atmospheric sound focusing. The Sound Intensity Prediction System computer code facilitates the implementation of this second approach by providing an automated, accurate and detailed prediction of the effects of an explosion.

A summary of the essential requirements for an effective noise abatement program utilizing prediction of atmospheric sound focusing includes: accurate and timely meteorological data; a rapid, accurate, detailed method of predicting atmospheric sound focusing effects (computer code); adequate computer facilities; a noise limit criterion; and integration of noise abatement information and procedures into overall operations. These essential elements were integrated to develop an effective noise abatement program as shown in Figure 1. Note that public relations is an integral part of the program.

As shown in Figure 1, the overall objective of the program is a reduction in the number of noise complaints received as a result of explosive operations. This is achieved (second row of blocks) by the actions of scheduling explosive operations as dictated by atmospheric sound focusing conditions, by modifying test procedures to reduce the output of acoustic energy, and by means of good public relations with the area population.

The basic tools required for these noise abatement actions are shown in the third row of blocks in Figure 1. "Effective prediction systems" are required, as previously mentioned, to predict the noise pollution effects of an explosion. "Noise limit criteria" are a set of guidelines for allowable noise levels, and may be established by law or ordinance or may be self-imposed. A description of the noise limit criteria in use at NSWC/DL is given later in this paper. Functionally, the noise limit criteria constitute the standard against which predicted noise levels are compared for the purpose of deciding whether to proceed with or postpone a scheduled explosive operation. "Problem programs identified" simply refers to the fact that it is desirable to know with some certainty which types of explosive operations are likely to result in noise disturbance. Such knowledge can help to minimize noise abatement cost and impact on operations without degrading the effectiveness of the noise

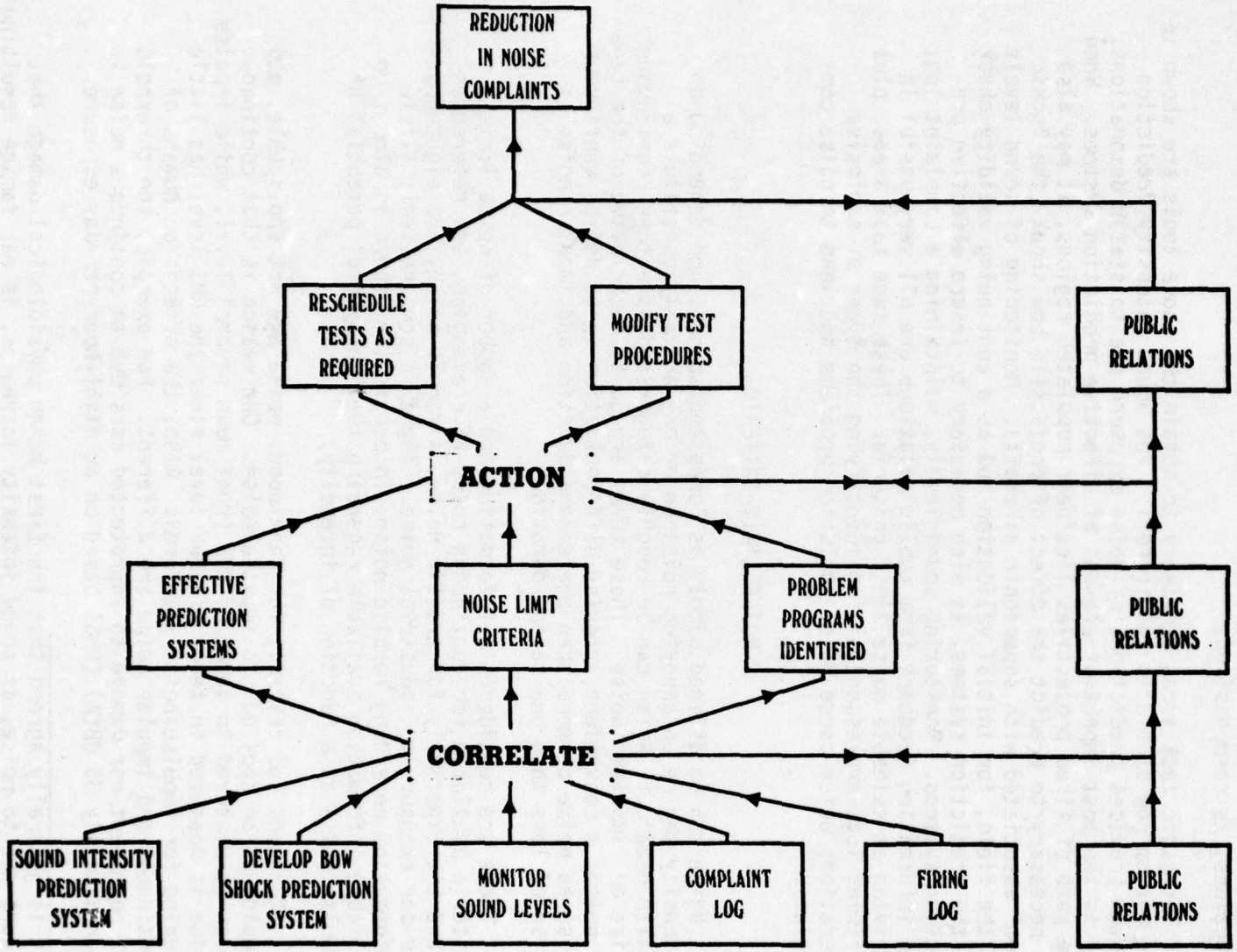


FIGURE 1. NSWC/DL NOISE ABATEMENT PROGRAM

abatement program. Finally, the importance of public relations, and the importance of information exchange between technical and public relations functions, is reemphasized.

The basic task areas necessary to obtain the above tools are shown in the bottom row of blocks in Figure 1. The Sound Intensity Prediction System provides predictions of noise exposure due to static detonations, and is the most important element of effective prediction systems. When the path of fired projectiles lies near populated regions, it may also be necessary to predict the effect of projectile bow shock (the "sonic boom" associated with supersonic aircraft). Monitoring of sound levels in the field, for initial validation and as a continuing validity check of the prediction systems, is also necessary to insure effective prediction systems. Monitoring sound levels, maintaining a complaint log, and information feedback from public relations are all very useful in arriving at suitable noise limit criteria. These same task areas, plus a firing log, are essential for identifying the types of explosive operations which cause noise pollution problems and lead to noise complaints.

NOISE LIMIT CRITERIA

Noise can be defined simply as "unwanted sound", and depending on intensity may be an annoying nuisance or may actually constitute a health hazard.* Noise can be roughly categorized as either "continuous" noise or "impulse" noise. These terms are quite descriptive of the type of noise; a convenient, precise differentiation is to define continuous noise as noise of more than one second duration and impulse noise as noise of less than one second duration.

There are considerable information and a number of noise limit criteria available for continuous noise (for examples, see references 4 and 5), especially for traffic noise, aircraft noise, and eight-hour-per-day exposure to industrial noise. There is comparatively little information regarding impulse noise; in particular, there is almost no reliable information available regarding the "annoyance" potential of impulse noise as a function of intensity.

Standards and criteria for continuous noise are not applicable, and should not be applied, to impulse noise. One reason is that continuous noise is measured in terms of RMS (root mean square) level, while impulse noise is measured in terms of peak level since the RMS level has little meaning for impulse noise waveforms. Also, the effects on humans of continuous and impulse noise are different. For example, the threshold for permanent ear damage to unprotected ears due to continuous noise is approximately 85 dB(A) (RMS) based on an eight-hour-per-day exposure

*It is generally agreed that the first human physiological damage that occurs due to noise, as sound intensity increases, is ear damage resulting in temporary or permanent impairment of hearing.

(references 4 and 5), while the threshold for permanent ear damage to unprotected ears due to impulse noise is approximately 140 dB (peak) based on 100 exposures per day (references 5 and 6).* Also, the spectral characteristics (intensity as a function of frequency) of continuous and impulse noise are in general greatly different. In summary, it can be concluded that standards and criteria for continuous noise cannot be applied to impulse noise.

When contemplating Noise Limit Criteria for impulse noise, then, one finds very little objective guidance available. Factors to be considered include the possibilities of structural damage to buildings and physiological damage to humans, and the likelihood of receiving annoyance noise complaints. It appears fairly certain that the first structural damage to occur as impulse sound intensity increases is window breakage (references 5, 8, 9, 10, 11), the threshold for which appears to be approximately 150 dB to crack a poorly mounted window pane (reference 10). The threshold for physiological damage, as mentioned earlier, is approximately 140 dB; this value was chosen as the maximum permissible sound level exposure for impulse noise. The threshold for annoyance is certainly lower than 140 dB, and varies greatly amond individuals. As summarized in reference 5, individual response of community members to noise depends on many factors. Some of these factors are of course the characteristics of the noise, including the intensity level and spectral characteristics, duration, repetitions, abruptness of onset or cessation, and the noise climate or background noise against which a particular noise event occurs. Social surveys have shown that other factors include the degree of interference of the noise with activity, the previous experience of the community with the particular noise, the time of day during which the intruding noise occurs, fear of personal danger associated with activities of noise sources, socioeconomic status and educational level of the community, the extent to which community members believe they are being treated fairly, the attitude of the community's residents regarding the contributions of the activities of the noise source to the general well-being of the community (for example, as a major employer), and the extent to which residents of the community believe that the noise output could be controlled.

---

*The units "dB", or decibels, are convenient units for pressure because of the wide range of sound pressure level that is of interest for noise, from 20 μPa (2.9×10^{-9} psi) to very high blast pressures of as much as 69,000 Pa (≈10 psi) or higher. The formula for sound pressure level expressed in dB is $SPL = 10 \log_{10} (\frac{P}{Po})^2 = 20 \log_{10} (\frac{P}{Po})$, where P is the gauge pressure (RMS for continuous noise, peak for impulse noise) of the sound wave and Po is a reference gauge pressure, the preferred value being (reference 7) 20 μPa, which is the lowest pressure detectable by normal, young human ears. Using the definition, 20 μPa = 0 dB and 69,000 Pa = 191 dB, yielding a more convenient range of numbers. The symbol (A) indicates the "A" frequency weighting scale, which simulates approximately the response of human ears at low sound intensity.

The approach used at NSWC/DL during derivation of Noise Limit Criteria for explosive operations was to use 140 dB as the absolute maximum allowable exposure level, and to estimate the risk of annoying community residents as a function of sound level exposure for sound levels of less than 140 dB, with some weighting according to the number of repetitions. These estimates were made by means of subjective judgements during field measurements of explosive operations noise events in the surrounding community.* The initial criteria were to be refined as needed based on noise complaints received. The resulting criteria, now in use at NSWC/DL, are shown in Table 1.

NOISE ABATEMENT PROCEDURES

Some reduction in noise output has been achieved by modification of explosive operations procedures. For example, routine disposal of excess or expired ordnance (for which the most practical and safe method is on-site detonation) is now limited in terms of explosive weight per detonation and number and frequency of detonations.

Noise abatement is more commonly effected at NSWC/DL by scheduling/rescheduling explosive operations according to atmospheric sound focusing conditions. Normal procedure is relatively straightforward. For any explosive operation for which noise abatement procedures are required, a balloon-suspended radiosonde is released shortly before the scheduled time of the test, to obtain meteorological data affecting sound speed as a function of altitude. The resulting data are input to the SIPS computer code, and the resulting sound level predictions are compared with the Noise Limit Criteria to determine whether to proceed with or postpone the scheduled explosive operation. The total elapsed time from balloon release to decision is usually about 20 minutes.** The cost of each prediction, including supplies and labor, is approximately $300.

The atmospheric conditions that cause sound focusing are dynamic and can change very rapidly. Time required to obtain the prediction is about 20 minutes, and further delays often occur before the explosive operation is fired. Thus, it is desirable to know, at the time the firing key is closed, that the sound focusing prediction is still valid. This is accomplished at NSWC/DL by means of a remote atmospheric sensing device, a Monostatic Acoustic Echo Sounder.*** This device emits bursts of sound and detects reflections (back-scattering) from anomalies in the atmosphere, especially temperature inversions (a prime cause of atmospheric sound focusing). The device is somewhat limited in that the vertical range is about 1 kilometer (3280 feet) and only a qualitative indication of the

---

*It is worth noting that these field measurements also showed that noise exposure levels due to NSWC/DL explosive operations only very rarely approached 140 dB.

**Reduction in this 20 minute turnaround time could be achieved by more sophisticated and automated (and costly) data gathering and data handling facilities and procedures.

*** Procured from Wave Propogation Laboratory, National Oceanic and Atmospheric Administration, Boulder, Colorado.

TABLE 1

NSWC/DL NOISE LIMIT CRITERIA

Predicted Exposure Sound Level (dB re 20 μPa)	Risk	Action
0-115	Low risk of noise complaints.	Fire all programs.
115-130	Moderate risk of noise complaints.	Fire important tests. Postpone non-critical testing, if feasible.
130-140	High risk of noise complaints, possibility of damage claims.	Only extremely important tests should be fired.
Greater than 140 dB	Threshold for permanent physiological damage to unprotected human ears. High risk of physiological and structural damage claims.	Postpone all explosive operations.

NOTE: For rapid fire test programs and/or programs that involve a large number of repetitions of impulse noise, reduce allowable sound levels by 15 dB.

strength of the back-scattering anomaly is obtained (location of the anomaly is obtained quite accurately). Nearly real-time data (the only delay is the transit time of a sound wave) is obtained, and is recorded on a strip-chart recorder, so that changes in atmospheric structure can be discerned at a glance. This device has proved to be very useful for indicating the continued validity of focusing predictions obtained earlier in the day.

Noise abatement procedures are not utilized for all explosive operations at NSWC/DL. Detonations of very small quantities of explosives have little potential for causing noise disturbance; utilization of noise abatement procedures for such programs would not be cost-effective. Parametric studies were performed to determine the minimum explosive weight for which noise abatement procedures would be required. These parametric studies utilized the SIPS computer code, a large number of actual and fabricated meteorological data profiles, and the Noise Limit Criteria. It was found, from examination of recent historical meteorological data records, that atmospheric structures that result in adverse atmospheric sound focusing occur quite frequently during the fall and winter months, and much less frequently during the spring and summer months. Accordingly, the following guidelines were selected:

> During the fall and winter months (October-March, January worst), when adverse atmospheric focusing is most likely to occur, focusing effect predictions may be required for firing of all guns larger than 5-inch and all explosives larger than (TNT equivalent) 10 lbs. During the spring and summer months, the requirements may be relaxed to guns larger than 8-inch and explosive weights larger than (TNT equivalent) 35 lbs. These requirements may be modified depending on circumstances (weather conditions, number of recent complaints, etc.) and/or on the basis of experience.

Another technique for reducing the cost without degrading the results of noise abatement has been to develop certain "rules of thumb". It has been found that, except possibly for very large explosions, normally only atmospheric conditions up to an altitude of 5000 feet or less are important in terms of atmospheric focusing.* Conditions at higher altitudes cause focusing, but the focal regions are at such extreme ranges that attenuation and energy spreading have adequately reduced the sound levels. Also, with experience it becomes possible to examine a meteorological data profile and sometimes determine that no adverse focusing effects will occur, thus obviating the need, delay and expense of carrying through with a complete focusing prediction.

*This conclusion has been confirmed by the Material Test Directorate, Aberdeen Proving Ground, Maryland (U.S. Army) during informal communication and information exchange.

RESULTS

The noise abatement program described in this paper was put into operation at NSWC/DL during May 1975. A measure of the success of the noise abatement program would be a comparison of the frequency of noise complaints received before and after initiation of the program. Unfortunately, prior to initiation of the program a noise complaint file had not been maintained and no single central point had been established for receiving noise complaints. Thus it was necessary to rely on the memory of individuals who had been associated with explosive operations prior to May 1975 to obtain an estimate of the frequency of noise complaints. Interviews with several such individuals have indicated that a conservative estimate is an average of three complaints per month, with as many as six received in a single month during the winter.

As of the writing of this paper, the noise abatement program has been in operation for 15 months. During that time, a total of 5 complaints have been received. One of these was found to be due to an aircraft sonic boom, and was hence invalid. Another was received within the first week after the program was initiated, and was due to an unforeseen procedural difficulty in utilization of the SIPS computer code. Two of the complaints were due to a type of testing (downrange fuze testing) for which noise abatement procedures were not utilized, and both were made by the same, apparently highly sensitive, citizen. The final complaint occurred during a 5-inch gun rapid-fire evaluation program, for which the sound level exposure was reasonably low (less than 115 dB) but which involved several hundred repetitions during a single day, indicating the validity of considering number and frequency, as well as magnitude, of impulse noise occurrences.

It can be seen that the number of noise complaints has been greatly reduced since the noise abatement program was initiated. Some of the reduction in the number of noise complaints may be attributable to a reduction in explosive operations at NSWC/DL, commensurate with the end of the Vietnam conflict. However, the evidence seems adequate to conclude that the NSWC/DL Noise Abatement Program has been very successful in reducing the amount and severity of community noise disturbance.

REFERENCES

1. Perkins, B., P. H. Lorrain and W. H. Townsend, "Forecasting the Focus of Air Blasts Due to Meteorological Conditions in the Lower Atmosphere," BRL Report No. 1118, October 1960.

2. Gholson, N. H., "An Analysis of Sound Ray Focusing," NWL Technical Report TR-2834, Naval Weapons Laboratory, Dahlgren, Virginia, January 1973.

3. Gholson, N. H., "Evaluation and Utilization of the NWL Sound Intensity Prediction System," NWL Technical Note TN-T-4/74, Naval Weapons Laboratory, Dahlgren, Virginia, October 1974.

4. "Fundamentals of Noise: Measurement, Rating Schemes, and Standards," U.S. Environmental Protection Agency Report No. NTID300.15, December 31, 1971.

5. "Public Health and Welfare Criteria for Noise," Environmental Protection Agency Report No. 550/9-73-002, July 27, 1973.

6. MIL-STD-1474(MI), "*Military Standard: Noise Limits for Army Material*," March 3, 1975.

7. "Preferred Reference Quantities for Acoustical Levels," American National Standard ANSI S1.8-1969.

8. Military Standardization Handbook MIL-HDBK-759, "Human Factors Engineering Design for Army Materiel," March 12, 1975.

9. Duvall, W. I. and D. E. Fogelson, "Review of Criteria for Estimating Damage to Residences from Blasting Vibrations," Report of Investigations No. 5968, Bureau of Mines, U.S. Dept. of the Interior, 1962.

10. Perkins, B., and W. F. Jackson, "Handbook for Prediction of Air Blast Focusing," BRL Report No. 1240, February 1964.

11. "Blasting Damage: A Guide for Adjustors and Engineers," Claims Bureau, Engineering and Safety Service and Property Claim Service of American Insurance Association, March, 1972.

"THE NOISE STANDARD REVISITED"

William V. Hollander
Winchester Group, Olin Corporation
New Haven, CT

Three weeks ago our moderator called my office to ensure that my talk was progressing satisfactorily, and my secretary assured him it was literally in the typewriter. Meanwhile, at another plant, I received a telephone call from our corporate loss prevention office: "Did you see today's Wall Street Journal"? "No." "You had better. We have lost our OSHA noise case before the Review Commission."

And there went my magnum opus!

The Continental Can (OSAHRC #3973 et als) and Turner (OSAHRC #3635) cases had been decided. Continental Can had won its review; Turner had lost.

The July issue of "Occupational Hazards" has an excellent summary of the Continental case, perceptively and accurately calling it out as a potential landmark decision. The involved Continental metal can manufacturing plants faced a $32 million cost to enclose 6300 machines in an attempt to bring the noise level down to 90 dB. The majority (Chairman Barnako and Commissioner Moran) found that this was not economically "feasible"; Commissioner Cleary flatly refused to accept the concept of economic feasibility.

The Turner metal can manufacturing plant was concerned with a $25,000 cost to enclose three machines in an attempt to bring the noise level down to 90 dB. (Commissioner Cleary and Chariman Barnako rejected the economics feasibility argument. After all, who could be concerned with so small an amount of money!)

With his usual elan, Commissioner Moran strongly dissented from the majority decision in Turner. I particularly commend to you the reading of his footnote number 28, where he points out that in Continental Chairman Barnako concluded that an expenditure of $494,000 to engineer

out the noise for 125 employees was not economically feasible, whereas in Turner it was concluded that $20 - 30,000 to protect nine employees was economically feasible. Thus, the per capita cost of reducing noise in both cases is approximately $3,000. 'The matter of economic feasibility is of vast importance to the industrial and commercial enterprises of this Nation. It is neither just, reasonable nor fair to have the law on this matter develop in such a willy-nilly fashion."

29 C.F.R. 1910. 95

OSHA is now in its fifth year of attempting to rewrite the noise standard, and at this writing nobody can truly forecast when the permanent standard will be finally issued and operational. The U. S. Chamber of Commerce publicly reviewed the proposed standard at a meeting in November, 1974 and stated that this was undoubtedly the most expensive standard in 29 CFR 1910. They committed that, if it was issued with engineering controls being mandatory and hearing protectors essentially being ignored, then they would contest the standard in the U. S. Court of Appeals under Article 6 (f) of the Act. They surely will be joined in that legal action by many organizations and companies. (And if the new standard is not set at 85 dB instead of the proposed 90 dB, then there will be unions who will challenge it in Federal court.)

It is a complete waste of time to elaborate on how noise "exposure" affects one's hearing. It does so not only at 90 dB, but also at 85 dB and at lesser noise levels.

High level noise is ubiquitous in industry: the man waving-in your jet plane at the Denver airport; the jack hammer operator breaking up the pavement; the skeet shooter at the Grand American; the policeman inside the Holland Tunnel. Even if they wear ear protectors, OSHA contends that this is not sufficient to protect them.

OSHA, of course, is concerned only with occupational noise. And they have chosen their battlegrounds most carefully. A night club or discotheque is an occupation so far as its employees are concerned--but have you ever seen a hostess with ear plugs?

Yet I will freely admit that noise emitted by any source can be engineered out--if unlimited funds are available. Even the noise of the jet plane being waved in to its dock can be "engineered out" so far as the solitary ramp employee is concerned.

The military services require action where noise exceeds 85 dB, and I personally have no problem with such a standard. Their action basically consists of ear protectors--not engineering out the noise. The position taken by the Department of the Army, for example, is seen in Technical Bulletin MED 251, 7 March 1972, paragraph 8:

> ... Little difficulty is experienced by persons with normal hearing in understanding speech when ear plugs or muffs are worn separately or in combination, if the voice is raised slightly above the level of ordinary conversation.

I personally find it much easier to understand speech when wearing E.A.R. plugs in a high noise area.

Even if there was an 85 dB OSHA standard, my position would be that ear protectors should be worn. As is now well known, a certain percentage of the population has a very low tolerance to noise--and that percentage should be as well protected as the 20% who will suffer a permanent loss of hearing at 90 dB.

I recently received a call from one of our plants: "What is our current policy on engineering out high noise levels?" "No change. If it will cost under $1,000, go ahead and do it. Otherwise, continue to rely on personal hearing protection. BUT: You must have a good hearing conservation program, with annual audiograms, review of audiograms, action taken on audiograms showing hearing deterioration; new employee training; policing the wearing of ear protectors."

This is taking a considered risk by us. Almost every manfuacturing plant has operations over 90 dB(A). An OSHA inspection could easily result in a citation under 29 CFR 1910. 95.

And we would fight such a citation in our multi-plant company as a matter of policy. Why?

OSHA has taken the position that a citation in one plant means that a company has been put on notice as to all of its plants. And we would be faced with a repeat violation. The ultimate citation could just as well be a wilful violation, with its Section 17 fine under the OSH Act of up to $10,000 for each violation.

The alternative to contesting your first noise citation is to accept the OSHA approach and engineer out the noise--irrespective of cost. Even if you know that you cannot reach 90 dB, spend the money anyhow. Then OSHA will let you protect employees with ear protectors--just as you have been doing all along. You have made the good try and OSHA now passes out your reward.

There is a booby trap in this approach. If OSHA comes back into the original plant and cites you for all the other equipment that is over 90 dB, then you probably will receive a repeat violation or even a wilful violation. The only solution is to "attempt" to engineer out all noise over 90 dB every place in the plant, and prove to the satisfaction of the OSHA inspector that you have made an honest engineering effort--and that you have an effective hearing conservation program. Of course, your company must have the money to do this.

HEARING CONSERVATION PROGRAM

Returning to the first noise inspection, if you do not have a "continuing, effective hearing conservation program" then expect to also receive a 1910. 95 (a) (3) citation as well as a 1910. 95 (a) (1) citation. While the standard does not refer to the "Guidelines to the Department of Labor's Occupational Noise Standard," Bulletin 334 (Revised 1971), this is what the inspector is looking for.

Interestingly enough, when we contested the 95 (a) (3) citation, the D.O.L. attorney waited until the hearing commenced to withdraw the citation. I would have much preferred to fight this one in court, as there had never been a Review Commission decision on just what was meant by this standard. If there ever was a vague standard, this one is it.

However, it is clear that if a plant does use ear protectors, then supervision is not the answer to an effective hearing conservation program. Baseline audiograms, annual audiograms, technical review of the audiograms, and the taking of action when there are negative indicators are all necessary. Incidentally, our large plants with all the necessary equipment to take audiograms have found that outside services do an excellent job of bringing in vans and initially testing employees. And for analysis of audiograms, whether in-house or outside, the computer services are invaluable time and money savers for even a small plant.

EXPOSURE

Let us assume that you have areas of over 90 dB (A), that the employees are in this environment for eight hours a day, that they properly wear ear protectors and that are correctly fitted. Are they "exposed" to noise as set forth in Table G-16?

Again, we are faced with a gray area in the law. Just what is meant by "exposure?" To me, merely being in a 100 dB environment does not mean a person is exposed to 100 dB sound. If he is in a sound-proofed enclosure while controlling his equipment, this is acceptable even to OSHA. If he is properly wearing correctly fitted ear protectors, then his ear drums are not exposed to 100 dB sound--at least that is my position. Many OSAHRC judges hold to the contrary.

Obviously, if the worker cuts off the tips of his ear plugs, he will be exposed to over 90 dB; or if he pokes holes in his ear muffs; I have even seen a person wearing his ear plugs in his ears--in a vertical position! Just what are the facts?

To the best of my knowledge, there is only one scientific and definitive published study on this subject. Du Pont in 1966 started a study of 2,770 employees out of a population of 18,758, in an environment of over 90 dB. In the February, 1973 issue of the Americal Industrial Hygiene Association Journal there appeared an article by S. Pell: "An Evaluation of a Hearing Conservation Program--a Five-Year Longitudinal Study." The noise was steady state and continuous throughout the working day, and the study showed "no indication of hearing loss" (id, p. 88.)

I have been unable to locate any similar scientific study setting forth an opposite conclusion. A doctoral disseration by a University of California student, apparently not having ever appeared in any scientific journal, concluded that ear protectors did not protect employees. (Actually, the paper only proved the case for the difficulty of getting people to use protection.)

CONTESTING THE CITATION

When Part 29 of the Code of Federal Regulations was issued in 1971 it was almost immediately clear that the standard which would have the greatest impact on industry was 1910. 95., "Occupational Noise Exposure." The problem was not so much the financial impact of engineering out noise from one machine due to an OSHA citation, but the legal result of doing so. In effect, every location within the plant would have to be similarly treated or else the plant would face a subsequent citation for a repeat or wilful violation, and a Section 17 fine can go to $10,000 for each violation.

(Today, of course, OSHA looks upon a citation in one plant as putting the employer on notice at all of the plants in the company.)

We recognized that with over 100 manufacturing plants within the United States we did not have the financial resources to engineer noise down to 90 dB. By 1972 we had agreed that the first plant to be cited for noise would not only contest the citation, but we would also appeal any

Review Commission decision going against us through the U. S. Court of Appeals and then through the U. S. Supreme Court.

In May 1973, our small Illinois plant engaged in making cans for propane gas was cited for noise. (The three employees involved were wearing personal hearing protection, and at the hearing the government attorney agreed that the plant did have an effective hearing conservation program.) Five months after our contesting the citation the government had two industrial hygienists survey the cited area with its three presses, and this was followed by their California noise consultant who prepared recommendations for engineering out the noise.

The hearing was held in June 1974. While the government testified as to noise between 90 and 100 dB, our arguments were based on a 100 dB level in the press room. The compliance officer saw only two presses in operation; we raised no objection to the industrial hygienists taking their subsequent readings with three presses in operation. Upon completion of the government's testimony, we waived our right to move for a dismissal. So you can see that we really wanted a legal resolution of 1910. 95.

Our objective was to obtain an ultimate judicial decision on the merits of the noise standard (1910. 95), and not invoke any legalistic gambit to win this case.

The OSH Review Commission noise cases selected for today's discussion all have the same factual situation, but undoubtedly the Continental and Turner cases will be applied to them:

1. Noise exceeded 90 dB
2. Employees were wearing personal hearing protectors.
3. An effective hearing conservation program was being followed, and there were no employees who had suffered a hearing loss as the result of their employment.
4. The case is currently on review before the Review Commission, following a decision by an OSAHRC judge.

The Goodrich Case (OSAHRC #2038)

Goodrich lost their citation contest and requested a hearing before the Review Commission, but this was denied. They then appealed to the U. S. Circuit Court of Appeals, where the case was returned to the Review Commission for "a more definite statement whether the feasible controls ordered will bring the noise level to or below 90 decibels during an eight hour day as required by 29 CFR 1910. 05 Table G-16 so that individual protective devices will not be required, and if not, the extent to which the feasible controls ordered will reduce the noise level." On April 1, 1976, the same OSAHRC judge found that "enclosures will bring the noise level to or below 90 dBA during an eight hour day." This time the Review Commission called the decision for review, to see if it was responsive to the Circuit Court's order of remand and supported by the evidence. (It is worthy of note that this is the only noise case that has reached a U. S. Circuit Court; there have been no Supreme Court cases.)

The Cox Enterprises Case (OSAHRC #12074)

Here the issue was whether engineering controls could be required for newspaper presses merely because they might reduce the noise level to Table 16 requirements. The judge ruled that an employer is not required to adopt engineering controls unless they will reduce noise below 90 dBA. The petition for review by OSHA submits that 1910. 95 (b) (1) requires such controls whether or not sound levels will be brought below the standard's requirement. (The proposed OSHA noise standard makes it crystal clear that this viewpoint of OSHA has prevailed--subject to a last minute change of heart or a reversal in a Federal court suit by employers or employer organizations such as the U. S. Chamber of Commerce.)

The Union Camp Case (OSAHRC #12203)

Union Camp won its case at the judge's level, and it was called for review by Commissioner Moran--but without Moran having stated what the issues were.

In the judge's decision are found the following:

Finding of Fact #7: "Employees of the respondent, by virtue of wearing ear protectors, are not exposed to noise in excess of Table G-16."

Conclusion of Law #6: "Engineering or administrative controls are not required unless it is established ... (they) will reduce the noise levels to the level permitted by Table G-16."

Conclusion of Law #9: "Respondent did not violate standard 29 C.F.R. 1910. 95 (b) (1) of the Act."

The West Point Pepperell Case (OSAHRC #8255)

The judge in this case, where the respondent argued that ear plugs meant he was not required to reduce the sound levels, held that the argument was in direct contradiction to the standard. A review has been ordered.

The Singer Co. Case (OSAHRC #7134)

Neither party petitioned for a review, and when it was ordered on the issue of vagueness of the standard neither party submitted a brief. The Review Commission in a 2-1 decision, declined to address the issues "in the absence of a compelling public interest." Commissioner Moran had written his usual erudite dissent, but the majority did not address the vagueness of the standard that he had raised as an issue.

Unfortunately, BNA and CCH seldom fully reproduce OSAHRC judge's decisions. If you are interested in reading any of the above cases, free copies may be obtained by writing or calling the Occupational Safety and Health Review Commission (1825 K Street, N.W., Washington DC 20006, Telephone 202-634-7943.)

ENVIRONMENTAL QUALITY STANDARDS FOR MUNITIONS-UNIQUE POLLUTANTS

John P. Glennon, CPT, MSC
LeRoy H. Reuter, LTC, MSC

U.S. Army Medical Bioengineering
Research and Development Laboratory
Fort Detrick, Frederick, Maryland 21701

INTRODUCTION

The U.S. Army Medical Research and Development Command is supporting research to determine the human health and environmental hazards associated with the Army's conventional munitions industry. The specific objective of this research program is to assemble the scientific data base from which environmental quality standards can be established. Primary emphasis in this program has been directed toward the evaluation of munitions-unique waste materials, in the form of air and water pollutants, that result from the manufacture, handling and demilitarization of conventional munitions. Additional efforts are being directed toward the industrial environment where the exposure of employees to toxic materials must be controlled to acceptable levels. This recently initiated research on potential occupational health hazards is evaluating the acceptability of Threshold Limit Values (TLVs) for certain munitions compounds and developing the criteria for TLVs where none exist.

Under this research program the human health and environmental concerns may be with the munitions product itself, the raw materials used in its manufacture, production or demilitarization by-products, or transformation products generated by pollution abatement facilities. Also addressed is the environmental fate of the waste materials following their discharge to the environment. This insures appropriate emphasis is placed on the stable pollutants or transformation products that persist in the environment and have the potential to pose long-term human health or environmental hazards.

Environmental quality standards are required to allow compliance with present and pending environmental legislation. The Federal Water Pollution Control Act as amended in 1972, the Clean Air Act as amended in 1974 and The National Environmental Policy Act all provide requirements to limit the discharge of pollutants and to assess their impact on the environment. In addition, considerable regulatory authority is delegated to the States and other local agencies who may establish additional pollutant discharge limitations. Research on munitions-unique water pollutants is specifically directed to the 1983 requirements of the 1972 amendments to the Federal Water Pollution Control Act to achieve water quality that will support

PRECEDING PAGE BLANK-NOT FILMED

fish and wildlife, be suitable for recreational uses, and insure human health is not adversely affected. The 1974 amendments to the Clean Air Act provide the principal goals for research on munitions-unique air pollutants. This Act requires national ambient air quality standards be established for specific air pollutants and that national emission standards be developed for hazardous air pollutants which have an adverse impact on human health. Also, environmental impact statements, required under the National Environmental Policy Act, require assessments of the projected impact new or modified munitions facilities will have on the environment. The absence of an adequate scientific data-base for many munitions pollutants precludes the preparation of complete impact statements. It is emphasized, however, that the availability of environmental quality standards does not constitute the complete package necessary for developing environmental impact statements. For example, many site specific factors of the proposed action must be evaluated to insure the proposed action is acceptable to the location in question.

Research to develop the criteria for new or revised TLVs for the industrial environment are being undertaken to allow Army compliance with the Occupational Safety and Health Act of 1970. This act requires safe and healthful working conditions be provided to all employees and that the Army maintain a safety and health program for all its employees. The absence of valid TLVs for most materials encountered in munitions industrial environments prevents compliance with many aspects of this Act. The research program under which occupational health standards are being developed will not be described in this paper. That program is sufficiently broad to warrant individual attention but is mentioned here because it is closely coordinated with the development of criteria for environmental quality standards and, in fact, borrows heavily from the mammalian toxicological data that has been generated under the environmental standards program.

The responsibility of establishing environmental quality standards lies principally with the U.S. Environmental Protection Agency (EPA) but also with several other Federal, State and local agencies. EPA's development of criteria for munitions standards, however, will not be timely to impact the Army's Munitions Production Base Modernization and Expansion Program. In addition, at the local level, individual Army ammunition plants are faced with increasingly stringent discharge limitations through the issuance of National Pollutant Discharge Elimination System Permits. Thus, it is urgent that the Army develops criteria for environmental quality standards. When sufficient data become available they are presented to EPA and other regulatory agencies for review, interpretation, and publication of Federal environmental quality standards. This requires close coordination of the Army's research program with the regulatory agencies, and the scientific community to insure the technical excellence and credibility of the research data. One method used to achieve this goal is by periodic review of the research by the National

Academy of Sciences Committee on Military Environmental Research. Participation at these research reviews by representatives from the regulatory agencies and scientific consultants facilitates the complex task of coordination. In addition, many of these nationally recognized experts are requested to serve on contractor selection boards which evaluate solicited research proposals and participate in the technical monitoring of on-going research efforts.

Accepted Environmental Quality Standards will have an impact on all levels of the Army's munitions industry. The impact to existing facilities will be by identifying unacceptable discharges and thereby directing advancements in pollution abatement technology research and implementation of available abatement technology. The standards should strongly influence site selection for new munitions facilities by providing a portion of the data package necessary for preparing environmental impact statements. This is especially true for munitions water pollutants where the level of stream dilution will be a significant factor in determining wastewater treatment requirements at specific locations. New and existing munitions facilities will be impacted by the identification of particularily toxic munitions compounds and related pollutants. This information may be used to determine the priority for process water recycling, select alternative production processes, or identify the need for substitute materials in specific munitions products. These alternatives should be considered along with the available air and water pollution abatement capabilities to insure that compliance with the eventual standards is achieved by the most economical and technically advantageous method.

While the research program is primarily directed to munitions production waste discharges, the resulting environmental quality standards will have direct application to munitions handling, use and demilitarization programs. Since many of the contaminants are of concern in both the industrial and general environment, the requirements for proper industrial hygiene practices and pollution abatement systems can be addressed concurrently. Scientifically based standards will provide the necessary justification for the development and implementation of cost-effective control measures that insure the protection of human health and the environment.

RESEARCH APPROACH

The research program under which the criteria for environmental quality standards are developed is multifaceted because environmental pollutants may cause adverse affects at many levels in the ecosystem. Of primary concern is the potential health hazard to man, however, evaluations of the hazards to aquatic and plant species are also required for various pollutants. These studies not only address the direct effects from these pollutants, but also their potential to be transferred or bioconcentrated through the food chain and ultimately be consumed by man.

Several sources of data are utilized to direct the hazard evaluation research. Through problem definition studies, information on the pollutant sources is collected to identify candidate chemical constituents and to document the conditions under which they are discharged to the environment. This is followed by a critical evaluation of the chemical and toxicological literature to define the physical and chemical properties of each pollutant and to assess the extent of the available toxicological data. Concurrently, chemical characterization of pollutant discharges may be required to confirm the identity of individual constituents, the magnitude and consistency of their occurrence and their stability and persistence in the environment. At this stage data are assembled to identify munitions-unique pollutants, to estimate their probable routes of exposure to man and other species and to assess the adequacy of prior toxicological studies to provide the criteria for environmental quality standards.

For the munitions-unique air and water pollutants, a relatively limited data-base usually exists, requiring additional toxicological evaluations to be initiated. Figures 1 and 2 represent the research strategy utilized for air and water pollutants, respectively. In both cases, mammalian toxicological studies are required to determine the pollutant's hazard to man. In addition, aquatic toxicity data are used to assess the impact of water pollutants in the receiving stream. Air pollutants, in addition to their potential effect on man, may also adversely impact natural and economically important vegetation. Therefore, an evaluation of the phytotoxic properties of munitions air pollutants is also required.

These toxicological studies are conducted under the framework of carefully designed research protocols which require data to be generated in sequential phases. In all cases the initial phase is designed to establish the general toxicological properties of individual compounds and, in certain cases, to determine their potential for bioconcentration. Later phases of the research require testing at lower, more environmentally relevant concentrations at which the subacute and chronic effects are expected during long-term exposure. During the chronic toxicological studies, not only are the threshold concentrations that initiate effects in mature test organisms determined, but included are mutagenic, teratogenic and carcinogenic studies to assess the more subtle, yet serious, long-term hazards to present and future generations.

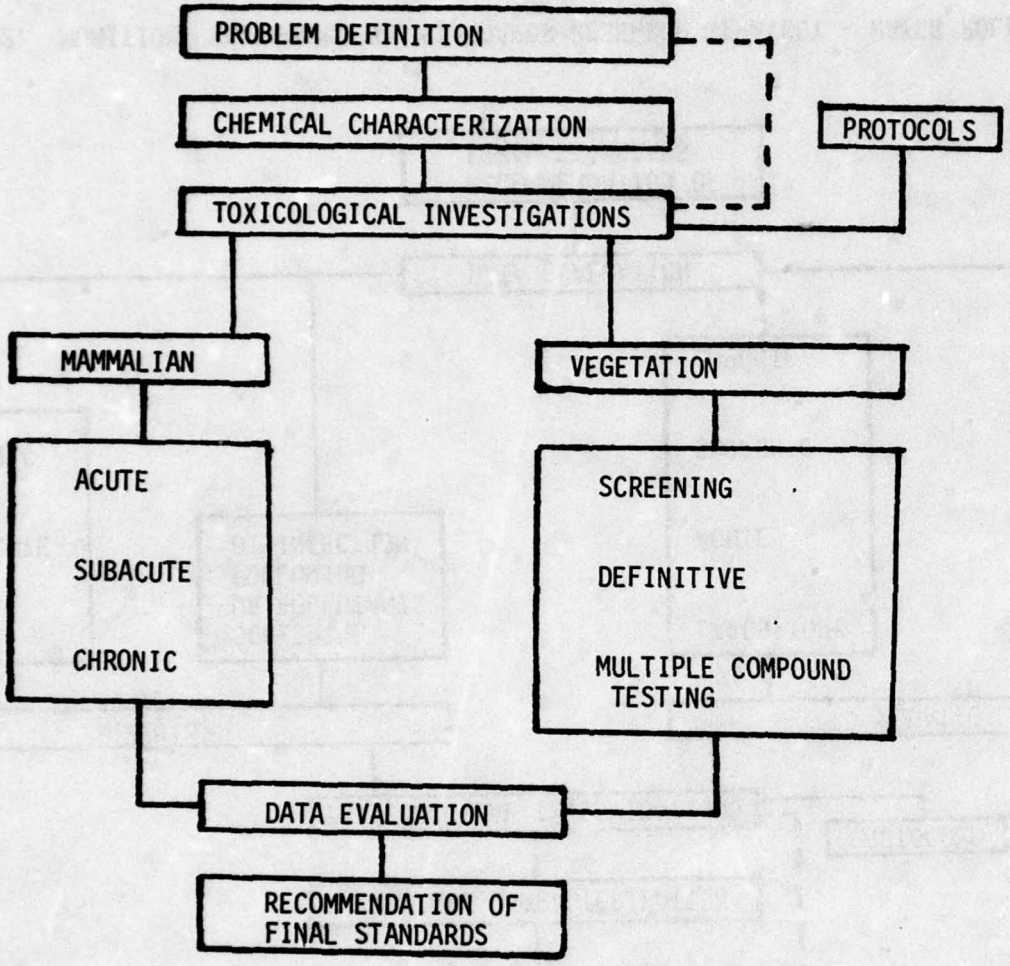


FIGURE 1. MUNITIONS ENVIRONMENTAL STANDARDS RESEARCH STRATEGY - AIR POLLUTANTS

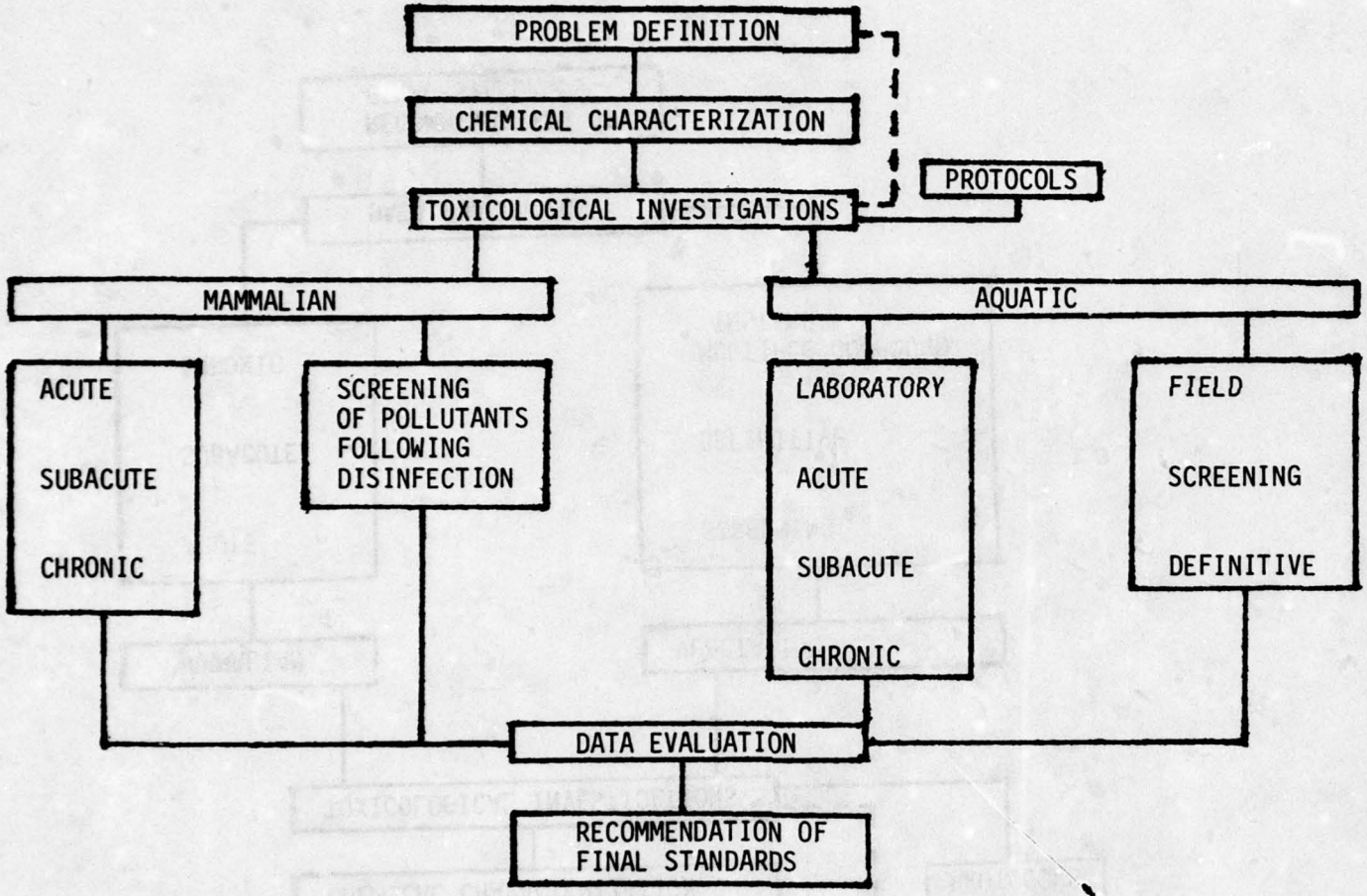


FIGURE 2. MUNITIONS ENVIRONMENTAL STANDARDS RESEARCH STRATEGY - WATER POLLUTANTS

The mammalian toxicity protocol is expanded for water pollutants to determine the chemical changes and assess the toxicological consequences resulting from their reaction with chemical disinfectants. This evaluates the possible impact of disinfection processes used for municipal water supplies on surface waters containing munitions pollutants. Under the aquatic toxicity protocol both laboratory studies on individual compounds or mixtures and aquatic field studies at Army ammunition plants are conducted. The field observations of naturally occurring aquatic species are used to verify the results of laboratory studies and, more importantly, aid in identifying possible synergistic effects when two or more pollutants are discharged into receiving streams. Under the phytotoxicity protocol the air pollutants are evaluated not only for their direct effects on vegetation, but also for possible synergistic effects in the presence of non-munitions-unique air pollutants (sulfur dioxide, oxides of nitrogen, etc.) which are discharged in greater quantities at munitions production facilities.

Coordination of research under each protocol is accomplished at the completion of each sequential phase. The emphasis here is on determining the relative sensitivity of various test species to the pollutant and to determine the requirements for continued evaluation under each individual protocol. Provisions are also made at this time to conduct preliminary evaluations of the available data and to recommend temporary guidelines for environmental quality standards. These guidelines will allow preliminary determinations of the adequacy of current pollution abatement systems and influence the priority for further developmental requirements to allow compliance with the anticipated discharge limitations. These guidelines are subject to change since they are based on an incomplete data-base. In certain cases, however, studies on an individual compound or under a specific protocol could be halted at an intermediate stage. This is done when a compound is found to have extremely low general toxicity or relatively low toxicity to a general class of organisms, e.g., aquatic, mammalian, or vegetation. The use of incomplete data to develop temporary guidelines requires the use of larger application factors. These application factors are used in an attempt to approximate the no-effect level that would be observed in subsequent research phases. Thus, as research progresses and the uncertainty in the true no-effect level diminishes, the application factors become less conservative. Under the aquatic and vegetation protocols, the no-effect levels defined during the final research phase (chronic studies) are generally used directly for the environmental quality standard. The no-effect level defined during mammalian chronic studies, however, is still used with a 0.01 safety factor for developing a human health standard. This approach toward translating mammalian toxicological data is warranted by the inability of standard laboratory test species to predict effects in humans. In addition, if compounds are found to be mutagenic or carcinogenic during mammalian testing, an even more conservative interpretation of the research data would result to preclude these extremely serious effects. The eventual

result of this research program will be the determination of "in-the-river" and ambient air concentrations that will not adversely effect human health and the environment.

Standards will be developed for only those pollutants unique to the conventional munitions industry. Conventional discharge parameters such as biochemical oxygen demand (BOD), chemical oxygen demand (COD), pH, sulfur dioxide (SO_2), oxides of nitrogen (NO_x), etc. also require limitations to prevent adverse effects resulting from their release into the environment. The effects of these materials are often known and standards for their discharge are generally in use. The combined availability of environmental quality standards for conventional and munitions-unique pollutants will insure compliance with the intent of Federal, State and local environmental legislation.

It is stressed that the concentrations presently developed as temporary guidelines are "in-the-river" and ambient air levels. The concentrations are not effluent (end-of-the-pipe or stack emission) limits. Site specific dilution factors must be utilized to arrive at appropriate discharge or emission limits for each pollutant at each location.

Current Research

The majority of the research initiated has been directed to pollutants resulting from the manufacture and handling of trinitrotoluene (TNT), cyclotetramethylene tetranitramine (HMX), cyclotrimethylene trinitramine (RDX), nitroglycerine, nitrocellulose, white phosphorus and priming compounds. Table I provides a detailed listing of individual air and water pollutants that have been identified from these production sources. As chemical characterization studies of pollutant discharges identify additional compounds of concern, their uniqueness to the munitions industry is determined and the compound is included in the hazard evaluation program. Recently, efforts have been initiated on pollutants associated with nitroguanidine, pyrotechnics, propellants and tracers. Table II provides a listing of these compounds.

As a general rule, not all compounds identified as munitions-unique air and water pollutants will receive complete evaluation under the hazard evaluation program described. Many of the individual compounds listed in Tables I and II are present in very small quantities in relation to the principal discharge component(s). For these minor pollutants, only the initial toxicological studies are initiated to determine their general toxicological properties relative to the major component(s). Only if these studies provide indications that the minor components are significantly more toxic than the major components, will more detailed toxicological evaluations be pursued. Thus, it should not be implied that a complete toxicological data-base and an environmental quality will be developed for each compound in Tables I and II. Attempts will be made to recommend environmental quality standards for classes of pollutant discharges based on the most toxic component(s).

TABLE I

MUNITIONS AIR AND WATER POLLUTANTS PRESENTLY UNDER EVALUATION

TNT Production

Condensate Water: 2,3-dinitrotoluene (DNT), 2,4-DNT, 2,5-DNT, 2,6-DNT, 3,4-DNT, 3,5-DNT, 4-amino-2,6-DNT, 2-amino-4,6-DNT, mononitrotoluene, 1,3,5-trinitrobenzene, 1,3-dinitrobenzene, 2,4,6-trinitrobenzonitrile, 2,4,6-trinitrobenzaldehyde, 4,6-dinitroanthranil, N-nitrosomorpholine.

Air Pollutants: Tetranitromethane, mononitrotoluene.

TNT Load, Assembly and Pack

Pink Water: 2,4,6-trinitrotoluene (TNT), 4-amino-2,6-DNT, 2-amino-4,6-DNT, 1,3,5-trinitrobenzene, 2,4,6-trinitrobenzaldehyde, 4,6-dinitroanthranil, 2,4,6-trinitrobenzyl alcohol, 4,6-dinitro[1,2] benzisoxazole, 1,3-dinitrobenzoate, 2,4,6-trinitrobenzaldoxime, 3,5-dinitrophenol.

RDX/HMX

Wastewaters: Cyclotrimethylene trinitramine (RDX), cyclotetramethylene tetranitramine (HMX), cyclohexanone, hexamine, methylamine, dimethylamine, hexahydro-1,3-dinitro-5-acetyl-S-triamine (TAX), Octahydro-1-acetyl-3,5,7-trinitro-S-tetramine (SEX).

Air Pollutants: Methyl nitrate, acetic acid, acetic anhydride.

Nitroglycerine Wastewaters

Trinitroglycerol, 1,2-dinitroglycerol, 1,3-dinitroglycerol, 1-mononitroglycerol, 2-mononitroglycerol, o-nitrodiphenylamine.

Nitrocellulose

White Phosphorus

Priming Compounds

Desensitized tetrazene, lead styphnate, trinitroresorcinol, pentaerythritol tetranitrate (PETN).

TABLE II

MUNITIONS COMPOUNDS UNDER EVALUATION - RECENT INITIATIONS

NITROGUANIDINE

PROPELLANTS:

Diphenylamine, Dibutyl Phthalate

TRACERS:

Red Phosphorus, Potassium Perchlorate

PYROTECHNICS:

Benzanthrone

1,4-Di-p-toluidinoanthraquinone

1,4-Diamino-2,3-dihydroanthraquinone

1-Methylaminoanthraquinone

Dibenz(b,def)chrysene-7,14-dione

Hexachloroethane

Hexachlorobenzene

Temporary Guidelines

As described earlier, provisions are made to conduct periodic evaluations of the available research data to provide temporary guidelines for environmental quality standards. Such an evaluation was conducted during November 1975 for the higher priority munitions compounds, for which a considerable data-base has been developed. Temporary guidelines were recommended for six classes of water pollutants: TNT pink water (from TNT load, assembly and pack operations); 0.05 ppm as alpha TNT; TNT condensate water (from TNT production) -0.025 ppm as 2,4-DNT; nitroglycerine -0.04 ppm; white phosphorus - 0.01 ppb; RDX and HMX - 0.25 ppm as RDX and nitrocellulose - no guideline due to relatively low toxicity. These temporary guidelines are more completely summarized in Table II, including the bases for these recommendations. The table shows whether the guideline was based on the compound's toxicity to mammalian species or to aquatic life. Table III also identifies the completeness of the research data-base from which the temporary guidelines were developed. The extent of completeness greatly impacts the certainty level applied to each temporary guideline and therefore, the general degree of confidence that the temporary guideline represents is the eventual environmental quality standard. Another factor impacting the certainty level, but not shown in Table III, is the chemical complexity of the actual pollution discharge from Army ammunition plants. In some cases the toxicological significance of minor components or environmental transformations of the parent compound are not fully identified and therefore, the relevance of the temporary guideline to the actual pollutants discharged may be unclear.

Several specific comments are required to clarify each temporary guideline. Two guidelines are provided for TNT related wastewaters due to the significant chemical differences of wastewaters from load, assembly and pack (LAP) operations and those from TNT production. The composition of LAP wastewater resembles the composition of the specific material being handled (TNT and RDX for Composition B). The photodecomposition of these materials (formation of pink water) adds significant complexity to the hazard evaluation since many compounds (some still unidentified) are formed in the environment. Condensate water is primarily a mixture of dinitrotoluene (DNT) isomers which are discharged from the red water treatment systems at TNT production facilities. Although a noticeable color is not formed, the DNT isomers also undergo complex photochemical reactions when discharged to surface waters and form many compounds of unknown toxicological properties.

For white phosphorus, an extremely low temporary guideline has been recommended. It should be noted that this extremely toxic material is of concern at only one location; Pine Bluff Arsenal, Arkansas. Also, since the Arkansas River is not used for municipal drinking water supplies, there is a reduced concern for potential human health effects from this material. A single temporary guideline is recommended for both RDX and HMX. Therefore, RDX would be the limiting factor in discharges containing both explosives. Where HMX alone is discharged, it is believed that

TABLE III

TEMPORARY GUIDELINES FOR ENVIRONMENTAL QUALITY STANDARDS

Wastewater	Temporary Guideline	Criteria	Estimated No Effect Level	Basis	Certainty
TNT Pink Water	0.05 ppm as TNT	Mammalian Tox.	No Estimate[a]	Partial Acute	--
		Aquatic Tox.	0.05 ppm	Partial Acute	Low
		Aquatic Field	0.01 to 0.3 ppm	Partial Definitive	Low
TNT Condensate Water	0.025 ppm as 2,4-DNT	Mammalian Tox.	0.025 ppm	Partial Chronic	Medium
		Aquatic Tox.	No Estimate[a]	Partial Acute	--
		Aquatic Field	0.03 to 0.3 ppm	Partial Definitive	Low
Nitroglycerine	0.04 ppm	Mammalian Tox.	0.18 ppm	Subacute	High
		Aquatic Tox.	0.04 ppm	Partial Chronic	High
		Aquatic Field	No Estimate[b]	Screening	--
White Phosphorus	0.1 ppb	Mammalian Tox.	0.1 ppm	Acute	Low
		Aquatic Tox.	0.6 ppb	Partial Chronic	High
		Aquatic Field	0.01 ppb	Definitive	High
RDX/HMX	0.25 ppm as RDX	Mammalian Tox.	0.25 ppm	Partial Chronic	Medium
		Aquatic Tox.	0.5 ppm	Partial Chronic	High
		Aquatic Field	0.02 ppm	Screening	Low
Nitrocellulose	Non Related To Toxicity [c]	Mammalian Tox.	> 100 ppm	Subacute	High
		Aquatic Tox.	>1000 ppm	Acute	High
		Aquatic Field	> 20 ppm	Partial Definitive	Low

a. No estimate of no effect level due to insufficient data.
b. No estimate of no effect level due to lack of a satisfactory site to measure nitroglycerine specific effects in the environment.
c. Suspended solids and nutrient concentrations in wastewaters will probably be controlling factors for environmental standards.

control to the equivalent level of RDX would be more than adequate to protect human health and the aquatic environment. As shown in Table III, no temporary guideline is recommended for nitrocellulose wastewaters. Nitrocellulose has not been found to cause toxicological effects at concentrations up to 100 ppm in mammalian species and 1000 ppm in aquatic organisms. Thus, on the basis of incomplete evaluations, it appears that an environmental quality standard for nitrocellulose discharges will be based on conventional water quality factors, i.e., suspended solids and nutrient loading rates.

These temporary guidelines are the first products of this research program. Updates of these guidelines and/or the recommendation of final standards will be accomplished annually. Estimates of the completion dates for the six wastewater classes for which interim guidelines have been developed are shown in Table IV. Forecasts of the completion dates for other munitions related air and water pollutants must await the completion of problem definition studies and, in most cases, the generation of initial toxicological data.

We reemphasize that the temporary guidelines provided are estimates of river concentrations at which no adverse effects on human health or aquatic organisms would be expected. Translation of these guidelines to effluent concentrations requires consideration of several site-specific factors, such as: total wastewater flow, river flow, definition of allowable mixing zones, etc. It is not the objective of this research program to provide those conversions. Rather, this research will identify the average, long-term concentrations that must be achieved in surface waters or the atmosphere to insure the protection of human health and the environment. These data will then provide a scientific basis for environmental quality standards development and the implementation of effective pollution abatement systems.

TABLE IV

MUNITIONS STANDARDS RESEARCH COMPLETION DATES

WASTEWATER	DATE
TNT PRODUCTION - CONDENSATE WATER	SEPTEMBER 79
TNT LAP - PINK WATER	SEPTEMBER 79
RDX/HMX	APRIL 77
NITROGLYCERINE	FEBRUARY 78
NITROCELLULOSE	DECEMBER 77
WHITE PHOSPHORUS	DECEMBER 76

GUIDELINES FOR ENVIRONMENTAL IMPACT STATEMENTS ON NOISE (Airblast)

Jack W. Reed
Sandia Laboratories
Albuquerque, New Mexico

Introduction

The National Academy of Sciences - National Research Council, through its Assembly of Behavioral and Social Sciences, operates a Committee on Hearing, Bioacoustics and Biomechanics called CHABA. At the request of the Environmental Protection Agency, Office of Noise Abatement, with support from the Departments of Transportation and Defense, CHABA commissioned Working Group 69 to prepare "Guidelines for Preparing Environmental Impact Statements on Noise." A third, and hopefully, final draft report has recently been assembled and submitted for agency reviews [1].

Acousticians have made considerable progress in unifying their concepts for prediction, measurement, and assessment of injury and annoyance resulting from many kinds of continuous tone noises. There have also been numerous attempts to transform impulse type noise parameters into regular acoustic terms, particularly for evaluating explosion waves and sonic booms. This has been attempted so that a single integrated annoyance parameter could be stated for all acoustic insults. It is not clear that this is possible or appropriate for amplitudes which threaten damages, as opposed to annoyances.

CHABA "Guidelines" addresses impulse noises in terms of a "C-weighted" sound level, [2] that can be measured through appropriate frequency-dependent filter systems. This sound level bears some relationship to human auditory response characteristics. This weighting gives essentially flat response from about 100Hz to 3kHz with drop-off to 15dB attenuation near 10Hz and 30kHz. On the low frequency end there is little response to much of the wave energy emitted by explosions of more than a few kilograms in TNT equivalent yield.

For low overpressures from explosions, well below the eardrum injury threshold of 35kPa (5 psi), environmental concern is primarily with minor damage thresholds, rather than annoyance

from single events or events widely spaced in time. Low frequency components cannot be ignored in this context, so a compromise has been reached in the guidelines. Blast wave analyses, rather than acoustic analyses, will be made when sound pressure levels above 140dB (200Pa, 0.03psi overpressures) are expected. The remaining difficulty is in specifying how to predict this relatively low overpressure level and thus, where to delineate between the two environmental analysis systems.

A conservative evaluation, relating an explosion yield limit to exposed population and distance, has been developed to allow simple decision-making, regarding the analysis system to be used. This paper will describe the derivation of this yield-limit relationship.

Yield-Limit Derivation

The approach here taken begins with the standard explosion overpressure (Δp) versus distance (R) and yield (W) relationship, $\Delta p(R, W)$. Atmospheric propagation is assumed to be enhanced by an extreme focus factor (F) so that observed incident overpressure is $F\Delta p$. An empirical relationship between incident airblast overpressures and window breakage probability is then used to give a maximized estimate of breakage probability in terms of explosion yield and distance. An approximation for the number of exposed window panes per capita then allows derivation of a yield limit needed to hold expected damage to less than one-half pane, depending only on population and distance, for specified communities. Additional relationships are provided for contained underground explosions and for relatively uniform population distributions in a rural area.

A standard 1kt nuclear explosion (NE) burst in free air without nearby reflecting surfaces, and in a sea level standard atmosphere, was recently defined by the Air Force Weapons Laboratory (AFWL) [3] to show various blast wave parameters as functions of distance. This result from sophisticated and modern hydro-code calculations is in good agreement with most previously accepted models and empirical data. In the far field, where low overpressures are of concern to environmental nuisance analyses, the standard overpressure-distance relationship can be approximated by an $R^{-1.1}$ decay law supplanting an $R^{-1.2}$ decay often used previously for distant blast predictions [4]. Applying the common explosion scaling laws leads to

$$\Delta p = K\left(W^{1/3}/R\right)^{1.1} \qquad (1)$$

where K = 6526 for pascal overpressures, kilometer ranges, R, and kiloton NE yield, W, free air burst. For kilograms of high-explosives (HE), where a 1kt NE blast yield may be approximated by a 0.5kt HE blast yield, and a typical surface burst with hemispherical rather than spherical wave expansion, the coefficient becomes 70.944. Equation (1) applies only for propagation in a uniform, calm atmosphere, that causes no blast wave refraction.

In a real atmosphere, wind and temperature strata may bend, distort, and even focus blast waves to considerably magnify overpressures in restricted areas. A fairly conservative upper bound for this magnification or focus factor is F = 3.6, obtained by experiment [5], to be multiplied by the AFWL model overpressure. This corresponds to F = 5 used with the old IBM Problem M [6] explosion parameters, or overpressures shown in The Effects of Nuclear Weapons [7]. Thus, when weather is ignored, as it is for many small explosion operations, incident overpressures may reach to

$$\Delta p \text{ max} = 254\left(W^{1/3}/R\right)^{1.1}, \qquad (2)$$

with units of pascals, kilograms HE, and kilometers. Note that ground reflection will usually cause doubling for gaged pressures from atmospheric ducted waves which strike ground at some elevated incidence angle.

A primary source of window damage data from explosions has been the accidental detonation at Medina Facility, near San Antonio, Texas, in 1963 [8]. A relationship was obtained for the number of broken panes (Q) that

$$Q = 8.28 \times 10^{-10} N(\Delta p)^{2.78} \qquad (3)$$

for pascal overpressures and exposed population, or number of people exposed, N. This incorporates the mix of pressures, window pane dimensions, and damage claims of that city, which might be assumed typical of other communities, lacking specific details. Large windows are usually most vulnerable, so their local popularity may be a strong consideration.

By substitution of Eq. (2) into Eq. (3), an upper bound on damage, in terms of yield, distance, and population is obtained. By assuming that no damage occurs when Q < 1/2, the result may be transformed into an inequality to be satisfied that

$$W < 114\ R^3/N, \text{ surface burst.} \qquad (4a)$$

At 1km from a community of 100 people, a 1kg HE surface burst limitation appears necessary for all-weather operation.

In mining and quarrying operations it might be assumed that explosion containment will be insured for economy and maximized rock breaking. For such buried shots, airblast in the far field will probably not exceed about 20 percent of the overpressure from a surface burst of the same yield. Many geologic materials will give even smaller transmissivities, but a quick safety estimate is obtained from multiplying overpressure in Eq. (2) by 0.2 and carrying through the previous manipulations to give

$$W < 9154\ R^3/N, \text{ contained underground burst.} \qquad (4b)$$

Limits for 1 person at 1km would not be realized because a typical unit residence houses 4 persons. The population variable is presented because it is most likely available from census statistics.

A more lenient limit, that allows almost tripling these yields, can be justified on the basis of integrating a probability distribution of scatter in gaged overpressures under adverse weather (propagation) conditions. An experiment with calculated caustic propagation [5] showed that the geometric average magnification of overpressure was $\overline{F} = 1.68$, with a lognormal scatter factor or geometric standard deviation of 1.67 ($\sigma = \ln 1.67 = 0.513$). Thus, near caustics,

$$\Delta p = 119\left(W^{1/3}/R\right)^{1.1} \times \left(1.67\right)^{\pm 1}. \qquad (5)$$

Window damage by this statistical overpressure may be estimated [9] by

$$Q = (2\pi)^{-\frac{1}{2}}\sigma^{-1}\int_{-\infty}^{+\infty}\left[8.28 \times 10^{-10}\ N\ \Delta p^{2.78}\right]\left[e^{-\frac{\ln^2(\Delta p/\overline{\Delta p})}{2\sigma^2}}\right]d(\ln\Delta p)$$

$$= 8.28 \times 10^{-10}\ e^{(2.78\sigma)^2/2}\ N\ \overline{\Delta p}^{2.78}$$

$$= 2.29 \times 10^{-9} \, N \, \overline{\Delta p}^{2.78}$$

$$= 1.36 \times 10^{-3} \, N \, (W/R^3)^{1.019}. \qquad (6)$$

Again using the criterion of $Q < 1/2$, there should be (50 percent probability) no window damage when

$$W < 328 \, R^3/N, \text{ surface burst} \qquad (7a)$$

$$W < 26430 \, R^3/N, \text{ contained underground burst.} \qquad (7b)$$

Much blasting occurs in relatively open country with scattered farmhouses, and few other population concentrations. When the nearest farmhouse is identified, a probability model may be used to extrapolate damages at all greater distances with a relatively uniform random scattering of other houses. The hypergeometric probability equation was first used in deriving an exact solution, but some simplifying approximations were found suitable. In result, the expected nearest house range, R_1 kilometers, could be related to density per square kilometer of either houses, H, or population, n, where $n \approx 4H$, by

$$R_1 = 0.469H^{-\frac{1}{2}} = 0.937n^{-\frac{1}{2}}. \qquad (8)$$

Damages would accrue with increments of area to farther ranges according to

$$dQ = K_w \, R^{-3.058} ndA = K_w n R^{-2.058} dR d\theta, \qquad (9)$$

for polar coordinates (R, θ) and $K_w = 1.36 \times 10^{-3} W^{1.019}$. Integration of damage beyond R_1 then shows

$$Q_\infty = K_w n \int_0^{2\pi} \int_{R_1}^{\infty} R^{-2.058} dR d\theta = 8.67 \times 10^{-3} n^{1.529} W^{1.019}. \qquad (10)$$

Total damages, Q_t, would be the sum of damages at the first house, Q_1, plus Q_∞, or

$$Q_t = 0.0126\left(W/R^3\right)^{1.019}, \tag{11}$$

so that no damage ($Q_t < 1/2$) results from

$$W < 40R_1^3, \text{ surface burst,} \tag{12a}$$

$$W < 3200R_1^3, \text{ contained underground burst.} \tag{12b}$$

Thus, by comparison with Eq. (7) using N = 4, a factor of two yield reduction is needed to protect all residences other than the nearest one, in relatively uniform but randomly populated rural areas.

References

1. "Guidelines for Preparing Environmental Impact Statements on Noise," 2nd Draft, National Research Council CHABA-69 (H. E. Von Gierke, chairman), Washington, DC, Feb 1976.

2. "Standard for Single Point Explosions in Air," 3d Draft, ANSI S2-54 (J. W. Reed, Chairman), Albuquerque, NM, Aug 1976.

3. Needham, C. E., Havens, M. L., and Knauth, C. S. "Nuclear Blast Standard (1kt)," AFWL-TR-73-55 (Rev.), Air Force Weapons Laboratory, Kirtland AFB, NM, April 1975.

4. Reed, J. W., "Airblast Overpressure Decay at Long Range," J. Geophys. Res., 77, 9, May 1972.

5. Reed, J. W., "Explosion Wave Amplitude Statistics for a Caustic at Ranges of 30 to 45 Miles," SC-RR-67-860, Sandia Laboratories, Feb 1968.

6. Broyles, C. D., "IBM Problem M Curves," SC-TM-268-56(51), Sandia Laboratories, Dec 1956.

7. Glasstone, S. (Ed.), The Effects of Nuclear Weapons, Rev. Ed., Government Printing Office, Washington, DC, 1962.

8. Reed, J. W., Pape, B. J., Minor, J. E., and DeHart, R. C., "Evaluation of Window Pane Damage Intensity in San Antonio Resulting from Medina Facility Explosives on November 13, 1963." Ann. N.Y. Acad. Sci., 152, 1, Oct. 28, 1968, pp. 565-584.

9. Reed, J. W., "An Approach to Airblast Damage Estimation Near Calculated Caustics," SC-RR-67-870, Sandia Laboratories, Feb 1968.

DESIGN OF STEEL, MASONRY AND PRECAST CONCRETE STRUCTURES TO RESIST THE EFFECTS OF H.E. EXPLOSIONS

by

John J. Healey, Ammann & Whitney
Samuel Weissman, Ammann & Whitney
Norval Dobbs, Ammann & Whitney
Paul Price, Picatinny Arsenal

ABSTRACT

This paper summarizes recent and on-going Picatinny Arsenal efforts in the development of structural design criteria and procedures for acceptor structures located in the low to intermediate pressure range. Design data and general discussion are included for structural steel, masonry and precast concrete protective structures. The material presented supplements the data on reinforced concrete given in the tri-service design manual, "Structures to Resist the Effects of Accidental Explosions."

PRECEDING PAGE BLANK-NOT FILMED

INTRODUCTION

The design of facilities for the manufacture or storage of explosive materials requires special procedures and criteria in order to avoid mass detonation and explosion propagation in the event of an accidental explosion and to provide protection for personnel and equipment. The basic document in this area is the tri-service manual, TM 5-1300, "Structures to Resist the Effects of Accidental Explosions" (Ref. 1). This manual contains comprehensive information on the principles of protective design, the calculation of blast loadings, dynamic analysis, and detailed procedures for designing reinforced concrete protective structures.

However, since TM 5-1300 is directed primarily to the design of reinforced concrete structures, with particular emphasis on donor structures, supplementary material is required to treat acceptor structures which utilize other materials, such as structural steel, masonry and precast concrete construction. To fulfill this need, Picatinny Arsenal, as part of its overall Safety Engineering Support Program for the U. S. Army Armament Command, has undertaken the preparation of design criteria documents for acceptor structures, with the assistance of Ammann & Whitney, Consulting Engineers. These documents include References 2, 3, and 4 pertaining to structural steel structures, and design criteria reports presently under preparation dealing with masonry (Ref. 10) and precast construction (Ref. 19). The data in these reports, and the results of related current research and testing programs, which will be described in this paper, can be used for the design of acceptor structures subjected to the effects of accidental explosions.

In general, the design of acceptor structures relates to buildings located in pressure ranges of 10 psi or less. These buildings contain personnel and/or valuable equipment which require protection against the blast and fragment output of an accidental detonation, particularly where hazardous operations are involved. The selection of the appropriate structural system and materials for acceptor structure design depends on overpressure level, degree of fragment hazard, explosive contents of the acceptor building, and normal operational functions.

Structural steel buildings used for protective structures range from pre-engineered buildings for low overpressures (less than about 1 psi) to strengthened steel buildings utilizing standard structural shapes and panels for higher overpressures. One disadvantage of steel designs is that they provide little protection against fragment penetration, and may not be suitable where the contents or construction of the donor is such that a significant fragment hazard will be produced. On the other hand, when the structure may also be a donor structure, the designer must consider the effects of explosives contained within the building since in this case the use of structural steel (compared to masonry or concrete) minimizes the creation of fragments.

Thus, where fragment protection is required for the acceptor structure it is necessary to provide more massive construction for the exterior components of the structure. In such cases, cast-in-place reinforced concrete, masonry, and precast concrete construction can be utilized. Masonry and precast concrete are practical for blast resistant buildings located at relatively low overpressure ranges of 1 to 2 psi, although, under certain conditions both types of construction may be used at high overpressure levels. For higher overpressure levels cast-in-place reinforced concrete structures become economically competitive. Procedures for the design of cast-in-place reinforced concrete protective structures are relatively well known and the data and techniques contained in Reference 1 can be applied for this purpose.

As indicated, the main advantage of masonry and precast concrete construction, in comparison to structural steel, is its capacity to prevent penetration of fragments to the interior of the structure. At the pressure levels of interest, velocities and sizes of fragments will be of such a magnitude to penetrate structural steel roof and wall systems, but will be rejected by block or concrete panels. Because of their inherent characteristics, masonry blocks are only applicable to wall construction, whereas precast panels usually may be used for the construction of both walls and roofs or in combination with masonry walls.

Although masonry and concrete construction does provide fragment protection for acceptor structures, it is a potential source of secondary fragments for structures containing explosives (donor structures). Therefore, in those facilities where the occurrence of secondary fragments is a design factor, the use of masonry and precast concrete construction must be limited to office buildings, laboratories and other such structures containing inert material or a relatively small amount of explosive which will not destroy the building. In some designs the fragment hazard as a donor can be reduced by utilizing combined structural steel and concrete/masonry construction, e.g., concrete/masonry walls facing the donor structure, with structural steel roof and side walls.

This paper is organized in three main sections, namely, structural steel, masonry, and precast concrete. The section on structural steel summarizes and describes design criteria contained in Reference 2, including the application of References 3 and 4, and also discusses recent and planned testing undertaken to verify and refine this data. The sections on masonry and precast concrete more generally describe the special factors involved in the design and construction of protective structures utilizing these materials.

STRUCTURAL STEEL

General

The design of steel buildings subjected to blast loads involves three general structural systems: (1) The wall and roof panels; (2) Supporting members such as girts, purlins, diagonal bracing and other members which can be treated as individual elements; and, (3) The main structural frame. Due to the complex nature of the loadings and the dynamic aspects of the structural response, special procedures and criteria are necessary for the design of steel structures subjected to blast loads. To fulfill this need, Picatinny Arsenal Technical Report 4837, "Design of Steel Structures to Resist the Effects of HE Explosions" (Ref. 2) was developed. This portion of the paper summarizes and describes the data contained in that report, including a discussion of design stresses, criteria for deformations, ultimate strength of structural steel elements, cold-formed steel panels, and frames. The application of this material to pre-engineered buildings is also discussed

Design Stresses

The strength and ductility of structural steel make it an ideal building material for use in blast-resistant construction. The significant engineering properties of steel are strength expressed in terms of yield stress and ultimate tensile strength, ductility expressed in terms of percent elongation at rupture, and rigidity expressed in terms of modulus of elasticity. Under dynamic loading, there is an increase in the yield stress and ultimate tensile strength as a result of the rapid rate of strain, which further enhances the effectiveness of structural steel for blast design.

Structural steel essentially exhibits a linear stress-strain relationship up to the proportional limit, which is either close, or identical to, the yield point. Beyond the yield point, it can stretch substantially (yield plateau) without appreciable increase in stress, the amount of elongation reaching 10 to 15 times that needed to reach yield. Beyond this point, strain hardening occurs until the tensile strength is reached. The nominal stress then decreases accompanied by further elongation and followed by fracture at an elongation amounting to 20 to 30 percent of the specimen's original length. Some high-strength steels do not exhibit a sharp, well defined yield plateau, but show continuous yielding with a curved stress-strain relation. Such steels generally have a smaller elongation at rupture and must be used with caution when large ductilities are required.

Blast-resistant design is commonly associated with plastic design since protective structures are usually designed for plastic deformations. Consequently, the steels used should meet the requirements of the AISC Specification (Ref. 5) for plastic design. The application of plastic

design concepts to cold-formed steel, is treated in detail since these sections are not covered by conventional plastic design procedures.

The effects of rapid loading on the mechanical behavior of the steel material have been observed and measured in uniaxial tensile stress tests. In actual members subjected to blast loading, the dynamic effects resulting from rapid strain rates may be expressed as a function of the time to reach yield. The effects of increasing strain rates are illustrated in Figure 1 for A-7 steel. The most significant effect is the increase in the yield point and in the yield plateau, with increased strain rate. Figure 2 presents a chart of dynamic increase factor versus strain rate for A-7 steel. The dynamic increase factor is the ratio of the dynamic to static yield stress. Dynamic increase factors for A-7 steel are considered to apply equally well to A-36 steel, and to certain other structural steels.

Dynamic increase factors recommended for use in dynamic design are presented below:

DYNAMIC STRESS INCREASE FACTORS

Pressure Range	A-36 Steel	High Strength Low Alloy Steels
Low to Intermediate	1.1	1.1
High	1.1 or a higher value as determined from the actual strain rate (Fig. 2)	1.1

To summarize, the dynamic yield stress F_{dy} is equal to the dynamic increase factor c times the specified minimum yield stress of the steel. The dynamic yield stress in shear F_{dv} is taken equal to 0.55 F_{dy}:

Compression and tension $F_{dy} = cF_y$

Shear $F_{dv} = 0.55\ F_{dy}$

The dynamic yield stresses for rivets, bolts and welds are taken equal to 1.87 times the allowable stresses given in Part 1 of the AISC Specification (Ref. 5). This factor accounts for the safety factor of 1.7 used in deriving these allowable stresses and includes a dynamic increase factor of 1.1.

Deformation Criteria

Although plastic behavior is not generally permissible under service loading conditions, it is quite appropriate for design when the

structure is subjected to a severe dynamic loading only once or at most a few times during its life. Under blast pressures, it will usually be uneconomical to design a structure to remain elastic and, as a result, plastic behavior is permitted in order to utilize more fully the energy absorption capacity of the members. However, in order to restrict the amount of damage a structure will experience when subjected to blast loads, limiting values must be assigned to the appropriate response quantities.

In general, two different types of values are specified, namely, limits on the level of inelastic dynamic response and limits on the maximum deflections and rotations. In addition, deformation criteria are specified for two categories of damage, "reusable" and "non-reusable".

For members that can be analyzed as single-degree-of-freedom systems, the limiting response quantities are the maximum permissible deflection and/or support rotation or the ratio of these values to the maximum elastic deflection and/or support rotation (ductility ratio, μ). On the other hand, the criteria for frame structures are specified in terms of failure modes both for the individual members of the frame and for the overall sidesway mechanism. In both cases, the member support rotation, θ, is defined as the angle between the chord joining the member ends and the chord joining the support and a point on the member where the deflection is a maximum.

Deformation criteria abstracted from Reference 2 for beams, frame structures, and cold-formed steel panels are summarized below. A current test program has been undertaken by Picatinny Arsenal to test cold-formed steel panels and pre-engineered buildings, in order to verify and refine the design criteria.

Beam Elements (purlins, spandrels, girts, etc.)

a) Reusable structures:

$\theta_{max} = 1°$ or $\mu_{max} = 3$, whichever governs

b) Non-reusable structures:

$\theta_{max} = 2°$ or $\mu_{max} = 6$, whichever governs

Frame Structures

a) Reusable structures:

For sidesway, maximum $\delta/H = 1/50$

For individual frame members, $\theta_{max} = 1°$

b) Non-reusable structures:

For sidesway, maximum $\delta/H = 1/25$

For individual frame members, $\theta_{max} = 2°$

Cold-Formed Steel Roof and Wall Panels

a) Reusable structures:

$\theta_{max} = 0.9°$ or $\mu_{max} = 1.25$, whichever governs

b) Non-reusable structures:

$\theta_{max} = 1.8°$ or $\mu_{max} = 1.75$, whichever governs

For members subjected to both axial loads and bending moments, the specification of deformation criteria is more complex. However, data is available (Ref. 6) whereby the failure of beam-columns can be predicted in terms of member end rotations. In Reference 6 the maximum permissible member deformations are specified in terms of the rotation capacity of the member, which is defined as the ratio of the maximum plastic rotation to the maximum elastic rotation at the member end.

Ultimate Strength and Stability of Structural Steel Elements

The dynamic flexural capacity of a steel section is related to its static flexural capacity by the dynamic increase factor described previously. Thus, the ultimate dynamic moment resisting capacity of a steel section is given by:

$$M_{pu} = F_{dy}Z$$

where F_{dy} is the dynamic yield strength of the material and Z is the plastic section modulus. Figure 3 shows the stress distribution at various stages of deformation for a plastic hinge section. As the moment approaches the fully plastic moment M_{pu}, a rectangular stress distribution as shown in Figure 3(c) is approached. The ratio between the fully plastic moment to the yield moment M_y is equal to the ratio between the plastic and elastic section moduli.

For design purposes, a bilinear representation of the moment-curvature relationship is employed as shown by the dashed lines in Figure 4. The plastic moment capacity M_p to be used in design is assigned in recognition of the actual nature of the transition between the yield moment M_y and the fully plastic moment M_{pu}. Since a substantial amount of plastic deformation must occur before M_{pu} is attained, a reduced value of the plastic design moment (M_{p1} in Figure 4) is defined for beams with moderate curvature (ductility ratios equal to or less than 3). For larger amounts of plastic deformations, the full value of the plastic moment capacity ($M_{p2} = M_{pu}$) may be used.

In flexural response calculations for single span and continuous beams, a single-degree-of-freedom analysis is utilized which requires that the equivalent stiffness and ultimate resistance be defined. Formulas for determining the stiffness and resistance for one-way steel beam elements are presented in Table 1. The ultimate resistance values correspond to developing a full collapse mechanism. The equivalent stiffnesses correspond to load deflection relationships that have been idealized as bilinear functions with initial slopes so defined that the area under the idealized load deflection diagram is equal to the area under the actual diagram up to the point of inception of fully plastic behavior of the beam (see Fig. 5).

The basic relationships for defining the bilinear resistance function for multi-span continuous beams under uniform loading are summarized below. These expressions are predicated upon the formation of a three-hinge mechanism in each span, where the span lengths do not differ by more than 20 percent.

Two-span continuous beam:

$$R_u = r_u bL = 12\ M_p/L$$

$$K_E = 163\ EI/L^3$$

Exterior span of continuous beams with 3 or more spans:

$$R_u = r_u bL = 11.7\ M_p/L$$

$$K_E = 143\ EI/L^3$$

Interior span of continuous beam with 3 or more spans:

$$R_u = r_u bL = 16.0\ M_p/L$$

$$K_E = 300\ EI/L^3$$

The design of a structure to resist the blast of an accidental explosion consists essentially of the determination of the structural resistance required to limit calculated deflections to within tolerable values. In general, the resistance and deflection may be computed on the basis of flexure provided that the shear capacity of the web is not exceeded. Steel structures will generally respond either to pressure only or to the pressure-time relationship when they are situated in the low and intermediate pressure design ranges. For each case, the appropriate dynamic response charts and equations are given in Reference 1. To supplement this data, Table 2 gives the natural period of vibration of steel beams for several support conditions.

The yield capacity of steel beams in shear is given by:

$$V_p = F_{dv} A_w$$

where V_p is the shear capacity, F_{dv} is the dynamic shear yield strength and A_w is the area of the web. For I-shaped beams and similar sections, only the web area between flanges should be used in calculating A_w. Table 3 presents equations for the acting support shear V for one-way beams. With regard to the influence of shearing forces on plastic moment capacity, it has been found experimentally that I-shaped sections achieve their full plastic moment capacity provided that the acting shear V does not exceed V_p. However, for those sections where the web is relied upon to carry a significant portion of the moment capacity, such as rectangular cross-section beams, the influence of shear on the available moment capacity must be considered as described in Reference 2.

In order to insure that a steel beam will attain fully plastic behavior and possess the assumed ductility at plastic hinge locations, it is necessary that the elements of the beam cross-section meet minimum thickness requirements to prevent a local buckling failure. In addition, web stiffeners may be required to prevent web crippling at load points. Reference 2 presents criteria relevant to maximum flange width-thickness and web depth-thickness ratios, and for web stiffeners, as adapted from the AISC Specification (Ref. 5) for application to blast design. Due to the short duration of the dynamic loads this approach to local stability is considered conservative for blast design applications.

Members subjected to bending about their strong axis may be susceptible to lateral-torsional buckling in the direction of the weak axis if their compression flange is not laterally braced. Therefore, in order for a plastically-designed member to reach its collapse mechanism, lateral supports must be provided in the vicinity of the plastic hinge locations. Lateral bracing requirements for steel beams designed for blast loads are given in Reference 2.

Since many members within the structural framework will be subjected to axial loads, and certain members will be subjected to both axial load and bending, design criteria are required for columns and beam-columns. The buckling strength of columns subjected to dynamic loading is dependent not only upon the magnitude of the pressure pulse, but also upon the rise time of the loading and the duration of the loading pulse relative to the natural period of the member. For a short duration load, a column will sustain a greater load than under static conditions, since inertial forces retard the buckling process, thereby providing a stabilizing effect. Hence, in blast design, a reasonable approach has been taken in which calculations are based on the static formulas for steel columns presented in Part 2 of the AISC Specification (Ref. 5) with the modification that the static yield stress is replaced by the corresponding dynamic value.

Reference 2 presents detailed criteria for columns and beam-columns subjected to blast loads, including the ultimate strength of axially loaded compression members, members subjected to combined axial load and biaxial bending, and effective length ratios for beam-columns.

Other topics pertaining to ultimate strength of steel elements are also treated in Reference 2, including the design of steel plates, blast doors, open-web joists, connections and special provisions for unsymmetrical bending.

To aid engineers and designers in the selection of support members subjected to blast loadings, Reference 3 presents design charts for the selection of single-span and multi-span cold-formed steel panels and wide-flange beam systems. These charts were developed based on the procedures and criteria in Reference 2.

Cold-Formed Steel Panels

Cold-formed steel panels are widely used for roof and wall panels in the construction of industrial installations and pre-engineered buildings. The behavior of these panels differs significantly from that of hot-rolled structural members due to the cross-sectional shapes which are made up of thin plate elements having large width-thickness and depth-thickness ratios. For static design, the AISI Specification for the Design of Cold-Formed Members (Ref. 7) provides the necessary design guidelines. However, consideration of the blast-resistant capacity of such panels requires additional provisions.

Under static loading, it is known that the load-deflection curve for cold-formed members is markedly non-linear and strongly dependent on the extent of local instability. The effective flexural properties of cold-formed sections are obtained by accounting for the post-buckling strength of stiffened compression flanges.

Cold-formed panels are produced in either open sections forming continuous corrugations, or closed sections consisting of a flat sheet with a series of hat sections, as illustrated in Figure 6. The amount of deformation that a specific section can develop after reaching its maximum resistance depends on the width-thickness ratio of the flange, as illustrated in Figures 7(a) and 7(b). For values of $w/t \leq 40$, the behavior is "ductile" since strains several times those attained at the onset of yielding can be developed before failure. For larger w/t ratios and especially for values greater than 60, the load-carrying capacity may be reduced abruptly upon yielding of the most stressed fiber. For an open cross-section, the descending curve is unstable in nature; whereas for a closed section, the decrease is more gradual, and a certain reserve capacity for energy absorption may exist, enhanced by the catenary action of the flat sheet, as indicated in Figure 7(b)

Due to the large width-thickness and depth-thickness ratios which characterize cold-formed sections, normal plastic design tech-

niques are not directly applicable to cold-formed construction. However, for the purposes of blast design it is possible to account for a limited, but definite amount of plastic behavior in these shapes. Criteria has been developed for inelastic design of cold-formed sections, based on the concept of limited ductility and partial redistribution, for panels designed to resist blast overpressure. The formulas of the AISI Specification have been extended and applied for this purpose. This criteria is presented in detail in References 2 and 8, and includes equations for ultimate moment capacities, ultimate resistances of single and continuous spans, stiffnesses, periods of vibration, shear stresses, support reactions, and rebound effects.

Figure 7(c) illustrates the non-linear character of the resistance-deflection curve and the suggested bilinear approximation used as a basis for developing the deformation criteria previously discussed. X_1 is defined as the maximum deflection at maximum resistance, X_u is the ultimate deflection after the drop in load carrying capacity. Based on static test data, the ratio of X_1/X_E has been estimated to range between 2.0 and 2.5. The amount of plastic deformation which is acceptable in design will vary in magnitude depending on the intended reusability or non-reusability of the panel after an accidental explosion. The ductility ratio criteria recommended in Reference 2 (as derived from static test data) i.e. 1.25 for reusable and 1.75 for non-reusable panels, are indicated in Figure 7(c).

Blast tests of cold-formed steel panels have recently been conducted by Picatinny Arsenal to verify the design criteria and determine the dynamic capacity of various panel sections. In these tests, held at Dugway Proving Ground, single span and three-span continuous panels were subjected to the blast effects of 2,000 pounds of explosives. The panels were subjected to overpressures ranging from 1 to 14 psi with a positive phase duration of about 50 msec. Although the test results are still being reduced and evaluated, the following are interim conclusions:

1. The criteria presented in Reference 2 result in conservative designs for cold-formed steel panels.

2. The maximum ductility ratios of 1.25 (reusable) and 1.75 (non-reusable) can be increased to about 2.5 (reusable) and 5.0 (non-reusable).

3. It has been indicated that the increased member strengths observed in the tests are due, in part, to actual static yield stresses which were on the order of twenty percent greater than the specified minimum yield strength. Since this difference between actual and minimum yield is especially significant for cold-formed sections it may be advisable to calculate moment capacities on the basis of actual yield strength values when such

information is available. Moreover, with respect to connection design, it may be somewhat unconservative to ignore the corresponding increase in maximum support shear.

4. Consideration is being given to using the full section modulus and full moment of inertia rather than reduced values as used in static design. This is due to the indication that under the rapid dynamic loading elastic buckling may not occur.

5. Tests up to 5 psi have indicated that open hat sections (Fig. 6(a)) can be used for applications in the low pressure range rather than only closed sections (Fig. 6(b)) as recommended in Reference 2.

6. Standard screw-type connections performed satisfactorily in blast tests up to 5 psi.

Implementation of the above criteria revisions is pending blast tests of a pre-engineered building to be conducted shortly where cold-formed steel panels will be tested under the support and interaction conditions of an actual complete structure.

Frames

As previously noted, the design of panels and supporting members can be accomplished with analyses of single-degree-of-freedom systems, whereas the design of frames involves multi-degree-of-freedom analyses. The complexities inherent in this type of analysis combined with the effects produced by the transient loads and the inelastic action of a frame require the aid of high-speed computers for a solution.

A computer program titled "Dynamic Inelastic Frame Analysis" (DYNFA) (Ref. 4 and 9) was developed by Ammann & Whitney, in conjunction with Picatinny Arsenal's Safety Engineering Support Program. The program determines the response of general types of frame structures (Fig. 8), subjected to arbitrary blast loads, in terms of the overall building motions as well as local displacements of the frame components. Although DYNFA was developed primarily for use in the analysis of structural steel frame buildings, it can also be used for the analysis of reinforced concrete frame structures.

In order to compute the response of a frame to the blast loads, DYNFA utilizes an approach which couples a lumped parameter representation of the structure with a numerical computation procedure in which the equations of motion of the system are integrated directly using the linear acceleration method. Inelastic behavior of individual members

is introduced into the analysis by the formation of concentrated plastic hinges whenever the combined axial load and bending moment capacity of a section is reached.

The lumped parameter representation of a frame consists of an assemblage of structural elements interconnected at nodal points as shown in Figure 9. Each nodal point has three degrees of freedom; namely, horizontal translation D_H, vertical translation D_V, and rotation θ. The mass of the structure, as well as the applied loads, are assumed to be concentrated at the nodal points. In this analysis, individual members can be modeled as one or more elements.

The results of the analysis consist of the deformations of the structure and the axial loads, bending moments and shears in each of the members. End rotations of each member are computed and utilized to monitor the amount of plastic deformation occurring in the structure. The computed deformations of the frame are compared to the ductile mode criteria previously given and, if necessary, the structure members are modified and the analysis is rerun until the most economical frame is obtained.

Application to Pre-Engineered Buildings

Standard pre-engineered buildings and other conventional steel frame structures are designed only for wind, seismic, dead and live loads; however, they possess a significant inherent blast-resistant capability. This is particularly true when the ultimate dynamic strength is considered and inelastic deformations are permitted. Moreover, the blast-resistant capability of a pre-engineered building can be increased by decreasing the spacing of the frames or by utilizing a frame designed for a higher conventional loading, while still retaining standard pre-engineered building components. Significant factors in the evaluation of the blast capability of conventionally designed structures include the difference in the relative proportions of lateral to vertical loads for conventional loading as compared to blast loading, and the differences in dynamic response characteristics between the overall frame and the individual structural members. For these reasons, it has been found in many cases that for actual conventional designs the blast capacity of the frame is considerably greater than that of the secondary members and it is, therefore, necessary to increase the size and/or decrease the spacing of these members in order to obtain a complete building with compatible blast capacity in all the members.

Some special factors involved in the application of the criteria and procedures, described in this paper, to pre-engineered buildings are discussed below.

The wall and roof panels of pre-engineered buildings usually consist of cold-formed open corrugated sections of the types shown in Figure 6(a), and the criteria for cold-formed steel panels would apply

to these panels, at least for the low overpressure range where it has been determined that closed sections are not required. In the design or analysis of these panels, rebound effects must also be considered, particularly with regard to the design of the connections (Ref. 2).

Girts and purlins of typical pre-engineered buildings are usually specially fabricated, cold-formed Z or channel-shaped members, rather than standard hot-rolled sections. These sections usually do not meet the requirements for plastic design because of the large flange width-thickness and web depth-thickness ratios. Consequently, the ductility and rotational criteria for the cold-formed panels are considered to be more applicable to these members than the criteria for the hot-rolled beams. It is noted in this regard that because of the relatively long spans encountered for girts and purlins, the design of these members for blast loads is usually controlled by rotation rather than ductility, which is a less critical condition considering the local buckling problems associated with these thin-plate members.

The main rigid frames of pre-engineered buildings are usually fabricated from standard hot-rolled sections or from built-up members consisting of hot-rolled plates welded together to form the column and girder members. In some cases these members do not meet the plastic design requirements for compact sections because of the thin plate sections utilized. In addition, pre-engineered building frames are usually fabricated in sections to facilitate shipment to the site. These sections are then spliced together in the field with connections which may not conform to the plastic design requirements of the AISC Specification (Ref. 5). It may be necessary, therefore, to limit the ductility of such frames.

The DYNFA program is especially suitable for the analysis of pre-engineered frames subjected to blast overpressure to determine the structural response and to establish the ultimate blast load capacity of the frame. DYNFA accounts for the following characteristics of blast-loaded frames and hence leads to accuracy and economy in design:

1. By permitting inelastic behavior, a greater blast loading can be resisted by the frame as a result of redistribution of stress and increased energy absorption.

2. Pre-engineered building frame members are generally tapered for economy and it is important to use intermediate nodal points since plastic hinges are more apt to form between the member ends than in the case of members of constant section.

3. The period of vibration of the sidesway mode of the frame is generally longer than the load duration, thereby resulting in a low dynamic response.

4. After the blast wave engulfs the entire structure the net sidesway loading is reduced by the load acting on the back wall.

5. A rise time (gradual buildup) of the blast loading on the frame due to the time to fully load the secondary members (girts, purlins, panels) reduces the response of the frame. This is particularly important with regard to the response of the columns to axial loads.

In order to verify and refine the criteria as it applies to the design of pre-engineered buildings subjected to blast loads, the design shown in Figure 10 will be tested shortly by Picatinny Arsenal at Dugway Proving Ground. As a basis for establishing the overpressure range to be utilized in the test, the conventional structure was analyzed to determine its blast capacity. In addition, certain components were modified to obtain an overall structure with a more nearly consistent blast capacity.

The building consists of 12 ft. high, 20 ft. wide, standard pre-engineered building rigid frames spaced at 20 ft. to form an 80 ft. long structure. One end-frame consists of post and beam construction in which the wall panel is intended to resist lateral forces as a shear wall. Lateral bracing has been provided in the longitudinal direction. The building was designed for the following conventional loads: 20 psf live load; 25 psf wind load; 3 psf dead load.

It was determined by utilizing the DYNFA program that the rigid frames are capable of resisting a maximum incident blast loading of 1.0 psi (2 psi reflected pressure). The calculated peak sidesway was 6.0 inches with plastic action occurring at all of the nodal points. However, by analysis of the individual secondary members it was determined that the capacity of the wall and roof panels and Z-section girts and purlins was in the order of 0.3 psi (0.6 psi reflected). As a result, the following revisions were made to these members to increase their capacity:

1. Maximum girt spacing was reduced from 7 ft.-3 in. to 4 ft.-0 in., and the girt sections were increased from 8x3x0.064 Z to 9.75x4x0.1345 Z.

2. Purlin sections were increased from 8x3x0.064 Z to 8x3x0.084 Z.

3. Wall and roof panel thickness was increased from 26 to 24 gage.

4. The foundation was made heavier based on the reactions determined from the DYNFA analysis. In addition the column footings were tied together by the floor slab to prevent relative lateral displacement of the footings.

MASONRY

General

A wide range of acceptor structure applications and wall configurations must be provided for in the development of design criteria for masonry walls (Ref. 10). Masonry units may be used for both exterior walls (non-load bearing curtain walls set within or hung on a structural frame or load-bearing structural walls) subject to blast overpressures, and interior partition walls subjected to inertial effects due to overall building motions and/or to the internal buildup of pressure within the structure due to the leakage of blast pressure through openings. Basic variations in wall configurations may be related to the type of masonry unit (brick or concrete, solid or hollow), the manner in which the units are laid (running bond, stack bond, etc.), the number of wythes of block (single or multiple), the basic lateral load-carrying mechanism (reinforced or arched wall, one-way or two-way spanning).

In addition to their inherent advantages with respect to fire protection, acoustic and thermal insulation, structural mass, and resistance to flying debris, masonry walls - properly designed and detailed - can provide economical resistance to relatively low blast pressures. The limitations on their application include a limited capability for large deformations, reduced capacity in rebound due to tensile cracking in the primary phase of the response and obvious limitations on the amount and type of reinforcement which can be provided in masonry walls.

One of the chief difficulties in masonry wall design involves the realistic representation of the governing resistance function - particularly where arching is involved - since the resistances are dependent on the behavior of adjacent elements. For example, in dynamically loaded structures, additional restraint against lateral displacement is provided by precompression due to vertical loads or may be reduced by negative pressures or rebound of the roof members. Hence, the interaction between vertical and lateral load-carrying capacity must be considered in evaluating the capacity that can be developed and the consequences of collapse of a particular masonry panel or supporting member. For this reason, good workmanship and inspection are especially important in these applications. Since the blast load encompasses the entire structure, failure in a single weak area may propagate more widespread damage through the adjacent members and panels.

For blast design, masonry units laid in running bond and reinforced vertically and/or horizontally (Fig. 11) are most commonly used. The reinforcement provides additional strength, ductility and overall integrity under severe loadings. Due to the staggered placement of the units, running bond, as opposed to stack bond, avoids the development of a potential plane of failure through the mortar.

The dynamic aspects of the design of masonry walls are discussed below in the two general categories of reinforced and unreinforced walls. The conventional aspects of the design and construction follow the standard masonry specifications (Ref. 11 and 12).

Reinforced Masonry Walls

Blast design procedures and criteria are required both for the evaluation of the capacity of existing walls and for the design of walls specifically for blast. In many facility applications, the DOD seismic design requirement for two-way reinforcement in masonry walls provides the wall with substantial blast resistance.

Reinforcement in masonry walls can be of various types (See Fig. 11). In a vertically spanning wall, one, or perhaps two, reinforcing bars are inserted in a cell and the bars are then solidly grouted in place. For horizontal spanning and relatively low pressures (up to about 1 psi), reinforcement can be provided in the form of prefabricated truss bar reinforcement laid in every or alternate courses. Alternatively, horizontal reinforcing bars may be placed in bond beams or channel units and solidly grouted. The function of the grout is to insure sufficient bond and interaction between the reinforcement and the masonry unit and to protect the bars against corrosion. By definition, the term "reinforced masonry" indicates that masonry unit, reinforcement, grout and mortar are combined in such a way that these component materials act together in resisting load. The reinforcement provides (a) increased strength; (b) increased energy absorption capability and ductility; and (c) reduced likelihood of brittle failure of the masonry, i.e., the reinforcement will tend to hold together the masonry wall even though cracking of the masonry and mortar has occurred between the reinforcing bars.

It is important that the reinforcing bars be continuous or well-anchored for ductile response of the reinforced walls. Hence corners and intersections are provided with special splice and anchorage reinforcement details. Furthermore, in order to prevent failure at a support as a result of rebound and/or negative overpressures anchor straps are provided in block walls at the supporting beams or columns, in order to provide a positive connection for response in the rebound direction. Finally, in order to provide compatible fragment resistance in a structure designed with masonry walls, consideration should be given to the use of cast-in-place or precast concrete slabs, rather than metal panels, for the roof construction.

Reinforced masonry walls are designed on the basis of their response in the flexural mode. Moreover, additional shear capacity must be provided to guard against a premature failure due to diagonal tension stresses or direct shear at the support. Ultimate moment capacities and shear stress calculations are made on the basis of ultimate strength rela-

tionships for under-reinforced reinforced concrete sections, together with the recommended effective areas for masonry sections in shear, axial compression and flexure, as provided in Reference 13.

The dynamic flexural response of the walls is calculated on the basis of a single-degree-of-freedom analysis by representing the masonry wall with an idealized bilinear resistance function (Fig. 5) and treating the load as a triangular pulse with zero rise time. The effective stiffness and natural frequency of the wall are developed accounting for the support conditions, the section geometry and progressively non-linear nature of the load-deflection relationship which develops as the wall progresses through the uncracked elastic, cracked elastic, elasto-plastic (for indeterminate elements) and plastic regions of the response. The maximum response, determined in terms of ductility ratio, μ, from the charts in References 1 and 2, is limited to the maximum level (ductility ratio and absolute deflection) permitted for the particular type of wall and the particular application. The on-going development of this criteria must consider the ductile energy-absorption capability of the basic wall types, the hazard to nearby personnel and equipment due to the progressively more severe cracking and spalling as the wall approaches its ultimate capacity, and the post-accident condition of the wall, i.e., the ability of a previously-loaded wall, with minor or moderate cracking, to undergo another application of load and/or the repair time associated with reinstating the blast capacity of the wall. Another significant consideration is the rebound response of masonry walls. In this regard, several factors tend to reduce the amount of anticipated rebound, including the relatively longer load durations associated with acceptor structures, the short natural periods of these relatively stiff walls, and the inherent internal damping due to cracking. However, since the rebound capacity of a masonry wall involves the reloading in compression of the cracked masonry which was in tension in the initial phase of the wall's response, a more or less significant reduction in rebound capacity will result depending upon the level of response, and the associated damage which is tolerated in the primary direction.

Unreinforced Masonry Walls

With regard to blast design, the use of unreinforced masonry walls is limited to applications where their capacity to resist lateral loads by arching action is utilized. Where arching action is not developed, failure occurs at a low pressure level due either to a tensile failure in the mortar itself or at the interface between the mortar and the masonry unit. The capacity of an arched wall is considerably in excess of the pressure level associated with this type of brittle flexural failure (Ref. 14 and 15).

Arching occurs when a masonry wall is constrained between substantial rigid supports which resist outward movement in the plane of the wall as it deflects under the lateral blast load. The resistance to lateral load develops from the compressive forces set up in the plane of the panel as the masonry material tends to be crushed at midspan and at the end

supports. As shown in Figure 12, the subsequent motion consists of the rigid body rotation of each half of the wall about these points. The magnitude of the resulting force couple is dependent upon the support rigidity and the stress-strain properties of the masonry. This rotation continues until either the load is removed or failure occurs due to the development of a wall deflection large enough to cause the couple moment arm to vanish.

The resistance-deflection function for arched walls is shown schematically in Figure 13. It consists of an elastic phase up to the point where the concrete initially crushes, and a subsequent decaying or unstable phase during which the wall is acting as a flat arch. The analytical development of such resistance functions for arched walls is available in the literature (Ref. 15,16,17 & 18). The deflection time history of arched walls can be determined by performing a step-by-step numerical solution of the governing equation of motion.

In protective design, the analysis of arched walls pertains mainly to the evaluation of the ability of existing walls to survive a blast load. Generally speaking, current designs are more apt to consider the strength due to the reinforcing required for conventional loads. It may not be economical to provide the structural system required to obtain an increased strength due to arching, i.e., block units laid against relatively rigid beams or columns with little or no gap between the block and the support.

PRECAST CONCRETE

General

The use of precast concrete construction in blast resistant design has two advantages, namely; (1) erection time for precast construction will be significantly less than that required for cast-in-place concrete; and (2) precast construction will provide protection against primary and secondary missiles not usually afforded by steel construction. These advantages are applicable to both prestressed and conventionally reinforced concrete precast members. In addition, precast construction is usually more economical than cast-in-place concrete construction; particularly where standard precast shapes (Fig. 14) can be used. The economy in using the standard shapes is achieved by the fact that most precast manufacturers have available metal or other type forms for casting most of the more commonly used sections. The use of standard precast shapes will usually be restricted to the pressure levels in the order of several psi or less. For higher levels of pressures, the use of cast-in-place concrete will usually be the more economical means of construction.

This portion of the paper summarizes, in qualitative form, the procedures to be used for design of precast blast resistant structures as presented in Reference 21.

Design Considerations

Precast construction can consist either of prestressed or conventional reinforced members. Since smaller material quantities are associated with the higher strength materials (both steel and concrete) used in prestressing, this type of construction is generally more economical than the conventional reinforcing. Furthermore, because of its reduced weight a greater portion of the strength of a prestressed member is available to resist blast than would be available in a conventionally reinforced member. However, in certain design situations the use of prestressed members will be impractical and, therefore, standard reinforcement must be used. An example of this situation is the design of a precast panel having relatively large openings and/or a number of openings. In this particular case, the special provisions needed to obtain a smooth stress flow around the openings would not be economically achieved with prestressed construction.

The strength of precast members with conventional reinforcement can be determined in accordance with the procedures given in Reference 1, while the strength characteristics of prestressed members may be calculated based upon the relationships given in References 19 and 20. In the case of the latter, however, provisions for increase in strength due to the dynamic nature of the blast loads should be provided as indicated in Reference 1.

Unlike intermediate grade reinforcement and structural steel, which can sustain relatively large straining at ultimate strength, the steel strands used in prestressed concrete can only undergo maximum elongations of 3.5 to 4 percent of the original length before the ultimate strength of the steel is reached. Furthermore, prestressed concrete steel will not exhibit a sharp, well defined yield plateau, but rather a slow continuous yielding with a curved stress-strain relationship until its ultimate strength is developed (Fig. 15). This type of stress-strain relationship precludes the use of plastic deformations and, in general, requires prestressed members to be designed to remain in the elastic range of response. However, the energy absorption capabilities lost due to nonplastic action may in many instances be offset by the high tensile strength afforded by the prestressed steel.

Although precast concrete members which utilize intermediate grade reinforcement can undergo some plastic straining, the magnitude of plastic deformations must be limited because of the brittle characteristics of the connectors used to attach adjoining precast members. As will be described later, most of these connectors consist of embedded steel plates which are connected by field welding of "loose" steel plates and/or structural shapes to the embedded plates. The brittleness of the connectors is produced by the change in physical and chemical properties of the structural steel associated with the welding.

It is suggested that the connectors of both prestressed and conventionally reinforced precast concrete members be designed to have a capacity which exceeds by at least 10 percent those of the members being connected.

Snow, wind, seismic and other live loads are usually small in comparison to the dead weight of conventionally loaded precast buildings. However, in blast resistant design, the magnitude of the blast loads will usually be equal to or greater than that of the dead weight of the buildings. This increased live to dead weight ratio will be a significant factor in the design of both the individual members and the connectors of precast buildings. For example, in the erection of a precast building, roof panels are placed on supporting members before the connection between the panels and supports is made. This permits the dead weight of the panels to be resisted by the simple beam action of the panels without inducing stresses in the connectors due to the rotation of ends of the panels. The stresses induced in conventional connectors by the rotation of the panels due to normal live loads are small, whereas the stresses produced by the blast loads would be significantly larger and hence such connectors would be expensive. In general, therefore, connectors of precast members should be designed such that the blast loads are transmitted to supporting members through simple beam action. Illustrative examples of simple beam connectors are given later in this paper.

Other factors to be considered in blast design of precast members and, in particular, prestressed precast members, are the effects associated with reversal stresses produced by vibrating members and negative phase blast pressures. Both individual members and connectors must be designed to sustain these stresses.

Application of Precast Construction

To illustrate the above procedures, consider the design of the precast concrete structure illustrated in Figure 16. This building is an Operations Office Building designed for and constructed by Catalytic, Inc., Philadelphia, Pa.

The structure will not house explosives and has overall plan dimensions of 128 ft. by 40 ft. and the total wall height above the floor slab is 16 ft.-10 in. The highest point on the roof panel is 15 ft.-8 in. above the floor and is located above the precast concrete girder at the center line of the structure. The extension of the wall above the roof serves as a parapet around the building's periphery.

Both the roof and wall panels are 8 feet wide and have a double stem "Tee" shaped cross section as illustrated in Figure 14. The stems of the roof panels extend downward while those of the wall panels extend outward from the exterior of the building. At the periphery of the structure, the roof panels are supported on corbels which are cast monolithically into the wall panels. The interior end of each roof panel is supported by

previously mentioned precast girders which, in turn, are supported by precast columns (Fig. 17). Both the columns and wall panels are supported on a cast-in-place reinforced concrete floor slab.

Monolithic action between the intersecting members is achieved with the use of splice plates and angle connections which transfer both the vertical and horizontal blast loads to the concrete floor. The splice plate and angle connections are formed in the field by welding (Fig. 17). Plates are embedded in the individual members at the points of connections. In general, standard connections are used with slight modifications to insure that reversal loads are resisted and that the fixity between the roof and wall panels is not developed.

For precast construction, all horizontal forces produced by the blast pressures acting on the structure walls are resisted by shear wall action of the wall panels. Standard connections (Fig. 18) are used to transfer the horizontal forces between adjoining panels. A similar detail is used to develop the deep-beam action of the roof slab. As may be noted in Figure 17 all vertical forces, both direct load and rebound, are transferred through the so-called "loose" splice plates while the horizontal forces are transferred through the angle and bent plate connectors.

In this particular design, both roof and wall panels were constructed of prestressed concrete, whereas the columns and girders utilized conventional reinforcement. In the case of the prestressed members, prestressing strands were placed at both the top and bottom of each stem. The strands located near the top of the "Tees" provide the necessary strength to resist rebound and negative phase pressures. It may be noted that in order to achieve economy in design, straight rather than draped prestressed strands were used. A compressive strength of 5000 psi was used for all prestressed members.

REFERENCES

1. Department of the Army, "Structures to Resist the Effects of Accidental Explosions (with Addenda)", Technical Manual TM 5-1300, Washington, D.C., June 1969.

2. Healey, J.J., et al, "Design of Steel Structures to Resist the Effects of HE Explosions", Technical Report 4837, prepared by Ammann & Whitney, Consulting Engineers, New York, N.Y., for Picatinny Arsenal, Dover, N.J., 1975

3. Tseng, G.S., Weissman, S., and Dobbs, N., "Design Charts for Cold-Formed Steel Panels and Wide-Flange Beams Subjected to Blast Loads", Technical Report 4838, prepared by Ammann & Whitney, Consulting Engineers, New York, N.Y., for Picatinny Arsenal, Dover, N.J., 1975.

4. "Analysis of Frame Structures Subjected to Blast Overpressures", Technical Report TR 4839, prepared by Ammann & Whitney, Consulting Engineers, New York, N.Y., for Picatinny Arsenal, Dover, N.J. 1976.

5. American Institute of Steel Construction, "Specification for the Design, Fabrication and Erection of Structural Steel for Buildings" and "Commentary" thereon, New York, N. Y., 1969.

6. Galambos, T.V., and Lay, M.G., "End Moment-End Rotation Characteristics for Beam-Columns", Fritz Engineering Laboratory, Lehigh University, Bethlehem, Pa., May 1962.

7. American Iron and Steel Institute, "Specification for the Design of Cold-Formed Steel Structural Members" and "Commentary" thereon, New York, N.Y., 1968.

8. Ammar, A.R., Tseng, G.S., and Healey, J.J., "Blast-Resistant Design of Cold-Formed Steel Panels" Proceedings of the Third International Specialty Conference on Cold-Formed Steel Structures, University of Missouri-Rolla, November 1975.

9. Tseng, G.S., et al, "Elastic and Elasto-Plastic Computerized Dynamic Analysis of Frame Structures Subjected to Blast Overpressure", Proceedings, ASCE National Structural Engineering Conference, University of Wisconsin, Madison, August 1976.

10. "Design of Masonry Structures to Resist the Effects of HE Explosions", prepared by Ammann & Whitney, Consulting Engineers, New York, N.Y., for Picatinny Arsenal, Dover, N.J., Draft Report, 1976.

11. Structural Clay Products Institute, "Building Code Requirements for Engineered Brick Masonry", McLean, Va., 1969.

12. National Concrete Masonry Association, "Specification for the Design and Construction of Load-Bearing Concrete Masonry", Arlington, Va., 1970.

13. "Seismic Design for Buildings", Department of the Army Technical Manual TM 5-809-10, April 1973.

14. Wilton, C., and Gabrielson, B., "Shock Tunnel Tests of Preloaded and Arched Wall Panels", prepared by U.R.S. Research Company, San Mateo, Ca., for Defense Civil Preparedness Agency, Washington, D.C., June 1973.

15. Gabrielson, B., and Wilton, C., "Shock Tunnel Tests of Arched Wall Panels", prepared by U.R.S. Research Company, San Mateo, Ca., for Defense Civil Preparedness Agency, December 1974.

16. McDowell, E., McKee, K., and Sevin, E., "Arching Action Theory of Masonry Walls", Journal of the Structural Division, ASCE, Vol. 82, No. ST 2, March 1956.

17. "Design of Structures to Resist Atomic Blast" prepared by Ammann & Whitney, Consulting Engineers, New York, N.Y., for Chief of Engineers, Department of the Army, Volume 1, 1954.

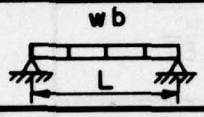
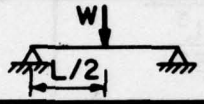
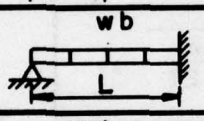
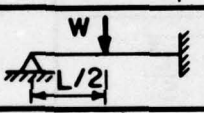
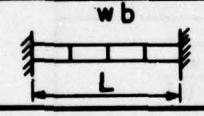
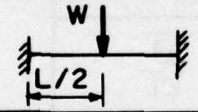
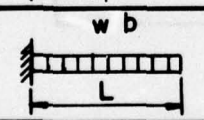
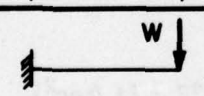
18. Whitney, C.S., Anderson, B.G. and Cohen, E., "Design of Blast Resistant Construction for Atomic Explosions", Journal of the American Concrete Institute, Volume 51, March 1955.

19. "Building Code Requirements for Reinforced Concrete", American Concrete Institute, ACI 318-71, 1971.

20. Lin, T.Y., "Design of Prestressed Concrete Structures", John Wiley & Sons, Inc., July 1955.

21. "Design of Precast Concrete Structures to Resist the Effects of HE Explosions" prepared by Ammann & Whitney, Consulting Engineers, New York, N.Y., for Picatinny Arsenal, Dover, N.J., Draft Report, 1976.

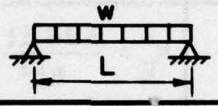
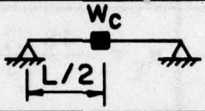
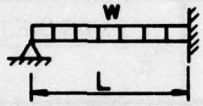
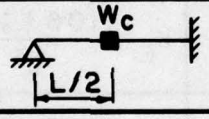
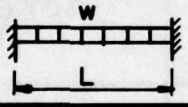
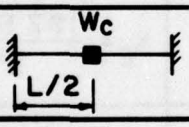
TABLE 1 ULTIMATE RESISTANCE AND STIFFNESS OF BEAM ELEMENTS

Member And Load Configuration	Ultimate Flexural Resistance	Equivalent Elastic Stiffness
	$r_u bL = 8.0 \frac{M_p}{L}$	$K_E = \frac{384 EI}{5L^3}$
	$R_u = 4.0 \frac{M_p}{L}$	$K_E = \frac{48 EI}{L^3}$
	$r_u bL = 12.0 \frac{M_p}{L}$	$K_E = \frac{160 EI}{L^3}$
	$R_u = 6.0 \frac{M_p}{L}$	$K_E = \frac{106 EI}{L^3}$
	$r_u bL = 16.0 \frac{M_p}{L}$	$K_E = \frac{307 EI}{L^3}$
	$R_u = 8.0 \frac{M_p}{L}$	$K_E = \frac{192 EI}{L^3}$
	$r_u bL = 2.0 \frac{M_p}{L}$	$K_E = \frac{8 EI}{L^3}$
	$R_u = \frac{M_p}{L}$	$K_E = \frac{3 EI}{L^3}$

Where:

b = Width Of Contributory Loading Area (ft)
M_p = Plastic Moment Capacity (lb-ft)
r_u = Ultimate Resistance per Unit Area (psf)
R_u = Ultimate Total Resistance (lb)
w = Load per Unit Area (psf)
W = Total Concentrated Load (lb)
L = Span Length (ft)

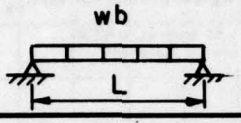
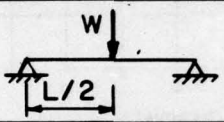
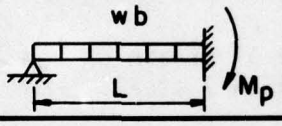
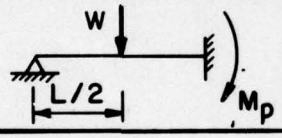
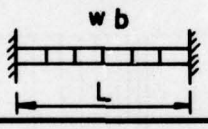
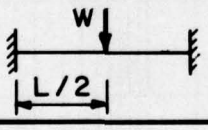
TABLE 2 EFFECTIVE NATURAL PERIOD OF VIBRATION FOR ELASTIC BEAM ELEMENTS

Member	Period
	$T_N = 0.64\ L^2 \sqrt{\frac{w}{gEI}}$
	$T_N = 0.91 \sqrt{\frac{W_c}{g} \frac{L^3}{EI}}$
	$T_N = 0.42\ L^2 \sqrt{\frac{w}{gEI}}$
	$T_N = 0.61 \sqrt{\frac{W_c}{g} \frac{L^3}{EI}}$
	$T_N = 0.28\ L^2 \sqrt{\frac{w}{gEI}}$
	$T_N = 0.45 \sqrt{\frac{W_c}{g} \frac{L^3}{EI}}$

Where:

w = Weight per unit length (lb/ft)
W_c = Total concentrated weight (lb)
L = Span length (ft)
g = Acceleration due to gravity (32.2 ft/sec^2)
E = Modulus of elasticity (psf)
I = Moment of inertia (ft^4)
T_N = Effective natural period (sec)

TABLE 3 SUPPORT SHEAR FOR BEAM ELEMENTS

Member And Load Configuration	Maximum Support Shear
	$V = \frac{r_u bL}{2}$
	$V = \frac{R_u}{2}$
	$V = \frac{r_u bL}{2} + \frac{M_p}{L}$
	$V = \frac{R_u}{2} + \frac{M_p}{L}$
	$V = \frac{wbL}{2}$
	$V = \frac{R_u}{2}$

Where:

b = Width Of Loaded Area (ft)
V = Support Shear (lb)
r_u = Ultimate Resistance per Unit Area (psf)
R_u = Ultimate Total Resistance (lb)
w = Load per Unit Area (psf)
W = Total Concentrated Load (lb)
L = Span Length (ft)

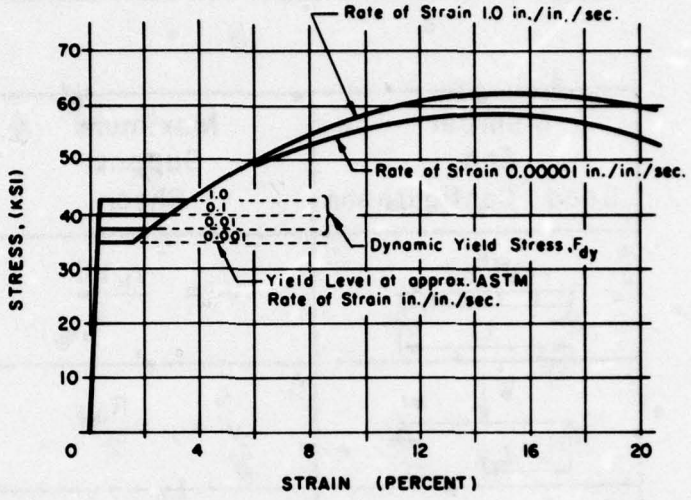


Figure 1 Effect of rate of strain on the stress - strain curve of A-7 steel.

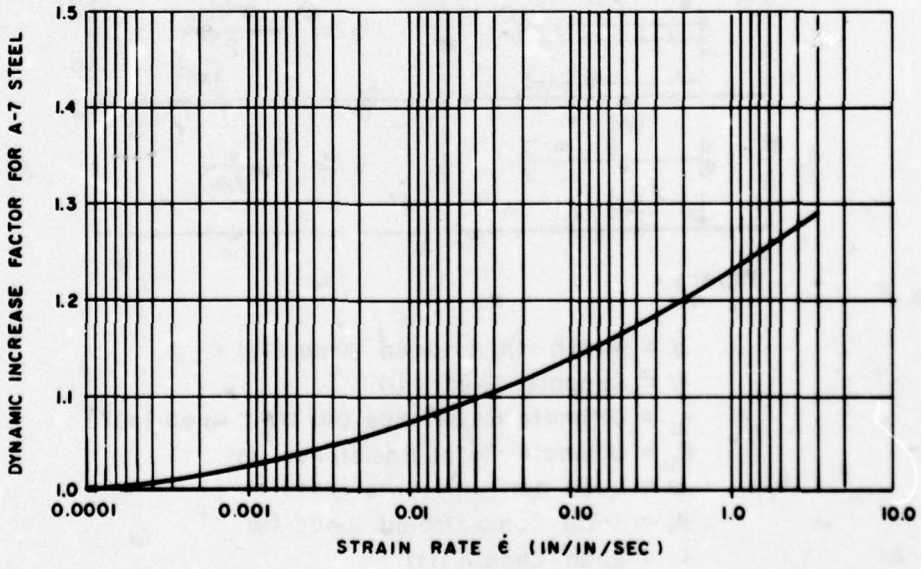


Figure 2 Values of dynamic increase factor at various strain rates.

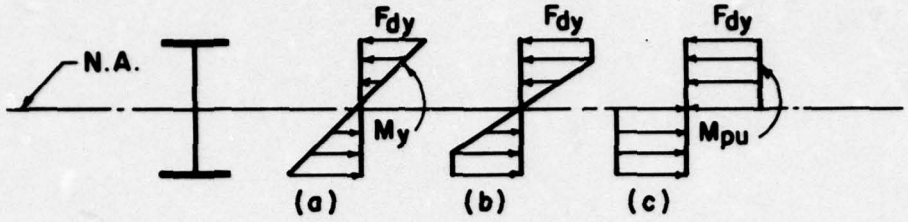


Figure 3 Theoretical stress distribution for pure bending at various stages of loading.

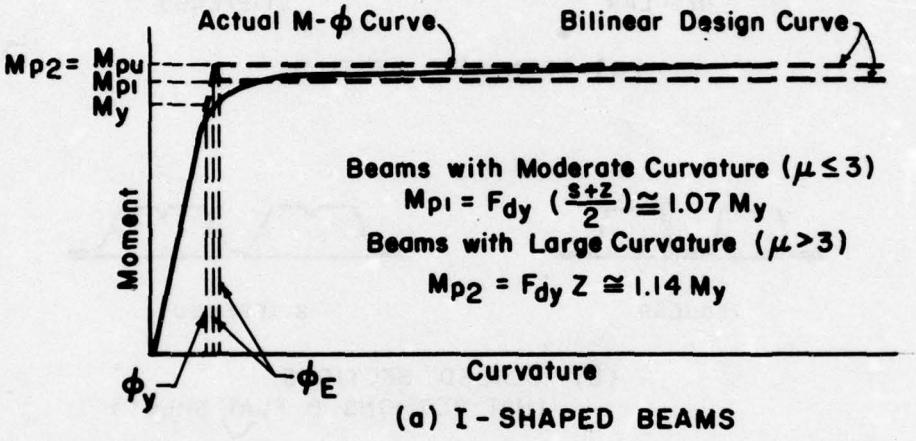


Figure 4 Dynamic moment-curvature diagrams for simply-supported beams.

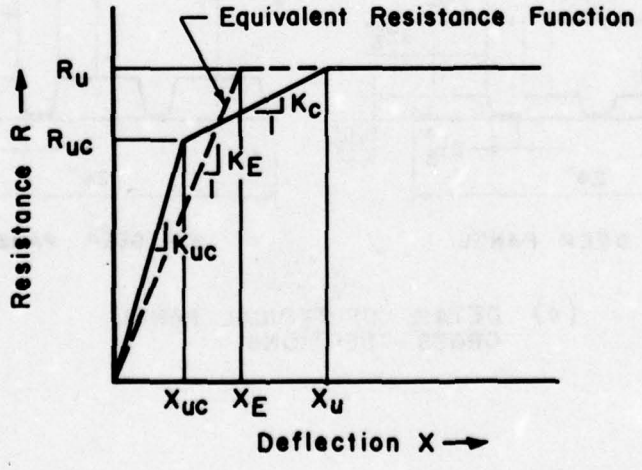
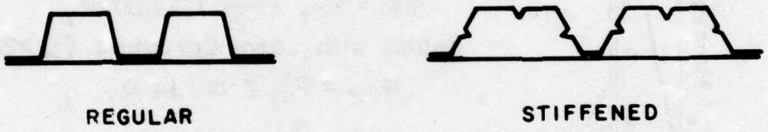


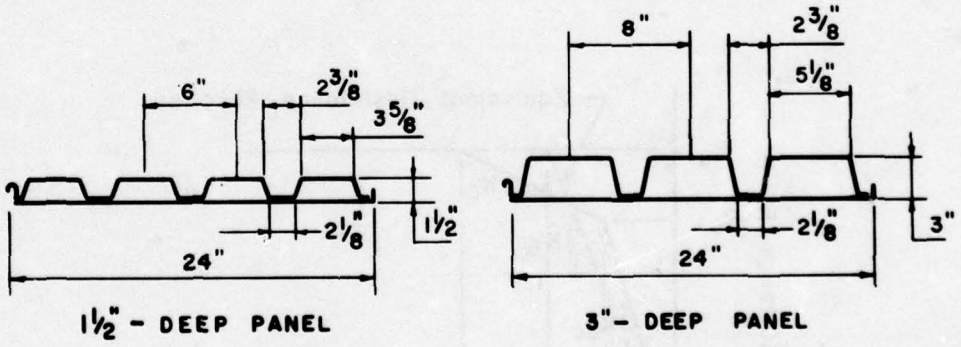
Figure 5 Bilinear resistance function.



(a) OPEN HAT SECTIONS

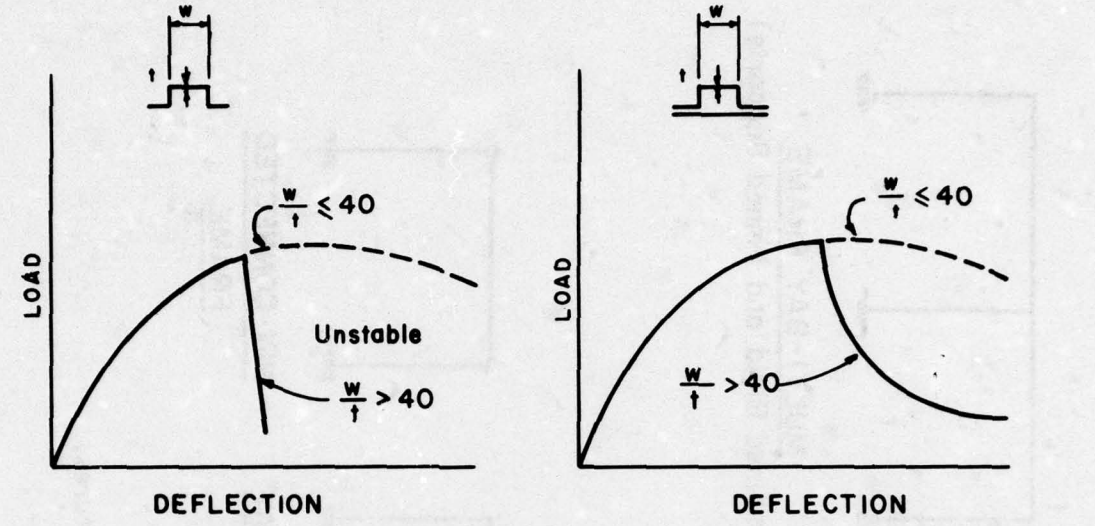


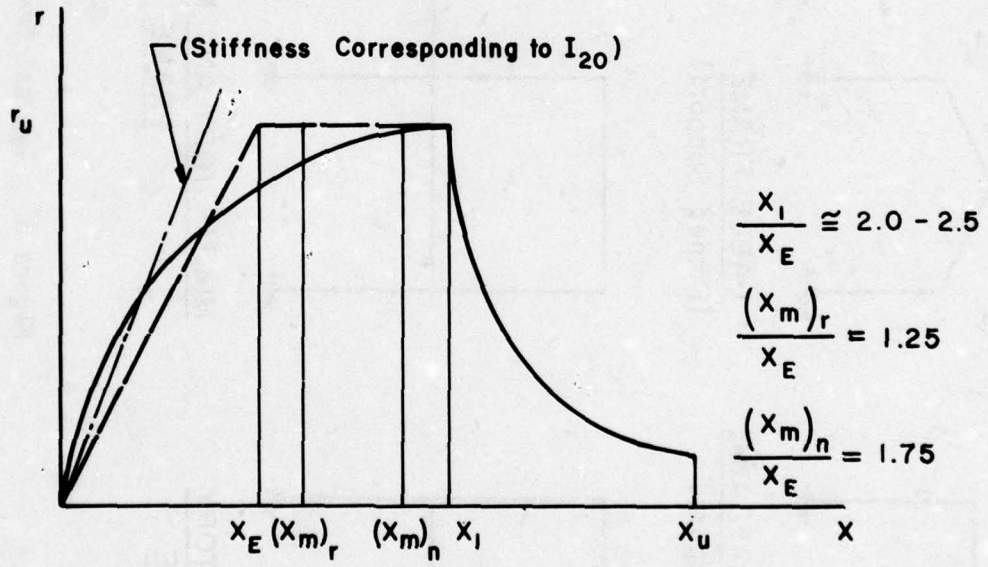
(b) CLOSED SECTIONS
(HAT SECTIONS & FLAT SHEET)



(c) DETAIL OF TYPICAL PANEL
CROSS - SECTIONS

Figure 6 Cold-formed sections and typical panel configurations.





(c) BILINEAR APPROXIMATION OF RESISTANCE-DEFLECTION CURVE FOR CLOSED SECTIONS.

Figure 7 Load-deflection characteristics of cold-formed, light-gage sections.

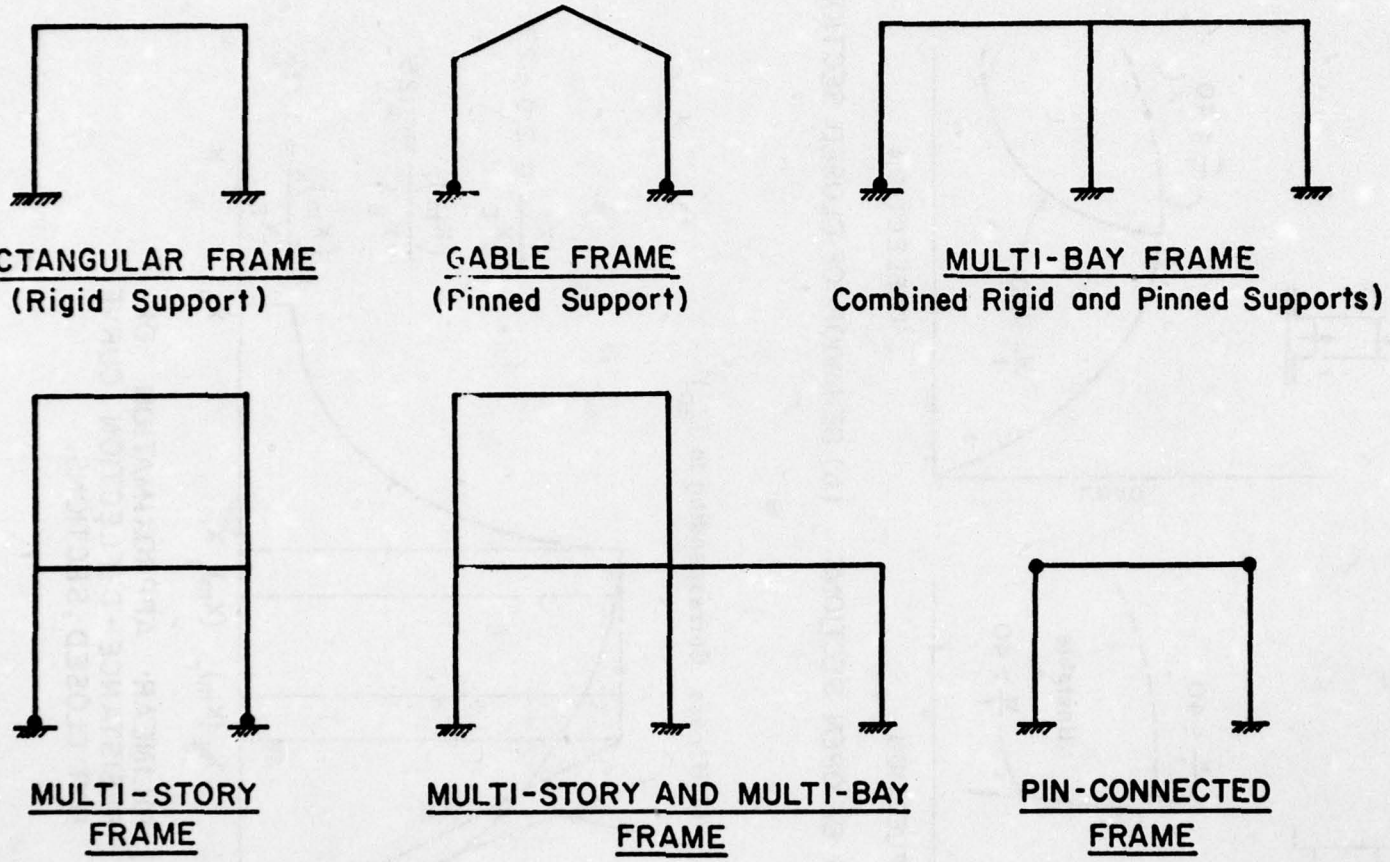


Figure 8 Typical frame structures.

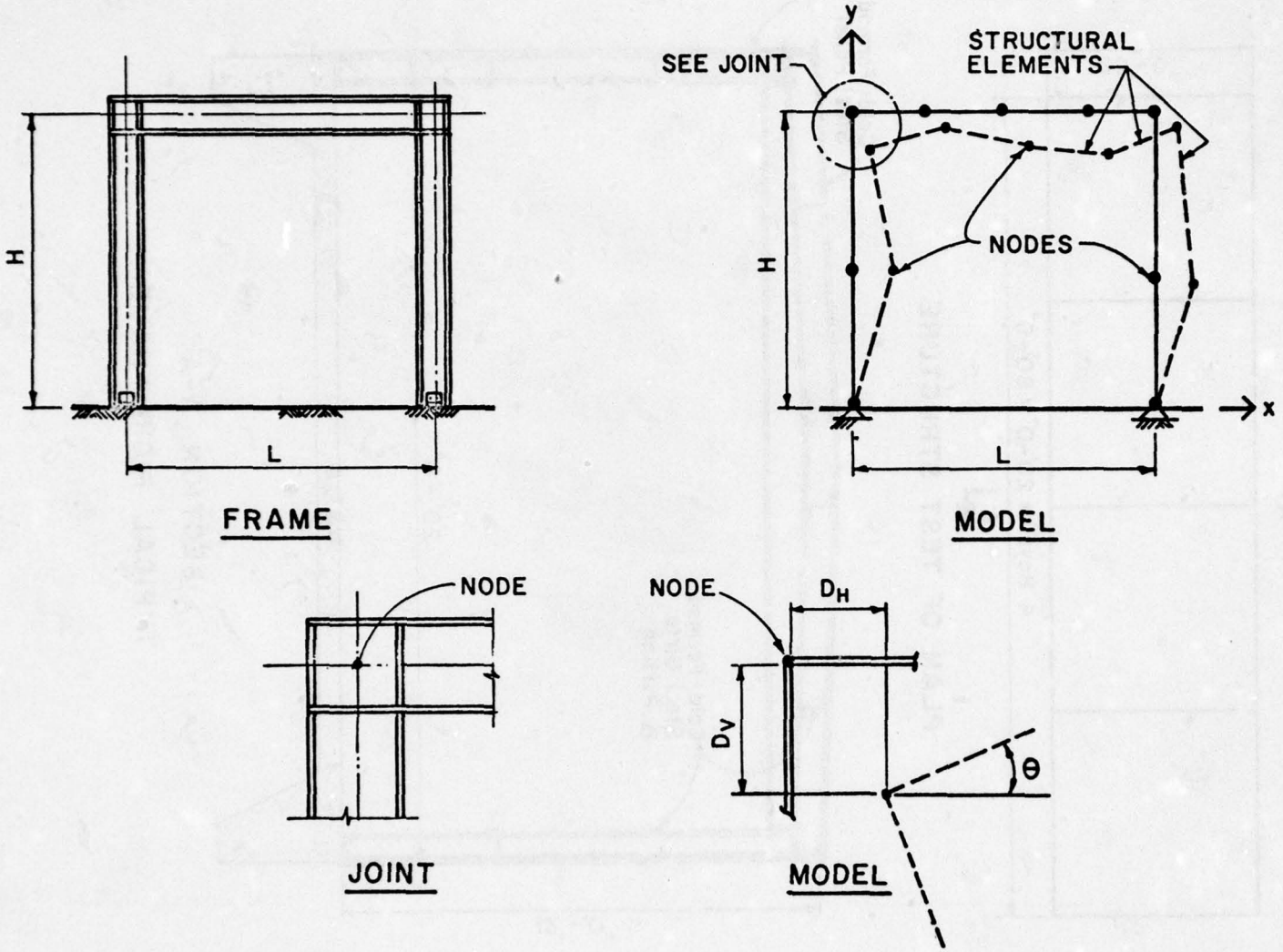
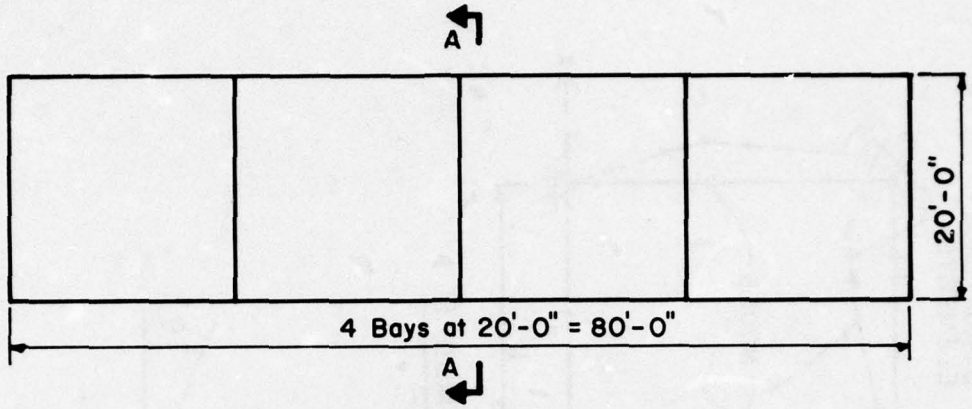
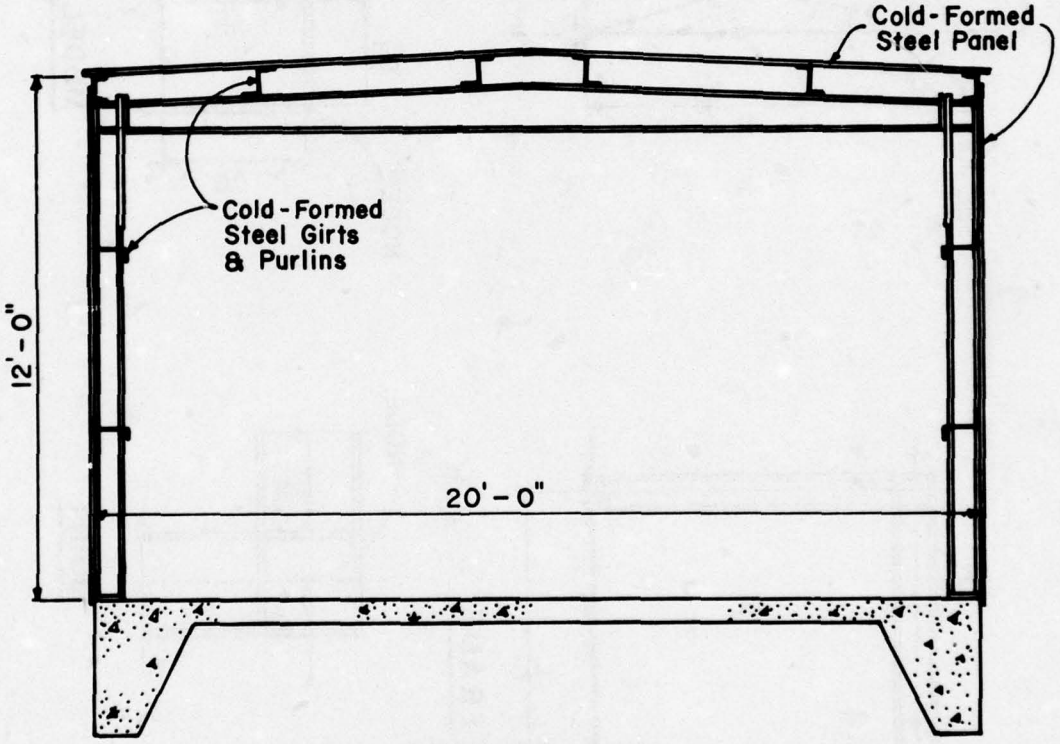


Figure 9 Lumped parameter representation of a frame.



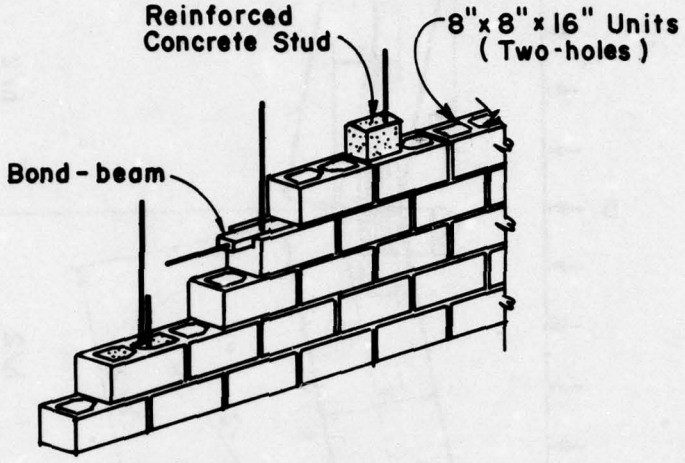
PLAN OF TEST STRUCTURE



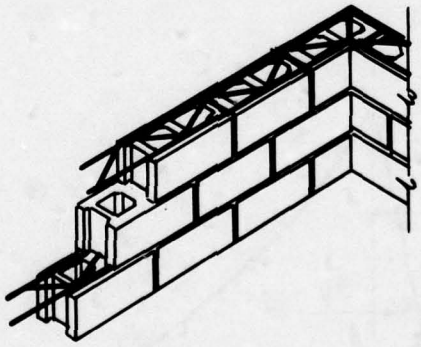
SECTION A-A

TYPICAL RIGID FRAME

Figure 10 Pre-engineered building test structure.



(a) CONCRETE BLOCK WITH VERTICAL REINFORCEMENT



(b) CONCRETE BLOCK WITH TRUSSED-BAR REINFORCEMENT AT 16" o.c.

Figure 11 Typical reinforced hollow masonry.

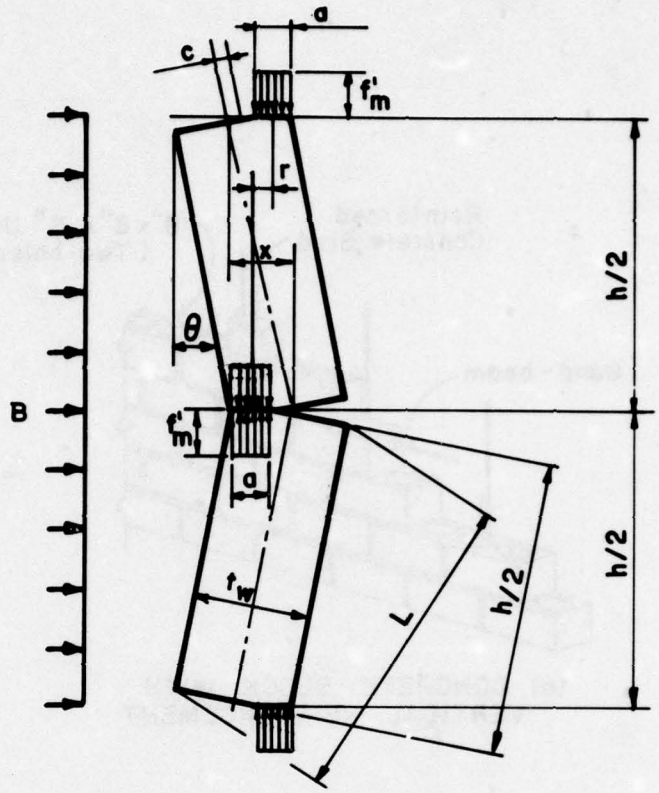


Figure 12 Arching behavior of masonry wall.

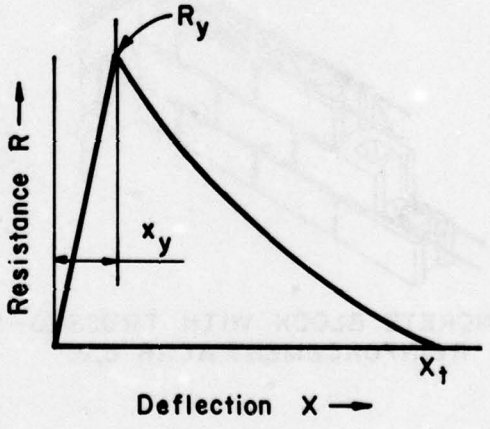
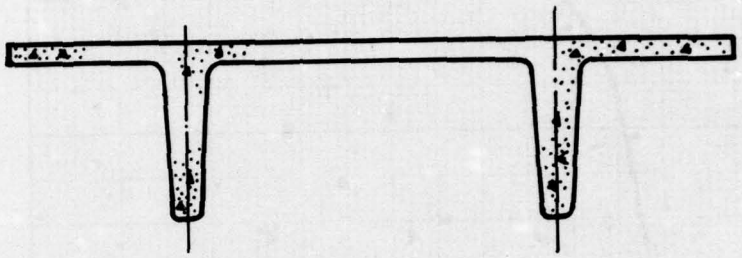
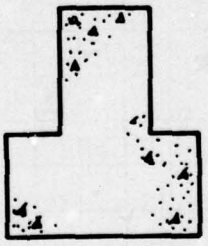


Figure 13 Resistance function for unreinforced solid masonry panel with rigid supports.



TYPICAL ROOF OR WALL PANEL



TYPICAL GIRDER

Figure 14 Standard precast concrete members.

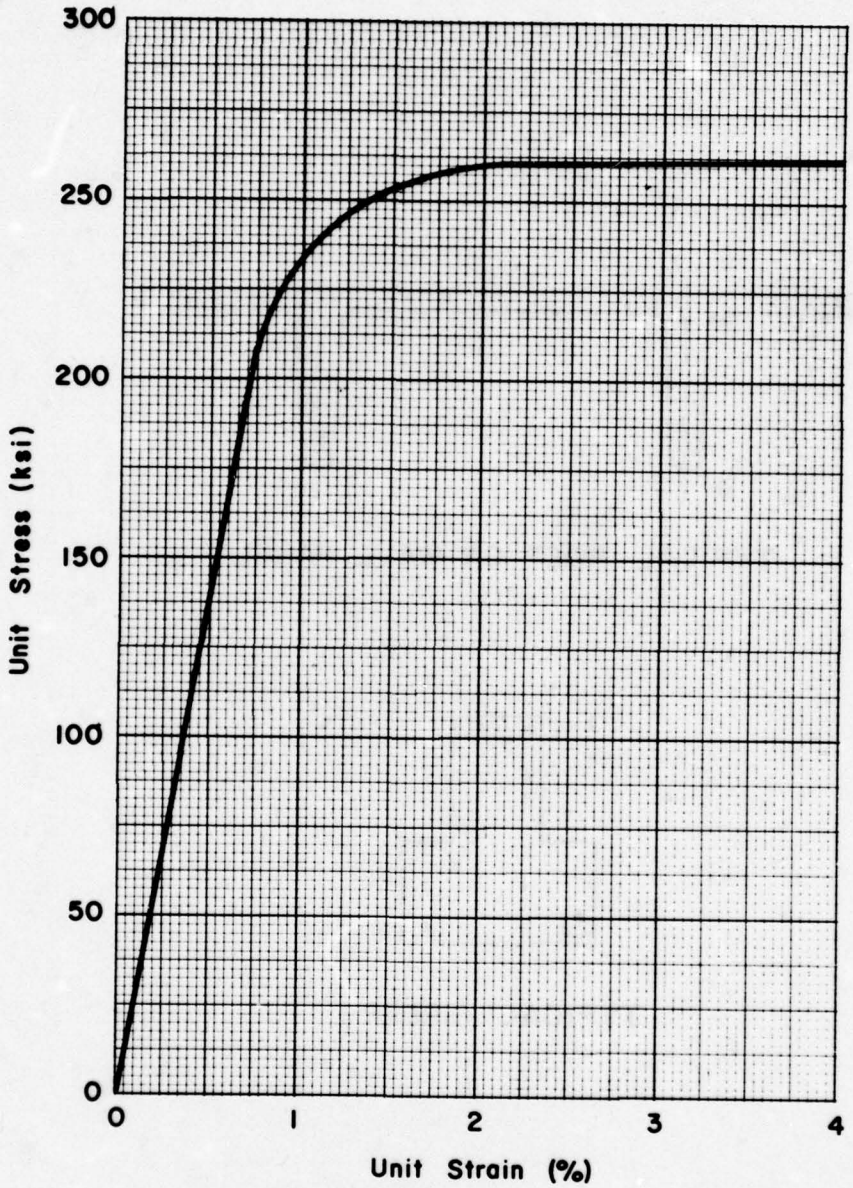


Figure 15 Typical stress-strain curve for high tension wire.

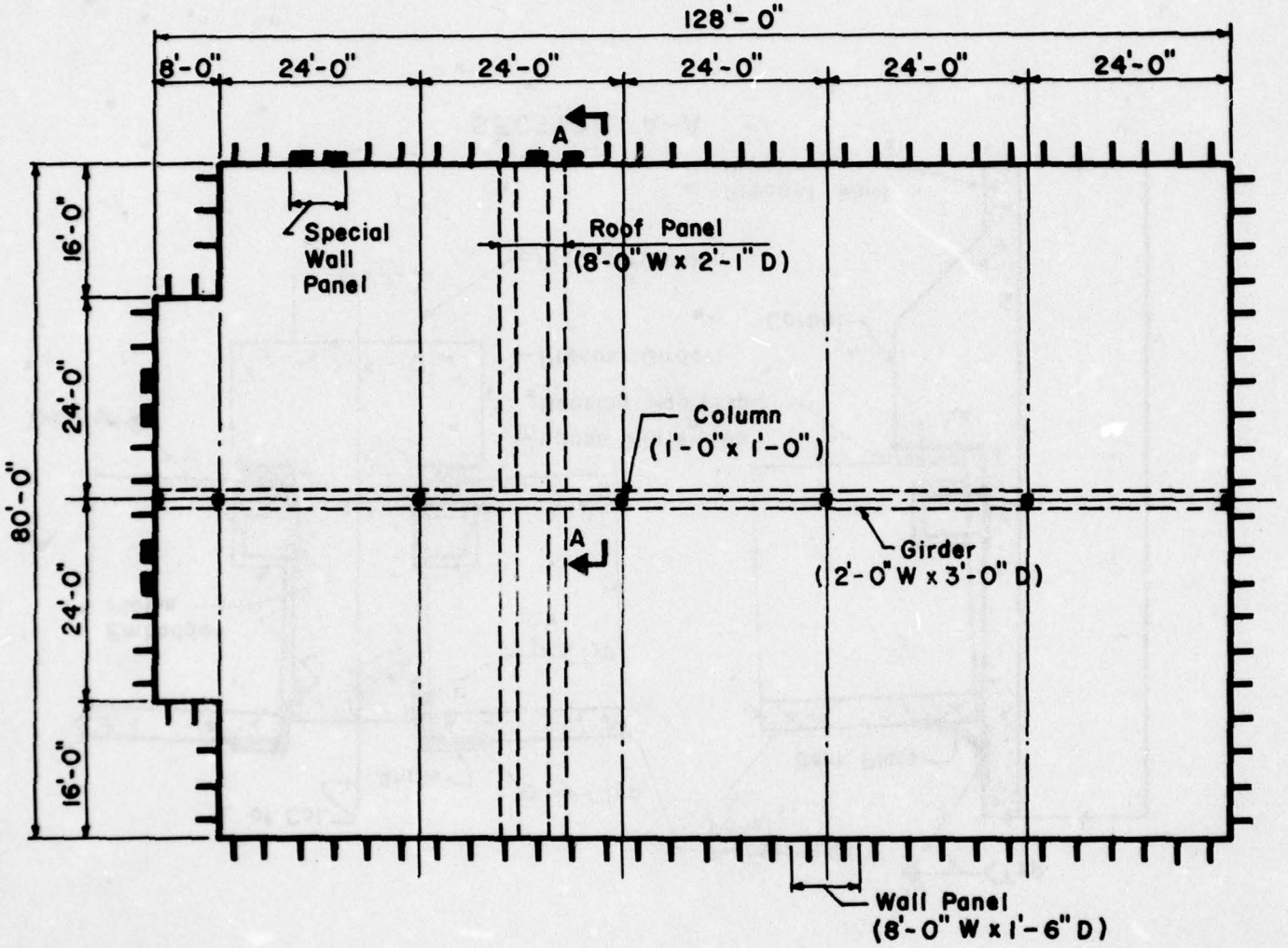


Figure 16 Typical building plan.

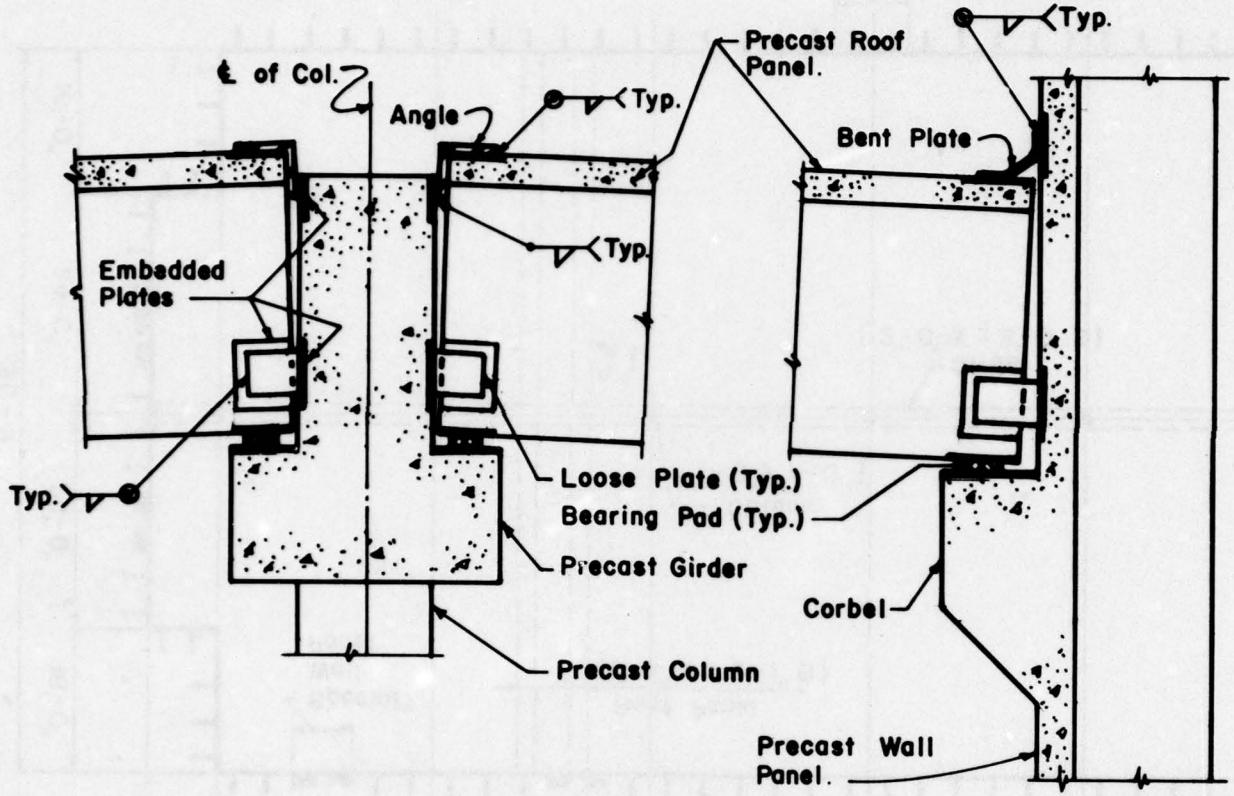


Figure 17 Typical building cross-section.

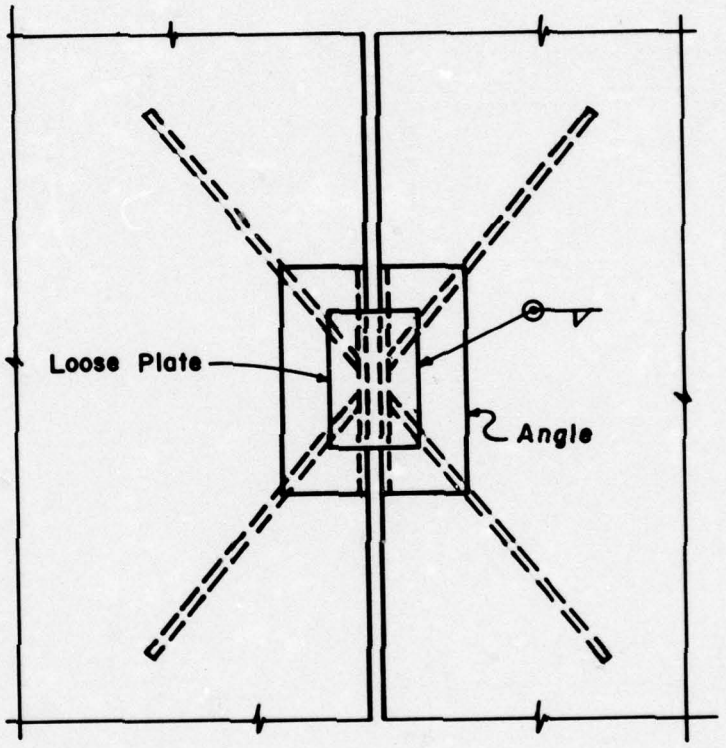


Figure 18 Typical panel splice.

SHEAR STRESS IN ONE-WAY SLABS SUBJECTED TO BLAST LOAD

W. A. Keenan
Civil Engineering Laboratory
Naval Construction Battalion Center
Port Hueneme, CA

INTRODUCTION

The NAVFAC P-397 Manual, "Structures to Resist the Effects of Accidental Explosions," outlines design procedures for resisting shear and diagonal tension in reinforced concrete slabs [1]. The design procedures are similar to procedures adopted by the ACI Building Code for static loads [2]. In practice, slabs are proportioned to provide enough dynamic flexural resistance and ductility to limit the maximum deflection under the blast load to a value less than some safe, *acceptable deflection*. Design procedures developed for static loads are then applied to provide the shear reinforcement needed to safely resist maximum shear stresses and prevent a premature shear failure. The procedure assumes that maximum shear stresses produced by the blast load are equivalent to maximum stresses produced by the dynamic flexural resistance applied as a static load to the slab. Whether this approach will prevent shear and diagonal tension failures depends on (a) the increase in applied shear stresses under blast loads, (b) the degree of conservatism in the ACI Code procedure for predicting the shear resistance of a reinforced concrete section, and (c) the increase, if any, in shear resistance under blast loads. If the effect of (a) exceeds the combined effects of (b) and (c), then a slab which fails in flexure under static load will fail prematurely in shear under blast load. This paper attempts to quantify each of these factors and evaluate the safety of current design procedures in the NAVFAC P-397 Manual for resisting shear and diagonal tension in one-way slabs.

This work is part of a current study at the Civil Engineering Laboratory (CEL) to examine current design procedures for resisting dynamic shear stresses in slabs. The study is being sponsored by the Naval Facilities Engineering Command.

DYNAMIC INCREASE FACTOR FOR SHEAR

Consider the simply supported, one-way slab shown in Figure 1a subjected to a uniformly distributed static load, r. The slab is adequately reinforced to prevent a premature failure in shear. The slab has a uniform stiffness, EI, and a uniform mass, m. The flexural resistance diagram for the slab is the relationship between the applied static load, r, and the resulting midspan deflection, x. Figure 1b is the idealized shape of the resistance diagram if the load is applied slowly to the slab. The slab behavior is elastic until the load reaches the static ultimate flexural resistance, r_u'. At this point, a plastic hinge forms at midspan at a static yield deflection, x_E'. The plastic hinge prevents the slab from mobilizing additional resistance. The slab continues to deflect with a resistance r_u' until it eventually fails in flexure at a collapse deflection, x_u. If the slab deflects rapidly, the rapid strain rates developed in the slab increase the yield strength of the reinforcing steel. Consequently, the flexural resistance of the slab increases from r_u' to the dynamic ultimate flexural resistance, r_u, and the yield deflection increases from x_E' to the dynamic yield deflection, x_E, as shown in Figure 1c.

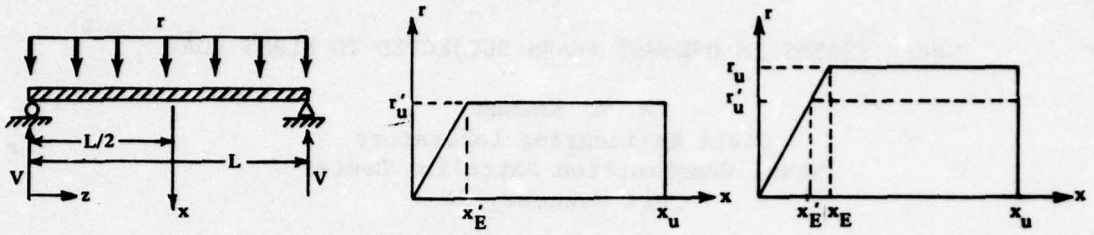
At any resistance, r, the applied shear, V, at a distance, z, from the supports is

$$V(z) = \frac{rL}{2}\left(1 - \frac{2z}{L}\right) \qquad (1a)$$

The maximum static shear, V_s, corresponds to the dynamic flexural resistance, r_u.

$$V_s(z) = \frac{r_u L}{2}\left(1 - \frac{2z}{L}\right) \qquad (1)$$

PRECEDING PAGE BLANK-NOT FILMED



(a) Simple slab under uniform static load.

(b) Static flexural resistance diagram.

(c) Dynamic flexural resistance diagram.

Figure 1. Simple slab subjected to uniform static load.

Now consider the same slab subjected to a blast load. If the resulting dynamic shear at any point, z, and any time, t, is $V_d(z, t)$, then the dynamic increase factor for shear, DIF, is defined as

$$DIF(z,t) = \frac{V_d(z,t)}{V_s(z)} \qquad (2)$$

DIF depends on the slab properties and the characteristics of the blast load and varies along the span with time. The maximum value of DIF is a measure of the maximum increase in applied shear stresses under the blast load. A slab designed to fail in flexure under a uniform static load will fail prematurely in shear under the blast load if DIF exceeds the factor of safety in the static design procedure. Expressions for DIF of one-way slabs in the elastic and plastic ranges of behavior are developed in the following sections.

Elastic Range of Behavior

Consider the simple slab in Figure 2a subjected to a uniformly distributed blast load of the type shown in Figure 2b. The slab has a uniform mass, m, and constant stiffness, EI. The flexural resistance diagram for the slab is shown in Figure 2c. The blast load, w(z, t), is a peak triangular pulse, and the time variation in the load is the same at any point, z. Therefore, the blast loading can be expressed as

$$w(z,t) = B\left(1 - \frac{t}{T}\right) \qquad (3)$$

where B is the peak blast load and T is the duration of the blast load. A free-body diagram showing the forces acting along an incremental length, dz, of the span at any time, t, is shown in Figure 3. Summing the forces acting on the free body, the governing equation of motion during elastic response ($x \leq x_E$) becomes

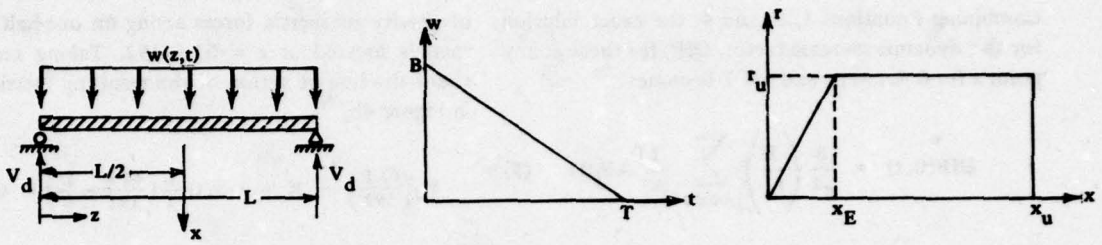
$$m\frac{\partial^2 y}{\partial t^2} + c\frac{\partial y}{\partial t} + EI\frac{\partial^4 y}{\partial z^4} = w(z,t) \qquad (4a)$$

Solving Equation 4a, the exact solution for the deflection at any point produced by the forcing function of Figure 2b for $0 \leq t \leq T$ and $t < t_E$ is

$$y(z,t) = \sum_{j=odd} C_j \phi_j(z) A F_j(t) \qquad (4b)$$

where $C_j = \frac{4BL^4}{j^5 \pi^5 EI} = 1.00386\left(\frac{B}{r_u}\right)\frac{EI x_E}{j^5}$

$$\phi_j(z) = \sin\left(j\frac{\pi z}{L}\right)$$



(a) Simple slab under uniform blast load.

(b) Blast loading.

(c) Dynamic flexural resistance diagram.

Figure 2. Simple slab subjected to uniform blast load.

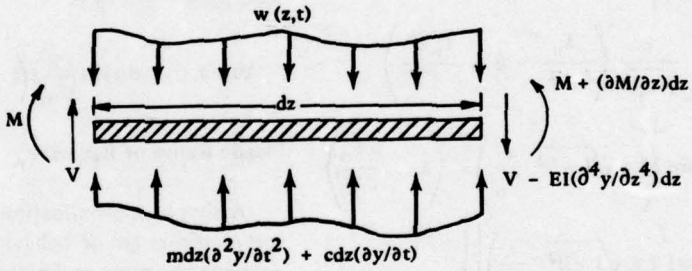


Figure 3. Free-body diagram of slab element.

$$A F_j(t) = 1 - \frac{t}{T} + \frac{\beta T_n}{j^2 \pi T} + e^{-2\pi\beta j^2 (t/T_n)} \left[\frac{1}{2\pi j^2 \sqrt{1-\beta^2}} \cdot \left(\frac{T_n}{T} - 2\pi j^2 \beta - \frac{2\beta^2 T_n}{T} \right) \cdot \sin\left(2\pi j^2 \sqrt{1-\beta^2}\, \frac{t}{T_n} \right) - \left(1 + \frac{\beta T_n}{\pi j^2 T} \right) \cdot \cos\left(2\pi j^2 \sqrt{1-\beta^2}\, \frac{t}{T_n} \right) \right]$$

The shear at any point and time is

$$V_d(z,t) = -EI \frac{\partial^3 x}{\partial z^3} \qquad (4c)$$

Therefore, from Equation 4b, the exact solution for the shear at any point for $0 \leq t \leq T$ and $t \leq t_E$ is

$$V_d(z,t) = \frac{4 r_u L}{\pi^2} \left(\frac{B}{r_u} \right) \sum_{j=\text{odd}} \frac{1}{j^2} A F_j(t) \cos\left(j\pi \frac{z}{L} \right) \qquad (4)$$

Combining Equations 1, 2, and 4, the exact solution for the dynamic increase factor, DIF, for shear at any point z for $0 \leq t \leq t_E$ and $t \leq T$ becomes

$$DIF(0,t) = \frac{8}{\pi^2}\left(\frac{B}{r_u}\right)\sum_{j=odd}\frac{1}{j^2}\,AF_j(t) \qquad (5)$$

From Equation 5, an approximate solution, including the shear contribution from the fundamental mode (j = 1) plus the average contribution from all higher modes, for the dynamic shear at the supports for $0 \leq t \leq t_E$ and $t \leq T$ is [3]

$$DIF(0,t) \simeq \left(\frac{B}{r_u}\right)\left\{1 - \frac{t}{T} + \frac{\beta t_n}{\pi T} + \frac{8}{\pi^2}e^{-2\pi\beta(t/T_n)} \cdot \left[\frac{1}{\sqrt{1-\beta^2}}\left(\frac{T_n}{2\pi T} - \beta - \frac{T_n\beta^2}{\pi T}\right) \cdot \sin\left(2\pi\sqrt{1-\beta^2}\,\frac{t}{T_n}\right) - \left(1 + \frac{\beta T_n}{\pi T}\right) \cdot \cos\left(2\pi\sqrt{1-\beta^2}\,\frac{t}{T_n}\right)\right]\right\} \qquad (6)$$

Another approximate solution for DIF in the elastic range of behavior is derived by approximating the shear contribution from the first mode of vibration and neglecting the contribution from all higher modes. A solution requires an assumed shape for the first mode. The assumed shape then defines the spanwise distribution of inertia forces acting on a slab with a uniform mass, m.

Referring to Figure 4, assume the deflected shape of the slab under a uniform blast load (Equation 3) is the same as the deflected shape produced by a uniform static load. Then the deflection, y, at any point z in terms of the midspan deflection, x, is

$$y = cxz(L^3 - 2Lz^2 + z^3) \qquad (7a)$$

Since the slab in Figure 4a has a uniform mass, Equation 7a describes the distribution of inertia forces along the span. For this distribution, the center of gravity of inertia forces acting on one-half of the span is located at z = 61 L/192. Taking moments about the line of action of the resulting inertia force in Figure 4b,

$$V_d\left(\frac{61L}{192}\right) - M - w(z,t)\frac{L}{2}\left(\frac{61L}{192} - \frac{L}{4}\right) = 0 \qquad (7b)$$

For a simple slab, the midspan moment, M, developed by a uniform resistance, r, is $M = rL^2/8$; so,

$$V_d(0,t) = 0.3934\,rL + 0.1065\,w(x,t)L \qquad (7c)$$

Combining Equations 1, 2, 3, and 7c, an approximate solution for the dynamic increase factor for the shear at supports of a simple slab under a uniform blast load for $0 < t < t_E$ is

$$DIF(0,t) = 0.2131\left(\frac{B}{r_u}\right)\left(1 - \frac{t}{T}\right) + 0.7868\left(\frac{x}{x_E}\right) \qquad (7)$$

Plastic Range of Behavior

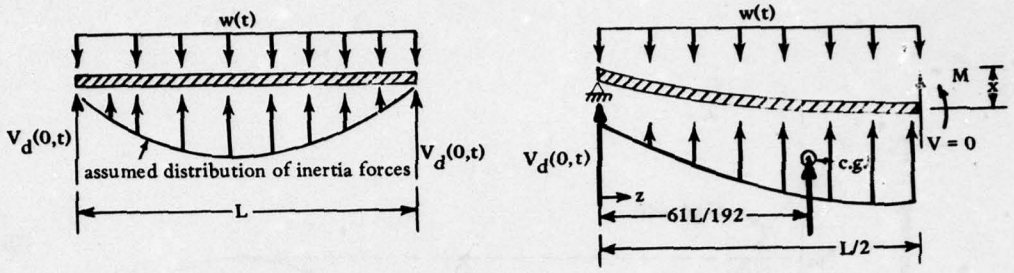
A simple approximation for the dynamic shear in the plastic range of behavior ($x > x_E$) is derived by applying the same technique used to derive Equation 7. In the plastic range, the slab is a linkage of two rigid bars with all rotations concentrated at the plastic hinge, as shown in Figure 5. Since the slab has a uniform mass and the deflected shape is linear, the spanwise distribution of inertia forces is linear. Considering the forces acting on one-half of the span (Figure 5b) and letting $M_p = r_u L^2/8$,

$$V_d(0,t) = 0.375\,r_u L + 0.125\,w(x,t)L \qquad (8a)$$

Combining Equations 1, 2, 3, and 8a, an approximate solution for the dynamic increase factor for the shear at supports of a simple slab under a uniform blast load for $t_E \leq t \leq t_m$ is

$$DIF(0,t) = 0.250\left(\frac{B}{r_u}\right)\left(1 - \frac{t}{T}\right) + 0.750 \qquad (8)$$

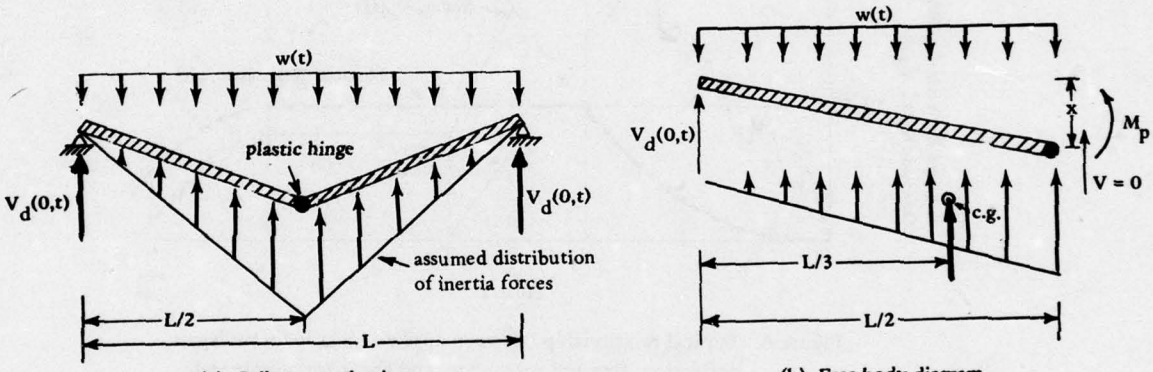
If the slab in Figure 5 is clamped at the supports, a collapse mechanism will eventually develop when



(a) Distribution of forces.

(b) Free-body diagram.

Figure 4. Forces acting on simple slab in elastic range of behavior.



(a) Collapse mechanism.

(b) Free-body diagram.

Figure 5. Forces acting on simple slab in plastic range of behavior.

plastic hinges form at the supports and midspan. At this stage of behavior, the deflected shape of the clamped slab is identical to the shape shown in Figure 5. Consequently, Equation 8 is also an approximate solution for the shear at supports of a clamped-clamped slab in the plastic range of behavior, provided the appropriate value of r_u is substituted in Equation 8. If the moment resistance of each support hinge is M_n then $r_u = (8/L^2)(M_n + M_p)$ for a clamped-clamped slab.

From Equation 4a, the governing equation of motion for the slab during plastic response ($x_E \leq x \leq x_m$) is

$$m \frac{d^2x}{dt^2} + c \frac{dx}{dt} + r_u = w(z,t) \qquad (9)$$

The solution of Equation 9 gives the midspan deflection, x, for $t_E \leq t \leq t_m$.

MAXIMUM DYNAMIC SHEAR

Consider the simple slab in Figure 2 subjected to a uniform blast load which produces inelastic deflections ($x_m > x_E$). Figure 6 shows the typical

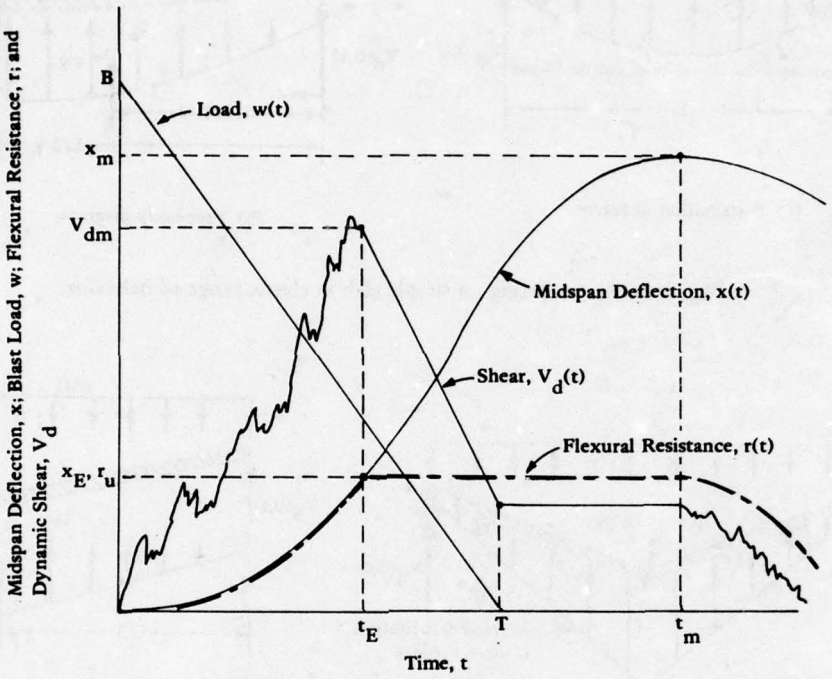


Figure 6. Typical relationship between applied blast load, midspan deflection, flexural resistance, and shear for simple slab.

relationship between the applied load, w, dynamic shear, V_d, flexural resistance, r, and midspan deflection, x. The load immediately rises to a peak load, B, and then decays to zero load at time T. The loading causes the slab to deflect, which, in turn, creates resistance in the slab and inertia forces along the span to oppose the motion. The applied load, slab resistance, and inertia forces together develop shear forces along the span. The shear forces and slab resistance increase with deflection until time t_E when a plastic hinge forms at midspan. Formation of the hinge developes a collapse mechanism which limits the maximum flexural resistance to r_u and the maximum shear at supports to V_{dm}.

$$V_{dm}(0) = V_s(0)\,DIF_m(0, t_E)$$

The maximum resistance, r_u, persists until the slab reaches its maximum deflection, x_m, while the shear, after reaching a maximum at t_E, decays with the applied load and then remains constant during the interval $T \leqslant t \leqslant t_m$. After the slab reaches a maximum deflection, the shear and resistance decrease as the slab begins to recover elastic deflections.

The exact and approximate solutions for the dynamic shear at supports, DIF, and midspan deflection, x, are plotted in Figure 7 for the simple slab and uniform blast load shown in Figure 2. Each graph represents a different peak blast load, B/r_u, and ductility factor, x_m/x_E, but the same blast load duration, $T/T_n = 1.5$. The elapsed time in each graph includes the time when the maximum dynamic shear, DIF_m, occurs at the supports. All graphs neglect effects of damping ($\beta = 0\%$). In the elastic range of response ($x \leqslant x_E$), the exact solution for shear (Equation 5) includes the shear contribution from the first 60 modes of vibration (j = 60). The solution for elastic deflections (Equation 4b) includes only the

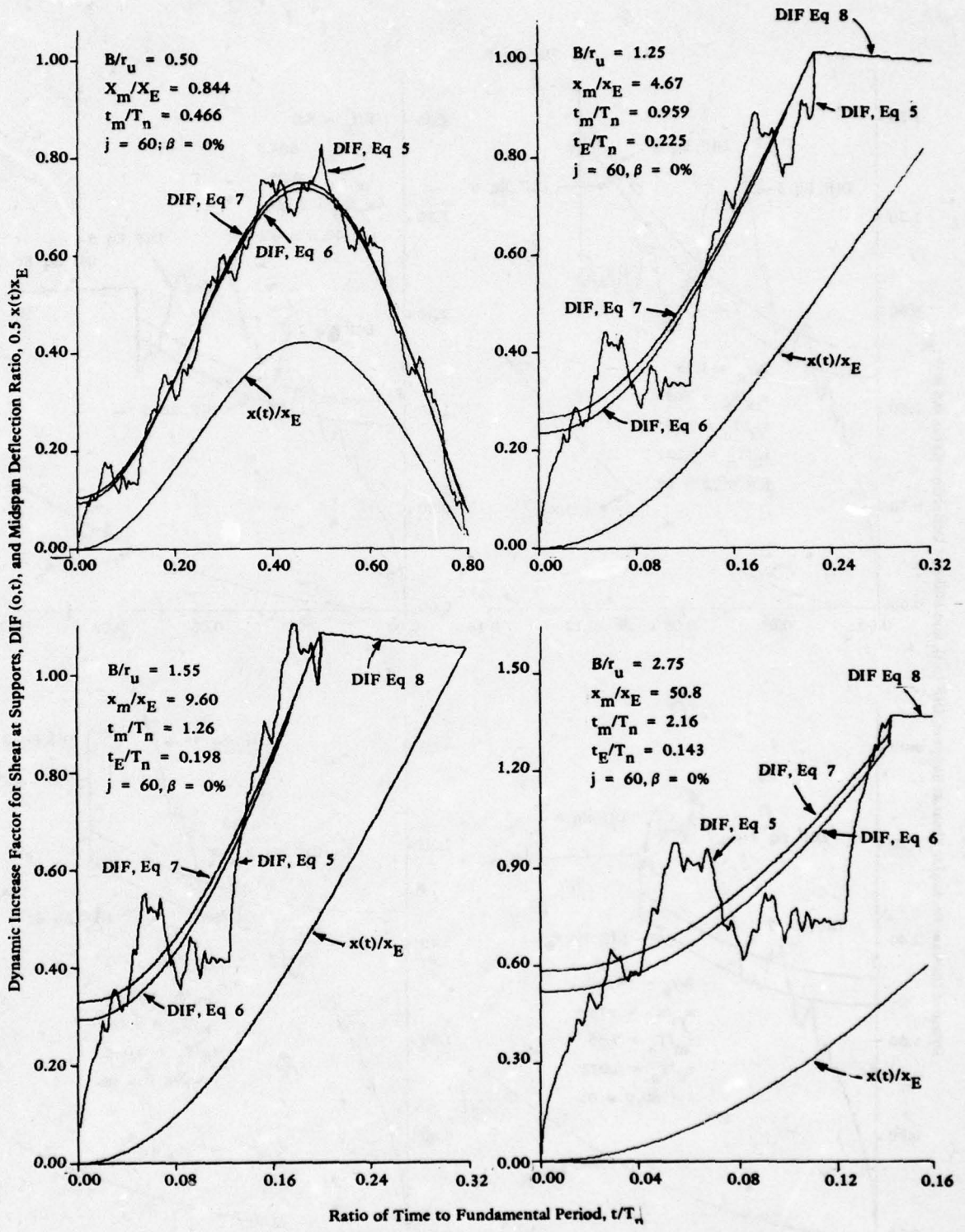


Figure 7a. Dynamic Increase Factor for shear at supports of simple, one-way slab under uniform blast load of short duration ($T/T_n = 1.5$).

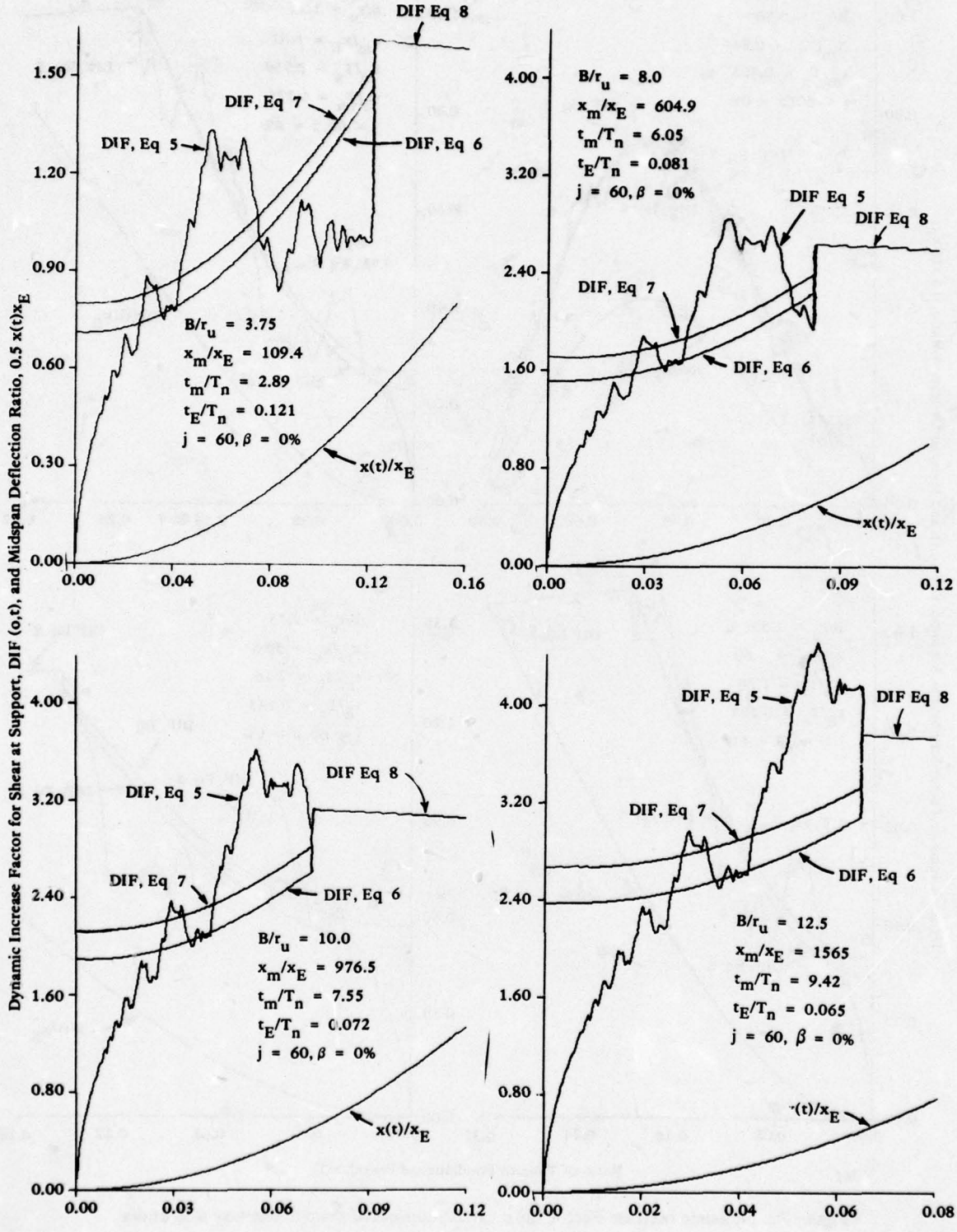


Figure 7b. Dynamic Increase Factor for shear at supports of simple, one-way slab under uniform blast load of short-duration ($T/T_n = 1.5$).

contribution from the first mode (j = 1). Deflections in the plastic range of behavior ($x > x_E$) are based on the solution for Equation 9 in which at $t = t_E$, initial conditions are $x = x_E$ and $\dot{x} = \dot{x}_E$.

Close examination of the graphs in Figure 7 leads to important conclusions concerning the dynamic shear in one-way slabs. If the slab remains elastic ($x_m/x_E < 1.0$), the maximum dynamic shear occurs at time t_m; $DIF(0, t_m)$ from Equation 7 is a good approximation of the maximum dynamic shear, DIF_m. If the slab undergoes inelastic deflections ($x_m/x_E \geq 1.0$), the maximum shear occurs at time t_E; $DIF(0, t_E)$ from Equation 8 is a good approximation of DIF_m. Also, DIF_m will be equal to or less than 1.0 if the slab response remains elastic, but if the slab undergoes inelastic deflections, DIF_m will be equal to or greater than 1.0 and will increase with B/r_u and x_m/x_E.

The impact of these findings on existing design procedures (outlined in the NAVFAC P-397 Manual) for safely resisting dynamic shear forces and preventing premature shear failure are discussed later.

THEORY VERSUS EXPERIMENT

In 1965, the Civil Engineering Laboratory (CEL) load-tested a series of reinforced concrete slabs to study shear and diagonal tension in one-way slabs subjected to blast loads [3]. The test slabs were simply supported and subjected to a uniform blast load in the CEL Atomic Blast Simulator Device. Some slabs were loaded statically to define the flexural resistance diagram. Companion slabs were subjected to blast loads, and the support shear, midspan deflection, and loading were recorded as a function of time.

These experimental results are compared with the theory in Figures 8, 9, and 10 for a short-, intermediate-, and long-duration load, respectively. The correlation between measured and predicted results is excellent. It is concluded that Equations 5, 6, 7, and 8 adequately describe the time variation in shear, and that $DIF(0, t_E)$ from Equation 8 adequately predicts the maximum dynamic shear, DIF_m.

All slabs which failed in flexure under static load also failed in flexure under the blast load; i.e., the blast load did not change the mode of failure from flexure to shear. This behavior is consistent with the theory since the theory predicts DIF_m to be less than 1.0 (see Figures 8, 9 and 10), while a DIF_m greater than 1.0 is required for the blast load to change the mode of failure. Recognizing this fact, CEL attempted to test slabs under blast loads sufficient to produce a DIF_m greater than 1.0. This requires a blast load corresponding to a large ratio of B/r_u and a small ratio of T/T_n, as illustrated in Figure 7. Unfortunately, the CEL Atomic Blast Simulator Device could not develop this type of loading and no other investigation could be found that had measured dynamic shear forces for this type of loading.

DESIGN CHART FOR MAXIMUM DYNAMIC SHEAR

It was demonstrated, both by theory and experiment, that a good approximation for the maximum dynamic shear in one-way slabs, either simply supported or clamped at the supports, is

$$DIF_m(0) = 0.250\left(\frac{B}{r_u}\right)\left[1 - \frac{t_E}{T_n}\left(\frac{T_n}{T}\right)\right] + 0.750 \quad (10)$$

Equation 10 was used to construct the design chart for $DIF_m(0)$ shown in Figure 11. The family of curves for constant values of B/r_u was generated by computing t_E/T_n from Equation 4b for $x/x_E = 1.0$, j = 1, and $\beta = 0\%$, and then substituting t_E/T_n and the associated values of B/r_u and T/T_n into Equation 10 to compute $DIF_m(0)$. The family of curves for constant values of x_m/x_E was generated by computing combinations of B/r_u and T/T_n associated with a fixed value of x_m/x_E and using Equations 4b and 9, assuming j = 1, $\beta = 0\%$, and the idealized resistance diagram shown in Figure 11.

The chart in Figure 11 facilitates computation of the maximum shear stress in one-way slabs. Simply enter Figure 11 with known values of the time ratio, T/T_n, and either the ductility factor, x_m/x_E, or the load ratio, B/r_u, and read from the chart the maximum dynamic increase factor for shear, DIF_m. The corresponding maximum dynamic shear at a distance z from the supports is approximately

$$V_{dm}(z) \cong DIF_m \left[\frac{r_u L}{2} \left(1 - \frac{2z}{L} \right) \right] \quad (11)$$

where $r_u = \frac{8 M_p}{L^2}$, simple-simple slab

$r_u = \frac{8}{L^2} (M_n + M_p)$, clamped-clamped slab

$r_u = \frac{2 M_n}{L^2}$, clamped-free slab

$r_u \cong \frac{4}{L^2} (M_n + 2 M_p)$, simple-clamped slab

Equation 11 assumes DIF_m to be constant across the span of the slab. Actually, DIF_m varies across the span as indicated by the form of Equation 4 and the distribution of forces shown in Figures 4 and 5. Inspection shows DIF_m increases with z, but the increase is slight. This is especially true for $0 \leq z/L \leq 0.2$, which is the critical region for pure shear and diagonal tension failure in one-way slabs subjected to a uniform load [3, 4]. The exact variation of DIF_m along the span is presently under study at CEL. Preliminary results indicate that the maximum shear never exceeds 125% of the shear given by Equation 11 for $0 < x/L < 0.1$. Until a definitive solution for $DIF_m(z)$ is developed, it is recommended that V_{dm} be based on the procedure given in Figure 11.

SAFETY OF CURRENT DESIGN PROCEDURE

Current design procedures in the NAVFAC P-397 for predicting the maximum applied shear in slabs under blast loads assume $DIF_m = 1.0$ [1]. According to Figure 11, DIF is greater than 1.0 for a wide range of the parameters. Figure 11 indicates that the P-397 procedure is adequate for long-duration blast loads (large ratios of T/T_n), regardless of the slabs ductility (x_m/x_E) or blast load ratio (B/r_u). However, the P-397 procedure grossly underestimates the maximum applied shear produced by short-duration loads (small ratios of T/T_n), especially for large ratios of x_m/x_E. For example, if $T/T_n = 1.0$ (typical for close-in explosions) and $x_m/x_E = 500$ (typical for laced slabs), then $DIF_m = 3.4$, according to Figure 11. Whether neglecting the proper values of DIF_m will result in a premature shear failure depends on the factor of safety in the P-397 design procedure for resisting shear stresses in slabs.

Current design procedures in the NAVFAC P-397 for resisting shear and diagonal tension are similar to procedures adopted by the 1971 ACI Building Code [2]. The ultimate shear resistance is calculated as [1]:

$$v_u = \phi [1.9 \sqrt{f'_c} + 2500 p + K r f_y] \quad (12)$$

where the capacity reduction factor, ϕ, equals 0.85 and K = 1.0 for vertical stirrups.

The degree of conservatism in Equation 12 is discussed in the ACI-ASCE Committee 326 report on shear and diagonal tension [4]. The report assumes $\phi = 1.0$ and shows that the present P-397 procedure (Equation 12) is conservative for one-way slabs subjected to static loads. For beams without shear reinforcement, the mean ratio of measured to calculated shear strength (for $\phi = 1.0$) was 1.192 for 64 beams tested under a uniform static load and 1.180 for 430 beams having various load patterns (concentrated and uniform load), cross sections, and support conditions. For beams with shear reinforcement, the mean ratio of measured to calculated shear strength under static load was 1.368 for 95 simply supported beams, 1.547 for 70 restrained beams, and 1.46 based on all beams. The mean ratio of measured to calculated static shear strength corresponding to $\phi = 0.85$ (Equation 12) would be 1.40 for beams without shear reinforcement and 1.72 for beams with shear reinforcement. In other words, the reserve shear strength in one-way slabs, designed using Equation 12, is approximately 40% for slabs without shear reinforcement and 72% for slabs with shear reinforcement.

In the shear tests described in Reference 3 it was observed that the shear resistance of slabs under blast load exceeded the shear resistance of companion slabs under static load. The shear resistance corresponding to formation of a critical diagonal tension crack increased approximately 60% in slabs without shear

reinforcement. The shear resistance at first yielding of stirrups increased approximately 45% in slabs with shear reinforcement (vertical stirrups). These increases in shear resistance were attributed to the increased tensile strength of the shear reinforcement and concrete as a result of rapid rates of straining near supports of slabs subjected to blast loads.

The degree of safety in the NAVFAC P-397 design procedure (Equation 12) for resisting dynamic shear stresses is equal to the product of the average increase in shear resistance from the blast load times the mean factor of safety in Equation 12 for static loads. In other words, the ratio of actual to predicted shear resistance of one-way slabs subjected to blast loads is approximately 1.60 x 1.40 = 2.24 for slabs without shear reinforcement and about 1.45 x 1.72 = 2.49 for slabs with shear reinforcement.

The degree of safety in the NAVFAC P-397 procedure (Equation 12) can be further refined by accounting for the fact that DIF_m at z/L = 0.1 (most probable location of a shear failure in one-way slabs under uniform load [4]) is approximately equal to 1.25 times the value of DIF_m given in Figure 11. By applying this increase to the above ratios, a one-way slab designed according to the NAVFAC P-397 procedures (Equation 12) can be expected to fail in shear if DIF_m from Figure 11 exceeds 2.24/1.25 = 1.79 for slabs without shear reinforcement and 2.49/1.25 = 1.99 for slabs with shear reinforcement. DIF_m can indeed exceed 1.79 and 1.99 according to the chart in Figure 11. DIF_m exceeds 1.79 and 1.99 for small values of T/T_n, especially if x_m/x_E or B/r_u is large, which is a common condition for flexural elements designed to resist close-in effects of H.E. explosions, i.e., substantial dividing walls and cubicles.

One-way slabs, with and without shear reinforcement, need to be tested to demonstrate the accuracy of Figure 11 for short-duration blast loads and the adequacy of the present design procedures (Equation 12) in the NAVFAC P-397 for resisting shear and diagonal tension in one-way slabs subjected to short-duration blast loads.

CONCLUSIONS AND RECOMMENDATIONS

1. The maximum shear stress produced by a blast load can exceed, by a wide margin, the maximum shear stress produced by the ultimate flexural resistance applied as a static load. The maximum dynamic shear stress can be predicted from Figure 11.

2. A one-way slab designed in accordance with the NAVFAC P-397 procedures can be expected to fail prematurely in shear if DIF_m from Figure 11 exceeds approximately 1.79 for slabs without shear reinforcement and 1.99 for slabs with shear reinforcement. DIF_m can indeed exceed these critical limits for a wide range of parameters, as indicated in Figure 11.

3. One-way slabs, with and without shear reinforcement, need to be subjected to blast loads from close-in H.E. explosions to demonstrate the accuracy of Figure 11 and the adequacy of the present design procedure in the NAVFAC P-397 for resisting shear and diagonal tension.

ACKNOWLEDGMENTS

Mr. Jerome S. Hopkins, mathematician at the Civil Engineering Laboratory, reviewed the derivation of shear equations, developed the equations for deflections, and computerized the theory.

REFERENCES

1. NAVFAC P-397 Manual. Structures to Resist the Effects of Accidental Explosions. Department of the Army, Navy and Air Force. Washington, DC. Jun 1969 (also Army TM 5-1300 and AFM 88-22).

2. American Concrete Institute. ACI 318-71: Building Code Requirements for Reinforced Concrete, Detroit, Feb 1971.

3. U. S. Naval Civil Engineering Laboratory. Technical Report R-395: Dynamic Shear Strength of Reinforced Concrete Beams, Part I, by W. A. Keenan. Port Hueneme, CA, Dec 1965.

4. ACI-ASCE Committee 326. "Shear and Diagonal Tension." American Concrete Institute, Journal Proceedings, vol. 59, no. 1 (General Principles, Jan 1962, pp 1-30), no. 2 (Beams and Frames, Feb 1962, pp 277-333), no. 3 (Slabs and Footings, Mar 1962, pp 353-395).

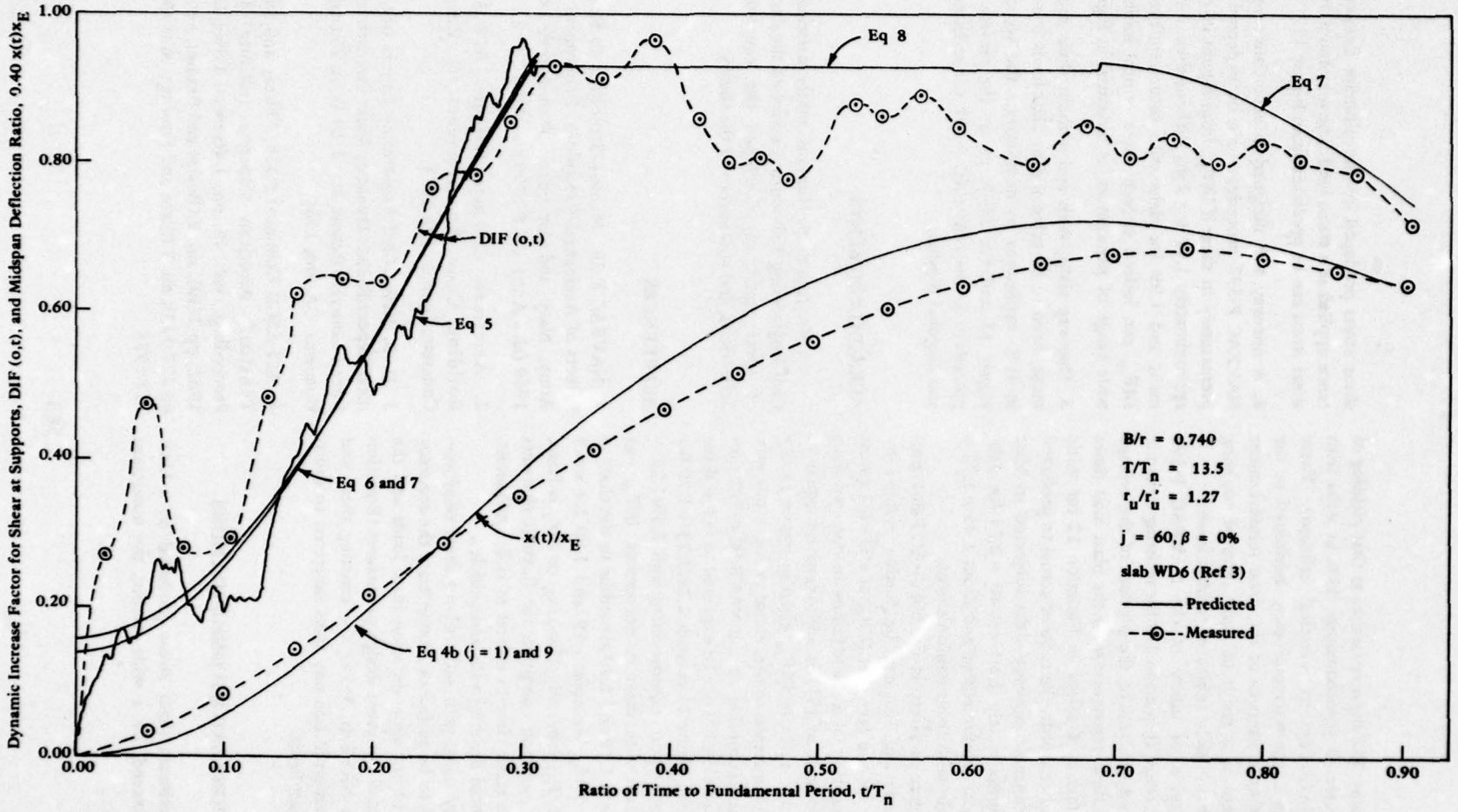


Figure 8. Comparison between measured and predicted shear at supports and deflection at midspan of simple slab under long duration blast load ($T/T_n = 13.5$).

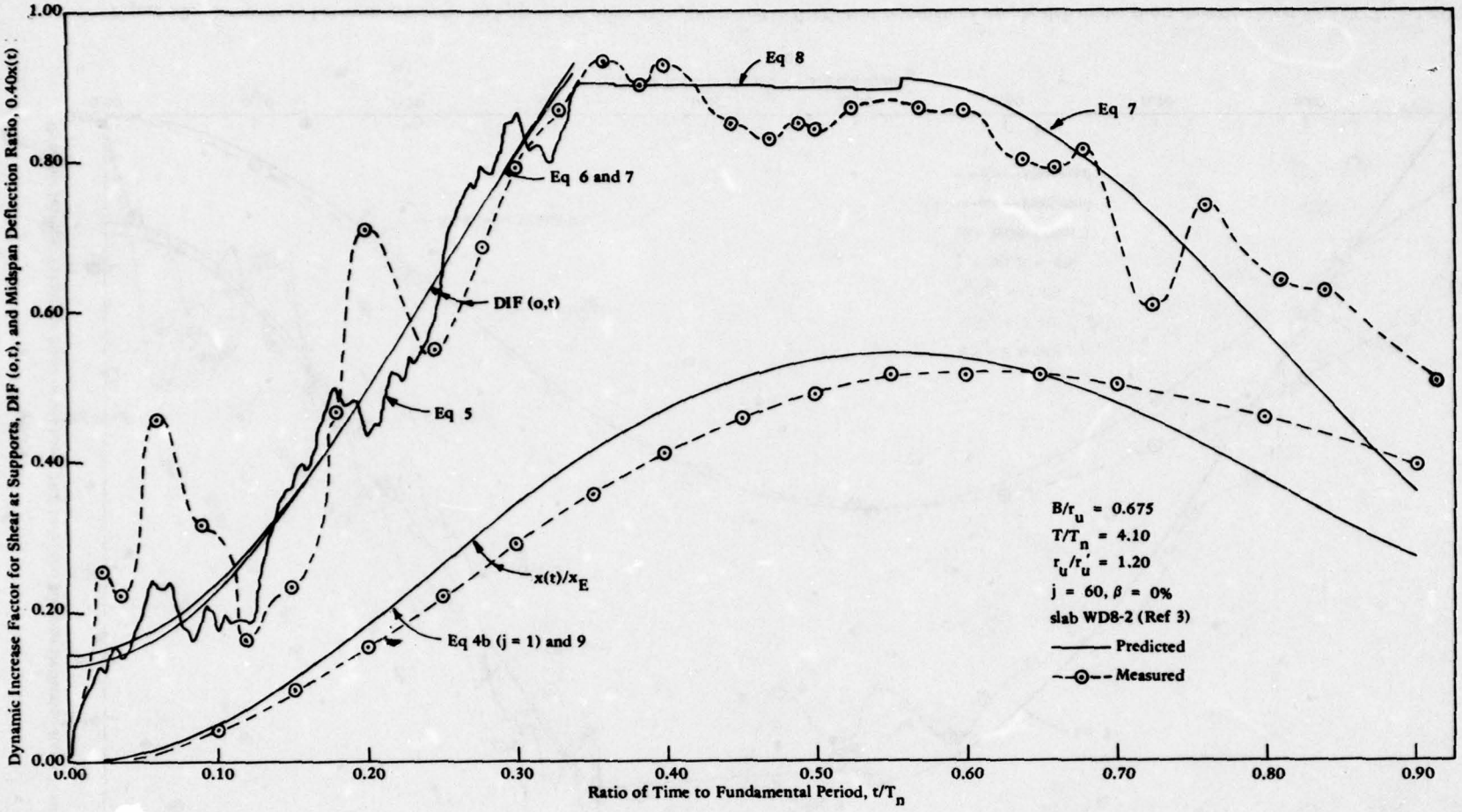


Figure 9. Comparison between measured and predicted shear at supports and deflection at midspan of simple slab under intermediate duration blast load ($T/T_n = 4.1$).

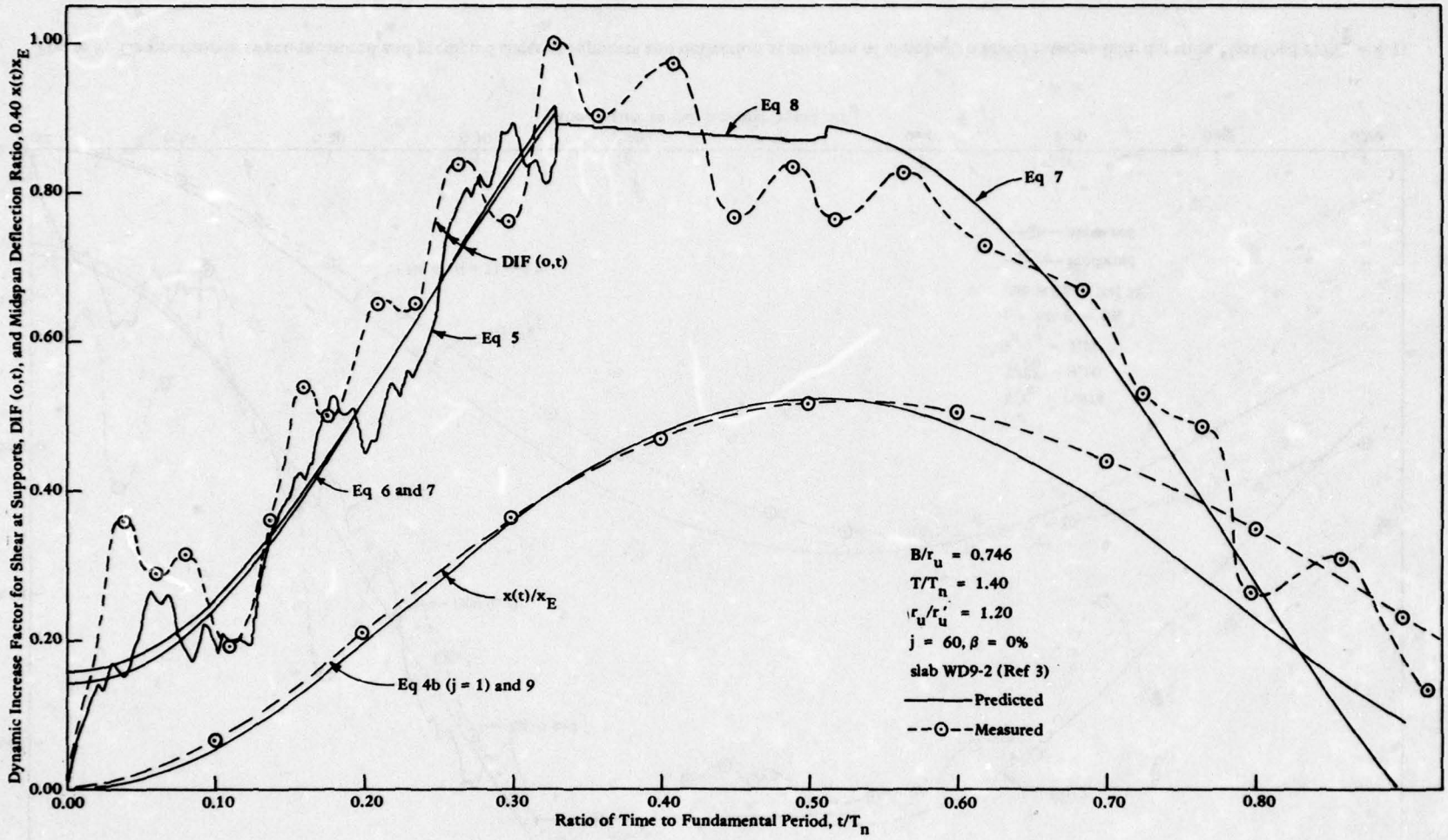


Figure 10. Comparison between measured and predicted shear at supports and deflection at midspan of simple slab under short duration blast load ($T/T_n = 1.40$).

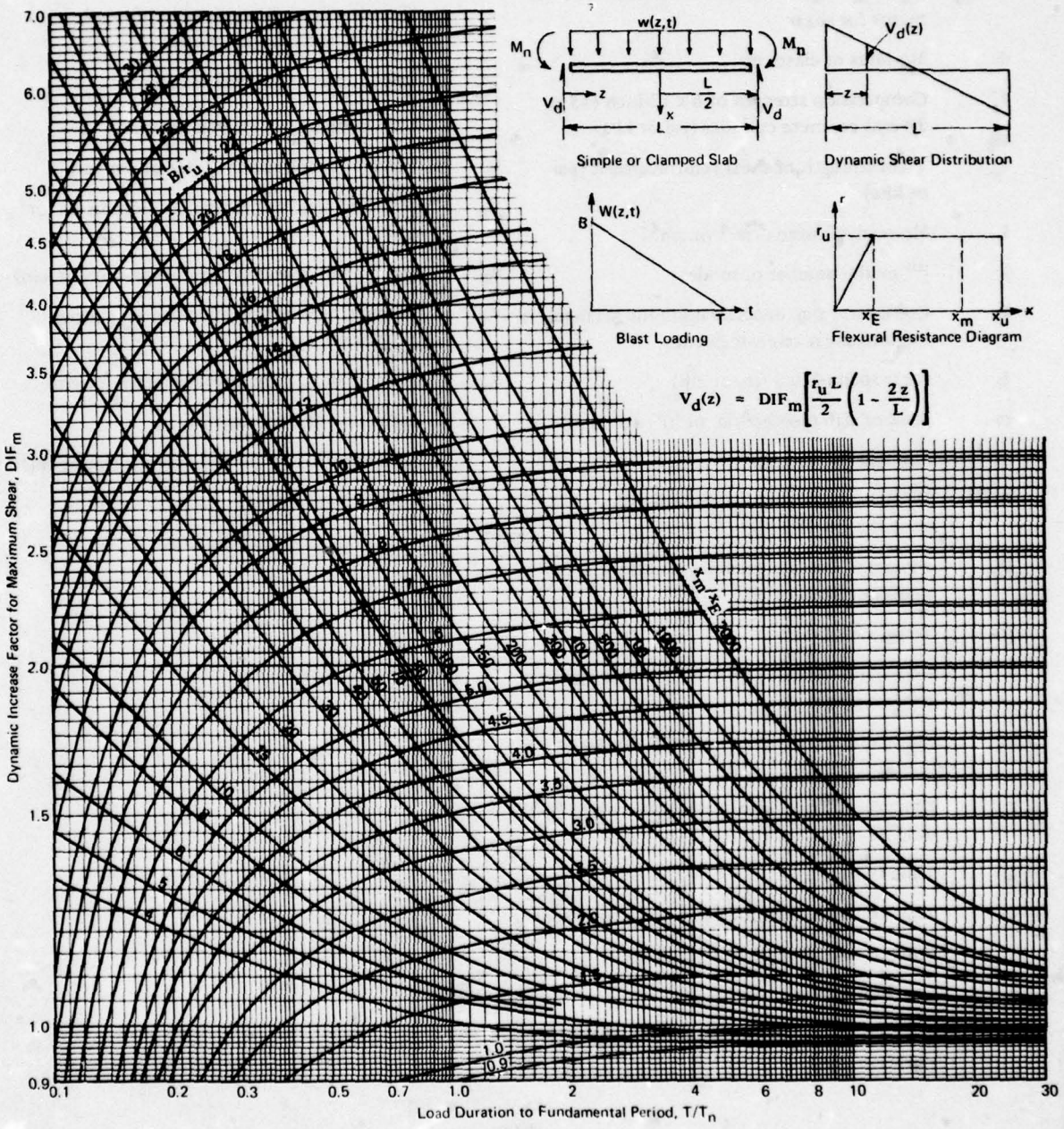


Figure 11. Design chart for maximum dynamic shear in a one-way slab.

LIST OF SYMBOLS

B	Peak blast load (psi or kPa)
c	Constant
DIF	$V_d(z, t)/V_s(z)$, dynamic increase factor for shear
DIF_m	$V_d(z, t_E)/V_s(z)$, maximum dynamic increase factor for shear
E	Modulus of elasticity
f'_c	Compression strength of 6 x 12-inch (15 x 30-cm) concrete cylinder (psi or kPa)
f_y	Yield strength of shear reinforcement (psi or kPa)
I	Moment of inertia (in.^{4} or cm^4)
j	j^{th} mode; number of modes
K	Constant, value depends upon the arrangement of shear reinforcement
L	Clear span of slab (in. or cm)
m	Mass of slab (psi-sec^2/in. or kPa-sec^2/cm)
M	Moment (in.-lb or N)
M_n	Dynamic ultimate moment resistance at supports (in.-lb or N)
M_p	Dynamic ultimate moment resistance at midspan (in.-lb or N)
p	Tensile steel ratio
r	Flexural resistance (psi or kPa); ratio of shear reinforcement
r'_u	Static ultimate flexural resistance or static load (psi or kPa)
r_u	Dynamic ultimate flexural resistance (psi or kPa)
t	Time (sec)
t_E	Time to reach dynamic yield deflection (sec)
t_m	Time to maximum deflection (sec)
T	Duration of blast load (sec)
T_n	$(2L^2/\pi)\sqrt{m/EI}$, fundamental period of vibration (sec)
V	Shear (lb or kg)
V_d	Dynamic shear (lb or kg)
V_{dm}	Maximum dynamic shear (lb or kg)
V_s	Static shear (lb or kg)
v_u	Ultimate shear strength of reinforced concrete section (psi or kPa)
w	Applied blast load (psi or kPa)
x	Deflection at midspan (in. or cm)
$\dot{x}$	Velocity at midspan (in./sec or cm/sec)
x_E	Dynamic yield deflection at midspan (in. or cm)
x'_E	Static yield deflection at midspan (in. or cm)
x_m	Maximum dynamic deflection at midspan (in. or cm)
x_u	Collapse deflection at midspan (in. or cm)
y	Deflection at z (in. or cm)
z	Horizontal distance from support (in. or cm)
ϕ	0.85, factor of safety
β	$= cT_n/4\pi j^2 m$ = damping ratio

AN ECONOMIC STUDY OF BLAST RESISTANT BUILDINGS

Charles C. Huang
U.S. Army Corps of Engineers, Huntsville Division
Huntsville, Al.

SUMMARY

Preengineered metal buildings have been studied to determine the feasibility of strengthening to withstand low overpressure levels up to 2.0 psi with reparable damage. This study also establishes guidelines, from a cost-effective viewpoint, for the use of strengthened preengineered buildings where a low potential overpressure is anticipated. Techniques for strengthening standard preengineered metal buildings is discussed.

INTRODUCTION

Support buildings that are located away from the production lines in an ammunitions plant would be subjected to potential incident overpressures ranging from 0.5 to 2.0 psi in the event of an accidental explosion. Designers have the option of selecting the types of construction for such buildings; reinforced concrete, steel frames made from rolled sections, or preengineered metal buildings, then incorporating the blast resistant requirement into their selected design. The tri-service design manual "Structures to Resist the Effects of Accidental Explosions," TM5-1300 (Ref 1) provides guidance for designing concrete structures. The Picatinny Arsenal Technical Report 4837, August 1975, "Design of Steel Structures to Resist the Effects of HE Explosions" (Ref 2) contains design criteria for steel frame structures. Procedures are not available to designers for strengthening commercially available (standard) preengineered metal buildings to attain desired blast resistance.

The relative cost-effectiveness of the three types of buildings as applied to withstand such low levels of blast loadings has been of interest to plant designers. Obviously, there is a cost increase in blast resistant buildings of any type. The question is that in such low overpressure levels which one would be the best choice - from the viewpoints of initial cost as well as down time for repair in the event of an accident. Some data on cost differential for concrete buildings are given in Ref 3. It indicates that on the average, a cost increase by a factor of 1.5 for a 1.5 psi design and about 2 for a 2.0 psi design. Similar information on specifically designed steel buildings is given in Ref 4, which

indicates that the added cost of steel for a 1.5 psi design would increase by a factor of about 2.0 and for a 2.0 psi design by a factor of 2.3. These factors present a trend, but are inadequate for cost effective evaluations because several other cost-influencing factors other than overpressure, particularly the building size, must also be taken into consideration.

To fill the data gap identified above, i.e., (1) the lack of procedures for strengthening conventional preengineered metal buildings, and (2) the need for guidelines for evaluating cost-effectiveness of different types of buildings to withstand low levels of external overpressure, this paper presents a summary of the findings of a study that addresses these issues. Readers who require the entire report are referred to the U.S. Army Corps of Engineers, Huntsville Division, Technical Report, HNDTR-75-23-ED-SR, 1 December 1975, "Overpressure Effects on Structures" (Ref 5), prepared for the Office of the DARCOM Project Manager for Munitions Production Base Modernization and Expansion.

PREENGINEERED BUILDING

Two factors, standardization and mass production, have made standard preengineered metal buildings (a typical version is shown in figure 1) attractive to users as compared with other types of construction. A large selection of stock items available enables the manufacturer to produce a structural system that meets building codes as well as client needs. As the word "preengineered" denotes, little engineering effort is involved for a particular application, and practically no lead time is required for structural design. Standard components (beams, columns, rigid frames, girts, purlins, wall and roof panels) are produced in large lots by automated processes which result in costs that are much lower than job-shop production. Preengineered buildings usually can be quickly erected in the field because of their light weight and ease of handling. In an emergency, repairs to damaged buildings in the wake of a tornado or a hurricane can be readily accomplished. In the main, preengineered buildings are cost effective. This has created a demanding market and a thriving industry since World War II.

In the early 1950's, in the interest of civil defense, preengineered buildings were tested to determine their resistance to overpressures induced by nuclear explosion. The U.S. Navy conducted similar tests on warehouse type buildings. The results of the tests, however, were applied only to the buildings of the sizes tested and were not conclusive enough to be generalized for the establishment of cost-effective or design criteria for blast resistant preengineered buildings in general. The need for blast resistant metal buildings in the ensuing years

apparently did not create a sufficient market to warrant manufacturers to pursue development further. To date, manufacturers are still reluctant to respond to an inquiry which calls for design loads other than the wind loads and live loads set forth in building codes.

Engineers who are not in the preengineered building industry and do not have intimate knowledge of preengineered components cannot possibly ascertain the blast resistance of preengineered buildings with confidence nor can they exploit the benefits such buildings may offer. The following sections provide: (1) an estimated blast resistance of standard preengineered buildings over a range of sizes, (2) the information concerning the feasibility of strengthening the standard buildings and (3) a comparison of the cost of standard and strengthened preengineered buildings with other types of construction, e.g., steel buildings made from rolled structural sections and reinforced concrete buildings.

DUCTILITY FACTOR

One consideration for the design of blast-resistant preengineered buildings is that the building damages resulting from an accidental explosion up to 2 psi overpressure should be rapidly and economically reparable. To this end, the rigid frame and the main bracing of a strengthened building are required to remain in the elastic range when the design blast load is applied. Thus, should an explosion occur, there would be no excessive twist or sag in the main structural members; and repair work, if any, would be minor and could be readily accomplished. The panels, girts and purlins, on the other hand, are permitted to go into the plastic range under design loads. It is thought that overdesign of these components would increase the initial building cost disproportionately to the extent that preengineered buildings would lose their competitive position. Replacing the panels, girts and purlins would be a comparatively easy task. All such components are standard items that can be readily supplied, and they are light and easy to handle at the site. Therefore, the proposed criteria for designing blast resistant preengineered buildings are (1) the ductility factor[1], μ for the main frames and bracing should be 1.0 and (2) μ for panels, girts and purlins should be 3.0. Tests of typical wall panels verified that the criteria of μ=3.0 is valid because the wall panels under test still could carry loads even though they had deflected considerably beyond their elastic range.

[1] Ductility factor is ratio of expected deflection under a dynamic load to the deflection corresponding to the yield strength of the material.

EQUIVALENT STATIC LOADS

To enable the manufacturers of preengineered buildings to design blast resistant buildings with their existing computational procedures and to fully utilize their standard components, a concept of equivalent static loads, which are analogous to live loads and wind loads in conventional designs, were developed. Thus, the manufacturers need not be concerned with the dynamic nature of blast loads to which they may not be accustomed. The blast loads acting on the walls and roof of a building were determined in accordance with the procedure given in TM5-1300 and based on estimated natural periods of building structural elements (e.g., girts and purlins, wall and roof panels, and rigid frames). The estimations of the natural periods could not be made with any accuracy since the spacing of the rigid frames and section properties of the structural components of the design were yet to be established. First order estimates based on data available in catalogs were made in order to gain a general idea of the ratio of pulse duration to the natural periods of the components. These ratios provided an insight into the behavior of structural response and the desired resistance function of the components. Figures 6 and 7 shown in TM5-1300 (Ref 1) and the procedures in Chapter IX of ASCE Manual 42 (Ref 6) are applicable in determining the equivalent static loading as depicted in figure 2. The load conditions thus derived, analogous to wind and live loads in conventional design, were given to the manufacturers (see figures 3 and 4). One manufacturer[2] responded and produced a preliminary design of several blast resistant preengineered buildings as shown in figures 5, 6, and 7. The values shown in figure 3 are for display purposes only because such values will change for different pulse durations associated with a design load and natural periods of selected components by manufacturers.

The commercial standard preengineered buildings having a spacing of 25 feet for rigid frames, 7 feet 6 inches for girts and 5 feet for purlins were analyzed and found that they can resist a blast loading up to 0.25 psi overpressure. This is expected because they are normally designed for 20 psf of wind load and 45 psf live load. However, their blast resistance can be readily increased to 0.5 psi overpressure without any modifications to the building system except for a closer spacing of girts and purlins. To further increase the blast resistance, the rigid frames would have to be spaced closer than 25 feet and add more girts, purlins, and substantial wind bracings. A summary of the strengthened preengineered metal buildings studied is given in table 1. It may be concluded that manufacturers can produce preengineered buildings provided a set of equivalent static loads similar to those in figures 3 and 4 are given. The responsibility for determining a set of equivalent static

[2] Mr. J. P. Steinman and Mr. D. L. Johnson of Butler Manufacturing Co. contributed the preliminary designs of the blast resistant preengineered buildings shown in figures 5, 6, and 7 based upon the given equivalent static loads.

loads from the design blast loading rests with the engineer. As stated earlier, the section properties of manufacturers' standard components must be known to accurately determine the equivalent static loads. Catalog information may be used as a first order estimate for the equivalent static loads that will be given to manufacturers to prepare a preliminary design. Based on the preliminary design, a dynamic response analysis[3] can be made to verify the adequacy of blast resistance. This procedure calls for a close coordination between the engineers and the manufacturer. Working together they will be able to arrive at a satisfactory design of a blast resistant preengineered metal building. This is an iterative process, which deviates from the normal procurement practice, but it must be done while manufacturers accumulate sufficient experience in producing blast resistant buildings. Figure 5 depicts the iterative process that was used and proven rather successful.

Our experience indicated that for blast resistant preengineered metal buildings all the manufacturers standard rigid frames, girts, purlins, and wall panels can be utilized with minor modifications which involves punching a number of additional holes for added fasteners. The only non-standard parts are the bracings that will have to be manufactured from special cold-rolled sections or be selected from steel sections listed in the AISC manual. The manufacturers' standard erection procedures apply to the blast resistant buildings because no significant change was made in the basic configuration of the structural system except for a number of added components. Therefore, the handling, transportation and erection costs for blast resistant buildings will increase accordingly to account for the increased steel requirement beyond that for standard buildings of the same size.

STEEL FRAME BUILDINGS DESIGNED FOR SPECIFIC USE

For the purpose of cost comparison, two steel frame buildings designed for specific use as a change house and maintenance shop in the Black Powder Manufacturing Facilities at Indiana Army Ammunition Plant were selected. They were made from standard steel sections and designed for an incident overpressure of 1.0 psi. Figures 8 and 9 show the configurations of the buildings. The buildings dimensions and floor areas do not correspond exactly with those of the preengineered buildings listed in table 1, but are close enough for cost comparison.

[3] Several structural dynamics computer programs are available. One of strengthened buildings designed by Butler Manufacturing Co. was analyzed by the program available at the Picatinny Arsenal under the supervision of Paul Price.

Table 1. Rigid Frame, Girt, And Purlin Spacing

Nominal Bldg. Size	Overpressure	Bent Spacing	Girt Spacing	Purlin Spacing
40' x 125'	0.25 Std. Bldg.	25'0"	7'6"	5'0"
	0.5 psi	25'0"	2'6"	4'0"
	1.0 psi	16'8"	2'6"	3'0"
	2.0 psi	8'4"	2'0"	2'6"
80' x 125'	0.25 Std. Bldg.	25'0"	7'6"	5'0"
	0.5 psi	25'0"	2'6"	4'0"
	1.0 psi	16'8"	2'6"	3'0"
	2.0 psi	8'4"	2'0"	2'6"
120' x 175'	0.25 Std. Bldg.	25'0"	7'6"	5'0"
	0.5 psi	25'0"	2'6"	4'0"
	1.0 psi	16'8"	2'6"	3'0"
	2.0 psi	8'4"	2'0"	2'6"

NOTE:

The above table is based on the use of a standard 8-in. Z section for the girts and purlins in combination with the exterior paneling (Butlerib II). Using heavier Z sections with the same depth and stronger panels than those used will change the spacings on the girts and purlins; however, the savings would probably be negligible because it would be difficult to remove more than one girt from the building at the pressure levels indicated.

REINFORCED CONCRETE BUILDINGS

Because of the lack of cost data on reinforced concrete structures in the 0.5 to 2.0 psi range, it was necessary to develop preliminary designs for cost estimating. The sizes of the structures developed were basically the same as the preengineered buildings to provide comparability. The three basic structures considered had nominal dimensions of 40- by 120-ft, 80- by 120-ft, and 120- by 180-ft as shown in figures 10, 11, and 12. The external dimensions were maintained while the wall thickness, beam depths and column sizes were varied as required for the imposed loads. The same design loads for the preengineered metal buildings were used for sizing the structural members of the reinforced concrete buildings. The reinforced concrete structures were designed in accordance with the ACI Code and the data in the CRSI Handbook. The following conditions were assumed:

Walls. All walls spanning between interior frames were considered to act as two-way slabs continuous over supports and fixed top and bottom. The walls at the end bays were considered the same as the interior spans except for the extreme end which was considered to be simply supported.

Frames. The frames, spaced at 20-foot centers, were considered to act as rigid frames supported by interior columns. The number of columns used was based on the width of the buildings. Parametric computer runs were made on each structure to optimize the frame configuration.

Roof. Pan joist construction was used for the roof to eliminate the need for additional beams between the rigid frames. The pan joist beams and associated slabs were considered to be continuous over the supports.

Reinforcing. Reinforcing steel requirements were determined for selected points of maximum load conditions. The steel requirements for these points varied from 0.75 percent to 1.25 percent. For estimating purposes, a uniform reinforcing steel requirement of 1.0 percent was used.

COST COMPARISON

For making a cost comparison, the costs for all the buildings described previously were developed and summarized in table 2 and figure 13. The costs shown in the table include costs for the structure, walls, and roof of the building, plus shipping, handling, and erection. Costs of electrical and mechanical systems, floor slabs, foundations, and site preparation are not included.

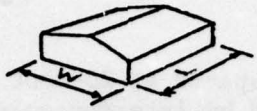
The costs are based on the 1975 market value for labor and materials.

CONCLUSIONS

Based on table 2 and figure 13, the following conclusions are drawn:

1. Steel frame buildings using structural sections designed to withstand low overpressure levels (0.5 to 2.0 psi) cost substantially more than reinforced concrete buildings.

Table 2. Cost Analysis Results



TYPE BUILDING	NOTES *	PSI [4]	W × L 40'x125' $/SF	W × L 80'x125' $/SF	W × L 120'x175' $/SF
STANDARD PREENGINEERED BUILDING	3	0.25	5.30	5.10	4.90
	2	1.0	—	—	—
	2	2.0	—	—	—
STRENGTHENED PREENGINEERED BUILDING	3	0.5	7.70	8.10	9.30
	3	1.0	9.40	9.90	12.40
	3	2.0	13.90	14.90	20.40
STEEL FRAME BUILDING-DESIGNED TO SPECIFIC REQUIREMENTS	1	0.5	—	—	—
	3	1.0	23.30	23.50	27.90
	1	2.0	—	—	—
REINFORCED CONCRETE BUILDING	3	0.5	13.40	10.70	10.60
	3	1.0	14.50	11.60	11.30
	3	2.0	15.65	12.55	12.00
STANDARD STRESSED SKIN BUILDING	5	—	6.10	5.60	5.10
	5	—	—	—	—
	5	—	—	—	—

* NOTES:

1 – COST DATA NOT AVAILABLE
2 – WILL NOT WITHSTAND OVERPRESSURE
3 – EXCLUDES SITE PREPARATION, ELECTRICAL, MECHANICAL, FOUNDATION, FLOOR SLAB AND MASONRY REQUIREMENTS
4 – OVERPRESSURES SHOWN ARE PEAK INCIDENT PRESSURES
5 – BUILDING OVERPRESSURE RESISTANCE NOT ASSESSED UNDER THIS STUDY

2. The standard preengineered metal buildings designed for 20 psf wind and 40 psf live load cost substantially less than any other type of building. It is estimated that they can survive an incident overpressure up to 0.25 psi with reparable damage.

3. Manufacturers can supply strengthened preengineered metal buildings if equivalent conventional wind loads and live loads are provided in lieu of blast loads, which are characterized by peak overpressure, pulse shape, and duration.

4. It is feasible to strengthen standard preengineered buildings by properly spacing the frames, girts and purlins, and by adding adequate wind bracing. The strengthened building can withstand an incident overpressure up to 2 psi with reparable damage. However, the close spacing of structural members may present architectural problems, e.g., the spacing between frames insufficient for large door openings. Special attention should be given to such details and to the connections between the building and its foundation.

5. Generally, preengineered buildings have cost advantages over concrete buildings of equivalent size under the following conditions:

a. Buildings having a frame span up to 120 feet and subjected to an incident overpressure of 0.7 psi or less.

b. Building having a frame span up to 80 feet and subjected to an incident overpressure of 1.5 psi or less.

c. Building having a frame span up to 40 feet and subjected to an incident overpressure of 2.4 psi or less.

d. Beyond the above conditions, the preengineered building loses its competitive position and reinforced concrete buildings become more cost-effective.

CAVEAT

The conclusions outlined above indicate a general trend as a guide for initial planning. Other cost factors which have not been addressed in this study must also be considered in the overall planning process, e.g., foundations, architectural considerations, life-cycle costs, and time constrains in design and construction. For example, projects having compressed schedules, consideration must be given to the lead time required for design and construction. It is estimated that it would take from 10 to 18 months to design and construct a typical concrete building but would only take 6 to 9 months for a similar size strengthened preengineered metal building.

Conventional doors and windows used in all types of buildings are the weakest elements in a blast environment. This has been demonstrated by explosive tests and evidenced in the wake of hurricanes and tornados. Interior partitions should be provided to protect personnel and contents against fragments of broken windows and doors. Alternatively, special doors capable of withstanding overpressure should be provided.

REFERENCES

1. TM5-1300, "Structures to Resist the Effects of Accidental Explosions," June 1969.

2. Healey, John; Price, Paul, et al, "Design of Steel Structures to Resist the Effects of HE Explosives," Picatinny Arsenal Technical Report 4837, August 1975, Dover, N.J.

3. Newark, et al, "Air Force Design Manual - Principles and Practices for Design of Hardened Structures," AFSWC-TDR-62-138, December 1962, The Kirkland Air Force Base, New Mexico.

4. Price, Paul and Dobbs, Norval, "Steel Structures to Resist the Effects of HE Explosives."

5. "Overpressure Effects on Structures," The U.S. Army Corps of Engineers, Huntsville, Division, Technical Report, HNDTR-75-23-ED-SR, December 1975, Huntsville, Al.

6. "Design of Structures to Resist Nuclear Weapons Effects," Manual of Engineering Practice, Number 42, ASCE, 1962, New York, N.Y.

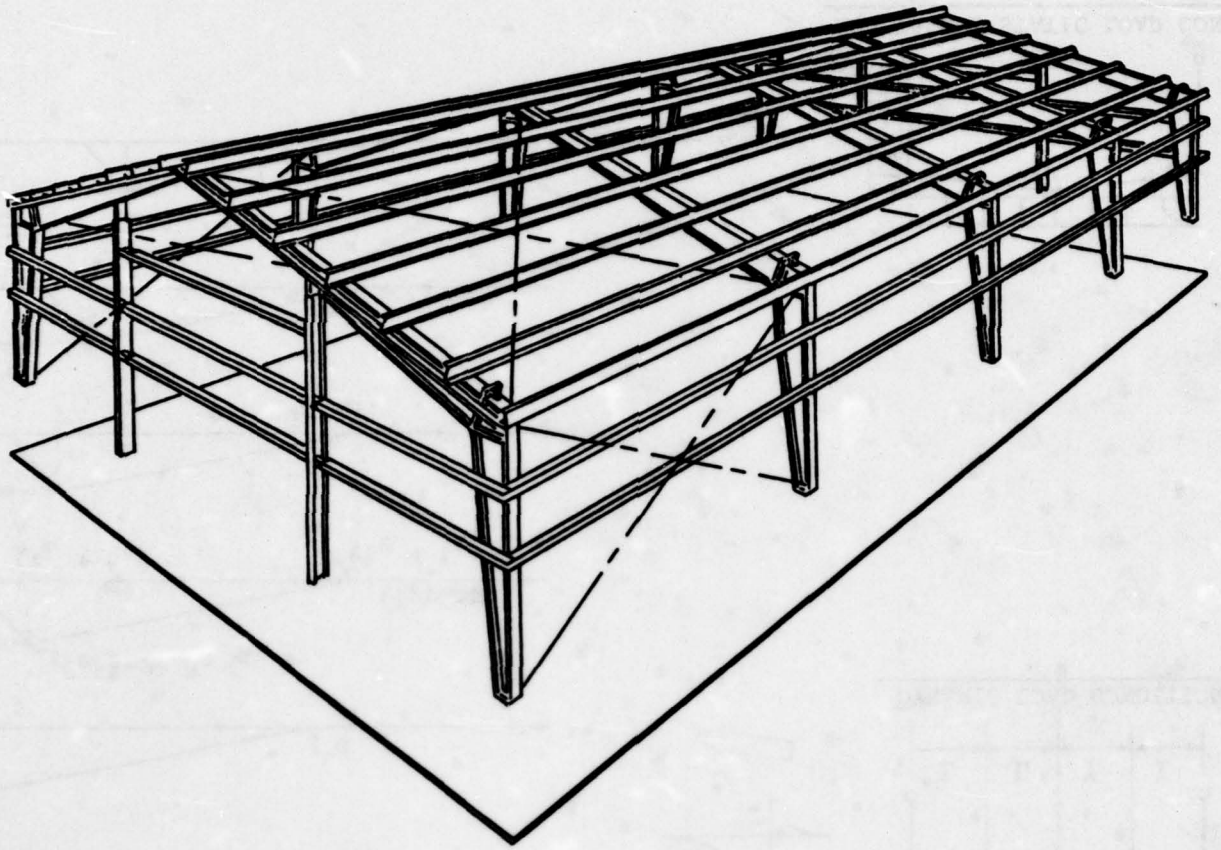


Figure 1. TYPICAL STANDARD PREENGINEERED BUILDING

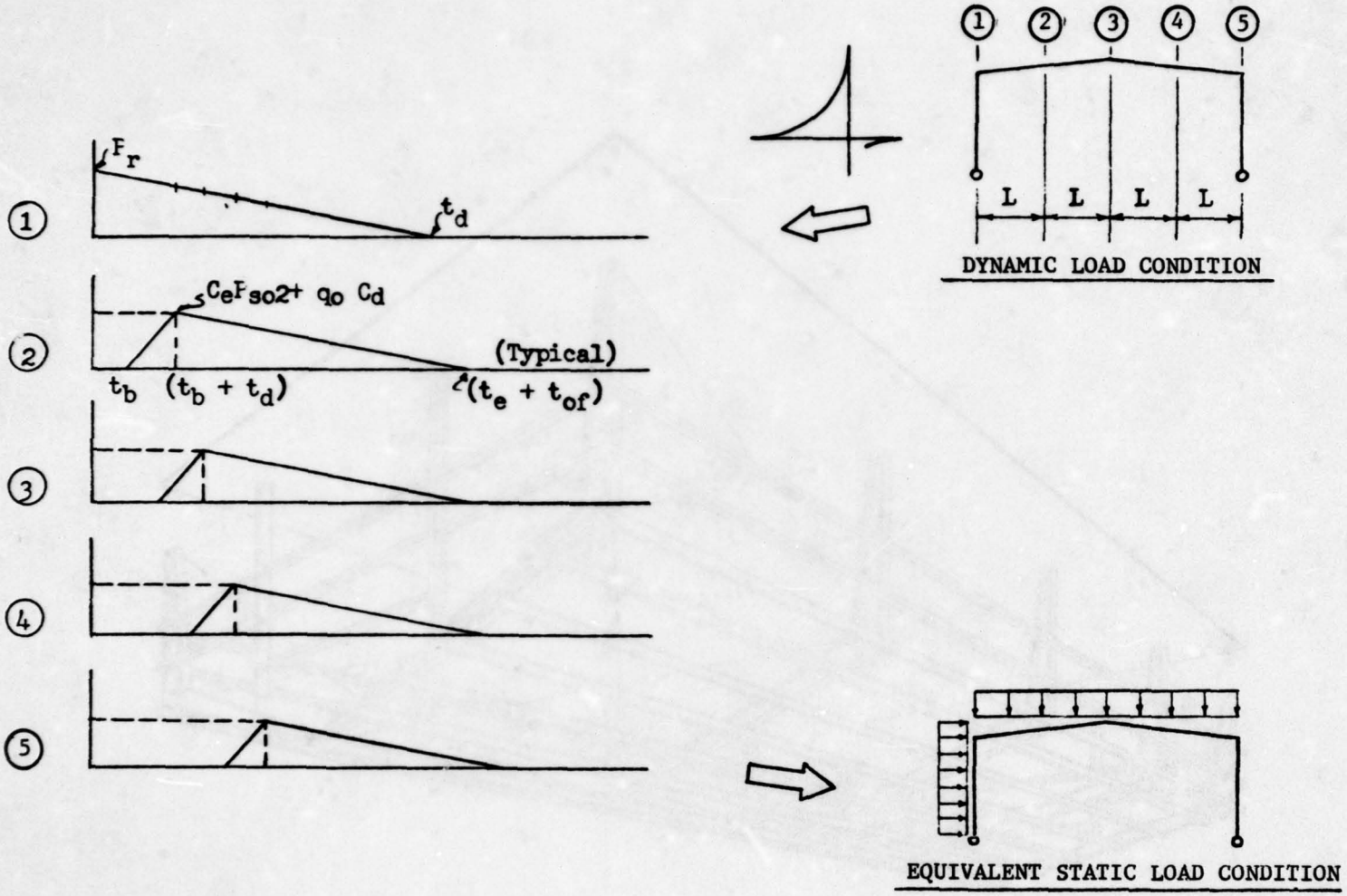


Figure 2. METHOD OF DETERMINING EQUIVALENT STATIC LOAD

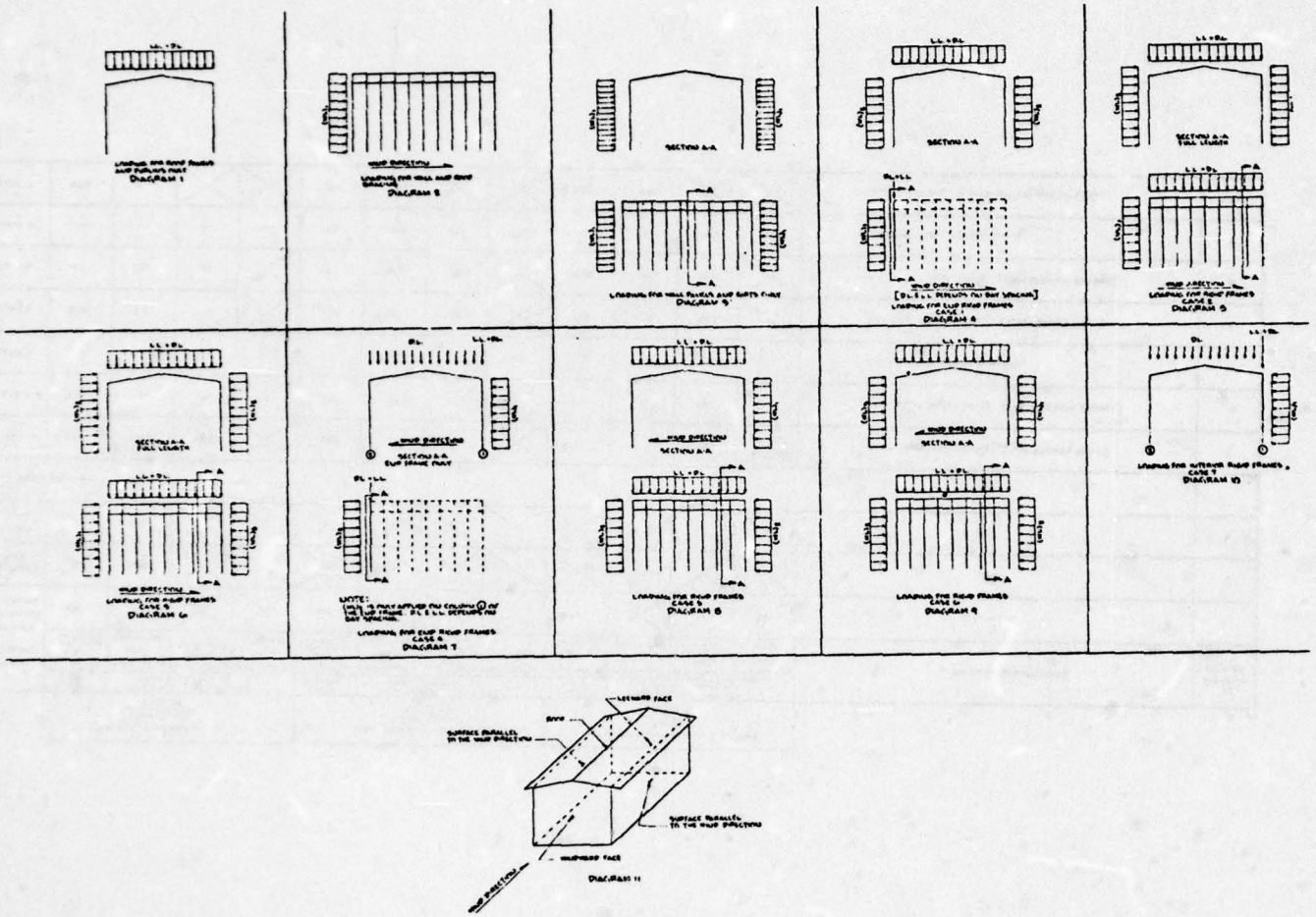


Figure 3. LOAD CONDITIONS ON RIGID FRAMES

ITEMS LOADED	BUILDING DIMENSIONS 120' × 175' Pan 2.5% & 10% m/s				BUILDING DIMENSIONS 80' × 125' Pan 2.5% & 10% m/s				BUILDING DIMENSIONS 40' × 125' Pan 2.5% & 10% m/s				DESIGN CONDITIONS	DIAGRAM NUMBER
	EQUIV LOAD	EQUIVALENT WIND LOAD (SEE DIAGRAM II)			EQUIV LOAD	EQUIVALENT WIND LOAD (SEE DIAGRAM II)			EQUIV LOAD	EQUIVALENT WIND LOAD (SEE DIAGRAM II)				
	LIVE LOAD % L.L. (SEE LOAD TABLE)	WIND LOAD % $(WL)_1$ (WINDWARD)	WIND LOAD % $(WL)_2$ (SURFACES ‖ TO WIND)	WIND LOAD % $(WL)_3$ (LEEWARD)	LIVE LOAD % L.L. (SEE LOAD TABLE)	WIND LOAD % $(WL)_1$ (WINDWARD)	WIND LOAD % $(WL)_2$ (SURFACES ‖ TO WIND)	WIND LOAD % $(WL)_3$ (LEEWARD)	LIVE LOAD % L.L. (SEE LOAD TABLE)	WIND LOAD % $(WL)_1$ (WINDWARD)	WIND LOAD % $(WL)_2$ (SURFACES ‖ TO WIND)	WIND LOAD % $(WL)_3$ (LEEWARD)		
ROOF PANELS & PURLINS	100				100				100				L.L. + D.L.	1
WALL PANELS & GIRTS		67%				67%				67%			$(WL)_1$	2
WALL & ROOF BRACING		57%				57%				57%			$(WL)_1$	3
RIGID FRAMES														
CASE 1	100	57%	100		100	57%	100		100	57%	100		D.L. + L.L. + $(WL)_1$ + $(WL)_3$ [END FRAMES ONLY]	4
CASE 2	100	0	100		100	0	100		100	0	100		D.L. + L.L. + $(WL)_1$ + $(WL)_3$ [FOR INTERIOR FRAMES]	5
CASE 3	—	—	—	—	—	—	—	—	—	—	—	—	D.L. + L.L. + $(WL)_1$ + $(WL)_2$ + $(WL)_3$	6
CASE 4	100	57%	100		100	57%	100		100	57%	100		D.L. + L.L. + $(WL)_1$ + $(WL)_3$ [END FRAMES ONLY]	7
CASE 5	100	57%	100		100	57%	100		100	57%	100		D.L. + L.L. + $(WL)_1$ + $(WL)_3$ [FOR INTERIOR FRAMES]	8
CASE 6	—	—	—	—	100	100	100	100	100	100	100	100	D.L. + L.L. + $(WL)_1$ + $(WL)_2$ + $(WL)_3$	9
CASE 7	100	57%			100	57%			100	57%			D.L. + L.L. + $(WL)_1$ [INTERIOR FRAMES ONLY]	10

Figure 4. DESIGN LOADS FOR PREENGINEERED METAL BUILDING

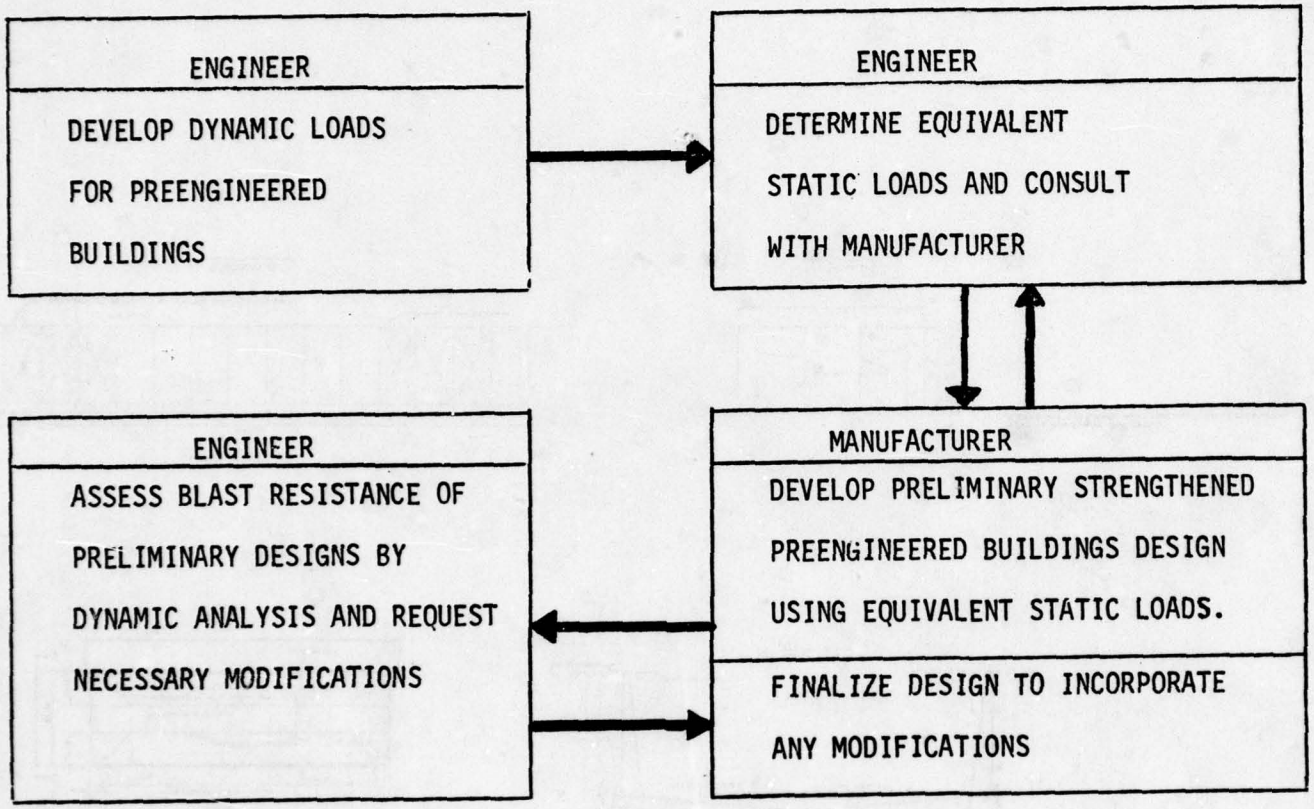


Figure 5. FLOW CHART FOR DEVELOPING STRENGTHENED PREENGINEERED BUILDINGS

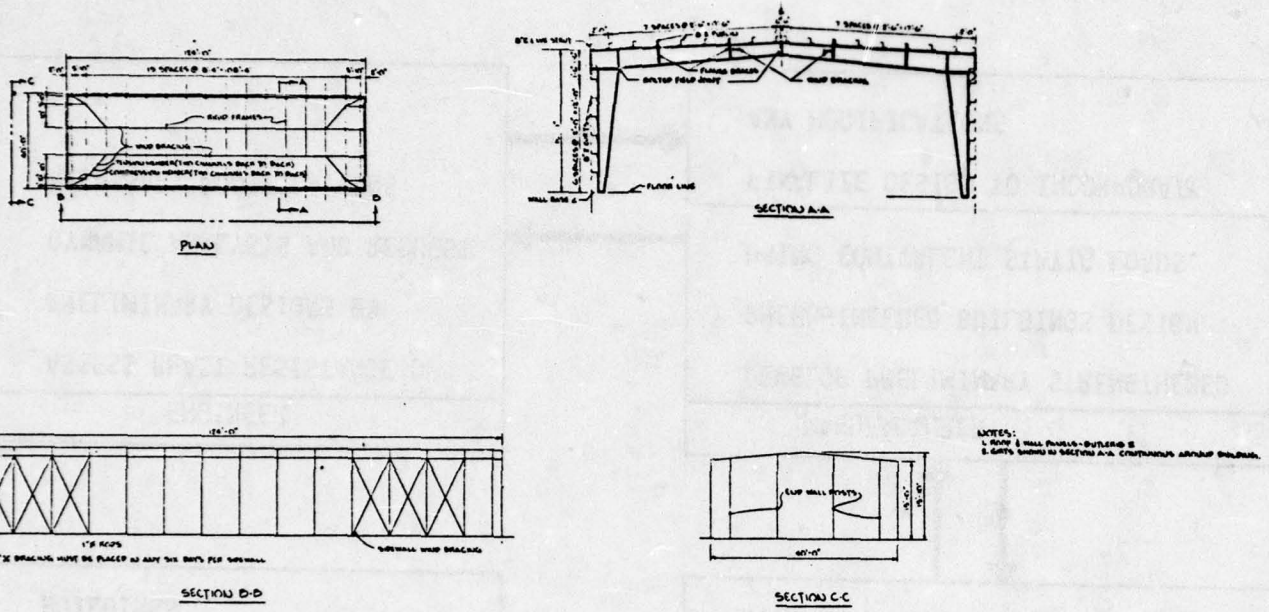


Figure 6. 40' X 125' STRENGTHENED PREENGINEERED BUILDING

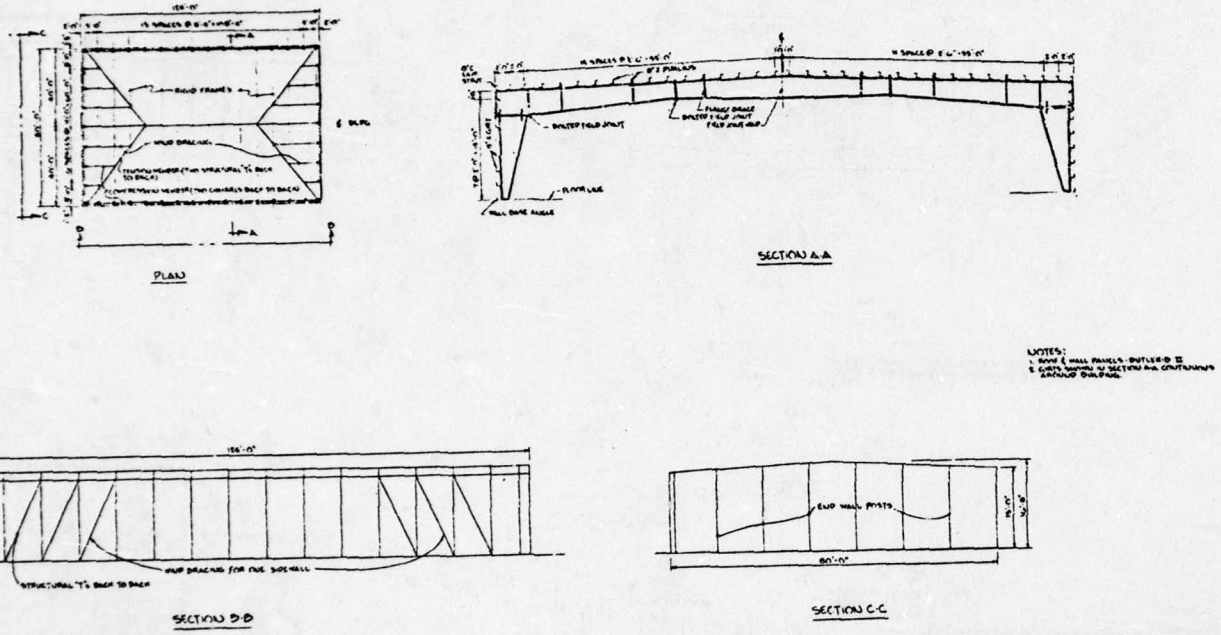
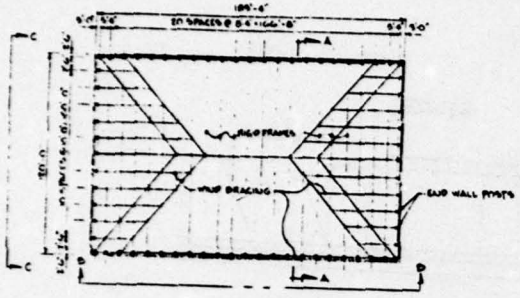
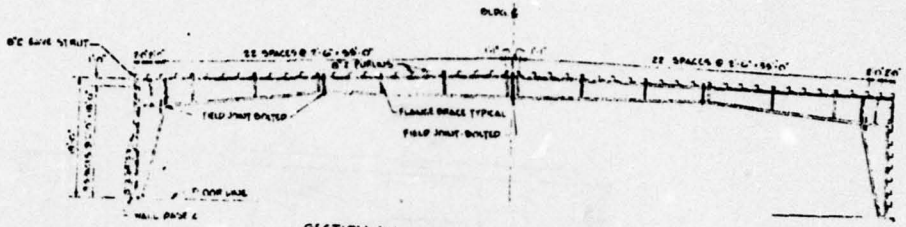


Figure 7. 80' X 120' STRENGTHENED PREENGINEERED BUILDING

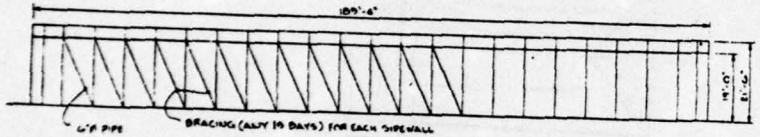


PLAN

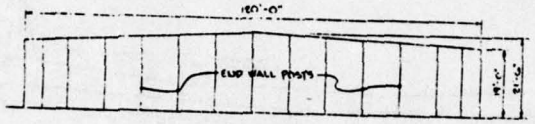


SECTION A-A

NOTES:
1. ROOF & WALL PANELS - OUTLERID II
2. GIRTS SHOWN IN SECTION A-A CONTINUOUS AROUND BUILDING.

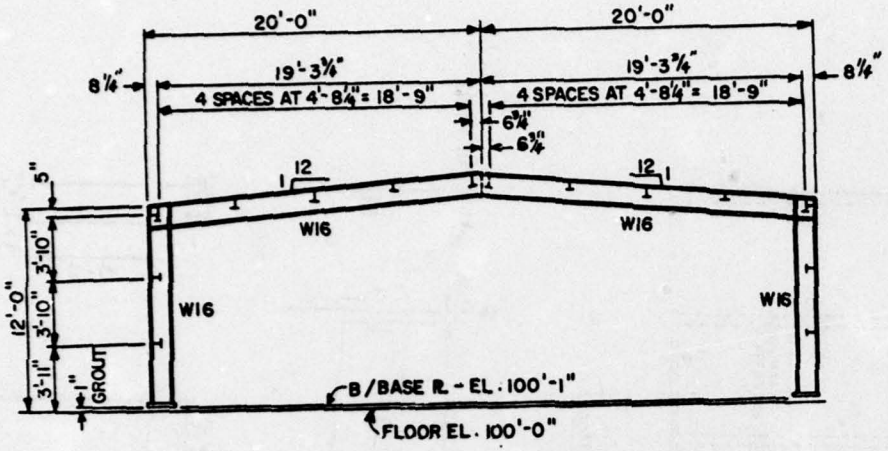


SECTION B-B

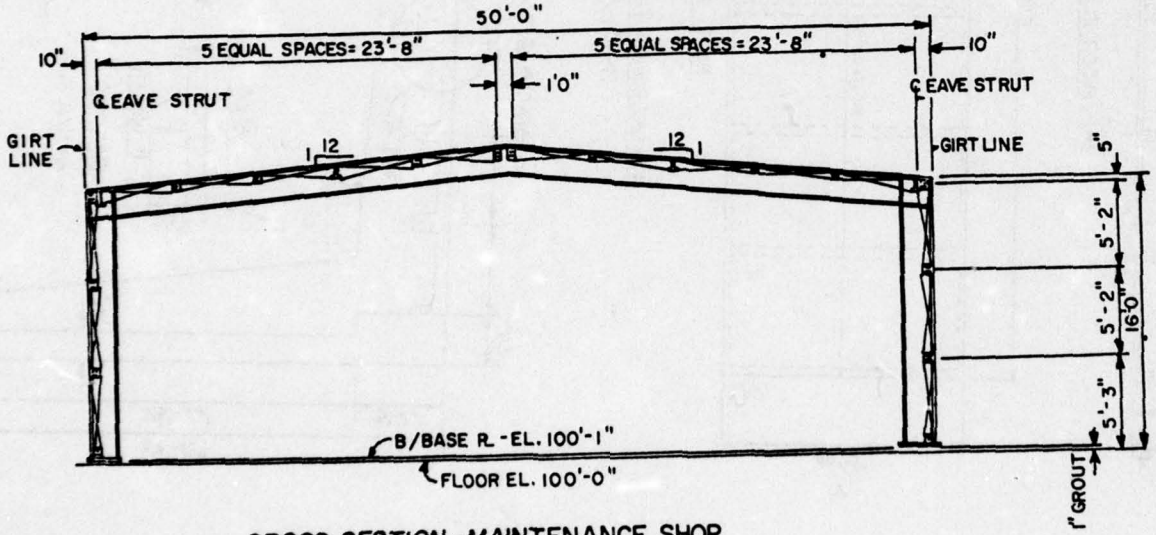


SECTION C-C

Figure 8. 120' X 180' STRENGTHENED PREENGINEERED BUILDING

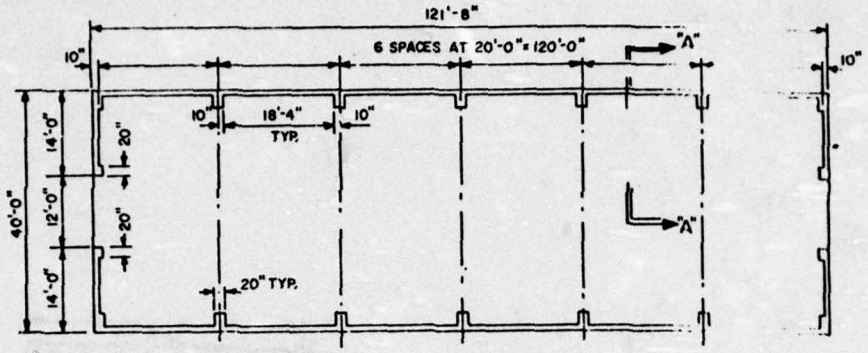


CROSS SECTION-CHANGE HOUSE

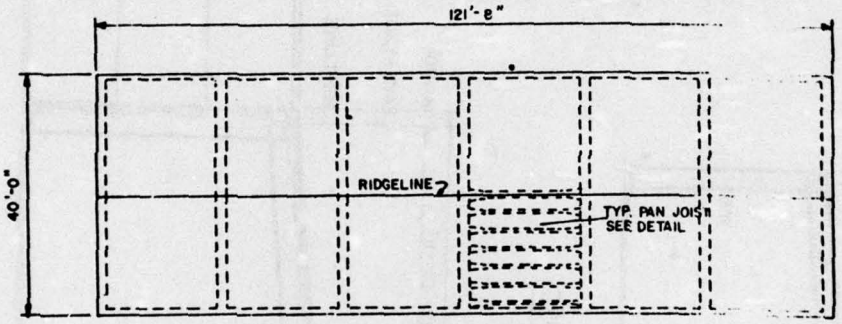


CROSS SECTION - MAINTENANCE SHOP

Figure 9. STEEL FRAME BUILDINGS



FLOOR PLAN



ROOF PLAN

40'x120' Building (Floor & Roof Plans)

(Pso = 2.0psi)

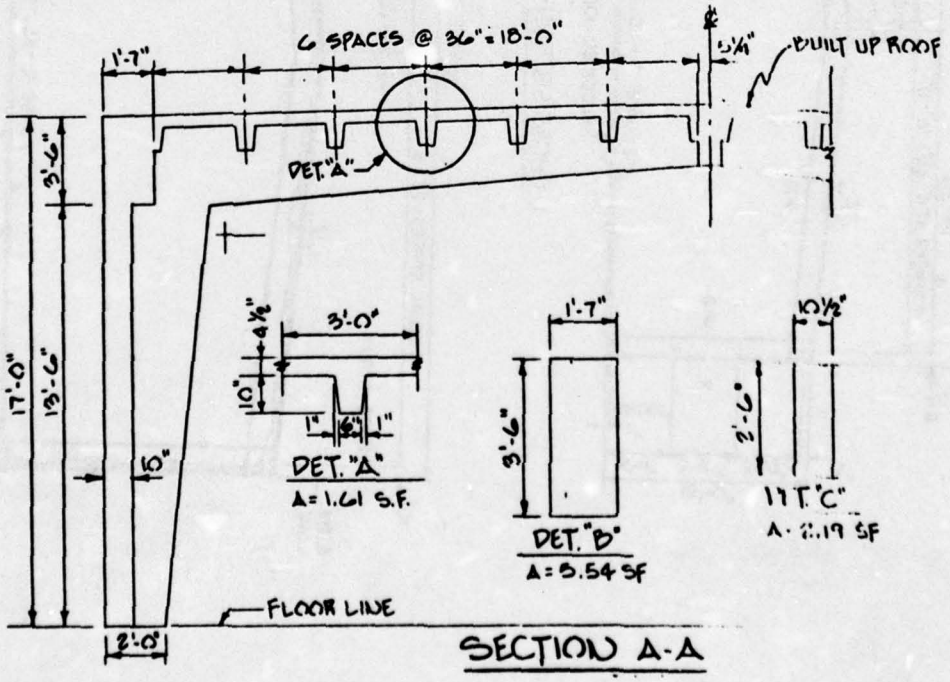
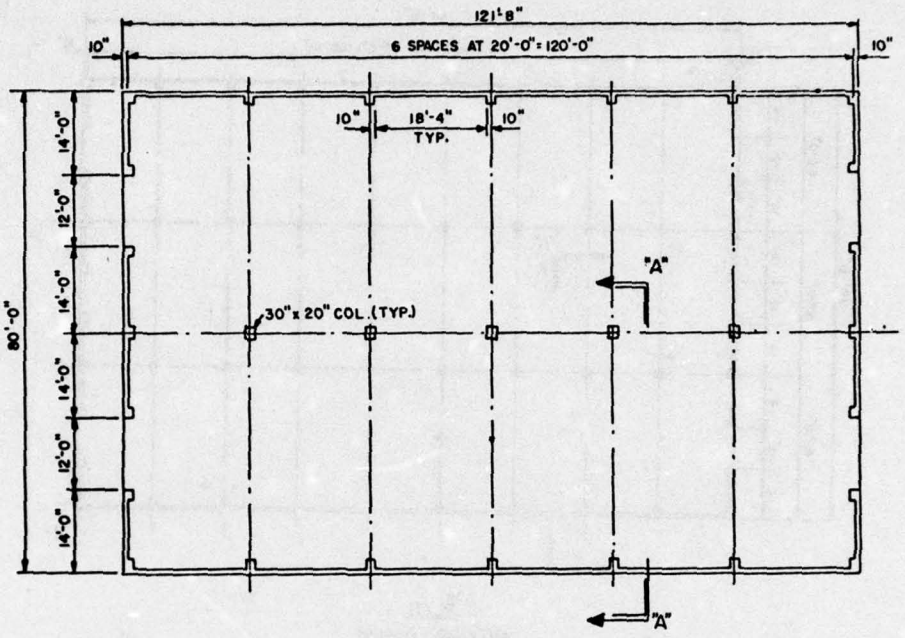
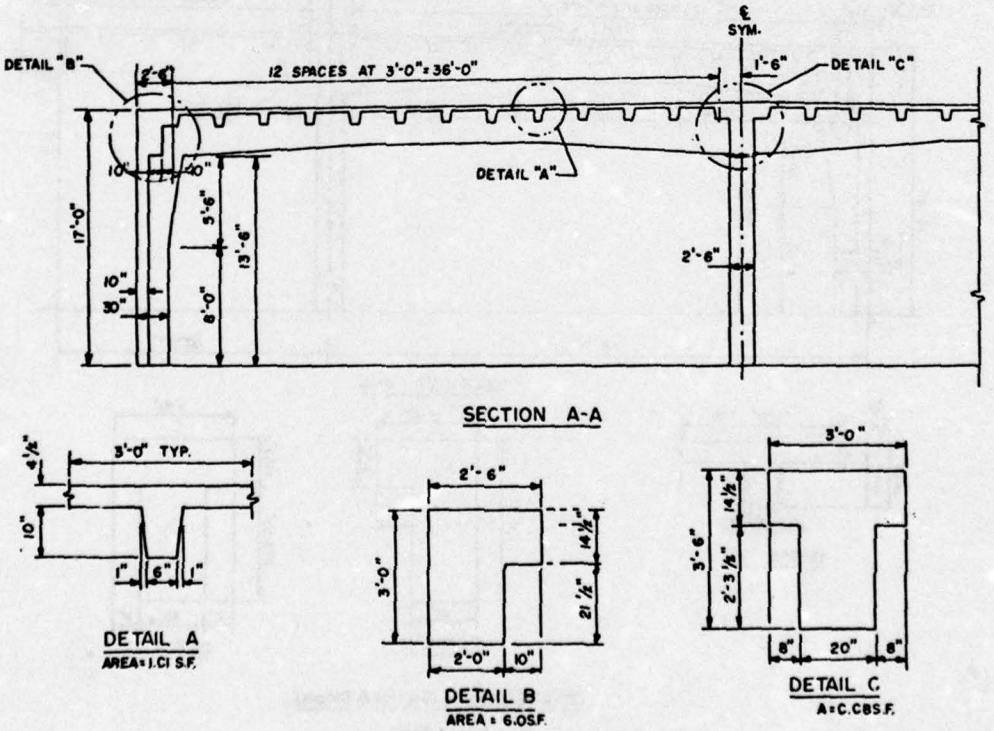


Figure 10. 40' X 120' REINFORCED CONCRETE BUILDING



PLAN
80'x120' Building
(Pso = 2psi)



SECTION A-A

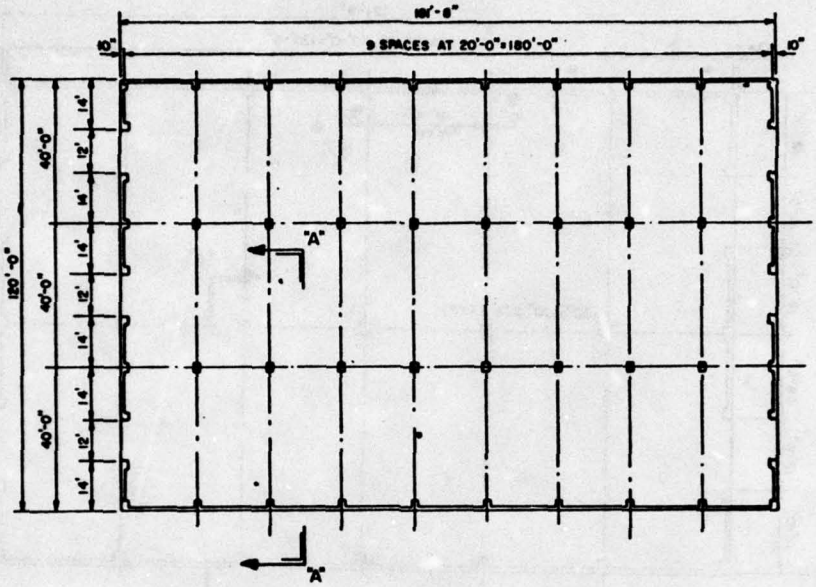
DETAIL A
AREA = 1.01 S.F.

DETAIL B
AREA = 6.05 S.F.

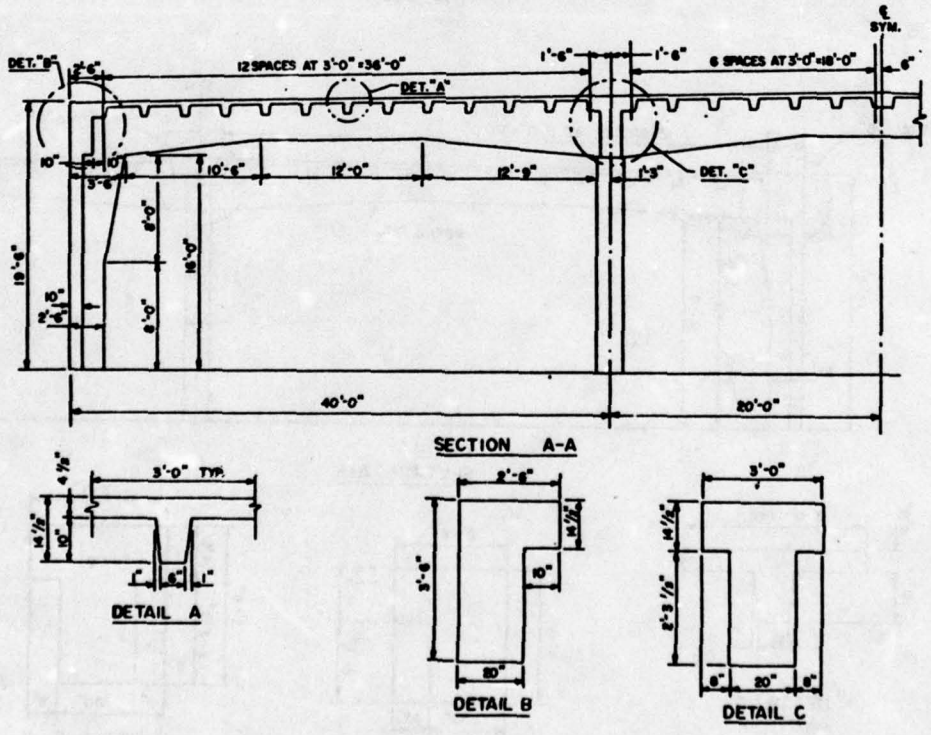
DETAIL C
A = C.CBS.F.

80'x120' Building (Section & Details)

Figure 11. 80' X 120' REINFORCED CONCRETE BUILDING



PLAN
120'x180' Building
(Pso = 2psi)



SECTION A-A

120'x180' Building (Section & Details)
(Pso = 2psi)

Figure 12. 120' X 180' REINFORCED CONCRETE BUILDING

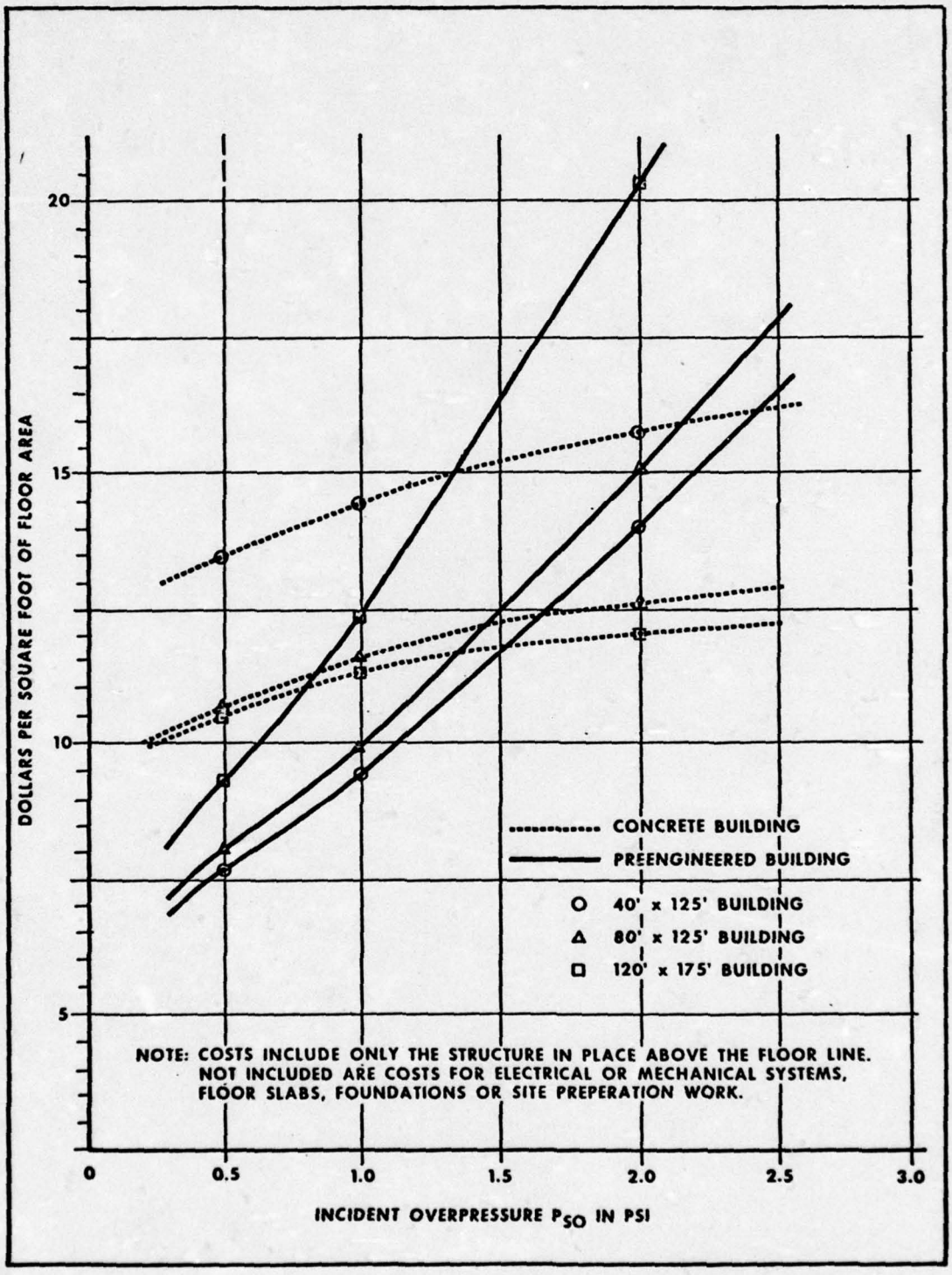


Figure 13. COST ANALYSIS RESULTS

METHODS FOR UPGRADING BLAST RESISTANCE OF EXISTING STRUCTURES

By

Kenneth Kaplan
Scientific Service, Inc., Redwood City, CA
and
Bernard L. Gabrielsen, Ph.D., Professor of Civil Engineering
San Jose State University, San Jose, CA

It is not the purpose of this paper to present a comprehensive review of all methods for strengthening existing structures. Rather, it is meant as a brief for trying to find the basic source of a structural deficiency before corrective measures are taken, and then seeking out (or at least not rejecting) new, novel, or non-standard solutions. Thus, there will be some emphasis on the unconventional, both in analysis and retrofit.

The material is divided into two parts: structural elements subject to out-of-plane loads (and therefore undergoing flexure); and those subject to in-plane loads (and therefore carrying shear). The basic functions of these structural elements is illustrated in Fig. 1 adopted from Ref. 1. The "side wall" of Fig. 1, which takes the blast loading head-on, must resist these loads in flexure, the "end wall" and "roof" carry the shear forces.

ELEMENTS SUBJECT TO OUT-OF-PLANE LOADS (FLEXURAL STRESS)

In concrete frame construction, infill walls, -- whether of masonry or light weight concrete -- can display very low resistance to an out-of-plane load such as that from a blast wave, because their basic design envisages them resisting wind loads of on the order of 30 lb/ft^2 (for a 100 mph wind) or less, equivalent to an incident blast pressure of only about 0.1 psi. Except for a few very special cases, such walls would fail in flexure at relatively low blast pressures because the tensile capacity of the wall materials, or of the wall's construction, is very low.

PRECEDING PAGE BLANK-NOT FILMED

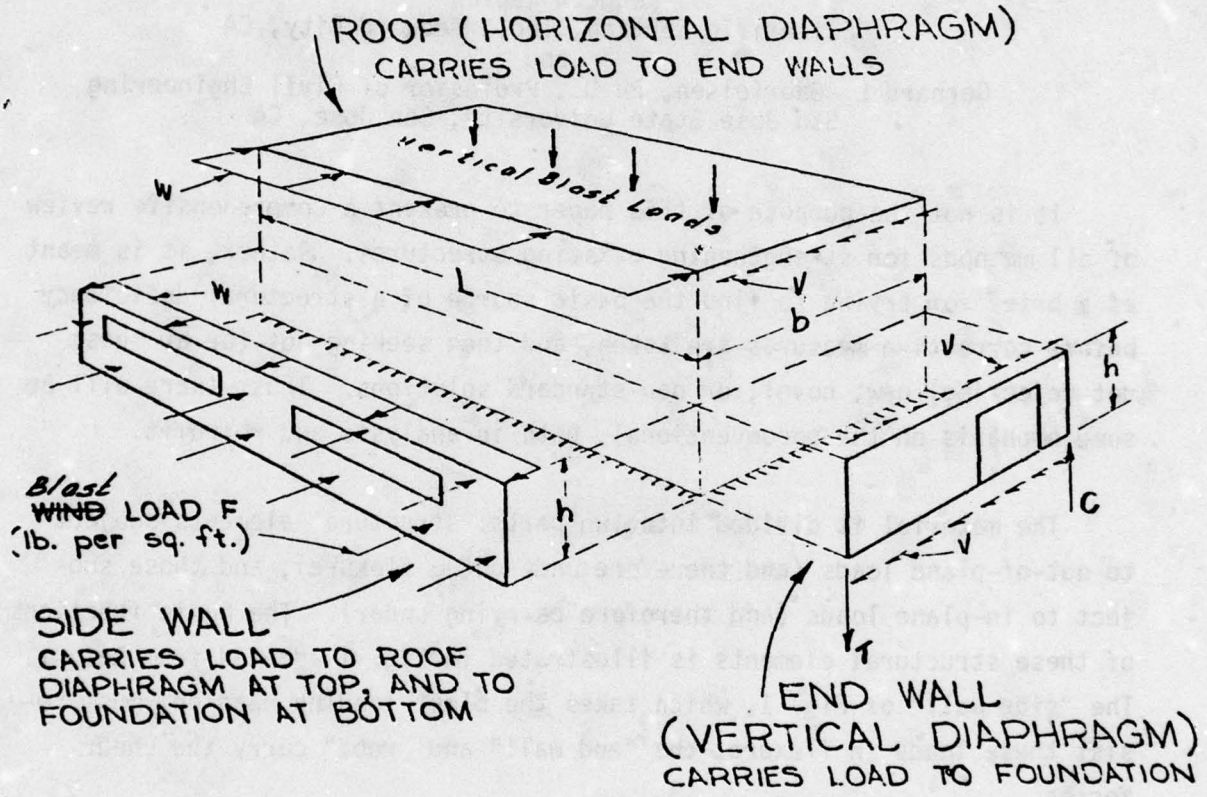


Fig. 1. Functions of Structural Elements.

Masonry Cantilevered Wall

A fairly common type of industrial and warehouse construction involves walls cantilevered from the floor with windows between the top of the wall and the beam above. Such a wall, 6 ft high, made of two wythes of unreinforced brick, and free-standing (that is, not well mortared to the columns on either side) could be expected to fail under a blast loading (reflected pressure) of only about 0.5 psi, or an incident pressure of about 0.25 psi. (This assumes brick mortar assemblage optimistic tensile strength of about 200 psi, some ten times typical code allowables.)

Assume, for the moment, that there is no practical way to tie the wall to the columns on either side. Increasing the blast resistance of the wall is then a matter of increasing its effective tensile strength. While it is not simple to increase the tensile strength of the brick mortar assemblage, its effective strength can be increased by putting the entire wall into vertical compression -- essentially pre-stressing the wall -- with steel straps in the manner shown in Fig. 2. Loading pressure is directly proportional to stress in the wall, thus if the stress required for failure to take place is trebeled, the blast pressure required to cause failure would also be trebeled. (This could be done with 4-in. wide straps, 1/8 in. thick positioned about 2 ft apart and tensioned to 80 ksi.)

Light Weight Concrete, Nonbearing Wall, Beam Mounted (Pin-Pin Support)

Such a wall frequently has only temperature steel running down the center of the wall, and again, the problem is the low tensile strength of the wall in flexure. (The steel being at the neutral axis contributes virtually nothing to the walls tensile strength.) Thus, very large increases in flexural strength could be achieved by adding steel to the tension of downstream face of the wall, since its flexural capacity is proportional to the area of steel that resists load, and the steel's effectiveness is heightened the closer it is to the area of maximum fiber stress (the downstream face).

An effective way of "incorporating" new steel into a wall is shown in Fig. 3. After preparation of the face of the wall to assure good bonding,

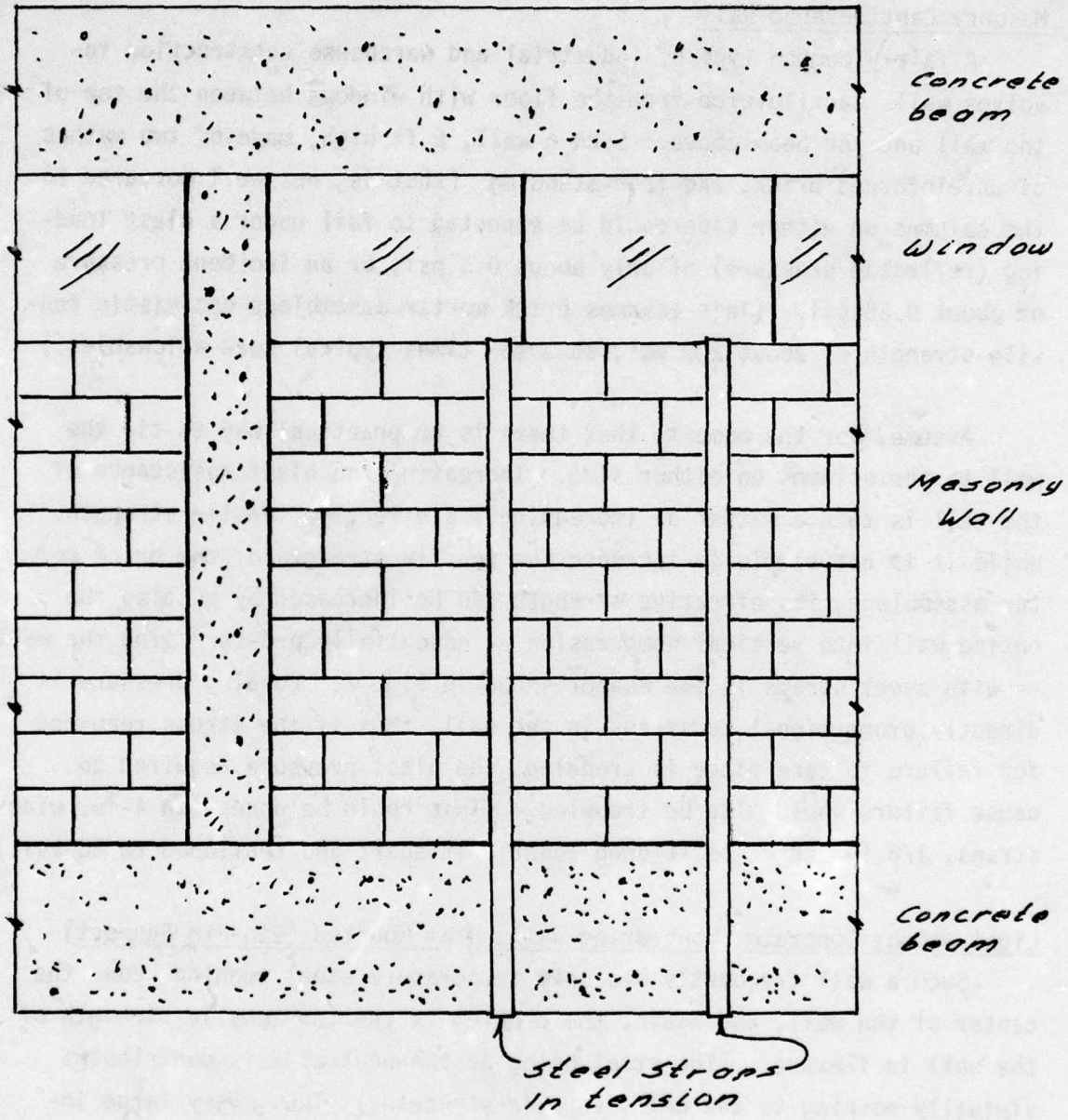


Fig. 2. Steel Straps Used to Place Masonry Cantilever Wall in Vertical Compression.

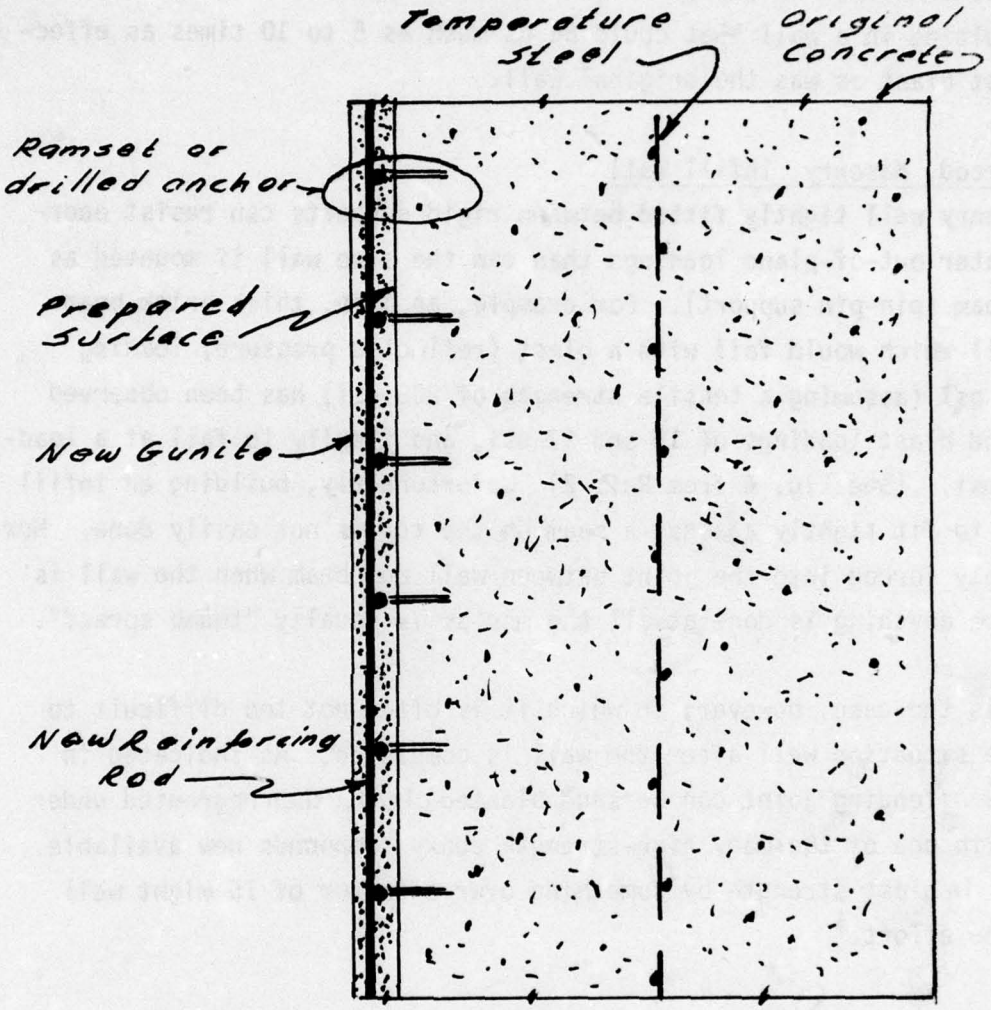


Fig. 3. Addition of Reinforcing and Gunite to Surface of Weak Concrete Wal to Increase Flexural Strength.

a grid of reinforcing rod or welded wire fabric is affixed to it (either ramset or with drilled anchors). Gunite is them applied to cover the steel, resulting in a wall that could be as much as 5 to 10 times as effective against blast as was the original wall.

Non-Reinforced, Masonry, Infill Wall

A masonry wall tightly fitted between rigid supports can resist enormously greater out-of-plane loadings than can the same wall if mounted as a simple beam (pin-pin support). For example, an 8-in. thick brick beam-mounted wall which would fail with a blast (reflected pressure) loading of about 1 psi (assuming a tensile strength of 200 psi) has been observed to withstand blast loadings of 15 and 17 psi, and finally to fail at a loading of 20 psi. (See Fig. 4 from Ref. 2) Unfortunately, building an infill wall so as to fit tightly against a beam on the top is not easily done. Mortar is rarely forced into the joint between wall and beam when the wall is built; where anything is done at all the mortar is usually "thumb spread".

This is the case, however, in which it is often not too difficult to improve the situation well after the wall is completed. As indicated in Fig. 5, the offending joint can be sand blasted clean, then regrouted under pressure with one of the many high-strength epoxy compounds now available. An increase in blast strength by something over a factor of 15 might well be worth the effort.

Timber Joist Floor or Roof

In much older bearing wall construction, the wooden covering over floor and roof joists serves mainly to distribute vertical load to the joists. Very large increases in resistance to vertical load can be achieved relatively simply by proper use of plywood.

Plywood Sheathing. If, for example, plywood only ½ in. thick were affixed to the bottom of 2" x 12" joists on 2-ft centers (preferably by gluing so that there is a stong bond between the two) the section modulus and therefore the moment capacity of the new "T" section would be almost

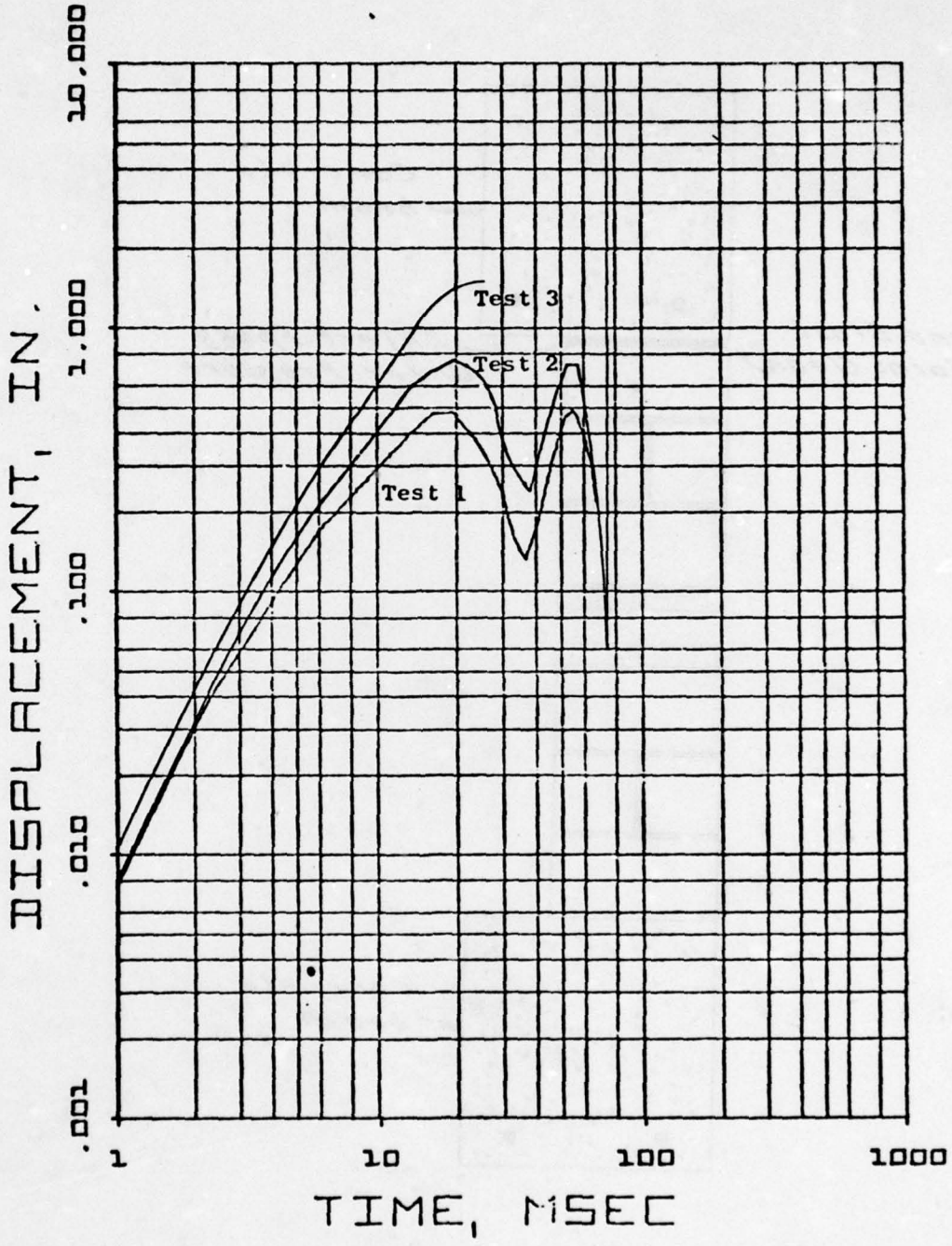


Fig. 4. Displacement as a Function of Time, Wall No. 87, Test 1, 13 psi; Test 2, 15 psi; Test 3, 20 psi.

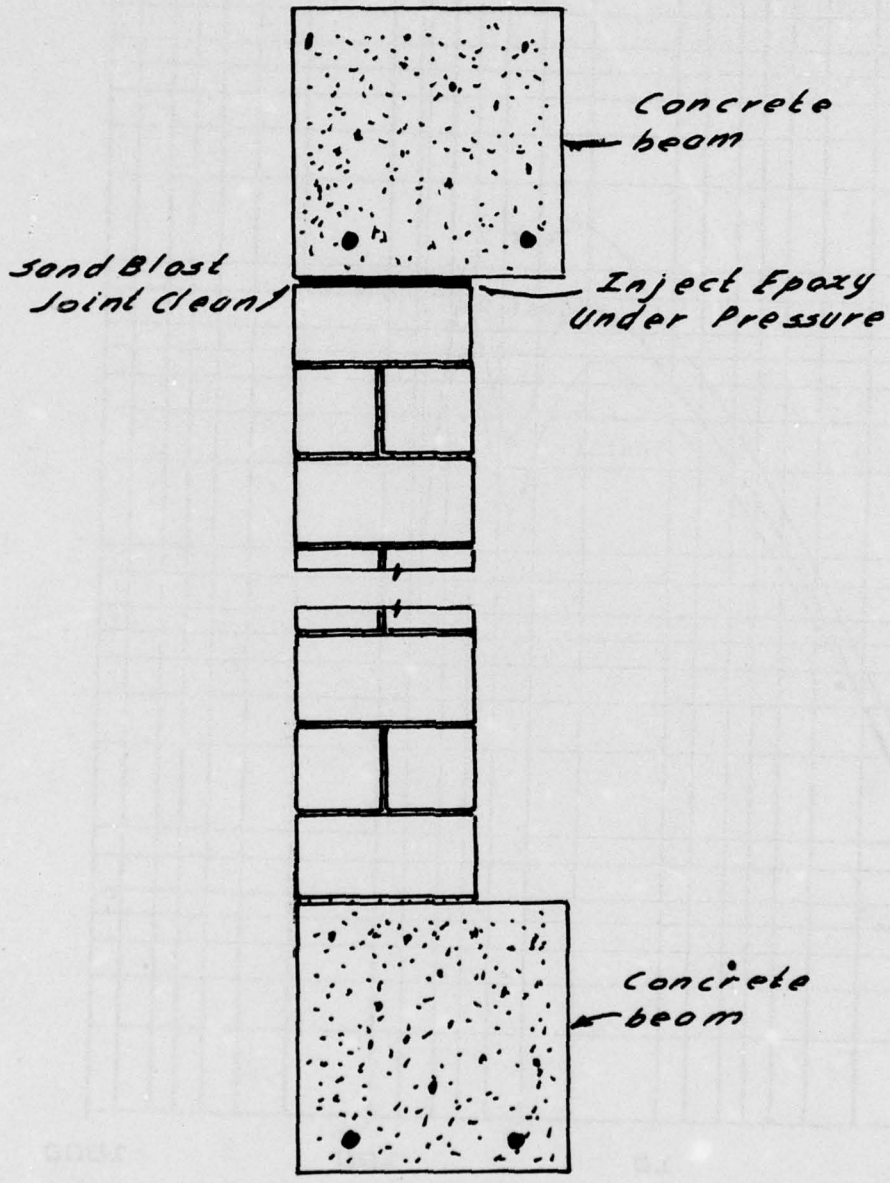


Fig. 5. Creating Conditions for Rigid Arching with Masonry Infill Wall.

doubled. Adding another ½ in. of plywood on top of the joists (converting each joist essentially to a wide-flange beam as illustrated in Fig. 6) would further increase the capacity by 50%, thus almost trebling the original capacity of the joist system.

Plywood Beams. The effective depth of a joist (or other member responding in flexure) can be readily increased by gluing a plywood-timber assemblage to the member to form a box beam. As an example of the strengths achievable by this method, in 1970, a box beam using 1-in. thick plywood, 32-ft long, 24-in. deep with flanges 3 in. deep and 12 in. wide, was designed, built and tested (Ref. 3) and displayed a moment capacity (300,000 ft lb) comparable to a reinforced concrete beam with similar outer dimensions. In Fig. 7, the two sections are compared. Fig. 8 shows the interior of the beam before assemblage; Fig. 9 shows the beam under test.

ELEMENTS SUBJECT TO IN-PLANE LOADS (SHEAR STRESS)

As with the previously discussed walls subject to out-of-plane loads, a basic problem with many wall and floor systems that must take shear under blast loadings (the end wall and roof in Fig. 1) is the fact that they were not originally designed to do so. The problem then is to find ways of increasing shear capacity without entirely rebuilding a structure.

Masonry Walls

In the first flexural example discussed, the flexural strength of a parapet or cantilever wall was increased by pre compressing the wall in the vertical direction. The same technique also increases the shear capacity of a wall, not by increasing its shear strength, but rather by reducing the shear caused by a particular horizontal load. This can be readily demonstrated by the construction of Mohr's circles for the uncompressed and compressed conditions.

For the uncompressed wall of Fig. 10a, for example, the Mohr's circle is shown in Fig. 10b. With τ being the shear stress, and no horizontal or

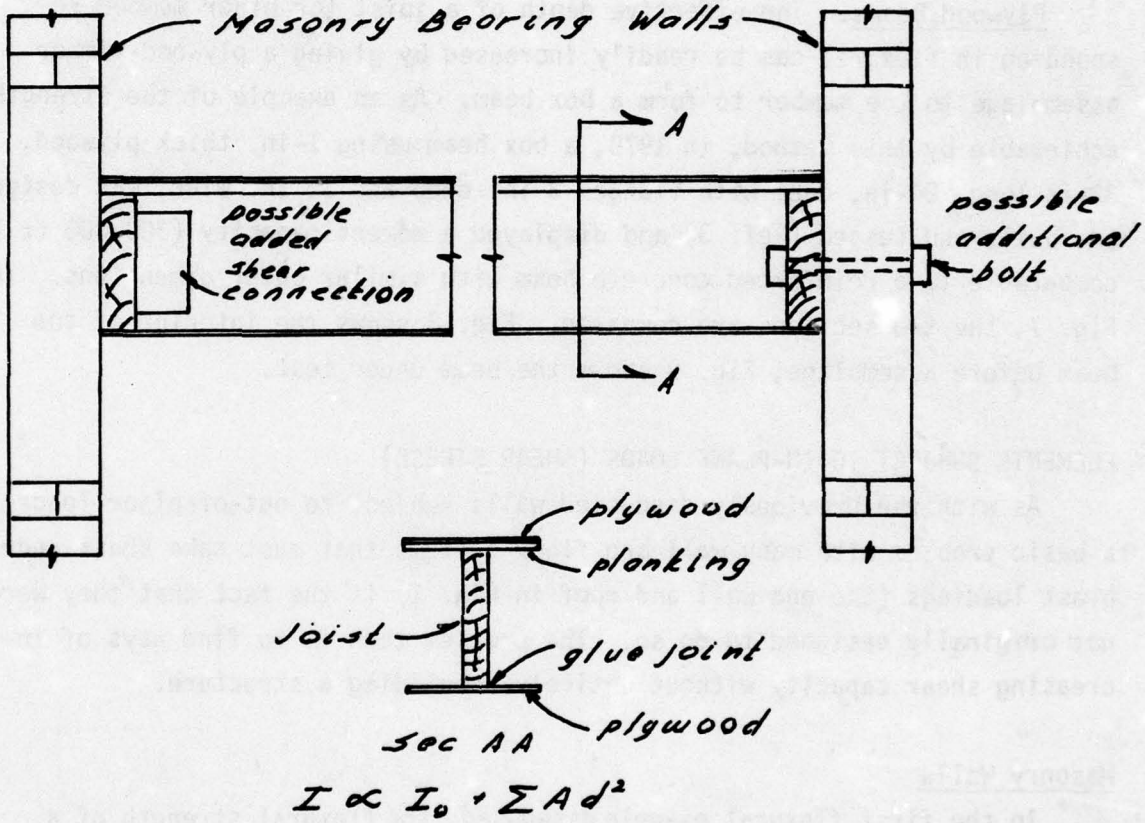


Fig. 6. Use of Plywood to Increase Moment Capacity of Joist. I = Moment of Inertia, I_o = I of Joist, A = Effective Area of Plywood, d = distance of Plywood from Centroidal Axis.

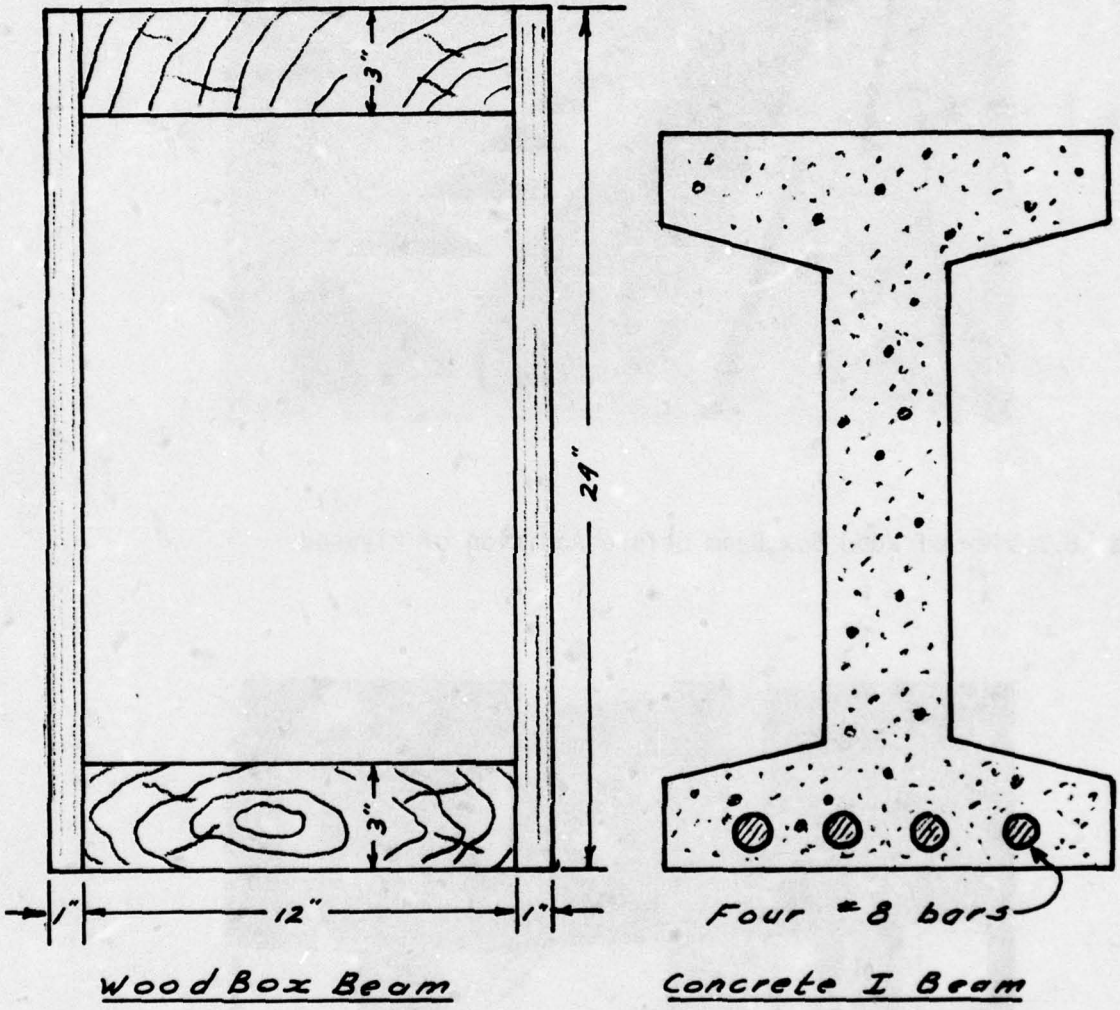


Fig. 7. Plywood Box and Concrete Beam Sections Compared.

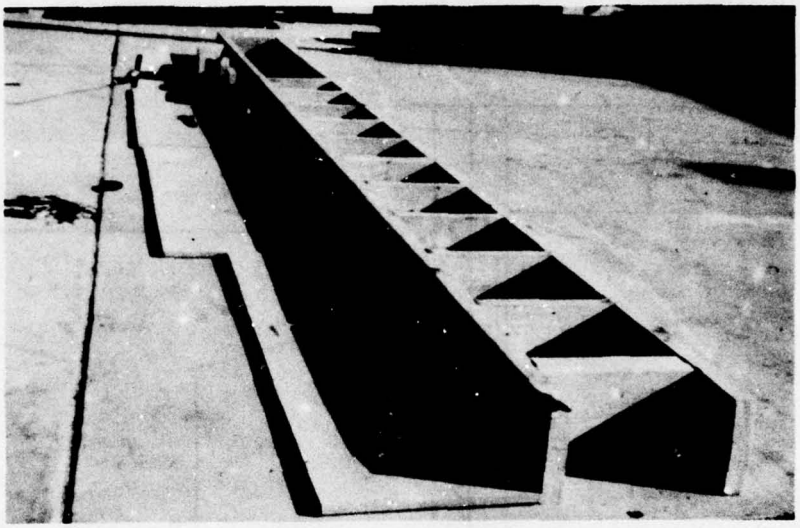


Fig. 8. View of Wood Box Beam Before Addition of Plywood.

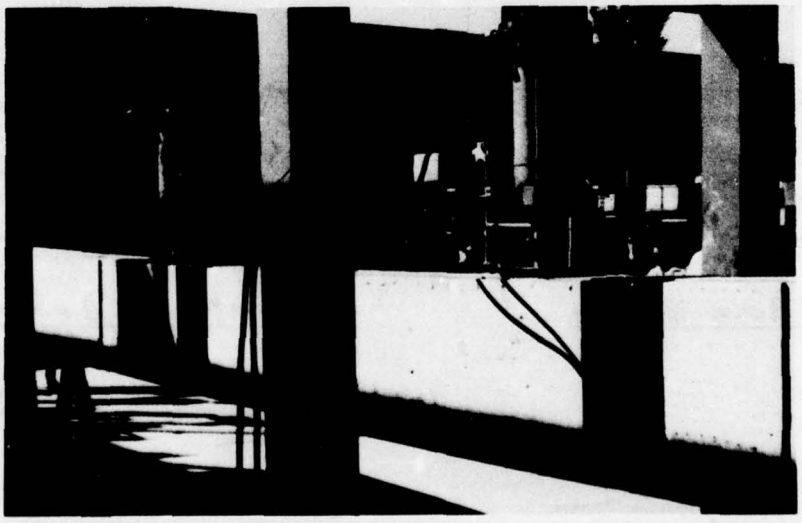


Fig. 9. Wood Box Beam During Flexure Strength Test.

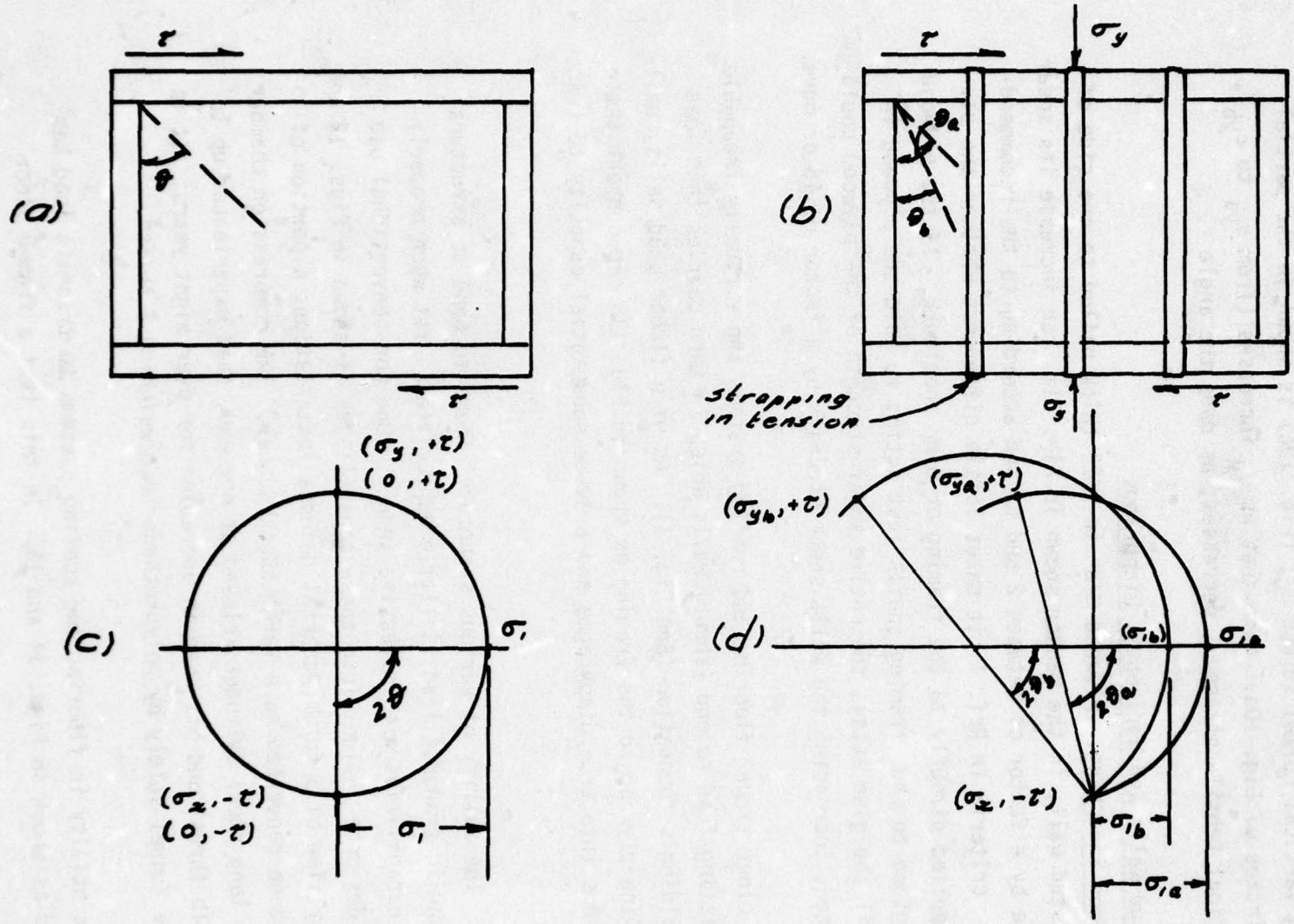


Fig. 10. Effect of Vertical Compression on Shearing Stress.

vertical normal stress, the principal tensile stress σ_1 is as shown. It acts normal to the plane forming an angle θ, with the vertical. The effect of adding vertical normal stress σ_y, (Fig. 10c) is shown in the partial Mohr's circles of Fig. 10d. Note that as σ_y increases (from σ_{ya} to σ_{yb}), the principal tensile stress σ_1 decreases, as does the angle θ.

Timber Stud Walls and Horizontal Diaphragms

Plywood Sheathing. Plywood 3/8" to 1/2" thick nailed to one side of a timber stud wall, in the manner shown in Fig. 11a can increase its shear resistance by a factor of between 2 and 5; and according to the recommended design criteria in Ref. 1, it makes little difference whether the plywood is applied directly to the framing or over sheetrock. If the plywood could be glued to the framing (nails just acting to hold the plywood in place until the glue sets), the entire shear strength of the plywood could be mobilized, increasing the walls shear strength by a factor of 15 or more.

Some older timber flooring and roofing systems are virtually incapable of transmitting load to end (shear) walls which in turn carries that load to the building's foundation (See Fig. 1). As with timber stud walls, nailing or gluing plywood to the framing as shown in Fig. 11b can convert these floor systems into true diaphragms and provide substantial capacity to transmit shear.

Foam. The ability of various structural foams to bond to structural members, and to transmit load is little appreciated. Yet when properly used, its capabilities are impressive indeed. One non-conventional use that provides some insight into these capabilities is shown in Figs. 12 and 13, cutaway view of a former coastal defense installation, a portion of which has been converted to a large shock tunnel. The compression chamber is a 63-ft long steel cylinder, closed at one end, that experiences up to 1,000,000 lb thrust and has been in operation for over eight years. It is held in the tunnel solely by polyurethane foam weighing 2 lb/ft^3.

Foam's utility in flooring and roofing systems to transmit load has been tested as shown in Figs. 14 and 15. In this test a framed floor

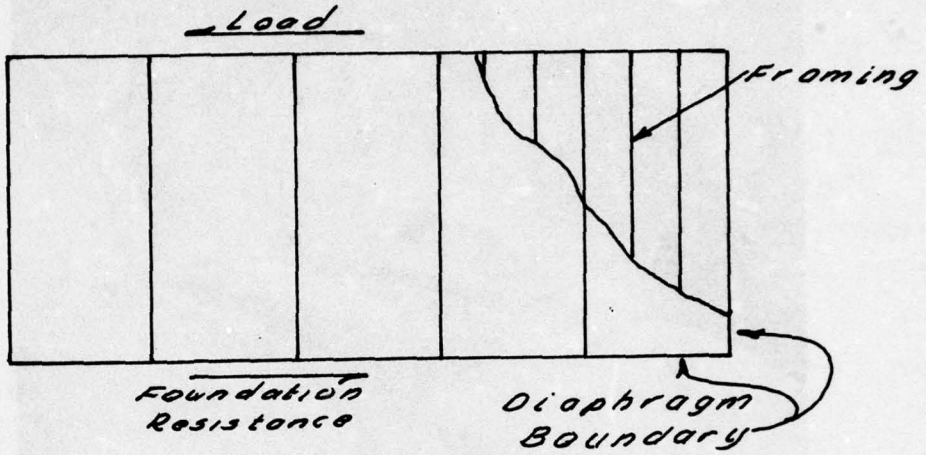


Fig. 11a. Plywood Shear Wall.

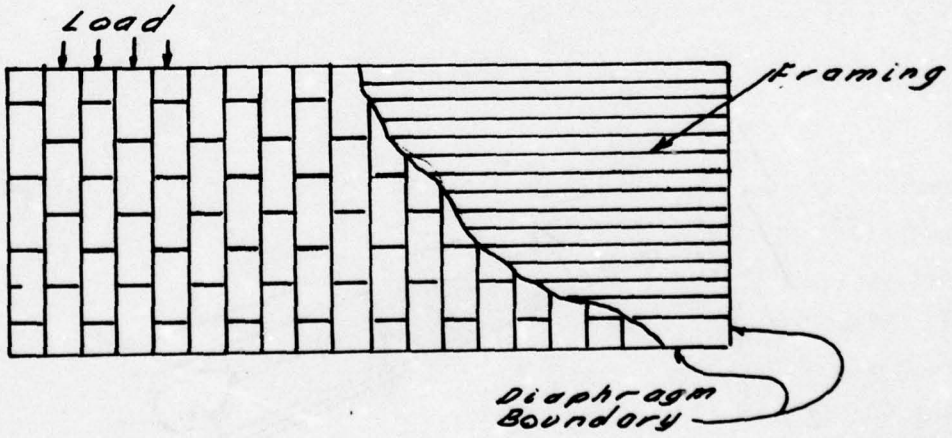


Fig. 11b. Horizontal Plywood Diaphragm.

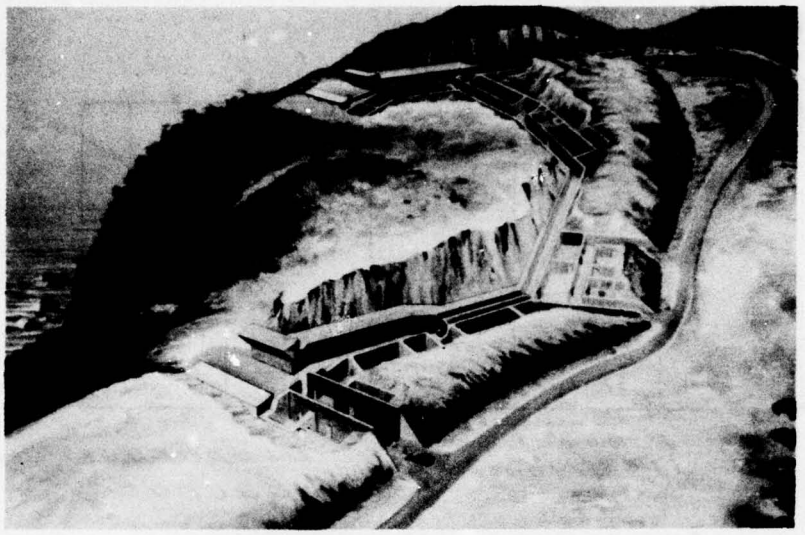


Fig. 12. Cutaway View of Former Coast Defense Battery Housing the Shock Tunnel (Foreground).

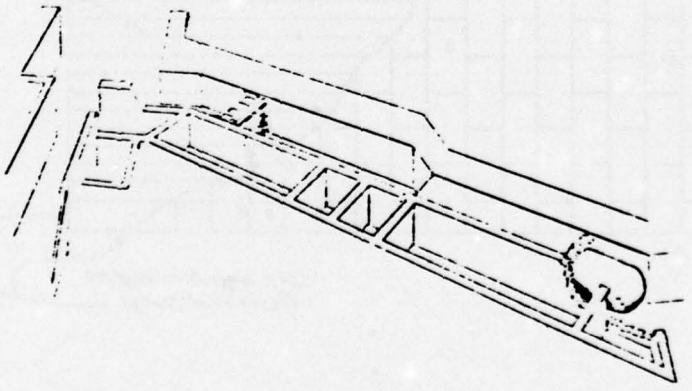


Fig. 13. Cutaway View of Shock Tunnel.

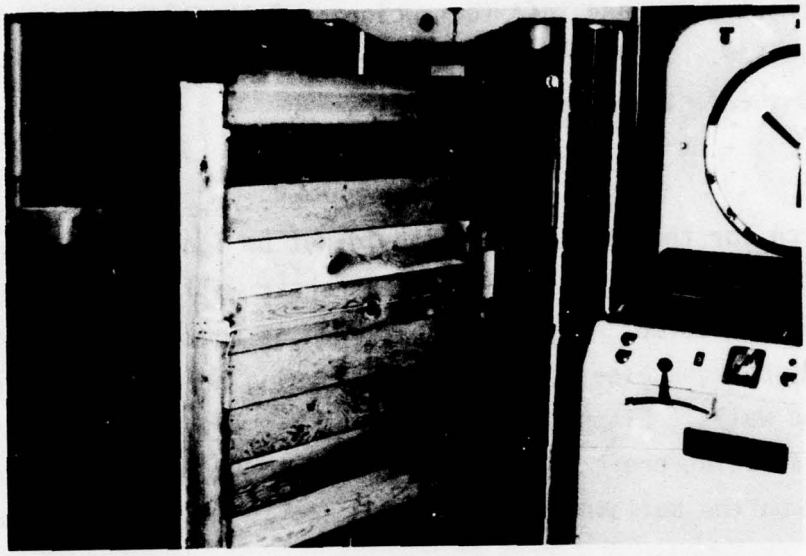


Fig. 14. Shear Test of Foamed Floor Diaphragm Section Showing 1-in. Wood Sheathing.

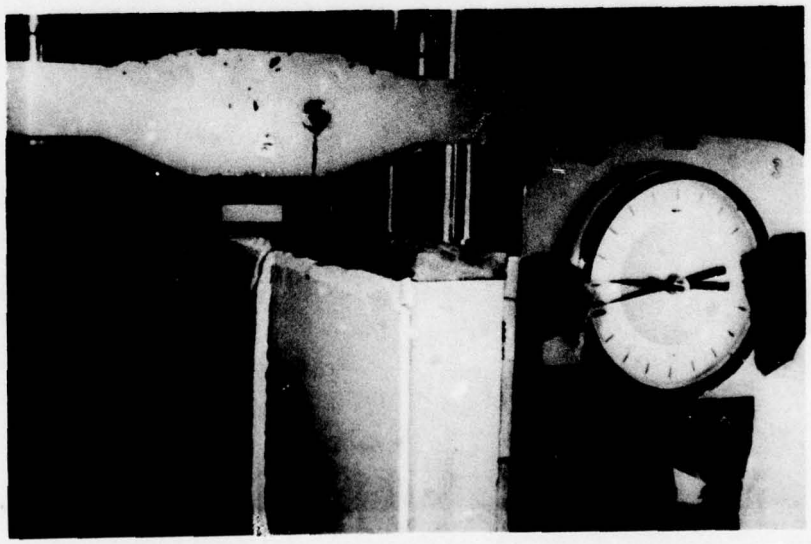


Fig. 15. Shear Test of Foamed Floor Diaphragm Section Showing Sheetrock Side.

system with sheetrock on one side and 1-in. thick planking on the other was first tested without foam, and then foam weighing 2 lb/ft^3 that was foamed (and formed) in place. Some results are shown in Fig. 16. The increase in stiffness and shear strength is dramatic.

Buttresses

In the search for the new, the old should not be ignored. Where it is impractical to strengthen walls to serve as shear walls, buttresses can provide a neat solution. Fig. 17 is a sketch of such a case in which the horizontal diaphragms also required strengthening because of the distance between end walls. Diaphragms were added in the form of balconies. These are shown as being pre-stressed with cables in an arc to put some compressive load on the building itself as a means of reducing any tendency to rattle.

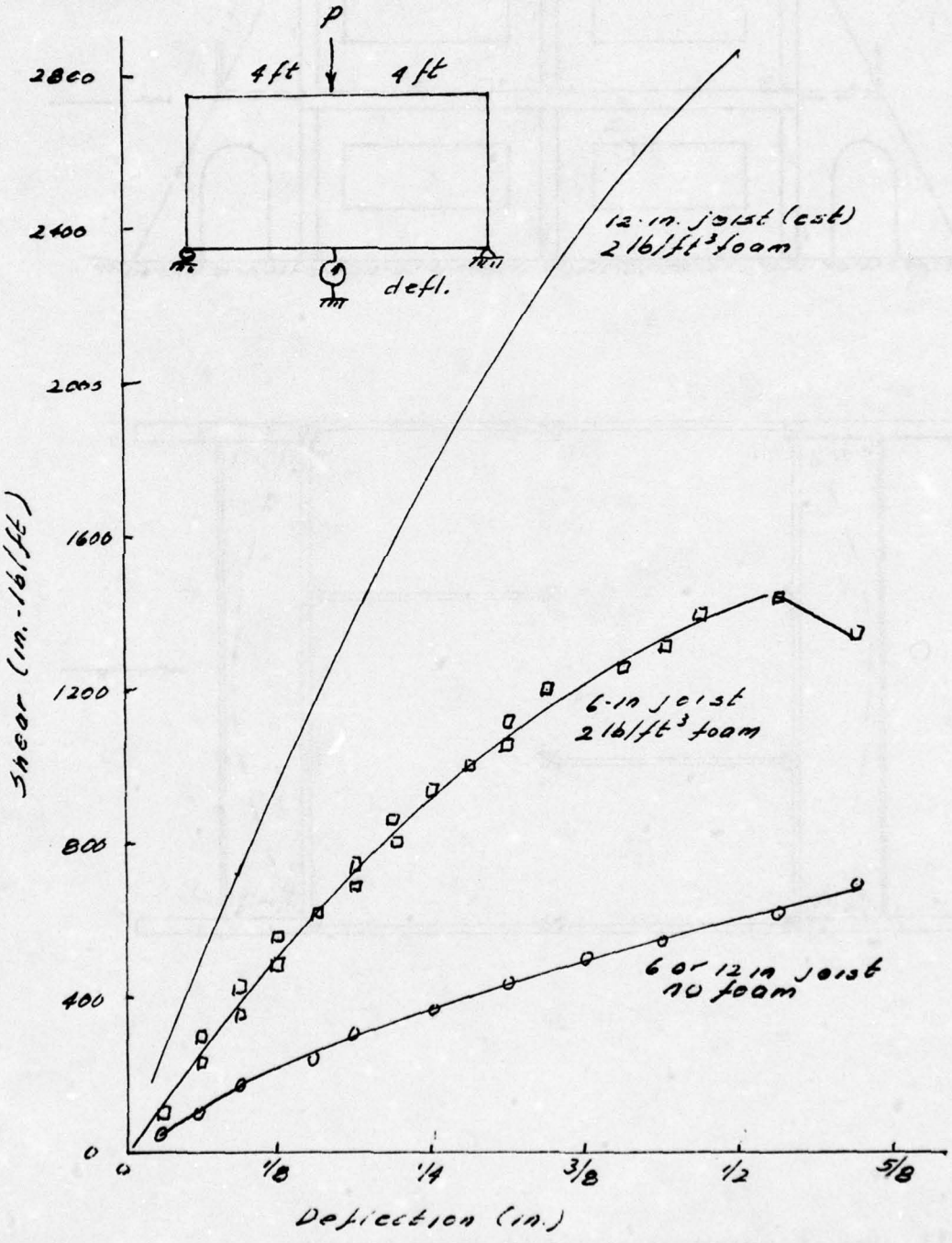
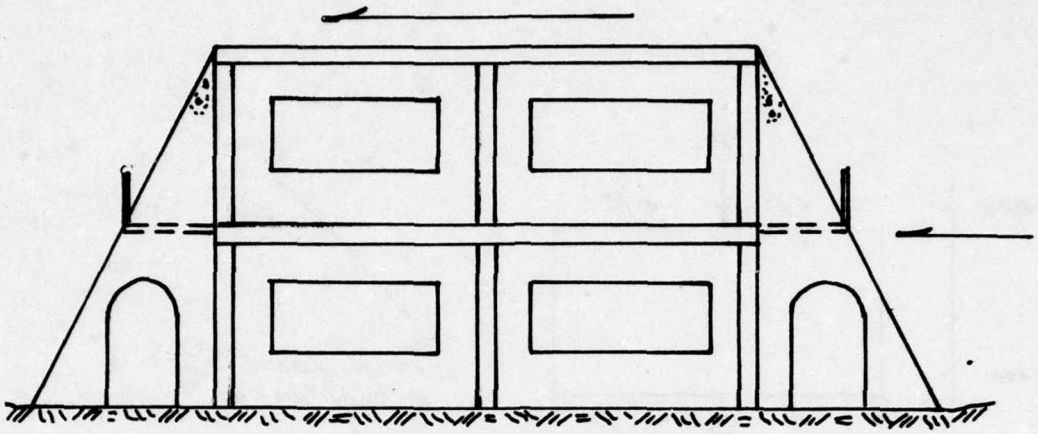
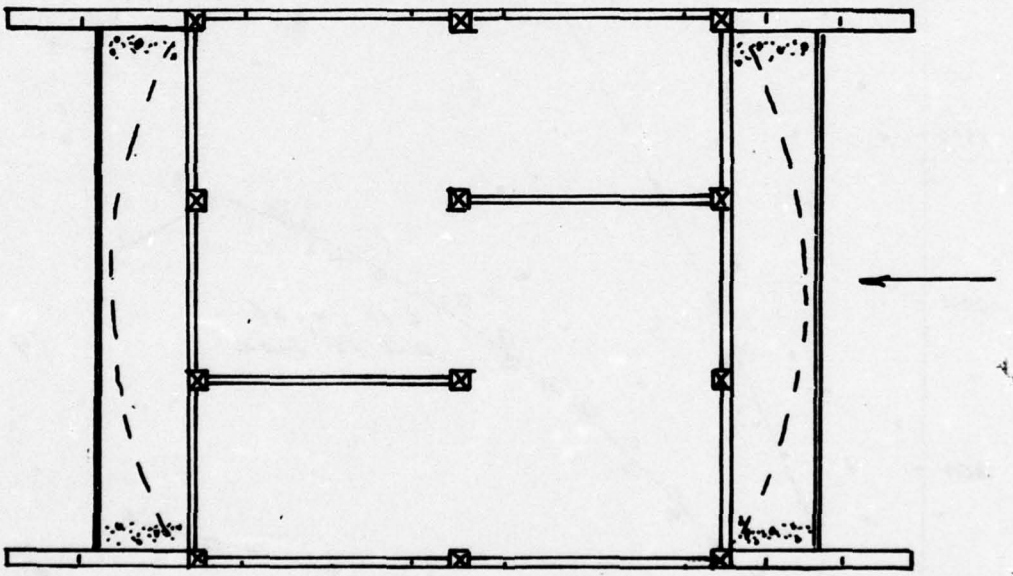


Fig. 16. Experimental Results with Floor Diaphragm Sections.





17. Use of Buttresses to Provide Shear Capacity.

REFERENCES

1. Carney, J.M., "Hurricane Resistant Plywood Construction", American Plywood Association, Tacoma, Washington.

2. Wilton, C., K. Kaplan, B. Gabrielsen, J. Zaccor, "Blast/Fire Interaction, Blast Translation, and Toxic Gases", SSI 742-8, Scientific Service, Inc. Redwood City, California, 1976 (in publication).

3. Meyers, J.A., "Design and Test of a 32-ft Plywood Box Beam", San Jose State University, 1970.

A REPORT ON U.S. COAST GUARD EXPLOSION-SUPPRESSION TESTS

by T. E. Larsen
Detector Electronics Corporation
Minneapolis, Minnesota

Extensive tests were conducted by the U.S. Coast Guard during 1975 in an attempt to find solutions to the control of gas/air ignitions of the type that have resulted in catastrophic fires and explosions aboard sea-going tankers. While it is true that gas ignitions are not ordinarly encountered in munitions production areas, the Coast Guard tests are of interest in that they demonstrate what can be accomplished through the use of very rapid detection and suppression systems. Before proceeding with a description of the Coast Guard tests, it seems advisable to explain the operating principle of UV detectors and to insure that both their limitations and advantages are understood.

In highly hazardous locations, instantaneous response to the presence of fire is essential, and in many cases, sensors responding to ultraviolet radiation are the only reliable means of detecting a fire. This is because UV sensors are not significantly affected by the presence of wind, rain, snow, salt spray, extremes of temperature and extremes of pressure. Using sophisticated processing techniques, it is also possible to produce UV detectors that are solar blind and can be used in direct sunlight. The spectral response of such a detector is illustrated in Figure I.

PRECEDING PAGE BLANK-NOT FILMED

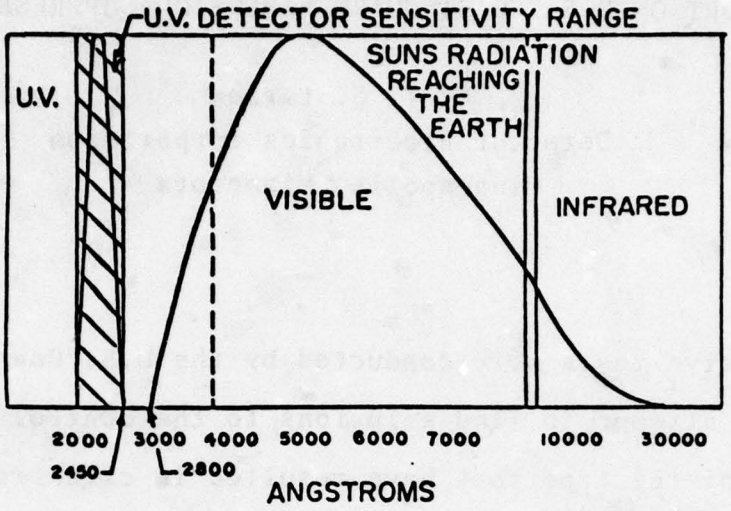


Figure I

Since there is no such thing as a "fire detector" per se, it must be expected that any type of detection equipment will have limitations when applied as a "fire detector." Ultraviolet sensors receive radiation at the speed of light, but they are dependent upon an unobstructed view of the fire. Devices commonly used for fire detection applications consist of Geiger-Mueller tubes mounted with suitable electronic circuitry in an explosion-proof enclosure. A typical UV system is illustrated schematically in Figure II.

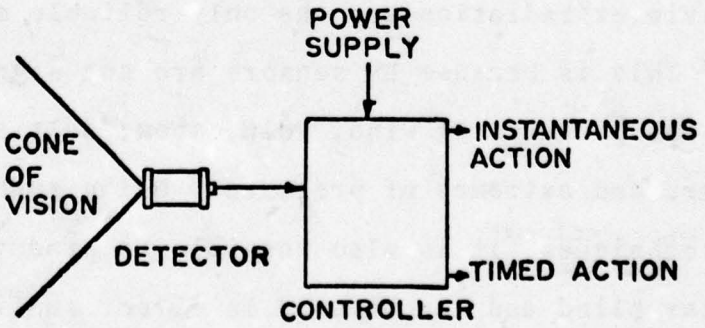


Figure II

As part of the enclosure, a quartz window is included to allow the transmission of ultraviolet radiation from the flame of a fire to the sensitive surfaces of the Geiger-Mueller tube. Should this quartz window become coated with ultraviolet absorbing materials, the radiation from the fire cannot be received by the detector, and a means of testing for this condition is essential.

Over the years, it has been the practice to check the transmission capabilities of UV detector optical surfaces by directing a hand-held radiation source at the detector in order to achieve a response of the total system. Although this testing system is highly reliable when actually performed, it becomes cumbersome when a large number of detectors must be tested under adverse weather conditions.

To overcome this and other problems, a method of testing ultraviolet detectors has been developed, which will reliably measure the radiation transmitting capabilities of the optical system from a remote location, such as a control center. Known as the "optical integrity" or "O_i" feature, it enables one person to check not only the optical surface of a UV detection system, but also the condition of the detectors and their electronic circuitry as well. The same basic O_i system can be incorporated in an automatic, self-checking circuit, thus removing the need for personnel involvement completely. The structure of the O_i detector is illustrated in Figure III.

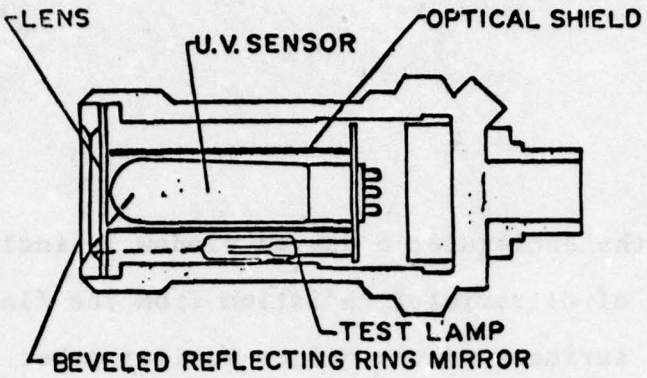


Figure III

The "test lamp" and "UV sensor" are mounted in the same explosion-proof enclosure, but are optically isolated from each other by the "optical shield." The only path by which radiation from the test lamp can reach the sensor is to pass out through the lens, reflect off the "mirror" and back through the lens as illustrated.

Recent tests conducted in cooperation with the U.S. Coast Guard demonstrate the extraordinary capability of UV detectors used with fast acting suppression systems. UV detectors were used to respond to propane/air ignitions in the pump room of a tanker, and the detectors were connected to actuate a suppression system, consisting of either Halon cylinders or dry chemical "cannons," illustrated in Figure IV.

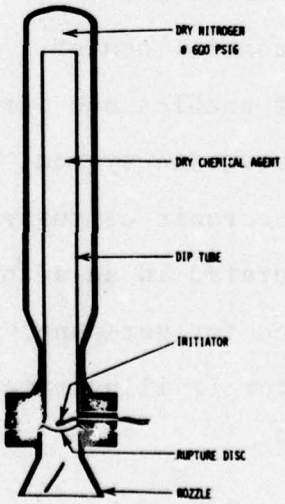


Figure IV - Cutaway view of Detector Electronics dry chemical cannon.

In all tests, the response time of the detectors to the presence of the propane fireball was between 18 and 25 milliseconds, and in each test shot, all detectors responded to the ignition. The dry chemical extinguishing agent successfully suppressed the explosions at an application density of 0.009 pound/cubic foot. While threshold application densities for all agents could not be determined from the tests, the data suggest that the following minimum application densities would provide sufficient suppression to limit the pressure rise to less than 1 psig.

	Minimum Application Density lb./cu.ft.
Water	0.15++
Purple K	0.007
Halon 1211	0.06+
Halon 1301	0.05+
Halon 2402	0.12+

What has been proven by these tests is that UV equipment is capable of detecting an ignition in propane/air atmospheres, and of transmitting a signal to release suppression agents in a very short period of time.

The speed of response of UV detection systems has also been proven during tests conducted for the U.S. Bureau of Mines. In these tests, methane/air ignitions in a simulated coal mine tunnel were effectively controlled by the use of UV detectors releasing dry chemical agent from "cannons" similar to those used in the Coast Guard tests.

The most serious problem that could develop within a UV detection system is one that would render the detectors insensitive to the presence of a developing fire or explosion. With the development of the "optical integrity" system it is now possible to determine from a remote control station whether or not the detectors' optical surfaces are capable of transmitting the radiation from a fire and if the detectors are functional. Another consideration in the application of UV detectors is the fact that dense accumulations of smoke may absorb or block the transmission of ultraviolet radiation from the fire to the detector. A simple extension of this "optical integrity" feature has been proven experimentally to allow also for the detection of such accumulations of smoke. The principle of operation is illustrated in Figure V.

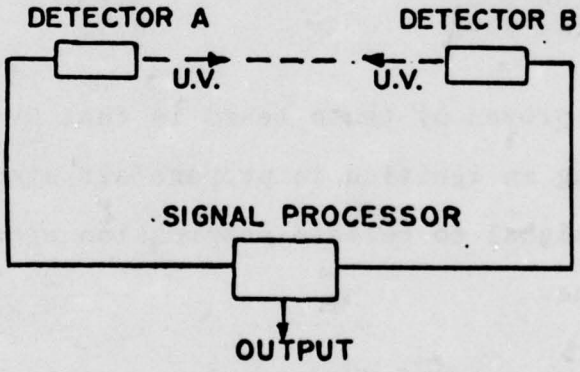


Figure V

Detectors A and B operate alternately, each one checking its own optical surfaces and transmitting a small UV signal to the other. Any contamination of the optical surfaces results in appropriate reset action in the Signal Processor. Thus, any reduction

in the net signal received by the detectors can be properly interpreted as due to UV absorbing materials coming between the detectors, such as would occur with the presence of smoke.

It must be noted that UV detectors will respond to any source of ultraviolet radiation that falls within their spectral response range. A source of intense radiation in the UV spectrum that can cause undesired detector response is that from electric are welding. The effects of arc welders on UV systems can be minimized by careful positioning of detectors and by insuring that welding operations are not carried out in areas where either direct or reflected radiation can reach the UV detection system, even from a distant source.

UV detection equipment has been proven to provide the rapid response to fire that is essential in highly hazardous areas, and such detectors are widely applied in munitions production. The limitations of UV detectors, which have been evidenced in the past, are being or have been reduced to the point that detectors equipped with proper discriminating features and circuitry are both reliable and virtually free of false discharge problems.

A WATER DELUGE FIRE SUPPRESSION SYSTEM FOR CONVEYOR LINES TRANSPORTING HIGH EXPLOSIVES

William H. McLain and Alex Wenzel
Southwest Research Institute, San Antonio, Texas

William O. Seals and Richard Rindner
Picatinny Arsenal, Dover, New Jersey

ABSTRACT

A program was conducted to design and demonstrate a rapid-response water deluge system for application to conveyor lines transporting high explosives. A prototype water deluge system was demonstrated capable of extinguishing fires that develop in 60-lb boxes of bulk Composition-B after a 60-lb detonation.

Using commercially available components a full-scale prototype water deluge system was designed and tested. The basic elements of the system include: (1) a UV detector and logic module, (2) piping, (3) straight stream water nozzles, and (4) a valving system. To provide protection from an initial 60-lb blast the water supply lines were buried in the ground adjacent to the simulated conveyor line. Water spray nozzles were installed just above ground level to maximize survivability. Narrow stream nozzles were used with each nozzle protecting an area approximately 3 ft wide by 15 to 45 ft long from the nozzle. The sprays were directed upwards to a height of 7 ft. The time required by the UV detector to respond to an HE detonation was less than 5 ms.

A series of qualification tests were performed to provide data on the statistical reliability of the overall system. The qualification tests were divided into two series of three tests in which all test variables were maintained constant with the exception of the water valving. Three qualification tests were made using a fast-response explosively-actuated valve. Three qualification tests were made using a conventional solenoid valve. All tests were successful. No major blast damage was sustained by the prototype demonstration under full-scale test conditions.

Based on this program a water deluge fire protection system using an unconventional design has been designed and developed. The system is economical and can survive the blast loading and shrapnel produced in a 60-lb HE blast. The system can extinguish fires in 60-lb boxes of flake Composition-B following a 60-lb HE explosion.

PRECEDING PAGE BLANK-NOT FILMED

INTRODUCTION

Bulk high explosives are moved from receiving magazines to the processing areas either on continuous belt conveyors or on overhead suspension carriers. While in transit these materials pose a significant hazard potential resulting from unwanted fires or explosions. In the past, plant designers have not provided fire protection systems along conveyor lines, partly because of installation cost and partly because of the assumption that adequate protection was maintained by using noncombustible building materials and safe separation distances. Unfortunately, not all munition plants are in fact constructed using noncombustible materials and a fire could propagate along the line into the processing area either via burning firebrands ejected from the explosion or by propagation along structures housing the conveyor line. The problem is further complicated by operating procedures for fire service personnel in fighting a fire involving high explosives. Such personnel are normally instructed not to operate in the immediate fire area because of the possibility of personnel injury.

Since these problems will continue to exist there is a need to develop a rapid-response fire protection system in order to isolate the fire and prevent further damage. It is necessary that such a system function following detonation of a 60-lb box of flake explosive.

The design of any fire protection system involves the following general considerations: (1) selection of a detection system, (2) choosing the best extinguishing agent, (3) determining proper extinguishing agent application rates, and (4) providing a delivery system which can assure extinguishment. For practical reasons additional factors which must be considered are cost, reliability, maintenance, freedom from false alarms, and response-time. Because of the specialized nature of the problem incurred in fires involving explosives, standard fire protection engineering practices designed for industrial plants either limit the choices available to the plant designer or do not apply.

A program of work was conducted to define the problem and to develop alternative solutions for these specialized fire protection engineering problems. The program emphasized the use of off-the-shelf fire protection hardware and equipment and was limited to the problem of fire suppression along conveyor lines transporting 60-lb boxes of high explosive from the plant unloading dock to the first plant processing area.

DESIGN CONCEPTS

The major problem was to provide both a rapid-response and adequate protection for water supply lines and nozzles from blast and fragment damage. A number of novel design concepts were employed to solve this problem.

To provide protection to water supply lines and nozzles, the water supply lines were buried in the ground and the nozzles were located close to floor level. This configuration provided maximum protection from blast effects and fragmentation damage.

As a result of locating the water supply system at this level, it was necessary to direct the water flow upward into the conveyor line housing structure rather than downward onto the area to be protected. For this purpose straight stream 0-deg nozzles were used. When these nozzles were directed upward to a maximum height of about 7-1/2 ft of stream elevation, the water pattern covered an area approximately 3-4 ft wide starting at 15-20 ft and extending to 40-45 ft from the nozzle. A major advantage of this system is that the nozzles are located at some considerable distance from the explosion.

This placement of nozzles resulted in a highly complex interlaced flow pattern. By adjusting pressures and elevations a water application rate of 0.7 to 0.5 gal/ft^2/min could be developed. An attempt was made to precalculate the elevation and azimuth angles but experience indicated it was preferable to experimentally test the system on site and adjust as necessary.

Initial program efforts evaluated the feasibility of developing steel armor for the nozzle assemblies. However, based on experimental results, these efforts were abandoned in favor of the more effective usage of heavy brass or steel straight-stream nozzles. Because of the low profile resulting from this ground location near the floor surface and because a right circular cylinder is one of the best shapes to reduce aerodynamic blast loading, armor for the water supply lines and the nozzles was unnecessary. During the tests no damage was sustained by impact of fragments into the metal water supply lines.

A second major problem was to develop a rapid-response detector system. The basic criteria used was that the detector unit must be able to detect an explosion and initiate water-deluge action prior to the time-of-arrival of a blast wave when located at a distance of 50 ft from the explosion center. In addition the detector must be sensitive to both fire and explosion. To accomplish this, a fast-response UV detector unit was installed. Modifications were made to reduce the delay circuits to provide 6-7 ms response time. Calculations indicate that this response time is on the order of the time required for the blast wave to travel 25 ft or half the distance specified above.

To provide rapid-response water deluge action, an explosive valve was used. This valve consisted of a scored aluminum diaphragm and dual detonator. The response time of the valve was on the order of 10 ms. However, the water delivery time to the explosion site was much longer because of the travel required for water sprays from the nozzles.

A second valve system was also evaluated. This valve used a standard off-the-shelf 3-in. solenoid valve. Although the estimated valve opening time is 3-5 seconds it was determined that this provided adequate protection for this application.

Specific design criteria on the system are outlined below.

- Detector Response Time . . . . 10 ms
- Valve Actuation Time . . . . 20 ms
- Exposed Waterline Shielding. . . . 1/2-oz Fragments Traveling at 1500 ft/sec
- Lowest Temperature . . . . -30°F
- Water Application Rate . . . . 0.5 gal./ft^2/min
- Component Availability . . . . Off-the-Shelf Hardware

The combination of rapid-response detectors, blast shielding of the waterlines by ground burial, and the use of an upward projected fire stream provided a highly cost-effective water deluge system. Although highly unconventional, this system was most effective. To make the system more cost effective a materials study was conducted with the result that heavy wall steel pipe initially specified and tested was replaced with standard schedule 40 steel pipe. Qualification tests were conducted with the steel schedule 40 pipe. A parallel study was conducted using PVC pipe. No effects of blast damage were observed in the main PVC pipes that were buried.

PROTOTYPE DEMONSTRATION TESTS

Two series of full-scale qualification tests were conducted to demonstrate the reliability of the water deluge design concepts under simulated large-scale field conditions. On the first series a rapid-response burst disk water valve was used. On the second series a standard 3-in. solenoid valve was used. All demonstration tests were conducted in a facility designed to simulate a full-scale conveyor system including associated housing structures. The results of these tests demonstrated that the design concepts used in this water deluge system can be applied to both present and future munitions plant modernization programs.

A. Test Facility

A schematic diagram of the overall test area is shown in Figure 1 together with an insert showing the simulated conveyor line. The test facility consisted of a concrete floor, a housing canopy (Figures 2 and 3), a series of fast-response fire detectors (Figure 8), a water supply system, a fast actuating blast valve (Figure 9). A 60-lb box of Composition-B was used as a donor, with a second 60-lb box as an acceptor. Instrumentation, observers and camera stations were located 450 ft from the test site. During preliminary testing a second camera station was located 325 ft from the test site to provide side-on viewing. During demonstration tests the number 2 camera station was relocated as indicated. Water was supplied from a reservoir using a rated 350-gpm pumper truck. Hose lines from the truck were attached to the steel pipe system approximately 20 ft from the end of the concrete test pad.

The simulated conveyor line consisted of a concrete paved surface 100 ft in length and 12-ft wide. The concrete was heavily reinforced to sustain multiple blast loadings. A combination of 2-1/2 and 3-in. steel pipe water supply lines were fabricated from schedule 40 steel. All unions and elbows were steel. A second dummy 3-in. PVC water system was fabricated and run parallel to the steel lines.

Straight stream nozzles were used to provide a complex interlaced cross-stream water deluge for extinguishment action. The nozzles were placed on uprisers at a spacing interval of 12 ft on alternate sides of the concrete floor. On each side the spacing was 25 ft. The nozzles were located at an elevation of approximately 1 ft above the surface of the concrete floor. Two nozzles were implaced on each upriser. During prototype demonstration tests, nine nozzles were used which provided full coverage for the area under the canopy.

High-speed motion picture photography was used to document blast wave effects and water deluge action during the blast survival tests. Two dual beam oscilloscopes recorded four channels of high-speed data.

For each test two detectors were used, one located at the edge of the 100 ft concrete test pad (50 ft from the explosion), the second located 25 ft from the first detector (75 ft from the explosion). In the first detector station, two detectors were used; (1) a standard detector, and (2) a modified detector system. The standard detector used commercially available UV sensor and housing assembly. The second detector used an aluminum parabolic mirror to focus UV radiation emitted from the explosion onto the end of the detector tube.

B. Test Results

A series of six qualification tests were conducted. Three tests were conducted to qualify the fast-response burst disk valve. Three tests were conducted to qualify the standard 3-in. solenoid water valve. The first series of tests were conducted inside a 24 ft section of a simulated conveyor housing. The second series of tests did not have a canopy housing. Additional tests were conducted to demonstrate the capability of the water deluge system to extinguish a "worst case" fire after a 60-lb HE explosion. All tests were successful.

The test results are best summarized by reference to Figures 1-12. Essentially similar results were obtained for all tests. Exterior and interior views of the simulated conveyor line are shown in Figure 2. The conveyor housing was of wood construction and had a nonfire retardant fiberglass exterior. Details of construction of the interior are shown in Figure 2. This construction represented a worst case housing structure in terms of flammability.

The placement of acceptor and donor boxes is shown in Figure 3b. Steel rollers were placed under the donor box. Extensive fragmentation of the rollers occurred and shrapnel was found up to 500 ft from the explosion center. Typical water sprays before each test are shown in Figure 3a.

A view of the actual blast during the first qualification test is shown in Figure 4. As can be seen, extensive destruction of the housing structure is in process.

Water deluge action after the first qualification test is shown in Figure 5. The complex interlaced water pattern can be clearly seen in these views. In this test the water deluge action was effective several seconds after the blast, the delay being caused by the time required for water stream travel. Water flows were adjusted by running the pumper fire truck at its maximum rate of 350 gpm which resulted in a delivered water pressure at 20 ft downstream of the valve of about 70 psig.

As anticipated, extensive damage was sustained by the housing structure (Figure 6). Damage to the nozzle assembly 4.5 ft from the explosion center is

shown in Figure 6a. This damage consisted of a translation of the upriser holding two spray nozzles about 30 deg from the vertical for the steel pipe. The results of this translation was a reduction of about one third in the water application rate to two areas 20-40 ft from the explosion. The immediate area in the vicinity of the explosion is still protected. With the exception of the single upriser 4.5 ft from the explosion, all other nozzles were fully effective, clearly demonstrating the effectiveness of the design concept.

Overall views of the test (Figure 7) clearly show the extensive damage to the building structure together with the damage sustained by the PVC upriser pipe. No damage to the PVC lines that were below the ground was observed.

During the test series, standard off-the-shelf UV detectors were used. These detectors were housed in an industrial "explosion proof" box. No damage was sustained by these detectors, although it is highly probable that fragments could destroy the unit. The reason this did not occur was the low cross section of the unit which is a statistical problem. However, as noted previously, the system was designed so that it would provide an alarm signal before the arrival of blast or fragments. A second detector unit was also investigated. The second unit consisted of a parabolic aluminum reflector to concentrate the UV emission from the fire/explosion zone. The sensitivity of this detector at 50 ft was 50-100 percent greater than the off-the-shelf hardware. Damage to the reflector unit is shown in Figure 8b.

A fast-response rupture disk valve and assembly is shown in Figures 9 and 10. This valve functioned effectively throughout both qualification test series. The system used a dual detonator connected in parallel to the detector system. In the preliminary tests, a failure occurred when a single detonator failed. Based on this failure, a dual detonator is required to provide a reliable system.

After the water deluge system was subjected to a series of 60-lb HE tests, one test was conducted to determine the capability of the system to extinguish a large fire after damage indicated earlier has been sustained. For this purpose, a fire test was conducted in which the fire detection system was deactivated. Fire was set to about 25 lbs of Composition-B scattered on a combustible table. After the fire had become fully involved, extinguishment action was initiated. The extinguishment action was successful (Figures 11 and 12).

SUMMARY AND CONCLUSIONS

- A prototype water deluge system capable of withstanding blast effects from a 60-lb HE charge has been designed and demonstrated.

- Test results have demonstrated the effectiveness of a number of unconventional design concepts which include:

  - use of a floor mounted overlapping water spray system
  - removal of the spray nozzles from the immediate blast area
  - use of rupture disk valves to initiate rapid-response water flow from the water deluge system.

- The UV detector selected can detect both fire and explosion. The response of a detector unit located 50 feet from an explosion is rapid relative to the blast wave velocities.

- The placement of water supply lines below ground level rather than overhead provides a highly cost effective method for protecting the water deluge system from large-scale blast effects.

- Standard construction components such as schedule 40 steel pipe and solenoid valves can be used.

- In principle, the system developed can provide cost effective fire protection to a wide range of special hazard areas found in munition plants.

ACKNOWLEDGEMENTS

The authors wish to acknowledge the following SwRI staff members for their contributions:

- Messrs. Lester Eggleston, George Commerford, and J. William Gehring, Jr., for their technical assistance.

- Messrs. Marvin Rumbaugh, Ernest Garcia, Jr., A.C. Garcia, Robert Marin, Dennis Scheidt, and John Weschler for implementing the field experiments.

The cooperation of these individuals and others is greatly appreciated.

The work reported was supported under U.S. Army Contract Nos. DAAA21-74-C-319 and DAAA21-75-C-0324 with Picatinny Arsenal.

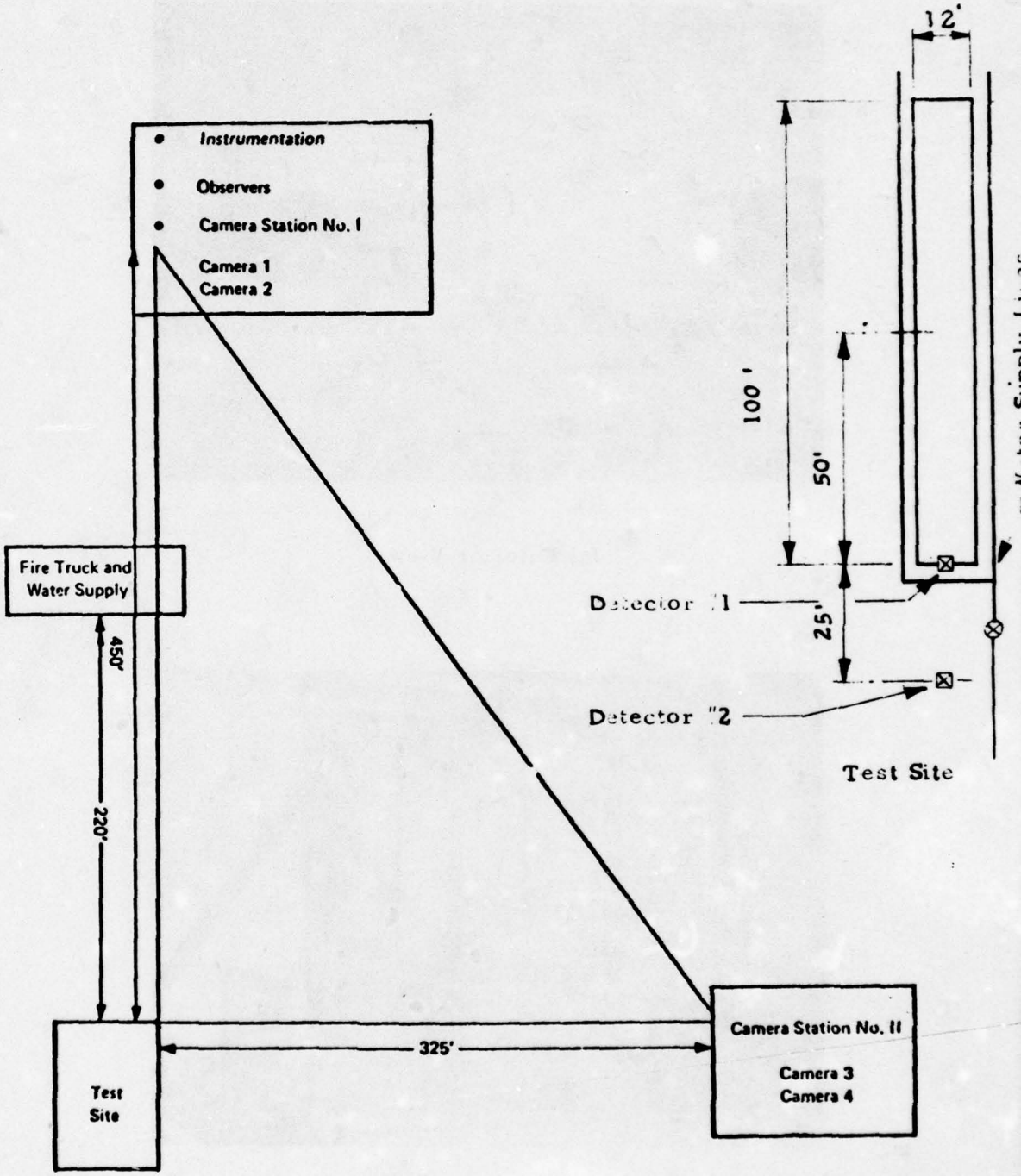
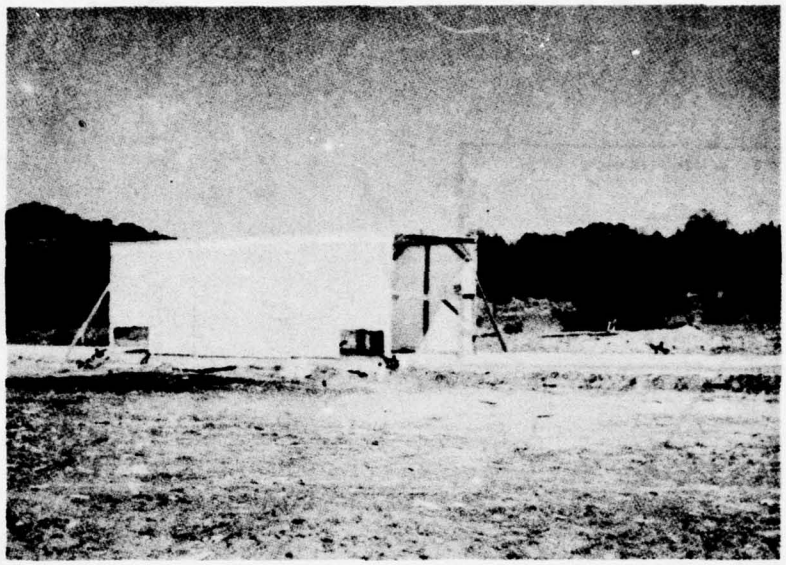
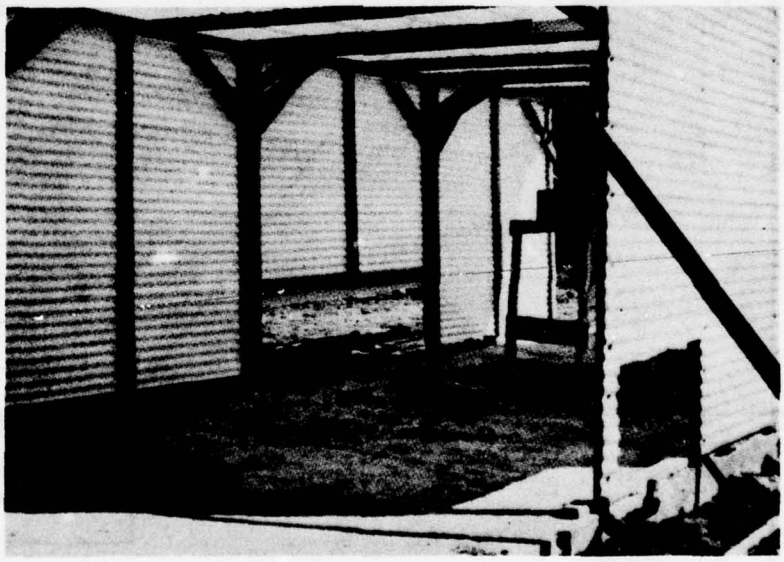


FIGURE 1. SCHEMATIC DIAGRAM OF TEST SITE

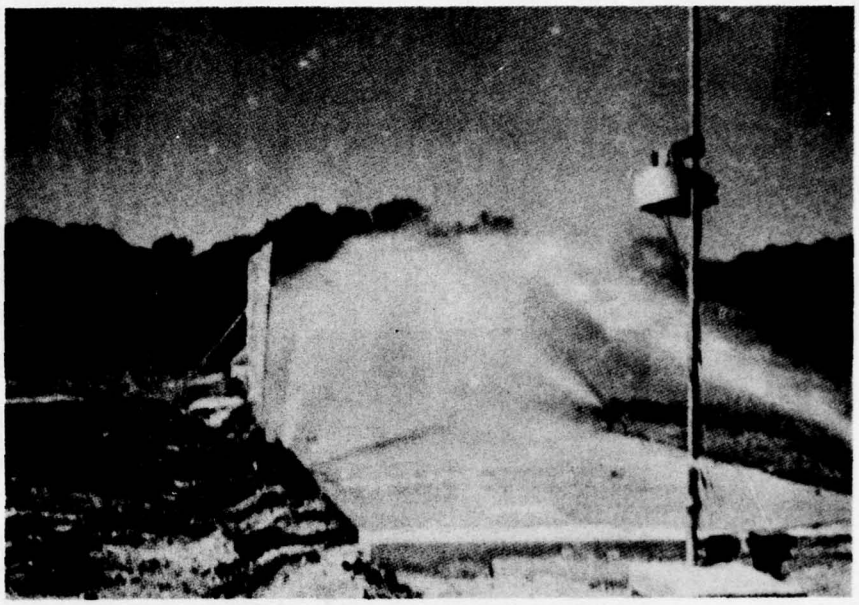


(a) Exterior View

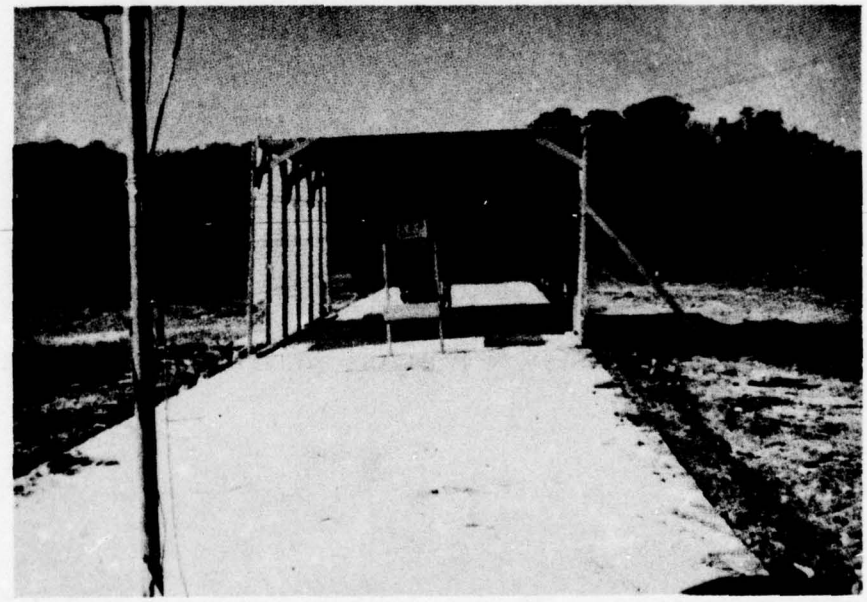


(b) Interior View

FIGURE 2. EXTERIOR AND INTERIOR VIEWS OF SIMULATED CONVEYOR LINE



(a) Water Spray and Station 1 Detector Assembly



(b) End View With Acceptor and Donor H. E. Boxes

FIGURE 3. END VIEWS OF SIMULATED CONVEYOR LINE

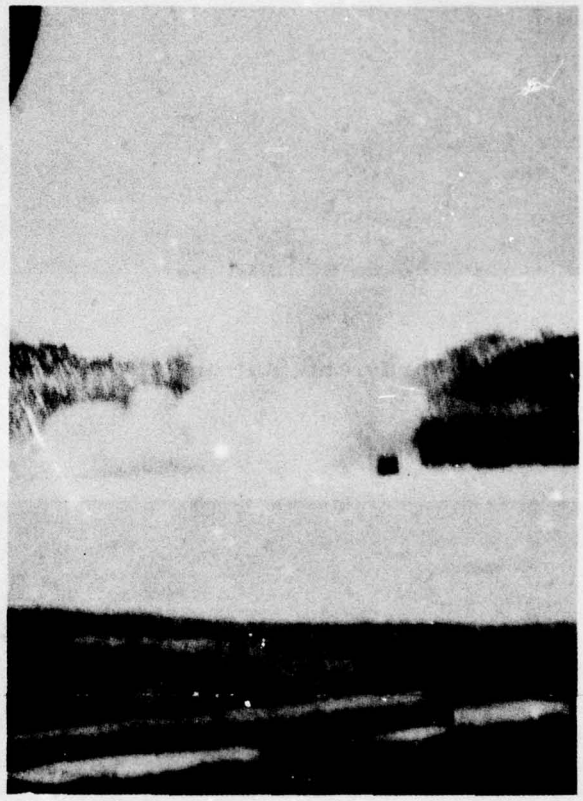


FIGURE 4. 60-lb COMPOSITION-B BLAST WITH SIMULATED CONVEYOR LINE

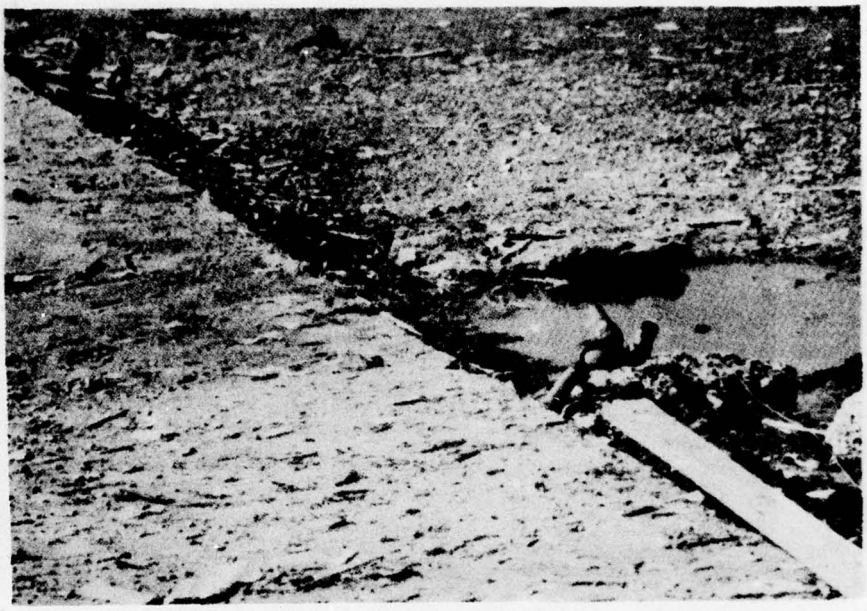


(a) End View

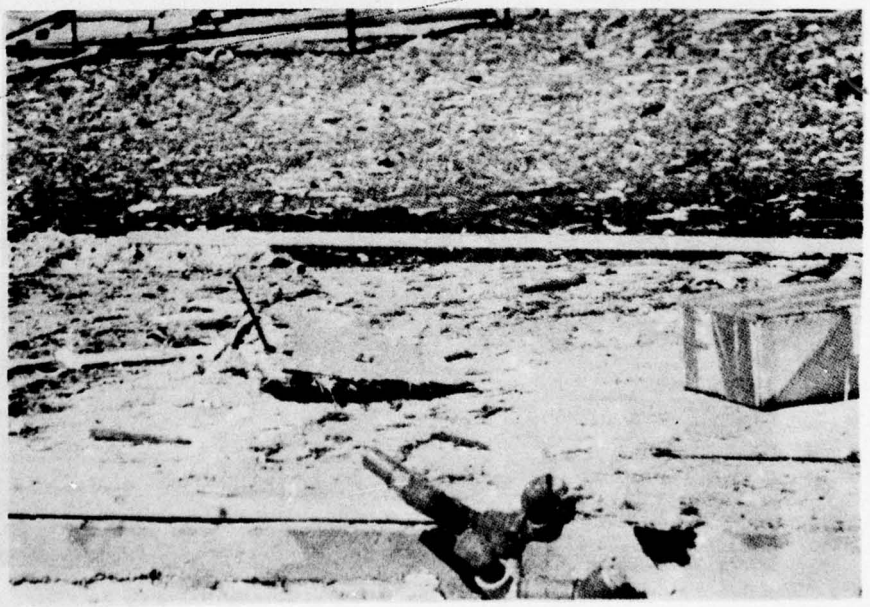


(b) Side View

'IGURE 5. WATER DELUGE ACTION AFTER 60-lb COMPOSITION-B BLAST

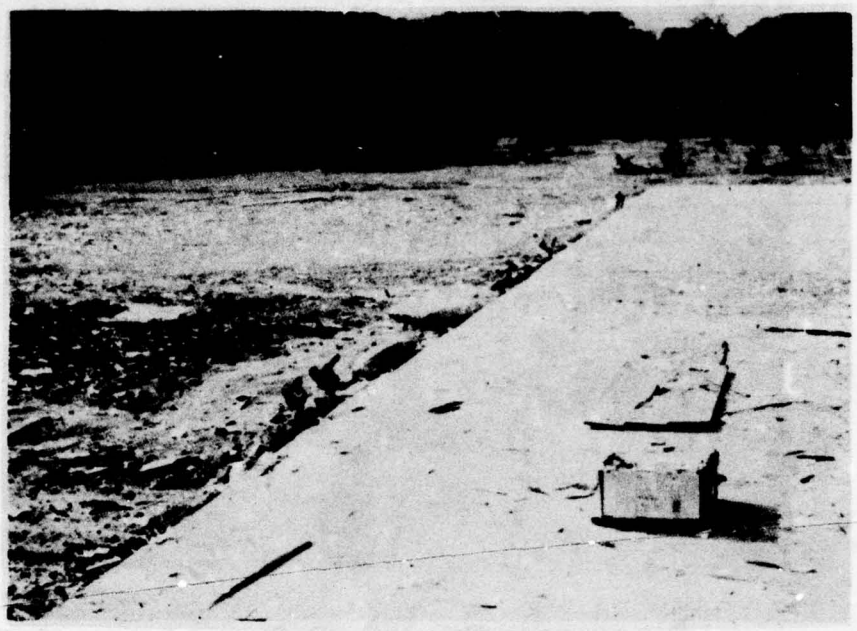


(a) Damage to Nozzle Assembly - 4.5 ft From Explosion Center

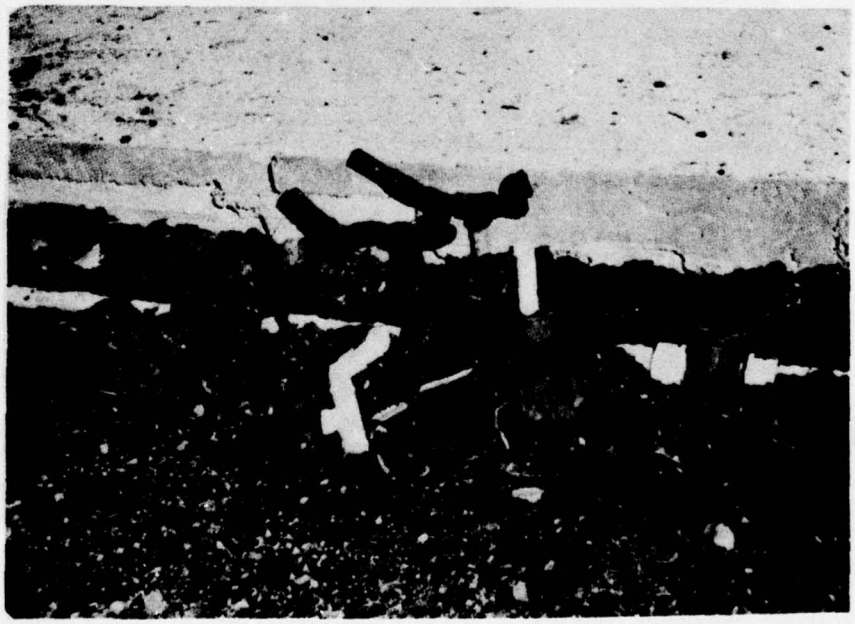


(b) Undamaged Nozzle Assembly

FIGURE 6. DAMAGE AFTER 60-lb COMPOSITION-B BLAST

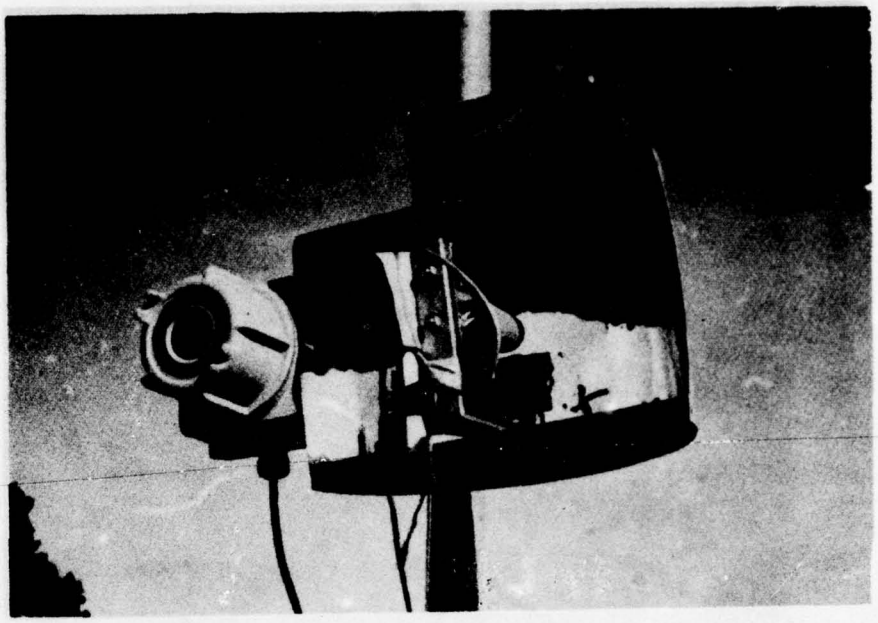


(a) Acceptor Box

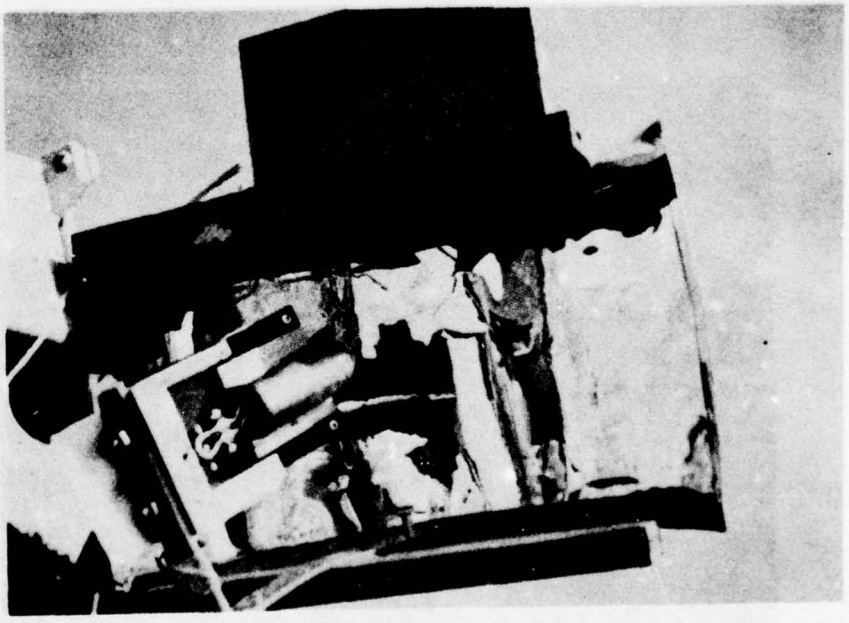


(b) Shear Damage to PVC Piping

FIGURE 7. AFTER BLAST

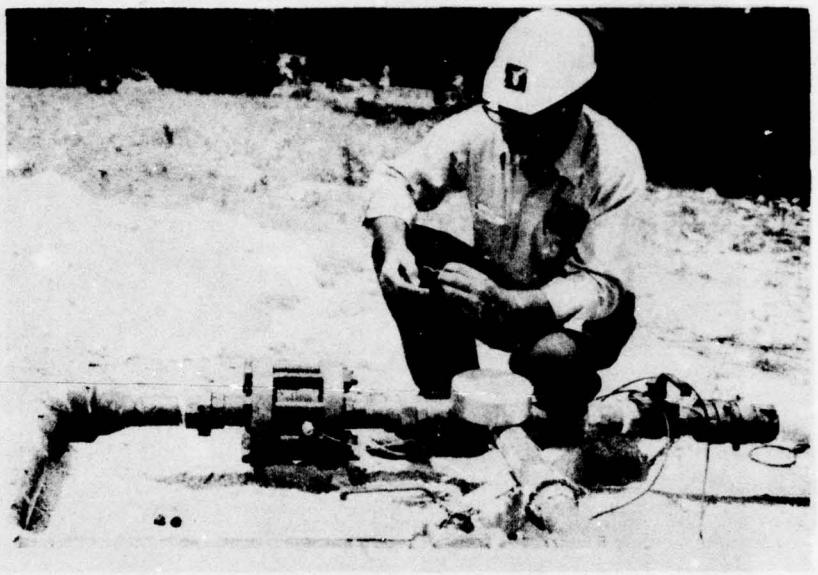


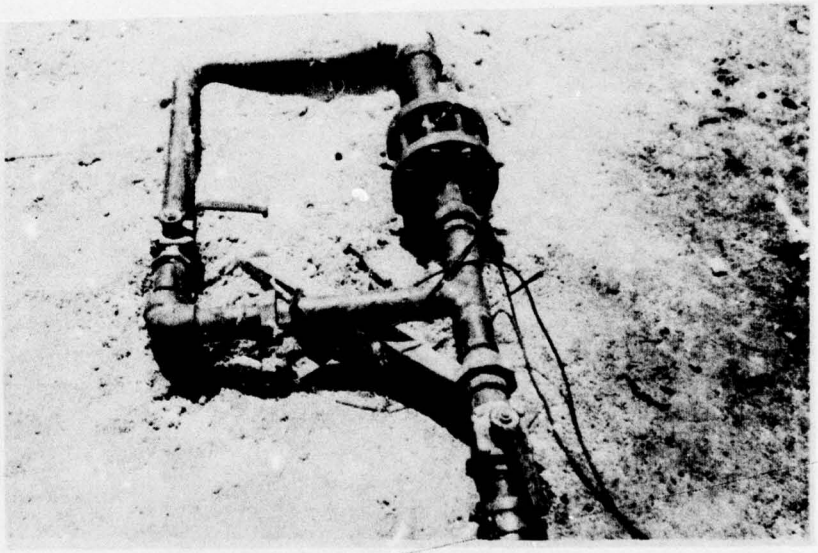
(a) Standard and Parabolic Reflector Before Test



(b) Damage to Parabolic Relector After Test

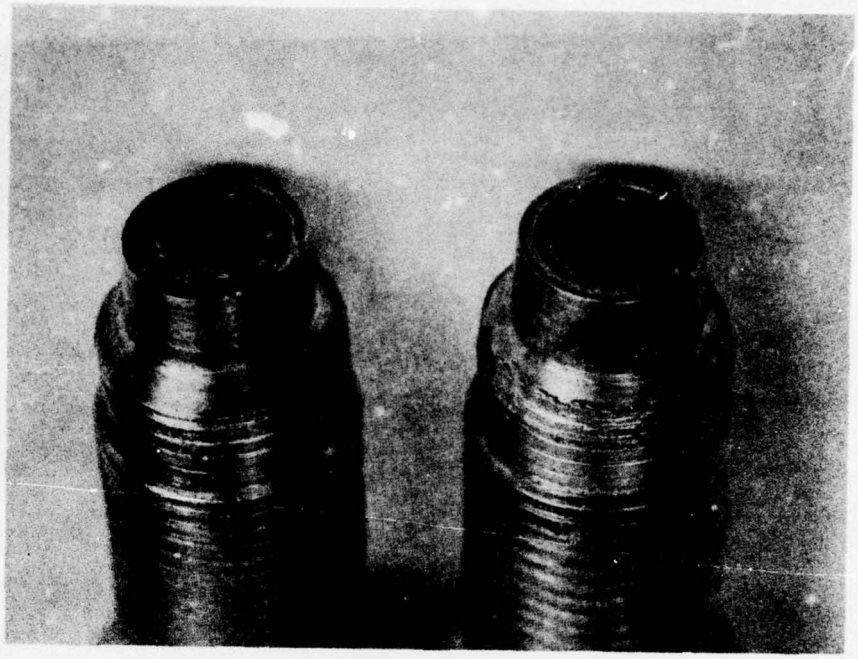
FIGURE 8. DETECTOR ASSEMBLY





(b) End View

FIGURE 9. RUPTURE DISK VALVE AND BYPASS VALVE FLOW LOOP

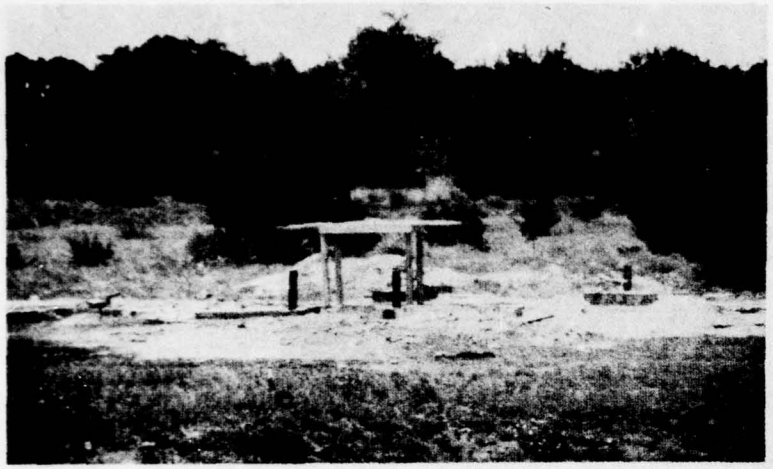


(a) Detonators After Operation

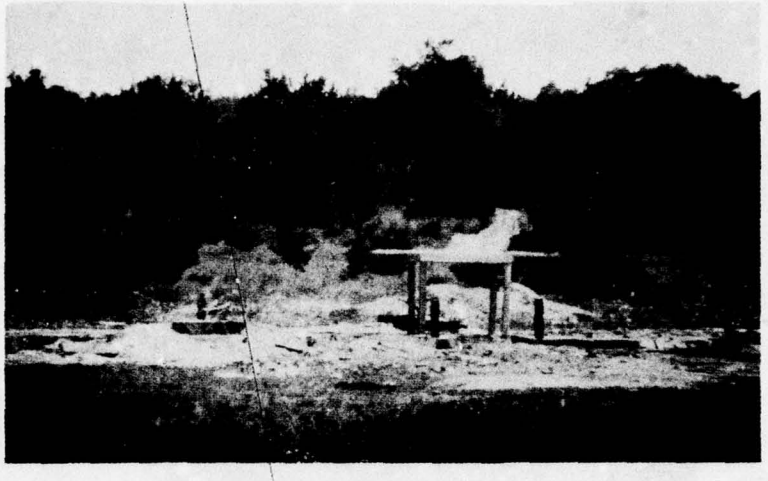


(b) After Operation

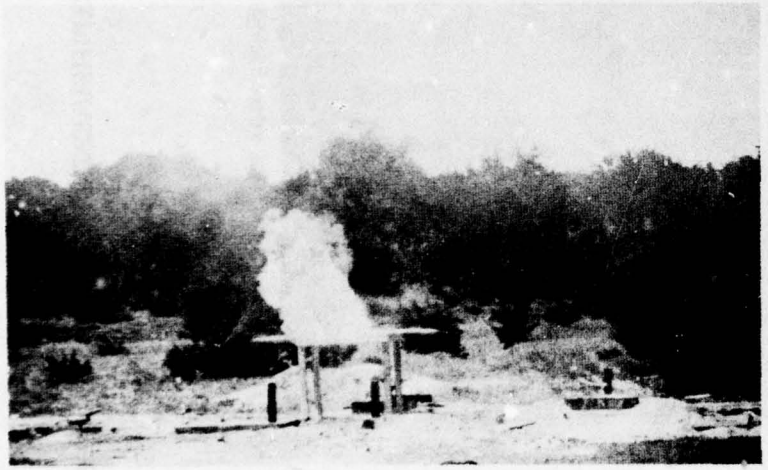
FIGURE 10. RUPTURE DISK VALVE



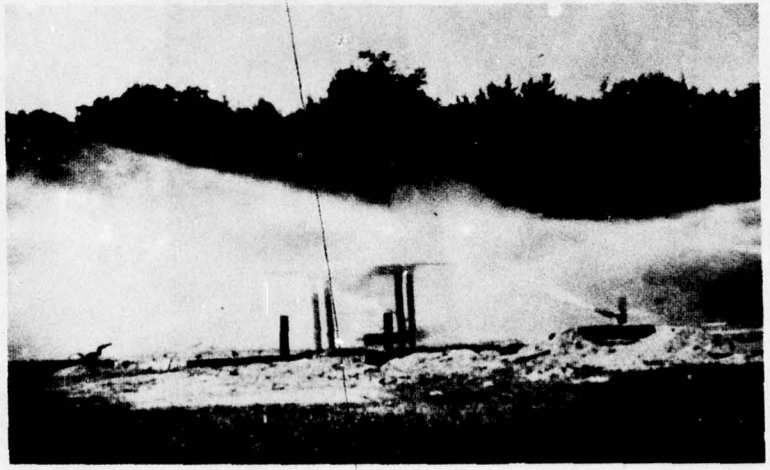
(a) Ignition



(b) Flame Spread



(c) Fire

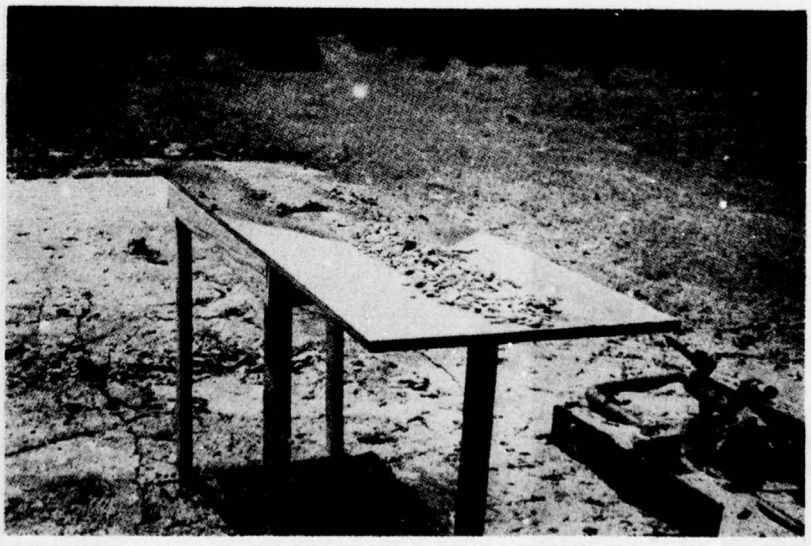


(d) Water Deluge Action

FIGURE 11. FIRE EXTINGUISHMENT FOR COMPOSITION-B AFTER 60-lb H. E. BLAST SURVIVAL TEST



(a) Before Extinguishment Action



(b) After Extinguishment Action

FIGURE 12. FIRE EXTINGUISHMENT TEST FOR COMPOSITION-B

DYNAMIC PROCESSES IMPORTANT TO THE SUPPRESSION OF PROPELLANTS AND EXPLOSIVES BY WATER DELUGE ACTION

William H. McLain
Southwest Research Institute, San Antonio, Texas

ABSTRACT

Dynamic processes important to the suppression of explosive and propellant fires by water deluge action are analyzed. Two types of fires are considered, RDX explosive fires and gun propellant fires. The description of these processes require a characterization of the nature of the fire threat and a determination of the fluid mechanical processes that are important to the delivery of water to a burning fuel bed. The characterization of the fire threat includes a description of its mass burning rate and plume characteristics. The characterization of the delivery system includes a description of the droplet size distributions for water spray nozzles and a method to calculate the rate of vaporization of water droplets with a fire plume. The relationship between these important fire and fluid mechanical factors is discussed in terms of the development of practical fire protection systems.

INTRODUCTION

Fire protection is an important consideration in the design of a modern munitions production facility. A number of special problems arise in plant areas processing explosives and propellants. In the past, the fire protection engineer has solved these problems by providing a water deluge extinguishment system designed in accordance with national concensus fire code standards. Such standards require the application of 0.25 to 0.30 gal./ft^2/min in hazardous industrial areas. These standards are based on general industrial plant experience and it is not obvious that they are adequate to meet the specialized fire threat present in a modern munitions production facility. Experimental data are not available to aid in the development of proper design criteria for RDX and gunpowder fires. However, in the absence of such direct experimental data it is possible to estimate the necessary water application rates using a theoretical engineering analysis. Such an analysis requires a description of the nature of the fire threat and the dynamic processes important in the penetration of a water stream through a fire plume. Some of the fire and fluid mechanical processes that must be considered are outlined.

THE FIRE THREAT

There are major differences in the nature of the fire threat posed by the deflagration of a box of flake high explosive and the threat posed by a gun propellant fire. These differences are the result of widely differing mass burning rates. For gun propellants, mass burning rates have been observed that are in excess of 10 lb/sec/ft^2 for a 9-ft^2 fire. For a bed of flake Composition-B explosive, the mass burning rate is estimated to be less than 0.5 lb/sec/ft^2.

The Composition-B high explosive fire is characterized as a liquid pool fire. It is difficult to ignite the fuel surface and once ignited the rate of flame spread across the surface is slow. The fire produces a heavy black smoke and the fire plume is relatively short and not well defined.

The gun propellant fire is a fire in which the chemical reaction zone is either on or very close to the solid fuel surface. The material is easily ignited and once ignited the rate of flame spread across the surface is very high. The fire is very intense. The fire plume is large and well defined, and, for a base fire size of 9 ft^2, the plume may reach heights up to 60 ft within 2-3 seconds.

Benreuven, et. al., have recently investigated the burning mechanism for the thermoplastic explosive RDX which is a major component of Composition-B. The mechanism proposed involves an initial pyrolysis to form the following products:

$$\begin{aligned} RDX \rightarrow\ & 1.25N_2 + 1.05N_2O + 0.51NO + 0.34NH_3 \\ & + 0.72CO_2 + 0.36CO + 1.04CH_2O \\ & + 0.37HCOOH + H_2O + (<0.1)H_2 \\ & + (<0.1)HOCH_2NHCHO \end{aligned} \quad (1)$$

The rate of reaction for RDX formulated in terms of an Arrhenius rate equation is:

$$k_{RDX} = 3 \times 10^{18} e^{\frac{-47.5}{RT}} (sec^{-1}) \quad (2)$$

Based on these products and this assignment of kinetic rates it can be concluded that the deflagration of RDX is very sensitive to the enthalpy of vaporization, the rate of vaporization of the fuel and the temperature. Assuming the model is correct, it is possible to estimate the effect of liquid water cooling on the burning rate. Also, it is possible to estimate the plume height and localized combustion gas-flow velocities providing burning rate data are available. Because of the high melting temperature of the thermoplastic explosive, it would be predicted that only a small amount of water delivered to the deflagrating surface would be required for extinguishment.

Two theoretical models can be used to describe the rate of fire spread in a liquid pool fire. One assumes that buoyancy forces dominate the heat transfer mechanism. For this model the flame spread rate (V) is given by:

$$V = \frac{(g)(h_\ell^3)}{\mu_\ell \ell}\left(\frac{d\rho_\ell}{dT}\right)(T_i - T_o) \quad (3)$$

The second model assumes that the horizontal rate of flame spread is dominated by the surface tension effects. For a shallow pool or thin film (Figure 1) the rate of flame spread is given by:

$$V = \sigma' h_\ell / \mu_\ell \quad (4)$$

where

$$\sigma' = \frac{\partial \sigma}{\partial T}\left(\frac{T_i - T_o}{\ell}\right) \quad (5)$$

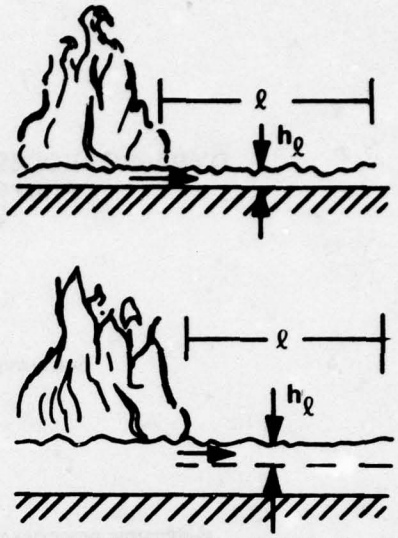


FIGURE 1. THERMOPLASTIC EXPLOSIVES–SHALLOW POOL MODEL

For a deep pool (Figure 2) the rate of flame spread is given by:

$$V = (\sigma')^{2/3} \left(\frac{\ell}{\mu_\ell \ell}\right)^{1/3} \quad (6)$$

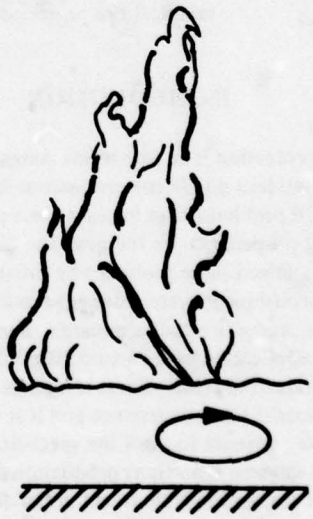


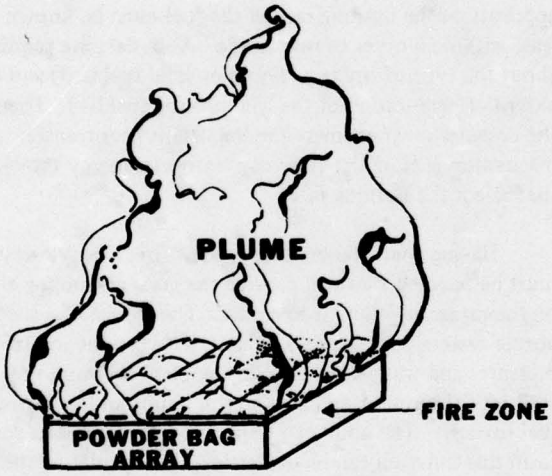
FIGURE 2. THERMOPLASTIC EXPLOSIVES–DEEP POOL MODEL

To extinguish a fire it is necessary to have conditions such that the rate of flame spread is negative. Using the above models the material properties of the propellant or explosive can be related to the relative difficulty of extinguishment. For example, the higher the surface tension of the liquid melt the less water would be required for extinguishment.

For gun propellants, in the absence of experimental kinetic rate data, rate estimates can be made for ambient pressure conditions by assuming that the burning rate is an exponentiation function of the combustion pressure. Kinetic rate data which are available from high pressure deflagration studies can then be used to estimate deflagration rates at ambient pressure conditions found in a munitions production facility.

In formulating an expression for the burning rate it is also necessary to use a model which can describe flame spread through porous fuel beds. An array of powder bags (Figure 3) corresponds to a porous fuel bed. For such a model the rate of flame spread is given by:

$$V = q^2/(\Delta h^2 \rho_s^2 \sigma^2 \kappa^2 \ell \lambda_s/\rho_s c) \qquad (7)$$



POWDER BAG PROPELLANTS

- THICK FIRE ZONE
- SOLID PHASE REACTIONS
- RADIANT AND CONVECTIVE HEAT TRANSFER FROM BURNING BED

FIGURE 3. POWDER BAG PROPELLANTS

Again, this formulation can be used to predict the relative fire threat posed by different types of fuel beds in terms of selected physical properties of the propellant. For example, as the packing fraction is increased the rate of flame spread is decreased and a smaller quantity of water is required for extinguishment.

The fire threat essentially results from the release of heat to the plant equipment and building structures. One aspect of the fire protection engineering design problem is to determine the changes in the nature of the fire threat that can result for different base fire sizes. This is particularly important for propellant fires which have very high burning rates. Two fire plume parameters which are of special importance are the plume temperatures and the centerline gas velocities. Unfortunately, very little data are available for these parameters for propellant fires. However, data are available for oil fires and it is useful to extrapolate these data to develop an empirical correlation.

Centerline gas velocities for a number of large oil fires are shown in Figure 4. Two baseline fire sizes are plotted, 10 ft^2 and 30 ft^2. The heat release rates are limited in range because of the nature of the fuels. From unpublished data of work at SwRI, it is known that an M-1 propellant fire (~ 10 ft^2) will release approximately 2×10^7 Btu/min and produce plume heights in excess of 50 ft within 1 to 2 sec after ignition. This data for the M-1 propellants is plotted in Figure 4 and correlates with the oil fire data. Similarly, the rate of heat release and the centerline gas temperature can be plotted (Figure 5). The theoretically calculated adiabatic flame temperature for an M-1 propellant (~ 2000°F) is also in good agreement with the extrapolated oil fire data. From this analysis it is concluded that two important parameters, the gas velocity and plume temperature, can be predicted with reasonable confidence for the M-1 propellants providing the burning rate at ambient pressure is known.

THE EXTINGUISHMENT ACTION

A water deluge system must be capable of delivering sufficient water to the burning surfaces to extinguish the fire. Since in an industrial plant an area is to be protected, the water flow must be distributed over a floor area. The essential action of the water is to change the rate of spread of the fire from a positive or steady state function to a negative function. As described in the previous section, a Composition-B fire is very sensitive to the heat of vaporization and, therefore, only a small amount of water is required to reduce the burning liquid surfaces below their ignition temperature.

For a propellant fire the fuel bed is distributed and burning occurs both on and below the surface. In this case much more water is required to distribute and wet the underlying burning surfaces. In addition, for propellant fires, radiant energy transfer from the combustion products to the surface is an important factor. Cooling of the fire plume reduces this energy transfer and therefore helps in the extinguishment action.

The major problem for the designer is the design of a water spray which can penetrate the fire plume. For the small plumes characteristic of Composition-B, this is relatively easy to accomplish. For high velocity plumes characteristic of propellant fires, this is much more difficult.

The penetration of a droplet through a fire plume depends on a number of engineering parameters. One of these parameters involves the hydraulic dispersion and breakup by a sprinkler water nozzle. The droplet size distribution function for a typical commercial spray nozzle is shown in Figure 6 for two line pressures (5 psi and 60 psi) at the same flow rate. As can be seen, the mean drop diameter is a function of operating pressures. Low pressures produce a large drop size that is more effective in penetrating the fire plume. Higher pressures produce a smaller drop size that is more effective in cooling the fire plume and reducing radiant energy flux to the surfaces. Figure 7 shows the drop size distribution function for a dual nozzle sprinkler designed to produce two distinct distributions, one to cool the plume and the second to penetrate to the fuel bed. Figure 8 shows a band of data for typical spray nozzles for the operating pressures ranging from 0 to 100 psi. As can be seen, the medium droplet size is in the range of 2000 to 2500 μ for a typical plant operating pressures of 60 to 80 psig. The designer has available a wide range of nozzles and must choose those which are most effective.

Having selected a nozzle, a second parameter that must be considered is the fraction of water that can penetrate the fire plume. The fraction of the quantity of liquid water that can be delivered to the burning surfaces can be calculated for a given drop size distribution providing the fire plume temperatures and gas flow velocities are known. The vaporization rate, W_A^m, for a pure liquid is given by:

$$W_A^m = (\pi D^2)(k_m)\left(\frac{X_{Ao} - X_{A\infty}}{1 - X_{Ao}}\right) \tag{8}$$

where

$$k_m = \frac{c_f \mathcal{D}_{AB_f}}{D}\left[2.0 + 0.60\left(\frac{Dv_\infty \rho_f}{\mu_f}\right)^{1/2}\left(\frac{\mu}{\rho \mathcal{D}_{AB}}\right)_f^{1/3}\right] \tag{9}$$

and

$$\mathcal{D}_{AB_f} = \frac{2.26 \times 10^{-5}\sqrt{T\left(\frac{1}{M_A} + \frac{1}{M_B}\right)}}{c\sigma_{AB}^2 \Omega \mathcal{D}_{,AB}} \tag{10}$$

To use these equations it is necessary to know the terminal velocity ($V\infty$) reached in free fall as a function of drop size. Figure 9 compares values for the terminal velocity calculated by the model developed by Kalelkar and Kunz with those found experimentally by Gunn and Krizer. The actual free-fall velocity that is used is the net velocity, i.e., the difference between the upward gas flows in the fire plume and the free-fall velocity. If the fire plume velocities are equal to or higher than the terminal free-fall velocity, the water cannot penetrate to the burning surface.

PRACTICAL DESIGN CONSIDERATIONS

The previous sections outlined the fundamental fire and fluid mechanical parameters that must be considered in the design of a fire protection system. For a specific application, the burning rate of the fuel must be known at least within an order of magnitude. Also, data are required about the type of fire (i.e., liquid or solid fuel bed) and the extent of penetration of the fire into the fuel bed. Then the designer must estimate the important heat transfer mechanism (i.e., radiative or convective to energy transport) that affect the burning rate.

Having characterized the type of fire, a nozzle system must be selected that will provide the greatest cooling effect on the rate controlling mechanism. The choice of a specific nozzle system depends on a balance between the available pressures and water-flow rates in the plant area and the ability of the system to cool the fire plume and/or burning fuel surfaces. The ability of a specific water spray to perform this function can be determined by calculating the rate of evaporation of droplets traveling through the fire plume. In general, the most effective spray will be one that can provide the maximum quantity of water to the surface. If the fire gas plume velocities are high the amount of water that can be delivered is reduced. Therefore, for very high burning rate materials it may be necessary to locate the spray nozzles on the side rather than above the fire. The optimum location for nozzle placement to maximize the area covered can be evaluated by analyzing the individual droplet trajectories.

LIST OF SYMBOLS

c	–average heat capacity
c_f	–average concentration of species A
D	–diameter
$\mathcal{D}_{AB_f}$	–average diffusiveness of species A in B
h_ℓ	–depth of heated fuel
Δh	–thermal enthalpy difference between the fuel at its ignition temperature and the virgin fuel
k_{xm}	–mass transfer coefficient
ℓ	–characteristic length
M_A	–molecular weight species A
M_B	–molecular weight species B
q	–net energy per unit area per second
R	–gas constant
T_i	–absolute temperature (°K)
T_o	–ignition temperature
T	–initial fuel temperature
V	–flame spread rate
W_A^m	–molar flow of species A crossing a mass transfer surface
X_{Ao}	–mole fraction of species A at surface
$X_{A\infty}$	–mole fraction of species A at a long distance from the surface
κ	–packing fraction
λ_s	–thermal conductivity of fuel
μ_f	–average viscosity
μ_ℓ	–viscosity of liquid
π	–3.14159···
ρ_f	–average density
ρ_ℓ	–liquid density
ρ_s	–specific gravity of fuel
σ	–surface to volume ratio
σ^1	–gradient in surface tension
σ_{AB}	–collision diameter for A, B
$\Omega\mathcal{D}_{AB}$	–collision integral for A, B

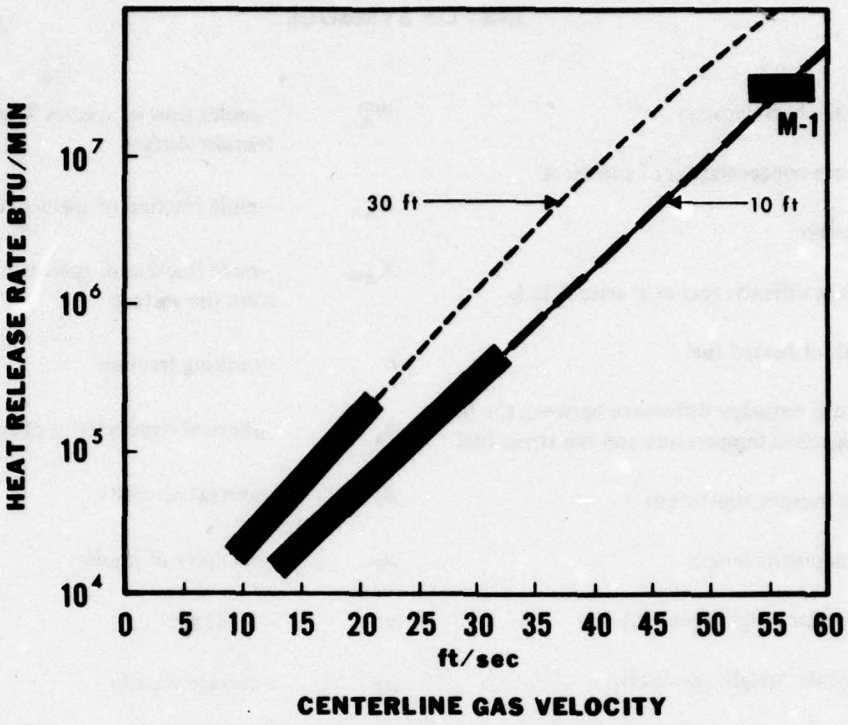


FIGURE 4. CENTERLINE GAS PLUME VELOCITIES VERSUS HEAT RELEASE RATES FOR SELECTED HEIGHTS ABOVE A 10-FT² FIRE

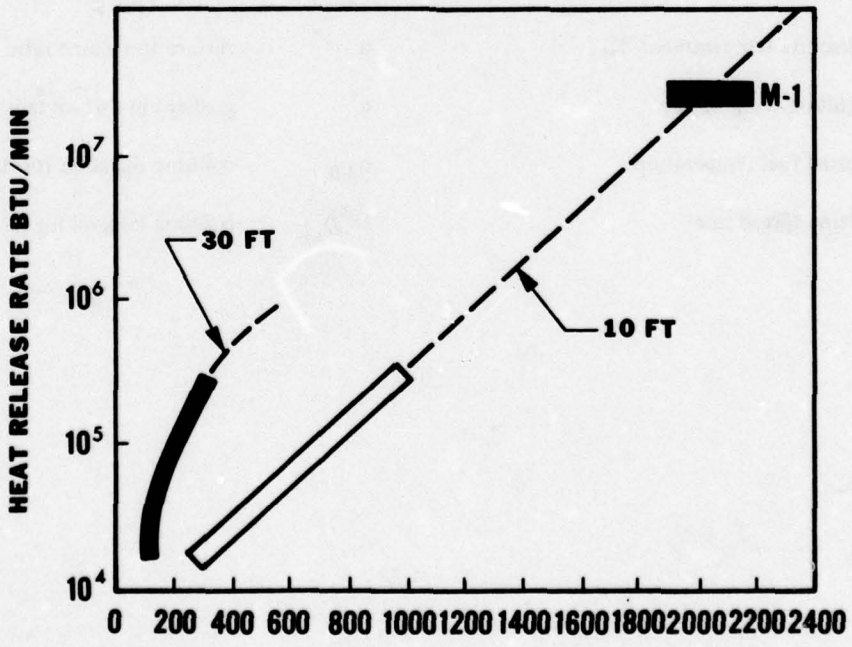


FIGURE 5. CENTERLINE GAS TEMPERATURES VERSUS HEAT RELEASE RATES AT SELECTED HEIGHTS ABOVE A 10-FT² FIRE

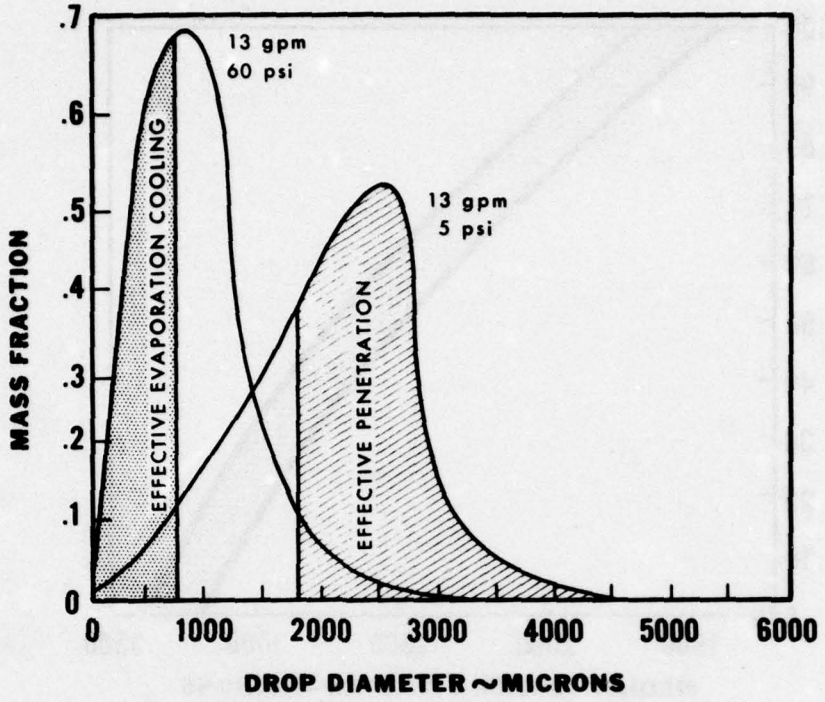


FIGURE 6. HISTOGRAM OF DROP SIZE AS A FUNCTION OF PRESSURE

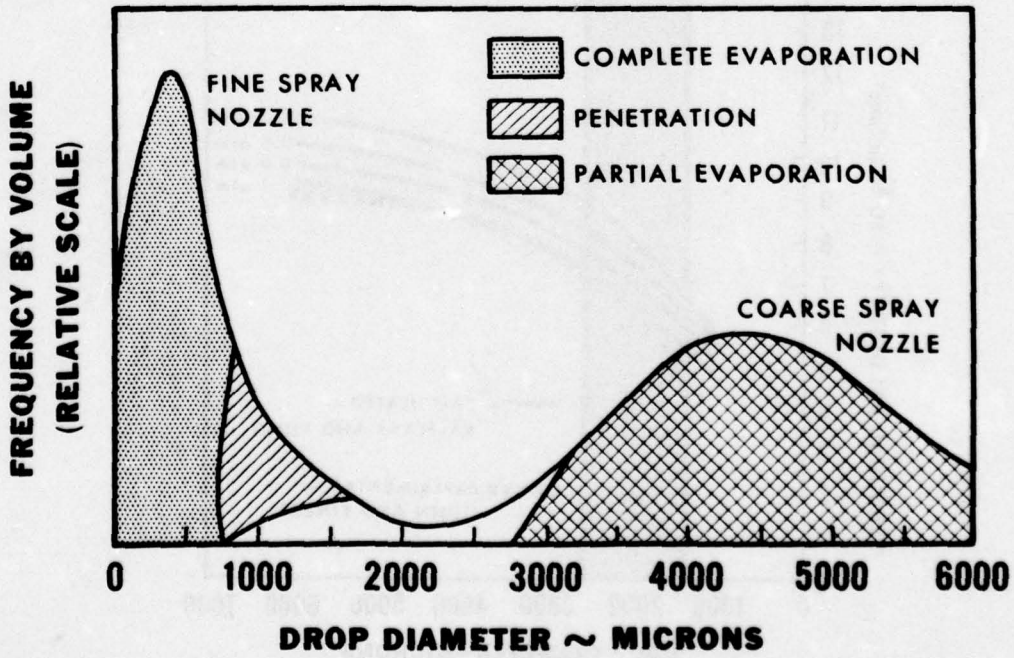


FIGURE 7. DROP SIZE DISTRIBUTION FOR DUAL NOZZLE SPRINKLER

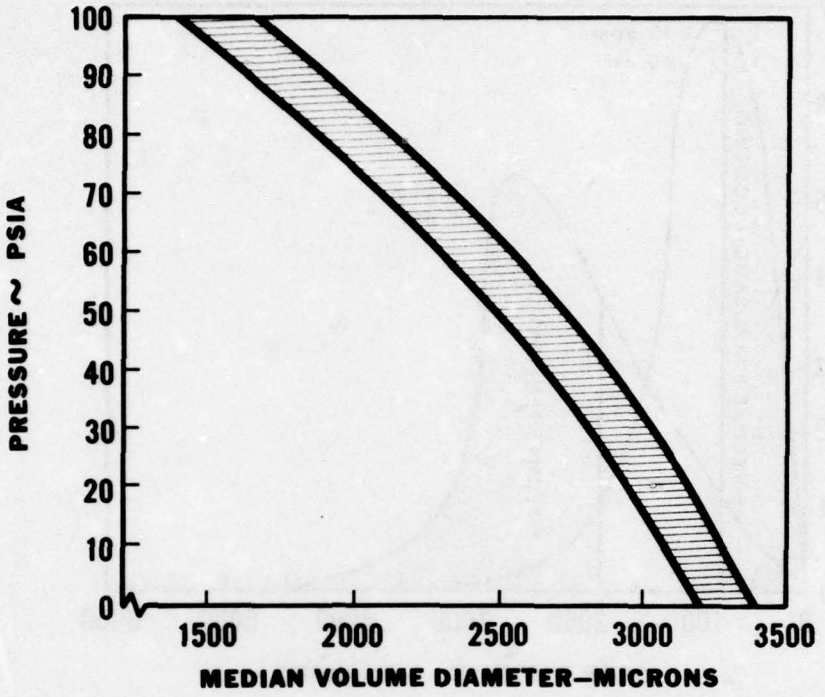


FIGURE 8. MEDIAN VOLUME DIAMETER FOR A COMMERCIAL SPRAY NOZZLE

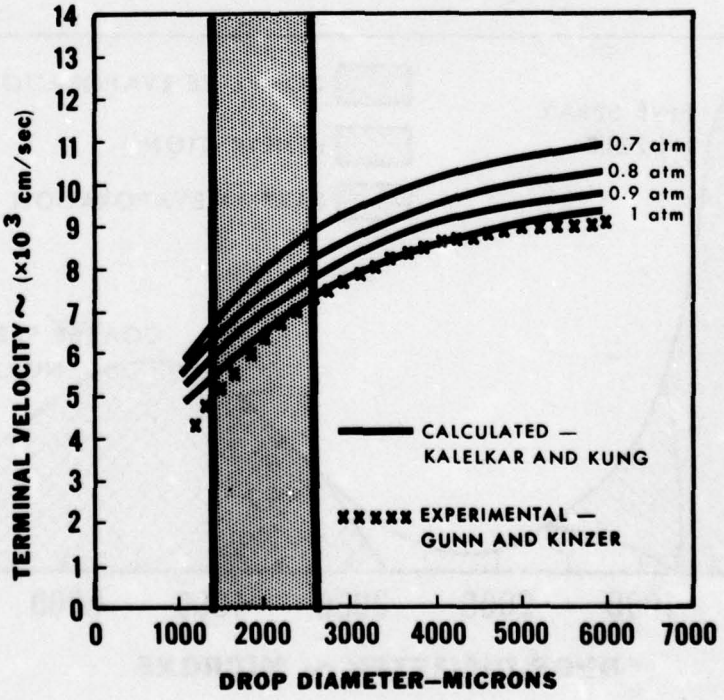


FIGURE 9. TERMINAL VELOCITY VERSUS DROPLET SIZE

THE CONTROL AND MONITORING OF EXPLOSIVES SAFETY IN THE BRITISH ARMY

Brigadier J H Lawrence-Archer
Chief Inspector Land Service Ammunition
United Kingdom

INTRODUCTION

1. I am Jim Lawrence-Archer and my appointment in the British Army is Chief Inspector Land Service Ammunition, CILSA for short.

2. I had the pleasure of showing Captain Klein one of our ammunition depots and of telling him how we are organised for explosive safety in the British Army when he visited UK in 1974. I was delighted to accept an invitation to talk to you on how the British Army tackles this important subject of explosive safety. I will concentrate on the salient points and keep the talk short. I hope you will find it interesting, most people enjoy hearing how other nations tackle their particular problems, if only to convince themselves that they do it better.

3. I hope you will be able to understand my British accent. I should perhaps therefore explain that whenever I use the term ammunition in this talk, I am using it in its widest sense to include all conventional ammunition, guided missiles and explosives used by the British Army. I believe you would call it Explosive Ordnance (EO).

LAW

4. The British laws which govern the general conditions of work and safety in factories and office and in the manufacture, storage, handling and movement of explosives are contained in the Acts of Parliament shown on Vufoil 1.

5. The first two that is the Factories Act and the Offices, Shops and Railway Premises Act lay down the conditions of work and safety rules to be followed in our factories and offices. Slide 1 shows some of the subjects which these Acts cover under the three generic headings of Health, Safety and Welfare.

6. These Acts apply to all factories and offices in the United Kingdom and as such equally apply to all military ammunition depots storehouses and workshops.

7. The Explosive Act as its name implies is the Act which governs the manufacture and storage of explosives in United Kingdom. It lays down all the safety rules which must be observed and also requires that all explosive factories and magazines are licenced by Her Majesty's Inspector of Explosives, who also has the right to inspect the premises at any time he wishes and in practice does so at regular intervals. If the Inspector finds any faults, he has the right to require the owner of the factory or magazine to put them right.

8. Unlike the first two Acts I mentioned, the Crown has exemption from the provision of the Explosive Act on the clear understanding that the Navy, Army and Air Force make and implement regulations which are at least equal to the provisions of Explosive Act. The reason for this exemption, granted in 1875, was that it was realised that to make the Services, who must manufacture and move explosives, subject to the Act would be too inhibiting and perhaps also because they realised that the Act which is written in legal jargon would not be easily understood by the simple soldiery. Slide 2 is an example from the Act, what it is saying is

that you may only store compatible groups of explosives together within the explosive limits of the particular store.

9. The three Services therefore issue their own Regulations governing the repair, handling, storage and transportation of explosives. Our three Services do not always, however, agree; a situation which I understand is also not uncommon in America. The Explosive Storage and Transport Committee was, therefore, established to act as referee or neutral adviser. It is made up of representatives of the three Services, scientists from the Government controlled explosives industry and civil ministries, including Her Majesty's Inspector of Explosives. The Army representatives are members of my Staff. This Committee issues recommendations on which the Service regulations are based and gives advice to the Services on request. I will not go any further into the role of this Committee as some of you will already have heard AVM Hedgeland talking about it in more detail.

10. The Robens Report identified that the main reasons for industrial accidents and bad working conditions generally were apathy and disinterest. To remedy this state of affairs, the Health and Safety at Work Act was passed through Parliament in 1974 and became law on 1 April 1975. It is the intention that all the Acts I have already mentioned will eventually be incorporated into this new Act, but this has not yet happened and it is hoped that the Crown will still enjoy exemption from those aspects which relate to the Explosives Act. The Act, however, does clearly define the responsibilities of employers to their employees. The Act also constitutes something of a revolution in the health and safety field in the United Kingdom in that for the first time in Section 3 as shown on Vufoil 2, it imposes general duties on employers in respect of persons other than their employees. In addition it contains a requirement to inform such persons of any effects upon them that the way an employer is running his business may have. It will be obvious to you that the implications of such changes as far as an ammunition depot and housing around it could be very considerable. These Sections of the Act are binding on all employers including the Services and any failings in this respect may be the subject of prosecution and damages.

11. You will see in a minute when I describe my responsibilities why I am concerned about these changes. At the moment the general opinion is that provided the Outside Quantity Distances are observed then, in law, all that is reasonably practicable will have been done for those living outside a depot and that there is no requirement to start telling people the risk to their property because of the proximity of the depot. This has not yet, however, been established by any case law.

12. Having explained to you the background of the United Kingdom law relating to safety I will now tell you where I fit into the picture by outlining my main responsibilities. Before I do that I will show you again Vufoil 3 which was used by AVM Hedgeland in his presentation. This I believe shows very well the organisation for explosive safety in UK. On the left hand side we have the civilian explosives, the safety of which is the responsibility of Her Majesty's Inspectors who are now part of the new Health and Safety Executive. The rest of the Chart covers military explosives and you will see that the focus for operational safety is the Ordnance Board and for storage and transport is the Explosive Storage and Transport Committee. All the major ministries concerned with storage and transport and explosives are represented on this Committee, which is chaired by the Vice President of the Ordnance Board, and which has on call technical advisers on all the relevant disciplines. The recommendations of the Committee are passed to the three Services and the Procurement Executive shown at the bottom on the Chart and I fit in under Army. Now on to my responsibilities.

EXPLOSIVE SAFETY

13. I am responsible within the British Army for writing and issuing the Army Regulations which govern the storage, handling and movement of Army ammunition. As I have explained these are based on the Acts I have mentioned and the recommendations made by the Explosive Storage and Transport Committee, and are known as Ammunition and Explosive Regulations. Slide 3 lists the Pamphlets issued and I think this perhaps gives you some idea of the comprehensive nature of the Regulations and they cover, I believe, most of the subjects you yourselves would expect them to include. Volume 2 is issued to all units and tells them how to store their ammunition, listing the safety precautions they must take.

14. Perhaps not surprisingly CILSA is the ultimate authority on the interpretation of these Regulations.

15. I not only issue the Regulations, but am also responsible for ensuring that they are implemented within the Army. This I achieve by:

a. Licencing. I licence all Army ammunition stores and workshops and any new projects must be submitted to my Headquarters for approval and licencing before building commences. Slide 4 shows the form of licencing document we use and I understand it is not very different from the one you use.

b. Staffing. Ammunition and explosives are stored both in our depots and in unit stores. I have technical staff, known as Ammunition Technical Officers and Ammunition Technicians, who have been specially trained in ammunition storage and safety matters. Some are positioned in all our depots and others are organised into small mobile sections known as Inspectorates with a responsibility for checking on unit ammunition stores. Those in depots are responsible for the day to day safety within the depot and for ensuring that all the regulations are being observed correctly and sensibly. Those responsible for unit stores cannot, of course, have such close control as there are too many unit stores. They do, however, visit and inspect the units in their areas regularly; some units, the bad ones, get visited more regularly than others.

c. Inspections. I personally inspect all RAOC depots every two years to ensure that Regulations are being observed. Unit ammunition stores are so many that I cannot inspect them all myself but the technical staff in the Inspectorates, I have already mentioned, are required to inspect each unit ammunition store at least once a year. I in turn inspect each Inspectorate every two years to ensure the Staff are carrying out their duties correctly.

d. Concessions. Only CILSA or Commanding Generals may authorise the disregard of mandatory storage and safety regulations, such authorisations are known as concessions and are carefully recorded by my Headquarters and have to be reviewed and renewed each year. Commanding Generals normally only give concessions in the case of operational necessity and even then only after consultation with my technical staff. I personally do not readily grant a concession especially in view of the new clauses in the Health and Safety at Work Act. Normally I make it a condition of granting a concession that action is being taken to render the concession unnecessary in the future.

16. I should perhaps have reminded you that like your Army, the British Army is not only stationed in the mother country. We have forces in many places such as

Germany, Canada, Cyprus and Hong Kong and my responsibilities extend to cover all these places. When abroad the British Army always observes the safety regulations of the land in which it is stationed, except that if our own regulations are tighter, then we observe our regulations. One of the big advantages from my point of view of the new NATO principles of storage is that in future the British Army should be able to observe the same regulations wherever it is stationed.

INVESTIGATION OF AMMUNITION AND DEFECTS

17. CILSA is responsible for coordinating all investigations into accidents and defects which may occur in Service with ammunition or explosives. The initial investigation will be made by one of my technical staff who will then send a report to my Headquarters. At the same time they may if they think it necessary ban the use of the ammunition pending further investigation. These incidents can, of course, range from the simple defect, such as blinds or misfires occurring on a range during firing practice, to a premature in a gun, where some of the gun crew are killed, or to a major explosion in a depot.

18. On receipt of the report in my Headquarters, my staff are responsible for calling in the help of outside agencies such as Government chemists, engineers and metullurgists to continue the investigation until the cause is established and then for taking such action as may be necessary to prevent a recurrence. This can take the form of withdrawing that particular ammunition from service, correcting an error in drill, repairing the ammunition or drafting and issuing new safety regulations.

19. An example of a major accident is one that occurred in an Ammunition Sub Depot in the Middle East. This Depot, although not a British one, was built to British Army Regulations in 1971 and when there was an accident there in 1973 I was asked to send an officer to investigate. The Depot was originally designed with strict explosive limits in mind, based on the types of ammunition to be stored in individual magazines.

20. Vufoil 4 shows the layout of the Depot. It is divided down the middle by a 27in brick wall intended as a receptor traverse. Please also note the fire hydrants sited along the centre line of the Depot. The Vufoil also shows the nature of ammunition that individual magazines were planned to hold. We have never been able to establish the quantities that were supposed to be held in each magazine. In the event at the time of the accident the magazine holdings by natures are also shown on the Vufoil.

21. You should note that Magazine 5 which was intended to hold basically Mortar ammunition and rockets, in fact contained bulk explosives, primers, detonators and HE armoured car complete rounds. I do not need to point out to you the incompatibility of these natures.

22. In the early evening of 1 May 1973, the guard noticed smoke coming out of Magazine 5 and about 10 minutes later there was a massive explosion and fragments and debris were thrown over a wide area. Slide 5 shows the scene after the explosion and as you can see the central blast wall was breeched.

23. Shortly after the explosion a second fire was noticed in Magazine 6. It is suspected that this fire was started by fragments from Magazine 5 thrown through the breeched central wall into Magazine 6. The fire was accompanied by sporadic low order detonations and unstable rockets flying out of the building.

24. A soldier visited Magazine 6 immediately after the Magazine 5 explosion occurred and soon after the start of the fires in Magazine 6. It is interesting to note that he was convinced that if he had had the necessary equipment, he could have put out these fires before they took proper hold. I am sad to say that although the Depot was provided with the good fire hydrant system shown on the

first Vufoil, they had never in fact been connected to water. I am sure there is a moral here somewhere.

25. Slide 6 shows what Magazine 6 looked like the next morning. It had been completely burnt out and all its contents had been lost.

26. As one would expect, Slide 7 shows that severe damage was occasioned to other parts of the Depot by flying fragments and blast. But no other ammunition was lost although recovery was a major task.

27. In summary, the IQDs in this case did what they were designed to do - they prevented sympathetic detonation, but as we always knew could happen we had indirect explosions caused by fragment attack.

28. We never clearly established the cause of the initial explosion in Magazine 5. Ignition of the gelignite associated with an electric fault in the air conditioning system, which was known to be faulty just prior to the incident, was suspected. Unfortunately the investigation left a number of questions unanswered, which will never be answered now.

29. Personally I am convinced that lack of safety discipline was a major contributing factor. It does not really matter how well you plan and layout a depot, if housekeeping is poor you will get accidents. The storage of incompatible groups together must never be allowed. One cannot overemphasise this.

30. Unfortunately the message has still not got through. In the same part of the world an open stack of ammunition on a forward storage site has recently been lost. It was reported to us that the stock contained 81mm WP bombs, but on investigation we found that the stock had also contained 81mm HE, Spanish 81mm Chemical Smoke, 2in HE, Coloured smoke and WP grenades: again you will have noted the incompatible groups; in addition a proportion of the ammunition was not in its packages. The Spanish smoke mortar bombs were filled titanium techrochloride and we found the locals quite happily putting these into 40 gallon drums of water during the clearing up operation. As you know titanium techrochloride and water do not make good bedmates.

31. The second accident I am going to describe concerns the 81mm Mortar. In March this year a battalion was training replacement crews at live HE firings in Germany. A bore premature occurred resulting in fatal injuries to two of the crew members. This is what safety is all about - it is not a pure scientific exercise as when we fail it can all too often result in a soldier being killed. At least four eye witnesses testified that the correct loading and safety drills had been complied with and that the bomb prior to the premature had definitely left the barrel. From this we inferred that the premature was attributable to faulty ammunition and therefore we placed a ban on all HE bombs of the same date and place of manufacture.

32. My investigating officer, as part of the normal procedure, collected all the fragments of metal at the site of the accident, labelled them and returned them to my Headquarters. These were pieced together by Government scientists and it was definitely established that they came from more than one bomb. Fortunately this was the first occasion that that particular firing site had been used for 81mm mortar firings and so we concluded the premature was due to a double feed and were able to release for training the stocks of bombs we had banned. It is our experience that in the event of prematures units always tend to blame the ammunition, it is only by means of detailed investigation and much detective work that we establish the real cause, which in practice is rarely due to ammunition faults.

33. You will all be familiar with the 175mm gun. In February 1972 and May 1972 bore prematures occurred whilst firing Shell HE M437A2 Fuzed PDM 572 with a German manufactured Charge 1, the DM 12A1. Luckily there were no casualties. This charge was on trial because the US Army had experienced blinds, short ranging and in flight prematures with the American Charge 1 and we did not therefore want to use it at training.

34. Examination of the recovered fragments proved that detonation of the shell had not occurred from the functioning of the fuze and also the absence of engraving on the driving band fragments showed that detonation had occurred before the shell had reached the Commencement of Rifling.

35. You will know that with this weapon when the shell is loaded the driving band is not engaged in the rifling but is retained in a tapered portion (the forcing cone) of the chamber which leads into the rifling. The amount of movement required for the band to engage the rifling is however minimal and this suggested therefore that perhaps the shell had slipped back after ramming.

36. The loading drill requires the use of a T stick to check that the shell is fully chambered. With the long leg of the T stick against the base of the shell the cross piece must rest flush with the face of the breech. Investigation showed however that it was possible to get a false reading if the stick missed the centre of the shell and slid down its boat tail. This would allow the cross piece to still rest flush with the breech when in fact the shell would be as much as 3 inches from being fully chambered.

37. It was then established that the effect of a shell not being fully chambered could be for it to fall back even further at even relatively low QEs, so that it was out of the forcing cone. Investigations showed that there were two reasons for the shell not being fully chambered:

The FIRST being that the interlock switches on the loading tray which control the application of the power rammer were unreliable. Due to wear, the switches intermittently opened for fractions of a second producing a "shunting" effect of the ram and shell. On the final "shunt" it was possible for the ram to rebound off the shell instead of forcing it fully home.

and SECOND that the profile of the forcing cone and the shape of the driving band were such that only the forward rib of the band was gripping in the cone. This was an American design fault which had been discovered and corrected in America but unfortunately the procedure for informing UK had been fouled up.

38. The problem was aggravated because we were using the German charge which was considerably shorter than the American Charge 1 and in addition was very much faster burning. This meant that when the shell fell back onto the German charge it was completely withdrawn from the forcing cone. On firing there was a very rapid rise in pressure and since the shell was not located in the forcing cone, it could get a very rough ride into the cone which could cause detonation in the extreme case.

39. We have introduced the following remedies to prevent this happening again:

FIRST: The T stick has been redesigned with a broader base.

SECOND: The driving band has been modified so that at least 3 ribs engage in the forcing cone; this is a similar modification to the one carried out by the American Army.

THIRD: The power rammer has been modified to produce consistently good ramming.

FOURTH: The German DM 12 charge was withdrawn from Service.

FIFTH: Steps have been taken to improve the technical channels of communications between our two nations.

40. I think this case was interesting because it illustrates the importance of ensuring that investigations are in depth. We must, I believe, always enquire into 'Why' an accident occurred and not only into 'How.' In this case the premature was caused by the fall back of the shell after loading. It is only when we ask ourselves why it happened that we find out that the design of the T stick is faulty and that something has gone wrong with the system of communications between our two nations.

41. Vufoil 5 shows a summary of the accidents that have occurred in the British Service by causes over the last few years. The Vufoil shows I am sorry to say that by far the major cause of accidents is human error, that is to say soldiers being stupid and or failing to follow the correct drill. I, therefore, work closely with those responsible for training to give publicity throughout the Army to the number of accidents that have occurred in an attempt to reduce the numbers of soldiers killed and injured entirely unnecessarily.

42. The big advantage of this involvement in the accident procedure is that my staff can keep our Safety Regulations up-to-date and can react quickly to any defect or new type of accident which may occur.

SURVEILLANCE, REPAIR AND DISPOSAL

43. My next responsibility is for the surveillance of our ammunition stocks, the repair of them when necessary and finally for their disposal when they have either become unserviceable or are no longer required. In each of these fields I am responsible for laying down the policy and procedure to be followed and for detailing the methods to be used.

44. In surveillance, we do, of course, still inspect samples from our stocks to determine quality, but our main method of determing quality is now by firing under controlled conditions samples from both our stocks of ammunition and guided missiles. The results of these firings are fed back to my Headquarters and using our computer we calculate a quality and sentence the ammunition accordingly.

45. With repair and disposal, my Headquarters says what is to be repaired or disposed of and the method to be used, for example, we may dispose of ammunition by detonation, burning or deep sea dumping. The detailed planning of the job is, of course, done at depot level by the ATOs I have already mentioned.

46. My Headquarters issues the Regulations which cover not only all this work but also gives the technical details of all the natures of ammunition in the British Service, some 204 pamphlets in all.

47. This means that all technical ammunition staff in the British Army wear two hats. With one on they are responsible for safety and with the other for organising repair etc. It has been argued that this divided responsibility is bad from a safety point of view, but all that I can say to this is that it seems to work. It does mean, of course, that all those employed on ammunition always have safety in the forefront of their minds. Ignoring unit ammunition storage where it is impossible for my staff to exercise effective day to day control, we have had

no major accidents in our depots worldwide over the last 20 years. Bearing in mind that we have between 15 and 25 depots, that is not too bad a record.

TRAINING

48. We train our ATOs and ATs on a course lasting a year at the Army School of Ammunition. I am responsible for the efficiency of the School and the syllabus of the ATO and AT courses.

EOD

49. My final responsibility is for the British Army's EOD organisation. Because of the depth of their knowledge of and experience with ammunition and explosives it is my ATOs and ATs who are tasked with rendering safe terrorist bombs and unexploded ordnance which is still being found in UK and elsewhere.

50. This is at the present time a very considerable task. In Northern Ireland which is the 1/10th size of Colorado we have dealt with over 2,500 terrorist devices since 1969 whilst in UK we still continue to handle over 4,000 UXOs each year in addition to a small number of bombs.

51. As technical head of this organisation I am, of course, deeply involved in the development of new equipment and techniques for dealing with bombs.

52. I hope this has given you some idea of what I do. I find it a fascinating job, with never a dull moment because of the breadth and scope of my responsibilities.

53. To illustrate one aspect of my responsibilities and sphere of influence I will now describe very briefly a project currently in hand in the United Kingdom. Vufoil 6 shows a major ammunition storage unit as it exists today, or perhaps more correctly as it existed last year. This depot was built at the beginning of the last war. You will notice that it extends over a considerable area in fact 4 sq miles with a perimeter of 17½ miles. As you will see there are very few roads and to get from one point in the depot to another can mean a long tortuous journey by rail car. In fact it is not uncommon to "loose" soldiers in the depot for the whole of a day. The present storage buildings are quite unsuitable for palletised ammunition and mechanical handling equipment, because of the numbers of pillars and in many cases the buildings are in urgent need of repair.

54. It does not take very much to realise that a major rebuild is required and this is exactly what is taking place at the moment. Now to describe briefly the steps in such a project and in particular how my Headquarters is responsible. A planning liaison officer was appointed. It was the job of this officer to gather together the requirements and justification for a case to be made to Treasury. The PLO gathered technical requirements from the specialist advisers on fire and security and for technical ammunition matters and factors affecting safety from my Headquarters. The user requirements were, of course, obtained from the depot. Having prepared a statement of requirement and justification it was then sent to the Ministry of Defence (MOD) and Treasury for approval and allocation of finance. The next stage was to set up a project team including architects, engineers, surveyors, etc who prepared sketch plans. At this stage close liaison was necessary between the user and specialist advisers in order that the design was correct. Following on the approved sketch plans detailed drawings were produced and eventually contract drawings. During the drawing stages my Headquarters had considerable influence and there was a strict requirement that all drawings must be given technical approval by my staff.

55. The first plan to be produced involved the construction of about 80 large free standing buildings of heavy concrete construction. The project was nearing contract stage when it was realised that we would be building a white elephant rather than an ammunition depot. This rather extraordinary revelation came about as a result of the Eskimo Series of Trials at China Lake, Trials at Shoeburyness in the United Kingdom and discussion within the NATO Group of Experts on safety and storage of ammunition.

56. As can be imagined this major upheaval caused a frenzy of activity in order not to let the programme slip. As well as a redesign of the storage complex it meant asking Treasury for an increase in financial cover. It was my Headquarters which became unpopular at the eleventh hour and instigated the change. However, it was necessary and the MOD could do nothing but accept my proposals and recommendations.

57. The new plan, which is shown on Vufoil 7, is to construct 100 small igloo type buildings and about 40 free standing brick buildings. We would have preferred to have the depot constructed completely of earth covered buildings but the cost became a prime factor and it must always be acknowledged that although flexibility is the key word, there will always be a requirement to store such natures as pyrotechnics, small arms ammunition, white phosphorus filled ammunition etc. Slide 8 shows a model of the new depot. The igloos can be clearly seen and also the free standing ESH which are located at such a distance as not to be a hazard from the mass exploding ammunition in the earth covered buildings. This new compact depot will show a significant saving in real estate. This project clearly illustrates the benefit achieved from international cooperation and exchange of ideas and the benefits which can accrue from a gathering such as this.

58. In conclusion I would like to sum up my thoughts on safety in just a few words under the headings Prevention, Minimisation and Investigation.

59. Our first task must be to try to prevent accidents occurring. To achieve this we must observe the safety rules using fail safe procedures wherever possible, our housekeeping must always be good and we must exercise strict control of the explosives area in terms of the entry of both men and materials.

60. But history has shown that human nature being what it is, accidents will happen. To this must be added in this day and age the very real danger of sabotage or of the unbalanced person who just likes bangs or who wants to commit suicide spectacularily. We must, therefore, always plan our depots and work to minimise the effects of any accident which occurs. This is not difficult to do, but almost inevitably it costs money or entails the inposition of some restriction which is not popular with either the field commander or the production manager. One becomes very unpopular on these occasions, but I have always found that if one spells out the risks in a way that is understood by the laymen, they nearly always accepts ones' advice.

61. And finally, when an accident has occurred there must always be a really detailed investigation to establish first how it occurred and secondly, even more important, why it occurred and thirdly, the prime reason for the investigation, what action must be taken to prevent it recurring.

62. That completes my presentation. Thank you for listening to me so patiently. If you have any questions, I will do my best to answer them.

ACTS OF PARLIAMENT

GOVERNING SAFETY

THE FACTORIES ACT 1961

THE OFFICES, SHOPS AND RAILWAYS PREMISES ACT 1963

THE EXPLOSIVES ACTS 1875 AND 1923

HEALTH AND SAFETY AT WORK ACT 1974

THE HEALTH AND SAFETY AT WORK ACT

SECTION 3(1)

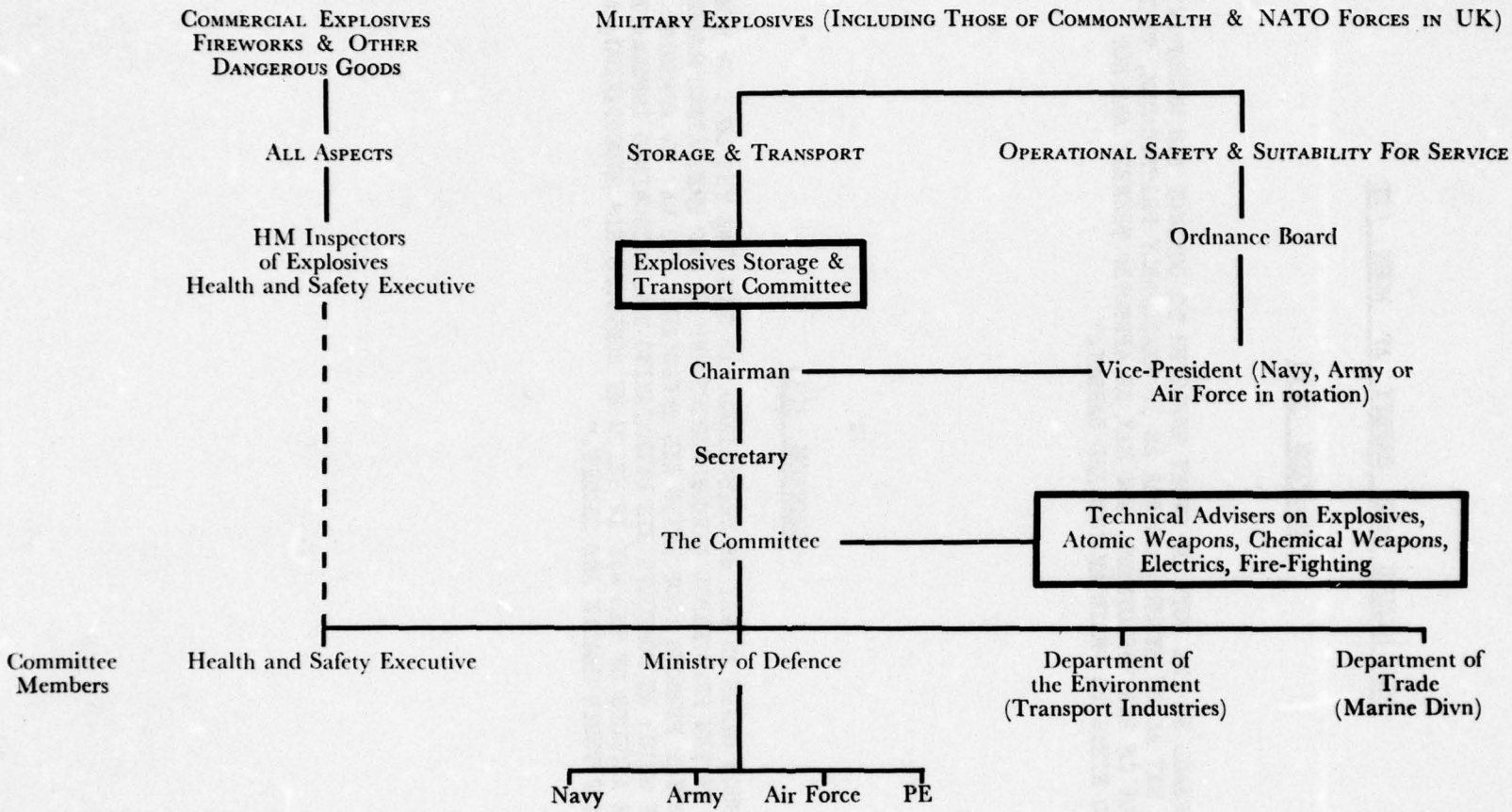
"IT SHALL BE THE DUTY OF EVERY EMPLOYER TO CONDUCT HIS UNDERTAKING IN SUCH A WAY AS TO ENSURE, SO FAR AS IS REASONABLY PRACTICABLE, THAT PERSONS NOT IN HIS EMPLOYMENT, WHO MAY BE AFFECTED THEREBY ARE NOT EXPOSED TO RISKS TO THEIR HEALTH AND SAFETY."

SECTION 3(3)

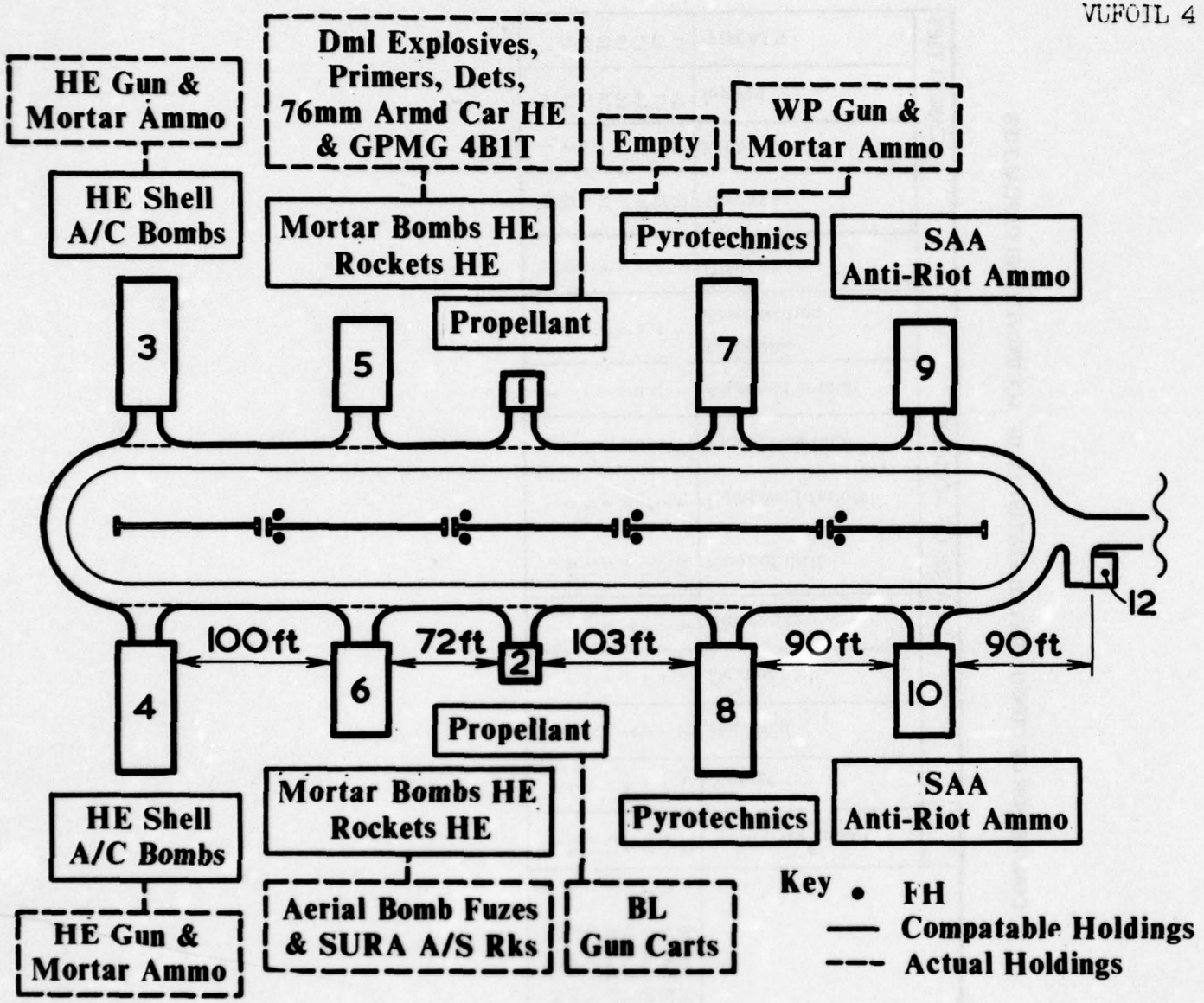
"IN SUCH CASES AS MAY BE PRESCRIBED, IT SHALL BE THE DUTY OF EVERY EMPLOYER, IN THE PRESCRIBED CIRCUMSTANCES AND IN THE PRESCRIBED MANNER, TO GIVE TO THE PERSONS (NOT BEING HIS EMPLOYEES) WHO MAY BE AFFECTED BY THE WAY IN WHICH HE CONDUCTS HIS UNDERTAKING THE PRESCRIBED INFORMATION ABOUT SUCH ASPECTS OF THE WAY IN WHICH HE CONDUCTS HIS UNDERTAKING, AS MIGHT AFFECT THEIR HEALTH AND SAFETY."

ORGANISATION CHART

EXPLOSIVES SAFETY IN THE UK



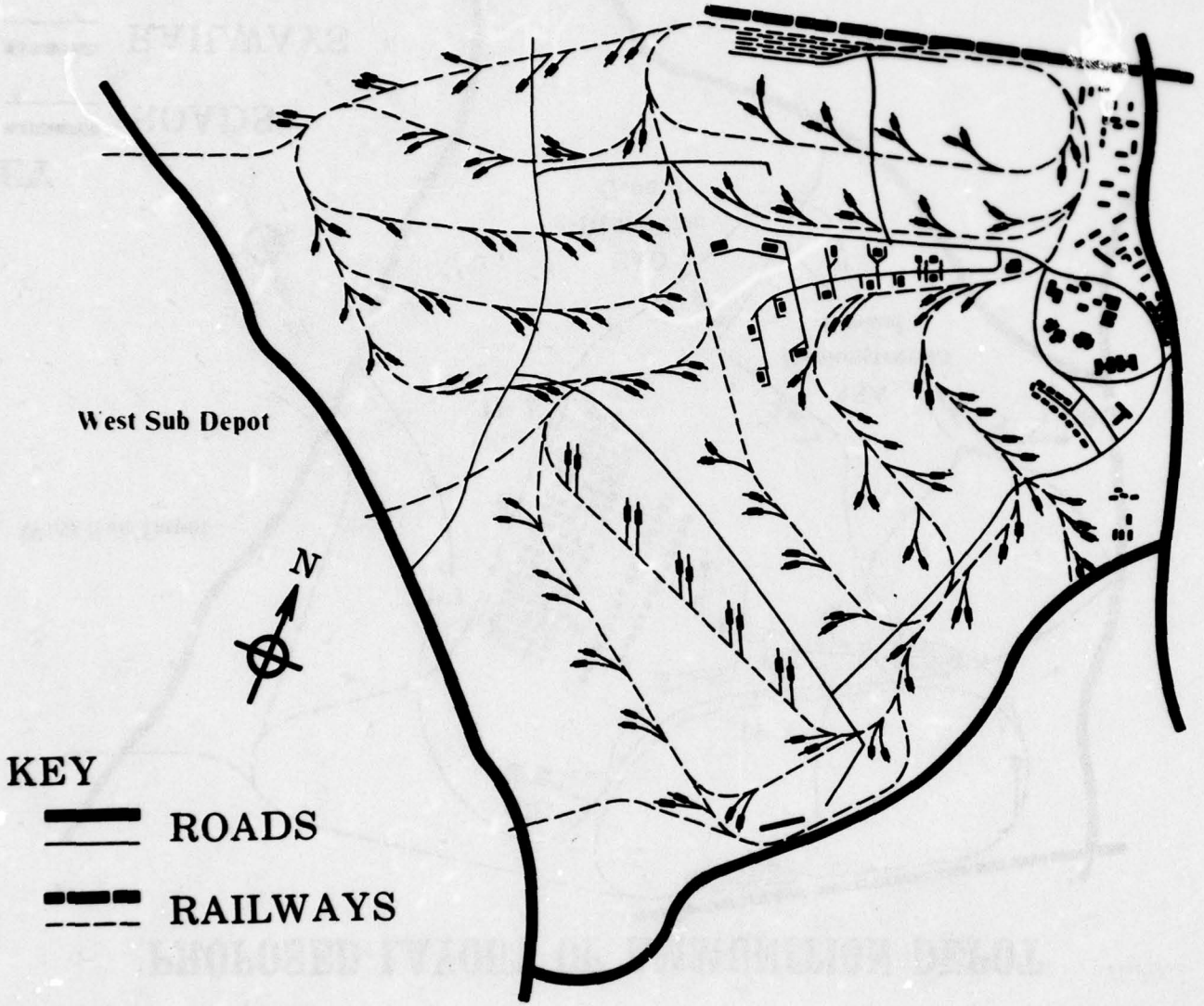
VUFOIL 4


HE Gun & Mortar Ammo
Dml Explosives, Primers, Dets, 76mm Armd Car HE & GPMG 4B1T
Empty
WP Gun & Mortar Ammo
HE Shell A/C Bombs
Mortar Bombs HE Rockets HE
Pyrotechnics
SAA Anti-Riot Ammo
Propellant
3
5
1
7
9
12
100ft
72ft
103ft
90ft
90ft
4
6
2
8
10
Propellant
HE Shell A/C Bombs
Mortar Bombs HE Rockets HE
Pyrotechnics
SAA Anti-Riot Ammo
HE Gun & Mortar Ammo
Aerial Bomb Fuzes & SURA A/S Rks
BL Gun Carts
Key • FH
Compatable Holdings
Actual Holdings

COMPARISON OF CONSOLIDATED STATISTICS OF ACCIDENTS AND CASUALTIES

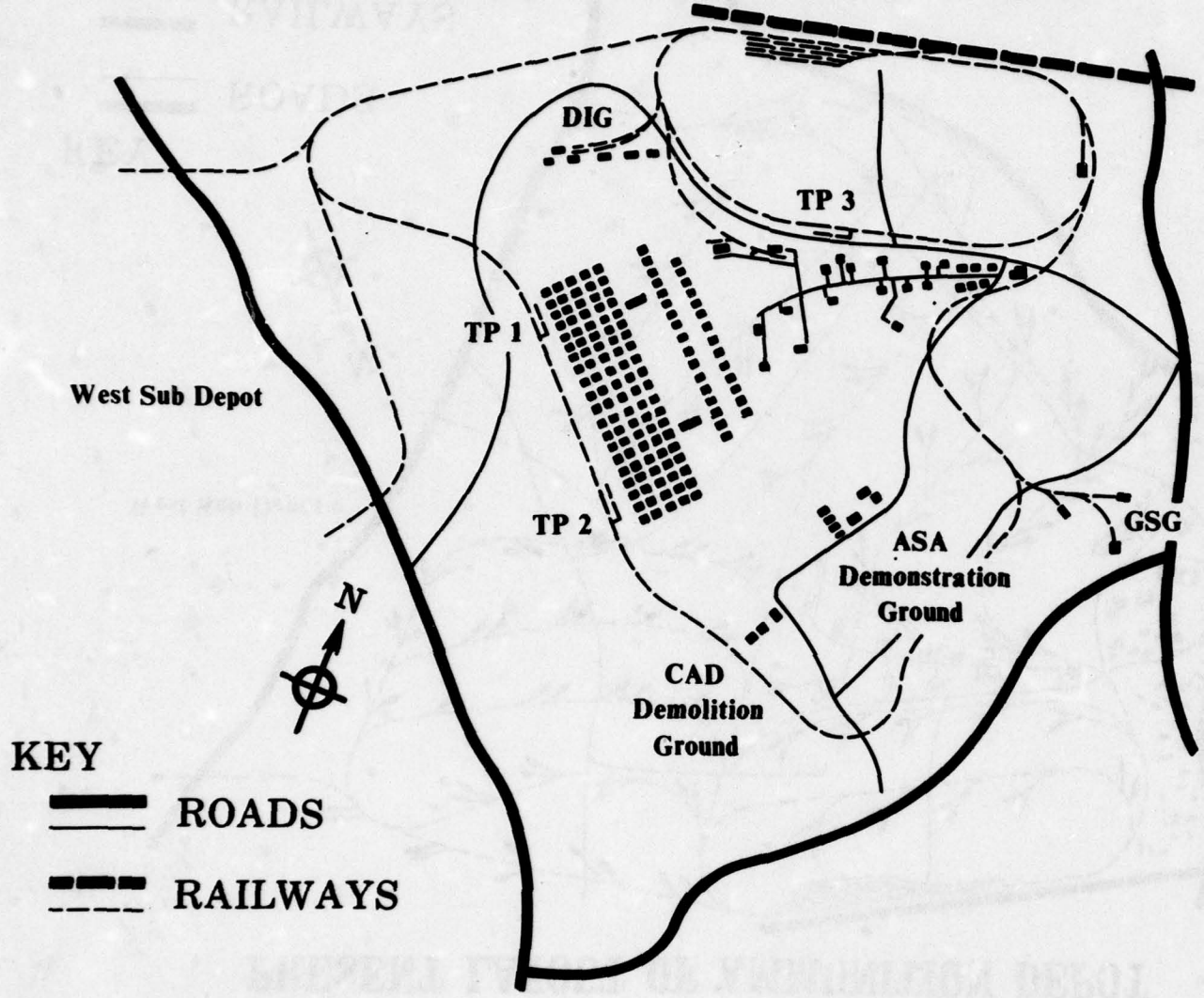
	CAUSE OF ACCIDENT												CASUALTIES		
	Not yet known	Storage	Handling	Design fault	Tampering	Error of drill	Equipment failure	Production fault	Ammunition fault	In Service deterioration	Other causes	TOTALS	Killed	Injured	TOTALS
30 Jun 76	18	–	3	–	3	17	1	1	1	1	5	50	2	29	31
31 Dec 75	8	–	3	–	5	25	3	–	–	–	6	50	1	41	42
30 Jun 75	14	–	3	–	3	13	2	–	–	–	1	36	1	16	17
31 Dec 74	12	–	3	–	2	9	6	–	–	2	1	35	1	16	17
30 Jun 74	19	–	1	–	3	4	4	–	–	–	1	32	–	24	24
31 Dec 73	15	–	1	–	1	13	10	–	–	1	3	4	1	27	27
30 Jun 73	21	–	1	–	6	14	6	1	–	–	3	52	3	44	47
31 Dec 72	6	–	2	–	5	17	2	–	1	–	7	40	1	16	17

PRESENT LAYOUT OF AMMUNITION DEPOT



665

PROPOSED LAYOUT OF AMMUNITION DEPOT



SLIDE 1

MATTERS COVERED BY FACTORY AND OFFICES, SHOPS AND RAILWAY PREMISES ACTS

HEALTH

CLEANLINESS

OVERCROWDING

TEMPERATURE

VENTILATION

LIGHTING

DRAINAGE OF FLOORS

SANITARY ACCOMMODATION

LIFTING

LEAD PROCESSES

NOTIFICATION OF INDUSTRIAL POISONING OR DISEASE

SAFETY

SAFETY MEASURES

a. MACHINERY

b. CORROSIVE OR BOILING LIQUID

TRAINING

MAINTENANCE AND TESTING OF LIFTS, HOISTS, CRANES, ETC.

PRECAUTIONS AGAINST GASSING, EXPLOSIONS OF FLAMMABLE DUST OR GAS

FIRE

PROTECTION OF EYES

WELFARE

PROVISION OF

a. DRINKING WATER

b. WASHING FACILITIES

FIRST AID

SLIDE 2

EXPLOSIVES ACT 1875

SECTION 40(5)

"TWO OR MORE DESCRIPTIONS OF EXPLOSIVES SHALL NOT BE KEPT IN THE SAME STORE OR REGISTERED PREMISES, EXCEPT SUCH DESCRIPTIONS AS MAY BE PRESCRIBED IN THAT BEHALF: AND, WHEN SO KEPT, SHALL BE KEPT SUBJECT TO THE PRESCRIBED CONDITIONS AND RESTRICTIONS"

AMMUNITION AND EXPLOSIVES REGULATIONS (LAND SERVICE)

VOLUME 1

PAMPHLET	
1.	INTRODUCTION, RESPONSIBILITIES, LEGAL ASPECTS AND CLASSIFICATION OF AMMUNITION
2.	SAFETY AND CONTROL OF EXPLOSIVES AREAS
3.	FIRE FIGHTING AND FIRE PRECAUTIONS IN EXPLOSIVES AREAS
4.	FIRST AID AND HEALTH MEASURES
5.	QUANTITY DISTANCES AND EXPLOSIVES LIMITS
6.	STORAGE IN DEPOTS AND UNITS
7.	MOVEMENT OF AMMUNITION
8.	SITING, PLANNING, DESIGN AND CONSTRUCTION OF BUILDING, FACILITIES AND DEPOTS
9.	ELECTRICAL INSTALLATIONS AND EQUIPMENT IN EXPLOSIVES AREAS
10.	INTERNAL COMBUSTION ENGINES FOR USE IN EXPLOSIVES AREAS
11.	ACTION IN CONNECTION WITH THE REPORTING OF DEFECTS, PERFORMANCE FAILURES AND ACCIDENTS

VOLUME 2

UNIT AMMUNITION STORAGE AND HANDLING

DOS FORM 723

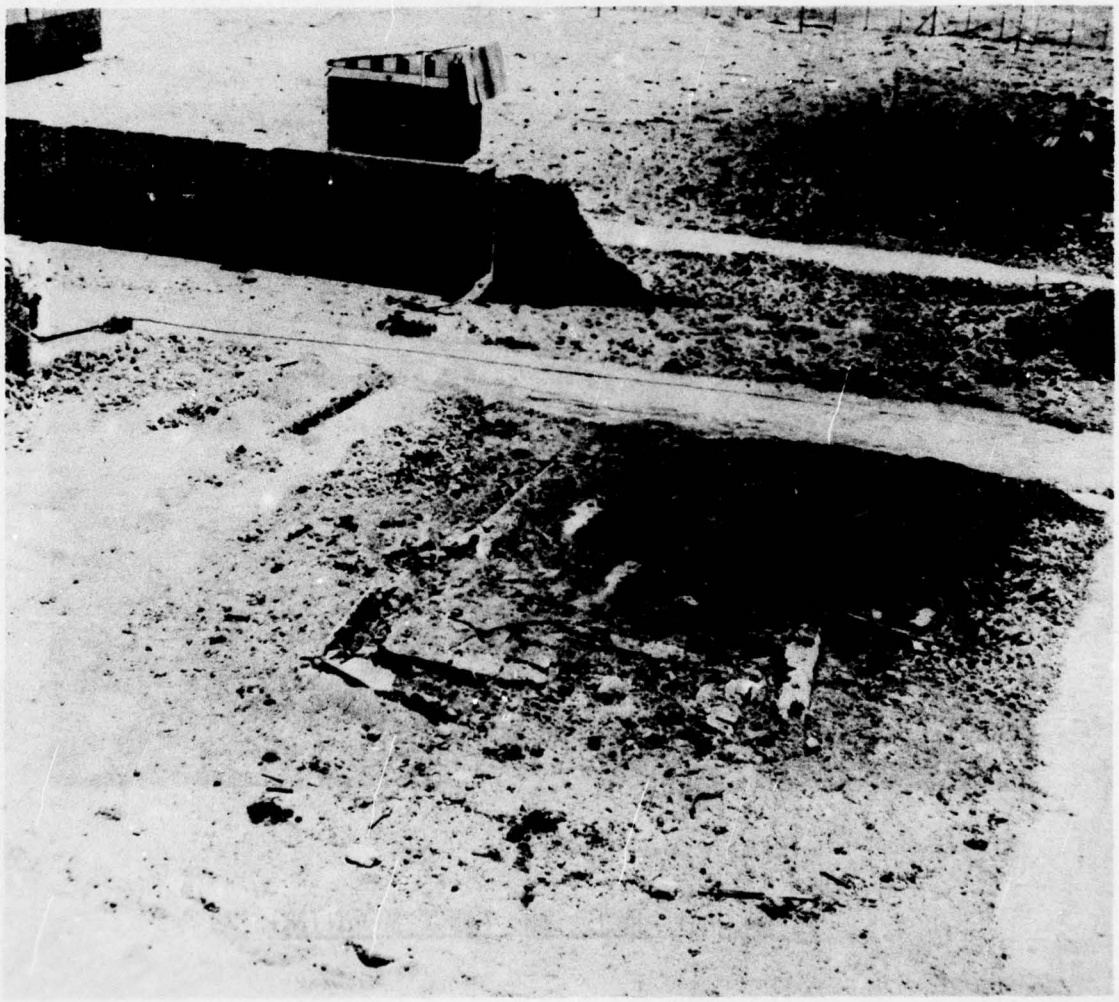
1. EXPLOSIVE LIMIT LICENCE	2. UNIT		3. LICENCE No.
4. SITE No. / NAME	5. FOR USE AS		6. ADEQUATE FIRE FIGHTING YES/NO
7. ELECTRICAL STANDARD A B C / WEATHERPROOF/OTHER	8. LIGHTNING PROTECTION YES/NO	9. AREA PLAN No.	10. SAFEGUARD PLAN No.
11. CONSTRUCTIONAL DETAILS			
12. HEADWALL & DOOR 7 BAR / 3 BAR / OTHER / FFR	13. TYPE OF FLOOR	14. TYPE OF HEATING	15. IAS YES/NO / 16. SITE DRAWING No.
17. TRAVERSE DETAILS			

18 EXPOSED SITE / POTENTIAL EXPLOSION SITE	QUANTITY DISTANCE (METRES)																OR GROUP 3			OR GROUP 4	OR GROUP 5	POL, RADIO TX, AIRFIELD, ELECT SUB
																OR GROUP 2 FACTOR						
ES No./NAME ON AREA PLAN																						
↗																						
↗																						
↗																						

19. NET EXPLOSIVE QUANTITY (10/100/1000 KILOGRAMMES)																						
HD 1·1																						
HD 1·21																						
HD 1·22																						
HD 1·33																						
HD 1·34																						

20 MAXIMUM NEQ (Kg) PERMITTED BY QUANTITY DISTANCE										21. CILSA USE ONLY
HD 1·1	OR	HD 1·21	OR	HD 1·22	OR	HD 1·33	OR	HD 1·34		
OR ANY COMBINATION OF HD NOT EXCEEDING ONE OF THESE FIGURES WHEN MIXED IN ACCORDANCE WITH A & ER VOL I PARAS 5 & 6										
AND/OR HD 1·4 TO PHYSICAL CAPACITY NOT EXCEEDING A TOTAL OF						UNITS OF SPACE IN ACCORDANCE WITH A & ER VOL I PARA 6				

SLIDE 5



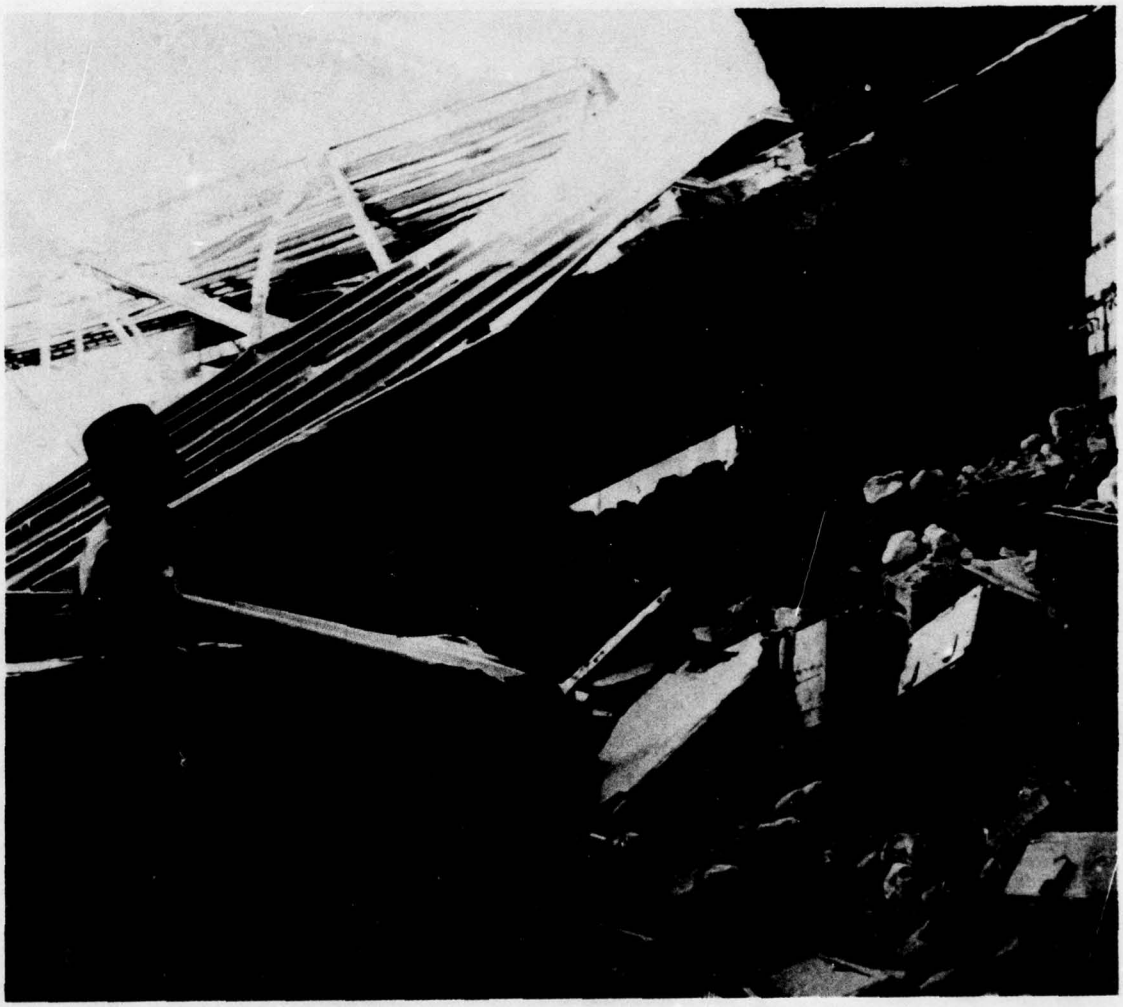
MAGAZINE 5 AFTER THE EXPLOSION

SLIDE 6



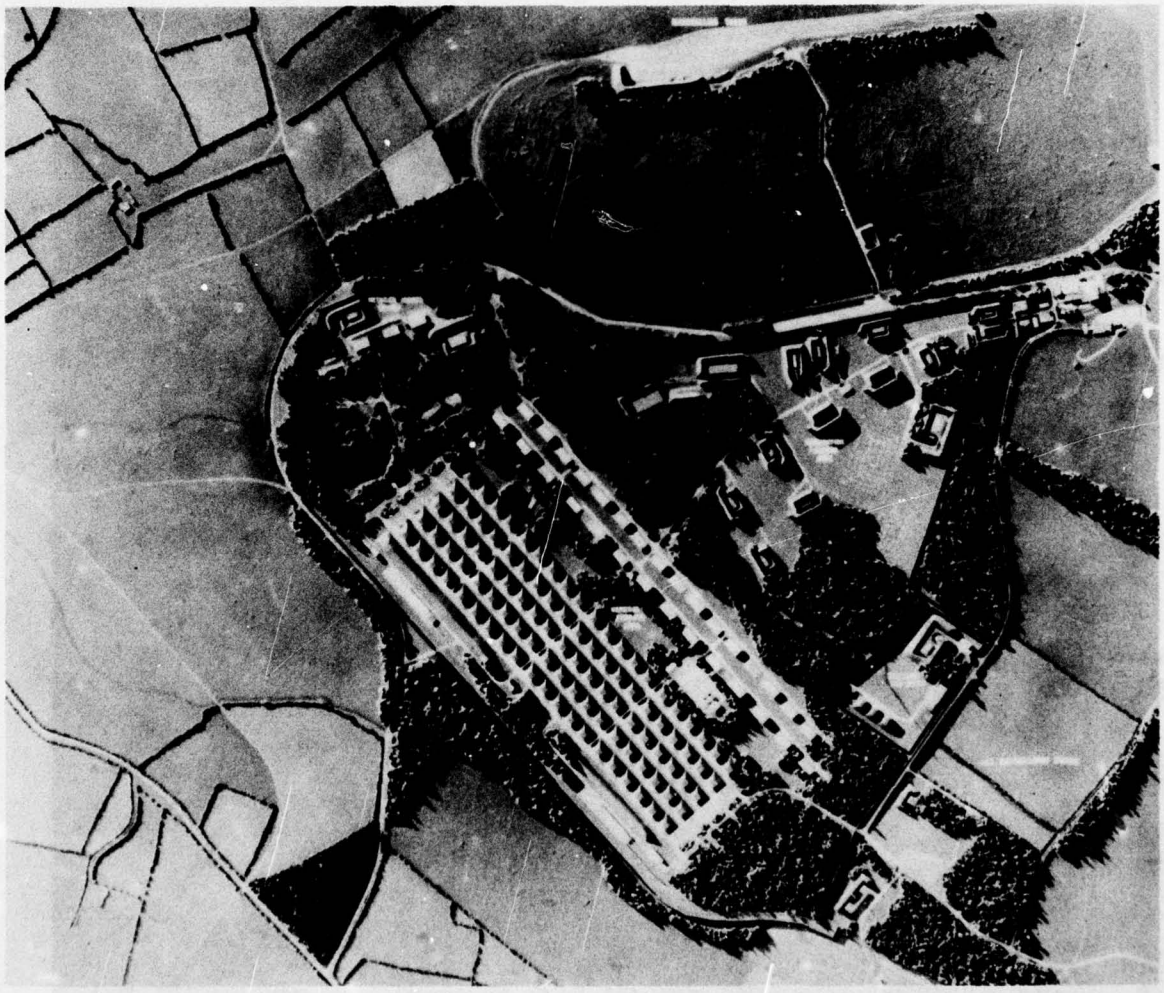
MAGAZINE 6 THE NEXT MORNING

SLIDE 7



OTHER DAMAGE IN THE DEPOT

SLIDE 8



MODEL OF NEW AMMUNITION DEPOT

PSYCHOLOGICAL BEHAVIOR OF EXPLOSIVE WORKERS

A. D. Workum
McDonnell Douglas Astronautics Company
Titusville, Florida

I INTRODUCTION

What I am about to talk about and offer to you is a concept. The explosive worker is better prepared mentally to perform his job in a safe manner than any other industrial employee. Although this is accomplished inadvertently by those responsible for his safety and by his peers, we can examine how his psychological behavior is modified and use this as a basis for reducing industrial injuries throughout industry.

This concept is based upon fact, but is not proven as such. There is not, to my knowledge, any experimental data which proves or strongly supports this concept, primarily because there is so little which has been done on the psychological behavior of workers as it relates to safety. The concept can be extended from the confines of explosive safety to industrial safety in general. It also deserves far more consideration than it is being given, regardless of the area of concern.

II BEHAVIOR

Before examining the explosive worker, let's look at basic human behavior. While the actions of living organisms can be observed and directly measured, the causes of such behavior can only be inferred albeit with a great deal of confidence in many cases. The phenomena of private experience is inaccessible to direct observation; the actions are easily accessible. Thus we can measure the number of times a child says "I love you" to her mother, the number of times she brings her a flower or the number of drawings she brings her from school. We cannot measure the "amount" of love that that child has for her mother - but those actions lead us to the conclusion that the child does in fact "love" her mother. We account for behavior by observing what actions take place; we can only conjecture as to why.

A. Human Behavior is caused and can be changed.

Human behavior is the result of our years of experience, environment, parental influences, peer pressures, social mores. It can be changed by our spouse, social climate, new experiences, our children's ideas, new peer pressures. Man acts as a change agent to other men - change being either temporary or permanent. Man is susceptible to group behavior. For example - you are the last of twenty students to be asked the same question. You are 100% convinced you have the correct answer. The 19 students preceding you all give an answer diametrically opposed to yours. The chances are very good that when called upon, you will conform to the group. Peer pressure and the need for approval can be devastating - whether at home, in school, in the office or in the factory.

B. Human Behavior is learned.

A child need not touch a hot stove more than once or twice before he "learns" that the stove can make his finger hurt. In fact, he may generalize and not want to touch the stove at all until he increases his store of knowledge about hot stoves. A child and an adult also learn that unfulfilled promises are meaningless and empty whether the promise be an ice cream cone, a promotion or better safety equipment.

C. Human Behavior can be predicted, but not guaranteed.

All eight-year old boys do not respond the same way to the same set of stimuli; neither do all 38-year old boys. Teachers learn to modify their course content to meet the needs and capabilities of the group of students. Supervisors must modify their training methods in like manner for the same reasons. It is simultaneously wonderful and frustrating that each of us is different.

D. Human Behavior can be manipulated.

Shaped may be a more palatable term. Parents can increase the frequency of a child's "good behavior" (i.e. approved behavior) and decrease the frequency of his unacceptable behavior and vice versa. Supervisors can increase the frequency of an employe's good workmanship and decrease the frequency of his poor performance or absenteeism, and vice versa. Praising the existence of good workmanship (or safe practices) and the lack of poor performance (or unsafe practices) is far more effective than expecting good work and punishing poor work. Accentuate the positive, eliminate the negative.

III SAFE BEHAVIOR

What does any or all of the preceding have to do with the explosive worker? The explosive worker is in fact a prime example of applying all of the foregoing behavioral concepts; in most cases however, the application is inadvertent or not understood. Understanding how his behavior is shaped, changed and learned should help us in making him a safer worker.

Nowhere in industry does safety play as important a role as it does in the handling and manufacture of explosives. The Army Safety Manual applies strictly to explosives but rivals the OSHA standards in bulk and detail. Explosive safety standards specify everything from the type of concrete to be used in construction of operating buildings to the resistance of ground cables. Operating procedures are highly detailed and specific with far less flexibility than other industrial standards. Explosive workers receive more safety training and re-training than any other group of industrial employes.

There is certainly no question that this emphasis on safety is essential. But this emphasis plays a critical role in influencing the explosive worker's behavior and is really the point of this discussion.

From the first day of employment, the explosive worker is treated different than fellow non-explosive workers. Look at the differences:

1. He receives special safety training, which might include a discussion of the unfortunate consequences of unacceptable safety performance.
2. He wears special coveralls, shoes and glasses - in many cases he changes clothes completely.
3. He works in a building that is built differently, looks unusual, has more exits and is rather drab - especially when again comparing it with that of his non-explosive counterpart. His building is a few hundred to a few thousand feet away from the main plant.
4. He eats, changes clothes and smokes in another separate building, together with all of his peers.
5. His performance is observed carefully, especially in the first few weeks - by his foreman, safety engineer, the worker on his left, the worker on his right.
6. He uses special hand tools and handling fixtures; special grounding devices, shields - he may work remotely behind a concrete blast wall.

Thus the worker is given almost as much attention in preparing him for his job as the facilities he is working in. In fact, he may be the only worker in industry whose attitudes and behavior are given any consideration in a safety program. He is encouraged (strongly) to question anything which he doesn't trust or doesn't believe. He is encouraged to treat explosives with respect but not to be immobilized by fear. He is encouraged to directly confront anyone immediately who is not following the procedure, be he a fellow worker or the vice-president. He is encouraged to question what he considers to be unsafe equipment or the lack of adequate safety gear. Realize it or not, the explosive worker's behavior is shaped (manipulated), changed, learned and predictable - and he is an excellent example ofthe value of participative management.

IV APPLICATIONS

A. We now have a worker who expects to be listened to; we have a worker who understands that his attitudes and behavior are important. Why? Because we have stroked him into believing that. By stroking we mean verbally acknowledging his feelings. Just as sure as mothers stroke little girls into being feminine and fathers stroke little boys into being masculine. Having done this to the worker initially, we have reinforced his good behavior. If we are not very careful, we can also extinguish (terminate) this good behavior by failing to reinforce it - just as a child will discontinue good behavior if we fail to reward it by praise or other tangible methods.

B. If he asks questions about his job or safety equipment or whatever, reinforcement is given by addressing the question, finding out why he asked the question and then answering it. If safety procedures or equipment are asked for, they are most probably needed. Failing to provide what is needed will extinguish the questions and the suggestions and eventually the good behavior. Workers will stop participating if they are asked but not listened to. How long do you think a porpoise will continue to jump through a hoop if the trainer stops giving it a fish?

C. More than any other worker, he needs to know not only that a certain procedure must be followed, but WHY. In fact, the "why" may be more important than the procedure itself. He is taught to expect this treatment - give it to him.

D. Remember that these workers are separated physically from management. You must make sure that this physical separation does not lead to separation of concern on the part of management. I am not suggesting that managers do not care - but face the reality that it is easier to walk out of your office into an adjoining non-explosive assembly area than it is to walk a few hundred feet or drive a mile or two to the explosive area. Encourage management to include the explosive workers in their tours - not only when there is a problem - but just to be seen. At the risk of sounding trite, most of us really want to know that someone really cares.

V CONCLUSION

In my opinion, the most overlooked aspect of safety in industry is the worker himself, specifically his behavior. Regardless of how safe we make the machines, the tools, the facilities and the atmosphere, the worker, if not included in this chain of concern, can, will and does cause injuries. He must be adequately prepared for his job, mentally and physically. We do this with the explosive worker. We train, shape and modify his behavior and attitudes. The reinforcement must be continued so that the good behavior will continue. There is no reason why this same approach cannot be taken in industry in general. We can't provide special clothing and change rooms and buildings for everyone. But we can consider the behavior and attitudes of all our employes. We can consider the stresses of every job and what effect this has on the worker. Safety is not an isolated discipline. It is affected by and in turn affects the functional areas of quality, production, human relations, cost and schedule. We can increase good performance by praising it and eliminate poor performance by praising the lack of it. And good performance is a good safety program.

REPORT OF ABSENCE OF HEALTH HAZARDS ASSOCIATED WITH RDX MANUFACTURE AND USE IN SHELL-LOADING PLANTS

James A. Hathaway, M.D.*
Charles R. Buck, M.D.†
U.S. Army Environmental Hygiene Agency
Aberdeen Proving Ground, MD 21010

---

* Chief, Occupational and Environmental Medicine Division, USAEHA.
† Currently, Medical Officer, Michigan Bell Telephone, Detroit, MI.

The opinions or assertions contained herein are the private views of the authors and are not to be construed as official or as reflecting the views of the Department of the Army or the Department of Defense.

PRECEDING PAGE BLANK-NOT FILMED

I. INTRODUCTION.

Cyclotrimethylene trinitramine (RDX) is a commonly used explosive. In 1972, production in Army plants was estimated at over 80,000 tons.[1] Work experience with RDX during World War II was considerably more favorable than with another explosive trinitrotoluene (TNT). No fatalities were experienced in RDX facilities as opposed to 22 fatalities from TNT.[2 3] Reported toxicity effects of RDX in man have been limited to the central nervous system and have been manifested as epileptic type seizures.[4 5] Toxic effects in animals in addition to central nervous system damage have included degeneration of renal tubular epithelium, fatty degeneration of the liver, and hyaline degeneration in heart muscle.[6]

These toxic effects in animals were produced by acute or chronic feeding studies using large doses of RDX. There appears to be no animal studies of inhalation toxicity and no low dosage studies that would be comparable to RDX levels in the workplace. Also, since methodology to measure airborne concentrations of RDX in the workplace has only recently been developed, older studies of RDX induced seizures were unable to correlate toxic effects to levels of RDX. The threshold limit value (TLV®) for RDX is 1.5 mg/m^3. This level appears to have been arbitrarily selected and based on the dubious assumption that toxic effect levels of RDX might be analagous to TNT, another cyclic, nitrated compound.[7]

The data presented in this paper include a separate analysis of medical tests performed on employees from Army ammunition plants who were originally part of a larger study looking at health effects of both TNT and RDX. Medical test results are compared to RDX levels expressed as time-weighted average exposures to airborne RDX dust. The findings of this paper provide support that the TLV of 1.5 mg/m^3 may indeed be a safe exposure level for RDX.[8]

II. BACKGROUND.

Between 1972 and 1974, three cases of systemic lupus erythmatosus (SLE) were noted in the employee population at one Army ammunition plant. The plant physician observed that this incidence greatly exceeded the incidence in the local community and the US Army Environmental Hygiene Agency (USAEHA) was asked to conduct an evaluation. Based on the structural similarity between RDX and various drugs known to provoke drug-induced SLE, 64 workers considered to have highest RDX exposures were screened. The fluorescent antinuclear antibody test (FANA) was used in an attempt to identify new cases or demonstrate evidence of autoimmune disease.[9] No new cases were identified; however, because of the small number of persons tested, lack of knowledge concerning prevalence of positive FANA results in the normal population and limited understanding of the toxic effects of RDX, additional studies were deemed necessary. The results of a subsequent study is discussed in this paper.

III. METHODS.

Approximately, 2,000 employees (1,000 controls and 1,000 exposed to RDX and/or TNT) at five different Army ammunition plants were randomly selected and asked to voluntarily participate in the study. Methods of selection and definition of exposure categories have been previously described.[8] Plants were selected based on the number of employees engaged in manufacture or load, assemble, pack (LAP) operations utilizing TNT, RDX, or cyclotetramethylenetetranitramine (HMX) or their mixtures.

A USAEHA team visited each plant over a 6-week period. Blood samples were collected, processed and shipped by air (at least daily) to a commercial laboratory. Essentially, all samples were processed by the laboratory within 24 hours of collection. Blood samples were analyzed for serum glutamic pyruvic transaminase (SGPT), serum glutamic oxaloacetic transaminase (SGOT), lactic dehydrogenase (LDH), alkaline phosphatase (ALK PHOS), Bilirubin (total and direct), albumin, glucose, cholesterol, blood urea nitrogen (BUN), total protein, hemoglobin (Hb), hematocrit (Hct), reticulocyte count, and fluorescent antinuclear antibodies (FANA).

FANA determinations were made using the indirect immunufluorescent technique. Frozen mouse liver was used as the substrate. Test results were considered positive if any pattern of nuclear staining was present. Titrations were performed by doubling dilutions of human sera starting at a 1:20 dilution. Both negative and positive controls were employed to validate the reactivity of the mouse liver substrate.

Atmospheric sampling of all types of operations involving exposure to open explosives was conducted at each plant. Because of the intermittent nature of many operations (e.g., pouring explosives), attempts were made to sample over as long as period as possible and generally averaged several hours. Paired samples were collected in the breathing zone of workers with 37-mm, type A, glass fiber filters. The calibrated air samplers were battery-operated MSA Model 6 or Bendix Model C115, belt-mounted pumps operating within a flow range of 1.5 to 2.5 liters per minute.

The filter cassettes were processed for analysis after sampling by extraction of each filter with 5 ml of chromatographic quality benzene. The resulting solutions were analyzed for RDX contents by use of gas chromatography. RDX was analyzed by taking the benzene solutions to dryness and redissolving the residue in 1 ml of chromatographic quality acetone. On microliter injections of the acetone solutions were made on a Tracor model 550 gas chromatograph equipped with an electron capture detector. Injection port temperature was maintained at 200°C, detector temperature at 240°C and column temperature at 210°C. The single column was an all glass system, 6-f

by 1/8-in packed with 3 percent OV-11 on 100-120 mesh GasChrom®Q. Carrier gas flow rate was maintained at 75 mg/minute and detector flow at 72 ml/minute.

IV. RESULTS AND ANALYSIS OF DATA.

Of the 2,022 employees selected for the study, 1,491 participated for an overall response rate of 73.7 percent. Of these, 558 were exposed to RDX alone or in combination with TNT and/or HMX, 863 were unexposed to explosives and the remaining were exposed to TNT only. A total of 69 were exposed to RDX only and 24 were exposed to RDX and HMX.

Table 1 shows the results of FANA tests by race and sex. There were no significant differences between positive results and exposure to explosives. In fact, prevalence of positive FANA tests was higher (3.5 percent) in nonexposed than RDX exposed employees (2.2 percent). Most FANA titers were low (either 1:20 or 1:40). There were four titers of 1:160 and one of 1:80. Of these five individuals, one was exposed only to HMX, one was exposed to RDX and TNT, and three had no exposure to explosives. No cases of SLE were found by followup tests on either exposed or unexposed employees conducted by the individual plants.

TABLE 1. PREVALENCE OF POSITIVE FANA BY RACE SEX GROUP AND EXPOSURE CATEGORY

Exposure Category	Males		Females		Total (n)
	White	Nonwhite	White	Nonwhite	
TNT alone	0.0	0.0	16.6*	0.0†	1.8 (57)
All Other Exposed‡	1.6	0.0	2.9	5.5	2.2 (558)
Nonexposed	3.3	1.7	4.3	4.1	3.5 (863)
Total	2.5	0.8	4.0	4.7	2.9

* One of six exposed.
† None exposed.
‡ Includes all exposures to RDX, HMX either alone or in combination with other explosives (including TNT).

®Chromosorb Q is a registered trademark of Johns-Manville Products Corp., New York, NY.
®GasChrome Q is a registered trademark of Applied Science Laboratories, Inc., State College, PA.

Because TNT exposure is known to have the potential for causing both hematologic and liver function abnormalities, employees having TNT exposure in addition to RDX are excluded from further analyses. Employees having mixed RDX and HMX exposures are included even though analysis of HMX air levels was not performed. Employees having RDX exposure are placed into two categories, those whose exposure was below detectable limits and those with exposures of 0.01 mg/m^3 or greater. Exposures ranged from undetectable to 1.57 mg/m^3. The mean exposure of those 70 employees with detectable exposure was 0.28 mg/m^3. Exposure to RDX alone or in combination with HMX was limited to two plants and involved only white employees. For this reason, a nonexposed control population was selected among white employees at these two plants only. The demographic distribution is shown in Table 2.

TABLE 2. DEMOGRAPHIC DISTRIBUTION OF RDX EXPOSED EMPLOYEES AND UNEXPOSED CONTROLS

Exposure	White Female	White Male
RDX only	26	43
RDX and HMX	0	24
Nonexposed	101	237

The results of blood chemistry determinations and hematological findings are presented in Table 3. Standard deviations were calculated and used in data analysis. They were omitted from the table to improve readability. There were no statistically significant differences between results from exposed and nonexposed workers.

TABLE 3. MEAN LABORATORY VALUES FOR RDX EXPOSED AND NONEXPOSED EMPLOYEES

Laboratory Determination	MALE			FEMALE		
	Non-exposed	RDX Exposure		Non-exposed	RDX Exposure	
		undetected*	0.1 mg/m^3 or over		undetected*	0.1 mg/m^3 or over
Number of Individuals	237	22	45	101	1	25
LDH	173	191	174	184	167	184
AL-PHOS	82	78	80	70	88	67
SGOT	22	25	21	21	10	20
SGPT	21	26	18	13	10	12
Bilirubin	0.5	0.4	0.4	0.4	0.4	0.4
Hb	15.2	14.7	15.2	13.8	13.9	13.8
Hct	47.0	45.6	47.0	41.7	43.3	41.4
Reticulocyte count	0.7	0.9	0.7	1.0	0.3	1.1
Total Protein	7.2	7.2	7.3	7.3	7.6	7.2
BUN	15.5	15.6	16.4	13.2	8.0	12.6
Glucose	94	91	93	92	67	92
Cholesterol	212	202	208	212	206	227

* Some exposure was felt to exist based on professional judgment but no RDX was detected by breathing zone sampling.

The results were also analyzed to determine if an excess of abnormal laboratory determinations might exist among exposed workers. The results of such a comparison for Hb levels is shown in Table 4.

TABLE 4. RELATIONSHIP BETWEEN HEMOGLOBIN VALUES AND RDX EXPOSURE

RDX Exposure	MALE Mean Hb	MALE Number Abnormal*	MALE Number Normal	FEMALE Mean Hb	FEMALE Number Abnormal*	FEMALE Number Normal
undetectable	14.7	3	19	13.9	0	1
0.1 mg/m^3 or over	15.2	4	41	13.8	0	25
not exposed	15.2	15	222	13.8	2	99

* Hb less than 14 gm/100 ml for males, less than 12 gm/100 ml for females.

Similar tables were also constructed for hematocrit, reticulocyte count, LDH, ALK PHOS, SGOT, SGPT, and bilirubin. There were no statistically significant differences between exposed and unexposed groups. Summaries of these results are shown in Tables 5 and 6.

TABLE 5. PROPORTION OF ABNORMAL LABORATORY DETERMINATIONS BY RDX EXPOSURE CATEGORY IN MALES

Determination	RDX EXPOSURE Not Exposed	Undetected	0.1 mg/m^3 or Over
Hb (<14)*	15/237	3/22†	4/45
Hct (<40)	1/237	1/22	1/45
Reticulocyte Count (>1.5)	18/237	3/22	2/45
LDH (>250)	2/237	1/22	0/45
ALK PHOS (>105)	34/237	1/22	6/45
SGOT (>35)	15/237	2/22	0/45
SGPT (>35)	20/237	4/22	2/45
Bilirubin (>1.0)	5/237	1/22	1/45

* Indicates abnormal range.
† Proportion of abnormal results to total number of individuals in exposure category.

TABLE 6. PROPORTION OF ABNORMAL LABORATORY DETERMINATIONS BY RDX EXPOSURE CATEGORY IN FEMALES

Determination	RDX EXPOSURE		
	Not Exposed	Undetected	0.1 mg/m^3 or Over
Hb (<12)*	2/101	0/1†	0/25
Hct (<37)	4/101	0/1	0/25
Reticulocyte Count (>1.5)	19/101	0/1	5/25
LDH (>250)	11/101	0/1	1/25
ALK PHOS (>105)	11/101	0/1	0/25
SGOT (>35)	4/101	0/1	1/25
SGPT (>35)	3/101	0/1	0/25
Bilirubin (>1.0)	4/101	0/1	0/25

* Indicates abnormal range.
† Proportion of abnormal results to total number of individuals in exposure category.

V. DISCUSSION.

The results of medical tests failed to reveal any abnormalities that could be related to RDX work exposure. This is in contrast to dose-related effects on hematologic function with TNT exposure.[8] Because of the state of the economy voluntary turnover of workers had been low and since the end of the Vietnam War, many workers have been involuntarily released leaving the more senior employees to participate in this study. Thus, these apparent nonhealth related variables have biased the study group towards chronically exposed workers. This bias would be expected to enhance the likelihood of identifying a chronic adverse health effect of RDX if it in fact existed. Although the average work exposure to RDX was only 0.28 mg/m^3,, many workers were exposed to levels of RDX between 0.5 and 1.5 mg/m^3. While these results do not prove that 1.5 mg/m^3 of RDX is a safe exposure, they do suggest that it may be a safe level. The results of the industrial hygiene sampling also indicates that it is quite feasible to maintain workplace levels of RDX below 1.5 mg/m^3 in these plants.

This study also failed to reveal any evidence that RDX work exposure might be responsible for induction of SLE. The FANA screening test used in this study has been reported to be positive preceding the development of

chemically-induced SLD.[10 11] An excess incidence of positive FANA titers would have been expected in RDX exposed workers compared to controls if it were responsible for the development of SLE. This did not occur; in fact, the incidence of positive FANA titers was actually found to be lower in exposed workers. Significant FANA titers have been reported to include those which are positive at dilutions of 1:160 or greater with a prevalence of 1/134 in normal blood donors.[12] The prevalence of significant titers in known or suspected cases of SLE was 19/24. Prevalence of significant FANA titers found by this study was 2/558 for RDX or HMX exposed employees and 2/863 for controls. This compares very closely to that found for normal blood donors.

Additional information on the three original cases of SLE at one plant also suggests that they are unrelated to exposure to RDX. Drug induced SLE is characterized by remission following discontinuation of the offending medication.[11] There was no remission of the disease in the three explosive workers who developed SLE following leave of absence from their jobs. If RDX had been responsible for the disease, clinical remission would have been expected. It appears that the three original cases of SLE were either coincidental or related to unknown factors other than RDX exposure at work.

VI. SUMMARY.

Medical testing of RDX exposed workers failed to reveal any evidence of adverse health effects among workers with RDX exposures of up to 1.57 mg/m^3 (0.28 mg/m^3 average). This study particularly attempted to identify abnormalities of the hematologic, hepatic, and renal systems and the presence of autoimmune disease. No differences in the number of abnormalities of these systems between RDX exposed workers and unexposed controls were found, and unexposed controls had a higher (although not statistically significant) prevalence of positive tests for fluorescent antinuclear antibodies than exposed workers.

REFERENCES

1. Small, M. J., and Rosenblatt, D. H., Munitions production products of potential concern as waterborne pollutants -- Phase II, US Army Bioengineering Research and Development Laboratory Technical Report 7404, Aberdeen Proving Ground (1974).

2. McConnel, W. J., Flinn, R. H., and Brandt, A. D., Summary of occupational disease in ordnance plants during World War II, Occup Med, 1:551 (1946).

3. McConnel, W. J., and Flinn, R. H., Summary of Twenty-two Trinitrotoluene Fatalities in World War II, J Ind Hyg Tox, 28:76 (1946).

4. Kaplan, A. S., Berghout, C. F., and Peczenik, A., Human intoxication from RDX, Arch Environ Health, 10:878-883 (1965).

5. Bargott, M., and Crotti, G., Epileptiform attacks as manifestations of professional poisoning with trimethylenetrinitramine (T4), Med Lavaro, 40:107-112 (1949).

6. Von Oettingen, W. F., et al., Toxicity and potential dangers of cyclotrimethylene trinitramine (RDX), J Ind Hyg, 31:21-31 (1949).

7. Documentation of the Threshold Limit Values for Substances in Workroom Air, American Conference of Governmental Industrial Hygienists (1971).

8. Buck, C. R., and Wilson, S. E., Adverse health effects of selected explosives (TNT, RDX), US Army Environmental Hygiene Agency - Occupational Health Special Study No. 32-049-75/76 (1975).

9. Cernik, J. J., Possible occupational disease in explosive workers, US Army Environmental Hygiene Agency - Occupational Health Special Study No. 99-051-73/75 (1974).

10. Alarcon-Segovia, D., and Fishbein, E., Patterns of antinuclear antibodies and lupus activating drugs, J Rheumatol, 2:167-171 (1975).

11. Lee, S. L. and Chase, P. H., Drug-induced systemic lupus erythematosus: A critical review, sem Ar Rheum 5:83-103 (1975).

12. Nisengard, R. J., Jablonska, S., Chorzelski, T. P., Blaszcyk, M., Jarrett, C., and Beutner, E. H., Diagnosis of systemic lupus erythematosus, Arch Dermatol 111:1298-1300 (1975).

TRINITROTOLUENE: A REVIEW OF REPORTED DOSE-RELATED EFFECTS PROVIDING DOCUMENTATION FOR A WORKPLACE STANDARD

JAMES A. HATHAWAY, M.D.
CHIEF, OCCUPATIONAL AND ENVIRONMENTAL MEDICINE DIVISION
US ARMY ENVIRONMENTAL HYGIENE AGENCY
ABERDEEN PROVING GROUND, MARYLAND 21010

The opinions or assertions contained herein are the private views of the author and are not to be construed as official or as reflecting the views of the Department of Army or the Department of Defense.

I. INTRODUCTION. This paper reviews the toxicity of trinitrotoluene (TNT) in both animals and man emphasizing recent studies conducted by the US Army Environmental Hygiene Agency (USAEHA) that are pertinent in establishing safe work exposure standards. Health effects that might be expected to be seen in manufacturing and shell-loading plants in the United States are described. Also, recent articles describing cataracts from low level TNT exposures and the results of screening tests identifying TNT as a mutagen are discussed.

II. TOXICITY OF TNT IN EXPERIMENTAL ANIMALS. Information available on the toxicity of TNT in mammals was extensively reviewed in 1974 by Dacre, et al., for the US Army Medical Bioengineering Research and Development Laboratory (USAMBRDL).[1] This review was updated by Hegyeli in 1976 (personal/communication). Toxic effects in animals include hemolysis of red blood cells, development of anemia, central and peripheral nervous system impairment including peripheral neuropathy, gastritis, disturbances in pancreatic function, fatty degeneration of the liver, hemosiderosis of the spleen, inhibition of phagocytosis, and elevated cholestrol levels in bile. While there is wide variability between species tested, cats and dogs appeared to be more susceptible than rabbits and rats. Hematological and liver function abnormalities occur in all species tested.

III. TOXICITY OF TNT IN MAN. TNT has been the most commonly used explosive since World War I. During World Wars I and II, many deaths were reported in TNT workers from aplastic anemia or toxic hepatitis. The nature of these toxic effects are well described in many articles published between 1920 and 1955.[2-6] Commonly reported but less serious medical problems include gastritis, dermatitis, and anemia.[3,6,7] Other reported toxic effects include hemolytic anemia,[8] nose and throat irritation,[9] red blood cell destruction,[6] methemoglobinemia,[6] leukopenia and leukocytosis,[9] peripheral neuritis,[10] myocardial irregularities,[10] pancreatic dysfunction,[11] and cataract formation.[12]

Occupational exposure to TNT has been reported to occur by inhalation, ingestion, and skin absorption. The relative importance of one route of exposure to the others appears to be variable and probably is dependent on the nature of the work operation, the physical state of TNT, and the personal hygiene and work practices of individual employees. Because skin absorption and accidental ingestion of TNT occurs, it is difficult to formulate dose-response relationships for airborne levels of TNT and observed toxic effects in man.

IV. REVIEW OF REPORTED DOSE-RELATED EFFECTS PROVIDING DOCUMENTATION FOR A WORKPLACE STANDARD. Older reports of adverse health effects often did not include information on workplace levels of TNT. This was particularly true for nonfatal effects which appear to have been accepted as an unfortunate but necessary risk of munitions production. In 1921, Voegtlin stated that 6.0 mg/m^3 of TNT could produce serious health effects implying toxic hepatitis or aplastic anemia.[13] One small, controlled study using pre and post exposure blood tests on 17 exposed workers reported transitory leukocytosis and

moderate eosinophilia from exposures to 0.5-2.0 mg/m^3 of TNT.[6] In an uncontrolled study by Ermakow, et al., published in 1969, it was reported that 122 out of 574 employees had chronic TNT poisoning.[14] Average TNT levels were reported as 1 mg/m^3 and work exposures ranged from 6 to 25 years. Most of the affected workers had functional disorders of the central nervous systems. Twenty-two percent of the affected workers (17) had normochromic anemia and leucopenia, 20 percent (24) had cataracts, and 12 percent (15) had symptoms of hepatitis. No comparisons to unexposed control populations were made. No breakdown of individual TNT exposures was given.

A number of case reports of aplastic anemia from various sources have included exposure levels and these are shown in Table 1.

TABLE 1. CASE REPORTS OF APLASTIC ANEMIA

Number of Cases	Reference Source	Exposure to TNT (mg/m^3)	Skin Contact	Other Exposures
13	3	*	yes	?
1	15	1.1-4.2	yes	no
1	15	2.1-3.4	yes	no
1	15	less than 0.5	yes	? benzene
1	16	nil	?	sulfanilamide
1	16	1.0-3.5	?	acetophenetidin
1	16	1.0-3.5	?	no
1	6	1.1-7.0	yes	no
1	6	3.7-10.7	yes	no
1	6	4.2	yes	no
1	6	5.3-7.0	yes	no

* One-third of persons exposed to TNT over 1.5 mg/m^3. Remaining two-thirds exposed to TNT at levels less than 1.5 mg/m^3. Exact exposure levels were not given.

A number of controlled studies have been reported that provide information on early and subclinical effects of TNT exposure. The first of these was reported by Stewart, et al., in 1945.[17] He obtained preexposure information concerning hematological and hepatic function on 62 students who then performed various jobs in a munitions loading plant. TNT exposure varied between jobs and included skin as well as inhalation exposures. The average exposure during the 4-11 week study period was reported as 0.3-0.6 mg/m^{3}TNT for 52 students working in fill shops and 0.3-1.3 mg/m^3 for 10 students working in both fill shops and melt houses. Coveralls were worn but gloves were not provided. Twenty-seven of 52 fill shop workers developed skin rashes indicating significant skin exposure to TNT. Skin exposure for the 10 students working primarily in the melt houses was minimal but TNT

exposure was generally nearer 1.3 mg/m^3 than 0.3 mg/m^3. Eighty-five percent of the students had decreases in their hemoglobin levels (9.6 percent for fill shop versus 14.2 percent for melt house). Comparable changes also occurred in red blood cell counts. Increases in reticulocyte counts (RTC) were minimal until approximately 48 hours following the termination of TNT exposure when larger increases developed. Both groups of students had significant increases in bilirubin levels. For fill shop workers the bilirubin increased 12 percent in females and 68 percent in males, primarily as indirect bilirubin. For melt house workers (all males) the bilirubin increased 179 percent (both indirect and direct fractions rose). Stewart[17] interpreted these findings to indicate that the hemolytic effects of TNT on red blood cells was more significant than a direct toxic effect on liver function.

A recent study by El Ghawabi, et al., reported Egyptian experience in a TNT manufacturing and shell-loading plant.[18] Thirty-eight TNT workers and 20 unexposed control workers were studied. TNT exposures for workers varied from 0.1-1.2 mg/m^3. Transient exposures at a crushing operation (performed less than daily) ranged from 2-10 mg/m^3. The mean exposure for most workers ranged from 0.2-1.0 mg/m^3. TNT workers had a greater number of upper respiratory (sneezing, sore throat, cough) and gastrointestinal complaints (stomachache, anorexia, constipation, flatulence, nausea and vomiting) than unexposed workers (highly statistically significant). Exposed workers also had significantly lower hemoglobin levels ($p<0.05$). Mean hemoglobin levels were reported as 85 percent (15 grams per 100 ml = 100 percent) in exposed versus 96 percent in controls. There were no significant differences in liver function tests and no cataracts were noted in exposed workers.

The remaining epidemiological studies to be discussed were conducted by USAEHA. In all studies conducted by USAEHA, most workers had potential skin exposure; however, because of the use of powder uniforms, head covers, gloves, clean underwear, double lockers, daily showers, and handwashing before meals, skin exposure was felt to be minimal.

The first study involved 24 TNT exposed workers and 20 unexposed control workers at a TNT washout facility.[19] Unfortunately TNT exposure levels were not calculated as time-weighted-average individual exposures. TNT exposure was undetectable (below 0.03-0.07 mg/m^3) at some operations and ranged from 0.10-2.52 mg/m^3 at other operations. Exposure at bagging operations performed intermittently varied from 0.62-4.00 mg/m^3. The study was initiated because of anemia developing in some workers. Findings included significantly ($p<0.05$) lower hemoglobin, hematocrit, and red blood cell levels in exposed workers and significantly higher reticulocyte counts, eosinophil counts, blood urea nitrogen levels, and glucose levels. Liver function tests were higher in exposed workers than controls but not significantly so.

A followup study at the same facility was performed following introduction of engineering controls to reduce exposures.[20] Twelve workers had liver function tests and hemoglobin levels compared before and after exposure. TNT exposed workers also had post exposure standard medical assessment (SMA-12) results compared to 12 age/race/sex matched controls. Time-weighted average TNT exposures were determined for each individual worker and ranged from 0.08-0.59 mg/m^3 for an 8-hour daily exposure. No differences were noted between pre and post exposure medical tests or compared to unexposed controls.

Another study was initiated at a shell-loading plant following complaints of upper respiratory irritation and dermatitis.[21] Concurrent industrial hygiene surveys noted levels of TNT above 1.5 mg/m^3 at some operations and engineering modifications were suggested and implemented. The study compared preplacement medical tests with tests performed monthly following institution of engineering controls. Forty-three TNT workers were followed for 5 months. During this period, average TNT exposures increased from 0.3 mg/m^3 to 0.8 mg/m^3 as the production rate of the plant was increased. The results of the tests are shown in Table 2.

TABLE 2. MEAN TNT DUST LEVELS, PRODUCTION RATE, AND MEAN LABORATORY TEST VALUES OF EMPLOYEES EXPOSED TO TNT BY MONTH

Test	Preemployment	Dec	Jan	Feb	Mar	Apr
Hgb*	15.6	15.0	15.2	15.1	14.8	14.9
SGOT†	35	35	32	39	58	54
LDH‡	64	53	52	51	106	103
Production Rate (% capacity)	N/A	75	75	75	126	100
Average TNT level (mg/m^3)	N/A	0.3	0.3	0.3	0.8	0.6

* Hemoglobin
† Serum glutamic oxalacetic transaminase
‡ Lactic dehydrogenase

A large number of individual employees were noted to have abnormal test results in March and April when average TNT levels reached 0.8 mg/m^3. These results are shown in Table 3.

TABLE 3. ABNORMAL LABORATORY TESTS BY MONTH

Test	Preemployment	Dec	Jan	Feb	Mar	Apr
Hgb	2	2	2	3	3	1
SGOT	3	1	2	2	10	7
LDH	4	0	0	0	23	13

Abnormal values: Hgb <13.5
SGOT >45
LDH >100

The changes in liver function tests were statistically significant at $P<0.005$ for LDH and at $P<0.01$ for SGOT. Although not statistically significant, hemoglobin levels dropped as exposure increased.

Because the results of studies at these two locations demonstrated significant biological effects from TNT at levels below the TLV of 1.5 mg/m^3, additional study to determine a threshold for effects was felt to be indicated. Such a study was completed and included 533 employees exposed to TNT and 865 employees not exposed to explosives.[22] Of the 533 exposed employees, 58 were exposed to both TNT and RDX (cyclotrimethylene-trinitramine). Concomittant exposure to RDX is not felt to influence TNT exposure on hematologic or hepatic function.[23] Also excellent matches were obtained for age, race, and sex between exposed workers and controls. Time-weighted average TNT exposures were determined for each job at each plant studied. They ranged from undetectable (below 0.01 mg/m^3) to 1.84 mg/m^3. Only 12.2 percent of workers were exposed above 0.5 mg/m^3. Significant findings were limited to the hematologic system even though laboratory tests were performed to check for abnormalities of carbohydrate metabolism, renal function, hepatic function, and the immunological system. Table 4 shows the relationship between Hgb values and TNT exposure.

TABLE 4. RELATIONSHIP BETWEEN HEMOGLOBIN (HGB) VALUES AND TNT EXPOSURE LEVELS BY SEX AND RACE

TNT Exposure Level*	White				Nonwhite			
	Mean HGS	Number Abnormal†	Number Normal	Relative Odds	Mean HGB	Number Abnormal	Number Normal	Relative Odds
				Males				
Not Exposed	15.2	48	495	1.0	14.7	17	42	1.0
0.01 or less	15.0	12	114	1.1	14.7	7	21	0.8
0.02-0.09	14.7	6	34	1.8	14.9	1	5	0.5
0.10-0.19	14.7	9	49	1.9	14.3	6	7	2.1
0.20-0.29	14.4	3	11	2.8	13.9	1	2	1.2
0.30-0.39	14.0	2	3	6.9	13.7	2	2	2.5
0.40-0.49	14.8	4	14	2.9	13.8	7	5	3.5
0.50-0.99	14.4	6	14	6.0	13.6	3	1	7.5
1.00-1.49	13.7	3	5	6.2	--	--	--	--
1.50 & over	--				13.1	1	--	--
				Females				
Not Exposed	13.7	4	160	1.0	13.1	9	88	1.0
0.01 or less	13.6	1	29	1.4	12.9	4	27	1.5
0.02-0.09	13.6	3	17	7.0	13.3	0	7	0.0
0.10-0.19	13.5	0	12	0.0	12.9	3	12	2.5
0.20-0.29	13.8	0	7	0.0	--	0	0	--
0.30-0.39	10.6	1	0	--	--	0	0	--
0.40-0.49	13.6	0	6	0.0	12.8	3	8	3.8
0.50-0.99	13.4	1	5	8.0	13.0	0	3	
1.00-1.49	--	--	--		--			
1.50 & over	12.4	0	1		--			

* in mg/m^3

† Males: abnormal is <14 gm Hgb/100 ml; Females: abnormal is <12 gm Hgb/100 ml.

‡ An estimate of relative risk of abnormal hemoglobin with increasing exposure to TNT. In all cases the odds are relative to those not exposed (e.g., for white males where TNT level is 0.02-0.09: R.O. = $\frac{6 \times 495}{48 \times 34} = 1.8$)

The combined results of all participants are shown in Table 5. Data should be valid, lumping all race/sex categories because of the excellent match of exposed workers to controls.

TABLE 5. RELATIONSHIP BETWEEN HEMOGLOBIN (HGB) and TNT EXPOSURE - ALL PARTICIPANTS

TNT EXPOSURE LEVEL*	NUMBER ABNORMAL†	NUMBER NORMAL	RELATIVE ODDS‡
NONE	78	785	1.0
0.01 or less	24	191	1.3
0.02-0.09	10	63	1.6
0.10-0.19	18	80	2.3
0.20-0.29	4	20	2.0
0.30-0.39	5	5	10.1
0.40-0.49	14	33	4.3
0.50-0.99	11	21	5.3
1.00-1.49	3	5	6.1
1.50+	1	1	10.1

* in mg/m^3

† Males: abnormal is less than 14 gm Hgb/100 ml blood
Females: abnormal is less than 12 gm Hgb/100 ml blood

‡ An estimate of relative risk of abnormal Hgb with increasing exposure to TNT. In all cases, the odds are relative to those not exposed.

$$\text{EXAMPLE: } 0.10\text{-}0.19\text{: R.O.} = \frac{18 \times 78}{80 \times 78} = 2.3$$

Reticulocyte counts (RTC) varied greatly both within exposed workers and controls. Many individuals had low RTC (below 0.5 percent) and many had elevated RTC (above 1.5 percent). Both low and high RTC tended to be more frequent in exposed workers and mean RTC were higher with higher TNT exposures.

V. DISCUSSION. The studies reviewed in this paper clearly demonstrate a need to lower the allowable exposure to TNT from 1.5 mg/m^3. The American Conferences of Governmental Industrial Hygienists proposed lowering the TLV for TNT to 0.5 mg/m^3 in 1976, based primarily on the results reported by Morton, et al.[21]

Case reports of aplastic anemia usually indicated a variable exposure to TNT between 1-10 mg/m^3. Time-weighted exposures were probably somewhere between these levels in the 2-3 mg/m^3 range (see Table 1). Reports of aplastic anemia from exposure to less than 1.5 mg/m^3 of TNT are difficult to evaluate. Two case reports[13 15] were complicated by other chemical exposures and McConnel's report[2] failed to give precise exposure data and was complicated by significant but unquantitified skin exposure. The implication made by Eddy[15] that TNT induced aplastic anemia is a rare response occurring only in unusually susceptible individuals may well be true. Wintrobe describes this phenomenon as occurring from exposure to an ever increasing number of compounds, the occurrence of aplastic anemia not appearing to be related to the amount of a chemical to which an individual has been exposed.[24] Even though TNT-induced aplastic anemia probably occurs in senstitive or susceptible workers, the history of munitions production suggests that for groups of workers as opposed to individuals, the level of TNT exposure is important. As work conditions improved from World War I to World War II, the number of cases of aplastic anemia declined dramatically. While it is impossible to determine an absolutely safe level of TNT exposure below which no aplastic anemia could develop, it appears that reduction of work exposures to TNT to generally below 1.5 mg/m^3 has nearly eliminated the problem over the past 25 years.

The most striking finding in reviewing all epidemiologic studies from Stewart[17] to Buck[22] is the occurrence of hematologic and hepatic abnormalities at TNT levels well below 1.5 mg/m^3. The most persistent findings are mild reductions in the hemoglobin, hematocrit, and red blood cell counts of exposed individuals. This reduction is probably due to destruction of red blood cells by hemolysis[6 13] and is a direct toxic effect of TNT and/or its metabolites. This effect appears to occur at quite low levels of TNT exposure and is compensated for by increased production of red blood cells reflected in higher reticulocyte counts. This compensatory factor may account for the minimal findings in the study by Buck[22] and the statistically insignificant hematological findings by Morton.[21] The more dramatic hematologic findings noted by Stewart[17] and Friedlander[19] occurred when previously unexposed employees started working with TNT either for the first time or following a long interval of no exposure. This observation coupled with the data presented in Tables 4 and 5 strongly suggests that exposure to 0.20 mg/m^3 or more of TNT may result in a slight reduction of hemoglobin levels. The results of El Ghawabi[18] and Stewart[17] tend to confirm this finding. At exposure levels below 0.5 mg/m^3 the minimal effects on hemoglobin, hematocrit, etc., appear to be well compensated and produces no apparent ill health.

Exposure to TNT above 0.5 mg/m^3, particularly as a new or sudden increased exposure, may result in liver function abnormalities. In Morton's study this occurred at 0.8 mg/m^3 and in Stewart's study was most pronounced at 1.3 mg/m^3. Whether or not liver function would have returned to normal if exposures continued longer was not clear from these studies but the absence of liver function abnormalities in Buck's[22] and El Ghawabi's[18] reports suggests that this may indeed happen.

Information on TNT produced cataracts is very scanty. All reports of TNT cataracts have come from the Russian or Eastern European literature. The studies appear to have identified the prevalence of disease states in TNT workers without comparison to unexposed controls. The absence of reported cataracts in western literature tends to cast doubt on the uncontrolled Russian studies but it is uncertain whether cataracts have been looked for except by El Ghawabi who did not find any.[18] However, the very high prevalence of cataracts of 45.3 percent reported in one article[25] suggests that this potential problem area should be explored further.

Biologic effects clearly occur from quite low TNT exposures. Effects appear to occur at 0.2 mg/m^3 and perhaps at even lower levels as well. Whether workplace standards should be set below the no effects level or not involves a philosophical decision. Morton and Buck have both proposed 0.5 mg/m^3 of TNT as an appropriate standard.[21 22] While this level is above a no effects level, it does appear to be satisfactory based on the "best available evidence, that no employee will suffer material impairment of health or functional capacity even if such employee has regular exposure to the hazard ... for the period of his working life."[26]

Future studies may pose different problems for TNT production and use. TNT has recently been identified as a bacterial mutagen.[27] Limited carcinogenicity testing of TNT has been reported with negative findings.[28 29] However, additional testing to more definitively determine the carcinogencity of TNT is under consideration by the US Army Medical Bioengineering Research and Development Laboratory and may be conducted in the near future. The finding of mutagenic effects of TNT is not surprising, as many other compounds which have produced aplastic anemia have been identified as carcinogens particularly likely to produce leukemia.[30 31] Should future research efforts demonstrate carcinogenic potential for TNT an exposure level which would effectively prevent cancer would have to be determined.

VI. SUMMARY. The toxicity of TNT was reviewed with emphasis on studies providing correlation between work exposures and adverse health effects. Numerous adverse health effects including upper respiratory and gastrointestinal complaints, anemia, liver function abnormalities, and possibly aplastic anemia have been noted at TNT levels below the current standard of 1.5 mg/m^3. Mild biological effects particularly reduction in hemoglobin levels or red blood cell counts (not generally producing anemia) have been noted at exposure as low as 0.2 mg/m^3. A workplace standard of 0.5 mg/m^3 is suggested for protection against adverse health effects.

REFERENCES

1. Dacre, J. C. and Rosenblatt, D. H., Mammalian Toxicology and Toxicity to Aquatic Organisms of Four Important Types of Waterborne Munition Propellants - An Extensive Literature Review, USAMBRDL Technical Report 7403 (1974).

2. McConnel, W. J. and R. H. Flinn, Summary of Twenty-two Trinitrotoluene Fatalities in World War II, *J Ind Hyg Tox*, 28:76-86 (1946).

3. Voegtin, C., C. W. Hooper and J. N. Johnson, Trinitrotoluene Poisoning - Its Nature, Diagnosis, and Prevention, *J Ind Hyg*, 3:280-292 (1921).

4. Crawford, M. A., Aplastic Anemia Due to Trinitrotoluene Intoxication, *Br Med J*, 2:430-437 (1954).

5. Hart, W. L., E. B. Ley, V. D. Scroggie, E. A. Johnson, and J. H. Eddy, A Report of Four Cases of Aplastic Anemia, *Ind Med*, 3:895-899 (1944).

6. Cone, T. E., A Review of the Effects of Trinitrotoluene (TNT) on the Formed Elements of Blood, *J Ind Hyg Tox*, 26:260-263 (1944).

7. Lawrence, R. D., Discussion on Trinitrotoluene Poisoning, *Proc Roy Soc Med*, 35:553-560 (1942).

8. Djerassi, L. S. and L. Vitany, Haemolytic Episode in G6 PD Deficient Workers Exposed to TNT, *Br J Indus Med*, 32:54-58 (1975).

9. Fairhill, L. T., *Industrial Toxicology*, 2nd Ed., Hafner Publishing Company, New York, pp 352-354 (1969).

10. Soboleva, L. P., State of the Myocardium During Chronic Trinitrotoluene Intoxication, *Gig Tr Prof Zabol*, 13:47-48 (1969).

11. Kleiner, A. I., N. M. Vasilenko, I. S. Sonkin, I. S. Ostrovskanya, L. N. Yashina and N. L. Liss, Functional Disturbances of the Pancreas of Toxico-chemical Etiology, *Gig Tr Prof Zabol*, 10:15-18 (1974).

12. Hassman, P. and J. Juran, Trinitrotoluene Cataract, *Sb Ved Pr Lek Fak Karlouya Univ*, 14:261 (1974).

13. Voegtlin, C., C. O. Hooper, and J. M. Johnson, Trinitrotoluene - Its Nature, Diagnosis, and Prevention, *J Ind Hyg Tox*, 28:239-254 (1921).

14. Ermakov, E. V., V. S. Aizenshadt, and B. B. Ventsenostsev, Chronic Trinitrotoluene Poisoning (Clinical Picture and Pathogenesis of Neuro-vegetative Disturbances), *Soviet Med*, 32:119-122 (1969).

15. Eddy, J. H., Aplastic Anemia from Responses Well Below 1.5 mg/m^3, *JAMA*, 125:1169-1172 (1944).

16. Sieves, R. F., R. L. Sturp, and A. R. Monaco, Aplastic Anemia Following Exposure to Trinitrotoluene, *Occup Med*, 1:351-382 (1946).

17. Stewart, A., L. T. Witts, G. Higgins, and J. R. P. O'Brien, Some Early Effects of Exposure to Trinitrotoluene, *Brit J Ind Med*, 2:74-82 (1945).

18. El Ghawabi, S. H., G. A. Ibrahim, M. F. Gaber, A. E. Harooni, M. B. Mansoor, R. El Owny, And M. M. Soudi, Trinitrotoluene Exposure, *Ain Shams Med J*, 25:545-549 (1974).

19. Friedlander, B. R., K. W. Vorphal, R. E. Glenn, and P. T. Jordan, Occupational Health Special Study No. 99-020-74, APE 1300 Wash-out Plant, USAEHA (1974).

20. Hathaway, J. A., Occupational Health Special Study No. 32-005-75, TNT Washout Facility, USAEHA (1975).

21. Morton, A. R., M. V. Ranadive, and J. A. Hathaway, Biological Effects of Trinitrotoluene from Exposure Below the Threshold Limit Value, *Am Ind Hyg Ass J*, 37:56-60 (1976).

22. Buck, C. R. and S. E. Wilson, Adverse Health Effects of Selected Explosives (TNT, RDX), Occupational Health Special Study No. 32-049-75/76, USAEHA (1975).

23. Hathaway, J. A. and C. R. Buck, Health Hazards Associated with RDX Manufacture and Use in Shell-loading Plants, Department of Defense Explosives Safety Seminar, 14-15 September 1976.

24. Wintrobe, M. M., et al., *Clinical Hematology*, 7th Ed., Lea & Febiger, Philadelphia, PA (1974).

25. Zakharova, P. and J. Juran, Clinical Picture in Chronic Trinitrotoluene Poisoning, *Gig Tr Prot Zabel*, 15:28-32 (1971).

26. Public Law 91-596, Williams-Steiger Occuational Safety and Health Act of 1970, Section 6(b)(5).

27. Won, W. D., L. H. DiSalvo, and J. Ng, Toxicity and Mutagenicity of 2,4,6-Trinitrotoluene and its Microbial Metabolites, *Appl Envir Microb*, 31:576-580 (1976).

28. Hartwell, J. L., *Survey of Compounds Which Have Been Tested for Carcinogenic Activity*, 2nd Ed., Public Health Service Publication No. 149, p 91 (1951).

29. Schepars, G. H., Lung Tumors of Primates and Rodents, *Ind Med*, 40(1):48-52 (April 1971), 40(2):23-31 (May 1971), 40(3):8-22 (June 1971).

30. Dameshek, W., Riddle: What do Aplastic Anemia, Paroxysmal Nocturnal Hemoglobinuria (PNH) and "Hypoplastic" Leukemia have in Common? *Blood*, 30:251-254 (1967).

31. Kjeldsberg, C. R. and H. P. Ward, Leukemia in Arsenic Poisoning, *Ann Int Med*, 77:935-937 (1972).

A DESIGN-AID & COST ESTIMATE MODEL FOR SUPPRESSIVE SHIELDING STRUCTURES

George D.C. Chiang
Richard S.K. Pei

USDARCOM Intern Training Center - ALMC
Red River Army Depot
Texarkana, Texas

ABSTRACT

A computer cost model of suppressive shielding structures has been constructed and is presented in this paper. This model consists of design-aid and cost estimation programs which, with proper inputs, calculates and outputs specific design and cost variables of suppressive structures. Design variables include the following: venting coefficient, plastic bending and yield moments of beams, penetration of primary fragments, and the total effective thickness of plates. Cost output variables include: material, fabrication, welding, and total costs of panels, frame, door, and foundation of a cubical suppressive structure. A description of the model and its construction details are briefly reviewed in the paper.

This design-aid and cost estimate model may be used to serve as an important base of the value engineering study for a suppressive structure.

INTRODUCTION

Suppressive shielding is a relatively new concept in safeguarding personnel and property in case of an accidental explosion during manufacturing, transporting, and storing of explosives.

A suppressive structure (sometimes called a suppressive shield) is an enclosure of a hazardous operation so that if an accidental explosion occurs, primary damage will be to the enclosed space. It can also be used in storing or transporting ammunitions and explosives of various strengths.

Most suppressive structures basically consist of four major structural components: frame, panel, door, and foundation. Except for the foundation which is mostly made of reinforced concrete, most of the other parts are made from structural steel. In the event of an explosion, the primary fragments are to be stopped by the steel and the pressure venting is done by using perforated plates and air spaces between structural elements such as angle bars, W beams, pipes, etc.

The economic value of suppressive structures must be determined before they can replace the other barriers. An economic feasibility analysis was

PRECEDING PAGE BLANK-NOT FILMED

conducted by the U.S. Army Material Systems Analysis Agency at Aberdeen Proving Ground in June 1974 (1)*. This study distinguished the effects of different levels of protection and inherent differences in costs between suppressive structures and concrete wall structures. Saving-to-investment ratios (S/I) are computed in this study upon foregoing walls and installing suppressive walls for the modernization of 105mm melt-pour complex at the Lone Star Army Ammunition Plant.

Parallel to the economic analysis is the value engineering study, which is the systematic application of recognized techniques to identify the function of a product or service, and establish a monetary value for that function and provide the necessary function reliably at the lowest overall cost (2). The most opportune time to apply value engineering is during research and development so that any cost savings can be realized throughout the complete life cycle of the end product (3).

The basic objectives in applying value engineering during research and development are to reduce the high cost of development, the subsequent cost of production, and the consequent costs related to operation and maintenance(3).

A design-aid and cost estimate model is developed in this paper to serve as an important base of the value engineering study for a suppressive structure. This computerized model can be separated into two parts, i.e., the design-aid model and the cost estimate model. The design-aid model includes the functional requirements parameters, the material parameters, and the geometric parameters while the cost estimate model handles the economic parameters of a suppressive structure.

The objective of the design-aid model is to assist the designer of a suppressive structure by rapidly changing quantities of various design variables in order to achieve an economic design and satisfy design criteria. Rather than manually calculating various design variables, existing equations are programmed in a computer language and results are obtained.

The same approach is used in the cost estimate model. Making use of the similarities between suppressive structures, the cost estimate model is developed based on the cost information obtained from the results of cost estimates of various suppressive structures (5,6,7,8). Through the use of this model, the designers of suppressive structure can possibly save some of their valuable time for decision making rather than performing repeated manual calculations of cost and design quantities.

---

*Denotes the number of reference used from list of references.

A COST MODEL FOR SUPPRESSIVE STRUCTURES

The importance of value engineering in the development stage of suppressive structures has been mentioned. A cost model is developed to serve as an important base of the value engineering study for a suppressive structure. This cost model consists of functional requirement parameters, material parameters, geometric parameters, and economic parameters.

Functional Requirement Parameters

The functional requirement parameters in a cost model are generally specified values from an analysis of the entire suppressive structure conducted before the actual design stage. These parameters are generated from the four basic requirements: safety, prevention of mechanical failure, environment and logistic support.

The primary parameters which are associated with safety requirements are the safe distance and pressure from the explosive charge to the person, structures, and equipment outside the suppressive structure. Other parameters such as degree of fire, chemical effects, etc., from any hazards produced by an explosion will also be considered.

The plastic yield strength of structural members and penetration of fragments are the basic design parameters which relate to the fracture failure mode.

Temperature, humidity, noise, and degree of ventilation are required environmental parameters.

Time between inspections, maintenance time (painting, joining), etc., are logistic support parameters.

These functional requirement parameters are primarily influenced by factors external to the structure, and, depending on which particular structure and its application, these parameters can possibly be dependent upon each other.

Geometric Parameters

Geometric parameters of the cost model include the following:

1. Geometric dimensions from selected configurations of steel angles, Z beams, W beams, tubes and panels which consist of single, stiffened, multibay and yawed shapes.

2. Geometric dimensions of frame, foundation and supporting structures such as doors, etc.

3. Spacing between panels, size and distribution of holes in panels, etc. The geometry of an element of suppressive structures can always be uniquely defined by specifying certain independent geometric parameters.

Material Parameters

Weight, density, yield strength, ultimate strength, elastic modulus, Poisson's ratio, toughness, unit cost, and temperature coefficient may be considered as the important material parameters. In conducting a design study, the selection of a material for a structural element will be, in general, based primarily on the material parameters which are explicitly defined. These parameters are mostly dependent on each other and on chemical and physical structures in available materials.

Economic Parameters

The economic parameters for a suppressive shield include the following:

1. The cost of structural steel shapes at the fabrication shop. The base price of the shapes varies with prices charged by the mills according to the size, weight, shape, quantity of steel required, and the cost of transporting the steel to the shop.

2. The cost of preparing drawings for use by the shop in fabricating the steel. The total cost of the drawings is charged to the steel supplied for a job. The cost per unit weight of steel will vary with the total cost of drawings and the quantity of steel supplied.

3. The cost of handling and fabricating the steel shapes into finished members. It will vary considerably with the operation performed, the sizes and shapes of the members, and the extent to which the operations are duplicated on similar members. For welded connections, the fabricating operations may include cutting, some punching for temporary bolt connections, milling, beveling, and shop welding.

4. The cost of shop painting, if required. The approximate costs of applying a coat of paint to structural steel for various types of members and structures and of the labor are included.

5. The cost of shop overhead, sales, and profits.

6. The cost of transporting structural steel. It will vary with the quantity of steel, the method of transporting, and the distance from the shop to the job site.

7. The cost of erection, including equipment, labor, bolts, rivets, or welding.

8. The cost of field painting the steel structure.

9. The cost of job overhead, general overhead, insurance, taxes and applications.

The Cost Equation

The cost parameters described above are closely related to design variables and parameters of a suppressive shield. With these costs parameters,

a cost equation (3) is given as below:

$$\text{Cost (\$)} = f\left[\begin{pmatrix}\text{Functional}\\ \text{requirement}\\ \text{parameters}\end{pmatrix}, \begin{pmatrix}\text{Material}\\ \text{parameters}\end{pmatrix}, \begin{pmatrix}\text{Geometric}\\ \text{parameters}\end{pmatrix}, \begin{pmatrix}\text{Economic}\\ \text{parameters}\end{pmatrix}\right]$$

This equation is used as the design-aid and cost estimate model in this report. The design-aid portion of this model will include most parameters of the functional requirement parameters, the material parameters, and the geometric parameters while the cost estimate portion handles the economic parameters of the cost equation.

The Model

The computerized model can be separated into two parts, i.e., the design-aid model and the cost estimate model. Figure 1 is a flow chart of the use of the model (3). According to a specific suppressive shielding application, some application requirements are established and a donor system can be prescribed. From this donor system, weight and speed of primary fragments (4,5,6), blast pressure loading (4,5,6), and venting requirements (4,5) are obtained. A suppressive shielding structure is designed and its structural elements are checked against their response to dynamic loading and functional design requirements. Detailed evaluations of the technical requirements are made and their effect on total performance is determined. Through design review some design alternatives are chosen, the evaluation of alternatives and cost effectiveness analysis are followed to produce a cost effective suppressive shield (3).

The objective of the design-aid model (a computer aided design of a suppressive structure) is to assist the designer of a suppressive structure by rapidly changing quantities of various design variables and parameters in order to achieve an economic design and to satisfy design requirements. Rather than manually calculating various design variables and parameters, existing design equations are programmed in a computer language and results are obtained.

The same approach is proposed for the cost estimation of suppressive structures. The conventional method of cost estimation is a mostly manual method. Such cost estimating processes are being used in estimating costs of various suppressive structures (7,8,9 & 10). This process is:

1. According to the drawings (blue prints) of a suppressive structure, its major components, i.e., panel, door, frame, and foundation are formed. All structural elements of each substructure together with their materials, major characteristics and geometric dimensions are listed on a table. The primary measuring quantities associated with these elements are dimensions, volume, material density, and weight from which the material cost can be priced.

2. The manufacturing costs related to making structural elements are estimated from suggested manufacturing processes of each structural element by reliable sources and references (11, 12, 13, 14). The most important quantities in estimating manufacturing costs are processing time, and use of equipment. These costs are obtained from experienced personnel and some reliable references for each measuring quantity.

Making use of the similarities between suppressive structures, a programmed cost estimate model is developed based on the cost information obtained from the results of the conventional method. This cost estimate model is combined with the design-aid model to form the general value cost model for suppressive structures. This model serves as an important tool for a value engineering study. Hopefully, through the use of this model, the designers of suppressive structures can save some of their valuable time for decision making rather than performing repeated manual calculation of cost and design quantities.

Model Testing

The validity of a computer model must be tested before it can be used confidently. Testing can be done by comparing results computed by use of the model to existing data. The design-aid model and the cost estimate model were tested separately against design and cost estimate results of the Categories III and IV suppressive shields obtained from references 9, 16, and 17. A comparison of computer model results and analytic results are shown in table 1 for the design-aid model, and table 2 for the cost estimate model. Result of comparison shows that the model outputs are, in most cases, in excellent agreement with analytic data.

MODEL DESCRIPTION

The computer model is formed by a main program and ten subroutines written in FORTRAN IV computer language (22). The main program contains the input and the output portions of the model. It coordinates the proper sequence of calculations by calling the appropriate subroutines. The proper sequence of calculations the program will execute depends on the options specified. The three options in the model are described below. Necessary inputs of each option and their formats and a user's guide can be obtained from reference 22.

Options

A. OPTION #1

This option will print a list of W beams, angle bars, and steel pipes, designated by beam type numbers 1, 2, and 3 (see figures 3, 4 and 5). These beams are tested in the model so that all the beams on the list are strong enough to withstand input pressure loading. These beams that are listed are standard size beams selected from reference 15. The advantages of using standard size beams in steel construction are that they are readily available

and are more economical than non-standard size beams. With the list provided by this option, the designer can choose the beam(s) after reviewing the economical and technical aspects of its usage in a suppressive structure.

The computer procedures for option number 1 are summarized as follows:

1. A deck of data cards containing dimensions for standard sized beams are inputted and stored.

2. Required inputs are read.

3. Plastic yield moment and plastic bending moment of each beam are calculated and compared (see description of subroutine BMDSN).

4. The beams whose plastic yield moment is greater than or equal to its plastic bending moment are listed.

B. OPTION #2

This option is used when direct cost estimation of a cubical suppressive structure is desired. Required inputs are the overall dimensions of the structure to be estimated, type of panel configuration of the structure, and cost parameters associated with each type of panel configuration. Cost quantities that will be calculated are listed below:

1. Material cost, fabrication cost, and welding cost for each component, i.e., frame, panel, door, and foundation.

2. Total material cost, total welding cost, and total fabrication cost.

3. Total frame cost, total panel cost, total door cost, total foundation cost, and total cost.

These cost quantities are calculated by the cost estimate model to be described later in this section.

C. OPTION #3

This option includes both suppressive shielding panel design and cost estimation. The design-aid model is first used to calculate design parameters such as venting coefficient (effective venting area ratio), plastic yield moment and plastic bending moment of beams, effective thickness of perforated plates required for both the quasi-static pressure and the impulsive pressure, and length of fragment penetration. These values are then used as inputs to the cost estimation model for cost estimation of the same cost quantities described in option #2.

Steps and calculation executed in this option are as follows:

1. Read the required input quantities.

2. Calculate venting coefficient required (call subrouting VENT).

3. Calculate and compare plastic yield moment and plastic bending moment of beams (call subroutine BMDSN).

4. Calculate effective thickness of perforated plates required and number of holes required for proper pressure venting (call subroutine PLDSN).

5. Calsulate length of fragment penetration in steel (call subroutine FRGPN).

6. Set total thickness of perforated plates to the larger of effective thickness of perforated plates from step 4 and length of fragment penetration calculated in step 5.

7. Calculate thickness of each perforated plate.

8. Estimate cost of structure using quantities from steps 1, 2, 3 and 7 (call subroutine COSTM).

Four types of panel configurations are programmed for use in options #2 and #3 (see figure 2). They are made of combinations of fragment stopping and pressure venting elements such as angle bars, W beams, pipes, and perforated plates.

Subroutines in the model are constructed for calculations of design and cost variables. They can be divided into two groups: The design-aid subroutines and the cost estimate subroutines. The design-aid subroutines are coordinated by the main program to form the design-aid model. The cost estimate subroutines themselves constitutes the cost estimate model.

The design-aid subroutines include: BMDSN (beam design), PLDSN (plate design), VENT (venting), FRGPN (fragment penetration), and RTPOL (root of polynomials). Except for the subroutine RTPOL which is adopted from the scientific subroutine package of the IBM 1130 computer, all the other design-aid subroutines are developed from design equations obtained primarily from references 4 and 20.

The cost estimate subroutines are: COSTM (cost model), FRAME (frame costs), PANEL (panel costs), DOOR (door costs) and FNDTN (foundation costs). These subroutines are based on estimates obtained from reference 6.

The Design-Aid Subroutines

A. SUBROUTINE BMDSN

This subroutine calculates, compares, and returns the plastic yield moment and the plastic bending moment of beams or bars of a suppressive panel. An error code of 0 will be returned if plastic yield moment of the beam is larger or equal to the plastic bending moment of the beam. Otherwise an error code of 1 will be returned. Equations for calculating plastic bending moment (M_p) and plastic yield moment (M_{py}) are given as follows * (4):

---

* All symbols used in equations in this section and their corresponding variable name used in the model are listed and explained in table 3.

$$M_p = \frac{i_r^2 b^2 L^2 S_f}{16N A_B W_o \rho} \quad (1)$$

$$M_{py} = 1.05 \times 41600.0 \times \frac{I_B}{C_B} \quad (2)$$

Three types of beams are considered in this subroutine. Their dimensions and the formula (21) for their moment of inertia (I_B), cross-sectional area (A_B), and section modulus (C_B) are shown in figures 3, 4, and 5. The correct formula for I_B, A_B, and C_B will be used when type of beam is specified.

The symbol b, in equation 1 stands for the stacking distance between two panel beams (see figures 6, 7, and 8). It is related to the venting area ratio (e_p) and the dimension of the beam. Formulas are found for all three types of beams (5, 19).

1. Type I - I beams (figure 6)

$$b = a + 1. \quad (3)$$

$$C_p = \frac{a}{2b}. \quad (4)$$

Substituting equation 4 into 3

$$b = 2 e_p b + 1. \quad (5)$$

Solving for b

$$b = \frac{1}{1-2e_p}. \quad (6)$$

2. Type II - Angle bars (figure 7)

$$b = 1.414 (t + a). \quad (7)$$

$$e_p = \frac{a}{b}. \quad (8)$$

Combining equations 7 and 8

$$b = 1.414 t + 1.414 e_p b. \quad (9)$$

Solving for b

$$b = \frac{1.414 t}{1 - 1.414 e_p}. \quad (10)$$

3. Type III - Pipes (figure 8)

$$e_p = \frac{a}{b} . \tag{11}$$

$$b = d_o + a. \tag{12}$$

Combining equations 11 and 12

$$b = d_o + b\, e_p. \tag{13}$$

$$b = \frac{d_o}{1 - e_p} . \tag{14}$$

B. SUBROUTINE PLDSN

Minimum effective thickness of perforated plates required to withstand blast pressure loading and number of holes necessary for pressure venting requirement are the output variables.

Minimum effective thickness (h_{ep}) is obtained by first calculating thickness for both impulsive pressure loading (h_d) and thickness for quasi-static loading (h_q). A relationship for h is given as below (20):

$$\left(\frac{\dot{\epsilon}_r X}{\sqrt{\sigma_y \rho h_d^2}}\right)^2 = \frac{\pi^{N-1}}{2N}\left\{1+\left[\frac{X}{Y}\right]^2\right\}\frac{W_o}{h_d} + \frac{2}{3}\left(\frac{X}{Y}\right)\frac{W_o}{h_d}$$

$$+ \frac{3^{N-1}\pi^2}{16N^2}\left[1+\left(\frac{X}{Y}\right)^2\right]\left(\frac{W_o}{h_d}\right)^2 + \frac{2N}{3}\left(\frac{X}{Y}\right)\left(\frac{W_o}{h_d}\right)^2. \tag{15}$$

Equation 15 can be simplified to:

$$Ah_d^3 + Bh_d^2 - C = 0 \tag{16}$$

Where

$$A = \left\{\frac{\pi^{N-1}}{2N}\left[1+\left(\frac{X}{Y}\right)^2\right] + \frac{2}{\sqrt{3}}\left(\frac{X}{Y}\right)\right\} W_o \rho\, \sigma_y ,$$

$$B = \left\{\frac{3^{N-1}\pi^2}{16N^2}\left[1+\left(\frac{X}{Y}\right)^2\right] + \frac{2N}{\sqrt{3}}\left(\frac{X}{Y}\right)\right\} W_o^2 \rho\, \sigma_y ,$$

$$C = i_r^2 X^2.$$

Roots of equation 16 are found by using subroutine RTPOL. Thickness for impulsive loading (h_d) is set equal to the largest positive root calculated by RTPOL.

As for h_q, it can be found from the following equation (20):

$$\frac{P_q}{\sigma_y}\left(\frac{X}{h_q}\right)^2 = \frac{\pi^{2/N}}{2^{4/N^2}}\left[1+\left(\frac{X}{Y}\right)^2\right] + \frac{4^{2N-3}}{\sqrt{3}\,\pi^{2(N-2)}}\left(\frac{X}{Y}\right)$$

$$+ \frac{3^{N-1}\,4^{N-2}\,\pi^{2(3-N)}}{32}\left[1+\left(\frac{X}{Y}\right)^2\right]\frac{W_o}{h_q}$$

$$+ \frac{2^{N-1}\,4^{2N-3}}{\sqrt{3}\,\pi^{2(N-2)}}\left(\frac{X}{Y}\right)\frac{W_o}{h_q}. \qquad (17)$$

Solving for h_q, equation 17 becomes:

$$D\,h_q^2 + E\,h_q + F = 0 \qquad (18)$$

Where

$$D = \frac{\pi^{2/N}}{2^{4/N^2}}\left[1+\left(\frac{X}{Y}\right)^2\right] + \frac{4^{2N-3}}{3\,\pi^{2(N-2)}}\left(\frac{X}{Y}\right),$$

$$E = \left\{\frac{3^{N-1}\,4^{N-2}\,\pi^{2(3-N)}}{32}\left[1+\left(\frac{X}{Y}\right)^2\right] + \frac{2^{N-1}\,4^{2N-3}}{\sqrt{3}\,\pi^{2(N-2)}}\left(\frac{X}{Y}\right)\right\}W_o,$$

$$F = -\frac{P_q X^2}{\sigma_y}.$$

The roots of quadratic equation 18 are:

$$h_{q\,1,2} = \frac{-E \pm \sqrt{E^2 - 4DF}}{2D} \tag{19}$$

We want h_q to be the largest positive root. Therefore:

$$h_q = \frac{-E + \sqrt{E^2 - 4DF}}{2D} \tag{20}$$

After both h_d and h_q are calculated using equations 16 and 20, minimum total thickness of panel plates (h_{min}) is then set equal to the larger of h_d and h_q.

$$h_{min} = \max \left[h_d , h_q \right]. \tag{21}$$

To compensate for the effect of venting space on perforated plates, h_{ep} (minimum effective thickness of each perforated plates) is found by (5):

$$h_{ep} = \frac{h_{min}}{n\,(1 - e_p)}. \tag{22}$$

Number of holes required for each perforated plate is calculated by dividing venting area by area of holes:

$$N_{hole} = \frac{A_p\, e_p}{A_{hole}}. \tag{23}$$

C. SUBROUTINE VENT

The venting coefficient (e) is calculated and returned in this subroutine. "e" is the total venting coefficient for all perforated plates or beams. For venting coefficient of each individual plate, the following formula is used (5):

$$\frac{1}{e} = \frac{1}{e_p} + \frac{1}{e_p} + \frac{1}{e_p} + \cdots\cdots \tag{24}$$

And for n plates

$$\frac{1}{e} = \frac{n}{e_p} \tag{25}$$

And therefore:

$$e_p = ne. \tag{26}$$

Relationship for "e" is given by (4):

$$P_s = 967.3 \frac{W_c^{2/3} \; e^{1/2}}{R^{3/2} \; X^{1/2}} \tag{27}$$

Solving for "e", equation 27 yields:

$$e = \left(\frac{P_s \; R^{3/2} \; X^{1/2}}{976.3 \; W_c^{2/3}} \right)^2 \tag{28}$$

The following constraints are imposed on equations (27) and (28):

$$0.0263 \leq e \leq 0.60. \tag{29a}$$

$$0.323 \leq \frac{X}{R} \leq 1.77. \tag{29b}$$

$$4.27 \leq \frac{R}{W_c^{1/3}} \leq 17.5 \tag{29c}$$

These limits are checked in the subroutine and if they are exceeded, corresponding error messages will be returned. For design purposes, "e" is set equal to 0.0263 if its value is less than 0.0263 and is set equal to 0.6 if its value is greater than 0.6.

D. SUBROUTINE FRGPN

With weight and velocity of primary fragments as input variables, depth of fragment penetration in steel is calculated. It is the thickness of steel that would be necessary to stop penetration of primary fragments. The equation used in its calculation is (5):

$$P = 0.112 \; M_f^{1/3} \; \frac{V_f^{4/3}}{1000}. \tag{30}$$

This subroutine is also programmed to return residual velocity (V_r) and residual weight of fragment (M_r) if the thickness of steel target is specified. The value of the residual fragment velocity will be negative if the target thickness is thicker than required. Formula for these two quantities are given as (5):

$$\log_{10} (M_f - M_r) = a_o + \sum_{i=1}^{4} a_i \log_{10} X_i \quad (31)$$

$$\log_{10} (V_f - V_r) = b_o + \sum_{j=1}^{4} b_j \log_{10} X_j \quad (32)$$

Where X_1 = Thickness of steel target.

X_2 = Weight of primary fragment.

X_3 = Secant of angle between direction of fragment and normal of the target.

X_4 = Velocity of primary fragment.

And $a_o = -2.2776$; $b_o = 3.9064$

$a_1 = 0.2885$; $b_1 = 0.9496$

$a_2 = 0.9145$; $b_2 = -0.3603$

$a_3 = 0.1958$; $b_3 = 1.2842$

$a_4 = 0.6394$; $b_4 = 0.1929$

Upon solving for M_r and V_r, equations 31 and 32 become:

$$M_r = M_f - 10^{(a_o + \sum_{i=1}^{4} a_i \log_{10} X_i)} \quad (33)$$

$$V_r = V_f - 10^{(b_o + \sum_{j=1}^{4} b_i \log_{10} X_j)} \quad (34)$$

Cost Estimate Subroutines

A. SUBROUTINE COSTM

This subroutine and the other cost subroutines constitutes the cost estimate model. It calls the other four cost subroutines (FRAME, DOOR, PANEL, and FNDTN) for material cost, welding cost, and fabrication cost of each of the four components of a cubical suppressive shield. With these cost quantities, it computes values for total welding cost, total material cost, total fabrication cost, total cost of door, total cost of frame, total cost of panels, total cost of foundation, and total cost of structure (grand total).

The cost estimate model is developed for cubical suppressive structures. Category IV suppressive shields represent a typical type of cubical suppressive structure with well defined features. Therefore, it is used as a base for the construction of the cost estimate model.

A few assumptions are made upon the construction of the cost estimate model:

1. All structures have the same basic structural components as the Category IV suppressive shield.

2. All dimensions of structural components varies linearly with the overall dimensions of the suppressive structures.

3. Fabrication cost and welding cost of structure are linearly related to the material cost of structure.

According to a cost estimate of a Category IV suppressive shield (9), 26¢ is a reasonable figure for average cost per lb. of steel of structure which includes such cost items as base price at mill, extras and delivery to shop, drafting, shop coat paint, trucking to job site, erect and plumb, crane and minor errection equipment, and a field coat paint. This figure does not include welding cost and fabrication cost of the structure. Welding cost includes cost of weld, welding equipment, and labor cost for welding. Fabrication cost is the cost of equipment and labor for cutting, grinding, and smoothing of structural members into proper shapes and sizes. The cost estimate (9) showed that the average welding cost and the average fabrication cost (per pound of steel) are 31¢ and 11¢ respectively.

In the cost estimate subroutines, the weight of each component of the suppressive structure will first be computed. Then the material cost of each component are determined by:

$$\text{Material Cost} = \text{Weight of structure} \times \text{Unit cost of steel} \tag{35}$$

where

Unit cost of steel = \$0.26 per pound (may be adjusted according to current price).

From material cost, fabrication cost and welding cost of each component can be calculated:

$$\text{Fabrication cost} = \text{Material cost} \times \text{Fabrication cost factor} \tag{36}$$

$$\text{Welding cost} = \text{Material cost} \times \text{Welding cost factor} \tag{37}$$

where

$$\text{Fabrication cost factor} = \frac{\$.11}{\$.26} = 0.39, \tag{38}$$

and

$$\text{Welding cost factor} = \frac{\$.31}{\$.26} = 1.16. \tag{39}$$

To compensate for the effects of inflation and other economic factors that may affect the cost of the structure, values for unit cost of steel, fabrication cost factor, and welding cost factor can be changed easily and accordingly.

B. SUBROUTINE FRAME

This subroutine computes and returns the material cost, the fabrication cost, and the welding cost of the frame of a cubical suppressive shield.

The frame of a cubical suppressive shield consists mainly of W beams, angle bars, and plates. Total weight of W beams constitutes approximately 49% of the total weight of frame (9). Therefore, if we can estimate the weight of W beams, then:

$$\text{Total weight of frame (lb)} = \text{Total weight of W beams} \times \frac{100}{49} . \quad (40)$$

Total weight of W beams is directly related to total volume of W beams:

$$\text{Total weight of W beams} = \text{Total volume of W beams} \times \text{density of steel} \quad (41)$$

where

$$\text{Density of steel} = 490 \text{ lb/cu. ft.} \quad (42)$$

Volume of W beam is calculated from length of W beam and its cross sectional area:

$$\text{Volume of W beam} = \text{Length of W beam} \times \text{cross section area.} \quad (43)$$

Fourteen vertically situated W beams account for 65.7% of total length of all W beams needed (9). Therefore, total length of W beams can be calculated by:

$$\text{Total length of W beam} = 14 \times \frac{100}{65.7} \times \text{Height of frame.} \quad (44)$$

By combining equations 41, 43, and 44, we have the equation for the total weight of frame.

$$\begin{aligned}\text{Total weight of frame} = 21.7 &\times \text{Height of frame} \\ &\times \text{Cross sectional area} \\ &\times \text{Density of steel} \\ &\times \frac{100}{49} . \end{aligned} \quad (45)$$

At this point, equations 35, 36, and 37 are used to calculate material cost, welding cost and fabrication cost of the frame.

C. SUBROUTINE PANEL

This subroutine is programmed to return material cost, fabrication cost, and welding cost of all the panels of a suppressive structure. Four types of panel configurations are also programmed to be consistent with the design-aid model (see figure 2).

Total weight of a panel is contributed by the following groups of structural elements:

1. Fragment stopping and pressure venting elements - W beams, angles, steel pipes, and perforated plates.

2. Channels.

3. Miscellaneous items - bars and plates.

The kind of fragment stopping and pressure venting elements used in a panel is determined by the panel configuration chosen. Two channels are used for the frame of a panel. Miscellaneous items such as lifting eyes and reinforcement bars are needed to complete the panel.

Miscellaneous items contribute very little to the total weight of a panel. It only amounts to about 13% of the total weight of panel (9). For an estimate of its weight, we will consider it as a percentage of the weight of channel:

$$\text{Weight of miscellaneous items} + \text{Weight of channel} = 2.8 \times \text{Weight channel}. \quad (46)$$

Thus, total weight of channel can be estimated by:

$$\text{Total weight per panel} = 2.8 \times \text{weight of channel} + \text{weight of fragment stopping and pressure venting elements.} \quad (47)$$

Weight of channel is computed as follows:

$$\text{Weight of channels} = \text{Number of channels} \times \text{Length of each channel} \times \text{Cross sectional area of channel} \times \text{Density of steel.} \quad (48)$$

A reasonable estimate of cross sectional area of channel is by its width:

$$\text{Cross sectional area} = 0.58 \times \text{Width of channel.} \quad (49)$$

Therefore, equation 48 becomes:

Weight of channel = Number of channels
x Length of channel x 0.58
x Width of channel
x Density of steel (50)

where

Length of channel = Height of panel.

Width of channel = Thickness of panel.

Number of channels = 2.

Weight of fragment stopping and pressure venting element (W_{fp}) varies with the type of panel configuration specified:

1. Panel configuration #1:

W_{fp} is equal to the sum of weight of angles 1, weight of angles 2, and weight of perforated plates.

W_{fp} = Weight of angles 1 + Weight of angles 2
+ Weight of perforated plates. (51)

where

Weight of angles 1 = Number of angles 1 x Cross sectional area 1
x Panel length x Density of steel. (52)

Weight of angles 2 = Number of angles 2 x Cross sectional area 2
x Panel length x Density of steel. (53)

Weight of perforated plates = Number of perforated plates
x Thickness of each plate
x Panel height
x Panel length
x Density of steel. (54)

2. Panel configuration #2:

In this configuration, W_{fp} equals to the weight of angles plus the weight of perforated plates.

$$W_{fp} = \text{Weight of angles} + \text{Weight of P. plates} \quad (55)$$

where

$$\text{Weight of angles} = \text{Number of angles} \times \text{Cross sectional area} \times \text{Panel length} \times \text{Density of steel.} \quad (56)$$

$$\text{Number of angles} = \text{Panel height}/b. \quad (57)$$

Number of perforated plates is computed using equation 54.

3. Panel configuration #3:

Only W beams are used in this configuration. Therefore, W_{fp} is equal to the weight of W beams.

$$W_{fp} = \text{Weight of W beams} = \text{Number of W beams} \times \text{Panel length} \times \text{Cross sectional area of W beam} \times \text{Density of steel} \quad (58)$$

where

$$\text{Number of W beams} = 2\,(\text{panel height}/b) - 1. \quad (59)$$

4. Panel configuration #4:

Two rows of steel pipes of the same size are used for stopping fragments and venting pressure. W_{fp} for this configuration can be calculated as follows:

$$W_{fp} = \text{Weight of pipes} = \text{Number of pipes} \times \text{Panel length} \times \text{Cross sectional area of pipe} \times \text{Density of steel} \quad (60)$$

where

Number of pipes = 2 (panel height/b) - 1. (61)

Now, total weight of the panel can be computed by using equations 47, 50, and the equations of W_{fp} for all four types of panel configurations. Welding and fabrication cost of panel can be found by using equations 35, 36, and 37.

D. SUBROUTINE DOOR

This subroutine calculates the material cost, welding cost and fabrication cost of a suppressive door. The structure of a suppressive door is basically the same as a panel. It has the same basic elements: fragment stopping and pressure venting elements, channels, and miscellaneous items. Due to these similarities, equations derived for panel costs are applicable for door costs also. All equations for W_{fp} (equations 51 to 61) will be the same with panel length and panel height changed to door length and door height. Extra channels are needed for the door edges. Therefore, the equation for weight of channel becomes:

Weight of channel = 2 (door height and door length)

x 0.58

x Door thickness

x Density of steel. (62)

Special items such as trolleys and trolley tracks, changes equation 46 to:

Weight of miscellaneous items
+ = 2.04 x Weight of channel. (63)
Weight of channel

Thus

Total weight of door = 2.04 x Weight of channel + W_{fp}. (64)

Material cost, welding cost, and fabrication cost of door are then computed using equation 35, 36, and 37.

E. SUBROUTINE FNDTN

This subroutine is used to estimate material cost, welding cost, and fabrication cost of the foundation of a cubical suppressive shield. Material cost includes cost of concrete and miscellaneous items. Cost of concrete can be calculated from the total volume of concrete used:

Cost of concrete = Volume of concrete x Unit cost of concrete. (65)

Where

Unit cost of concrete = $28.71 per cu. yd. of concrete.

Volume of concrete needed is computed by given length of foundation (l_f), width of foundation (w_f), and height of foundation (h_f). Figure 9 represents the concrete portion of the foundation and therefore:

$$\text{Volume of concrete} = (l_f\ w_f\ h_f) - (l_f - 2t_f) \times (w_f - 2t_f) \times (h_f - t_f). \quad (66)$$

Cost of miscellaneous items approximately equals to 33% of cost of concrete (9). Therefore:

$$\text{Total material cost of foundation} = 1.33 \times \text{Cost of concrete.} \quad (67)$$

Welding cost is equal to zero since no welding is necessary. Fabrication cost of foundation is obtained by using equations 67 and 36.

CONCLUSIONS

The design and cost information of a suppressive structure are the necessary backbones to support value engineering activities (3). The design-aid and cost estimate model presented in this paper provides a valuable mean for obtaining such informations. The advantages of using this model have been discussed previously. However, suppressive structures are still under development. New ideas and design concepts are continuously being generated by researchers and designers of suppressive projects. Therefore, the model must be periodically revised according to new technology and developments to provide up to date design and cost information. The design-aid model could be easily modified for new design concepts. Corresponding changes in the cost estimate model could also be done to provide a complete value model.

This model is developed only for cubical suppressive structures. The model can be modified to include design and cost estimates of different types of suppressive structures.

One should clearly define desired objectives, functions, or purposes that the suppressive structures are to be accomplished when applying this model. All functional requirements essential to the attainment of desired goals must then be identified. Furthermore, various alternatives of concepts for accomplishing the functions have to be reviewed and enhanced. A cost-effective suppressive shield should result through the use of this model and other value engineering activities outlined in reference 3.

LIST OF REFERENCES

1. Dean Westerman, Bruce Archer, Micholas Hagis, Charles Hoover, James Liu, James McKivigan, William Michael, Lambert Sebastiani, William Webster, "An Economic Feasibility Analysis of Suppressive Structures", U.S. Army Material Systems Analysis Agency, Aberdeen Proving Ground, Maryland, June 1974.

2. Definition by the Society of American Value Engineers.

3. George D. C. Chiang and Richard S. K. Pei, "Ground Work for Value Engineering in Development of Suppressive Structures", DARCOM Intern Training Center, RRAD, Texarkana, Texas, June 1975.

4. W. E. Baker, P. S. Westine, J. A. Cox and E. D. Esparza, "Analysis and Preliminary Design of A Suppressive Structure for A Melting Loading Operation", Technical Report No. 1, Contract No. DAAD 05-74-C-0751, SWRZ, San Antonio, Texas, March 1974.

5. J. Coutinho, N. Hagis, and J. Liu, "Current State of Design Procedures for Suppressive Structures", AMSAA Interim Note No. R-29, Aberdeen Proving Ground, Maryland, May 1974.

6. "Structures to Resist the Effects of Accidental Explosions", Army TM 5-1300, June 1969.

7. James R. Jones and George D. C. Chiang, "Cost Investigation of Suppressive Shielding Structures (Category I)", DARCOM Intern Training Center, RRAD, Texarkana, Texas, Jul7 1975.

8. George D. C. Chiang, "Cost Estimating for 1/4 Scale Category I Suppressive Structure", DARCOM Intern Training Center, RRAD, Texarkana, Texas, July 1975.

9. Phillip T. Haltom, "Cost Estimation of Category IV Suppressive Shield", DARCOM Intern Training Center, RRAD, Texarkana, Texas, July 1975.

10. Roy Zimmerman and George D. C. Chiang, "Category 6 Suppressive Structure Cost Estimate", DARCOM Intern Training Center, RRAD, Texarkana, Texas, May 1975.

11. Venon, I. R., "Realistic Cost Estimating for Manufacturing", Society of Manufacturing Engineering.

12. Peurifoy, "Estimating Construction Costs", McGraw-Hill

13. Miles, L. D., "Techniques of Value Analysis and Engineering", McGraw Hill

14. Department of Defense, "Army Programs Cost Estimating Guide (Methods and Factors)", LD 29764.

15. "Manual of Steel Construction", AISC.

16. P. O. Fassnacht, "Category 3 Suppressive Shielding Structure Preliminary Design", NASA-NSTL, Bay St. Louis, Mississippi, Sept 1974.

17. P. O. Fassnacht, "Category 4 Suppressive Shielding Structure Preliminary Design", NASA-NSTL, Bay St. Louis, Mississippi, Sept 1974.

18. Robert E. Wandrey, "Category 5 Suppressive Shielding Structure Preliminary Design", NASA-NSTL, Bay St. Louis, Mississippi, Sept 1974.

19. "SWRI Panel Designs", Southwest Research Institute, 1974.

20. P. S. Westine and W. E. Baker, "Energy Solutions for Predicting Deformations in Blast Loaded Structures", DOD 16th Annual Explosives Safety Seminar, Sept 1974.

21. Gerner A. Olsen, "Elements of Mechanics of Materials", third edition, Prentice Hall, Inc.

22. Richard S. K. Pei, "A Design-Aid and Cost Estimate Model for Suppressive Shielding Structures", ITC-02-08-76-413, DARCOM Intern Training Center, RRAD, Texarkana, Texas, Dec 1975. (An Engineering Report for Master of Engineering Degree from Texas A&M University).

ACKNOWLEDGMENTS

The authors express their deep appreciation to Dr. David Katsanis, who provided encouragement and generous assistance throughout the course of this study. Also, we gratefully acknowledge the members of the Suppressive Shielding Branch, Edgewood Arsenal, for their technical assistance. Sincere gratitude is extended to Dr. S. Bart Childs for his valuable suggestions and discussions during the study.

This work was supported in part by the Edgewood Arsenal.

DESIGN-AID MODEL

CATEGORY III

Variables	(Symbol)	Analytic	Computer Model
1. Venting Coefficient	e	0.0263	0.02629
2. Thickness (Impulsive realm)	h_d	0.404 in.	0.4349 in.
3. Thickness (Quasi-static realm)	h_q	0.335 in.	0.3545 in.
4. Dffective thickness/plate	h_{ep}	0.131 in.	0.1215 in.
5. Fragment Penetration	P	0.13 in.	0.10 in.
6. Plastic yield moment x Area	(M) x A_B	3800.0 lb.-in.^{3}	3793.5 lb.-in.^{3}
7. Plastic bending moment x Area	(M_p) x A_B	730.0 lb.-in.^{3}	830.9 lb.-in.^{3}

CATEGORY IV

1. Venting Coefficient	e	0.0263	0.0264
2. Thickness (Impulse)	h_d	0.160 in.	0.1717 in.
3. Thickness (Quasi-static)	h_q	0.178 in.	0.1874 in.
4. Effective thickness/plate	h_{ep}	0.055 in.	0.0528 in.
5. Plastic yield moment x Area	(M) x A_B	79000.0 lb.-in.^{3}	87002.0 lb.-in.^{3}
6. Plastic bending moment x Area	(M_p) x A_B	1200.0 lb.-in.^{3}	1024.0 lb.-in.^{3}

TABLE I. COMPARISON OF CALCULATIONS OF CATEGORY III AND IV DESIGNS

COST MODEL

CATEGORY IV

ELEMENT	PARAMETERS	ESTIMATED VALUES ($)	COMPUTER MODEL VALUES ($)
Panel	Material	14508	14577
	Welding	22540	16908
	Fabrication	7714	5685
Door	Material	1340	1350
	Welding	1293	1566
	Fabrication	291	526
Frame	Material	6381	6501
	Welding	2034	7541
	Fabrication	1578	2535
Foundation	Material	314	343
	Fabrication	100	33
Whole Structure	Material	22554	22772
	Welding	25867	26018
	Fabrication	9684	8881
	GRAND TOTAL	58106	57672

TABLE II. COMPARISON OF COST ESTIMATING FOR CATOGORY IV SUPPRESSIFE STRUCTURE

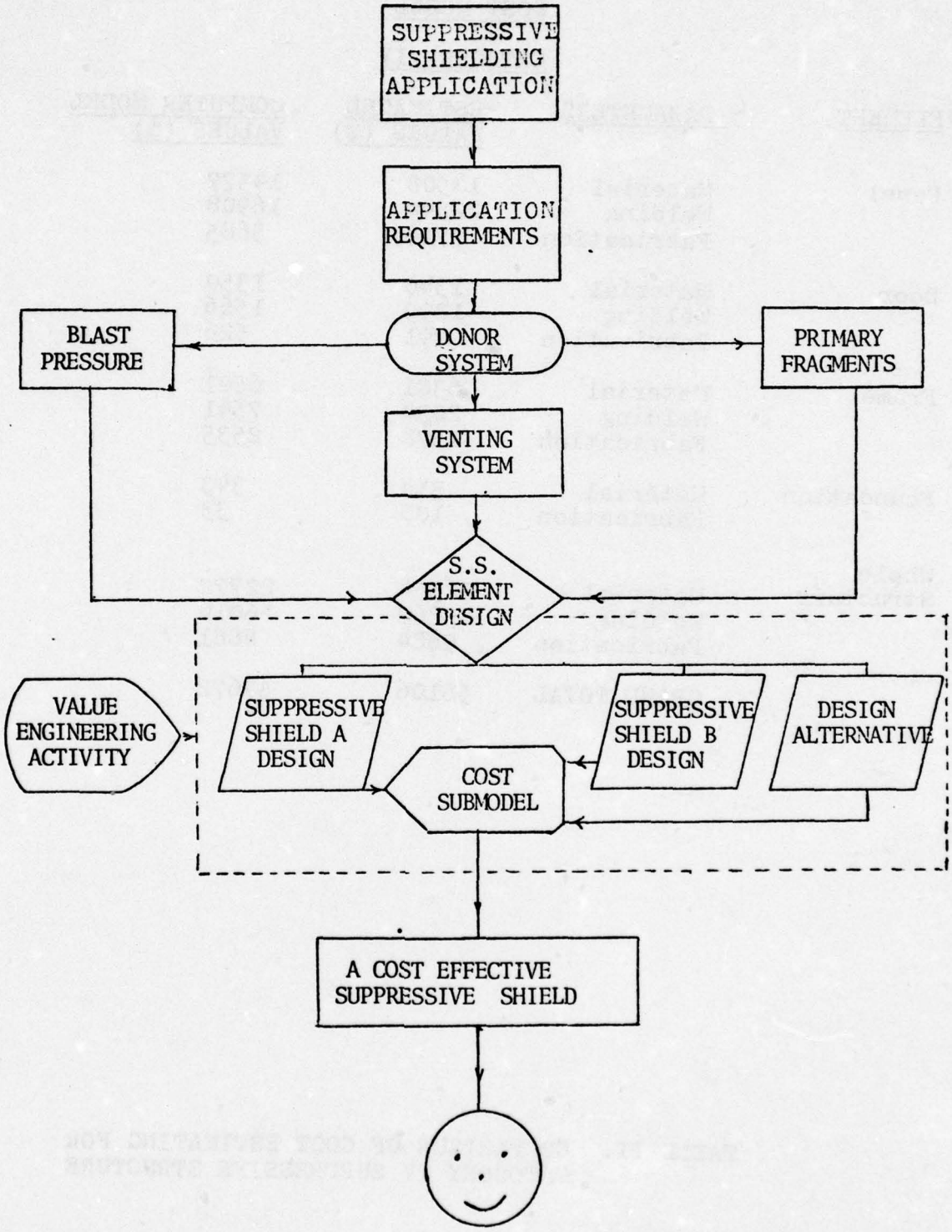
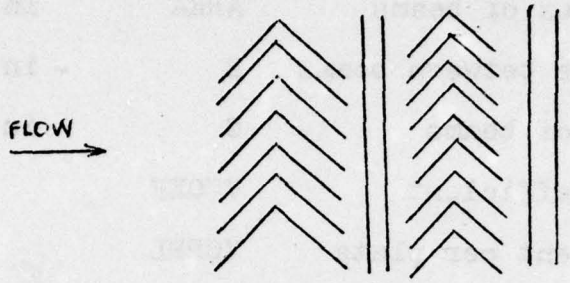
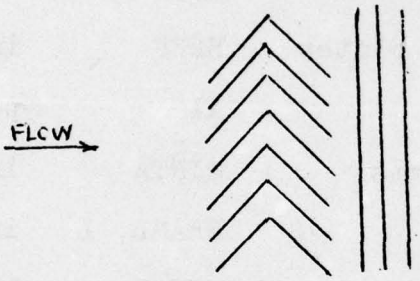


FIGURE 1 - A COST MODEL OF SUPPRESSIVE STRUCTURES

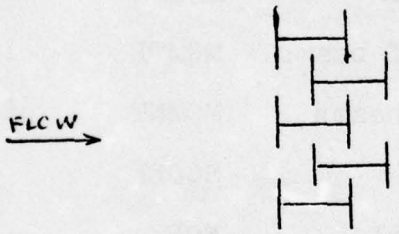
Panel Configuration #1 - Angles, Plate, Plate, Angles, Plate, Plate.



Panel Configuration #2 - Angles, Plate, Plate, Plate



Panel Configuration #3 - W Beams, W Beams



Panel Configuration #4 - Pipes, Pipes

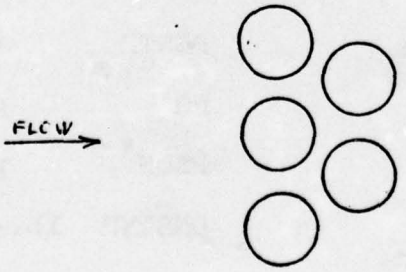


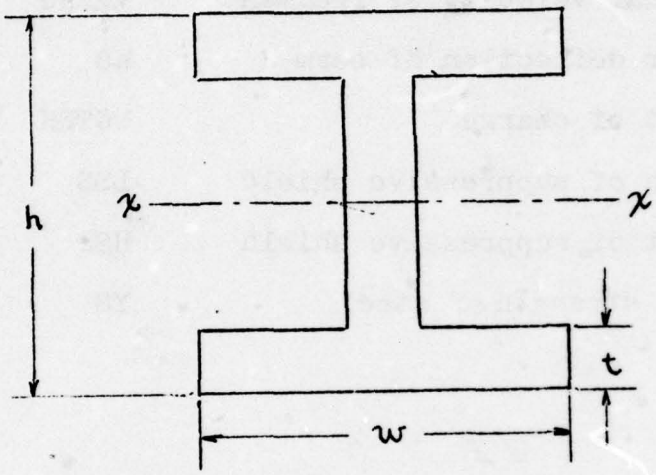
FIGURE 2 - PANEL CONFIGURATIONS

SYMBOL	EXPLANATION	MODEL NAME	DIMENSION
A_B	Cross-section area of beams	AREA	in^2
b	Stacking distance between beams	B	in
C_B	Section modulus of beams	C	in
e	Total venting coefficient	VCOEF	
e_p	Venting coefficient per plate	VCPPL	
h_d	Thickness for impulsive loading		in
h_{min}	Minimum thickness of plates	HMAX	in
h_{ep}	Effective thickness for plates	HEFF	in
i_r	Impulsive pressure	AI	psi-sec
I_B	Moment of inertia of beams	MINTA	in^4
L	Length of beam	BEAML, L	in
M_f	Weight of primary fragment	WPFAG	lb.
M_r	Weight of residual fragment	WRFAG	lb.
M_p	Plastic bending moment of beams	MOMTP	in-lb.
M_{py}	Plastic yield moment of beams	MOMNT	in-lb.
N	Support coefficent	SCOEF	
n	Number of plates per panel	NOP	
N_{hole}	Number of holes on plates	NHOLE	
P	Penetration of fragments	PENTH	in
P_q	Quasi-static pressure	PQ	psi
P_s	Side on safety pressure	PSON	psi
ρ	Mass density of steel	DNSTYM	$lb.-sec^2/in^4$

TABLE III. SYMBOLS FOR EQUATIONS

SYMBOL	EXPLANATION	MODEL NAME	DIMENSION
R	Safety distance to personnel	R	Ft.
S_f	Safety factor	SF	
V_f	Velocity of primary fragment	VPFAG	ft/sec
V_r	Residual velocity of fragment	VRFAG	ft/sec
W_o	Center deflection of beam	WO	in
W_c	Weight of charge	WGTCH	lb.
X	Length of suppressive shield	LSS	ft.
Y	Height of suppressive shield	HSS	ft.
σ_y	Yield strength of steel	YS	psi

TABLE III. SYMBOLS FOR EQUATIONS (CONTINUED)

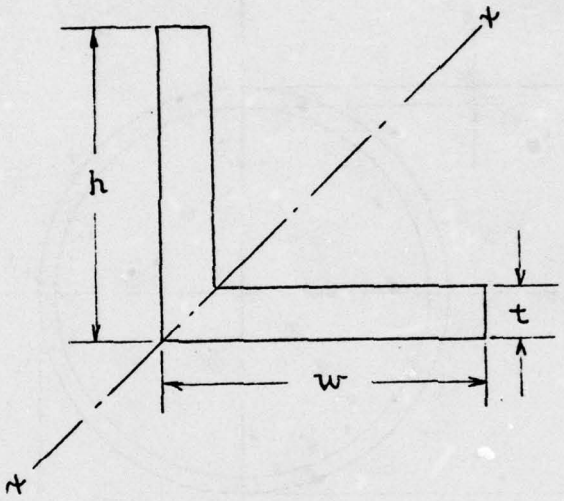


$$A_B = wh - (h - 2t)(w-t)$$

$$I_B = I_{xx} = 2\left[\frac{wt^3}{12} + (wt)\left(\frac{h-t}{2}\right)^2 + \frac{t\left(\frac{h-2t}{2}\right)^3}{12}\right]$$

$$C_B = \frac{h}{2}$$

FIGURE 3 - TYPE I BEAM - W BEAM



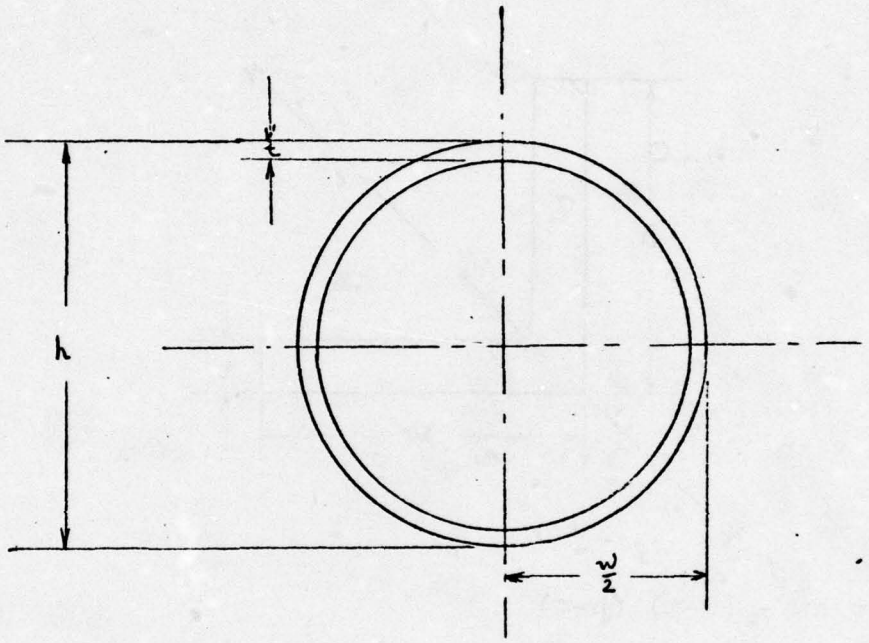
$$A_B = hw - (w-t)\,(h-t)$$

$$I_B = I_{xx}$$

$$= (0.70711)^2 \; \frac{2}{3} \left(h^3 t + w t^3\right) - \frac{w^2 h^2 t}{4\,(h+w)}$$

$$C_B = \frac{w}{1.414}$$

FIGURE 4 - TYPE II BEAM - ANGLE BAR



$$A_B = \frac{3.1416}{2} \quad h^2 - (h-2t)^2$$

$$I_B = \frac{3.1416}{64} \quad h^4 - (h-2t)^4$$

$$C_B = \frac{h}{2}$$

FIGURE 5 - TYPE III BEAM - PIPE

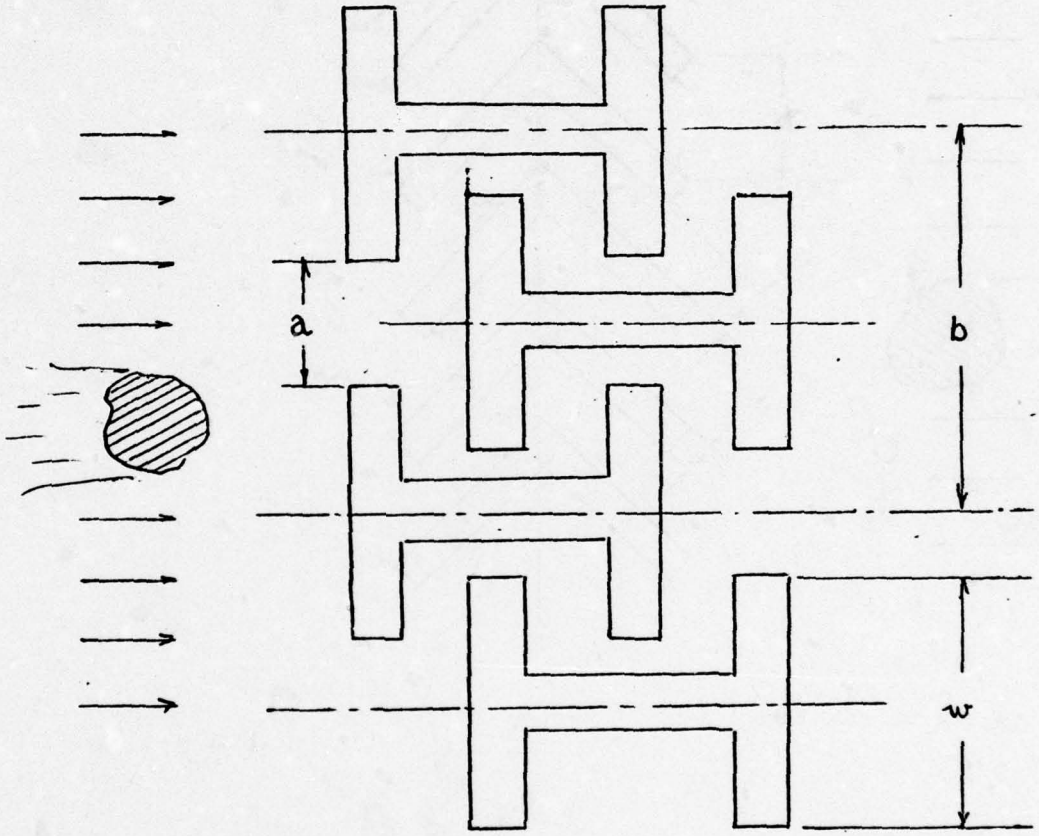


FIGURE 6 - TYPE I PANEL BEAMS

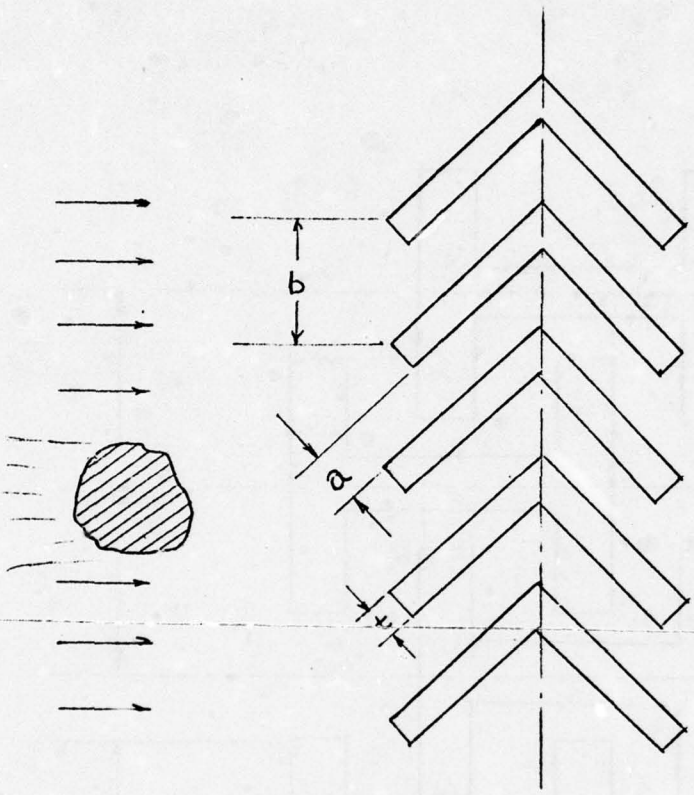


FIGURE 7 - TYPE II PANEL BEAMS

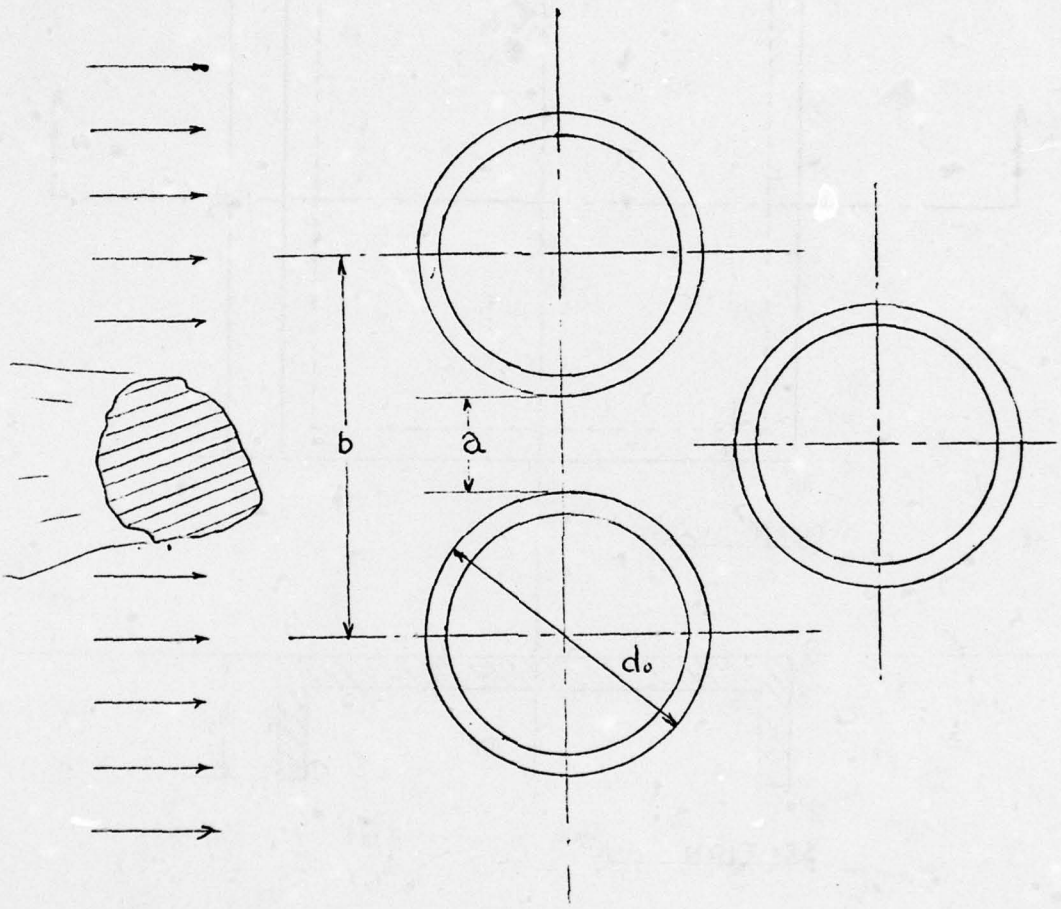


FIGURE 8 - TYPE II PANEL BEAMS

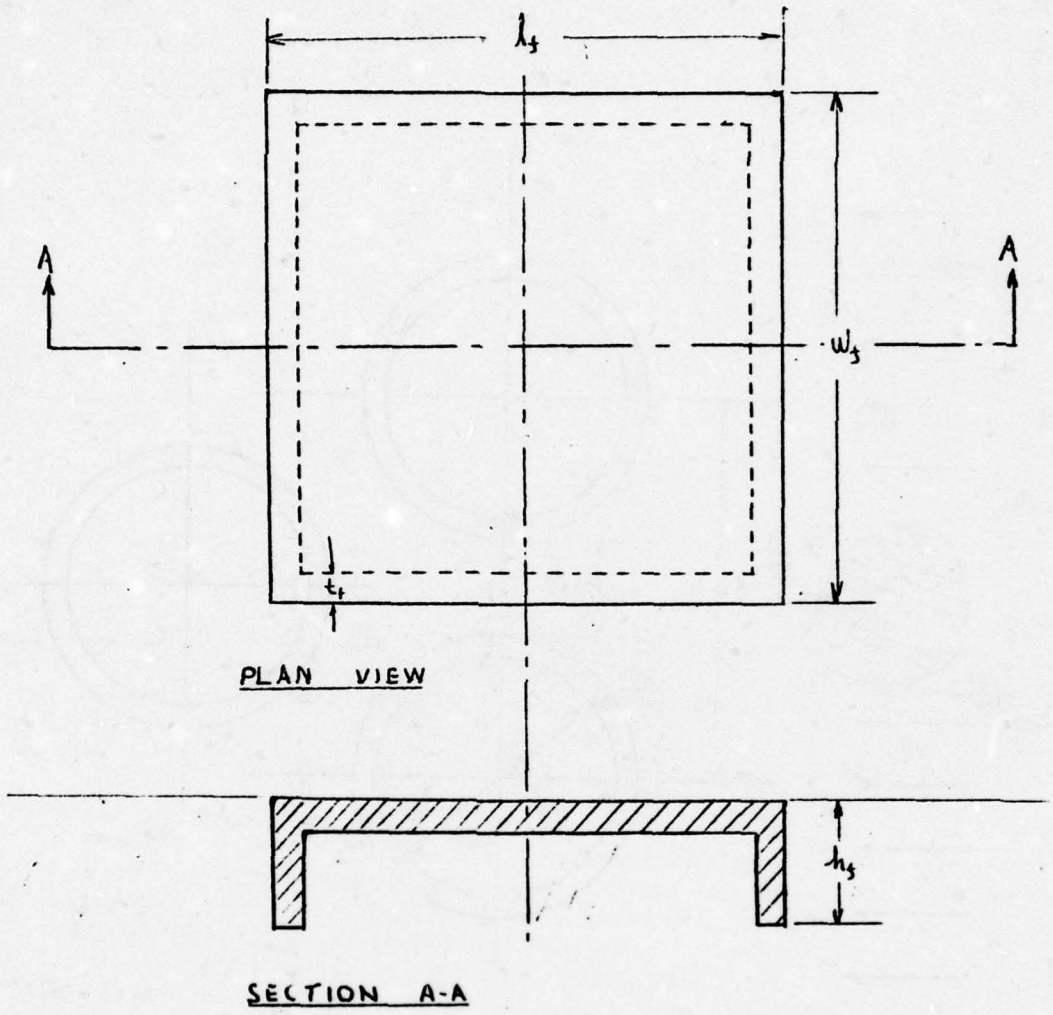


FIGURE 9 - FOUNDATION OF SUPPRESSIVE SHIELD

ANALYSIS OF THE LOADING AND RESPONSE OF A SUPPRESIVE SHIELD WHEN SUBJECTED TO AN INTERNAL EXPLOSION

by

Frederick H. Gregory
Ballistic Research Laboratory

The topic of this paper is an analysis of the ¼ Scale Category I Suppressive Shield which has been under test at the Ballistic Research Laboratory during the past year. This work is a part of the Suppressive Shielding Project of the Army's Munitions Production Base Modernization and Expansion Program which is managed by Edgewood Arsenal. The results of this subtask will be used in the formulation of a Handbook of Design Principles for Suppressive Structures. The overall objective is shown in Figure 1 and is to provide structures with lower construction and maintenance costs and at the same time provide increased safety and efficiency for ammunition processing and storage facilities.

Figure 2 is a photograph of the Shield taken at BRL. The sidewalls are composed of vertical interlocking I-beams around which are positioned three laminated steel rings that provide hoop strength. The top and bottom are constructed of reinforced concrete cast in the shape of a disc.

A cross section of the configuration is shown in Figure 3 as it exists during test with an explosive charge positioned at the geometrical center. The shock strikes the ceiling and floor first, then the sidewall next. These shocks reverberate and interact inside the chamber. It is these transient pressures which are applied to the interior surfaces which must be obtained from computer calculations. These calculated loads are then included in the structural response calculations.

Two different areas of analysis were required in the course of this task. These were modeling of the loading and modeling of the structural response. First, I will talk about the loading, then about the structural response. The loading calculations were made in two parts as shown in Figure 4. One load model was based on experimental data and empirical fits to available data. The other model was obtained from computer codes. The structural response calculations were made with an augmented version of the finite difference code REPSIL. With the REPSIL code we examined the performance of a series of configurations similar to the ¼ Scale Shield.

The load is composed of two basic components -- the blast or shock load and the quasi-static load. I have referred to the blast load previously. The quasi-static load is the slowly decaying pressure pulse

whose magnitude is determined by the energy of the explosive and the volume of the shield. Its decay rate is controlled primarily by the rate at which gases are vented from the interior to the outside.

The formulation of the loading model from empirical and experimental data served two purposes. It served as a reference for comparison with that of the model developed from the computer calculation. It also allowed us to initiate the structural response calculations at nearly the same time as the computer generated load prescription. This transient load was developed from such parameters as shock magnitude, time of arrival, and shock decay rate. These data were obtained from (a) detonation of pentolite charges in free air, (b) detonation of pentolite charges above reflecting planes (i.e. height-of-burst curves), and (c) from actual measurements of pressure pulses in the tests conducted in the ¼ Scale Suppressive Shield.

The tests conducted at BRL on the ¼ Scale structure included pressure measurements at only three locations in the interior. This is not enough to specify the load in a reasonable approximation for a comprehensive structural calculation. Thus, we anticipated the need for a more comprehensive prediction of this highly transient and complex load. Two hydrodynamic computer codes were used to generate these data. The WUNDY code is a 1-D Lagrangian code which has extensive equations-of-state routines for explosives and air. It represents an efficient means of generating the flow variables for spherical shocks in these media.

As the shock wave approached the nearest surface (which happened to be the top), the WUNDY code was stopped and the results of this calculation were used in the DORF code to follow the reflections on the interior surfaces. The DORF code is a 2-D Eulerian hydrocode which has been used for impact and shock wave problems. One can follow the motion of material boundaries and other physical quantities of interest by the use of tracer particles in the flow field.

Due to symmetry considerations, one need be concerned with only one quarter of the vertical cross section of the interior space. This space was divided into a grid and the appropriate variables were determined from the WUNDY calculations. Figure 5 shows the pressure distribution in this grid shortly after the shock strikes the ceiling. The axial or z-coordinate is plotted on the right and the radial coordinate is on the left. The pressure is the vertical axis. Figure 6 shows the pressure distribution after the shock has reflected from the ceiling and sidewall and has coalesced into a shock approaching the center of the Shield. The particle velocity at this time is shown in Figure 7. The jagged line is the interface between the explosive gas and the air. These types of maps are generated automatically to see how the shock fronts interact with one another.

A comparison of the pressure-time curve between the DORF calculations and the experimentally measured data is shown in Figure 8. These data are for a point on the sidewall near the mid-height. The first peak is the initial shock reflection from the sidewall. The second pulse comes from a shock reflection off the ceiling. The third is a reflection from the center of the structure. The overlay shows the measured pressure-time trace for the same point. Note that the quasi-static pressure level is approximately 1.25 MPa (180 psi).

The data generated from the foregoing two loading models were used as the forcing function in the REPSIL Code. The REPSIL Code is a finite difference structural response code which has a number of desirable features as indicated in Figure 9. However, for this particular problem, a number of additions were made as indicated by the asterisks. An equation-of-motion for the concrete cap was provided to determine the force on the fixed-sliding end condition applied at the top of the I-beams. The interaction of the rings or bands with the I-beams was modeled by including both hoop and inertia forces.

We found that strain rate effects had a significant influence on the structural response. The strain rate model is one which considers the strain rate to be dependent on the dynamic overstress. The stress-strain curve for several strain rates is given in Figure 10. For the strain rates which were experienced in the ¼ Scale Shield with the 20 kg charge, the increase in the yield stress was typically 50%. The stress-strain curves shown here are for mild steel.

The original reason for using interlocking I-beams in the sidewall of the Shield was to allow for venting of the gases inside the Shield. The idea was that in passing through the tortuous path between the I-beam flanges, the gases would be allowed to escape to reduce the inside pressure, but not at such a fast rate that the exterior blast and fireball would be too great. In order to check the relative importance of the blast pulse and the quasi-static transient, a numerical experiment was conducted. Figure 11 shows an idealized exponential shock and nearly constant quasi-static pressure. Three separate structural response calculations were made. One was for the shock pulse alone, one was for the quasi-static pressure alone, and a third for the combination of the two. The deflection of the sidewall with a 20.8 kg charge for these three loads is shown in Figure 12. The solid line shows the deflection as a function of time for the blast pulse, the lower dashed line is for the quasi-static load and the upper dashed line shows the combined response. The shock pulse causes a significantly greater deflection than the quasi-static load. The response to the total load is much larger than that to either component of the load acting alone due to the nonlinearity of stress-strain property. From this, one concludes that venting of this structure is of only secondary importance.

Table 1 presents a summary of some numerical results on several configurations for which structural response calculations were made. The first case is for the standard configuration ¼ Scale Suppressive Structure of which I showed you a photograph. The second and third cases show the results when some of the rings are removed. Notice the extremely large deflection and strain when all the rings are removed. This gives an indication of the radial stiffness provided by the rings. Case number four is for a 30% increase in charge weight. Again, notice the nonlinear response. The deflection is nearly four times the deflection as that for the standard charge. Case number five is a configuration in which one-half of the I-beams have been eliminated. The deflection increases modestly and the peak hoop strain increases only a small amount. The increase in the axial strain is due to the decreased bending stiffness. This would be alleviated by the gussets at the intersection of the sidewall and the ceiling. The last case is for a structure in which one half the I-beams and the three rings are replaced with a uniform thickness cylindrical shell of equivalent weight. Note that the radial deflection and strain are reduced to about one half of those for the standard configuration. Also in this last configuration, the minimum thickness for fragment penetration is increased by 22%.

Table 2 presents the more important results which are pertinent to the Category I Shield. The blast load is a more severe load than the quasi-static load. The structural response time is such that it responds relatively quickly to the blast load. Within the external blast restrictions imposed on the Category I Shield, there cannot be enough venting area to reduce this blast load significantly before the structure attains maximum deflection. For this reason, the requirement for an integral venting design can be eliminated. We believe that it is more practical to allow venting through engineering penetrations such as utility tunnels and cracks around doors, etc. Third, a more efficient structure from a blast and fragment viewpoint can be designed by reducing the number of longitudinal elements and replacing them by circumferential reinforcement.

There are some conclusions which are of a general nature. These conclusions will apply to a large class of suppressive shields. We expect significant response of the structure to occur before there is sufficient venting to relieve the load in most configurations. Second, the circumferential hoop or else a shell structure is more efficient than the longitudinal stiffener. So we should use these types of construction where other restrictions permit it.

OBJECTIVE

FORMULATION OF DESIGN PRINCIPLES

$\Longrightarrow$ INPUT TO HANDBOOK

DESIGN IMPROVEMENT – CATEGORY I

- LOWER INITIAL COSTS
- LOWER MAINTENANCE COSTS
- LOWER EXTERIOR BLAST PRESSURE

Figure 1. Objective of Suppressive Shielding Structural Analysis Subtask

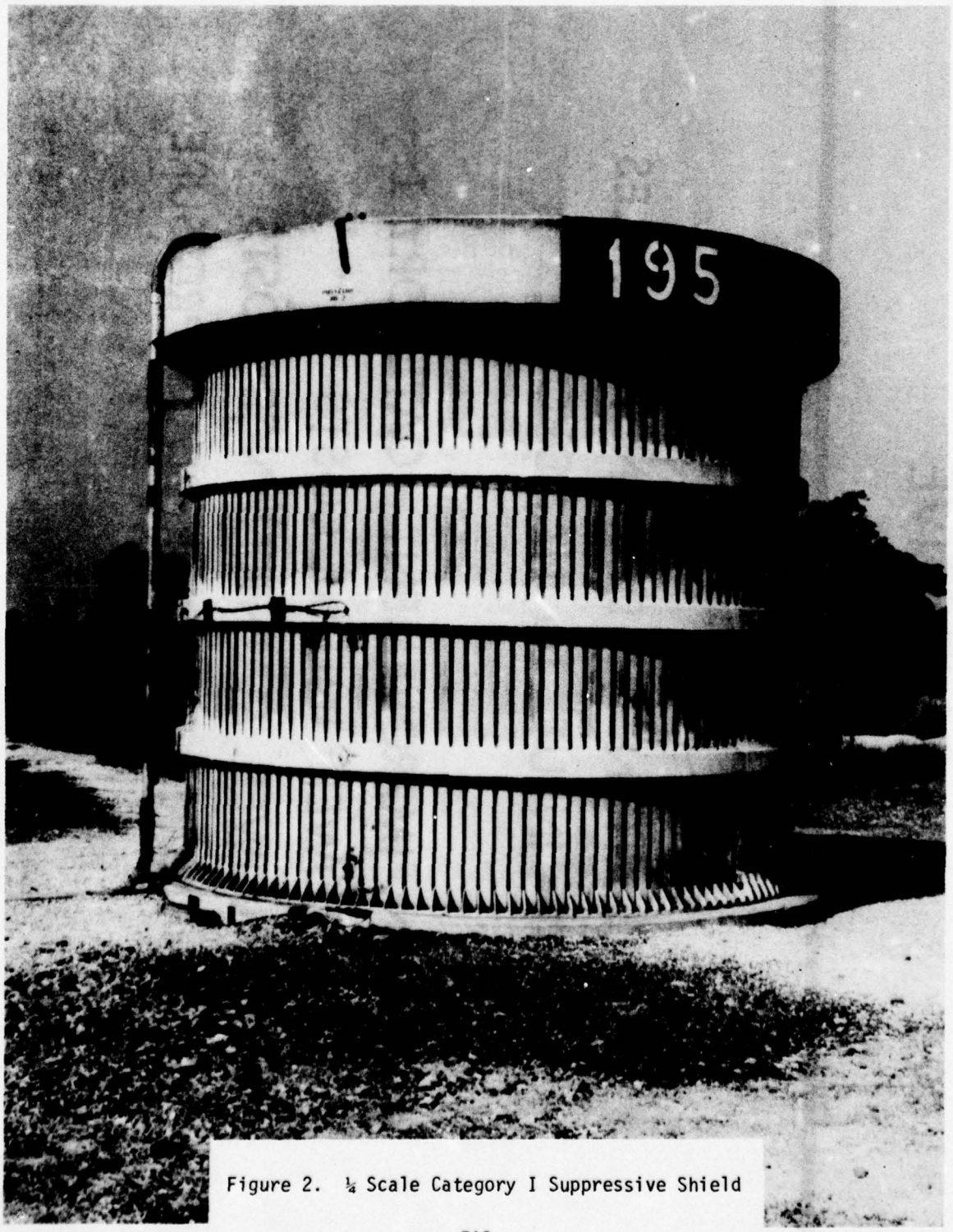


Figure 2. ¼ Scale Category I Suppressive Shield

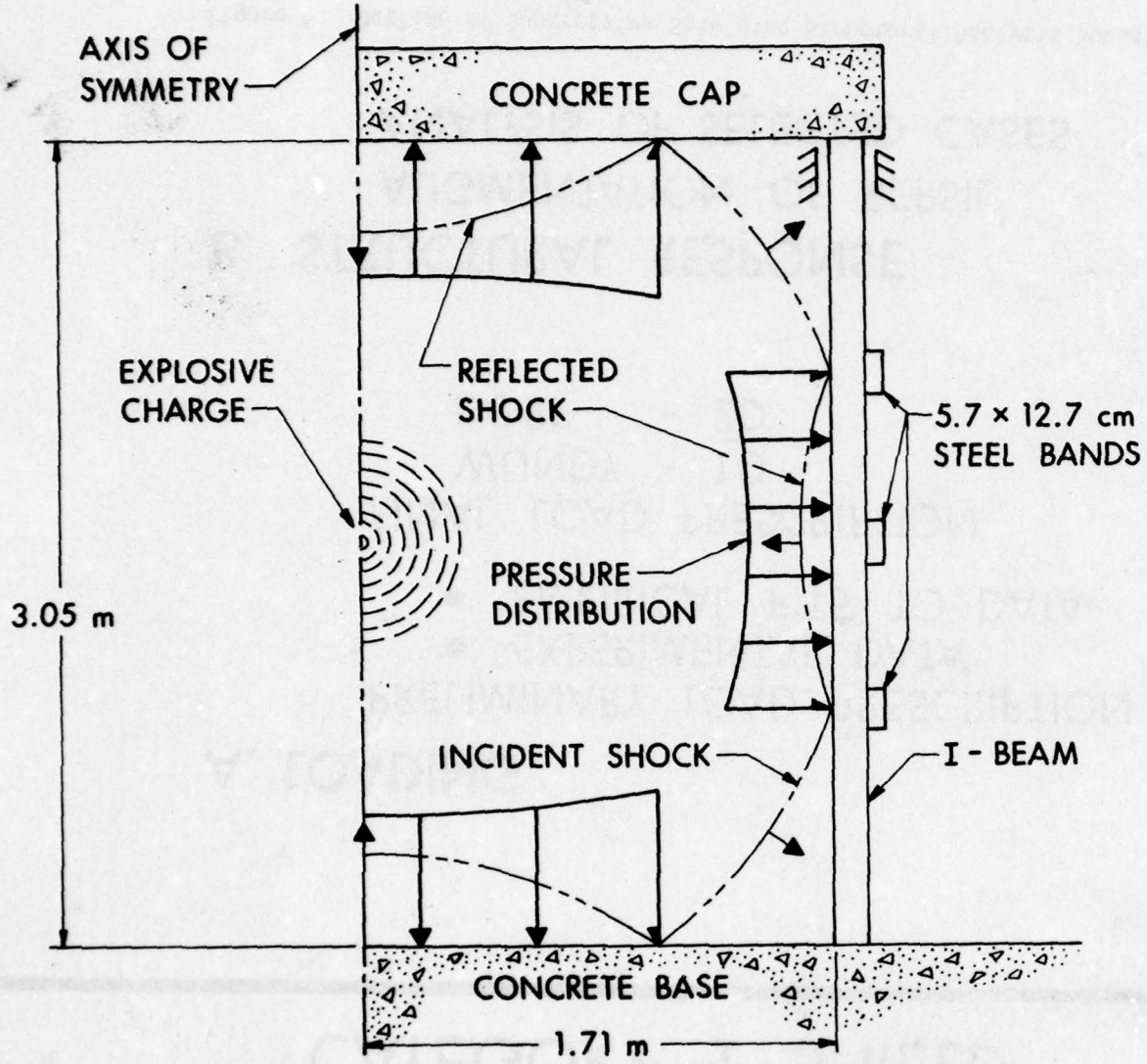


Figure 3. Schematic Representation of Shock Reflections from Interior Walls of ¼ Scale Category I Suppressive Shield

ANALYSIS OF CATEGORY I SHIELD

A. LOADING

PRELIMINARY LOAD PRESCRIPTION

- EXPERIMENTAL DATA
- EMPIRICAL FITS TO DATA

FINAL LOAD PRESCRIPTION

WUNDY - 1D
DORF - 2D

B. STRUCTURAL RESPONSE

AUGMENTATION OF REPSIL

ANALYSIS OF SELECTED CASES

Figure 4. Outline of Suppressive Shielding Structural Analysis Subtask

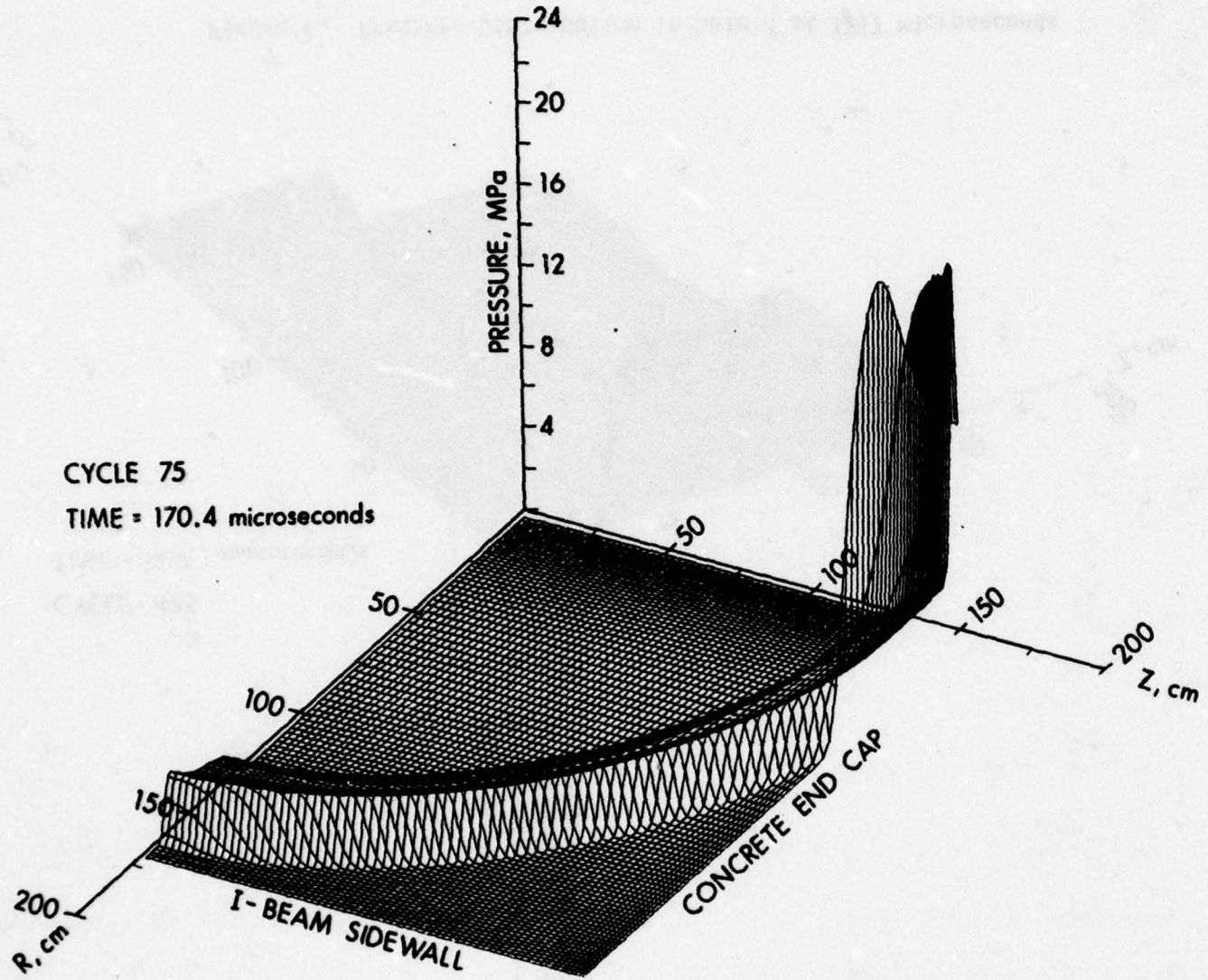


Figure 5. Pressure Distribution in Shield at 170 Microseconds

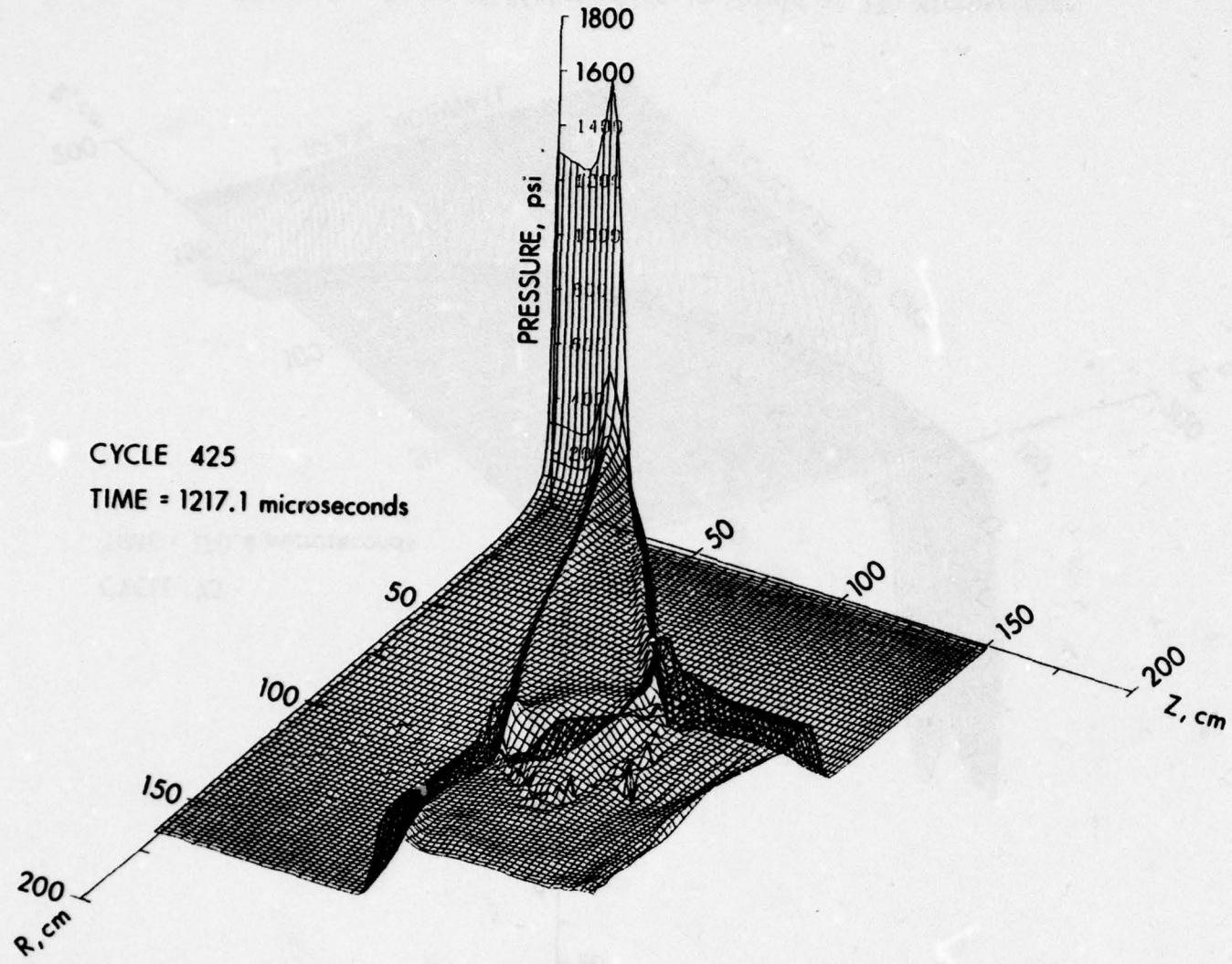


Figure 6. Pressure Distribution in Shield at 1217 Microseconds

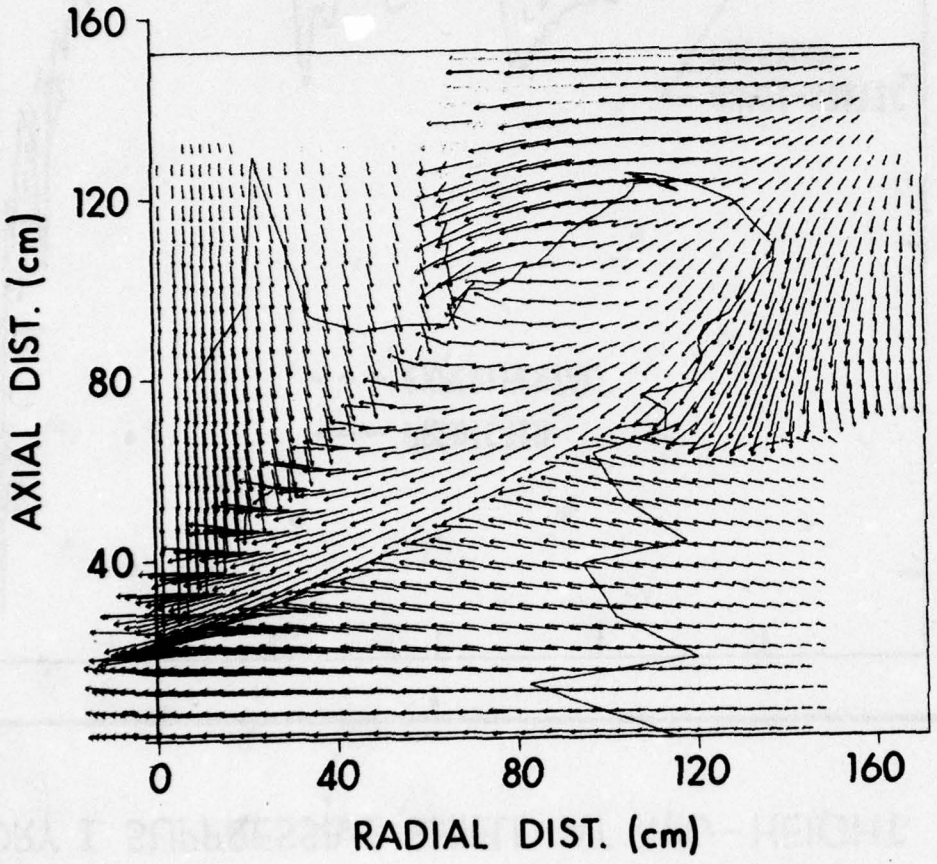


Figure 7. Particle Velocity Distribution in Shield at 1217 Microseconds

LOADING ON SIDEWALL OF QUARTER SCALE CATEGORY I SUPPRESSIVE SHIELD AT MID-HEIGHT

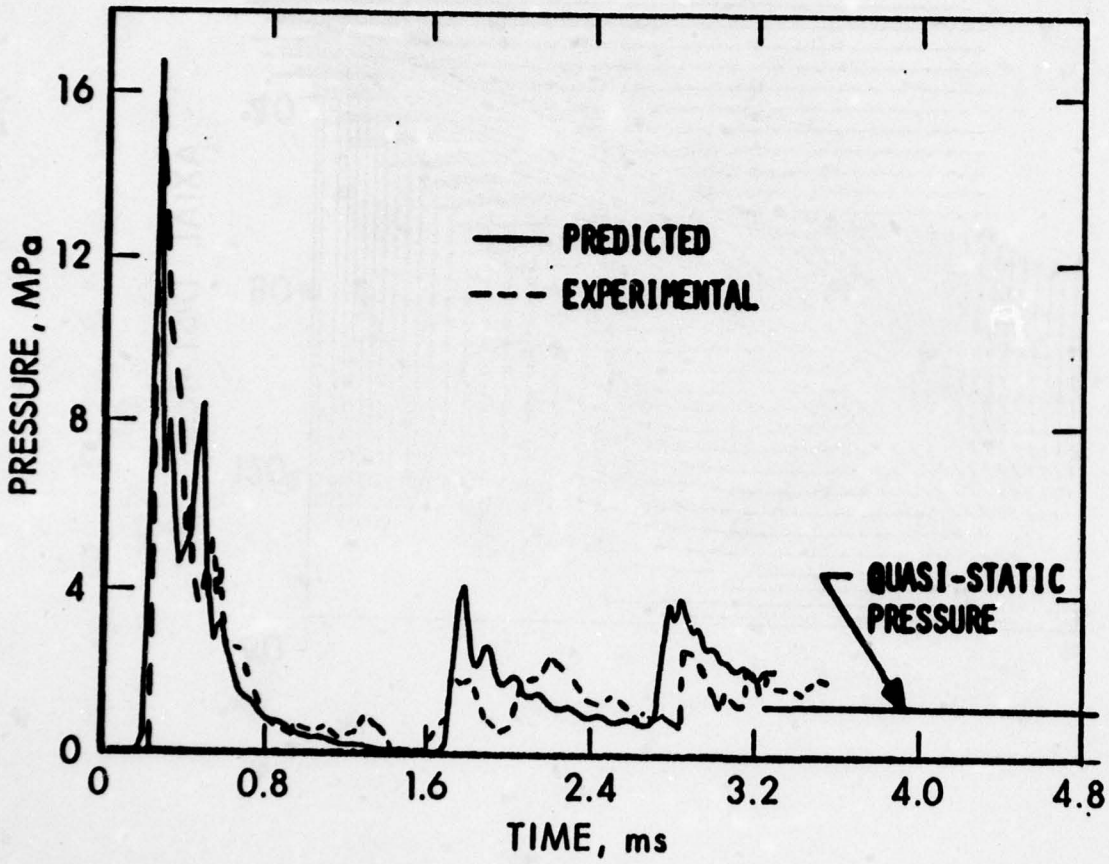


Figure 8. Comparison of Predicted and Measured Pressure Pulse at Point on Sidewall at Mid-Height

STRUCTURAL RESPONSE
REPSIL CODE

TRANSIENT LARGE DEFLECTION ELASTOPLASTIC RESPONSE FOR BEAM-COLUMN

STRAIN RATE AND STRAIN HARDENING MATERIALS

* COUPLED MOVEMENT OF CONCRETE CAP AS A RIGID BODY

* INTERACTION OF BANDS WITH I-BEAMS (BOTH INERTIA FORCES AND HOOP FORCES)

* TRANSIENT BLAST LOAD SPECIFICATION

Figure 9. Major Features of REPSIL Structural Response Calculations

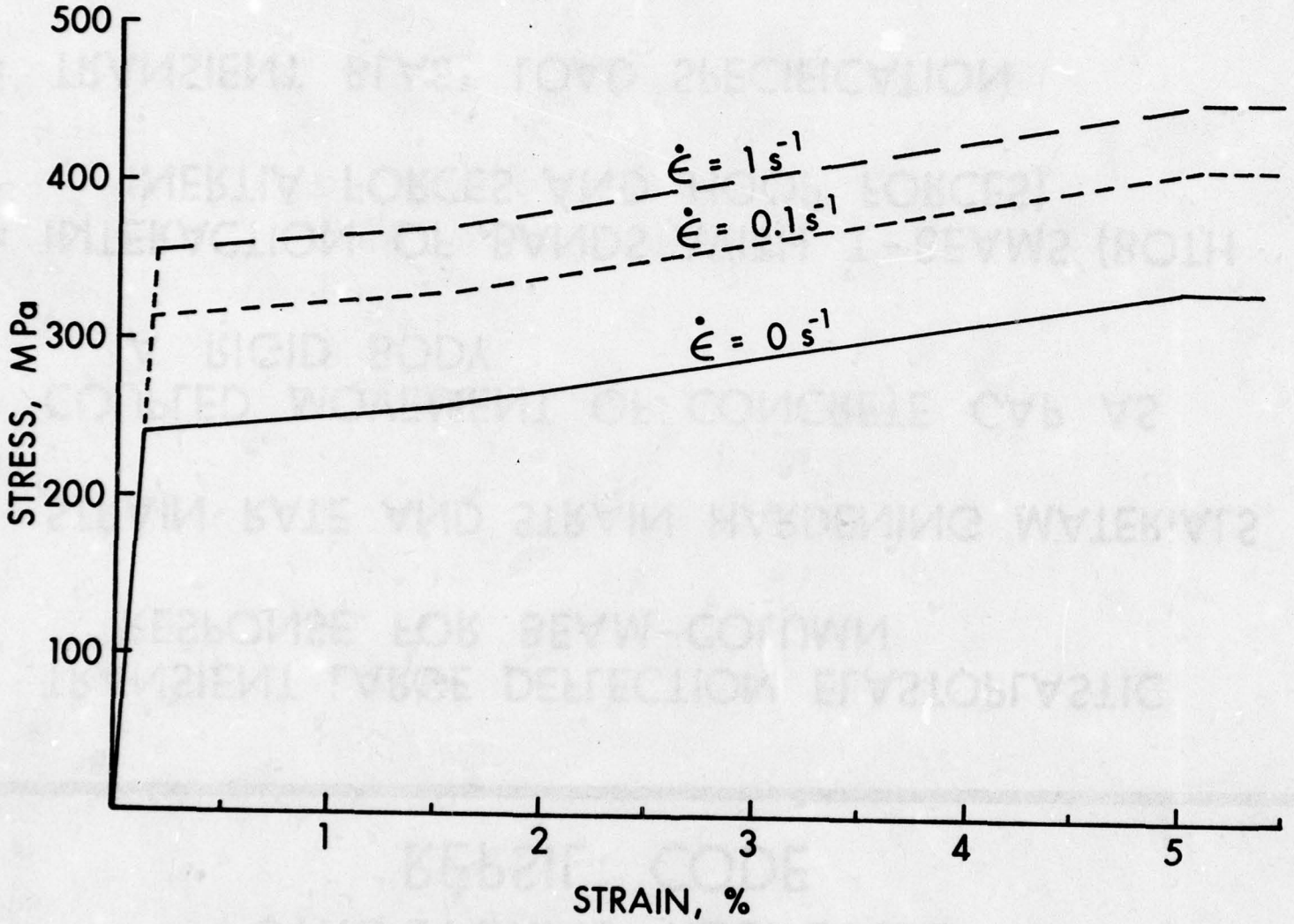


Figure 10. Dynamic Stress-Strain Curves for Mild Steel

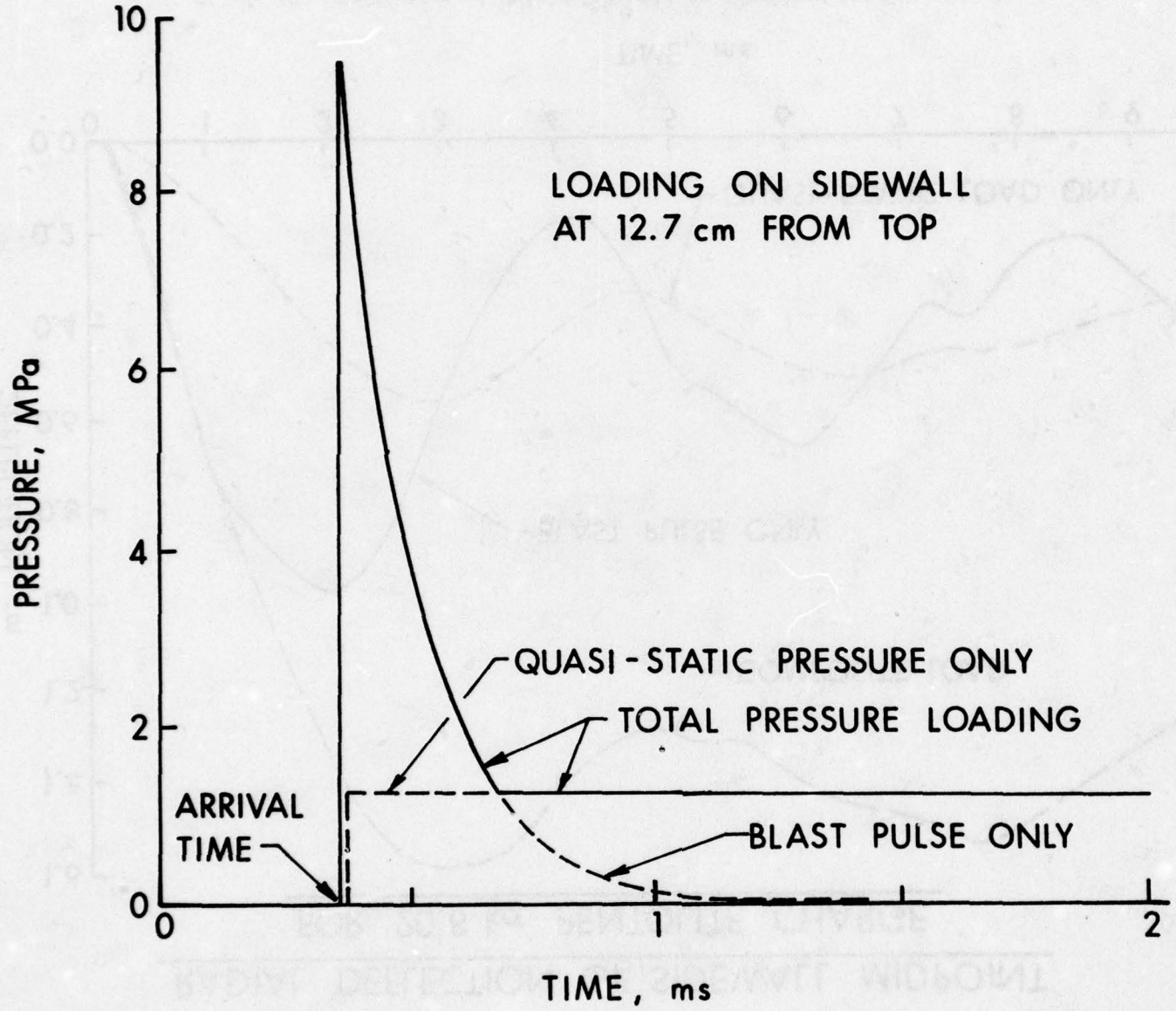


Figure 11. Idealized Load Components on Shield Surface

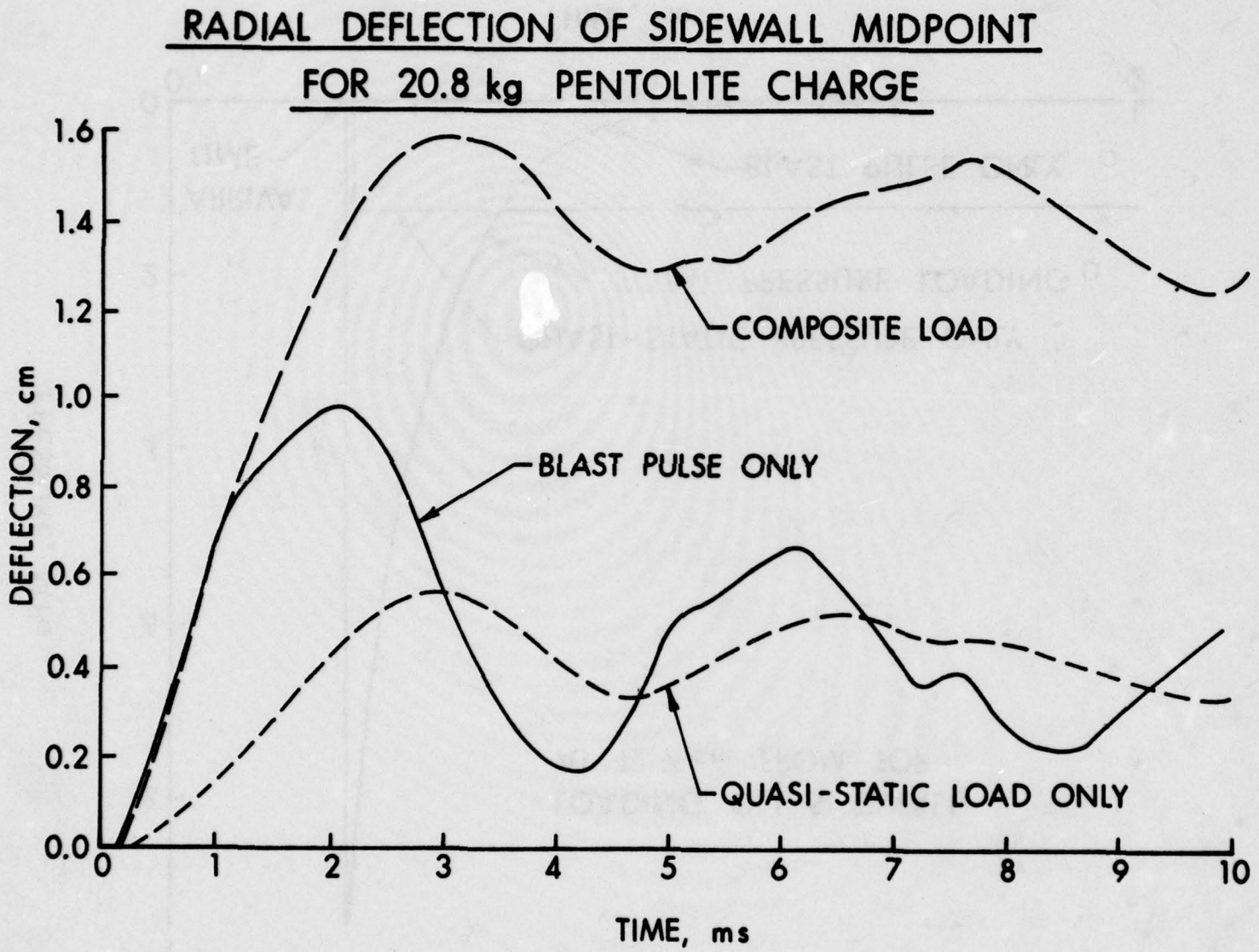


Figure 12. Deflection of Shield Sidewall to Idealized Load Components

TABLE 1. SUMMARY OF RESULTS

CASE	CHARGE WEIGHT (KG)	NO. OF RINGS	NO. OF BEAMS	PEAK DEFL. CENTER (CM)	TIME AT PEAK DEFL. (MSEC)	PEAK HOOP STRAIN CENTER RING (%)	PEAK AXIAL STRAIN INSIDE FLANGES (%)
I	20.8	3	296	1.1	2.8	0.6	1.0
II	20.8	1	296	5.9	8.6	3.2	3.5
III	20.8	0	296	34.8	23.5	—	14.3
IV	27.3	3	296	4.0	4.4	2.2	1.7
V	20.8	3	148	1.5	2.8	0.7	3.0
VI	20.8	–	148	0.6	4.1	0.3	1.1

Table 2. Significant Results for Category I Suppressive Shield

- BLAST PULSE IS THE MORE SEVERE LOAD
- ELIMINATE VENTING BETWEEN I-BEAMS
- REDUCE THE NUMBER OF I-BEAMS FOR A DESIGN CAPACITY OF 1150 kg OF HE (FULL SCALE CATEGORY I DESIGN LIMIT)

Virtual Velocity-Stationary Mode Techniques for the Design of Suppressive Shield Structures

by

Alan S. Kushner
and
Michael E. Giltrud

Naval Surface Weapons Center
White Oak, Silver Spring, Maryland 20910

Abstract

Approximate solution methods for beams and plates dynamically loaded into the plastic range are presented. These methods use stationary mode solutions in the principle of virtual velocities to develop solution procedures capable of including strain rate effects and the influence of moderately large deflections. The method assumes the material can be adequately modeled with a rigid-plastic material model, however arbitrary time varying loads can be included. A comparison of analytical predictions with existing experimental results for impulsively loaded beams and plates shows a very good correlation.

List of Symbols

Symbol	Definition
b	width of I-beam flange
d	width of I-beam web
ℓ	half length of beam
m	mass per unit length of beam
p	force per unit length on beam
$\dot{q}$	generalized strain rate
t	time
$\dot{u}_i$	i'th component of velocity vector
$\underline{X}$	position vector
$\dot{D}$	dissipation rate function
H	distance from centroid to flange of I-beam
HT	distance from centroid to top of I-beam
M	bending moment in beam hinge region
M_y	fully plastic bending moment of section
N	membrane stress resultant
N_y	fully plastic membrane stress resultant
P	coefficient of load term
Q_j	generalized stress
S	surface of structure
V	volume of structure
V_o	initial velocity
W	displacement amplitude of stationary mode
ds	differential of surface area
dv	differential of volume
$\dot{\varepsilon}$	average membrane strain rate
σ	spatial component of generalized stress
σ_y	dynamic yield stress
σ_{yo}	static yield stress
ϕ_i	spatial component of displacement
ψ_i	spatial component of generalized strain
$\dot{\psi}$	average rotation rate
Σ	amplitude of generalized stress
Ψ	amplitude of generalized strain

1. Introduction

Efficient structural design techniques are needed for the design of structures used for the containment and suppression of the explosions resulting from the accidental detonation of explosives during their manufacture, handling, and storage. These structures must provide total containment of fragments, partial suppression of the shock wave, and a controlled release of the internal quasi-static pressure. Because of the relatively low frequency of accidental detonations, the most cost effective approach to the design of such structures appears to be one utilizing inexpensive and easily erectable structures which can be replaced after an explosion.

There are several approaches which one could take in designing structures to contain the internal explosion while undergoing large plastic deformation. The most sophisticated approach would involve the use of a large scale finite element computer code to model the complete structure and solve for the dynamic response using an elastic-plastic, strain rate dependent material model. In addition to being beyond the capabilities of most structural analysis computer codes, such analyses are very expensive and time consuming especially when being used in a design iteration mode. At the other end of the spectrum, a designer could utilize simple handbook type of equations to analyze individual components of the structure independently. Such a design procedure would be very quick and inexpensive, however the resulting design would be highly conservative and would involve a large weight and cost penalty in its construction. The objective of the current work is to provide the designer with easy to use design tools which will enable him to simplify the design procedure without paying a large weight and cost penalty.

To be weight and cost effective, structures should be designed so as to undergo large plastic deformations under the loading due to an accidental explosion. In designing structures for large deflection dynamic, plastic response, a useful simplification is to neglect elastic effects and treat the material as a rigid-plastic material. It will be demonstrated that theories based on such simplifications can provide highly accurate design procedures for designing suppressive shield structures.

2. Analytical Development

In formulating approximate theories for the behavior of structural systems, three basic criterion must be addressed.

First, an equation which expresses an equilibrium balance must be stated. In order to apply this equilibrium equation it is necessary to invoke a constitutive equation to relate the forces and displacements contained in the equilibrium equation. To complete the formulation, it is necessary to invoke boundary conditions which constrain the possible stress and displacement fields. Problems involving dynamic, plastic deformation of common structural elements are generally much too complex to solve analytically and are beyond the capabilities of most structural analysis computer codes. In developing approximate solutions for such problems, it is essential to have a clear formulation in which the influences of the approximations can be clearly assessed.

A dynamic equilibrium equation which is very useful for formulating approximate solutions in plasticity is the principle of virtual velocities (1):

$$\int_S P_i \dot{u}_i ds - \int_V m\ddot{u}_i \dot{u}_i dv = \int_V Q_j \dot{q}_j dv \qquad (1)$$

where $\dot{u}_i$ and $\dot{q}_j$ are kinematically admissible velocity and generalized strain rate fields. The generalized stress field Q_j and the acceleration field $\ddot{u}_i$ are statically admissible. Statically admissible fields are those which satisfy the equilibrium constraints of forces and accelerations, while kinematically admissible fields are those which satisfy the kinematic boundary conditions and constraints of the problem. More comprehensive dicussions of the these features can be found in Martin (2) and Save and Massonnet (3). Equation (1) is a statement of instantaneous power balance. The first integral represents the rate at which the external forces are doing work. The power of the inertial forces is expressed by the second integral or alternately this can be interpreted as the rate of change of kinetic energy. The last integral represents the instantaneous rate at which energy is being dissipated in plastic work. It is important to emphasize that the set of $\dot{u}_i$ and $\dot{q}_j$ is independent of the set of Q_j and $\ddot{u}_i$. Formally we may say that the kinematically admissible field is independent of the dynamically admissible field. If the two fields are associated, that is $\dot{u}_i$ are the actual velocities caused by the loads P_i, then equation (1) reduces to a direct energy balance. However, the great utility of the principle of virtual velocities is that it does hold when the fields are not associated.

A useful approximation often utilized in developing solutions for dynamic response problems involving large plastic deformations is to neglect elastic effects. Such rigid-plastic approximations greatly simplify the problem formulation and solution. An excellent review of the range of validity for the use of rigid-plastic theories in structural dynamics was given by Symonds (4). One of the most successful applications of limit analysis to rigid plastic structural elements has been the use of stationary mode solutions (5). Martin (1), has given several results useful for determining the "best" stationary mode. However, his results are applicable only to impulsively loaded linear problems in which no interaction between components of the generalized stress vector, Q_j, occurs. Very little analytical work has been done on problems involving finite duration loading and interacting dissipation mechanisms.

For any particular problem, once a stationary mode of the form

$$U_i(\underline{x},t) = \phi_i\ (\underline{x})W(t) \tag{2}$$

has been chosen, a suitable set of generalized strain rates

$$\dot{q}_i(\underline{x},t) = \psi_i(\underline{x})\Psi(W(t)) \tag{3}$$

consistent with the assumed mode can be determined. The generalized stresses are chosen in a manner such that $Q_j\dot{q}_j$ is a rate of energy dissipation and we assume

$$Q(\underline{x},t) = \sigma(\underline{x})\Sigma(W(t)). \tag{4}$$

W is the displacement of a reference point in the structural element. The form chosen for the generalized stresses implies they are independent of the generalized strain rates. For many materials this is a valid assumption, however, most common grades of structural steel show a very strong influence of strain rate on the value of the uniaxial yield stress. Bodner (6) has assessed the significance of strain rate effects in solving dynamic plasticity problems. He concluded that for structures with relatively simple dissipation modes, such as a cantilever beam, the accuracy of rigid plastic solutions could be greatly improved by using an increased yield stress based on the rate of generalized strain. However, he also concluded that for the case of structures with complex interacting dissipation modes, extra care must be taken in assessing the influence of the interacting generalized strain rates. Manjoine (7), correlated the existing experimental data for experiments on mild steel and found that the empirical formula,

$$\sigma_y = \sigma_{yo}\ (1 + \dot{\varepsilon}/40.4)^{0.20} \tag{5}$$

gave a very good approximation for the value of the dynamic yield stress.

If the stationary mode solution, equation (2), is substituted into the virtual velocity equation, (1), one obtains,

$$\dot{W}(t) \int_S P_i \phi_i(\underline{x})\, ds - \dot{W}(t)\ddot{W}(t) \int_V m\phi_i(\underline{x})\, \phi_i(\underline{x})\, dv \qquad (6)$$
$$= \int_V Q_j\, \dot{q}_j\, dv$$

Equation (6) can be rewritten as a non-linear, ordinary differential equation,

$$P(t)\dot{W}(t) - M\,\dot{W}(t)\ddot{W}(t) = \dot{D}(W,\dot{W}) \qquad (7)$$

where,

$$P(t) = \int_S P_i(t)\, \phi_i(\underline{x})\, ds \qquad (7a)$$
$$M = \int_V m\phi_i(\underline{x})\, \phi_i(\underline{x})\, dv \qquad (7b)$$
$$\dot{D} = \int_V Q_j\, \dot{q}_j\, dv \qquad (7c)$$

The only step now remaining to complete the problem formulation is the selection of an admissible generalized stress field.

It has been found that in many cases, the static collapse mode gives a very good approximation to the final deformed shape of a structure loaded dynamically into the plastic range. Static collapse modes can be found by examining the displacement pattern for an elastic-perfectly plastic structure and passing to the limit as the elastic component of the displacement becomes negligible.

As an example of how the preceding is applied to actual structure elements, the development for an I-beam will be outlined. The details of this development and applications to other structural members can be found in reference (8). The ends of the I-beam will be assumed to be restrained against both normal displacement and in-plane motion. Deformation is assumed to take place within "hinge regions" at the center and ends. Gross motion of the beam can be described by the kinematically admissible mode shape

$$\phi(x) = \begin{cases} x/\ell\,, & 0<x<\ell \\ \dfrac{1-(x-\ell)}{\ell}\,, & \ell<x<2\ell \end{cases} \qquad (8)$$

while dissipation is related to the generalized strain rates,

$$\dot{\varepsilon} = \frac{2\dot{W}}{W} \qquad (9)$$

$$\dot{\psi} = \frac{4\dot{W}}{W^2} \qquad (10)$$

As the beam deflects, the stress resultant versus displacement relation can be described in three stages. The first two stages represent regions of combined bending and membrane stress, while the third stage represents a region of pure membrane stress. The stress versus displacement relations and governing differential equation for each region can be summarized.

Region 1:

$$0 \leq W \leq 2H$$

$$N = \frac{dN_y}{[bHT - H(b-d)]} W \tag{11}$$

$$M = M_y - \left[\frac{dM_y}{4[b(HT^2 - H^2) + dH^2]}\right] W^2 \tag{12}$$

$$\ell p(t) - \frac{2}{3} m\ell\ddot{W} = \frac{4M_y}{\ell} + \left[\frac{dN_y}{[bHT - H(b-d)]} - \frac{dM_y}{4[b(HT^2 - H^2) + dH^2]}\right]\frac{W^2}{\ell} \tag{13}$$

Region 2:

$$2H \leq W \leq 2HT$$

$$N = \left[\frac{H(b-d) - b\,W/2}{H(b-d) - bHT}\right] N_y \tag{14}$$

$$M = \left[\frac{bHT^2 - b\,W^2/4}{b(HT^2 - H^2) + dH^2}\right] M_y \tag{15}$$

$$\ell p(t) - \frac{2}{3} m\ell\ddot{W} = \left[\frac{N_y b}{(bHT - H(b-d)} - \frac{M_y b}{b(HT^2 - H^2) + dH^2}\right]\frac{W^2}{\ell} - \left[\frac{2H(b-d)N_y}{bHT - H(b-d)}\right]\frac{W}{\ell} + \left[\frac{4bHT^2\,M_y}{(b(HT^2 - H^2) + dH^2)\ell}\right] \tag{16}$$

Region 3:

$$2HT \leq W$$

$$N = N_y \tag{17}$$

$$M = 0 \tag{18}$$

$$\ell p(t) - \frac{2}{3} m\ell\ddot{W} = \frac{2N_y}{\ell} W \tag{19}$$

Equations (13), (16), and (19) must be solved to describe the beam response. For simplicity, the loading function, p(t), is assumed to be expressed as a series of linear segments, and a solution of the pertinent governing equation is defined for the time interval corresponding to the load segment. Equations (13) and (16) are nonlinear, ordinary differential equations for which no analytical solution can be written, however a solution for each has been developed in the form of a truncated power series. It has been found that retaining eight terms in the power series gives satisfactory accuracy. Equation (19) is an inhomogeneous, harmonic equation and an analytical solution can be written for it. Once a solution for a given time interval has been obtained one must check to see if the velocity goes to zero during this interval. In addition a check must be made to see that the deflection does not exceed the limiting value of applicability for the governing equation during the time interval. Both of these problems can be reduced to problems of finding the root of the solution function or its derivative. Newton's method (9) was used to solve these problems and in general convergence to the desired results was obtained in less than four iterations.

3. Results

The methods described in this report offer the designer of suppressive shield structures a powerful tool to be utilized in the preliminary design phase of his work. In order to demonstrate the accuracy of these methods and also to point out several significant results a series of sample solutions will now be presented.

Humphreys (10) performed a series of experiments to determine the permanent deformations of explosively loaded beams of rectangular cross sections whose ends were restrained against both normal and in-plane displacements. In our analysis the loading was assumed to be impulsive and the beam was assumed to have an initial velocity imparted to it. A discussion of how one chooses the best initial velocity for the stationary mode can be found in (8). Figure 1 shows a comparison of the computed results and Humphreys' experimental results. In addition, the results of a bending only solution and a non-stationary mode solution (11) due to Symonds and Mentel are shown. As may be seen, the current theory shows a good correlation to the experimental data.

In addition to the solution for beams presented in this report, an analogous formulation for rectangular plates has

been developed (8). A comparison of the results obtained from this solution with the experimental results of Jones, Uran, and Tekin (12) is shown in Figure 2. As can be seen, the present theory provides an excellent prediction of the maximum permanent deflection of the plates.

Very often in developing approximate solution procedures the exact form of the interaction relations for the generalized stresses is not followed. To illustrate one of the dangers in such an assumption a comparison was made of the maximum deflection of I-beams to that of rectangular cross section beams which had identical values of fully plastic stress resultant and bending moment. The results of two such analyses are shown in Figures 3 and 4. While the results show a fairly good correlation, it is significant to note that treating the I-beam as an equivalent rectangular cross section beam under predicts the true solution and hence, can not be said to represent a conservative design approach.

In addition to correctly modeling the interaction of the generalized stresses it is also important to assess the influence on the response of the time variation of the loading. To illustrate how significant this effect can be, a 40 foot long rectangular cross section beam with properties identical to those of a W 10 X 77 I-beam was analyzed under the loading shown in Figure 5. The loading under the first curve, $t \leq 4$ msec was first applied as an impulsive load. The resulting displacement was calculated to be 33.4 inches. When the same load was applied as a time-varying pressure the final displacement was found to be 25.3 inches. When the complete loading curve was applied to the beam the final displacement was 85.7 inches. However, if the beam was assumed to have an initial displacement of 25.3 inches and a zero initial velocity and was then subjected to the second part of the loading curve, the final displacement was found to be only 63.5 inches. This example illustrates the fact that uncoupling of the impulsive and quasi-static loads may not be an acceptable design procedure.

5. Conclusions

It has been demonstrated that stationary mode solutions developed from the Principle of Virtual Velocities and including the effects of finite deflections and dependence of yield stress on strain rate offer the designer of suppressive shield structures a powerful design tool. Through the use of solutions generated by such procedures it has been shown that conservative design procedures should in general, include the actual form of the interaction relation among the generalized stresses and the time variation of the loading function.

References

1. Martin, J. B., "Mode Approximations for Impulsively Loaded Structures in the Inelastic Range," in Structure, Solid Mechanics, and Engineering Design, edited by M. TE'ENI, Wiley Interscience, 1969, pp. 1227-1248.

2. Martin, J. B., Plasticity, Fundamentals and General Results, the MIT Press, 1975.

3. Save, M. A., and Massonnet, C. E., Plastic Analysis and Design of Plates, Shells, and Disks, North Holland Publishing Company, 1972.

4. Symonds, P. S., "Survey of Methods of Analysis for Plastic Deformation of Structures Under Dynamic Loading," Technical Report BU/NSRDC/1-67, Division of Engineering, Brown University, 1967.

5. Martin, J. B., and Symonds, P. S., "Mode Approximations for Impulsively-Loaded Rigid-Plastic Structures," Journal of the Engineering Mechanics Division, ASCE, Vol. 92, pp. 43-66 EM 5, 43, 1966.

6. Bodner, S. R., "Strain Rate Effects in Dynamic Loading of Structures," in Behavior of Materials under Dynamic Loading, edited by N. J. Huffington, Jr., ASME, 1965.

7. Manjoine, M. J., "Influence of Rate of Strain and Temperature on Yield Stresses of Mild Steel," Journal of Applied Mechanics, Vol. 11, Trans ASME, Vol. 66, Ser. A, 1944 pp. 211-218.

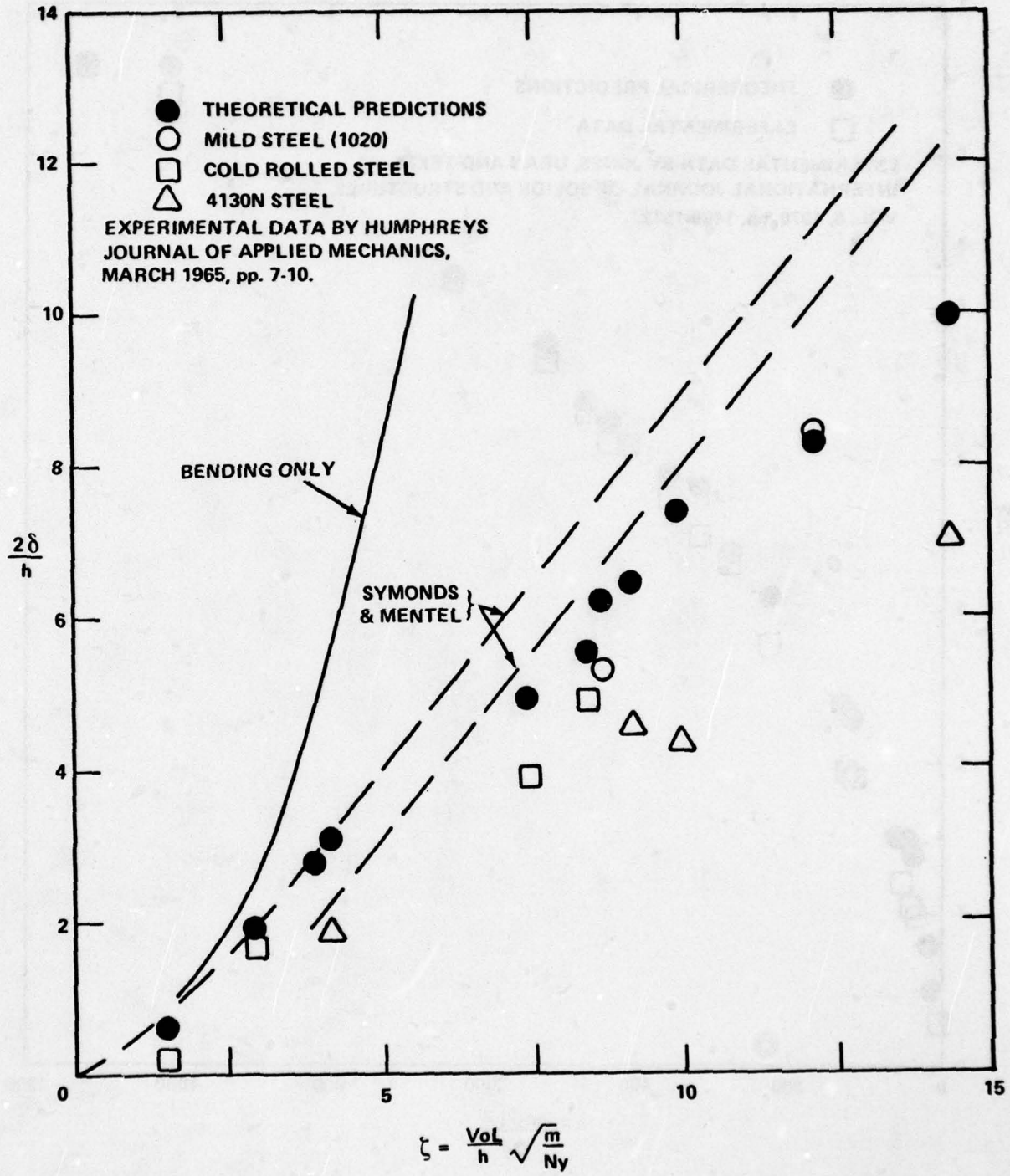
8. Kushner, A. S., and Giltrud, M. E., "Recommended Design and Analysis Procedures for Suppressive Shield Structures," NSWC/WOL/TR 76-112, in preparation.

9. Isaacson, E., and Keller, H. B., Analysis of Numerical Methods, John Wiley and Sons, Inc., 1966.

10. Humphreys, J. A., "Plastic Deformation of Impulsively Loaded Straight Clamped Beams," Journal of Applied Mechanics, Vol. 32, 1965, pp. 7-10.

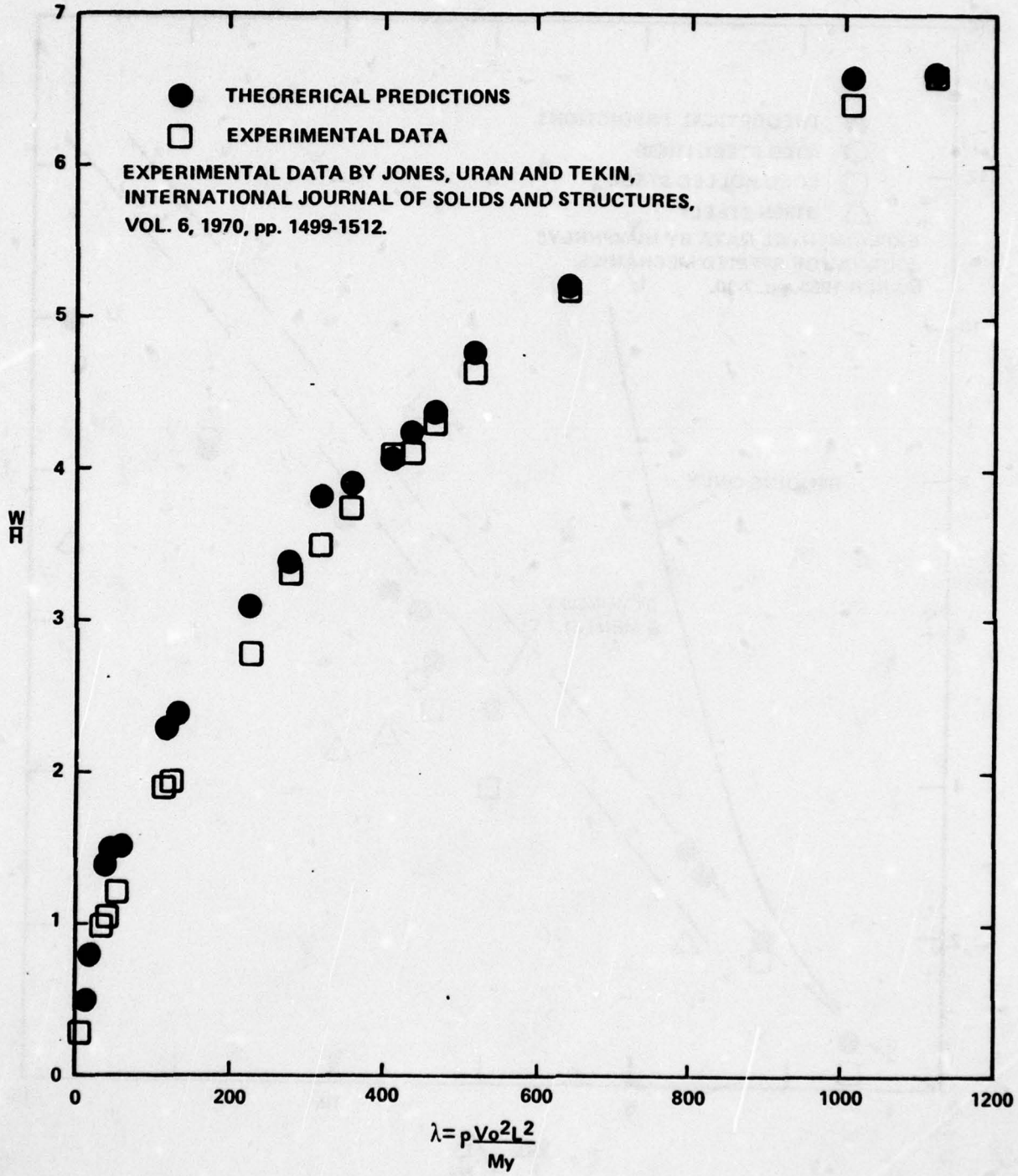
11. Symonds, P. S. and Mentel, T. S., "Impulsive Loading of Plastic Beams with Axial Constraints," Journal of the Mechanics and Physics of Solids, Vol. 6, 1958, pp. 106-202.

12. Jones, N., Uran, T. O., and Tekin, S. A., "The Dynamic Plastic Behavior of Fully Clamped Rectangular Plates," Int. Journal of Solids and Structures, Vol. 6, 1970, pp. 1499-1512.



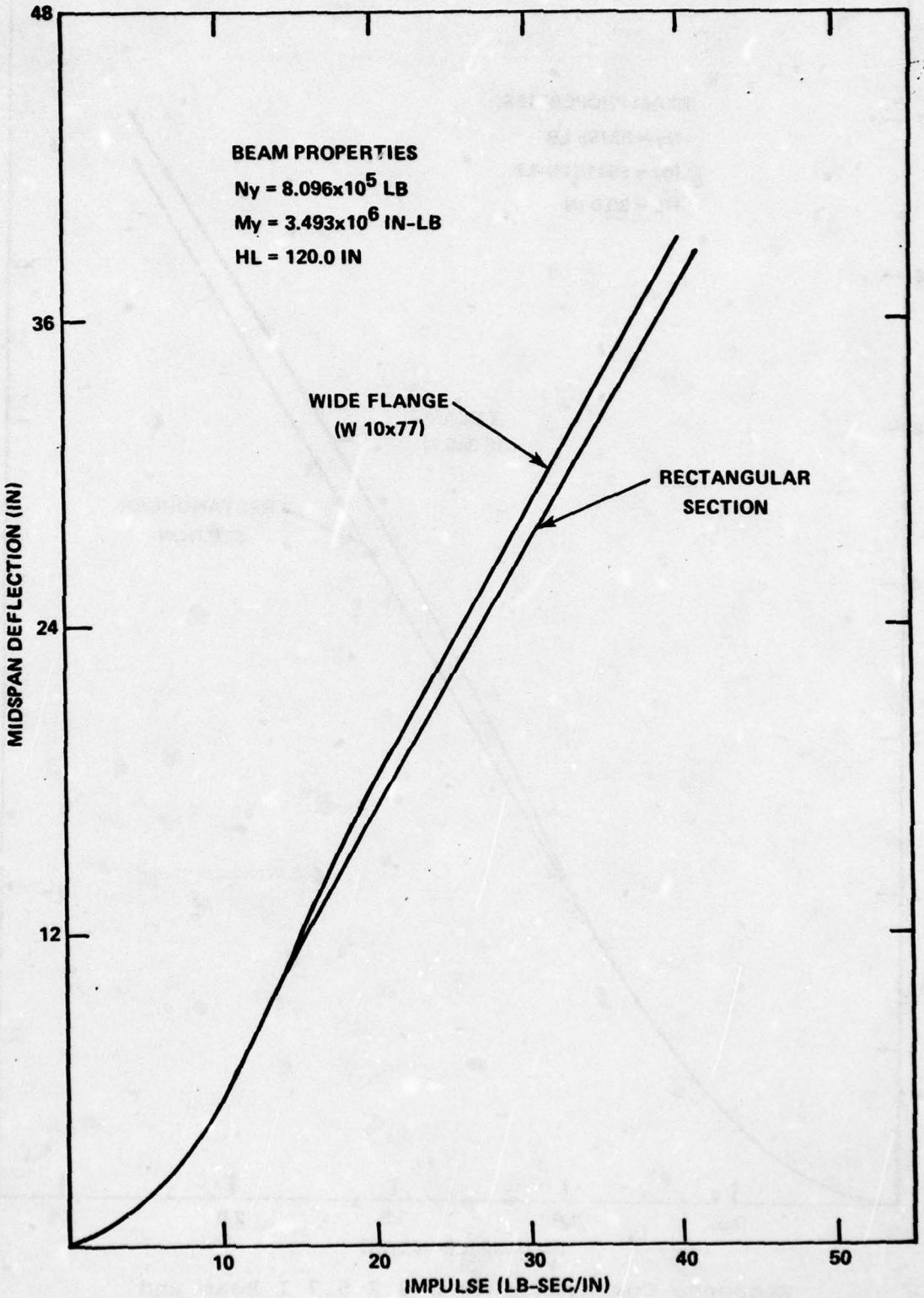
IMPULSIVE RESPONSE OF BEAMS WITH BUILT IN ENDS

Figure 1



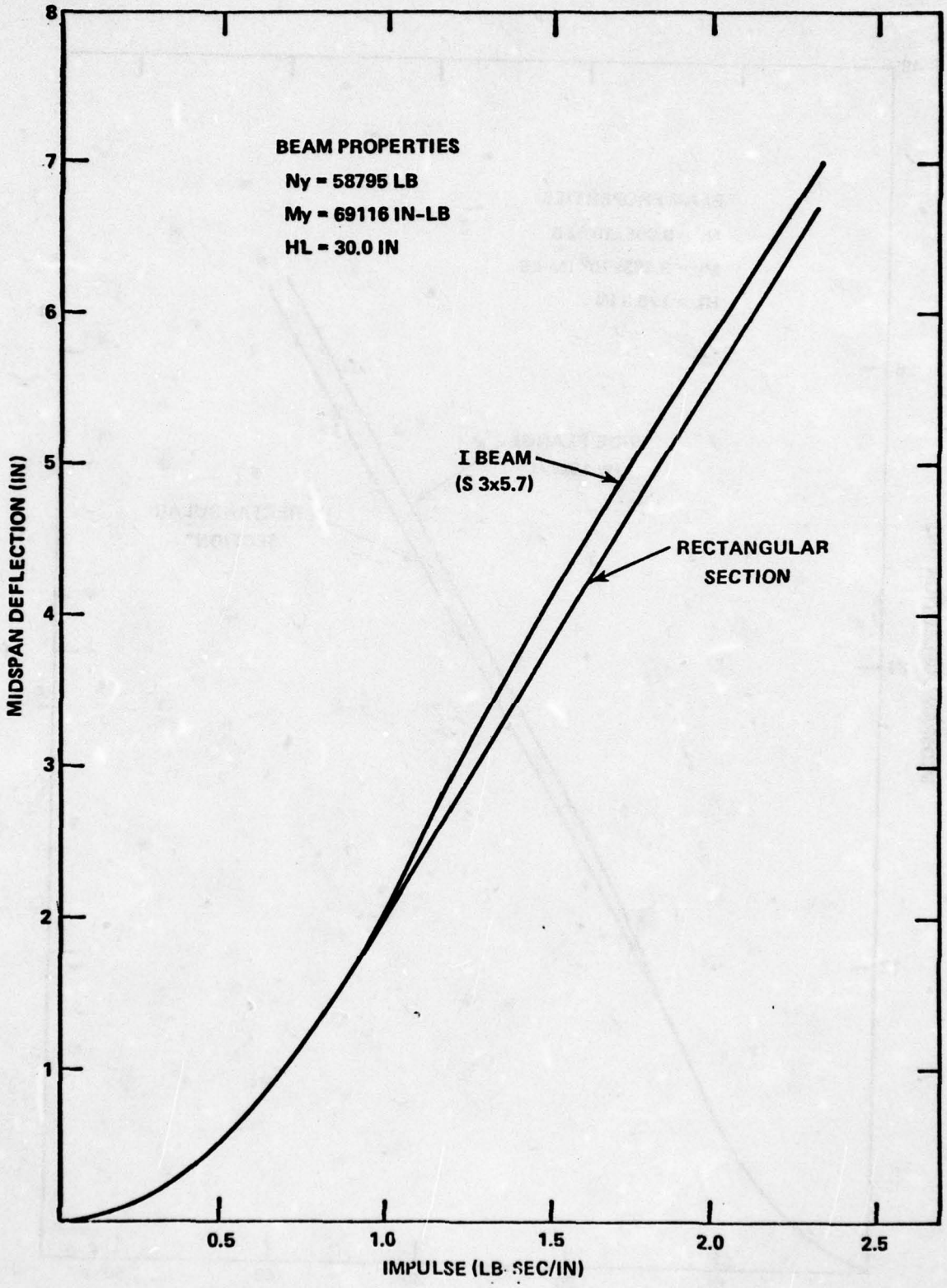
IMPULSIVE RESPONSE OF A RECTANGULAR PLATE WITH BUILT-IN EDGES

Figure 2



Response Comparison of W 10 X 77 I Beam and Rectangular Section with Equivalent Properties

Figure 3



Response Comparison of S 3 X 5.7 I Beam and Rectangular Section with Equivalent Properties

Figure 4

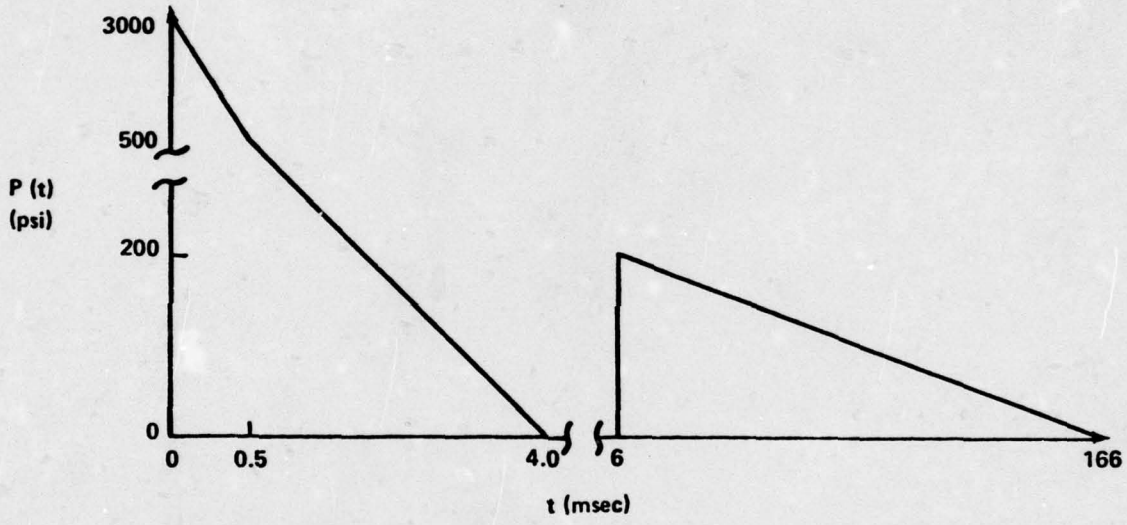


FIGURE 5. TYPICAL COMBINED LOADING FUNCTION

STRUCTURAL ANALYSIS EMPHASIZING ENERGY METHODS: SOME COMPARISONS WITH SUPPRESSIVE SHIELD EXPERIMENTS

by

P. S. Westine
P. A. Cox
E. D. Esparza

Southwest Research Institute
San Antonio, Texas

ABSTRACT

Energy methods yield closed-form solutions permitting estimates of maximum strains and deflections in structural components with various boundary conditions. Because these solutions can be presented graphically or in simple algebraic formats, they are of great value to designers. In the suppressive structures program, energy solutions were developed and used to predict elastic-plastic response in structures exposed to both shock waves and the quasi-static pressure buildup from detonations in an enclosed volume. If responding components are supported by other systems which also deform, coupled energy solutions are required for more accurate estimates of strains and deflections in both structures.

Comparisons are made with measured strain and displacement data for both simple blast loaded components and the complex configuration of the Category I shield in the suppressive structures program. These comparisons include results obtained with the simplified energy solutions as well as results obtained using elastic-plastic finite element computer programs.

INTRODUCTION

Energy solutions and other approximate analysis techniques are generally applied to fundamental structural components, such as beams, plates, strings and membranes. Furthermore, boundary conditions are idealized as completely clamped or hinged without friction and attached to perfectly rigid foundations. As this paper shows, these ideal solutions quickly break down when applied to real structures where supports are not rigid and deflections in the support structure greatly influence the response of the component and vice versa. To handle this more complex problem coupled energy solutions have been developed to complement the energy solutions presented for simple components. Solutions obtained

PRECEDING PAGE BLANK-NOT FILMED

with both methods are applied to an actual structure and comparison with experiments are made. The structure chosen for these comparisons is the 1/4-scale model of the Category I shield from the Suppressive Shielding Program[1]. Additionally, more rigorous solutions are obtained by finite element methods for comparison with the energy solutions and experiment.

GENERAL ENERGY SOLUTIONS

As discussed in previous papers[2,3], approximate energy solutions for blast loaded structures are obtained by the following procedures:

(1) An appropriate deformed shape is assumed to describe the final shape of the structure

(2) The strain energy stored in the structure is derived for the assumed deformed shape.

(3) Expressions are derived for the kinetic energy imparted to the structure by the blast loading and/or for the external work done by the quasi-static pressure during deformation.

(4) A solution for deflection in the impulsive loading realm is obtained by equating the kinetic energy to the strain energy.

(5) The asymptote for deflection in the quasi-static loading realm is obtained by equating strain energy to the external work.

(6) Maximum bending strains are then calculated from the second derivative of deflections.

Energy solutions do not give transient results; only the final (maximum) deformation or strain is obtained. For elastic behavior, the solution gives the peak elastic response. For rigid-plastic behavior, the peak residual deformation is obtained. The simplicity of the procedure and the results makes the method ideally suited for design work. In addition energy solutions are easy to apply because a single graphical solution can give answers to an entire class of problems, as in Figure 1.

Figure 1 is a nondimensional load-impulse (p - i) diagram for determining the maximum strain and deflection in beams loaded by a blast wave. The blast wave is characterized by its peak applied pressure p and impulse i, which are either side-on or reflected values dependent upon the orientation of the building relative to the enveloping wave. In this graph, we assume that the load is uniform over the entire span length ℓ.

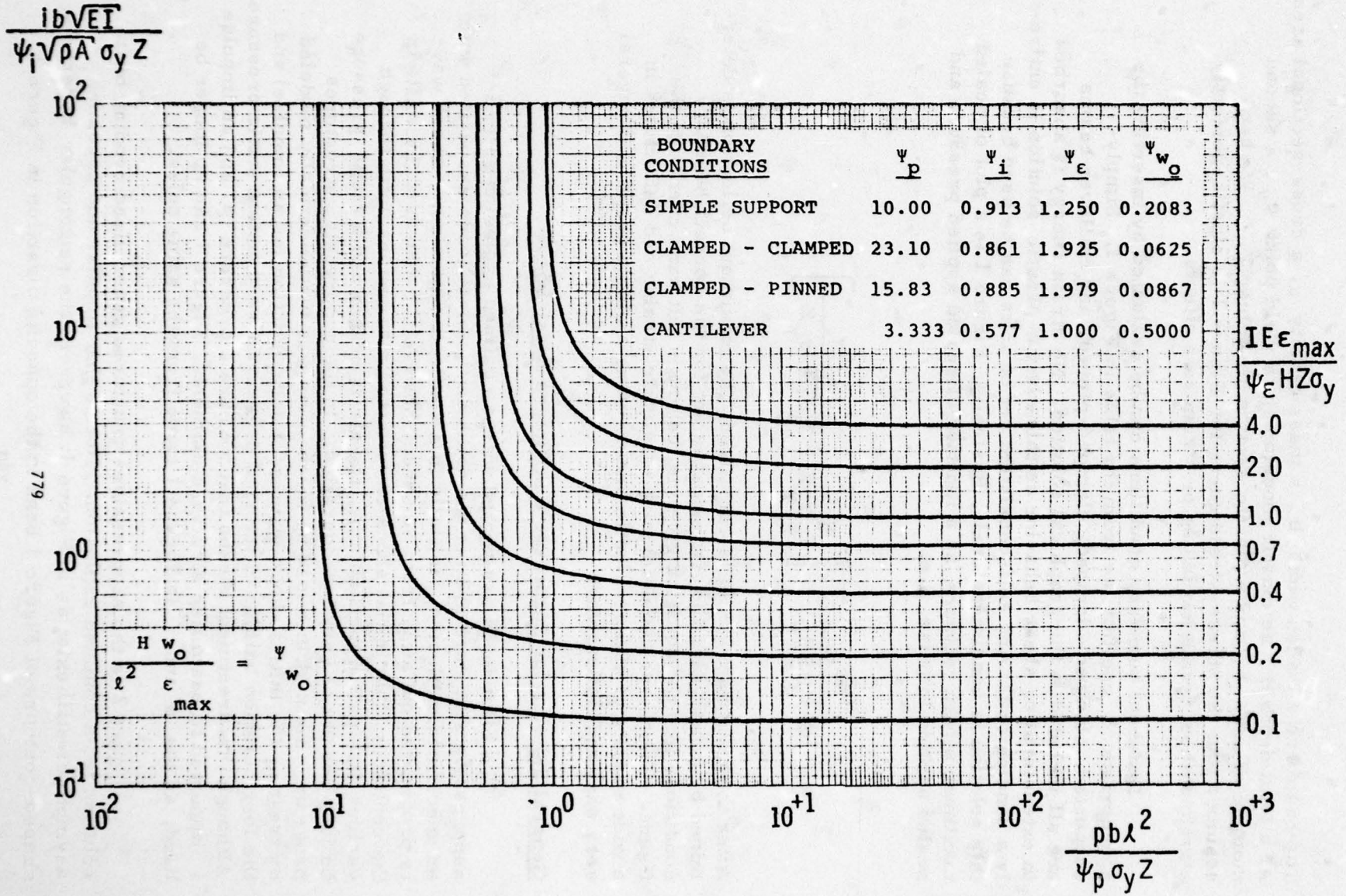


FIGURE 1. ELASTIC-PLASTIC SOLUTION FOR BLAST LOADED BEAMS

The beam has a loaded width b , a mass density ρ, a cross-sectional area A, a total depth H , an elastic modulus E, a yield point σ_y , a second moment of area I , and a plastic section modulus Z. We have assumed that the stress-strain curve for Figure 1 is elastic-perfectly plastic without strain hardening or strain rate effects.

Different boundary conditions can be evaluated by inserting the appropriate Ψ coefficients from the table in Figure 1. Simply-supported, clamped-clamped, clamped-pinned, and catilever beams are all included in the graphical solution. No strain energy is absorbed in extensional or shear behavior as this elastic-plastic solution is entirely a bending one. Any self-consistent set of units can be used because this solution is nondimensional. Basically, Figure 1 is a plot of scaled maximum strain contours as a function of scaled applied pressure and scaled applied impulse, i. e.

$$\frac{IE\epsilon_{max}}{\Psi_\epsilon HZ\sigma_y} = f\left[\frac{pb\ell^2}{\Psi_p \sigma_y Z} , \frac{ib\sqrt{EI}}{\Psi_i \sqrt{\rho A}\, \sigma_y Z}\right]$$

After the maximum strain is calculated, the maximum deflection is determined by substituting the Ψw_p coefficient for the correct boundary conditions into the equation given in the lower left hand corner of the figure. Thus, one can determine maximum strains and deflections in a wide variety of elastic-plastic beams using a single graph and several very easy multiplications.

General Solution for Suppressive Structure Blast Loads

The blast loads associated with a confined explosion as in a suppressive structure are not the same as the blast loads associated with an unconfined explosion. Initially in a confined explosion, a shock wave is propagated out away from a source; however, because of the walls in the container this initial shock is reflected many times until through various dissipation mechanisms, the air is heated and a static pressure buildup results of very long duration. In the suppressive structures program, this multiple loading mechanism was mathematically modeled by treating the initial shock wave as a delta function (as an impulse) and the long duration buildup of internal pressure as a constant static pressure. Although this treatment means that we have a pressure p and an impulse i imparted to beam like structure elements, Figure 1 can no longer be used, as the p and i in Figure 1 came from the same pulse.

Figure 2 is the suppressive-structures generalized bending beam solution for a confined explosion. Notice that impulse and pressure asymptotes still exist as in Figure 1; however, the rectangular hyperbola shaped contours of Figure 1 bend in the opposite direction in Figure 2.

Boundary Conditions	α_p	α_i	α_ϵ	α_{w_o}
Simple Support	10.00	3.652	1.250	0.2083
Clamped-Clamped	23.09	3.444	1.925	0.0625
Clamped-Pinned	15.83	3.540	1.979	0.0867

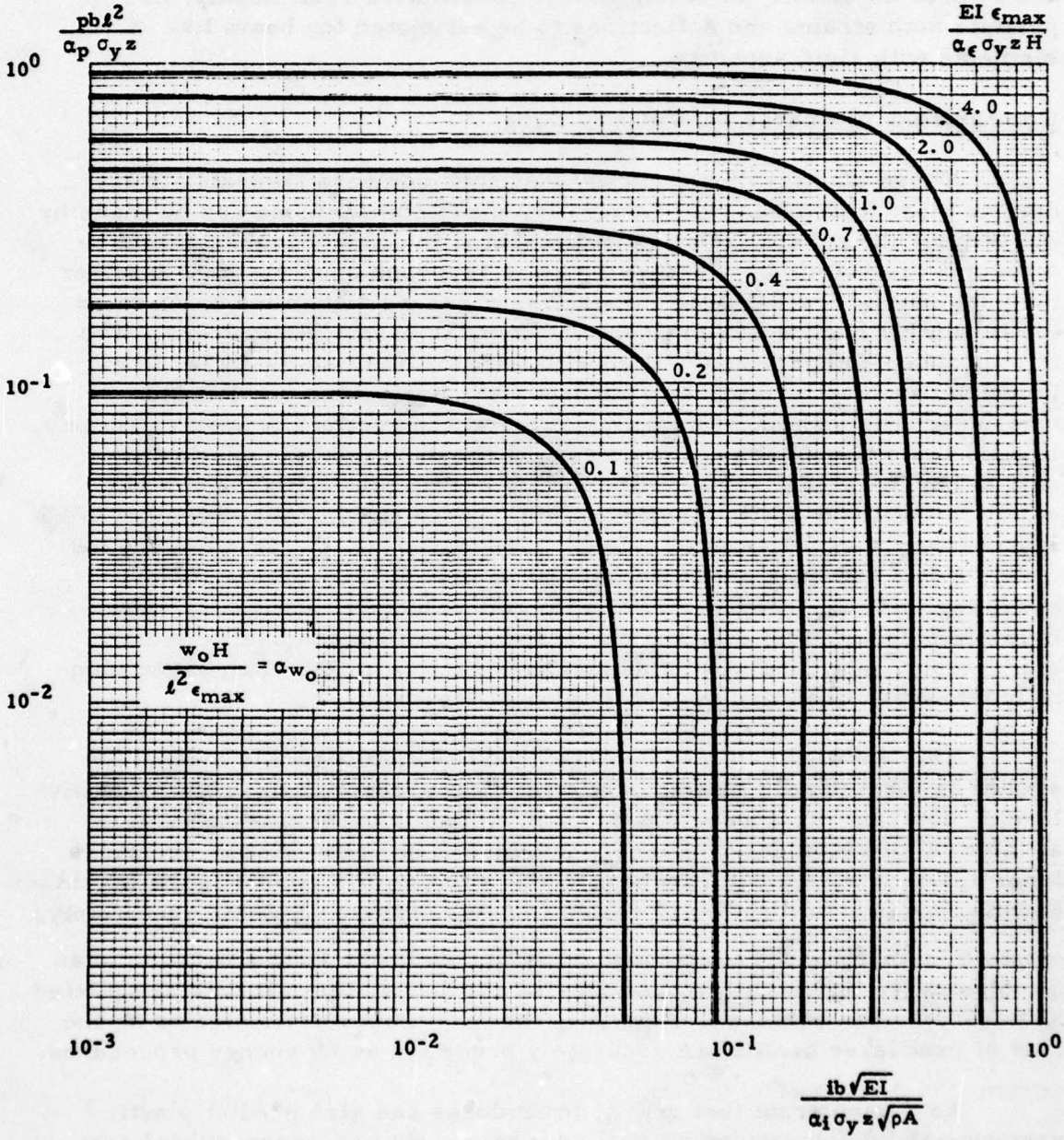


FIGURE 2. SUPPRESSIVE STRUCTURES ELASTIC-PLASTIC BEAM SOLUTION

Figure 2 was developed by equating the sum of the kinetic energy associated with the initial shock plus the maximum possible work associated with the static pressure buildup to the strain energy in a beam with an assumed deformed shape. The parameters in Figure 2 are as defined in Figure 1 and the α coefficients are the counterparts of the Ψ coefficients in Figure 1 to account for various boundary conditions. Figure 2 also uses an elastic-perfectly plastic constitutive relationship, and permits both strains and deflections to be estimated for beam like elements with rigid supports.

Comparisons of Energy Solutions to Date

These elastic-plastic energy solutions compare favorably to test data on blast loaded beams. Generally, these comparisons can be made by simplifying the general solution as presented in either Figures 1 or 2 to a special case of either elastic or plastic response and response in either the quasi-static loading realm where the pressure asymptote matters or the impulsive loading realm where the impulse asymptote matters. The first of these comparisons will be with unreported tests by J. D. Day in which five blast loading experiments were performed on clamped cantilever steel beams with strain gauges at the root of the beam. These limited tests are extremely important as they are the only ones to the best of our knowledge to be performed on beams whose response was solely in the quasi-static loading realm. These steel beams were 6 x 3/4 x 3/4 inch and were exposed to side-on overpressures p_s as summarized in Table 1. The drag pressure Q can be calculated from p_s, and assuming that C_D equals 1.75, we obtain calculated strains as shown in the last column of Table 1. The response of all these beams are elastic only. Calculated strains compare very favorably with experimentally measured observed maximum elastic strains.

This solution can also be compared to experimentally measured strains in blast-loaded elastic cantilever beams responding in the impulsive loading domain. Reference 4 reports maximum elastic bending strains at the root of rectangular 6061-T6 aluminum cantilever beams 12 inches long, 1.0 inch wide, 0.051 inches thick. Plotted in Figure 3 is the maximum bending strain as a function of scaled impulse $\frac{i}{\sqrt{\rho E}\, L}$. Some uncertainty exists in computing the exact impulse imparted to the beams because of an air blast wave diffracting around the beams; hence, the test data are plotted as bars. As can be seen in Figure 3, the maximum elastic strains at the root of cantilever beams are accurately predicted using energy procedures.

To demonstrate that energy procedures can also predict plastic response and deformations as well as strains, we use experimental test data taken by Florence and Firth[5]. All of the beams tested by Florence and Firth were of rectangular cross-section and had a length to thickness ratio ℓ/h of 36. Both clamped and pinned beams made of 2024-T4 aluminum,

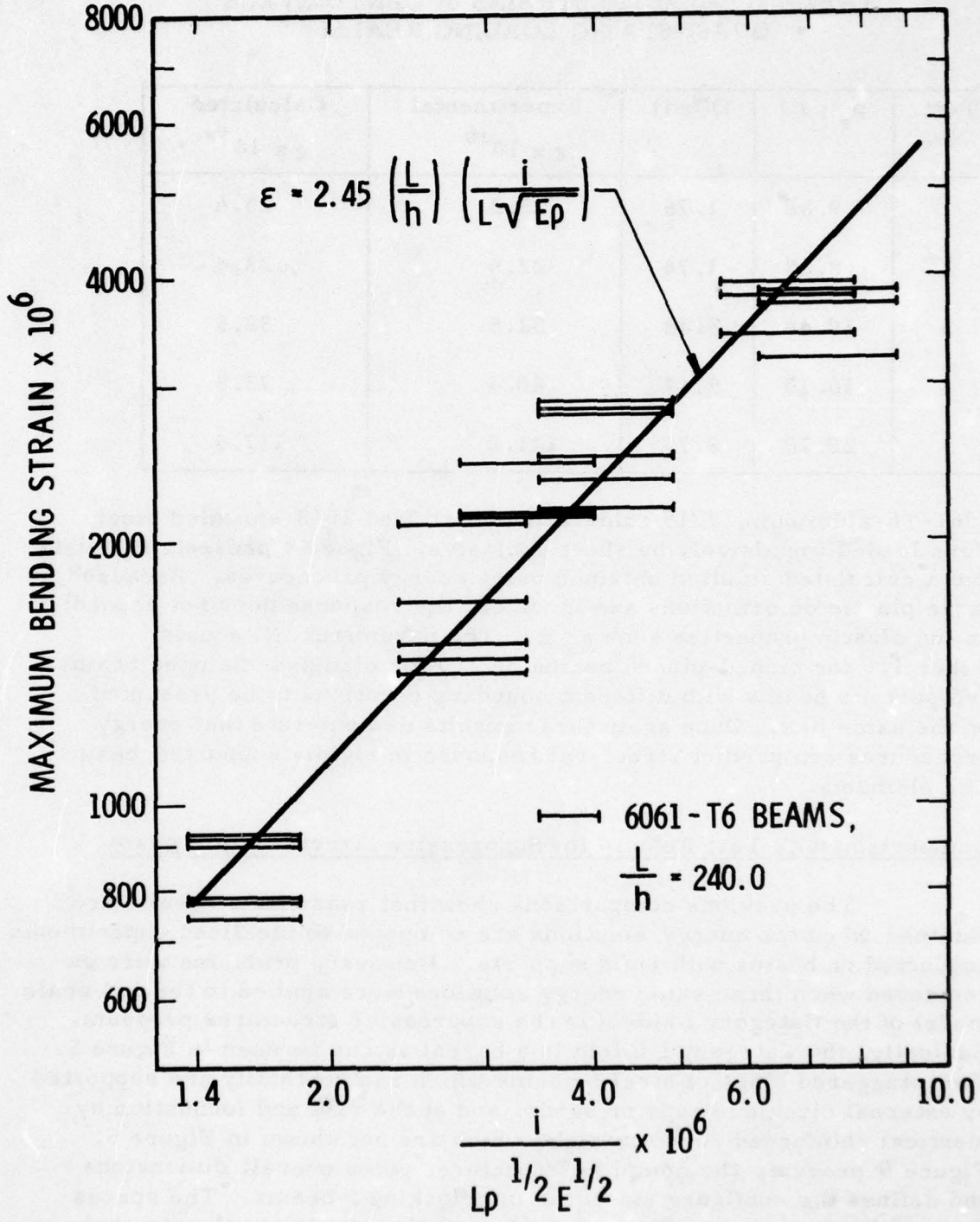


FIGURE 3. ELASTIC RESPONSE OF CANTILEVERS, IMPULSIVE LOADING REALM

TABLE 1. ELASTIC STRAINS IN CANTILEVERS
QUASI-STATIC LOADING REALM

Test No.	p_s(psi)	Q(psi)	Experimental $\epsilon \times 10^{+6}$	Calculated $\epsilon \times 10^{+6}$
1	8.80	1.76	23.2	23.6
2	8.68	1.74	22.9	23.4
3	10.48	2.42	32.5	32.5
4	16.10	5.47	80.4	73.5
5	20.78	8.73	141.0	117.5

6061-T6 aluminum, 1018 cold-rolled steel, and 1018 annealed steel were loaded impulsively by sheet explosive. Figure 4 presents this data and a calculated solution obtained using energy procedures. Because large plastic deformations are involved, the response does not depend on the elastic properties such as E. The parameter N equals either 1.0 for pinned-pinned beams or 2.0 for clamped-clamped beams and permits beams with different boundary condtions to be presented on the same plot. Once again these results demonstrate that energy procedures can predict structural response in rigidly supported beam like elements.

Comparison with Test Results for Suppressive Structures Program

The previous comparisons show that reasonable results are obtained when the energy solutions are compared to idealized experiments conducted on beams with rigid supports. However, problems were encountered when these same energy solutions were applied to the 1/4 scale model of the Category I shield in the suppressive structures program. Basically, the Category I shield is a barrel as can be seen in Figure 5. Two staggered rings of steel I-beams which run vertically are supported by external circular hoops or bands, and at the roof and foundation by identical reinforced concrete slabs which are not shown in Figure 5. Figure 6 presents the complete structure, gives overall dimensions and defines the configuration of the interlocking I-beams. The spaces between the beams were to permit a controlled venting to the atmosphere of the explosive products. In all the comparisons which we will make, these vents were closed with a liner.

The intent of the designers was to have both the I-beams and the supporting hoops deform plastically for large internal explosions. Provided these structural members deformed but did not rupture, the structure

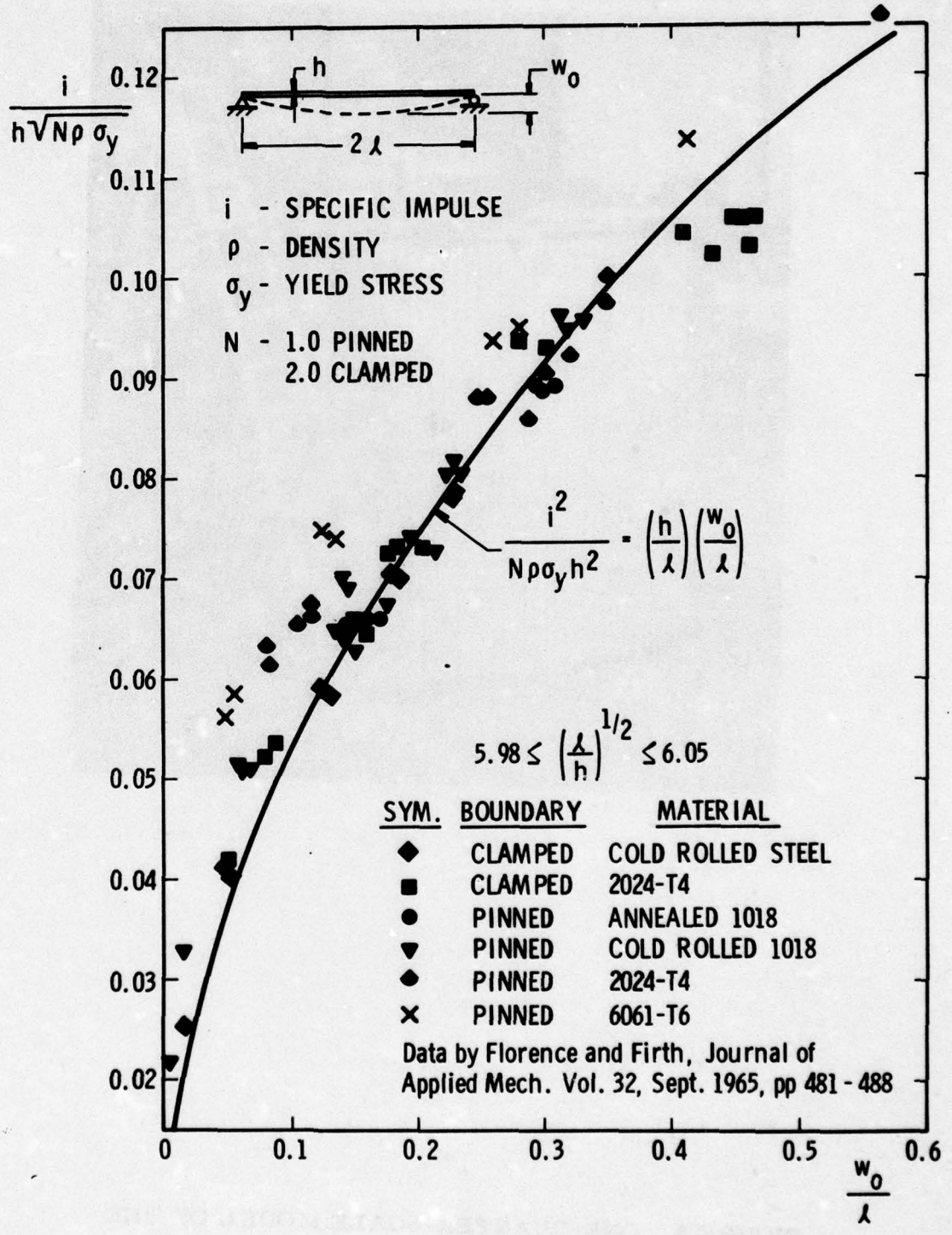


FIGURE 4. BEAM BENDING IN THE IMPULSIVE LOADING REALM

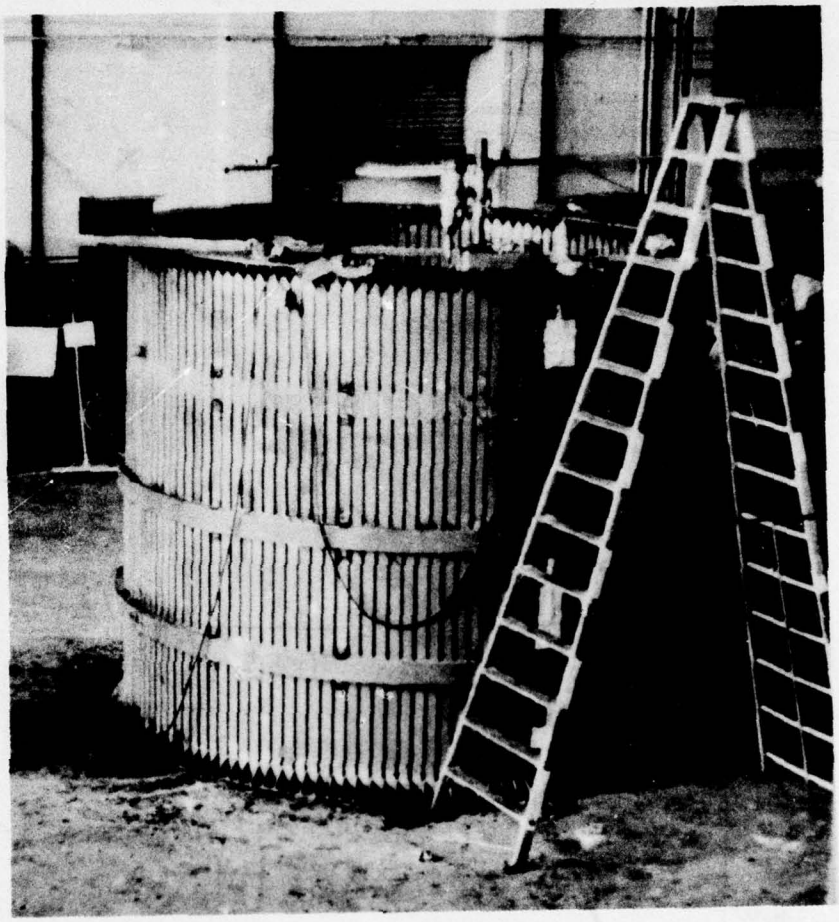


FIGURE 5. ONE-QUARTER-SCALE MODEL OF THE CATEGORY I SUPPRESSIVE SHIELD

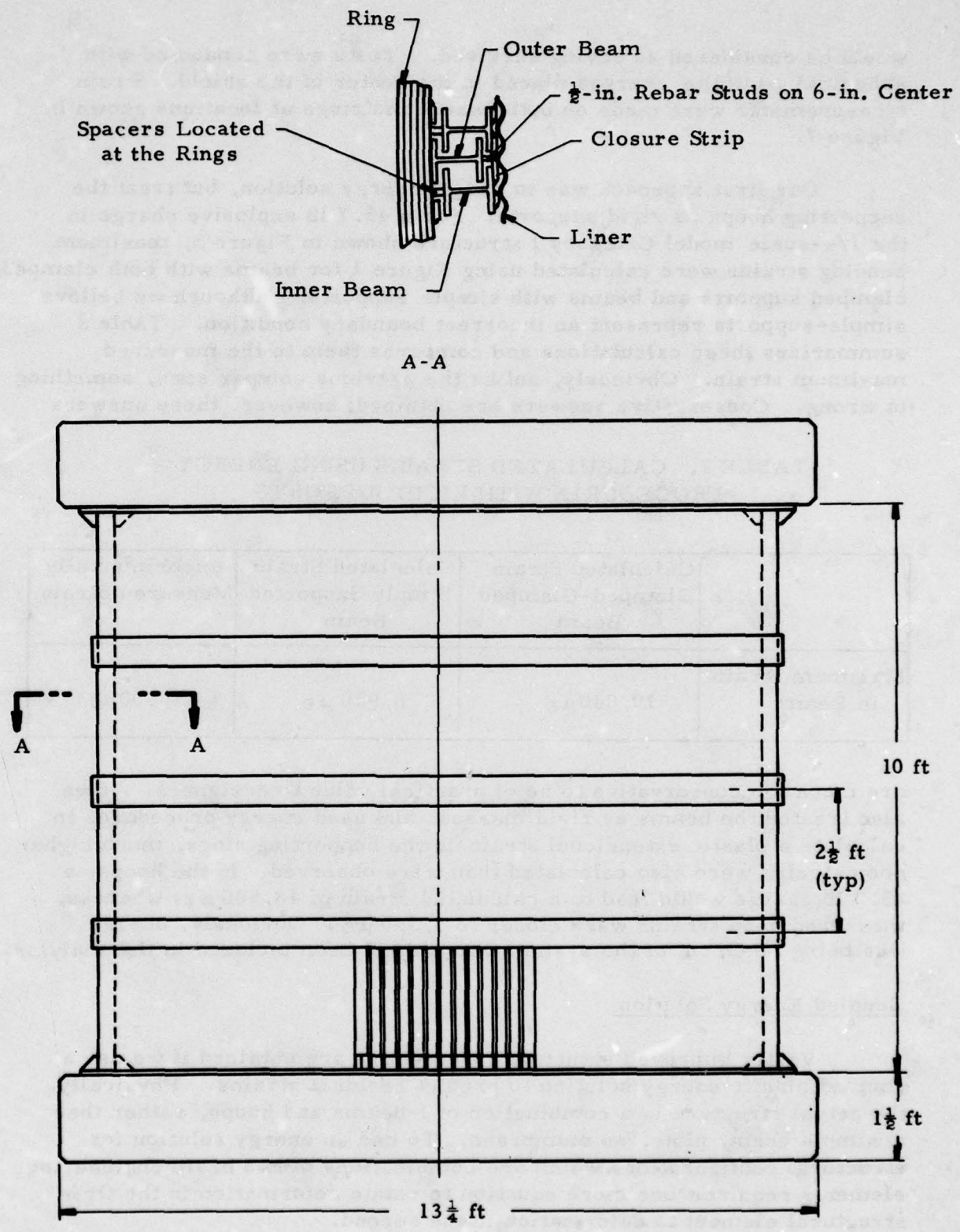


FIGURE 6. DIMENSIONS AND DETAILS OF THE CATEGORY I ¼-SCALE MODEL

would be considered as having survived. Tests were conducted with spherical pentolite charges placed in the center of the shield. Strain measurements were made on both beams and rings at locations shown in Figure 7.

Our first approach was to use an energy solution, but treat the supporting hoops as rigid supports. For a 45.7 lb explosive charge in the 1/4-scale model Category I structure shown in Figure 5, maximum bending strains were calculated using Figure 1 for beams with both clamped-clamped supports and beams with simple supports, although we believe simple-supports represent an incorrect boundary condition. Table 2 summarizes these calculations and compares them to the measured maximum strain. Obviously, unlike the previous comparisons, something is wrong. Conservative answers are obtained; however, these answers

TABLE 2. CALCULATED STRAINS USING ENERGY PROCEDURES WITH RIGID SUPPORTS

	Calculated Strain Clamped-Clamped Beam	Calculated Strain Simply Supported Beam	Experimentally Measured Strain
Maximum Strain in Beam	10,040 $\mu\epsilon$	6,950 $\mu\epsilon$	1,600 $\mu\epsilon$

are much too conservative to be of practical value to designers. If we also treated the beams as rigid masses, and used energy procedures to calculate a plastic extensional strain in the supporting rings, much higher hoop strains were also calculated than were observed. In the hoops, a 45.7 lb charge would lead to a calculated strain of 18,500 $\mu\epsilon$; whereas, measured hoop strains were closer to 3,350 $\mu\epsilon$. Obviously, energy was being taken out of the system that had not been included in the analysis.

Coupled Energy Solution

Vastly improved structural predictions are obtained if we use a coupled plastic energy solution to predict residual strains. Physically, the actual structure is a combination of I-beams and hoops, rather than a simple beam, plate, or membrane. To use an energy solution for structural configurations which are combinations of two basic engineering elements requires one more equation to relate deformation in the first structural element to deformation in the second.

Coupled plastic systems can be visualized by a rigid-plastic, rheological model as in Figure 8. In Figure 8, the yield force f_1 must

Location	Gage Nos.			
	0°	90°	180°	270°
Upper Band	90	95	91	94
Middle Band	92	96	93	97
Lower Band	Not instrumented			

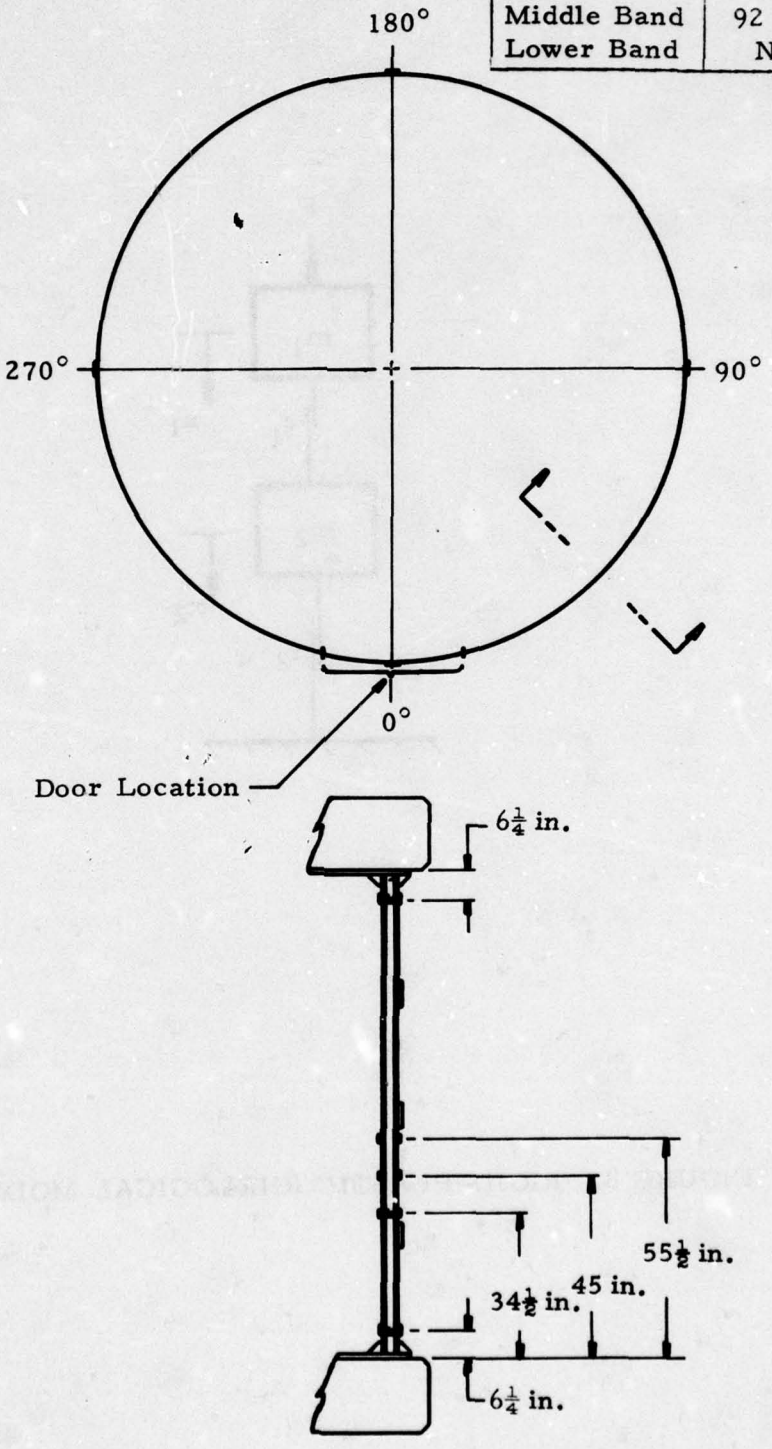


FIGURE 7. STRAIN GAGE LOCATIONS ON THE BEAMS AND RINGS FOR THE CATEGORY I ¼-SCALE MODEL TESTS

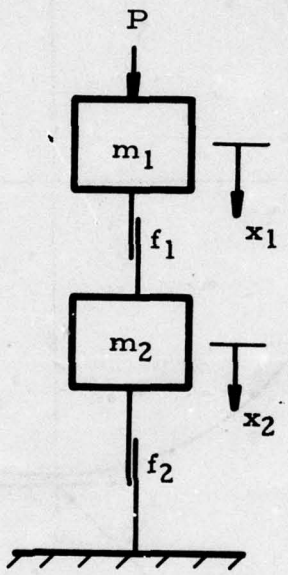


FIGURE 8. RIGID-PLASTIC RHELOGICAL MODEL

must exceed f_2, and the quasi-static force P must be less than both f_1 and f_2; otherwise, the system will not act as a coupled one. The relative residual deformation $(X_1 - X_2)$ is related to the residual deformation X_2 through an impedance match involving the parameters m_1, m_2, f_1, f_2, and P.

The coupling equation is obtained by writing the two equations of motion for the masses m_1 and m_2 in Figure 8. The initial conditions are no initial displacement, no initial velocity for m_2, and an initial velocity for m_1 equal to the impulse I divided by the mass m_1. Solving these equations for the maximum relative deformation $(X_1 - X_2)$ and for the displacement X_2 yields the coupling equation, Equation 1, after $(X_1 - X_2)$ is divided by X_2.

$$\frac{(X_1 - X_2)}{X_2} = \frac{m_2(f_2 - P)}{m_1(f_1 - f_2)} \tag{1}$$

Equation (1) is this coupling relationship. To complete an energy solution, one now only has to equate the kinetic energy from the impulse in the initial shock plus the maximum possible work from the static pressure buildup in a suppressive shield to the sum of the strain energies in both structural components to obtain estimates of the deformation in a dynamically loaded suppressive shield. In a coupled system as in Figure 5, the strain energy S. E. is given by:

$$\text{S. E.} = f_1(X_1 - X_2) + f_2 X_2 \tag{2}$$

Because two equations now exist for X_1 and X_2, they can be solved simultaneously. We will illustrate the use of this approach by using the 1/4 scale Category I suppressive shield as an example.

As has already been seen, external circular hoops provide restraint for longitudinal I-beams. The I-beams represent the $m_1 - f_1$ structure, and the hoops are the $m_2 - f_2$ structure. If we treat the I-beams as clamped-clamped beams, an appropriate assumed deformation pattern for this structural component is given by:

$$y = \frac{w_o}{2}\left(1 + \cos\frac{2\pi x}{\ell}\right) \tag{3}$$

where

w_o = maximum mid-span deformation relative to the supports

ℓ = total span

x = coordinate system with its origin at mid-span

y = deformation anywhere at some value of x

Differentiating Equation (3) twice gives:

$$\frac{d^2y}{dx^2} = \frac{-2\pi^2 w_o}{\ell^2} \cos\frac{2\pi x}{\ell} \tag{4}$$

The strain energy S. E. $_{①}$ in a plastic system is given by the integral

$$\text{S. E.}_{①} = 2\int_0^{\ell/2} M_y \frac{d^2y}{dx^2}\, dx \tag{5}$$

where

M_y = plastic yield moment

Substituting Equation (4) into Equation (5) and completing the desired integration gives:

$$\text{S. E.}_{①} = \frac{4\pi M_y w_o}{\ell} \tag{6}$$

The average deformation y_{AVG} must be calculated next. It is obtained by the integral

$$[\ell]\, y_{AVG} = 2\int_0^{\ell/2} \frac{w_o}{2}\left(1 + \cos\frac{2\pi x}{\ell}\right) dx \tag{7}$$

or

$$y_{AVG} = \frac{w_o}{2} \tag{8}$$

The force f_1 in one beam equals S. E.$_{①}$ divided by the average deformation, or:

$$f_1 = \frac{8\pi M_y}{\ell} \tag{9}$$

The mass m_1 equals:

$$m_1 = \rho_b A_b \ell \tag{10}$$

where

ρ_b = mass density of a beam

A_b = cross-sectional area of a beam

Next f_2 and m_2 must be calculated for the hoops. If we assume hoops of equal cross-sectional area on each end, the deformation will be a symmetric change in radius ΔR. The strain energy for both hoops is two times the stress times the strain $\frac{\Delta R}{R}$ times the volume $2\pi R A_h$ or:

$$\text{S. E.}_{②} = 4\pi\sigma_h A_h \Delta R \tag{11}$$

The average deflection in a hoop is the deflection ΔR. This means that the force f_2 is given by S. E.$_{②}$ $/\Delta R$ or:

$$f_2 = 4\pi\sigma_h A_h \tag{12}$$

The mass m_2 equals two times the mass density ρ_h times the area A_h times the circumference $2\pi R$ or

$$m_2 = 4\pi\rho_h A_h R \tag{13}$$

The quasi-static force P equals the pressure p times the internal circumference times the length or:

$$P = 2\pi r \ell p \tag{14}$$

Now the coupling equation can be used to relate the average deformation of the beams $(\frac{w_o}{2})$ to the deformation in the hoops ΔR. Substituting for m_1, m_2, f_1, f_2, and P then yields:

$$\frac{\frac{w_o}{2}}{\Delta R} = \frac{(4\pi\rho_h A_h R)\left[(4\pi\sigma_h A_h) - 2\pi r \ell p\right]}{(N\rho_b A_b \ell)\left(\frac{8\pi N \sigma_b z}{\ell} - 4\pi\sigma_h A_h\right)} \tag{15}$$

The parameter N stands for the number of beams. The mass of the beams and force equals N times m_1 or f_1 for a single beam in Equation (15). In addition, the yield stress σ_b times the plastic section modulus z was substituted for the yield moment in the beam force equation, Equation (9). Reducing Equation (15) algebraically gives the ratio for the maximum deformation in the beams relative to the change in hoop radius.

$$\frac{w_o}{\Delta R} = \frac{8\pi\left(\frac{\rho_h A_h R}{N\rho_b A_b \ell}\right)\left(1 - \frac{p r \ell}{2\sigma_h A_h}\right)}{\left[2\left(\frac{N\sigma_b z}{\sigma_h A_h \ell}\right) - 1\right]} \tag{16}$$

The solution proceeds by writing the strain energy S. E. for the entire system. This energy equals the sum of Equations (6) and (11) or:

$$S.E. = \frac{4\pi N \sigma_b z w_o}{\ell} + 4\pi\sigma_h A_h \Delta R \tag{17}$$

Substituting Equation (16) for ΔR in Equation (17) gives:

$$S.E. = \frac{4\pi N \sigma_b z w_o}{\ell} + \frac{N \rho_b A_b \sigma_h \ell w_o}{2 \rho_h R} \times \frac{\left[2\left(\frac{N \sigma_b z}{\sigma_h A_h \ell}\right) - 1\right]}{\left(1 - \frac{p r \ell}{2 \sigma_h A_h}\right)} \tag{18}$$

Next the energy imparted to the structure must be estimated. This energy comes from the kinetic energy imparted through blast waves and the work from the quasi-static pressure buildup within a suppressive shield. Algebraically, this energy E_N equals Equation (19) if we assume all loads are imparted to the beams.

$$E_N = \frac{N I^2}{2 m_1} + p b \ell (y_{AVG} + \Delta R) \tag{19}$$

where

b = loaded width of the beams.

Substituting for I, m_1, y_{AVG}, and Equation (16) for ΔR yields, after collecting Terms:

$$E_N = \frac{N i^2 b^2 \ell}{2 \rho_b A_b} + \frac{p b \ell w_o}{2} \left[1.0 + \frac{N \rho_b A_b \ell}{4\pi \rho_h A_h R} \frac{\left(\frac{2 N \sigma_b z}{\sigma_h A_h \ell} - 1\right)}{\left(1 - \frac{p r \ell}{2 \sigma_h A_h}\right)}\right] \tag{20}$$

Finally, equating E_N, Equation (20) to S.E., Equation (18), and gathering terms yields an equation which can be solved for w_o, the maximum deflection in the beams.

$$\frac{i^2 b^2 \ell^2}{\rho_b A_b \sigma_b z w_o} + \frac{p b \ell^2}{N \sigma_b z} \left[1.0 + \frac{N \rho_b A_b \ell}{4 \pi \rho_h A_h R} \frac{\left(\frac{2 N \sigma_b z}{\sigma_h A_h \ell} - 1 \right)}{\left(1 - \frac{p r \ell}{2 \sigma_h A_h} \right)} \right] \tag{21}$$

$$= 8\pi + \frac{\sigma_h \rho_b A_b \ell^2}{\sigma_b \rho_h z R} \frac{\left(\frac{2 N \sigma_b z}{\sigma_h A_h \ell} - 1 \right)}{\left(1 - \frac{p r \ell}{2 \sigma_h A_h} \right)}$$

This solution can be checked against experimental results from the one-quarter scale Category I structure. Equation (21) yields w_o, the maximum beam deformation relative to the rings, and subsequent substitution in Equation (16) yields ΔR, the change in hoop radius. Strains can also be estimated. The residual hoop strain equals $\frac{\Delta R}{R}$ as in Equation (22a), and the maximum residual bending strain in the beams equals half the beam depth $\frac{H}{2}$ times the maximum beam curvature as given by Equation (4). Equation (22b) is the maximum residual strain in the beams.

$$\epsilon_{hoop} = \frac{\Delta R}{R} \tag{22a}$$

$$\epsilon_{beams} = \frac{\pi^2 w_o H}{\ell^2} \tag{22b}$$

The following values from the one-quarter scale Category I tests were substituted into the preceding equations.

$$\sigma_b = \sigma_h = 45,000 \text{ psi}$$

$$\rho_b = \rho_h = 7.332 \times 10^{-4} \frac{\text{lb-sec}^2}{\text{in}^4}$$

A_b = 1.67 in^2

z = 1.95 in^3

i_R = 0.478 psi-sec

p = 194 psi

N = 296

A_h = 5.625 in^2 (this is half of a ring area, as another half handles another bay)

b = 1.43 in. (this is less than the flange width because of overlap)

ℓ = 30.0 in.

R = 72.25 in. (this is the radius to the center of a ring)

r = 67.25 in. (this is the internal radius)

H = 3.0 in.

These values yield the following estimates for residual deformations and residual strains. Because of rebound, the maximum strain observed could equal $\epsilon_{residual}$ plus $\frac{\sigma_y}{E}$.

w_o = 0.0118 in.

ΔR = 0.497 in.

$\epsilon_{\substack{beam \\ residual}} = 388\,\mu\,\frac{in}{in}$ $\qquad$ $\epsilon_{\substack{beam \\ maximum}} = 1,888\,\mu\,\frac{in}{in}$

$\epsilon_{\substack{hoop \\ residual}} = 6,878\,\mu\,\frac{in}{in}$ $\qquad$ $\epsilon_{\substack{hoop \\ maximum}} = 8,378\,\mu\,\frac{in}{in}$

All estimates are reasonable relative to measured results in Category I model tests. Remember, to distinguish whether strains are residual or maximum ones. In addition, we assume beams respond in a bending mode, an assumption which may or may not be true. In the experiments, the I-beams deformed very little; this is as predicted. Many hoops broke near welds, but this may be an embrittlement problem of construction. Other fabrication problems existed which make this structure a poor one for evaluating analysis. For example, the bands

making up a hoop were not in contact. This observation means high strains in inner bands and lower strains in outer bands where measurements are being made. Yield stress has never been measured in the structural materials, and results are sensitive to yield stress and ring area. If we double the ring area so the total area rather than the half area acts, the following results show how sensitive the response is to the A_h parameter.

$w_o = 0.05756$ in.

$\Delta R = 0.168$ in.

$\epsilon_{\text{beam residual}} = 1,894\ \mu \frac{\text{in}}{\text{in}}$ $\epsilon_{\text{beam maximum}} = 3,394\ \mu \frac{\text{in}}{\text{in}}$

$\epsilon_{\text{hoop residual}} = 2,328\ \mu \frac{\text{in}}{\text{in}}$ $\epsilon_{\text{hoop maximum}} = 3,828\ \mu \frac{\text{in}}{\text{in}}$

By way of a summary, Table 3 has been created to compare calculated and observed strains in this coupled energy solution. As can be seen through comparison with Table 2, the influence of coupling or flexible supports is to reduce greatly the calculated estimates. Although estimates are still not in agreement, they are much closer to measured values on the actual structure. A strong possiblity exists that the hoops never reach the maximum possible strain, as they did rupture near embrittled welds.

TABLE 3. CALCULATED STRAINS USING COUPLED ENERGY PROCEDURES

	Calculated Strain	Experimentally Measured Strain
Maximum Strains In Beam	1,888 $\mu\epsilon$	1,600 $\mu\epsilon$
Maximum Strains In Hoop	8,378 $\mu\epsilon$	3,350 $\mu\epsilon$

Finite Element Solutions

In addition to the energy solutions, a small two-dimensional (2-D) finite element computer program, developed specifically for the dynamic-transient analysis of beams to blast loading, was used to predict structural

response of the Category I 1/4-scale model. The equations of motion are cast in finite difference form and integrated step-wise in time using a predictor-corrector method. The program treats material behavior as bi-linear with hysteretic recovery, including the effects of strain rate and strain hardening. Calculations of the response were made with and without strain rate to show the significant effect strain rate has on displacements and strains. Strain hardening effects were found to be negligible and are not discussed.

The finite element model used for the calculations is shown in Figure 9. It is drawn schematically along side one of the beams from the cylinder. The structure is idealized by assuming axial symmetry and symmetry about a horizontal plane through the center of the shield. This amounts to neglecting the presence of the door on the response of the beams away from its immediate vicinity, and neglecting axial loading and response. Although there is some connection between the beams through the closure strips, which are tack welded to the face of the inner beam and to the studs on the outer beam (see Figure 6), the beams are assumed to respond individually. Thus, only the lower half of one beam is represented in the model.

Bi-linear springs have been used to model the rings and radial flexibility in the foundation. The resistance of the rings is divided into two parts to spread the support over the ring width. Guided end conditions permit lateral displacements but no rotation, and the first beam element above the foundation has been sized to represent the combined bending stiffness of the slab foundation and the bolted connection. Although the closure strips will contribute to the beam stiffness, they are not welded continuously to the beams and so their contribution is ignored; however, mass of the closure strips and the liners is added to the beam mass.

As for the energy solutions, the pressure loading was assumed to be uniformly distributed over the beam. The loading is composed of an initial impulse and near constant (quasi-static) pressure. Two loading conditions were analyzed. They are:

19.3 lb charge:	$i_r = .199$ psi-sec
	$p_{qs} = 73$ psi
45.7 lb charge:	$i_r = .478$ psi-sec
	$p_{qs} = 194$ psi

Basic beam and ring parameters used in computing input for the program are:

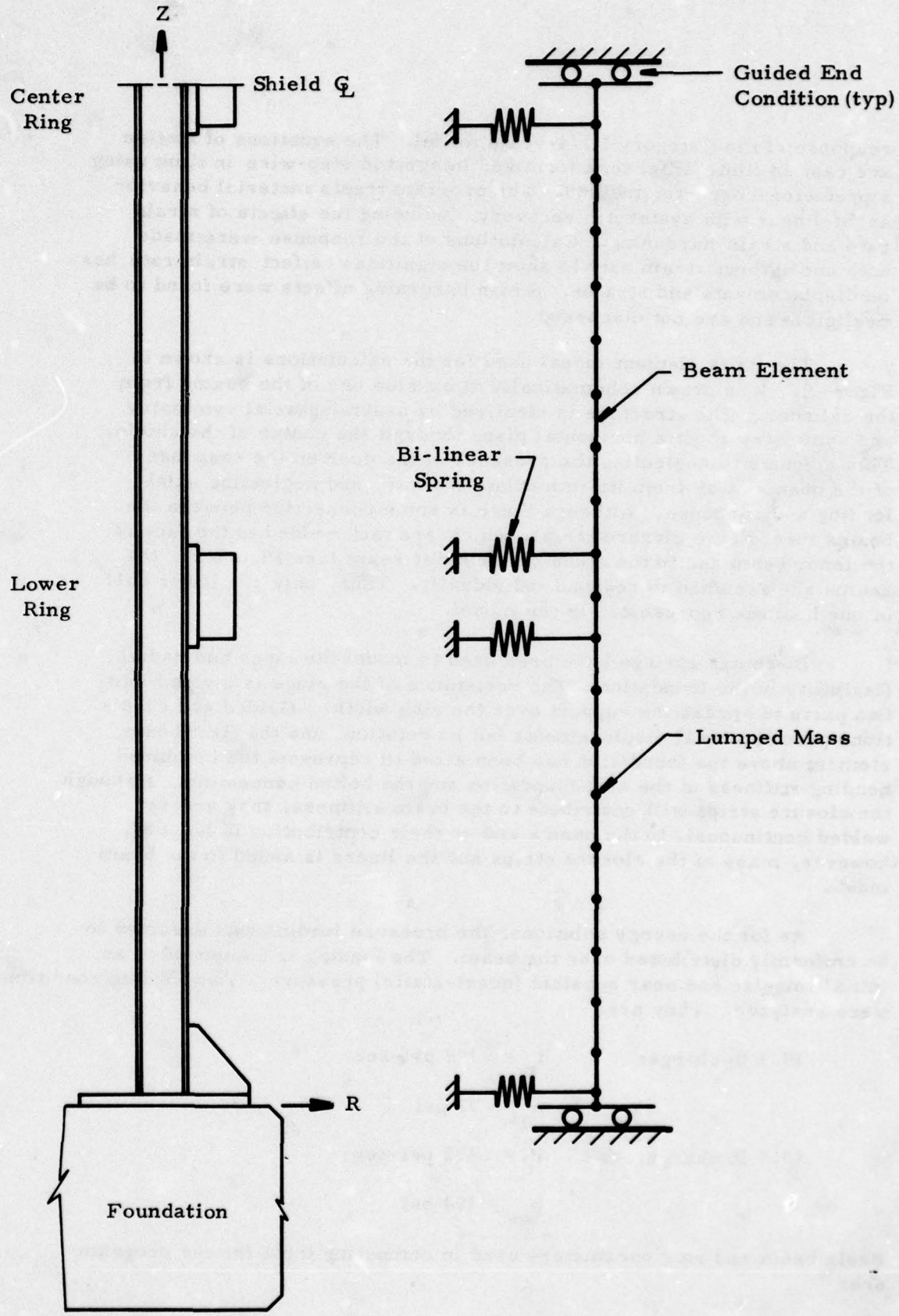


FIGURE 9. SCHEMATIC OF THE FINITE ELEMENT MODEL OF THE STRUCTURE

- S3 x 5.7 beam geometry
- mass per unit length (including closure strips and liners),

  $\rho A = 1.46 \times 10^{-3}$ lb sec/in^2
- foundation effective modulus, $E_c = 4.5 \times 10^6$ psi
- beam plastic moment, $M_y = 87,750$ in/lb
- beam elastic modulus, $E = 30 \times 10^6$ psi
- beam plastic modulus = 1% of elastic modulus
- beam loaded width, b = 1.43 in.

Although the details will not be given, stiffness of the reinforcing gussets at the foundation and of the spacers at the rings were added to the beam. Also, estimates were made of the bending stiffness of the beam attachment to the foundation. Strain rate effects are based on the well known relationship[6] for mild steel given in Equation (23)

$$\sigma_d = \sigma_y \left[1 + \left(\frac{\dot{\epsilon}}{40.4}\right)^{.2} \right] \tag{23}$$

where σ_d is the dynamic yield stress and $\dot{\epsilon}$ is the strain rate.

Results for the 19.3 lb charge are given in Figure 10. Strain rate effects are included. This figure shows the distribution of maximum values of displacement, bending strain and shear stress along the beam. The shear stress is based on the shear reactions in the beam rather than on shearing strains, and is computed as

$$\sigma_s \approx \frac{V}{dt_w} \tag{24}$$

where V is the shear reaction in the beam, d is the beam depth and t_w is the beam web thickness. Data points are shown as circles. Three observations can be made from this comparison:

(1) The distribution of peak strains in the beam is irregular and not what one would expect if only a section of the beam between two rings were analyzed.

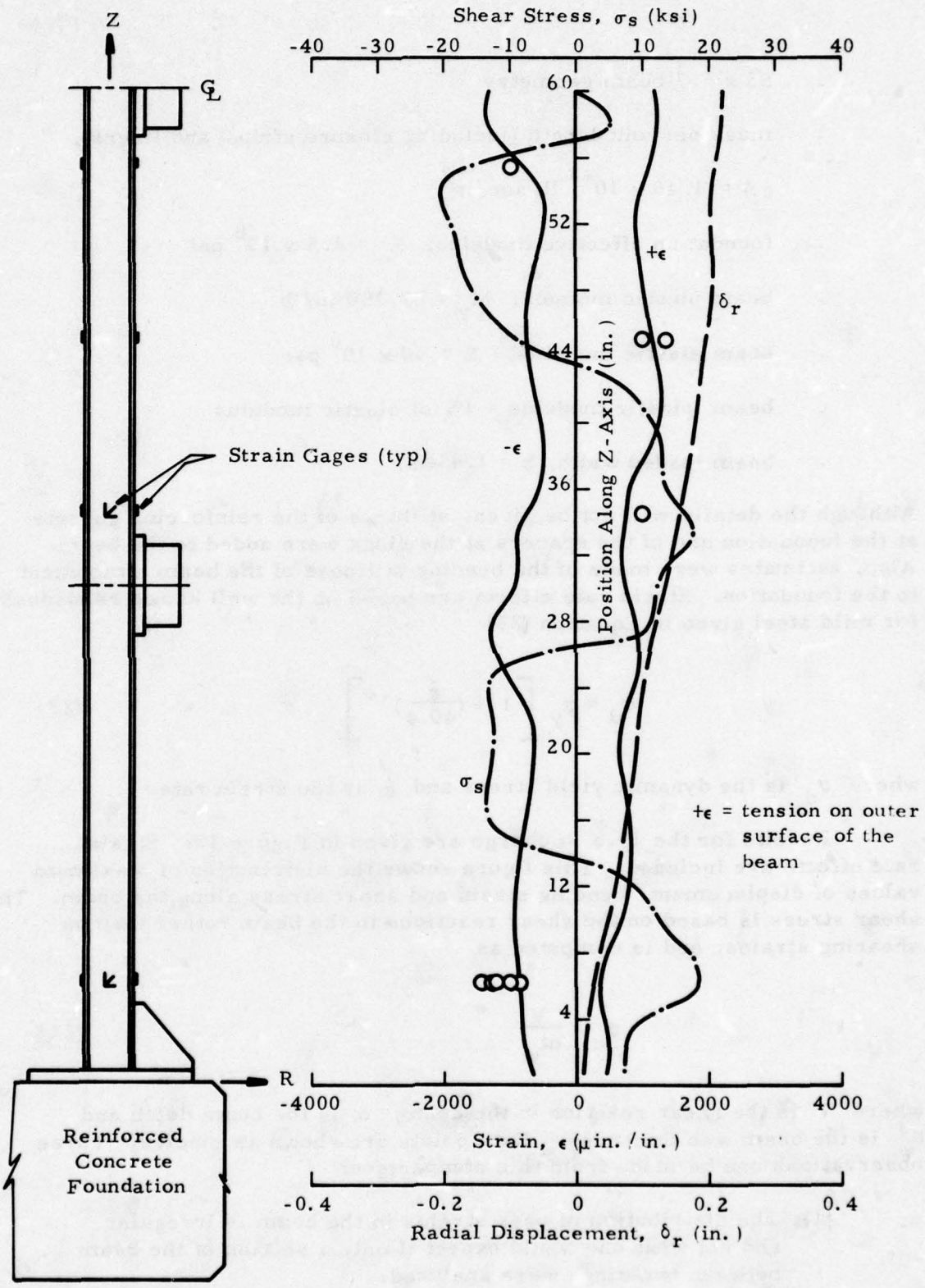


FIGURE 10. DISTRIBUTION OF MAXIMUM DEFLECTION, STRAIN AND SHEAR STRESS VALUES (19.3 lb charge)

(2) Computed results for bending strains underestimate the measured values for this charge weight.

(3) If the computed distribution of strain is accurate, the measurement point may not have recorded the maximum values.

Figure 11 gives similar results for the 45.7 lb charge. The same observations can be made for this case as were made for the smaller charge except that, in this instance, the computed strains are higher than measured values. Also, for this charge weight the shearing stresses exceed the shear yield stress of the material at many points along the beam. We estimate that the allowable shear stress values for the material are:

$$\sigma_{sy} = 21,600 - 27,000 \text{ psi}$$

$$\sigma_{su} = 34,800 - 49,800 \text{ psi}$$

These compare to peak calculated values of 44,000 psi, which indicates that substantial yielding of the beam in shear should have occurred and perhaps the beam was near a shear failure.

Although strain comparisons cannot be made because shearing strains were not computed by the program, Table IV lists measured shear strains versus the computed stress. The measured results do confirm that substantial yielding occurred in shear for the 45.7 lb charge. Shear strains slightly beyond yield were also recorded for the 19.3 lb test. These results plus the results in Figure 11 indicate that the beam is not properly proportioned for highly impulsive short duration loading. Higher shear area relative to bending stiffness is needed to bring the shearing and bending strains into better balance. This observation is true for almost all commercially available beams because they have been designed for high efficiency under static loads.

Only results, which included strain rate effects, were presented in Figures 10 and 11. The effects of strain rate on the overall structural response are best demonstrated by the variation in ring strains. Measured and calculated strains are given in Table V. Calculated values include those obtained by energy formulas as well as by the finite element program. For the energy solutions, both coupled and uncoupled results are included. The coupled solution was obtained from Equation (21); the equation for uncoupled response is given in Reference 7 which presents a plastic limiting solution to the solution shown in Figure 2.

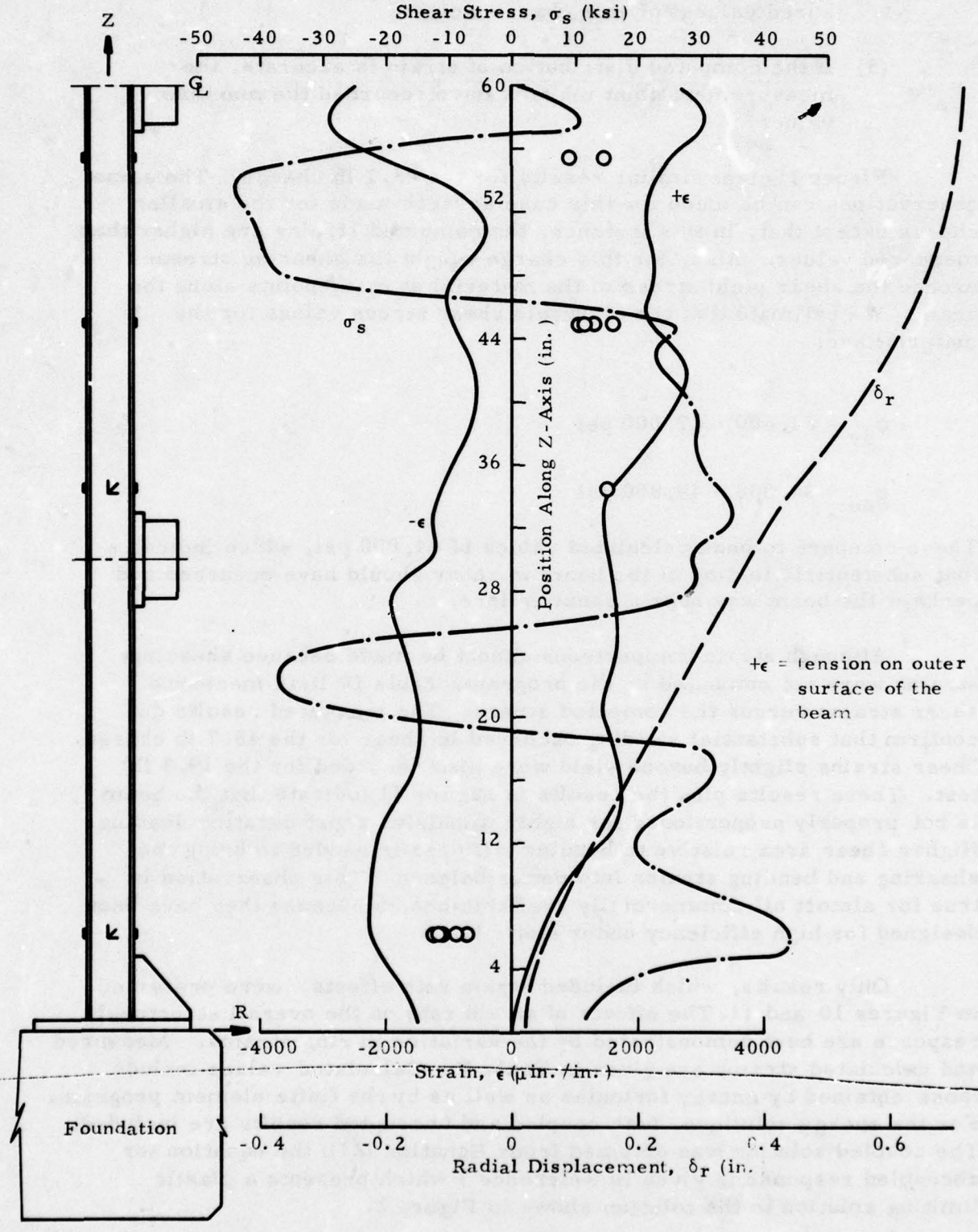


FIGURE 11. DISTRIBUTION OF MAXIMUM DEFLECTION, STRAIN AND SHEAR STRESS VALUES (45.7 lb charge)

TABLE IV. BEAM SHEAR DATA

Location	19.3 lb		45.7 lb			
	Meas. Strain Test 194	Calc. Stress F.E. Prog	Measured Strain Test 195	Measured Strain Test 196	Measured Strain Test 197	Calc. Stress F.E. Prog
Outer beam 34 1/2" from foundation	2,650*	18,000**	3,250	--	--	35,000
Outer beam 6 1/4" from roof	1,550	20,000	2,400	--	--	44,000
Inner beam-6 1/4" from roof	2,000	20,000	2,500	7,500	--	44,000
Inner beam-6 1/4" from roof	2,350	20,000	7,000	14,000	14,800	44,000

*Strain μ in/in
**Stress psi

TABLE V. MEASURED AND CALCULATED STRAINS IN THE RINGS

	19.3 lb	45.7 lb		
	Test 194	Test 195	Test 196	Test 197
Top Ring				
Measured				
Gage 90*	1100**	2200	2400	2200
Gage 91	--	3100	2400	4200
F. E.+ Solution				
No S.R.++	5315		13630	
With S.R.	1840		5110	
Energy Formulas				
No coupling	3100		18490	
With coupling	2460		6820	
Center Ring				
Measured				
Gage 92	1600	--	3300	3400
Gage 93	2300	--	2100	3100
F. E. Solution				
No S.R.	10360		21530	
With S.R.	3000		9740	
Energy Formulas				
No coupling	3100		18490	
With coupling	2490		6824	

*refer to Figure 7 for gage locations
**strains are in μ in/in
+finite element 2-D program
++ strain rate effects

The most obvious conclusion to be reached from the results in Table V is that the calculated values overestimate measured ring response in every case. For the two comparisons available, it appears that the difference between computed and measured values increase as charge weight increases; hence, the analytical results should always be conservative. The effects of strain rate and coupling are pronounced, reducing calculated values by approximately a factor of 3 for the large charge weight. Still, the calculated values are far above measured values. It should be noted that the energy solution does not include strain rate or strain hardening effects and yet gives a result which is the same order of magnitude as the more rigorous finite element method. One reason for this is that the energy solution forces plastic deformation in the beams whereas the finite element solution does not. It is apparent from Figure 11 that predicted plastic straining in the beams was minimal so that energy absorption by the beams was small.

Reasons for the disagreement between predictions and measurements of ring response are not clear. However, two factors may have effected the results:

(1) The closure strips shown in Figure 6 were tack welded to the inner beams and provided some circumferential restraint. Thus, they acted in a manner similar to rings but were distributed over the full eight of the shield. This effect was neglected in the response calculations.

(2) Properties of the ring material were never measured. It proved to be a brittle material because fractures were noted during the testing. The calculations were performed assuming a mild steel which may not represent true ring properties.

One final comparison of measured and calculated results is given in Table VI. It compares peak measured strains in the beam to strains and shearing stresses computed by both the energy and finite element methods. From this comparison it is obvious that both the finite element solution with strain rate effects and the coupled energy solution give results which are consistent with the measured values. Additionally, the finite element method provides useful information on shear in beams by providing shear reactions which predict the presence of large shearing strains. From the finite element solution it is also apparent that strain rate effects play little part in the beam bending response. By stiffening the ring, however, strain rate does cause higher shear stresses. This stiffening of the ring was demonstrated in Table V by the sharp reduction in the ring strain.

TABLE VI. COMPARISON OF PEAK VALUES IN THE BEAMS

	19.3 lb charge			45.7 lb charge		
	Bending Strain μ in/in	Shear Strain μ in/in	Shear Stress psi	Bending Strain μ in/in	Shear Strain μ in/in	Shear Stress psi
Measured	1450	2650		1600	14,800	
F.E. Method						
No SR	--		--	3010		36,900
With SR	1400		20,000	3000		44,000
Energy Solution						
Uncoupled	3325			10040		
Coupled	1700			1890		

CONCLUSIONS

The conclusions to be derived from these comparisons of analysis and experiment are five fold:

(1) Energy methods give quick easy solutions to elastic, plastic or elastic-plastic dynamic problems if time histories are not required and only the peak values of displacement, strain and stress are required.

(2) Energy formulas can be cast in convenient graphical form to give solutions to a large class of problems.

(3) Energy solutions can be derived even for the problem of coupled response in complex structures.

(4) Comparisons with experiment for complex structures show that the energy solutions give reasonable answers which, if in error, tend to over estimate strains and deflections.

(5) The finite element computer solution infers that strain rate and coupling should not be ignored in calculations of structural response to high intensity blast loading. If these effects are ignored the solution is an upper bound which may over estimate the true response by an order of magnitude.

ACKNOWLEDGEMENTS

This work was performed under Contract Number DAAA15-75-C-0083 with Edgewood Arsenal, Aberdeen Proving Grounds, Maryland. The Army's technical monitor was Mr. Bruce W. Jezek. Both Mr. Jezek and Mr. James McKivrigan of the Edgewood staff provided technical direction, suggestions, and information to our program.

At SwRI, we are indebted to Drs. Wilfred E. Baker and William Ko for suggestions on the development of energy procedures. Special thanks are extended to Mr. James Hokanson for computer programming and other technical assistance. Mrs. Sue Miller typed this paper and Mr. Victor Hernandez drafted all figures.

REFERENCES

(1) W. E. Baker, P. A. Cox, E. D. Esparza and P. S. Westine, Design Study of a Suppressive Structure for a Melt-Loading Operation, Edgewood Arsenal Contractor Report EM-CR-76043, T.R. No. 9, December 1975.

(2) P. W. Westine and W. E. Baker, "Energy Solutions for Predicting Deformations in Blast Loaded Structures," Minutes of the Sixteenth Explosives Safety Seminar, Vol. II, Hollywood, Florida, September 1974, pp. 849-878.

(3) P. S. Westine and W. E. Baker, Energy Solutions for Predicting Deformations in Blast-Loaded Structures, Edgewood Arsenal Contractors Report EM-CR-76027, Report No. 6, November 1975.

(4) W. E. Baker, W. D. Ewing, Jr., and J. W. Hanna, Laws for Large Elastic and Permanent Deformation of Model Structures Subjected to Blast Loading, Ballistic Research Laboratories Report No. 1060, December 1958.

(5) A. L. Florence and R. D. Firth, "Rigid-Plastic Beams Under Uniformly Distributed Impulses," Journal of Applied Mechanics, Vol. 32, Series E1, March 1965, pp. 7-10.

(6) P. S. Symons, Survey of Methods for Plastic Deformation of Structures Under Dynamic Loading, Dept. of the Navy, Contract Nonr 3248(01)(X), Naval Ship Research and Development Center, June 1967.

(7) P. S. Westine and P. A. Cox, Additional Energy Solutions for Predicting Structural Deformations, Edgewood Arsenal Contractor Report EM-CR-76031, T.R. No. 4, November 1975.

Airblast and Structural Response Testing of a 1/4 Scale Category I Suppressive Shield

by

R. N. Schumacher
C. N. Kingery

Abstract

This report presents the results of an experimental program that was conducted to evaluate one design concept of a 1/4 scale Category I Suppressive Shield subjected to internal blast loading. The shield evaluated was cylindrical in shape, had nonvented floor and roof sections, and a vented wall made up of nested I-beams.

The experiment consisted of detonating bare spherical 50/50 pentolite charges in the geometric center of the shield and measuring (1) the shields capability to attenuate blast pressures outside the structure, (2) blast loading inside the structure, (3) fireball size and (4) structural response of the shield. Three weights of explosive charge were utilized (nominally 8, 19, and 45 lb) and the vented area of the structure was varied over a wide range.

The test data were analyzed and are presented in tabular, graphic, and equation form. The test results indicate that the shield satisfied the specified design requirements investigated during the test program.

USA Ballistic Research Laboratory
Aberdeen Proving Ground, Maryland 21005

PRECEDING PAGE BLANK-NOT FILMED

I. DESCRIPTION OF EXPERIMENT

A. Introduction

This series of tests was part of the Category Shield Program and specifically related to Category I. The Category I Shield is being designed to contain the fragments and attenuate the airblast from an accidental explosion in a melt-pour operation containing 2500 pounds of explosive. The peak airblast overpressure outside of the structure must be attenuated to 50 percent of that expected at an intraline distance of 18 $W^{1/3}$ feet (W is explosive weight in pounds) without shielding.

In order to construct a cost-effective Category I Shield, critical design information was needed that was not available. Both BRL and a contractor (SWRI) recommended that a 1/4 scale structure be designed and tested with instrumentation to determine the structural loading and response, the venting characteristics, and the airblast attenuation. With the results from this experiment and the test results from the previously conducted 1/16 size Category I Shield experimental program[1,2] a full scale structure could be designed with greater confidence.

B. Objectives

The objectives of the 1/4 scale tests of the Category I Shield program were: (1) to document and present in a useable format the ground level free-field blast overpressure versus time data outside the test structure for different charge weights and venting areas; (2) to present the overpressure reduction obtained for the various test configurations at the required scaled intraline distance (Z) of 18 ft/$lb^{1/3}$; (3) to document the peak reflected pressure and impulse impinging on the roof and walls of the structure; (4) to document the quasi-static pressure inside the structure as a function of time; (5) to document the structural response for the various configurations tested; (6) to document the fireball radius observed for the various configurations tested.

[1] *"Blast Attenuation Outside Critical Enclosures Made Up of Selected Suppressive Structure Panel Configurations," R. N. Schumacher and W. O. Ewing, Jr., Ballistic Research Laboratories Memorandum Report No. 2537, September 1975, Aberdeen Proving Ground, MD AD B007711L.*

[2] *"Internal Pressure from Explosions in Suppressive Structures," C. Kingery, R. Schumacher and W. Ewing, Ballistic Research Laboratories Interim Memorandum Report No. 403, June 1975, Aberdeen Proving Ground, MD.*

II. TEST PROCEDURE

A. Test Structure

The test structure consisted of three primary parts. The reinforced concrete floor, the interlocked I-beam cylindrical body, and a reinforced concrete roof. The three parts were fabricated by Global Associates at the National Space Technology Laboratory, Bay St. Louis, Mississippi, from design drawings prepared by the U.S. Army Engineer Division, Huntsville, Alabama[3]. The three parts were shipped by truck to the BRL test site at Aberdeen Proving Ground and assembled by Aircraft Armaments Inc. of Cockeysville, Maryland. A photograph showing the test structure assembled and ready for testing is presented in Figure 1. The detailed design drawings are presented in the Appendix.

1. Structure Roof and Floor. The concrete roof and floor were of similar construction with the exception of a mild steel spallation fragment shield 1/2 inch thick and 61 inches in diameter mounted on the top surface of the roof. Both roof and floor were constructed of reinforced concrete. The rods were number 4 size and were tied together with 1/4 inch vertical stirrups. The roof and floor were 18 inches thick and 13 feet 4 inches in diameter.

2. Structure Body. The body of the structure is cylindrical with an internal radius of 5 feet 7-1/2 inches and a height of 10 feet. It was fabricated utilizing 296, S 3X5.7 interlocking I beams. The inner layer of I-beams (148) had an internal radius of 5 feet 7-1/2 inches, while the outer layer (148) had an internal radius of 5 feet 8-1/8 inches. Each I-beam end was welded to a ring which was bolted to the floor and roof using 3/4 inch bolts tightened with a torque of 300 foot-pounds.

There were three layered reinforcing rings placed around the outer circumference of the structure body. These were located at 2.5, 5.0, and 7.5 feet above the floor. Each ring consisted of nine concentric bands of steel, five inches wide and 1/4 inch thick. The three rings, in the as-delivered and assembled configuration at BRL, were not closely fitted against the I-beam structure body. It appeared that the structure body and rings were not of true circular shape, therefore variations in gap between the I-beams and rings ranged between 1/16 inch and 7/16 inches at various locations around the circumference. This situation was corrected, but not until after the fourth test had been conducted.

3. Effective Vent Area. The vent area for this structure was obtained almost entirely from the structure body portion of the test structure. The venting through the small drain tubes in the concrete

[3] *"Suppressive Shield Quarter Scale Model Category I Drawings," File Numbers 6000 through 6004, U.S. Army Engineer Division Huntsville, Corps of Engineers, Huntsville, Alabama.*

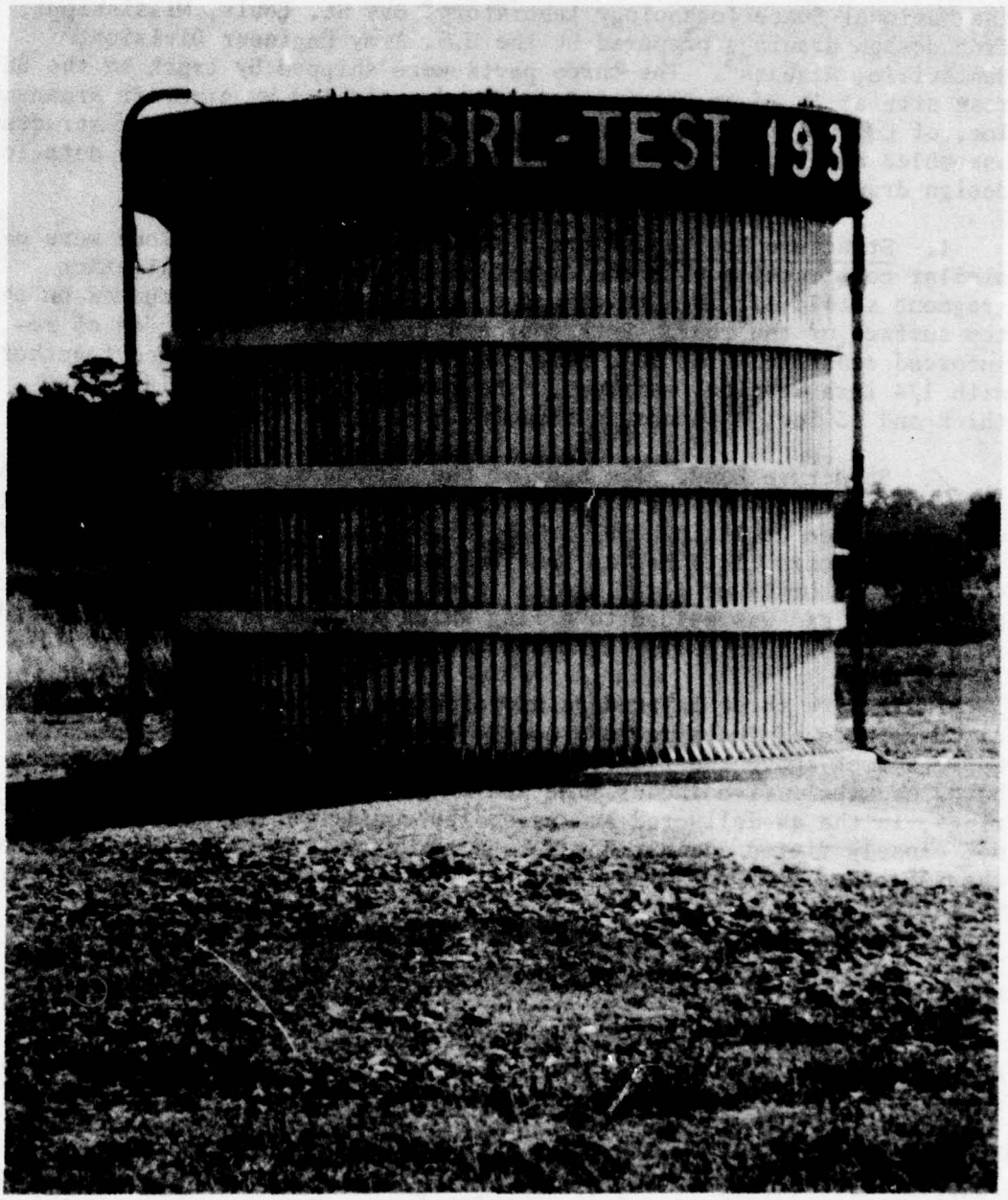


Figure 1. Test Structure Assembled and Ready for Test.

floor and around the threads of the pressure transducers screwed into the roof was considered to be insignificant and therefore was not considered.

In order to determine the effective vent area for the I-beam structure body an equation developed and recommended for use by Southwest Research Institute (SWRI)[4] was utilized. The equation used and the subsequent calculations are presented below.

$$\frac{1}{A_{eff}} = \frac{1}{A_1} + \frac{1}{A_2} + \frac{1}{A_3} + \frac{1}{A_4} \qquad (1)$$

A_1 = vent area between flanges of the first layer = 8720 in.^{2}

A_2 = vent area between flange and webs of the second layer = 6965 in.^{2}

A_3 = vent area between flange and webs of the third layer = 8755 in.^{2}

A_4 = vent area between flanges of the fourth layer = 9694 in.^{2}

A_{eff} = 2102 in.^{2} = 14.60 ft^2

Wall Surface Area	= 50894 in.^{2}	= 353.4 ft^2
Roof Surface Area	= 14314 in.^{2}	= 99.4 ft^2
Floor Surface Area	= 14314 in.^{2}	= 99.4 ft^2
Total Surface Area	79522 in.^{2}	= 552.2 ft^2

In order to determine the vent area as a fraction or percent, one must determine, or arbitrarily establish a reference surface area. There are three reference areas that are considered to be of interest in evaluating suppressive structures. These are (1) the total internal surface area; (2) the wall surface area (the only vented portion of the structure); (3) the surface area of the wall plus roof. The vent areas indicated as a percentage for the above reference areas are: 2.64%, 4.33%, and 3.22% respectively.

On occasion, the vent area to volume ratio is used when comparing the results of quasi-static pressure decay or blast attenuation. Based

[4] *"Analysis and Preliminary Design of a Suppressive Structure for a Melt Loading Operation," Baker, Westine, Cox, Esparza, Technical Report No. 1, Southwest Research Institute, San Antonio, Texas, March 4, 1974.*

on a volume of 994 ft^3 the vent area to volume ratio (VA/V) for the structure as delivered was calculated to be 0.01469 ft^{-1}.

B. Test Schedule

There were five tests planned for this phase of the 1/4 scale Category I Shield program. Two additional tests were conducted after the completion of the five planned tests. The sequence and configuration for each test are presented in Table I.

1. Test Number 191. Test number 1 consisted of the detonation of an 8.3 pound Pentolite sphere in the geometric center of the structure. Structural loading and response was documented as well as internal and external pressure. The test was conducted with the vent area of the structure as delivered. This test was a calibration shot and no damage to the structure was anticipated. Figure 2 shows a typical portion of the internal surface area of the structure body in the as-delivered condition.

2. Test Number 192. The second test was conducted with the structure in the as-delivered condition and with an explosive charge weight slightly over twice that for the first test. This test was to check the structural response prediction methods and establish a basis for comparison for the results of tests 193 and 194.

3. Test Number 193. The primary objective of the test was to document the change in the loading and response of the structure as the venting was reduced. The venting was reduced by approximately fifty percent by welding steel blocking strips over one-half of the spaces between the flanges on the inside of the structure. Figure 3 shows a typical portion of the internal surface area of the structure body with half of the blocking strips in place.

Other objectives were to record the changes in decay rate and duration of the quasi-static pressure and to establish the blast attenuation characteristics outside of the structure with the decreased venting area. The charge weight and location was the same as used for test 192.

4. Test Nubmer 194. The results obtained from test 193 gave confidence in the soundness of the structure; therefore, the metal blocking strips were placed over the remaining internal gaps between I-beam flanges to minimize the structure venting area. The same charge weight and placement was used as for the two preceding tests. Structural loading and response data were recorded to determine changes in structural response for the reduced venting area. The internal and external pressures were recorded to determine structural loading and blast attenuation characteristics for the reduced venting condition.

Table I. Test Description

Test Sequence	Test Number	Charge* Weight (Pounds)	Structural Configuration
1	191	8.3	Structure as delivered.
2	192	19.3	Structure as delivered.
3	193	19.3	50% of vent area blocking strips installed.
4	194	19.3	All vent area blocking strips installed.
5	195	45.7	All vent area blocking strips installed.
6	196	45.7	Light corrugated liner inside structure body.
7	197	45.1	Heavy corrugated liner inside structure body.

*Charge weight of bare spherical 50/50 Pentolite detonated in the geometric center of the structure.

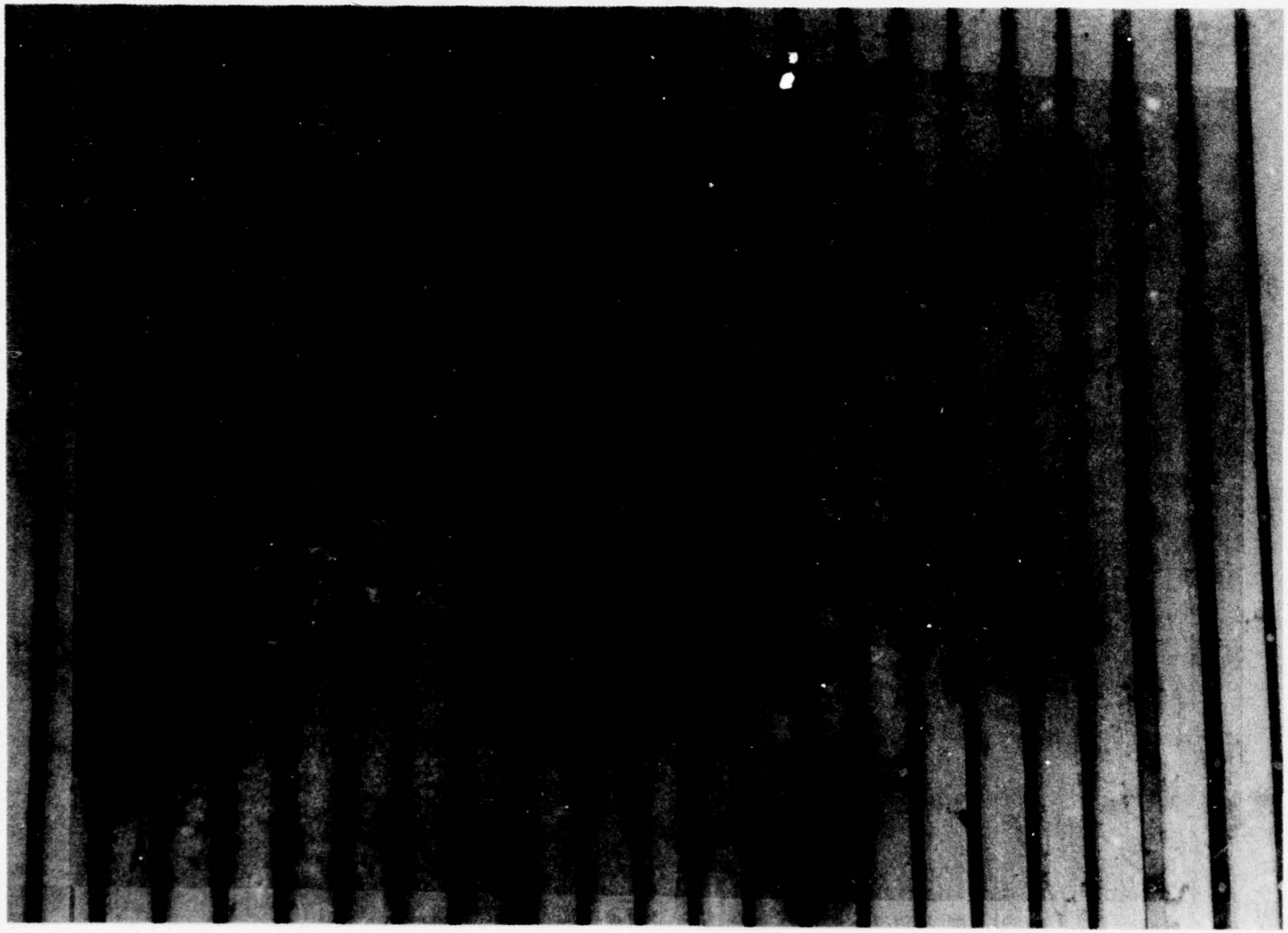


Figure 2. Typical View of Inside Wall Surface as Delivered

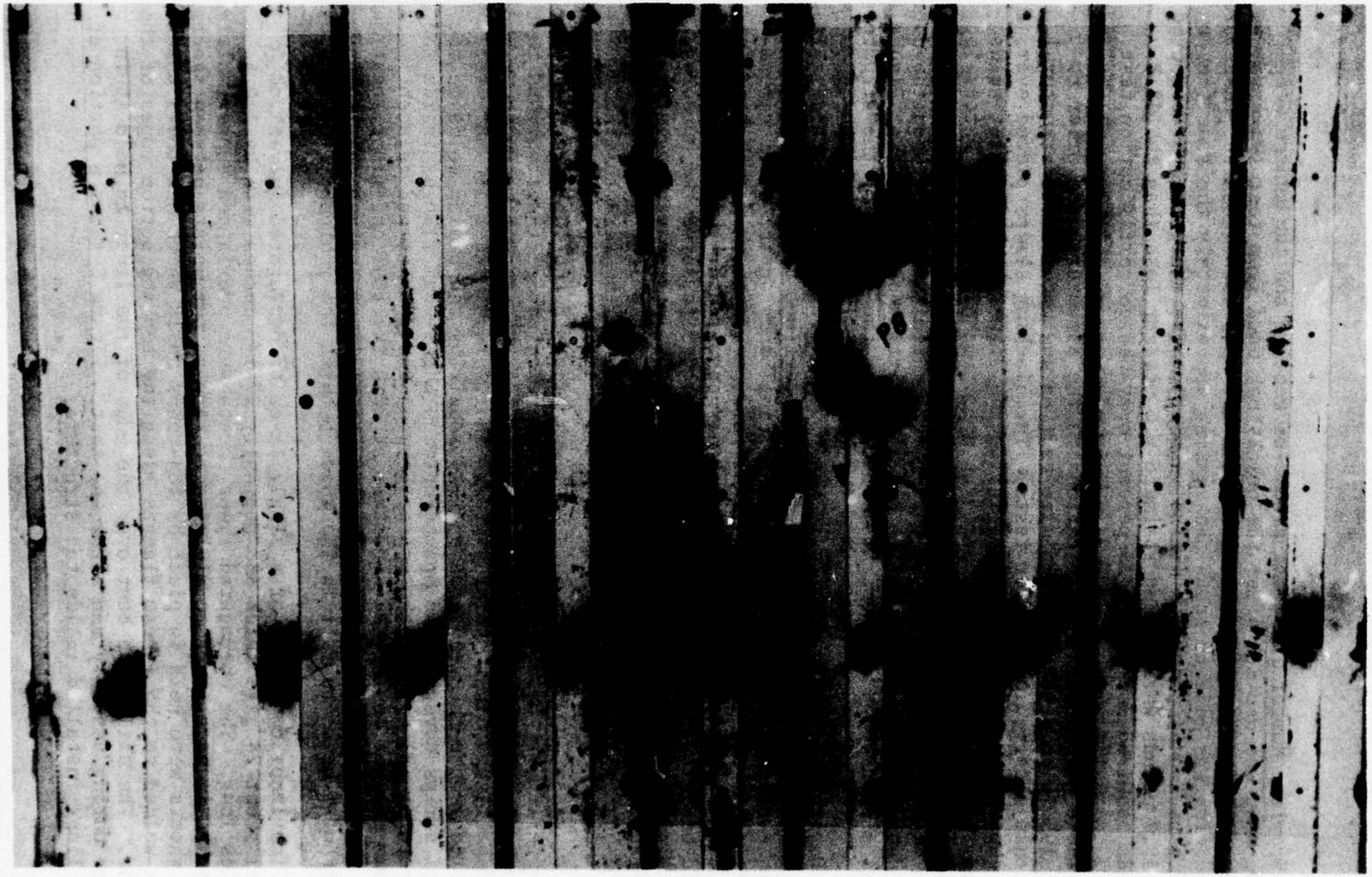


Figure 3. Typical View of Inside Wall Surface with 1/2 of Blocking Strips Installed.

5. Test Number 195. The amount of venting and the charge weight to be used was decided after the quick-look data from test 194 were analyzed. The strain levels from test 194 were not excessive, therefore a decision was made to leave the venting approximately the same (cover some gaps around door to minimize venting). The charge weight selected was 45.7 pounds which is approximately 6 percent less than the 48.8 pounds required for a full 25 percent over-charge certification test.

There were several modifications to the structure made prior to test 195 in an attempt to minimize venting and undesirable structural response observed on earlier tests. The blocking strips placed over the gaps between I-beam flanges inside the structure had fillet welds added to both sides of each strip at approximately six inch intervals. In addition, pieces of plate 1/16 inch thick were welded to the inside edge of the entrance doors so that they covered the gap between the door and door frame in an attempt to minimize jetting of hot gases. Figure 4 shows a photograph of these modifications to the inside of the structure.

During the previous tests it was noted that there was considerable motion of the I-beam elements before they deflected outward enough to make contact with the three reinforcing bands on the outer circumference of the structure body. Therefore, prior to this test, it was decided to shim all spaces such that no gaps greater than 1/16 inch would be left. This modification was expected to serve two purposes, (1) minimize I-beam outward travel and thus help keep venting areas constant and (2) provide more symmetric loading of the reinforcing rings and I-beam elements around the circumference of the structure body.

6. Test Number 196. This test was added to the test program after the preliminary results from test 5 were examined. It was obvious that there was still considerable venting of the hot gaseous products (fireball) and blast overpressures. Therefore, further attampts were made to reduce the vent area by, (1) repairing the broken welds on the metal strips covering the spaces between the I-beam flanges inside the structure; (2) welding the spaces between the gussets and adjacent I-beam flanges inside the structure at both the roof and floor locations; (3) inserting a corrugated galvanized steel liner against the inner layer of I-beams to fill in the space between the roof and floor gussets.

The liner consisted of a single layer of corrugated galvanized steel sheet 24 gage thick and nominally 27-1/2 inches wide by 110.5 inches long. The corrugated liner sheets were overlapped approximately 6 inches in an attempt to minimize leakage at the joints between sheets. The sheets were held in place by ten-penny nails which had their heads tack welded to the I-beam flanges along the top and bottom edges of the liner. The nails were bent over the edge of the liner to hold it in place during assembly and after the test. Figure 5 shows a portion of the liner installed inside the structure.

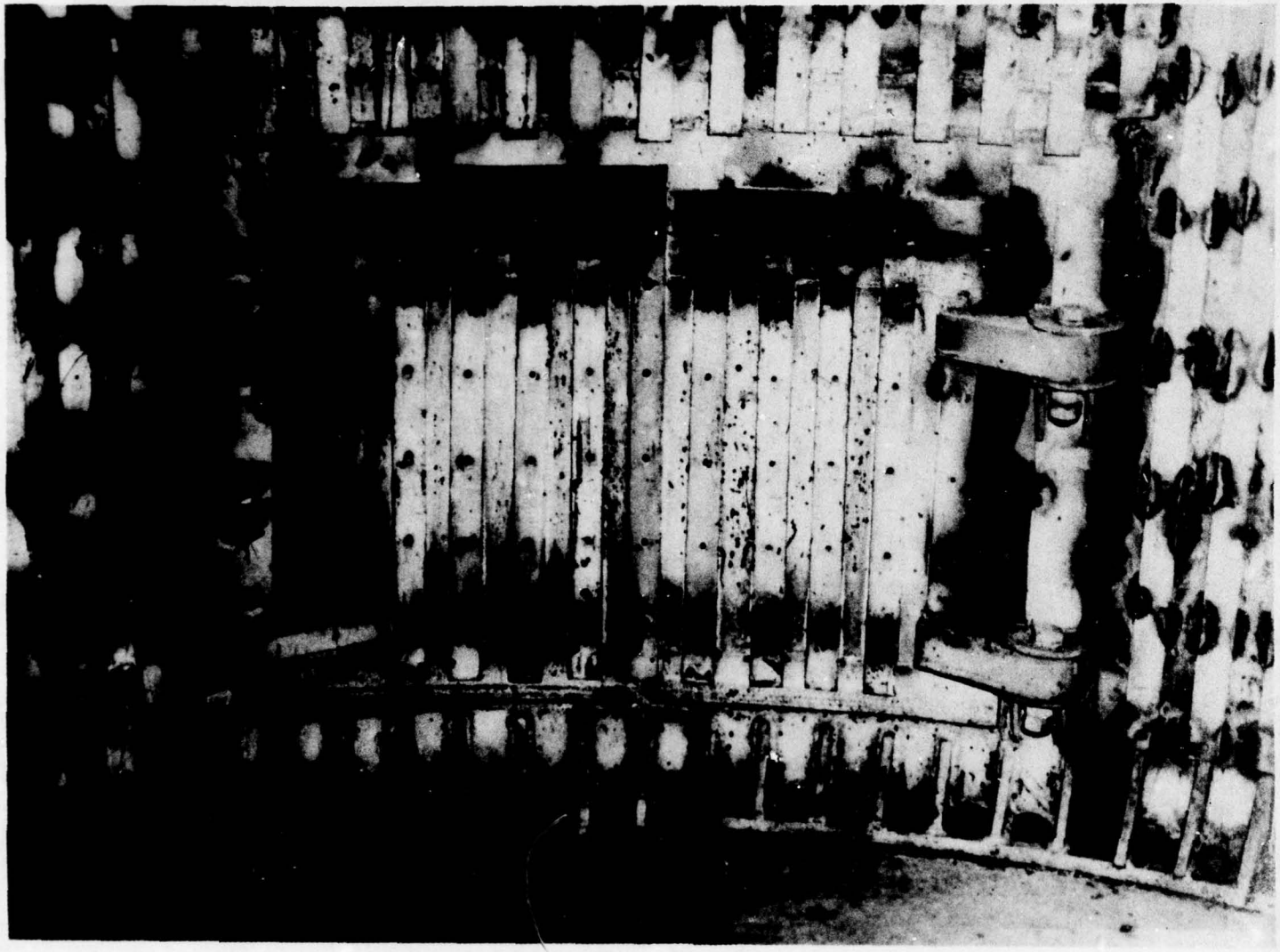


Figure 4. Typical View of Inside Wall Surface with Door Lip Seal and All Blocking Installed.

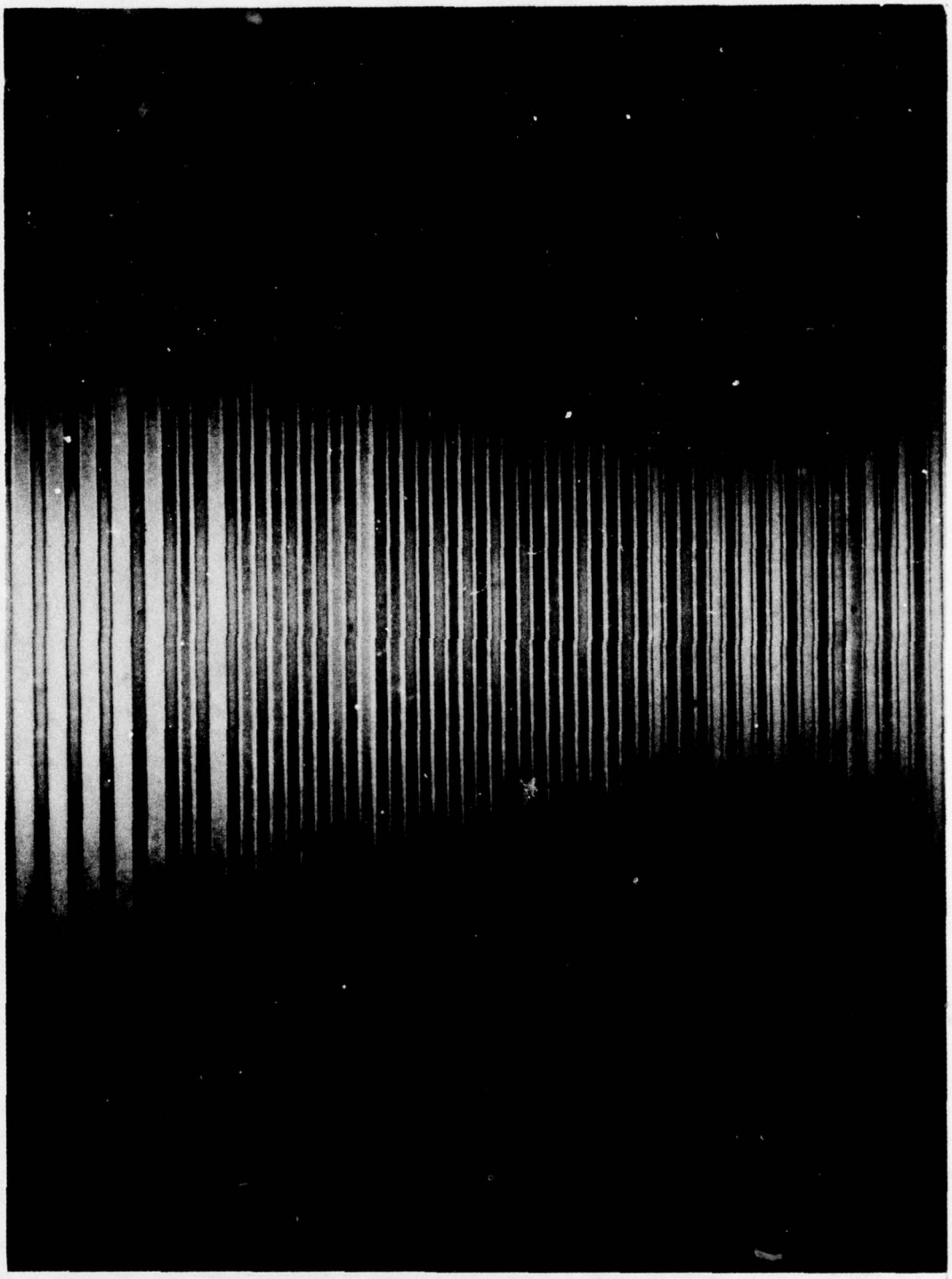


Figure 5. Typical View of Corrugated Steel Liner Installation

Most of the broken bands in the three reinforcing rings were repaired for this test and an additional outer band was added to each ring in an attempt to increase the ring strength and assure that the inner bands if broken would stay in place.

The existing 9 bands of the middle ring were repaired by rewelding as required and a tenth band was added to the outside. The outer band had a doubler plate (4 inches wide x 12 inches long x 0.25 inches thick) welded over the butt-splice welds to assure that the outer band would have the greatest strength. The doublers were welded along their upper and lower edges only with a continuous fillet weld.

The upper ring location was reinforced by adding a tenth band to the outer existing band, and again, doublers were utilized to maximize strength in the outer band. The broken inner band was left in place and was not repaired.

The lower ring location was repaired by removing and then rewelding the existing outer three bands. One broken band was not repaired for this test. Again, a tenth band was added to the outside and doubler plates welded on.

A 45.7 pound pentolite charge was detonated in the geometric center of the structure and the subsequent structural response and pressure data recorded. This test was a repeat of test 195 with an expected reduction in vent area.

7. Test Number 197. This was the last of the current series of tests on the 1/4 scale test structure. The charge weight was nominally the same as for tests 195 and 196 (45.1 pounds instead of 45.7 pounds) and was located at the geometric center of the structure. For this test major modification and/or repair was undertaken so that an attempt could be made to test an even tighter structure (less venting) than was provided for test 196.

For this test, the liner from test 196 was removed and replaced with two layers of heavier corrugated galvanized steel sheet (22 gage) to minimize significant venting through the central portion of the wall area. The two layers had their lap joints staggered so that they were approximately 13 inches apart. The panels were lapped approximately six inches and attached to the wall in the same manner as for test 196.

All of the outer retaining bands at all three locations were removed and replaced prior to this test. All band splices were made at an angle of 30 degrees from the horizontal instead of vertical as on the original as-delivered condition. Again ten bands per ring location were utilized and the outer band at each location had a doubler added to assure maximum strength in the outer band.

C. Instrumentation Locations

A sketch showing the locations of the pressure transducers and their notation is presented in Figure 6. The locations of the strain gages installed on the test structure are presented in the appendix. The drawing in the appendix is a copy of the instrumentation drawings provided by the U.S. Army Engineer Division, Huntsville, AL.

1. External Pressure Measurements. A gage line was established outside of the structure to document the airblast attenuation provided by the test structure. The free-field side-on overpressure measurements were made at fixed distances from the center of the floor of the structure (see Figure 6). Each transducer was flush mounted inside of a large aluminum block that was buried in the ground so that the upper transducer surface was flush with the ground surface. The aluminum block provided a hard surface adjacent to the transducer so that shock wave disturbances would be minimized. Black plastic electrical tape was put over the sensing elements at locations P1 through P6 to minimize the thermal effect on the transducer while having a negligible effect on the operation of the transducer. Figure 7 shows a close-up picture of a typical gage installation. Gage positions P1 through P5 were located at ground ranges of 12 ft, 18 ft, 26 ft, 35.7 ft, and 48 ft, respectively. Location P6 was set at 61 ft for tests 191 through 194 and then relocated at 64.4 ft for tests 195 through 197. Location P12 was set at 122 ft for all tests. Black plastic tape over this gage was not required since this gage has a thermal shield as part of its construction.

2. Quasi-Static Pressure Measurements. There were two locations selected for measuring the quasi-static pressure inside the test structure. Position P9 was 54 inches up from the floor on the interior of the cylindrical body structure and position P11 was located near the center of the roof. The pressure transducers were mounted in a shock-isolation and thermal protection mount to minimize the effects of the severe environment on the transducer operation. Figure 8 shows the design details of the gage mount utilized.

3. Reflected Pressure Measurements. There were three gage locations utilized for documenting the peak reflected pressure and impulse loading on the wall and roof of the structure. Gage number P7 was located on the interior wall of the structure 8 inches up from the floor. Gage P8 was located 54 inches up the interior wall of the structure (adjacent to measurement P9) and gage P10 was located near the center of the roof adjacent to the quasi-static pressure gage P11.

---

[5] *"Suppressive Shield Quarter Scale Model Category I Instrumentation Drawings," File Numbers 6005 through 6009, U.S. Army Engineer Division Huntsville, Corps of Engineers, Huntsville, Alabama.*

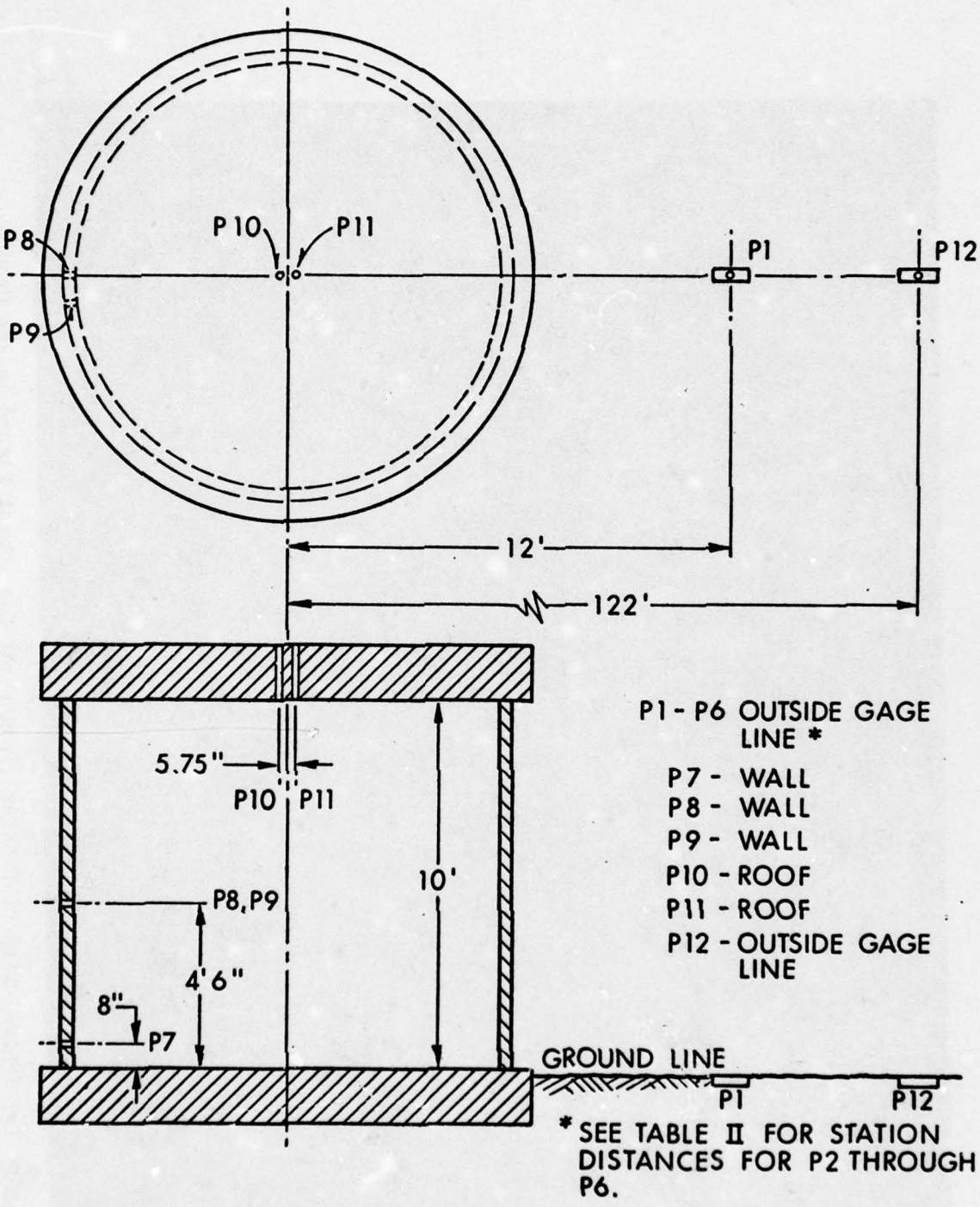


Figure 6. Locations of Pressure Gages

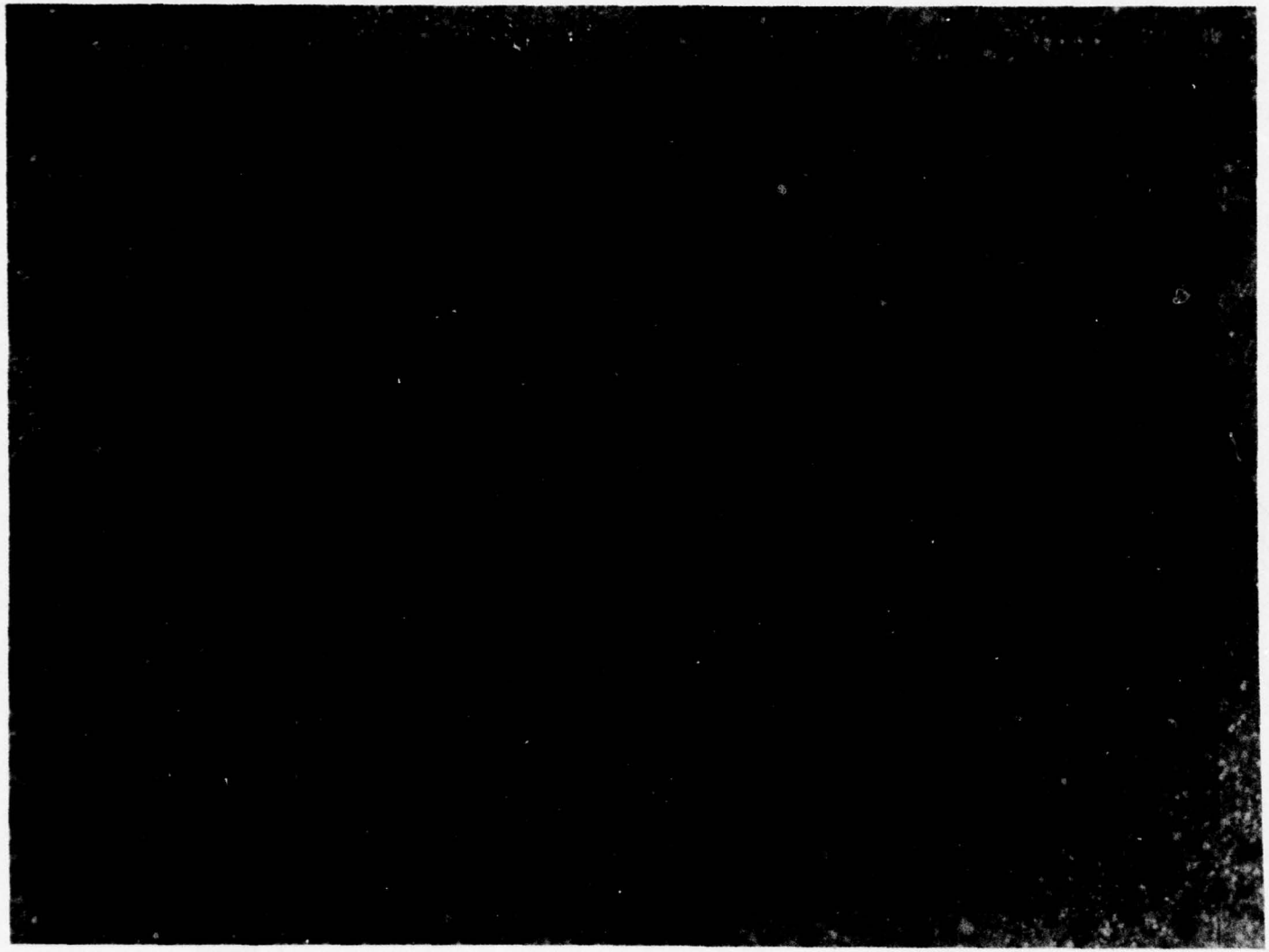


Figure 7. Typical View of Pressure Transducer Gage Mount Placed in the Ground

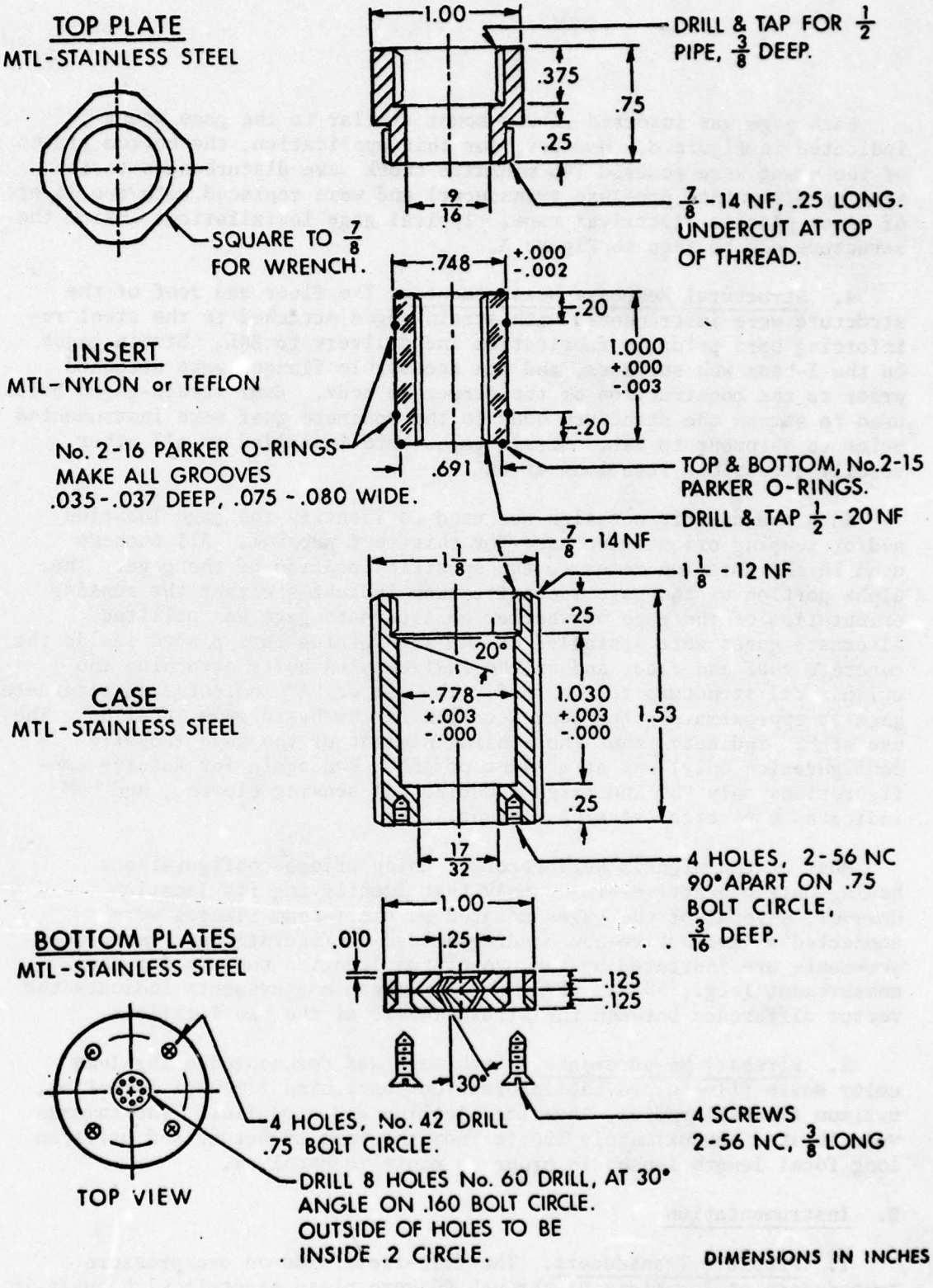


Figure 8. BRL Shock Isolation Transducer Mounts

Each gage was inserted into a mount similar to the gage mount indicated in Figure 8. However, for this application, the bottom plates of the mount were removed (to minimize shock wave disturbances to the sensing element of pressure transducer) and were replaced with two layers of black plastic electrical tape. Typical gage installations inside the structure can be seen in Figure 3.

4. Structural Response Measurements. The floor and roof of the structure were instrumented with strain gages attached to the steel reinforcing bars prior to fabrication and delivery to BRL. Strain gages on the I-beam web surfaces, and non accessible flanges were attached prior to the construction of the structure body. Four strain-gaged bolts used to attach the structure body to the concrete roof were instrumented prior to shipment to BRL. Strain gages were installed at all other readily accessible locations at BRL.

An alpha-numeric notation was used to identify the gage location and/or sensing orientation used for this test program. All numbers used in the notation refer to the specific location of the gage. The alpha portion of the gage identification indicates either the sensing orientation of the gage or whether an alternate gage was utilized. Alternate gages were installed on the reinforcing bars placed inside the concrete roof and floor and on the instrumented bolts attaching the cylindrical structure to the roof. The use of "A" indicates an alternate gage at approximately the same location as the basic gage location. The use of "S" indicates that the sensing element of the gage (Rosette configuration only) was at a slant of 45°. And again for Rosette configurations only "H" indicates a horizontal sensing element, and "V" indicates a vertical sensing element.

Most of the signals were recorded using bridge configurations having only one-active-arm, namely that identifying its location. However, several of the gages mounted on the I-beam flanges were connected as two-active-arm bending-bridge configurations. These measurements are indicated by the use of two location numbers for the measurement (e.g., 50/51, 58/59 etc.). These measurements indicate the vector difference between the strain levels at the two locations.

5. Fireball Measurements. Each test was documented using 16mm color movie film to provide information concerning fireball formation, maximum fireball radius, localized jetting and anomalies. The cameras were located approximately 500 ft from the test structure and utilized long focal length lenses in order to minimize parallax.

D. Instrumentation

1. Pressure Transducers. The free-field side-on overpressure transducers at locations P1 through P6 were piezo-electric with built-in source followers. They were Susquehanna Instruments Model ST-2 gages.

Location P12 was instrumented with a Bytrex Model HF6 pressure transducer. The gage has a four-arm wheatstone bridge configuration with two active semiconductor arms and two dummy arms. Stations P7 through P11 were instrumented with quartz sensing element piezo-electric type pressure transducers with attached source followers. The gages were PCB Electronics Inc., Model 113A22.

2. Strain Gages. The strain gages were all purchased from Micro-Measurements Inc. Model CEA-06-250VW-350 gages were mounted on the reinforcing rods in the concrete roof and floor, on the I-beam flanges, and on the reinforcing ring outer bands. The Rosette strain gages located on the I-beam webs were Model CEA-06-125UR-350. The retaining ring outer bands were instrumented with Model EP-08-250BR-350 strain gages for tests 195 through 197 to measure the high elongation that was expected at these locations.

3. Recorders. All pressure data were recorded on a tape recorder having a frequency response capability from D.C. to 80 kH_z.

All strain data were recorded on tape recorders having a frequency response from D.C. to 20 kH .

4. Motion Picture Cameras. Two different types of motion picture cameras were utilized to document the test program. A standard documentary film was made at a frame rate of 24 pictures per second. In addition, moderate speed movies were made (400 pictures per second).

III. RESULTS

The results obtained from the seven tests will be discussed and presented in both tabular and graphic form. The results and discussion will be grouped according to phenomenon or subject matter established by the test objectives indicated previously.

A. General Observations and Structural Damage

1. Test Number 191. There was no structural damage observed after this test. There was some indication of significant motion of the I-beams. The painted outer surface of the I-beams (behind the reinforcing rings) showed marks of impact with and/or rubbing against the rings. This was primarily indicated at the location where the gaps were relatively small.

2. Test Number 192. There was no structural damage observed after this test. There was an indication that the I-beam motion was greater for this test than that indicated above. All of the I-beams showed marks of impact with and/or rubbing against the reinforcing rings.

3. Test Number 193. There was no structural damage observed after this test. There was some indication of relative motion between the I-beams making up the cylindrical body. The blocking strips attached inside the structure caused scrape marks on the flanges of the inside row of I-beams. This could be caused by several types of motion: (1) twisting of the I-beams; (2) radial deflection of the I-beams; and (3) lateral motion of the I-beams, or some combination of all three. The scrape marks at mid-span were found to vary from no scratches at some locations up to about 1/4 inch beyond the edge of the blocking strips at other locations.

4. Test Number 194. There was no structural damage observed after this test. There was some localized failure of the small lugs to which the blocking strips were welded. These lugs were only tack welded to the inner flange of the outer I-beam row and thus did not appear to have significant strength. This would indicate that there was significant relative motion between the I-beams as there was for the previous test. It should be remembered that the outer reinforcing rings were not always in contact with the I-beams, and in fact at some locations considerable gaps were present for this as well as for the first four tests, as was previously noted.

5. Test Number 195. Structural damage was sustained during this test, which was the first one at 117% of the design maximum charge weight. There was considerable failure of bands making up the three reinforcing rings, cracked concrete in the floor and roof sections, and failed welds on the blocking strip attachments.

The upper reinforcing ring had only one broken band. All the bands of this ring location stayed in place.

The middle reinforcing ring had six broken bands and the lower reinforcing ring had three broken bands (all adjacent to butt welds).

Figure 9 shows the test structure and the final position of the bands that fell to the ground. This test indicated the necessity to make provision to try and keep the bands in place even if some bands failed. The technique selected for the test program was to reinforce the outer bands at the welds in an attempt to assure that the outer bands would have the greatest strength and therefore be the ones least likely to fail.

The concrete roof had indications of localized failure on the inner surface at four locations inside the structure in the vicinity of the attachment to the cylindrical body (see Figures 10, 11, and 12). In Figures 10, 11, and 12 the crack sizes can be estimated by comparison with the nominal bolt spacing (3 inches) of the cylinder body to roof attachment. In general, the cracks did not extend more than three inches

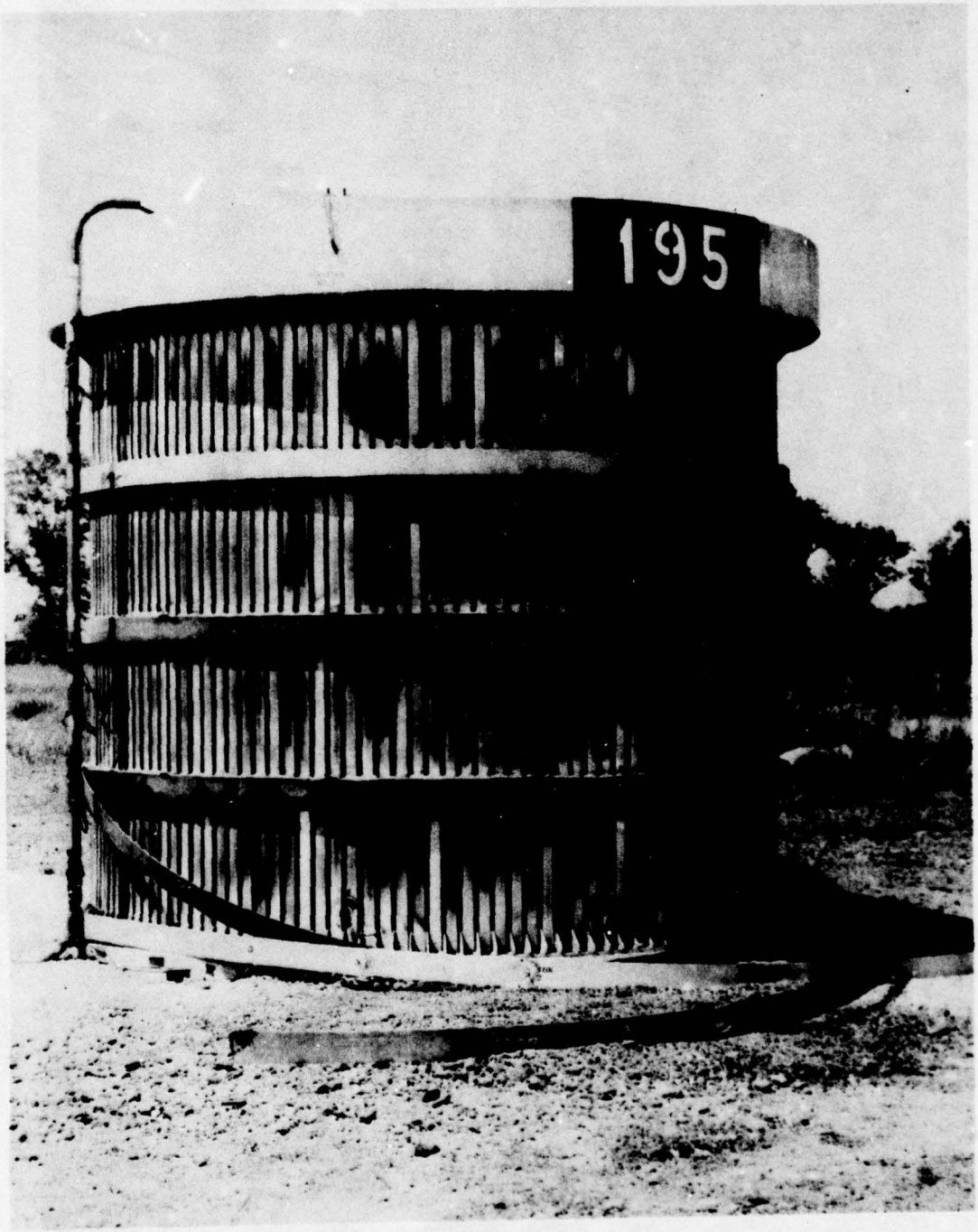


Figure 9. Reinforcing Ring Damage After Test 195

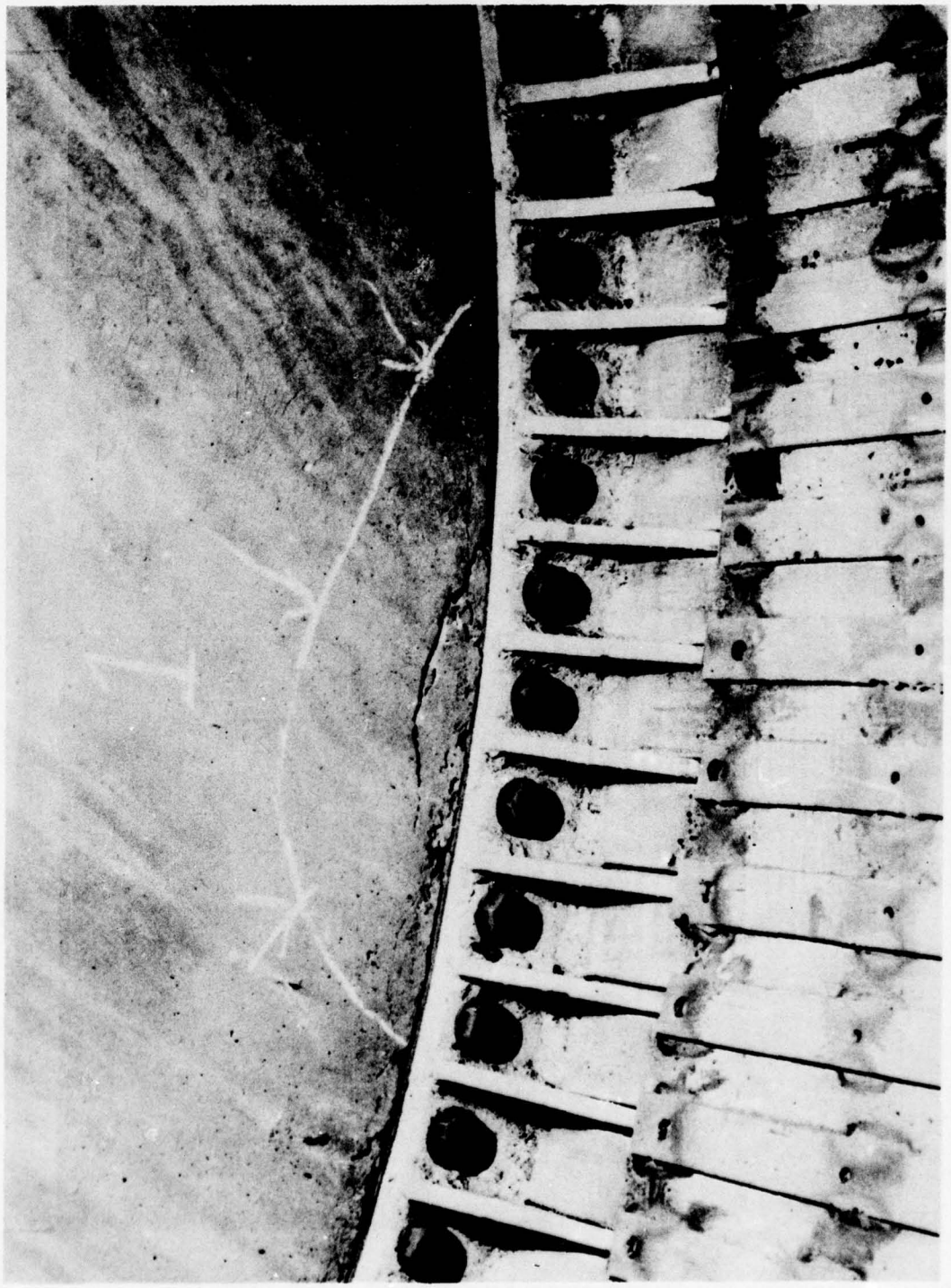


Figure 10. Roof Damage at Location 1 After Test 195

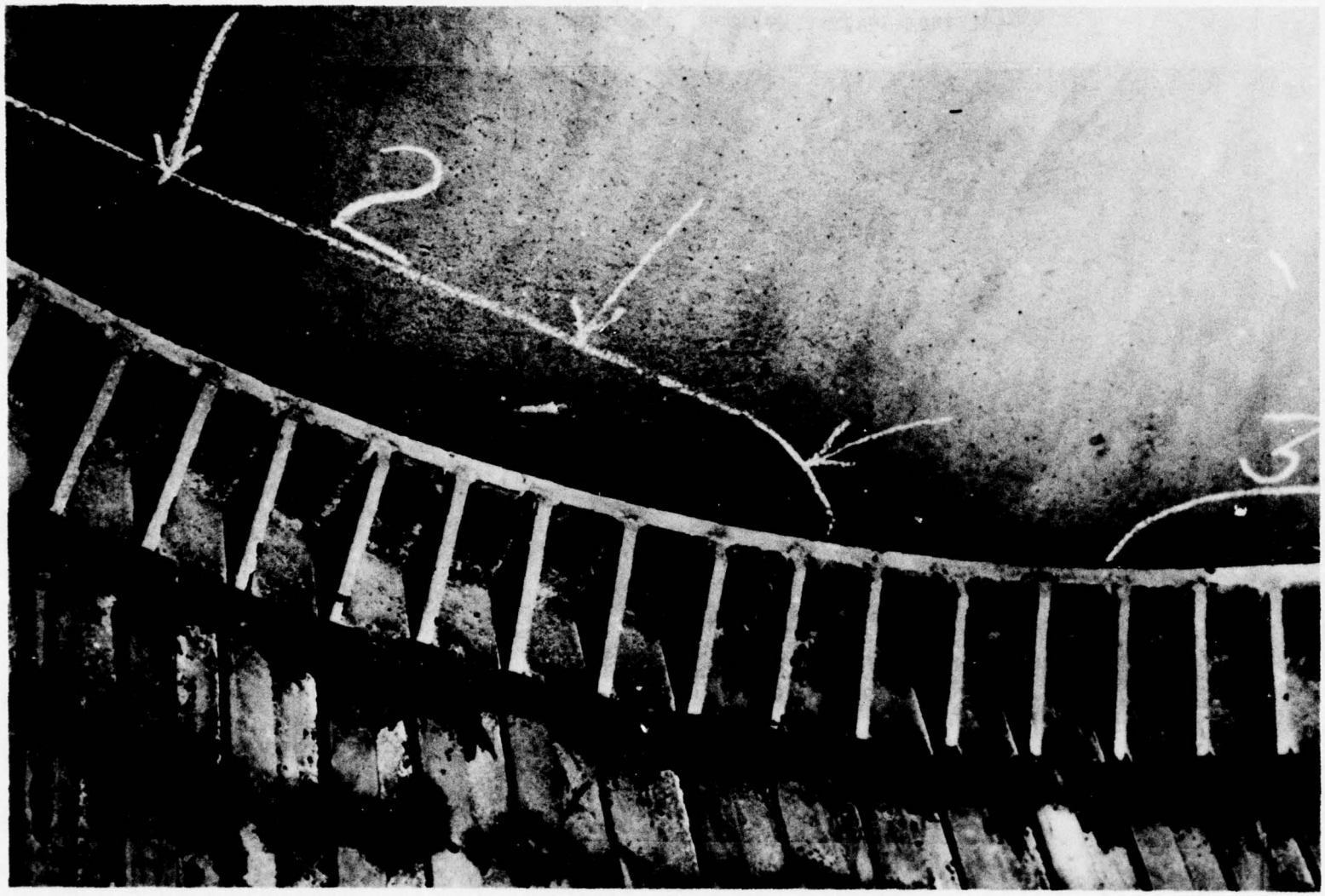


Figure 11. Roof Damage at Locations 2 and 3 After Test 195



Figure 12. Roof Damage at Location 4 After Test 195

from the cylindrical body steel end rings. These cracks did not go all the way through to the outer surface of the roof. There was one hair-line crack on the upper surface which extended between the two pressure transducer steel tube inserts.

The failure of the concrete floor was limited primarily to an oval section near the center of the floor. There were large cracks and a depression in the center of the damaged area with small cracks at the perimeter of the depression. Figure 13 shows the damage to the floor. As an indication of the extent of damage the maximum depression was approximately 3/8 inch below the normal floor surface. No estimate of the damage to the floor lower surface could be made.

6. Test Number 196. Structural damage was sustained during this test, which was the second test at 117% of the design maximum charge weight. There was considerable failure of the bands making up the reinforcing rings, additional damage to the cracked concrete floor and roof, failed welds on the blocking strip attachments, and considerable failure of the corrugated liner placed inside the cylindrical body.

The upper reinforcing ring had four broken bands. The middle ring had eight broken bands. The lower reinforcing ring had five bands failed during this test. The outer bands at all three ring locations did not fail and therefore all bands stayed in place.

The concrete roof section appeared to have an increase in the width of the crack openings on the inside surface of the roof section. There did not appear to be additional cracking. The hair line crack on the upper surface from the previous test did not appear to get any larger. The concrete floor section sustained additional damage during this test. The previous cracks got wider and the depression in the floor was found to be approximately 7/8 inch deep after the test. The size of the damaged area did not appear to increase noticeably from the previous test.

The corrugated liner placed inside the structure sustained considerable failure. There was considerable shearing of the liner along the edges of the blocking strips, punching through of the liner at the holes drilled in the blocking strips, and localized areas where the liner was torn and pulled away from the wall surface. Figure 14 shows a typical portion of the damage sustained by the liner. In general, the mid-sections of the panels sustained the greatest damage. This would be expected because this is the wall area that is loaded with the highest reflected shock wave pressures.

7. Test Number 197. Structural damage was also sustained during this test, which was 115% of the design maximum charge weight. There was considerable failure of the bands making up the reinforcing rings, additional damage to the floor and roof sections, and minor (expected) damage to the corrugated liner placed inside the cylindrical body section of the test structure.

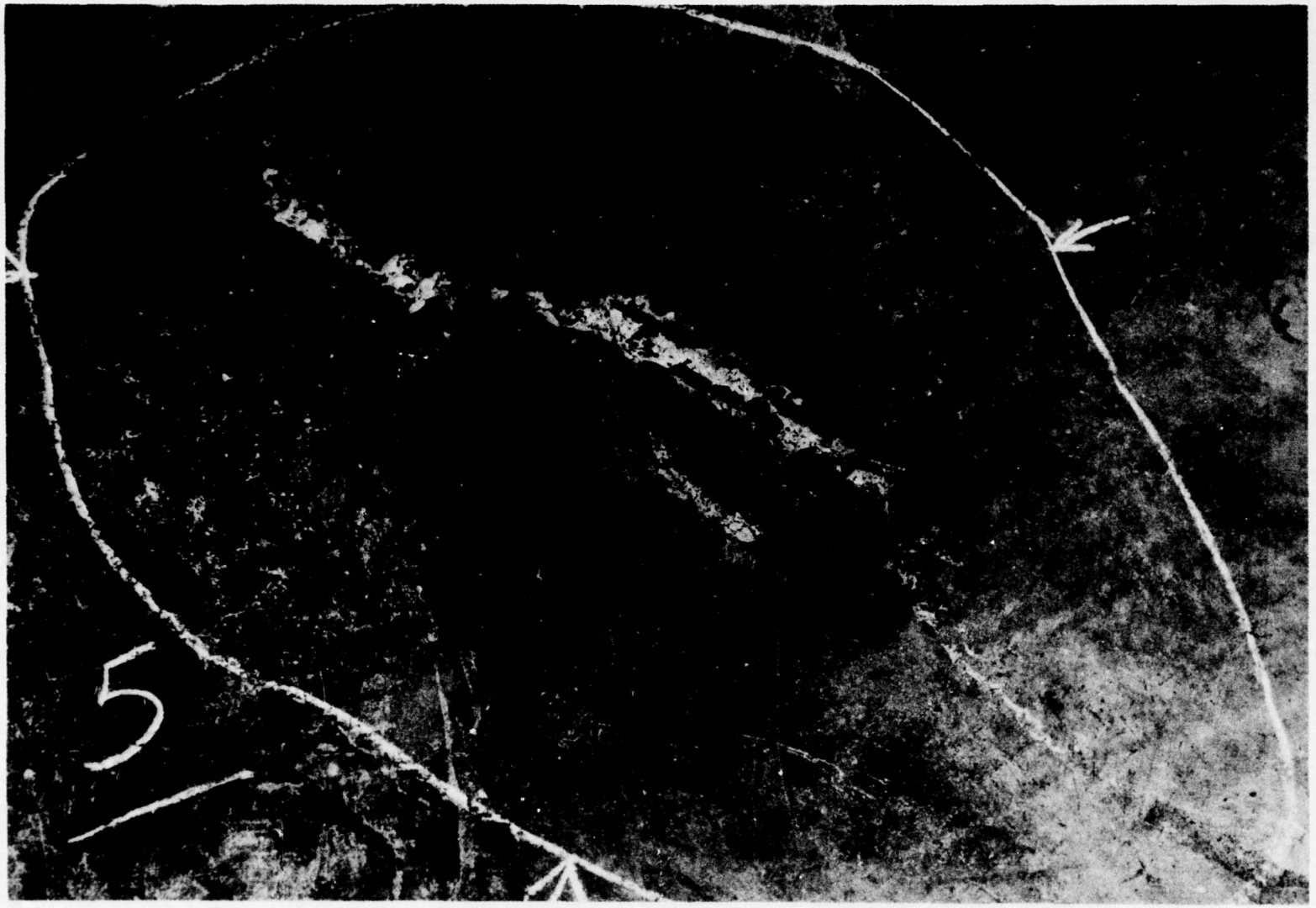


Figure 13. Floor Damage at Location 5 After Test 195

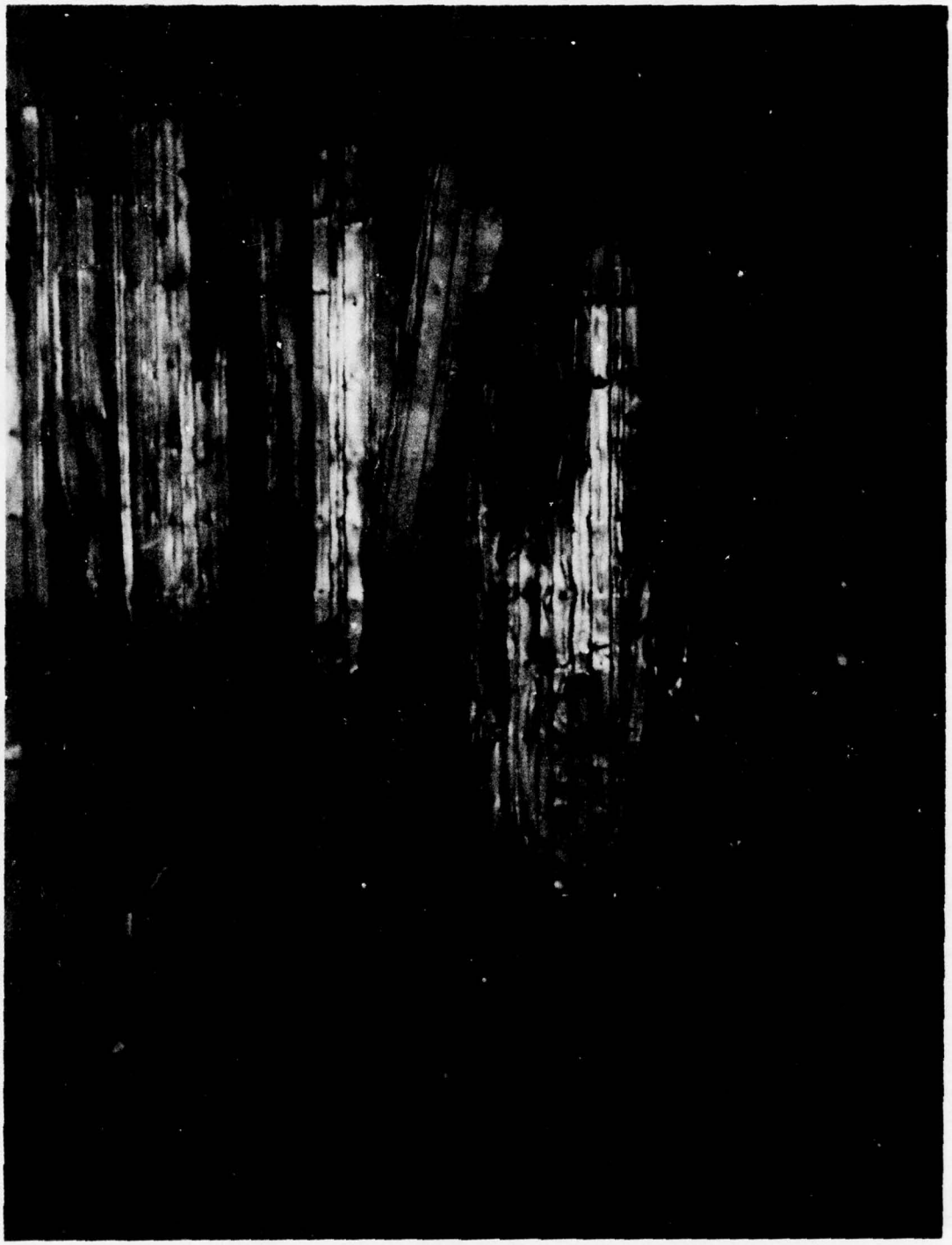


Figure 14. Corrugated Steel Liner Damage After Test 196

The upper reinforcing ring had seven broken bands. The middle reinforcing ring had all of the bands except the outer one broken. The lower ring location had seven broken bands. None of the outer bands broke, therefore all bands stayed in place. A close look at the failed welds of all the broken bands indicated that the field welds (welds made in place to complete ring segments) were generally of very poor quality. Therefore, the weld failures cannot be used as an indication of excessive loading, but rather that the strength of the elements is only as good as the best welds.

The concrete roof appeared to have a slight increase in the width of the cracks previously sustained. The outer surface hair line crack did not appear to get any larger. The floor section sustained additional deformation to the previously damaged area. The cracks opened up a little and the depression was approximately 1-1/4 inch below the normal floor level. There did not appear to be a noticeable increase in the size of the damaged area of the floor.

The corrugated steel liner sustained only minor damage during this test. It was flattened against the cylindrical wall (as was expected) and there was some bulging inward at several locations. There was no indication of shearing or tearing of the corrugated liner as was observed on the previous test. The liner stayed in place after the test.

B. Free-Field Overpressure Data

1. Maximum Overpressure. The maximum overpressures at each station along the blast line outside the structure are presented in Table II. An examination of the pressure versus time data indicated that the maximum overpressure was not always associated with the first pressure rise. This same phenomenon was also observed on the tests associated with the 1/16 size Category I shield. Pressure time history plots for the seven gage locations for test 195 are presented in Figures 15 through 21. These plots show the variations that were generally recorded as the multiple shock waves propagating outside the structure catch up with preceding shocks. Figures 22 and 23 present the pressure time histories for gages at the scaled intraline distance for tests 196 and 197. At this distance the first shock is also the biggest one, however, there is considerable difference to be noted between the tests in regard to the time it takes for the positive overpressure to decay to less than ambient.

In this report the term "scaled ground range" (Z) is the ground range indicated in Figure 6 divided by the cube root of the explosive charge weight utilized ($ft/lb^{1/3}$).

Table II. Maximum Overpressure Data Outside Suppressive Structure

Gage Location	Ground Range (ft)	Maximum Overpressure (psi) Test 191	Test 192	Test 193	Test 194	Test 195	Test 196	Test 197
P1	12.0	6.71	13.3	10.96	7.01	7.69	3.25	3.15
P2	18.0	6.55	9.97	9.23	5.17	8.60	2.80	1.74
P3	26.0	3.35	7.25	5.46	N.R.	3.93	1.67	1.32
P4	35.7	2.03	3.79	2.85	N.R.	3.26	1.16	N.R.
P5	48.0	1.27	2.66	2.13	1.41	2.06	0.80	N.R.
P6	61.0*	0.90	1.90	1.45	1.12	1.15	0.61	0.59
P12	122.0	N.R.	0.68	0.53	0.38	0.45	0.25	N.R.

*Ground range changed to 64.4 ft for tests 195 through 197

Table III. Maximum Overpressure Coefficients for Use With Equation (2)

Test Number	Standard Deviation (%)	Coefficient α	Coefficient β
191	16.0	117	-1.425
192	12.2	125	-1.347
193	12.2	114	-1.400
194	9.4	52.3	-1.263
195	20.2	64.0	-1.383
196	9.6	16.1	-1.161
197	7.5	9.4	-0.970

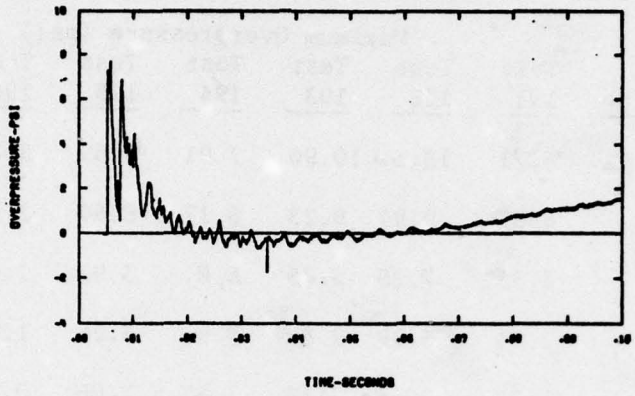


Figure 15. Overpressure Time History for Measurement P1 During Test 195

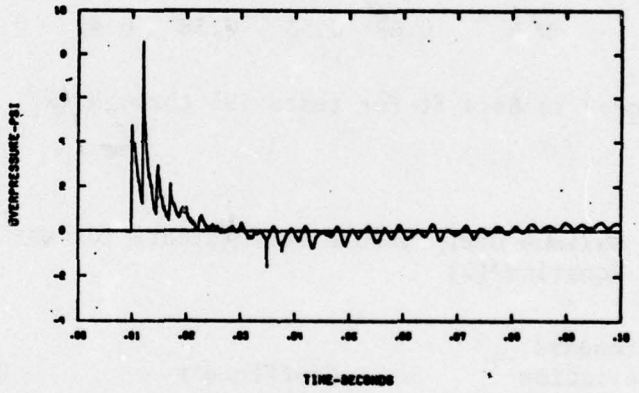


Figure 16. Overpressure Time History for Measurement P2 During Test 195

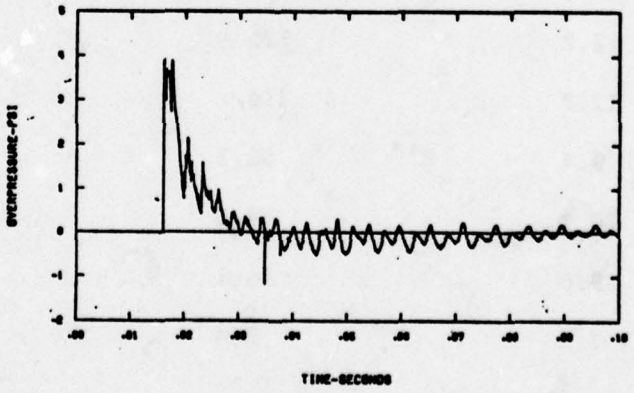


Figure 17. Overpressure Time History for Measurement P3 During Test 195

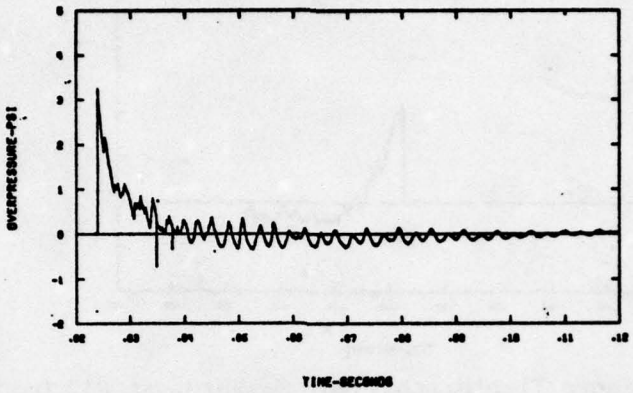


Figure 18. Overpressure Time History for Measurement P4 During Test 195

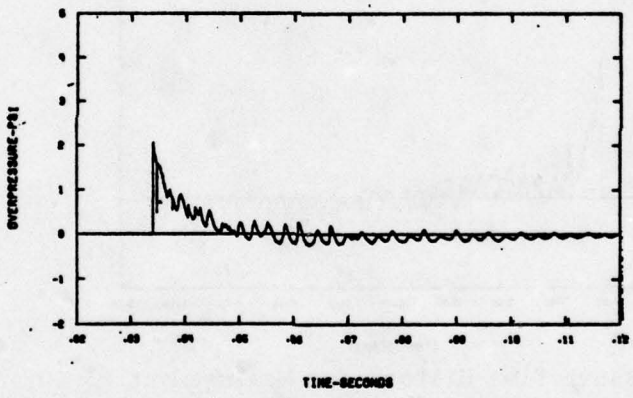


Figure 19. Overpressure Time History for Measurement P5 During Test 195

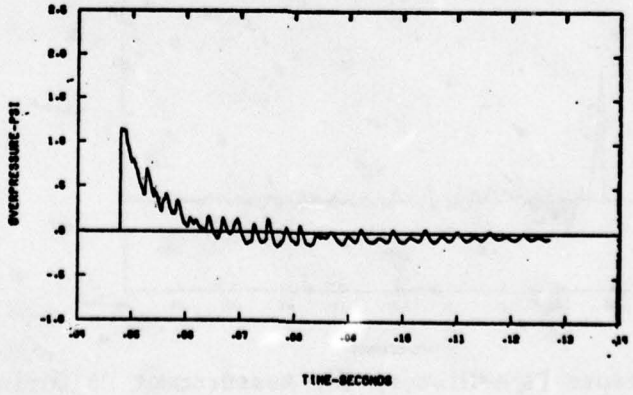


Figure 20. Overpressure Time History for Measurement P6 During Test 195

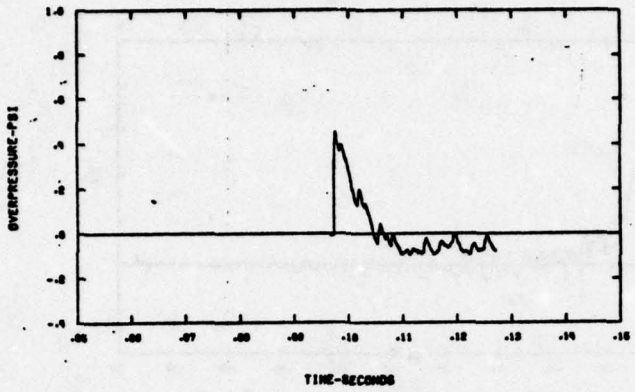


Figure 21. Overpressure Time History for Measurement P12 During Test 195

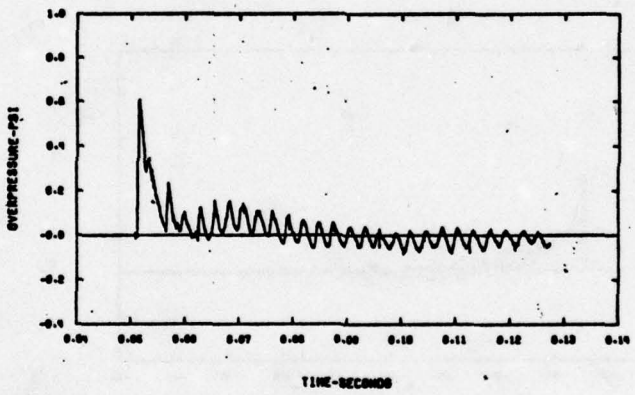


Figure 22. Overpressure Time History for Measurement P6 During Test 196

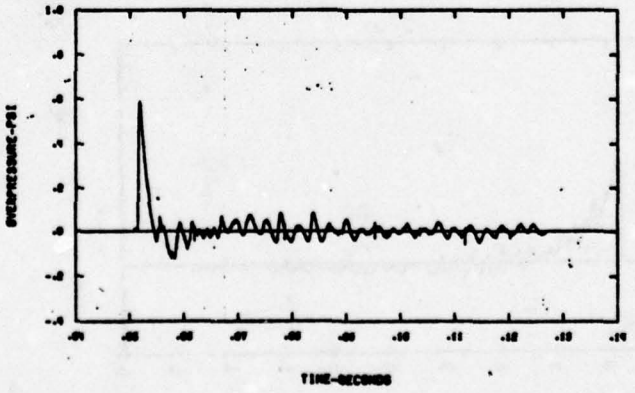


Figure 23. Overpressure Time History for Measurement P6 During Test 197

An examination of the test data indicated that a plot of the maximum overpressure vs. scaled ground range (in the log-log plane) would result in a linear relationship over the range of the test data. Therefore the data for each test can be represented by an equation of the form:

$$P = \alpha Z^{\beta}. \qquad (2)$$

Here; P is the maximum overpressure (psi) and Z is the scaled ground range ($ft/lb^{1/3}$).

A least squares analysis was performed to determine the coefficients α and β. The results of this analysis are presented in Table III.

In order to determine the overpressure reduction as a function of scaled ground range, a relationship describing overpressure vs scaled ground range without a suppressive structure is required. The free-field blast parameters for bare spherical 50/50 pentolite charges was determined by BRL during the 1/16 size Category I shield program and therefore it was considered unnecessary to duplicate the tests. The test data in Reference 1 were found to be adequately described (standard deviation of 8.8%) by Equation (2) with $\alpha = 1386$ and $\beta = -2.07$.

Using Equation (2) and the coefficients indicated above, plots of the percent reduction of maximum overpressure vs. scaled ground range for each test were determined and are presented in Figure 24. These data indicate a greater reduction of free-field overpressure close-in to the structure than for greater ranges. This was also observed during the 1/16 size tests. From the plots in Figure 24 it can be seen that tests 194 through 197 satisfied the criteria for at least 50% overpressure reduction at a scaled ground range of 18 $ft/lb^{1/3}$.

For the first three tests, the free-field overpressure reduction at the scaled intraline distance was less than 50%. For test 191 it was 43.7%, for test 192 it was 24.5%, and for test 193 it was 40.7%. For all subsequent tests the overpressure reduction at the scaled intraline distance exceeded 50%. For test 194 it was 59.6%, for test 195 it was 65.1%, for test 196 it was 83.3% and for test 197 it was 83.2%. This indicates that the overpressure reduction requirement was not met by the shield in the as-delivered configuration nor with only half of the blocking strips installed.

Figure 24 also indicates a large difference in venting between tests 191 and 192 which utilized two different charge weights inside the structure in the as-delivered condition. This indicates that the gaps between the I-beams and reinforcing rings did permit the vent area to increase with increased charge weight. The amount of increase was approximately the same as the reduction provided by installation of half of the blocking strips inside the structure. This is indicated by the

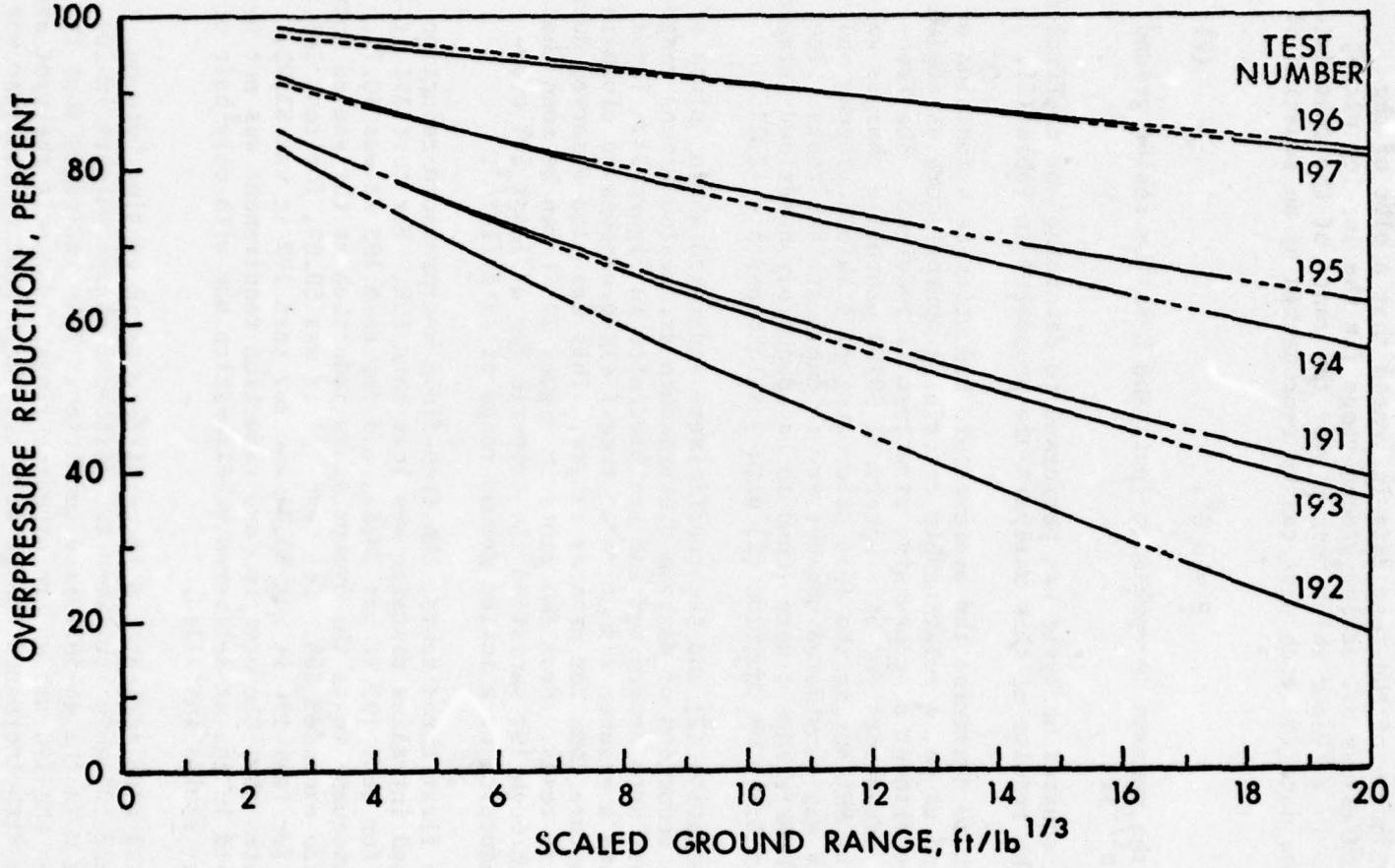


Figure 24. Percent Reduction of Maximum Overpressure versus Scaled Ground Range

relative closeness of the curves for tests 191 and 193. Figure 24 also indicates that there was not a significant reduction in overpressure obtained by using a heavy liner inside the structure instead of the light one that failed. This indicates that the liner was effective during the time of the first few shock reflections inside the structure and less effective thereafter.

2. Overpressure Impulse. The overpressure impulse data was obtained by integrating the overpressure time histories recorded on magnetic tape using a digital computer. The maximum positive overpressure impulse calculated for each measurement is presented in Table IV.

An examination of the test data indicated that the scaled impulse for measurements P1 through P6 could be represented by an equation having a form similar to that for the maximum overpressure. The impulse for measurement P12 was consistently found to be significantly less than expected using a relationship based on the data for measurements P1 through P6. It would appear that this phenomena is related to either instrumentation problems, or to a considerable change in impulse decay for scaled ground ranges between 30 and 35 $ft/lb^{1/3}$. A check of the instrumentation indicated no apparent problems, especially since the peak overpressure data appear to be acceptable. Measurement P12 has a better low frequency response than measurements P1 through P6 and therefore would not be expected to indicate low impulse values. It is therefore recommended that the impulse data for measurement P12 be used with caution.

The data from measurements P1 through P6 for each test were represented by an equation of the form:

$$I_s = \gamma Z^{\delta} \qquad (3)$$

where, I_s is the scaled impulse $\left(\frac{psi\text{-}ms}{lb^{1/3}}\right)$ and Z is the scaled ground range $(ft/lb^{1/3})$ which should be limited to values of 32 or less.

A least squares analysis was performed to determine the coefficients γ and δ. The results of this analysis are presented in Table V.

In order to determine the scaled impulse reduction as a function of scaled ground range, the free-field blast parameters presented in Reference 1 were used. The coefficients for the reference scaled impulse relationship using Equation (3) are $\gamma = 59.7$ and $\delta = -0.843$. The standard deviation of the reference data was 5.7%. Using the above relationships, the percent reduction of scaled impulse versus scaled ground range for each test was determined and is presented in Figure 25.

Table IV. Impulse Data Outside Suppressive Structure

Gage Location	Ground Range (ft)	Maximum Overpressure Impulse (psi-ms) Test 191	Test 192	Test 193	Test 194	Test 195	Test 196	Test 197
P1	12.0	18.19	39.10	34.20	19.6	30.80	10.50	4.40
P2	18.0	12.79	28.90	22.40	13.7	21.60	4.25	2.87
P3	26.0	9.55	22.70	18.90	N.R.	18.20	3.58	2.41
P4	35.7	6.52	15.30	12.20	N.R.	12.20	3.00	N.R.
P5	48.0	4.76	11.20	9.54	5.83	9.09	2.02	N.R.
P6	61.0*	3.57	8.99	6.97	4.76	6.72	1.75	0.82
P12	122.0	N.R.	2.50	1.81	1.18	1.62	0.48	N.R.

*Ground range changed to 64.4 ft for tests 195 through 197

Table V. Scaled Impulse Coefficients for Use With Equation (3)

Test Number	Standard* Deviation (%)	Coefficient* γ	Coefficient* δ
191	4.5	56.2	-1.003
192	5.6	62.2	-0.926
193	6.4	54.5	-0.955
194	2.4	26.8	-0.868
195	6.3	27.1	-0.907
196	15.5	8.42	-1.031
197	8.2	4.23	-0.989

*Values based on measurements P1 through P6 only.

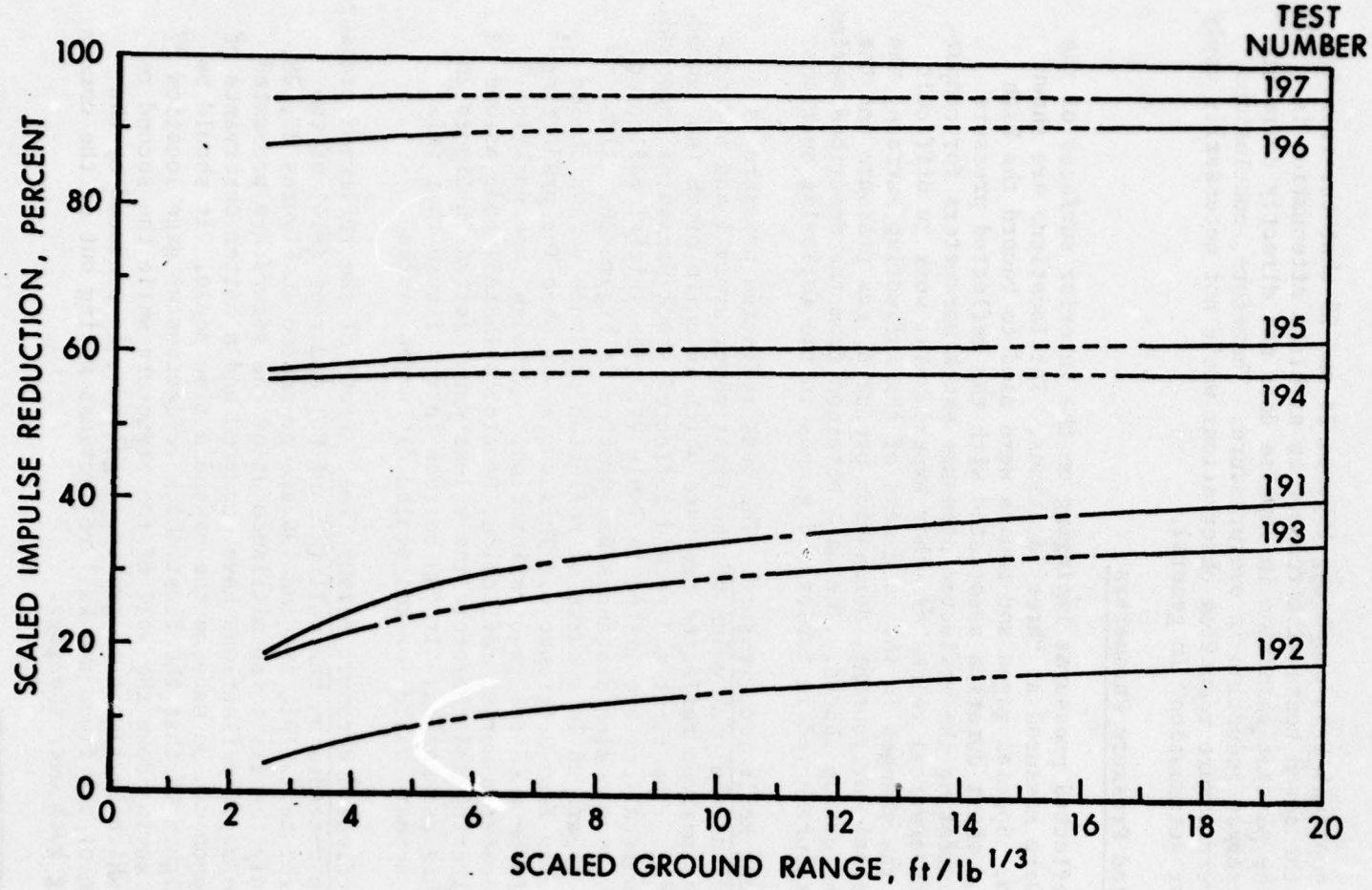


Figure 25. Percent Reduction of Scaled Impulse versus Scaled Ground Range

It is apparent from comparing Figures 24 and 25 that the relative ranking of the seven tests with respect to airblast attenuation is similar. The percent reduction in impulse does not directly correlate with the observed reduction in overpressure. Therefore, conclusions based on overpressure reduction observations would not necessarily apply to "airblast attenuation" in general.

C. Reflected Pressure Parameters

The reflected pressures impinging on the interior surfaces of the structure were measured at three locations. The locations are shown in Figure 6. Special gages and mounts were used to record the high pressure and short duration associated with the reflected pressure pulse. Documenting the reflected pressure shock parameters for comparison with theoretical values or other experimental work is difficult because of the changes in the roughness of the reflecting surface, the extreme thermal environment, detonation products, gas pressure and the repeated reflecting shocks. The data obtained from the described series of tests are presented in tables and graphs in the following sections.

1. Peak Reflected Pressure. The peak reflected pressure is defined here as the peak value of the first shock arrival and not necessarily the maximum reflected pressure which is quite often the second shock arrival. The first and second reflected shock pressures recorded at two gage locations are listed in Table VI. The initial reflected pressures versus scaled distances are plotted in Figure 26. Also plotted in Figure 26 is a curve of reflected pressure versus scaled distance taken from Reference 6. This curve was used for predicting pressures to be used for gage calibration. Although gage position 7 does not receive a normal reflection, Proctor's INBLAST code assumes a normal reflection and therefore the values were plotted in Figure 26 to check this assumption. It can be seen in the figure that this assumption appears valid for the scaled distances plotted.

2. Reflected Pressure Versus Time. Plots of the reflected pressure versus time recorded on the wall (P7 and P8) and roof (P10) of the structure for tests 191, 194 and 196 are presented in Figures 27, 28, and 29. Only the first ten milliseconds of the record are presented because the major reflections have occurred and a better observance of the phenomenon can be made on the expanded time scale. It should be noted in Figure 27 that the first shock reflection at gage location P7 is the one moving down the wall of the structure while the second reflection, which is always of greater magnitude, is produced by the interaction of the floor and wall reflections moving out of the corner and passing back over the gage.

---

[6] *"Parametric Analysis of Regular Reflection of Air Blast," C. Kingery and B. Pannill, Report Number 1249, Ballistic Research Laboratories, Aberdeen Proving Ground, MD, June 1964. AD 444997.*

Table VI. Reflected Pressure Parameters

Gage Location	Distance Feet	Gage Location	Test 191	Test 192	Test 193	Test 194	Test 195	Test 196	Test 197
					Pressure (psi)				
P7	7.10	Wall	391/499	900/1230	543/893	744/1040	1680/1720	1990/2370	1561/2086
P8	5.63	Wall	718	1570	1170	1550	2600	2220	2337
P10	5.00	Roof	1735/810	2015/3270	2005/2930	1880/2660	4960/4200	4390/3230	2216/2777
					Reflected Pressure Duration (ms)				
P8	5.63	Wall	1.20	1.10	1.10	1.00	1.00	1.10	1.10
P10	5.00	Roof	.85	1.00	1.05	1.00	.85	.90	.90
					Reflected Pressure Impulse (psi-ms)				
P8	5.63	Wall	124	202	188	210	388	465	450
P10	5.00	Roof	196	258	261	253	464	361	363

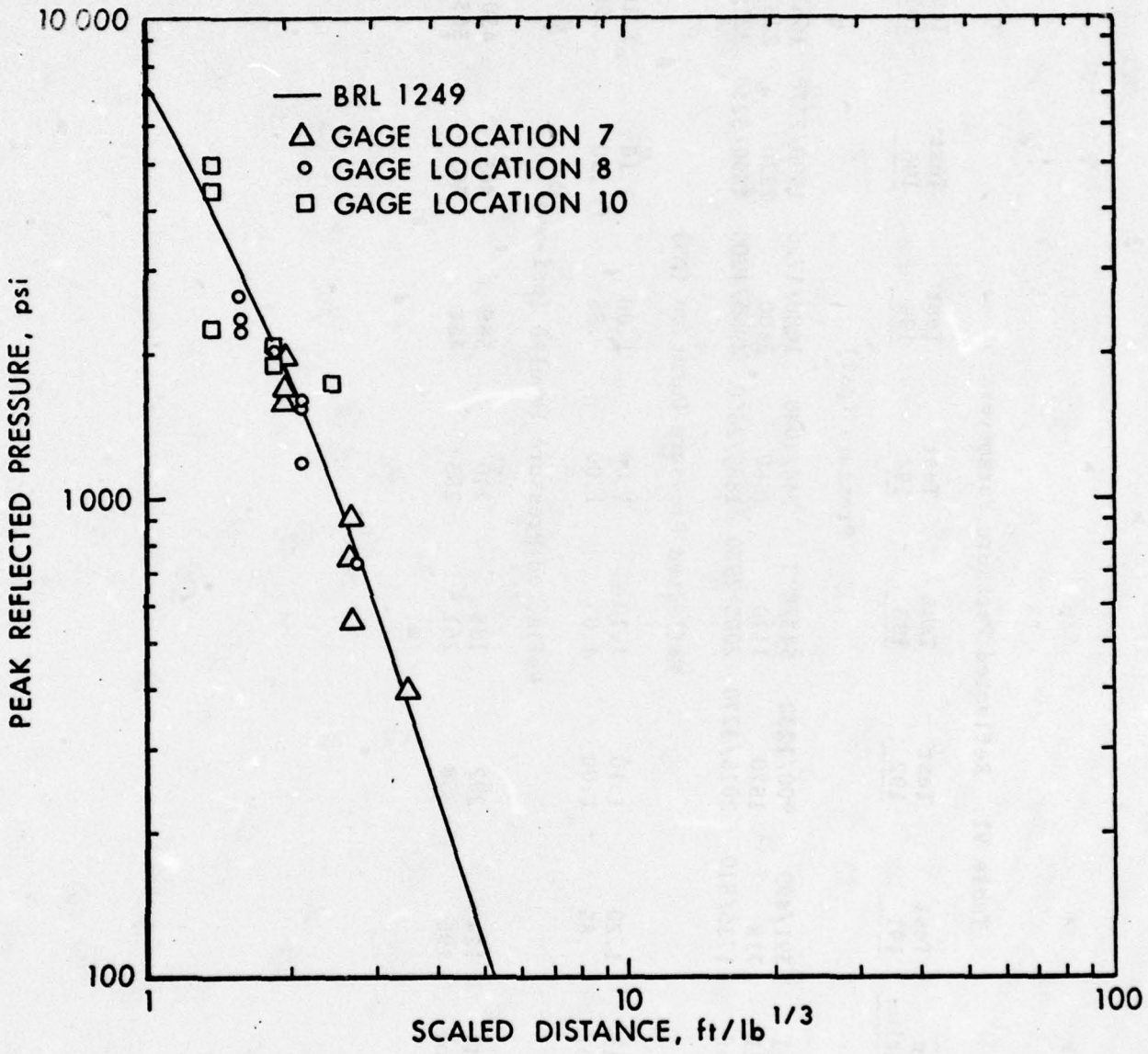


Figure 26. Peak Reflected Pressure Versus Scaled Distance

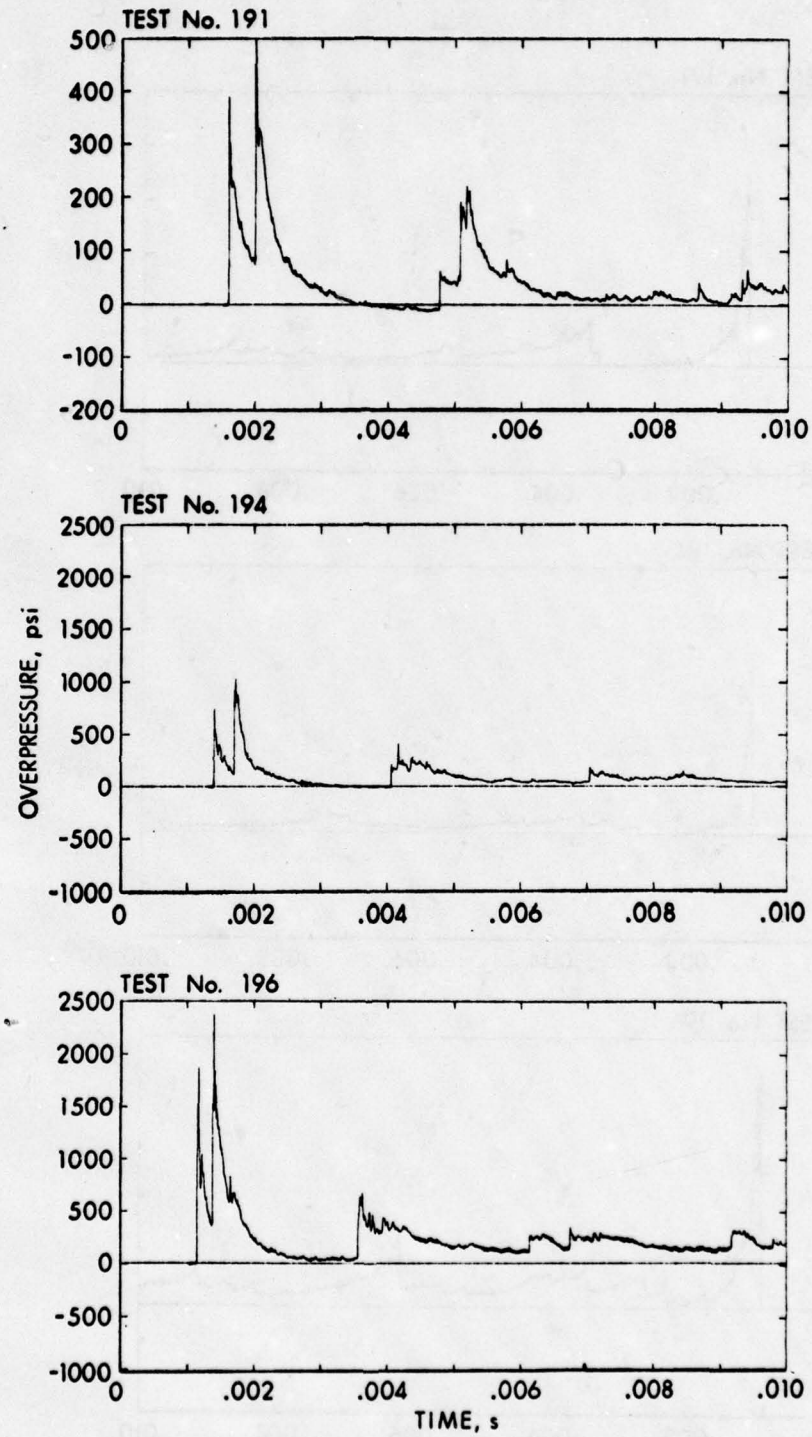


Figure 27. Reflected Pressure Versus Time at Gage Location P7 for Tests 191, 194, and 196

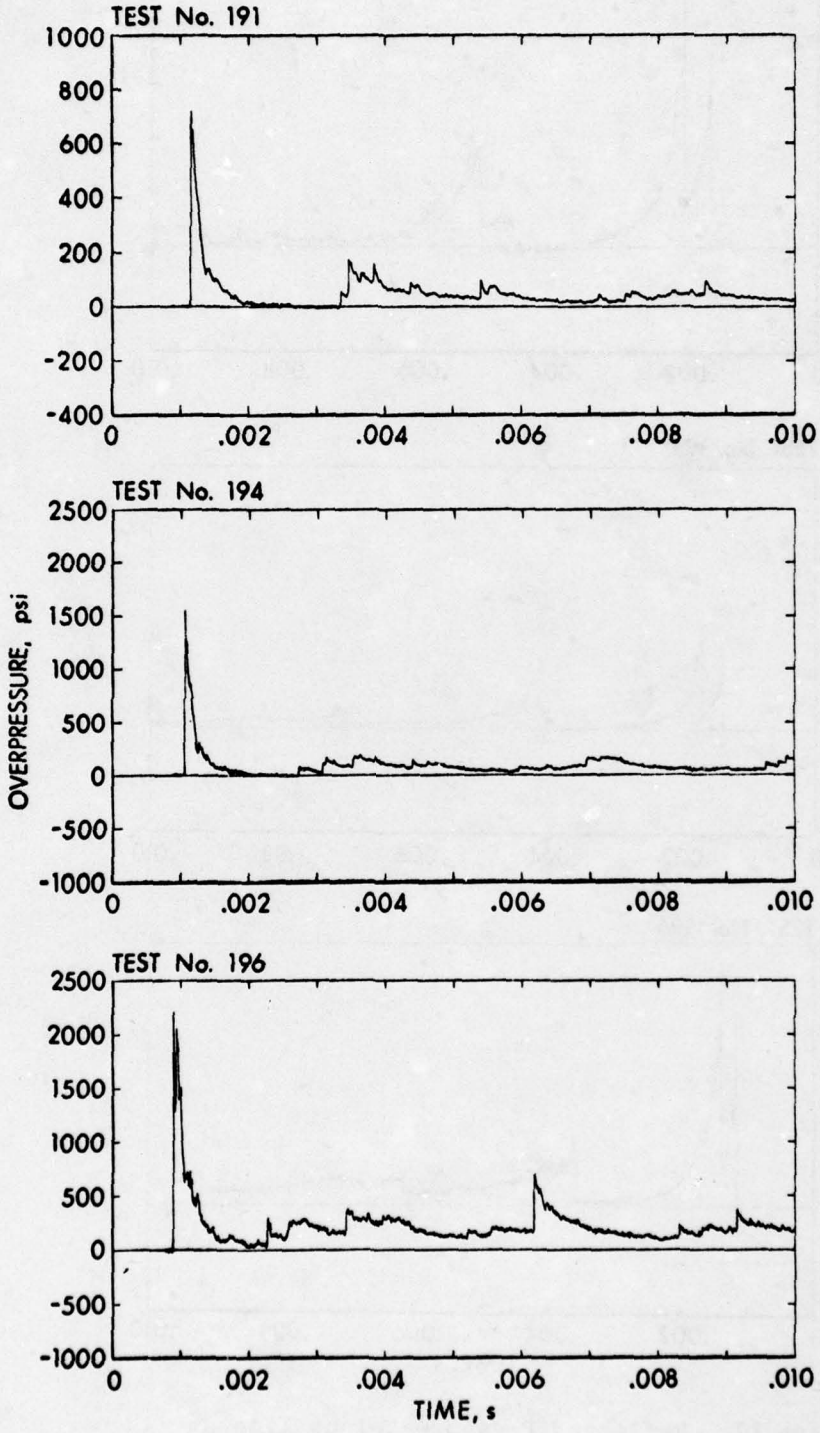


Figure 28. Reflected Pressure Versus Time at Gage Location P8 for Tests 191, 194, and 196

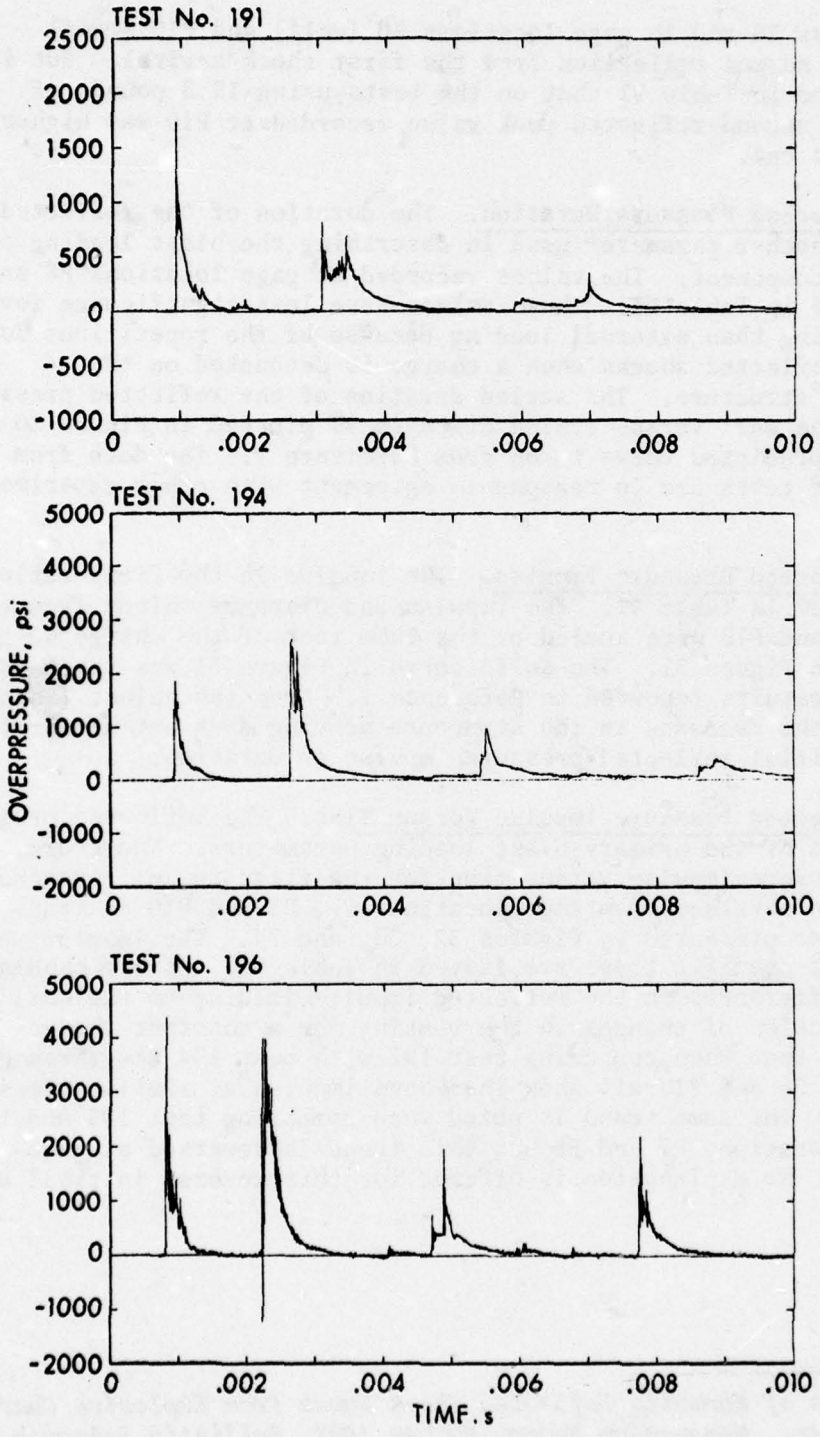


Figure 29. Reflected Pressure Versus Time at Gage Location P10 for Tests 191, 194, and 196

In Figures 28 and 29 gage locations P8 (wall) and P10 (roof) both record a normal reflection from the first shock arrival. But it should be noted in Table VI that on the tests using 19.3 pounds of pentolite the second reflected peak value recorded at P10 was higher than the first one.

3. Reflected Pressure Duration. The duration of the reflected pressure is another parameter used in describing the blast loading on a structural component. The values recorded at gage locations P8 and P10 are listed in Table VI. These values have less significance for internal loading than external loading because of the repetitious loading of the many reflected shocks when a charge is detonated on the interior of a structure. The scaled duration of the reflected pressure measured on the wall versus scaled distance is plotted in Figure 30 along with a predicted curve taken from Reference 7. The data from this series of tests are in reasonable agreement with other experimental results.

4. Reflected Pressure Impulse. The impulse in the first reflected shock is listed in Table VI. The impulse and distance values from gage locations P8 and P10 were scaled by the cube root of the charge weights and plotted in Figure 31. The solid curve in Figure 31 was taken from experimental results reported in Reference 7. From the values listed in Table VI, the decrease in the structure venting does not appear to affect the initial reflected pressure impulse or duration.

5. Reflected Pressure Impulse Versus Time. The reflected pressure impulse is one of the primary blast loading parameters. Therefore, the reflected pressure impulse versus time for the first ten milliseconds of the records obtained from gage locations P7, P8 and P10 on tests 191, 194 and 196 are presented in Figures 32, 33, and 34. The impulse values accumulated at specific times are listed in Table VII. These tabulations show differences in the reflected impulse loading on the wall and roof as a function of changes in the venting for a constant charge weight. Note that when comparing test 192 with test 194 the three gage locations P7, P8 and P10 all show increased impulse at similar times for test 194. The same trand is noted when comparing test 195 and test 197 at gage locations P7 and P8 but this trend is reversed at gage location P10. No explanation is offered for this reverse in trend at this time.

---

[7] *"Measurements of Normally Reflected Shock Waves from Explosive Charges," W. H. Jack, Jr., Memorandum Report Number 1499, Ballistic Research Laboratories, Aberdeen Proving Ground, MD, July 1963. AD 422886.*

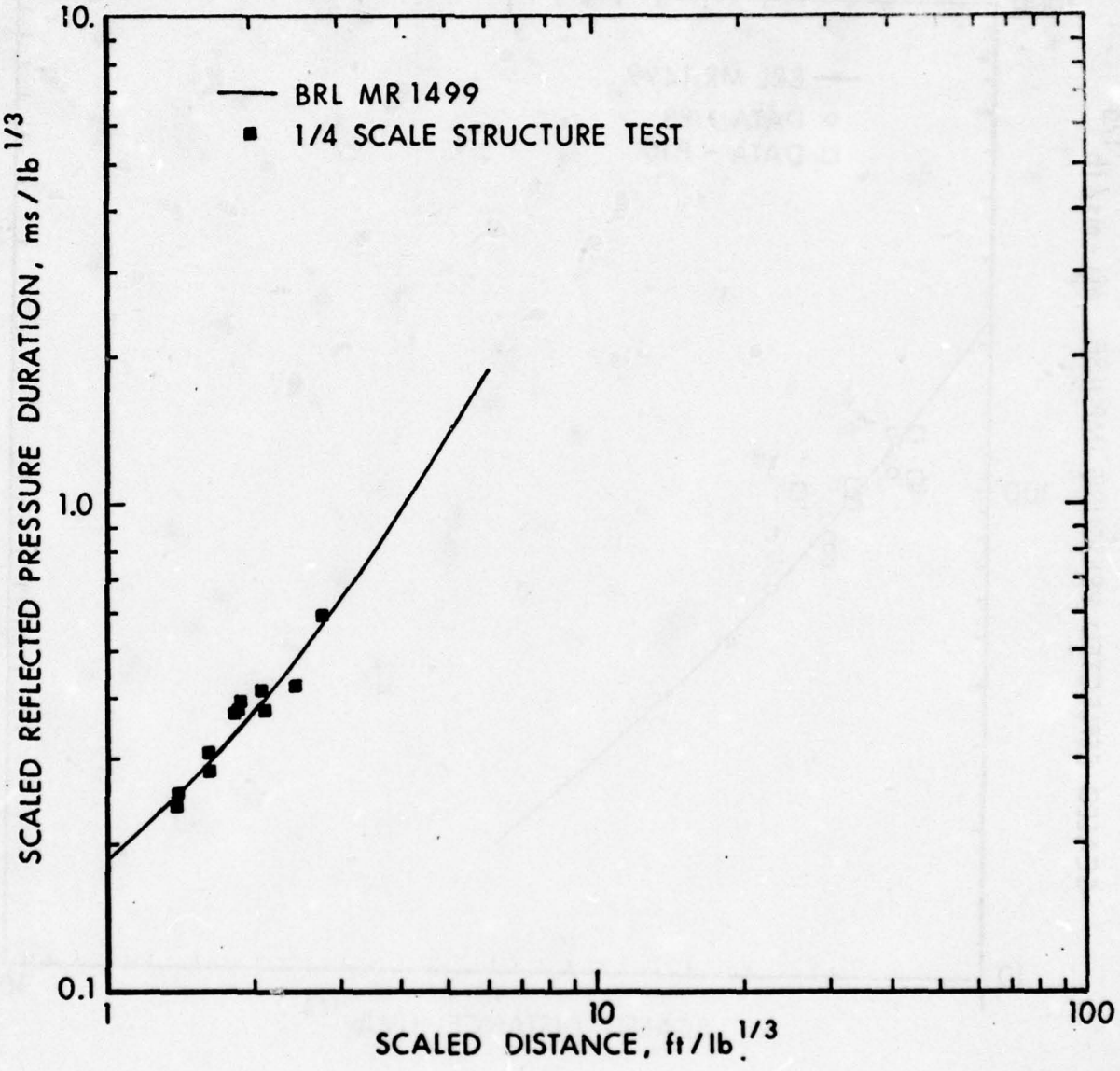


Figure 30. Scaled Reflected Pressure Duration Versus Scaled Distance

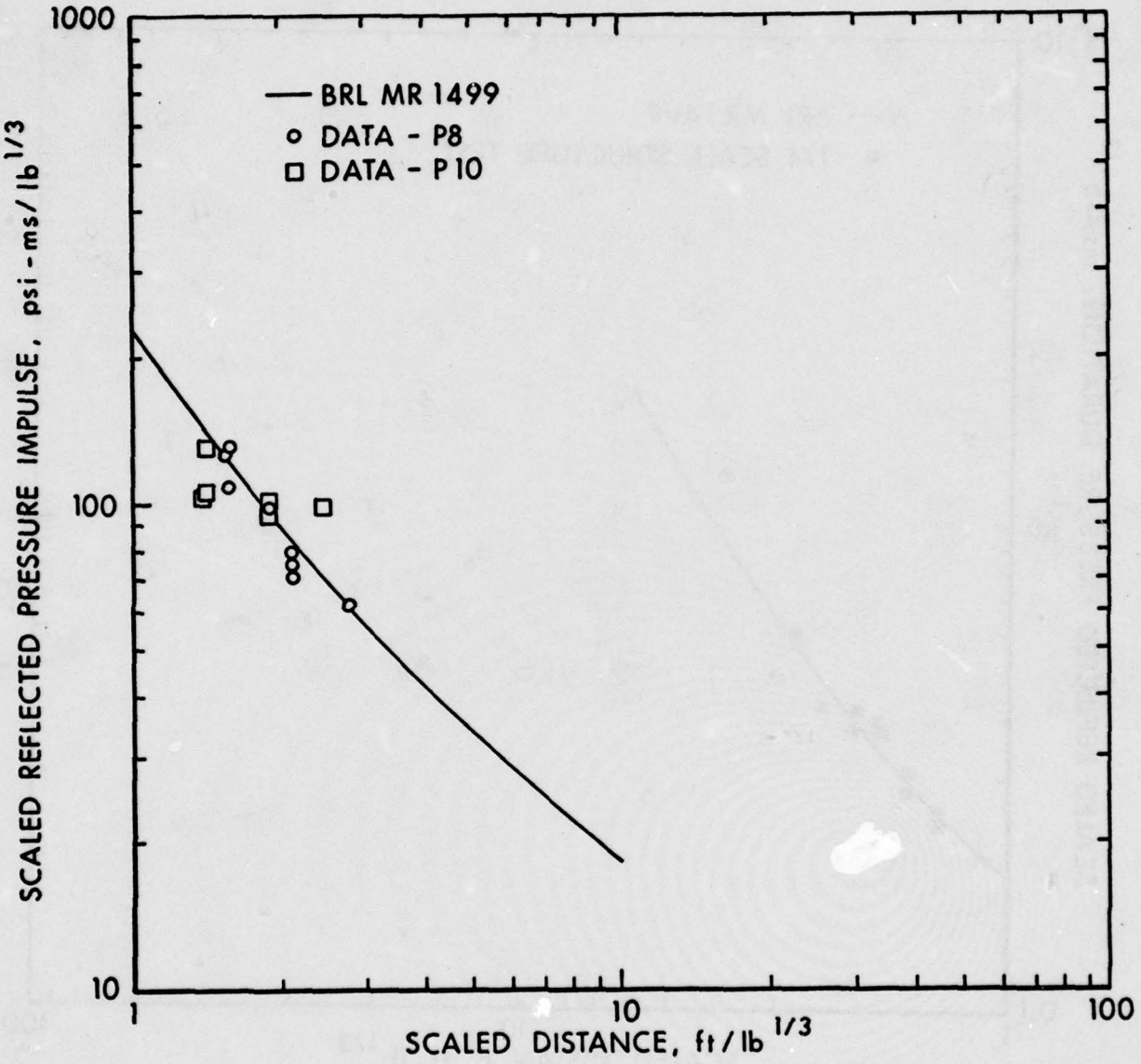


Figure 31. Scaled Reflected Pressure Impulse Versus Scaled Distance

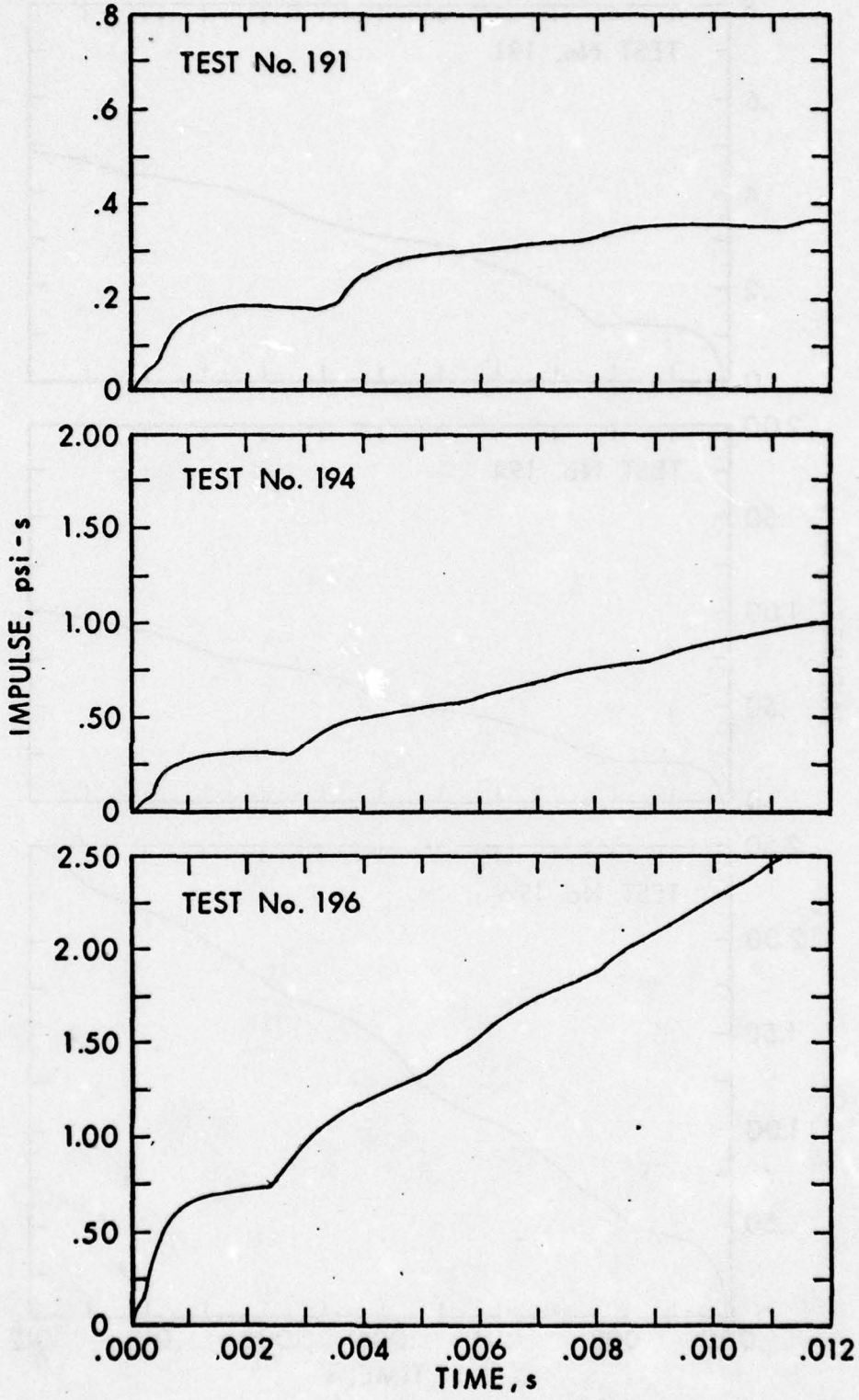


Figure 32. Reflected Pressure Impulse Versus Time at Location P7 for Tests 191, 194, and 196

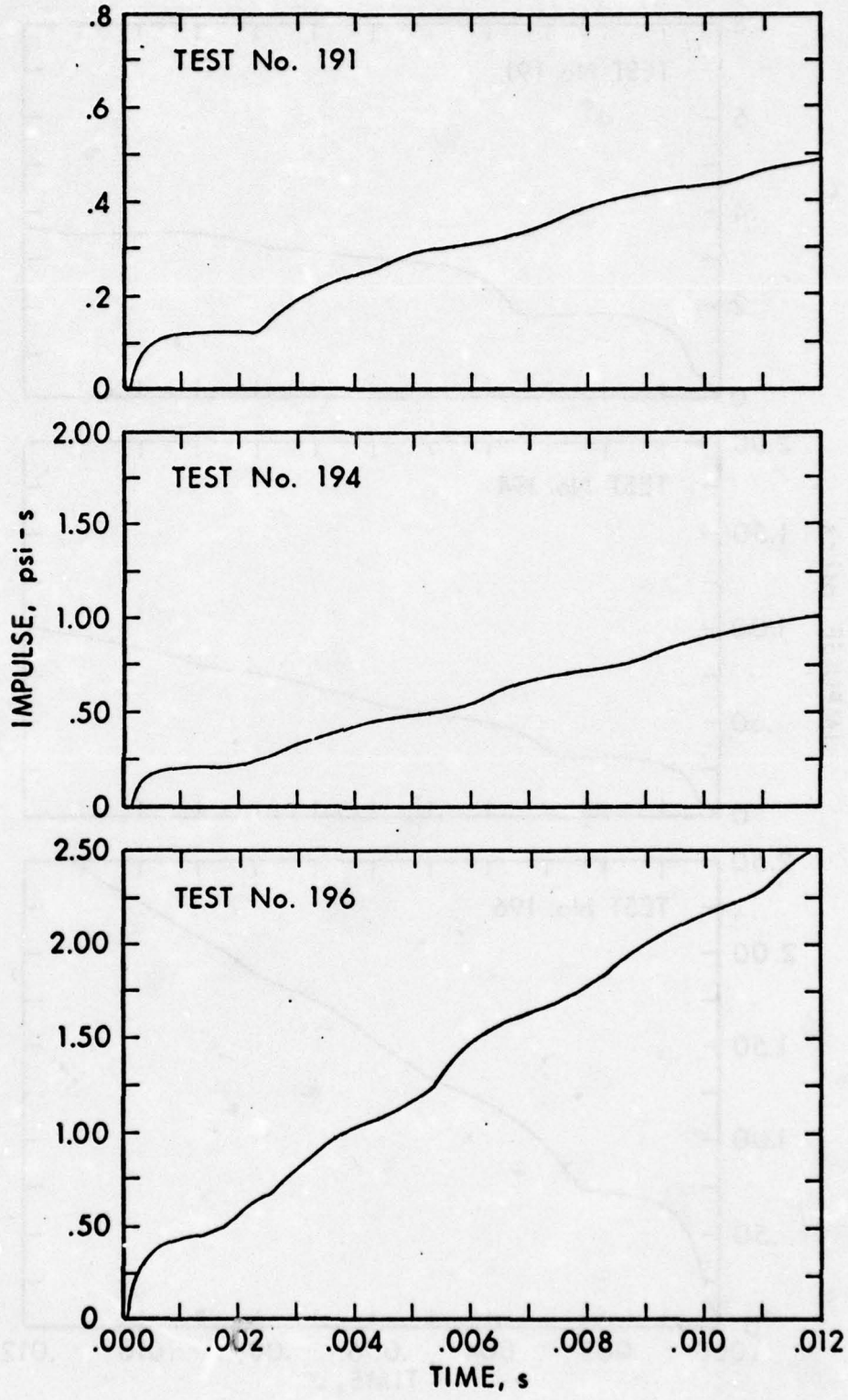


Figure 33. Reflected Pressure Impulse Versus Time at Location P8 for Tests 191, 194 and 196

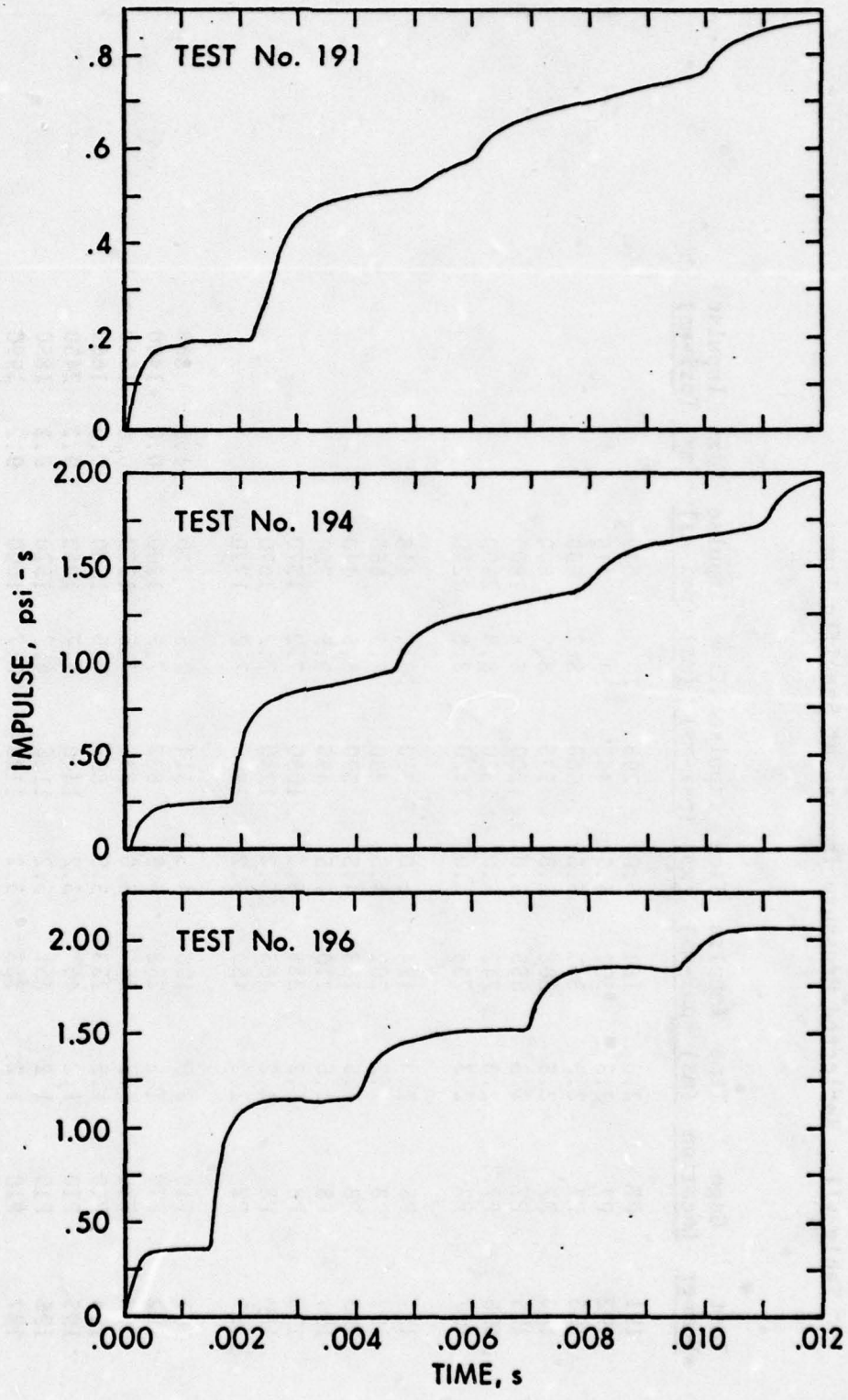


Figure 34. Reflected Pressure Impulse Versus Time at Location P10 for Tests 191, 194, and 196

Table VII. Reflected Pressure Impulse at Specific Times

Test Number	Gage Location	Time (ms)	Impulse (psi-ms)	Time (ms)	Impulse (psi-ms)	Time (ms)	Impulse (psi-ms)	Time (ms)	Impulse (psi-ms)
191	P7	2.0	181	6.0	298	10	349		
192	P7	2.5	307	5.5	445	10	416		
193	P7	2.5	347	5.5	660	8.7	890		
194	P7	2.5	308	5.5	575	8.7	800		
195	P7	2.3	655	5.0	1200	8.8	1800		
196	P7	2.3	742	5.0	1320	8.8	2100		
197	P7	2.3	738	5.0	1420	8.8	2270		
191	P8	2.0	124	6.0	310	10	418		
192	P8	1.5	202	4.5	400	8.5	555		
193	P8	1.5	188	4.5	390	8.5	440		
194	P8	1.5	210	4.5	455	8.5	750		
195	P8	1.2	388	5.2	1050	7.2	1370		
196	P8	1.2	465	5.2	1240	7.2	1670		
197	P8	1.2	450	5.2	1296	7.2	1720		
191	P10	2.0	196	4.5	514	9.5	730	11.5	868
192	P10	1.5	258	3.5	832	7.5	1200	10.0	1400
193	P10	1.5	261	3.5	890	7.5	1270	10.0	1510
194	P10	1.5	253	3.5	895	7.5	1380	10.0	1660
195	P10	1.2	464	3.2	1340	6.7	1980	9.2	2450
196	P10	1.2	361	3.2	1150	6.7	1520	9.2	1850
197	P10	1.2	363	3.2	1120	6.7	1600	9.2	1990

D. Quasi-Static Pressure Parameters

The quasi-static pressure is the term used to define the over-pressure generated from the gaseous by-products when an explosion occurs in a closed vessel. The magnitude of the quasi-static pressure is a function of the ratio of charge weight to structure volume. The duration of the quasi-static pressure is a function of the ratio of the vent area to volume of the structure.

1. Peak Quasi-Static Pressure. The peak quasi-static pressure is a difficult parameter to interpret because it usually occurs in a vented structure while the repeated shock reflections are still in evidence. Two values for the quasi-static pressure are listed in Table VIII. The first value (P_{QE}) is an extrapolation of the quasi-static pressure versus time back to a zero rise time. A second value (P_{Qt_r}) is also listed in Table VIII. It is an average pressure determined at a time t equal to $W^{2/3}$, where W is the charge weight in pounds and t is the time in milli seconds. This second value should be the maximum gas pressure prior to any decay due to venting of the structure. An example of the method used to determine the two values is given in Figure 35. Although gage locations P7, P8 and P10 were designed primarily to document the reflected pressure parameters they were also used to determine quasi-static pressure. They were not used to determine duration or impulse because they were not protected from the thermal environment which can cause signal distortion before the pressure has decayed to atmospheric conditions. The average values of P_{QA} for each test are plotted in Figure 36. Also plotted in Figure 36 are experimental results from the 1/16 size structure, Reference 2. Data from the Naval Civil Engineering Laboratory (NCEL) and Naval Ordnance Laboratory (NOL) taken from Reference 8 are also plotted in Figure 36. The results from the BRL tests fill an important data gap between the two sets of data from NOL and NCEL.

The quasi-static pressures P_{QE} listed in Table VIII are presented in Figure 37. These values are higher than the P_{QA} values and agree with a curve calculated from Proctor's computer code INBLAST described in Reference 9. There is excellent correlation between the predictions from the NOL computer program and the experimental data obtained by BRL.

2. Quasi-Static Pressure Duration. The duration (t_g) of the quasi-static pressure is listed in Table VIII. The values listed for tests 196 and 197 are questionable because the thermal environment is beginning to affect the pressure gages. The duration of the quasi-static

8 *"Effects of Venting and Frangibility on Blast Environment from Explosions in Cubicles," W. A. Keenan and J. E. Tancreto, Minutes of Fourteenth Explosive Safety Seminar, pp. 125-161, New Orleans, LA, November 1973.*

9 *"Internal Blast Damage Mechanism Computer Program," J. F. Proctor, Report 61 JTCG/ME-73-3, Joint Technical Coordinating Group for Munitions Effectiveness, April 1973.*

Table VIII. Quasi-Static Pressure Parameters

Gage Station	Distance (Feet)	Gage Location	Test 191	Test 192	Test 193	Test 194	Test 195	Test 196	Test 197
			Pressure (psi) - Extrapolated (P_{QE})						
P7	7.10	Wall	75	-	140	120	250	260	280
P8	5.63	Wall	70	140	140	110	240	280	255
P9	5.63	Wall	70	130	135	130	-	285	290
P10	5.00	Roof	80	150	160	150	260		250
P11	5.00	Roof	70	140	140	150	-	290	300
		Average	73	140	143	132	250	279	275
			Pressure (psi) at $t = w^{2/3}$ (P_{QA})						
P7	7.10	Wall	70	130	120	100	170	180	240
P8	5.63	Wall	60	100	100	105	175	180	195
P9	5.63	Wall	60	100	100	110	-	185	200
P10	5.00	Roof	75	140	120	120	170	-	150
P11	5.00	Roof	60	120	110	120	-	200	200
		Average	65	118	110	111	172	191	197
			Time Duration (ms)						
P9	5.63	Wall	40	35	50	100	-	380	715
P11	5.00	Roof	42	40	65	95	-	260	470
		Average	41	38	58	98	-	320	593
			Maximum Impulse (psi-ms)						
P9	5.63	Wall	721	1145	1640	3860	-	22300	63200
P11	5.00	Roof	939	-	2470	4440	-	22200	34500
		Average	830	1145	2055	4150	-	22250	48850
			Time Duration from Strain Data (ms)						
		Average	35	40	60	150	200	430	1450

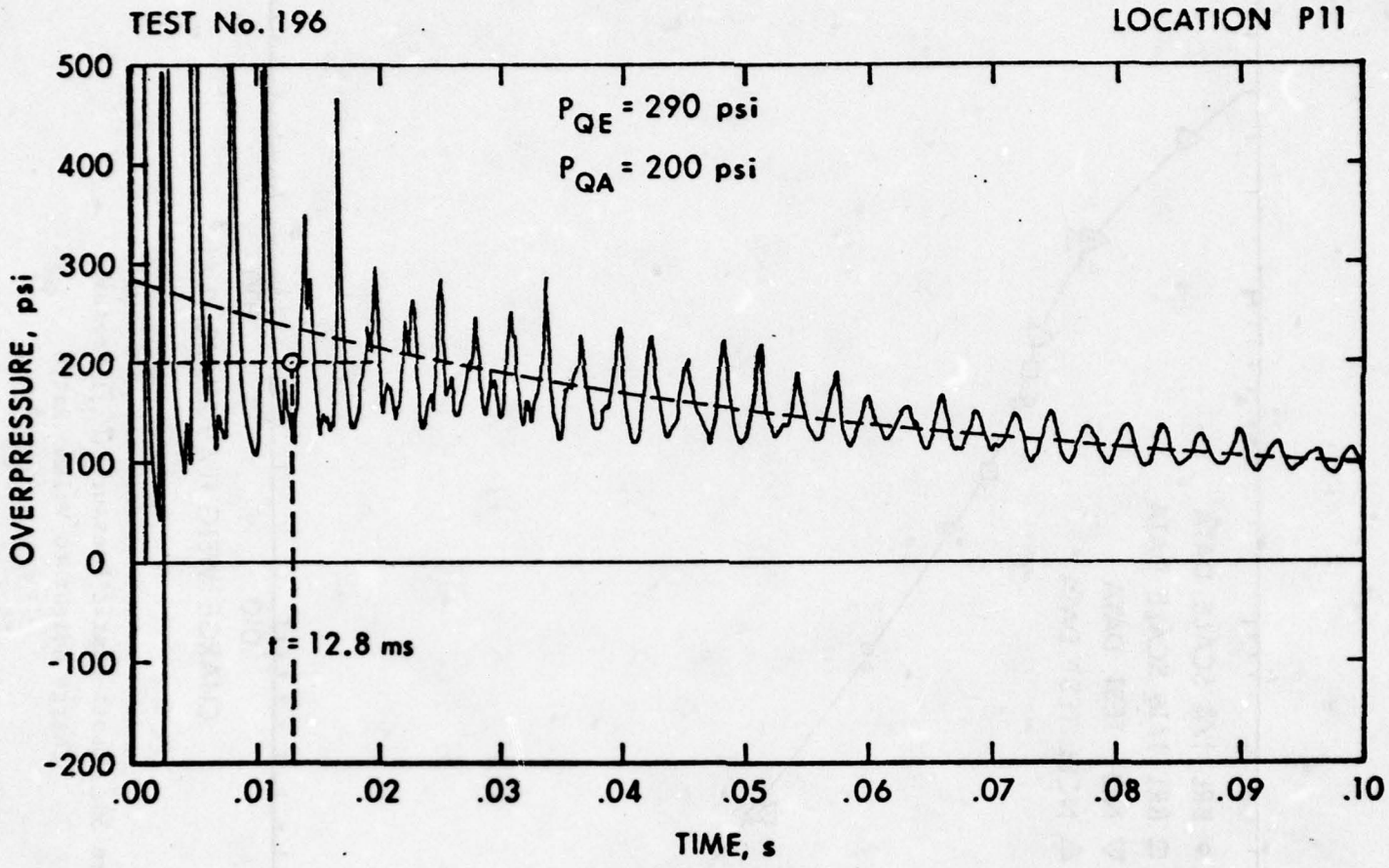


Figure 35. Method of Determining P_{QE} and P_{QA}

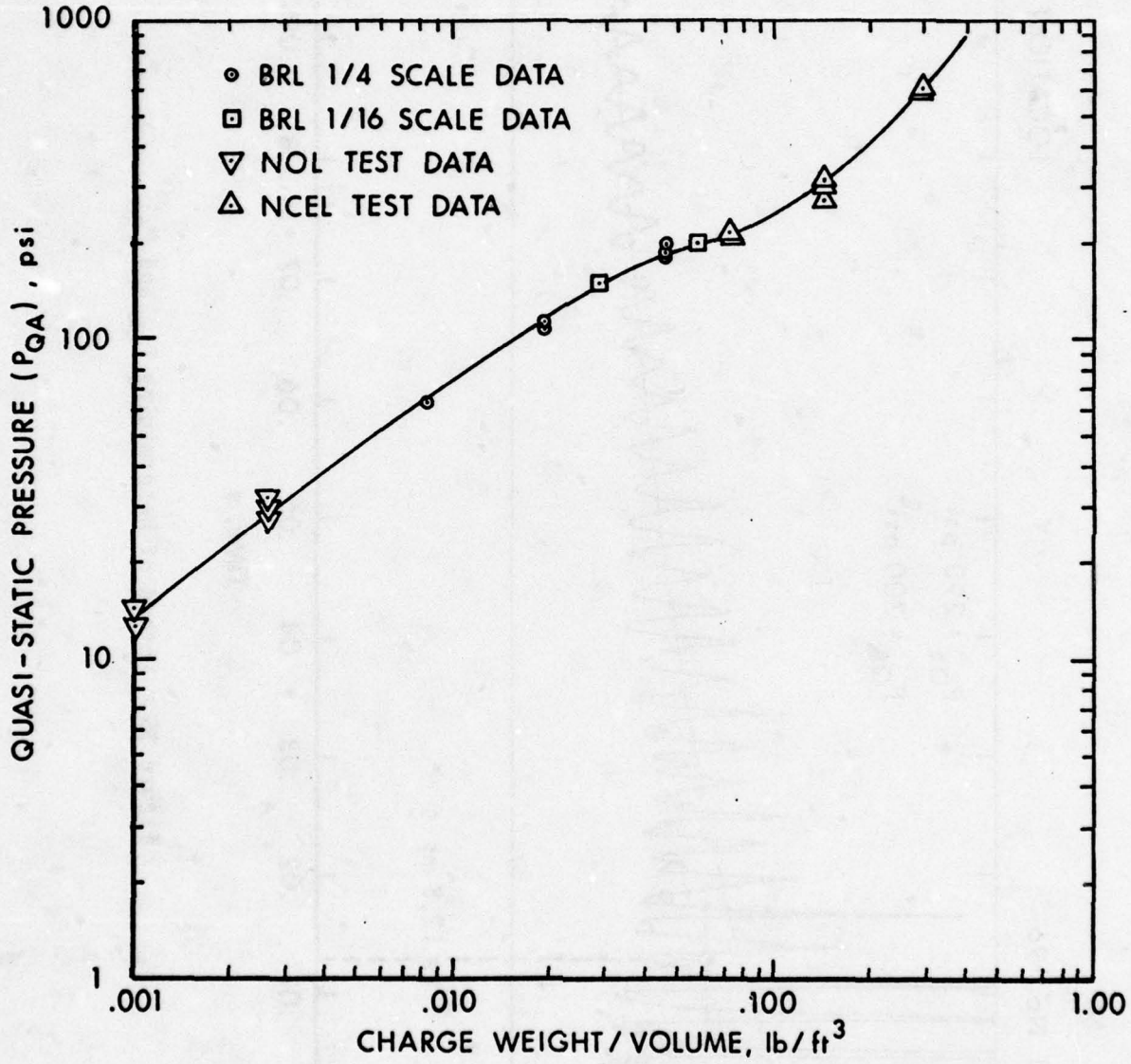


Figure 36. Quasi-Static Pressure (P_{QA}) Versus Charge Weight to Volume Ratio

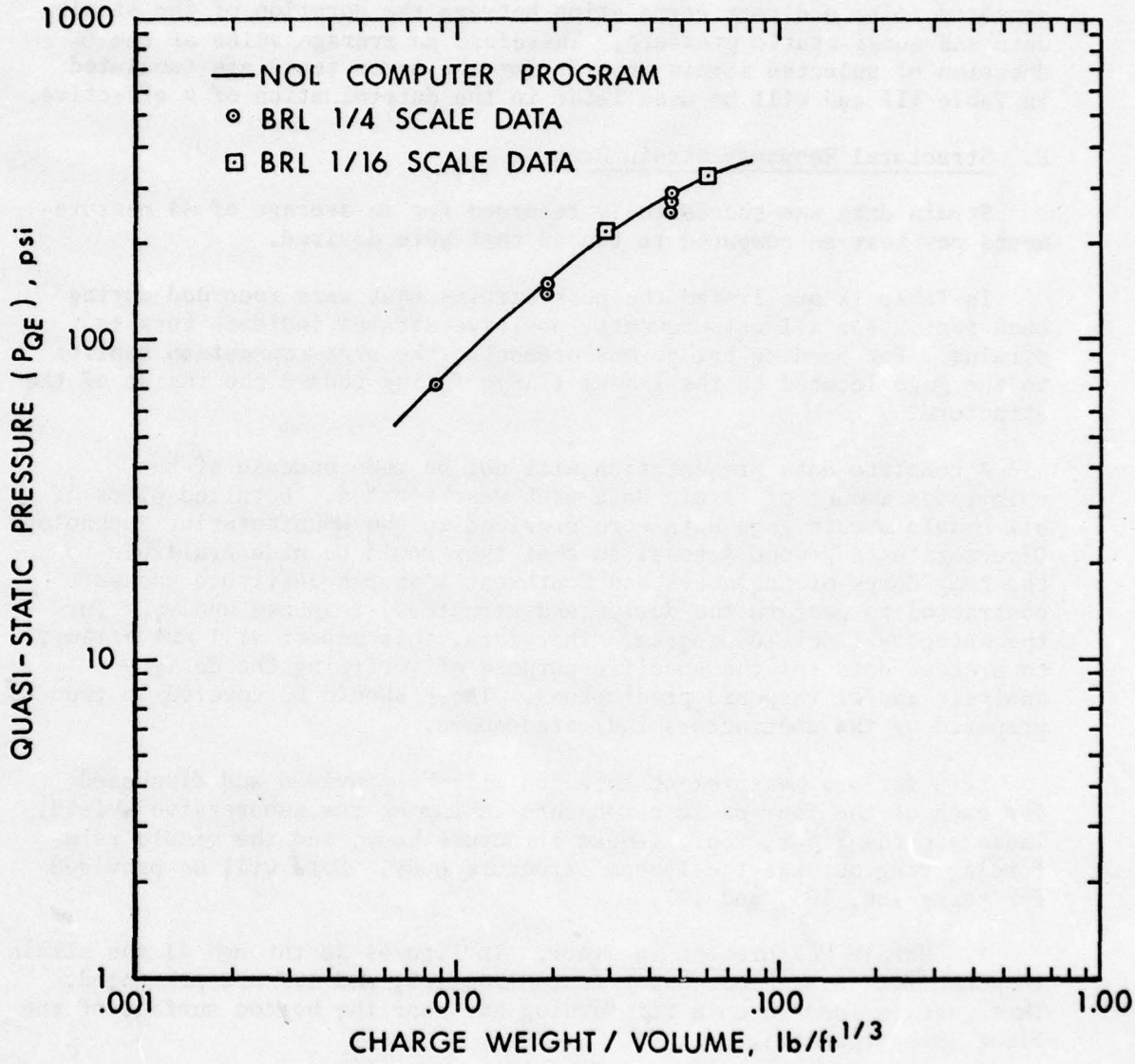


Figure 37. Quasi-Static Pressure (P_{QE}) Versus Charge Weight to Volume Ratio

pressure in a suppressive structure is a function of the area vented or α effective. Therefore a discussion of duration and impulse of the quasi-static pressure will be included in a later section of this report.

Upon the examination of many of the strain gage records there appeared to be a direct correlation between the duration of the strain data and quasi-static pressure. Therefore an average value of the duration of selected strain records for the seven tests are tabulated in Table VII and will be used later in the determination of α effective.

E. Structural Response Strain Data

Strain data was successfully recorded for an average of 44 measurements per test as compared to the 48 that were desired.

In Table IX are listed the peak strains that were recorded during each test. For all measurements, positive strains indicate tensile strains. For bending bridge measurements, the sign convention applies to the gage located on the I-beam flange facing toward the inside of the structure.

A complete data presentation will not be made because of the voluminous amount of strain data that was recorded. Detailed plots of all usable strain gage data were provided to the Manufacturing Technology Directorate, Edgewood Arsenal so that they could be made available to the Army Corps of Engineers and Southwest Research Institute who were contracted to perform the design and structural response analysis for the Category I Shield program. Therefore, this report will not attempt to present data for the specific purpose of verifying the design analysis and/or response predictions. These should be covered in reports prepared by the contractors indicated above.

Data for one measurement location will be provided and discussed for each of the four basic components making up the suppressive shield. These are the floor, roof, I-beam structure body, and the middle reinforcing ring outside the I-beam structure body. Data will be provided for tests 194, 195, and 197.

1. Strain Measurement in Floor. In Figures 38 through 41 the strain response for gage number 6 for tests 194, 195, and 197 are presented. This gage is located on a reinforcing bar near the bottom surface of the floor (see Appendix).

In Figure 38 it can be seen that the large damped oscillations occur for approximately 60 ms. Note the presence of the higher oscillation frequency (approximately 4 times the fundamental) superimposed onto the fundamental frequency. For tests 195 and 197 (Figures 39 through 41) the higher frequency response is suppressed but still evident for the first 20 ms and the fundamental frequency is seen to dampen out between 80 and 120 ms after being excited.

Table IX. Measured Peak Strain

Strain Gage Number	Peak Strain (Microstrain) Test 191	Test 192	Test 193	Test 194	Test 195	Test 196	Test 197
1	940	1600	1880	1910	2400	2900	2670
5	211	570	625	725	2050	----	----
6	382	850	915	935	2500	2600	3150
20	-215	-325	-380	-400	-685	-585	-460
21A	145	370	418	480	2400	3000	3100
22	372	1350	3200	4800	----	----	----
22A	----	----	----	----	----	----	----
23	----	----	530	630	3100	3420	1750
24	358	-340	-395	-425	-335	330	475
27	320	950	1520	1950	----	----	----
27A	----	----	----	----	----	1100	4000
31	530	1000	1190	1120	1400	2070	2020
32	118	-255	-295	-320	-770	-900	-850
33	-360	-740	-720	-800	-1750	-1990	-1960
35	705	2100	2400	2600	2900	1620	5520
36A	-222	-400	-400	-430	-770	850	800
37	250	440	505	500	650	1020	1100
38	-238	----	----	-310	-750	750	742
38A	----	----	-240	----	----	----	----
39	440	860	940	1240	1270	1970	2040
50/51	1570	1900	1620	1700	1450	2200	2500
52/53	-1220	-2470	-2140	-2000	-2270	-6150	-2100
54	-960	-1200	-1100	-1200	-980	-1120	-932
55	1080	1400	1350	1250	1200	1200	1340
56/57	2150	2350	2160	2400	----	1760	----
58/59	-1500	-1960	-1180	-2020	-2900	----	----
60/61	-2050	-3750	----	----	----	----	----
62/63	-1880	-1980	-1780	-2000	-1810	-----	-2910
64	-770	-1000	-1500	-1200	-770	1180	-770

Table IX. (Cont'd) Measured Peak Strain

Strain Gage Number	Peak Strain (Microstrain) Test 191	Test 192	Test 193	Test 194	Test 195	Test 196	Test 197
65	1070	1200	1140	1300	----	----	----
74/75	----	----	----	-2750	-2330	-3650	-3190
76	-980	-1080	-1080	-1400	840	1150	1510
77	1000	1600	1650	1550	880	1150	670
78H	----	-950	-660	-980	-1450	----	----
78S	----	900	1230	990	1100	----	----
78V	----	310	340	375	575	----	----
80H	-250	-760	----	----	----	----	----
80S	-530	-870	----	----	----	----	----
80V	290	460	----	----	----	----	----
83H	-328	-450	-940	-620	-615	1080	800
83S	-830	-1100	-1120	-1200	-2370	-3400	-2820
83V	-330	----	-440	340	2000	-420	-930
84H	----	----	320	495	590	----	----
84S	----	----	-670	-670	-1100	----	-1190
84V	----	----	318	300	680	----	600
85H	270	710	670	-640	1350	1950	1940
85S	-690	-1420	-1450	-1080	-3450	-6800	-7600
85V	-250	-395	-312	-500	-690	-2000	-2650
86	495	530	640	550	730	-945	----
90	-460	-850	1030	1060	2580	2420	2250
91	-880	-1430	-570	-920	3100	2400	4220
92	515	1450	3250	3300	10000	3200	3460
93	470	1120	1650	2700	2800	2120	3100
98	430	780	860	810	3250	1770	1820
99	760	1460	1220	----	1320	1390	----

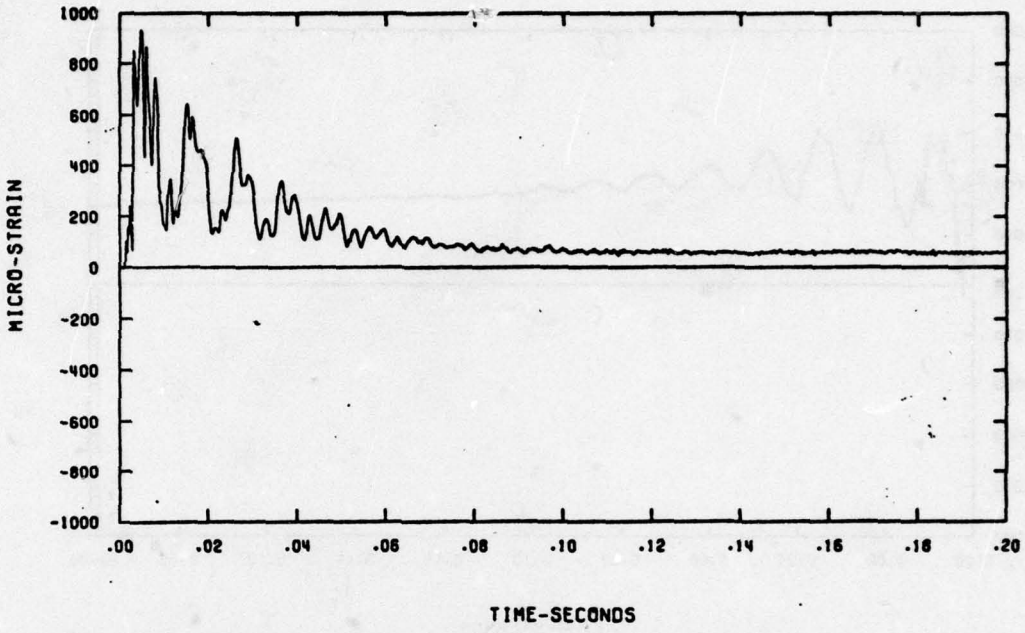


Figure 38. Strain Gage Number 6 Time History During Test 194

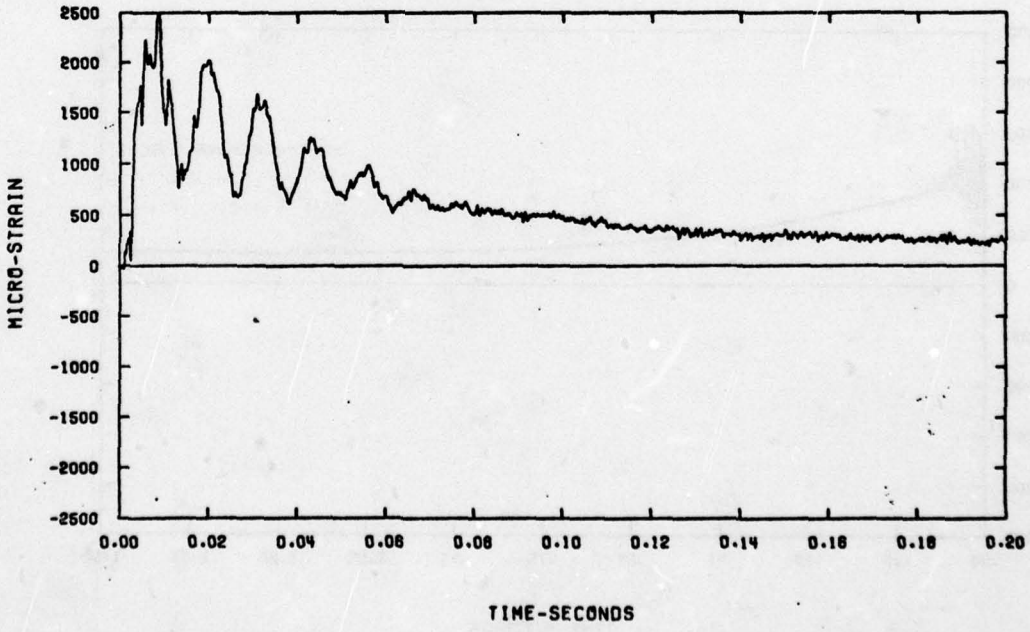


Figure 39. Strain Gage Number 6 Time History During Test 195

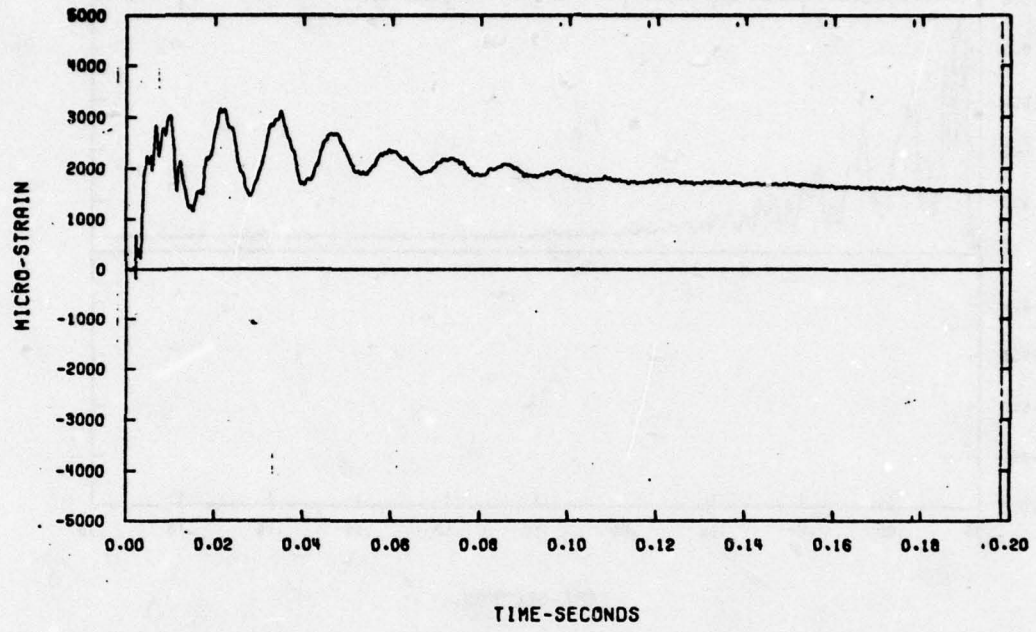


Figure 40. Strain Gage Number 6 Early Time History During Test 197

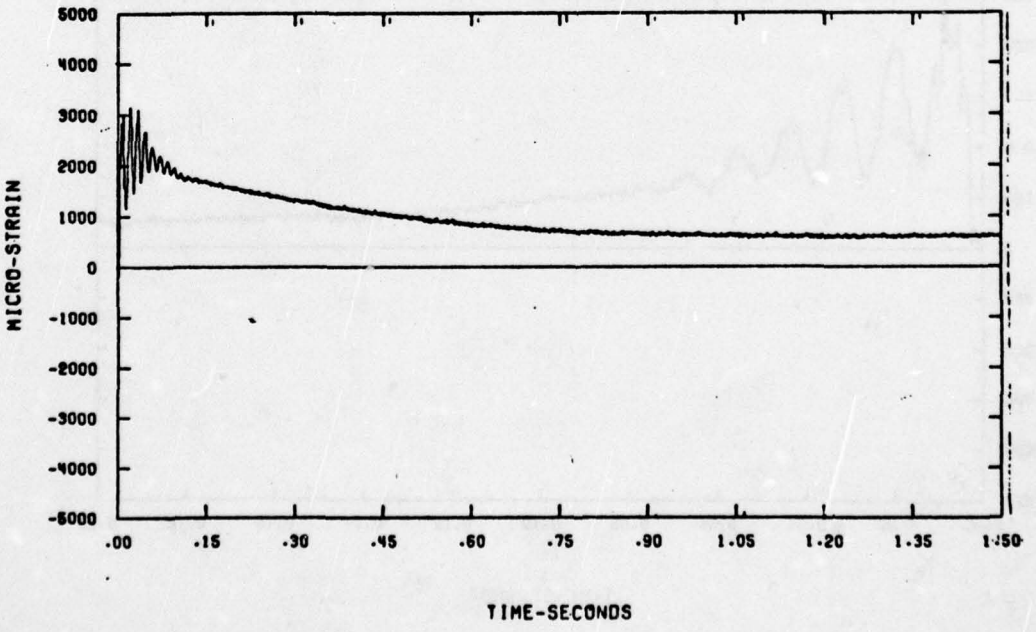


Figure 41. Strain Gage Number 6 Long Duration Time History During Test 197

2. Strain Measurement in Roof. In Figures 42 through 45 the strain response for gage number 21A for tests 194, 195, and 197 are presented. This gage is located on a reinforcing bar near the upper surface of the roof (see Appendix).

An examination of these figures indicates a similarity to the response indicated for measurement 6 in the floor. The amplitude of response for gage 21A is less than that for gage 6, however this may be accounted for by the different location of the gage elements in their respective concrete slabs. The presence of the higher frequency components and their rather rapid decay for tests 195 and 197 is similar for the roof and floor locations. This would indicate that the ground (4 inch sand layer) had only a minor effect on the frequency of oscillation and damping of the relatively massive concrete slab.

3. Strain Measurement on I-Beam Structure Body, In Figures 46 through 49 the strain response for one I-beam bending bridge configuration for tests 194, 195, and 197 is presented. For this gage configuration, which is located midway between the lower and middle reinforcing rings, positive strain indicates bending strains such that gage 75 is in tension. The exact location of the gage elements are shown in the Appendix.

In Figure 46 an effect resulting from the gaps (free play) between the I-beams and reinforcing rings is evident. The strain level oscillates about a nominal bending strain of -1000 microstrain for approximately 0.05 seconds then decays gradually to zero. For test 195, where the gaps were shimmed, this type of response is not apparent. In Figure 47 there appears to be an indication of bands failing during the first three milliseconds of the record. This is indicated by the gradual increase of the maximum response during the first three oscillations of loading followed by a gradual decline in the bending strains. In Figure 48 the band failures for test 197 appear to occur during the first six milliseconds of time.

4. Strain Measurements on Center Reinforcing Ring. In Figures 50 through 53 the strain response for gage 92, located on the outer band of the center reinforcing ring, is presented for tests 194, 195, and 197.

In Figure 50 the strain level for test 194 is seen to decay to the steady state zero value at about 0.05 seconds. This correlates with the I-beam data indicated above. In Figure 51 the initial high strains for test 195 drop to a semi-steady-state value after approximately 0.004 seconds. This is most likely the time at which this band broke, and the strains thereafter caused by flexing of the band until the strain gage leads broke. During the first 0.004 seconds there are four large strain oscillations evident; these most likely are related

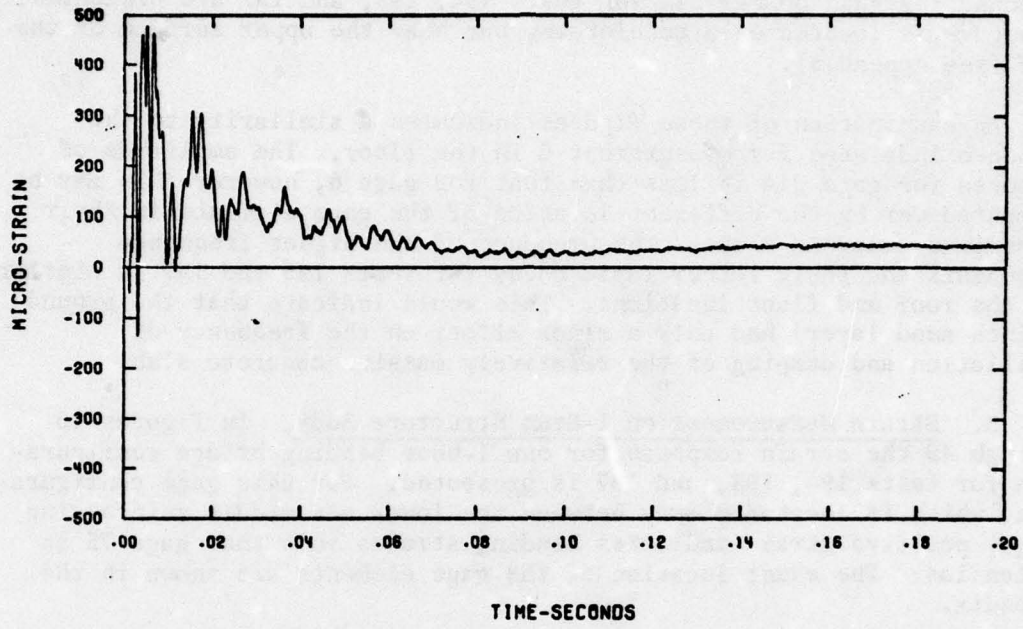


Figure 42. Strain Gage Number 21A Time History During Test 194

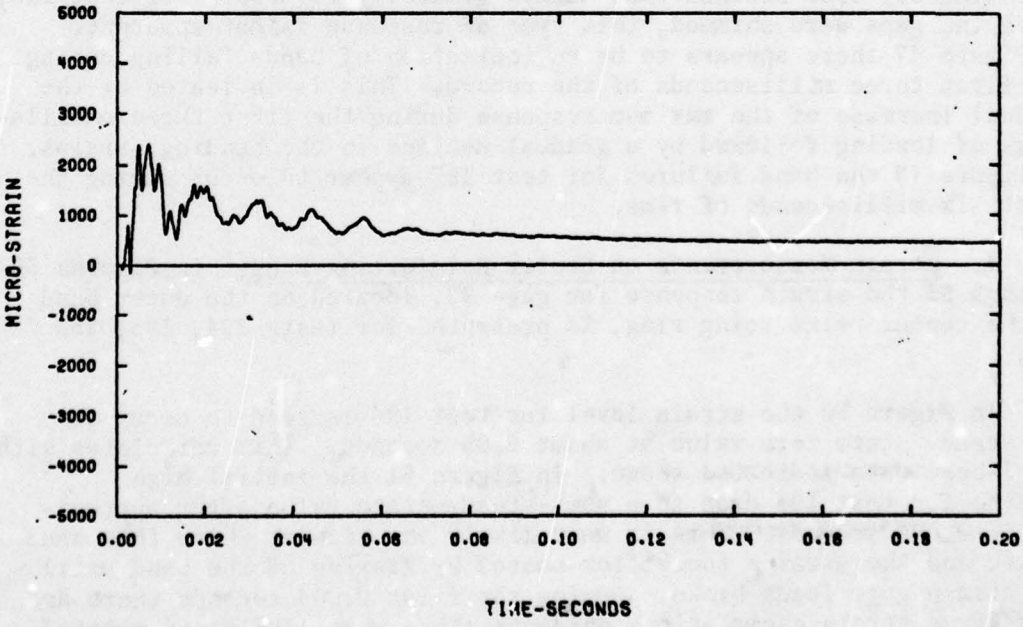


Figure 43. Strain Gage Number 21A Time History During Test 195

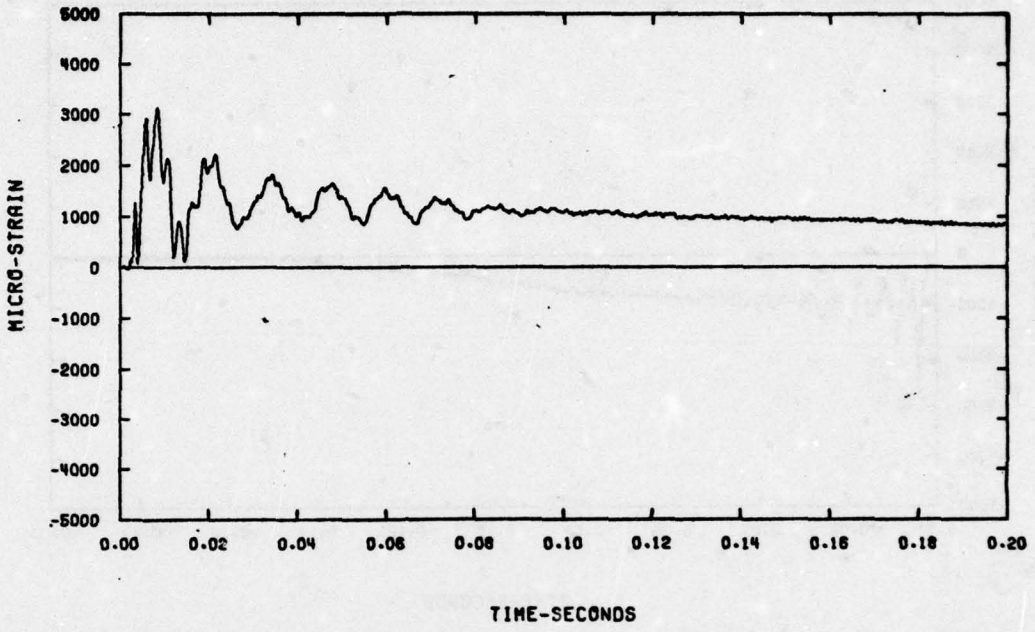


Figure 44. Strain Gage Number 21A Time History During Test 197

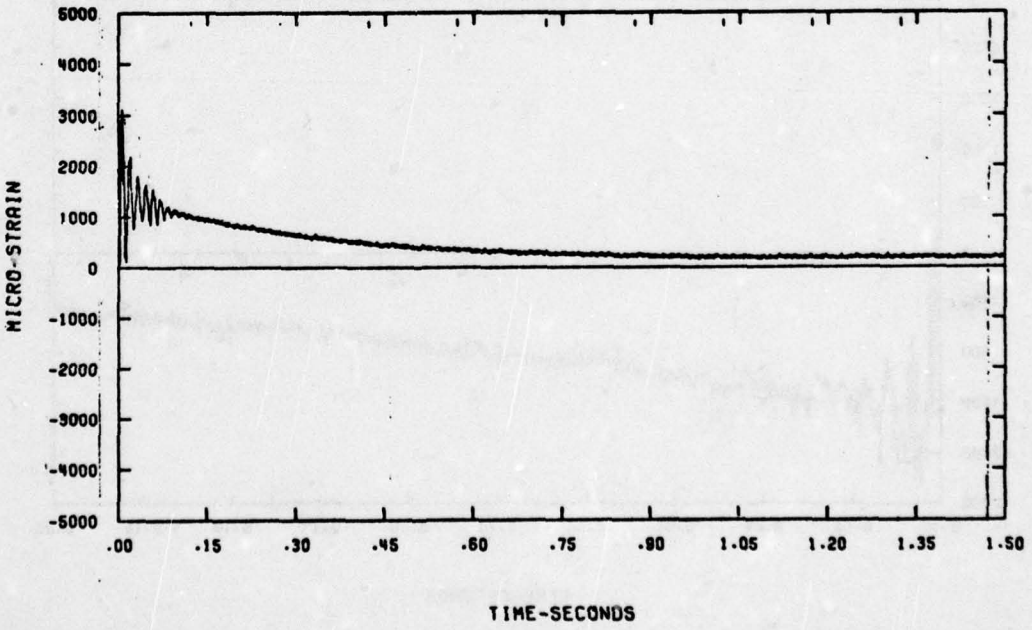


Figure 45. Strain Gage Number 21A Long Duration Time History During Test 197

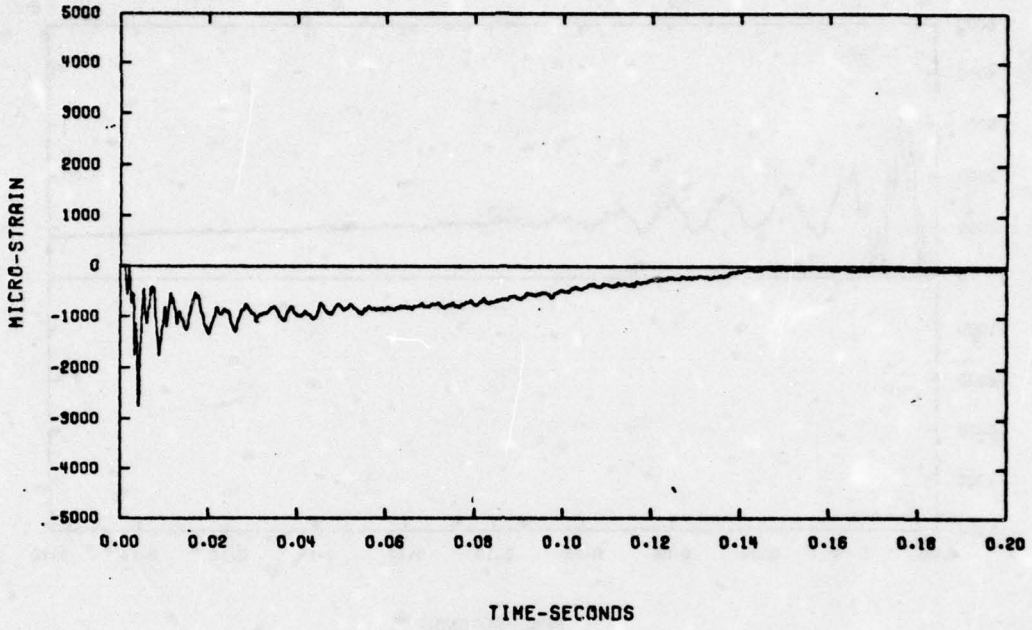


Figure 46. Bending Strain Measurement 74/75 Time History During Test 194

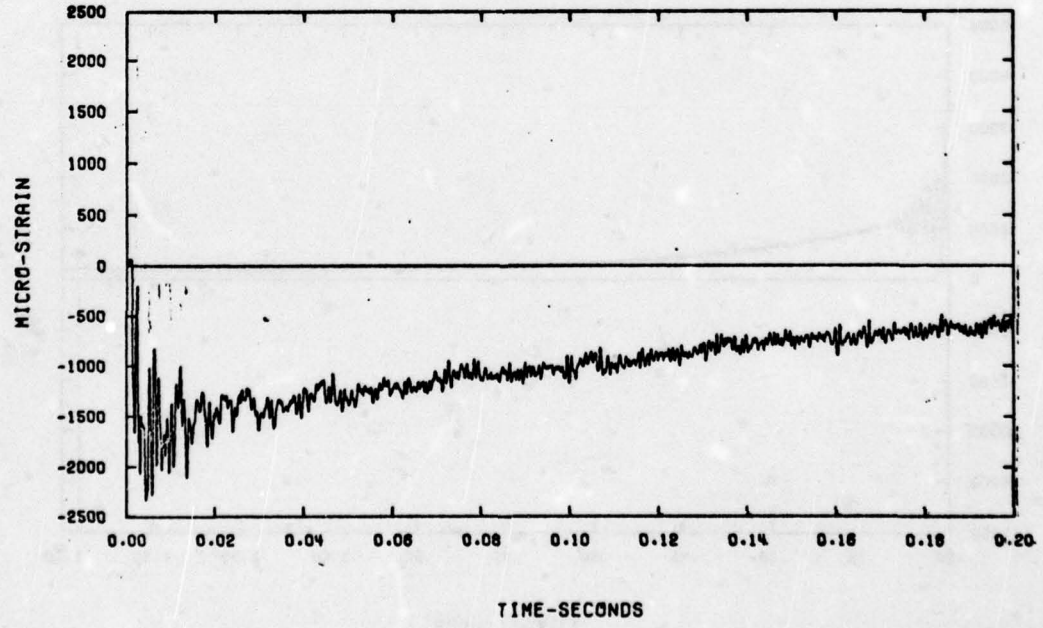


Figure 47. Bending Strain Measurement 74/75 Time History During Test 195

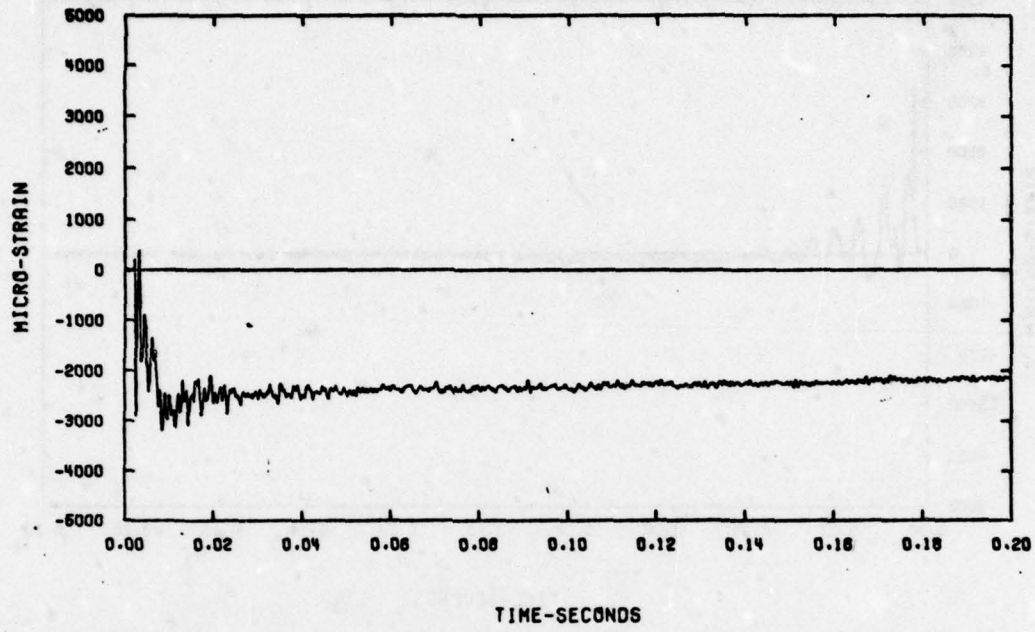


Figure 48. Bending Strain Measurement 74/75 Early Time History During Test 197

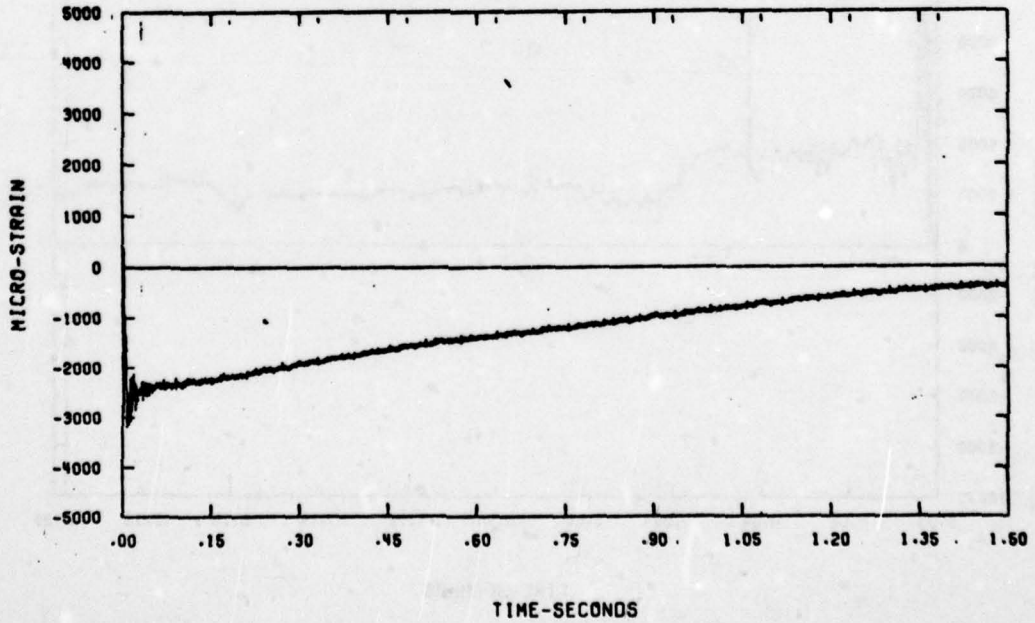


Figure 49. Bending Strain Measurement 74/75 Long Duration Time History During Test 197

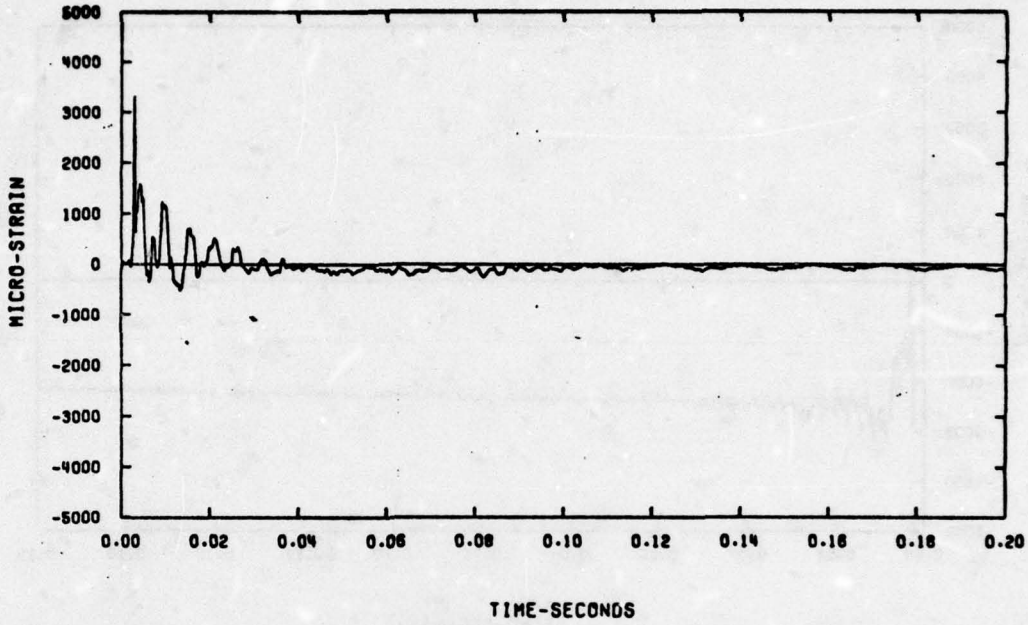


Figure 50. Strain Gage Number 92 Time History During Test 194

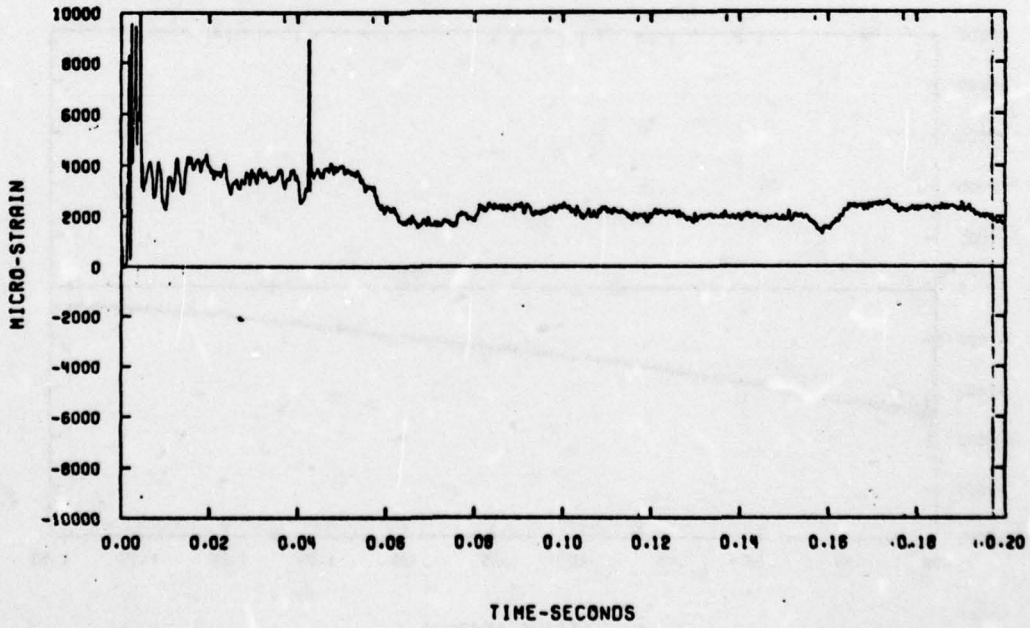


Figure 51. Strain Gage Number 92 Time History During Test 195

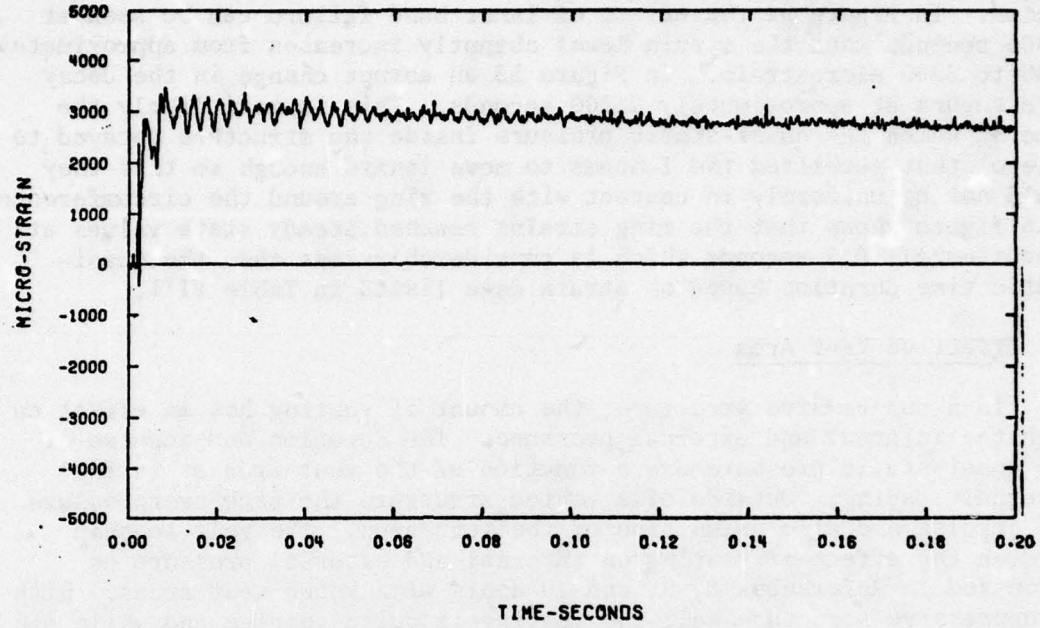


Figure 52. Strain Gage Number 92 Early Time History During Test 197

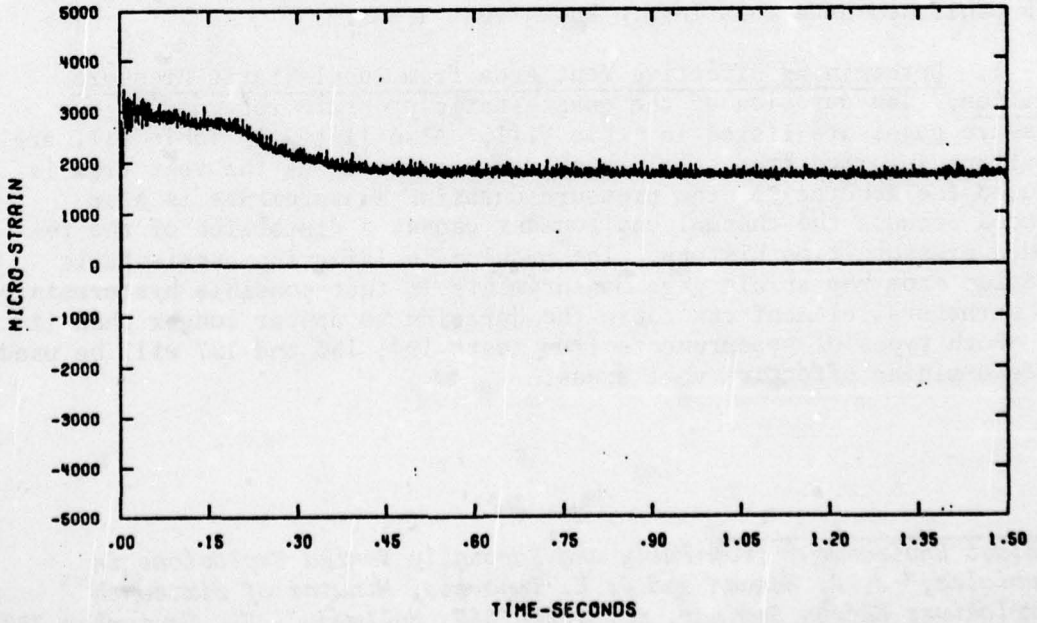


Figure 53. Strain Gage Number 92 Long Duration Time History During Test 197

to strain changes due to band failures of the nine bands before the outer one failed. In Figures 52 and 53 the data for test 197 are presented. In Figure 52 the effect of inner band failure can be seen at 0.006 seconds when the strain level abruptly increases from approximately 2000 to 3300 microstrain. In Figure 53 an abrupt change in the decay rate occurs at approximately 0.200 seconds. This is most likely the time at which the quasi-static pressure inside the structure decayed to a level that permitted the I-beams to move inward enough so that they would not be uniformly in contact with the ring around the circumference. This figure shows that the ring strains reached steady state values at approximately 0.5 seconds which is considerably less than the quasi-static time duration based on strain data listed in Table VIII.

F. Effective Vent Area

In a suppressive structure, the amount of venting has an effect on both the internal and external pressure. The duration and impulse of the quasi-static pressure are a function of the vent area as in the internal loading. Outside of a vented structure the peak overpressure and impulse are also a function of the vent area. The relationship between the effect of venting on internal and external pressure as discussed in References 8, 9, and 10 deals with known vent areas. With a suppressive structure wall the venting is quite complex and while one method was proposed in Reference 4 for calculating an effective vent area it has not been consistent when used to predict both internal and external blast parameters. The results of these seven tests will be used in an attempt to determine an effective vent area by comparison with published data relating to known vent areas.

1. Determining Effective Vent Area from Quasi-Static Pressure Duration. The duration of the quasi-static pressure recorded by the pressure gages are listed in Table VIII. Also listed in Table VIII are durations inferred from strain gage measurements. As the vent area is reduced the accuracy of the pressure duration measurements is also reduced because the thermal environment causes a distortion of the recorded pressure-time history. The problem in inferring quasi-static duration from the strain gage measurements is that possible hysteresis of the structural element can cause the duration to appear longer than it is. Both types of measurements from tests 194, 196 and 197 will be used in determining effective vent areas.

[10] *"Blast Environment from Fully and Partially Vented Explosions in Cubicles," W. A. Keenan and J. E. Tancreto, Minutes of Sixteenth Explosives Safety Seminar, pp. 1527-1559, Hollywood, FL, September 1974.*

In Reference 4 a relationship is established by Southwest Research Institute (SWRI) showing that the blowdown time or quasi-static pressure duration can be described as

$$\frac{t_g}{p^{1/6} V^{1/3}} = f \left\{ \frac{(\text{eff } A)^{3/2}}{v} \right\} \qquad (4)$$

using the graph in Figure 6 of Reference 4 the effective vent areas were calculated for the durations listed in Table VIII and the results are listed in column 1 of Table X. The pressures used in teh calculations were the average P_{QA} values listed in Table VIII.

Work has been conducted by Keenan and Tancreto of the Naval Civil Engineering Laboratory (NCEL)[10], in describing the blast environment in a partially vented structure. An equation was developed relating the duration of the quasi-static pressure and the vent area for $A/V^{2/3} < 0.21$,

$$t_g/w^{1/3} = 2.26 \ (AW^{1/3}/v)^{-0.86} \qquad (5)$$

For the 1/4 scale structure this equation should be valid for vent areas less than 21 ft^2. Using the recorded durations listed in Table VIII the vent area A was calculated and listed in column 2 of Table X for all tests except tests 191, 192, and 193. The calculations for these tests imply vent areas greater than 21 ft^2. Values of the vent areas for tests 191, 192, and 193 were determined from Figure 2 of Reference 10 and are also listed in column 2 of Table X.

A third method used for calculating the effective vent area from the measured duration is based on a family of curves developed by Proctor of the Naval Surface Weapons Center (NSWC) and published in Reference 11. Figure 9 of Reference 11 presents the scaled duration of the gas pressure versus scaled venting for a family of curves of different charge weight to structure volume (w/v) ratios. Based on these curves a simple equation was established for three w/v ratios which allowed a quick calculation of the effective vent areas versus quasi-static duration.

---

11 *"Internal Blast Computer Program," J. Proctor and R. A. Lorenz, Naval Surface Weapons Center (WOL) Report No. TR75-183 (to be published).*

Table X. Effective Vent Areas - Based on Duration (t_g)

Number	SWRI Vent Area (ft^2)	NCEL Vent Area (ft^2)	NSWC Vent Area (ft^2)	K+S Vent Area (ft^2)	Average Vent Area (ft^2)
191	35.7	32.9	28.6	18.2	28.9
192	44.6	36.0	33.2	25.8	34.9
193	25.6	25.9	21.8	17.1	22.6
194	13.0	14.6	12.9	9.81	12.6
194s	7.70	8.87	8.42	6.40	7.85
195s	6.06	6.66	6.74	6.04	6.38
196	3.64	3.86	4.21	3.92	3.91
196s	2.67	2.74	3.13	2.90	2.86
197	1.93	1.88	2.27	2.09	2.04
197s	.928	.671	.929	.861	.847

Note: s after test number denotes the quasi-static duration was inferred from strain gage measurements

SWRI - Southwest Research Institute - Reference 4

NCEL - Naval Civil Engineering Laboratory - Reference 10

NSWC - Naval Surface Weapons Center - Reference 11

K+S - Kenny and Sewel - Reference 12

$$A = \frac{KV}{t_g} \quad \text{where} \ldots\ldots \tag{6}$$

$K = 1.356$ ms/ft for w/v = .0460 lb/ft^3

$K = 1.270$ ms/ft for w/v = .0194 lb/ft^3

$K = 1.180$ ms/ft for w/v = .0084 lb/ft^3

The effective vent area A calculated for the measured duration (t_g) are listed in column 3 of Table X. Correlation with values in column 1 and 2 is very good for the smaller vent areas but the scatter is greater for the larger vent areas.

A fourth method relating vent area to quasi-static pressure duration was developed by Kenny and Sewell in Reference 12. In this reference an equation was derived to describe the quasi-static pressure variation versus time.

$$\text{Log } P = \text{Log Pmax} - .315 \frac{A}{V} t_g \tag{7}$$

where P = absolute pressure-bars

A = vent area - square metres

V = volume - cubic metres

t_g = Time - milliseconds

Arranging the terms to calculate A when P = 1 (Log P = 0) the equation becomes:

$$A = (\text{Log Pmax})\ (V)\ /.315\ t_g \tag{8}$$

A value for A was calculated for the seven tests using the quasi-static durations (t_g) listed in Table VIII. The results are listed in column 4 of Table X. The calculated areas are lower than the other three methods for the first four tests but show good comparisons for the last three tests.

An average value of effective vent area determined from the four described methods for each test is listed in column 5. It should be noted that although the structure remained the same, the effective vent area increased on test 192. It is surmised that the larger charge

[12] *"Venting of Explosions," G. F. Kinney and R. G. S. Sewell, Naval Weapons Center Technical Memorandum 2448, July 1974.*

weight on test 192 allowed larger I-beam deflections thus allowing the quasi-static pressure to decay more rapidly giving a shorter duration.

Using a relationship established in Figure 5 of Reference 10, scaled duration $t_g/w^{1/3}$ was plotted versus scaled venting $A\ w^{1/3}/v$ in Figure 54. The data are best represented by a straight line (in the log-log plane) with a slope of - 1.0. An equation of the form

$$t_g/w^{1/3} = 1.25\left(\frac{A\ w^{1/3}}{V}\right)^{-1.0} \tag{9}$$

gave a good fit to the data points. For this specific structure the equation can also be written as

$$t_g = 1.25\ (\frac{V}{A}) \tag{10}$$

Knowing the duration the effective vent area can be determined from

$$A = \frac{1.25V}{t_g} \quad \text{or} \quad \frac{1243}{t_g} \tag{11}$$

This is similar to the expression developed from Proctors' work[11].

2. Determining Effective Vent Area from Quasi-Static Impulse. Relationships have been established between the duration of the quasi-static pressure and the vent area of a suppressive structure; therefore it is reasonable to assume that a similar relationship can be developed between the impulse of the quasi-static pressure and the vent area.

The primary source of data showing quasi-static impulse as a function of known vent area is Reference 10. In this reference an equation

$$I_g/W^{1/3} = 569\ (A/W^{2/3})^{-7.8}\ (W/V)^{-.38} \quad \text{for } A/V^{2/3} < 0.21 \tag{12}$$

was developed as well as a family of curves which can be used where $A/V^{2/3}$ is > 0.21. By substituting the values of quasi-static impulse from Table VIII into the above equation the effective vent area can be calculated for $A/V^{2/3} < 0.21$. These calculations were made and the values are listed in Table XI for tests 194, 196, and 197. Reliable impulse measurements were not obtained on test 195. On tests 191, 192, and 193 the effective vent areas were determined from the family of curves presented in Figure 4 of Reference 10. These values are also listed in Table XI.

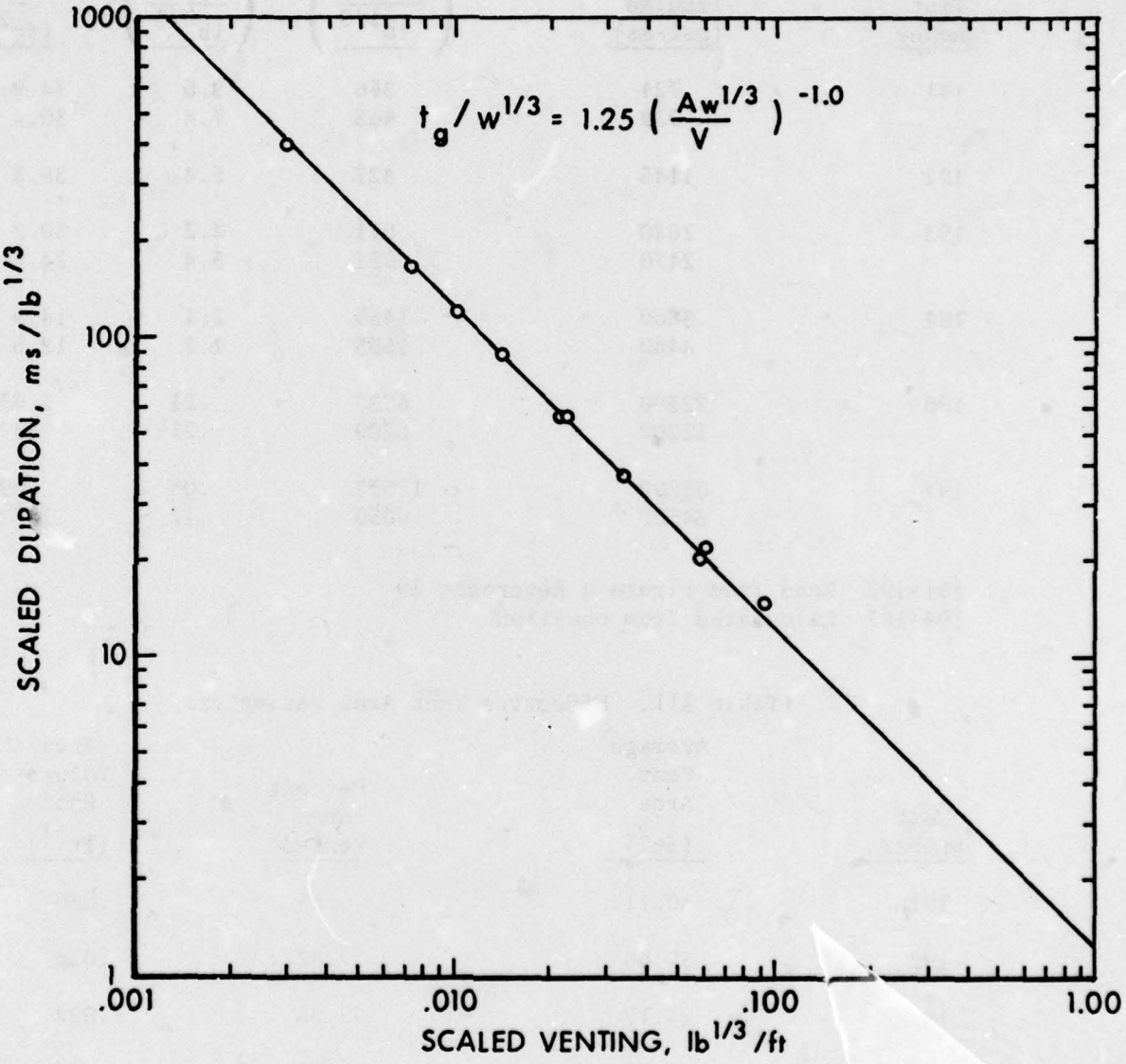


Figure 54. Scaled Quasi-Static Duration Versus Scaled Venting

Table XI. Effective Vent Areas from Impulse (I_g)

Test Number	Impulse (psi-ms)	$\frac{\text{Impulse}}{W^{1/3}}$ $\left(\frac{\text{psi-ms}}{\text{lb}^{1/3}}\right)$	$\frac{A/_w 2/3}{}$ $\left(\frac{\text{ft}^2}{\text{lb}^{2/3}}\right)$	$\frac{A}{(\text{ft}^2)}$
191	721	356	8.5	34.9
	939	463	7.4	30.4
192	1145	427	5.4	38.8
193	1640	611	4.2	30.2
	2470	921	3.4	24.4
194	3860	1439	2.1	14.9
	4440	1655	1.7	12.5
196	22300	6237	.21	2.65
	22200	6209	.21	2.67
197	63200	17677	.05	.699
	34500	9650	.12	1.52

191-193 Read from Figure 4 Reference 10
194-197 Calculated from equation

Table XII. Effective Vent Area Parameters

Test Number	Average Vent Area (ft^2)	Percent Area Vented*	Area/ Volume Ratio (ft^{-1})
191	30.11	6.65	.030
192	35.68	7.87	.036
193	24.17	5.33	.024
194	12.95	2.86	.013
195	6.38	1.41	.006
196	3.49	.77	.0035
197	1.73	.38	.0017

*Based on roof and wall area only (452.8 ft^2)

3. Summation of Effective Vent Area Determinations from Quasi-Static Parameters. Effective vent areas were determined for each test using the measured quasi-static duration and impulse when available. These values are listed in Tables X and XI. Data obtained from the pressure gage recordings of duration and impulse are plotted in Figure 55. The solid line is drawn through an average of the pressure data in Tables X and XI and the duration inferred from strain measurements on test 195. The average values of effective vent areas are listed in Table XII along with percentage of area vented and vent area to volume ratios.

4. Determining Effective Vent Area From Free-Field Pressure Data. The use of free-field pressure data to estimate an effective vent area is not considered to be reliable because of a paucity of applicable test data. The only data available, based on known vent areas, is presented in Reference 10. This data is for concentrated vent areas in the roofs of enclosures and for three wall barricades. This data showed that the free-field blast parameters are a function of the ground range from the center of the structure and the orientation of the vented area with respect to the free-field gage location. There is no data available for structures having a known uniformly distributed vent area. Testing has been done on suppressive structures having distributed venting but in all cases the venting was obtained through complex multi-layered panels for which effective vent areas were estimated (i.e., References 1 and 4). The problem is further complicated for the case where the vent area can change during internal blast loading due to structural deflections. This situation was most likely the case for tests 191 through 194.

In an attempt to estimate effective vent areas based on the free-field data it was concluded that the relationships established for cubicle enclosures[10] with venting in the center of the roof, approach at relatively long ground ranges, the values expected from our experiment. Therefore, in Table XIII are listed the vent areas based on the data from measurements P4 through P6 as determined from Figures 6 and 7 in Reference 10. A comparison of the values listed in Table X with those in Table XIII indicates relatively close agreement for all tests except test 192. For that test a considerably larger value of vent area based on free-field pressure data is indicated. It is recommended that less reliance be placed upon the vent areas indicated in Table XIII than in Table X because of the considerations indicated earlier in this section.

In general, the problem of determining a single effective vent area based on free-field blast parameters is not an easy one. This is especially true for structures which permit the vent area to change as a function of time or have a non-uniformly-distributed vent area. Based on the test observations indicated in Section III A, it appears that the biggest change in vent area during a given test occurred during test 192. The smallest variation in vent area was expected to occur during test 197. Also, during the test program the distribution of vent area changed considerably. For tests 191 through 195 the vent area

Table XIII. Effective Vent Areas Based on Free-Field Overpressure Data

Test Number	Average Effective Vent Area (ft^2) From Overpressure Data*	From Impulse Data**
191	44.4	30.8
192	68.9	60.6
193	34.4	32.9
194	16.4	12.2
195	7.22	8.25
196	0.71	1.40
197	0.78	0.56

*Calculated from Figure 6 of Reference 10 using P4 through P6 data only.
**Calculated from Figure 7 of Reference 10 using P4 through P6 data only.

Table XIV. Maximum Fireball Data

Test Number	Average Maximum Diameter (ft)	Average Maximum Scaled Diameter ($ft/lb^{1/3}$)
191	19.0	9.38
192	39.1	14.6
193	39.1	14.6
194	35.9	13.4
195	48.4	13.5
196	29.5	8.25
197	23.7	6.66

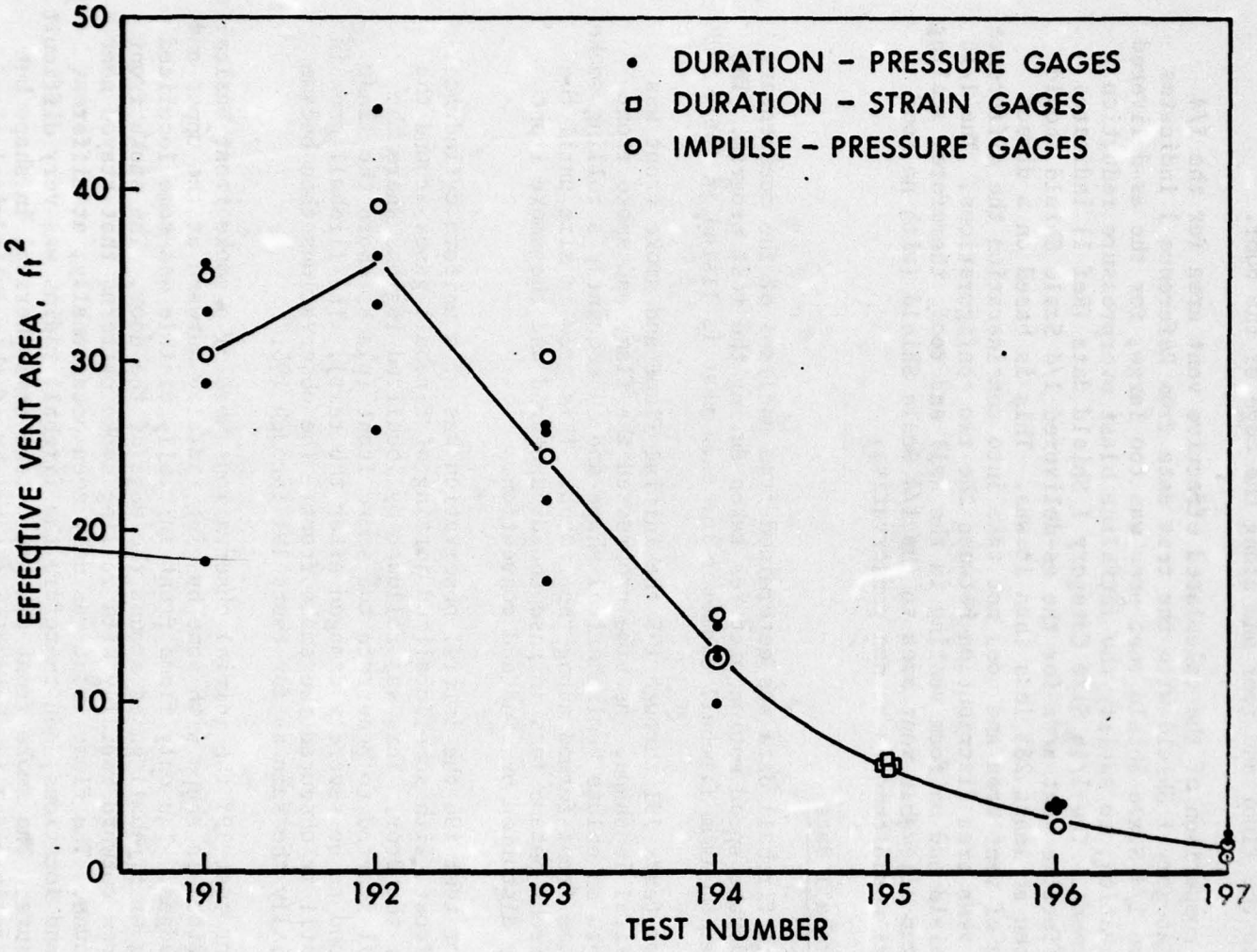


Figure 55. Effective Vent Area Versus Test Number

might be considered to be "uniform" over the wall area, whereas for test 196 and 197 the area would tend to be concentrated along wall regions close to the floor and roof and along the edge of the door.

A comparison of the calculated effective vent area for the 1/4 Scale Category I Shield with the test data from Reference 1 indicates that the 1/4 Scale Shield vent area was too large, for the as-delivered configuration, to satisfy the intraline blast overpressure reduction requirement. The 1/16 Size Category I Shield data (Ref 1) indicates that effective vent area for the as-delivered 1/4 Scale Shield should have been at least 28% less than it was. This is based on a direct scaling of vent area and does not take into consideration the difference in the vent area distribution between the two configurations. The 1/16 size Shield had uniform venting in the wall and roof, therefore, scaling a maximum allowable vent area to the 1/4 Scale Shield (with no roof venting) would tend to be non-conservative.

G. Fireball Data

The fireball data was determined from analyses of the documentary and moderate speed motion pictures taken during the test program. The averaged maximum fireball diameter for each test is listed in Table XIV.

For tests 191 through 195 the initial flame and smoke front was cylindrical in shape. As time progressed the flame and smoke front grew into an oblate hemispherical shape and subsequently a rolling smoke and flame front formed along the ground. This grew in size until the flame front became less intense and disappeared and the smoke front heavily distorted by wind and convection.

For test 196 the initial observation was of a uniform cylindrical smoke front, with some localized jetting of fireball gases around the edge of the door. This was followed by localized regions where the fireball started to penetrate the smoke front (places where the liner was found to be severely damaged after the test). The fireball grew in size until it obscured the smoke front. The observations then became essentially the same as for tests 191 through 195.

For test 197 the initial observations were of a smoke front basically cylindrical in shape with some bulging radially outward at the upper and lower edges. The only flame front initially visible was some localized jetting of fireball gases around the edge of the door. The smoke front then grew outward radially with rolling smoke patterns that stayed near the ground. The flame front was only seen occasionally, at different times and locations, and therefore the fireball radius was very difficult to measure. The smoke front did not become hemispherical in shape but rather cylindrical in shape with the height of this cylindrical cloud not exceeding ten feet. The fireball radius indicated in Table XIV for this test could not readily be determined as indicated above, and from one camera orientation, no fireball was observed at all. Therefore, the radius listed is only an estimate of the maximum radius.

Fireball growth for tests 195 and 197 during the first 7.5 ms are shown in Figure 56 and for elapsed times of 25 ms and 150 ms in Figure 57.

IV. CONCLUSIONS

The conclusions to be drawn from the results obtained during the series of tests are as follows:

1. The free-field peak overpressures versus distance outside of the structure were documented for each test. The rate of decay of pressure with distance was not constant as the venting area was decreased, i.e., the slope changed on each shot. The conclusion to be reached from this is that the attenuation of blast outside of the structure is influenced by both the amount of venting and the method of venting.

2. The 1/4 Scale Category Shield (in the as-delivered configuration) did not satisfy the free-field overpressure reduction requirement at the scaled intraline distance. However, the shield did satisfy the requirement when blocking strips were placed over all of the slots between the I-beams.

3. The measured peak reflected pressure and impulse impinging on the wall and roof of the structure agreed with the predicted values within acceptable limits. Based on the measurements of reflected pressure versus time it was concluded that the repeated reflections should be accounted for in inputs to structural response computer codes, because, for some tests the second recorded reflected pressure and impulse were of greater magnitude than the first ones.

4. The decrease in the venting area of the shield had no significant influence on the peak quasi-static pressure, although it did increase the duration of the pressure and hence increased the impulse.

5. There was no significant increase in peak strain response or observed structural damage as the vented area was decreased from that required to satisfy the intraline blast requirement to one approaching total containment.

6. The results show that the general fireball radius is reduced as the venting is decreased. If the fireball reduction is an established criteria then special attention must be given to sealing entrances and exits because fireball jetting could pose a hazard.

7. The 1/4 Scale Category I Shield demonstrated its ability to satisfy the structural integrity requirements for the established internal blast loading criteria. This ability was demonstrated for venting that satisfied the design requirement, as well as for the case where venting was reduced to the minimum attainable.

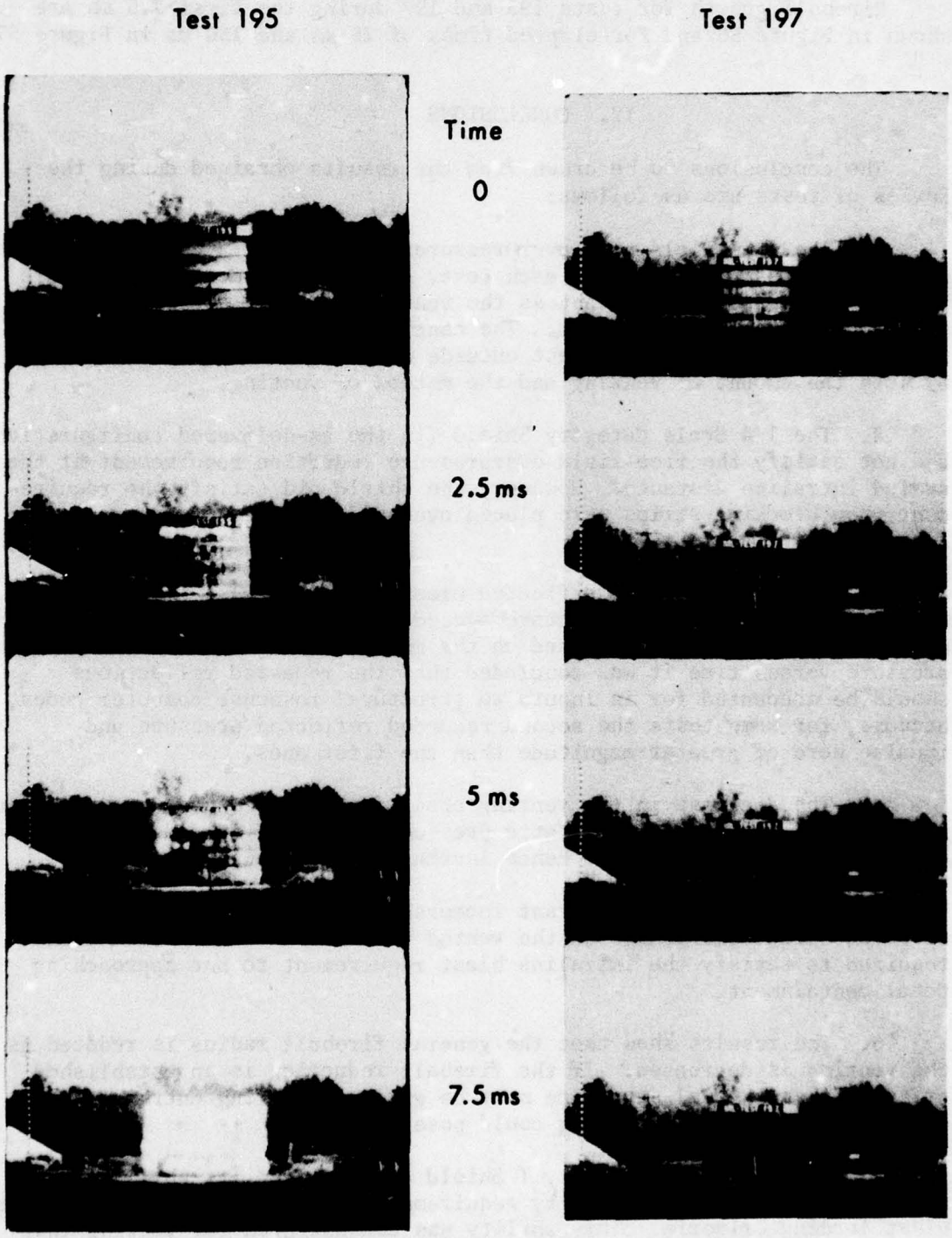


Figure 56. Fireball Formation for Tests 195 and 197 During the First 7.5 ms After Detonation

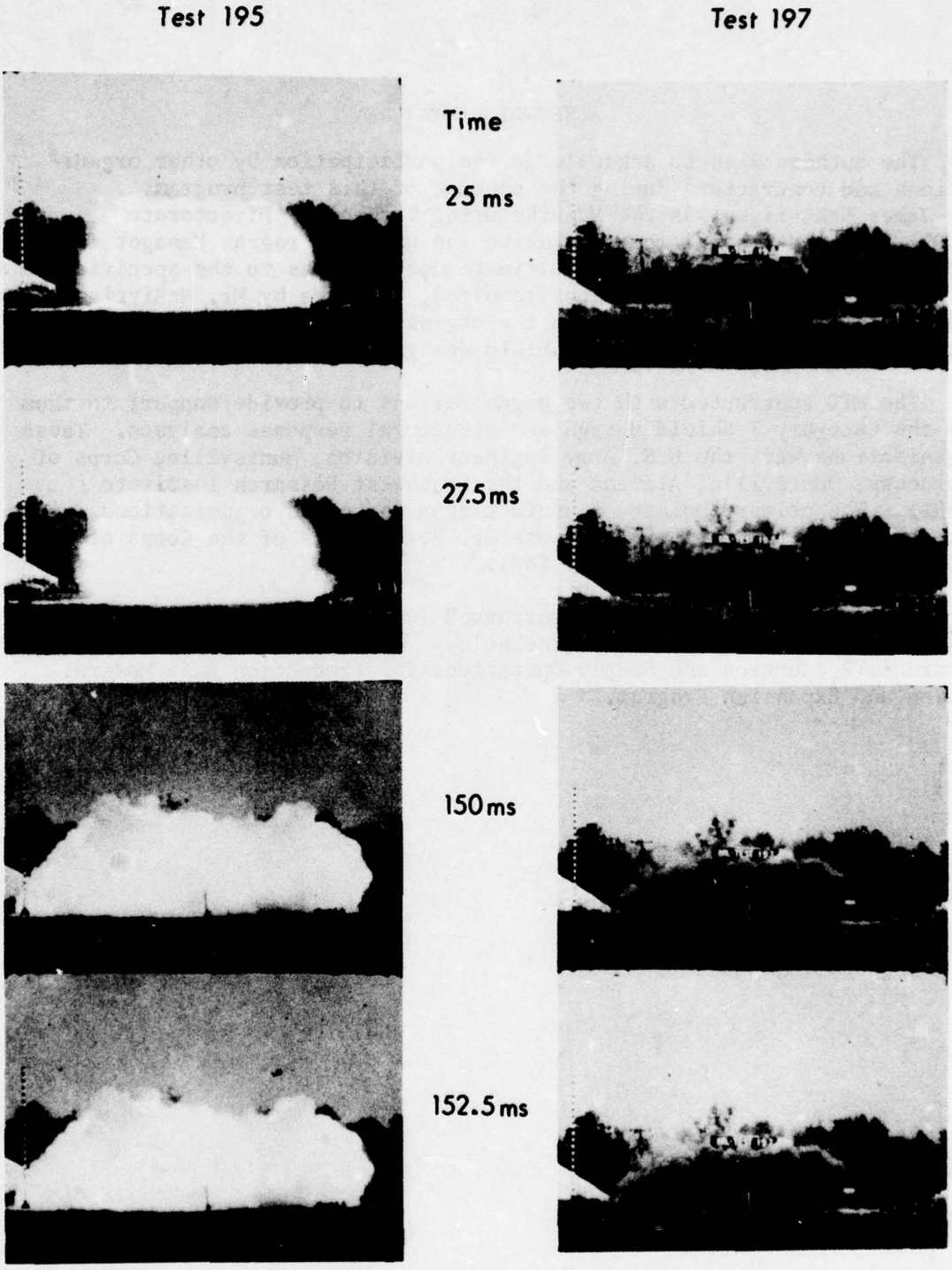


Figure 57. Fireball Shape for Tests 195 and 197 at 25 ms and 150 ms after Detonation

ACKNOWLEDGEMENT

The authors wish to acknowledge the participation by other organizations and contractors during the conduct of this test program. Mr. James McKivrigan was the Manufacturing Technology Directorate (MTD), Edgewood Arsenal representative and was the Program Manager for the Category I Shield program. The ultimate decision, as to the specific tests to be conducted and modifications required, was made by Mr. McKivrigan and/or other representatives from the organization after concultation with the BRL and the Category I Shield designers.

The MTD contracted with two organizations to provide support to them for the Category I Shield design and structural response analyses. These organizations were the U.S. Army Engineer Division, Huntsville, Corps of Engineers, Huntsville, Alabama and the Southwest Research Institute (SWRI). The primary points of contact from these two organizations during the conduct of the test program were Mr. E. Williams of the Corps of Engineers, and Mr. E. Esparza of SWRI.

The work reported here was performed for, and funded by PA, A 4932 MM&T Project #5751264, Advanced Technology for Suppressive Shielding of Hazardous Production and Supply Operations for Production Base Modernization and Expansion Program.

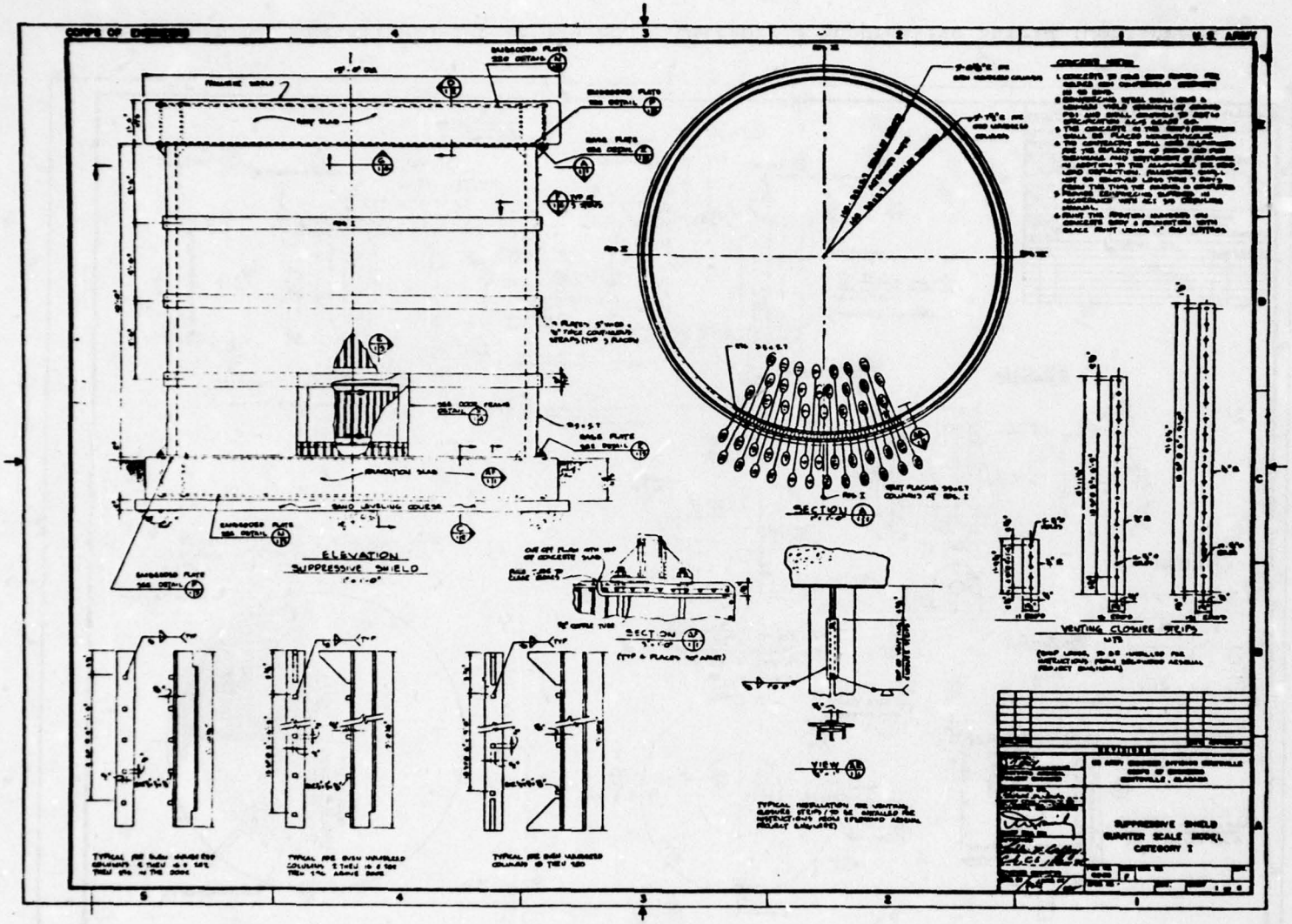


Figure A1. Detail Drawing of 1/4 Scale Category I Suppressive Shield

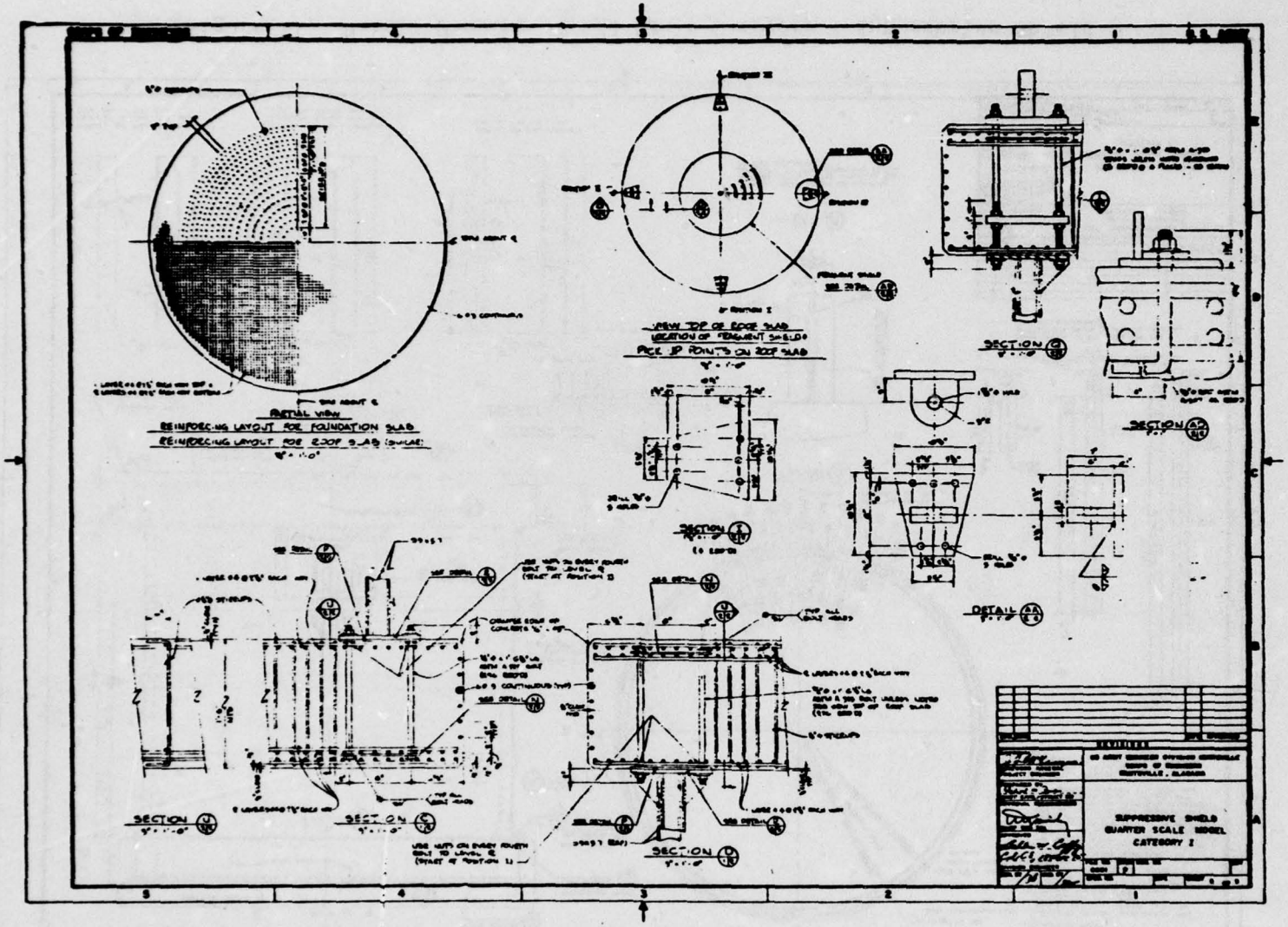


Figure A1. Detail Drawing of 1/4 Scale Category I Suppressive Shield (Continued)

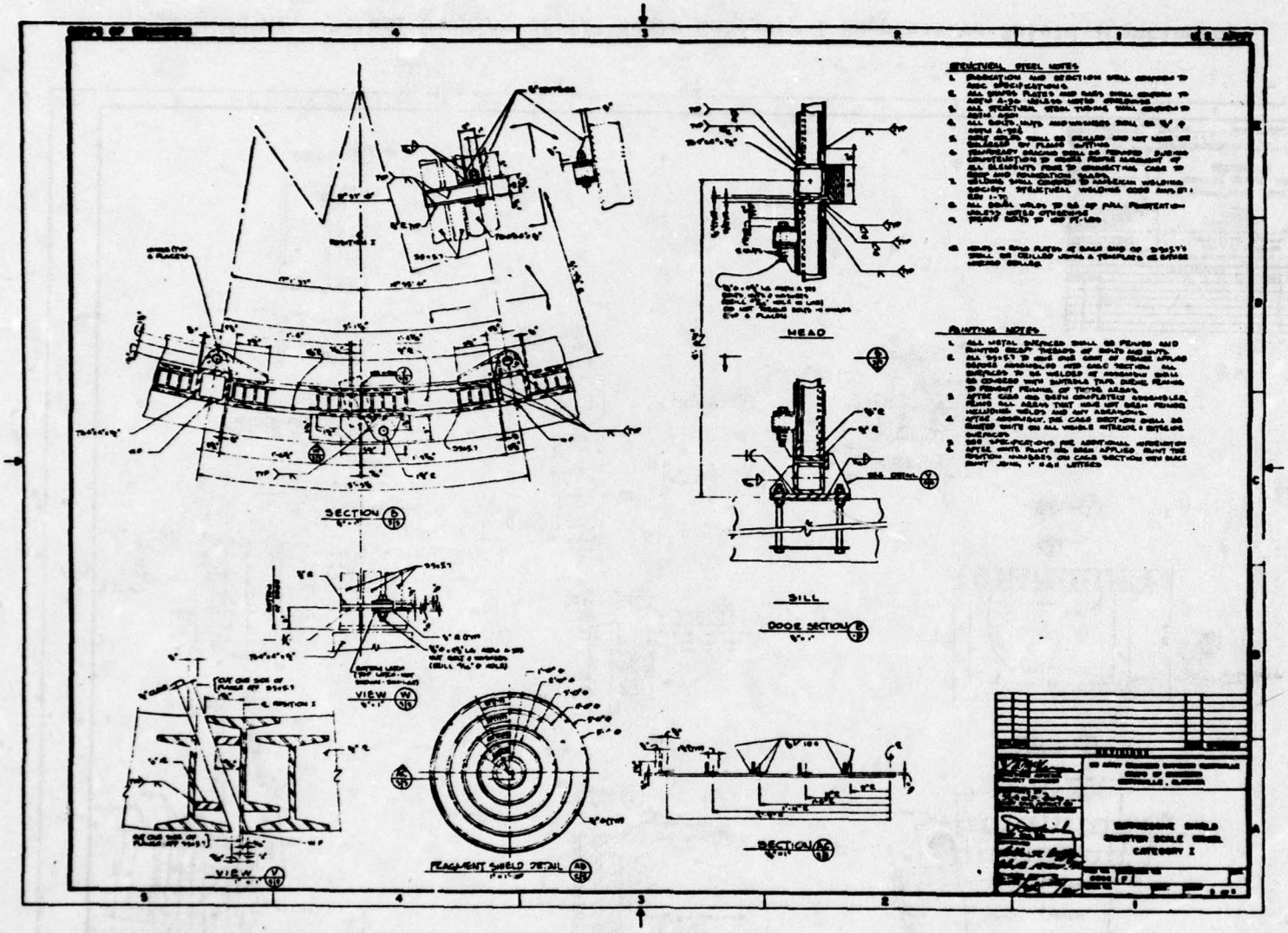


Figure A1. Detail Drawing of 1/4 Scale Category I Suppressive Shield (Continued)

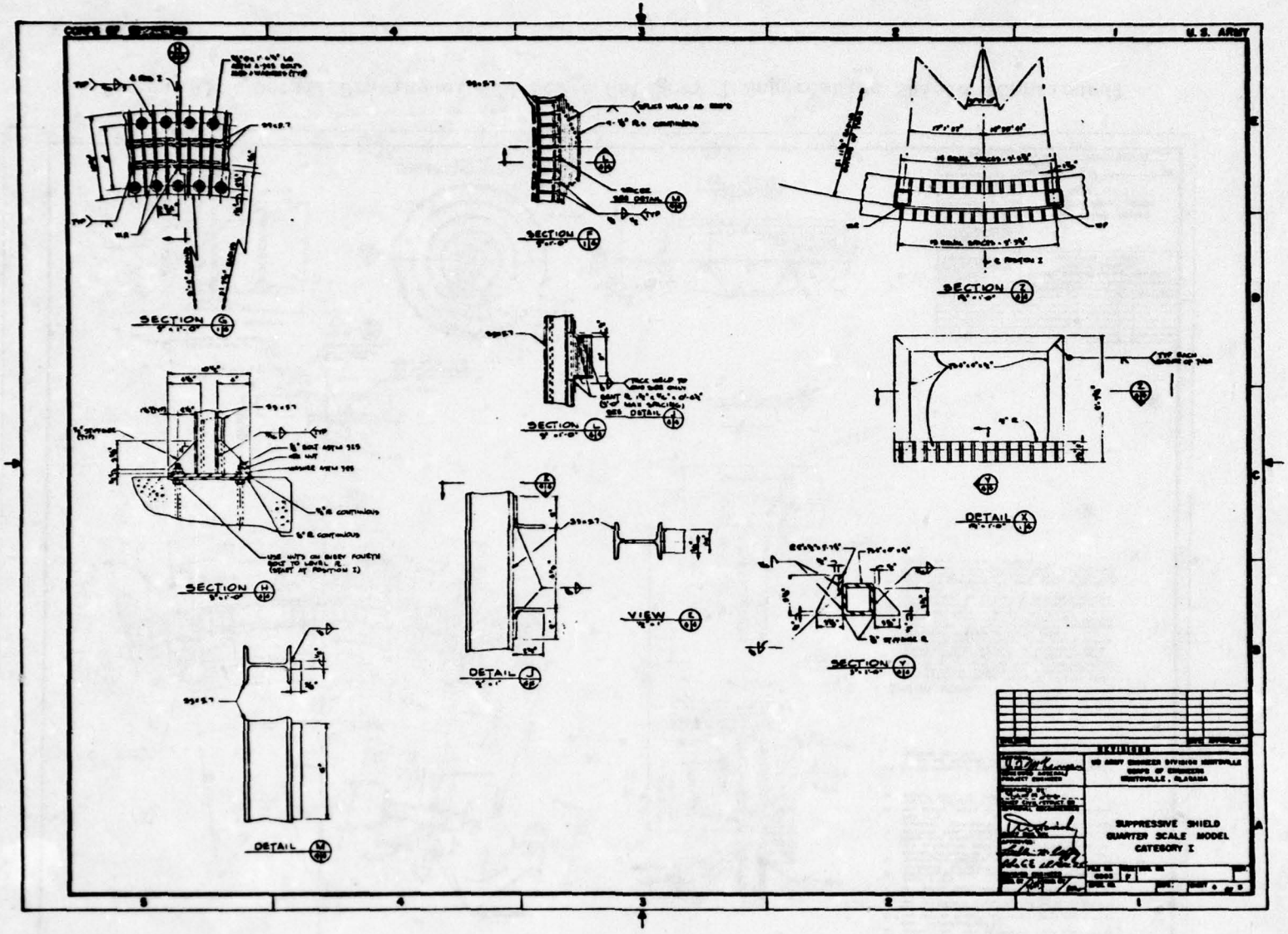


Figure A1. Detail Drawing of 1/4 Scale Category I Suppressive Shield (Continued)

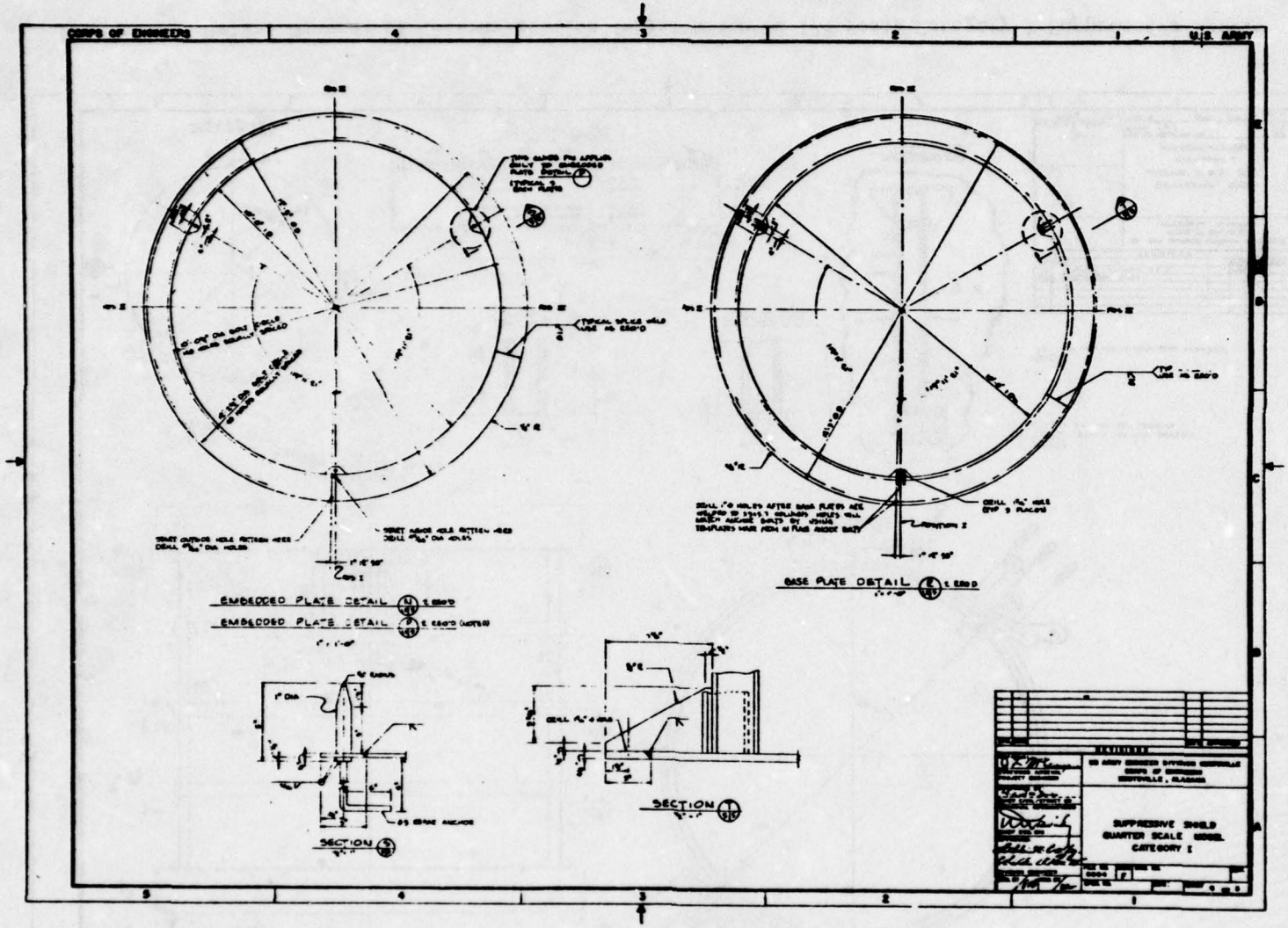


Figure A1. Detail Drawing of 1/4 Scale Category I Suppressive Shield (Continued)

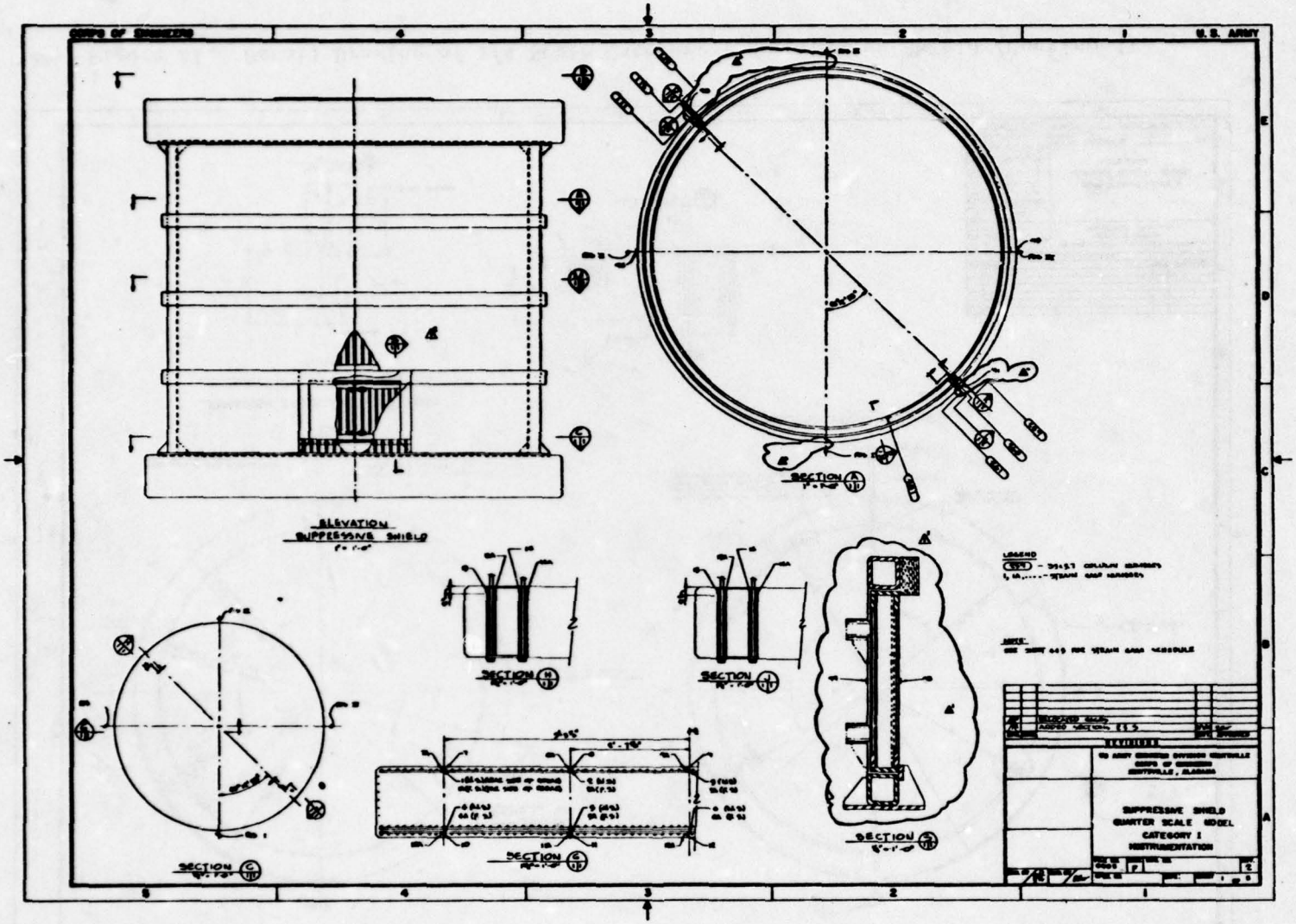


Figure A2. Detail Drawing of Instrumentation Installation on 1/4 Scale Category I Suppressive Shield.

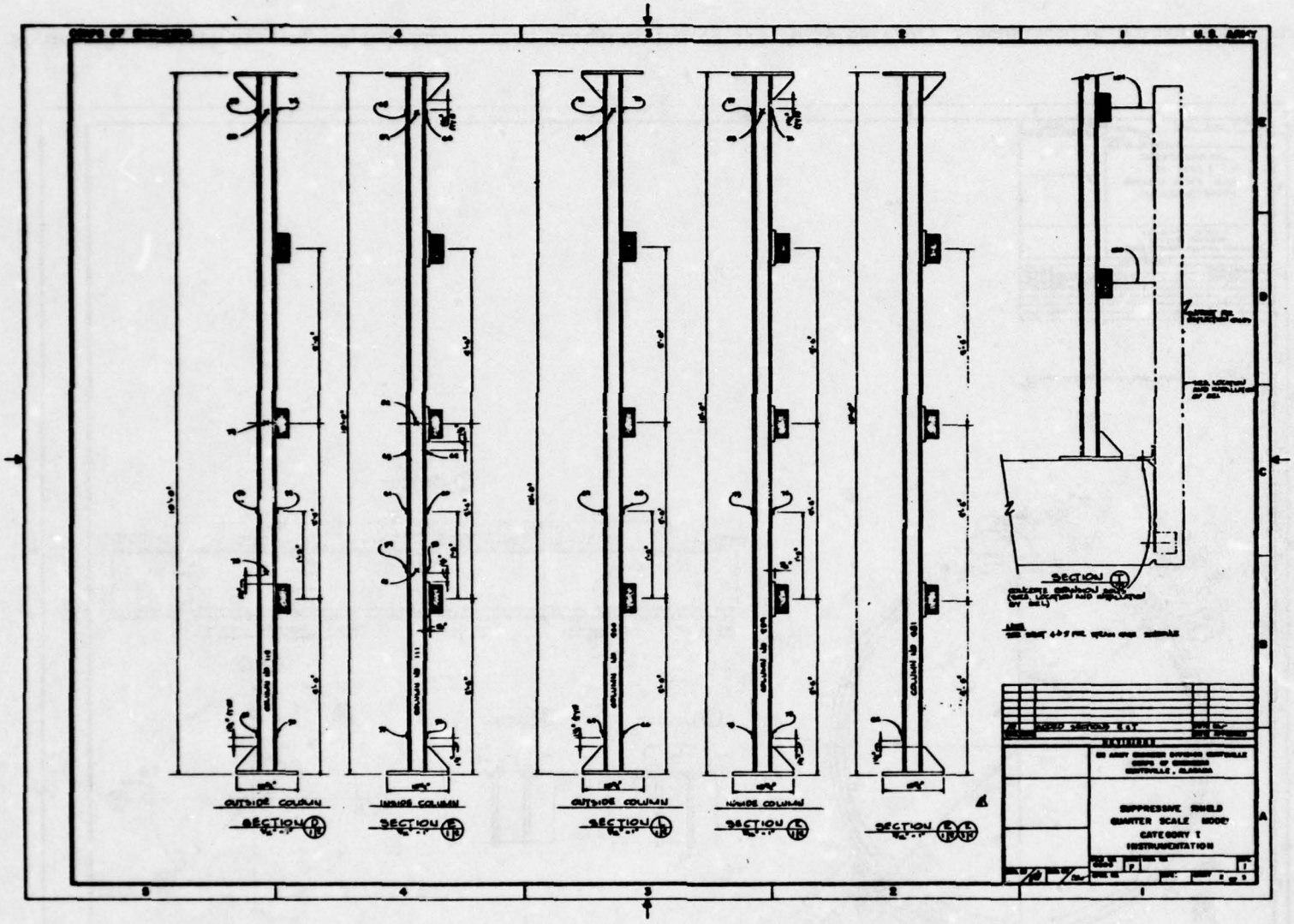


Figure A2. Detail Drawing of Instrumentation Installation on 1/4 Scale Category I Suppressive Shield (Continued)

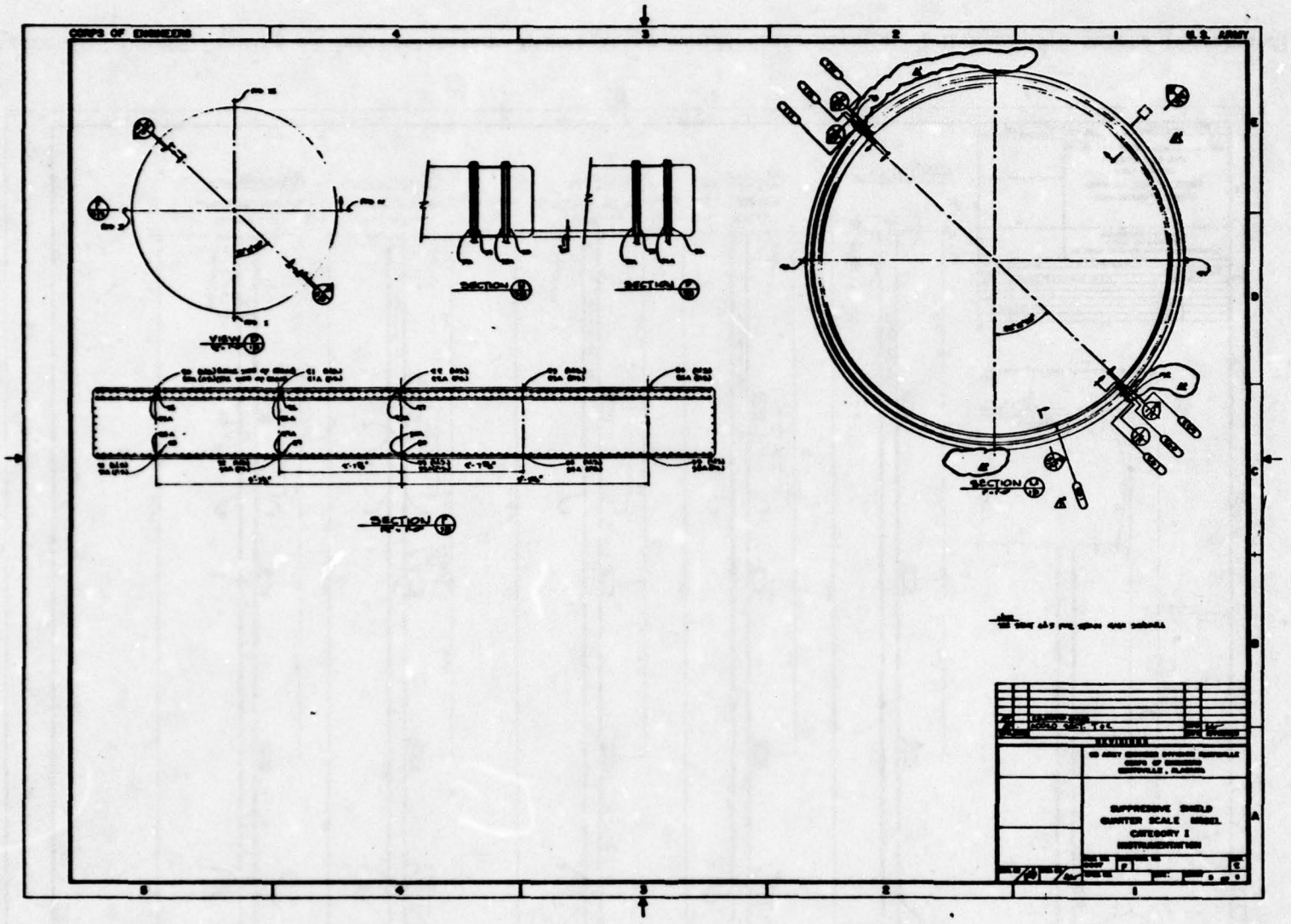


Figure A2. Detail Drawing of Instrumentation Installation on 1/4 Scale Category I Suppressive Shield (Continued)

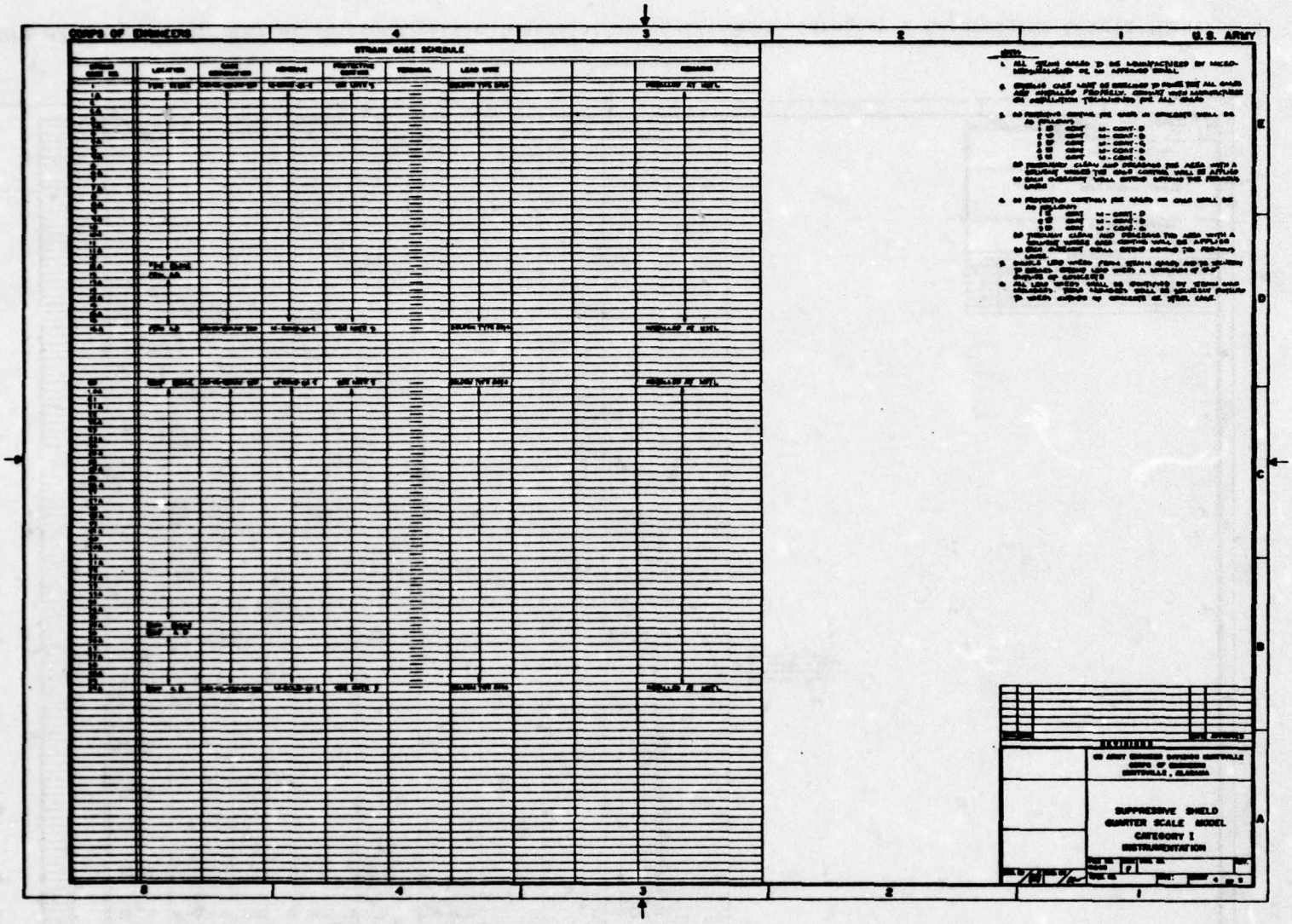


Figure A2. Detail Drawing of Instrumentation Installation on 1/4 Scale Category I Suppressive Shield (Continued)

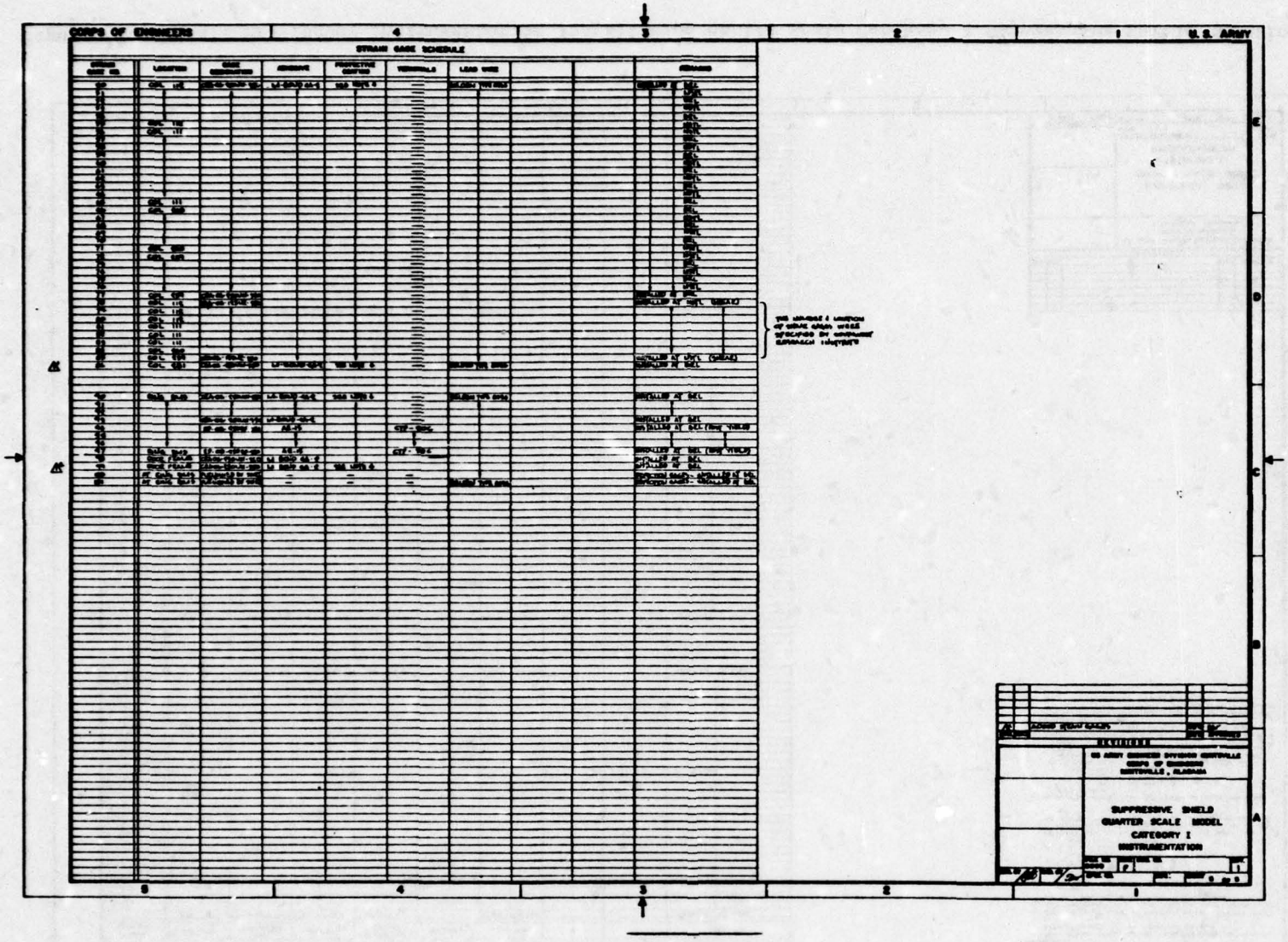


Figure A2. Detail Drawing of Instrumentation Installation on 1/4 Scale Category I Suppressive Shield (Continued)

S Y S T E M S A F E T Y

THE KEY TO EFFECTIVE ACCIDENT PREVENTION ON R&D PROJECTS

Rex B. Gordon
Aeronutronic Ford Corporation
Newport Beach, California

ACCIDENTS - WHO WANTS THEM?

In my professional safety career, extending over some 20 years, I have yet to find anyone in authority who wanted even a single accident associated with his program. Accidents are often expensive and painful, always wasteful and occasionally catastrophic. Nobody really wants them to happen, yet effective accident prevention techniques are often misused, downgraded or simply overlooked due to emphasis on performance, schedule and cost demands which Program Management must often contend.

If you are seeking a simple, magic formula that assures a completely accident free environment, in balance with performance, schedule and cost requirements - I'm sure I don't have it. However, from my varied safety experiences with numerous weapon Research & Development (R&D) projects, I feel confident that the effective application of System Safety Engineering principles, in a timely and comprehensive manner, is the best available approach to accident risk reduction. I have emphasized the terms "timely" and "comprehensive" because I often find these characteristics lacking in many non-effective System Safety activities. It is the primary purpose of this paper to share some of the insights I have gained during the past 20 years, which I trust will be of interest to those concerned with efforts to further reduce the accident risks normally associated with the development of new ordnance related weapons. These remarks are oriented to the program/project management level, where inadvertent restrictions to system safety program effectiveness can be most easily corrected.

THE SYSTEM SAFETY CONCEPT

Before proceeding into a discussion of what I feel are the key elements of an effective R&D ordnance system safety effort, I would like to establish a common frame of reference for my use of the term system safety.

In my view,, the "System Safety Concept" envisions a pre-planned, organized effort which has as its primary goal the prevention of accidents and conservation of resources associated with a given system, product or operation. Its basic elements include:

(a) The early identification of potential hazards, assessment of accident risks, and all safety related interface problems.

(b) The timely incorporation of safety-related design, facility, procedural, training and test requirements and/or criteria.

(c) The systematic evaluation of designs, facilities, and procedures for compliance with applicable safety criteria.

(d) Maintaining coordination with all applicable safety related interfacing functions, organizations and regulatory agencies.

(e) Continuing surveillance over safety related production, handling, shipping, testing, use and disposal through the entire life span of a product, to audit conformance with established safety criteria.

Although this encompassing concept of system safety has been well documented in MIL STD 882[1], various technical papers[2][3], documents[4] and text books[5] on this subject, there often arises considerable confusion, when system safety engineering is removed from its more natural environment (i.e., the large aerospace systems programs), and placed into a relatively unfamiliar habitat such as ordnance related Research and Development projects.

Unfamiliarity with the comprehensive nature of the system safety concept may lead project management to questions like:

- Why have a system safety effort when we can reference existing explosive, occupational, fire protection, transportation and range safety manuals?

- Why have system safety if there is no complex weapon system or field application involved in the R&D phase?

Let us see if with some further discussion, the answer to these and similar questions do not become self-evident.

WHAT IS THE SCOPE OF SYSTEM SAFETY?

For the purpose of this presentation, I will be considering that the term system safety encompasses all identified accident prevention activities specifically required by contractual provisions of any ordnance related weapon development or procurement program.

This concept of system safety places a critical spotlight on the specific clauses and statements of the contractual document which defines what the buyer (usually a DOD organization) and the seller (usually a defense/weapons contractor) have agreed upon relative to the safety effort to be implemented; along with technical performance, schedule and cost parameters. This spotlight is intentional, as I consider established contractual clauses and requirements to be a critical factor leading to effective system safety efforts.

WHY BOTHER WITH SYSTEM SAFETY?

There are many compelling reasons for both the customer and contractor to insist on an effective, coordinated system safety activity on every significant ordnance weapon development/procurement program. The consequences for not doing so can be most embarrassing, to say the least. For example:

- An uncoordinated, after-the-fact safety effort cannot be relied on to provide early identification of unique hazard in a manner which would permit a timely and cost effective engineering correction.

- The unchallenged use of inappropriate and over restricted "cookbook" safety criteria may cost the program unnecessary expense, delays and performance restrictions.

- o Unplanned safety constraints imposed by other activities, i.e., explosive hazard classification requirements, range safety approvals, quantity-distance limitation, transportation regulations, can cause frustrating delays at critical times in an R&D project.

- o Accidents during development phases can cause schedule delays, expensive redesign, and in some cases cancellation of the project. Sometimes these decisions are made under the influence of the emotional environment of a severe accident, and are not truly reasonable or objective.

- o Failure to properly identify and correct unacceptable accident risks in the design phase may result in embarrassing and expensive litigation against the Company due to product liability, claims and/or adverse publicity.

HOW COULD SYSTEM SAFETY EFFORTS BE OVERLOOKED?

It would seem that with so many compelling reasons for having an effective system safety program, that no responsible program manager or contracting officer would be willing to enter into an agreement without a careful evaluation of the adequacy of the Safety Engineering provisions of the contract. Unfortunately, such is not always the case. Often, early in the developmental phase of a new weapon, the risk of failure to meet performance objectives shadows all considerations to reduce accident potential. Because it represents a negative aspect, the accident risk potential is quite often overlooked in the glare of management optimism. Often, even when not ignored completely, the appraisal of accident risks may be at such a shallow level that no significant safety input for effective decision making are developed.

ACCIDENT RISK PRINCIPLES

Program Managers, who have the responsibility for the allocation of available resources on a given project, must be cognizant of the basic principles of accident risk evaluation, if he or she is to properly determine the type and extent of any formalized system safety effort that is needed.

Too often, we in the safety profession do not communicate our trade very effectively to program managers. Part of this difficulty is the confusing use of some key terms that are commonly used in our field. I feel some simple definitions and principles advanced by G. A. Peters[2] and C. O. Miller[3] are worthy of our consideration when attempting to explain to management and each other, what we are attempting to accomplish.

In essence, we must be clear in our use of at least four basic terms - accident, hazard, risk and unsafe. These terms, as you can see, are the basic building blocks of the system safety approach to our common goal, the conservation of available resources to accomplish a given objective.

An accident, according to Miller[3] is "... an unplanned but controllable combination of events which causes injury or harm to someone or something -- It is not just a matter of luck or, perhaps more accurately a matter of misfortune." In virtually every case, an accident is the combination of many causitive factors, conditions and actions - most of which should have been predictable and controlled.

We should use the term hazard when referring to these causitive factors of accidents. Accidents are relatively rare events in comparison to the many hazards which are present in most explosive related activities. Miller[3] puts it this way - "A hazard is simply an accident element that has not yet happened. Except for the damage incurred, the only real difference between an accident and a hazard is that the latter is usually a single cause-effect relationship envisioned before-the-accident fact. It can be treated individually and often is.

The difficulty arises when hazards are confused with total accident causation. They are degraded because there is not operational experience or investigative proof that the particular hazard in and of itself was significant."

This situation, i.e., failure to appreciate the importance of a new, unfamiliar hazard, should be of high concern during the R&D phase of new ordnance items or systems. The use of accident statistics is of little value, and may lead to false assumptions. It must be remembered that the number of accidents of interest that have occurred is very small compared to the spectrum of hazards that can produce them. Hazards, therefore need the emphasis in an effective system safety program, not accidents per se.

The next term we need to define is "Risk." Although this term is found in many different contexts - such as insurance management, financial planning, gambling, etc., we in system safety tend to limit its use as suggested by Peters[2] to "... the qualitative degree of possible harm likely to occur." This includes both the statistical probability (estimate of likelihood of occurrence), together with an estimate of severity of injury or loss. In other words, risk is the foreseeable or predictable amount of harm likely to result from a given combination of hazards.

The fourth and final basic term we need to consider is "unsafe." When a decision has been made that there is a special peril, unusual harm, or unexpected risk beyond that considered tolerable or permissible under the circumstances at hand, then it should be called unsafe, and immediate corrective action taken to prevent injury or loss. A value judgement must be made, since what may be acceptable in, say a combat situation, may be totally unacceptable in a commercial plant. This subjective judgement, as to when a given risk is unsafe (i.e., unacceptable in the specific situation being considered) should not normally be considered as being totally the system safety engineers' responsibility. This determination must be made at a high management level, where all pertinent factors can be seen in perspective. The system safety engineers' task should be to properly identify the hazards and evaluate the risks in an objective manner. This information is then passed on to appropriate management for the judgement decision as to whether or not the risks presented are acceptable or should be identified as being "unsafe."

The specific techniques and methods used by system safety engineers for the identification and evaluation of hazards and risks have been fully documented by myself[4][5] and others[2][3], and will not be expanded in this discussion. Suffice to state that effective hazard identification and risk evaluation requires a detailed knowledge of all contemplated uses and design features, and therefore is not a matter to be dealt with by cookbook or casual attention by program managers when allocating resources for safety efforts to be performed. For if program managers short change the system safety hazard identification and risk analysis effort to be performed, how will they be able to make good judgement decisions on what risks are acceptable or not? This type of judgement could well be one of the most critical decisions a program manager may have to make during a project; certainly one that has the highest potential for involving him or her in legal or higher management attention should severe accidental injuries result.

CONTRACTING FOR SYSTEM SAFETY

Based on these previous comments, with what I consider to be reasonable justification for the placement of primary attention on hazard identification and risk evaluation, rather than a statistical study of past accidents; one would perhaps expect to find appropriate contractual coverage for system safety engineering efforts included in all ordnance/explosive related work statements.

Although I have been observing an encouraging trend in this direction, I have not always seen what I would consider to be truly effective work statement requirements for system safety, particularly in the smaller ordnance/explosive related R&D proposal. I feel this is often the result of two factors: (1) the lack of enough experienced system safety engineers in procuring functions to write effective system safety work statements tailored to the specific problems associated with a given project; and (2) the lack of understanding by program managers (on both sides of the negotiating table), as to what constitutes a minimum cost, but effective contractor effort to assure the early identification of hazards and evaluation of risks on R&D programs.

As a minimum, most ordnance/explosive related RFPs and contracts contain "Armed Services Procurement Regulations (ASPR) 7-104.79 - Safety Precautions for Ammunition and Explosives." This clause requires the contractor to comply with DOD Contractor Safety Manual for Ammunition, Explosive and Related Dangerous Material (DOD Manual 4145.26M). It also stipulates that the contractor is to notify the Contracting Officer should any serious accident occur involving ammunition or explosives in the performance of the contract.

It further stipulates that non-compliance with the DOD Safety Manual on the part of the contractor is grounds for stop-work direction from the Contracting Officer. The provisions of ASPR 7-104.79 are to flow down to applicable subcontractors and suppliers.

While this clause has been used for a number of years, and is of positive value, particularly in production and manufacturing type programs, it has some shortcomings when applied as the basic safety provision in an R&D project. These include:

(a) No provisions for a timely pre-accident hazard identification and risk evaluation study.

(b) DOD 4145.26M is basically oriented toward large scale ordnance production efforts. For many smaller R&D projects, full compliance with the manual is neither cost or safety effective.

(c) It tends to place reporting emphasis on major accidents, rather than on identified hazards and risks.

(d) Being located in the ASPR section of the contract, it often does not receive the full attention of the program manager as being a safety effort that should be initiated, funded and monitored by the program manager.

(e) It is limited in scope to only defined explosive and ammunition items. There are often other hazardous components on a given system which are also dangerous, and deserve system safety attention.

To overcome these and other possible deficiencies relative to effective system safety efforts on R&D projects, Requests for Proposals (RFPs), and contracts, often contain other safety related requirements besides the ASPR 7-104.79. These tend to be copies or extracts from basic "boiler-plate" safety work statements which have been adopted by a specific procuring activity or command. Since my job requires me to respond to these safety work statement requirements, I have made it a practice to keep file copies of all such safety requirements to evaluate in a somewhat more subjective viewpoint, once the panic rush of getting the proposal prepared has passed.

From this review I have noticed that few work statement provisions are written so as to gain the attention and support from the program managers (on both sides) to actively support the implementation of an effective system safety effort as part of the mainstream of the contracted effort.

Most safety requirements written into R&D contracts tend to be rather passive and "cookbook" oriented. That is, they may stipulate that the contractor shall comply with a various assortment of Army, Navy or Air Force safety manuals (few of which were written with R&D contractors in mind), and submit a safety plan per MIL STD-882. In some cases (usually when new explosive items are involved), a requirement to submit a "hazard classification" report per a Contractor Data Requirement List (CDRL) format at the completion of the design effort, is included in the contract.

I believe it is becoming evident that what I am discussing here is that there appears to be a considerable disparity between what the system safety engineering practitioners are reporting as being effective accident prevention principles in new R&D projects, and what is commonly being incorporated in R&D contractual requirements.

I therefore would like to present for your consideration a few comments and recommendations that I think might prove effective in reducing the gap between good theory and actual day to day practice in this area of accident prevention:

(a) It should be recognized by those responsible for the safety aspects of the procurement of R&D ordnance/explosive contracted efforts, that there does not currently exist a suitable criteria document oriented specifically toward the unique safety problems associated with R&D of new ordnance/explosive related systems. MIL-STD-882 is too general and "large system" procurement oriented. ASPR 7-104.79 and DOD Manual 4145.26M do not adequately address the problems unique to small R&D efforts or hazard identification and evaluation type activities. Current CDRL Data Item Descriptions (DIDs) do not address the subject of small R&D System Safety data inputs adequately. A System Safety Plan designed to meet all of MIL-STD-882 requirements would be probably too expensive to be cost effective on small (under $10 million) R&D efforts, CDRL inputs for "Hazard Classification," "Accident/Incident Reports," "Safety Statements," etc., are not normally effectively tied with timely and comprehensive system safety engineering task requirements.

(b) It would appear timely for the DOD to formulate and implement use of a new system safety oriented ASPR clause to supplement ASPR 7-104.79 for R&D type projects.

(c) It is suggested that the DOD Explosive Safety Board prepare some model examples of appropriate System Safety oriented work statement inputs to be used by the various DOD procurement activities when preparing R&D ordnance/explosive related RFP and contracts.

(d) It is also suggested that provisions be included into the ASPR clause and/or work statement models inputs to deal with the professional qualifications and organizational structure and functional responsibilities of the Contractors safety engineers who will be conducting the hazard identification and risk analysis. Bidders should be required to demonstrate suitable safety engineering organization and capability as a provision of contract award.

(e) My final point is that some suitable provision should be incorporated in the above noted requirements that will require that joint customer/contractor management review all significant identified risks, accomplished in a formal manner so that a well documented record is maintained of what risks have been judged "unsafe" (i.e., unacceptable), and the status of corrective actions assigned.

Consideration should be given to assigning this risk acceptance responsibility to a separate board who is not under the direct control of either the customer or contractor program managers, since the overriding pressures of meeting assigned schedules and cost goals may make it difficult for effective objective judgement decisions relative of the intangibles or risk acceptance.

In summary, what I have attempted to convey in this paper is that because of the unique, or not previously encountered hazards which are often confronted in ordnance/explosive related R&D programs by contractors, some special considerations in the contracting for system safety efforts appear appropriate. These considerations include the emphasis on hazard identification and risk evaluation rather than cookbook safety manuals and accident reporting. Assurance that qualified safety specialists will perform the hazard analysis effort should be a formal condition of contract award. The determination of "acceptable" versus "unsafe" risks should be accomplished in a formal and objective manner.

There are few if any decisions associated with a program that may have the long term legal and emotional consequences than those of risk acceptance or rejection. Who of us would want to make such critical decisions on skimpy or hastily developed data and information? The best way for program managers to avoid being caught in such an undesirable position is to demand that effective system safety studies and activities be performed throughout the entire development cycle of each weapons system project, including, and most importantly, during tne R&D phases of weapon/explosive related programs.

REFERENCES

1. "Requirements for System Safety Program for System and Associated Subsystem and Equipment," (MIL-STD-882).

2. Peter, G. A., "Systematic Safety." National Safety News, September 1975. National Safety Council, 425 N. Michigan Ave., Chicago, IL. 60611.

3. Miller, C. O., "Aviation Accident Prevention." Hazard Prevention, Jan/Feb, 1976. System Safety Society, P.O. Box A, Newport Beach, CA 92663.

4. Gordon, R. B., "System Safety Analytical Techniques." Safety Engineering Bulletin No. 3, Electronic Industries Association, 2001 Eye St., N.W., Washington, D. C. 20006.

5. Gordon, R. B., "System Safety." Chapter 16, Loss Control Management, Bird and Loftus, Institute Press. P.O. Box 345, Logan Ville, Georgia 30249.

HARPOON SYSTEM SAFETY PROGRAM

by

William J. Smith

Effectiveness Engineering Department

McDonnell Douglas Astronautics Company-East

McDonnell Douglas Corporation

St. Louis, Missouri 63166

ABSTRACT — This paper describes the MDAC-EAST Hazard Identification and Control System instituted for the U. S. Navy Harpoon Program. Basic elements of analyses, reporting, and hazard dispositioning are reviewed. Emphasis is given to the organization and activities of the System Safety Working Group (SSWG) in the hazard control process, and several hazard reports are included to serve as examples of the system's effectiveness.

INTRODUCTION

Harpoon Weapon System — The Harpoon Weapon System was designed and developed by the McDonnell Douglas Astronautics Company-East for the U.S. Naval Air Systems Command, Washington, D.C. The Specific Operational Requirement (SOR) for the Harpoon missile was prepared in July 1969. Initiating design in July 1971, the Harpoon Weapon System (HWS) is now in Operational Evaluation (OPEVAL) and entering production.

The Harpoon is an all-weather, anti-ship weapon system designed for use by aircraft, ships and submarines. The missile employs a low-level cruise trajectory, and active radar guidance with counter-counter-measures to assure maximum weapon effectiveness from beyond-the-horizon ranges. Typical Harpoon trajectories are depicted in Figure 1.

The missile external shape is designed for compatibility with several different launchers. The missile features a common body to which the appropriate aerodynamic surfaces and booster section are added, as required. The missile body consists of a guidance section; GFE warhead section; sustainer section; and control section. All sections are interchangeable with like sections. An exercise section is also provided as an interchangeable substitute for the warhead section. The missile inboard profile is shown in Figure 2.

The missile Command and Launch System (CLS) interfaces with existing sensors, and various fire control equipment of the designated launch platforms to make maximum use of existing hardware. While differing to some degree from platform to platform, the CLS equipment typically consists of control and displays, data processor computer, data convertors, and power supply.

The Harpoon Weapon System's designated mission is target destruction and therefore is a potentially hazardous item. Its potential for equipment destruction and personnel hazard is dramatically illustrated in Figure 3, which shows the remains of a DD target ship following a direct hit by the Harpoon missile.

System Safety Program — To control the inherent potential hazard, a continuous concentrated effort by MDAC-EAST and the involved U.S. Navy agencies was maintained to assure inherent safeguards were incorporated in the weapon system and its operational procedures. A key element of this effort was the implementation of a System Safety Program that provided for continuous assessment of the adequacy of the incorporated safeguards and the identification of areas requiring improvement.

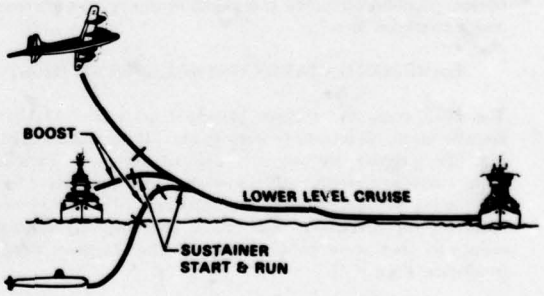
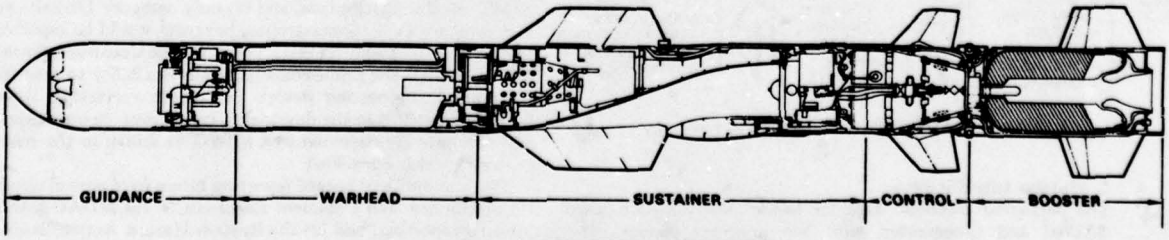


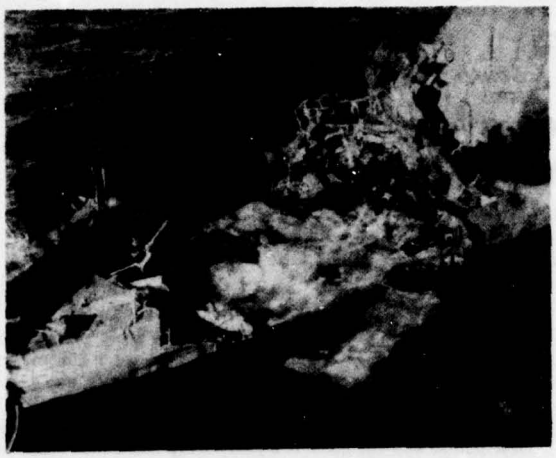
FIGURE 1 –



	AIR LAUNCH	SHIP LAUNCH
MISSILE LENGTH	151.2 IN.	182.2 IN.
MISSILE DIAMETER	13.5 IN.	13.5 IN.
MISSILE WINGSPAN	36 IN.	36 IN.
MISSILE WEIGHT	1168 LB	1468 LB

FIGURE 2 – MISSILE SUBSYSTEM

PRECEDING PAGE BLANK-NOT FILMED



PM-21 WARHEAD DAMAGE – EX-USS GUNASON

FIGURE 3 – WARHEAD MISSILE SINKS TARGET SHIP

The System Safety Program was initiated at inception of the Harpoon Program, and has been maintained throughout the design, development and on-going pilot production phases. The safety program included the elements of MIL-STD-882 and was conducted in accordance with customer approved System Safety Program Plans. As with all System Safety programs, the primary objective was to identify and eliminate/or control hazards to personnel and equipment. It is this activity of the Safety Program that is the subject to this paper, and is hereafter referred to as the Hazard Control System (HCS). The term "hazard" as used herein is defined to be any real or potential condition which can result in injury to personnel or major material loss.

HARPOON HAZARD CONTROL SYSTEM (HCS)

The HCS consists of three principal activities: (1) hazard identification, (2) hazard reporting, and (3) hazard dispositioning. The activities by necessity are not exclusive. Timeliness requirements can frequently dictate a nearly concurrent identification-reporting-dispositioning process. For convenience, however, the discussion will follow the normal sequence of events as they were implemented for the Harpoon Program (reference Figure 4).

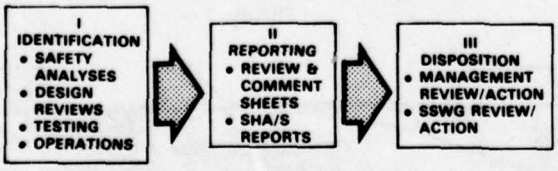


FIGURE 4 – HARPOON HAZARD CONTROL SYSTEM

I. Hazard Identification

The particular methods used for hazard identification were tailored and time-phased with the program phases. The efficacy of the technique depended largely upon what stage of development the weapon was in at the time of application. The techniques applied and proved effective for the various Harpoon Program phases are summarized as follows:

Program Phase	Hazard Identification Sources
Design Phase	• Design Reviews • Safety Analysis(PHA,OHA,FHA & FTA) • Verification Testing
Development Phase	• Design Reviews • Safety Analyses (OHA, FHA & FTA) • Preliminary Procedures/Manual Reviews • ECP Reviews • Flight and Qualification Testing
Pilot Production Phase	• Procedure/Manual Reviews • ECP Reviews • Operational Exercises

Fundamental to the Harpoon hazard identification process were the safety analyses, typically consisting of Preliminary Hazard Analyses (PHA's), Operating Hazard Analyses (OHA's), Fault Hazard Analyses (FHA's) and Fault Tree Analyses (FTA's), see reference (a) for analyses descriptions. These analyses were strongly concentrated in the Design and Development Phases of the Program. It is during these phases that the system's inherent safety was developed through the identification and elimination of hazards from the system design. At this time in the program the most positive corrective actions could be implemented with minimum potential cost and schedule impact. For this reason, the HCS was afforded its major funding and staffing during this period.

Other sources of hazard identification included review of testing results, procedural reviews, and operational experience gained through the assembly, test, checkout, and flight testing of the weapon system. These sources proved effective in identifying those hazards more related to the operational and testing aspects of the system. It should be noted that the sources for hazard identification were not limited to the contractors activities, but also included the contributions of the Navy agencies represented on the Harpoon System Safety Working Group (SSWG). The SSWG and its activities will be discussed later under Hazard Dispositioning.

II Hazard Reporting

It was recognized early in the program that an expedient method of reporting must be established to effect timely management and customer notification of identified hazards. Publication of all the safety analyses was quickly judged inefficient due to the sheer volume of paper involved and that the reporting of all hazards regardless of criticality category would tend to mask those requiring prompt attention and action. Consequently, a procedure was devised which provided two significant features to promote efficiency in critical hazard reporting; (1) there would be two levels of reporting; one level being restricted to MDAC-EAST internal distribution and the second level being expanded to include the customer and SSWG on the distribution, and (2) only category III-Critical, and category IV – Castastrophic hazards[1] would be reported to the customer and SSWG. These unique features allowed MDAC-EAST, the prime contractor, the flexibility to exercise its normal engineering design process in correcting those hazards identified in the day-to-day inter-group co-ordination, and still provide customer and SSWG visibility to the more critical hazards identified.

Two standardized hazard reporting forms were agreed upon: (1) the Review and Comment Sheet (RCS) for MDAC-EAST internal reporting, and (2) the System Hazard Action/Status (SHA/S) report for customer and SSWG reporting. Sample formats of each are shown in Figure 5. See appendix for completed examples.

[1] Category III – Critical (will cause personnel injury or major system damage, or will require immediate corrective action for personnel or system survival) Category IV – Catastrophic (will cause death or severe injury to personnel, or system loss)

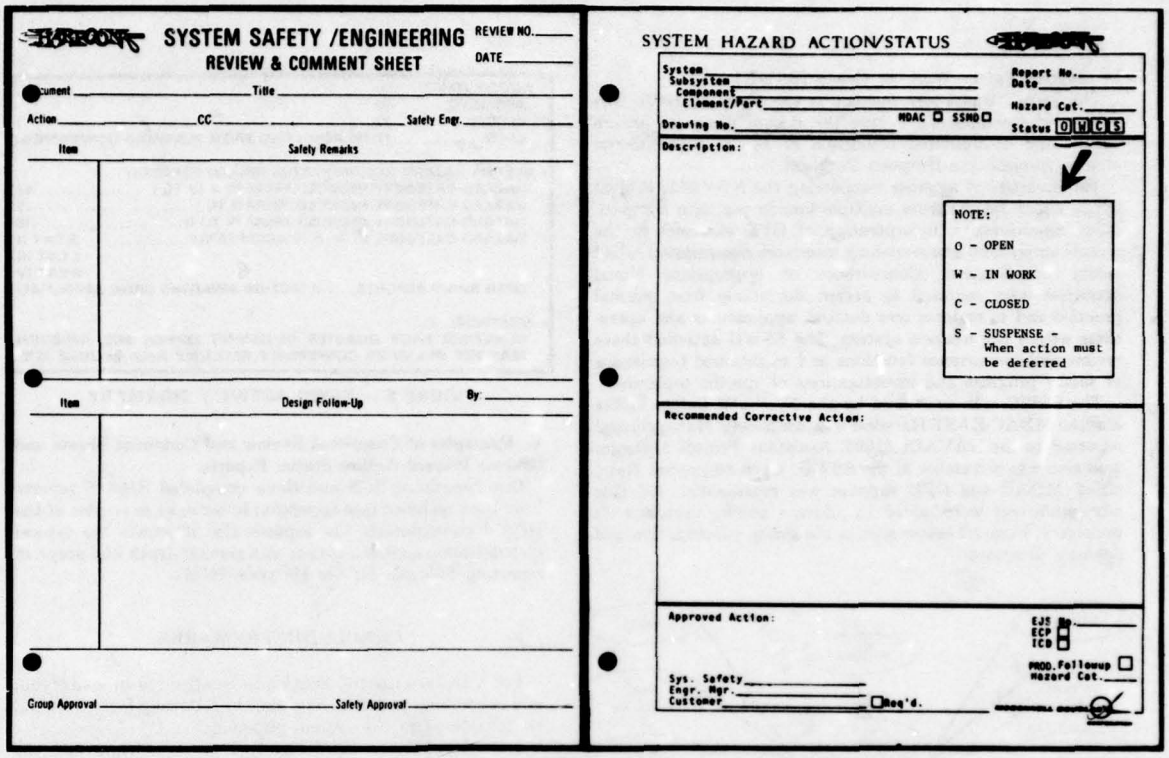


FIGURE 5 –

To ensure reporting was maintained to the mutual satisfaction of both MDAC-EAST and the customer, copies of all RCS's and SHA/S's were kept on file at MDAC-EAST for customer review upon request. The criteria followed prior to design release in the preparation of the RCS's and SHA/S were as follows; as hazards were identified, a RCS with recommended corrective action was prepared and coordinated with the appropriate design or test group. This was accomplished by head-to-head meetings in which the conditions contributing to the hazard were reviewed and corrective action recommendations discussed. For hazards which could not be resolved in this manner, SHA/S reports were prepared and submitted to the customer and SSWG. Following design release, SHA/S reports were prepared for all hazards identified.

The SHA/S reports were normally prepared by MDAC-EAST (or subcontractors), although their intended use was to be the standard reporting form for any agency wishing to report a hazard for HCS processing.

III Hazard Dispositioning

Co-ordination was considered the main issue in obtaining proper dispositioning of unresolved hazards. As previously noted, unresolved hazards and hazards identified after design release required the preparation of an SHA/S report. The SHA/S report corrective action required review and approval by: the responsible action group, MDAC-EAST safety personnel, MDAC-EAST Harpoon Program Management, and one or more U.S. Naval agencies depending upon the nature of hazard.

The requirement for timely review and coordination among the several U.S. Navy agencies posed a potential problem. MDAC-EAST internal review/co-ordination could be expedited and controlled. The Navy review, however, was beyond MDAC-EAST control. To resolve the problem of timely Navy co-ordination, the Navy review responsibility for SHA/S reports was delegated to the Harpoon System Safety Working Group (SSWG). The approval cycles for the RCS and SHA/S report are depicted in Figure 6.

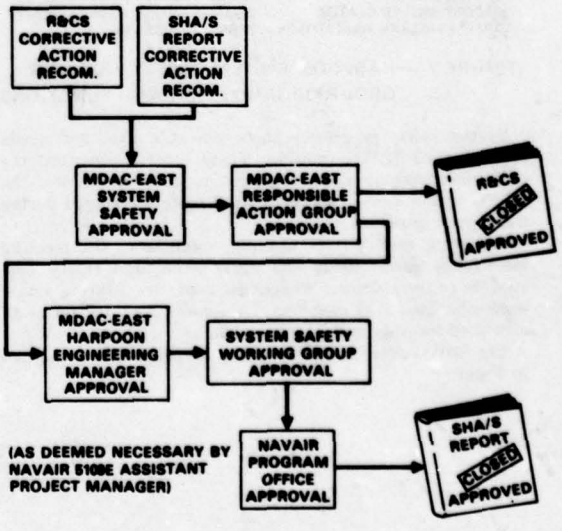


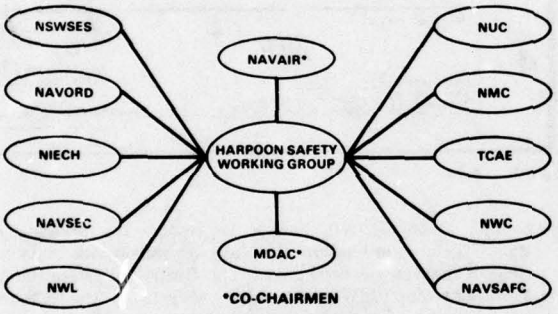
FIGURE 6 – RCS & SHA/S APPROVAL CYCLE

IV System Safety Working Group [SSWG]

The SSWG was a key element in the Harpoon HCS. The SSWG was established during the design phase to ensure timely and co-ordinated resolution of safety requirements arising through the Harpoon Program.

The diversity of agencies supporting the NAVAIR Project Office which results from multiple launch platform compatibility requirements, incorporation of GFE elements in the missile subsystem and numerous interfaces necessitated broad safety coordination. Concurrence of appropriate Naval activities were required to accept deviations from normal practice and to endorse new devices, applications and operations within the weapon system. The SSWG satisfied these review and concurrence functions and maintained cognizance of safety progress and investigations of specific problems.

The SSWG was co-chaired by the NAVAIR Safety Office and the MDAC-EAST Harpoon System Safety Manager, and reported to the NAVAIR 5109E Assistant Project Manager who also was a member of the SSWG. Each concerned Navy office, MDAC and GFE supplier was represented. Ad Hoc representatives were added to address unique problems as necessary. Figure 7 below depicts the group participation and primary functions.



FUNCTIONS:

PROGRAM REVIEW	REVIEW SAFETY PLANS
DESIGN REVIEW	REVIEW AND APPROVE SHA/S
REPORT SAFETY STATUS	ASSIGN ACTION RESPONSIBILITY
SAFETY HAZARD RESOLUTION	SUPPORT WSESRB

FIGURE 7 – HARPOON SYSTEM SAFETY WORKING GROUP ORGANIZATION AND FUNCTIONS

System safety progress reports were submitted two weeks prior to each SSWG meeting. These reports described the milestones accomplished, the system safety activities, the SSWG action items, and the SHA/S reports prepared during the reporting period.

Following each SSWG meeting, minutes of the meeting identifying action items and agreements, and safety constraints to the Harpoon Weapon System necessitating action were submitted to all members. The minutes denoted review of identified hazards and actions taken.

The SSWG activity summary for the program is presented in Figure 8.

- ACTION ITEMS:
  - ASSIGNED.....89
  - CLOSED.....72
  - OPEN.....17 (16 RESULTING FROM PLANNING CONFERENCE)
- SYSTEM HAZARD ACTION/STATUS (SHA/S) REPORTS:
  - HAZARD CATEGORY REDUCED FROM III & IV TO I.....53
  - HAZARD CATEGORY REDUCED FROM II TO I.....22
  - HAZARD CATEGORY REDUCED FROM IV TO II.....10
  - HAZARD CATEGORY II, III, & IV ACCEPTABLE.....3 CAT II, 1 CAT III, 0 CAT IV
  - OPEN SHA/S REPORTS.....4 (ACTION AWAITING SSWG APPROVAL)
- MEETINGS:
  - CONVENED EACH QUARTER BEGINNING MARCH 1972 THROUGH MAY 1975. PLANNING CONFERENCE RECENTLY HELD 24 JUNE 1976.

FIGURE 8 – SSWG ACTIVITY SUMMARY

V. Examples of Completed Review and Comment Sheets and System Hazard Action/Status Reports

One completed RCS and three completed SHA/S reports have been included (see appendix) to serve as examples of the HCS documentation. The reports also illustrate the typical distributions, approval cycles, and general depth and scope of reporting followed for the Harpoon HCS.

CONCLUDING REMARKS

For a Hazard Control System to be effective in identifying and controlling potential hazards, the following factors should be considered in the system planning:

- Safety analyses and design reviews must begin with the start of design activity and be performed by competent analysts.
- Funding and staffing must be concentrated through the Design and Development Phases.
- Hazard reporting criteria must be defined and agreed upon by all involved agencies
- Hazard reporting must include management levels with direction authority.
- Working Groups, or equivalent, must be established for timely co-ordination whenever several agencies are involved.

Reference (a) NAVORD 44942 Part III, Weapon System Safety Guidelines Handbook, Hazard Control for Explosive Ordnance Production.

APPENDIX (REMOVED)

Example Review & Comment Sheet (RCS) and System Hazard/Status (SHA/S) Reports

– CONTENTS –

1. Review & Comment Sheet, Review No. 21, 17 July 1973.
2. System Hazard/Status Report No. LTV-123, 15 April 1974.
3. System Hazard/Status Report No. SCL-125, 1 May 1974.
4. System Hazard/Status Report No. SCL-206, 14 July 1976.

IMPROVED SAFETY FOR SMALL ARMS AMMUNITION ASSEMBLY, INSPECTION AND PACKAGING

BY

CHARLES S. SKINNER
VICE PRESIDENT
BOOZ, ALLEN & HAMILTON, INC.
DESIGN AND DEVELOPMENT DIVISION
CLEVELAND, OHIO 44131

In the development of high-speed automated plant equipment for the assembly, inspection and packaging of small arms linked ammunition, numerous innovations have been developed in order to improve safety in both the ammunition plant and the field.

1. AUTOMATING AND INCREASING THE RATE OF THE PROCESS REMOVES PERSONNEL FROM EXPLOSIVE HAZARDS EXPOSURE.

A current 7.62 MM assembly, inspection and packaging line can process at about 400 cartridges per minute and requires about 8 people. The assembly operation which paces the process, consists of feeding M13 links and 7.62 MM cartridges, both ball and tracer, to an intermixing and linking subsystem which intermixes the ball and tracer cartridges and assembles them with the links, as illustrated in Exhibit I. With the development of an automated, high-speed assembly, inspection and packaging line under sponsorship of Frankford Arsenal, 7.62 MM is assembled, inspected and packaged at 1200 cartridges per minute and requires 7 people. Therefore, in equivalent production units, there is a reduction in personnel from 24 to 7 to assemble, inspect and package at a rate of 1200 cartridges per minute. The high-speed intermixing and assembly subsystem is illustrated in Exhibit II. A similar piece of equipment, illustrated in Exhibit III, was also developed for 20 MM ammunition, increasing the rate per line from 150 to 600 cartridges per minute, with similar explosive hazard exposure reduction benefits.

2. ON-LINE, ONE-HUNDRED PERCENT INSPECTION OF VENDOR SUPPLIED COMPONENTS REDUCES EQUIPMENT JAM HAZARDS, INCREASES THE PRODUCTION RATE AND IMPROVES PRODUCT QUALITY.

The subsystem which orients and feeds metallic ammunition links from bulk at a rate up to 1200 cartridges per minute is illustrated as Exhibit IV. This subsystem has two inspection stations, as illustrated in Exhibit V, which inspects each link for diameter and hardness, and rejects those links which fail inspection. Because

EXHIBIT I
Booz, Allen & Hamilton, Inc.
Design and Development Division
Cleveland, Ohio 44131
INTERMIX AND ASSEMBLY OF
7.62 MM LINKED AMMUNITION

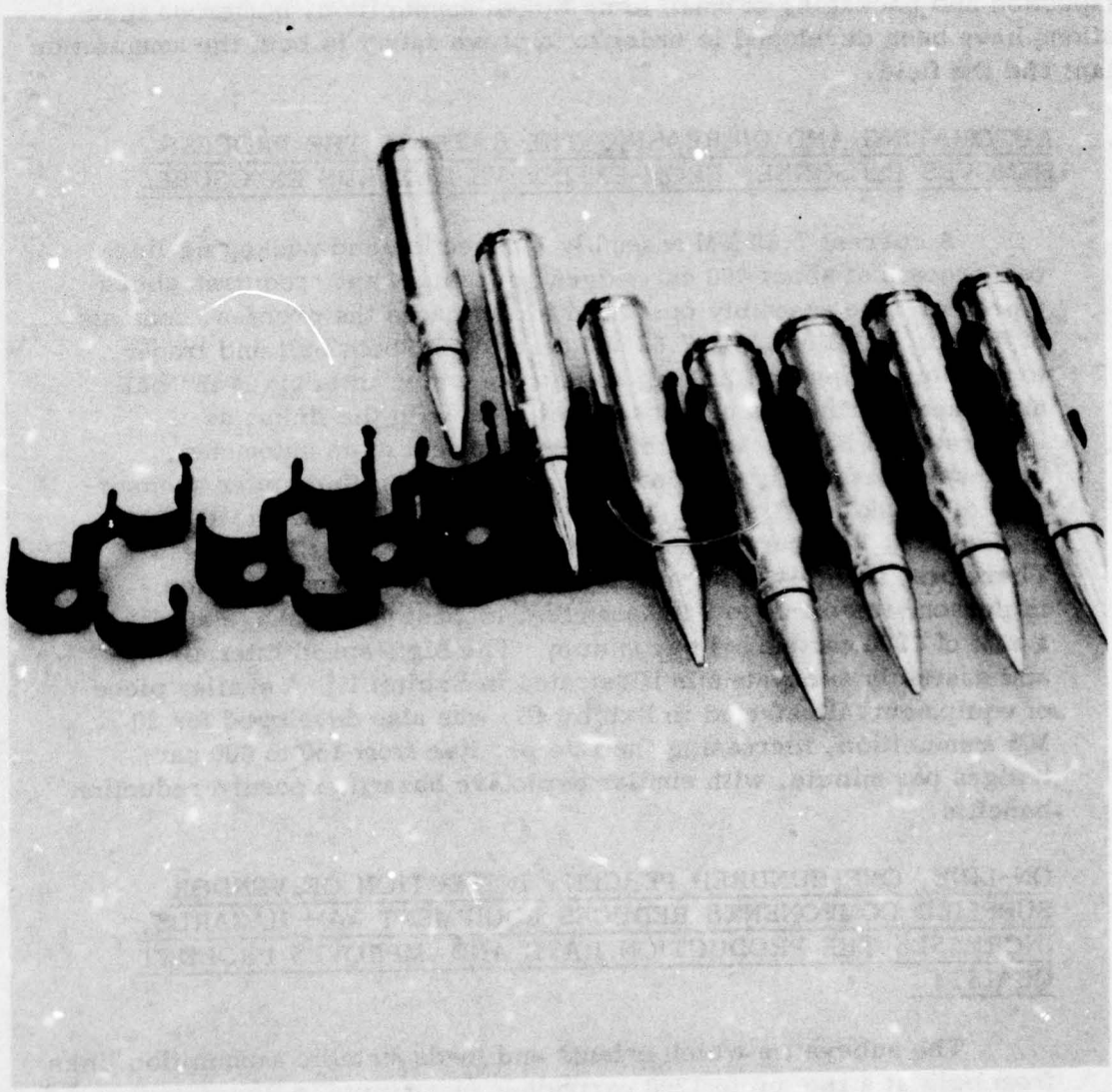


EXHIBIT II
Booz, Allen & Hamilton, Inc.
Design and Development Division
Cleveland, Ohio 44131
HIGH-SPEED INTERMIX AND LINKING
SUBSYSTEM FOR 7.62 MM AMMUNITIO

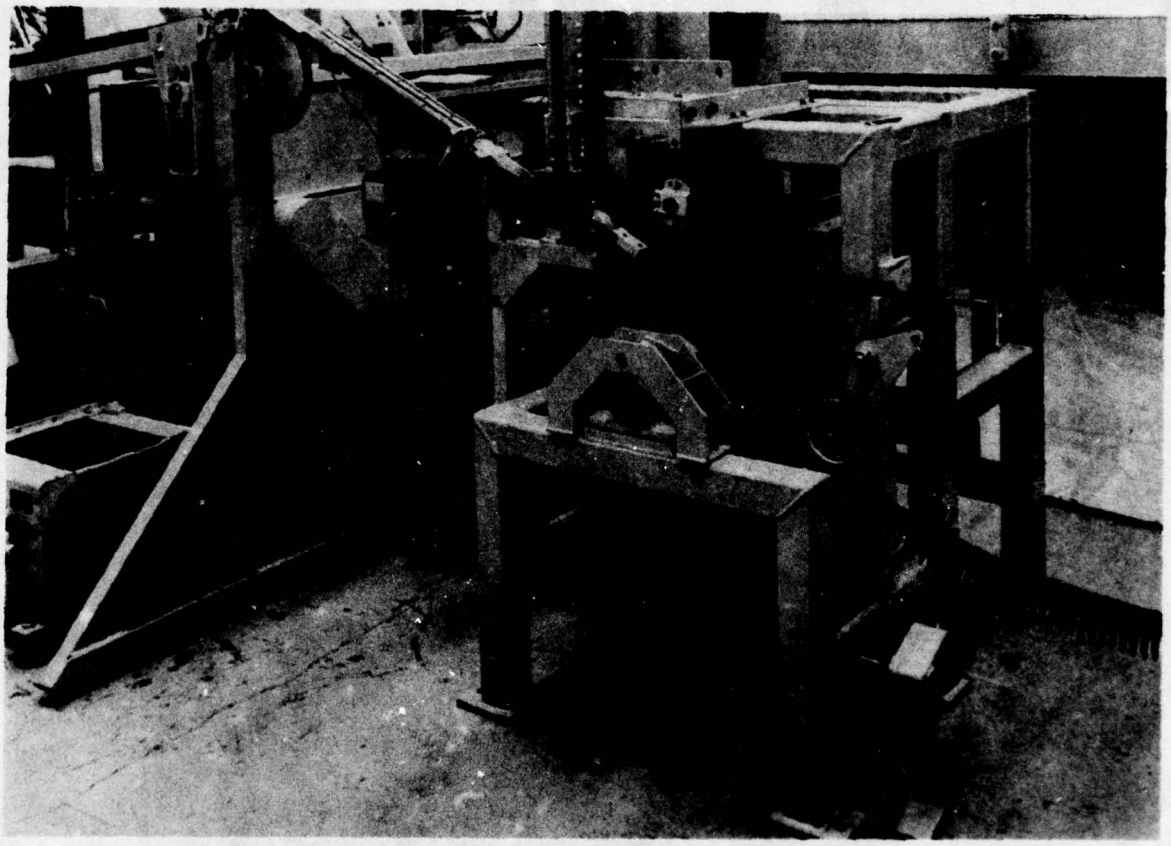


EXHIBIT III
Booz, Allen & Hamilton, Inc.
Design and Development Division
Cleveland, Ohio 44131
HIGH-SPEED INTERMIX AND LINKING
SUBSYSTEM FOR 20 MM AMMUNITION

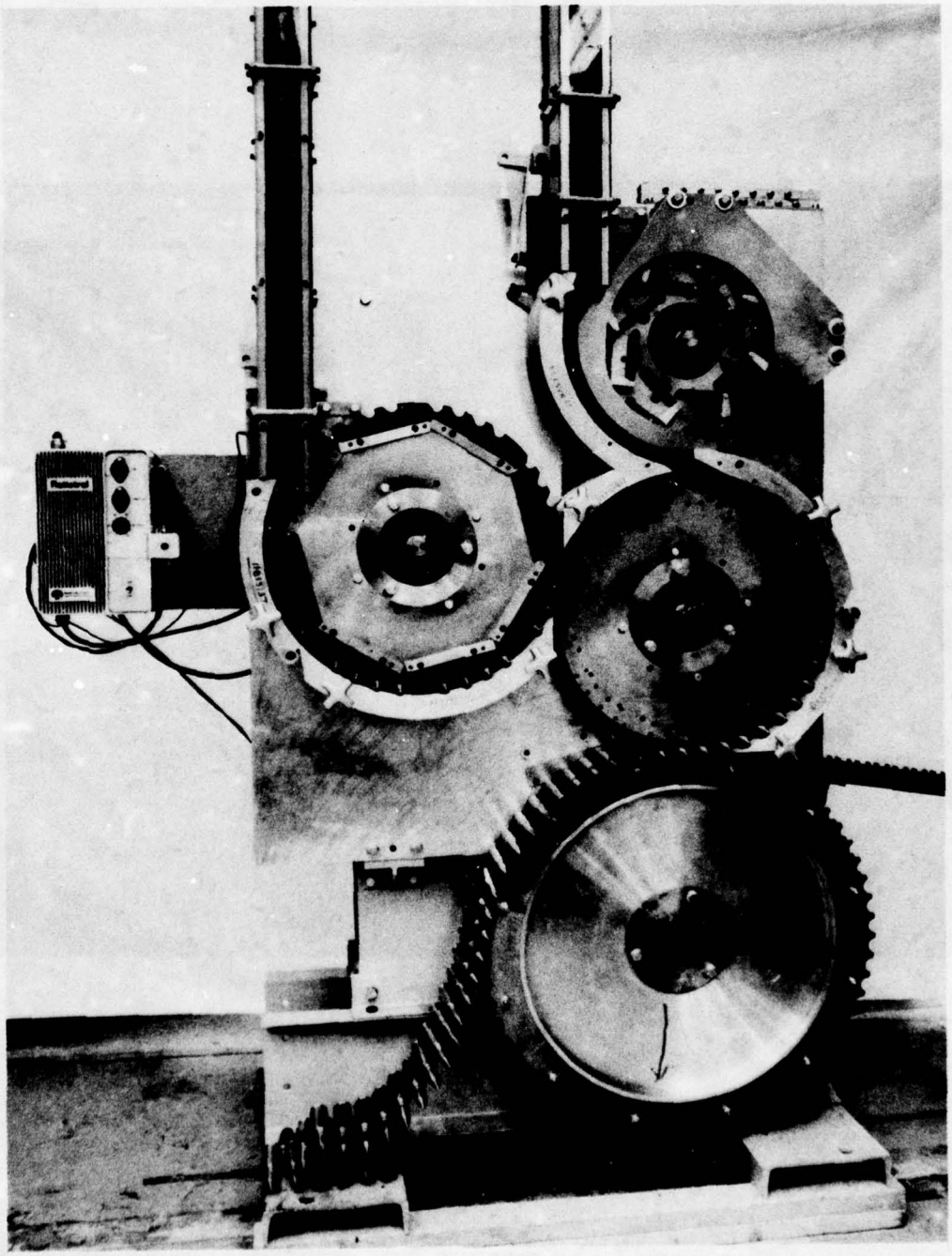


EXHIBIT IV
Booz, Allen & Hamilton, Inc.
Design and Development Division
Cleveland, Ohio 44131
M 13 LINK ORIENTATION, FEED AND
INSPECT SUBSYSTEM

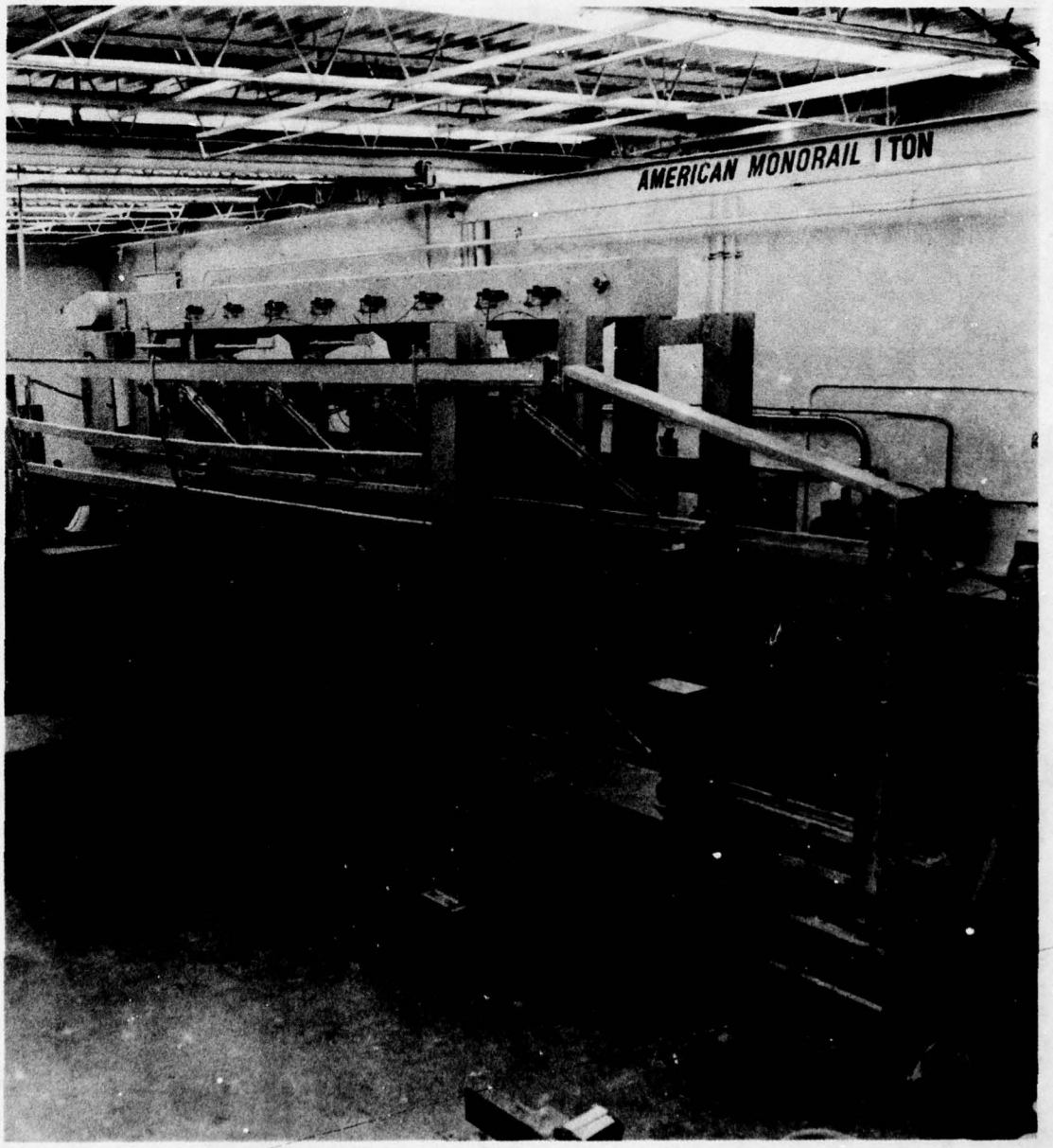
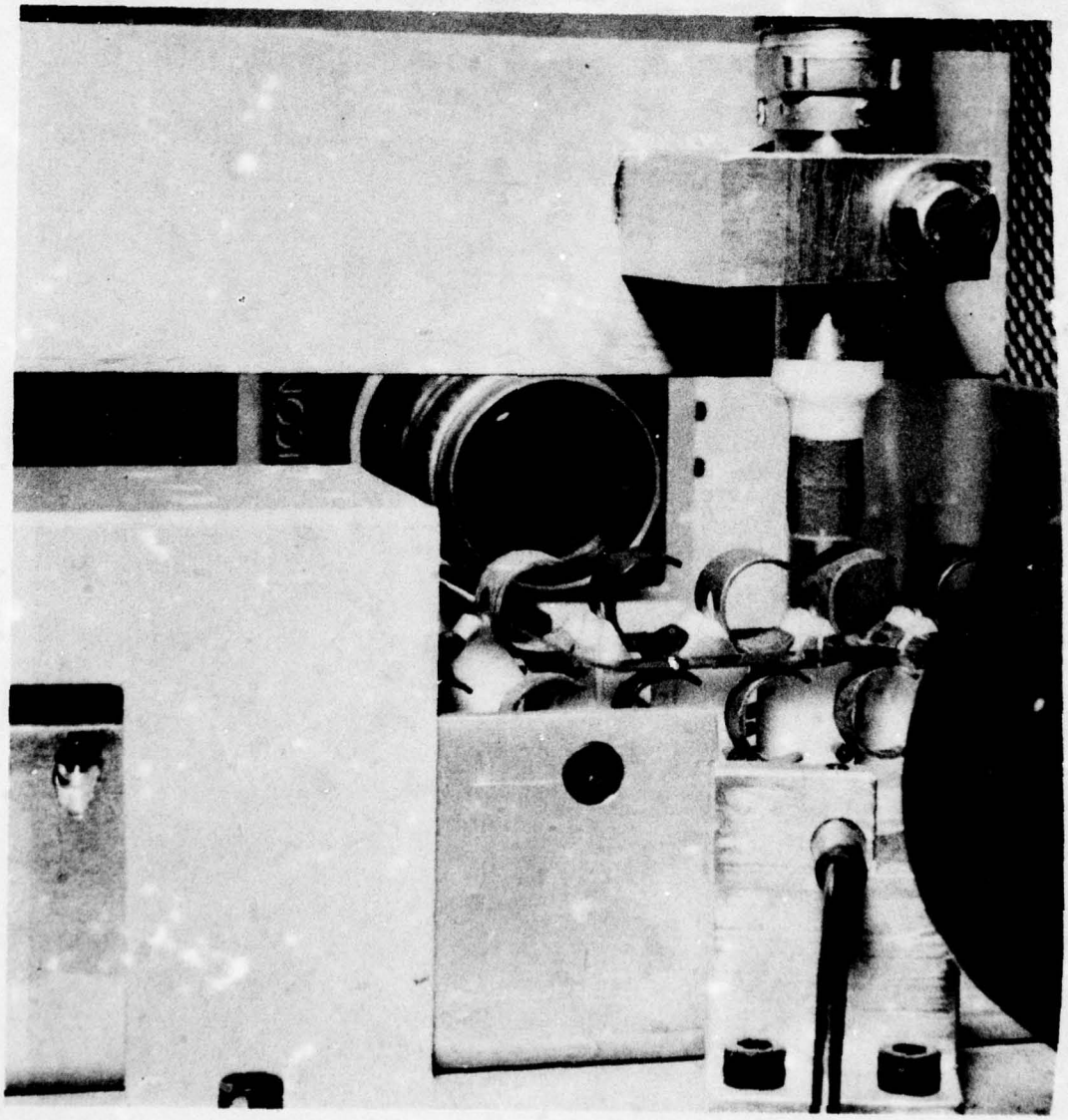


EXHIBIT V
Booz, Allen & Hamilton, Inc.
Design and Development Division
Cleveland, Ohio 44131
M 13 LINK DIAMETER AND
HARDNESS INSPECTION STATION



defective parts are pulled out of the system, equipment jam hazards are reduced, equipment stoppages are reduced, thus increasing the overall production rate and product quality is improved, thus providing safer product in the field.

3. ON-LINE, ONE-HUNDRED PERCENT QUALITY ASSURANCE INSPECTION OF THE FINISHED PRODUCT REDUCES SUBSEQUENT PACKAGING JAM HAZARDS AND SAFE FUNCTIONAL AMMUNITION IN THE FIELD.

Linked ammunition is currently inspected visually on line, and by quality assurance testing on a sampling basis. The automated high-speed assembly and packaging line will perform a one-hundred percent inspection test continuously on-line. The inspection subsystem as illustrated in Exhibit VI, performs all the required quality assurance tests and marks and records the faulty rounds. Subsequent discrete belts containing faulty rounds are rejected for rework, allowing only acceptable belts to be packaged. This contributes to reducing packaging equipment jam hazards and assures safe functional ammunition in the field.

4. EQUIPMENT SAFETY DEVICES CONTRIBUTE TO SAFER PLANT OPERATIONS

Equipment safety devices, such as the disengaging clutches on the drive of the 20 MM intermixing and linking machine illustrated as Exhibit VII, reduce the safety hazards in the event of equipment jams. Equipment jam detectors are employed extensively to assure safe equipment operation, as illustrated in the automatic belt folding subsystem of Exhibit VIII. Sensors are employed to insure each operation is complete before proceeding to the next, as with the 7.62 MM cloth bandoleer and metal container packaging subsystem illustrated as Exhibit IX. The centralized control of the more than 150 sensors and commands are accomplished with a programmable process controller, as illustrated in Exhibit X.

5. INNOVATIVE IN-PLANT AMMUNITION HANDLING DEVICES INCORPORATING CONTROLLED MOTION, REDUCE HAZARDS OF FEEDING PROCESSING EQUIPMENT.

Equipment specifically designed to feed and orient cartridges incorporating gentle handling techniques, such as the 7.62 MM cartridge feeder illustrated as Exhibit XI, reduce the hazards associated with feeding explosive components to processing equipment. This feeder is an adaptation of a feeder employed in the food processing industry to handle fragile bread sticks and pretzels. The feeder first singularizes and aligns the cartridges, then orients them end-for-end. There is no cartridge recycling, as with current cartridge feeders, which reduces product process damage and explosive hazard.

EXHIBIT VI
Booz, Allen & Hamilton, Inc.
Design and Development Division
Cleveland, Ohio 44131
ON-LINE AMMUNITION INSPECTION
SUBSYSTEM

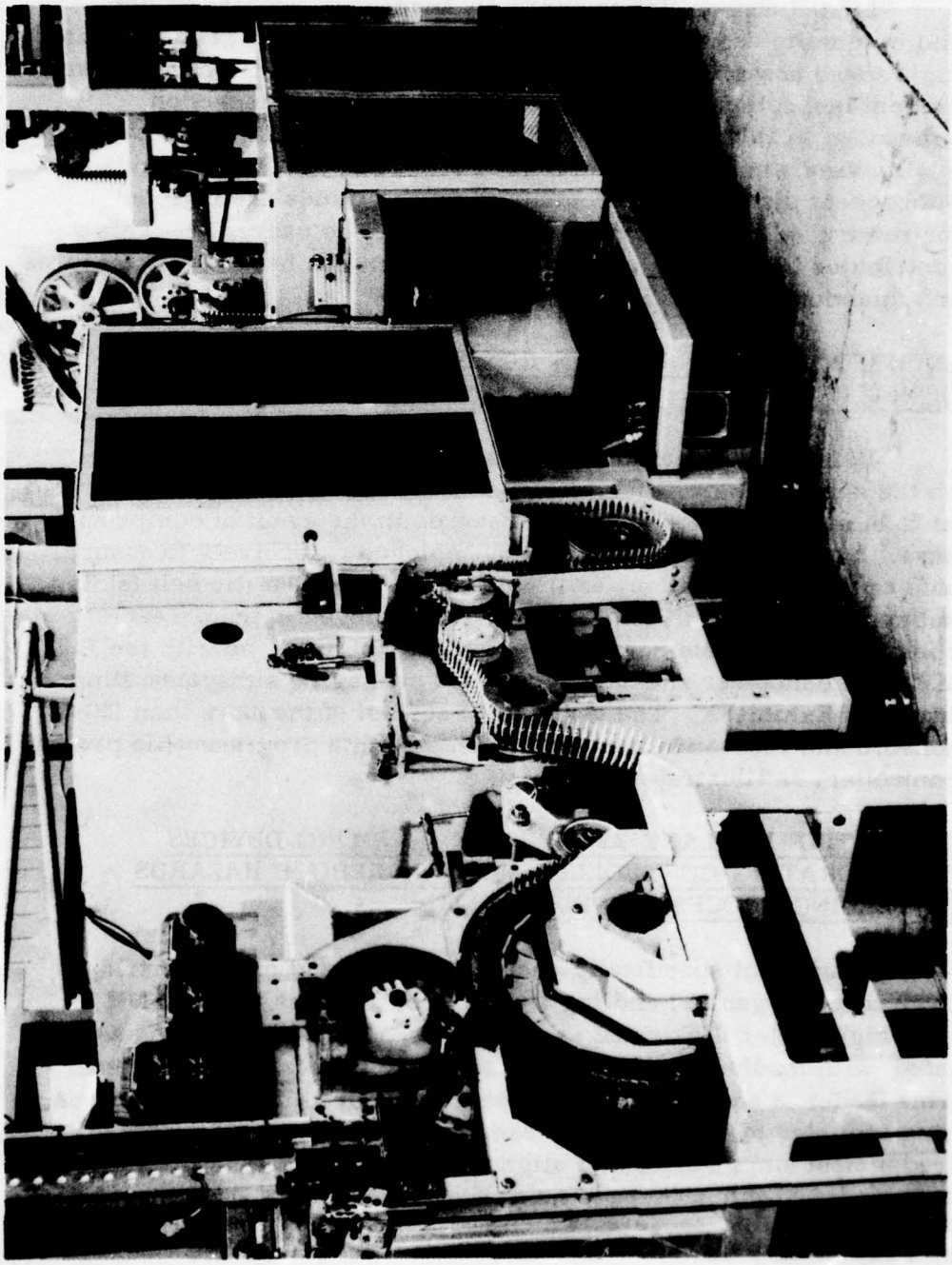


EXHIBIT VII
Booz, Allen & Hamilton, Inc.
Design and Development Division
Cleveland, Ohio 44131
EQUIPMENT SAFETY DEVICES ON
20 MM INTERMIXING AND LINKING MACHINE

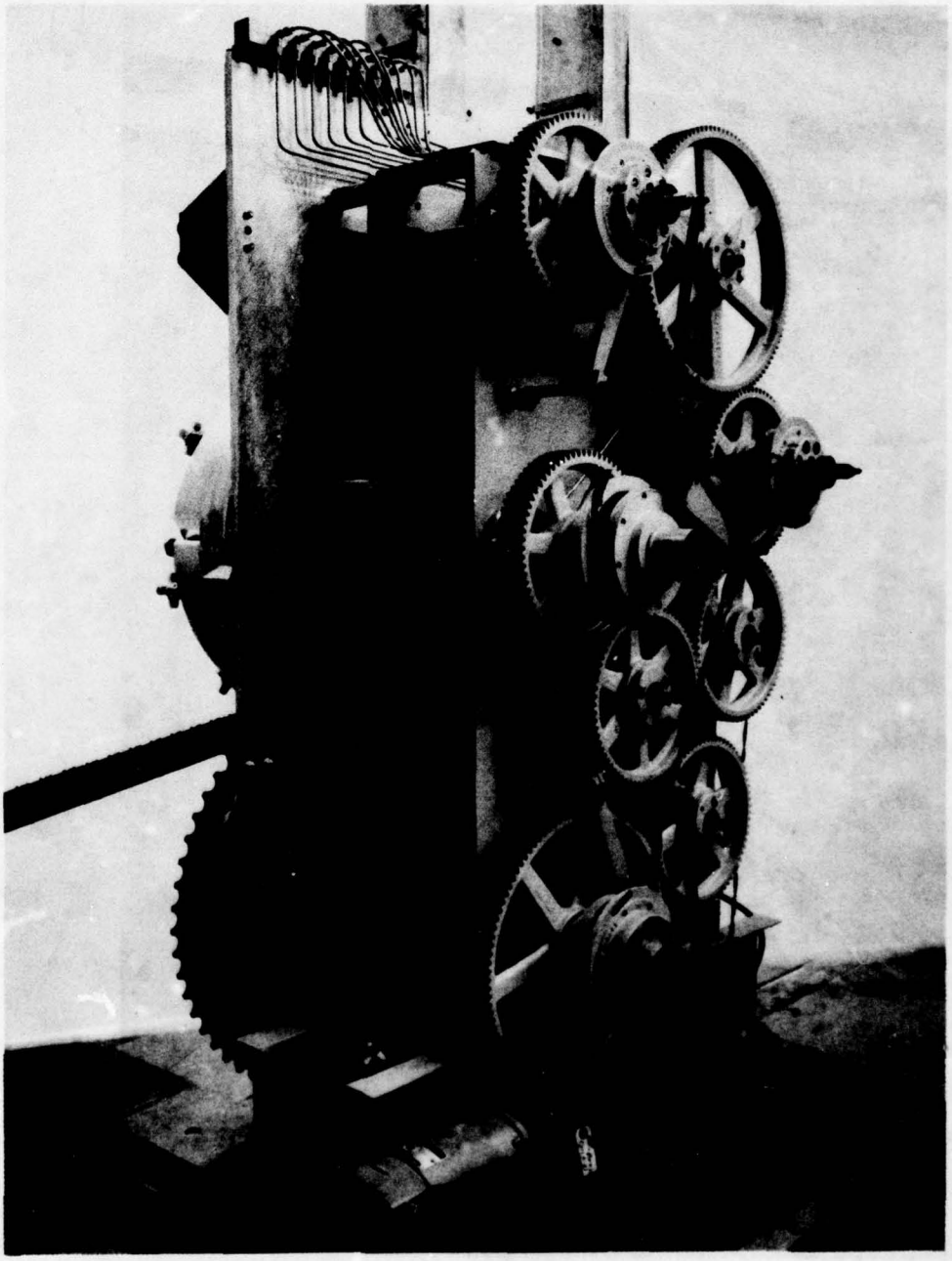


EXHIBIT VIII
Booz, Allen & Hamilton, Inc.
Design and Development Division
Cleveland, Ohio 44131
EQUIPMENT JAM DETECTORS EMPLOYED
WITH 7.62 MM BELT FOLDING SUBSYSTEM

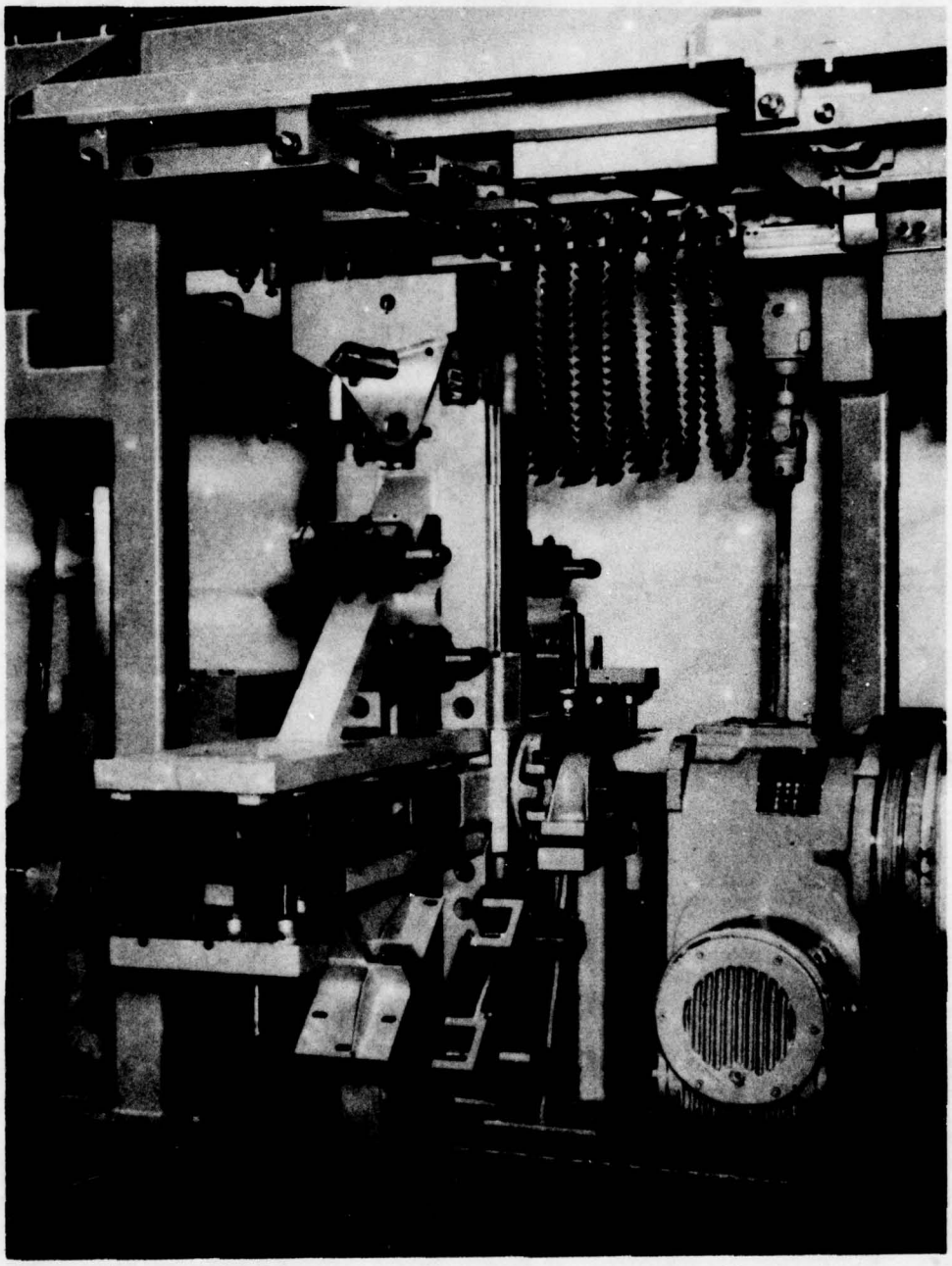


EXHIBIT IX
Booz, Allen & Hamilton, Inc
Design and Development Division
Cleveland, Ohio 44131
OPERATION COMPLETE SENSORS EMPLOYED
ON 7.62 MM CLOTH BANDOLEER AND
METAL CONTAINER PACKAGING SUBSYSTEM

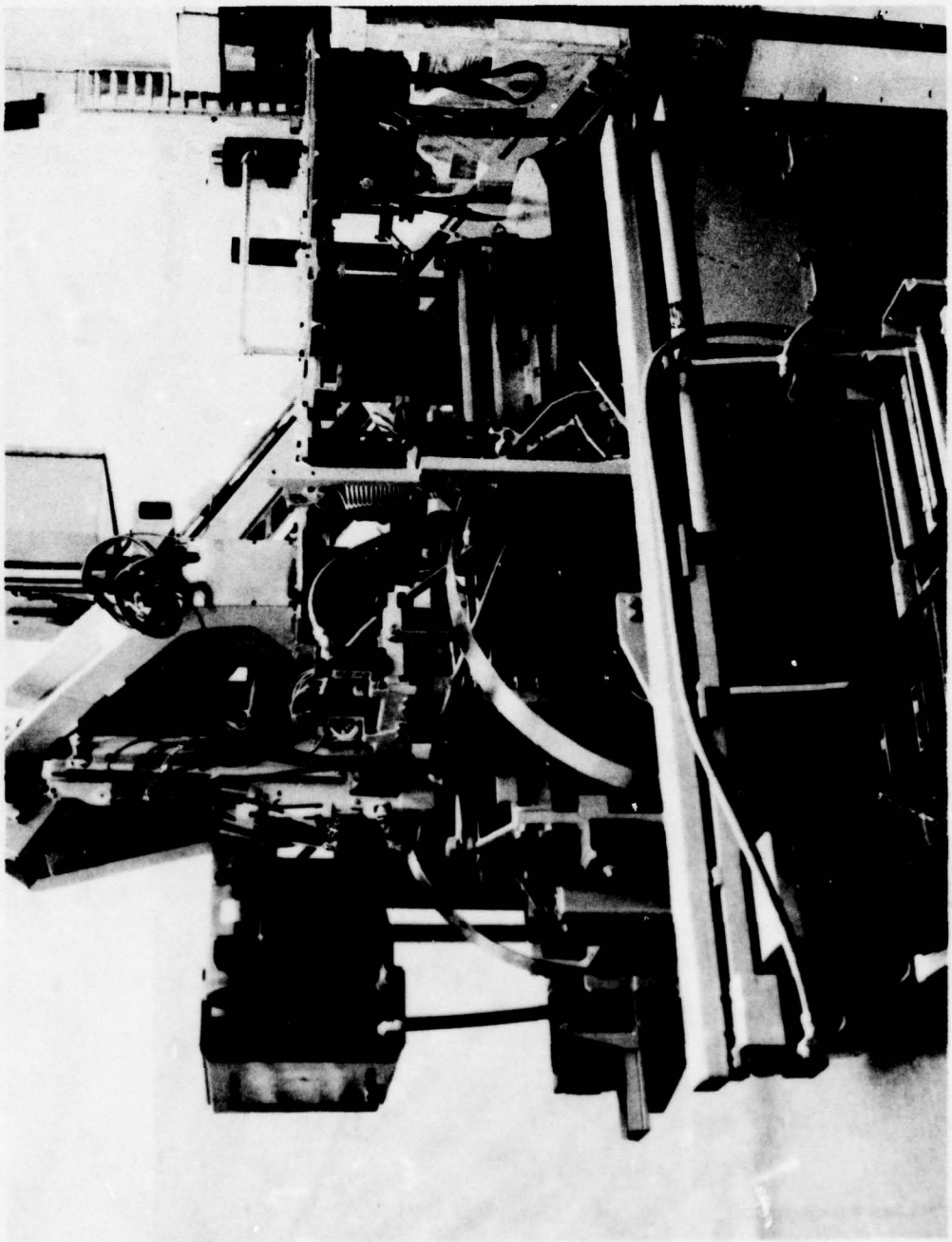


EXHIBIT X
Booz, Allen & Hamilton, Inc.
Design and Development Division
Cleveland, Ohio 44131
EQUIPMENT SAFETY DEVICES AND
OPERATIONS ARE CONTROLLED BY
A PROGRAMMABLE PROCESS CONTROLLER

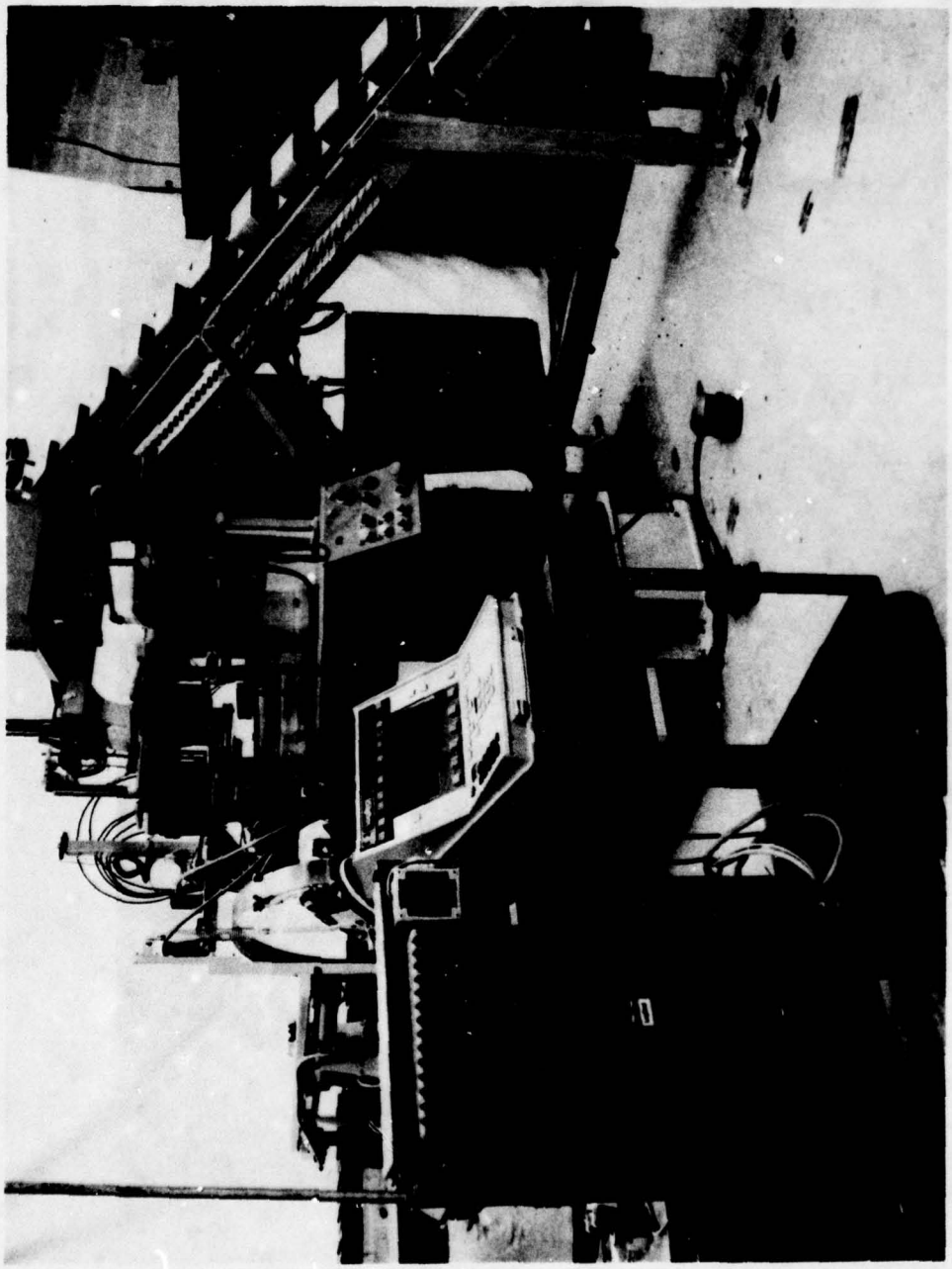
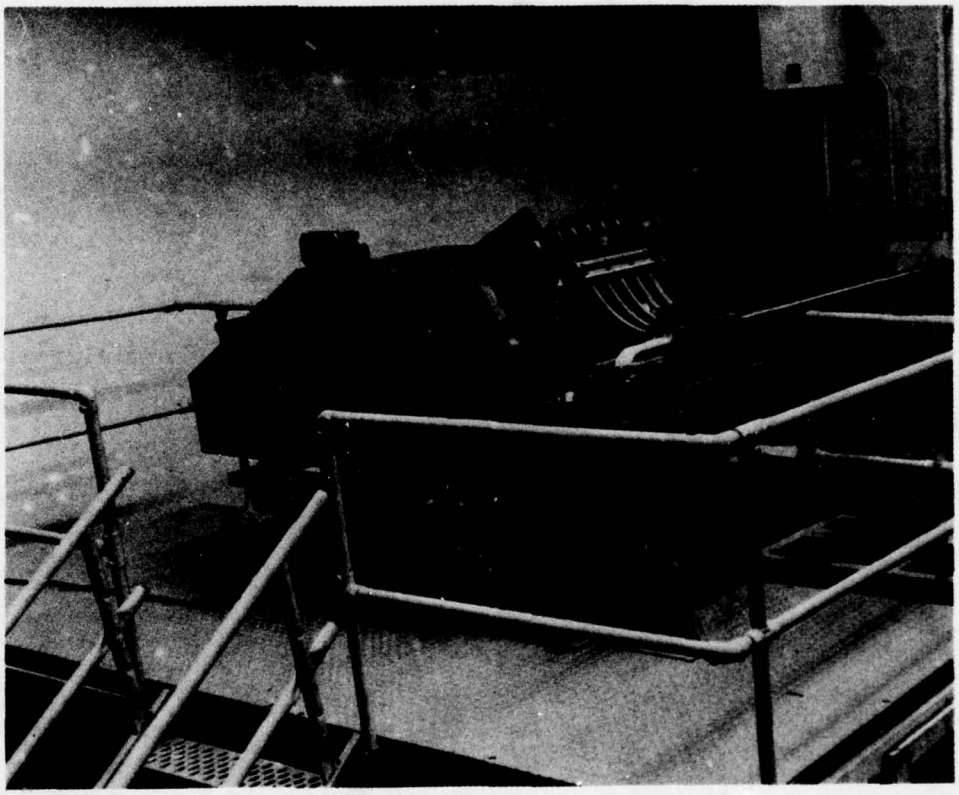


EXHIBIT XI
Booz, Allen & Hamilton, Inc.
Design and Development Division
Cleveland, Ohio 44131
INNOVATIVE CARTRIDGE FEEDER
FOR GENTLE HANDLING OF 7.62 MM
CARTRIDGES



THE THERMAL PROTECTION OF IN-SERVICE AIR LAUNCHED NAVAL WEAPONS

Paul B. McQuaide
Pacific Missile Test Center
Point Mugu, CA

THIS PRESENTATION WILL DISCUSS THE NATURE OF COOK-OFF, THE INTERFACES BETWEEN WEAPONS AND FIRE, THE ONGOING NAVY WEAPONS COOK-OFF PROGRAM AND SOME NEW CONCEPTS THAT MAY BE INCORPORATED INTO FUTURE WEAPON DESIGN.

THE INITIAL QUESTION OFTEN PROMPTED BY OUR PROGRAM IS 'WHAT IS COOK-OFF"? COOK-OFF, WITH RESPECT TO WEAPONS, IS THAT EXPLOSIVE REACTION WHICH OCCURS WHEN AN ORDNANCE ITEM IS SUBJECTED TO A HEAT SOURCE SUCH AS AN ACCIDENTAL FUEL FIRE ON AN AIRCRAFT CARRIER. THE INSUING FIRE FROM AN AIRCRAFT ACCIDENT OR ASHORE AMMUNITION STORAGE DUMP FIRE.

AS YOU UNDOUBTEDLY REMEMBER, THE NAVY EXPERIENCED TWO AIRCRAFT CARRIER FIRES IN THE RECENT PAST, ONE ABOARD THE USS ENTERPRISE IN 1969 AND THE OTHER ABOARD THE USS FORRESTAL IN 1967 DUE TO COOKING OFF OF AIR-LAUNCHED ORDNANCE. THESE ACCIDENTS FOCUSED THE ATTENTION ON THE PROBLEM WHICH RESULTED IN THE CURRENT WEAPON COOK-OFF PROGRAMS.

TO PREVENT CONFUSION RESULTING FROM LOCALIZED USE OF TERMINOLOGY DESCRIBING VIOLENT REACTIONS, PRACTICAL AND STANDARDIZED DEFINITIONS OF REACTIONS HAVE BEEN PROMULGATED IN NAVORD OP5, VOLUME 1. THESE DESCRIBE REACTIONS IN TERMS OF EXPLOSIVE REACTIONS, BLAST, FRAGMENTATION, AND ENVIRONMENTAL EFFECTS.

A "DETONATION" HAS OCCURRED WHEN THE MUNITION PERFORMS IN ITS DESIGN MODE. THE MAXIMUM POSSIBLE AIR SHOCK IS FORMED AND ESSENTIALLY ALL OF THE CASE IS BROKEN INTO SMALL FRAGMENTS.

PRECEDING PAGE BLANK-NOT FILMED

IN AN "EXPLOSION", VIOLENT PRESSURE RUPTURE AND FRAGMENTATION OF THE MUNITION CASE WITH RESULTING AIR SHOCK OCCURS. MOST OF METAL CASE BREAKS INTO LARGE PIECES WHICH ARE THROWN ABOUT WITH UNREACTED OR BURNING EXPLOSIVE.

IN AN "DEFLAGRATION", THE ORDNANCE ENERGETIC MATERIAL IN THE MUNITION BURNS RAPIDLY. THE CASE MAY RUPTURE OR THE ENDPLATES BLOW OUT, HOWEVER, THERE IS NO FRAGMENTATION OF THE CASE.

IN ADDITION, MIL-STD 1648 WHICH ESTABLISHES THE COOK-OFF REQUIREMENTS FOR NAVY ORDNANCE FURTHER DEFINES A DEFLAGRATION AS A REACTION WHICH EXPELLS ANY PORTION OF THE MUNITION 25 FEET OR MORE FROM GROUND ZERO. IT ALSO DEFINES A BURNING REACTION WHERE THE ORDNANCE ENERGETIC MATERIAL MAY, AS A RESULT OF CASE BURN THROUGH OR RUPTURE, BURN OR JET.

THESE STANDARDIZED DEFINITIONS FOR DESCRIBING COOK-OFF REACTIONS HAVE ASSISTED IN CLARIFYING MUCH OF THE AMBIGUITY RELATED TO COOK-OFF TESTING.

THE NAVY WEAPON COOK-OFF PROGRAM ADDRESSES THREE AREAS:

THE FIRST OF THESE IS THE "BASELINE" COOK-OFF TESTING OF THE WEAPONS IN THE INVENTORY TO DETERMINE RELATIVE HAZARDS AND PROMULGATE THIS INFORMATION TO THE OPERATING FORCES.

THE SECOND AREA IS IMPROVEMENT OF THE COOK-OFF CHARACTERISTICS OF IN-SERVICE WEAPONS. THE THIRD AREA IS THAT OF ADVANCED COOK-OFF PROTECTION CONCEPTS WHICH ADDRESSES THE DEVELOPMENT OF THE MEANS TO IMPROVE THE COOK-OFF CHARACTERISTICS OF WEAPONS UNDER DEVELOPMENT.

THE NAVAL WEAPONS LABORATORY, DAHLGREN, VIRGINIA WAS TASKED TO ACCOMPLISH THE BASELINE TESTING AND NAVAL WEAPONS CENTER, CHINA LAKE, WAS TASKED WITH THE ADVANCED CONCEPTS.

THE PACIFIC MISSILE TEST CENTER (PACMISTESTCEN) WAS TASKED AS THE LEAD NAVAL FIELD ACTIVITY IN 1969 FOR THE WEAPONS COOK-OFF IMPROVEMENT PROGRAM BECAUSE OF ITS ENGINEERING COGNIZANT FUNCTION ON IN-SERVICE WEAPONS. AS THE LEAD FIELD ACTIVITY THE PACMISTESTCEN COORDINATES THE EFFORTS OF APPROXIMATELY SEVEN PARTICIPATING NAVY FIELD ACTIVITIES, OTHER DOD ACTIVITIES AND CONTRACTORS IN ACHIEVING THE PROGRAM OBJECTIVES.

THE OBJECTIVE OF THE NAVAL WEAPONS COOK-OFF IMPROVEMENT PROGRAM IS TO PROVIDE A FIVE MINUTE MINIMUM THERMAL PROTECTION AND DECREASE THE EXPLOSIVE REACTION OF THOSE IN-SERVICE WEAPONS WHEN SUBJECTED TO A FUEL FIRE.

THE PROGRAM IS DIVIDED INTO FOUR MAJOR AREAS; BOMBS, UNGUIDED ROCKETS, AIRCRAFT GUNS SYSTEMS AND MISSILES. EACH OF THESE WEAPON TYPES PRESENTS A DIFFERENT SET OF PROBLEMS WHEN DEVELOPING A SUITABLE THERMAL PROTECTION SYSTEM.

IT WOULD NOW BE APPROPRIATE TO DISCUSS OUR APPROACH TO MEETING PROGRAM OBJECTIVES, HOWEVER, I AM GOING TO DEFER THIS FOR NOW AND INCLUDE IT AS A PART OF THE DISCUSSION OF THE AIR-LAUNCHED MISSILE PORTION OF THE PROGRAM.

THE FOLLOWING BAR CHARTS BRIEFLY SUMMARIZE THE STATUS OF THE DIFFERENT WEAPON COOK-OFF PROGRAMS:

BOMBS

WITH RESPECT TO THE BOMBS, THE NAVY'S MK 80 SERIES HAS BEEN THERMALLY PROTECTED, THE 500 POUND MK 82 IS IN USE IN THE FLEET AND THE MK 83 AND MK 84 HAVE BEEN RELEASED FOR PRODUCTION. COOK-OFF TIMES FOR THESE BOMBS ARE NINE TO TEN MINUTES. OVER 300,000 THERMALLY PROTECTED MK 82'S HAVE BEEN PRODUCED TO DATE. THE THERMAL CONCEPT USED WAS AN ACTIVE EXTERNAL COATING POSSESSING ABLATIVE CHARACTERISTICS, AN INCREASED INTERNAL HOT MELT THICKNESS AND A SOLID INTERNAL BASE PAD.

THE FUZING SYSTEMS FOR THESE BOMBS ALSO REQUIRED THERMAL PROTECTION. IN ORDER TO ENSURE A DEFLAGRATION REACTION OF THE BOMB, THE FUZE SYSTEM MUST HAVE A LONGER COOK-OFF TIME THAN THE BOMB ITSELF. FOR THIS REASON A MINIMUM OF 12 MINUTES HAS BEEN ESTABLISHED FOR GENERAL PURPOSE BOMB FUZING SYSTEMS. THE M904 AND MK 346 ARE MECHANICAL FUZES WHILE THE MK 344 AND MK 75 ARE ELECTRICAL. ELECTRICAL FUZES INHERENTLY POSSESS GREATER COOK-OFF TIMES AND AS A RESULT DID NOT REQUIRE MODIFICATION AS DID THE M904 OR MK 346. THERMAL PROTECTIVE SLEEVES WERE DEVELOPED TO INCREASE COOK-OFF TIME OF THE TWO MECHANICAL FUZES THE ADAPTER BOOSTERS ARE A PART OF THE FUZE EXPLOSIVE TRAIN AND MUST MEET THE SAME REQUIREMENTS AS THE FUZES FOR SAFETY.

ROCKEYE

THE MK 20 ROCKEYE IS A CLUSTER BOMB UNIT. IT CONSISTS OF THE MK 7 DISPENSER WHICH CONTAINS APPROXIMATELY 250 MK 118 BOMBLETS. THE MK 339 FUZE IS ATTACHED TO THE NOSE OF THE DISPENSER AND INITIATES A LINEAR SHAPE CHARGE WHICH OPENS THE DISPENSER AFTER AIRCRAFT RELEASE.

A THERMALLY PROTECTED VERSION OF THE MK 20 ROCKEYE HAS BEEN RELEASED TO PRODUCTION. THIS VERSION, THE MK 20 MOD 6 UTILIZES AN INTUMESCENT EXTERIOR COATING OF APPROXIMATELY 100 MILS WHICH PROVIDES SIX MINUTES MINIMUM COOK-OFF PROTECTION VERSUS APPROXIMATELY ONE MINUTE FOR THE UNPROTECTED MK 20 MOD 3. PRODUCTION VERSIONS OF THIS WEAPON WILL REACH THE FLEET DURING FY 77.

ROCKETS

THE APPROACH USED ON UNGUIDED ROCKET SYSTEMS WAS TO THERMALLY PROTECT THE LAUNCHER VICE THE INDIVIDUAL ROCKET COMPONENTS. THE COOK-OFF TIMES SHOWN IN FIGURE 8 ARE FOR THE MOTORS AND WARHEADS IN A STANDARD AND THEN THERMALLY PROTECTED LAUNCHER. THE ZUNI THERMALLY PROTECTED LAU-10D/A LAUNCHER HAS BEEN RELEASED FOR PRODUCTION WHICH COMMENCED EARLY IN CALENDAR YEAR 1974. A THERMAL PROTECTION SYSTEM HAS BEEN DEVELOPED FOR THE 2.75 INCH ROCKET SYSTEM, HOWEVER, QUALIFICATION FOR FLEET USE IS REQUIRED. THE THERMAL PROTECTION SYSTEM DEVELOPED FOR THE LAU-10D/A CONSISTS OF AN EXTERNAL LAUNCHER INTUMESCENT COATING, AN INTUMESCENT PAINTED FORWARD FAIRING AND THE ADDITION OF THE AFT THERMAL SHIELD MADE OF ALUMINA SILICA FIBER.

THE DIFFERENCE IN THE ROCKET WARHEAD COOK-OFF TIME IS DUE TO THE DIFFERENT WARHEADS CONFIGURATION AND POSITION IN THE LAUNCHER.

FIGURE 10 SHOWS THE LOCATION OF THE WARHEADS IN THE LAUNCHER. THE MK 32 WARHEAD REACTS FASTER BECAUSE OF THE HEAT INPUT FROM THE FORWARD END OF THE LAUNCHER.

GUNS

THE MAIN AIRCRAFT GUN USED ABOARD THE CARRIERS IS THE M61A1 GUN SYSTEM. A TEST TO DETERMINE ITS HAZARD IN A FUEL FIRE WAS CONDUCTED. THE TEST SETUP UTILIZED A SIMULATED A-7 AIRCRAFT WITH THE ALL UP GUN INSTALLED. THE RESULTS OF THE TEST INDICATED THAT THE INITIAL REACTION OCCURRED AT 130 SECONDS, THE INITIAL MAGAZINE REACTIONS OCCURRED AT 240 SECONDS. APPROXIMATELY 750 REACTIONS OCCURRED (MAINLY DEFLAGRATION), BETWEEN TWO AND ONE-HALF AND TEN MINUTES NO SYMPATHETIC REACTIONS OCCURRED. ANALYSIS OF THE TEST DATA INDICATED THE COOK-OFF HAZARD OF THE M61A1 GUN SYSTEM IS LESS THAN THAT OF BOMBS, ROCKETS AND MISSILES.

COOK-OFF IMPROVEMENT MATERIALS

DURING THE BOMB AND ROCKET PROGRAMS APPROXIMATELY 50 EXTERNAL THERMAL PROTECTIVE MATERIALS WERE EVALUATED, THE MATERIALS CONSIDERED INCLUDED MODIFIED RUBBERS, ABLATIVE COATINGS, INTUMESCENT PAINTS AND COATINGS, FILLED PLASTICS, METAL CLOTHS, INORGANIC COATINGS, METAL OXIDES AND VARIOUS COMBINATIONS. BECAUSE OF THEIR COST, APPLICATION, THERMAL, PHYSICAL AND ENVIRONMENTAL PROPERTIES, ORGANIC COATINGS WHICH ACT THROUGH ABLATION AND OR INTUMESCENCE HAVE BEEN SELECTED IN MOST CASES FOR FINAL QUALIFICATION.

NUMEROUS INTERNAL LINERS WERE CONSIDERED IN THE BOMB PROGRAM. THEY RANGED FROM FILLED POLYESTER SYSTEMS TO A VARIETY OF HOT MELTS. THE MAJORITY OF THEM EXHIBITED EXPLOSIVE COMPATIBILITY PROBLEMS AND OTHERS ACTUALLY INCREASED THE EXPLOSIVE REACTION FROM COOK-OFF.

A MODIFIED ASPHALT WAS SELECTED BECAUSE IT ADDED TO THE COOK-OFF TIME AND DECREASED THE COOK-OFF REACTION.

HEAT PATH INTERRUPTERS HAVE BEEN EFFECTIVELY UTILIZED IN SEVERING THE DIRECT HEAT PATH TO THE EXPLOSIVE. IN THE M148 ADAPTER BOOSTER PHENOLIC WAS USED IN THE FORM OF A DISK AND WASHER IN THE ASSEMBLY OF THE ADAPTER BOOSTER TO REMOVE THE DIRECT HEAT PATH.

DESIGN CHANGES IN WHICH ADDITIONAL PARTS ARE UTILIZED HAVE BEEN EFFECTIVELY UTILIZED IN THE BOMB FUZES AND ROCKETS. AN ACRYLONITRILE BUTADIENE RUBBER SLEEVE WAS DESIGNED TO INCREASE THE COOK-OFF TIME OF THE M904E4 BOMB FUZE FROM 5 TO 12 MINUTES. A PHENOLIC SLEEVE TO ACCOMPLISH THE SAME AS DESIGNED FOR THE MK 346 FUZE.

THE APPROACHES UTILIZED FOR COOK-OFF IMPROVEMENT IN FREEFALL WEAPONS AS WELL AS OTHERS ARE CURRENTLY BEING USED IN THE MISSILE COOK-OFF IMPROVEMENT PROGRAM.

AS WE CAN SEE IN THIS CHART, ALL IN-SERVICE AIR LAUNCHED MISSILE MOTORS AND WARHEADS REACT IN LESS THAN FIVE MINUTES. MOST MOTOR REACTIONS OCCUR IN LESS THAN TWO MINUTES. MOST COMMON COOK-OFF REACTIONS FOR WARHEADS ARE:

DEFLAGRATION - SIDEWINDER, SPARROW, WALLEYE

EXPLOSION - SHRIKE, BULLPUP

DETONATION - STANDARD ARM

MOST COMMON MOTOR REACTIONS ARE DEFLAGRATIONS. HOWEVER SOME STANDARD ARM MOTORS HAVE EXPLODED DURING FAST COOK-OFF TESTS.

THE SIGNIFICANCE OF THESE REACTIONS IS DEMONSTRATED BY RESULTS OF THE NAVY LABORATORY RESEARCH PLANNING PANEL INVESTIGATING THE USS FORRESTAL FIRE OF JULY 1967. THEIR REPORT CONCLUDED THAT A HIGH PERCENTAGE OF MISSILE HARDWARE ON THE AFT DECK AT THE TIME OF THE FIRE REACTED CAUSING DAMAGE, SPREADING THE FIRE, AND POSSIBLY CAUSING SOME GP BOMBS TO DETONATE. FOUR SHRIKE MISSILES FOR EXAMPLE WERE ON THE AFT DECK DURING THE FIRE. TWO ARE KNOWN TO HAVE EXPLODED. ONE WAS JETTISONED AND THE STATUS OF THE FOURTH WAS NEVER DETERMINED.

THE OBJECTIVES OF THE MISSILE COOK-OFF PROGRAM ARE MUCH THE SAME AS FOR OTHER WEAPONS WITH PARTICULAR ATTENTION DEVOTED TO REACHING THE FIVE MINUTE MINIMUM TIME TO REACTION AND ELIMINATING PROPULSIVE REACTIONS.

THE APPROACH TO COOK-OFF IMPROVEMENT INVOLVES:

"BASELINE" TESTING DESIGNED TO DEFINE CRITICAL HEAT PATHS, TEMPERATURE PROFILES, AND FAILURE MODES IN ADDITION TO COOK-OFF TIMES AND REACTIONS. USING THIS DATA, IMPROVEMENT CONCEPTS AND MATERIALS ARE DEVELOPED BY VARIOUS AGENCIES FOR MISSILE APPLICATIONS. DEFINED THERMAL PROTECTION SYSTEMS ARE THEN QUALIFIED PRODUCED AND RELEASED TO THE FLEET.

BASELINE TESTS

IN ORDER TO DEVELOP THE REQUIRED THERMAL PROTECTION SYSTEMS FOR IN-SERVICE MISSILES, INSTRUMENTED FAST COOK-OFF TESTS OF UNPROTECTED HARDWARE MUST BE CONDUCTED. THESE BASELINE TESTS ARE DESIGNED TO DEFINE CRITICAL HEAT PATHS, TEMPERATURE PROFILES, AND FAILURE MODES IN ADDITION TO COOK-OFF TIMES AND REACTIONS. USING THIS DATA, IMPROVEMENT CONCEPTS AND MATERIALS ARE BEING DEVELOPED BY VARIOUS AGENCIES FOR MISSILE APPLICATIONS.

SHOWN IN THESE VIEWS ARE THE TYPE OF FACILITIES USED FOR OUR COOK-OFF TESTING. THIS FACILITY IS LOCATED AT NAVWPNCEN, CHINA LAKE. IT CONSISTS OF A FUEL PIT 24 FEET SQUARE OR OCTOGON WHICH IS LINED WITH POLYETHYLENE PLASTIC TO PREVENT FUEL LOSS INTO THE GROUND. TRANSDUCER LEADS PROTRUDING FROM THE TEST ITEMS ARE SEALED, INSULATED AND RUN UNDER GROUND TO RECORDING EQUIPMENT. THE FUEL PIT IS FILLED WITH 1,000 GALLONS OF JP-5 AND THIRTY GALLONS OF GASOLINE ARE POURED OVER THE FUEL SURFACE TO PROMOTE RAPID FUEL IGNITION. THERMITE GRENADES ARE PLACED AROUND THE TEST PIT AND ARE ELECTRICALLY INITIATED TO IGNITE THE FUEL.

A WIND BARRIER APPROXIMATELY THREE FEET HIGH ENCLOSES THE PIT TO REDUCE AFFECTS OF SURFACE WINDS. THE TEST ITEM IS SUPPORTED BY AN A-FRAME SO THAT THE DISTANCE FROM THE FUEL SURFACE TO THE CENTERLINE OF THE TEST ITEM IS 36 INCHES. POOL FIRE STUDIES HAVE SHOWN THAT THIS IS THE HOTTEST AREA IN A J.P. POOL FIRE WITH TEMPERATURES RANGING FROM 1,700 TO 2,000°F

SKYTOP WHICH IS ALSO LOCATED AT NAVWPNCEN, CHINA LAKE WAS DESIGNED AS A RETENTION STRUCTURE. THE STRUCTURE INCORPORATES TWO SIDE SOLID STEEL-PLATED FIREWALLS WITH SUPPORTING REVETMENTS, AND TWO OPEN SCREENED ENDS AND ROOF WHICH ALLOW FREE AIR FLOW BUT RESTRAIN MISSILE MOTORS WHICH MAY REACT PROPULSIVELY. THE STRUCTURE IS 63 FEET LONG, 47 FEET WIDE AND 31 FEET HIGH. THE FUEL PIT AND DATA ACQUISITION SYSTEM ARE SIMILAR TO THAT USED IN THE OUT DOOR FACILITY.

DATA COLLECTED DURING TESTS ARE IN THE FORM OF THERMOCOUPLE RESPONSE, REAL TIME MOTION PICTURES, VIDEO TAPES WITH AUDIO RECORDERS AND STILL PHOTOS. ONE ADDITIONAL FACILITY ESPECIALLY HELPFUL IN DETERMINING FAILURE MODE DURING A FULL SCALE TEST IS THE FIRE PIT WITH SMOKE ABATEMENT. SHOWN HERE IS A MK 20 ROCKEYE UNDERGOING FIRE TEST. THIS FACILITY ALLOWS THE TEST CONDUCTOR TO REMOVE THE FLAME AND SMOKE ASSOCIATED WITH A FULL SCALE FIRE SO THAT THE TEST ITEM CAN BE VIEWED AND PHOTOGRAPHED DURING A TEST. THE SPRINKLER SYSTEM CAN THEN BE SHUT OFF AND THE FIRE RESUMES. BECAUSE THE J.P. FUEL IS LIGHTER THAN WATER, THE FIRE WILL QUICKLY REBUILD UNLESS IT HAS BEEN COMPLETELY EXTINGUISHED.

THE FOLLOWING FILM SHOWS A RECENT TEST OF A MK 20 ROCKEYE.

A SUMMARY OF THE RESULTS OF BASELINE TESTING PERFORMED TO DATE FOLLOWS: SIDEWINDER BASELINE COOK-OFF TESTS WERE CONDUCTED FROM JANUARY TO AUGUST 1972 AND REPORTED IN NAVMISCEN TP 73-20 OF 14 MARCH 1973. BASELINE COOK-OFF TEST OF SHRIKE AND SPARROW MISSILES WERE COMPLETED IN JUNE OF 1974 AND A REPORT RELEASED IN OCTOBER. STANDARD ARM TESTS ARE BEING CONDUCTED IN FY 76/77.

AS NOTED EARLIER, DATA FROM THE BASELINE SERIES ARE USED IN THE DEVELOPMENT OF THERMAL PROTECTION SYSTEMS. ONE OF THE INTERMEDIATE STEPS IN THE DEVELOPMENT OF THERMAL PROTECTION SYSTEMS IS COOK-OFF IMPROVEMENT CONCEPT FEASIBILITY STUDIES.

THE THERMAL PROTECTION CONCEPTS CURRENTLY BEING INVESTIGATED INCLUDED HEAT PATH INTERRUPTERS, EXTERNAL COATINGS, INTERNAL INSULATORS OR IMPROVED LINERS AND VARIOUS DESIGN MODIFICATIONS.

EXTERNAL COATINGS HAVE BEEN TESTED ON SIDEWINDER MOTORS AND WARHEADS AND HAVE DEMONSTRATED THAT THEY CAN INCREASE COOK-OFF TIME. SIDEWINDER MOTOR REACTION TIMES WERE INCREASED FROM APPROXIMATELY ONE TO FIVE MINUTES UTILIZING 60 MILS OF AN EXTERNAL INTUMESER. SIDEWINDER WARHEAD REACTIONS WERE INCREASED FROM APPROXIMATELY THREE TO NINE MINUTES USING THE SAME COATING. NO NOTICEABLE CHANGE IN TYPE OF REACTION OCCURRED.

AT THE END OF THE SIDEWINDER AND SPARROW BASELINE SERIES INTERNAL INSULATORS WERE TESTED TO DETERMINE THEIR FEASIBILITY. IN THE SIDEWINDER WARHEAD 80 MILS OF ALUMINA SILICA FIBER WAS INSERTED BETWEEN THE WARHEAD EXPLOSIVE BILLET AND THE ROD BUNDLE TO ACT AS AN INTERNAL INSULATOR. IN CONCEPT FEASIBILITY TESTS OF SHRIKE WARHEADS AND MOTORS, EXTERNAL STRESS RISERS WERE EMPLOYED IN AN ATTEMPT TO REDUCE THE VIOLENCE OF THE COOK-OFF REACTION WHICH IS AN EXPLOSION. IN THE CASE OF THE MK 30 MOTOR. TESTS DEMONSTRATED THAT REDUCTION TO A DEFLAGRATION IS POSSIBLE. IT IS IMPORTANT TO NOTE, HOWEVER, THAT BOTH INTERNAL INSULATORS AND DESIGN MODIFICATIONS ARE CONSIDERABLY MORE DIFFICULT TO QUALIFY AND RETROFIT THAN EXTERIOR COATINGS. FOR THIS REASON THE MAJOR TRUST OF PRODUCTION SYSTEM DEVELOPMENT AT THIS TIME IS OCCURRING IN THE EXTERNAL COATINGS AREA.

THE SIDEWINDER TESTS MENTIONED EARLIER WERE CONDUCTED USING AN INTUMESCENT COATING MATERIAL DESIGNATED NASA 313. ALTHOUGH THIS MATERIAL DEMONSTRATED THAT EXTERNAL COATINGS CAN PROVIDE ADEQUATE THERMAL PROTECTION TO MISSILES, IT ALSO DEMONSTRATED THAT A NUMBER OF MATERIAL PROBLEMS NEED TO BE SOLVED BEFORE AN EXTERNAL COATING CAN BE CONSIDERED PRACTICAL FOR MISSILE APPLICATIONS. THESE PROBLEMS INCLUDE: INCREASED THERMAL PERFORMANCE TO PROVIDE FOR A MINIMUM THICKNESS, THICKNESS CONTROL, FINISH, APPLICATION TECHNIQUE, ADHESION AND ENVIRONMENTAL CHARACTERISTICS.

THE CURRENT PROTECTION SYSTEM DEVELOPMENT EFFORTS ARE DESIGNED TO OVERCOME SUCH DEFICIENCIES. CURRENT EFFORTS INCLUDE FLEXIBLE WRAP COATINGS AND IMPROVED INTUMESCENT COATINGS BEING DEVELOPED UNDER NAVY DIRECTION, COATING, BEING DEVELOPED IN-HOUSE BY THE NAVY, AND COATINGS BEING DEVELOPED BY PRIVATE INDUSTRY NOT UNDER NAVY DIRECTION WHO SEE MARKETING POTENTIAL IN OUR PROGRAM.

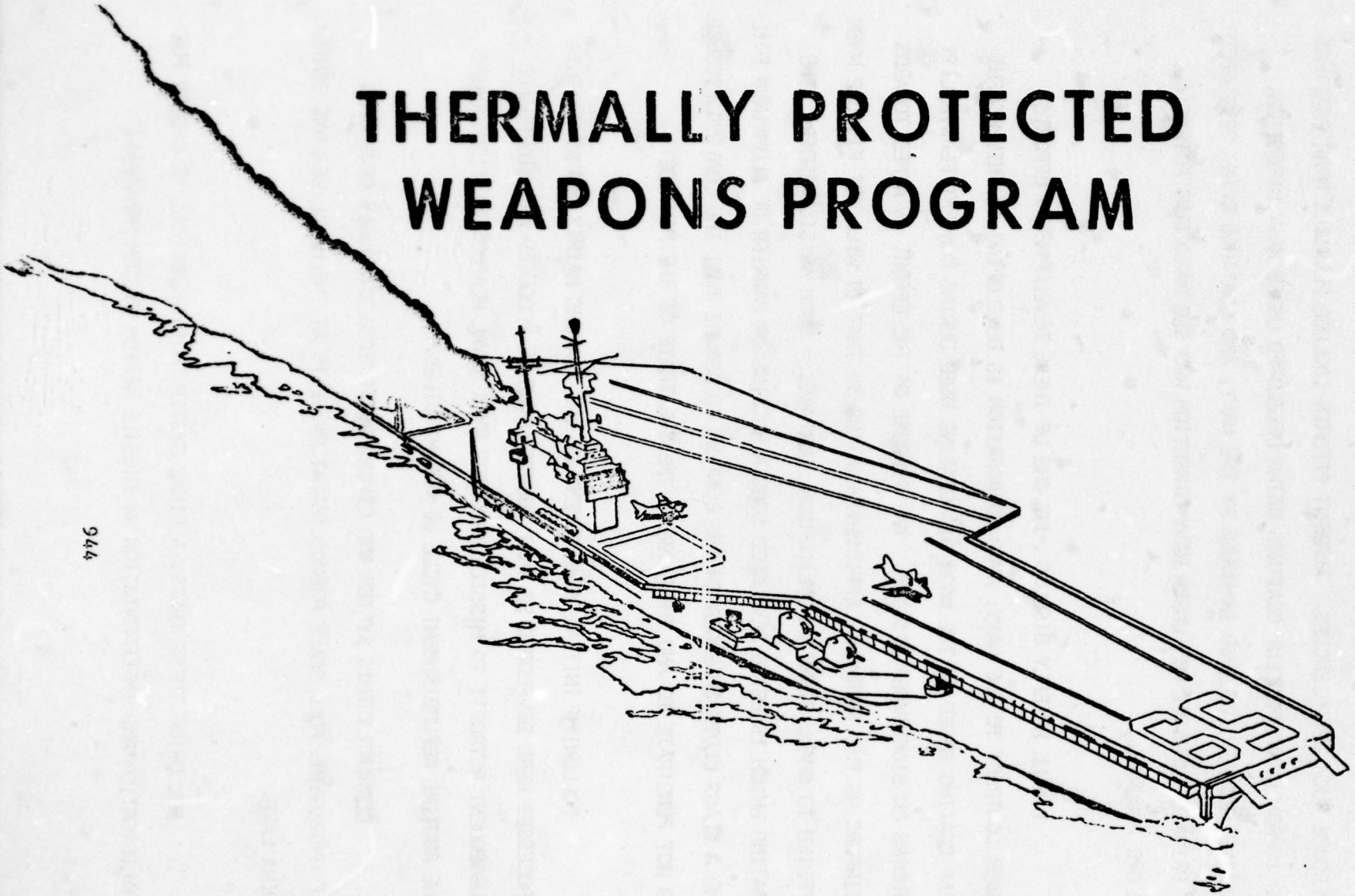
I WILL BRIEFLY DISCUSS JUST ONE OF THESE DEVELOPMENTS EFFORTS. UNDER CONTRACT TO THE NAVY, AVCO CORPORATION IS DEVELOPING AN INTUMESCENT WRAP COATING BASED ON THE NASA 313 COATING USED DURING CONCEPT FEASIBILITY STUDIES ON SIDEWINDER MISSILE. THE PURPOSE OF THE EFFORT IS AIMED TOWARDS REINFORCING THE THERMALLY EFFICIENT COATING SO THAT IT WILL NOT FISSURE WHEN APPLIED TO SMALL DIAMETER CYLINDRICAL SURFACES - SUCH AS SIDEWINDER. THE COATING WHICH IS BEING DEVELOPED USES A BACKING OR CARRIER OF ALUMNINUM FOIL AND A GLASS CLOTH IMBEDDED IN THE COATING TO ASSURE THAT THE COATING FISSURE, DO NOT PENETRATE TO AND THEN EXPOSE THE SUBSTRATE OF THE MISSILE.

FOLLOWING INITIAL DEVELOPMENT OF THE COATING MATRIX, MANUFACTURING PROCESSES WERE DEVELOPED SO THAT SHEETS COULD BE PRODUCED AND STORED FOR SUBSEQUENT RETROFIT TO MISSILE HARDWARE BY A NAVAL WEAPONS STATION DURING THE ROUTINE REFURBISHMENT CYCLE OF OUR MISSILES.

CURRENTLY THIS SYSTEM AND OTHERS BEING SIMULTANEOUSLY DEVELOPED ARE UNDERGOING FULL SCALE PREQUALIFICATION TESTS AT THE NAVAL WEAPONS CENTER CHINA LAKE.

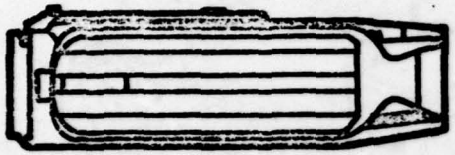
FOLLOWING THESE TESTS, A FINAL SYSTEM OR SYSTEMS WILL BE CHOSEN FOR QUALIFICATION AND IMPLEMENTATION BY MISSILE WEAPON SYSTEM MANAGERS.

THERMALLY PROTECTED WEAPONS PROGRAM



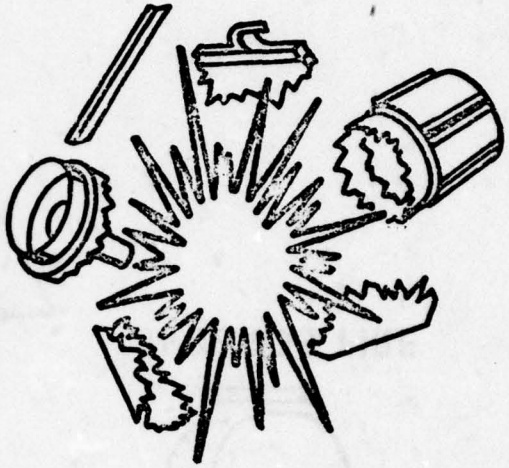
944

COOK-OFF



ORDNANCE





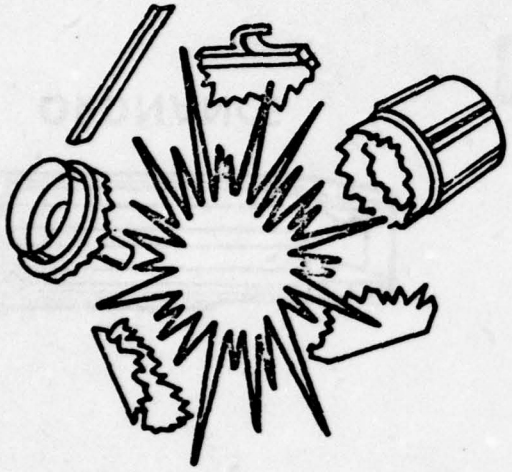
REACTION



FIRE

945

CARRIER SURVIVABILITY



VIOLENT COOK-OFF





SPREADS FIRE

KILLS OR INJURES

946

COOK-OFF DEFINITIONS

DETONATION: MUNITION REACTS IN IT'S DESIGN MODE

EXPLOSION: VIOLENT PRESSURE RUPTURE WITH FRAGMENTATION AND RESULTING SHOCK WAVE

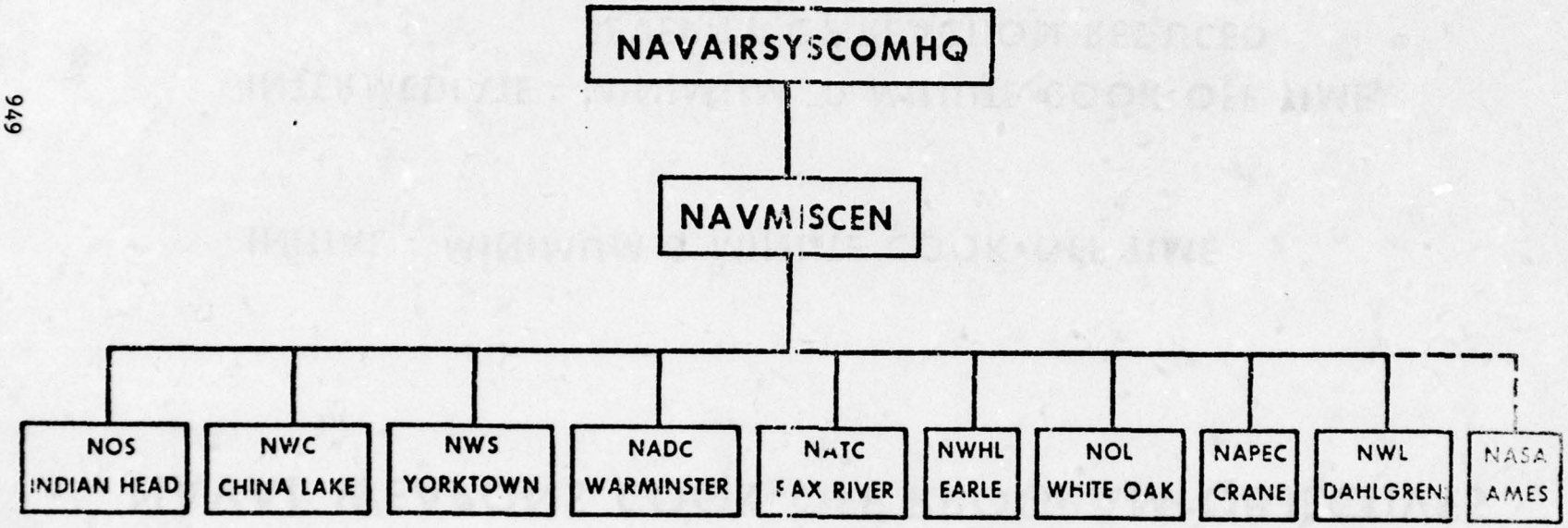
DEFLAGRATION: PRESSURE RUPTURE OR BURNING WITH NO FRAGMENTATION OR SHOCK WAVE

NAVY WEAPON COOK-OFF PROGRAM

- "BASELINE" COOK-OFF OF WEAPONS IN INVENTORY
- IN-SERVICE WEAPONS COOK-OFF IMPROVEMENT
- ADVANCED COOK-OFF PROTECTION CONCEPTS

WEAPON COOK-OFF IMPROVEMENT PROGRAM

ORGANIZATION



NAVAL WEAPONS COOK-OFF PROGRAM OBJECTIVES

INITIAL - MINIMUM 5 MINUTE COOK-OFF TIME

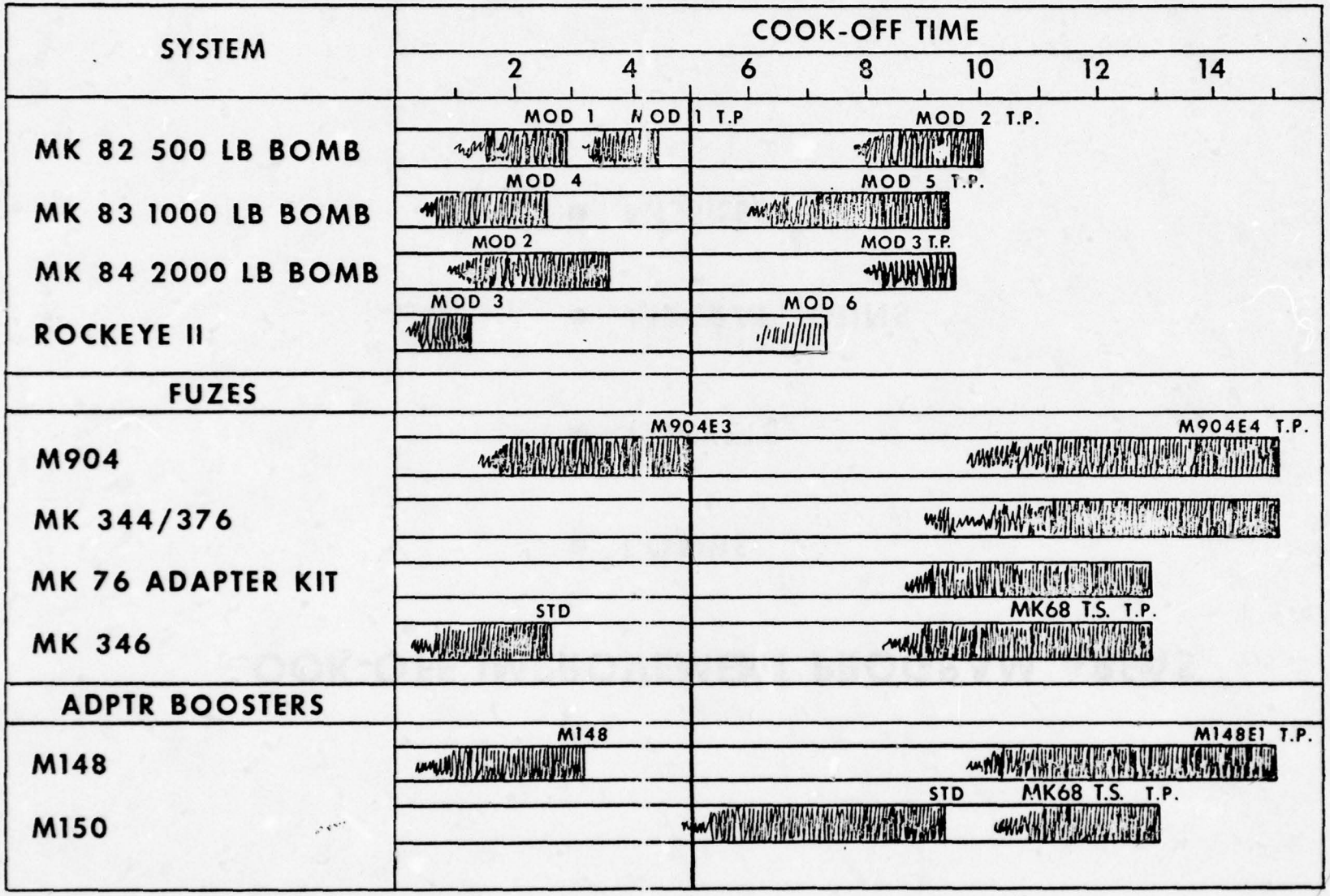
INTERMEDIATE - MINIMUM 10 MINUTE COOK-OFF TIME,
SEVERITY OF REACTION REDUCED

ULTIMATE - PROVIDE WEAPONS THAT WILL NEITHER
DETONATE NOR EXPLODE

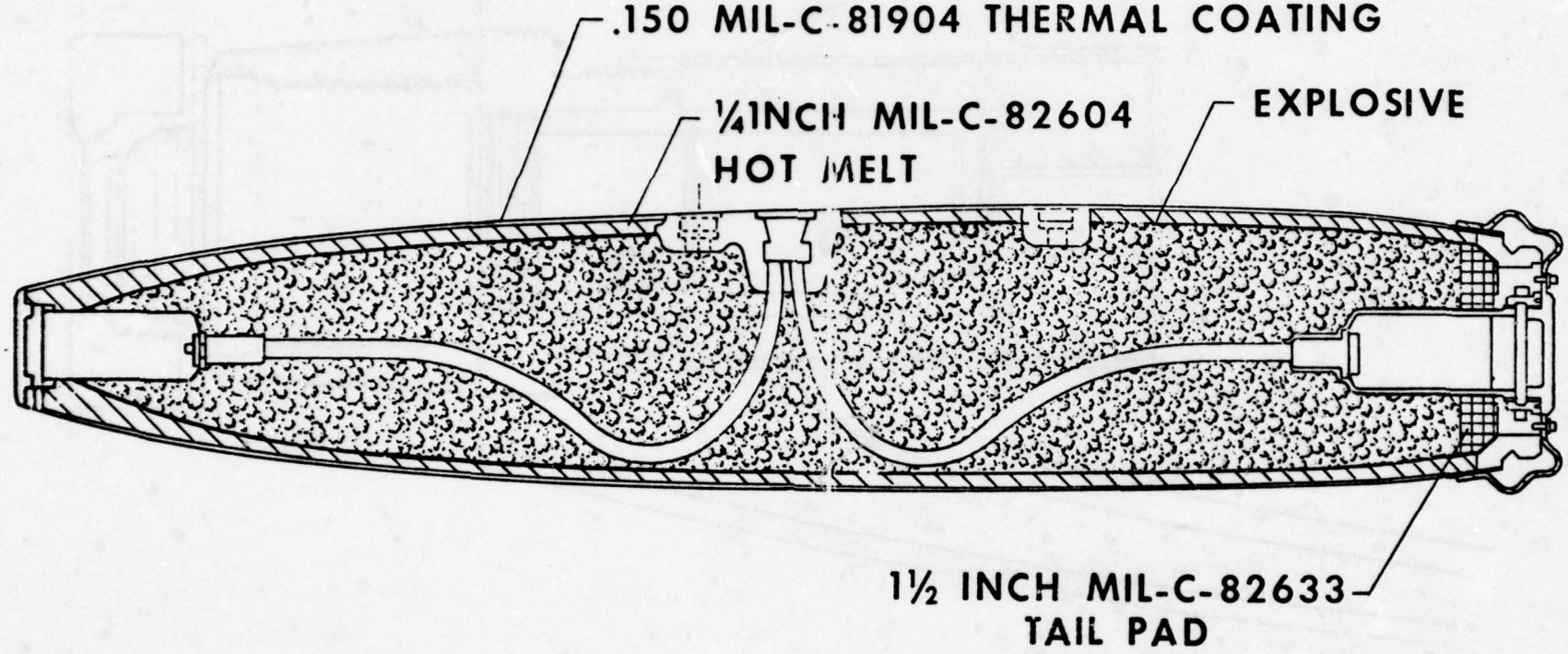
COOK-OFF IMPROVEMENT PROGRAM AREAS

- BOMBS
- ROCKETS
- AIRCRAFT GUNS
- MISSILES

BOMB COOK-OFF IMPROVEMENT PROGRAM STATUS

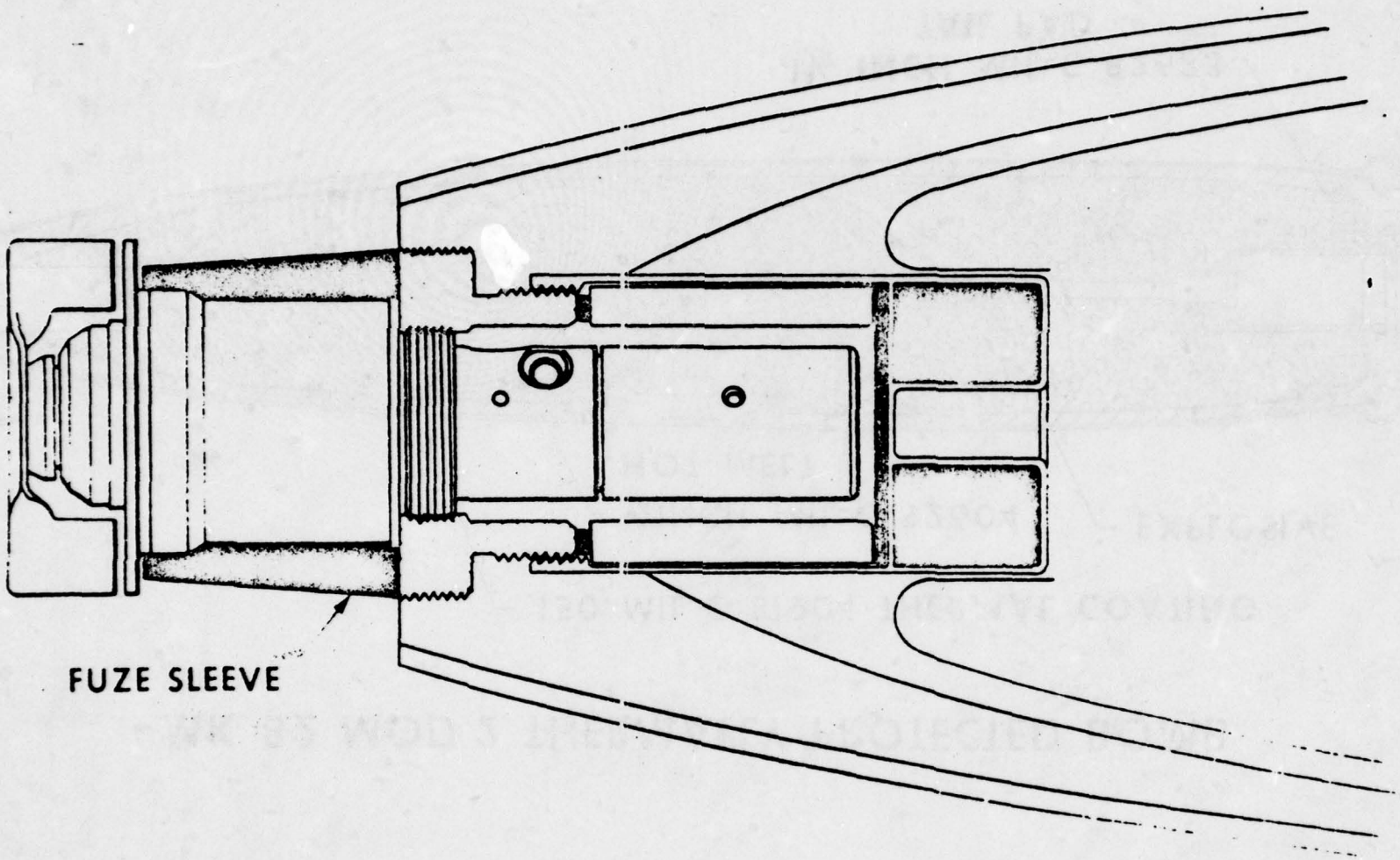


MK 82 MOD 2 THERMALLY PROTECTED BOMB

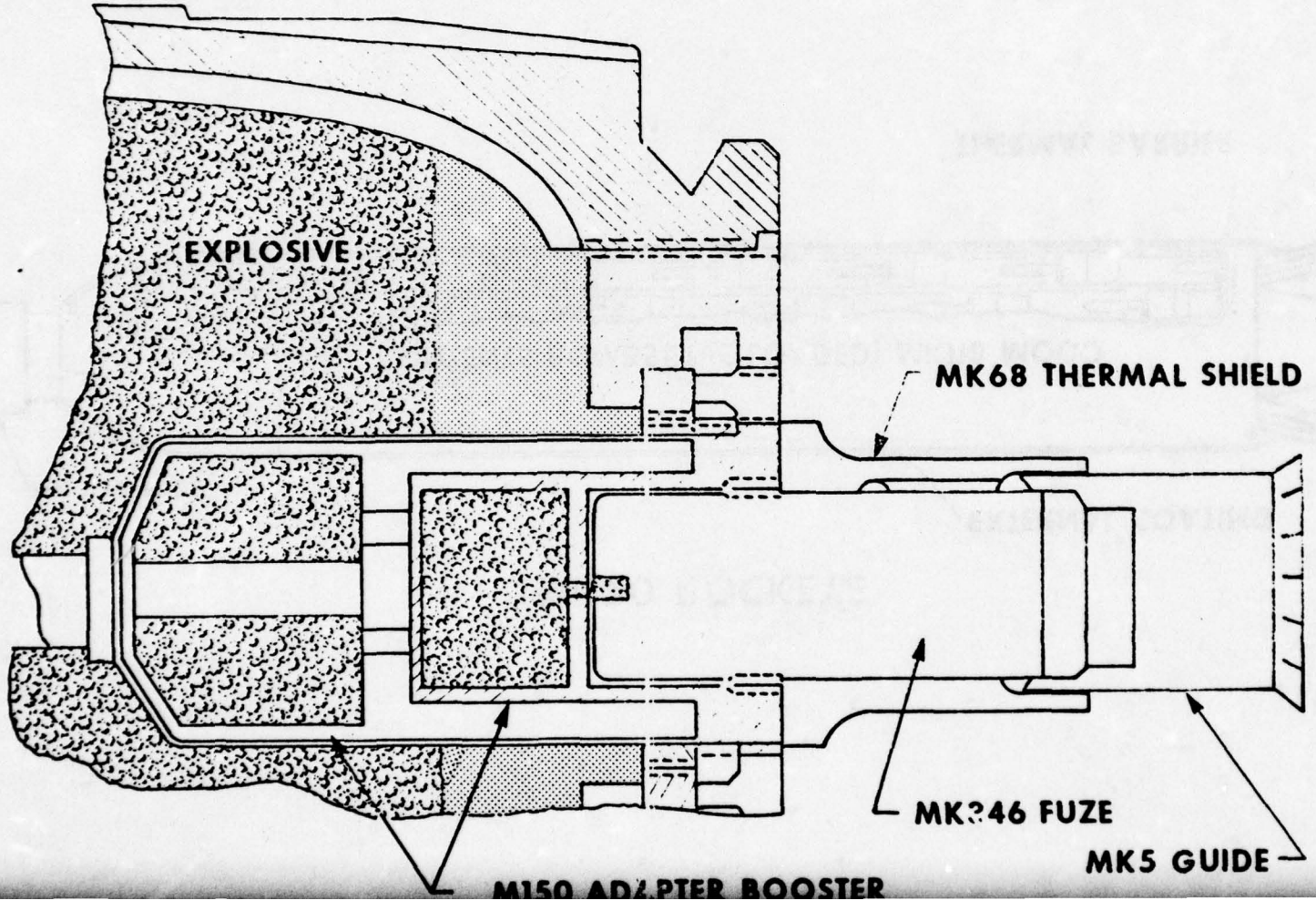


953

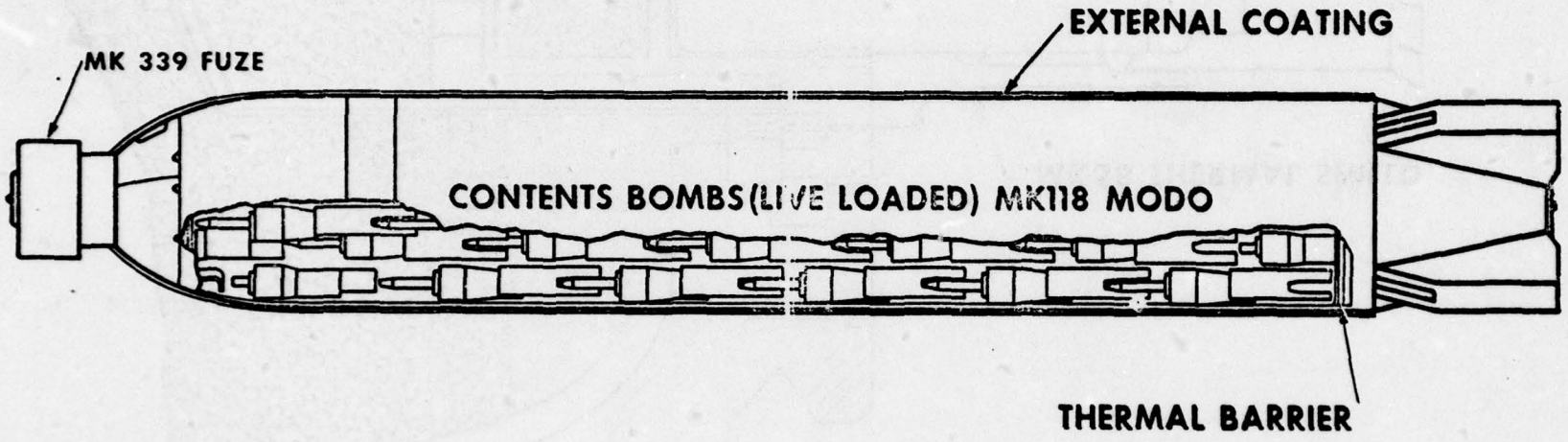
M904E4 FUZE/M148E1 ADAPTER BOOSTER COMBINATION



MK346 AND M150 ADAPTER BOOSTER WITH MK68 THERMAL SHIELD

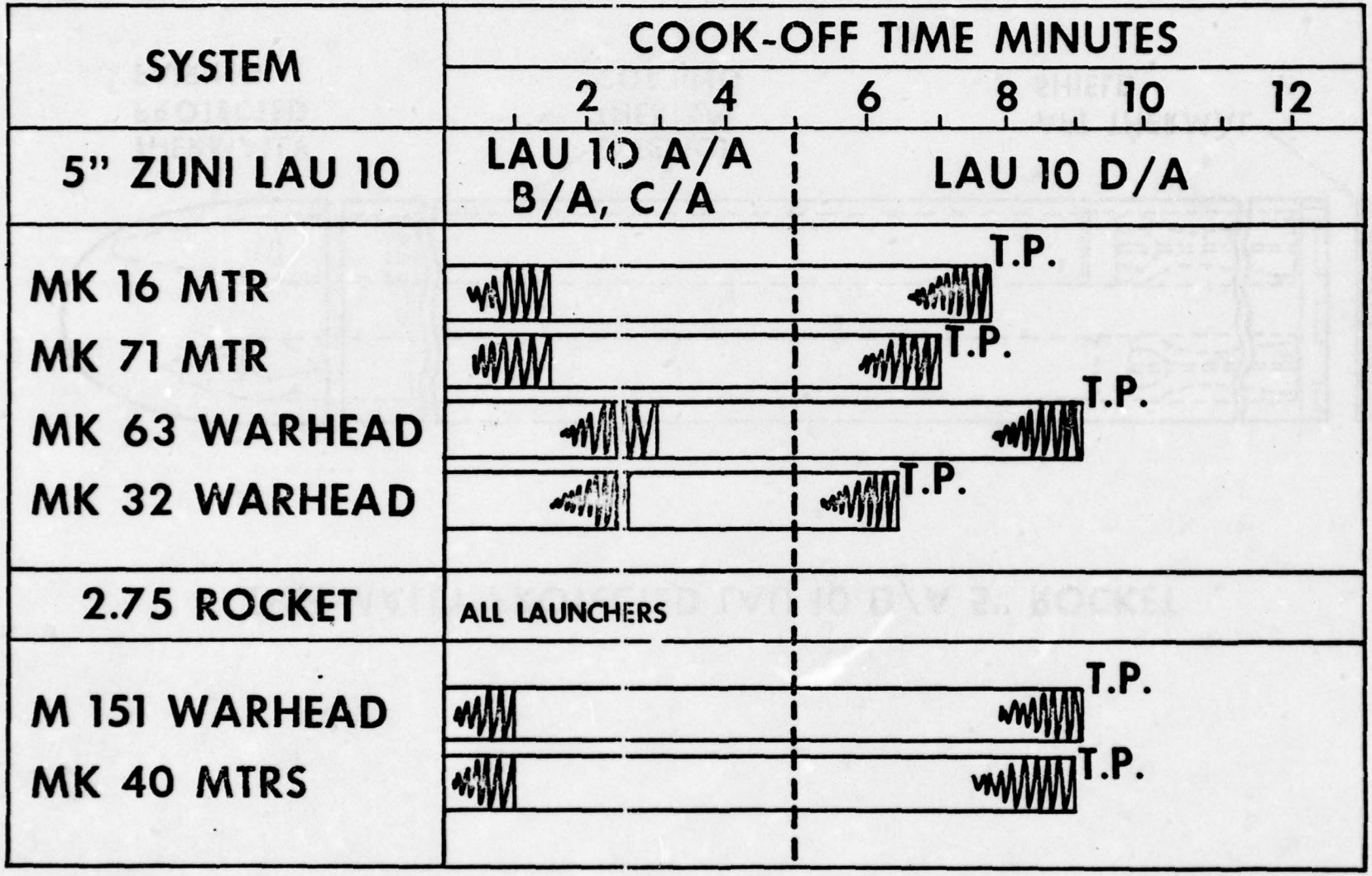


MK20 ROCKEYE

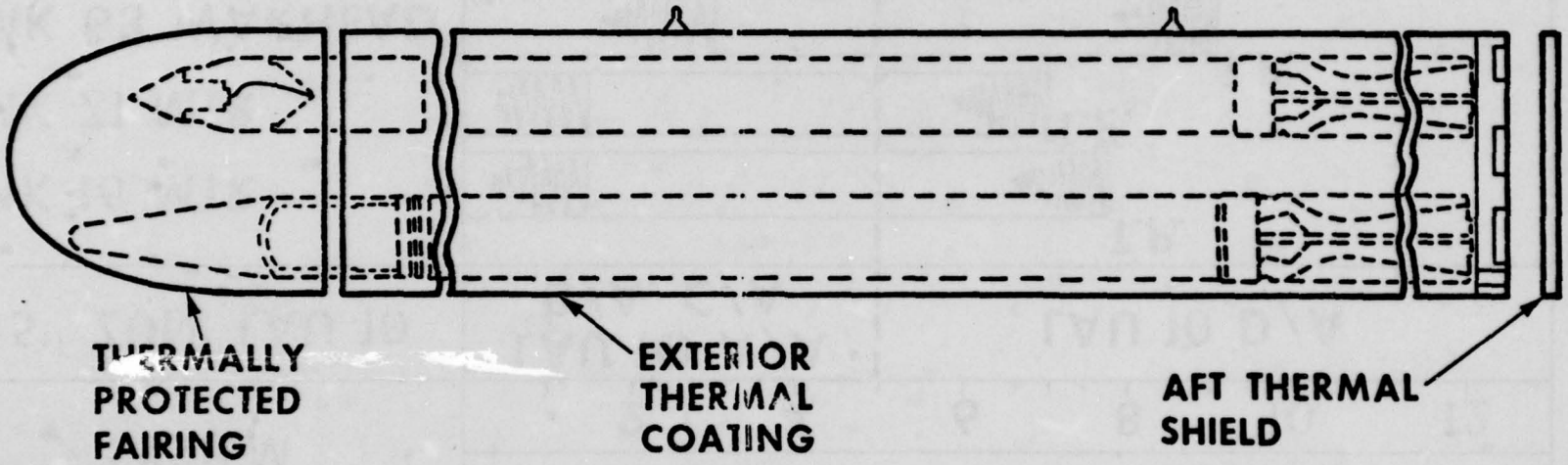


956

ROCKET COOK-OFF IMPROVEMENT PROGRAM STATUS



THERMALLY PROTECTED LAU 10 D/A 5" ROCKET



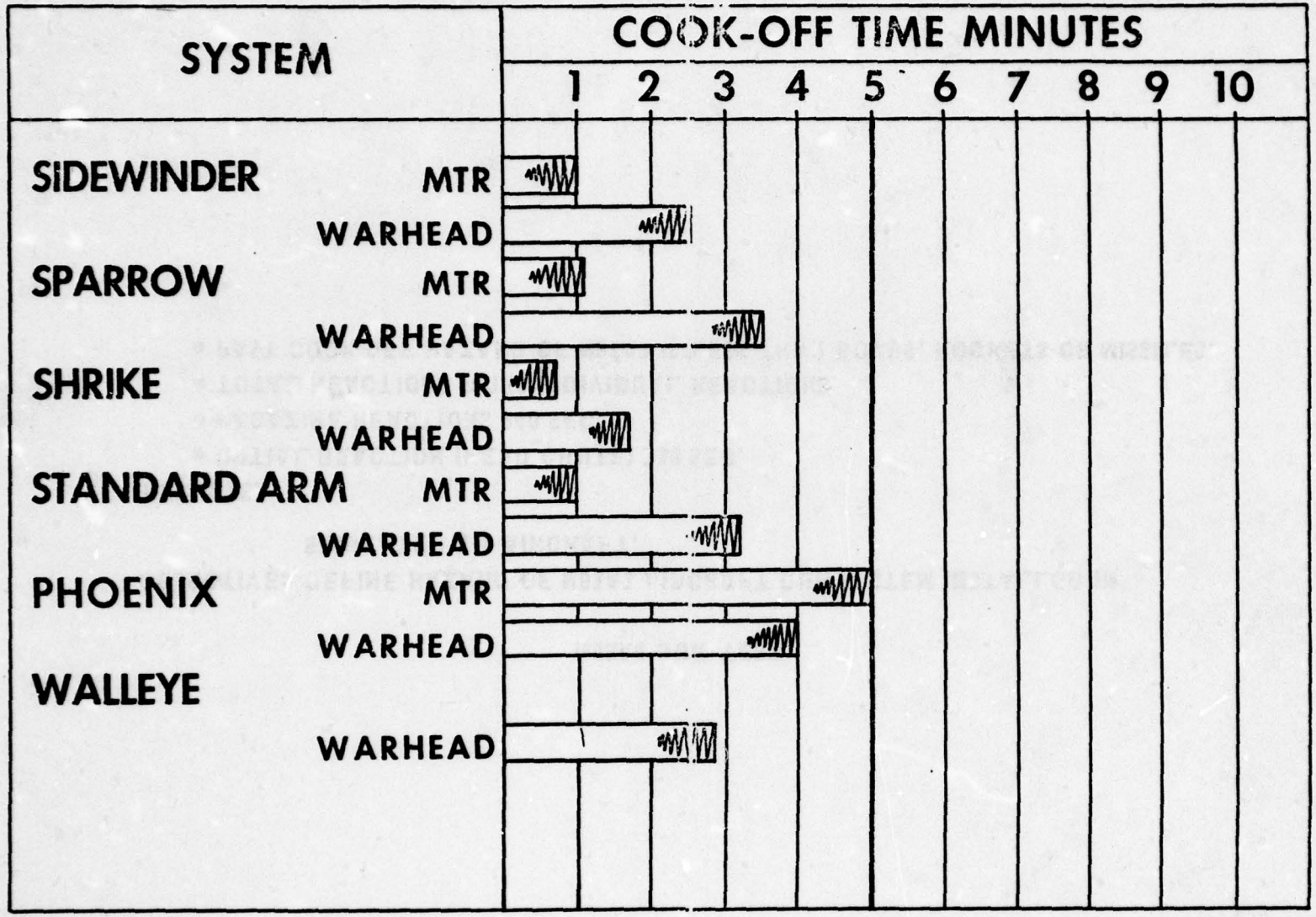
M61A1 GUN TEST

OBJECTIVE: DEFINE HAZARD OF M61A1 AIRCRAFT GUN SYSTEM INSTALLED IN SIMULATED A-7 AIRCRAFT.

RESULTS:

- INITIAL REACTION (FEED CHUTE) 130 SEC.
- MAGAZINE REACTIONS 240 SEC.
- TOTAL REACTIONS ≈ 750 INDIVIDUAL REACTIONS.
- FAST COOK-OFF HAZARD OF M61A1 IS LESS THAN BOMBS, ROCKETS OR MISSILES.

MISSILE COOK-OFF IMPROVEMENT PROGRAM

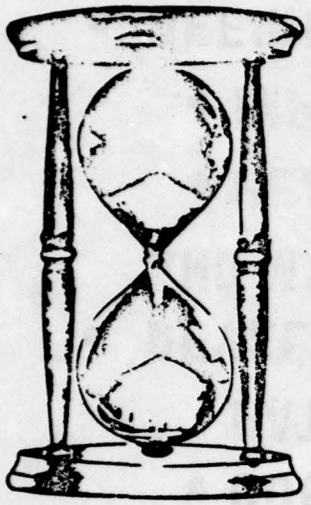


960

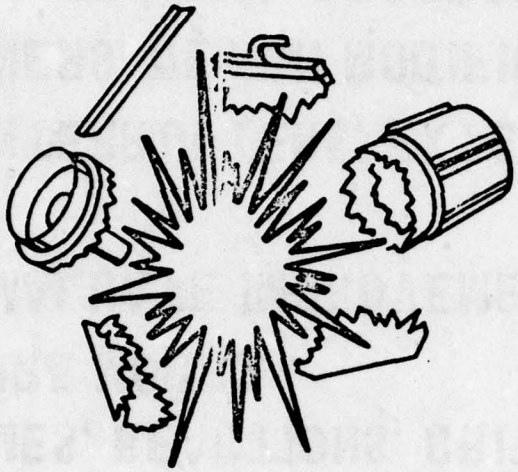
APPROACH

- DEFINE BASELINE CHARACTERISTICS:
  - COOK-OFF TIMES, REACTIONS, CRITICAL HEAT PATHS, FAILURE MODES.
- DEVELOP AND EVALUATE IMPROVEMENT CONCEPTS AND MATERIALS:
  - HEAT PATH INTERRUPTERS, EXTERNAL COATINGS.
  - IMPROVED LINERS, DESIGN MODIFICATIONS.
- DEFINE RETROFIT THERMAL PROTECTION SYSTEM THROUGH TEST AND EVALUATION:
  - NAVY TECHNICAL EVALUATION.
  - PROCESS ECP'S.

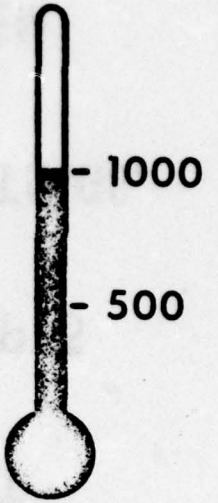
BASELINE TESTING



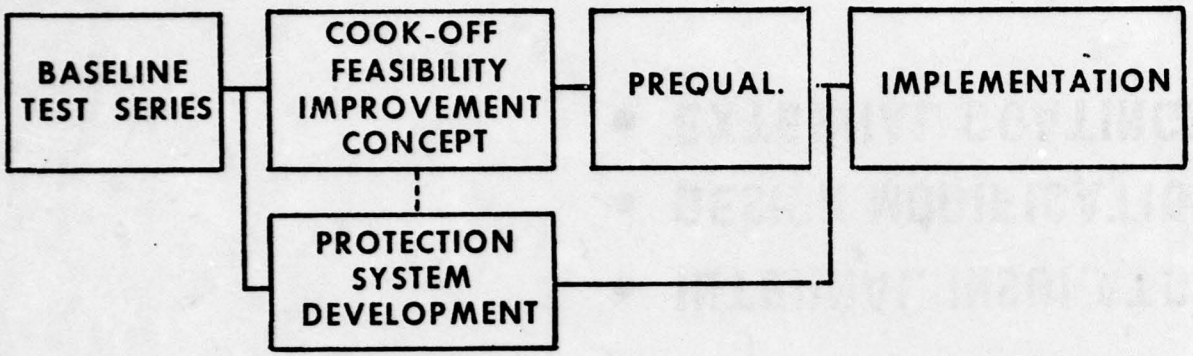
TIME



REACTION TYPE



T.C. DATA



BASELINE TESTING

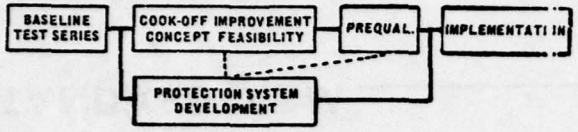
963

SIDEWINDER _____ MAR 1973

SHRIKE/SPARROW _____ OCT 1974

STANDARD ARM _____ FY 1975/FY 1976

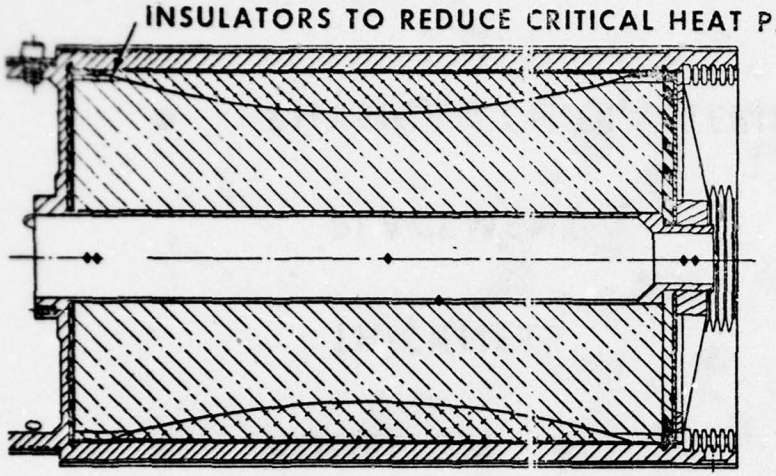
SUPPLEMENTED BY NSWC DAHLGREN DATA. ___ 1969 - 72

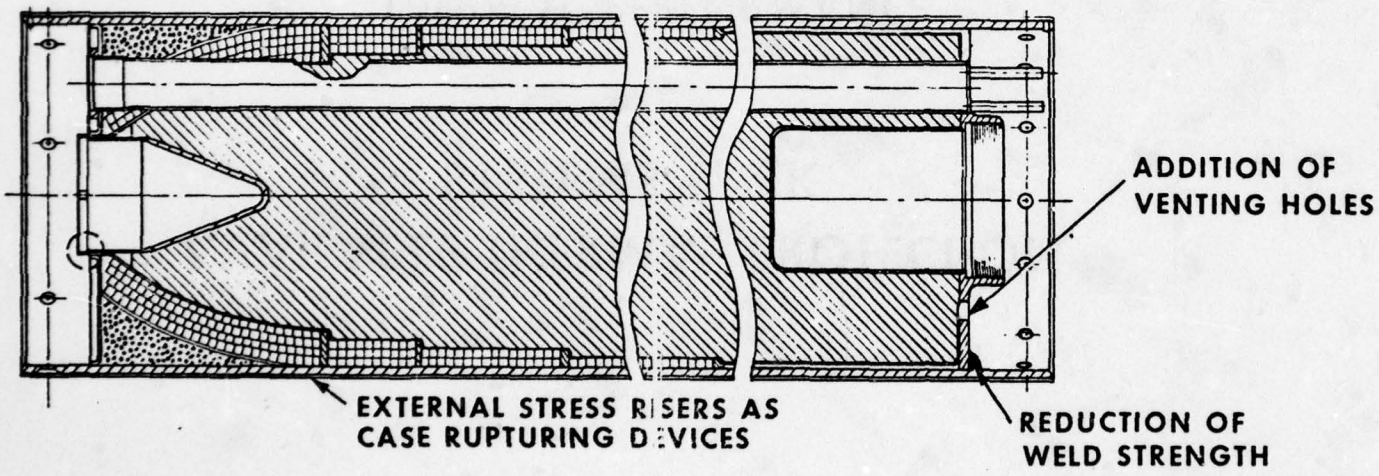


COOK-OFF IMPROVEMENT CONCEPT FEASIBILITY

- INTERNAL INSULATORS
- DESIGN MODIFICATIONS
- EXTERNAL COATINGS

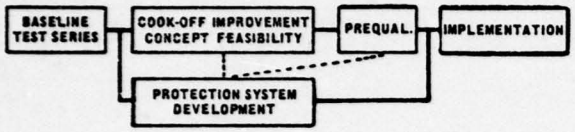
INTERNAL INSULATORS AND DESIGN MODIFICATIONS





AVAILABLE THERMAL PROTECTION SYSTEMS LACK

- THERMAL PERFORMANCE
- APPLICATION CONTROLS
- ADHESION
  - THICKNESS
  - PLACEMENT
- PHYSICAL CHARACTERISTICS



THERMAL PROTECTION SYSTEM DEVELOPMENT

- FLEXIBLE WRAP COATING
- NAVY DEVELOPED INTUMESCENT COATING
- IMPROVED NASA INTUMESCENT PAINT
- PROPRIETARY THERMAL COATINGS
- SUPPORTING STUDIES

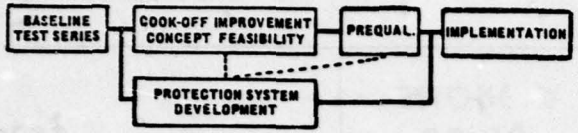
FLEXIBLE WRAP COATING DEVELOPMENT

- REINFORCEMENT TO REDUCE FISSURING
- ADHESIVES STUDY
- APPLICATION TECHNIQUE DEVELOPMENT
- MANUFACTURING AND PRODUCTION SPECIFICATIONS

EXTERIOR COATINGS

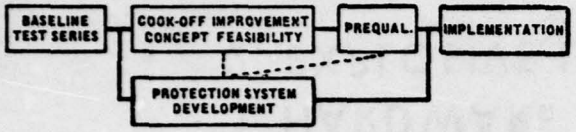
	FLEXIBLE WRAP COATING	NAVY DEVELOPED LIQUID INTUMESCENT COATING	IMPROVED NASA PAINT	MIL-C-81945
APPLICATION	WRAP SHEETS	SPRAY	BOND FREE FILM	SPRAY*
COATING EFFICIENCY				
SEC/MIL TO 500° F	2.7	3.2	2.7+	2.3
SEC/MIL TO 1000° F	5.2	5.0	6.0	5.0
TOP COAT REQUIRED	YES	YES	YES	YES
FINISH	VERY GOOD	VERY GOOD	GOOD	FAIR
DIR. IMPACT STRENGTH	100 IN-LBS	48 IN-LBS	45 IN-LBS	100 IN-LBS
REV. IMPACT STRENGTH	15 IN-LBS	8 IN-LBS	5 IN-LBS	4 IN-LBS
HARDNESS	80-90 SHORE A	77-80 SHORE A	90-95 SHORE A	90-95 SHORE A

*CURRENT METHOD



PREQUALIFICATION EVALUATION OF THERMAL PROTECTION SYSTEM

- SYSTEM APPLICATION EVALUATION
- FAST COOK-OFF
- CAPTIVE FLIGHT
- ENVIRONMENTAL
- LOGISTICS CYCLE EVALUATION



THERMAL PROTECTION SYSTEM IMPLEMENTATION

- INTERIM QUALIFIED SYSTEMS AVAILABLE FOR MISSILE PROGRAM MANAGERS
- FINAL QUALIFICATION AND IMPLEMENTATION TO BE ACCOMPLISHED BY PROGRAM MANAGERS

QUALIFICATION TESTS

CONFIGURATION DEFINITION COOK-OFF TESTS
ENVIRONMENTAL SAFETY EVALUATION
SHIP SUITABILITY
BALLISTICS
EXPOSURE
    1. SHIPMENT
    2. ENVIRONMENT
APPLICATION DEMONSTRATION
INTERFACES
DOCUMENTATION
    1. HARDWARE
    2. EXPLOSIVE LOADING